

Fall 1997

Modeling study on the neopentyl+ O₂ reaction system and experimental and modeling study on MTBE pyrolysis and oxidation

Ru Wei

New Jersey Institute of Technology

Follow this and additional works at: <https://digitalcommons.njit.edu/dissertations>



Part of the [Environmental Sciences Commons](#)

Recommended Citation

Wei, Ru, "Modeling study on the neopentyl+ O₂ reaction system and experimental and modeling study on MTBE pyrolysis and oxidation" (1997). *Dissertations*. 1071.

<https://digitalcommons.njit.edu/dissertations/1071>

This Dissertation is brought to you for free and open access by the Theses and Dissertations at Digital Commons @ NJIT. It has been accepted for inclusion in Dissertations by an authorized administrator of Digital Commons @ NJIT. For more information, please contact digitalcommons@njit.edu.

Copyright Warning & Restrictions

The copyright law of the United States (Title 17, United States Code) governs the making of photocopies or other reproductions of copyrighted material.

Under certain conditions specified in the law, libraries and archives are authorized to furnish a photocopy or other reproduction. One of these specified conditions is that the photocopy or reproduction is not to be “used for any purpose other than private study, scholarship, or research.” If a user makes a request for, or later uses, a photocopy or reproduction for purposes in excess of “fair use” that user may be liable for copyright infringement,

This institution reserves the right to refuse to accept a copying order if, in its judgment, fulfillment of the order would involve violation of copyright law.

Please Note: The author retains the copyright while the New Jersey Institute of Technology reserves the right to distribute this thesis or dissertation

Printing note: If you do not wish to print this page, then select “Pages from: first page # to: last page #” on the print dialog screen

The Van Houten library has removed some of the personal information and all signatures from the approval page and biographical sketches of theses and dissertations in order to protect the identity of NJIT graduates and faculty.

INFORMATION TO USERS

This manuscript has been reproduced from the microfilm master. UMI films the text directly from the original or copy submitted. Thus, some thesis and dissertation copies are in typewriter face, while others may be from any type of computer printer.

The quality of this reproduction is dependent upon the quality of the copy submitted. Broken or indistinct print, colored or poor quality illustrations and photographs, print bleedthrough, substandard margins, and improper alignment can adversely affect reproduction.

In the unlikely event that the author did not send UMI a complete manuscript and there are missing pages, these will be noted. Also, if unauthorized copyright material had to be removed, a note will indicate the deletion.

Oversize materials (e.g., maps, drawings, charts) are reproduced by sectioning the original, beginning at the upper left-hand corner and continuing from left to right in equal sections with small overlaps. Each original is also photographed in one exposure and is included in reduced form at the back of the book.

Photographs included in the original manuscript have been reproduced xerographically in this copy. Higher quality 6" x 9" black and white photographic prints are available for any photographs or illustrations appearing in this copy for an additional charge. Contact UMI directly to order.

UMI

A Bell & Howell Information Company
300 North Zeeb Road, Ann Arbor MI 48106-1346 USA
313/761-4700 800/521-0600

UMI Number: 9822283

**Copyright 1997 by
Wei, Ru**

All rights reserved.

**UMI Microform 9822283
Copyright 1998, by UMI Company. All rights reserved.**

**This microform edition is protected against unauthorized
copying under Title 17, United States Code.**

UMI
300 North Zeeb Road
Ann Arbor, MI 48103

**MODELING STUDY ON THE NEOPENTYL + O₂ REACTION SYSTEM
AND
EXPERIMENTAL AND MODELING STUDY ON MTBE PYROLYSIS AND
OXIDATION**

**by
Ru Wei**

**A Dissertation
Submitted to the Faculty of
New Jersey Institute of Technology
in Partial Fulfillment of the Requirements for the Degree of
Doctor of Philosophy**

**Department of Chemical Engineering,
Chemistry, and Environmental Science**

October 1997

Copyright © 1997 by Ru Wei
ALL RIGHTS RESERVED

APPROVAL PAGE

**MODELING STUDY ON THE NEOPENTYL + O₂ REACTION SYSTEM
AND
EXPERIMENTAL AND MODELING STUDY ON MTBE PYROLYSIS AND
OXIDATION**

by
Ru Wei

Dr. Joseph W. Bozzelli, Dissertation Advisor Date
Distinguished Professor of Chemistry, NJIT, Newark, New Jersey

Dr. Richard B. Trattner, Committee Member Date
Professor of Chemistry and Environmental Science, NJIT, Newark, New Jersey

Dr. Barbara B. Kebbekus, Committee Member Date
Professor of Chemistry, NJIT, Newark, New Jersey

Dr. Carol A. Venanzi, Committee Member Date
Distinguished Professor of Chemistry, NJIT, Newark, New Jersey

Dr. Ernst U. Monse, Committee Member Date
Professor of Chemistry, Rutgers at Newark, Newark, New Jersey

ABSTRACT

MODELING STUDY ON THE NEOPENTYL + O₂ REACTION SYSTEM AND EXPERIMENTAL AND MODELING STUDY ON MTBE PYROLYSIS AND OXIDATION

**by
Ru Wei**

A modeling study on neopentyl radical + O₂ reaction system is conducted in this study. Thermodynamic parameters on all species and important transition states are calculated. A thermochemical kinetic analysis is performed.

Thermodynamic parameters are estimated using group additivity with HBI groups. Transition state energies are evaluated from experimental and theoretical data in the literature, combined with elementary reaction modeling to account for temperature effects. Transition state structures, vibration frequencies and entropies are determined from semi-empirical calculations, MOPAC PM3. Kinetics are analyzed with quantum RRK theory for $k(E)$ coupled with modified strong collision analysis of Gilbert et al for fall-off. An elementary reaction mechanism is constructed to model experimental data in the literature focusing on this neopentyl + O₂ reaction system.

Experimental and modeling studies are conducted for methyl *tert*-butyl ether (MTBE) pyrolysis and oxidation. Experimental data are presented in argon diluent in a high pressure, flow reactor over a wide temperature range and at three pressures of 4, 7, 10 atm. Three equivalence ratios were selected for the study of oxidation of MTBE. On-

line GC-FID was used to analyze reacted mixture from flow reactor. Iso-butene and methanol are observed as major products from both oxidation and pyrolysis of MTBE experiments. Acetone, formaldehyde, propene and methane are additional important products.

A detailed, pressure and temperature dependent, kinetic model is developed for the pyrolysis and oxidation of MTBE. The mechanism includes oxidation and thermal decomposition of the major products and other important intermediates. Thermodynamic parameters, transition states and kinetics are estimated, evaluated and analyzed as in the neopentyl modeling work.

Chebyshev polynomials (7×3) incorporate the pressure and temperature dependence into rate constant expressions. A modified Chemkin Interpreter is used to incorporate the combined pressure and temperature dependent rate expressions into the Chemkin integrators.

A specific reaction series: one of β -scission of $C.CR'COOH$, hydroperoxy alkyl radical to form an olefin plus a hydroperoxy methyl radical $RC.OOH$. This $RC.OOH$ rapidly decompose to lower energy products: $RCHO + OH$. Little or no evidence is observed for formation of the final products in the transition state of the first β -scission step.

BIOGRAPHICAL SKETCH

Author: Ru Wei

Degree: Doctor of Philosophy in Environmental Science

Date: October 1997

Undergraduate and Graduate Education:

- Doctor of Philosophy in Environmental Science,
New Jersey Institute of Technology, Newark, NJ, 1997
- Master of Science in Chemistry,
East Normal University of China, ShangHai, People's Republic of China, 1988
- Bachelor of Science in Analytical Chemistry,
Jiang Xi University, Nan Chang, People's Republic of China, 1985

Major: Environmental Science

Presentations and Publications:

Wei, Ru; Bozzelli, Joseph W. "Kinetic Study on Neopentyl + O₂ Reaction System", "CHEMICAL AND PHYSICAL PROCESSES IN COMBUSTION" 1995 fall technical Meeting,, The Eastern Section of The Combustion Institute, Worcester Polytechnic Institute, Worcester, Massachusetts, USA, October 16-18, 1995.

Wei, Ru; Bozzelli, Joseph W. "Kinetic Study on Neopentyl + O₂ Reaction System", J. Phys. Chem., submitted, 1997.

Wei, Ru; Bozzelli, Joseph W. "Modeling Study on MTBE Pyrolysis and Oxidation", The Fourth International Conference on Chemical Kinetics, National Institute of Standard Technologies, Washington, D. C., 1997.

**This dissertation is dedicated to
my beloved family**

ACKNOWLEDGMENT

I wish to express my appreciation to Prof. Joseph W. Bozzelli, my advisor, not only for his professional advice but also his encouragement, patience, and kindness. I am deeply indebted to him for the opportunities which he made available to me.

I would also like to thank to my dissertation committee members, Dr. Richard B. Trattner, Dr. Barbara B. Kebbekus, Dr. Carol A. Venanzi, and Dr. Ernst Monse, for their helpful corrections and productive comments.

It is my pleasure to thank Dr. Wen-Jiun Ing, who installed the high pressure experimental apparatus during his thesis work and shared his experiences with me of working on that high pressure experimental system. In addition, I like to thank my coworkers at NJIT, Xian Zhong, Chiung-Ju Chen, Samuel Chern and Takahiro Yamada, for having dealt with me as a colleague, which has made my time at NJIT much more enjoyable and productive.

For love and inspiration I shall be eternally grateful to my family and my friends. Without their constant support and encouragement, I truly believe all of this would not have been possible.

TABLE OF CONTENTS

Chapter	Page
PART I THERMO CHEMICAL AND THERMO CHEMICAL KINETIC MODELING	1
1 RADICAL AND MOLECULE THERMO CHEMICAL KINETICS	2
1.1 Overview.....	2
1.2 Group Additivities (THERM).....	3
1.2.1 Molecules.....	4
1.2.2 Radicals.....	5
1.2.2.1 Methods.....	5
1.2.2.2 Example of HBI Group Application.....	8
1.3 Mopac	9
1.3.1 Molecules.....	10
1.3.2 Radicals.....	11
1.3.3 Transition States.....	11
1.4 Thermodynamic Analysis	12
2 KINETICS	13
2.1 Types of Reaction on Kinetics Estimation	13
2.1.1 Abstraction Reactions (Metathesis)	13
2.1.2 Addition Reactions.....	15
2.1.3 Elimination Reactions (Beta Scission).....	15

TABLE OF CONTENTS (Continued)

Chapter	Page
2.1.4 Isomerization reactions (Special Unimolecular)	15
2.1.5 Dissociation Reactions (Simple Unimolecular)	17
2.1.6 Combination Reactions	17
2.2 Quantum RRK Calculations	17
2.2.1 RRK Theory	18
2.2.1.1 Lindemann-Hinshelwood Mechanism for Unimolecular Reactions	19
2.2.1.2 RRK Theory of Unimolecular Reactions	21
2.2.1.3 Chemically Activation Reactions	23
2.2.2 QRRK Analysis for Unimolecular and Chemical Activation Reactions	26
2.2.2.1 Input Data Requirements for the QRRK Calculations	27
2.2.2.2 Modifications	28
PART II MODELING STUDY ON THE NEOPENTYL RADICAL + O ₂ REACTION SYSTEM	30
3 INTRODUCTION	31
3.1 Overview	31
3.2 Objective of this Study	33
3.3 General Approach	33
3.4 Literature Review	34
4 KINETIC MODELLING FOR THE NEO-C ₅ H ₁₁ + O ₂ SYSTEM	42
4.1 Thermodynamic Properties	42

TABLE OF CONTENTS (Continued)

Chapter	Page
4.2 Important Transition States.....	43
4.2.1 C3CCOO. → TS(1) → C3.CCOOH.....	44
4.2.2 C3.CCOOH → TS(2) → C2CyCCOC + OH	45
4.2.3 C3CCOO. → TS(x) → C2C=C + C.H ₂ OOH.....	45
4.3 Quantum RRK Analysis	45
4.3.1 Chemical Activation Reaction System: C3CC. + O ₂ → Products	47
4.3.2 Chemical Activation Reaction System: C3.CCOOH + O ₂ → Products	49
4.3.3 Chemical Activation Reaction System: C2C=C + OH, O ₂ → Products	50
4.3.4 Fate of Stabilized Peroxy and Hydroperoxide Adducts.....	51
4.3.4.1 C3CCOO. and C3.CCOOH	51
4.3.4.2 C2C(COOH)COO., C2.C(COOH)COOH, C2C(COOH)C.OOH	51
4.3.4.3 C2C(OH)COO., C2C(O.)COOH, C2C(OOH)CO., C2C(OO.)COH.....	52
4.3.5 Unimolecular Dissociation Reaction Systems	52
4.3.6 Summary	53
5 MODELLING VALIDATION FOR THE NEO-C5H ₁₁ + O ₂ SYSTEM	55
5.1 Basic Model of Neopentyl + O ₂ System	55
5.2 Validation by Hughes' Data.....	55
5.3 Validation and Comparison with Literature Data for Important Reactions.....	57
5.3.1 Comparison with Slagle's Data for C3CC. → C2C=C + CH ₃ (k ₁).....	57

TABLE OF CONTENTS (Continued)

Chapter	Page
5.3.2 Fall-Off Analysis for $C_3CC. + O_2 \rightarrow C_3CCOO. (k_2/k_{-2}=K_2)$	59
5.3.3 MOPAC Calculation for $C_3CCOO. \rightarrow C_3.CCOOH$	61
5.3.4 Rate Constant for $C_3.CCOOH \rightarrow C_2CyCCOC + OH (k_4)$	62
5.3.5 Beta Scission Reaction $C_3.CCOOH \rightarrow C_2C=C + C.H_2OOH$	63
5.4 Conclusion for Neo-C ₅ H ₁₁ + O ₂ System	63
PART III FUNDAMENTAL STUDY ON MTBE PYROLYSIS AND OXIDATION	65
6 INTRODUCTION	66
6.1 Overview.....	66
6.2 Objective of this Study	69
6.3 Literature Review.....	70
6.3.1 MTBE Pyrolysis.....	71
6.3.2 Abstraction Reactions of MTBE by OH Radical.....	72
6.3.3 MTBE Oxidation	74
7 EXPERIMENTAL STUDY ON MTBE.....	77
7.1 Experimental Conditions	77
7.2 Experimental Apparatus.....	77
7.3 Flow Control and Measurement	78
7.4 Temperature Control and Measurement	79
7.5 Qualitative and Quantitative Analysis	79

TABLE OF CONTENTS (Continued)

Chapter	Page
7.6 Experimental Results	81
7.6.1 MTBE Oxidation	81
7.6.1.1 Fuel Lean Environments	81
7.6.1.2 Stoichiometric Environments.....	83
7.6.1.3 Fuel Rich Environments	86
7.6.2 MTBE Pyrolysis.....	88
7.6.2.1 At the Pressure of 4 Atm.....	89
7.6.2.2 At the Pressure of 7 Atm.....	90
7.6.2.3 At the Pressure of 10 Atm.....	91
7.6.3 Temperature and Pressure Dependence of Product Distributions.....	92
7.6.4 Conclusion	92
8 MODELLING STUDY ON MTBE.....	93
8.1 Overview.....	93
8.2 Methods for Kinetic Modeling Study	94
8.3 Important Transition States.....	95
8.4 Quantum RRK Analysis of Important Pathways.....	97
8.4.1 Abstraction and Dissociation Reactions of MTBE	98
8.4.1.1 Abstraction Reaction of MTBE	98
8.4.1.2 Unimolecular Dissociation of MTBE	101

TABLE OF CONTENTS (Continued)

Chapter	Page
8.4.1.3 $C_3C. + O_2 \rightarrow$ Products	103
8.4.2 Oxidation Of Iso-Butene	105
8.4.2.1 Reactions between $C_2C=C$ and $OH, O, H, CH_3, CH_3O, HO_2, O_2$	107
8.4.2.2 $C_2C=C + HO_2 \rightarrow C_3.COOH/C_2C.COOH, + O_2 \rightarrow$ Products	109
8.4.2.3 $C_2C=C + OH \rightarrow C_3.COH/C_2C.COH, + O_2 \rightarrow$ Products	111
8.4.2.4 Further Reactions of Intermediates from Iso-Butene Oxidation	112
8.4.2.5 Stable Molecules $C_2CyCOC, C_2C=O$ and $C=C(C)CHO$	113
8.4.2.6 $C_2C.CHO$ and $C_2C.CHO + O_2$	114
8.4.2.7 Reaction of Allylic Iso-Butenyl Radical with O_2	114
8.4.3 Oxidation and Unimolecular Dissociation Reactions of Methanol	116
8.4.3.1 Abstractions Reactions Involving Methanol	116
8.4.3.2 Unimolecular Dissociation Reactions of Methanol	118
8.4.3.3 Reactions of CH_2OH / CH_3O and CH_2O / CHO	118
8.4.4 Reactions of CH_4, C_2 and C_3	119
8.5 Conclusion	121
9 MODEL VALIDATION FOR MTBE SYSTEM	124
9.1 Available Literature Data	124
9.2 Comparison With Experimental Data at 4, 7 and 10 Atm	125
9.2.1 Fuel Lean Mixture	126

TABLE OF CONTENTS

(Continued)

Chapter	Page
9.2.2 Chemical Stoichiometric Fuel.....	127
9.2.3 Fuel Rich Mixture.....	128
9.2.4 MTBE Pyrolysis.....	129
9.3 Comparison to Experimental Data at 1 atm.....	130
PART IV TRANSITION STATES FOR $R_1R_2C.CCOOH \rightarrow R_1R_2C=C$ + $C.H_2OOH$	132
10 STUDY ON $R_1R_2C.CCOOH \rightarrow R_1R_2C=C + C.H_2OOH$	133
10.1 Overview.....	133
10.2 $C.CCOOH \rightarrow C=C + C.H_2OOH$	135
10.3 $C_2.CCOOH \rightarrow CC=C + C.H_2OOH$	135
10.4 $C_3.CCOOH \rightarrow C_2C=C + C.H_2OOH$	136
10.5 $C.H_2OOH \rightarrow CH_2O + OH$	137
10.6 Thermodynamic Analysis and QRRK Analysis	138
10.7 Conclusion	140
APPENDIX IA TABLES IN THE NEO-C ₅ H ₁₁ + O ₂ SYSTEM	141
APPENDIX IB TRANSITION STATES IN THE NEO-C ₅ H ₁₁ + O ₂ SYSTEM	148
TS IB. 1 Thermodynamic Properties from MOPAC PM3 and THERM.....	148
TS IB. 2 Thermodynamic Analysis of Transition State Related Reactions.....	149
TS IB. 3 Transition State (TS1) Structure and its Properties.....	150
TS IB. 4 Transition State's Z-Matrix (TS1) for MOPAC Calculation.....	151

TABLE OF CONTENTS (Continued)

Chapter	Page
TS IB. 5 Interatomic Distances (TS1) from MOPAC Calculation	152
TS IB. 6 Transition State Structure (TS2) and its Properties.....	154
TS IB. 7 Transition State (TS2) Z-Matrix for MOPAC Calculation	155
TS IB. 8 Interatomic Distance of TS2 from MOPAC Calculation	156
APPENDIX IC FIGURES IN THE NEO-C ₅ H ₁₁ + O ₂ SYSTEM	158
APPENDIX ID QRRK INPUT PARAMETERS IN THE NEO-C ₅ H ₁₁ + O ₂ SYSTEM	180
ID. 1 C ₃ CC.+ O ₂ → Products	180
ID. 2 C ₃ .CCOOH + O ₂ → Products	182
ID. 3 C ₂ C=C + OH → Products	184
ID. 4 C ₂ C=C + OH → C ₂ C.CO ₂ H	185
ID. 5 C ₃ .COH + O ₂ → Products	186
ID. 6 C ₂ C.CO ₂ H + O ₂ → Products	187
ID. 7 C ₃ CC. → C ₂ C=C + CH ₃	188
ID. 8 CH ₂ OOH → CH ₂ O + OH	189
ID. 9 C=C(C)COOH → C=C(C)CO. + OH.....	190
ID. 10 C=C(C)CO. → C=C(C)CHO + H	191
ID. 11 C ₂ C(COOH)CHO → C ₂ C(CO.)CHO + OH.....	192
ID. 12 C ₂ C(CO.)CHO → C ₂ C.CHO + CH ₂ O.....	193
ID. 13 C ₂ C.CHO → Products	194

TABLE OF CONTENTS (Continued)

Chapter	Page
ID. 14 $C_2C.OOH \rightarrow C_2C=O + OH$	195
APPENDIX IIA TABLES IN MTBE SYSTEM.....	196
APPENDIX IIB TRANSITION STATES IN THE MTBE SYSTEM.....	246
TS IIB. 1 Thermodynamic Properties from MOPAC PM3	247
TS IIB. 2 TS Information for $MTBE \rightarrow C_2C=C + CH_3OH$	250
TS IIB. 3 Information for $C_2C=C$ Related Transition States	252
TS IIB. 4 Transition State Information for Reaction $CH_3OH \rightarrow CH_2O + H_2$	262
TS IIB. 5 Thermodynamic Analysis for $C_3COC \rightarrow C_2C=C + CH_3OH$	264
TS IIB. 6 Thermodynamic Analysis for $CH_3OH \rightarrow CH_2O + H_2$	265
APPENDIX IIC FIGURES IN THE MTBE SYSTEM.....	266
APPENDIX IID QRRK INPUT PARAMETERS IN THE MTBE SYSTEM	418
IID. 1 $MTBE \rightarrow$ Products.....	418
IID. 2 $C_3.COC/C_3COC. \rightarrow$ Products	420
IID. 3 $C_2.COC \rightarrow$ Products	422
IID. 4 $C_3C./C_3.C \rightarrow$ Products	424
IID. 5 $C_3C. + O_2 \rightarrow$ Products	426
IID. 6 $C=C(OOH)C \rightarrow C_2.C=O (C=C(O.)C) + OH$	428
IID. 7 $C_2C=C \rightarrow CC.=C + CH_3$	429
IID. 8 $CC.=C \rightarrow$ Products.....	430

TABLE OF CONTENTS (Continued)

Chapter	Page
IID. 9 $C_2C=C + HO_2 \rightarrow [C_3.COOH]^* \rightarrow \text{Products}$	432
IID. 10 $C_2C=C + HO_2 \rightarrow [C_2C.COOH]^* \rightarrow \text{Products}$	434
IID. 11 $C_3.COOH + O_2 \rightarrow \text{Products}$	437
IID. 12 $C_2C.COOH + O_2 \rightarrow \text{Products}$	440
IID. 13 $C_2C=C + OH \rightarrow [C_3.COH]^* \rightarrow \text{Products}$	443
IID. 14 $C_2C=C + OH \rightarrow [C_2C.COH]^* \rightarrow \text{Products}$	445
IID. 15 $C_3.COH + O_2 \rightarrow \text{Products}$	447
IID. 16 $C_2C.COH + O_2 \rightarrow \text{Products}$	450
IID. 17 $C_2C=COOH \rightarrow C_2C.CHO (C_2C=CO.) + OH$	453
IID. 18 $C_2.C=C + HO_2 \rightarrow C=C(C)COOH \rightarrow C=C(C)CO. + OH$	454
IID. 19 $C=C(C)CO. \rightarrow \text{Products}$	455
IID. 20 $C_2C(OOH)CHO \rightarrow \text{Products}$	456
IID. 21 $C_2C(OH)CHO \rightarrow \text{Products}$	458
IID. 22 $C_2C(OH)C.=O \rightarrow C_2C.OH + CO$	459
IID. 23 $C_2C(OOH)C.=O \rightarrow C_2C.OOH + CO$	460
IID. 24 $CCyCOC(COOH) \rightarrow \text{Products}$	461
IID. 25 $CCyCOC(COH) \rightarrow \text{Products}$	462
IID. 26 $C_2C.OOH \rightarrow C_2C=O + OH$	463
IID. 27 $CCyC.OC \rightarrow C_2.C=O$	464

TABLE OF CONTENTS (Continued)

Chapter	Page
IID. 28 $C_2CyCOC \rightarrow CCyC.OC + CH_3$	465
IID. 29 $C_2C=O \rightarrow CH_3C.=O$	466
IID. 30 $C=C(C)CHO \rightarrow$ Products.....	467
IID. 31 $C=C(C)C.=O \rightarrow CC.=C + CO$	468
IID. 32 $C_2.C=O \rightarrow C=C=O + CH_3$	469
IID. 33 $C_2CyCOC. \rightarrow C_2C.CHO \rightarrow$ Products.....	470
IID. 34 $C_2C.CHO + O_2 \rightarrow$ Products.....	472
IID. 35 $C_2.C=C \rightarrow$ Products.....	474
IID. 36 $C_2.C=C + O_2 \rightarrow$ Products	475
IID. 37 $CC.CHO \rightarrow$ Products	479
IID. 38 $CH_3OH \rightarrow$ Products	481
IID. 39 $CH_3O/CH_2OH \rightarrow$ Products.....	483
IID. 40 $CH_2OH + O_2 \rightarrow$ Products	485
IID. 41 $CHO + O_2 \rightarrow$ Products	487
IID. 42 $HC(OOH)=O \rightarrow HC(O.)=O + OH$	489
IID. 43 $HC(O.)=O \rightarrow$ Products.....	490
IID. 44 $HCO_2H \rightarrow$ Products	492
IID. 45 $CH_2O \rightarrow$ Products	493
IID. 46 $CH_4 \rightarrow CH_3 + H$	494

TABLE OF CONTENTS

(Continued)

Chapter	Page
IID. 47 $\text{CH}_3 + \text{O}_2 \rightarrow \text{Products}$	495
IID. 48 $\text{CH}_3 + \text{CH}_3 \rightarrow \text{Products}$	497
IID. 49 $\text{C}_2\text{H}_4 + \text{OH} \rightarrow \text{Products}$	499
IID. 50 $\text{C.CO} + \text{O}_2 \rightarrow \text{Products}$	501
IID. 51 $\text{C}_2\text{H}_4 + \text{HO}_2 \rightarrow \text{Products}$	503
IID. 52 $\text{C.CO} + \text{O}_2 \rightarrow \text{Products}$	505
IID. 53 $\text{C(OOH)CHO} \rightarrow \text{Products}$	507
IID. 54 $\text{C(OOH)C=O} \rightarrow \text{CH}_2\text{OOH} + \text{CO}$	509
IID. 55 $\text{CHOCHO} \rightarrow \text{Products}$	510
IID. 56 $\text{CHOC=O} \rightarrow \text{CHO} + \text{CO}$	511
IID. 57 $\text{C=COOH} \rightarrow \text{C=CO} + \text{OH}$	512
IID. 58 $\text{C(O.CO)OH} \rightarrow \text{CH}_2\text{O} + \text{CH}_2\text{OH}$	513
IID. 59 $\text{C}_2\text{H}_5 \rightarrow \text{C}_2\text{H}_4 + \text{H}$	514
IID. 60 $\text{C}_2\text{H}_5 + \text{O}_2 \rightarrow \text{Products}$	515
IID. 61 $\text{C}_2\text{H}_3 \rightarrow \text{C}_2\text{H}_2 + \text{H}$	517
IID. 62 $\text{C}_2\text{H}_3 + \text{O}_2 \rightarrow \text{Products}$	518
IID. 63 $\text{C}_2\text{H}_2 + \text{OH} \rightarrow \text{Products}$	520
IID. 64 $\text{COC} \rightarrow \text{Products}$	522
IID. 65 $\text{COC} \rightarrow \text{CH}_2\text{O} + \text{CH}_3$	523

TABLE OF CONTENTS (Continued)

Chapter	Page
IID. 66 COC. + O ₂ → Products	524
IID. 67 CC.C + O ₂ → Products.....	526
IID. 68 C=CC. + O ₂ → Products	528
IID. 69 CC.C → CC=C + H.....	533
IID. 70 CC=C + HO ₂ → [C2C.OOH]* → Products.....	534
IID. 71 CC=C + HO ₂ → [CC.COOH]* → Products	536
IID. 72 C2.COOH + O ₂ → Products.....	538
IID. 73 CC.COOH + O ₂ → Products	541
IID. 74 CC=C + OH → [C2.COH]* → Products.....	544
IID. 75 C2.COH + O ₂ → Products.....	546
IID. 76 CC=C + OH → [CC.COH]* → Products	549
IID. 77 CC.COH + O ₂ → Products.....	552
IID. 78 CyCOC(C)OOH → CCyCOC. + HO ₂	555
IID. 79 CyCOC(C)OH → CCyC.OC + OH	556
IID. 80 CC(OOH)CHO → Products.....	557
IID. 81 CC(OH)CHO → Products.....	559
IID. 82 CC(OH)C.=O → CC.OH + CO	560
IID. 83 CC(OOH)C.=O → CC.OOH + CO.....	561
IID. 84 CC(=O)COOH → CC(=O)CO. + OH.....	562

TABLE OF CONTENTS (Continued)

Chapter	Page
IID. 85 $\text{CC}(=\text{O})\text{CO} \rightarrow \text{Products}$	563
IID. 86 $\text{C}=\text{CC}=\text{O} \rightarrow \text{C}_2\text{H}_3 + \text{CO}$	565
APPENDIX III TS INFORMATION AND QRRK ANALYSIS IN CH_2OOH ELIMINATION REACTION SYSTEM	566
TS III. 1 TS Information for $\text{C.CCOOH} \rightarrow \text{C}_2\text{H}_4 + \text{CH}_2\text{OOH}$	567
TS III. 2 TS Information for $\text{C2.CCOOH} \rightarrow \text{CC}=\text{C} + \text{CH}_2\text{OOH}$	569
TS III. 3 TS Information for $\text{C3.CCOOH} \rightarrow \text{C2C}=\text{C} + \text{CH}_2\text{OOH}$	571
TS III. 4 TS Information for $\text{CH}_2\text{OOH} \rightarrow \text{CH}_2\text{O} + \text{OH}$	573
TS III. 5 Summary of the Important Bond Lengths	574
TS III. 6 Thermodynamic Properties from MOPAC Calculation	575
TS III. 7 Thermodynamic Analysis for $\text{C.CCOOH} \rightarrow \text{C}=\text{C} + \text{CH}_2\text{OOH}$	576
TS III. 8 Thermodynamic Analysis for $\text{C2.CCOOH} \rightarrow \text{CC}=\text{C} + \text{CH}_2\text{OOH}$	577
TS III. 9 Thermodynamic Analysis for $\text{C3.CCOOH} \rightarrow \text{C2C}=\text{C} + \text{CH}_2\text{OOH}$	578
TS III. 10 Thermodynamic Analysis for $\text{CH}_2\text{OOH} \rightarrow \text{CH}_2\text{O} + \text{OH}$	579
TS III. 11 Potential Energy Diagrams for $(\text{R1R2C})\text{CCOOH} \rightarrow \text{R1R2C}=\text{C}$ $+ \text{CH}_2\text{OOH}$	580
TS III. 12 Temperature Dependence of Rate Constants at 1 Atm	581
TS III. 13 Pressure Dependence of Rate Constants at 700 K	582
TS III. 14 Pressure Dependence of Rate Constants at 1100 K	583
TS III. 15 Activation Energy Analysis	584

LIST OF TABLES

Table	Page
IA. 1 Thermodynamic Properties for Species in the Neo-C ₅ H ₁₁ + O ₂ System.....	141
IA. 2 Comparison of Current Rates with Literature Recommendations.....	143
IA. 3 Important Reactions Responsible for the Formation of OH.....	144
IA. 4 The Reaction Mechanism for Neopentyl Radical + O ₂	145
IA. 5 Important Reaction Flux	147
IIA. 1 Experimental Conditions of MTBE Oxidation and Pyrolysis	196
IIA. 2 Retention Time of Species	197
IIA. 3 Thermodynamic Properties for Species in MTBE Model.....	198

LIST OF FIGURES

Figure	Page
IC. 1 Temperature and pressure dependence of rate constants of the various channels of $C_3CC. + O_2$ with He as bath gas.....	159
IC. 2 Temperature and pressure dependence of rate constants of the various channels of $C_3.CCOOH + O_2$ with He as bath gas.....	160
IC. 3 Temperature and pressure dependence of reaction $C_2C=C + OH \rightarrow C_3.COH$ with He as bath gas	161
IC. 4 Temperature and pressure dependence of reaction $C_2C=C + OH \rightarrow C_3.COH$ with He as bath gas	162
IC. 5 Temperature and pressure dependence of rate constants of the various channels of $C_3.COH + O_2$ with He as bath gas.....	163
IC. 6 Temperature and pressure dependence of rate constants of the various channels of $C_2C.COH + O_2$ with He as bath gas	164
IC. 7 Temperature dependence of rate constants of the various channels of stabilized adducts $C_3CCOO. / C_3.CCOOH$ with He as bath gas.....	165
IC. 8 Temperature dependence of rate constants of the various channels of stabilized adducts $C_2C(COOH)COO. / C_2.C(COOH)COOH / C_2C(COOH)C.OOH$ with He as bath gas	166
IC. 9 Temperature dependence of rate constants of the various channels of stabilized adducts $C_2C(OH)COO. / C_2C(O.)COOH$ with He as bath gas.....	167
IC. 10 Temperature dependence of rate constants of the various channels of stabilized adducts $C_2C(OO.)COH / C_2C(OOH)CO.$ with He as bath gas.....	168
IC. 11 Temperature and pressure dependence of reaction $C_3CC. \rightarrow C_2C=C + CH_3$ with He as bath gas	169
IC. 12 Temperature and pressure dependence of reaction $CH_2OOH \rightarrow CH_2O + OH$ with He as bath gas.....	170

LIST OF FIGURES (Continued)

Figure	Page
IC. 13 Temperature and pressure dependence of reaction $C=C(C)COOH$ → $C=C(C)CO.$ + OH with He as bath gas	171
IC. 14 Temperature and pressure dependence of reaction $C=C(C)CO.$ → $C=C(C)CHO$ + H with He as bath gas	172
IC. 15 Temperature and pressure dependence of reaction $C_2C(COOH)CHO$ → $C_2C(CO.)CHO$ + OH with He as bath gas	173
IC. 16 Temperature and pressure dependence of reaction $C_2C(CO.)CHO$ → $C_2C.CHO$ + CH_2O with He as bath gas	174
IC. 17 Temperature and pressure dependence of reaction $C_2C.CHO$ → Products with He as bath gas	175
IC. 18 Fall-off in the reaction $C_3CC. + O_2 \rightarrow C_3CCOO.$	176
IC. 19 Comparison with Gutman's experimental result	177
IC. 20 OH formation comparison of model with Hughes experiment	178
IC. 21 Log k of OH formation vs 1000/T comparison of model with experiment	179
IIC. 1 Experimental Apparatus.....	267
IIC. 2 Calibration curve of mass flow controller 1 (AR) with inlet pressure of 200 psi.....	268
IIC. 3 Calibration curve of mass flow controller 2 (AR) with inlet pressure of 200 psi.....	269
IIC. 4 Calibration curve of mass flow controller 3 (O_2) with inlet pressure of 200 psi.....	270
IIC. 5 Reactor temperature profile at 1.3 gm Ar / min.	271
IIC. 6 Reactor temperature profiles at 1 atm.	272

LIST OF FIGURES (Continued)

Figure	Page
IIC. 7 Experimental result of 0.5% MTBE oxidation product distribution at $\phi = 0.75$, $P = 4$ atm, $T = 823$ K	273
IIC. 8 Experimental result of 0.5% MTBE oxidation product distribution at $\phi = 0.75$, $P = 4$ atm, $T = 873$ K	274
IIC. 9 Experimental result of 0.5% MTBE oxidation product distribution at $\phi = 0.75$, $P = 4$ atm, $T = 898$ K	275
IIC. 10 Experimental result of 0.5% MTBE oxidation product distribution at $\phi = 0.75$, $P = 4$ atm, $T = 923$ K	276
IIC. 11 Experimental result of 0.5% MTBE oxidation product distribution at $\phi = 0.75$, $P = 7$ atm, $T = 798$ K	277
IIC. 12 Experimental result of 0.5% MTBE oxidation product distribution at $\phi = 0.75$, $P = 7$ atm, $T = 823$ K	278
IIC. 13 Experimental result of 0.5% MTBE oxidation product distribution at $\phi = 0.75$, $P = 7$ atm, $T = 873$ K	279
IIC. 14 Experimental result of 0.5% MTBE oxidation product distribution at $\phi = 0.75$, $P = 10$ atm, $T = 798$ K.....	280
IIC. 15 Experimental result of 0.5% MTBE oxidation product distribution at $\phi = 0.75$, $P = 10$ atm, $T = 823$ K.....	281
IIC. 16 Experimental result of 0.5% MTBE oxidation product distribution at $\phi = 0.75$, $P = 10$ atm, $T = 873$ K.....	282
IIC. 17 Experimental result of 0.5% MTBE oxidation product distribution at $\phi = 1.00$, $P = 4$ atm, $T = 823$ K	283
IIC. 18 Experimental result of 0.5% MTBE oxidation product distribution at $\phi = 1.00$, $P = 4$ atm, $T = 848$ K	284
IIC. 19 Experimental result of 0.5% MTBE oxidation product distribution at $\phi = 1.00$, $P = 4$ atm, $T = 873$ K	285

LIST OF FIGURES (Continued)

Figure	Page
IIC. 20 Experimental result of 0.5% MTBE oxidation product distribution at $\phi = 1.00$, $P = 4$ atm, $T = 923$ K	286
IIC. 21 Experimental result of 0.5% MTBE oxidation product distribution at $\phi = 1.00$, $P = 4$ atm, $T = 973$ K	287
IIC. 22 Experimental result of 0.5% MTBE oxidation product distribution at $\phi = 1.00$, $P = 4$ atm, $T = 1023$ K.....	288
IIC. 23 Experimental result of 0.5% MTBE oxidation product distribution at $\phi = 1.00$, $P = 4$ atm, $T = 1073$ K.....	289
IIC. 24 Experimental result of 0.5% MTBE oxidation product distribution at $\phi = 1.00$, $P = 7$ atm, $T = 798$ K	290
IIC. 25 Experimental result of 0.5% MTBE oxidation product distribution at $\phi = 1.00$, $P = 7$ atm, $T = 823$ K	291
IIC. 26 Experimental result of 0.5% MTBE oxidation product distribution at $\phi = 1.00$, $P = 7$ atm, $T = 873$ K	292
IIC. 27 Experimental result of 0.5% MTBE oxidation product distribution at $\phi = 1.00$, $P = 7$ atm, $T = 923$ K	293
IIC. 28 Experimental result of 0.5% MTBE oxidation product distribution at $\phi = 1.00$, $P = 7$ atm, $T = 1023$ K.....	294
IIC. 29 Experimental result of 0.5% MTBE oxidation product distribution at $\phi = 1.00$, $P = 7$ atm, $T = 1073$ K.....	295
IIC. 30 Experimental result of 0.5% MTBE oxidation product distribution at $\phi = 1.00$, $P = 10$ atm, $T = 798$ K.....	296
IIC. 31 Experimental result of 0.5% MTBE oxidation product distribution at $\phi = 1.00$, $P = 10$ atm, $T = 823$ K.....	297
IIC. 32 Experimental result of 0.5% MTBE oxidation product distribution at $\phi = 1.00$, $P = 10$ atm, $T = 873$ K.....	298

LIST OF FIGURES (Continued)

Figure	Page
IIC. 33 Experimental result of 0.5% MTBE oxidation product distribution at $\phi = 1.00$, $P = 10$ atm, $T = 923$ K.....	299
IIC. 34 Experimental result of 0.5% MTBE oxidation product distribution at $\phi = 1.00$, $P = 10$ atm, $T = 973$ K.....	300
IIC. 35 Experimental result of 0.5% MTBE oxidation product distribution at $\phi = 1.00$, $P = 10$ atm, $T = 1023$ K.....	301
IIC. 36 Experimental result of 0.5% MTBE oxidation product distribution at $\phi = 1.00$, $P = 10$ atm, $T = 1073$ K.....	302
IIC. 37 Experimental result of 0.5% MTBE oxidation product distribution at $\phi = 1.50$, $P = 4$ atm, $T = 823$ K	303
IIC. 38 Experimental result of 0.5% MTBE oxidation product distribution at $\phi = 1.50$, $P = 4$ atm, $T = 848$ K	304
IIC. 39 Experimental result of 0.5% MTBE oxidation product distribution at $\phi = 1.50$, $P = 4$ atm, $T = 873$ K	305
IIC. 40 Experimental result of 0.5% MTBE oxidation product distribution at $\phi = 1.50$, $P = 4$ atm, $T = 898$ K	306
IIC. 41 Experimental result of 0.5% MTBE oxidation product distribution at $\phi = 1.50$, $P = 4$ atm, $T = 923$ K	307
IIC. 42 Experimental result of 0.5% MTBE oxidation product distribution at $\phi = 1.50$, $P = 4$ atm, $T = 998$ K	308
IIC. 43 Experimental result of 0.5% MTBE oxidation product distribution at $\phi = 1.50$, $P = 4$ atm, $T = 1048$ K.....	309
IIC. 44 Experimental result of 0.5% MTBE oxidation product distribution at $\phi = 1.50$, $P = 7$ atm, $T = 798$ K	310
IIC. 45 Experimental result of 0.5% MTBE oxidation product distribution at $\phi = 1.50$, $P = 7$ atm, $T = 823$ K	311

LIST OF FIGURES (Continued)

Figure	Page
II.C. 46 Experimental result of 0.5% MTBE oxidation product distribution at $\phi = 1.50$, $P = 7$ atm, $T = 848$ K	312
II.C. 47 Experimental result of 0.5% MTBE oxidation product distribution at $\phi = 1.50$, $P = 7$ atm, $T = 873$ K	313
II.C. 48 Experimental result of 0.5% MTBE oxidation product distribution at $\phi = 1.50$, $P = 7$ atm, $T = 898$ K	314
II.C. 49 Experimental result of 0.5% MTBE oxidation product distribution at $\phi = 1.50$, $P = 7$ atm, $T = 923$ K	315
II.C. 50 Experimental result of 0.5% MTBE oxidation product distribution at $\phi = 1.50$, $P = 7$ atm, $T = 973$ K	316
II.C. 51 Experimental result of 0.5% MTBE oxidation product distribution at $\phi = 1.50$, $P = 7$ atm, $T = 998$ K	317
II.C. 52 Experimental result of 0.5% MTBE oxidation product distribution at $\phi = 1.50$, $P = 7$ atm, $T = 1048$ K.....	318
II.C. 53 Experimental result of 0.5% MTBE oxidation product distribution at $\phi = 1.50$, $P = 10$ atm, $T = 798$ K.....	319
II.C. 54 Experimental result of 0.5% MTBE oxidation product distribution at $\phi = 1.50$, $P = 10$ atm, $T = 823$ K.....	320
II.C. 55 Experimental result of 0.5% MTBE oxidation product distribution at $\phi = 1.50$, $P = 10$ atm, $T = 848$ K.....	321
II.C. 56 Experimental result of 0.5% MTBE oxidation product distribution at $\phi = 1.50$, $P = 10$ atm, $T = 873$ K.....	322
II.C. 57 Experimental result of 0.5% MTBE oxidation product distribution at $\phi = 1.50$, $P = 10$ atm, $T = 898$ K.....	323
II.C. 58 Experimental result of 0.5% MTBE oxidation product distribution at $\phi = 1.50$, $P = 10$ atm, $T = 923$ K.....	324

LIST OF FIGURES (Continued)

Figure	Page
II.C. 59 Experimental result of 0.5% MTBE oxidation product distribution at $\phi = 1.50$, $P = 10$ atm, $T = 973$ K.....	325
II.C. 60 Experimental result of 0.5% MTBE oxidation product distribution at $\phi = 1.50$, $P = 10$ atm, $T = 998$ K.....	326
II.C. 61 Experimental result of 0.5% MTBE oxidation product distribution at $\phi = 1.50$, $P = 10$ atm, $T = 1048$ K.....	327
II.C. 62 Experimental result of 0.5% MTBE pyrolysis product distribution at $P = 4$ atm, $T = 823$ K.....	328
II.C. 63 Experimental result of 0.5% MTBE pyrolysis product distribution at $P = 4$ atm, $T = 873$ K.....	329
II.C. 64 Experimental result of 0.5% MTBE pyrolysis product distribution at $P = 4$ atm, $T = 923$ K.....	330
II.C. 65 Experimental result of 0.5% MTBE pyrolysis product distribution at $P = 4$ atm, $T = 973$ K.....	331
II.C. 66 Experimental result of 0.5% MTBE pyrolysis product distribution at $P = 4$ atm, $T = 1023$ K.....	332
II.C. 67 Experimental result of 0.5% MTBE pyrolysis product distribution at $P = 4$ atm, $T = 1048$ K.....	333
II.C. 68 Experimental result of 0.5% MTBE pyrolysis product distribution at $P = 4$ atm, $T = 1073$ K.....	334
II.C. 69 Experimental result of 0.5% MTBE pyrolysis product distribution at $P = 4$ atm, $T = 1123$ K.....	335
II.C. 70 Experimental result of 0.5% MTBE pyrolysis product distribution at $P = 7$ atm, $T = 873$ K.....	336
II.C. 71 Experimental result of 0.5% MTBE pyrolysis product distribution at $P = 7$ atm, $T = 923$ K.....	337

LIST OF FIGURES (Continued)

Figure	Page
IIC. 72 Experimental result of 0.5% MTBE pyrolysis product distribution at P = 7 atm, T = 973 K.....	338
IIC. 73 Experimental result of 0.5% MTBE pyrolysis product distribution at P = 7 atm, T = 998 K.....	339
IIC. 74 Experimental result of 0.5% MTBE pyrolysis product distribution at P = 7 atm, T = 1023 K.....	340
IIC. 75 Experimental result of 0.5% MTBE pyrolysis product distribution at P = 7 atm, T = 1048 K.....	341
IIC. 76 Experimental result of 0.5% MTBE pyrolysis product distribution at P = 7 atm, T = 1073 K.....	342
IIC. 77 Experimental result of 0.5% MTBE pyrolysis product distribution at P = 7 atm, T = 1123 K.....	343
IIC. 78 Experimental result of 0.5% MTBE pyrolysis product distribution at P = 10 atm, T = 873 K.....	344
IIC. 79 Experimental result of 0.5% MTBE pyrolysis product distribution at P = 10 atm, T = 923 K.....	345
IIC. 80 Experimental result of 0.5% MTBE pyrolysis product distribution at P = 10 atm, T = 973 K.....	346
IIC. 81 Experimental result of 0.5% MTBE pyrolysis product distribution at P = 10 atm, T = 998 K.....	347
IIC. 82 Experimental result of 0.5% MTBE pyrolysis product distribution at P = 10 atm, T = 1023 K.....	348
IIC. 83 Experimental result of 0.5% MTBE pyrolysis product distribution at P = 10 atm, T = 1048 K.....	349
IIC. 84 Experimental result of 0.5% MTBE pyrolysis product distribution at P = 10 atm, T = 1073 K.....	350

LIST OF FIGURES (Continued)

Figure	Page
IIC. 85 Experimental result of 0.5% MTBE pyrolysis product distribution at P = 10 atm, T = 1123 K.....	351
IIC. 86 Experimental result of 0.5% MTBE oxidation: temperature and pressure dependence of MTBE at $\phi = 0.75$	352
IIC. 87 Experimental result of 0.5% MTBE oxidation: temperature and pressure dependence of MTBE at $\phi = 1.00$	353
IIC. 88 Experimental result of 0.5% MTBE oxidation: temperature and pressure dependence of MTBE at $\phi = 1.50$	354
IIC. 89 Experimental result of 0.5% MTBE pyrolysis: temperature and pressure dependence of MTBE.....	355
IIC. 90 Experimental result of 0.5% MTBE oxidation: temperature and pressure dependence of $C_2C=C$ at $\phi = 0.75$	356
IIC. 91 Experimental result of 0.5% MTBE oxidation: temperature and pressure dependence of $C_2C=C$ at $\phi = 1.00$	357
IIC. 92 Experimental result of 0.5% MTBE oxidation: temperature and pressure dependence of $C_2C=C$ at $\phi = 1.50$	358
IIC. 93 Experimental result of 0.5% MTBE pyrolysis: temperature and pressure dependence of $C_2C=C$	359
IIC. 94 Experimental result of 0.5% MTBE oxidation: temperature and pressure dependence of CH_3OH at $\phi = 0.75$	360
IIC. 95 Experimental result of 0.5% MTBE oxidation: temperature and pressure dependence of CH_3OH at $\phi = 1.00$	361
IIC. 96 Experimental result of 0.5% MTBE oxidation: temperature and pressure dependence of CH_3OH at $\phi = 1.50$	362
IIC. 97 Experimental result of 0.5% MTBE pyrolysis: temperature and pressure dependence of CH_3OH	363

xxx

LIST OF FIGURES (Continued)

Figure	Page
IIC. 98 Experimental result of 0.5% MTBE oxidation: temperature and pressure dependence of CH_2O at $\phi = 0.75$	364
IIC. 99 Experimental result of 0.5% MTBE oxidation: temperature and pressure dependence of CH_2O at $\phi = 1.00$	365
IIC. 100 Experimental result of 0.5% MTBE oxidation: temperature and pressure dependence of CH_2O at $\phi = 1.50$	366
IIC. 101 Experimental result of 0.5% MTBE pyrolysis: temperature and pressure dependence of CH_2O	367
IIC. 102 Experimental result of 0.5% MTBE oxidation: temperature and pressure dependence of $\text{C}_2\text{C}=\text{O}$ at $\phi = 0.75$	368
IIC. 103 Experimental result of 0.5% MTBE oxidation: temperature and pressure dependence of $\text{C}_2\text{C}=\text{O}$ at $\phi = 1.00$	369
IIC. 104 Experimental result of 0.5% MTBE oxidation: temperature and pressure dependence of $\text{C}_2\text{C}=\text{O}$ at $\phi = 1.50$	370
IIC. 105 Experimental result of 0.5% MTBE pyrolysis: temperature and pressure dependence of $\text{C}_2\text{C}=\text{O}$	371
IIC. 106 Experimental result of 0.5% MTBE oxidation: temperature and pressure dependence of C_3H_6 at $\phi = 0.75$	372
IIC. 107 Experimental result of 0.5% MTBE oxidation: temperature and pressure dependence of C_3H_6 at $\phi = 1.00$	373
IIC. 108 Experimental result of 0.5% MTBE oxidation: temperature and pressure dependence of C_3H_6 at $\phi = 1.50$	374
IIC. 109 Experimental result of 0.5% MTBE pyrolysis: temperature and pressure dependence of C_3H_6	475
IIC. 110 Experimental result of 0.5% MTBE oxidation: temperature and pressure dependence of C_2H_4 at $\phi = 0.75$	376

LIST OF FIGURES (Continued)

Figure	Page
IIC. 111 Experimental result of 0.5% MTBE oxidation: temperature and pressure dependence of C_2H_4 at $\phi = 1.00$	377
IIC. 112 Experimental result of 0.5% MTBE oxidation: temperature and pressure dependence of C_2H_4 at $\phi = 1.50$	378
IIC. 113 Experimental result of 0.5% MTBE pyrolysis: temperature and pressure dependence of C_2H_4	379
IIC. 114 Experimental result of 0.5% MTBE oxidation: temperature and pressure dependence of CH_4 at $\phi = 0.75$	380
IIC. 115 Experimental result of 0.5% MTBE oxidation: temperature and pressure dependence of CH_4 at $\phi = 1.00$	381
IIC. 116 Experimental result of 0.5% MTBE oxidation: temperature and pressure dependence of CH_4 at $\phi = 1.50$	382
IIC. 117 Experimental result of 0.5% MTBE pyrolysis: temperature and pressure dependence of CH_4	383
IIC. 118 Experimental result of 0.5% MTBE oxidation: temperature and pressure dependence of CO at $\phi = 0.75$	384
IIC. 119 Experimental result of 0.5% MTBE oxidation: temperature and pressure dependence of CO at $\phi = 1.00$	385
IIC. 120 Experimental result of 0.5% MTBE oxidation: temperature and pressure dependence of CO at $\phi = 1.50$	386
IIC. 121 Experimental result of 0.5% MTBE pyrolysis: temperature and pressure dependence of CO.....	387
IIC. 122 Experimental result of 0.5% MTBE oxidation: temperature and pressure dependence of CO_2 at $\phi = 0.75$	388
IIC. 123 Experimental result of 0.5% MTBE oxidation: temperature and pressure dependence of CO_2 at $\phi = 1.00$	389

LIST OF FIGURES (Continued)

Figure	Page
IIC. 124 Experimental result of 0.5% MTBE oxidation: temperature and pressure dependence of CO ₂ at $\phi = 1.50$	390
IIC. 125 Comparison of experiment and modeling result $\phi = 0.75$, $P = 4$ atm, $T = 873$ K	391
IIC. 126 Comparison of experiment and modeling result $\phi = 0.75$, $P = 4$ atm, $T = 923$ K	392
IIC. 127 Comparison of experiment and modeling result $\phi = 0.75$, $P = 7$ atm, $T = 823$ K	393
IIC. 128 Comparison of experiment and modeling result $\phi = 0.75$, $P = 7$ atm, $T = 873$ K	394
IIC. 129 Comparison of experiment and modeling result $\phi = 0.75$, $P = 10$ atm, $T = 798$ K	395
IIC. 130 Comparison of experiment and modeling result $\phi = 0.75$, $P = 10$ atm, $T = 873$ K	396
IIC. 131 Comparison of experiment and modeling result $\phi = 1.0$, $P = 4$ atm, $T = 873$ K	397
IIC. 132 Comparison of experiment and modeling result $\phi = 1.0$, $P = 4$ atm, $T = 1023$ K	398
IIC. 133 Comparison of experiment and modeling result $\phi = 1.0$, $P = 7$ atm, $T = 873$ K	399
IIC. 134 Comparison of experiment and modeling result $\phi = 1.0$, $P = 7$ atm, $T = 1023$ K	400
IIC. 135 Comparison of experiment and modeling result $\phi = 1.0$, $P = 10$ atm, $T = 873$ K	401
IIC. 136 Comparison of experiment and modeling result $\phi = 1.0$, $P = 10$ atm, $T = 1023$ K	402

LIST OF FIGURES (Continued)

Figure	Page
II.C. 137 Comparison of experiment and modeling result $\phi = 1.5$, $P = 4$ atm, $T = 873$ K	403
II.C. 138 Comparison of experiment and modeling result $\phi = 1.5$, $P = 4$ atm, $T = 998$ K	404
II.C. 139 Comparison of experiment and modeling result $\phi = 1.5$, $P = 7$ atm, $T = 873$ K	405
II.C. 140 Comparison of experiment and modeling result $\phi = 1.5$, $P = 7$ atm, $T = 998$ K	406
II.C. 141 Comparison of experiment and modeling result $\phi = 1.5$, $P = 10$ atm, $T = 873$ K	407
II.C. 142 Comparison of experiment and modeling result $\phi = 1.5$, $P = 10$ atm, $T = 998$ K	408
II.C. 143 Comparison of experiment and modeling result Pyrolysis, $P = 4$ atm, $T = 873$ K	409
II.C. 144 Comparison of experiment and modeling result Pyrolysis, $P = 4$ atm, $T = 1023$ K	410
II.C. 145 Comparison of experiment and modeling result Pyrolysis, $P = 7$ atm, $T = 873$ K	411
II.C. 146 Comparison of experiment and modeling result Pyrolysis, $P = 7$ atm, $T = 1023$ K	412
II.C. 147 Comparison of experiment and modeling result Pyrolysis, $P = 10$ atm, $T = 873$ K	413
II.C. 148 Comparison of experiment and modeling result Pyrolysis, $P = 10$ atm, $T = 1023$ K	414
II.C. 149 Comparison of experiment and modeling result $\phi = 1.0$, $P = 1$ atm, $T = 923$ K	415

LIST OF FIGURES (Continued)

Figure	Page
II.C. 150 Comparison of experiment and modeling result Pyrolysis, $P = 1 \text{ atm}$, $T = 923 \text{ K}$	416
II.C. 151 Comparison of experiment and modeling result $\phi = 0.96$, $P = 1 \text{ atm}$, $T = 1028 \text{ K}$	417

PART I

THERMO CHEMICAL AND THERMO CHEMICAL KINETIC MODELING

CHAPTER 1

RADICAL AND MOLECULE THERMO CHEMICAL KINETICS

1.1 Overview

Thermodynamic properties of molecules and radicals are important in many fields of science and research. Several important applications of these thermodynamic properties include: calculation of energy balance; equilibrium considerations; stability; reaction path analysis; spontaneity of reaction; kinetics versus thermodynamic control; theoretical reaction yields and detailed chemical reaction mechanism integration (reverse rate calculation).

An important era in chemical engineering optimization calculations and reactor design techniques is rapidly developing. It entails incorporation and use of detailed reaction kinetic mechanisms, which are based on fundamental thermodynamic and kinetic principles into a comprehensive computer code to model an entire reaction system and reactor using: (1) detailed mass balance from elemental composition; (2) energy conservation based on specific heat capacities and reactor heat flow; (3) thermodynamic properties of each species (atoms, molecules and radicals) incorporated into the mechanism for assurance of correct equilibrium determination; and (4) numerical integration of stiff Ordinary Differential Equations (ODE) describing the reaction for appropriate time, pressure and temperature profile(s), yielding complete product distribution and reagent conversion information. The code will also calculate sensitivity to input reagent concentrations and specific reactions in the mechanism, at different reaction time, should one wish to further optimize a mechanism using new experiment data.

Thermodynamic data on stable species, radicals and reaction transition states is critical in determining energy balance in chemical reactions and in calculation of the Gibbs Free Energy of a reaction and thus the equilibrium constant as a function of temperature, as well as to kinetic paths.

The use of detailed reaction kinetic mechanisms, based on fundamental principles in chemical kinetic theory, e.g. Transition State Theory, and on thermodynamic properties of the reacting species ($\Delta H_f(T)$, $\Delta S(T)$, and $C_p(T)$), allows the code (integration of reaction mechanism) to accurately predict results into regimes well outside those in the calibration experiments under which the mechanism was developed. Further more those codes can be reduced to reasonable numbers of detailed reaction steps by use of available computer sensitivity analysis codes for elimination of non-important reactions. This yields strong insight into the important elementary reaction steps and allows the optimizer code to function in a reasonable computer time requirement. To implement these computer codes, one has to have developed an accurate reaction mechanism and the thermodynamic database. The first step in derivation of the kinetic mechanism is development of the thermo database, which stress the key position of thermo database in the computer modeling work for related fields.

The way used to obtain thermodynamic properties for involved species in the current study is Group Additivity (THERM) and MOPAC calculation. Group database was developed by the Bozzelli group in NJIT. Enthalpies of formation of groups were obtained by evaluation of literature data. Entropies and heat capacities for stable species were calculated using the Rigid Rotor Harmonic Oscillator approximation taking into account the contributions from translation, rotations, vibrations and internal rotations.

Proper account was also taken of symmetry and optical isomers. Moments of inertia and fundamental frequencies were obtained using semi-empirical MNDO/PM3 calculations in the MOPAC 6.0 package. Barriers for internal rotations were adopted from appropriate experimental data or ab initio studies. Pitzer and Gwinn's approach was used to calculate the contributions of hindered rotors.

1.2 Group Additivities (THERM)

The Group Additivity methods was initially developed by Benson and Buss [1], from which one can often determine easier and faster than if one needed to search through the literature. This exists as a basis data set of reasonable and easily accessible size, from which one can determine thermodynamic parameters for a very large number of organic molecules and radicals.

The computer program THERM [2] performs group additivity calculations. The basic principle of calculations for molecules and radicals are illustrated as following.

1.2.1 Molecules

In the Group Additivity method, molecules are broken up into groups on the central atoms. The central atoms are those with more than one bond. Each C, O, N, S in a molecule is a group atom while H, Cl and F are not central atoms or group atoms. Each group is further identified by the specific species that are bonded to it. For example, the neopentane molecule, $(\text{CH}_3)_4\text{C}$ can be divided into 5 groups, they are: one group "C/C4", which means 4 carbon atoms bonded to central carbon atom which is located in the first

position of the group ID, and four identical groups “C/C/H3”, which means one carbon atom and three hydrogen atoms bonded to central carbon atom.

Thermodynamic properties of a molecule can then be attributed to the sum of the properties of all groups within the molecule. The entropy obtained from group additivity is an Intrinsic Entropy, which does not consider the symmetry of the molecules. To get the actual entropy (Extrinsic Entropy) of stable molecules one needs to correct for symmetry. This is done by subtracting a term $-R\ln\sigma$ (R is $1.987 \text{ cal}\cdot\text{mol}^{-1}$, \ln is natural log and σ is the symmetry of the molecule), from the intrinsic entropy (S_i) which results from adding the group values, that is $S = S_i - R\ln\sigma$. Enthalpies and heat capacities are obtained directly from Group Additivity.

1.2.2 Radicals

Radical species are extremely important intermediates and reaction initiators in gas phase chemical systems. Accurate knowledge of their thermodynamic properties permits estimation of kinetic activation energies, calculation of important equilibrium values and, from the principles of microscopic reversibility, calculation of reverse reaction rates. All of these parameters are requirements for the kinetic modeling study.

1.2.2.1 Methods

Thermodynamic properties of radicals can be obtained in two ways. One of the methods, similar to molecules, is addition of values from all groups plus symmetry correct for entropies. This method needs one special group with a radical site on one central atom,

and it is difficult to find or assign thermodynamic parameters for such groups based on literature and experimental results.

The method used to calculate almost all radical species involved in current studies (Part II and Part III) is based on the Hydrogen atom Bond Increment (HBI) technique developed in this research group [3–4]. The HBI group technique is based on known thermodynamic properties of the parent molecule and the calculated changes that occur upon formation of a radical via loss of a H atom. The HBI group incorporates evaluated carbon hydrogen (C—H) or oxygen hydrogen (O—H) bond energies, for $\Delta H_f(298)$ of the respective radical, and entropy and heat capacity changes that result from loss or changes in vibration frequencies, internal rotation, and spin degeneracy when a hydrogen atom is removed from the specific carbon site.

Enthalpies of radicals are calculated by considering the following homologous reaction:



Then, the radical enthalpies of formation can be written as:

$$\Delta H^\circ_{rxn,298}(R.) = D(R-H) + \Delta H^\circ_{rxn,298}(RH) - 52.1 \text{ kcal}\cdot\text{mol}^{-1}$$

One can calculate $\Delta H^\circ_{rxn,298}(R.)$ if one knows the bond strength for the R—H bond being broken to form the radical and H atom, and $\Delta H^\circ_{rxn,298}(RH)$.

Entropy and heat capacity can also be estimated, to a reasonable degree from those of the parent molecule. The molecular structure of a radical (R.) can be considered, to some extent, to be similar to that of the corresponding stable molecule (RH). The unpaired electron on the radical-centered atom is replaced by a bond to a H atom in the stable molecule while most of molecule sequence and chemical bonds basically remain the same

in the two species. If the differences in molecular structure and properties for R. and RH are properly taken into account, one can calculate S°_{298} and $C_p(T)$ values for R. from properties of the corresponding RH parent plus increment values for $\Delta C_p(T)$ and ΔS°_{298} that account for these changes:

$$S^{\circ}_{\text{int},298}(\text{R.}) = S^{\circ}_{\text{int},298}(\text{RH}) + \Delta S^{\circ}_{298}$$

$$C_p(T)(\text{R.}) = C_p(T)(\text{RH}) + \Delta C_p(T)$$

where S°_{int} represents the intrinsic entropy (excluding symmetry).

These ΔS°_{298} and $\Delta C_p(T)$ ($300 \leq T/K \leq 1500$) increments are group (HBI) values for estimating entropy and heat capacity for radical from the parent. The real entropy for radical species should consider symmetry correction. So if one calculates entropy and heat capacity for a radical based on the parent molecule, one should incorporate the followings:

- (1) Entropy and heat capacity increments accounting for loss and for the differences in vibration frequencies of a parent molecule losing a H atom to form the radical.
- (2) Gain of inversion frequencies at radical centers of carbon atoms.
- (3) Entropy and heat capacity corrections accounting for the differences of rotational barriers of internal rotors in parent and radical.
- (4) Entropy corrections for electron spin degeneracy
- (5) Entropy corrections for changes in symmetry between parent and radical (this is not included in the HBI groups but is done in THERM)
- (6) Changes of mass (about accounting for $0.1 \text{ cal}\cdot\text{mol}^{-1}$)

The calculation of entropy and heat capacity for a radical are:

$$S^{\circ}_{298}(\text{R.}) = S^{\circ}_{298}(\text{RH}) + \Delta S^{\circ}_{298}(\text{HBI}) + R \ln(\sigma_{\text{radical}}/\sigma_{\text{parent}})$$

where σ_{radical} and σ_{parent} are the symmetry number for radical and the corresponding parent molecule. No further correction is required for the calculation of heat capacity using the HBI term value:

$$C_p(T)(\text{R.}) = C_p(T)(\text{RH}) + \Delta C_p(T)$$

1.2.2.2 Example of HBI Group Application

As an example, we consider formation of C_2H_3 from C_2H_6 .

Loss of H atom results in the loss of one C-H stretch, two H-C-H bends and one H-C-C bend, and gain of one inversion motion of radical center because the normal rigid tetrahedral structure has been replaced with a more flexible, non-planar configuration. This loss of four frequencies and gain of one are used to account for the vibration frequency differences for HBI group, via the equation: $S/R = -\ln(1-e^{-x}) + x/(e^x - 1)$, $x = h\nu/kT$, ν is frequencies and other have common meanings, between the ethyl radical and ethane parent, and get a value of $0.336 \text{ cal}\cdot\text{mol}^{-1}$.

The difference in rotation barriers, $2.9 \text{ kcal}\cdot\text{mol}^{-1}$ and $0.1 \text{ kcal}\cdot\text{mol}^{-1}$, for ethane and ethyl radical respectively, accounts for a significant fraction of ΔS°_{298} and $\Delta C_p(T)$ contribution to HBI values via "Pitzer and Gwinn Tables"[5 - 8], and results in a value of $0.892 \text{ cal}\cdot\text{mol}^{-1}$ for $\Delta S^{\circ}_{298, \text{int-rot}}$.

Because all free radicals estimated in HBI techniques are considered to have only one unpaired electron (doublet) and assumed spin degeneracy equal to 2. Term $R\ln 2$ (1.38 cal-mol⁻¹) is already included into the HBI group.

The other very important correction for entropy is symmetry, which is not included in the HBI group but is done with computer code THERM. In ethyl radical and ethane molecule case, σ_{radical} is 6 and σ_{parent} is 18, the $R\ln(\sigma_{\text{radical}}/\sigma_{\text{parent}})$ turn out value of 2.18 cal-mol⁻¹.

So, the entropy of ethyl radical is:

$$\begin{aligned} S^{\circ}_{298}(\text{C}_2\text{H}_5\cdot) &= S^{\circ}_{298}(\text{C}_2\text{H}_6) + \Delta S^{\circ}_{298}(\text{HBI}) + R\ln(\sigma_{\text{radical}}/\sigma_{\text{parent}}) \\ &= S^{\circ}_{298}(\text{C}_2\text{H}_6) + (0.336 + 0.892 + 1.38) + 2.18 + 0.1 \\ &= S^{\circ}_{298}(\text{C}_2\text{H}_6) + 4.888 \text{ (cal-mol}^{-1}\text{-K}^{-1}\text{)} \end{aligned}$$

1.3 MOPAC

MOPAC is a general-purpose semi-empirical molecular orbital package for the study of chemical structures and reactions. MOPAC [9-10] calculates the vibration spectra, thermodynamic quantities, isotopic substitution effects and force constants for molecules, radicals, ions, and polymers. MOPAC is also available for locating a transition-state for the chemical reactions. As a relatively higher level calculation method in this study, MOPAC has been used for obtaining thermodynamic properties for molecules, radicals and transition states when it becomes necessary to find transition states for some important reactions, such as isomerization reaction, beta scission reactions and cyclic product formation reactions, involved in this modeling studies. MOPAC is also used as a more accurate and precise calculation tool to calculate thermodynamic properties for some species when THERM is not available or is not accurate enough.

Entropies, heat capacities and frequencies are calculated by using semi-empirical (MOPAC PM3) calculations modified by separately including the contributions from internal rotors, spin degeneracy (for radicals and transition states) and correction for optical isomers. The semi-empirical (MOPAC PM3) calculations can also be used to define transition state structures and obtain Arrhenius A factors for reactions including Isomerization, Elimination (Beta scission), Addition and Epoxide + OH (oxetan formation). These data are coupled into the QRRK fall-off calculations to determine the A factors as a function of temperature.

1.3.1 Molecules

The first step to calculate thermodynamic properties for molecules is to define the geometry of species, and build up a Z-matrix as calculation input file manually or using the computer program "CHEMSITE". Thermodynamic properties can be calculated by running computer program "MOPAC 6.0" with keyword "THERMO" and parameters (number of symmetry considered and number of internal rotors not included). The keyword "PRECISE" is usually used to set up a more strict criteria for the self-consistent-field (SCF) convergence in the geometry optimization process. Thermodynamic properties from MOPAC calculations then combine with some corrections for entropies and heat capacities. The most important one is the correction for entropy and heat capacity contributions from internal rotors. A computer program "VIBIR", developed by Bozzelli's group in NJIT, is used to obtain the value of entropy and heat capacity from internal rotors, which is not included in MOPAC calculations. This part of the contribution for entropy can account for up to 1/3 or 1/4 of total entropy of species. The

entropy contribution from optical isomers such as -OOH groups, is also combined to final result for specific species, a value of $R\ln 2$ is usually assigned to each of optical isomer.

1.3.2 Radicals

The calculations of thermodynamic properties of radicals are also based on radical's optimized geometry. The parent's geometry can be used with replacing H, which does not exist on radical, with dummy atom (X). The calculation should combine the keyword "UHF" (Unrestricted Hartree-Fock), especially for the calculations of open shell such as radicals. One more correction for entropy in addition to those for molecule is entropy contribution from electron spin ($R\ln 2$) because there is one unpaired electron on radical.

1.3.3 Transition States

The calculations of thermodynamic properties $H_{f,298}$, S_{298} and $C_p(T)$ of transition states are carried out by first defining the transition states using semi-empirical (MOPAC PM3) method. Thermodynamic properties as well as vibration frequencies, moments of inertia of transition states can then be calculated by adding the keyword "THERMO" with parameters (number of symmetry considered and number of internal rotors not included) to optimize geometric input files. The keywords "UHF" in addition "PRICISE" is often used.

There are different ways to find transition states for specific reactions. One of methods used in this study is to use the optimized geometry of reactant (radical or molecule), adjust certain bond length, bond angle or dihedral angle and use keyword "TS". The "SIGMA" or "NLLSQ" is used sometime to help find transition states. Identifying of a transition

state is usually carried by an image vibration frequency (with a minus sign) and reasonable internal atom distances in optimized geometry found. That the geometry will have no change after adding keyword "THERMO" is also helpful for identifying a transition state.

1.4 Thermodynamic Analysis

Thermodynamic analysis is carried out by computer program "THERMRXN" and "AFACT2F", developed by Bozzelli's group in NJIT. Based upon thermodynamic properties, $\Delta H_{f,298}$, S_{298} and $C_p(T)$ ($T = 300, 400, 500, 600, 800, 1000$ and 1500), thermodynamic analysis (THERMRXN) calculates thermodynamic properties for reaction such as ΔH_{rxn} , ΔU_{rxn} , ΔS_{rxn} , ΔG_{rxn} , and reaction equilibrium constant (K_c) or the ratio of forward Arrhenius A factor to reverse Arrhenius A factor (A_f/A_r) at temperature range from 298 to 1500 K. The ΔH_{rxn} and ΔU_{rxn} are used to calculate activation energies for isomerization reaction and unimolecular dissociation (elimination or beta scission) reactions based on activation energies for reverse addition reactions. Thermodynamic analysis (AFACT2F) can also calculate A factors in the form of $A'T^n$ using ΔS^\ddagger ($S_{\text{reactant}} - S_{\text{transition state}}$) based on transition state theory. The fit value of A factor is also obtained from thermodynamic analysis for the temperature range from 300 K to 2000 K. Thermodynamic analysis also reports the temperature dependence of thermodynamic properties and shows negative temperature effects for some reactions.

CHAPTER 2

KINETICS

2.1 Types of Reaction on Kinetics Estimation

Many reactions are considered and covered in this study for modeling a real reaction system. Abstraction reactions are always the initial reaction and play key role in the low to intermediate temperature range. Thermal unimolecular dissociation and chemical activation addition reactions are the most important reactions considered in this study. Reaction to other new product channels as well as isomerization, stabilization and reverse reaction are included in this calculation. This is an important aspect of the reaction analysis for both combination as well as addition reactions that other modelers do not usually incorporate. This leads to a more correct treatment of fall-off and pressure dependence for these non-elementary reaction systems. Rate constants inclusion in for the model are obtained which incorporate the calculated pressure dependency and therefore make the model more fundamentally correct.

As for better organization of this thesis, we summarize several important reaction types here, including abstraction reaction (metathesis), addition reaction, elimination reaction (beta scission), isomerization reactions (especially unimolecular), simple dissociation reactions, and recombination reactions.

2.1.1 Abstraction Reactions (Metathesis)

Abstraction reaction rate constants are not pressure dependent and usually taken from evaluated literature when available. If estimation is required, a generic reaction is utilized

as a model and adjusted for steric effects. Evans Polanyi analysis is used on the reaction in the exothermic direction to estimate the energy of activation (E_a) for rate constant. An Evan Polanyi plot, E_a versus ΔH_{rxn} , allows use of a known ΔH_{rxn} to obtain E_a for these reactions. The abstraction reaction in an endothermic reaction must incorporate the ΔH_{rxn} , or thermodynamics will be violated.

When no literature data are available, an alternative estimation procedure from Dean and Bozzelli [11] is also used in this study but limited to abstraction by H, O, OH, NH_2 and CH_3 . This estimation procedure is based on a reference reaction. For example, for abstraction by H to form a carbon-centered radical, the reaction $C_2H_6 + H \rightarrow C_2H_5 + H_2$ serves as a reference reaction with a well known rate constant taken from literature. Rate constant is expressed in modified Arrhenius form:

$$k = n_H A T^n \exp (-E_a/RT) = n_H A T^n \exp \{ -[E_0 - f(\Delta H_0 - \Delta H)]/RT \} \text{ cm}^3\text{-mol}^{-1}\text{-s}^{-1}$$

Where n_H is the number of hydrogen atoms which can be abstracted from molecule, E_0 is the activation energy for reference reaction, ΔH_0 and ΔH are reaction heat formations for specific abstraction reaction and reference reaction respectively. The f is a fraction assigned by authors from several set of calculated value fitted to literature data. The A , n , f , E_0 and ΔH_0 as a reference value is list below.

R	A	n	E_0 (kcal-mol ⁻¹)	ΔH_0 (kcal-mol ⁻¹)	f
H	2.4×10^8	1.5	7.4	-3.1	0.65
O		1.5	5.8	-1.1	0.75
OH		2.0	0.86	-18.3	0.50
NH_2		1.94	7.2	-7.5	0.23
CH_3		1.87	10.6	-3.7	0.65

2.1.2 Addition Reactions

Addition reactions are treated with the quantum RRK formalism for $k(E)$ and modified strong collision theory of Gilbert et al. for falloff. The QRRK analysis will be described in the following section. The reaction involves addition of an atom or radical to an unsaturated species. Addition reactions typically form an energized adduct with ca. 20 to 50 kcal-mol⁻¹ of energy above the ground state. This energy is often sufficient to allow the adduct to react to other reaction products (lower energy) before stabilization occurs.

2.1.3 Elimination Reactions (Beta Scission)

These reactions are the reverse of addition reactions and utilize the quantum RRK formalism for $k(E)$ and modified strong collision theory of Gilbert et al. for falloff and are treated in two ways. In the first way, a unimolecular quantum RRK formalism for $k(E)$ and modified strong collision theory of Gilbert et al. for falloff is employed where reverse high-pressure reaction (addition) parameters are determined. The corresponding high-pressure unimolecular beta scission rate constants using microscopic reversibility are then calculated. These high pressure unimolecular elimination parameters are then input to the QRRK formalism to calculate the rate constants at the appropriate pressure. An alternate method is to use the reverse rate constants from the QRRK - modified strong collision reaction calculations for the corresponding addition reaction.

2.1.4 Isomerization Reactions (Special Unimolecular)

This reaction represents intramolecular, endothermic transfer of a H atom from a primary methyl carbon atom to the peroxy O radical. The activation energy (E_a) for the forward

rate of this reaction was estimated using the calculations, from analysis of the ethyl +O₂ reaction [12], and more recent comparisons to the experimental and calculation data base for this ethyl system. The data utilize:

$$E_a = \text{Ring strain} + E_{\text{abst}} + \Delta H_{\text{rxn}}$$

where ΔH_{rxn} is the enthalpy of reaction (only included if reaction is endothermic). The ring strains are 28.0, 26.0, 6.0, 1.0 or 0, and 6.0 kcal-mol⁻¹ for rings containing three, four, five, six, and seven members, respectively. Energies of abstraction E_{abst} are taken from Evans Polanyi plots of carbon atoms abstracting a hydrogen, where a abstraction by carbon atom is the reverse reaction in this system. These compared to an E_a of 12.5 kcal-mol⁻¹ for a thermo neutral reaction and a decrease in E_a of 0.33 kcal-mol⁻¹ for each 1 kcal in exothermicity.

Pre-exponential factors (A factors) for the ROO isomerization (unimolecular reaction) were obtained using Transition State Theory (TST):

$$A(T) = (ek/h) \exp(\Delta S^\ddagger(T)/R) \text{ in } AT^n \text{ form}$$

where ΔS^\ddagger is calculated from $S^\ddagger_{(\text{transition state})} - S_{(\text{reactants})}$ which is obtained from semi-empirical calculation (MOPAC PM3) modified with entropy $S(T)$ contributions from the internal rotors, electron spin of radicals and correction for optimal isomers, or from empirical estimations, which consider the number of lost rotors, and each rotor account for -4.3 kcal-mol⁻¹.

2.1.5 Dissociation Reactions (Simple Unimolecular)

Simple unimolecular (dissociation) reactions are the reverse of two radical recombination reactions. The rate constants are determined by two methods similar to beta scission reactions. The reverse high-pressure reaction (combination) parameters are determined. The corresponding high-pressure unimolecular dissociation rate constants are then calculated using microscopic reversibility. These high pressure unimolecular dissociation parameters are then input to the QRRK formalism to calculate the rate constants at the appropriate pressure and temperature. The reverse rate constant from the QRRK combination reaction calculation can also be used for the respective reaction.

2.1.6 Combination Reactions

These reactions involve the combination of two radicals or an atom with a radical. The energy of the adduct formed before stabilization is equal to the bond energy of the new bond(s) formed and this is typically on the order of 80 to 120 kcal-mol⁻¹. This is often sufficient under combustion conditions for an adduct, with this initial energy above its ground state energy, to react to lower energy products before stabilization occurs. The high pressure limit rate constant for combination is obtained from literature or estimated from known generic combination reactions. The QRRK chemical activation formalism is then used to calculate the rate constants at the appropriate pressure and temperature to all the recognized available channels.

2.2 Quantum RRK Calculations

Quantum RRK calculations are performed, through the whole study, to evaluate energy dependent rate constants, $k(E)$, of the adduct to the various channels for the calculations

of branching ratios of the adduct formed from combination, addition or insertion reactions to various product channels. The RRK theory is then outlined below.

2.2.1 RRK Theory

Most modern theories of unimolecular reaction rates, including the Slater theory, the RRK (Rice and Ramsperger and Kassel) theory and the RRKM (Marcus Rice) theory, are based on the fundamental Lindemann mechanism involving collision energization of the reactant molecules, and more specifically on Hinshelwood's development of the original treatment.

The Slater theory [13-14] is a dynamical theory concerned with the detailed treatment of molecular vibrations and the behavior of particular molecular coordinates as a function of time. Reaction is postulated to occur in Slater theory when a chosen coordinate achieves a critical extension by the phase-coincidence of certain modes of vibration. The rate constant of energized molecule dissociation to product(s) (k_s) is related to a "specific dissociation probability" L ; this is the frequency with which a chosen coordinate in the molecule reaches a critical value, and can be calculated for the case in which the vibrations of the molecule are assumed to be harmonic. The L is actually a function of the energies in the individual oscillators and not simply of the total energy E of the molecule.

In RRK theory the assumption is made that the rate of conversion of energized molecules into products is related to the chance that the critical energy E_0 is concentrated in one part of the molecule, e.g. in one oscillator (Kassel theory) or in one squared term (Rice-Ramsperger theory). This probability is clearly a function of the total energy E of the energized molecule.

The Marcus Rice theory, is known as RRKM theory since its basic model is RRK model. The main developments are the calculation of the rate constant of energization by quantum-statistical mechanisms and the application of ideas related to the Absolute Rate Theory for the calculation of the rate of conversion of energized molecules into products.

2.2.1.1 Lindemann-Hinshelwood Mechanism for Unimolecular Reactions

The theory known as Lindemann theory forms the basis for all modern theories of unimolecular reactions and has been developed from ideas published almost simultaneously by Lindemann [15] and Christiansen [16]. The main concept is that: (a) by collision, a certain fraction of the molecules become energized, i.e. gain energy in excess of a critical quantity E_0 . The rate of the energization process depends upon the rate of bimolecular collision. (b) energized molecules are de-energized by collision, which is a reverse reaction. This de-energized rate is taken to be energy-independent and is equated with the collision number Z_2 by assuming that every collision of A^* leads to a de-energized start. (c) there is a time-lag between the energization and unimolecular dissociation or isomerization of the energized molecules. This unimolecular dissociation also occurs with a rate constant k_3 independent of the energy content of A^* . The whole idea can be expressed by the following equations.



where M can represent a product molecule, an added “inert” gas molecule, or a second molecule of reactant. In the simple Lindemann theory k_1 , along with k_2 and k_3 is taken to be energy-independent and is calculated from the simple collision theory equation.

By application of the steady-state hypothesis to the concentration of A^* , the unimolecular rate constant and high pressure limit and low pressure limit rate and rate constants are then given as following:

High pressure limit rate $\nu_{\infty} = (k_1 k_3 / k_2) [A] = k_{\infty} [A]$

Low pressure limit rate $\nu_0 = \nu_{\text{bim}} = k_1 [A] [M] = k_{\text{bim}} [A] [M]$

Unimolecular rate constant $k_{\text{uni}} = (k_1 k_3 / k_2) / (1 + k_3 / k_2 [M]) = k_{\infty} / (1 + k_{\infty} / k_1 p)$

Fall-off $k_{\text{uni}} / k_{\infty} = 1 / (1 + k_{\infty} / k_1 p)$ -

One can expect that the Lindemann theory predicts a change in the order of the initial rate of a unimolecular reaction with respect to concentration at low pressure.

The k_1 in original Lindemann theory is taken from the collision theory expression ($k_1 = Z_1 \exp(-E_0/kT)$ with $Z_1 = (\sigma_d^2 N_A / R) (8\pi N_A k / \mu)^{1/2} (1/T)^{1/2}$, where Z_1 will be in $\text{Torr}^{-1} \cdot \text{s}^{-1}$ (consistent with $[M]$ in Torr and k_3 in s^{-1}) when σ_d = collision diameter in cm; μ = reduced molar mass in $\text{g} \cdot \text{mol}^{-1} = (1/M_A + 1/M_B)^{-1}$; T = temperature in K; $N_A = 6.0225 \times 10^{23} \text{ mol}^{-1}$; $R = 6.2326 \times 10^4 \text{ cm}^3 \cdot \text{Torr} \cdot \text{K}^{-1} \cdot \text{mol}^{-1}$; $k = 1.3805 \times 10^{-16} \text{ erg} \cdot \text{K}^{-1}$).

Based on the Lindemann's suggestion that k_1 could be increased by assuming that the required energy (energize molecules) could be drawn in part from the internal degrees of freedom (mainly vibration) of the reactant molecule, Hinshelwood [17] increases k^1 by using a much higher chance of a molecule possessing total energy $\geq E_0$ in s classical degrees of freedom, $(E_0/kT)^{s-1} \exp(-E_0/kT) / (s-1)!$, than one, $\exp(-E_0/kT)$ Lindemann used.

So the $k_1 = [Z_1/(s-1)!] (E_0/kT)^{s-1} \exp(-E_0/kT)$ with k_1 a function of energy and replace k_1 and A^* as $k_{1(E \rightarrow E-\delta E)}$ and $A^*_{(E \rightarrow E-\delta E)}$ in mechanism above.

2.2.1.2 RRK Theory of Unimolecular Reactions

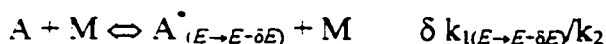
In order to make accurate quantitative predictions of the fall-off behavior of a unimolecular reaction it is essential to take into account the energy dependence of the rate constant k_1 (k_3) for the conversion of energized molecules into activated complexes and hence products. One of accepted theories is the RRK theory, a statistical theory used in this thesis because it is more computable and needed parameters are readily obtained.

The RRK theory due to Rice and Ramsperger [18] and Kassel [19-20] was developed virtually simultaneously and very similar in their approach. Both consider that for reaction to occur a critical energy E_0 must become concentrated in one part of the molecule. They used the basic Lindemann-Hinshelwood mechanism of collision energization and de-energization, but assume more realistically that the rate constant of conversion of an energized molecule to products is proportional to a specific probability, a finite statistical probability that E_0 will be found in the relevant part of the energized molecule which contains E greater than E_0 since E of the molecule under consideration is assumed to be rapidly redistributed around the molecule. Obviously this probability will increase with E and make k_1 a function of its energy content.

The difference between these two models is twofold. Firstly, Rice and Ramsperger used classical statistical mechanics throughout, while Kassel used classical method but also developed a quantum treatment; the latter is very much more realistic and accurate. Secondly, different assumptions were made about the part of the molecule into which the

critical energy E_0 has to be concentrated. The Kassel's model seems slightly more realistic by assuming the energy had to be concentrated into one oscillator. The quantum version of the Kassel theory serves as a theoretical basis for calculation performed in this thesis.

The mechanism of RRK theory is written as:



The quantum version of version of Kassel's theory is based on the calculation of the probability that a system of s quantum oscillators, while the classical version considered s classical oscillators, with total energy E should have energy $\geq E_0$ in one chosen oscillator. It assume that there are s identical quantum oscillators, all having frequencies ν and hence energy $h\nu$, and so the critical energy E_0 is expressed as the critical number of quanta being $m = E_0/h\nu$, and the energy E of energized molecule is expressed as a total of n quanta with $n = E/h\nu$. The probability of that one oscillator contains at least m quanta, probability (energy $\geq m$ quanta in one chosen oscillator) is then equal to:

$$\text{Probability (energy} \geq m \text{ quanta in one chosen oscillator)} = \frac{n!(n - m + s - 1)!}{(n - m)!(n + s - 1)!}$$

Hence,

$$k_s(nh\nu) = A \frac{n!(n - m + s - 1)!}{(n - m)!(n + s - 1)!}$$

where A is proportion constant here and actually the same as the classical one.

Corresponding $k_1(E)$ of Hinshelwood expression is derived, refereed to energization into a specific quantum state rather than into an energy range E to $E + \delta E$, as

$$k_1(nh\nu) = k_2 \alpha^{n-1} (1-\alpha)^{s-n} \frac{(n+s-1)!}{n!(s-1)!}$$

where $\alpha = \exp(-h\nu/kT)$.

2.2.1.3 Chemically Activation Reactions

Molecules undergo thermal unimolecular reactions as a result of energization by molecular collision. This molecular collision at a given temperature produces energized molecules with an equilibrium distribution of energy which enables the fraction of molecules energized into a particular energy range or quantum state. The energization methods other than by molecular collision, such as photoactivation and chemical activation, may produce a non-equilibrium situation in which molecules acquire energies far in excess of the average thermal energy. This amount of excess of energy contained in energized adduct makes chemical activation reactions much more important in a particular system, and a much different treatment for the rate of conversion decomposition of energized adduct to product (including back to reactant) which is very competing with the rate of its collision stabilization.

A example of chemically activated reaction system is neopentyl radical + O₂ system. As we will discussed in part II, C₃CC₃ radical reacts with O₂ to form a chemically activated, energized adduct [C₃CCOO.^{*}], this process of forming adduct is much more efficient than that by thermal molecular collision, and adduct contains excess energy from the chemical reaction. The energized adduct [C₃CCOO.^{*}] could go back to reactant C₃CC₃ + O₂, or could directly go to products C₂CyCCOC + OH via a intramolecular H shift. The QRRK calculation (see chapter 4 in part II) shows that the chemical activation process is more

important than thermal dissociation process. Another example of chemically activated reaction system is the addition reaction of OH to unsaturated double in iso-butene ($C_2C=C$). The channel of forming a chemically activated adduct $[C_2C=C\cdots OH]^*$ followed by a dissociation to various products is an important pathway in iso-butene oxidation system to explain product distribution and this chemical activation channel is very competing with abstraction reaction.

The basic idea of the treatment of a chemical activation system is that a vibration excited molecule A^* by an association of reactants can reform reactants with a rate constant $k'_a(E)$, form decomposition products with a rate constant $k_a(E)$ or be de-energized to stable molecules A.

On the strong collision assumption the first order rate constant for de-energization is equal to the collision frequency, $\omega = Zp$ where p is the total pressure and Z is collision number (see "2.2.1.1 Lindemann-Hinshelwood Mechanism for Unimolecular Reactions" on page 19).

Suppose that the fraction of molecules which are energized per unit time into the energy range between E and $E+\delta E$ is $f(E)\delta E$. To simplify, one can consider only one decomposition path (back to reactant can be considered as one of decomposition paths), then the fraction of A^* decomposing (say path D) compared with those stabilized (say path S) is $k_a(E)/[k_a(E)+\omega]$. The fraction of molecules in the energy range between E and $E+\delta E$ decomposing to products is therefore $\{k_a(E)/[k_a(E)+\omega]\}f(E)\delta E$, and the total number of molecules decomposing per unit time (D), at all energies above the critical energy E_0 , is:

$$D = \int_{E_0}^{\infty} \frac{k_d(E)}{k_d(E) + \omega} f(E) dE$$

corresponding, the total rate of stabilization (S) is:

$$S = \int_{E_0}^{\infty} \frac{\omega}{k_d(E) + \omega} f(E) dE$$

Considering an average rate constant $\langle k_d \rangle$ for all energies above E_0 , there have:

$$\frac{\langle k_d \rangle}{\omega} = \frac{D}{S} = \frac{\text{No. molecules decomposing per unit time}}{\text{No. of molecules being stabilized per unit time}}$$

So,

$$\langle k_d \rangle = \omega \frac{\int_{E_0}^{\infty} \{k_d(E) / [k_d(E) + \omega]\} f(E) dE}{\int_{E_0}^{\infty} \{\omega / [k_d(E) + \omega]\} f(E) dE}$$

The $f(E)$ is the distribution function of energized molecules in the energy range between E and $E+\delta E$. In the thermal energization systems, this distribution function is simply the thermal quantum Boltzmann distribution $K(E)$ and the rate of energization into the energy range between E and $E+\delta E$ is $K(E)\delta E = \delta k_1/k_2$. For the chemically activated system described here, the distribution function can be derived by applying the principle of detailed balancing to the reverse process to reactants. Consider a situation in which the processes D and S can be ignored and equilibrium is established between A^{\bullet} and reactants, then the fraction of molecules with energy between E and $E+\delta E$ is Boltzmann distribution $K(E)\delta E$, so the rate of dissociation to reactants is then $K'_d(E)K(E)\delta E$, and by the principle of detailed balancing this also gives the rate of combination of reactants to give A^{\bullet} in this energy range. The total rate of energization to all levels above the minimum energy E_{\min} (the minimum energy of A^{\bullet}) is:

$$\text{Total rate of energization} = \int_{E_0}^{\infty} k'_s(E)K(E)dE$$

Therefore, the distribution function is given by:

$$f(E)\delta E = \frac{k'_s(E)K(E)\delta E}{\int_{E_0}^{\infty} k'_s(E)K(E)dE}$$

The $f(E)\delta E$ can be incorporated into QRRK theory for $k_s(E)$ and $k_t(E)$ (see “2.2.1.2 RRK Theory of Unimolecular Reactions on page 21) serves as a basis for the calculations for chemical activation reaction systems.

2.2.2 QRRK Analysis for Unimolecular and Chemical Activation Reactions

QRRK analysis, as initially presented by Dean [21 - 23] combined with the modified strong collision approach of Gilbert et al [24], are used to compute rate constants for both chemical activation and unimolecular reactions, over a range of temperature and pressure. The computer program CHEMDIS, based on the QRRK theory outlined as above, and unimolecular dissociation and chemical activation formalism carries out all unimolecular and chemical activation reactions involved in this thesis. The input parameters for CHEMDIS are: (1) High pressure limit rate constants (Arrhenius A factor and activation energy E_a) for each reaction included for analysis; (2) A reduced set of three vibration frequencies and their associated degeneracy; (3) Lennard-Jones transport parameters, (σ (Angstroms) and ϵ/k (Kelvin)), and (4) molecular weight of well species. All these input parameters are readily available or straightforward to estimate.

2.2.2.1 Input Data Requirements for the QRRK Calculations

It is important to have accurate input data for the calculations, without this aspect the accuracy or assumption in the calculations of fall-off or chemical activation rate constants are of less value.

Pre-exponential factors (Arrhenius A factors) in the high pressure limits, are obtained from calculations and the literature or are estimated from generic reactions for combinations and additions. Transition state theory is utilized for isomerization using the methods Benson [25] and Dean [21].

Activation energies come from endothermicity of reaction ΔU_{rxn} and from analogy to similar reactions with known energetics.

A reduced set of three vibration frequencies and their associated degeneracy are computed from fits to heat capacity data, as described by Ritter [2]. These have been shown by Ritter to accurately reproduce molecular heat capacities, $C_p(T)$, and by Bozzelli et al [26] to yield accurate density of states $\rho(E)$ to partition coefficient (Q) ratios.

Lennard-Jones transport parameters, s (Angstroms) and ϵ/k (Kelvin), are obtained from tabulations [27] and from a calculation method based on molar volumes and compressibility [28]. The calculation formula is: $\sigma = (2.3551 - 0.087w)/(P_c/T_c)^{1/3}$ and $\epsilon/k = (0.7915 + 0.1693w)T_c$, where w is molecular weight in gram-mol^{-1} , P_c and T_c are the critical temperature and the critical pressure respectively.

Arrhenius A factors for the radical bimolecular combination at the high pressure limit are obtained from literature, and from trends in homologous series of these type reactions.

When necessary, estimation is done in a consistent and uniform manner with reference to

literature, experiment and / or calculation in all cases. The input parameters and references are important, and data are listed in the tables associated with each calculation.

2.2.2.2 Modifications

A significant number of modifications have been made since the initial descriptions of the quantum RRK and fall-off calculations were published [21 - 24]. These modifications [23] include:

- Use of a manifold of three vibration frequencies and respective degeneracy, plus incorporation of energies from one external rotation mode for the calculation of the ratio of the density of states to the partition coefficient $\rho(E)/Q(T)$ and for calculation of $k(E)$ and of $F(E)$.
- The F_E factor is now explicitly calculated for use in determining the collision efficiency β_c [24] in place of the previously assigned 1.15 value. The β_c is calculated from Gilbert et al. eqn. 4.7 [24].
- The Lennard-Jones collision frequency Z_{LJ} is calculated by: $Z_{LJ} \equiv Z \Omega^{(2,2)}$ integral [27, 29, 30], Ω is obtained from fit of Reid et al [27].

The QRRK analysis with the modified strong collision approach and constant F_E for fall-off has been used to analyze a variety of chemical activation reaction systems [31 - 40]. It is shown to yield reasonable results in these applications; and provides a mechanism by which the effects of temperature and pressure can be evaluated and included in the kinetics.

Chebyshev polynomials (7×3) incorporate the pressure and temperature dependence into rate constant expression. A modified Chemkin Interpreter is used to incorporate the combined pressure and temperature dependent rate expression into the Chemkin integrators.

PART II

MODELING STUDY ON THE NEOPENTYL RADICAL + O₂ REACTION

SYSTEM

CHAPTER 3

INTRODUCTION

3.1 Overview

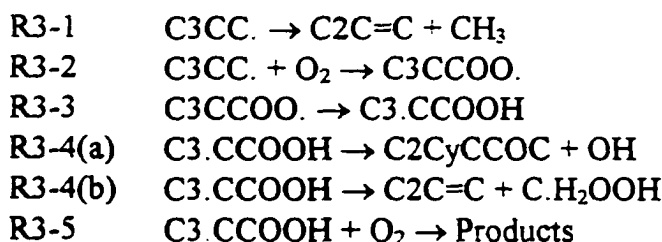
Atmospheric and combustion reactions forming alkyl radicals are well-characterized relative to the subsequent reactions of the alkyl radicals with O_2 . The reactions of alkyl radicals with O_2 are, however important and often rate limiting processes in the low temperature chemistry (below 1000 K) of hydrocarbons oxidation, especially the chemistry which occurs prior to ignition in internal combustion engines and cool flames. The reaction processes are, unfortunately, relatively complex and the analysis presents a source of some controversy [41-42]. This oxidation process involves formation of a peroxy radical, which contains ca 35 kcal-mole⁻¹ of excess internal energy, this can either be lost via collision process or used for further reaction (including dissociation back to reactants) before stabilization occurs [31,43].

The overall reaction of alkyl radicals with O_2 to form the conjugate alkene plus HO_2 is considered the dominate process over the temperature range 500 to 900 K; it is often treated as one step by many modelers [44-45]. There is, however, a significant quantity of data from the elementary kinetics community which shows (for the reaction systems studied) that the reactions occur by formation of a peroxy adduct, which undergoes a unimolecular isomerization and the hydroperoxy alkyl isomer undergoes further reactions to products. While this reaction process is more complex due to pressure dependent stabilization channels, proper inclusion of it in kinetic models for combustion processes will make them more accurate and meaningful for use in optimization. It will, in addition,

extend their range of validity. For example, it is the subsequent reactions of the alkyl peroxy radical intermediate that are determined essential, by combustion modelers, to predict negative temperature coefficient behavior [41,46].

Two features of neopentane facilitate a simpler interpretation of results, relative to most alkyl radical - oxygen reaction systems. (i) All the C-H bonds are identical so that only one species of alkyl radical is involved. (ii) The carbon atom radical site is connected to a carbon with no hydrogen atoms, thus, unlike the majority of alkyl radicals, the formation of the conjugate alkene by a more direct abstraction of H by O₂, not involving radical isomerization, is structurally impossible. Reactions of stabilization, reverse dissociation, isomerization and isomer decomposition are dominant here.

Only few studies focus on reactions of neopentane + O₂ system, and the basic reaction scheme expressed as following:



The fundamental chemical kinetic study of neopentane and/or neopentyl radical will certainly help to understand fundamental chemistry of combustion at the low and intermediate temperatures. Only one full mechanism exists for oxidation of neopentane by Curran (see 3.4 Literature Review starting on page 34), but it is too complex with about 1570 reactions included, few of which account for fall-off, and it may not be used as sub-mechanism in the other model. So, it's really make sense for us to build a reduced but more accurate mechanism for neopentane combustion under the intermediate temperature.

3.2 Objective of this Study

- Development and advancement of the understanding of the reaction of neopentyl + O₂ system under intermediate temperature conditions.
- Identification of important reactions and key species in the intermediate temperature chemistry of neopentyl + O₂ system.
- Development of a reduced kinetics model for neopentyl + O₂ system, based on thermochemical kinetic principles, supported by literature data. Particular importance will be directed to reactions of primary radical intermediates with O₂, plus and OH addition reactions to olefins and carbonyl species, and then subsequent reactions of these radical adducts with O₂.

3.3 General Approach

The reaction mechanism is based upon fundamental principles of thermochemical kinetics including Transition State Theory (TST), and accurate molecular thermodynamic properties. The mechanism consists of elementary reactions with each reaction based on literature evaluation, or if it is estimated, on thermochemical kinetics principles.

Chemical activation analysis to determine rate constants as a function of temperature and pressure will be performed on combination reactions of radical intermediates with O₂ and on radical (OH) addition to unsaturated species, olefins and carbonyls. Unimolecular dissociation analysis will be performed to determine temperature and pressure dependence, especially fall-off, for beta scission and important unimolecular decomposition reactions.

Quantum Kassel Analysis (see part I) is also utilized to account for fall-off effects in unimolecular reactions and in chemical activation processes such as addition or combination reactions. We apply this analysis to rate constants which are pressure dependent that are reported in the literature from measurements at other pressures, as well as our estimated rate constants for these type of reactions.

The reaction mechanism consisting of all involved elementary reactions will finally be validated by experimental results or literature data and therefore be used to predict product distribution for experimental or real chemical reaction systems by performing special species concentrations interpretation by some computer programs.

3.4 Literature Review

Over 70% of these studies was focused on abstraction reactions of hydrogen from neopentane by OH, CH₃, Cl, O, H, CH₃O, CN, (CH₃)₃CH₂O, C₂H₅, D, Br, F, CD₂, NF₂, CF₃, CH₃CHCH₃, CH, CD₃, C₂D₅ and NH₂. Most groups interested in radical abstraction reactions from alkane and tried to obtain bimolecular rate constants for one particular reaction or a series of abstraction reactions with experimental or theoretical studies.

The previous important studies which focused on neopentane goes in two ways, one of which is the neopentane pyrolysis reactions and unimolecular decomposition of neopentyl radical, the other focused on the oxidation reactions of neopentyl radical by few groups.

There were three studies specialized on the unimolecular decomposition of neopentyl radical, (R1) which is an important competitive reaction in the oxidation environment in the intermediate temperature range.

Anderson and Benson [47] investigated the reaction R3-1 in a study of the pyrolysis of neopentane in the presence and absence of HCl at 489 °C and gave an initial rate, $k_1 = 10^{3.3 \pm 0.3} \text{ s}^{-1}$ and $E_a = 17.0 \pm 0.2 \text{ kcal-mol}^{-1}$ from the rate. It is a pretty low rate compared to later studies.

Furimsky and Laidler [48] studied unimolecular decomposition of neopentyl radical (R3-1), during their experimental and kinetics study on the mercury-photosensitized decomposition of neopentane over the temperature range 230-335 °C and at pressures from 3 to 280 Torr. They obtained a high pressure limit rate constant, $k_\infty = 2.5 \times 10^{13} \exp(-29.0/RT) \text{ s}^{-1}$, directly based on rate constants for the abstraction reaction between CH_3 radicals and neopentane and for the combination of CH_3 radicals with $t\text{-C}_4\text{H}_9$ radicals. They also found the fall-off at low pressures ($P_{\text{neopentyl}} < 2 \text{ Torr}$) and a low pressure limit rate constant, $k^0 = 5.8 \times 10^{10} \exp(-17.1/RT) \text{ ml-mol}^{-1}\text{-s}^{-1}$.

About 20 years later, Slagle et al [49] studied the loss of neopentyl radical using a heated tubular reactor coupled to a photoionization mass spectrometer over a 1 to 10 Torr pressure range and a 287 to 377 °C temperature range. They produced neopentyl radical indirectly by pulsed excimer laser photolysis of CCl_4 (to produce $\text{CCl}_3 + \text{Cl}$) followed by the rapid reaction between the Cl atoms and neopentane to produce $\text{neo-C}_5\text{H}_{11} + \text{HCl}$. $\text{Neo-C}_5\text{H}_{12}$ concentrations were high enough to “convert” the Cl atoms to $\text{neo-C}_5\text{H}_{11}$ radicals within 0.5 ms and $\text{neo-C}_5\text{H}_{11}$ concentrations were low (typically in the range $(1\text{-}6) \times 10^{10} \text{ molecules cm}^{-3}$). This was achieved by selecting the initial conditions (CCl_4 concentration and laser intensity) so that reactions between photolysis products (including the $\text{C}_5\text{H}_{11} + \text{C}_5\text{H}_{11}$ recombination reaction) had negligible rates compared to that of the

unimolecular decomposition process under study. They monitored decomposition of neo- C_5H_{11} radical at various temperatures (287 to 377 °C) allowing an enthalpy of reaction to be derived. Unimolecular rate constants were determined as a function of bath gas (He, N_2 and Ar), temperature and bath gas densities ($(3-30) \times 10^{16}$ molecules- cm^{-3} for He and $(6-12) \times 10^{16}$ molecules- cm^{-3} for N_2 and Ar). They modeled (RRKM) the unimolecular decomposition of neo- C_5H_{11} to iso-butene + methyl radical and determined a (30.9 ± 1.0) kcal-mole $^{-1}$ barrier and an A factor of $10^{13.9 \pm 0.5}$ (7.94×10^{13}), both the E_a and A factor compare well with data obtained by Baldwin [50] and Furimsky [48].

More recently, Mitchell and Benson [51] conducted a modeling study of the neopentane pyrolysis and reinvestigated unimolecular decomposition of neopentyl radical with the aid of computer simulation and sensitivity analysis techniques, over the temperature range of 477 to 527 °C (750 to 800 K) in the absence and presence of additives iso-butene, HCl and HBr. They concluded that the apparent discrepancy between Anderson et al [47] and other reports [48-49 50] for reaction R3-1 is due to the use of an incomplete mechanism in the former determination. The experimental data from Anderson et al [47] are fully consistent with the use of a k_1 value determined by Slagle et al [49] when the data are interpreted using their more detailed mechanism.

The research group of Bayes et al [52-53] was focusing on kinetics of the initial neopentyl peroxy radical formation at low pressure and on the equilibrium and thermodynamic aspects of the oxygen addition reaction. They studied the rate constants on reaction of neopentyl radical with O_2 (R3-2) at 266 to 374 K and low pressure, 3 to 3.5 Torr. They monitored the pseudo-first-order decay of the neopentyl radicals as a function of oxygen,

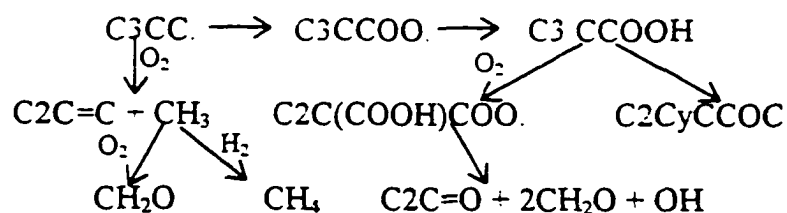
using a mass spectrometer as a detector. Neopentyl radicals were produced by the laser flash photolysis of neopentyl bromide using an ArF laser at 193 nm, or by the two step method described above in Slagle's experiment (first, chlorine atom, then neopentyl radicals)[49]. Their experimental results show a negative temperature dependence for the rate constant of neopentyl radical with O₂. They used adiabatic channel model calculation to interpret their results and reported the rate constant of this reaction as $k = \{2.1 \times 10^{-12} \text{ cm}^3 \text{ molecules}^{-1} \text{ s}^{-1}\} (T/300 \text{ K})^{-(2.1 \pm 0.4)}$, with no fall-off analysis.

Hughes et al [54] conducted a direct measurements of the neopentyl -peroxy-hydroperoxy radical isomerization (R3-3). They studied the formation of OH radical from thermal decomposition of neopentyl iodide in a bath of He with varied concentrations of O₂ at pressures of 575 to 660 Torr and at temperatures from 660 to 750 K. OH radical product concentration profile versus time was monitored and fit to bi-exponential growth curves. An exact analytical solution was postulated incorporating peroxy formation, reverse dissociation, isomerization (hydrogen atom transfer, but non-reversible), and only one isomer decomposition product channel – cyclic ether + OH. Hughes et al concluded that the above reaction processes were the only important components to include in their analysis, that the isomerization process had the barrier controlling the overall reaction process(es) and that the kinetics and pathways for adduct formation, reverse decomposition, isomerization and subsequent hydroperoxide alkyl radical decomposition were in good agreement with previous studies of the Baldwin and Walker research group [50]. Hughes et al reported rate constants for the isomerization with A of 1.58×10^{12} and E_a of 29 kcal mole⁻¹, where the E_a is needed to correlate with a combined ring strain plus E_a abstraction of 17 kcal mole⁻¹.

Except above studies on individual reaction involved in the oxidation of neopentyl radical, there were several investigations on the oxidation of neopentane or neopentyl radical by few groups.

The earliest investigations on the oxidation of neopentane or neopentyl radical were conducted by several workers [55 - 59] over the temperature range 260 - 350 °C. Zeelenberg [55] examined the products formed during the very early stages of reaction at 260 °C, but reported results for only one mixture composition. Antonik and Lucquin [56-57] studied the cool flame and explosion limits, and carried out a partial analysis of the products in the presence and absence of HBr at 298 °C. Drysdale and Norrish [58] determined the products over a wide extent of reaction at 280 °C, but the results were limited to one mixture and appear incomplete; for instance, the yield of the important product 3,3-dimethyloxetan was not given. Fish [59], in a study of the non-isothermal oxidation of neopentane at 300 - 350 °C, gave only a qualitative distribution of products. There were no or little mechanism and kinetic information reported in this early stage.

In 1970's, Baker et al [60 - 62] conducted a more completely experimental study on neopentyl radical by adding neopentane and the primary products to slowly reacting mixtures of hydrogen and oxygen at 480 °C, in a flow reactor (an aged boric-acid-coated Pyrex vessel) with reaction times ranging up to 200 seconds. They reported all products detected by colorimetry for formaldehyde and gas chromatography for all others under their experimental conditions and proposed a simple mechanism as follows to explain the formation of primary and secondary products.



Several years later, the same research group of Baldwin and Walker reworked on the oxidation reactions of neopentyl radical derived from neopentane in an atmosphere of hydrogen and oxygen at temperature range from 380 to 520 °C (653 to 793 K), in a flow reactor (an aged boric-acid-coated Pyrex vessel) with reaction times ranging up to several tens of seconds and gave the first complete experimental and kinetics study on the oxidation of neopentyl radical [50]. They analyzed stable products as a function of the concentration of oxygen at temperature from 380 to 520 °C (653 to 793 K) and analyzed the data using steady state and equilibrium relationships. They concluded that the reactions of neopentyl radicals in an oxidizing environment involve a relatively simple mechanism which gave a quantitative interpretation of the product yields; and that the only detectable initial products at their experimental temperature were 3,3-dimethyloxetan (DMO), acetone, iso-butene, and formaldehyde. They determined Arrhenius parameters for those elementary reactions included in their mechanism by extrapolating the product ratios $([\text{acetone}] + [\text{DMO}]) / [\text{i-butene}]$ and $[\text{acetone}] / [\text{DMO}]$ which were measured using gas chromatograph coupled to an integrator at each temperature, and reported a $k_1 = 10^{13.65 \pm 0.2} \exp(-127.4 \pm 6 \text{ kJ}\cdot\text{mol}^{-1}/RT) \text{ s}^{-1}$ by thermochemical method for reaction R3-1; $k_2/k_3 = 2.7 \times 10^{-5} \exp(+105.1 \text{ kJ}\cdot\text{mol}^{-1}/RT) \text{ dm}^3\cdot\text{s}^{-1}$ by using of Benson's additivity data [50] for reaction R3-2; $k_3 = 10^{13.08} \exp(-120.0 \pm 6 \text{ kJ}\cdot\text{mol}^{-1}/RT) \text{ s}^{-1}$ for reaction R3-3; $k_{4a} = 10^{11.30} \exp(-73.0 \text{ kJ}\cdot\text{mol}^{-1}/RT) \text{ s}^{-1}$ and $k_{4b} = 10^{13.65} \exp(-116.0 \text{ kJ}\cdot\text{mol}^{-1}/RT) \text{ s}^{-1}$ for

reaction R3-4(a) and R3-4(b). They also combined Arrhenius expressions for their 1.5p H-atom transfer (where p represents primary) in neopentyl peroxy radical and 1,4p H-atom transfer in ethyl peroxy radical [63], with thermochemical calculations to estimate a set of Arrhenius parameters for primary, secondary and tertiary intramolecular H-atom transfers in alkyl peroxy radicals involving 4 to 8 member cyclic transition states (at 753 K).

The only other complete study, which is a pure kinetics modeling study, on neopentane oxidation was conducted by Curran et al [64]. They have recently published a detailed chemical kinetic model to analyze experimental results, obtained by Baker et al [61-62], on the oxidation of neopentane in a closed reactor at 500 Torr pressure and one temperature, 480 °C (753 K). The important rate parameters in Curran's mechanism were based on empirical estimations and literature data. They used Slagle's data [49] for R1; Xi's data [53] for reaction R3-2. They calculated rate constant for isomerization reaction (R3-3) based on the theoretical methods of Bozzelli [41] and gave $k_3 = 10^{12.35} \exp(-23.9 \text{ kcal-mol}^{-1}/RT) \text{ s}^{-1}$ for reaction R3-3; evaluated rate parameters for the cyclic ether formation reaction based on their earlier study [65] for the formation of oxetan species from an alkyl hydroperoxide radical and gave a $k_{4a} = 10^{10.40} \exp(-15.25 \text{ kcal-mol}^{-1}/RT) \text{ s}^{-1}$ for reaction R3-4(a). Curran et al calculated rate constants for β -scission reaction by considering methyl radical addition to iso-butene and taking Slagle's data [49] for this reverse reaction and gave $k_{4b} = 10^{13.70} \exp(-29.0 \text{ kcal-mol}^{-1}/RT) \text{ s}^{-1}$ for reaction R3-4(b). The rate constants model stable species profile well and are presented as part of a very large, - several thousand reactions, general hydrocarbon oxidation model. The paper developed detailed reaction paths, but with no calculations of transition state

thermochemical properties. no performance of fall-off analysis as a function of temperature and pressure for chemical activation or unimolecular reaction system.

CHAPTER 4

KINETIC MODELLING FOR THE NEO-C₅H₁₁ + O₂ SYSTEM

4.1 Thermodynamic Properties

All species involved in the modeling mechanism have to have assigned thermodynamic parameters to support all reaction rate constant estimations or QRRK calculations and species concentration interpretations. Thermodynamic parameters ΔH_{f298} , S_{298} and $C_p(300)$ to $C_p(\text{infinity})$ for these species in the neopentyl radical + O₂ system are listed in Table IA. 1. The thermodynamic properties for the relevant radicals and stable parents were obtained by group additivity using THERM (see section “1.2 Group Additivities (THERM)” on page 4) with recently published peroxy groups and Hydrogen Bond Increment groups [66 - 68]. The OO symbol is a new group notation for peroxides, groups were developed using Ab Initio (Gaussian 94 6-31G** and MP2) and semi-empirical calculations on isodesmic reactions. The thermochemical data allow calculation of reverse reaction rate constants by microscopic reversibility [69]. Entropies and $C_p(T)$ values of radicals are from use of Hydrogen Bond Increments (HBI) [3]. The thermodynamic property entropy and heat capacity for species C3CCOO., C3.CCOOH and C2CyCCOC were calculated from semi-empirical calculation method MOPAC PM3 (see section “1.3 MOPAC on page 9) to consistent with corresponding reaction transition state calculations for reaction analysis.

4.2 Important Transition States

Three important transition states were defined and calculated for this modeling study system. Isomerization reaction of neopentyl peroxy radical (C3CCOO.) to neopentyl hydroperoxide radical (C3.CCOOH) had been combined into modeling mechanism, in totally different way from previous study, we consider this reaction as a faster-established equilibrium reaction (see section “5.3 Validation and Comparison with Literature Data), which does not affect the formation of OH radical a lot. Hughes et al [54] considered this reaction as rate control step and obtained a pretty high activation energy from their experimental result of the OH profile. The second important transition state defined in this neopentyl system is one of the cyclic compound, oxetan (C2CyCCOC), formation reaction from neopentyl hydroperoxide radical (C3.CCOOH). This is a OH elimination and cyclic compound formation reaction, which accounts for over 80% of OH formation while Hughes et al [54] used this reaction to account for all OH formation to obtain the rate constant for isomerization reaction. The last important transition state defined is for a beta scission of neopentyl hydroperoxide radical (C3.CCOOH) to iso-butene and methyl hydroperoxide radical (C.H₂OOH) which will rapidly dissociated to formaldehyde and OH radical. This reaction will account for part of total yield of iso-butene, a major product in neopentyl radical + O₂ system, this is the first try to use higher level calculation method to study this type of reaction and the detail will be discussed in chapter 10 of part IV on page 136.

Thermodynamic properties of transition states, related species and thermodynamic analysis are listed in TS IB. 1 and TS IB. 2. The S_{298} and $C_p(T)$ on transition states and relevant species calculated by using semi-empirical (MOPAC PM3) (see section 1.3 MOPAC).

Enthalpies of transition states are from evaluation of activation energies from kinetics, experiments and calculations in the literature on similar reactions. Enthalpies of relevant species are calculated from group additivity (THERM). Equilibrium constants $K_{eq}(T)$ are calculated from thermodynamic properties of reactants and products or reactants and transition states as a function of temperature. Reverse rate constants are calculated from $K_{eq}(T)$ and $k_f(T)$ values.

Semi-empirical (MOPAC PM3) calculations are also used to define transition state structures so provide bond distance information. These data are coupled into the QRRK fall-off calculations to determine the A factors as a function of temperature.

4.2.1 C3CCOO. \rightarrow TS(1) \rightarrow C3.CCOOH

The structure of transition state for isomerization of neopentyl peroxy radical (C3CCOO) to neopentyl hydroperoxide radical (C3.CCOOH), determined by semi-empirical (MOPAC PM3) calculation, is shown in TS IB. 3 along with frequencies, moments of inertia and barriers for internal rotors. TS IB. 4 and TS IB. 5 give the transition state's Z-matrix, containing bond angles and dihedral angles and the interatomic distances. TS IB. 3 shows that the breaking C-H bond stretches to 1.268 angstroms from 1.09 angstroms, and the forming O-H bond length is 1.292 angstroms which is longer than regular O-H bond length 0.95 angstroms.

TS IB. 2 shows temperature dependence of the properties of H transfer (isomerization) from thermodynamic analysis. Entropies of the reaction increase with temperature. The A factor increase with temperature, which indicate that transition state gets looser when temperature goes higher. E_a from this MOPAC calculation is usually larger than that from

the evaluation of kinetics, experiments and calculations in the literature on similar reactions. The latter one have been used in the studies.

4.2.2 $\text{C3.CCOOH} \rightarrow \text{TS(2)} \rightarrow \text{C2CyCCOC} + \text{OH}$

The structure of the transition state for this oxetan formation reaction along with frequencies, moments of inertia and barriers of internal rotors for transition state are shown in TS IB. 6. The breaking O-O bond length is 1.630 angstroms and the forming C-O bond length is 1.866 angstroms; 1.253 and 1.310 times longer than normal RO-O. and R-OO. bond lengths of 1.3008 and 1.4249 angstroms respectively [70].

A thermodynamic analysis (TS IB. 2) shows that $\Delta S^\ddagger(T)$ for this reaction decreases with temperature — negative temperature effect, thus on a relative scale, the transition state gets tighter with increased temperature.

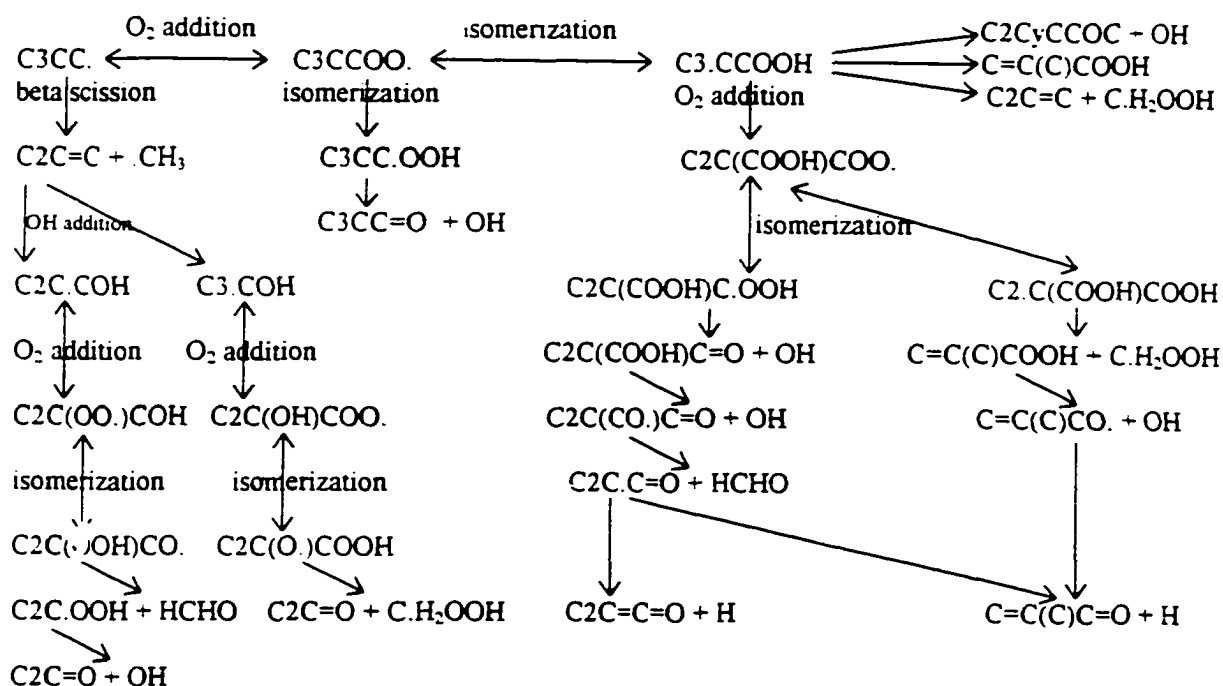
TS IB. 7 and TS IB. 8 show the transition state's Z-matrix, containing bond angles and dihedral angles and the interatomic distances.

4.2.3 $\text{C3CCOO.} \rightarrow \text{TS(x)} \rightarrow \text{C2C=C} + \text{C.H}_2\text{OOH}$

We could not find a transition state for this direct elimination channel. The reaction would have a carbon - hydrogen - oxygen bond being formed, and both a carbon and an oxygen leaving from a near planar iso-butene structure. We do not include this reaction in the analysis. If the reaction occurred the $\text{C.H}_2\text{OOH}$ would rapidly form $\text{OH} + \text{CH}_2\text{O}$.

4.3 Quantum RRK Analysis

The elementary reaction mechanism of the neopentyl radical + O_2 system is outlined as:



There are several dominant pathways here. At the intermediate temperature, the unimolecular dissociation of neopentyl radical is very competitive with the addition of O_2 to it, which are two major pathways for neopentyl radical.

The O_2 addition reaction pathway accounts for the primary major products other than isobutene such as oxetan ($C_2CyCCOC$) and part of iso-butene. Treatment of the chemically energized complex reactions allows analysis of decomposition back to reactants, intramolecular transfer of hydrogen atoms to form hydroperoxy radicals which further decompose to primary and secondary products before stabilization to ground state peroxy or hydroperoxy radicals. Further reactions of the stabilized peroxy radicals include: dissociation to reactants, or isomerization to hydroperoxy via H shift and then beta scission to final products, or addition of a second O_2 .

7

The unimolecular dissociation of neopentyl radical is certainly responsible for the production of most of iso-butene, whose further reactions, the attacking of OH and HO₂ radicals and then O₂ addition to hydroxide and hydroperoxide radicals, may account for many other secondary or minor products.

All reaction pathways of addition reactions and unimolecular isomerization or dissociation reactions are analyzed by construction of potential energy diagrams of the systems. and a assignment of sets of high pressure limit rate constants based on existing experimental data, literature data, theoretical calculation data, and on group additivity estimation techniques, thermodynamic analysis and chemical reaction microscopic reversibility. The most important reactions in this system, such as the reversible peroxy formation, the isomerization channels as well as the OH formation path, are discussed as follows.

4.3.1 Chemical Activation Reaction System: C₃CC. + O₂ → Products

An energy level diagram of the pathway that the O₂ addition to neopentyl radical and subsequent dissociation reactions, and data for each high pressure limit rate constant are shown and listed in Appendix ID. 1. Reaction channels for the energized adduct C₃CCOO.* include dissociation back to reactants, stabilization to C₃CCOO., and isomerization via hydrogen transfer to hydroperoxide radical. The energized isomer C₃.CCOOH* can undergoes cyclic ether formation to C₂CyCCOC + OH, elimination (beta scission) to C=C(C)COOH + CH₃ and C₂C=C + C.H₂OOH or stabilization to C₃.CCOOH radical. The other energized isomer C₃CC.OOH* will rapidly dissociate to C₃CCHO + OH. The barrier for isomerization to C₃.CCOOH is evaluated as 11.39 kcal-mol⁻¹, some lower than dissociation back to reactants (Appendix ID. 1). There is

sufficient energy in the adduct C3CCOO^{\bullet} to allow isomerization to occur before it is stabilized – i.e. a chemically activated reaction path.

Figure IC. 1(a) shows the apparent rate constants for the product channels of $\text{C3CC}^{\bullet} + \text{O}_2$ versus temperature from 300 to 1300 K at atmospheric pressure. It shows that the dominant product channel for $\text{C3CC}^{\bullet} + \text{O}_2$ chemical activation pathways is stabilization to C3CCOO^{\bullet} (filled squares) at and below 800 K. When temperature rises above 800 K, the chemically activated unimolecular dissociation to isomer C3.CCOOH , products $\text{C2CyCCOC} + \text{OH}$, $\text{C2C}=\text{C} + \text{C.H}_2\text{OOH}$, $\text{C}=\text{C}(\text{C})\text{COOH} + \text{.CH}_3$ and back to reactants $\text{C3CC}^{\bullet} + \text{O}_2$ become very competitive with stabilization channel while the rate of stabilization decreases. Also the rate of isomerization to C3.CCOOH decreases a little with increasing temperature. This is because the A factor becomes dominant rate controller. For the same reason, direct dissociation to $\text{C3CCO}^{\bullet} + \text{O}$ from chemically activated C3CCOO^{\bullet} will have the largest increase of the reaction rate with increasing temperature. At 700 K, a fraction (approximately 10 % at 1.0 atm) of the chemically activated C3CCOO^{\bullet} directly reacts to products via the isomerization to C3.CCOOH channel. This is responsible for formation of C2CyCCOC , one of major products. The other isomerization channel to C3CC.OOH has a low rate at 700 K while the channel of C3CC.OOH to product $\text{C3CCHO} + \text{OH}$ has a very high rate (E_a is only ca. $2.5 \text{ kcal}\cdot\text{mol}^{-1}$), so almost all energized $\text{C3CC.OOH}^{\bullet}$ adduct goes to product with almost no reverse reaction. The chemical activation channel $\text{C3CC}^{\bullet} + \text{O}_2 \rightarrow \text{C3CCHO} + \text{OH}$ also contributes to OH formation.

Figure IC. 1(b) illustrates the pressure dependence for the rate constants of the chemically activated reactions. In the pressure range from 0.1 to 100 atm, the channels of

stabilization, dissociation back to reactants, isomerization to C3.CCOOH and its dissociation products have much higher rates than other channels. Stabilization to C3CCOO. is the dominant product channel over almost all pressures. The back to reactants channel will be dominant when pressure is lower than 0.1 atm. The stabilization and isomerization to C3.CCOOH have almost the same increasing rate below atmospheric pressures while isomerization decreases when pressure increases to above atmospheric pressure. Other product channels decrease too relative to stabilization as the pressure increases.

4.3.2 Chemical Activation Reaction System: C3.CCOOH + O₂ → Products

The second O₂ addition to neopentyl hydroperoxide radical is important at low temperature and high O₂ concentration conditions and it is responsible for the production of acetone [50,64], a second major product from neopentyl radical oxidation.

The energy level diagram and input parameters for addition of a second O₂ to hydroperoxide isomer and subsequent reactions are shown in Appendix ID. 2. The reaction channels for C2C(COOH)COO.* radical are similar to C3CCOO.*, reverse reaction, isomerization and stabilization. Two isomers result from intramolecular hydrogen transfer, and are important in this second O₂ addition. C2.C(COOH)COOH will eliminate a C.H₂OOH to form hydroperoxide olefin (C=C(C)COOH) and the C.H₂OOH rapidly undergoes elimination (exothermic) to CH₂O + OH. This isomer can also form an epoxide + OH as in the first O₂ addition. C2C(COOH)C.OOH will rapidly eliminate OH to form hydroperoxide carbonyl (C2C(COOH)C=O). Both the hydroperoxide carbonyl and olefin will undergo dissociation, cleavage of the weak O-O bond in the peroxy moiety with

products OH and alkoxy, serving to accelerate the oxidation (chain branching reaction). These alkoxy radicals are important sources to form 2-methyl-2-propenal ($\text{C}=\text{C}(\text{C})\text{CHO}$) which was identified as an important products from oxidation of neopentyl radical [50]. The sensitivity analysis shows that this second O_2 addition reaction pathway also contributes to the OH formation.

The apparent rates of chemical activation channels from $\text{C}_3\text{CCOOH} + \text{O}_2$ to various products shows a similar tendency to the first O_2 addition $\text{C}_3\text{CC} + \text{O}_2$ (Figure IC. 1).

4.3.3 Chemical Activation Reaction System: $\text{C}_2\text{C}=\text{C} + \text{OH}, \text{O}_2 \rightarrow \text{Products}$

The OH addition to iso-butene, followed by O_2 addition to intermediate radical, is the key reaction pathway to account for secondary product formation. OH can add to each side of carbon double bond in iso-butene to form two intermediate radicals C_3COH and $\text{C}_2\text{C}\cdot\text{COH}$. Temperature and pressure dependence of these two addition reactions are in Appendix Figure IC. 1 and Figure IC. 1, which show they are pressure dependent reactions at the temperature above 700 K and are negative temperature dependent reactions in the all pressure range. The C_3COH and $\text{C}_2\text{C}\cdot\text{COH}$ radicals will quickly react with O_2 with no barrier to form chemically activated, energized adduct $[\text{C}_2\text{C}(\text{OH})\text{COO}]^*$ and $[\text{C}_2\text{C}(\text{OO})\text{COH}]^*$, which then undergo stabilization, isomerization and further beta scission, or dissociation back to reactant. The QRRK analysis (Appendix Figure IC. 1 and Figure IC. 1 shows that the adducts will most go back to reactant at temperature above 700 K, pressure below 1 atm. With the decreasing temperature and increasing pressure, stabilization becomes dominant channel and certain fraction of adduct can directly go to product $\text{C}_2\text{C}=\text{O}$ and CH_2O (from dissociation of $\text{C}_2\text{H}_2\text{OOH}$)

4.3.4 Fate of Stabilized Peroxy and Hydroperoxide Adducts

The computed results for the rate of O₂ addition to neopentyl radical as well as other O₂ additional chemical activation pathways above show that the main product path of chemically activated adducts is stabilization for almost all pressures and at intermediate or above temperatures. It is, therefore, important to determine the fate of the stabilized peroxy and hydroperoxide adduct as a function of temperature. QRRK analysis results for these stabilized adducts and some of their products are shown in Appendix Figure IC. 1.

4.3.4.1 C3CCOO. and C3.CCOOH

C3CCOO. peroxy radical and C3.CCOOH hydroperoxide radical are from major reaction pathway C3CC. + O₂ and are responsible for the major product C2CyCCOC formation. Our results (Appendix Figure IC. 1 show that at atmospheric pressure, the dominant reaction of stabilized C3CCOO. is dissociation to C3CC. + O₂ when temperature is above 900 K; is isomerization via a H atom shift followed by a beta scission to a cyclic ether + OH when temperature is below 700 K. This account for the formation of C2CyCCOC, while major product channel of stabilized C3.CCOOH is C2C=C + C.H₂OOH, which account for a part of C2C=C formation.

4.3.4.2 C2C(COOH)COO., C2.C(COOH)COOH, C2C(COOH)C.OOH

The dominant path for stabilized C2C(COOH)COO. radical is dissociation back to C3.CCOOH + O₂. The dominant product channel from this peroxy radical is C=C(C)COOH + C.H₂OOH (these can further form C=C(C)CHO, CH₂O). Two hydroperoxide radicals C2.C(COOH)COOH and C2C(COOH)C.OOH are intermediates resulting from isomerization of stabilized C2C(COOH)COO. radical or directly from

chemically activated adduct $[C_2C(COOH)COO.]^*$ ($C_3.CCOOH + O_2$). They both can go back or go further as beta scission reactions. QRRK analysis (Appendix Figure IC. 1) shows that the $C_2.C(COOH)COOH$ will mainly undergo reverse reaction with a small fraction undergoing beta scission to $C=C(C)COOH + C.H_2OOH$, while the product channel of $C_2C(COOH)CHO + OH$ from $C_2C(COOH)C.OOH$ is dominant over the temperature range because of very low or no barrier for this type beta scission with carbonyl formation. The secondary product $C=C(C)CHO$ is from these pathways.

4.3.4.3 $C_2C(OH)COO.$, $C_2C(O.)COOH$, $C_2C(OOH)CO.$, $C_2C(OO.)COH$

These four stabilized adducts $C_2C(OH)COO.$, $C_2C(O.)COOH$, $C_2C(OOH)CO.$ and $C_2C(OO.)COH$ are from OH / O_2 addition to iso-butene. The QRRK analysis (Appendix Figure IC. 1) show that the $C_2C(OH)COO.$ and $C_2C(OO.)COH$ will mostly go back to reactants and have certain fractions to product $C_2C=O + C.H_2OOH$ (from $C_2C(OH)COO.$) and $C_2C.OOH + CH_2O$ (from $C_2C(OO.)COH$) in the temperature range of 500 to 1300 K, and isomerization to $C_2C(O.)COOH$, $C_2C(OOH)CO.$ will be dominant at temperature below 500 K. The $C_2C(O.)COOH$, $C_2C(OOH)CO.$ will go to product $C_2C=O + C.H_2OOH$, $C_2C.OOH + CH_2O$ separately at temperature above 700 K and go back to their isomers at temperature below 700 K.

4.3.5 Unimolecular Dissociation Reaction Systems

The most important unimolecular dissociation reaction in neopentyl radical + O_2 system is neopentyl radical dissociation to iso-butene and methyl radical. The QRRK analysis (Appendix Figure IC. 1) show that it is pressure dependent reaction at temperature above 700 K. This reaction will be discussed in more detail in the following chapter.

4.3.6 Summary

The QRRK analysis have showed that the two primary major products: (1) 3,3-dimethyloxetan (DMO, C2CyCCOC) (2) iso-butene (C2C=C) from the oxidation of neopentyl radical under the molecular oxygen atmosphere and at intermediate temperature were produced by chemically activated reaction pathway of C3CC. + O₂ via the neopentyl hydroperoxide isomer C3.CCOOH, and unimolecular dissociation of neopentyl radical.

The OH formation will be accounted by product channel of the first O₂ addition to neopentyl radical. C2CyCCOC + OH, C3CCHO + OH, as well as the second O₂ addition to neopentyl hydroperoxide isomer.

The reactions C3CC. → C2C=C + CH₃ and C3.CCOOH → C=C(C)COOH + CH₃ are responsible for the formation of methane (CH₄), and the reaction C3.CCOOH → C2C=C + C.H₂OOH may account for the formation of formaldehyde (CH₂O) because all C.H₂OOH rapidly undergoes dissociation with a ca. 2.5 kcal·mol⁻¹ activation energy to form CH₂O.

The QRRK analysis also shows that the dominant product channel of a chemically activated adduct above 0.1 atm and below 900 K is, stabilization, because isomerization has a relative low A factor (tight transition state). Fall off at 700 K occurs because of adduct dissociation (reverse reaction). The important isomer (C3.CCOOH) product channel is C2CyCCOC + OH, and next important product channels are C2C=C + C.H₂OOH and C=C(C)COOH + .CH₃. Subsequent reactions of this stabilized isomer with O₂ will also be important at conditions where stabilization occurs and O₂ is present. The

channel to $\text{C}_3\text{CC}=\text{O} + \text{OH}$ (endothermic, beta scission of the $\text{C}_3\text{CC.OOH}$) also has some significance.

CHAPTER 5

MODELLING VALIDATION FOR THE NEO-C₅H₁₁ + O₂ SYSTEM

5.1 Basic Model of Neopentyl + O₂ System

The model contains 58 reactions and 39 species and the mechanism is listed in Table I.A. 4. It has been shown to describe set of experimental data well; but it is significantly different in description of the neopentyl + O₂ reaction from that of Hughes et al [54], and of Baldwin and Walker [50]. It also comparable to literature data for important reactions. We conclude an isomerization barrier height some 7 kcal mole⁻¹ lower than that of the above two research groups and that subsequent barriers are responsible for the apparent barrier reported by Hughes et al. We also show that while one reaction is responsible for a major fraction of the OH formation - (more than half), the total OH is actual by the result of several reaction paths. The importance of these paths will change with varied conditions (oxygen concentration, pressure and temperature). And we show that reactions of the hydroperoxy-neopentyl radical with oxygen can have significant contributions to the OH profile.

5.2 Validation by Hughes' Data

Hughes et al [54] conducted a direct measurements of the neopentyl peroxy-hydroperoxide radical isomerization over the temperature range 660 - 750 K in 1992. They obtained their results by monitoring the OH profile. In this work we have attempted to model set of their experimental result and thus validate our mechanism.

The Senkin [71] computer code from Sandia is used to integrate the kinetic equations and calculate reverse rate constants from the forward rate constants and thermodynamic parameters. A comparison of the time dependence of the OH radical formation to data published by Hughes et al is illustrated in Figure IC. 20 and a comparison of the energy of activation vs. temperature to the experiment results of Hughes is shown in Figure IC. 21. The results for OH profile and the temperature dependence of rate constants show very good agreement with experimental data of Hughes et al [54]. Sensitivity analysis on OH profile at the mean experimental temperature indicates that the A factor for the formation of C2CyCCOC and the well depth (Enthalpy of neopentyl peroxy) of the adduct are important. The most important reactions for the OH profile are C3CC. radical reaction with O₂ (chemical activation) and unimolecular decomposition.

Table IA. 3 shows that there are several reactions responsible for the OH formation. The OH radical is generated by three major paths: (i) Dissociation of hydroperoxy alkyl isomer to OH + a cyclic ether and others (Appendix ID. 1); (ii) The addition of a second O₂ to hydroperoxy alkyl radical with isomerization and subsequent reaction of the isomer (Appendix ID. 2); (iii) Methyl radical oxidation and subsequent reactions. Table IA. 3 shows that at pressure near 1 atm and 700 K, the formation of epoxide is the most important channel to form OH radical. The addition of O₂ to C3.COH and C2C.COH with isomerization and subsequent reaction of the isomers (Appendix ID. 5, ID. 6) does not show an importance to the OH profile; but our analysis shows that C3.COH and C2C.COH are important intermediates in this reaction system. These species are produced by addition of OH radical to iso-butene, a major initial product from neopentyl radical decomposition and some from the neopentyl radical + O₂ reaction paths. These

hydroxyl adducts undergo addition reaction with O_2 , isomerization (hydrogen transfer of the OH hydrogen to the peroxy group) and unimolecular decomposition of the alkoxy radical to an alkyl- $C.H_2OOH$, which rapidly undergoes exothermic reaction to a ketone or aldehyde + OH (Appendix ID. 5, ID. 6). The hydrogen shift in these isomers is facilitated via hydrogen bonding between the peroxy oxygen radical and the OH group and may be responsible for an important and stable product, acetone, formation in neopentyl oxidation.

Some important reaction fluxes are listed in Table IA. 5. The data shows that addition of O_2 to alkyl radicals are in near equilibrium and the epoxide formation is faster than other dissociation paths excluding reverse isomerization of the hydroperoxy radical by a factor of 10.

5.3 Validation and Comparison with Literature Data for Important Reactions

5.3.1 Comparison with Slagle's Data for $C_3CC. \rightarrow C_2C=C + CH_3$ (k_1)

Our QRRK analysis is shown to describe Slagle et al's experimental data [49] well for neopentyl radical decomposition reaction.

The unimolecular dissociation of neopentyl radical has been widely investigated with the studies of the pyrolysis of neopentane. Furimsky and Laidler [48] investigated this reaction as a special part of the whole study for neopentane pyrolysis and reported the first set of experimentally based high pressure limit rate constant, $2.5 \times 10^{13} \exp(-29.001 \text{ kcal} \cdot \text{mol}^{-1}/RT) \text{ s}^{-1}$, by extrapolating their experimental data obtained at the temperature of 529 to 608 K and pressure of 0.0355 to 0.296 atm with neo- C_5H_{12} as bath gas. This rate has

been considered too high because they assigned a too high A factor for the reference reaction they used for derived absolute rate constant. A two set of rate constants of $2.0 \times 10^{13} \exp(-29.8 \text{ kcal-mol}^{-1}/RT) \text{ s}^{-1}$ (in 1975), $2.51 \times 10^{13} \exp(-29.637 \text{ kcal-mol}^{-1}/RT) \text{ s}^{-1}$ (in 1979), for unimolecular dissociation of neopentyl radical to iso-butene and methyl radical were derived, by Szirovicza and Marta [72], from fitting a complex mechanism of neopentane pyrolysis under the temperature range from 512 to 571 K, and pressure range from 0.0158 to 0.259 atm. Muller et al [73] reported a rate constant of $1.00 \times 10^{13} \exp(-30.00 \text{ kcal-mol}^{-1}/RT) \text{ s}^{-1}$ derived from fitting a complex mechanism while they investigated the influences of HCl and HBr on the pyrolysis of neopentane and ethane at small extents of reaction. More recently, Baldwin et al [50] calculated a rate of $10^{13.65 \pm 0.2} \exp(-30.474 \text{ kcal-mol}^{-1}/RT) \text{ s}^{-1}$ for their neopentane oxidation mechanism in 1982 while Tsang [74] derived a rate of $1.07 \times 10^{13} \exp(-29.808 \text{ kcal-mol}^{-1}/RT) \text{ s}^{-1}$ from detailed balance and reverse rate in 1985. The latest report for neopentyl radical decomposition is $10^{13.9} \exp(-31.5 \text{ kcal-mol}^{-1}/RT) \text{ s}^{-1}$ by Mitchell and Benson [51] when they reinvestigated the apparent discrepancy between previous reports.

Only one particular study on unimolecular decomposition of the neopentyl radical is conducted by Slagle et al [49]. They directly monitored the decomposition of neopentyl radical by using a heatable tubular reactor coupled to a photoionization mass spectrometer. Their experimental temperature and pressure were 560 - 650 K and 0.00132 - 0.0118 atm.

The rate of $10^{13.9} \exp(-30.76 \text{ kcal-mol}^{-1}/RT) \text{ s}^{-1}$ in this study derived from fitting a simple mechanism for oxidation of neopentyl radical in the O_2 atmosphere and quite comparable

to other studies (Table IA. 2). A comparison of our QRRK calculation result to the experimental data reported Slagle et al [49] is made and shown in Figure IC. 19. A very good agreement between our QRRK calculation under their experimental condition and their experiment data is obvious while the rate becomes lower when we directly took their high pressure limit rate constant for our QRRK analysis.

5.3.2 Fall-Off Analysis for $\text{C3CC.} + \text{O}_2 \rightarrow \text{C3CCOO.}$ ($k_2/k_{-2}=K_2$)

The reaction of O_2 addition to neopentyl radical was studied only by Bayes group [52, 53] at a very low pressure of 3 Torr and they found high pressure rate constant, $\{2.1 \times 10^{12} \text{ cm}^3\text{-molecule}^{-1}\text{-s}^{-1}\}(T/300 \text{ K})^{-(2.1 \pm 0.4)}$ for $\text{C3CC.} + \text{O}_2$, a negative temperature dependence (rate constant decrease with increase temperature), k ranged from $1.7 \times 10^{12} \text{ cm}^3\text{-mol}^{-1}\text{-sec}^{-1}$ at 266 K to $6.91 \times 10^{11} \text{ cm}^3\text{-mol}^{-1}\text{-sec}^{-1}$ at 374 K. The rate constants used by Hughes et al [54] and Curran et al [64] and this study are originally referenced to Bayes et al experimental study on this particular reaction but in different way. We took the average k reported by Bayes et al, using $1.0 \times 10^{12} \text{ cm}^3\text{-mole}^{-1}\text{-sec}^{-1}$ as the high pressure limit k_{∞} for our QRRK analysis while Hughes et al and Curran et al directly extrapolated Bayes' low pressure and low temperature data for their modeling studies without fall-off considerations. Baldwin et al [50] used Benson's additivity data with an assumed internal rotational energy barrier of 10 kJ-mol⁻¹ for the $t\text{-C}_4\text{H}_9$ group to get an equilibrium constant of $2.7 \times 10^{-5} \exp(+105.1 \text{ kJ-mol}^{-1} / RT) \text{ dm}^3\text{-mol}^{-1}$.

A full fall-off analysis is illustrated in Figure IC. 18. Figure IC. 18 (a) shows a negative temperature dependence of the rate of reaction $\text{C3CC.} + \text{O}_2 \rightarrow \text{C3CCOO.}$ and this dependence goes smaller when pressure goes higher. Figure IC. 18 (b) shows that almost

no fall-off at 300 K but the rates go down with decreasing pressures more rapidly at higher temperatures. above 700 K. At 300 K, we calculated only 1.8% fall off from the high pressure limit using $1.0 \times 10^{12} \text{ cm}^3\text{-mole}^{-1}\text{-sec}^{-1}$ to 3.0 Torr. If one extrapolates the low pressure data of Bayes' to 700 K, $k_{(\text{C3CC.} + \text{O}_2)}$ is $2.13 \times 10^{11} \text{ cm}^3\text{-mole}^{-1}\text{-sec}^{-1}$; to 753 K, $k_{(\text{C3CC.} + \text{O}_2)}$ is $1.83 \times 10^{11} \text{ cm}^3\text{-mole}^{-1}\text{-sec}^{-1}$. Hughes et al [54], whose experiment are at 550 Torr, 700 K and Curran et al [64], who modeled the experimental data reported by Baker et al [61, 62] at 500 Torr, 753 K, both used this low k ($2.13 \times 10^{11} \text{ cm}^3\text{-mole}^{-1}\text{-sec}^{-1}$ and $1.83 \times 10^{11} \text{ cm}^3\text{-mole}^{-1}\text{-sec}^{-1}$) in their modeling. At 700 K, we calculated a 90.9% decrease in k due to fall off at 3 Torr, 38.9% at 550 Torr from the average high pressure limit k ($k_{\infty(\text{avg.})}$, $1 \times 10^{12} \text{ cm}^3\text{-mole}^{-1}$) so there is about 50% increase in k from 3 Torr to 550 Torr at 700 K due to fall-off. At 753 K, we calculated a 95.7% fall off at 3 Torr, 57.5% at 500 Torr from high pressure limit k (k_{∞}) so 35% difference between 3 Torr and 500 Torr at 753 K. So a direct (temperature only) extrapolation of Bayes' low pressure data to 700 K or 753 K for higher pressure experiment is not justified. Our QRRK analysis yields an $A_{700 \text{ K}}$ of 4.54×10^{11} at 550 Torr and 4.75×10^{11} at 1 atm with A_{∞} as estimated $1.0 \times 10^{12} \text{ cm}^3 \text{ mole}^{-1} \text{ sec}^{-1}$.

The flux of this reactions is calculated and shown in Table IA. 5, which shows that reaction $\text{C3CC.} + \text{O}_2 \rightleftharpoons \text{C3CCOO.}$ is effectively at equilibrium in the modeling (conditions: 700 K, 550 Torr) with forward rate of $1.02 \times 10^{-9} \text{ cm}^3 \text{ mole}^{-1} \text{ sec}^{-1}$ and reverse rate of $1.07 \times 10^{-9} \text{ cm}^3 \text{ mole}^{-1} \text{ sec}^{-1}$ at 1.0 millisecond, and forward rate of $3.67 \times 10^{-10} \text{ cm}^3 \text{ mole}^{-1} \text{ sec}^{-1}$ and reverse rate of $3.82 \times 10^{-10} \text{ cm}^3 \text{ mole}^{-1} \text{ sec}^{-1}$ at 1.8 millisecond. The kinetic aspect of this reaction is well controlled by the thermodynamic properties. A sensitivity

analysis on our mechanism has also been performed by varying A_r from $1.0 \times 10^{12} \text{ cm}^3 \text{ mole}^{-1} \text{ sec}^{-1}$ to $6.0 \times 10^{12} \text{ cm}^3 \text{ mole}^{-1} \text{ sec}^{-1}$, and found the results shown in Figure IC. 21, which shows only small differences.

5.3.3 MOPAC Calculation for $\text{C3CCOO} \rightarrow \text{C3.CCOOH}$

There were no specialized study except Hughes et al [54] focused on this isomerization reaction, a intramolecular H transfer via a 6 member ring transition state. The different sets of A factor and activation energy for this isomerization reaction are listed in Table IA. 2 Transition State theory incorporated semi-empirical calculation method MOPAC PM3 is used in this study to describe this H transfer reaction (see section 1.3 MOPAC) and we calculated an A factor of $10^{9.77} T^{0.71}$ and activation energy of $22.7 \text{ kcal-mol}^{-1}$ as high pressure limit rate constants for QRRK analysis.

Hughes et al [54] obtained an A_∞ factor of 1.585×10^{12} and $E_{a,\infty}$ of $29.4 \text{ kcal-mol}^{-1}$ derived from experimentally determined rate constants versus temperature. Their result was based on their assumption that only one reaction $\text{C3.CCOOH} \rightarrow \text{C2CyCCOC} + \text{OH}$ responsible for the formation of OH and the isomerization is the rate-determining step, so they monitor OH profile and plot time constants obtained from bi-exponential fits to the OH profile versus O_2 concentration, then obtained their experimentally determined rate constants by fitted into this curve with assigned rate constants for k_1 ($\text{C3CC} \cdot \rightarrow \text{C2C}=\text{C} + \text{CH}_3$), K_2 ($\text{C3CC} \cdot + \text{O}_2 \rightarrow \text{C3CCOO} \cdot$) (see section “5.3.1 Comparison with Slagle’s Data for $\text{C3CC} \cdot \rightarrow \text{C2C}=\text{C} + \text{CH}_3$ ” and “5.3.2 Fall-Off Analysis for $\text{C3CC} \cdot + \text{O}_2 \rightarrow \text{C3CCOO} \cdot$ ”).

Baldwin et al [50] obtained rate of $10^{13.08} \exp(-28.7 \text{ kcal-mol}^{-1} / RT)$ from their experimental determined value of $k_2 k_3 / k_2 k_1$ ($A_2 A_3 / A_2 A_1$ and $E_{23} E_{33} / E_{21} E_{31}$) with their calculated k_1 and K_2 . The $k_2 k_3 / k_2 k_1$ values were determined by applying stationary-state treatment to the equation $d([\text{acetone}] + [\text{DMO}]) / d[\text{iso-butene}] = K_2 k_3 [\text{O}_2] / k_1$ and found the initial product yield ratio $R = ([\text{acetone}] + [\text{DMO}]) / [\text{iso-butene}]$ by extrapolating experimental determinations. Their result was based on their proposed simple mechanism: iso-butene is accounted by neopentyl radical dissociation, DMO is accounted by neopentyl hydroperoxide radical dissociation and acetone is from a second O_2 addition to neopentyl hydroperoxide isomer.

Curran et al [63] calculated a rate of $10^{12.35} \exp(-23.9 \text{ kcal-mol}^{-1} / RT)$ by using transition state theory but without MOPAC calculations for A factor.

5.3.4 Rate Constant for $\text{C3.CCOOH} \rightarrow \text{C2CyCCOC} + \text{OH}$ (k_4)

Table IA. 2 lists set of Arrhenius parameters for this epoxide formation reaction. This is a somewhat faster reaction and account for most of OH formation. Baldwin et al calculated a rate constant of $10^{11.30} \exp(-17.46 \text{ kcal-mol}^{-1} / RT)$ based on their experimental determined value for k_4 / k_6 (k_6 is the rate of reaction $\text{C3.CCOOH} \rightarrow \text{C2C}=\text{C} + \text{CH}_2\text{O} + \text{OH}$, see following discussion). Curran et al get their self-consistent rate of $10^{10.40} \exp(-15.25 \text{ kcal-mol}^{-1} / RT)$ based on their previous on the formation of oxetan species from an alkyl hydroperoxide radical. We calculated an A factor of $10^{7.76}$ using MOPAC PM3 (see section 1.3 MOPAC) and obtain a n of 0.71 and E_a of $14.0 \text{ kcal-mol}^{-1}$ by best fitting Hughes experimental results.

5.3.5 Beta Scission Reaction $\text{C3.CCOOH} \rightarrow \text{C2C}=\text{C} + \text{C.H}_2\text{OOH}$

The sensitivity analysis in our mechanism shows that the β -scission of C3 CCOOH to $\text{C2C}=\text{C} + \text{C.H}_2\text{OOH}$ is account for a part of iso-butene. The rate of this reaction is also important in the explanation of products distribution. Baldwin et al took the same A factor as one they calculated for neopentyl radical dissociation but lower about $12 \text{ kJ}\cdot\text{mol}^{-1}$ for activation energy for consideration of the presence of less effective OOH group Curran et al and this study calculated the rate constants based on reverse reaction and considered a methyl likened radical $\text{C.H}_2\text{OOH}$ addition to the double bond in iso-butene. Curran et al directly took rate constant of the reverse reaction of neopentyl dissociation from Slagle [49]. We took the same E_a as methyl addition to ethylene and lower A factor to $10^{11.2}$ from $10^{11.5}$.

5.4 Conclusion for Neo- $\text{C}_5\text{H}_{11} + \text{O}_2$ System

We have evaluated thermodynamic properties, reaction paths and kinetic parameters for the neopentyl radical + oxygen reaction system and the sub-system of neopentyl peroxy isomer: neopentyl hydroperoxide radical + O_2 reaction system as well as neopentyl unimolecular decomposition reaction and further iso-butene reaction system. Quantum RRK theory is used to calculate $k(E)$ with the modified strong collision of Gilbert et al used to calculate fall off effects in a kinetic analysis on the chemical activation reaction systems. The rate constants are incorporated into a detailed, elementary reaction mechanism, which is used to model the set of experimental results.

Enthalpies of reactants, intermediates, products and transition states for the elementary reactions resulting from addition of neopentyl radical to molecular oxygen are evaluated in

this study and are illustrated in Appendix IA, Appendix IB. Potential energy diagrams are constructed for QRRK analysis, and high pressure rate constants are taken from evaluated literature data or estimated as described above, they are illustrated in Appendix ID.

The temperature and pressure dependencies of reactions are calculated with QRRK analysis and are illustrated in Appendix IC.

We also defined transition states for two important reactions — isomerization of neopentyl peroxy radical to neopentyl hydroperoxide radical and the formation of cyclic ether from neopentyl hydroperoxide isomer (C3.CCOOH) and calculate pre-exponential A factors from transition state theory. All information for these two transition states are summarized in Appendix IB. We calculate transition state structures and evaluate barriers to isomerization and epoxide formation reactions as 22.7 and 14.0 kcal mole⁻¹ respectively. Flux analysis indicates that a number of these peroxy dissociation and isomerization reactions are at or near equilibrium. Thermodynamic equilibrium and bleed reactions such as: slow epoxide + OH formation relative to reverse isomerization, addition of a second O₂ to the neopentyl hydroperoxide primary alkyl radical, isomerization and subsequent dissociation of this second peroxy, serve to control oxidation rate in this 700 K, 550 Torr reaction system.

PART III

FUNDAMENTAL STUDY ON MTBE PYROLYSIS AND OXIDATION

CHAPTER 6

INTRODUCTION

6.1 Overview

MTBE, Chemically named 2-methoxy-2-methyl-propane or methyl tert-butyl ether ($C_5H_{12}O$), CAS NO. 1634-04-4, is a combustible, but relatively stable (in storage), clear and colorless liquid of low viscosity. It has a distinct odor that is responded to be neither pleasant nor nauseating. It's other chemical/physical properties are MW = 88.15; MP = -109 °C; BP = 55.2 °C; $d = 0.7404 \text{ g}\cdot\text{ml}^{-1}$ (20/4 °C) and VP (vapor pressure) = 245 mmHg at; RVP (Reid Vapor Pressure) = 4.7 psi at 25 °C.

As it is more commonly known, MTBE is a motor fuel oxygenate and octane enhancer. It has been a preferred choice of petroleum industry as an octane enhancer in gasoline since 1980's because it seems to be an efficient way [75] to meet the emission control and fuel composition requirements of the 1990 Clean Air Act with no additional capital investment to change the additive main manufacture route. It is currently being blended with gasoline up to 15 volume percent and the amount may be raised up to 30 volume percent according to legislation and regulations under the Clean Air Act Amendments (CAAA) of 1990. MTBE is accepted as oxygenate in the reformulated gasoline and oxygenated gasoline by US Environmental Protection Agency (EPA), to improve and ameliorate the air quality of the ozone non-attainment areas and carbon monoxide non-attainment areas, because it allows the gasoline to burn more cleanly [76] in the engine and significantly reduces exhaust emissions (CO and hydrocarbon) [77].

The effect of MTBE blending on the properties of gasoline has been reviewed by Mamid et al [78]. MTBE effectively boosts the octane number of gasoline without adversely affecting its other properties, and it provides a much higher FEON, (Front End Octane Number) which becomes more important in cold start conditions and characterizes the efficiency of the engine, to the gasoline pool. It is not affected by the lead (Pb) concentrations in the gasoline so it can readily make up the lost of octane number due to elimination of lead in the gasoline. MTBE has favorable effect on the vapor pressure and distillation characteristics of the gasoline because it has lower RVP (Reid Vapor Pressure) relative to other octane enhancers such as butane. MTBE addition lowers the distillation temperature, which improves driveability, carburation, and cold engine operation. MTBE-gasoline blend are free of gums and peroxides after long term storage and it is more stable during handling and storage than alcohols. It has a good water tolerance and poses no phase separation problems, blending in just like a hydrocarbon in distribution systems and in the presence of water. MTBE appears to be the most economical way to increase octane number while accomplishing environmentally desirable goals, and enhancing octane rating.

MTBE's chemical, physical and thermal properties, are compatible with that of gasoline, especially in the boiling range where gasoline typically shows the lowest antiknock characteristics, this makes it one of the fastest growing chemicals in the world and by far the largest-volume oxygenate used in US. The rapidly increasing demand for MTBE is also due to the lower production cost related to that of alcohol and the lead-phase down regulations of the CAAA of 1990.

Many practical benefits are shown from related studies done on MTBE-gasolines. However, concerns and questions about its environmental and health effects [79 - 81] arose, in recent years, from scientists, researchers, occupational workers and consumers. The environmental concerns focus on the products and by-products after combustion of MTBE and reactions in atmosphere after evaporation from motor fuel distribution, storage and fueling operations plus products after combustion.

MTBE is an effective octane booster and volume extender for unleaded gasoline, but it is not as efficient as tetra-alkyl lead compounds, whose antiknock characteristics had been identified by [82] as a chain breaking mechanism (chain termination), as far as specific octane number improvements are concerned. The improvement of blending properties by the addition of MTBE has been evaluated to depend not only on characteristics of the base gasoline (composition of gasoline which contains hundreds of components in different concentrations) but also on the relative concentration of MTBE.

New questions arise such as: How does MTBE behavior change in gasoline, so as to become an octane enhancer? Does it produce toxic by-products? How MTBE-gasoline will affect the environment can be evaluated from the actual elementary chemical process, what is the reaction mechanism and the product distribution of MTBE oxidation under the real or near typically combustion conditions in the internal combustion chamber. The fundamental combustion chemistry of oxygenated hydrocarbons (OHC's) such as MTBE is becoming more and more important as federal, state and community as well as individuals become more concerned about the environment in which they live. Answering to these questions are becoming more urgent as the EPA continues to propose more restrictive regulations or mandates on petroleum industry.

The more scientists and researchers understand the fundamentals of why MTBE has good anti-knocking properties, the better refiners and engineers can control the combustion and improve engine design to obtain more clean burning in the internal combustion chamber

Development of a fundamentally based, pressure dependent, reaction mechanism for MTBE to use in modeling combustion and low temperature oxidation is becoming more important and necessary because the combustion of hydrocarbon and OHC's in practical devices such as internal combustion engines occurs at pressure well above atmospheric conditions, i.e. pressures up to 40 atm.

6.2 Objective of this Study

The goals of this part study are :

- Development and advancement of the understanding of oxidation and pyrolysis processes on MTBE under high pressure conditions.
- Identification of important reactions and key species in the high temperature chemistry of MTBE.
- Identify product distributions of MTBE oxidation and pyrolysis under the experimental conditions by acquisition of experimental data from lab experiments on oxidation and pyrolysis of methyl tert-butyl ether (MTBE).
- Development of a pressure and temperature dependent elementary kinetic model for MTBE, based on thermochemical kinetic principles, tested against experimental data.

This will allow computer experiments to suggest trends for future experimental testing

and preferred fuel compositions that can lead to reduced hydrocarbon emissions while hopefully maintaining or improving engine performance.

A fundamentally based, and pressure and temperature dependent elementary reaction model is targeted to describe both literature and experimental data from this lab for MTBE in the combustion and low temperature oxidation regimes. This includes detailed reaction paths for the major products and for the second major products. A pressure dependent analysis is performed by QRRK calculation coupled with beta collision analysis for fall-off effects on unimolecular decomposition and isomerization reaction and on bimolecular chemical activation reactions [83]., for rate constants under the experimental pressure (1 to 10 atm) conditions. The concentration of reactants, intermediates and final products predicted by the mechanism are coupled (tested) against experimental data. Particular importance is directed to reactions of primary radical intermediates with O_2 , such as $C_3C\cdot + O_2$, $C_2C=C\cdot + O_2$ and $C=CC\cdot + O_2$, plus HO_2 and OH addition reactions with isobutene, which is a major product of MTBE pyrolysis and oxidation and then subsequent reactions of these radical adducts with O_2 . A second importance is directed to the reactions of methanol, an other major product from MTBE pyrolysis and oxidation.

The experiments are conducted in tubular flow reactors to obtain reactant loss and intermediate species profiles versus reaction time, pressure and temperature for pathway analysis and model validation.

6.3 Literature Review

There are a number of studies on 1 atm oxidation and pyrolysis of MTBE for the overall reaction reactants, stable products, as well as some studies on total rate of OH abstraction.

A more limited number of health effect studies have been reported [81]. There are no published studies, however, on a detailed reaction mechanism that focus on both pressure and temperature effects of initial reactions of MTBE coupled with detailed analysis of primary and secondary products from the initial processes. A fundamental study on high temperature chemistry of MTBE is necessary to understand important aspects of fuel combustion in internal engine combustion chamber such as emission or knock.

6.3.1 MTBE Pyrolysis

Early studies on thermal pyrolysis of MTBE were all conducted at temperature below 800 K and all concluded that MTBE decomposes nearly exclusively through the formation of a four-center transition state, followed by the decomposition to iso-butene and methanol.

Daly and Wentrup [84] reported that the thermal decomposition of MTBE produced iso-butene and methanol with no iso-butane formation and with unimolecular rate constant of $10^{14.38} \exp(-61.54 \text{ kcal-mol}^{-1}/RT) \text{ s}^{-1}$ over the temperature range from 706 to 768 K. The fact that added excess iso-butylene did not change the rate of iso-butene production led them first to suggest that four-center transition states for the decomposition of MTBE and lack of any radical intermediates.

Choo et al [85] conducted thermal decomposition of MTBE in a VLPP (Very Low-Pressure Pyrolysis) reactor coupled with a quadrupole residual gas analyzer for product and reactant identification. They confirmed a four-center transition state mechanism for MTBE decomposition to iso-butene and methanol by their experimental conduction and RRKM calculations. They recommend a value of $10^{13.9} \exp((-59.0 \pm 1.0 \text{ kcal-mol}^{-1})/RT) \text{ s}^{-1}$ over the temperature range from 888 to 1158 K.

One study on pyrolysis of MTBE was done by Brocard and Baronnet [86]. MTBE was decomposed thermally in a static or low flow reactor over the temperature range from 623 to 763 K at the low pressures of 0.0658 to 0.197 atm. They used gas chromatography to analyze products and reactants and reported an absolute rate constant value of $10^{14.0} \exp(-59.6 \text{ kcal-mol}^{-1}/RT) \text{ s}^{-1}$ for reaction $\text{C3COC} \rightarrow \text{C2C}=\text{C} + \text{CH}_3\text{OH}$. They also concluded a four-center unimolecular elimination path accounts for the homogenous thermal decomposition of MTBE over the temperature and pressure range of their study.

A summary of these pyrolysis data (rate constant for $\text{C3COC} \rightarrow \text{C2C}=\text{C} + \text{CH}_3\text{OH}$) includes:

<u>Dalyand Wentrup [84]</u>	$k = 10^{14.38} \exp(-61.54 \text{ kcal-mol}^{-1}/RT) \text{ s}^{-1}$ $E_a - \Delta H_{\text{rxn}} = 46.35 \text{ kcal-mol}^{-1}$ $k_{600} = 9.0 \times 10^{-9}$; $k_{800} = 3.69 \times 10^{-3}$; $k_{1000} = 8.50 \times 10^0 (\text{s}^{-1})$
<u>Choo [85]</u>	$k = 10^{13.9} \exp((-59.0 \pm 1.0 \text{ kcal-mol}^{-1})/RT) \text{ s}^{-1}$ $E_a - \Delta H_{\text{rxn}} = 43.18 \text{ kcal-mol}^{-1}$ $k_{600} = 2.5 \times 10^{-8}$; $k_{800} = 6.03 \times 10^{-3}$; $k_{1000} = 1.01 \times 10^1 (\text{s}^{-1})$
<u>Brocard and Baronnet [86]</u>	$k = 10^{14.0} \exp(-59.6 \text{ kcal-mol}^{-1}/RT) \text{ s}^{-1}$ $E_a - \Delta H_{\text{rxn}} = 44.41 \text{ kcal-mol}^{-1}$ $k_{600} = 1.9 \times 10^{-8}$; $k_{800} = 5.21 \times 10^{-3}$; $k_{1000} = 9.40 \times 10^0 (\text{s}^{-1})$
<u>Average</u>	$k = 10^{14.03} \exp(-60.05 \text{ kcal-mol}^{-1}/RT) \text{ s}^{-1}$ $E_a - \Delta H_{\text{rxn}} = 44.65 \text{ kcal-mol}^{-1}$ $k_{600} = 1.77 \times 10^{-8}$; $k_{800} = 4.98 \times 10^{-3}$; $k_{1000} = 9.33 \times 10^0 (\text{s}^{-1})$

6.3.2 Abstraction Reactions of MTBE by OH Radical

The abstraction reaction of Hydrogen atom from MTBE by OH radical, serves an important role in the oxidation of MTBE process at intermediate temperatures, and has been widely studied since MTBE was introduced in large quantities as a gasoline additive to increase the octane and reduce CO emissions in the late 1980's.

Cox and Goldstone [87] measured the total abstraction rate constant of reaction from MTBE by OH radical using the relative rate technique at temperature of 295 K and 1 atm pressure. Their experiments were conducted in a static reaction system with gas chromatography to examine the products and reactants. They reported rate ratio of 0.44 relative to a reference reaction between OH radical and n-hexane and obtained a normalized overall value of $1.51 \times 10^{-12} \text{ cm}^3\text{-molecule}^{-1}\text{s}^{-1}$.

Wallington et al [88] conducted a flash photolysis resonance fluorescence study on the kinetics of the reaction of OH radical with MTBE and reported an overall value of rate constant as $k = (5.1 \pm 1.6) \times 10^{-12} \exp[-(155 \pm 100)/T] \text{ cm}^3\text{-molecule}^{-1}\text{s}^{-1}$ over the temperature range 240 - 440 K at total pressure between 25 to 50 Torr. This rate constant includes abstractions from both the methyl ether hydrogen and the primary methyl tert-butyl hydrogen by OH radical. They produced OH radicals, at an initial concentration estimated as $10^{10} \leq [\text{OH}]_0 \leq 10^{11} \text{ molecules-cm}^3$, by the vacuum ultraviolet ($\lambda \geq 165 \text{ nm}$) photolysis of H_2O ($\approx 0.1 \text{ Torr}$). They monitored OH radicals as a function of time under pseudo-first-order kinetic conditions by fluorescence at 300 nm excited by a microwave OH resonance lamp. Reaction was in Pyrex reaction cell and the reactant mixture flowed through the reaction vessel to avoid the accumulation of photolysis or reaction products. The initial concentration of MTBE, $(0.5\text{--}4.0) \times 10^{14} \text{ molecules-cm}^3$ was high enough to assure pseudo-first-order kinetic conditions with respect to the radical decay.

Wallington et al [89] investigated the abstraction reaction between OH radical and MTBE again but under different conditions by relative rate measurement method. The OH radicals were formed through the photolysis of methyl nitrite (CH_3ONO) in reactant

mixture, a synthetic air consisting a reference organic (n-butene or diethylether), MTBE and CH_3ONO , at atmospheric pressure (about 740 Torr). Analysis was carried out on a gas chromatograph equipped with a split/splitless injector and FID and fitted with either a 30 m \times 0.25 mm (film thickness 0.25 μm) DB-5 column or a 30 m \times 0.53 mm GS-Q column. They used 10 to 20 ppm as typically initial concentrations for both the reference and reactants and 50-100 ppm concentration for methylnitrite. They reported a consistent overall value of $(3.24 \pm 0.08) \times 10^{-12} \text{ cm}^3\text{-molecule}^{-1}\text{s}^{-1}$ with their previous value [88]. We note again that these experiments present only the overall rate not on analysis of the tert-butyl versus methoxy C---H hydrogen.

6.3.3 MTBE Oxidation

In 1991, Tuazon et al [90] first focused on the product investigation from the OH radical-initiated oxidation of MTBE under atmospheric (lower troposphere) conditions. They reported the major products are t-butyl formate (TBF), formaldehyde (CH_2O), methyl acetate ($\text{CH}_3\text{C}(=\text{O})\text{OCH}_3$), acetone ($\text{CH}_3\text{C}(=\text{O})\text{CH}_3$), acetaldehyde (CH_3CHO), peroxyacetyl nitrate ($\text{CH}_3\text{C}(=\text{O})\text{OONO}_2$, PAN) and NO_2 in the presence of NO_x , products were identified by on-line Fourier transform infrared absorption spectroscopy and/or on batch gas chromatography.

Smith et al [91] investigated the OH radical-initiated oxidation of MTBE, with methyl nitrite as the source of OH radical by a photolysis technique. They reported a product distribution consistent with Tuazon [90]. An overall value of $(2.99 \pm 0.12) \times 10^{-12} \text{ cm}^3\text{-molecule}^{-1}\text{s}^{-1}$ at 298 K for abstraction reaction between OH radical and MTBE with n-butane as a reference is reported.

Dunphy and Simmie's[92] reported on oxidation of MTBE conducted in reflected shock waves over a temperature range from 1024 to 1850 K and a pressure of 3.5 bar in an argon diluent. The reactant mixture composition varied widely, with equivalence ratios varying from 0.25 for a fuel-lean, 1.0 for a stoichiometric, to 2.5 for a fuel-rich mix. Measurements of the ignition delay times, characterized by chemiluminescence and pressure increase, led them to conclude that high temperature oxidation of MTBE is, in essence, that of methanol and iso-butene production for stoichiometric and fuel-rich mixtures, but is not for fuel-lean mixture. The probable reason is that the rate of oxidation of MTBE at high concentration of O₂ is much faster than the rate of MTBE via only reaction $C_3COC \rightarrow C_2C=C + CH_3OH$, and then the faster rate of oxidation of methanol + iso-butene.

Norton and Dryer [93] presented experimental results for flow reactor oxidation of MTBE at equivalence ratio 0.96, initial temperature of 1024 K and atmospheric pressure. Gas samples extracted at fifteen positions along the reactor duct centerline were quenched in the hot-water-cooled probe and stored at 343 K for subsequent gas chromatographic analysis. The purity of the MTBE was only 97%. The main products they observed are iso-butene and methanol. At 1024 K, 50% MTBE is converted in a time of about 5 msec, and 90% of conversion is achieved at about 40 msec. Iso-butene and methanol are generated at up to 75% and 40% of initial MTBE concentration, and decay slowly compared to the MTBE decomposition rate. At 1024 K and residence times to 100 msec, increased amounts of carbon monoxide, acetone, propyne and C₅ are produced with increased MTBE conversion. Methane and propene are observed at about 10% of MTBE initial concentration. Other observed, low concentration, products (less than 10% of

MTBE initial concentration) are C_2H_2 , C_2H_4 , C_2H_6 and CO_2 . Norton and Dryer describe the result of MTBE decay by the unimolecular elimination reaction only, which occurs through a four-center activated complex.

An experimental and kinetic modeling study on oxidation of MTBE was recently reported by Held, Dryer et al [94] again using the Princeton atmospheric pressure flow reactor (Δ PFR), the same apparatus as that used by Norton and Dryer [93], but at two temperatures of 1028 K and 1119 K, and at equivalence ratios near one. The concentrations of the hydrocarbon intermediates, plus CO and CO_2 were determined by gas chromatograph with SP-1000 and Porapak Q and R packed columns, FID and TCD detectors. They found significant quantities of acetone in the intermediates and again larger quantities of iso-butene than methanol. A detailed chemical mechanism was developed to describe their experimental results. They explained acetone production by considering the MTBE decomposition reactions other than four-center elimination: specially by cleavage of the methyl-ether C-O bond to form $(CH_3)_3O\cdot$ radical and then invoke this oxy radical's decomposition to form acetone. The non-unity ratio of iso-butene and methanol was accounted for by the abstraction reactions of methyl-ether hydrogen in MTBE to form $(CH_3)_3OCH_2\cdot$ radical followed by formaldehyde elimination from this radical to produce excess iso-butene without formation of methanol. This abstraction pathway accounts for approximately 10-15% of the fuel consumption for the low temperature conditions and 5-10% for the 1119 K experiment.

CHAPTER 7

EXPERIMENTAL STUDY ON MTBE PYROLYSIS AND OXIDATION

7.1 Experimental Conditions

Pyrolysis and oxidation of MTBE under high pressure conditions (4 to 10 atm) are conducted over the temperature range 798 to 1123 K at four equivalence ratios. The temperature range represents MTBE conversion from 0 to 100 percent in a 6 second time regime. The pressures are 4, 7 and 10 atm. Residence times range from 0.3 to 6 seconds and are limited by the required flow rate for ensuring needed amount of MTBE entering the reactor. Three reaction ratios for oxidation of MTBE represent fuel lean, stoichiometric and fuel rich. Pyrolysis of MTBE, the fourth, is carried out in the same way by varying temperature, pressure and residence time. The specific experimental conditions are listed in Appendix Table IIA. 1.

7.2 Experimental Apparatus

Reactions of MTBE in argon bath gas are carried out in a high pressure reactor which is a heavy wall (6 mm) quartz tube with 6 mm ID, housed in 75 cm length of three zone Chemshell 1.25" ID electric tube furnace equipped with three independent Omega Model CN-310 digital temperature controllers. A Neon Controls BPS 26G2501, 200 psi back pressure regulator is used to maintain the desired pressure within the reactor.

A diagram of the experimental apparatus is shown in Appendix Figure IIC. 1. Reactant MTBE is HPLC grade supplied by Fisher Co. Methane, argon and helium gases are reagent grade supplied by Liquid Carbonic Co. and filtered (activated carbon and

molecular sieve) of O₂, H₂O, and hydrocarbon impurities before entering the reactor system.

7.3 Flow Control and Measurement

The carrier gas (argon) is passed through 273 K saturator for feed of vapor MTBE. Sufficient contact time is achieved, by increasing the length of the saturation column, to insure saturation of MTBE in the Argon carrier. A second argon stream is used as additional make-up gas to control the desired mole fraction between reagents. Methane and oxygen were brought into the flow stream as required. The flow rate for each gas is controlled by Union Carbide LINDE Model FM-4550 mass flowmeter-flowcontroller with individual mass flow control module which is well calibrated before experiment. The calibration curves of mass flow controllers are in Appendix Figure IIC. 2 - Figure IIC. 4.

The reactants (feed mixture) are mixed in about 20 cm of the flow tube located upstream of the furnace and preheated to about 373 K to prevent condensation and to improve reactor temperature control. The reactants can either flow through the reactor or flow directly to a GC sampling valve via a bypass line. The bypass is used to determine the initial concentration of reactants without going through the high temperature reactor. All gas lines to the analytical equipment are held at 373 ± 10 °K to limit condensation. A fraction (5%) of the outlet gases from the reactor is passed to the analytical device through a Tee connector while the bulk of the effluent flows through a sodium bicarbonate (NaHCO₃) flask for neutralization before being released to the atmosphere via exhaust into a fume hood.

Gas samples are drawn through a separate sampling line by means of a mechanical vacuum pump, from the reacted flow to fume hood, with a constant flow rate of $45 \text{ cm}^3 \text{ min}^{-1}$. An HP-5890 Series II gas chromatograph with two flame ionization detectors (FID) is used on-line for analysis.

7.4 Temperature Control and Measurement

Temperature profiles are obtained at each flow using a shielded type K thermocouple probe moved axially within the 75 cm length reactor with a representative flow of inert. Thermocouple error caused by furnace wall radiation is minimized by using a sheath. The darkened outside surface of the quartz tube reactor also served as a second radiation shield. Heater control resulted in temperature profiles isothermal to within $\pm 5 \text{ K}$ over 80 - 85% of the furnace length for each temperature. Temperature gradients of 500 K in 5 cm at the inlet and outlet of the reactor occur. Uncertainty in absolute temperature measurements is estimated to be $\pm 1\%$ (i.e. $\pm 8\text{-}12 \text{ K}$) but relative temperatures are measured to within $\pm 5 \text{ K}$. The temperature profiles are shown in Appendix Figure IIC. 5 and Figure IIC. 6 with and without reactions present.

7.5 Qualitative and Quantitative Analysis

The reaction time was measured as: $t = V / F_{T,P} = \pi (D/2)^2 L_{\text{eff}} / F_{T,P}$, where V is the effective volume of reactor, $F_{T,P}$ is flow rate (cm^3 / sec) at reactor temperature and pressure, D is the diameter of reactor in cm, L_{eff} is effective length of the constant high temperature zone of the reactor in cm. L_{eff} is obtained from temperature profiles. $F_{T,P}$ is calculated from flow rate at room temperature and atmospheric pressure ($F_{298\text{K}, 1\text{atm}}$), which

is controlled by mass flowmeter. A small computer code was used to calculate the flow of each reagent for the desired residence times at each temperature and pressure.

An HP-5890 Series II gas chromatograph with two flame ionization detectors is used on-line to determine the concentrations of reactants and products. A ten-port VALCO gas sampling valve is employed to introduce the gas samples into the GC columns. Gas samples are passed through two sampling loops, 1.0 cm³ and 0.25 cm³, at a constant flow rate of 45 cm³ per minute, and then injected into a packed column and a capillary column, respectively.

Two columns, one packed and one capillary, are used to perform separations of the hydrocarbons, oxy-hydrocarbons and CO + CO₂. The 6' × 1/8" stainless steel column packed with 50% 80/100 Poropak T and 50% 80/100 Poropak Q is used for the separation of CO, CO₂ and light hydrocarbons. A catalytic converter containing 5% of 80/100 ruthenium on alumina catalyst with constant flow (about 24.4 cc / min) of H₂, connected in series after the packed column and held at about 300 C°, is used to convert the CO and CO₂ to methane after GC column separation therefore CO and CO₂ can be quantitatively analyzed by FID. A 90 m × 0.53 mm Hewlett Packard fused silica capillary column is used for heavier hydrocarbon and oxy-hydrocarbon separation. The chromatogram peaks are analyzed with two HP 3396A integrators. The carrier flow was about 24 cc / min for packed column and 9 cc / min for capillary column.

Calibration to obtaining appropriate molar response factors and retention times of relevant compounds is performed by injecting known concentrations of standard gases and known

quantities of liquid samples. The average retention times and relative response factors are shown in Appendix Tables IIA. 2.

Product identifications are also verified by HP 5899A GC/Mass Spectrometry, with a HP 90 m \times 0.53 mm fused silica capillary, on batch samples of reactor gas drawn from the reactor exit into evacuated 25 cm³ stainless steel sample cylinders for later analysis.

7.6 Experimental Results

7.6.1 MTBE Oxidation

7.6.1.1 Fuel Lean Environment

Experimental results of 0.5% MTBE pyrolysis and oxidation under three pressures and selected temperatures are presented in Appendix IIC Figure IIC. 7 to Figure IIC. 16.

Fuel lean P = 4 atm:

Figure IIC. 7 - Figure IIC. 10 present the results of oxidation of MTBE in the fuel lean ($\phi = 0.75$) environment, a pressure of 4 atm, and three temperatures of 823, 873 and 923 K.

70-80% of MTBE decays in about 1.0 second at 823 K. Significant amount of C₂C=C, CH₃OH ($1 - 6 \times 10^{-3}$ mole fraction), CH₂O, C₃H₆ ($1 - 2 \times 10^{-4}$ mole fraction), and some C₂C=O, and C=C(C)CHO ($1 - 5 \times 10^{-5}$ mole fraction), are produced. A steadily increasing amount of CO is observed, at low level (less than 2×10^{-4} mole fraction) with increased MTBE conversion. No CH₄ or CO₂ is observed at this temperature. When temperature increase to 873 K, over 80 % of the MTBE is converted to products with

similar product distribution in the same time scale of 0.6 - 1.2 sec. Both $C_2C=C$, and CH_3OH have a lower concentration level at 873 K than that at 823 K and reach a peak at 0.85 sec. The level of formaldehyde (CH_2O) appears constant (stable) in this temperature range of 823 to 873 K, while C_2H_4 , C_3H_6 , $C_2C=O$ and $C=C(C)CHO$ increase with time but show no change with time at 823 K. Results at 823 K and at 873 K suggest that the further oxidation of major products $C_2C=C$ and CH_3OH start as early as at 873 K in the fuel lean mixture (equivalence ratio = 0.75) and result in formation of products C_2H_4 , C_3H_6 , $C_2C=O$ and $C=C(C)CHO$ but not significant quantities of CH_2O . At 923 K, all intermediate products presented in the 823 and 873 K conditions are converted to final product CO_2 at about 0.6 second, the only detected product at this temperature is CO_2 .

Fuel lean $P = 7$ atm:

Figure IIC. 11 - Figure IIC. 13 present oxidation of MTBE, $\phi = 0.75$, at pressures of 7 atm and residence time to 4.0 sec. At about 1.0 sec, the conversion of MTBE is lower than 40% at 798 K, over 40% at 823 K and 100% at 873 K. Higher concentration of major products $C_2C=C$ and CH_3OH are produced when temperature increases from 798 to 823 at about 1.0 sec. None of $C_2C=C$ or CH_3OH , two major products are observed at 873 K, CO_2 is the only detected product. At 4 atm, the concentration of both $C_2C=C$ and CH_3OH start to decrease at 873 K (as at 4 atm) and they completely convert to final product at 923 K in less than 0.2 sec. The increased pressure is observed to speed oxidation of $C_2C=C$ and CH_3OH as well as the overall rate of MTBE decay to final product CO_2 . Increasing the pressure will lower the temperature for complete conversion of MTBE.

Fuel lean $P = 10$ atm:

Figure IIC. 14 - Figure IIC. 16 show the results at 10 atm. MTBE is completely converted to CO_2 at 823 K. Comparing results at 10 atm to those at 7 atm at 798 K (Figure IIC. 11) and residence time about 1.6 sec, the highest peak or concentration points of $\text{C}_2\text{C}=\text{C}$, CH_3OH , CH_2O and C_3H_6 are about 1.6 sec at 10 atm, and 2.6 sec at 7 atm; Increasing pressure speeds the overall reaction rate.

Higher level of $\text{C}_2\text{C}=\text{C}$ related to CH_3OH are produced from fuel lean mixtures as is observed in all pressures and temperatures. For these fuel lean conditions, at 4 atm, complete loss of MTBE occurs at 898 K, 0.65 sec, complete conversion of MTBE and major products occurs at 923 K, in less than 0.4 sec; at 7 atm, complete conversion of MTBE and major products occurs at 873 K and in less than 0.8 sec; at 10 atm, complete loss of MTBE occurs at 823 K, 1.60 sec, complete conversion of MTBE and major products occurs at 873 K and in less than 1.6 sec.

7.6.1.2 Stoichiometric Environment

Figure IIC. 17 - Figure IIC. 36 in Appendix IIC show MTBE oxidation results at stoichiometric environments and three pressures of 4 (residence time 0.4 to 1.2), 7 (residence time 0.8 to 3.4), and 10 atm (residence time 1.2 to 5.6 seconds).

Stoichiometric $P = 4$ atm:

Product distributions over temperature range from 823 to 1073 K at 4 atm are presented in Figure IIC. 17 to Figure IIC. 23. Conversion of MTBE at 0.7 sec is about 40% at 823 K, 70% at 873 K, and 100% at the temperatures of 923 K or above. When temperature increases from 823 to 873 K, the amount of major products $\text{C}_2\text{C}=\text{C}$ and CH_3OH increase

30% for 0.8 sec residence time. They reach a maximum concentration point at 0.85 sec at 873 K. At 823 K the concentration level of major products continue to increase with residence time and did not yet reach a maximum at 1.2 sec. CH_2O , C_3H_6 , $\text{C}_2\text{C}=\text{O}$ and $\text{C}=\text{C}(\text{C})\text{CHO}$ as well as C_2H_4 , C_2H_2 , and C_2H_6 all have higher concentration levels at 873 K than that at 823 K in the same residence time range. The concentration level of all these products increase with residence time and have not yet reached a maximum in observed time range. A faster increase of CO with time accompanies the MTBE conversion at 873 K.

A different product distribution is found when temperature is increased to 923 K from 873 K. We note the difference in Figure IIC. 20 to Figure IIC. 19. Higher concentrations of CO and much higher levels of CO_2 , and CH_4 along with much lower levels of major products are observed at 923 K. The second observation is that much more C_2H_4 (100 times at 0.55 sec) and more $\text{C}_2\text{C}=\text{O}$ (2 times at 0.5 sec), C_2H_2 (100 times at 0.5 - 0.6 sec), and C_2H_6 (100 times at 0.5 - 0.6 sec), are produced. $\text{C}_2\text{C}=\text{C}$ and CH_3OH are at much lower level (100 times at 0.6 sec), CH_2O levels remain similar at 873 K and 923 K. A third observation is that all product levels start to decrease with time at 923 K. The fourth observation is that $\text{C}_2\text{C}=\text{C}$ and CH_3OH are now approximately equal in level. Figure IIC. 21 (973 K) and Figure IIC. 23 (1073 K) show that at increased temperature, an increase of CO_2 level occurs with a continuous decrease in level of all products are observed at 973 K, and a complete conversion to CO_2 with some CO of all products at 1073 K is observed. An important change is the new ratio of $\text{C}_2\text{C}=\text{C}$ to CH_3OH at 973 K. The ratio of $\text{C}_2\text{C}=\text{C}$ to CH_3OH is larger than 1 below 923 K, almost equal to 1 at 923 K, and less than 1 at 973 K.

A summary for stoichiometric oxidation of MTBE at 4 atm, with reactant MTBE decay, major products $C_2C=C$ and CH_3OH produced first increase, then decrease with residence time, the levels of these two products increase from 0.4 to 1.2 sec, below 873 K, reach a maxima at 0.8 sec and start to decrease at 873 K, and undergoes rapidly decay above 873 K. complete conversion to CO_2 occurs at 1073 K in less than 0.5 sec.. Oxidation of the major products $C_2C=C$ and CH_3OH , lead to C_2H_4 , $C_2C=O$, C_2H_2 , C_2H_6 , this indicates that the oxidation of $C_2C=C$ and CH_3OH is one of the major sources responsible for these products.

Comparing fuel lean oxidation of MTBE at 4 atm and 0.7 to 1.0 sec, to stoichiometric oxidation, 70% of conversion of MTBE occurs at 823 K for fuel lean environment, only 40% at 823 K for stoichiometric; 70% conversion occurs at 873 K for stoichiometric. Complete conversion to CO_2 from MTBE occurs at 923 K (fuel lean) and 1073 K (stoichiometric) respectively. This indicates that increased O_2 (more fuel lean) increases the overall rate of MTBE decay. Higher concentrations of major products $C_2C=C$, and CH_3OH are observed in stoichiometric than that in fuel lean environment (Figure IIC. 8 and Figure IIC. 19). This indicates that high $[O_2]$ results in faster oxidation of major products. In both fuel lean and stoichiometric environments maximum concentration levels of $C_2C=C$ and CH_3OH occur at 873 K indicates that temperature (798 to 1073 K) does not affect the point on time frame for relative levels of the major product distribution, this is also seen from other product distributions.

Stoichiometric P = 7 atm:

Figure IIC. 24 -29 present the experimental results at the pressure of 7 atm and at 798 K, 823 K, 873K, 923 K, 1023 K and 1073 K respectively. Conversion of MTBE is about

40% at about 1.0 sec at 798 K, 50% at 823 K, almost 100% at 873 K (100% conversion does not occur until 923 K at 4 atm). The maximum concentration levels of $C_2C=C$, CH_3OH and CH_2O (7 atm, $\phi = 1$) are located at 823 K, and at 873 K for 4 atm in both fuel lean and stoichiometric environments). Maxima of $C_2C=O$, C_3H_6 , C_2H_4 are at 873 K in this 7 atm case. Figure IIC. 26 shows that $C_2C=C$ is lower than CH_3OH at this 873 K temperature. This reverse of the ratio of $C_2C=C$ to CH_3OH at 4 atm occurs at 973 K. Complete oxidation of CH_3OH at 7 atm occurs at 1073 K in less than 0.8 sec (Figure IIC. 29).

Stoichiometric P = 10 atm:

Results at 10 atm are shown Figure IIC. 30 to Figure IIC. 36. Similar product distributions are observed to data at 4 and 7 atm, with maximum levels of products observed at lower temperature at 798 K.

One difference between the data at 7 atm versus 10 atm in this stoichiometric environment is that small HC's such as CH_4 , C_2H_4 , C_2H_6 , C_2H_2 appear more stable at higher temperatures and pressures.

7.6.1.3 Fuel Rich Environment

Reducing the O_2 level in the reactant fuel mixtures decreases reactant decay and different trends of product distribution occur as shown in Figure IIC. 37 - 61.

At 4 atm and about 1.0 sec, MTBE conversion is near 50% at 823 K, 85% at 873 K, and complete at 898 K in 0.7 sec. At 823 K (Figure IIC. 37), observed products are $C_2C=C$, CH_3OH and CH_2O , C_3H_6 with $C_2C=C$ and CH_3OH at higher levels than CH_2O , C_3H_6 (50 - 100 times at 0.6 sec). At 873 K Figure IIC. 39, $C_2C=C$ and CH_3OH reach a maxima at

0.75 sec and start to decrease with residence time. CH_2O , C_3H_6 , $\text{C}_2\text{C}=\text{O}$ and $\text{C}=\text{CC}(\text{C})\text{CHO}$ as well as C_2H_4 increase with time in 0.5 - 1.2 sec but C_2H_4 is 100 times lower than CH_2O . At 923 K (Figure IIC. 41, CO is high with little CO_2 and CH_4 observed. All other product levels start to decrease with increased residence time (0.5 - 1.2 sec) except C_2H_4 remains at the same level. The ratio of $\text{C}_2\text{C}=\text{O}$ to CH_3OH becomes less than 1 at 973 K. Continuing increase of temperature to 1048 K from 998 K. CO increases about 10%, CO_2 increase by 50%, and CH_4 remain unchanged in 0.5 - 1.2 sec. No $\text{C}_2\text{C}=\text{C}$ was observed at 1048 K, 0.5 - 1.2 sec, CH_3OH is much lower in concentration (mole fraction less than 3×10^{-6}), the major product in addition to CO, CH_4 and CO_2 now is C_2H_4 and C_2H_2 , C_2H_6 , CH_2O are at higher concentration levels than CH_3OH and C_3H_6 (ca 10 times). $\text{C}_2\text{C}=\text{C}$ and $\text{C}_2\text{C}=\text{O}$ as well as $\text{C}=\text{C}(\text{C})\text{CHO}$ are not observed at this 1048 K, 4 atm and fuel rich environment.

Affects of pressure increase to 7 atm and 10 atm, at 1.0 sec, MTBE conversion is about 10% at 798 K and quickly goes to 100% at 823 K at 7 atm; 20% at 798 K and 100% at 823 K at 10 atm. Figure IIC. 44 - 61 show that CO increases quickly with residence time and temperature, and reaches a maxima at 898 K (mole fraction 0.021) at both 7 atm and 10 atm while the maximum concentration level of CO at 4 atm is observed at 1048 K (mole fraction 0.017). A larger overall rate is shown under the higher pressure conditions, which is similar to that in other two oxidation environments ($\phi = 0.75, 1.0$). The reverse of the ratio of $\text{C}_2\text{C}=\text{C}$ to CH_3OH , from, greater than 1, to, less than 1, occurs with increase temperatures, 973 K at 7 atm; 998 K at 10 atm.

Comparing to other two oxidation environments ($\phi = 0.75, 1.0$) which have higher $[O_2]$ in the reactant fuel mixtures, the obvious change is that the levels of CO_2 increase with $[O_2]$ as shown as following data (in mole fractions):

	4 atm (0.4 - 1.2 sec)	7 atm (0.8 - 3.4 sec)	10 atm (1.2 - 5.6 sec)
$\phi = 1.5$	0.0025 at $T = 1048$ K	0.003 at $T = 1048$ K	0.003 at $T = 1048$ K
$\phi = 1.0$	0.02 at $T = 1023$ K	0.01 at $T = 923$ K	0.01 at $T = 873$ K
$\phi = 0.75$	> 0.025 at $T = 923$ K	> 0.025 at $T = 873$ K	> 0.025 at $T = 823$ K

CO and CH_4 show higher concentrations than in fuel lean and stoichiometric environments. C_2H_4 , C_2H_2 , and C_2H_6 become dominant products under the higher pressures and fuel rich environment. Major products $C_2C=C$ and CH_3OH further react faster when O_2 is present. This affects the concentration levels of both $C_2C=C$ and CH_3OH in relative higher temperatures ($\phi = 0.75$: > 873 K at 4 atm; > 798 K at both 7 atm and 10 atm. $\phi = 1.0$: > 873 K at 4 atm; > 798 K at both 7 atm and 10 atm. $\phi = 1.5$: > 873 K at 4 atm; > 823 K at 7 atm and > 798 K at 10 atm). The ratio of $C_2C=C$ to CH_3OH also changes with decreased temperature, pressure and oxygen level in fuel mixture. Pressure change affects the overall rate and product distribution, but not temperature dependence of the relative product ratio.

7.6.2 MTBE Pyrolysis

Experimental results on MTBE pyrolysis over temperature range from 823 to 1123 K at 4 atm, 7 atm, and 10 atm are presented. The distribution of major and important products profiles is illustrated in Appendix Figure IIC. 62 - 85.. These figures show that under the experimental conditions of pyrolysis: (1) $C_2C=C$ and CH_3OH are unique major products up to temperature at 1123 (4 atm), 1048 K (7 atm), 998 K (10 atm); (2) CH_4 is a much

more important product than CO and CO₂ and is at a high concentration level at high temperatures; and (3) Differences between C₂C=C and CH₃OH are smaller compared to those in the three oxidation environments; and (4) less CH₂O, C₂C=O and C=C(C)CHO are observed from pyrolysis, which indicates that much of these carbonyl species are from oxidation paths of reactant and major products.

7.6.2.1 At the Pressure of 4 Atm, Pyrolysis

Figure IIC. 62 -69 present the pyrolysis results of MTBE at 4 atm over temperature of 823 K to 1123 K. At 1.0 sec, MTBE decay is about 30% at 823 K, 55% at 873 K, 80% at 923 K and complete loss at 973 K in 0.9 sec. At 823 K, C₂C=C and CH₃OH are major products with only two minor products CH₂O and C₃H₆ at very low concentration (1000 times lower). At 873 K, the MTBE conversion is higher and C₂C=C and CH₃OH increase 15% in 0.5 - 1.1 sec, mole fraction of CH₂O increases to 9×10^{-6} at 873 K from 3×10^{-6} at 823 K at 0.8 sec, mole fraction of C₃H₆ increases to 3×10^{-6} at 873 K from 5×10^{-7} at 823 K at 0.8 sec, and C₂C=O is observed at $1 - 2 \times 10^{-6}$ (mole fraction, in 0.5 - 1.0 sec) as the third minor. When temperature continues to increase to 923 K, the levels of three minor products C₂C=O, CH₂O and C₃H₆ increase by about 8 - 12 times in 0.5 - 1.0 sec, while major products C₂C=C and CH₃OH increase by only 5%. C₂C=O increases faster than all others and CH₂O increases slower than C₂C=O and C₃H₆, which may due to the greater stability of C₂C=O than CH₂O at higher temperatures. At 973 K, all products continue to increase with four more products CH₄, C₂H₄, C₂H₆ and C₂H₂ observed in very low concentration levels. The latter three are new members in minor products group and there is a large difference between the higher levels of C₂C=O, C₃H₆, CH₂O and lower

levels of these new species (C_2H_4 , C_2H_6 , C_2H_2). At 1023 K, CH_4 has a higher concentration level (0.004 - 0.009 in mole fraction in 0.4 - 1.0 sec) and all other products remain almost the same level as that at 973 K except C_3H_6 , C_2H_4 , C_2H_6 and C_2H_2 increases by 2 - 5 times in 10 sec. Increasing the temperature to 1048 K from 1023 K, $C_2C=C$ (0.0014 mole fraction) and CH_3OH (0.00117 mole fraction) remain unchanged in 0.5 - 1.1 sec. Changes are observed in minor product distribution, CH_4 has significant increase (mole fraction is 0.0016 at 1048 K and 0.0008 at 1023 K, at 0.8 sec) and start to compete with $C_2C=C$ and CH_3OH . Little difference is now observed between the other members of the minor products group, C_3H_6 has the highest level and C_2H_4 , C_2H_6 , C_2H_2 increase by about 0.5 - 1.5 time in 0.5 sec. At 1073 K, CH_4 continues to increase and is similar to $C_2C=C$ and CH_3O , which start to decrease with the residence time (0.5 - 1.0 sec.), $C_2C=O$ decreases with the time and CH_2O reaches a maxima at 0.7 sec then start to decrease with the time. Further increasing temperature to 1123 K, show all products except $C_2C=O$ and $C=C(C)CHO$ are competing (similar in concentration) with CH_4 , all products decrease with the residence time (0.5 - 1.1 sec).

7.6.2.2 At the Pressure of 7 Atm, Pyrolysis

Experimental results at 7 atm are presented in Appendix Figure IIC. 70 - 77. Conversion of MTBE, at 1 sec, is about 25% at 873 K, 75% at 923 K, 100% at 973 K. Major products are $C_2C=C$ and CH_3OH , and minor products are C_3H_6 , $C_2C=O$ and CH_2O at 873 K. C_2H_4 is observed at 923 K in very low concentration (1.1×10^{-6} mole fraction). CH_4 , C_2H_2 and C_2H_6 are observed at 973 K. All products increase with the increasing temperature (873 K to 923 K to 973 K), $C_2C=O$ and C_3H_6 increase faster than the others.

At 998 K and 1023 K (Figure IIC. 73 - 74), major products $C_2C=C$, CH_3OH and two minor products $C_2C=O$, CH_2O decrease with residence time (0.6 - 3.0 sec), while small HC's CH_4 , C_2H_4 and C_3H_6 still increase with residence time. When temperature increases to 1048 K (Figure IIC. 75), CH_4 start to compete with major products and rapidly increase with the residence time (0.6 - 3.0 sec), CO is observed to increase with time. At 1123 K, experiment show that CH_4 decrease and CO increase with residence time (0.6 - 3.0 sec); $C_2C=C$ rapidly decreases with residence time; CH_3OH , C_3H_6 decrease with residence time and their concentration are higher than that of $C_2C=C$. C_2H_4 does not change with the time.

7.6.2.3 At the Pressure of 10 Atm, Pyrolysis

Figure IIC. 78 - 85 are experimental results at 10 atm under the conditions of pyrolysis. MTBE conversion at 1.0 sec, is about 20% at 873 K, 60% at 923 K, 100% at 973 K. The product distribution profiles observed at 10 atm are very similar to that at 7 atm with faster overall reaction rate.

Comparison of pyrolysis results at the three pressures, at the same temperature, we can see that with the higher pressure, MTBE decay becomes slower (not much); products have a little bit higher concentrations (in the unit of mole fraction); overall reaction rates are faster. Pressure change does not affect product distribution profiles nearly as much as in case of oxidation but does affect concentration levels a little.

7.6.3 Temperature and Pressure Dependence of Product Distributions

Temperature and pressure dependence of important product decay are showed in Appendix Figure IIC. 86 - 124. The discussion above has illustrated temperature and pressure dependence of important product profiles. Increasing temperature always change product distribution profiles. This change becomes more complicated in oxidation environments and is smoother in pyrolysis case. Temperatures always bring faster decay of reactant MTBE, and speeds oxidation of products when O_2 is present. Pressure seems to shift product distribution profiles versus residence time but does not change temperature dependence of product distribution profiles. In the pyrolysis environment, pressure has less effect on overall reaction than that in oxidation environments.

MTBE decay in the presence of O_2 becomes faster at about 873 K and is complete at 923 K in fuel lean environment. The more O_2 , the shorter time needed for MTBE complete oxidation in three pressures. The pyrolysis of MTBE shows very similar temperature decay curves at three pressures. Not like oxidation in which case there seems be a certain temperature point at which oxidation becomes very rapid. Pyrolysis shows a smooth change with temperature.

7.6.4 Conclusion

Experimental data were collected at 4, 7, 10 atm, temperatures of 798 K to 1123 K, and 0.4 sec to 1.2 sec (4 atm), to 3.8 sec (7 atm), to 5.6 sec (10 atm). The major products from both oxidation and pyrolysis of MTBE are iso-butene and methanol, with acetone and formaldehyde as important minor species at relative low temperatures. Small hydrocarbons, C_3H_6 , C_2H_4 , CH_4 , are present along with $C_2C=C$ and CH_3OH or dominate

at low $[O_2]$ and high temperature conditions. CO_2 is produced with more O_2 in reactant fuel mixture and there is no CO_2 observed in pyrolysis environment. Little CH_4 is produced in fuel lean environment and high levels (0.008 in mole fraction) are observed in pyrolysis environment. CO is observed in all environments and its concentration level is dependent on $[O_2]$ and temperatures. Important secondary products are $C_2C=O$, CH_2O , CH_4 , C_2H_4 , C_3H_6 , C_2CyCOC , $C=C(C)CHO$, $C_2C=C=O$, $C=C(C)COH$, C_2CCOH , CO and CO_2 . More iso-butene than methanol is produced under the conditions of high O_2 levels and relative lower temperatures, the ratio of $C_2C=C$ to CH_3OH changes from, greater than 1, to near 1, to less than 1 with increased temperature. The difference between the amount of this two major products becomes small in pyrolysis environment compared to oxidation. Experimental data also show MTBE decay is much faster as expected in high O_2 concentration (more fuel lean) mixtures than pyrolysis environments and product distributions are more complex in oxidation than pyrolysis. Formaldehyde and iso-butene are more dominant in the low temperatures in the pyrolysis situation. MTBE conversion increases with increased temperature at constant pressure and stoichiometry; increases with decreased stoichiometry (more fuel lean) at constant temperature and pressure; increases with increased pressure at constant temperature and stoichiometry.

CHAPTER 8

MODELLING STUDY ON MTBE PYROLYSIS AND OXIDATION

8.1 Overview

What is the reaction mechanism and product distribution of MTBE decay under the real or near typically combustion conditions and how the pressures affect the mechanism become a valuable research topic after many experiments conducted by several research groups. Only a few research groups provide kinetic information for this system as we discussed in chapter 6. One of the goal of this study is to build a detailed, pressure and temperature dependent, kinetic mechanism for MTBE pyrolysis and oxidation. Specific emphasis has been placed on understanding and properly treat using the pressure dependent reactions and identifying important reactions and key species in the high temperature chemistry so the model can be applied to both atmospheric and internal engine oxidation / combustion.

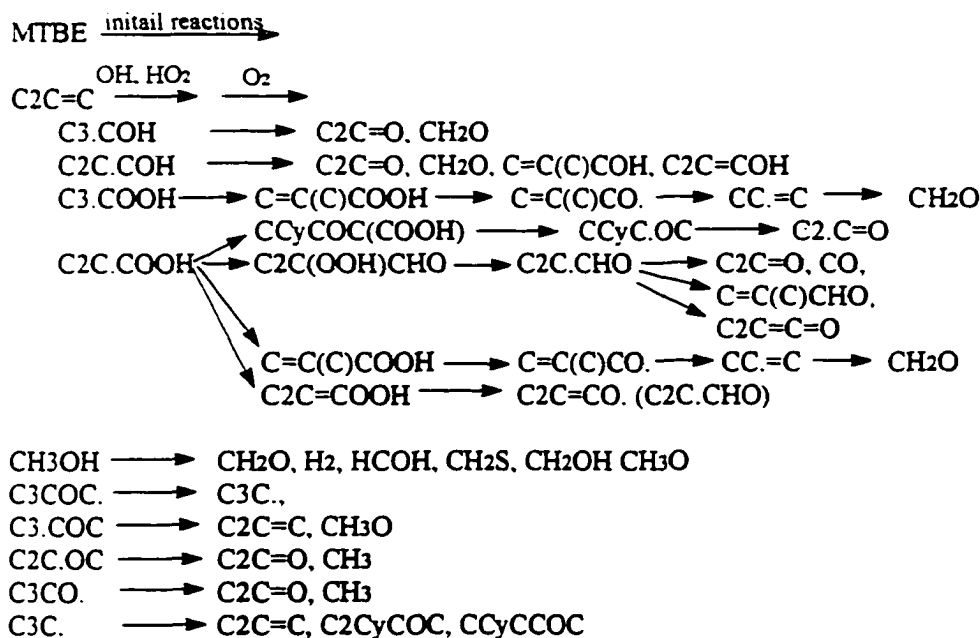
In this study, we consider the dissociation and abstraction by O_2 as the initial reactions of MTBE oxidation. Specific abstraction reactions between MTBE and OH, H, O, HO_2 , CH_3 are also considered in the initial reaction part.

MTBE decomposes at lower temperatures, up to 1000 K, primarily by molecular elimination reaction, to products iso-butene + methanol. Iso-butene has six allylic type carbon - hydrogen bonds, bond energy ca $88 \text{ kcal}\cdot\text{mol}^{-1}$, which are readily attacked by primary, secondary, and tertiary alkyl radicals as well as by H, O, OH radicals, all of which have stronger C---H bond energies, so the abstraction reactions are exothermic.



The weak C---H bonds in iso-butene serves to capture the more active radicals, noted above, and produce the relatively non-reactive allylic iso-butenyl radicals. Reactions of allylic like radicals with O₂, for example, form an adduct which has a very shallow well, only 18.5 kcal-mol⁻¹, and the dominant adduct reaction is reverse to the allylic radical and O₂.

The initial radicals from MTBE dissociation reactions are C3C., C3CO., C3COC., C3.COC, and C2C.OC, which all have further reactions to stable products or other radicals. The important product formation pathways are illustrated as follows.



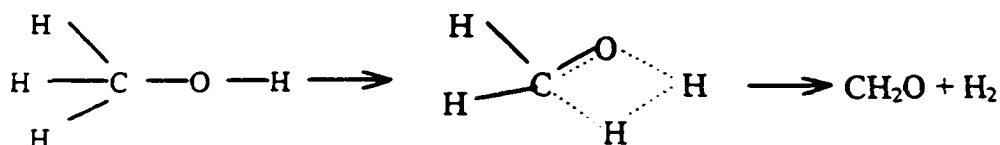
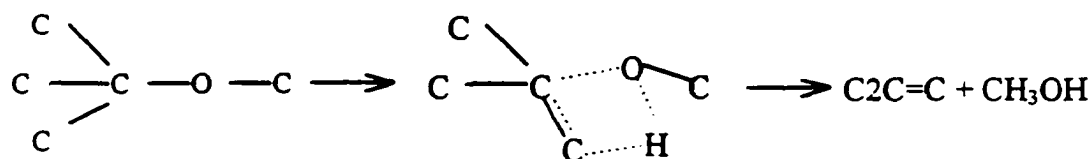
8.2 Methods for Kinetic Modeling Study

Thermodynamic parameters ΔH_{298} , S_{298} and $C_p(300)$ to $C_p(\text{infinity})$ for all species involved in the modeling mechanism are listed in Table IIA 1. The calculation methods and rules obtaining these thermodynamic properties are described in chapter 1. The principle of

obtaining and/or estimations of input parameters for QRRK calculations are also described in chapter 2. One extra ordinary feature here, however, is that QRRK calculations with beta collision for fall off incorporate not only temperature but also pressure dependence (0.001 to 100 atm, 200 to 2500 K) into rate constant expressions by employing Chebyshev polynomials (7×3). A modified Chemkin Interpreter is used to incorporate the combined pressure and temperature dependent rate expression into the Senkin or Chemkin integrators [83].

8.3 Important Transition States

The semi-empirical calculation method MOPAC PM3 is used to find the transition states thus rate constants (A factor) for many important reactions including isomerization reaction, elimination reactions and β -scission reactions in this modeling study. Most of transition state structures and their thermodynamic properties are directly taken from reference [95] or calculated by Bozzelli's research group in NJIT. Transition states for MTBE dissociation to $C_2C=C + CH_3OH$ and CH_3OH to $CH_2O + H_2$ are calculated in this study and listed in Appendix IIB along with the information for the transition states related to MTBE, $C_2C=C$ and CH_3OH reaction.



The transition states for MTBE and CH₃OH dissociation will be discussed in the following section. The transition states for the important C₂C=C related reactions are listed in here and detailed in Appendix IIB.

	<u>ID</u>	<u>Reactions</u>
TS 1	TC2C*JCXH	C ₃ C. → C ₂ C=C + H
TS 2	TC2YCQC	C ₃ COO. → C ₃ .COOH
TS 3	TC2YCXQC*	C ₃ COO. → C ₂ C=C + HO ₂
TS 4	TC3*CXQ	C ₃ .COOH → C=C(C)OOH + CH ₃
TS 5	TC2YC2OXP	C ₃ .COOH → C ₂ CyCOC + OH
TS 6	TC2CJ*CXQ	C ₂ C=C + HO ₂ → C ₂ C.COOH
TS 7	TC2YCCOXP	C ₂ C.COOH → C ₂ CyCOC + OH
TS 8	TC2YCCQ	C ₂ C.COOH → C ₂ CCOO.
TS 9	TC2YC*CXQ	C ₂ CCOO. → C ₂ C=C + HO ₂
TS 10	TCYCCQC	C ₂ CCOO. → C ₂ .CCOOH
TS 11	TC2YCCQO	C ₂ C(OH)COO. → C ₂ C(O.)COOH
TS 12	TICPYCCQC	C ₂ C(OH)COO. → C ₂ .C(OH)COOH
TS 13	TC2CPYCQ	C ₂ C(OH)COO. → C ₂ C(OH)C.OOH
TS 14	TICCQYCPC	C ₂ C(O.)COOH → C ₂ .C(OH)COOH
TS 15	TC2YCPCIQ	C ₂ C(O.)COOH → C ₂ C(OH)C.OOH
TS 16	TICPYC3OXP	C ₂ .C(OH)COOH → CCyC3O(OH) + OH
TS 17	TC2YCQOC	C ₂ C(OO.)COH → C ₂ C(OOH)CO.
TS 18	TICCPYCQC	C ₂ C(OO.)COH → C ₂ .C(OOH)COH
TS 19	TC2YCQCIP	C ₂ C(OO.)COH → C ₂ C(OOH)C.OH
TS 20	TICCQYCQC	C ₂ C(OO.)COOH → C ₂ .C(OOH)COOH
TS 21	TC2YCQOOC	C ₂ C(OO.)COOH → C ₂ C(OOH)COO.
TS 22	TC2YCQCIQ	C ₂ C(OO.)COOH → C ₂ C(OOH)C.OOH
TS 23	TICQYCCQC	C ₂ C(OOH)COO. → C ₂ .C(OOH)COOH
TS 24	TC2*CYCQ	C=C(C)COO. → C=C(C)C.OOH
TS 25	TC*YCCQC	C=C(C)COO. → C=C(C.)COOH
TS 26	TC2*YCOOC	C=C(C)COO. → C ₂ .CyCOOC
TS 27	TCYC*COOC	C=C(C)COO. → CCyC.COOC
TS 28	TC*YC3OXP	C=C(C.)COOH → C=CyCCOC + OH

The first 10 transition states are related to C₃C. dissociation, C₃C. + O₂, C₂C=C + HO₂, the next 9 transition states are for (C₂C=C)-OH + O₂ and the following 4 are for (C₂C=C)-OOH + O₂ sub system. The last 5 transition states are related to C₂.C=C + O₂

sub system. These are important reactions for the further oxidation of $C_2C=C$ to secondary products and will be described in the following sections.

Thermodynamic properties of transition states are listed in Appendix IIB. 1. The transition state structures and corresponding internal atom bond lengths are showed in Appendix IIB. 2-4 along with frequencies, moment of inertia for transition states of MTBE and CH_3OH dissociation in IIB. 2, IIB. 4 respectively, and important thermodynamic reaction analysis information for $C_2C=C$ related reactions in IIB. 3. The values of A and n from thermodynamic analysis have been used as high pressure limit input parameters for each corresponding reactions above. While the E_a are still estimated using the methods described in chapter 2 with ΔH or ΔU from thermodynamic reaction analysis (performed by using computer program THERMRXN) which be also shown in IIB. 3.

8.4 Quantum RRK Analysis of Important Pathways

QRRK analysis are performed for all chemical activation and unimolecular dissociation pathways in MTBE system. The QRRK input parameters and reference sources are listed in Appendix IID. 1-86 along with potential energy level diagrams. The most important pathways, abstraction and unimolecular dissociation of MTBE, oxidation of iso-butene, and dissociation of methanol, are described below.

8.4.1 Abstraction and Dissociation Reactions of MTBE

8.4.1.1 Abstraction Reaction of MTBE

In the $MTBE + O_2 + Ar$ atmosphere, the initial reactions are H abstraction of MBTE by O_2 as well as O, H, OH, and HO_2 radicals or atoms, or thermal dissociation reactions at

relatively high temperatures ($> 900\text{ K}$) There are two types of hydrogen on MTBE, the methyl-ether group H, C3COC--H , and tert-butyl-ether group H, H--C3COC . The C-H bond (or $\text{CH}_2 - \text{H}$ bond) strengths of the methyl-ether group on MTBE are approximately $97.5\text{ kcal}\cdot\text{mol}^{-1}$, which is similar to a tertiary C-H bond ($96.3\text{ kcal}\cdot\text{mol}^{-1}$), thus it can be easily abstracted by a number of other radicals. The C-H bond strengths of the tert-butyl-ether group on MTBE is about the same as a C-H bond on neo-C5 ($101.1\text{ kcal}\cdot\text{mol}^{-1}$). Two types of hydrogen on MTBE can be abstracted by atoms, radicals and molecular O_2 :

	<u>Reactions</u>	<u>$k\text{ (cm}^3\text{ mol}^{-1}\text{ s}^{-1}\text{)}$</u>
R 8-1	$\text{C3COC} + \text{O} \rightarrow \text{C3COC.} + \text{OH}$	$5.351 \times 10^{12} T^0 \exp(-3.031\text{ kcal}\cdot\text{mol}^{-1}/RT)$
R 8-2	$\text{C3COC} + \text{O} \rightarrow \text{C3.COC} + \text{OH}$	$1.53 \times 10^9 T^{1.5} \exp(-5.305\text{ kcal}\cdot\text{mol}^{-1}/RT)$
R 8-3	$\text{C3COC} + \text{H} \rightarrow \text{C3COC.} + \text{OH}$	$7.2 \times 10^8 T^{1.5} \exp(-4.3515\text{ kcal}\cdot\text{mol}^{-1}/RT)$
R 8-4	$\text{C3COC} + \text{H} \rightarrow \text{C3.COC} + \text{OH}$	$2.16 \times 10^9 T^{1.5} \exp(-6.997\text{ kcal}\cdot\text{mol}^{-1}/RT)$
R 8-5	$\text{C3COC} + \text{OH} \rightarrow \text{C3COC.} + \text{H}_2\text{O}$	$6.27 \times 10^9 T^0 \exp(-0.739\text{ kcal}\cdot\text{mol}^{-1}/RT)$
R 8-6	$\text{C3COC} + \text{OH} \rightarrow \text{C3.COC} + \text{H}_2\text{O}$	$1.08 \times 10^7 T^{2.0} \exp(-0.525\text{ kcal}\cdot\text{mol}^{-1}/RT)$
R 8-7	$\text{C3COC} + \text{HO}_2 \rightarrow \text{C3COC.} + \text{H}_2\text{O}_2$	$9.64 \times 10^{10} T^0 \exp(-14.536\text{ kcal}\cdot\text{mol}^{-1}/RT)$
R 8-8	$\text{C3COC} + \text{HO}_2 \rightarrow \text{C3.COC} + \text{H}_2\text{O}_2$	$3.01 \times 10^4 T^{2.55} \exp(-15.5\text{ kcal}\cdot\text{mol}^{-1}/RT)$
R 8-9	$\text{C3COC} + \text{CH}_3 \rightarrow \text{C3COC.} + \text{CH}_4$	$1.31 \times 10^0 T^{4.0} \exp(-11.567\text{ kcal}\cdot\text{mol}^{-1}/RT)$
R 8-10	$\text{C3COC} + \text{CH}_3 \rightarrow \text{C3.COC} + \text{CH}_4$	$1.36 \times 10^0 T^{3.65} \exp(-7.154\text{ kcal}\cdot\text{mol}^{-1}/RT) \text{ cm}^3\text{ mol}^{-1}\text{ s}^{-1}$
R 8-11	$\text{C3COC} + \text{CH}_3\text{O} \rightarrow \text{C3COC.} + \text{CH}_3\text{OH}$	$3.01 \times 10^{11} T^0 \exp(-5.266\text{ kcal}\cdot\text{mol}^{-1}/RT)$
R 8-12	$\text{C3COC} + \text{CH}_3\text{O} \rightarrow \text{C3.COC} + \text{CH}_3\text{OH}$	$9.03 \times 10^{11} T^0 \exp(-7.866\text{ kcal}\cdot\text{mol}^{-1}/RT)$
R 8-13	$\text{C3COC} + \text{O}_2 \rightarrow \text{C3COC.} + \text{HO}_2$	$2.05 \times 10^{13} T^0 \exp(-38.392\text{ kcal}\cdot\text{mol}^{-1}/RT)$
R 8-14	$\text{C3COC} + \text{O}_2 \rightarrow \text{C3.COC} + \text{HO}_2$	$4.04 \times 10^{13} T^0 \exp(-39.432\text{ kcal}\cdot\text{mol}^{-1}/RT)$

We use Dean and Bozzelli's method described in chapter 2 to calculate a rate of $1.53 \times 10^9 T^{1.5} \exp(-5.305 \text{ kcal}\cdot\text{mol}^{-1}/RT) \text{ cm}^3 \text{ mol}^{-1} \text{ s}^{-1}$ for reaction (R 8-2). The NIST fitted value of $5.351 \times 10^{12} T^0 \exp(-3.031 \text{ kcal}\cdot\text{mol}^{-1}/RT) \text{ cm}^3 \text{ mol}^{-1} \text{ s}^{-1}$ for reaction $\text{COC} + \text{O} \rightarrow \text{COC} + \text{OH}$ is used for the rate of reaction (R 8-1).

The rates for reaction (R 8-3,4,6,10) are calculated using Dean and Bozzelli's method described in chapter 2. The rate of reaction (R 8-5) is taken directly to be that of $\text{COC} + \text{OH} \rightarrow \text{prod}$ (86 ATK). The A factor of reaction (R 8-7) is taken to be that of $\text{CH}_3\text{OH} + \text{HO}_2 \rightarrow \text{CH}_2\text{OH} + \text{H}_2\text{O}_2$ (87 TSA), and E_a is taken as the average of the E_a of above reaction ($E_a = 12.579 \text{ kcal mol}^{-1}$) and the reaction $\text{CCC} + \text{HO}_2 \rightarrow \text{CCC} + \text{H}_2\text{O}_2$ ($E_a = 16.494 \text{ kcal mol}^{-1}$, 88 TSA). The rate constant of reaction (R 8-8) is taken to be that of $\text{C3C} + \text{HO}_2 \rightarrow \text{C3.C} + \text{H}_2\text{O}_2$ (90 TSA).

CH_3 radical plays an important role in the MTBE decay, especially in the pyrolysis case. The fitted value from NIST for $\text{COC} + \text{CH}_3 \rightarrow \text{COC} + \text{CH}_4$ and the calculation value from Dean and Bozzelli's method were used for reaction 9 (R 8-9) and 10 (R 8-10) respectively. The current values of rates used for these two reactions are directly taken from 90 ZHA/BAC of NIST (National Institute of Standard Technology Database) for reaction 9 (R 8-9) and 90 TSA for $\text{C3C} + \text{CH}_3 \rightarrow \text{C3.C} + \text{CH}_4$ respectively. The lower rates of NIST give better modeling results to fit experimental data.

The A factor for reaction 11 (R 8-11) is taken that of $\text{CH}_3\text{OH} + \text{CH}_3\text{O} \rightarrow \text{CH}_2\text{OH} + \text{CH}_3\text{OH}$ (87 TSA), and E_a is taken as the average of the E_a of above reaction ($E_a = 4.074 \text{ kcal mol}^{-1}$) and the reaction $\text{CCC} + \text{CH}_3\text{O} \rightarrow \text{CCC} + \text{CH}_3\text{OH}$ ($E_a = 6.458 \text{ kcal mol}^{-1}$, 88 TSA). Taking reaction 11 (R 8-11) as a reference, we use Dean and Bozzelli's method to

calculate the rate constant of reaction 12 (R 8-12) as $k = n_H A^n \exp(-[E_{\text{ref}} - f(\Delta H_{\text{ref}} - \Delta H)] / RT \text{ cm}^3 \text{ mol}^{-1} \text{ s}^{-1}$. The number of abstractable hydrogen $n_H = 9$, A is from reference reaction ($A/(\text{per H}) = A_{(\text{R 8-21})} / 3 = 3.01 \times 10^{11} / 3 = 1.003 \times 10^{11}$), and $E_a = 5.266 - 0.65 [-7.56 - (-3.5)] = 7.866 \text{ kcal mol}^{-1}$. The f is taken as that of CH_3 radical.

The abstraction reactions between MTBE and O_2 are initial reaction and very important in the oxidation of MTBE system. Two sets of rate values for reaction 13 (R 8-13) and reaction 14 (R 8-14) are tested in this study. A literature data of $4.04 \times 10^{13} T^0 \exp(-50.932 \text{ kcal-mol}^{-1} / RT) \text{ cm}^3 \text{ mol}^{-1} \text{ s}^{-1}$ (90 TSA for $\text{C}_3\text{C} + \text{O}_2 \rightarrow \text{C}_3\text{C} + \text{HO}_2$) for reaction 13 (R 8-13), and an evaluated rate constant of $2.05 \times 10^{13} T^0 \exp(-47.892 \text{ kcal-mol}^{-1} / RT) \text{ cm}^3 \text{ mol}^{-1} \text{ s}^{-1}$ for reaction 14 (R 8-14), (based on two reference reaction: $\text{CCC} + \text{O}_2 \rightarrow \text{CCC} + \text{HO}_2$, $3.97 \times 10^{13} T^0 \exp(-50.872 \text{ kcal-mol}^{-1} / RT) \text{ cm}^3 \text{ mol}^{-1} \text{ s}^{-1}$, 88 TSA; $\text{CH}_3\text{OH} + \text{O}_2 \rightarrow \text{CH}_2\text{OH} + \text{HO}_2$, $2.05 \times 10^{13} T^0 \exp(-44.911 \text{ kcal-mol}^{-1} / RT) \text{ cm}^3 \text{ mol}^{-1} \text{ s}^{-1}$, 87 TSA), are tested and modeling results suggest the higher values should be used for these two reactions. The alternative E_a 's, $38.392 \text{ kcal-mol}^{-1}$ for reaction 13 (R 8-13) and $39.432 \text{ kcal-mol}^{-1}$ for reaction 14 (R 8-14), are estimated based on the recent evaluated activation energies: $38.56 \text{ kcal-mol}^{-1}$ for reaction $\text{C}_2\text{C}=\text{C} + \text{O}_2 \rightarrow \text{C}_2\text{C}=\text{C} + \text{HO}_2$, and $39.11 \text{ kcal-mol}^{-1}$ for reaction $\text{CC}=\text{C} + \text{O}_2 \rightarrow \text{C.C}=\text{C} + \text{HO}_2$, by Walker research group, which lead to faster reaction than corresponding NIST evaluation. This set of rate constant gives reasonable modeling results.

8.4.1.2 Unimolecular Dissociation of MTBE

The Unimolecular decomposition reactions of MTBE are initial reactions in MTBE pyrolysis and become possible and more important initial reactions in MTBE oxidation at

higher temperatures. The energy diagram and input parameters with reference sources for unimolecular dissociation calculations on the decomposition reactions of MTBE are detailed in Appendix IID. 1. There are six possible product channels as following:

R 8-15	$\text{C3COC} \rightarrow \text{C2C}=\text{C} + \text{CH}_3\text{OH}$	$\Delta H_{\text{rxn}} = 15.19 \text{ kcal mol}^{-1}$
R 8-16	$\text{C3COC} \rightarrow \text{C3CO.} + \text{CH}_3$	$\Delta H_{\text{rxn}} = 80.08 \text{ kcal mol}^{-1}$
R 8-17	$\text{C3COC} \rightarrow \text{C2C.OC} + \text{CH}_3$	$\Delta H_{\text{rxn}} = 82.45 \text{ kcal mol}^{-1}$
R 8-18	$\text{C3COC} \rightarrow \text{C3C.} + \text{CH}_3\text{O}$	$\Delta H_{\text{rxn}} = 82.55 \text{ kcal mol}^{-1}$
R 8-19	$\text{C3COC} \rightarrow \text{C3COC.} + \text{H}$	$\Delta H_{\text{rxn}} = 97.90 \text{ kcal mol}^{-1}$
R 8-20	$\text{C3COC} \rightarrow \text{C3.COC} + \text{H}$	$\Delta H_{\text{rxn}} = 100.96 \text{ kcal mol}^{-1}$

ΔH_{rxn} values are at average temperature from 300 K to 1500 K. The rates of these channels at 873 K and 1123 K are:

		$k_{873 \text{ K}} (\text{s}^{-1})$	$k_{1123 \text{ K}} (\text{s}^{-1})$
R 8-15	$\text{C3COC} \rightarrow \text{C2C}=\text{C} + \text{CH}_3\text{OH}$	1.056×10^{-1}	8.158×10^{-1}
R 8-16	$\text{C3COC} \rightarrow \text{C3CO.} + \text{CH}_3$	1.769×10^{-4}	7.967×10^{-1}
R 8-17	$\text{C3COC} \rightarrow \text{C2C.OC} + \text{CH}_3$	3.206×10^{-5}	9.641×10^{-2}
R 8-18	$\text{C3COC} \rightarrow \text{C3C.} + \text{CH}_3\text{O}$	3.614×10^{-4}	2.122×10^0
R 8-19	$\text{C3COC} \rightarrow \text{C3COC.} + \text{H}$	1.000×10^{-9}	3.187×10^{-5}
R 8-20	$\text{C3COC} \rightarrow \text{C3.COC} + \text{H}$	1.000×10^{-9}	6.119×10^{-5}

The rate constants and the sources for these reactions are listed in Appendix IID. 1.

The most important product channel is iso-butene and methanol formation pathway. The four-center transition state for this reaction had been proposed from several literature references (see chapter 6). We use semi-empirical MOPAC PM3 to define the transition state for this elimination reaction and confirm the four center elimination mechanism. The important information about this transition state is listed in Appendix IIB. 2. One of three methyl carbons on MTBE (C3COC) is ready to lose one of three H attached on it, this methyl H attach to oxygen to get ready to be hydroxyl H for methanol and compose two of four bonds for transition ring C---H---O. The tetra C on MTBE (C3COC) collect one electron from methyl C (lose H) and the other one from oxygen by break C-O bond to

form a π bond, thus double bond for forming iso-butene, this compose the other two bonds of transition ring $O\cdots C=C$. In this four member transition ring $(tC)=pC\cdots H\cdots O\cdots tC$ (tC means tetra C, pC means primary C), the forming carbon double bond has a 1.440 Å of bond length, longer than regular carbon double bond length, 1.334 Å, in iso-butene, and shorter than regular single carbon bond, 1.539 Å, in MTBE. The other forming O-H bond has a 1.143 Å of bond length while a regular O-H bond in methanol has a 0.949 Å of bond length. The breaking C-O bond, making it possible to form methanol directly from MTBE, has a 1.657 Å of bond length, much longer than normal C-O bond, 1.442 Å, in MTBE. The last bond in the four member transition ring is C-H bond, breaking to take methyl-H away from forming iso-butene and give it to forming methanol as a hydroxy-H to close the formation of two separated species from MTBE. This breaking C-H bond length is found, 1.529 Å, much much longer than methyl-H bond length, 1.098 Å, in MTBE. The bond lengths in four member transition ring shows a loose transition structure which gives a relative high A factor and low E_a for this reaction. All other bonds besides transition ring are only having little change, 0.01-0.02 Å.

Other reaction paths of MTBE dissociation give intermediate radical, $C_3COC\cdot$, $C_3\cdot COC$, $C_2C\cdot OC$, $C_3CO\cdot$, which all rapidly undergo further dissociation to give $C_2C=C$, $C_2C=O$, $CC=C$, CH_2O ; radicals $C_3C\cdot$, $CH_3\cdot$, $CH_3O\cdot$ and other species (see detailed pathways in Appendix IID. 2-3 and 11).

8.4.1.3 $C_3C\cdot + O_2 \rightarrow$ Products

There are several important radical products from high temperature, unimolecular dissociation of MTBE, tertiary butyl and methoxy radicals from dissociation of MTBE

(C3COC) to $\text{C3C}\cdot + \text{CH}_3\text{O}$ ($\Delta H_{\text{rxn}} = 82.55 \text{ kcal mol}^{-1}$), and tert-butoxy plus methyl radicals from $\text{C3COC} \rightarrow \text{C3CO}\cdot + \text{CH}_3$ ($\Delta H_{\text{rxn}} = 80.08 \text{ kcal mol}^{-1}$).

T-butyl radical $\text{C3C}\cdot$ is an important intermediate radical from MTBE dissociation, it can also form from dissociation of $\text{C3COC}\cdot$ radical and H atom addition to $\text{C2C}=\text{C}$. The $\text{C3C}\cdot$ radical is relatively more stable than other intermediate radicals because of its tertiary structure and because its beta scission reaction all require scission of primary C---H bond rather than a weaker C---C bond or C---O bond, it can accumulate up to a relative high concentration level in the intermediate temperatures. The $\text{C3C}\cdot$ radical can lose a H to form iso-butene (Appendix IID. 4) via beta scission reaction. The $\text{C3C}\cdot$ can also react with O_2 to form chemically activated energized adduct $[\text{C3COO}\cdot]^*$, which can be stabilized or undergo isomerization reaction via a intramolecular H transfer and this alkyl hydroperoxide radical ($\text{C3}\cdot\text{CCOOH}$) can further react by addition to an oxygen or by β -scission reaction to $\text{C2CyCOC} + \text{OH}$, $\text{C2C}=\text{C} + \text{HO}_2$ and $\text{C}=\text{C}(\text{C})\text{OOH} + \text{CH}_3$ (see Appendix IID. 5), $\text{C}=\text{C}(\text{C})\text{OOH}$ will rapidly dissociate to $\text{C2}\cdot\text{C}=\text{O}$ radical (Appendix IID. 6). The chemically activated adduct $[\text{C3COO}\cdot]^*$ can also eliminate one HO_2 radical directly to form iso-butene. Transition states are found for the isomerization and elimination reactions separately (see Appendix IIB. 3, TS2 and TS3).

Bond lengths in transition states for four related reactions ($\text{C3COO}\cdot \rightarrow \text{C2C}=\text{C} + \text{HO}_2$; $\text{C3COO}\cdot \rightarrow \text{C3}\cdot\text{CCOOH}$, $\text{C3}\cdot\text{CCOOH} \rightarrow \text{C2C}=\text{C} + \text{HO}_2$, $\text{C3}\cdot\text{CCOOH} \rightarrow \text{C2CyCOC} + \text{OH}$) are listed in Appendix IIB. 2 - 5). Transition states show that $\text{C3COO}\cdot$ radical can undergo isomerization to alkyl hydroperoxide radical $\text{C3}\cdot\text{CCOOH}$, or eliminate one HO_2 directly from $\text{C3COO}\cdot$ radical via two different transition states [95], and hydroperoxide

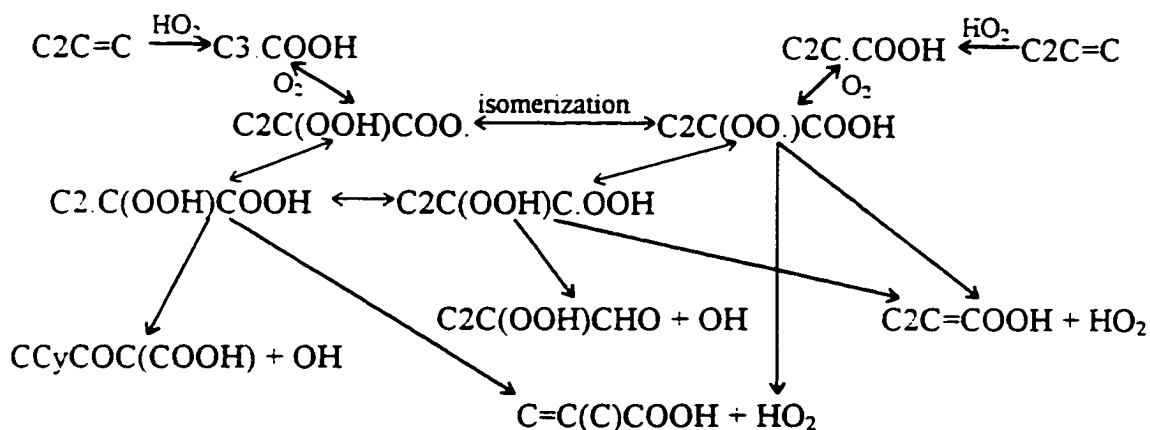
isomer C3 COOH then undergoes β -scission to $C_2C=C + HO_2$, or to epoxide $C_2CyCOC + OH$ via different transition states. In the transition state for isomerization reaction (IIB. 3, TS 2), two “unusual” bonds are involved, one is breaking bond C-H which has a 1.266 Å bond length instead of normal bond length 1.098 Å, the other is forming bond O-H which has a 1.321 Å bond length instead of normal bond length 0.943 Å. In the transition ring for HO_2 direct elimination (IIB. 3 - TS 3), four bonds are involved. The breaking C-H bond and forming O-H bond similar to isomerization transition ring, that the C-O bond length is extended to 2.030 Å from 1.497 Å indicates a breaking; the C-C bond reduces to a 1.404 Å from 1.527 Å, which indicates two electrons from C-H breaking bond and C-O breaking bond is forming a π double bond for $C=C$. In the transition state for reaction $C_3.COOH \rightarrow C_2C=C + HO_2$ (Appendix IIB. 4), $C_3.C---OOH$ bond is extended to 1.923 Å from 1.431 Å, $C_3CO---OH$ bond here is 1.351 Å, while in the transition state for reaction $C_3.COOH \rightarrow C_2CyCOC + OH$ (Appendix IIB. 5), $C_3.C---OOH$ bond is 1.477 Å and $C_3CO---OH$ is extended to 1.679 Å from 1.514 Å. In addition to these two bonds involved in the transition state for reaction $C_3.COOH \rightarrow C_2CyCOC + OH$ (Appendix IIB. 5), a new C---O bond in the length of 1.779 Å is being formed to close the three member ring for C_2CyCOC .

The reaction of O_2 addition to $C_3C.$ and further dissociation of peroxy and/or hydroperoxide radicals is an important reaction system in the oxidation of the MTBE intermediate $C_3C.$ at low to mid range temperatures up to 1300 K since both O_2 and $C_3C.$ are present at relative high levels. The products from $C_3C. + O_2$ are $C_2C=C$, C_2CyCOC and $C_2.C=O$ radical, along with HO_2 , CH_3 and OH radicals.

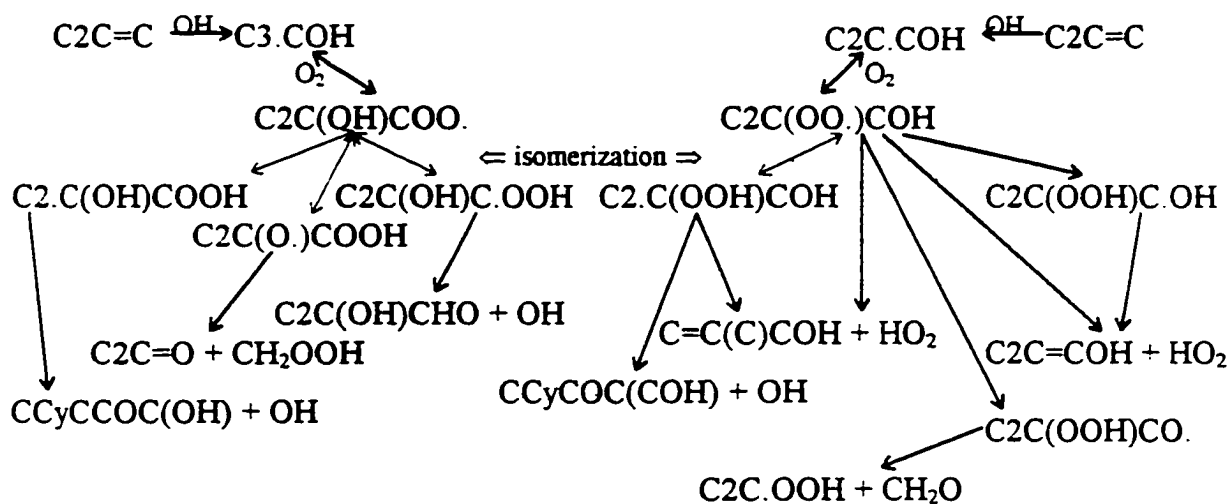
8.4.2 Oxidation of Iso-Butene

Iso-butene is a noted major product from MTBE oxidation and pyrolysis as demonstrated from all reported experiments done by several groups [84-93]. As discussed above, iso-butene can be formed from directly dissociation of MTBE ($\text{C}_3\text{COC} \rightarrow \text{C}_2\text{C}=\text{C} + \text{CH}_3\text{OH}$), dissociation of intermediate radicals C_3COC ($\text{C}_3\text{COC} \rightarrow \text{C}_2\text{C}=\text{C} + \text{CH}_3\text{O}$), C_3C . ($\text{C}_3\text{C} \cdot \rightarrow \text{C}_2\text{C}=\text{C} + \text{H}$) and also from O_2 addition to C_3C . radical. Further oxidation of iso-butene is important on the explanation of important, secondary product formation.

One of the 6 allylic H can be abstracted from iso-butene by OH, O, H, CH_3 and other radicals to form allylic iso-butenyl radical, which can react with O_2 , see section 8.4.2.4. Direct dissociation reaction of iso-butene can occur at high temperatures. (Appendix IID. 7) to form $\text{CC}=\text{C} + \text{CH}_3$ ($\Delta H_{\text{rxn}} = 97.46 \text{ kcal}\cdot\text{mol}^{-1}$), the $\text{CC}=\text{C}$ then (Appendix IID. 8) either dissociate to $\text{C}=\text{C}=\text{C} + \text{H}$, or isomerize to allyl radical ($\text{C}=\text{CC}\cdot$), which can react with O_2 (Appendix IID. 68), like $\text{C}_2\text{C}=\text{C}$ does (see section “8.4.2.4”). The most important reaction pathways for iso-butene oxidation are additions of OH and HO_2 radicals to form hydroxyl and peroxy radicals, these intermediate radicals can further react with O_2 as follows:



And



We discuss abstraction reactions of iso-butene first, then OH, HO₂ and O₂ addition reactions (C₂C=C + OH/HO₂, + O₂) and the further reactions of secondary important products from those addition reactions, and complete the iso-butene oxidation with the reaction of allylic iso-butenyl radical with O₂.

8.4.2.1 Reactions between C₂C=C and OH, O, H, CH₃, CH₃O, HO₂, O₂

The abstraction reaction of iso-butene is important not only because of C₂C=C's relatively high concentration levels but also the resonance stabilized structure of allylic iso-butenyl radical. The dissociation energy of weakly allylic C-H bond on C₂C=C is only 88.2 kcal·mol⁻¹, which is ca 12.9 kcal·mol⁻¹ less than normal C-H bond on alkane. The 6 allylic H can be abstracted by OH, H, O, etc. reactive radicals, also by intermediate reactive radical or molecule such as HO₂ and O₂. We consider the following abstraction reactions of C₂C=C in this system.

	Reactions	$k \text{ (cm}^3\text{-mol}^{-1}\text{-s}^{-1}\text{)}$
R 8-21	$\text{C}_2\text{C}=\text{C} + \text{O} \rightarrow \text{C}_2.\text{C}=\text{C} + \text{OH}$	$1.21 \times 10^{11} T^{0.7} \exp(-7.633 \text{ kcal-mol}^{-1}/\text{RT})$
R 8-22*	$\text{C}_2\text{C}=\text{C} + \text{O} \rightarrow \text{C}_2\text{CyCOC}$	$4.20 \times 10^{12} T^0 \exp(-0.503 \text{ kcal-mol}^{-1}/\text{RT})$
R 8-23	$\text{C}_2\text{C}=\text{C} + \text{H} \rightarrow \text{C}_2.\text{C}=\text{C} + \text{H}_2$	$3.50 \times 10^5 T^{2.5} \exp(-2.492 \text{ kcal-mol}^{-1}/\text{RT})$
R 8-24	$\text{C}_2\text{C}=\text{C} + \text{H} \rightarrow \text{CC}=\text{C} + \text{CH}_3$	$1.45 \times 10^{13} T^0 \exp(-1.302 \text{ kcal-mol}^{-1}/\text{RT})$
R 8-25	$\text{C}_2\text{C}=\text{C} + \text{OH} \rightarrow \text{C}_2.\text{C}=\text{C} + \text{H}_2\text{O}$	$6.24 \times 10^6 T^{2.0} \exp(-(-0.298) \text{ kcal-mol}^{-1}/\text{RT})$
R 8-26	$\text{C}_2\text{C}=\text{C} + \text{CH}_3 \rightarrow \text{C}_2.\text{C}=\text{C} + \text{CH}_4$	$4.42 \times 10^0 T^{3.5} \exp(-5.675 \text{ kcal-mol}^{-1}/\text{RT})$
R 8-27	$\text{C}_2\text{C}=\text{C} + \text{CH}_3\text{O} \rightarrow \text{C}_2.\text{C}=\text{C} + \text{CH}_3\text{OH}$	$4.42 \times 10^0 T^{3.5} \exp(-5.675 \text{ kcal-mol}^{-1}/\text{RT})$
R 8-28	$\text{C}_2\text{C}=\text{C} + \text{HO}_2 \rightarrow \text{C}_2.\text{C}=\text{C} + \text{H}_2\text{O}_2$	$1.93 \times 10^4 T^{2.6} \exp(-13.91 \text{ kcal-mol}^{-1}/\text{RT})$
R 8-29*	$\text{C}_2\text{C}=\text{C} + \text{HO}_2 \rightarrow \text{C}_2\text{CyCOC} + \text{OH}$	$1.05 \times 10^{12} T^0 \exp(-14.206 \text{ kcal-mol}^{-1}/\text{RT})$
R 8-30	$\text{C}_2\text{C}=\text{C} + \text{O}_2 \rightarrow \text{C}_2.\text{C}=\text{C} + \text{HO}_2$	$4.79 \times 10^{12} T^0 \exp(-38.56 \text{ kcal-mol}^{-1}/\text{RT})$

* reaction (R 8-22) is a n addition reaction and reaction (R 8-29) is an addition and then epoxide formation reaction.

There are no available data for reaction (R 8-21) $\text{C}_2\text{C}=\text{C} + \text{O} \rightarrow \text{C}_2.\text{C}=\text{C} + \text{OH}$. The rate constant of $6.03 \times 10^{10} T^{0.7} \exp(7.633 \text{ kcal-mol}^{-1}/\text{RT}) \text{ cm}^3\text{-mol}^{-1}\text{-s}^{-1}$ for reaction $\text{CC}=\text{C} +$

$O \rightarrow C.C=C + OH$ (91 TSA) had been taken as reference and multiplied by a factor of 2 is considering 6 allylic H on $C_2C=C$ while 3 allylic H on $CC=C$. A triplet O atom can also add to carbon double, via “triplet \rightarrow singlet” conversion by collision, to form 2,2-dimethyloxerine which is a important product from oxidation of $C_2C=C$. The rate constant is also referenced from reaction $O + CC=C \rightarrow CCyCOC$ (73 HER).

The H atom can abstract one allylic H from $C_2C=C$ to form $C_2.C=C$ radical similar to reaction $CC=C + H \rightarrow H_2 + C.C=C$, which has a rate constant of $1.73 \times 10^5 T^{2.5} \exp(2.492 \text{ kcal-mol}^{-1} / RT) \text{ cm}^3\text{-mol}^{-1}\text{-s}^{-1}$ (91 TSA). We use this rate constant by timing a factor of 2. The H can also replace a methyl radical from $C_2C=C$ to form $CC=C + CH_3$, a rate constant of reaction $CC=C + H \rightarrow CH_3 + C=C$ is used by multiplying by a factor of 2.

The OH radical is other most important one in the oxidation reaction systems. One report in literature data is from Walker's group [96]. A rate constant of $7.80 \times 10^{12} T^0 \exp(0.0 \text{ kcal-mol}^{-1} / RT) \text{ cm}^3\text{-mol}^{-1}\text{-s}^{-1}$ (78 BAK/BAL) was obtained using relative rate technique at 0.658 atm and one temperature, 753 K in N_2 bath. Considering wide range of temperature, we choose data for propene and multiplied by a factor of 2 for the increased number of H's.

The CH_3 as well as CH_3O radical can accumulate to relatively high concentration level. The abstraction of allylic H on $C_2C=C$ by CH_3 or CH_3O is considered to be analogous to abstraction reaction by CH_3 or CH_3O from $CC=C$. A factor of 2 is multiplied to account for 6 allylic H on $C_2C=C$.

The HO_2 radical is not as an strong abstracting agent as O, OH or H because the $HOO \cdots H$ bond is only 88 kcal-mol^{-1} . HO_2 exists in relative high concentrations at moderate

temperature, up to 1200 K in oxidation environments especially in intermediate temperature range 600 K to 1000K. The abstraction of allylic H from C2C=C is compete with the reaction of addition of peroxy radical to carbon double bond, epoxide formation and the releasing of OH radical. The propene's data are taken as reference data for both reactions of iso-butene.

The abstraction reaction between C2C=C and O₂ is considered in this system because both species are present at high concentrations. Walker's group conducted a series of O₂ abstraction reaction studies and found a rate constant of $4.79 \times 10^{12} T^0 \exp(38.56 \text{ kcal-mol}^{-1} / RT) \text{ cm}^3\text{-mol}^{-1}\text{-s}^{-1}$ for C2C=C and of $1.95 \times 10^{12} T^0 \exp(39.11 \text{ kcal-mol}^{-1} / RT) \text{ cm}^3\text{-mol}^{-1}\text{-s}^{-1}$ for CC=C, which is much faster than NIST data of $6.03 \times 10^{13} T^0 \exp(47.59 \text{ kcal-mol}^{-1} / RT) \text{ cm}^3\text{-mol}^{-1}\text{-s}^{-1}$ for CC=C at intermediate temperature. We chose Walker's data.

8.4.2.2 C2C=C + HO₂ → C3.COOH/C2C.COOH, + O₂ → Products

The C2C=C + HO₂ reaction system becomes more important in the intermediate temperature because of high concentration of C2C=C and HO₂ produced from MTBE dissociation and further reactions of resulted intermediate radicals. The HO₂ radical can attach to either side of carbon double bond on C2C=C and results in two peroxy radicals C3.COOH and C2C.COOH. Both of these two radicals can form 2,2-dimethyloxirane by releasing one OH radical, or undergo isomerization reaction via intramolecular H transfer and further β-scission or HO₂ elimination reactions. C3.COOH radical is also formed from C3COO. isomer via C3C. + O₂ (we discussed above), which shows a reverse reaction chain: C2C=C + HO₂ ⇌ C3.COOH ⇌ C3COO. ⇌ C3C. + O₂. An equilibrium

exists between both molecules ($C_2C=C$, O_2) and radicals. The potential energy level diagrams of $C_2C=C + HO_2 \rightarrow C_3.COOH \rightarrow$ products (Appendix IID. 9) show the chemical activation reaction system for $C_2C=C + HO_2$, and the $C_3.COOH$ radical can be formed from both $C_2C=C + HO_2$ and $C_3C. + O_2$.

The potential energy level diagram in Appendix IID. 10 shows the addition of HO_2 to the terminal carbon (CD/ H_2 carbon) of double bond in $C_2C=C$. Several product channels exist for further reactions of $C_2C.COOH$ since there are 4 types of H on $C_2C.COOH$. These hydrogens can be transferred to form different isomers, one of the isomers being $C_2CCOO.$ radical, which can eliminate directly H-O-O group (as HO_2) just like $C_3COO.$ radical we discussed in section 8.4.1.3. An equilibrium, $C_2C=C + HO_2 \rightleftharpoons C_2C.COOH \rightleftharpoons C_2CCOO. \rightleftharpoons C_3.C + O_2$, may not exist for $C_2C.COOH$ because of low concentration level of $C_3.C$ radical. The potential energy level diagrams of $C_2C.COOH$ (Appendix IID. 10) shows that: 2,2-dimethyloxirane (C_2CyCOC) formation from $C_2C.COOH$, $C_2C=C$ formation with HO_2 elimination directly from $C_2CCOO.$ isomer, and methyloxetane ($CCyCCOC$) formation are important product channels.

The reactions of O_2 addition to both $C_3.COOH$ and $C_2C.COOH$ radicals (Appendix IID. 11-12) are important in the high O_2 environment. The resulting intermediate radicals $C_2C(OOH)COO.$, $C_2C(OO.)COOH$, $C_2.C(OOH)COOH$ and $C_2C(OOH)C.OOH$ undergo HO_2 direct elimination reaction, isomerization and epoxide formation, HO_2 β -scission and CH_3 elimination reactions, to form products $CCyCOC(COOH)$, $C_2C=COOH$, $C=C(C)COOH$ and $C_2C(OOH)CHO$, which further reactions will be discussed in section

8.4.2.4. An equilibrium exist in $C_3.COOH + O_2 \rightleftharpoons C_2C(OOH)COO. \rightleftharpoons C_2C(OO.)COOH \rightleftharpoons C_2C.COOH + O_2$ system.

8.4.2.3 $C_2C=C + OH \rightarrow C_3.CO\dot{H}/C_2C.CO\dot{H}, + O_2 \rightarrow$ Products

The addition of OH to $C_2C=C$ produces important stabilized intermediates $C_3.CO\dot{H}$ and $C_2C.CO\dot{H}$. The potential energy level diagram (Appendix IID. 13) shows that chemically activated adduct $[C_3.CO\dot{H}]^*$ has enough energy to go directly to $C=C(OH)C$, which is the end isomer of $C_2C=O$. The acetone product $C_2C=O + CH_3$, via $C_3CO.$ isomer becomes more important at higher temperatures since adduct $[C_3.CO\dot{H}]^*$ is more exothermic and this channel needs ca 10 kcal-mol⁻¹ more energy. The direct dissociation to products from energized $[C_2C.CO\dot{H}]^*$ adduct are less important (see Appendix IID. 14).

The stabilized or energized $C_3.CO\dot{H}$ radical can both react with O_2 to form $[C_2C(OH)COO.]^*$ adduct, which can directly go to products: $C_2C=O + CH_2OOH$ via $C_2C(O.)COOH$ isomer; $CCyCCOC(OH) + OH$ via $C_2.C(OH)COOH$ isomer; $C_2C(OH)CHO + OH$ via $C_2C(OH)C.OOH$ isomer (see Appendix IID. 15), in addition to stabilized to $C_2C(OH)COO.$ radical. The further reactions of $CCyCCOC(OH)$ and $C_2C(OH)CHO$ will discussed in section 8.4.2.4.

The chemically activated adduct $[C_2C(OO.)CO\dot{H}]^*$ from reaction of $C_2C.CO\dot{H}$ with O_2 can be stabilized to $C_2C(OO.)CO\dot{H}$ radical, or dissociate to products $C_2C=COH + HO_2$ via the $C_2C(OOH)C.OH$ isomer, to products $CCyCOC(COH) + HO_2$ and $C=C(C)COH + HO_2$ via $C_2.C(OOH)COH$ isomer, to products $C_2C.OOH + CH_2O$ via $C_2C(OOH)CO.$ isomer, or undergo direct HO_2 elimination to $C=C(C)COH / C_2C=COH$. The $C_2C.OOH$ will rapidly dissociate to $C_2C=O + OH$ (see Appendix IID. 26). The potential energy

level diagram (Appendix IID. 16) shows all the above product channels are important since the dissociation back to reactants had the highest activation energy, that is, the adduct has enough energy to go directly to products.

8.4.2.4 Further Reactions of Intermediates from Iso-Butene Oxidation

The important intermediates from the very exothermic product channels of the iso-butene oxidation reaction system ($C_2C=C + OH/HO_2 + O_2$) are $C_2C=COOH$, $C=C(C)COOH$, $C_2C(OOH)CHO$, $C_2C(OH)CHO$, $CCyCOC(COH)$ and $CCyCOC(COOH)$. The potential energy level diagrams are shown in Appendix IID. 17-25. All these species can undergo β -scission reactions as discussed below.

$C_2C=COOH$ produces, (see Appendix IID. 17), an $OH + C_2C=CO\cdot$, the $C_2C=CO\cdot$ radical instantly rearranges to $C_2C\cdot CHO$ radical. The reactions of $C_2C\cdot CHO$ is discussed later in this section. $C=C(C)COOH$, see Appendix IID. 18, produces an $OH + C=C(C)CO\cdot$, the $C=C(C)CO\cdot$ radical can further undergoes dissociation to $C=C(C)CHO$ (Appendix IID. 19), an important minor product found from experiments, by losing a H, or undergoes beta scission to $CC=C + CH_2O$, which is higher in E_a than H atom elimination.

Decomposition of both $C_2C(OOH)CHO$ and $C_2C(OH)CHO$ (Appendix IID. 20-21) produce $C_2C\cdot CHO$ radicals by elimination of OH or HO_2 radical. The $C_2C(OOH)CHO$ have the other product channel $C_2C\cdot OOH + CHO$, $C_2C(O\cdot)CHO + OH$, the $C_2C\cdot OOH$ quickly dissociate to $C_2C=O + OH$ (Appendix IID. 26) and the $C_2C(O\cdot)CHO$ dissociate to $C_2C=O + CHO$. The alternative product channel from $C_2C(OH)CHO$ is $C_2C\cdot OH + CHO$. The $C_2C\cdot CHO$ radical can either dissociate to $CC\cdot C + CO$ via isomerization to

$C_2CC=O$, or react with O_2 to give product $C=C(C)CHO$, $C_2C=C=O$, $C_2C=O$ and CO , the reactions related to the $C_2C.CHO$ radical will discuss later in section 8.4.2.6.

Both $CCyCOC(COOH)$ and $CCyCOC(COH)$ will decompose to $CCyC.OC$ (Appendix IID 24-25), and then to $C_2C=O$ (Appendix IID. 27). Two steps are needed for $CCyC.OC$ radical formation from $CCyCOC(COOH)$ by first releasing OH to form $CCyCOC(CO.)$ radical, then eliminating CH_2O (beta scission) from $CCyCOC(CO.)$ radical (Appendix IID. 24).

8.4.2.5 Stable Molecules C_2CyCOC , $C_2C=O$ and $C=C(C)CHO$

The most stable secondary products are C_2CyCOC , $C_2C=O$ and $C=C(C)CHO$ from oxidation of $C_2C=C$. At high temperature, these species can thermally decompose to $CCyC.OC + CH_3$ from C_2CyCOC (Appendix IID. 28); to $CH_3C=O + CH_3$ from $C_2C=O$ (Appendix IID. 29); to $C=C(C)C=O + H$ and $CC=C + CHO$ from $C=C(C)CHO$ (Appendix IID. 30). At low and intermediate temperatures, these species can undergo abstraction reactions to form $C_2CyCOC.$, $C_2C=O$ and $C=C(C)C=O$. The $C_2CyCOC.$ then undergoes isomerization reaction to $C_2C.CHO$ radical (see Appendix IID. 33), $C_2C=O$ can further dissociate to $C=C=O + CH_3$ (see Appendix IID. 32), and $C=C(C)C=O$ can eliminate CO molecule with $CC=C$ radical (see Appendix IID. 31). The $CCyC.OC$ radical from thermal decomposition of C_2CyCOC will rapidly isomerize to $C_2C=O$ radical (see Appendix IID. 27). The $CH_3C=O$ radical from $C_2C=O$ will rapidly decompose to $CH_3 + CO$. The $C=C(C)C=O$ radical from $C=C(C)CHO$ via abstraction reactions with radical pool or decomposition reaction at high temperatures will further dissociate to $CO + CC=C$. The $CC=C$ from both $C=C(C)CHO$ molecule and

$\text{C}=\text{C}(\text{C})\text{C}=\text{O}$ radical have relative more reaction pathways, one of the most important is $\text{CC}=\text{C}$ radical reacts with O_2 (see section 8.4.4)

In summary, these stable species can convert to CH_3 , CO , H , $\text{CC}=\text{C}$, $\text{C}_2\text{C}\cdot\text{CHO}$ radical and $\text{C}=\text{C}=\text{O}$.

8.4.2.6 $\text{C}_2\text{C}\cdot\text{CHO}$ and $\text{C}_2\text{C}\cdot\text{CHO} + \text{O}_2$

The radical $\text{C}_2\text{C}\cdot\text{CHO}$ can be formed in several ways. The ring opening (β -scission) reaction of $\text{C}_2\text{CyCOC}\cdot$ radical is the major source for $\text{C}_2\text{C}\cdot\text{CHO}$ formation here. It can also be formed from unimolecular decomposition of $\text{C}_2\text{C}=\text{COOH}$, $\text{C}_2\text{C}(\text{OOH})\text{CHO}$, $\text{C}_2\text{C}(\text{OH})\text{CHO}$, and by abstraction reactions. The potential energy level diagram (Appendix IID. 33) shows that the $\text{C}_2\text{C}\cdot\text{CHO}$ radical can undergoes unimolecular dissociation reaction or isomerization reaction followed by further β -scission reaction to $\text{CC}\cdot\text{C} + \text{CO}$ at high temperatures. $\text{C}_2\text{C}\cdot\text{CHO}$ radical will also react with O_2 . This O_2 addition reaction is much more important at low and intermediate temperatures and fuel lean conditions (see Appendix IID. 34). The favored low energy products from $\text{C}_2\text{C}\cdot\text{CHO} + \text{O}_2$ are $\text{C}=\text{C}(\text{C})\text{CHO}$, $\text{C}_2\text{C}=\text{C}=\text{O}$, $\text{C}_2\text{C}\cdot\text{OOH}$ ($\rightarrow \text{C}_2\text{C}=\text{O} + \text{OH}$), HO_2 and CO .

8.4.2.7 Reaction of Allylic Iso-Butenyl Radical with O_2

As noted in the previous discussion, an important secondary product from reactions of iso-butene is allylic iso-butenyl radical $\text{C}_2\cdot\text{C}=\text{C}$, formed from abstraction reactions of iso-butene due to the weakly bonded hydrogen atom (the allylic C-H bond is only 88.3 kcal mol^{-1}). The allylic iso-butene radical $\text{C}_2\cdot\text{C}=\text{C}$ could accumulate to higher levels because of its low reactivity which is due to its high resonance stabilization energy. It can

dissociate to $C=C=C + CH_3$ (Appendix IID. 35), abstract H from other species to form $C_2C=C$, or react with molecule oxygen.

The $C_2C=C$ radical can also recombine HO_2 to form $C=C(C)COOH$. This reaction becomes more important at the intermediate temperatures, because that the HO_2 concentration becomes sufficiently large. The allylic iso-butenyl radical is resonantly stabilized, and its thermal decomposition and reaction with O_2 are slow (see below). The energy level diagram and input parameters for the chemical activation calculations on allylic iso-butenyl radical + HO_2 are shown in Appendix IID 18-19. The combination of $C_2C=C$ and HO_2 produce a chemically activated adduct $[C=C(C)COOH]^*$, which has sufficient energy (ca 12 kcal more) to decompose to radical $C=C(C)CO\cdot + OH$ radicals. The $C=C(C)CO\cdot$ radical can then loss one H to form methacrolein $C=C(C)CHO$ with 13.54 kcal mol⁻¹ activation energy and formaldehyde $CH_2O + CC=C$ with 23.5 kcal mol⁻¹ activation energy.

The addition of O_2 to the allylic iso-butene radical is analyzed in this study by using semi-empirical calculations for transition states of the isomerization reactions. The potential energy level diagram is shown in Appendix IID. 36. The chemically activated energized adduct $[C=C(C)COO\cdot]^*$ can most easily dissociate back to $C_2C=C + O_2$ but a number of channels with activation energies above that of initial reactant energy are of importance. The important pathways considered in this work are (1) $C=C(C)COO\cdot \rightleftharpoons C=C(C)COOH \Rightarrow C=C(C)COOC + OH$; (2) $C=C(C)COO\cdot \rightleftharpoons C=C(C)C.OOH \Rightarrow C=C(C)CHO + OH$; (3) $C=C(C)COO\cdot \rightleftharpoons CCyC.COOC \rightleftharpoons CCyCC.OOC \rightleftharpoons CC(CO)CHO \Rightarrow CC.CHO + CH_2O$; (4) $C=C(C)COO\cdot \rightleftharpoons CCyC.COOC \rightleftharpoons CCyCOC(CO\cdot) \Rightarrow CCyC.OC + CH_2O$; (5)

$C=C(C)COO. \rightleftharpoons C2.CyCOOC \rightleftharpoons C2CyCOOC. \rightleftharpoons C2C(O.)CHO \Rightarrow C2C=O + CHO; (6)$
 $C=C(C)COO. \rightleftharpoons C2.CyCOOC \rightleftharpoons CCyCOC(CO.) \Rightarrow CCyC.OC + CH_2O.$ Almost all product channels are very exothermic and have relatively much higher barriers for isomerization processes. Several of the isomerization channels have similar energies for isomerization reactions and are in competition. The reactivity towards O_2 of $C2.C=C$ will increase with temperature, due to exothermic nature of these channels.

8.4.3 Oxidation and Unimolecular Dissociation Reactions of Methanol

Methanol, as a major product from MTBE oxidation, is mainly formed from MTBE dissociation. Some abstraction reactions also result in methanol production. Compared to iso-butene, methanol has relatively simple reaction pathways to go to the final products CH_4 or CH_2O or CO / CO_2 . At the intermediate temperature or low temperature, methanol decays mainly by abstraction reactions while its thermal decomposition also plays important role at the high temperature. The important pathways for methanol decay are discussed below.

8.4.3.1 Abstractions Reactions Involving Methanol

There are two types of hydrogen on methanol, methyl H ($H---CH_2OH$ bond energy = 97.5 kcal mol⁻¹) and hydroxy H (CH_3O---H bond energy = 104.0 kcal mol⁻¹). At low temperatures, more CH_2OH than CH_3O can be produced from methanol abstraction reactions by other radicals in the system because of relatively weak C-H bond compared to O-H bond.



R 8-32	$\text{CH}_3\text{OH} + \text{O} \rightarrow \text{CH}_3\text{O} + \text{OH}$	$\frac{1.00 \times 10^{13}}{\text{RT}} T^0 \exp(-5.129 \text{ kcal-mol}^{-1})$
R 8-33	$\text{CH}_3\text{OH} + \text{H} \rightarrow \text{CH}_2\text{OH} + \text{OH}$	$\frac{3.40 \times 10^{13}}{\text{RT}} T^0 \exp(-5.497 \text{ kcal-mol}^{-1})$
R 8-34	$\text{CH}_3\text{OH} + \text{H} \rightarrow \text{CH}_3\text{O} + \text{OH}$	$\frac{4.00 \times 10^{13}}{\text{RT}} T^0 \exp(-6.095 \text{ kcal-mol}^{-1})$
R 8-35	$\text{CH}_3\text{OH} + \text{OH} \rightarrow \text{CH}_2\text{OH} + \text{H}_2\text{O}$	$\frac{1.35 \times 10^{13}}{\text{RT}} T^0 \exp(-1.881 \text{ kcal-mol}^{-1})$
R 8-36	$\text{CH}_3\text{OH} + \text{OH} \rightarrow \text{CH}_3\text{O} + \text{H}_2\text{O}$	$\frac{1.00 \times 10^{13}}{\text{RT}} T^0 \exp(-1.953 \text{ kcal-mol}^{-1})$
R 8-37	$\text{CH}_3\text{OH} + \text{CH}_3 \rightarrow \text{CH}_2\text{OH} + \text{CH}_4$	$\frac{3.19 \times 10^1}{\text{RT}} T^{3.2} \exp(-7.172 \text{ kcal-mol}^{-1})$
R 8-38	$\text{CH}_3\text{OH} + \text{CH}_3 \rightarrow \text{CH}_3\text{O} + \text{CH}_4$	$\frac{1.44 \times 10^1}{\text{RT}} T^{3.1} \exp(-6.935 \text{ kcal-mol}^{-1})$
R 8-39	$\text{CH}_3\text{OH} + \text{CH}_3\text{O} \rightarrow \text{CH}_2\text{OH} + \text{CH}_3\text{OH}$	$\frac{3.01 \times 10^{11}}{\text{RT}} T^0 \exp(-4.074 \text{ kcal-mol}^{-1})$
R 8-40	$\text{CH}_3\text{OH} + \text{HO}_2 \rightarrow \text{CH}_2\text{OH} + \text{H}_2\text{O}_2$	$\frac{9.64 \times 10^{10}}{\text{RT}} T^0 \exp(-12.579 \text{ kcal-mol}^{-1})$
R 8-41	$\text{CH}_3\text{OH} + \text{O}_2 \rightarrow \text{CH}_2\text{OH} + \text{HO}_2$	$\frac{2.05 \times 10^{13}}{\text{RT}} T^0 \exp(-44.911 \text{ kcal-mol}^{-1})$

The OH, O and H radical or atoms can abstract the two types of H from CH₃OH (R 8-31 to R 8-36). The NIST fit values are used for reaction (R 8-31) and reaction (R 8-35), both of which form CH₂OH radical. The A factors of reaction (R 8-32) and reaction (R 8-36) (form CH₃O radical) are both taken from literature (84 WAR, NIST) while their E_a are calculated based on Bozzelli and Dean's equation using corresponding CH₂OH radical formation reaction (R 8-31, R 8-35) as reference separately. The difference of ΔH_{rxn} between CH₂OH and CH₃O formation reaction are the same as 7.16 kcal-mol⁻¹. The f is estimated as 0.03 and 0.01 for O abstraction and OH abstraction separately. Rate constants of abstractions by H are taken from the NIST database, 81 VAN/VAN and 81 HOY/SIE for reaction (R 8-33), 84 WAR for reaction (R 8-34). The rate constants of other abstraction reaction (R 8-37 to R 8-41) are from the NIST recommended data (87 TSA).

8.4.3.2 Unimolecular Dissociation Reactions of Methanol

The decomposition steps of methanol are estimated by QRRK / beta collision analysis as previous described. The potential energy diagram and high pressure limit rate constants for QRRK analysis are illustrated in Appendix IID. 38.

	Reactions	$\Delta H_{\text{rxn}, 298 \text{ K}}$	$E_a \text{ (kcal-mol}^{-1}\text{)}$
R 8-42	$\text{CH}_3\text{OH} \rightarrow \text{CH}_2\text{O} + \text{H}_2$	22.00 kcal mol ⁻¹	90.11
R 8-43	$\text{CH}_3\text{OH} \rightarrow \text{HCOH} + \text{H}_2$	70.56 kcal mol ⁻¹	86.97
R 8-44	$\text{CH}_3\text{OH} \rightarrow {}^1\text{CH}_2 + \text{H}_2\text{O}$	91.65 kcal mol ⁻¹	90.33
R 8-45	$\text{CH}_3\text{OH} \rightarrow \text{CH}_3 + \text{OH}$	92.30 kcal mol ⁻¹	91.03
R 8-46	$\text{CH}_3\text{OH} \rightarrow \text{CH}_2\text{OH} + \text{H}$	96.50 kcal mol ⁻¹	96.52
R 8-47	$\text{CH}_3\text{OH} \rightarrow \text{CH}_3\text{O} + \text{H}$	104.60 kcal mol ⁻¹	103.76

The barriers of reaction (R 8-42 to R 8-44) are taken from the study of Walch [96] using complete-active-space self-consistent-field (CASSCF) / internally contracted configuration-interaction (CCI), Ab Initio calculations. The reverse channel of reaction (R 8-44) is found to have no barrier. The barriers of the reverse of reaction (R 8-42, R 8-43) are calculated as 1.7 and -5.2 kcal-mol⁻¹ with respect to the energy level of CH₃ + OH channel (44.3 kcal-mol⁻¹). The barriers of these three reactions are then derived as 93.11, 86.97 and 90.33 kcal-mol⁻¹ for reaction R 8-42, R 8-43 and R 8-44 respectively. The A factors are taken from Dean [21, 82]. The rate constants of three simple dissociation reactions are calculated from reverse reactions by MR.

8.4.3.3 Reactions of CH₂OH / CH₃O and CH₂O / CHO

More CH₂OH radical is formed from methanol dissociation because of relatively weak bond H---CH₂OH and three methyl H's compared to the one hydroxyl H. Both radicals can undergo β-scission to form formaldehyde with a barrier of 22.83 kcal-mol⁻¹ from CH₃O and 30.99 kcal-mol⁻¹ from CH₂OH (Appendix IID. 39).

Because of high concentration level of CH_2OH radical, the reaction system of $\text{CH}_2\text{OH} + \text{O}_2$ plays an important role in the methanol decay to formaldehyde. The potential energy level diagram with QRRK input parameters are listed in Appendix IID. 40. The chemically activated adduct $[\text{C}(\text{OO}\cdot)\text{H}_2\text{OH}]^*$ has enough energy to go to $\text{CH}_2\text{O} + \text{HO}_2$, $\text{HCO}_2\text{H} + \text{OH}$ and $\text{HC}(\text{OOH})=\text{O} + \text{H}$ product channels via two hydroperoxide isomers $\text{C}(\text{OOH})\text{H}_2\text{O}$ and $\text{C}\cdot(\text{OOH})\text{HOH}$. The $\text{HC}(\text{OOH})=\text{O}$ will undergoes β -scission to $\text{HC}(\text{O}\cdot)=\text{O} + \text{OH}$, and the $\text{HC}(\text{O}\cdot)=\text{O}$ radical soon go to carbon monoxide by releasing OH radical and carbon dioxide by losing H atom (see Appendix IID. 42-43). The HCO_2H decay via $\text{C}\cdot(\text{OH})=\text{O}$ and $\text{HC}(\text{O}\cdot)=\text{O}$ radical by abstraction reaction, or directly decompose to $\text{CO} + \text{H}_2\text{O}$ and $\text{CO}_2 + \text{H}_2$ at high temperatures (see Appendix IID. 44).

Formaldehyde, important intermediate from oxidation of iso-butene and methanol, decays mostly by abstraction reactions of H, O, OH, and CH_3 radicals or atoms to CHO radical, which easily decomposes to carbon monoxide or is converted through reaction with O_2 to final products $\text{CO} + \text{HO}_2$ and $\text{CO}_2 + \text{OH}$ (see Appendix IID. 41). The direct dissociation of CH_2O to $\text{CO} + \text{H}_2$ can also be important at high temperatures. The barrier for $\text{CH}_2\text{O} \rightarrow \text{CO} + \text{H}_2$ is ca $35.3 \text{ kcal}\cdot\text{mol}^{-1}$ based on the NIST fit value (Appendix IID. 45).

8.4.4 Reactions of CH_4 , C_2 and C_3

Methane, ethylene and propene are observed as important products from MTBE oxidation and pyrolysis at intermediate temperatures. The reaction system are described below, the potential energy level diagrams and the high pressure limit input parameters for QRRK calculations are documented in Appendix IID. 46 - 86.

The initial intermediate radical from methane decay is methyl radical, which can be formed from abstraction reactions of methane by H, O, OH and CH₃. The methyl radical can react with O₂ to go to formaldehyde (Appendix IID. 47) or CH₃O + O and therefore go to the final product CO and CO₂.

The most important C₂ product from MTBE oxidation and pyrolysis is ethylene (C₂H₄), which can also be formed from methyl radical recombination and ethyl radical reacting with O₂. The potential energy level diagrams in Appendix IID. 49-52 show that the OH or HO₂ radical addition to ethylene followed by O₂ additions can convert C₂H₄ to CH₃CHO, CH₂O, C=COH, C=COOH and C(OOH)CHO, which can undergo further abstraction, β-scission reactions to final products CO and CO₂. The other important reaction pathways included in this study for C₂ species are C₂H₅ + O₂, C₂H₃ + O₂, and C₂H₂ + O₂, the products from these reactions are C₂H₄, CH₃CHO, CHOCHO, CH₂O, CO, C=C=O, CHO, HO₂, OH, CH₃, and H. The potential energy level diagrams are in Appendix IID. 59-63. The abstraction and dissociation reactions of dimethylether (COC) and O₂ addition to COC. radical are included and potential energy level diagrams are in Appendix IID. 64-66. The decay of COC is via dissociation to the COC. radical or O₂ addition to COC. radical to go to formaldehyde therefore final CO and CO₂. The potential energy level diagrams and QRRK input parameters are detailed in Appendix IID. 49 - 66.

The reactions of C₃ species are focused on (1) CC.C + O₂ → CC=C, CCyCOC, C₂C=O and HO₂, OH radicals (Appendix IID. 67); (2) C=CC. + O₂ → C=CC=O, CH₂O, CyCOC, C.CHO, CH₃C.=O, CC.OH, OH (Appendix IID. 68); (3) C=CC + HO₂/OH, O₂ → CCyCOC, CC(OOH)CHO, CC(OH)CHO, CyCOC(C)OOH, CyCOC(C)OOH,

CC(=O)COOH, CC(=O)COH, CH₃CHO, C₂C=O, C=C(OH)C, C=CCOOH, CC=COOH, C=CCOH, CC=COH, C=COH, CCCHO, CH₂O, CC.OOH, C₂H₃, CH₂OH, CH₃, OH, HO₂, H. The potential energy level diagrams for (3) are in Appendix IID. 70-77, and relative intermediate reactions are illustrated in Appendix IID. 78-86.

8.5 Conclusion

Chemical activation and unimolecular dissociation reactions in MTBE oxidation and pyrolysis system have been analyzed with QRRK calculations incorporated pressure dependence. The initial reactions of MTBE in the presence of O₂ are unimolecular dissociation and abstraction reactions while OH, O, HO₂ and CH₃ are the most important radicals, and initial thermal decomposition of MTBE becomes more important with increasing temperature. The major products from initial oxidation of MTBE are iso-butene, methanol, acetone, propene and formaldehyde. The most important pathways in the MTBE oxidation are (1) unimolecular dissociation of MTBE to iso-butene and methanol, (2) abstraction reactions between MTBE and H, CH₃, OH, O₂ radicals, and between CH₂O and HO₂, (3) dissociation of formaldehyde, (4) further oxidation of iso-butene via C₂C=C + OH/HO₂ → intermediates, intermediates + O₂, and (5) further oxidation of methanol via CH₃OH → CH₂OH (abstraction), CH₂OH + O₂, and (6) further oxidation of formaldehyde via CH₂O → CHO (abstraction), CHO + O₂. The secondary important products from further oxidation of major products are C₂C=C, C₂C=O, CH₂O, CH₄, C₂H₄, C₃H₆, C₂CyCOC, C=C(C)CHO, C₂C=C=O, C=C(C)COH, C₂CCOH, CO and CO₂.

The initial step in MTBE pyrolysis is thermal dissociation of MTBE. The thermal decomposition of CH_2O and abstraction and addition reactions are responsible for the concentration level of CH_2O . The H atom and CH_3 radical plays key role in all abstraction reactions after MTBE dissociation, while the most important products are almost the same as those from MTBE oxidation with no CO_2 and more CH_4 . The formaldehyde and isobutene are more stable at the low temperatures in the pyrolysis situation.

CHAPTER 9

MODEL VALIDATION FOR MTBE SYSTEM

9. 1 Available Literature Data

Few literature data are available for validation of MTBE model on pyrolysis and oxidation. Previous studies on MTBE pyrolysis focused on MTBE unimolecular dissociation reaction $C_3COC \rightarrow C_2C=C + CH_3OH$, the rate constant we used in this study is compared to literature data as below.

	$k \text{ (s}^{-1}\text{)} (E_a \text{ in kcal-mol}^{-1}\text{)}$	$k_{600 \text{ K}} \text{ (s}^{-1}\text{)}$	$k_{800 \text{ K}} \text{ (s}^{-1}\text{)}$	$k_{1000 \text{ K}} \text{ (s}^{-1}\text{)}$
<u>Daly [84]</u>	$10^{14.38} \exp(-61.54 / RT)$	9.0×10^{-9}	3.69×10^{-3}	8.50×10^0
<u>Choo [85]</u>	$10^{13.9} \exp((-59.0 \pm 1.0) / RT)$	2.5×10^{-8}	6.03×10^{-3}	1.01×10^1
<u>Brocard [86]</u>	$10^{14.0} \exp(-59.6 / RT)$	1.9×10^{-8}	5.21×10^{-3}	9.40×10^0
<u>Average</u>	$10^{14.03} \exp(-60.05 / RT)$	1.77×10^{-8}	4.98×10^{-3}	9.33×10^0
This study	$10^{10.34} T^{1.22} \exp(-59.54 / RT)$	1.00×10^{-8}	4.12×10^{-3}	9.69×10^0

The second focus of previous study on MTBE was abstraction reactions of MTBE by OH radical. The overall rate constants reported are $1.51 \times 10^{-12} \text{ cm}^3\text{-molecule}^{-1}\text{s}^{-1}$ by Cox et al [87]; $(5.1 \pm 1.6) \times 10^{-12} \exp[-(155 \pm 100) / T] \text{ cm}^3\text{-molecule}^{-1}\text{s}^{-1}$ by Wallington et al [88]; $(3.24 \pm 0.08) \times 10^{-12} \text{ cm}^3\text{-molecule}^{-1}\text{s}^{-1}$ by Wallington et al [89]; $(2.99 \pm 0.12) \times 10^{-12} \text{ cm}^3\text{-molecule}^{-1}\text{s}^{-1}$ by Smith et al [91], and our rate constants are $10^{7.03} T^{2.0} \exp(-0.525 \text{ kcal-mol}^{-1} / RT) \text{ cm}^3\text{-mol}^{-1}\text{s}^{-1}$ for $C_3COC + OH \rightarrow C_3.COC + H_2O$ ($k_{600 \text{ K}} = 4.16 \times 10^{-12} \text{ cm}^3\text{-molecule}^{-1}\text{s}^{-1}$; $k_{800 \text{ K}} = 8.25 \times 10^{-12} \text{ cm}^3\text{-molecule}^{-1}\text{s}^{-1}$; $k_{1000 \text{ K}} = 1.38 \times 10^{-11} \text{ cm}^3\text{-molecule}^{-1}\text{s}^{-1}$) and $10^{12.8} T^0 \exp(-0.739 \text{ kcal-mol}^{-1} / RT) \text{ cm}^3\text{-mol}^{-1}\text{s}^{-1}$ for $C_3COC + OH \rightarrow C_3COC. + H_2O$ ($k_{600 \text{ K}} = 5.60 \times 10^{-12} \text{ cm}^3\text{-molecule}^{-1}\text{s}^{-1}$; $k_{800 \text{ K}} = 6.54 \times 10^{-12} \text{ cm}^3\text{-molecule}^{-1}\text{s}^{-1}$; $k_{1000 \text{ K}} = 7.18 \times 10^{-12} \text{ cm}^3\text{-molecule}^{-1}\text{s}^{-1}$).

Early investigations on product distribution of MTBE oxidation were conducted by Tuazon et al [90] and Smith et al [91] in the presence of NO_x (see chapter 6). Dunphy and Simmie's[92] studied on the oxidation of MTBE but did not report any product distributions except ignition delay times verse temperatures.

Only available literature data in our knowledge are from Norton et al [93] and Held et al [94]. Please see discussion in section 9.3.

9.2 Comparison With Experimental Data at 4, 7 and 10 Atm

The modified CHEMKIN [83] computer code, which employs Chebyshev polynomials (7×3) to incorporate the pressure and temperature dependence (0.001 to 100 atm, 200 to 2500 K) into rate constant expressions, is used to integrate the kinetic equations and to calculate reverse rate constants from the forward rate constants and thermodynamic parameters. The pressure and temperature combined mechanism includes 1265 reactions and 268 species.

As shown in previous chapters, important products of MTBE decay under either pyrolysis or oxidation conditions are C₂C=C, CH₃OH, C₂C=O, C₃H₆, C₂H₄, CH₄, C=C(C)CHO, CO and CO₂. In current stage, model calculations agree with experimental results under some conditions and predict the trend of product distribution.

Comparisons of model calculations, on the time dependence of the reactant (MTBE) decay and major products (C₂C=C, CH₃OH, CH₄, C₂C=O and C₃H₆) formation, to experimental data collected in this study under the pyrolysis and oxidation conditions are illustrated in Appendix IIC Figure 125 - 148.

9.2.1 Fuel Lean Mixture

A comparison of experimental results and model calculations for fuel lean mixtures at different temperatures and pressures are shown in Appendix Figure IIC. 125 - 130. At pressure of 4 atm and 873 K (see Appendix Figure IIC. 125), the model predicts a slower MTBE decay than experimental data. Model calculations for $C_2C=C$, $C_2C=O$ and CH_4 agree well with experimental results, while production of C_3H_6 , CH_3OH and CH_2O from model calculations are higher than experimental results. Over-production of C_3H_6 , CH_3OH and CH_2O from model along with slower MTBE decay indicate a slower reaction proceeding, which may be due to a wall effect that is not considered in the model. A difference between $C_2C=C$ and CH_3OH concentration level is shown from model but it is smaller than that from experiment. When temperature increases to 923 K, experimental data shows that MTBE quickly decays and no those major products observed or detected under the experiment conditions in 0.5 - 1.0 sec (see Appendix Figure IIC. 126). When pressure increases to 7 atm and 10 atm from 4 atm (Appendix Figure IIC. 128, Figure IIC. 129), at 873 K, similar product distributions are predicted by model calculations. Better agreement on MTBE decay and CH_4 formation, as well as CH_2O and C_3H_6 formation at 7 atm and 823 K is shown Appendix Figure IIC. 127. A trend of product distribution is predicted from model at 10 atm and 798 K. At relatively lower temperatures and higher pressures, model gives better agreement for MTBE decay and CH_4 formation while only a trend could be predicted from model for other products $C_2C=C$ and CH_3OH as well as CH_2O , C_3H_6 and $C_2C=O$ formation (Appendix Figure IIC. 127, Figure IIC. 129).

9.2.2 Chemical Stoichiometric Fuel

A better agreement between experiment and model calculation for reactant decay and product formations is obtained at 873 K and 4 atm in the stoichiometric fuel environment (Appendix IIC Figure IIC. 131). Experiment data shows that major products $C_2C=C$ and CH_3OH reach maximum levels at the early reaction stage, then start to decrease at 0.9 sec, and other products $C_2C=O$, C_3H_6 , CH_4 , CH_2O increase with the reaction proceeding (0.5 - 1.2 sec). The difference between $C_2C=C$ and CH_3OH concentration levels from model calculation is smaller than that from experimental results. $C_2C=O$ and CH_4 are predicted well by model calculations, while model gives higher productions of C_3H_6 and CH_2O than that from experiments. Sensitivity analysis shows that at these conditions (873 K, 4 atm, 0.5 - 1.2 sec), MTBE decay and product formation are controlled by decomposition and oxidation of MTBE, and abstraction reactions of MTBE by radical pools, as well as further reactions of intermediate radicals and molecules. MTBE thermal decomposition, abstraction reaction of MTBE by O_2 , abstraction reaction of CH_2O by HO_2 are important pathways and reactions for controlling the overall rate of reaction system and product distribution under 4 atm and 873 K. Chemical activation pathways $C_3C. + CH_3O \rightarrow [C_3COC]^* \rightarrow \text{products}$ and $C_3CO. + CH_3 \rightarrow [C_3COC]^* \rightarrow \text{products}$ have important effects on product distribution, this is because chemically activated transition adducts contain more energy than thermally activated adducts do. At 873 K, experimental data become more disperse at 7 and 10 atm, which suggests a more sensitive experimental conditions. Good matches on MTBE decay and CH_4 formation between model calculation and experiment are obtained at 7 atm, 873 K, and become worse at 10 atm, 873 K. At 873 K, model calculations only predict product distribution trends but much

higher concentration levels for $\text{C}_2\text{C}=\text{O}$, C_3H_6 at both 7 and 10 atm, for $\text{C}_2\text{C}=\text{C}$, CH_3OH , CH_2O , model predicts down trends with residence time (1.0 - 5.6 sec) while experimental data show an up - top - down trend. At higher temperature (1023 K), model calculations seem to be differ from with experimental data, this suggest that more complex reaction pathways are involved in the reaction process. At 1023 K, few products are observed from experiment which should be accounted for by faster conversion of those products to final CO and CO_2 .

9.2.3 Fuel Rich Mixture

Because of reduced O_2 concentration in the fuel mixture, both experimental data and modeling results show that more CH_4 is produced from MTBE decay. Similar predictions by model to that in stoichiometric fuel mixtures are shown in Appendix Figure IIC. 137 - 142. Model gives good fit to experimental data at 873 K and 4 atm, and under predict CH_4 at 7atm and 10 atm for both lower and higher temperatures. Model predictions on CH_3OH , C_3H_6 , $\text{C}_2\text{C}=\text{O}$, and CH_2O are higher than those from experiment at 7 atm and have better fits to experimental data at 10 atm. Under prediction on $\text{C}_2\text{C}=\text{C}$ is the case for both 7 and 10 atm at 873 K. When temperature increases, a difference occurs between model and experiments just like the case in the stoichiometric fuel environments.

9.2.4 MTBE Pyrolysis

Comparisons of model calculations to experiment data are shown in Appendix Figure IIC. 143 - 148. Good agreements for MTBE decay and major products $\text{C}_2\text{C}=\text{C}$ and CH_3OH as well as $\text{C}_2\text{C}=\text{O}$, CH_2O and C_3H_6 formations between model calculation and

experimental data at 873 K and 4 atm are shown in Figure IIC. 143. Sensitivity analysis shows that under relatively low temperature (873 K) and pyrolysis condition only thermal decomposition of MTBE, and abstraction between MTBE and H, CH₃ radicals are important to MTBE decay. A deviation of model calculations from experiment data at 873 K and 4 atm is that more iso-butene is produced than CH₃OH from experiment while model predicts almost the same quantities of both C₂C=C and CH₃OH. Also modeling result gives a little bit higher C₃H₆ production. When temperature goes to 1023 K at 4 atm, fits are seen on MTBE decay and major product C₂C=C, CH₃OH formations but not on other products formation. Figure IIC. 144 (4atm and 1023 K) in Appendix IIC shows that modeling results are agree well with the experimental results for MTBE decay and C₂C=C formation, CH₃OH production is a little bit lower than C₂C=C in the model in contrast to a little higher CH₃OH than C₂C=C at 873 K. The productions of CH₄, C₂C=O, C₃H₆, and CH₂O are much lower in the model than that from experiment. In the pyrolysis environment, thermal decomposition reactions play uniquely important roles at intermediate and high temperatures, C₂C=C and CH₃OH are mainly from MTBE decomposition by a four-center elimination mechanism in the almost equal amount. The chemical activation channel $C_3C. + CH_3O \rightarrow [C_3COC]^* \rightarrow \text{products}$ and $C_3CO. + CH_3 \rightarrow [C_3COC]^* \rightarrow \text{products}$ are important to CH₄ and C₃H₆ as well as C₂C=O levels at 1023 K in MTBE pyrolysis system. Lower C₂C=O, C₃H₆ and CH₄ levels are predicted from model calculations than that are observed, this may be accounted for by assignments of rate constants of abstraction reactions of MTBE by H, CH₃ radicals. The other major source responsible for C₂C=O, C₃H₆ and CH₄ productions are the dissociation of intermediate radicals which are from MTBE thermal decomposition, sensitivity analysis

show that these intermediate's decomposition affect little on the $\text{C}_2\text{C}=\text{O}$, C_3H_6 and CH_4 production. At 873 K, thermal decomposition of CH_2O , abstraction reactions of CH_2O by H , CH_3 radicals are responsible for concentration levels of CH_2O from MTBE decay. At 1023 K, much lower levels of formaldehyde (CH_2O) may have a little bit more complicated reasons since CH_2O can be formed from many ways.

At 873 K, when pressure goes up to 7 atm and 10 atm (Appendix Figure IIC. 145, Figure IIC. 147), much faster decay of MTBE, a little bit higher level of CH_3OH , and higher level of C_3H_6 , lower levels of $\text{C}_2\text{C}=\text{O}$ and CH_2O , are observed in the model.

At 1023 K, when pressure goes higher, the discrepancies of model calculations from experimental results become larger for CH_4 and $\text{C}_2\text{C}=\text{O}$, smaller for C_3H_6 , and no change for CH_2O . Sensitivity analysis shows that the under predictions by model is due to lower productions of these species and is not due to dissociation of these species, nor by abstraction consuming of produced species. So, one of the reasons responsible for these discrepancies may be that we missed some other reaction pathways.

9.3 Comparison to Experimental Data at 1 Atm

Model calculations are also compared to experimental data at 1 atm. Experimental data at 1 atm, 923 K, and in both pyrolysis and stoichiometric oxidation environments were taken from this laboratory's previous work, and experimental data at 1 atm, 1028 K in oxidation ($\phi = 0.96$) environment were taken from Princeton's work, Held et al [94]. The comparisons with these experimental data at 1 atm are shown in Appendix Figure IIC. 49 - 51. The better fit is obtained at the condition of 1 atm, 923 K and stoichiometric oxidation environment. Faster decay of MTBE along with higher levels of $\text{C}_2\text{C}=\text{C}$ and

CH_3OH are observed in the model for experimental data at the conditions of 1 atm, 923 K and pyrolysis. Finally, model predicts much higher levels of $\text{C}_2\text{C}=\text{C}$ and CH_3OH , and much lower levels of CH_4 , C_2H_6 , C_3H_4 , C_3H_6 , $\text{C}_2\text{C}=\text{O}$ and CO for the experimental data under the conditions of 1 atm, 1028 K and oxidation ($\phi = 0.96$).

PART IV

TRANSITION STATES FOR $R_1R_2C.CCOOH \rightarrow R_1R_2C=C + C.H_2OOH$

CHAPTER 10

STUDY ON $R_1R_2C.CCOOH \rightarrow R_1R_2C=C + C.H_2OOH$

10.1 Overview

One interest and thrill of physical chemistry lies not so much in what reactants turn into which products but in the intricacies of the journey from one to the other- a journey that almost always involves a transition state, the heart of a chemical reaction.

A specific reaction series: one of beta scission of $C.CR'COOH$, hydroperoxy alkyl radical to form an olefin plus a hydroperoxy methyl radical $RC.OOH$. This $RC.OOH$ radical rapidly decomposes to lower energy products: $RCHO + OH$. Little or no evidence is observed for formation of the final products in the transition state of the first beta scission step. The primary alkyl radical is represented as $RC\cdot$, where R is alkyl group with at least one C (alkyl group such as CH_3 or C_2H_5) attached. It can be represented as $(R_1R_2C)C\cdot$ (R_1 and R_2 are either alkyl groups or H). $RC\cdot$ reacts with O_2 to form peroxide radical $(R_1R_2C)CCOO\cdot$. because of the high relative concentration of O_2 in combustion and that the reaction occurs with no energy of activation, and further undergoes isomerization reaction to form hydroperoxide radical $(R_1R_2C).C-CH_2OOH$: $C_3.CCOOH$ ($R_1 = R_2 = CH_3$), $C_2.CCOOH$ ($R_1 = CH_3$, $R_2 = H$), and $C.CCOOH$ ($R_1 = R_2 = H$). β -scission occurs to release $C.R_1R_2OOH$ radical and form an alkene species. The peroxide radical $(R_1R_2C)CCOO\cdot$ can also form $(R_1R_2C)CC.HOOH$ ($RC.HOOH$) radical. Note here and in all cases where a $C.H_2OOH$ or a $R-C.HOOH$ is formed; this type carbon radical when centered adjacent to a peroxy group will rapidly decompose to $CH_2O + OH$ or $RCHO + OH$ as the reaction is ca $30 \text{ kcal mole}^{-1}$ exothermic and has little or no barrier ([96] Page,

1990). The geometric structure of $\text{C.H}_2\text{OOH}$ radical, please see, as shown in figure in Appendix TS III. 5, calculated by MOPAC PM3 also indicates that it is a very unstable radical. The $\text{CH}_2\text{O--OH}$ bond has a 1.93 Å of bond length in the individual molecule which is much longer than normal O--O bond and in breaking status, the $\text{CH}_2\text{--OOH}$ bond, on the contrary, has a 1.207 Å of bond length which is very close to normal bond length in CH_2O (1.202 Å).

One of the concerns is the rate constant for $\text{C.H}_2\text{OOH}$ elimination reactions and the other one is whether there are two steps for hydroperoxide alkyl radical go to final products alkene + CH_2O + OH . or, is the entire reaction process the one step where the transition state sees the intermediate. The rate constants for $\text{C.H}_2\text{OOH}$ radical elimination reactions are usually estimated from reverse addition reaction, and the addition reaction of CH_3 radical to ethylene ($\text{C}=\text{C}$) has been taken as reference reaction since no literature data for $\text{C.H}_2\text{OOH}$ radical addition to alkene is available. Knowing the steps for a hydroperoxide alkyl radical to go to final products CH_2O + OH + alkene is important for understanding this $\text{C.H}_2\text{OOH}$ elimination or R.C.HOOH formation reactions.

In this study, we calculate three transition states which are the first examples of such a system where a $\text{C.H}_2\text{OOH}$ or a R-C.HOOH is formed, using semi-empirical (MOPAC PM3) method. Transition state theory and thermodynamic analysis are employed to obtain A factors for reactions. Thermodynamic properties of transition states and related species are listed in Appendix 3 TS III. 1. The bond lengths in reactants, transition states and products are listed in Appendix 3 along thermodynamic analysis information thus A factors.

10.2 C.CCOOH \rightarrow C=C + C.H₂OOH

Transition state for reaction C.CCOOH \rightarrow C=C + C.H₂OOH has been found and shown in Appendix TS III. 1. We notice that three bond lengths suffer large change between reactant, transition state and products. The forming carbon double bond, which has one carbon with radical site on and another carbon with C.H₂OOH radical on, has a 1.462 Å of bond length in reactant (C.CCOOH), a 1.347 Å of bond length in transition state and a 1.322 Å of bond length as a typical double bond in alkene (C=C). The breaking bond CC - COOH has a normal bond length of 1.530 Å in reactant (C.CCOOH), a 2.096 Å bond length is observed in the transition state. The much longer bond length in transition state of this breaking bond combining the bond length of the forming double bond which is very close to a typical double bond length indicates that the transition state is ready for forming products, a 2.80×10^{13} of A factor at 800 K is obtained from the calculation employing transition state theory based on ΔS^\ddagger from thermodynamic analysis for reaction C.CCOOH \rightarrow TS. With the increasing temperature, ΔS^\ddagger increases quickly from 8.45×10^{-16} at 300 K to 3.34×10^{-3} at 2000 K, which indicates increasing A factor therefore rate of reaction.

10.3 C2.CCOOH \rightarrow CC=C + C.H₂OOH

Transition state for reaction C2.CCOOH \rightarrow CC=C + C.H₂OOH is shown in Appendix TS III. 2. In transition state we found similar bond lengths to that for reaction C.CCOOH \rightarrow C=C + C.H₂OOH. The forming double bond has its bond length change from 1.471 Å in reactant to 1.357 Å in transition state, and 1.328 Å in final propene (CC=C). The breaking C2.C-COOH bond has its bond length change from 1.540 Å in the reactant to 2.090 Å in the transition state. The A factor of 3.48×10^{13} at 800 K is calculated the

same way as that for reaction $C.CCOOH \rightarrow C=C + C.H_2OOH$, and is a little bit larger than that of reaction $C.CCOOH \rightarrow C=C + C.H_2OOH$ (2.80×10^{13} at 800 K). A increasing ΔS^\ddagger with temperature, thus an increasing A factor, a positive temperature dependence of rate constant is found for this reaction.

10.4 $C3.CCOOH \rightarrow C2C=C + C.H_2OOH$

Calculation for $C3.CCOOH \rightarrow C2C=C + C.H_2OOH$ shows consistent data with the above ($C.CCOOH$, $C2.CCOOH$) two reactions. The forming carbon double bond change its bond length from 1.488 Å in the reactant to 1.364 Å in the transition state, and to 1.334 Å as a typical carbon double bond in iso-butene, and the breaking $C3.C - COOH$ bond has a 2.096 Å bond length in the transition state while a 1.548 Å in the reactant radical $C3.CCOOH$ (Appendix TS III. 3). The bond lengths in the transition state well consistent with that in the above two reaction transition states (Appendix TS III. 5). A positive temperature dependence of rate constants is seen from increasing ΔS^\ddagger with temperature via thermal reaction analysis (Appendix TS III. 9).

The other interesting bond lengths in the three transition states is $RC--OOH$ bond and $RCO--OH$ bond. We notice that the three transition states have almost the same $RC--OOH$ bond length of 1.345 Å, which are a little bit shorter than that in the reactants (1.411 Å, 1.412 Å and 1.394 Å for $C.CCOOH$, $C2.CCOOH$ and $C3.CCOOH$ respectively), much longer than a $C=O$ double bond in CH_2O (1.202 Å). Almost the same bond lengths of 1.534 Å are found in the three transition states for $RCO--OH$ bond, which is longer than a typical $O--O$ bond length (1.40 Å). But we do not see a trend of final products $CH_2O + OH$ being formed at the same time of beta scission.

At this point, we also conclude that the MOPAC PM3 calculation does not show any change in the bond length in the transition states when the substitutes on the carbon connected to both C.H₂OOH and radical site (carbon) change from two H to two methyl groups. This indicates a similar A factor could be used for this type reactions.

10.5 C.H₂OOH → CH₂O + OH

Comparing bond lengths of RC--OOH and RCO--OH in the transition states to that in the reactants (see discussion above), we do not see any evidence of the one step process for hydroperoxy alkyl radical to go directly to final product alkene + CH₂O + OH. The C=O bond length in CH₂O is 1.202 Å, the C.H₂OOH radical (Appendix III. 1-4) has a bond length of 1.930 Å for CO--OH bond and a bond length of 1.207 Å for C--OOH bond, this indicates the CH₂O + OH must be rapidly formed after formation of C.H₂OOH. Appendix III. 4 shows MOPAC calculation information for reactant and products of reaction C.H₂OOH → CH₂O + OH, we did not find transition state for this reaction. Thermodynamic analysis was performed for this reaction (Appendix III. 10) and the temperature dependence of reaction thermodynamic properties are small. And we may conclude here again that there are two steps instead of one step for hydroperoxide alkyl radical to go to the final products CH₂O + OH + alkene, and the first step is rate controlling step.

10.6 Thermodynamic Analysis and QRRK Analysis

One of the reason for us to concern this specific type of beta scission – C.H₂OOH elimination reactions, was to obtain the rate constants because they are important

reactions in combustion conditions: high O₂ level and the following dissociation of C.H₂OOH radical occurs with no energy of activation as we discussed above.

Thermodynamic properties of related reactants, transition states and products were calculated using MOPAC PM3 method and listed in Appendix III. 6. Thermodynamic analysis performed for three reactions are shown in Appendix TS III. 7-9. The A factor is calculated by use of transition state structures and the fit value in the temperature range 300 K to 2000 K is used as high pressure limit parameter for QRRK calculation. The activation energy is estimated in usual way as we mentioned in chapter 2 for β -scission reaction. A 7.8 kcal-mol⁻¹ of E_{a,r} is used for reverse addition reaction of the C.H₂OOH to the alkene double bond. The E_{a,f} for β -scission reaction can then be calculated using the principle of microscopic reversibility ($E_{a,f} = E_{a,r} + \Delta U_{\text{rxn}}$). The potential energy level diagram in Appendix TS III.11 shows a small decrease on E_{a,f} for dissociation of C.CCOOH, C2.CCOOH and C3.CCOOH respectively. This is due to the decrease on ΔU_{rxn} . The ΔU_{rxn} avg. (298, 1500 K) of dissociation reaction of C.CCOOH, C2.CCOOH and C3.CCOOH are 22.03, 20.77 and 19.56 kcal-mol⁻¹ respectively, and the calculated E_{a,f} are 29.8, 28.57 and 27.36 kcal-mol⁻¹. The temperature dependence of rate constants of these three reactions shown in Appendix TS III.12 illustrate a similar trend for three reactions. A slightly higher rate constant is observed for the higher substituted hydroperoxide radicals ($k_{\text{C3.CCOOH}} > k_{\text{C2.CCOOH}} > k_{\text{C.CCOOH}}$).

Appendix TS III.13-14 shows the pressure dependence of rate constants of three reactions. At 700 K, the high pressure limit rate constant (k_{∞}) is observed at about 1 atm for reaction C.CCOOH \rightarrow TS \rightarrow C=C + C.H₂OOH and C2.CCOOH \rightarrow TS \rightarrow CC=C +

C.H₂OOH, 10 atm for reaction C3.CCOOH → TS → C2C=C + C.H₂OOH. At higher temperature (1100 K), the pressure dependence of rate constants is observed in a wide pressure range for all three reactions (k_{∞} is not observed even at 100 atm), which indicates the pressure dependence of rate constant becomes much more important under the higher temperature conditions such as combustion. Appendix TS III.13-14 also show that the higher substitute (C3.CCOOH), the larger dependence of rate constant on pressure.

One other interesting trend for this type of reaction is the estimation of activation energy directly from MOPAC calculations. The heat of formations for three radicals and three alkene from THERM (group additivity) and MOPAC calculations (including corrections) are illustrated in Appendix TS III. 15 along with the activation energies from two methods (MOPAC and thermo chemical kinetics). We see a linear trend in the three sets of data, and a certain percent of overestimation for E_a . In this case, 16-18% of overestimation for E_a is found. Also we notice the lower heat of formation the hydroperoxide alkyl radical has, the lower ΔU_{rxn} thus lower E_a whether the E_a is from THERM or MOPAC, and the less overestimation for E_a . This suggest that direct estimation of E_a from MOPAC may be possible after more reactions are analyzed in order to get a more accurate value of percent of overestimation. But higher level of calculation such as Gaussian 94 (MP2) or density function are needed to verify MOPAC results.

10.7 Conclusion

Three examples for C.H₂OOH elimination reactions are analyzed in this study. Transition states, thermodynamic properties, A factors are calculated from MOPAC PM3 method. QRRK analysis is performed and shows a similar trend in the temperature and pressure

dependence of rate constants. Analysis also shows that MOPAC calculation for heat of formation of species could also be able to used with consideration of over- or under-estimations, therefore E_a can be directly obtained from MOPAC calculations. More analysis on this type of reactions need to be done.

APPENDIX IA

TABLES IN THE NEO-C₅H₁₁ + O₂ SYSTEM

Table IA. 1 Thermodynamic Properties for Species in the Neo-C₅H₁₁ + O₂ System

SPECIES	H ₂₉₈	S ₂₉₈	C _p							
			300	400	500	600	800	1000	1500	
HE	0.00	30.12	4.97	4.97	4.97	4.97	4.97	4.97	4.97	a
O ₂	0.00	49.00	6.86	7.10	7.33	7.54	7.89	8.18	8.70	a
H	52.10	27.30	4.90	4.90	4.90	4.90	4.90	4.90	4.90	a
OH	9.50	43.80	6.79	6.86	6.93	7.00	7.14	7.28		a
CH ₃	34.80	46.30	9.12	9.91	10.68	11.41	12.75	13.9	16	a
C ₂ H ₆	-20.40	55.08	12.38	15.68	18.80	21.58	26.04	29.54	35.16	c
I	25.50	43.20	5.00	5.00	5.00	5.00	5.00	5.00	5.00	b
C2C(COOH)COO.	-46.58	114.55	43.74	52.59	60.17	67.15	76.37	83.75		c
C2.C(COOH)COOH	-33.68	119.55	45.20	54.11	61.67	68.59	77.59	84.66		c
C=C(C)COOH	-24.38	90.10	30.23	36.16	41.22	45.79	52.26	57.51		c
C=C(C)CO.	13.70	80.55	23.83	28.87	33.43	37.38	43.75	48.41	55.38	c
C2C(COOH)C=O	-79.49	103.12	37.92	46.40	53.83	60.29	69.30	75.91		c
C2C(CO.)C=O	-42.14	94.04	31.71	39.64	46.56	52.29	60.91	66.84		c
C=C(C)C=O	-27.34	74.64	23.14	28.34	32.66	36.17	41.73	45.56		c
C2C=O	-51.56	70.09	17.97	22.00	25.89	29.34	34.93	39.15		c
CH ₂ O	-26.00	50.92	8.47	9.38	10.46	11.52	13.37	14.81		c
CH3O	3.96	55.84	9.51	11.04	12.61	14.13	16.67	18.58	21.43	c
C3.CO	-26.10	85.40	26.61	32.89	38.22	42.65	49.78	55.10		c
C2C(OH)COO.	-60.19	98.67	33.48	40.34	46.10	51.19	58.68	64.63		c
C2C(O.)COOH	-44.33	96.99	34.55	41.88	48.04	53.39	61.02	66.80		c
C2C.CO	-24.10	88.49	25.43	30.55	35.54	40.14	47.73	53.51		c
C2C(OO.)COH	-59.38	97.27	33.38	40.26	45.97	51.04	58.32	64.16		c
C2C(OOH)CO.	-43.52	95.59	34.45	41.80	47.91	53.24	60.66	66.33		c
C2C.OOH	-8.48	87.31	26.55	30.69	34.50	38.21	43.48	47.93		c
CH ₂ OOH	14.60	68.25	16.55	18.40	19.87	21.44	23.20	24.93		c
CH ₃ OO	4.30	65.18	13.88	15.47	16.85	18.44	20.49	22.71		c
C2CyCCOC	-33.33	77.34	26.78	35.56	43.27	49.57	58.91	65.50	75.54	d
C4C	-40.30	72.87	29.13	37.49	44.96	51.28	60.85	67.84	78.44	c
C3CC.	8.70	80.84	28.54	36.17	42.91	48.63	57.35	63.78	73.57	c
C3CCOO.	-25.39	93.62	34.19	42.97	50.69	57.01	66.47	73.23	83.65	d
C3.CCOOH	-12.49	101.74	36.32	45.45	53.22	59.42	68.32	74.46	83.82	d
C3CC.OOH	-17.59	97.71	37.60	45.62	52.68	58.96	67.79	74.49		c
C2C=C	-3.80	69.99	21.58	26.65	31.30	35.34	41.91	46.89	54.71	c
C=C(C)COOH	-24.38	90.10	30.23	36.16	41.22	45.79	52.26	57.51		c
C3CC=O	-58.30	82.68	29.59	37.43	44.45	50.31	59.18	65.47		c
C2C=C=O	-28.06	73.97	24.08	28.58	33.01	36.14	41.27	45.33	51.36	c
C3CCI	-22.10	90.40	32.14	40.65	48.46	54.39	63.63	70.27		c

**Table IA. 1 Thermodynamic Properties for Species in the Neo-C₅H₁₁ + O₂ System
(Cont')**

SPECIES	H _{f298}	S ₂₉₈	C _p						
			300	400	500	600	800	1000	1500
C3.CCI	26.90	97.79	31.55	39.33	46.41	51.74	60.13	66.21	c
C3CC.I	26.90	93.43	31.55	39.33	46.41	51.74	60.13	66.21	c

- a. *JANAF Thermochemical Tables* 3rd ed. NSRDS-NBS, 37, 1986.
b. Benson, S. W. *Thermochemical Kinetics* 2nd ed. Wiley, New York, 1976.
c. THERM: Computer Code for Thermodynamic Properties Estimation Ritter, E. R., Bozzelli, J. W. *Intl. J. Chem. kinet.* 23, 767, 1991.
d. H_{f298} are from THERM, S²⁹⁸ and C_p(T) is sourced from MOPAC PM3 calculations.

Table IA. 2 Comparison of Current Rates with Literature Recommendations

Sources	High Pressure limit parameters	Rate Constant ^(h)
Unimolecular Dissociation of Neopentyl: C3CC . → C2C=C + CH₃		
Hughes ^(a)	$k(s^{-1}) = 10^{13.9 \pm 0.5} \exp(-30.90 \pm 1.0 \text{ kcal-mol}^{-1} / RT)^{(d)}$	1.49×10^4
Baldwin ^(b)	$k(s^{-1}) = 10^{13.65 \pm 0.2} \exp(-30.48 \pm 1.44 \text{ kcal-mol}^{-1} / RT)$	1.36×10^4
Curran ^(c)	$k(s^{-1}) = 10^{13.98} \exp(-30.90 \text{ kcal-mol}^{-1} / RT)$	8.92×10^3
NJIT	$k(s^{-1}) = 10^{13.90} \exp(-30.76 \text{ kcal-mol}^{-1} / RT)^{(e)}$	$1.09 \times 10^4^{(i)}$
Isomerization of Neopentyl: C3CCOO. → C3.CCOOH		
Hughes	$k(s^{-1}) = 10^{12.2} \exp(-29.4 \text{ kcal-mol}^{-1} / RT)$	$1.23 \times 10^3^{(j)}$
Baldwin	$k(s^{-1}) = 10^{13.08} \exp(-28.7 \text{ kcal-mol}^{-1} / RT)$	1.31×10^4
Curran	$k(s^{-1}) = 10^{12.35} \exp(-23.9 \text{ kcal-mol}^{-1} / RT)$	7.66×10^4
NJIT	$k(s^{-1}) = 10^{9.7} T^{1.0} \exp(-22.7 \text{ kcal-mol}^{-1} / RT)^{(f)}$	1.15×10^5 (forward) 1.10×10^7 (reverse) ⁽ⁱ⁾
Epoxide Formation from Neopentyl Hydroperoxide: C3.CCOOH → C2CyCCOC + OH		
Hughes		
Baldwin	$k(s^{-1}) = 10^{11.30} \exp(-17.46 \text{ kcal-mol}^{-1} / RT)$	7.05×10^5
Curran	$k(s^{-1}) = 10^{10.40} \exp(-15.25 \text{ kcal-mol}^{-1} / RT)$	4.33×10^5
NJIT	$k(s^{-1}) = 10^{7.7} T^{0.71} \exp(-14.0 \text{ kcal-mol}^{-1} / RT)^{(f)}$	$9.77 \times 10^4^{(i)}$
Dissociation of Neopentyl Hydroperoxide: C3.CCOOH → C2C=C + CH₂OOH		
Hughes		
Baldwin	$k(s^{-1}) = 10^{13.65} \exp(-27.75 \text{ kcal-mol}^{-1} / RT)$	9.73×10^4
Curran	$k(s^{-1}) = 10^{13.70} \exp(-29.00 \text{ kcal-mol}^{-1} / RT)$	4.41×10^4
NJIT	$k(s^{-1}) = 10^{13.72} \exp(-28.18 \text{ kcal-mol}^{-1} / RT)^{(g)}$	$1.87 \times 10^4^{(i)}$

- (a) Hughes, Kevin J.; Halford-maw, Peter A.; Lightfoot, Phillip D.; Turanyi, Tamas and Pilling, Michael J., 24th Symposium (International) on Combustion/The Combustion Institute, 645-652 (1992)
- Hughes, K. J.; Lightfoot, P. D.; and Pilling, M. J., Chemical Physics Letters, 191(6), 581-586 (1992)
- (b) Baldwin, R. R.; Hisham, M. W. M. and Walker, R. W., J. Chem. Faraday Trans. I, 78, 1615-1627 (1982)
- (c) Curran, H. J.; Pitz, W. J.; Westbrook, C. K.; Hisham, M. W. M. and Walker, R. W., for The 26th International Symposium on Combustion, Naples, Italy.
- (d) Slagle, I. R.; Batt, L.; Gmurczyk, G. W. Gutman, D. and Tsang, W., The Journal of Physical Chemistry, 95(20), 7732-7739 (1991)
- (e) Fit to Gutman's (d) experimental data for rate constant
- (f) Based on TST. $\Delta S^\ddagger(T)$ was taken from semi-empirical and Ab Initio calculations. see text for detail
- (g) Calculated from reverse reaction. $A_r = 10^{11.2} \text{ s}^{-1}$, $E_{a_r} = 7.8 \text{ kcal mole}^{-1}$ (this work)
- (h) Calculated from rate constant expression at 700 K
- (i) Result from RRK calculation
- (j) Experimental value from (a)

Table IA. 3 Important Reactions Responsible for the Formation of OH

Reactions ^(a)	Percent (%) ^(b)
$\text{C}_3\text{CC.} + \text{O}_2 \Rightarrow \text{C}_2\text{CyCCOC} + \text{OH}$	69.65
$\text{C}_3\text{CC.} + \text{O}_2 \Rightarrow \text{C}_3\text{CC=O} + \text{OH}$	7.39
$\text{C}_3\text{CCOOH} + \text{O}_2 \Rightarrow \text{C=C(C)COOH} + \text{CH}_2\text{OOH}$	22.96
$\text{C}_3\text{CC.} + \text{O}_2 \Rightarrow \text{C}_2\text{C=C} + \text{CH}_2\text{OOH}$	
$\text{CH}_3 + \text{O}_2 \Rightarrow \text{CH}_2\text{O} + \text{OH}$	

(a) Conditions: $T = 700 \text{ K}$, $P_{\text{total}} = 0.807 \text{ atm}$, $[\text{C}_5\text{H}_{11}] = 7 \times 10^{12} \text{ cm}^{-3}$, $[\text{C}_5\text{H}_{11}]_0 = 3 \times 10^{11} \text{ cm}^{-3}$, $P_{\text{O}_2} = 63.3 \text{ Torr}$, Bath gas = He

(b) data were taken at the top point of OH growth curve

Table IA. 4 The Reaction Mechanism for Neopentyl Radical + O₂

Reactions	A ^a	n	E ^b	
C3CCI <=> C3CC. + I	1.00E+16	0	52100	c
C3CCI + OH <=> C3.CCI + H ₂ O	6.80E+08	1.42	899.6	c
C3CCI + OH <=> C3CC.I + H ₂ O	1.16E+08	1.55	204.7	c
C3CC.+ O ₂ <=> C3CCOO.	5.32E+45	-10.99	8972	d
C3CC.+ O ₂ <=> C3.CCOOH	9.58E+38	-8.31	13555	d
C3CC.+ O ₂ <=> C2C=C + CH ₂ OOH	4.91E+42	-8.65	27178	d
C3CC.+ O ₂ <=> C2CyCCOC + OH	1.31E+41	-8.82	20996	d
C3CC.+ O ₂ <=> C=C(C)COOH + CH ₃	5.41E+42	-8.66	26991	d
C3CC.+ O ₂ <=> C3CC.OOH	1.90E+15	-2.31	19285	d
C3CC.+ O ₂ <=> C3CC=O + OH	3.80E+21	-2.92	21244	d
C3CCOO. <=> C3.CCOOH	6.07E+42	-9.81	31384	d
C3CCOO. <=> C2C=C + CH ₂ OOH	1.90E+61	-14.69	56786	d
C3CCOO. <=> C2CyCCOC + OH	2.56E+50	-12.01	43926	d
C3CCOO. <=> C=C(C)COOH + CH ₃	1.60E+61	-14.67	56501	d
C3CCOO. <=> C3CC.OOH	1.90E+40	-10.41	51004	d
C3CCOO. <=> C3CC=O + OH	4.68E+46	-11.07	52949	d
C3.CCOOH <=> C2C=C + CH ₂ OOH	2.15E+29	-5.34	31508	d
C3.CCOOH <=> C2CyCCOC + OH	1.25E+19	-3.14	16575	d
C3.CCOOH <=> C=C(C)COOH + CH ₃	1.70E+29	-5.32	31177	d
C3CC.OOH <=> C3.CCOOH	5.01E+17	-4.94	575	d
C3CC.OOH <=> C3CC=O + OH	1.19E+05	1.07	-1948	d
CH ₂ OOH <=> HCHO + OH	3.63E+10	-0.66	595	d
C3CC. <=> C2C=C+CH ₃	2.04E+47	-10.85	39743	d
CH ₃ + O ₂ <=> CH ₃ OO	8.61E+31	-6.59	4931	d
CH ₃ + O ₂ <=> HCHO + OH	2.85E+08	1	12526	d
C3.CCOOH + O ₂ <=> C2C(COOH)COO.	4.88E+39	-9	7456	d
C3.CCOOH + O ₂ <=> C2.C(COOH)COOH	6.91E+38	-8.43	13957	d
C3.CCOOH + O ₂ <=> C=C(C)COOH + CH ₂ OOH	1.16E+45	-9.38	29174	d
C3.CCOOH + O ₂ <=> C2C(COOH)C=O + OH	6.01E+18	-3.24	21727	d
C2C(COOH)COO. <=> C2.C(COOH)COOH	7.59E+36	-8.18	28541	d
C2C(COOH)COO. <=> C=C(C)COOH + CH ₂ OOH	7.81E+56	-13.26	56447	d
C2C(COOH)COO. <=> C2C(COOH)C=O + OH	6.20E+35	-8.79	50582	d
C2.C(COOH)COOH <=> C=C(C)COOH + CH ₂ OOH	1.54E+26	-4.21	31584	d
C2.C(COOH)COOH <=> C2C(COOH)C=O + OH	4.00E+32	-8.05	40578	d
C=C(C)COOH <=> C=C(C)CO. + OH	2.33E+45	-9.68	53233	d
C=C(C)CO. <=> C=C(C)C=O + H	5.11E+43	-10.62	20054	d
C2C(COOH)C=O <=> C2C(CO.)CO + OH	1.45E+43	-8.92	52055	d
C2C(CO.)CO <=> C2C.C=O + HCHO	1.12E+10	-0.55	426	d
C2C.C=O <=> C=C(C)C=O + H	3.29E+29	-5.25	45282	d
C2C.C=O <=> C2C=C=O + H	7.26E+28	-5.08	44459	d
C2C=C + OH <=> C3.COH	9.34E+41	-9.52	8698	d
C3.COH + O ₂ <=> C2C(OH)COO.	1.78E+47	-11.4	9255	d

Table IA. 4 The Reaction Mechanism for the Neopentyl Radical + O₂ (Cont')

Reactions	A ^a	n	E ^b	
C3.CO ₂ H + O ₂ <=> C2C(O.)COOH	6.30E+32	-7.74	8612	d
C3.CO ₂ H + O ₂ <=> C2C=O + CH ₂ OOH	4.71E+34	-6.98	13531	d
C2C(OH)COO. <=> C2C(O.)COOH	6.03E+44	-11.5	29831	d
C2C(OH)COO. <=> C2C=O + CH ₂ OOH	2.62E+55	-13.57	41747	d
C2C(O.)COOH <=> C2C=O + CH ₂ OOH	8.87E+29	-6.16	14484	d
C2C=C + OH <=> C2C.CO ₂ H	3.38E+38	-8.4	8284	d
C2C.CO ₂ H + O ₂ <=> C2C(OO.)CO ₂ H	1.71E+55	-14.06	11164	d
C2C.CO ₂ H + O ₂ <=> C2C(OOH)CO.	2.47E+37	-9.41	9477	d
C2C.CO ₂ H + O ₂ <=> C2C.OOH + HCHO	7.86E+37	-8.22	13561	d
C2C(OO.)CO ₂ H <=> C2C(OOH)CO.	3.55E+47	-12.47	30351	d
C2C(OO.)CO ₂ H <=> C2C.OOH + HCHO	2.24E+58	-14.64	41636	d
C2C(OOH)CO. <=> C2C.OOH + HCHO	8.40E+28	-5.91	13365	d
C2C.OOH <=> C2C=O + OH	1.47E+07	0.38	-1166	d
OH <=> Y	8.80E+01	0	0	e
CH ₃ + CH ₃ <=> C ₂ H ₆	2.63E+65	-17.28	12709	d
CH ₃ OO. + CH ₃ <=> CH ₃ O + CH ₃ O	9.00E+12	0	0	d

a Unit is cm³/mole-s or s⁻¹

b Unit is cal/mole

c From reference 37

d Result from QRRK calculations

e Wall loss reaction and rate constant is taken from reference 8

Table IA. 5 Important Reaction Flux

Reactions	k^a	Flux at Indicated Time ^b	
		1.0 (ms)	1.8 (ms)
$C_3CC. \rightarrow C_2C=C + CH_3$	1.07E+04	1.87E-11	7.09E-12
$C_3CC.+ O_2 \rightarrow C_3CCOO.$	4.54E+11	1.14E-09	4.34E-10
$C_3CCOO. \rightarrow C_3CC.+ O_2$	1.19E+04	1.28E-09	4.81E-10
$C_3CCOO. \rightarrow C_3.CCOOH$	1.18E+05	1.27E-08	4.78E-09
$C_3.CCOOH \rightarrow C_3CCOO.$	1.14E+07	5.23E-09	1.96E-09
$C_3.CCOOH \rightarrow C_2C\gamma CCOC + OH$	9.73E+04	4.44E-11	1.67E-11
$C_3.CCOOH \rightarrow C_2C=C + C.H_2OOH$	2.00E+04	9.14E-12	3.43E-12
$C_3.CCOOH \rightarrow C=C(C)COOH + CH_3$	2.29E+04	1.05E-11	3.93E-12
$C_3.CCOOH + O_2 \rightarrow C_2C(COOH)COO.$	5.68E+11	3.75E-10	1.41E-10
$C_2C(COOH)COO. \rightarrow C_3.CCOOH + O_2$	1.53E+04	3.57E-10	1.33E-10
$C_2C(COOH)COO. \rightarrow C_2.C(COOH)COOH$	4.96E+04	1.16E-09	4.33E-10
$C_2.C(COOH)COOH \rightarrow C_2C(COOH)COO.$	3.41E+07	1.10E-09	4.12E-10
$CH_3 + O_2 \rightarrow CH_3OO.$	4.43E+11	1.22E-09	1.46E-09
$CH_3OO. \rightarrow CH_3 + O_2$	3.91E+04	4.20E-09	5.14E-09

a k is in unit of s^{-1} or $cm^3\text{-mole}^{-1}\text{-s}^{-1}$ and at 700 K and 0.807 atm

b Flux is in unit of $\text{mole}\text{-sec}\text{-cm}^{-3}$

APPENDIX IB
TRANSITION STATES IN THE NEO-C₅H₁₁ + O₂ SYSTEM

TS IB. 1 Thermodynamic Properties from MOPAC PM3 and THERM

SPECIES	H _{f298} ^a	S ₂₉₈ ^b	C _p ^b						
			300	400	500	600	800	1000	1500
MOPAC Calculations									
C2CyCCOC	-41.02	77.34	26.78	35.56	43.27	49.57	58.91	65.5	75.54
C3.CCOOH	-20.65	101.74 ^c	36.32	45.45	53.22	59.42	68.32	74.46	83.82
C3CCOO.	-16.93	93.62 ^d	34.19	42.97	50.69	57.01	66.47	73.23	83.65
TS(1) ^e	1.35	89.83 ^d	32.94	42.16	50.06	56.44	65.88	72.62	83.09
TS(2) ^f	15.25	84.06 ^d	32.61	42.47	50.9	57.69	67.65	74.59	85.03
THERM Calculations									
C2CyCCOC	-33.33	76.78	26.77	35.71	42.96	49.17	59.1	65.9	0
C3.CCOOH	-12.49	101.28	36.87	45.14	52.29	58.61	67.47	74.22	0
C3CCOO.	-25.39	94.11	35.41	43.62	50.79	57.17	66.25	73.31	0

a Unit in kcal-mol⁻¹.

b Unit in cal-mol⁻¹.

c correct for OI & spin degeneracy (Rln2)

d correct for spin degeneracy (Rln2)

e Transition state for reaction C3CCOO. <=> C3.CCOOH

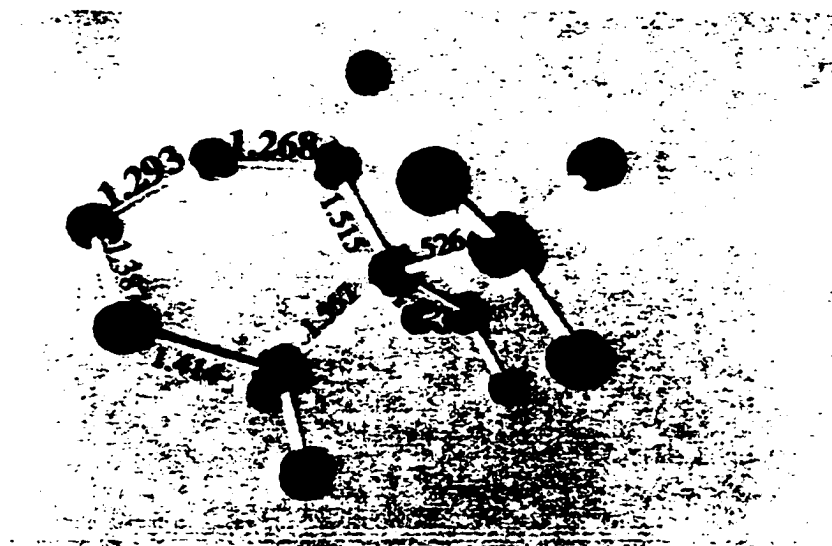
f Transition state for reaction C3.CCOOH <=> C2CyCCOC + OH

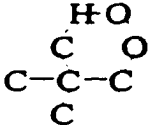
TS IB. 2 Thermodynamic Analysis of Transition State Related Reactions

Rx C3CCOO. = TS(1)*					
H_{f298} {kcal/mol}	-25.390		-2.690		
S_{298} {cal/mol-K}	93.620		84.060		
ΔH_r {kcal/mol} (298K) = 22.70			ΔH_r avg (298., 1500. K) = 23.23		
ΔS_r {cal/mol K} (298K) = -9.56			ΔS_r avg (298., 1500. K) = -9.13		
A_f/A_r (298 K) = 8.137E-03			A_f/A_r avg (298., 1500. K) = 1.01E-02		
Fit A_f/A_r	$A = 2.869E-02n = -.28$		$\alpha = -7.961E-04$		
T (K)	ΔH (kcal/mol)	ΔU (kcal/mol)	ΔS (cal/mol-K)	(A_f/A_r)	ΔG (kcal/mol)
300.00	2.270E+01	2.270E+01	-9.570E+00	8.096E-03	2.557E+01
400.00	2.259E+01	2.259E+01	-9.877E+00	6.937E-03	2.654E+01
500.00	2.258E+01	2.258E+01	-9.908E+00	6.829E-03	2.753E+01
600.00	2.263E+01	2.263E+01	-9.819E+00	7.144E-03	2.852E+01
800.00	2.283E+01	2.283E+01	-9.529E+00	8.267E-03	3.046E+01
1000.00	2.309E+01	2.309E+01	-9.242E+00	9.548E-03	3.233E+01
1200.00	2.335E+01	2.335E+01	-9.002E+00	1.078E-02	3.416E+01
1500.00	2.376E+01	2.376E+01	-8.701E+00	1.254E-02	3.681E+01
2000.00	2.453E+01	2.453E+01	-8.260E+00	1.565E-02	4.105E+01
Rx C3.CCOOH = TS(2)*					
H_{f298} {kcal/mol}	-12.490		1.510		
S_{298} {cal/mol-K}	101.740		89.830		
ΔH_r {kcal/mol} (298K) = 14.00			ΔH_r avg (298., 1500. K) = 12.71		
ΔS_r {cal/mol K} (298K) = -11.91			ΔS_r avg (298., 1500. K) = -13.95		
A_f/A_r (298K) = 2.494E-03			A_f/A_r avg (298., 1500. K) = 8.943E-04		
Fit A_f/A_r	$A = 4.026E+02$ $n = -2.17$		$\alpha = -1.197E-03$		
T (K)	ΔH (kcal/mol)	ΔU (kcal/mol)	ΔS (cal/mol-K)	(A_f/A_r)	ΔG (kcal/mol)
300.00	1.399E+01	1.399E+01	-1.193E+01	2.467E-03	1.757E+01
400.00	1.365E+01	1.365E+01	-1.291E+01	1.508E-03	1.882E+01
500.00	1.333E+01	1.333E+01	-1.363E+01	1.047E-03	2.015E+01
600.00	1.303E+01	1.303E+01	-1.419E+01	7.925E-04	2.154E+01
800.00	1.249E+01	1.249E+01	-1.496E+01	5.368E-04	2.446E+01
1000.00	1.206E+01	1.206E+01	-1.545E+01	4.206E-04	2.750E+01
1200.00	1.173E+01	1.173E+01	-1.575E+01	3.613E-04	3.063E+01
1500.00	1.141E+01	1.141E+01	-1.599E+01	3.207E-04	3.539E+01
2000.00	1.132E+01	1.132E+01	-1.605E+01	3.112E-04	4.341E+01

* TS(1) & TS(2) are the same as in Table 2a and Table 2b

TS IB. 3 Transition State (TS1) Structure and its Properties



Properties Of Transition State (TS1)							
TS(1)			Principal Moments of Inertial (cm^{-1})				
			A = 0.1336 B = 0.0643 C = 0.0614				
			Principal Moments of Initial (10^{-40} g-cm^2)				
			A = 209.510 B = 435.256 C = 455.821				
			Symmetry = 9				
			Barrier for Rotors				
			CH3--(CC3OOH) = 4.7 kJ/mole				
Frequencies (cm^{-1})							
-2767	81	178	203	264	309	330	418
448	464	496	548	672	690	875	946
959	965	977	988	1009	1057	1096	1126
1148	1235	1280	1320	1331	1360	1378	1400
1401	1402	1406	1413	1415	1417	2959	3038
3080	3080	3084	3085	3111	3134	3177	3178

TS IB. 4 Transition State's Z-Matrix (TS1) for MOPAC Calculation

PM3 PRECISE TS THERMO(298,1498,100) ROT=9 TRANS=3

Input Z-Matrix for MOPAC Calculation

Transition States for Reaction C3CCOO. → C3.CCOOH

	ATOM	CHEMICAL	BOND LENGTH	BOND ANGLE	TWIST ANGLE
	NUMBER	SYMBOL	(ANGSTROMS)	(DEGREES)	(DEGREES)
(I)		NA:I	NB:NA:I	NC:NB:NA:I	NA NB NC

1	C				
2	C	1.52517 *		1	
3	C	1.52638 *	109.34890 *	2 1	
4	C	1.55659 *	108.60235 *	-119.74564 *	2 1 3
5	C	1.51519 *	110.36392 *	121.35379 *	2 1 3
6	H	1.26814 *	107.69587 *	138.24071 *	5 2 1
7	O	1.29247 *	144.06736 *	-22.25409 *	6 5 2
8	O	1.41415 *	111.58871 *	-164.70251 *	4 2 1
9	H	1.09854 *	111.78460 *	-179.48823 *	1 2 3
10	H	1.09798 *	111.18068 *	60.28528 *	1 2 3
11	H	1.09783 *	111.09187 *	-59.41340 *	1 2 3
12	H	1.09821 *	111.25955 *	60.63817 *	3 2 1
13	H	1.09827 *	111.36133 *	-59.15849 *	3 2 1
14	H	1.09780 *	111.38918 *	-179.30266 *	3 2 1
15	H	1.10306 *	112.40537 *	81.98248 *	4 2 1
16	H	1.10663 *	110.69537 *	-39.79590 *	4 2 1
17	H	1.09202 *	115.26263 *	23.95895 *	5 2 1
18	H	1.09182 *	115.66422 *	-107.95967 *	5 2 1

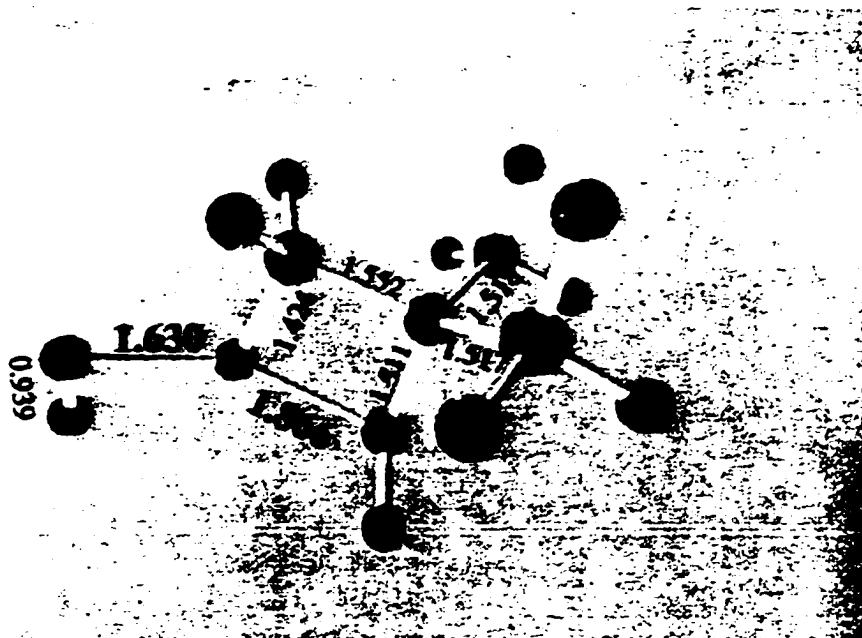
TS IB. 5 Interatomic Distances (TS1) from MOPAC Calculation

	C1	C2	C 3	C4	C 5	H 6	
C 1	.000000						
C 2	1.525169	.000000					
C 3	2.489701	1.526384	.000000				
C 4	2.502746	1.556586	2.521677	.000000			
C 5	2.496047	1.515188	2.494243	2.494134	.000000		
H 6	3.463071	2.252127	3.171443	2.452441	1.268136	.000000	
O 7	4.113112	2.886904	3.796703	2.297329	2.435755	1.292468	
O 8	3.749201	2.458179	3.096599	1.414151	2.767027	2.086142	
H 9	1.098543	2.185526	3.464022	2.765698	2.753286	3.563122	
H 10	1.097983	2.177570	2.748419	2.745619	3.460014	4.308334	
H 11	1.097830	2.176342	2.739946	3.476815	2.772790	3.953867	
H 12	2.752895	2.179799	1.098206	3.492593	2.764087	3.686681	
H 13	2.742481	2.181121	1.098272	2.775461	3.460634	4.079607	
H 14	3.460109	2.181115	1.097805	2.778882	2.753146	3.052027	
H 15	2.964337	2.224546	2.644636	1.103061	3.445008	3.453726	
H 16	2.605179	2.205694	3.462164	1.106627	2.921558	2.852976	
H 17	2.597860	2.213725	3.410232	3.088626	1.092020	1.850047	
H 18	3.197650	2.218292	2.568179	3.361477	1.091820	1.842622	
	O7	O8	H9	H 10	H 11	H 12	
O 7	.000000						
O 8	1.387168	.000000					
H 9	4.113133	3.981394	.000000				
H 10	4.762313	4.115381	1.772121	.000000			
H 11	4.836175	4.599323	1.771191	1.770999	.000000		
H 12	4.556924	4.070258	3.766989	3.114295	2.545435	.000000	
H 13	4.497554	3.531583	3.763930	2.543197	3.085103	1.770324	
H 14	3.534835	2.824883	4.329862	3.759807	3.758861	1.772126	
H 15	3.182593	1.959723	3.395241	2.796200	3.935739	3.701705	
H 16	2.576883	2.091746	2.420250	2.842782	3.662412	4.328535	
H 17	2.922361	3.501154	2.457203	3.668958	2.769106	3.550266	
H 18	3.087107	3.433577	3.633149	4.131434	3.165453	2.502324	

TS IB. 5 Interatomic Distances (TS1) from MOPAC Calculation (Cont')

	H13	H14	H15	H16H17	H18
H 13	.000000				
H 14	1.772320	.000000			
H 15	2.461169	2.878459	.000000		
H 16	3.670986	3.846308	1.795679	.000000	
H 17	4.296174	3.815352	4.112881	3.143349	.000000
H 18	3.653773	2.634277	4.183693	3.951492	1.800672 .000000

TS IB. 6 Transition State Structure (TS2) and its Properties



Properties Of Transition State (TS2)							
TS(2)	<div>OH C--O C-C-C C</div>		Principal Moments of Initial (cm ⁻¹)				
			A = 0.1568 B = 0.0529 C = 0.0512				
			Principal Moments of Initial (10 ⁻⁴⁰ g-cm ²)				
			A = 178.544 B = 529.411 C = 546.385				
			Symmetry = 9				
			Barrier for Rotors:				
			CH3--(CC3OOH) = 4.7 kJ/mole				
			OH--(C2CyCCOC) = 0.0 kJ/mole				
Frequencies (cm ⁻¹)							
-998	63	145	157	158	183	270	326
345	449	454	515	653	714	915	932
937	945	964	971	991	1004	1027	1074
1173	1241	1288	1321	1321	1370	1393	1400
1402	1403	1412	1415	1427	2968	3017	3081
3083	3083	3084	3122	3143	3177	3178	4001

TS IB. 7 Transition State (TS2) Z-Matrix for MOPAC Calculation

PM3 T=36000 PRECISE TS THERMO(298,1498,100) ROT=6 TRANS=4
 TSC2YC3O.DAT=TC2YC3OB.ARC+thermo see if get the same result as PC

ATOM NUMBER (I)	CHEMICAL SYMBOL	BOND LENGTH (ANGSTROMS) NA:I	BOND ANGLE (DEGREES) NB:NA:I	TWIST ANGLE (DEGREES) NC:NB:NA:I	NA	NB	NC
1	C						
2	C	1.51803 *			1		
3	C	1.51794 *	110.43310 *		2	1	
4	C	1.55149 *	112.42165 *	-126.49523 *	2	1	3
5	C	1.51128 *	112.69436 *	127.05850 *	2	1	3
6	O	1.86516 *	81.76388 *	114.76459 *	5	2	1
7	O	1.63063 *	151.14749 *	122.80247 *	6	5	2
8	H	1.09816 *	111.69155 *	-179.67800 *	1	2	3
9	H	1.09784 *	111.02266 *	60.25231 *	1	2	3
10	H	1.09778 *	111.11311 *	-59.53770 *	1	2	3
11	H	1.09778 *	111.11429 *	59.32907 *	3	2	1
12	H	1.09780 *	111.02746 *	-60.48985 *	3	2	1
13	H	1.09824 *	111.64831 *	179.43962 *	3	2	1
14	H	1.10412 *	113.93878 *	127.49080 *	4	2	1
15	H	1.10309 *	114.64780 *	1.81371 *	4	2	1
16	H	1.08920 *	119.72112 *	12.13858 *	5	2	1
17	H	1.08854 *	119.41148 *	-138.80923 *	5	2	1
18	H	0.93888 *	91.99001 *	70.99032 *	7	6	5

TS IB. 8 Interatomic Distance of TS2 from MOPAC Calculation

	C 1	C 2	C 3	C 4	C 5	O 6

C 1	.000000					
C 2	1.518041	.000000				
C 3	2.549899	1.551652	.000000			
C 4	2.493865	1.517850	2.552322	.000000		
C 5	2.522112	1.511203	2.265579	2.521621	.000000	
O 6	3.297928	2.226444	1.424285	3.356076	1.865534	.000000
H 7	1.097762	2.170367	3.507204	2.746716	2.857376	4.094420
H 8	1.097869	2.169141	2.855994	2.759682	3.471522	3.933033
H 9	1.098164	2.177824	2.777116	3.462720	2.743016	3.242497
H 10	2.619543	2.247583	1.103113	3.353695	3.062035	2.082843
H 11	3.369477	2.239857	1.104108	2.610736	3.027075	2.109135
H 12	2.756034	2.169899	3.507861	1.097773	2.846695	4.134907
H 13	3.462514	2.177138	2.771680	1.098236	2.750004	3.341459
H 14	2.750474	2.169222	2.868225	1.097803	3.472352	3.992638
H 15	3.433370	2.254514	2.967182	2.682426	1.088550	2.437927
H 16	2.687493	2.258884	2.977427	3.431399	1.089183	2.391726
O 17	4.814153	3.687595	2.469663	4.536300	3.386186	1.630273
H 18	5.188222	4.110177	3.105625	5.055716	3.467762	1.909510

	H 7	H 8	H 9	H 10	H 11	H 12

H 7	.000000					
H 8	1.772402	.000000				
H 9	1.771870	1.771857	.000000			
H 10	3.703394	2.680394	2.560526	.000000		
H 11	4.273396	3.455621	3.778347	1.789889	.000000	
H 12	2.552332	3.125320	3.766009	4.267523	3.691170	.000000
H 13	3.764063	3.770644	4.324130	3.752412	2.516166	1.771883
H 14	3.096044	2.560443	3.768856	3.428796	2.711632	1.772698
H 15	3.595268	4.332995	3.792852	3.926168	3.441690	2.854660
H 16	2.869779	3.753330	2.544106	3.504394	3.907682	3.580120
O 17	5.678565	5.279233	4.734729	2.907811	2.531641	5.431803
H 18	5.968555	5.793310	4.993579	3.538239	3.355151	5.841028

TS IB. 8 Interatomic Distance of TS2 from MOPAC Calculation

	H 13	H 14	H 15	H 16	O 17	H 18
H 13	.000000					
H 14	1.772143	.000000				
H 15	2.547123	3.749952	.000000			
H 16	3.798785	4.331582	1.833478	.000000		
O 17	4.225636	5.033353	3.645269	3.912016	.000000	
H 18	4.748895	5.683758	3.652430	3.798991	.938890	.000000

APPENDIX IC

FIGURES IN THE NEO-C₅H₁₁ + O₂ SYSTEM

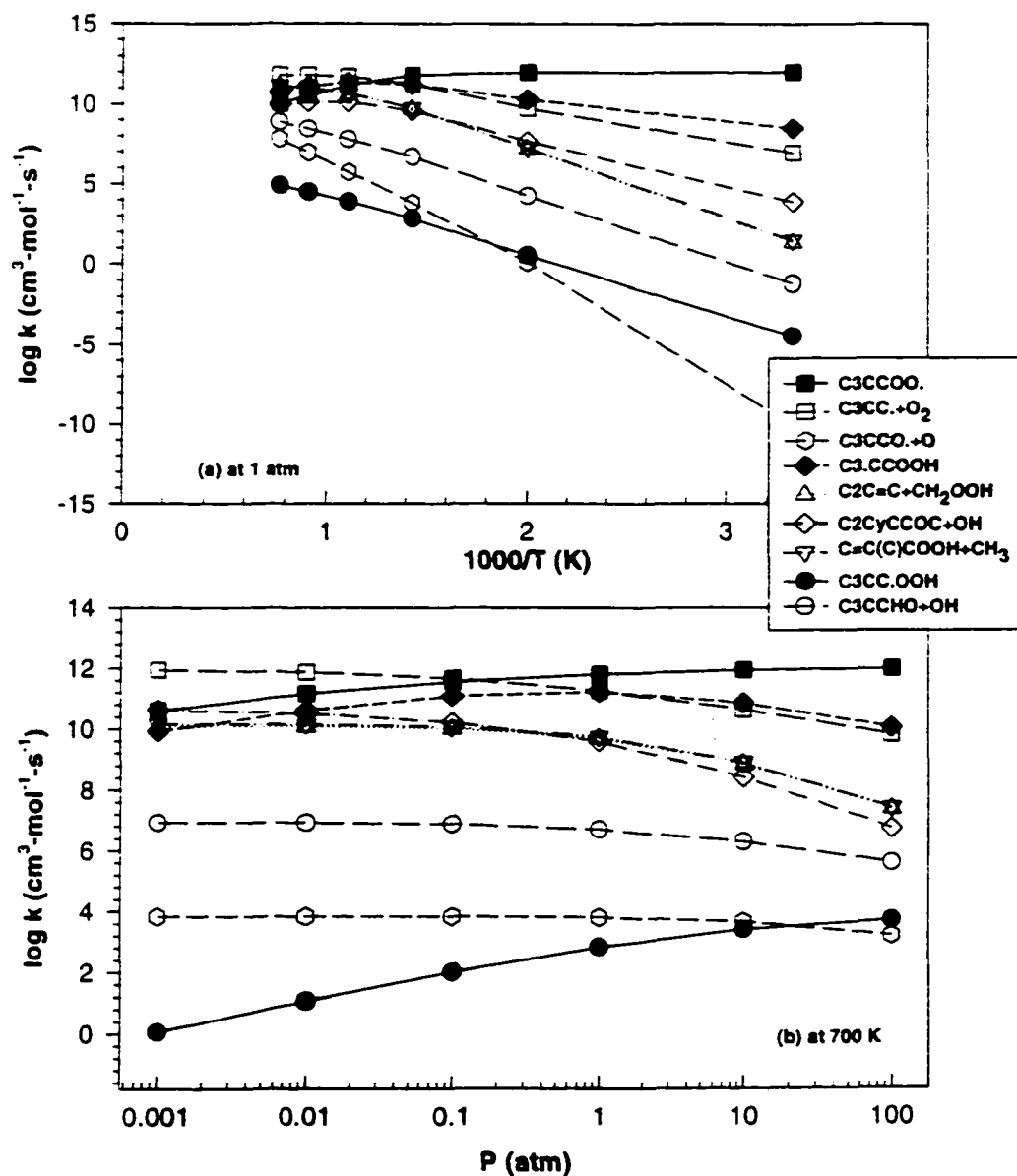


Figure IC. 1 Temperature and pressure dependence of rate constants of the various channels of $C_3CC. + O_2$ with He as bath gas

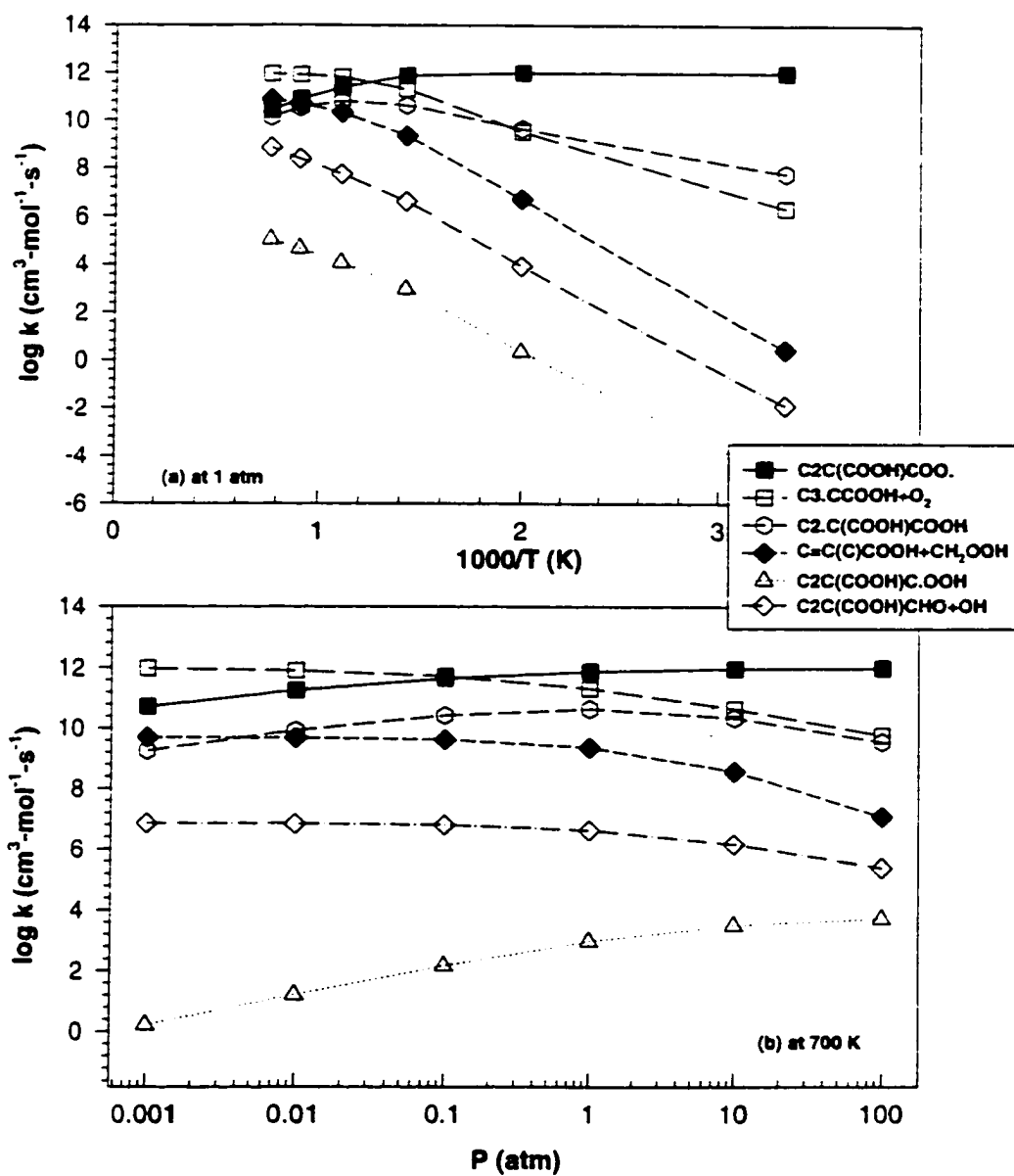


Figure IC. 2 Temperature and pressure dependence of rate constants of the various channels of $\text{C}_3\text{CCOOH} + \text{O}_2$ with He as bath gas

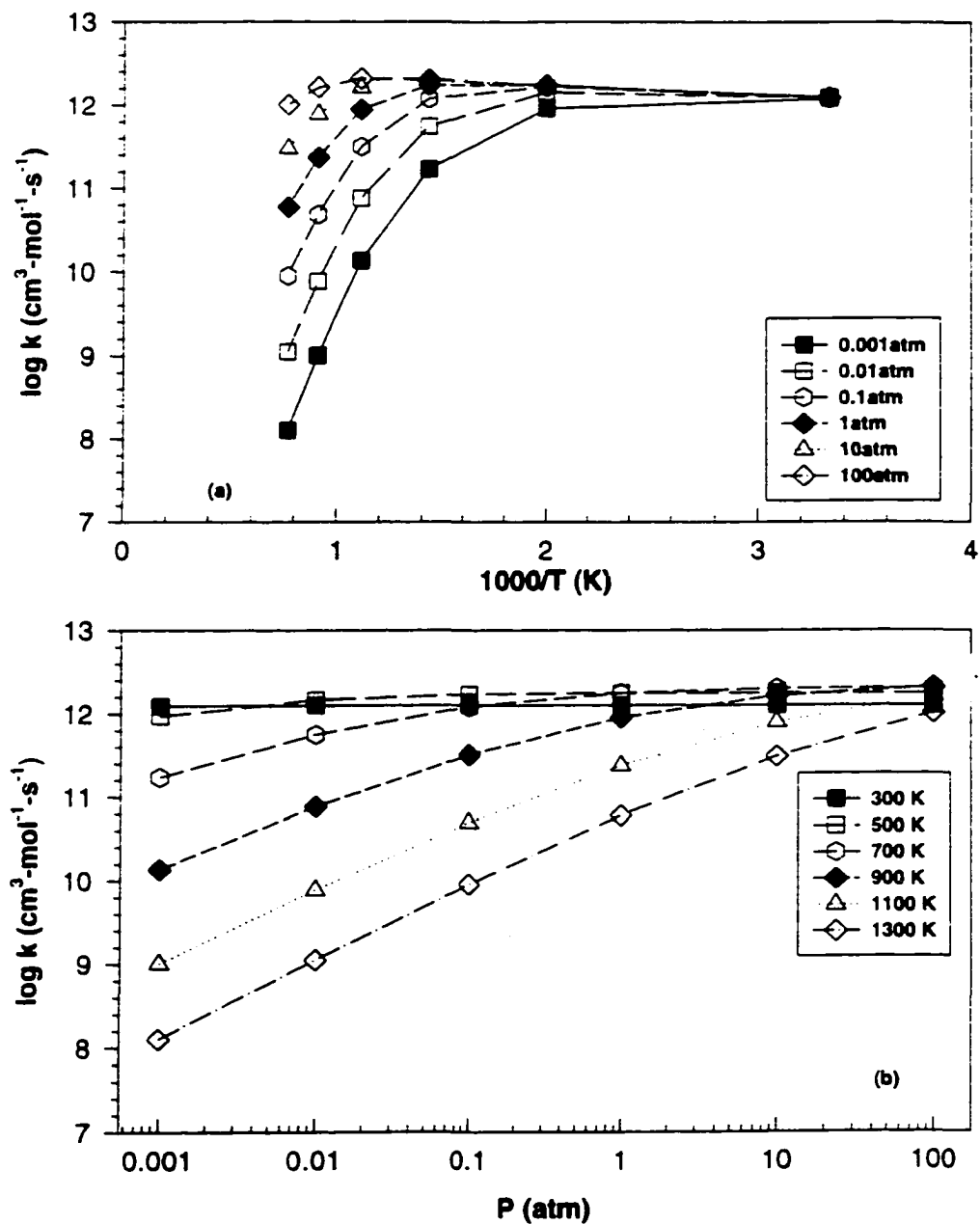


Figure IC. 3 Temperature and pressure dependence of reaction $\text{C}_2\text{C}=\text{C} + \text{OH} \rightarrow \text{C}_3.\text{COH}$ with He as bath gas

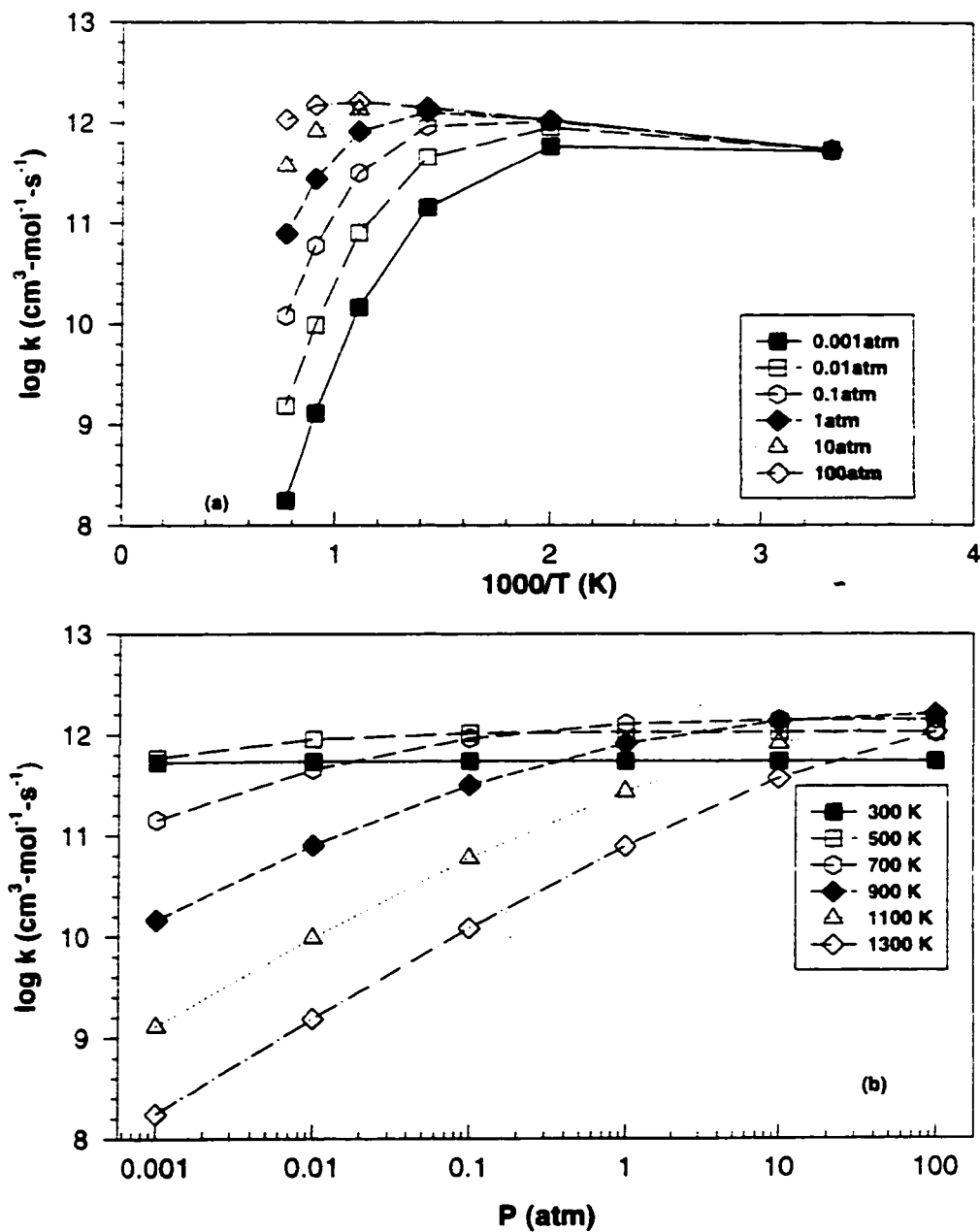


Figure IC. 4 Temperature and pressure dependence of reaction $\text{C}_2\text{C}=\text{C} + \text{OH} \rightarrow \text{C}_3.\text{COH}$ with He as bath gas

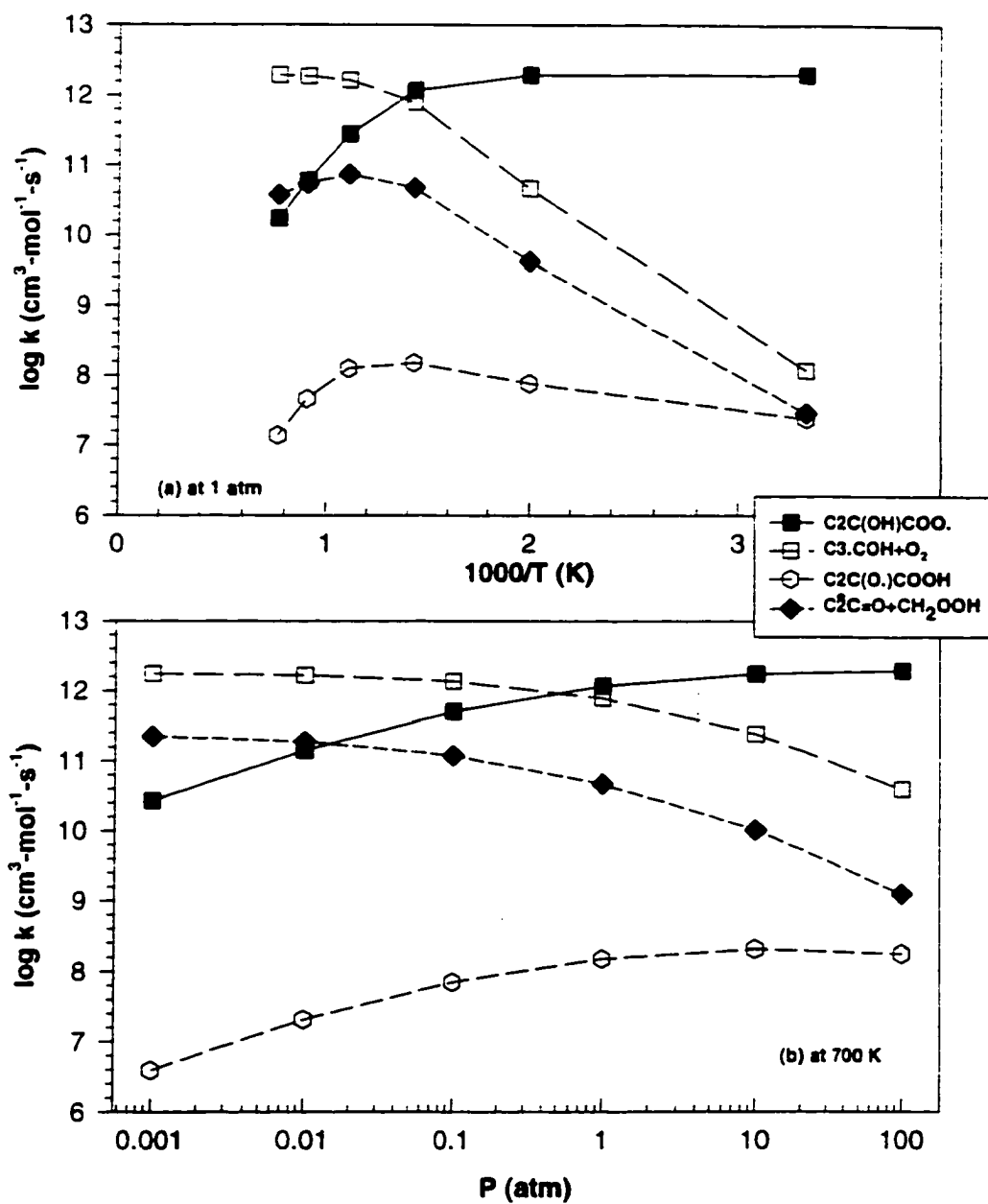


Figure IC.5 Temperature and pressure dependence of rate constants of the various channels of $\text{C}_3\text{COH} + \text{O}_2$ with He as bath gas

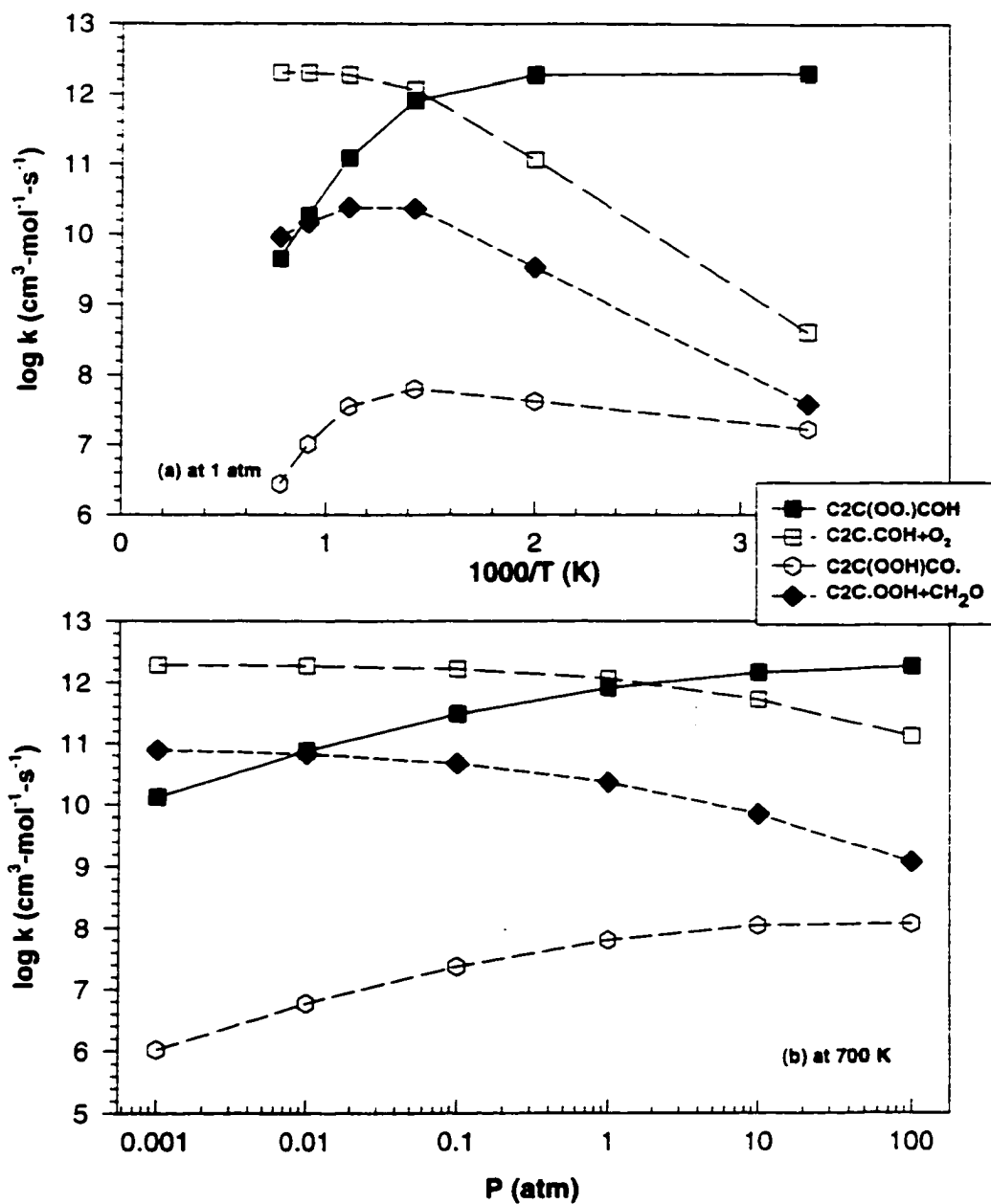


Figure IC. 6 Temperature and pressure dependence of rate constants of the various channels of $\text{C}_2\text{C.COH} + \text{O}_2$ with He as bath gas

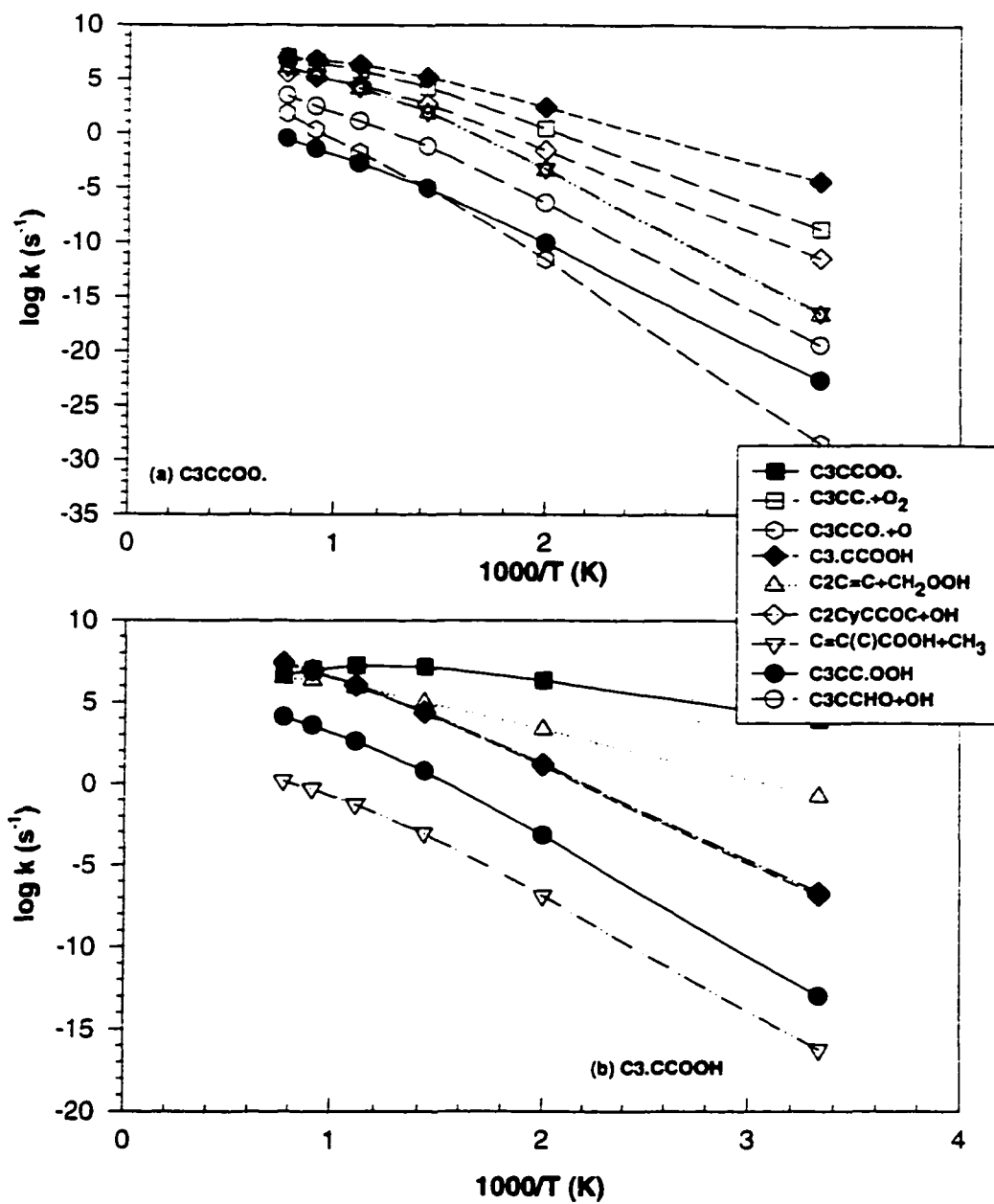


Figure IC. 7 Temperature dependence of rate constants of the various channels of stabilized adducts $C_3CCOO.$ / $C_3.CCOOH$ with He as bath gas

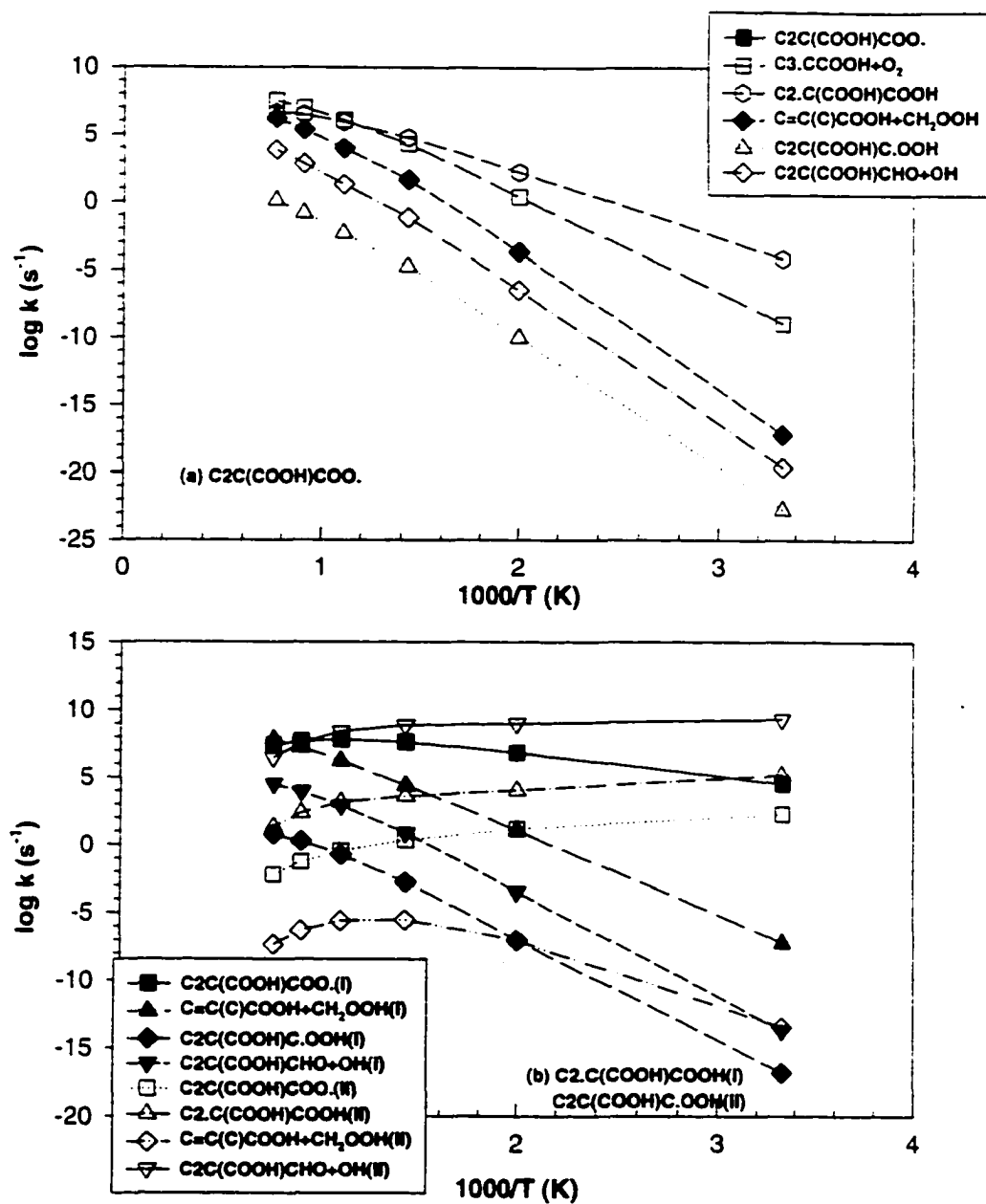


Figure IC. 8 Temperature dependence of rate constants of the various channels of stabilized adducts $C_2C(COOH)COO.$ / $C_2.C(COOH)COOH$ / $C_2C(COOH)C.OOH$ with He as bath gas

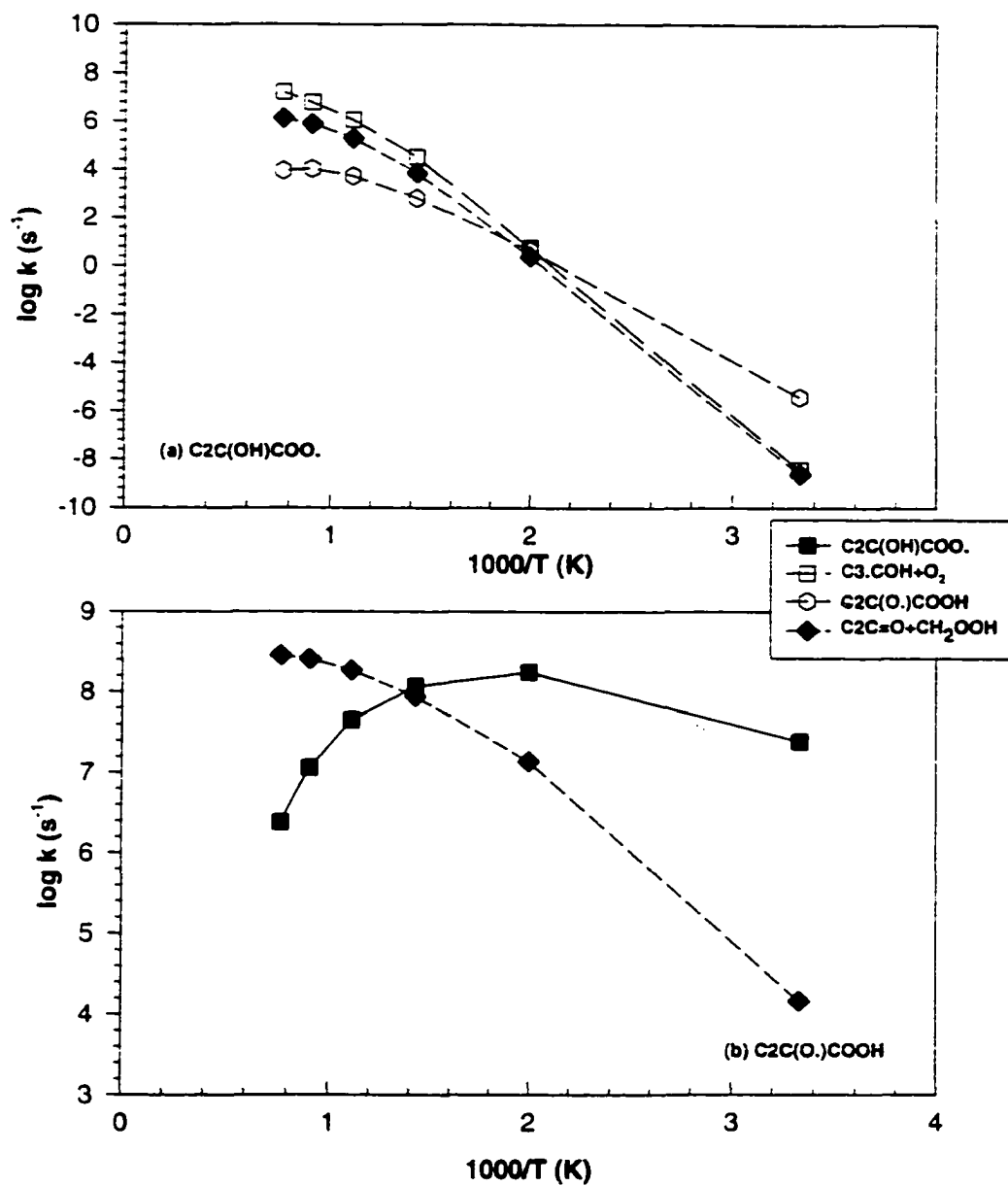


Figure IC. 9 Temperature dependence of rate constants of the various channels of stabilized adducts $\text{C}_2\text{C(OH)COO.} / \text{C}_2\text{C(O.)COOH}$ with He as bath gas

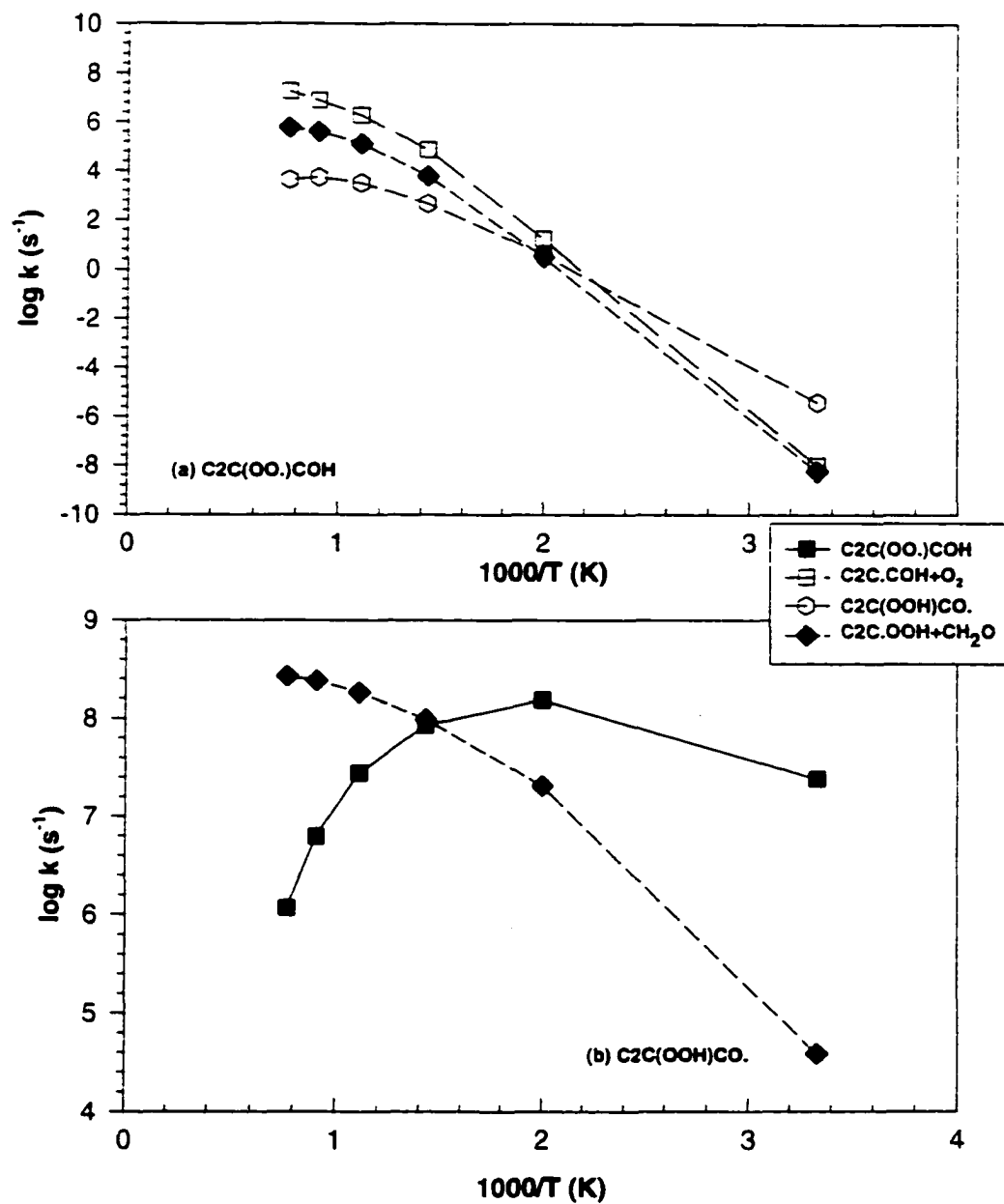


Figure IC. 10 Temperature dependence of rate constants of the various channels of stabilized adducts C2C(OO.)COH / C2C(OOH)CO. with He as bath gas

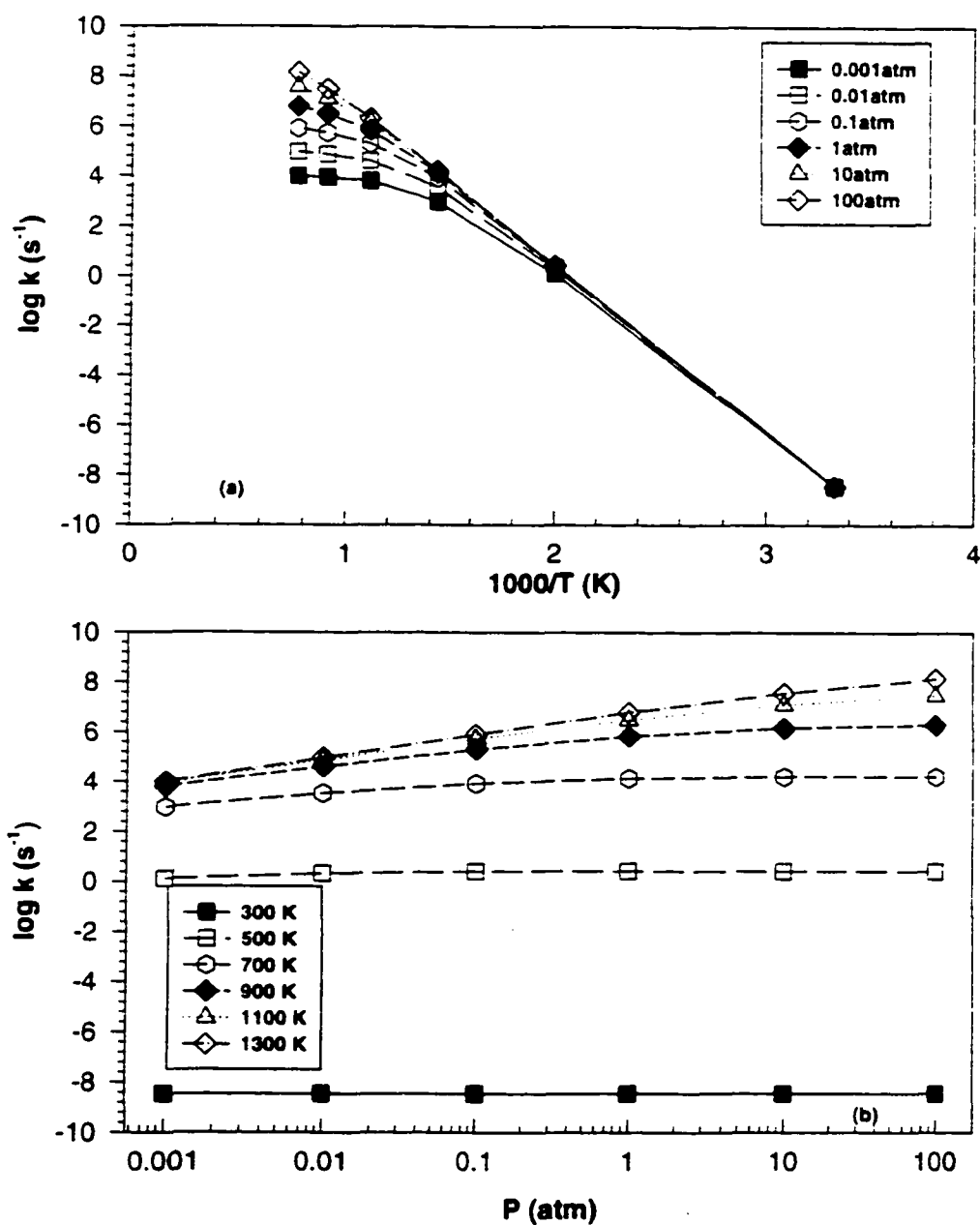


Figure IC. 11 Temperature and pressure dependence of reaction $\text{C}_3\text{CC} \cdot \rightarrow \text{C}_2\text{C}=\text{C} + \text{CH}_3$ with He as bath gas

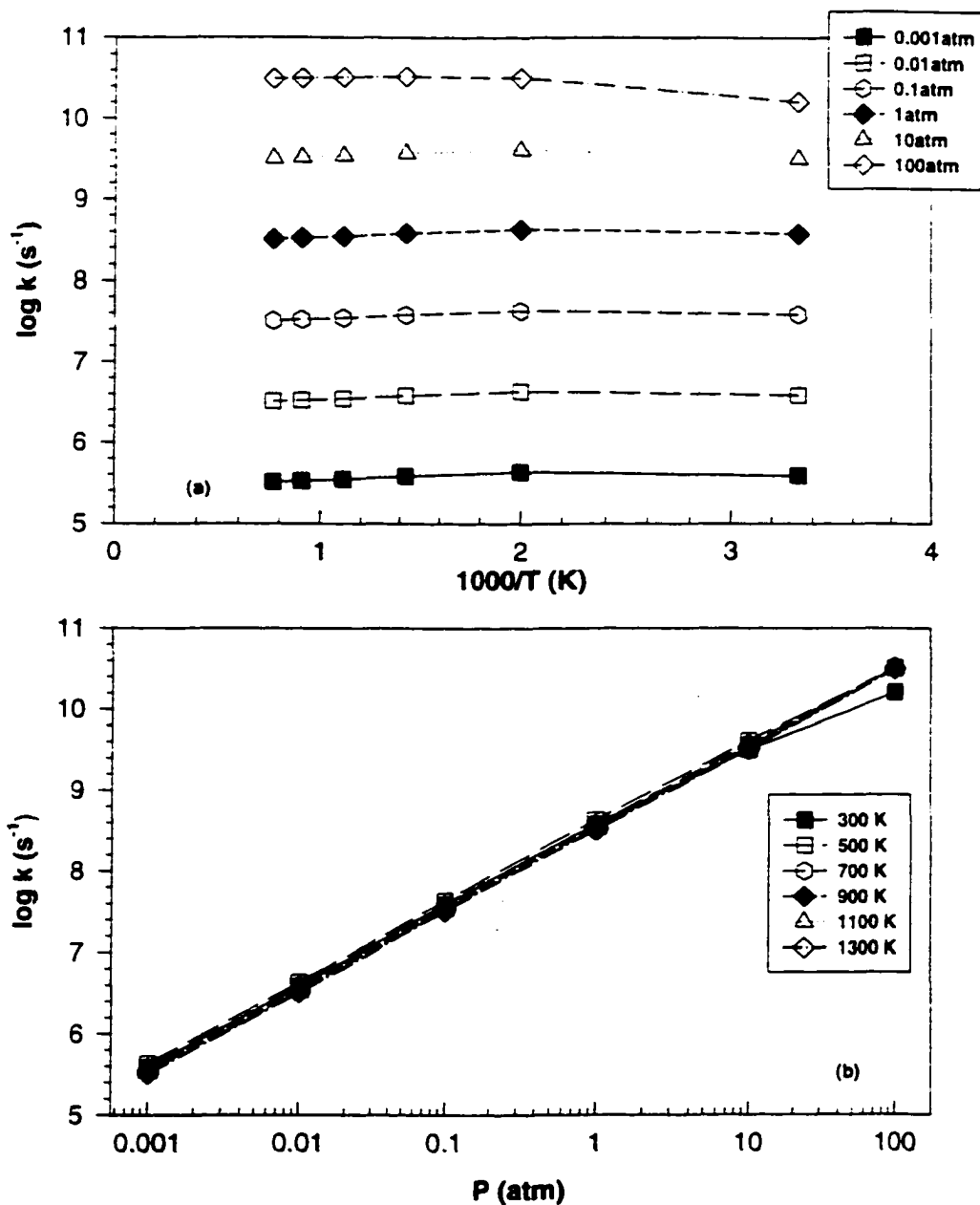


Figure IC. 12 Temperature and pressure dependence of reaction $\text{CH}_2\text{OOH} \rightarrow \text{CH}_2\text{O} + \text{OH}$ with He as bath gas

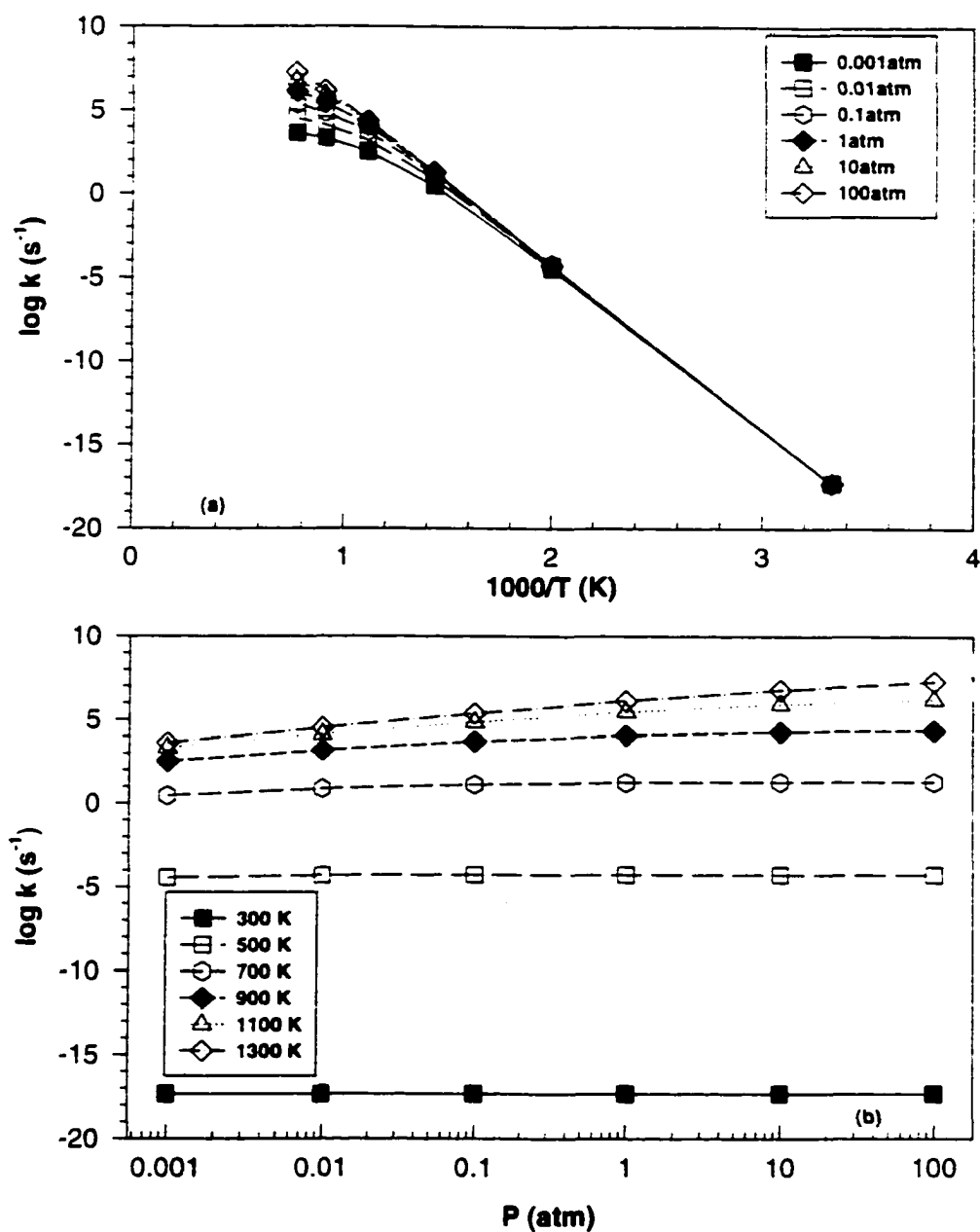


Figure IC. 13 Temperature and pressure dependence of reaction $\text{C}=\text{C}(\text{C})\text{COOH} \rightarrow \text{C}=\text{C}(\text{C})\text{CO.} + \text{OH}$ with He as bath gas

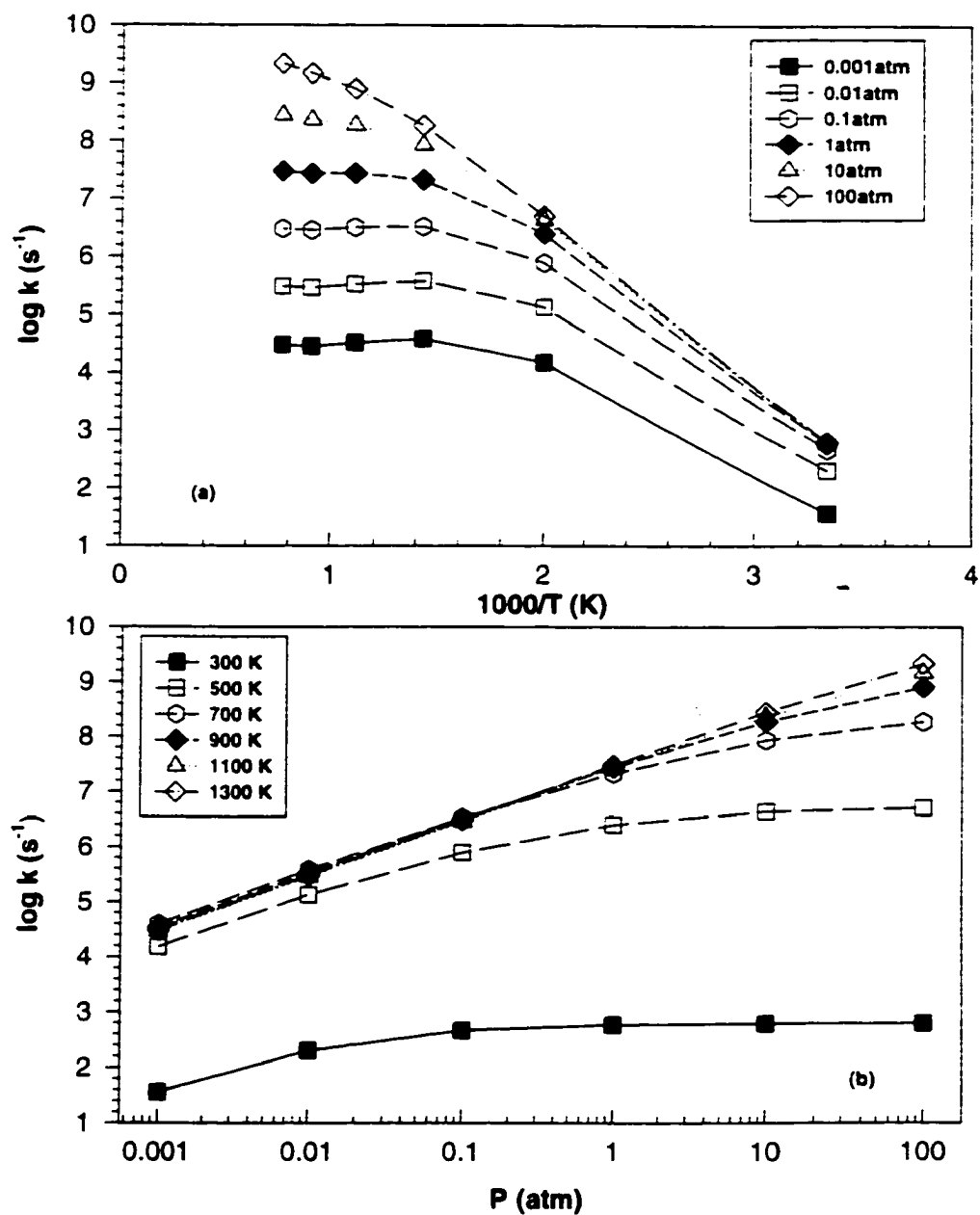


Figure IC. 14 Temperature and pressure dependence of reaction $\text{C}=\text{C}(\text{C})\text{CO} \cdot \rightarrow \text{C}=\text{C}(\text{C})\text{CHO} + \text{H}$ with He as bath gas

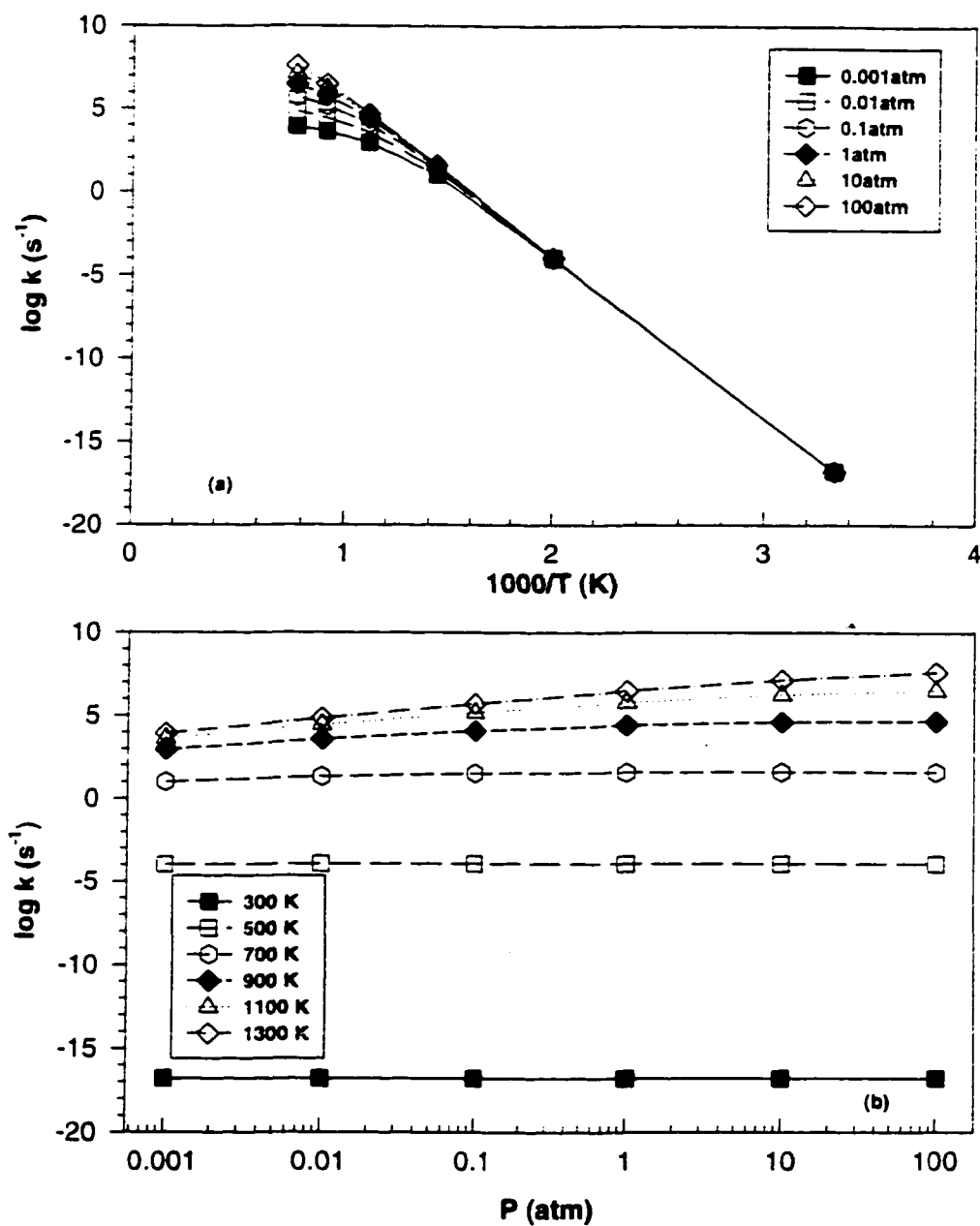


Figure IC. 15 Temperature and pressure dependence of reaction $\text{C}_2\text{C}(\text{COOH})\text{CHO} \rightarrow \text{C}_2\text{C}(\text{CO.})\text{CHO} + \text{OH}$ with He as bath gas

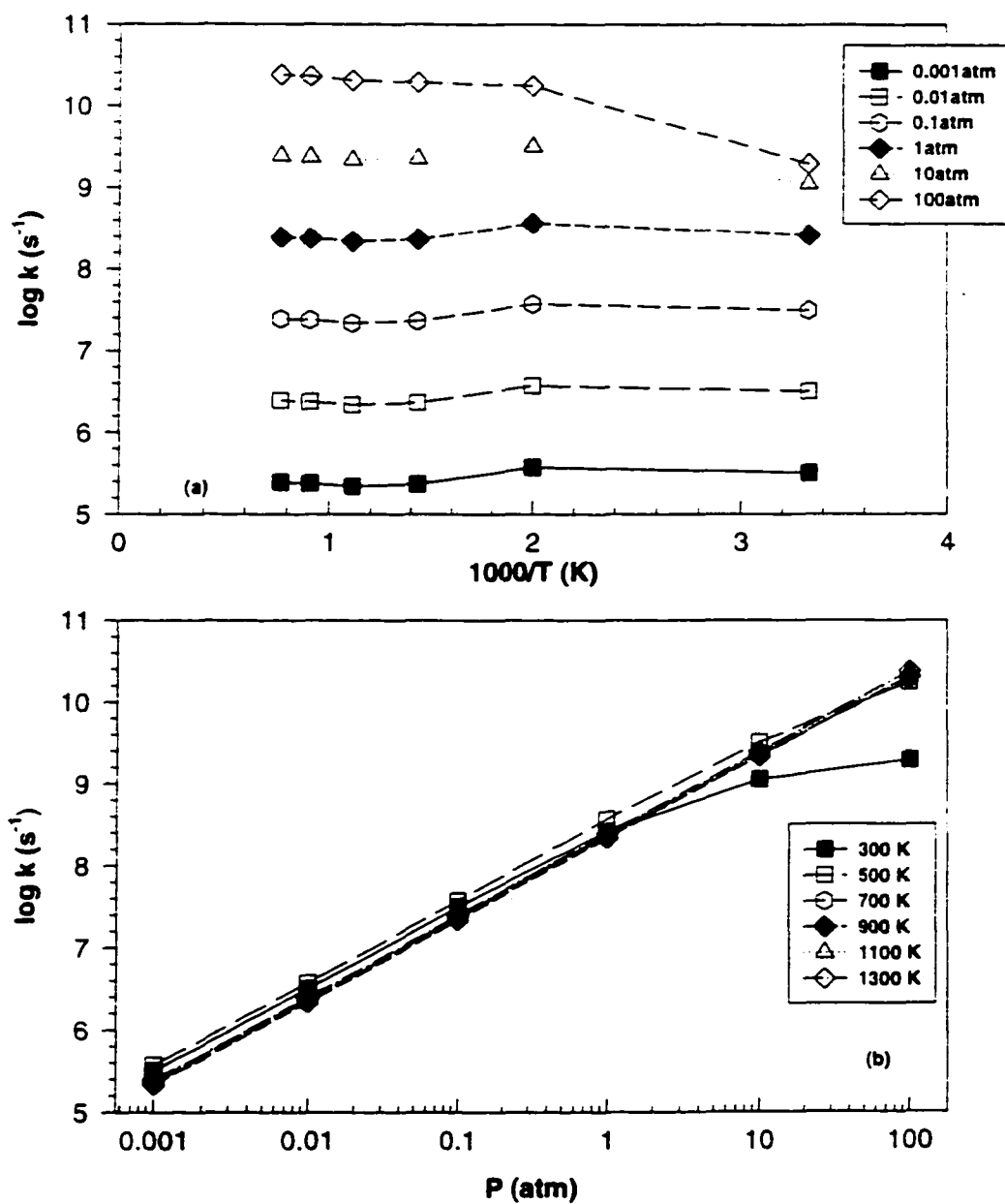


Figure IC. 16 Temperature and pressure dependence of reaction $\text{C}_2\text{C}(\text{CO})\text{CHO} \rightarrow \text{C}_2\text{C.CHO} + \text{CH}_2\text{O}$ with He as bath gas

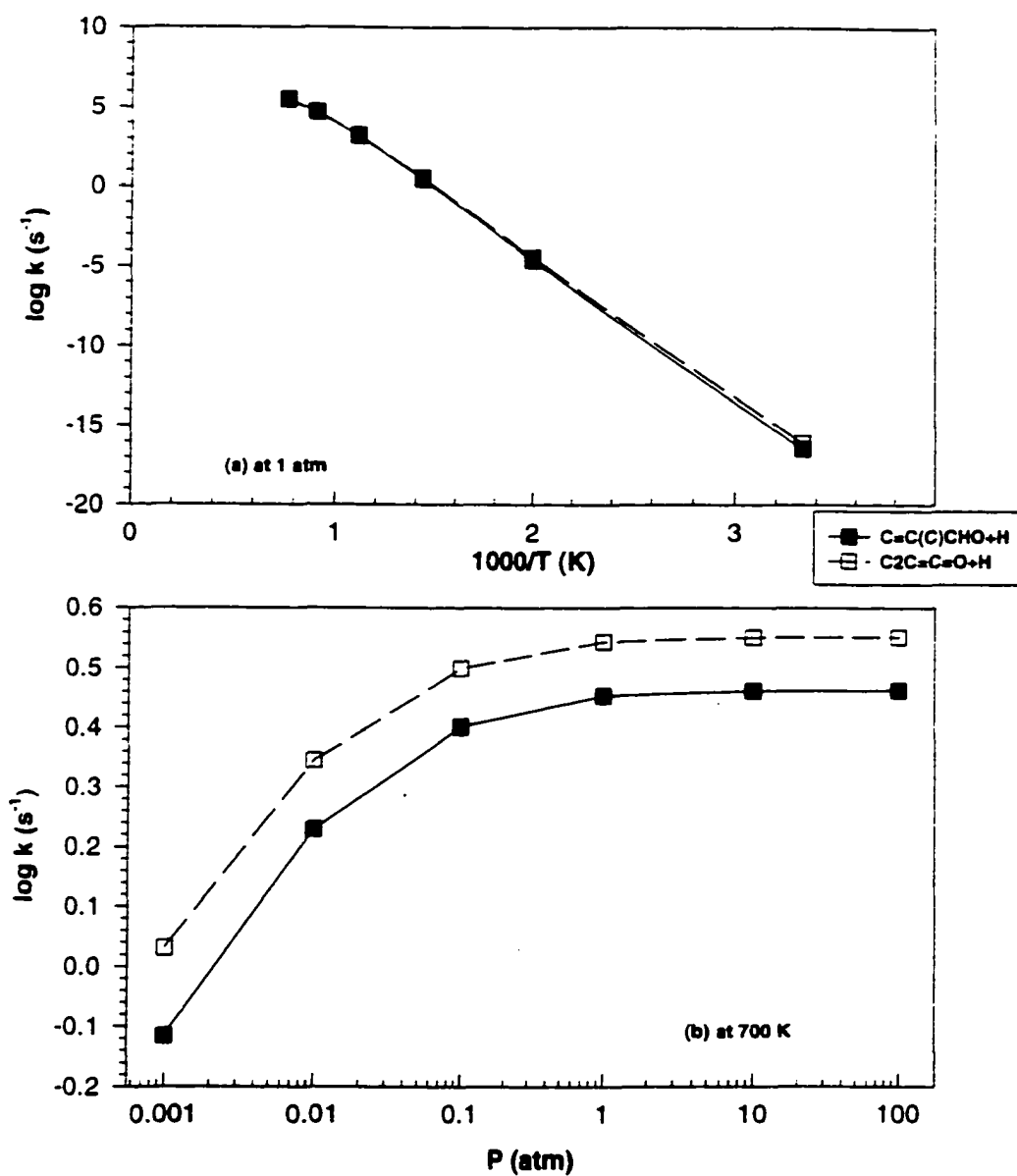


Figure IC. 17 Temperature and pressure dependence of reaction $\text{C}_2\text{C}.\text{CHO} \rightarrow \text{Products}$ with He as bath gas

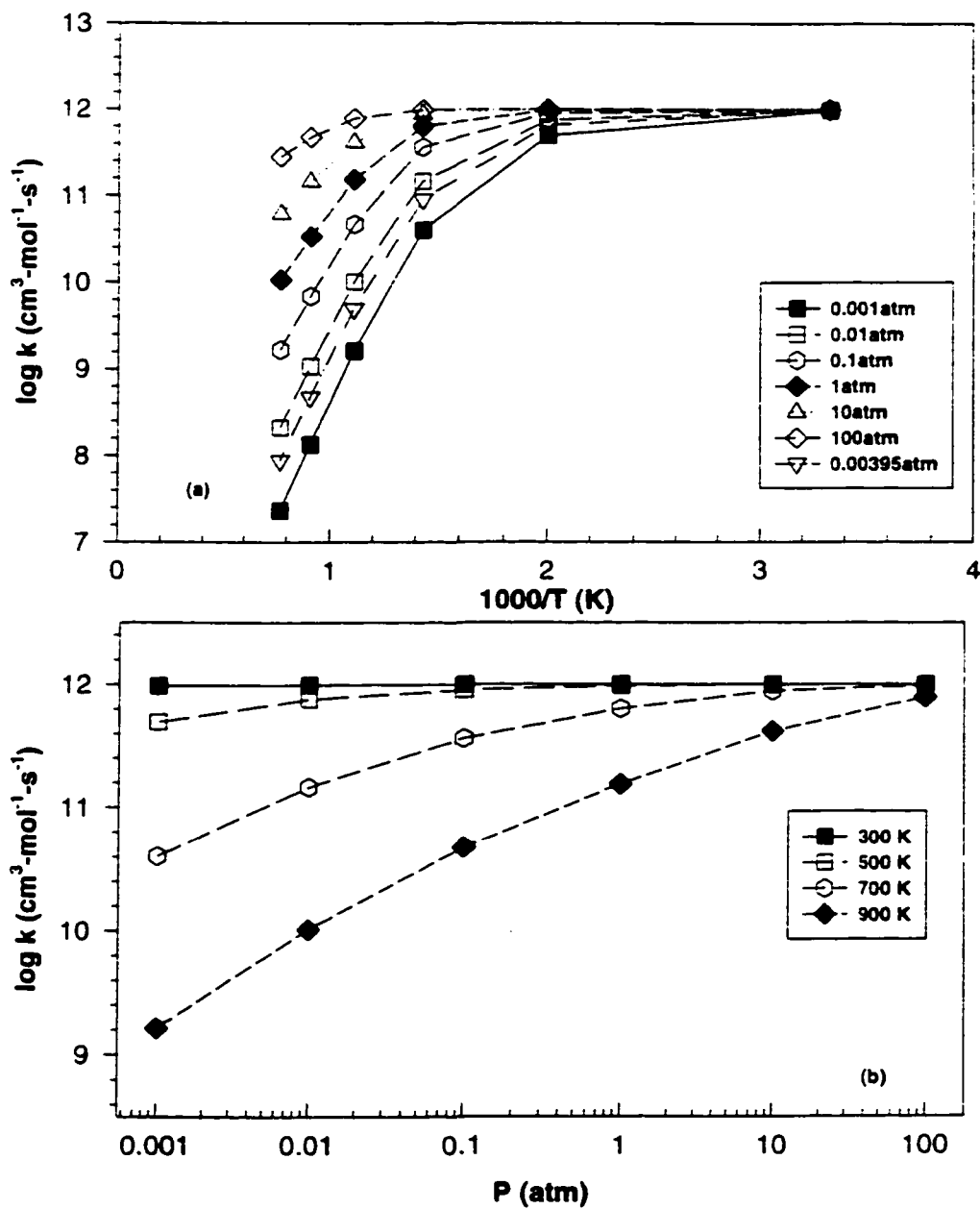


Figure IC. 18 Fall-off in the reaction $\text{C}_3\text{CC.} + \text{O}_2 \rightarrow \text{C}_3\text{CCOO.}$

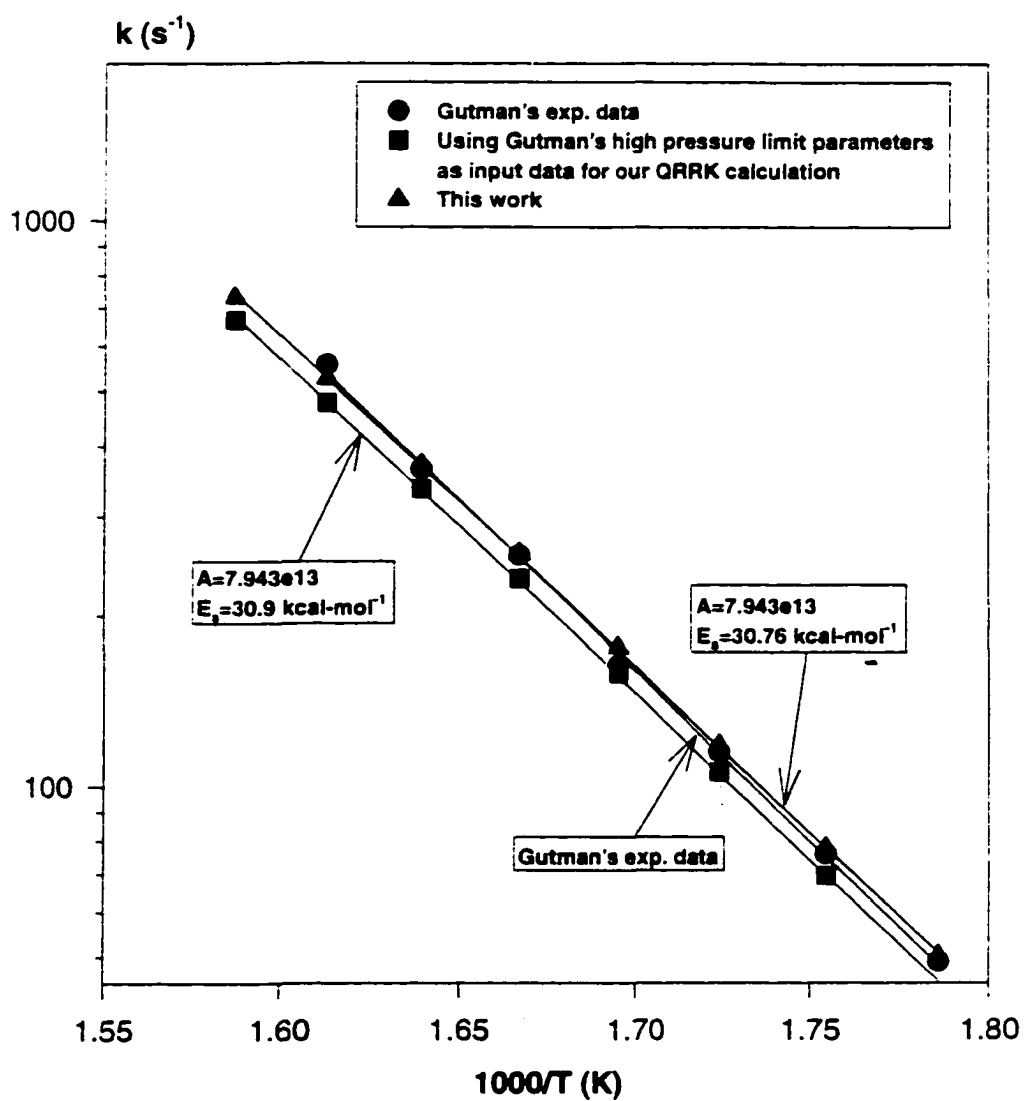


Figure IC. 19 Comparison with Gutman's experimental result

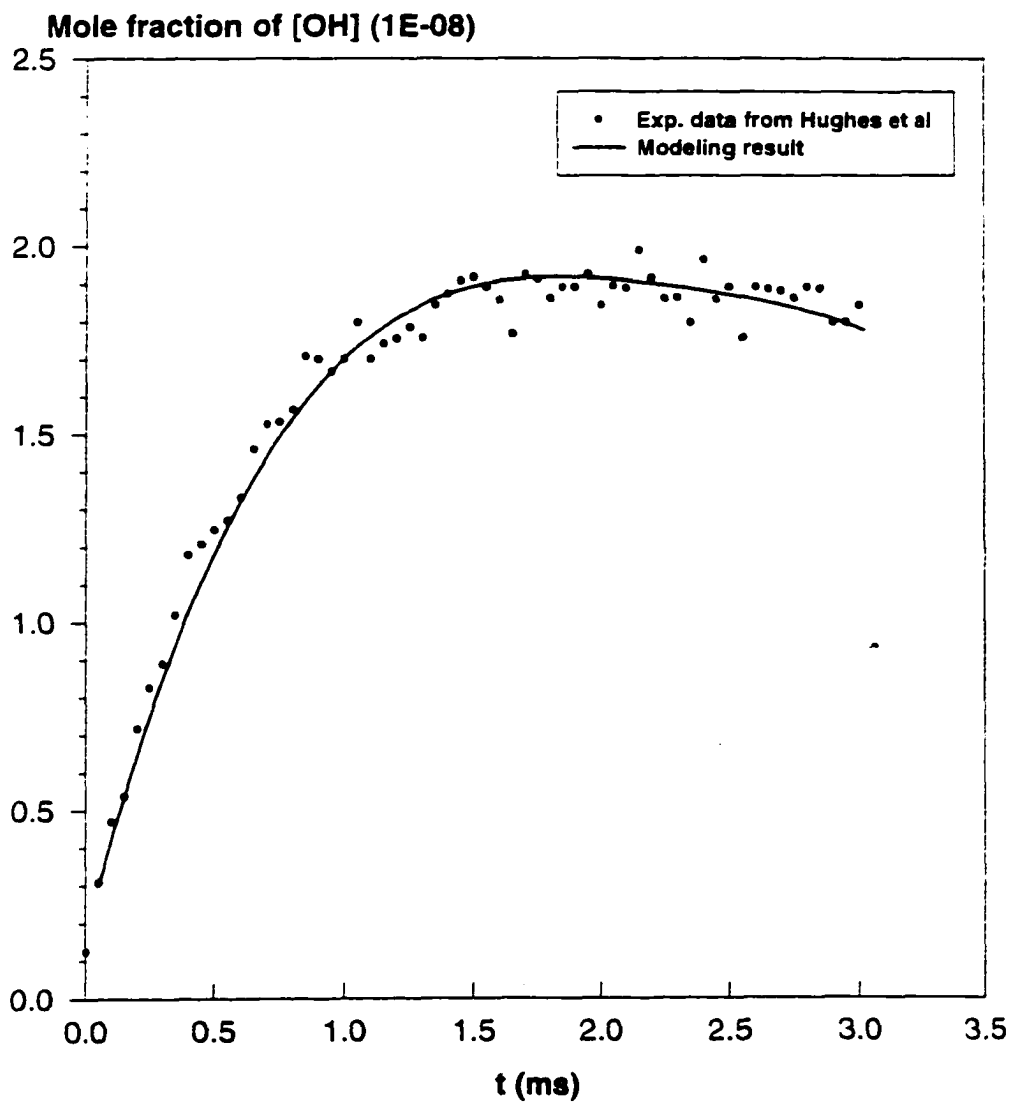


Figure IC. 20 OH formation comparison of model with Hughes experiment

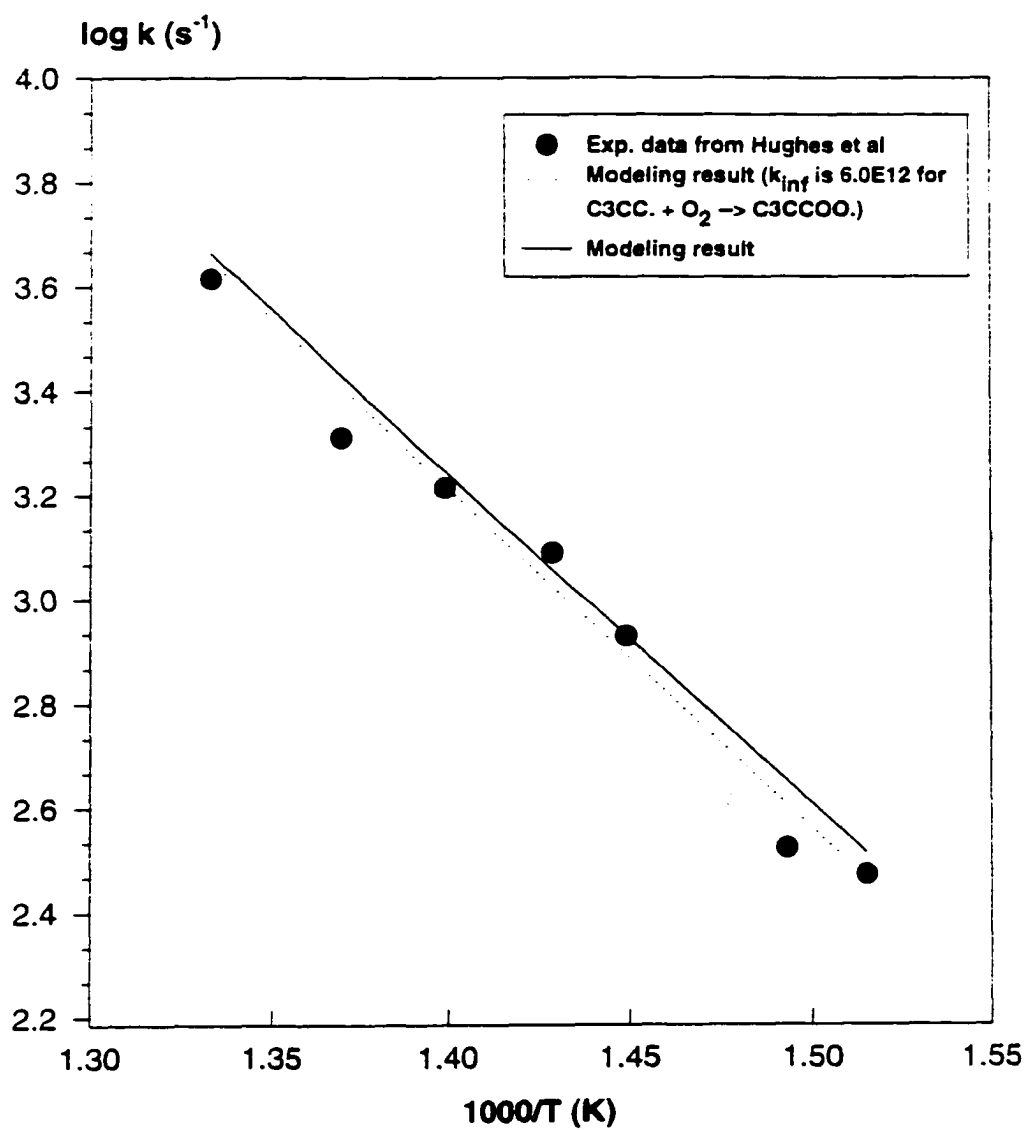
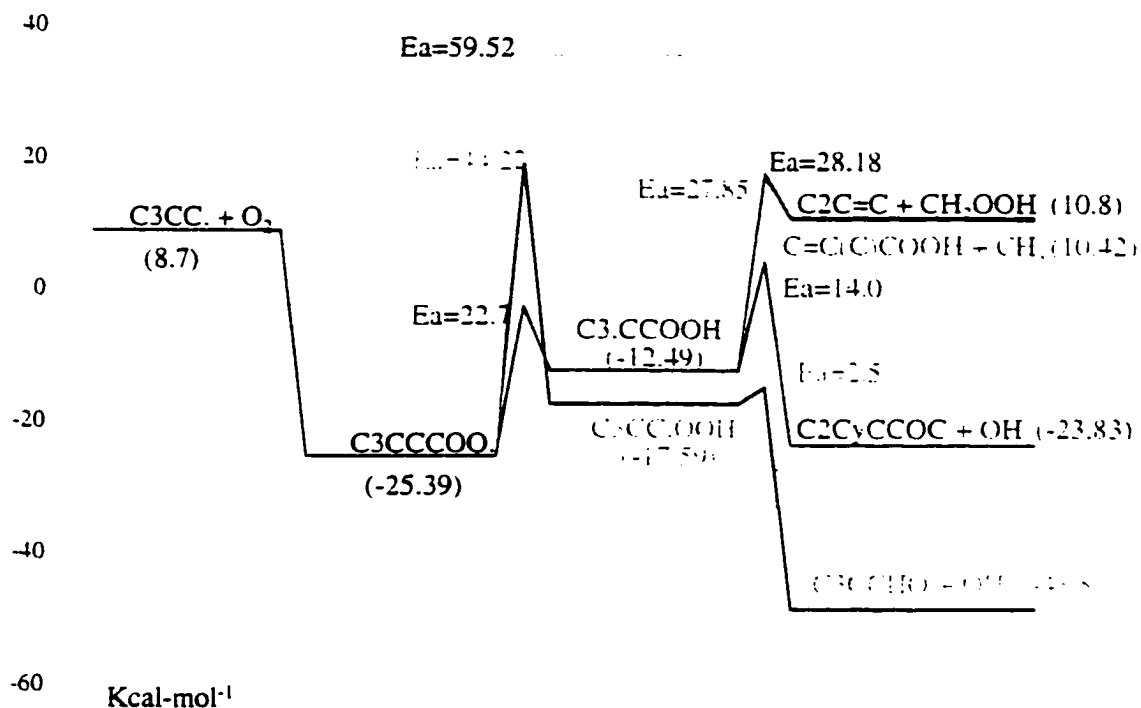


Figure IC. 21 Log k of OH formation vs 1000/T comparison of model with experiment

APPENDIX ID

QRRK INPUT PARAMETERS IN THE NEO-C₃H₁₁ + O₂ SYSTEM

ID. 1 C3CC.+ O₂ → Products



Reaction	A (s ⁻¹ or cm ³ /mol-s)	n	Ea (kcal/mol)
k ₁ C3CC + O ₂ → C3CCOO.	1.00E12	0.00	0.00
k ₋₁ C3CCOO. → C3CC + O ₂	2.27E14	0.00	31.68
k ₂ C3CCOO. → C3.CCOOH	5.15E09	1.00	22.70
k ₋₂ C3.CCOOH → C3CCOO.	1.29E12	-0.74	8.90
k ₃ C3.CCOOH → C2CyCCOC + OH	5.06E07	0.71	14.00
k ₄ C3.CCOOH → C2C=C + CH ₂ OOH	5.23E13	0.00	28.18
k ₅ C3.CCOOH → C=C(C)COOH + CH ₃	4.77E13	0.00	27.85
k ₆ C3CCOO. → C3CC.OOH	2.60E10	1.00	44.22
k ₋₆ C3CC.OOH → C3CCOO.	7.50E12	-0.35	35.64
k ₇ C3CC.OOH → C3CC=O + OH	1.43E13	0.00	2.50
k ₈ C3CCOO. → C3CCO + O	1.03E15	0.00	59.52

frequency/degeneracy (CPFIT):

C3CCOO.: 952.2/45.5; C3.CCOOH: 898.2/45.0; C3CC.OOH: 880.6/45.0

Lennard-Jones parameter:

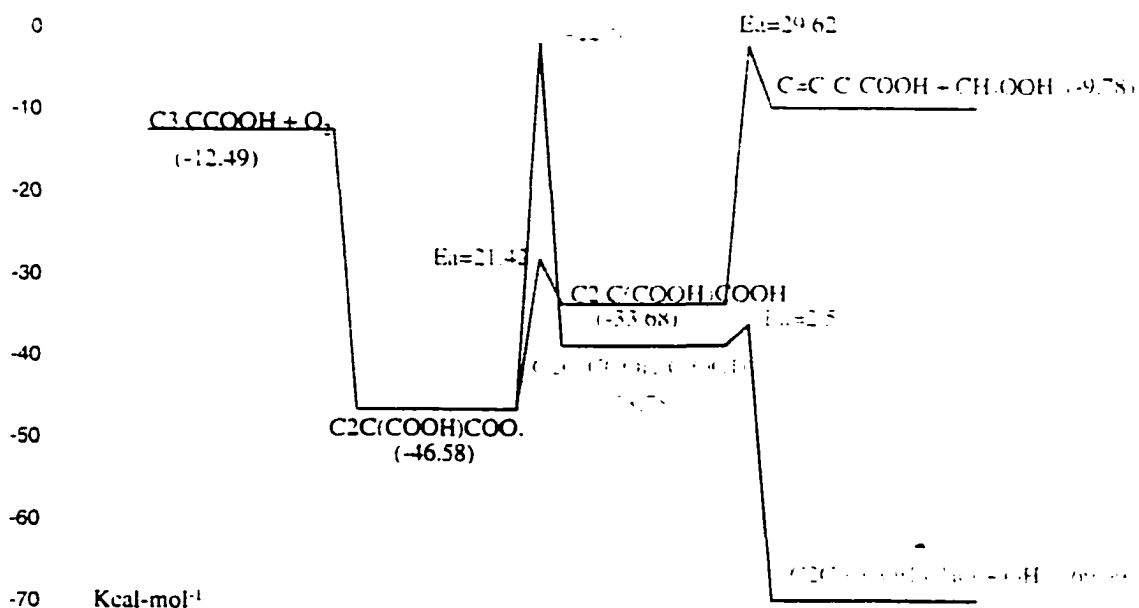
$\sigma(a) = 5.86$ ϵ/k (K) = 632

Beta values for QRRK calculations:

Temp.(K)	300	600	900	1200	1500	1800	2100	2400
Beta	0.117	0.018	0.004	0.004	0.008	0.011	0.014	0.016

- k_1 $A_1 = 1.0E12$, take average value of high pressure limit data from Bayes et al.; $E_{a1} = 0$
- k_{-1} Via k_1 and MR; $E_{a-1} = E_{a1} + \Delta U_{rxn}$
- k_2 A_2 estimated using TST, $A = (\text{deg.})(ek_b/h)\exp(\Delta S^*(T)/R)$, $\Delta S^*(T)$ is taken from MOPAC PM3 calculation, here $\Delta S^*_{avg}(298., 1500. \text{ K}) = -9.13 \text{ cal/mole-K}$, $\text{deg.} = 9$; $E_{a2} = RS + E_{abst} + \Delta H_{rxn}$, 6 member ring ($RS = 1$), $E_{abst} = 12.5 - (\Delta H_{rxn}/3)$, $\Delta H_{rxn} = 13.80 \text{ kcal./mole}$
- k_{-2} Via k_2 and MR; $E_{a-2} = E_{a2} - \Delta H_{rxn}$
- k_3 A_3 estimated using TST, $A = 5.66 \times 10^{10} \exp(\Delta S^*(T)/R)$ in $AT^n \exp(-E_a/RT)$ form, $\Delta S^*(T)$ is taken from MOPAC PM3 calculation, here $\Delta S^*_{avg}(298., 1500. \text{ K}) = -13.95 \text{ cal/mole-K}$; E_{a3} estimated in this study
- k_4 A_4 via A_{-4} (NIST), and MR; $E_{a4} = \Delta U_{rxn} + E_{a-4}$
- k_5 A_5 via A_{-5} (NIST), and MR; $E_{a5} = \Delta U_{rxn} + E_{a-5}$
- k_6 A_6 estimated using TST, loss of one rotors (4.3×1), gain of OI ($R \ln 2$), $\text{deg.} = 2$; $E_{a6} = RS + E_{abst} + \Delta H_{rxn}$, 4 member ring ($RS=26$), $E_{abst} = 12.5 + (\Delta H_{rxn}/3)$, $\Delta H_{rxn} = 8.58$
- k_{-6} Via k_6 and MR; $E_{a-6} = E_{a6} - \Delta H_{rxn}$
- k_7 A_7 via A_{-7} which estimated from $1/2(\text{OH} + \text{C}=\text{C})$, and MR; $E_{a7} = 2.5$ (NIST),
- k_8 A_8 via A_{-8} (NIST), and MR; $E_{a8} = 0.0$

ID. 2 C3.CCOOH + O₂ → Products



	Reaction	A (s ⁻¹ or cm ³ /mol-s)	n	Ea (kcal/mol)
k ₁	C3.CCOOH + O ₂ → C2C(COOH)COO.	1.00E12	0.00	0.00
k ₋₁	C2C(COOH)COO. → C3.CCOOH + O ₂	3.54E14	0.00	32.21
k ₂	C2C(COOH)COO. → C2.C(COOH)COOH	1.03E09	1.00	21.42
k ₋₂	C2.C(COOH)COOH → C2C(COOH)COO.	1.10E10	0.12	8.04
k ₃	C2.C(COOH)COOH → C=C(C)COOH + CH ₂ OOH	2.63E14	0.00	29.62
k ₄	C2C(COOH)COO. → C2C(COOH)C.OOH	2.60E10	1.00	44.56
k ₋₄	C2C(COOH)C.OOH → C2C(COOH)COO.	2.19E15	-1.39	35.47
k ₅	C2C(COOH)C.OOH → C2C(COOH)C=O + OH	1.43E13	0.00	2.50

frequency/degeneracy (CPFIT):

C2C(COOH)COO.: 863.1/50.5; C2.C(COOH)COOH: 823.2/50.0;

C2C(COOH)C.OOH: 616.8/50.0

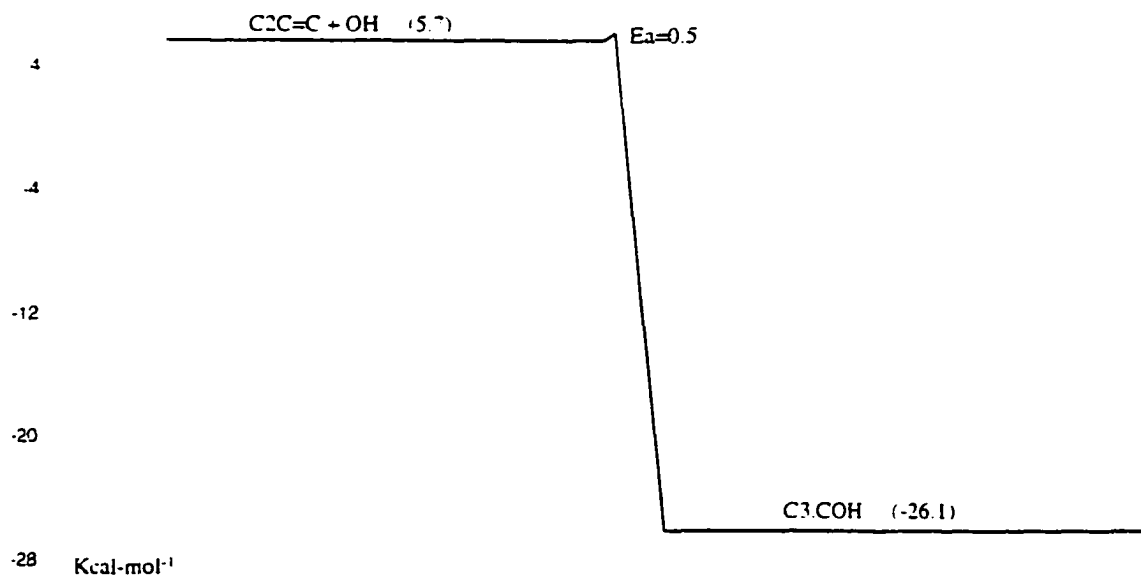
Lennard-Jones parameter:

σ(a) = 6.40 ε/k (K) = 720.5

Beta values for QRRK calculations for adduct C2C(COOH)COO.

Temp.(K)	300	600	900	1200	1500	1800	2100	2400
Beta	0.111	0.014	0.004	0.008	0.013	0.018	0.019	0.019

- k_1 $A_1 = 1.0E12$, take average value of high pressure limit data from Bayes et al.: $E_{a1} = 0$.
 k_{-1} Via k_1 and MR: $E_{a_{-1}} = E_{a1} + \Delta U_{rxn}$
 k_2 A_2 estimated using TST, loss of three rotors (4.3×3), gain of OI ($R \ln 2$), deg. = 6: $E_{a2} = RS + E_{abst} + \Delta H_{rxn}$, 6 member ring ($RS = 1$), $E_{abst} = 12.5 + (\Delta H_{rxn}/3)$, $\Delta H_{rxn} = 13.38$
 k_{-2} Via k_2 and MR: $E_{a_{-2}} = E_{a2} - \Delta H_{rxn}$
 k_3 A_3 via $A_3 = 1E11.2$ (NIST), and MR: $E_{a3} = \Delta U_{rxn} + E_{a_{-3}}$, $E_{a_{-3}} = 7.8$, $\Delta U_{rxn} = 21.82$
 k_4 A_4 estimated using TST, loss of one rotors (4.3×1), gain of OI ($R \ln 2$), deg. = 2: $E_4 = RS + E_{abst} + \Delta H_{rxn}$, 4 member ring ($RS = 26$), $E_{abst} = 12.5 + (\Delta H_{rxn}/3)$ or 5, $\Delta H_{rxn} = 9.09$
 k_{-4} Via k_4 and MR: $E_{a_{-4}} = E_{a4} - \Delta H_{rxn}$
 k_5 A_5 via $A_5 = 2.75E12$, estimated from $1/2$ ($OH + C=C$), and MR: $E_{a5} = 2.5$

ID. 3 $\text{C}_2\text{C}=\text{C} + \text{OH} \rightarrow \text{Products}$ 

	Reaction	A (s^{-1} or $\text{cm}^3/\text{mol}\cdot\text{s}$)	n	E_a (kcal/mol)
k_1	$\text{C}_2\text{C}=\text{C} + \text{OH} \rightarrow \text{C}_3.\text{COH}$	2.92E12	0.0	0.5
k_{-1}	$\text{C}_3.\text{COH} \rightarrow \text{C}_2\text{C}=\text{C} + \text{OH}$	4.22E13	0.0	31.95

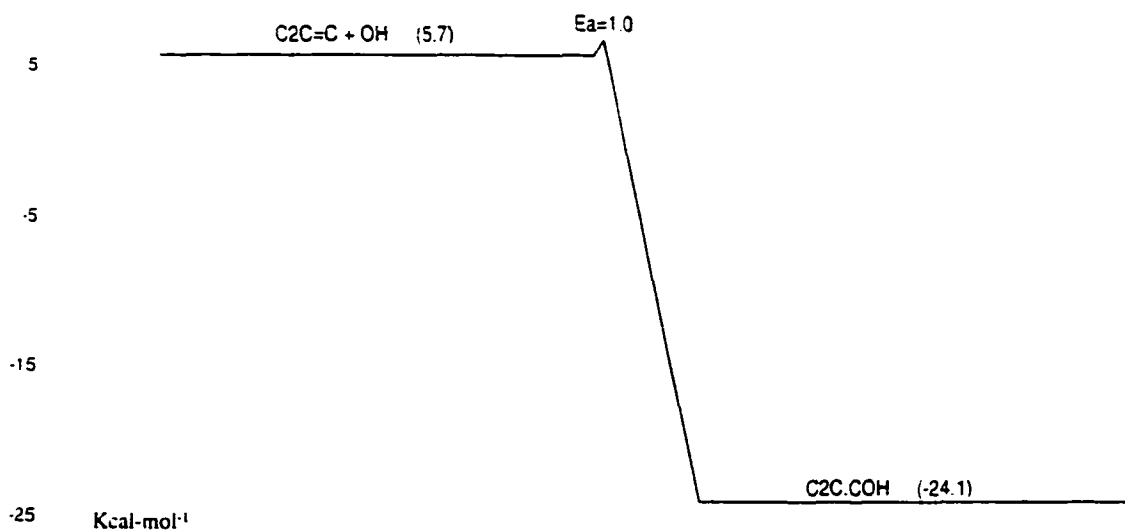
frequency/degeneracy (CPFIT):

 $\text{C}_3.\text{COH}$: 1105.1/34.0

Lennard-Jones parameter:

 $\sigma(a) = 5.20$ ϵ/k (K) = 533.1 k_1 $A_1 = 2.92\text{E}12$, estimated from ($\text{C}_3\text{H}_6 + \text{OH}$, 91 TSA), and MR; $E_{a1} = 0.5$ (NIST) k_{-1} Via k_1 and MR; $E_{a,-1} = E_{a1} + \Delta U_{\text{rxn}}$

ID. 4 $\text{C}_2\text{C}=\text{C} + \text{OH} \rightarrow \text{C}_2\text{C}.\text{COH}$



	Reaction	A (s^{-1} or $\text{cm}^3/\text{mol}\cdot\text{s}$)	n	E_a (kcal/mol)
k_1	$\text{C}_2\text{C}=\text{C} + \text{OH} \rightarrow \text{C}_2\text{C}.\text{COH}$	$2.92\text{E}12$	0.0	1.0
k_{-1}	$\text{C}_2\text{C}.\text{COH} \rightarrow \text{C}_2\text{C}=\text{C} + \text{OH}$	$1.95\text{E}13$	0.0	31.51

frequency/degeneracy (CPFIT):

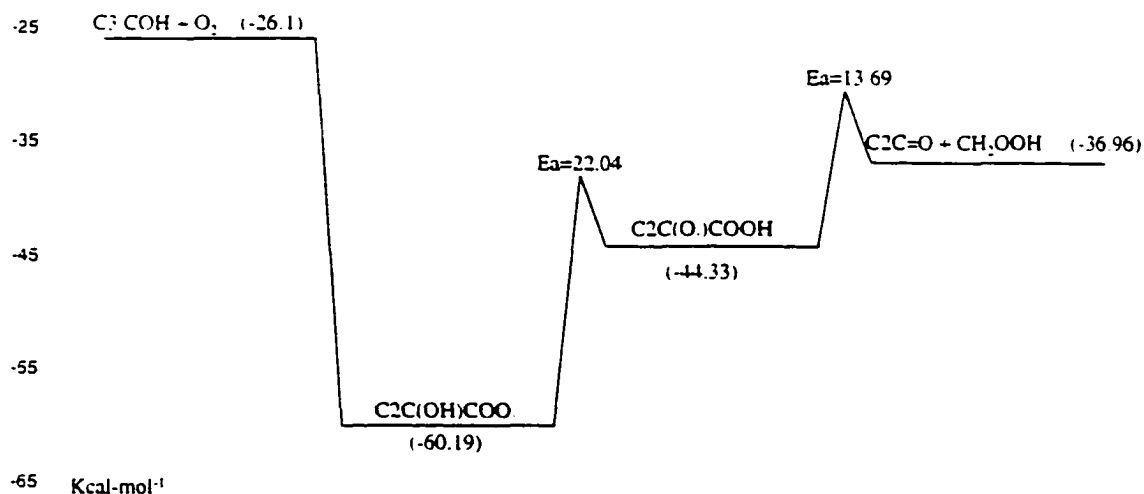
$\text{C}_2\text{C}.\text{COH}$: 1153.5/34.0

Lennard-Jones parameter:

$\sigma(a) = 5.20$ ϵ/k (K) = 533.1

k_1 $A_1 = 2.92\text{E}12$, estimated from ($\text{C}_3\text{H}_6 + \text{OH}$, 91 TSA), and MR; $E_1 = 1.0$ (NIST)

k_{-1} Via k_1 and MR; $E_{a-1} = E_{a1} + \Delta U_{\text{rxn}}$

ID. 5 C3.COH + O₂ → Products

	Reaction	A (s ⁻¹ or cm ³ /mol-s)	n	Ea (kcal/mol)
k ₁	C ₃ .COH + O ₂ → C ₂ C(OH)COO.	2.0E12	0.0	0.00
k ₋₁	C ₂ C(OH)COO. → C ₃ .COH + O ₂	4.589E14	0.0	31.71
k ₂	C ₂ C(OH)COO. → C ₂ C(O.)COOH	1.72E8	1.0	22.04
k ₋₂	C ₂ C(O.)COOH → C ₂ C(OH)COO.	1.73E11	-0.06	5.00
k ₃	C ₂ C(O.)COOH → C ₂ C=O + CH ₂ OOH	3.492E14	0.0	13.69

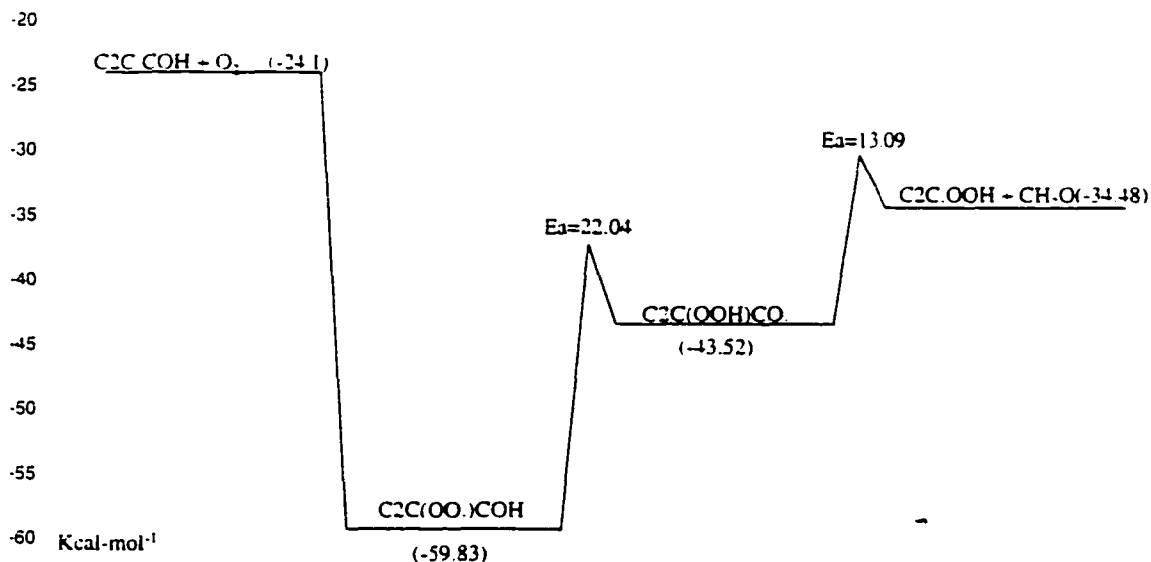
frequency/degeneracy (CPFIT):

C₂C(OH)COO.: 933.1/39.5; C₂C(O.)COOH: 882.4/395

Lennard-Jones parameter:

σ(a) = 5.86 ε/k (K) = 632.1

k₁ A₁ = 2.0E12, estimated from R. + O₂ → ROO.; Ea₁ = 0.0k₋₁ Via k₁ and MR; Ea₋₁ = Ea₁ + ΔU_{rxn}k₂ A₂ estimated using TST, loss of three rotors (4.3*3), gain of OI (Rln2), deg. = 1;
Ea₂ = RS + E_{abst} + ΔH_{rxn}, 6 member ring (RS = 0), E_{abst} = 5 (NIST), ΔH_{rxn} = 17.04k₋₂ Via k₂ and MR; Ea₋₂ = Ea₂ - ΔH_{rxn}k₃ A₃ via A₃ = 1E11.2 (NIST), and MR; Ea₃ = ΔH_{rxn} + Ea₋₃, Ea₃ = 7.8, ΔH_{rxn} = 5.89

ID. 6 C2C.CO₂H + O₂ → Products

	Reaction	A (s ⁻¹ or cm ³ /mol-s)	n	E _a (kcal/mol)
k ₁	C2C.CO ₂ H + O ₂ → C2C(OO.)COH	2.0E12	0.0	0.0
k ₋₁	C2C(OO.)COH → C2C.CO ₂ H + O ₂	2.252E15	0.0	32.05
k ₂	C2C(OO.)COH → C2C(OOH)CO.	1.72E8	1.0	22.04
k ₋₂	C2C(OOH)CO. → C2C(OO.)COH	1.71E11	-0.06	5.0
k ₃	C2C(OOH)CO. → C2C.OOH + HCHO	3.42E14	0.0	13.09

frequency/degeneracy (CPFIT):

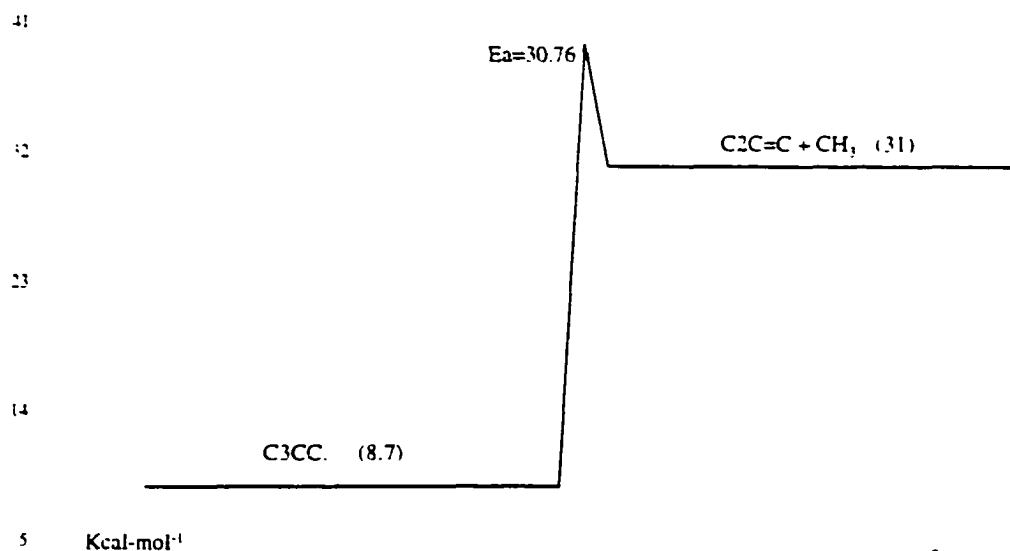
C2C(OO.)COH: 955.2/39.5; C2C(OOH)CO.: 901.6/39.5

Lennard-Jones parameter:

σ(a) = 5.86 ε/k (K) = 632.1

k₁ A₁ = 2.0E12, estimated from R. + O₂ → ROO.; Ea₁ = 0.0k₋₁ Via k₁ and MR; Ea₋₁ = Ea₁ + ΔH_{rxn}k₂ A₂ estimated using TST, loss of three rotors (4.3*3), gain of OI (Rln2), deg. = 1;
Ea₂ = RS + E_{abst} + ΔH_{rxn}, 6 member ring (RS = 0), E_{abst} = 5 (NIST), ΔH_{rxn} = 17.04k₋₂ Via k₂ and MR; Ea₋₂ = Ea₂ - ΔH_{rxn}k₃ A₃ via A₃ = 1E11.0 (NIST), and MR; Ea₃ = ΔH_{rxn} + Ea₃, Ea₃ = 5.9 which
estimated from (CH₃ + CH₂O, 84 WAR),, ΔH_{rxn} = 7.19

ID. 7 $\text{C3CC.} \rightarrow \text{C2C=C} + \text{CH}_3$



	Reaction	$A(\text{s}^{-1})$	n	$E_a(\text{kcal/mol})$
k_1	$\text{C3CC.} \rightarrow \text{C2C=C} + \text{CH}_3$	9.572E13		30.76

frequency/degeneracy (CPFIT):

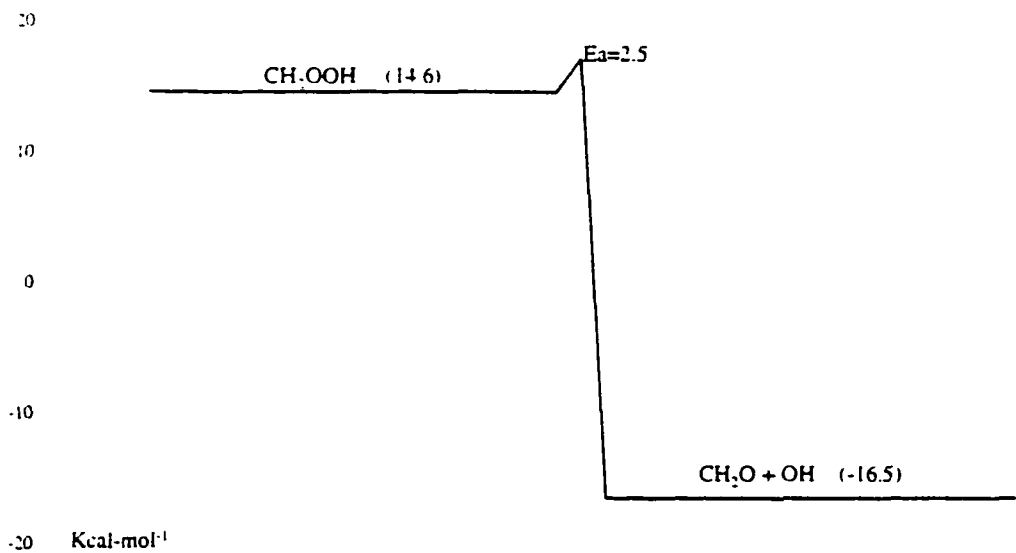
$\text{C3CC.}: 1123.5/40.0$

Lennard-Jones parameter:

$\sigma(\text{\AA}) = 5.50 \quad \epsilon/k(\text{K}) = 443$

k_1 A_1 via A_{-1} (1E11.5), estimated by NIST, and MR; $E_{a1} = E_{a-1} + \Delta H_{\text{rxn}}$, $E_{a-1} = 7.8$, $\Delta H_{\text{rxn}} = 21.03$

ID. 8 CH₂OOH → CH₂O + OH

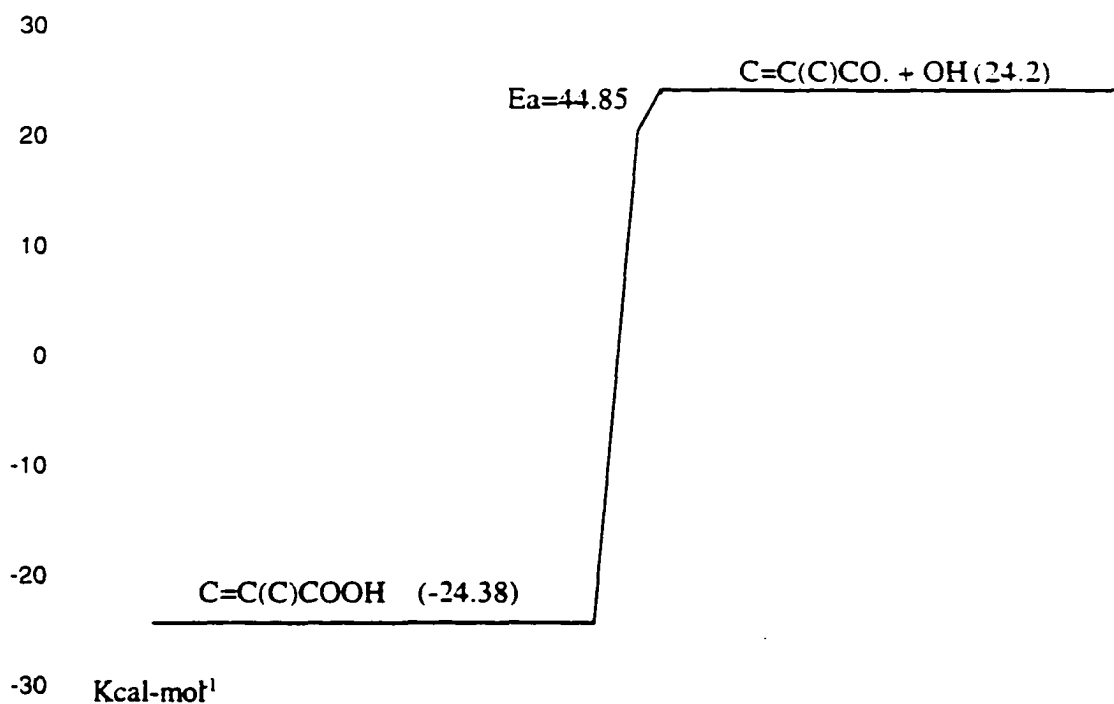


	Reaction	A(s ⁻¹)	n	E _a (kcal/mol)
k ₁	CH ₂ OOH → HCHO + OH	3.069E12	0.0	2.5

frequency/degeneracy (CPFIT):
CH₂OOH: 613.7/11.0
Lennard-Jones parameter:
σ(a) = 4.34 ε/k (K) = 432

k₁ A₁ via A₋₁ which estimated from 1/2 (OH + C=C), and MR, Ea₁ = 2.5 (NIST)

ID. 9 $\text{C}=\text{C}(\text{C})\text{COOH} \rightarrow \text{C}=\text{C}(\text{C})\text{CO} \cdot + \text{OH}$



	Reaction	$A(\text{s}^{-1})$	n	$E_a(\text{kcal/mol})$
k_1	$\text{C}=\text{C}(\text{C})\text{COOH} \rightarrow \text{C}=\text{C}(\text{C})\text{CO} \cdot + \text{OH}$	$2.21\text{E}15$	0.0	44.85

frequency/degeneracy (CPFIT):

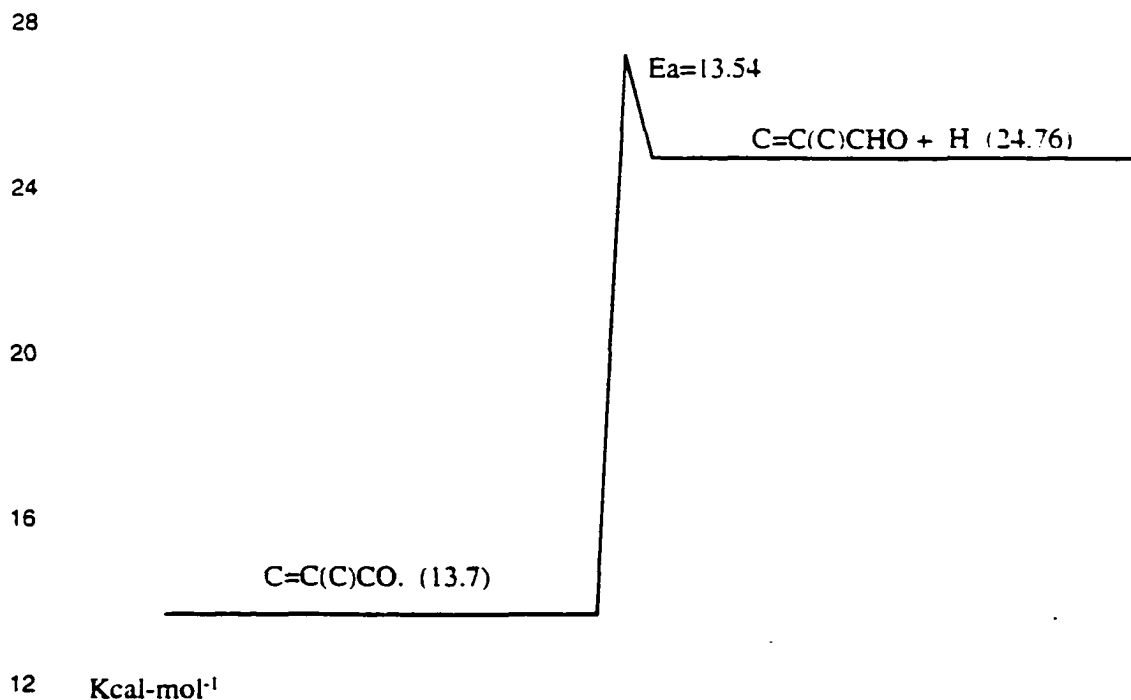
$\text{C}=\text{C}(\text{C})\text{COOH}$: 898.2/34.0

Lennard-Jones parameter:

$\sigma(a) = 5.55$ ϵ/k (K) = 584.9

k_1 Via k_1 estimated from ($n\text{-C}_3\text{H}_7 + \text{OH} = n\text{-C}_3\text{H}_7\text{OH}$, 88 TSA), and MR

ID. 10 $\text{C}=\text{C}(\text{C})\text{CO.} \rightarrow \text{C}=\text{C}(\text{C})\text{CHO} + \text{H}$



	Reaction	$A(\text{s}^{-1})$	n	$E_a(\text{kcal/mol})$
k_1	$\text{C}=\text{C}(\text{C})\text{CO.} \rightarrow \text{C}=\text{C}(\text{C})\text{C}=\text{O.} + \text{H}$	$4.175\text{e}12$	0.0	13.54

frequency/degeneracy (CPFIT):

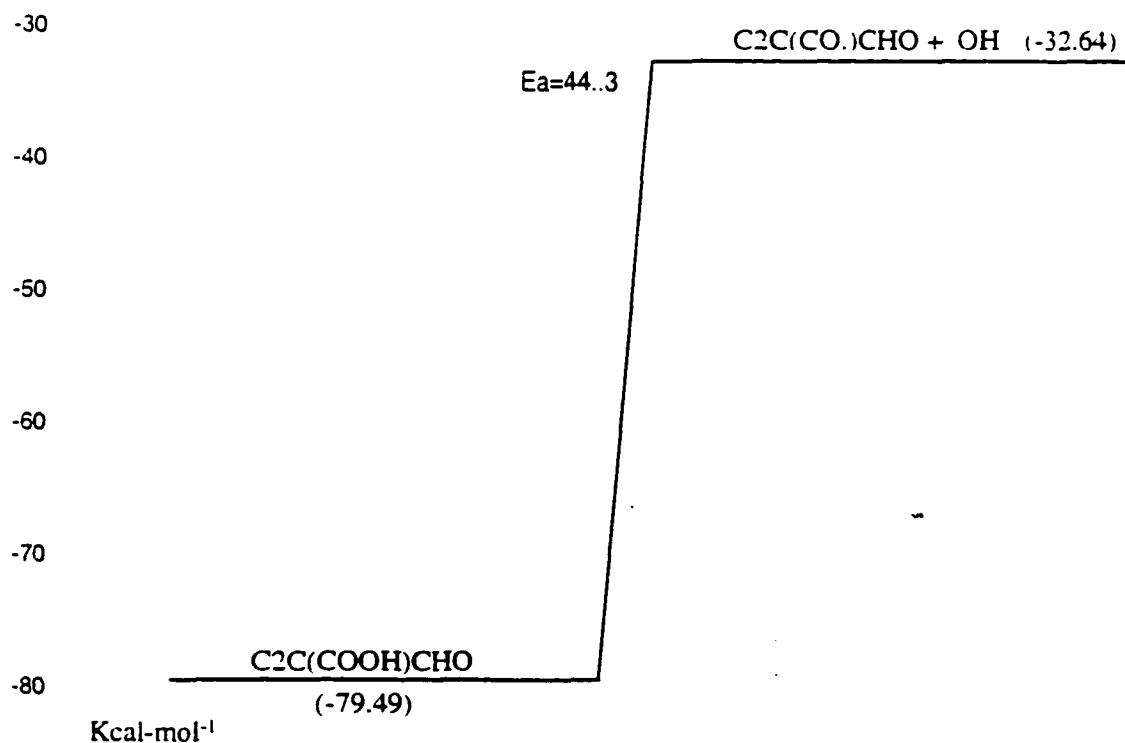
$\text{C}=\text{C}(\text{C})\text{CO.}: 1110.9/29.0$

Lennard-Jones parameter:

$\sigma(a) = 5.20 \quad \epsilon/k (K) = 533.1$

k_1 A_1 via $A_{-1} = 5\text{E}12$ which estimated from $1/2(\text{C}_2\text{H}_4 + \text{H}$, 91 TSA), and MR:
 $E_{a1} = E_{a-1} + \Delta H_{\text{rxn}}$, $\Delta H_{\text{rxn}} = 12.63$, $E_{a1} = 2.7$ (NIST)

ID. 11 $\text{C}_2\text{C}(\text{COOH})\text{CHO} \rightarrow \text{C}_2\text{C}(\text{CO.})\text{CHO} + \text{OH}$



	Reaction	A (s^{-1})	n	$E_a(\text{kcal/mol})$
k_1	$\text{C}_2\text{C}(\text{COOH})\text{C}=\text{O} \rightarrow \text{C}_2\text{C}(\text{CO.})\text{C}=\text{O} + \text{OH}$	$3.222\text{E}15$	0.0	44.30

frequency/degeneracy (CPFIT):

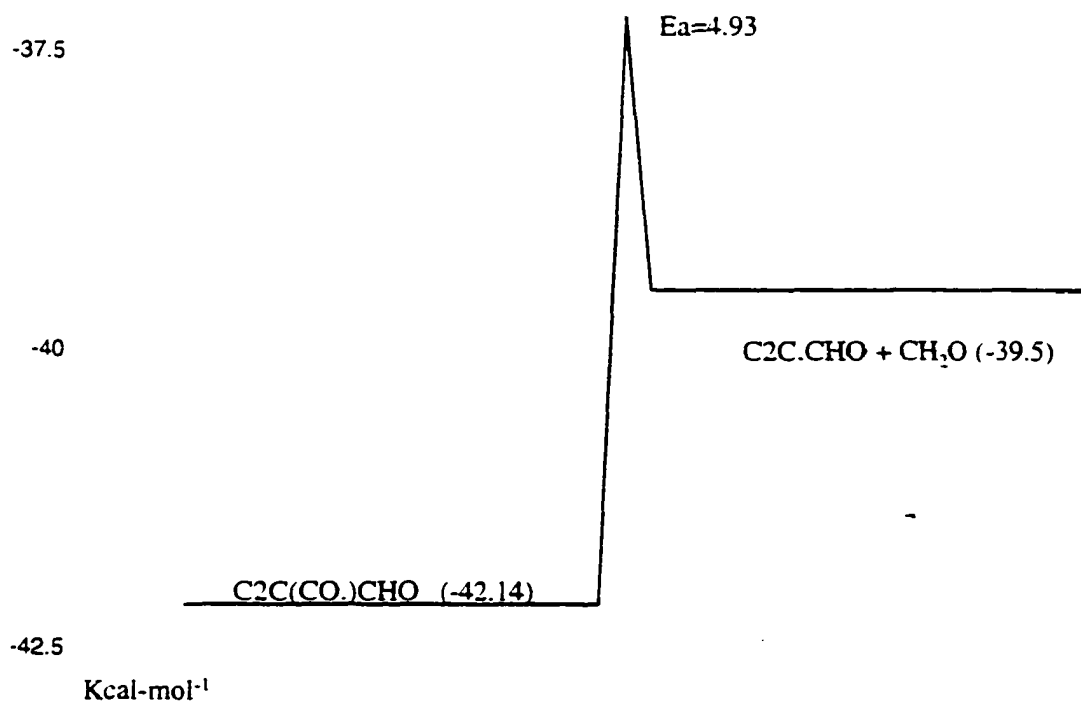
$\text{C}_2\text{C}(\text{COOH})\text{C}=\text{O}$: 857.1/45.0

Lennard-Jones parameter:

$\sigma(a) = 6.14$ ϵ/k (K) = 678.6

k_1 Via k_1 estimated from $(n\text{-C}_3\text{H}_7 + \text{OH} = n\text{-C}_3\text{H}_7\text{OH}, 88 \text{ TSA})$, and MR

ID. 12 $\text{C}_2\text{C}(\text{CO.})\text{CHO} \rightarrow \text{C}_2\text{C}.\text{CHO} + \text{CH}_2\text{O}$



	Reaction	$A(\text{s}^{-1})$	n	$E_a(\text{kcal/mol})$
k_1	$\text{C}_2\text{C}(\text{CO.})\text{C}=\text{O} \rightarrow \text{C}_2\text{C}.\text{C}=\text{O} + \text{HCHO}$	$7.295\text{E}12$	0.0	4.932

frequency/degeneracy (CPFIT):

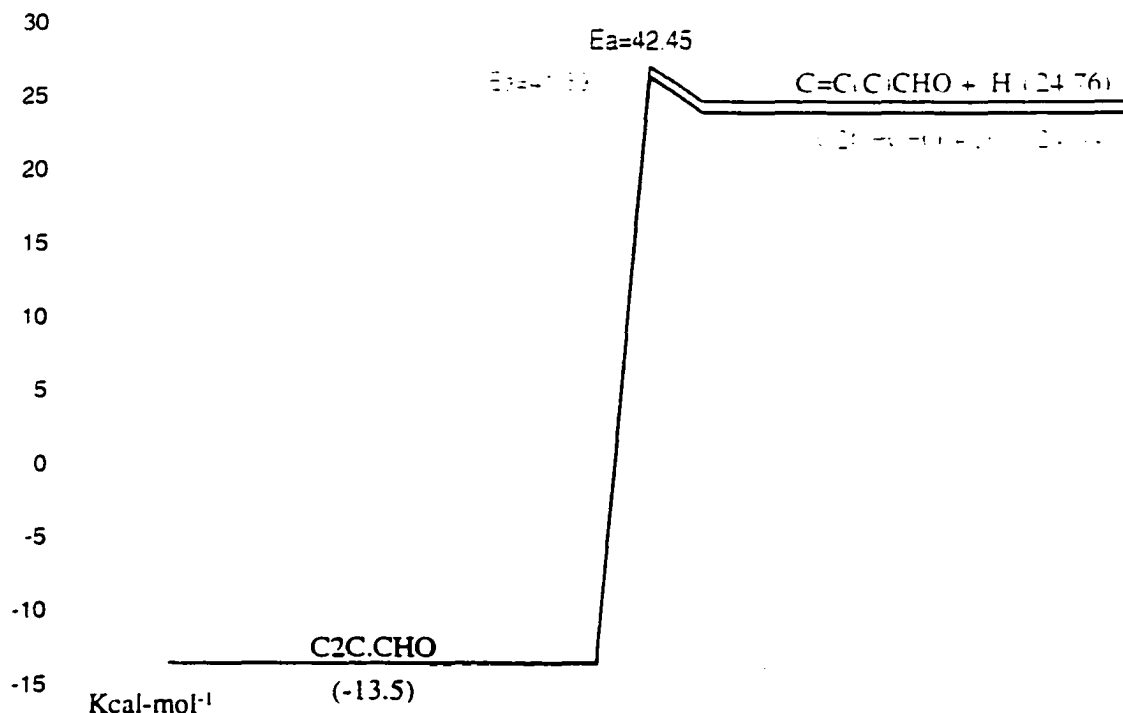
$\text{C}_2\text{C}(\text{CO.})\text{C}=\text{O}$: 1010.9/40.0

Lennard-Jones parameter:

$\sigma(a) = 5.86$ ϵ/k (K) = 632.7

k_1 Via k_1 estimated from ($\text{HCHO} + \text{CH}_3$, 84 WAR), and MR

ID. 13 C2C.CHO → Products



	Reaction	A(s ⁻¹)	n	E _a (kcal/mol)
k ₁	C2C.C=O → C=C(C)C=O + H	1.442E13	0	42.45
k ₂	C2C.C=O → C2C=C=O + H	1.076E13	0	41.69

frequency/degeneracy (CPFIT):

C2C.C=O: 1047.8/28.5

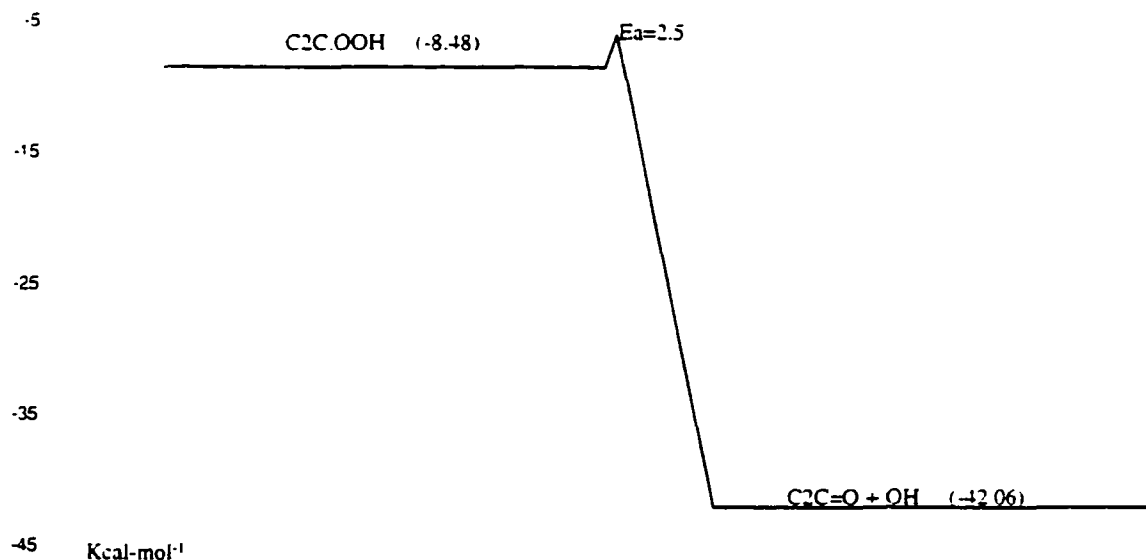
Lennard-Jones parameter:

σ(a) = 5.20 ε/k (K) = 533.1

k₁ A₁ via A₁ = 5E12 which estimated from 1/2(C₂H₄ + H, 91 TSA), and MR; Ea₁ = Ea₁ + ΔH_{rxn}, ΔH_{rxn} = 39.75, Ea₁ = 2.7 (NIST)

k₂ A₂ via A₂ = 5E12 which estimated from 1/2(C₂H₄ + H, 91 TSA), and MR; Ea₂ = Ea₂ + ΔH_{rxn}, ΔH_{rxn} = 38.99, Ea₁ = 2.7 (NIST)

ID. 14 $\text{C}_2\text{C.OOH} \rightarrow \text{C}_2\text{C=O} + \text{OH}$



	Reaction	$A(\text{s}^{-1})$	n	$E_a(\text{kcal/mol})$
k_1	$\text{C}_2\text{C.OOH} \rightarrow \text{C}_2\text{C=O} + \text{OH}$	4.485E12	0.0	2.5

frequency/degeneracy (CPFIT):

$\text{C}_2\text{C.OOH}$: 750.2/28.0

Lennard-Jones parameter:

$\sigma(a) = 5.20$ ϵ/k (K) = 533.1

k_1 A_1 via $A_{-1} = 2.75\text{E}12$ which estimated from $1/2(\text{C}=\text{C} + \text{OH})$, and MR; $E_{a1} = 2.5$ (NIST)

APPENDIX IIA
TABLES IN MTBE SYSTEM

Table IIA. 1 Experimental Conditions of MTBE Oxidation and Pyrolysis

4 atm		7 atm		10 atm	
Temp. (°C)	RT (second)	Temp. (°C)	RT (second)	Temp. (°C)	RT (second)
MTBE Oxidation At $\phi = 0.75$					
750	0.45-0.90	750	0.80-2.90	750	1.00-4.90
700	0.45-1.00	700	0.80-3.10	700	1.10-5.10
650	0.50-0.90	650	0.90-3.30	650	1.10-5.30
625	0.50-1.10	600	0.80-3.50	600	1.70-5.70
600	0.55-1.10	550	1.00-3.40	550	1.30-5.70
575	0.60-1.10	525	1.00-3.80	525	1.60-5.80
550	0.60-1.20				
MTBE Oxidation At $\phi = 1.00$					
800	0.3-0.9	800	0.7-2.7	800	0.9-4.7
750	0.45-0.9	750	0.8-2.9	750	1-4.9
700	0.45-1.0	700	0.8-3.1	700	1.1-5.1
650	0.5-1.0	650	0.9-3.3	650	1.3-5.5
600	0.55-1.1	600	0.9-3.5	600	1.3-5.7
575	0.6-1.1	550	1-3.4	550	1.3-5.7
550	0.6-1.2	525	1-3.8	525	1.4-6.2
MTBE Oxidation At $\phi = 1.50$					
775	0.5-0.9	775	0.8-2.8	775	1-3.6
725	0.5-1.0	725	0.8-3	725	1.2-5.2
700	0.45-1.0	700	0.8-3.1	700	1.1-5.1
650	0.5-1.0	650	0.9-3.3	650	1.3-5.5
625	0.5-1.1	625	1-3.4	625	1.3-4.5
600	0.55-1.1	600	0.9-3.5	600	1.3-5.7
575	0.6-1.1	575	1-3.4	575	1.4-6.2
550	0.6-1.2	550	1-3.4	550	1.3-5.7
		525	1-3.8	525	1.4-6.2
MTBE Pyrolysis					
850	0.45-0.85	850	0.8-2.6	850	1-3.6
800	0.3-0.9	800	0.7-2.7	800	1-4.9
775	0.5-0.9	775	0.8-2.8	775	1-3.6
750	0.45-0.9	750	0.8-2.9	750	1-4.9
725	0.5-1.0	725	0.8-3	725	1.2-5.2
700	0.45-1.0	700	0.8-3.1	700	1.1-5.5
650	0.5-1.0	650	0.9-3.3	650	1.1-5.7
600	0.55-1.1	600	1-3.5	600	1.3-5.7
550	0.6-1.2				

Table IIA. 2 Retention Time of Species

Species	RT (A) (min)	RRF (A)	RT (B) (min)	RRF (B)
CO	1.01	0.906		
CH ₄	1.28	1.000	3.18	1.000
CO ₂	3.24	0.906		
C ₂ H ₄	4.53	1.591	3.27	1.740
C ₂ H ₆	5.64	1.975	3.30	1.798
C ₂ H ₂	6.87	0.777	3.27	1.744
CH ₂ O	10.70	0.864	3.50	<0.1
C ₃ H ₆	11.39	2.479	3.55	2.656
C ₃ H ₈	11.62	2.938	3.55	2.747
C ₃ H ₄	12.92	1.387	3.76	2.488
CH ₃ OCH ₃	13.01		3.90	
CH ₃ OH	14.55	1.075	4.15	0.784
CH ₃ CHO	14.85		4.27	
(CH ₃) ₃ CH	15.31	4.15	3.81	4.061
CH ₂ =CHCH ₂ CH ₃	15.77	3.129	4.21	3.476
CCCC	16.03	3.924	4.27	3.714
(CH ₃) ₄ C	18.36	5.073	4.28	5.325
C=CCHO	19.70	2.962	6.15	1.807
C ₂ CCC	20.54	5.2	5.25	5.097
C=CCCC	21.05	4.242	5.76	4.481
C ₂ C=O	21.07	3.00	6.30	1.654
CCCCC	21.55	4.822	5.91	4.583
COCOC	21.90	3.097	6.83	1.324
C=C(C)CHO	27.80	3.150	8.40	2.058
C ₂ CCHO	28.20	3.690	8.10	3.128
CCC(C)CC	28.54	5.36	6.65	5.850
MTBE (C ₃ COC)	30.778	5.472	8.12	3.830
C ₃ CCC	31.741	5.378	7.57	5.929
C ₂ CCCC	32.928	5.4	8.03	6.000
C=CCCCC	33.867	4.708	8.42	5.583
CCCCCC	34.826	5.585	8.61	5.350

Table IIA. 3 Thermodynamic Properties for Species in MTBE Model

SPECIES	Hf	S	Cp 300	400	500	600	800	1000	1500	DATE	ELEME	N	TS			
AR		0.00	36.98	4.97	4.97	4.97	4.97	4.97	4.97	7/12/93		0	0	0	AR	1 G 0
HE		0.00	30.12	4.97	4.97	4.97	4.97	4.97	4.97		HE	1	0	0	0 G 0	
I		25.50	43.20	5.00	5.00	5.00	5.00	5.00	5.00	BENSON	I	1	0	0	0 G 0	
N2		0.00	45.70	6.67	6.83	6.97	7.11	7.36	7.57	Xi	N	2	0	0	0 G 0	
O		59.51	38.40	5.00	5.00	5.00	5.00	5.00	5.00		120186 O	1	0	0	0 G 0	
X		59.51	38.40	5.00	5.00	5.00	5.00	5.00	5.00		120186 O	1	0	0	0 G 0	
O2		0.00	49.00	6.86	7.10	7.33	7.54	7.89	8.18	8.70	O	2	0	0	0 G 0	
H		52.10	27.30	4.90	4.90	4.90	4.90	4.90	4.90		H	1	0	0	0 G 0	
OH		9.50	43.80	6.79	6.86	6.93	7.00	7.14	7.28	0.00	H	1 O	1	0	0 G 0	
Y		9.50	43.80	6.79	6.86	6.93	7.00	7.14	7.28	0.00	H	1 O	1	0	0 G 0	
HO2		3.50	54.73	8.37	8.95	9.48	9.96	10.78	11.43	12.47	JANAF	H	1 O	2	0	0 G 0
H2		0.00	31.20	6.89	6.97	7.05	7.12	7.27	7.41	7.69		H	2	0	0	0 G 0
H2O		-57.80	45.10	8.02	8.19	8.41	8.66	9.24	9.85	11.23	BSN	H	2 O	1	0	0 G 0
H2O2		-32.60	55.70	10.53	11.76	12.74	13.50	14.58	15.29	16.50	5/7/91 THERM	H	2 O	2	0	0 G 1
C		170.88	38.31	4.98	4.97	4.97	4.97	4.97	4.97	4.97	J 3/61	C	1	0	0	0 G 0
C(S)		0.00	21.83	2.06	2.86	3.50	4.02	4.73	5.16	5.65	J 3/61	C	1	0	0	0 G 0
CO		-26.40	47.20	6.71	6.89	7.06	7.23	7.53	7.79	8.29		121286 C	1 O	1	0	0 G 0
CO2		-94.01	51.00	8.90	9.81	10.57	11.20	12.17	12.84	13.77		121286 C	1 O	2	0	0 G 0
CH		142.00	43.72	6.97	6.97	7.03	7.12	7.41	7.77	8.74	J12/67	C	1 H	1	0	0 G 0
CHO		10.90	53.42	7.64	7.95	8.50	9.10	10.21	11.08	0.00		10/31/96 C	1 H	1 O	1	0 G 0
O.C*O		-38.30	65.04	9.52	11.00	12.30	13.29	15.12	16.26	0.00		10/31/96 C	1 H	1 O	2	0 G 0
HCO2.		-38.30	65.04	9.52	11.00	12.30	13.29	15.12	16.26	0.00		12/31/96 C	1 H	1 O	2	0 G 0
C.O2H		-35.80	66.11	10.87	12.14	13.17	13.94	15.47	16.42	0.00		1/7/97 C	1 H	1 O	2	0 G 1
HCQ.*O		-31.30	74.08	13.22	14.83	16.12	17.17	19.11	20.51	0.00	12/31/96 THERM	C	1 H	1 O	3	0 G 1
C.Q*O		-30.50	74.98	14.44	16.24	17.71	18.84	20.67	21.75	0.00	12/31/96 THERM	C	1 H	1 O	3	0 G 2
CH2S		101.45	44.15	8.33	8.77	9.21	9.64	10.45	11.16	12.47	K	C	1 H	2	0	0 G 0
CH2		92.36	46.32	8.33	8.77	9.21	9.64	10.45	11.16	12.47	K	C	1 H	2	0	0 G 0
HCHO		-26.00	50.92	8.47	9.38	10.46	11.52	13.37	14.81	0.00		10/31/96 C	1 H	2 O	1	0 G 0
HCOHT		48.36	60.95	10.79	11.97	12.81	13.58	14.84	15.81	17.26		10/9/95 C	1 H	2 O	1	0 G 1
HCOH		22.56	58.19	10.79	11.97	12.81	13.58	14.84	15.81	17.26		10/9/95 C	1 H	2 O	1	0 G 1

Table II.A. 3 Thermodynamic Properties for Species in MTBE System (Cont')

SPECIES	Hf	S	Cp	300	400	500	600	800	1000	1500	DATE	ELEME	N	TS
OC*O	-90.20	64.25	10.83	12.87	14.62	15.98	18.40	20.00	0.00	10/31/96	C	1	H	2 O 2 O G 1
HCO2H	-90.20	64.25	10.83	12.87	14.62	15.98	18.40	20.00	0.00	12/30/96	THERM C	1	H	2 O 2 O G 1
HOC.HO.	2.83	65.50	13.45	14.35	15.26	16.25	18.06	19.37	0.00	1/2/97	C	1	H	2 O 2 O G 1
HCQ*O	-67.40	73.86	15.27	17.67	19.67	21.26	23.83	25.48	0.00	12/31/96	THERM C	1	H	2 O 3 O G 2
C.(OH)2O.	-42.27	78.15	15.69	16.27	17.20	18.44	20.87	22.55	0.00	1/2/97	C	1	H	2 O 3 O G 2
HOCHO.O.	-31.01	72.22	15.48	16.90	18.41	19.96	22.61	24.28	0.00	1/2/97	C	1	H	2 O 3 O G 1
HOC.HQ.	1.54	74.82	17.19	18.34	19.27	20.32	22.17	24.00	0.00	1/2/97	C	1	H	2 O 3 O G 2
HOC.HQ.T	-13.00	77.58	17.19	18.34	19.27	20.32	22.17	24.00	0.00	1/2/97	C	1	H	2 O 3 O G 2
O.C.HQ	17.40	73.14	18.26	19.88	21.21	22.52	24.51	26.17	0.00	1/2/97	C	1	H	2 O 3 O G 2
O.C.HQT	4.86	76.52	18.26	19.88	21.21	22.52	24.51	26.17	0.00	1/2/97	C	1	H	2 O 3 O G 2
CH3	34.80	46.30	9.12	9.91	10.68	11.41	12.75	13.90	16.00	J 6/69	C	1	H	3 0 O G 0
CH2OH	-3.60	59.03	11.77	13.27	14.42	15.47	17.22	18.61	20.85	10/31/96	C	1	H	3 O 1 O G 1
CH3O	3.96	54.87	9.01	10.77	12.44	14.02	16.61	18.55	21.42	1/ 3/97	THERM C	1	H	3 O 1 O G 0
CH2OOH	14.60	68.25	16.55	18.40	19.87	21.44	23.20	24.93	0.00	10/31/96	C	1	H	3 O 2 O G 2
CH3OO	4.30	65.18	13.88	15.47	16.85	18.44	20.49	22.71	0.00	10/31/96	C	1	H	3 O 2 O G 1
HOCH2O.	-39.07	66.10	13.12	14.65	16.28	17.92	20.73	22.76	0.00	1/2/97	C	1	H	3 O 2 O G 1
C.H(OH)2	-49.13	68.34	14.43	15.65	16.87	18.14	20.44	22.17	0.00	1/2/97	C	1	H	3 O 2 O G 2
C.(OH)3	-94.23	79.61	16.67	17.57	18.81	20.33	23.25	25.35	0.00	1/2/97	C	1	H	3 O 3 O G 3
CH(OH)2O.	-82.97	73.68	16.46	18.20	20.02	21.85	24.99	27.08	0.00	1/2/97	C	1	H	3 O 3 O G 2
HOC.HQ	-34.56	77.36	19.24	21.18	22.82	24.41	26.89	28.97	0.00	1/2/97	C	1	H	3 O 3 O G 3
CQH2O.	-24.50	75.12	17.93	20.18	22.23	24.19	27.18	29.56	0.00	1/2/97	C	1	H	3 O 3 O G 2
CQ.H2OH	-40.36	76.80	16.86	18.64	20.29	21.99	24.84	27.39	0.00	1/2/97	C	1	H	3 O 3 O G 2
CH2OHOO	-30.30	81.70	19.68	21.49	23.31	24.97	27.72	29.82	33.11	rayez,lev 11/	C	1	H	3 O 3 O G 2
CH4	-17.90	44.40	8.71	9.82	10.99	12.19	14.52	16.60	20.17	J 3/61	C	1	H	4 0 O G 0
CH3OH	-48.00	57.30	10.49	12.34	14.22	16.02	19.05	21.38	25.02	10/31/96	C	1	H	4 O 1 O G 1
CH3OOH	-31.80	64.96	15.93	18.31	20.40	22.53	25.21	27.68	0.00	10/31/96	C	1	H	4 O 2 O G 2
CH2(OH)2	-91.03	66.18	14.10	15.95	17.89	19.81	23.11	25.56	0.00	1/2/97	C	1	H	4 O 2 O G 2
CH(OH)3	-134.93	75.14	17.44	19.50	21.63	23.74	27.37	29.88	0.00	1/2/97	C	1	H	4 O 3 O G 3
CQH2OH	-76.46	76.58	18.91	21.48	23.84	26.08	29.56	32.36	0.00	1/2/97	C	1	H	4 O 3 O G 3
C2H	134.46	51.51	10.05	10.42	10.71	10.96	11.47	11.95	12.92	10/31/96	C	2	H	1 0 O G 0
C#CO.	56.33	57.60	11.88	12.79	13.68	14.94	16.02	16.97	0.00	1/ 2/97	THERM C	2	H	1 O 1 O G 0

Table IIA. 3 Thermodynamic Properties for Species in MTBE System (Cont')

SPECIES	Hf	S	Cp 300	400	500	600	800	1000	1500	DATE	ELEME	N	TS
C.#COH	101.03	60.82	12.71	13.22	13.89	14.95	15.68	16.33	0.00	1/ 2/97 THERM	C	2 H	1 O 1 G 1
C.*C*O	41.36	60.49	12.25	13.60	15.09	15.65	16.52	17.38	0.00	1/2/97 C	C	2 H	1 O 1 G 0
O*CC.*O	-19.70	65.41	14.71	16.69	18.05	19.19	21.07	21.91	0.00	1/ 2/97 THERM	C	2 H	1 O 2 O G 1
C2H2	53.86	48.02	10.56	11.98	12.98	13.74	14.94	15.92	17.70	10/31/96 C	C	2 H	2 0 O G 0
C*C*O	-11.74	56.45	12.70	14.65	16.73	17.80	19.50	20.98	23.03	10/31/96 C	C	2 H	2 O 1 O G 0
C#COH	20.43	58.71	13.22	14.78	16.16	17.73	19.15	20.30	0.00	1/ 2/97 THERM	C	2 H	2 O 1 O G 1
O*CC*O	-50.60	65.42	14.90	17.54	19.64	21.40	24.28	25.80	0.00	1/ 2/97 THERM	C	2 H	2 O 2 O G 1
C2H3	71.62	55.23	10.01	11.97	13.66	15.08	17.32	19.05	21.85	10/31/96 C	C	2 H	3 0 O G 0
CH3C.*O	-2.28	64.25	12.39	14.28	16.26	18.05	21.06	23.24	0.00	10/31/96 C	C	2 H	3 O 1 O G 1
C*CO.	6.29	60.42	12.81	15.33	17.49	19.29	22.06	24.11	27.30	1/ 2/97 THERM	C	2 H	3 O 1 O G 0
C.*COH	29.49	64.30	13.96	16.57	18.61	20.16	22.37	23.95	26.56	1/ 2/97 THERM	C	2 H	3 O 1 O G 1
C*C.OH	24.79	63.39	14.19	16.59	18.52	20.04	22.26	23.86	26.51	1/ 2/97 THERM	C	2 H	3 O 1 O G 1
CYC.OC	29.32	61.23	11.75	14.62	17.10	19.10	22.07	24.19	0.00	1/ 2/97 THERM	C	2 H	3 O 1 O G 0
C.CHO	3.12	60.40	12.92	15.31	17.44	19.24	22.10	24.12	0.00	1/2/97 C	C	2 H	3 O 1 O G 1
C*CQ.	28.50	69.96	16.35	19.17	21.54	23.49	26.52	28.77	0.00	1/ 2/97 THERM	C	2 H	3 O 2 O G 1
C*C.Q	49.30	71.55	18.06	20.80	23.15	25.06	27.90	29.83	0.00	1/ 2/97 THERM	C	2 H	3 O 2 O G 2
C.*CQ	51.50	72.51	18.21	21.26	23.73	25.66	28.42	30.25	0.00	1/ 2/97 THERM	C	2 H	3 O 2 O G 2
O*CCO.	-21.54	72.11	16.55	18.77	20.73	22.52	25.94	28.21	0.00	1/ 2/97 THERM	C	2 H	3 O 2 O G 1
O*CC.OH	-34.60	67.38	15.54	18.62	21.25	23.40	26.66	29.00	0.00	1/ 2/97 THERM	C	2 H	3 O 2 O G 2
O*C.COH	-36.60	74.69	16.70	18.64	20.38	21.99	25.16	27.28	0.00	1/ 2/97 THERM	C	2 H	3 O 2 O G 2
CYC.OOC	41.61	65.24	13.99	18.16	21.83	24.57	28.22	31.21	0.00	1/ 2/97 THERM	C	2 H	3 O 2 O G 0
C2H4	12.52	52.47	10.20	12.72	15.02	17.00	20.14	22.54	26.38	10/31/96 C	C	2 H	4 0 O G 0
CH3CHO	-39.18	63.13	13.22	15.71	18.22	20.47	24.22	26.97	0.00	10/31/96 C	C	2 H	4 O 1 O G 1
C*COH	-29.61	61.53	14.15	17.32	19.97	22.08	25.19	27.44	31.09	1/ 2/97 THERM	C	2 H	4 O 1 O G 1
CYCOC	-12.58	58.14	11.58	15.09	18.25	20.85	24.78	27.60	0.00	1/ 2/97 THERM	C	2 H	4 O 1 O G 0
C*CQ	-7.60	69.74	18.40	22.01	25.09	27.58	31.24	33.74	0.00	1/ 2/97 THERM	C	2 H	4 O 2 O G 2
O*CCOH	-73.50	73.57	17.53	20.07	22.34	24.41	28.32	31.01	0.00	1/ 2/97 THERM	C	2 H	4 O 2 O G 2
CYCOOC	-2.29	60.77	14.05	18.68	22.94	26.31	31.07	34.90	0.00	1/ 2/97 THERM	C	2 H	4 O 2 O G 0
CQCHO	-58.93	82.59	22.34	25.60	28.29	30.68	34.77	37.81	0.00	2/ 9/97 THERM	C	2 H	4 O 3 O G 3
C2H5	28.60	59.87	11.61	14.32	16.89	19.18	22.88	25.80	30.50	10/31/96 C	C	2 H	5 0 O G 1
CCO.	-4.24	65.64	14.50	17.89	20.91	23.56	27.77	30.91	0.00	1/ 2/97 THERM	C	2 H	5 O 1 O G 1

Table IIA. 3 Thermodynamic Properties for Species in MTBE System (Cont')

SPECIES	Hf	S	Cp 300	400	500	600	800	1000	1500	DATE	ELEME	N	TS
C.CO _H	-7.20	71.89	14.71	17.83	20.61	23.05	26.99	29.97	0.00	1/ 2/97 THERM	C	2 H	5 O 1 O G 2
CC.OH	-14.30	67.88	15.81	18.89	21.50	23.78	27.48	30.32	0.00	1/ 2/97 THERM	C	2 H	5 O 1 O G 2
COC.	1.00	67.28	16.30	19.30	21.70	23.93	27.96	30.87	0.00	1/ 2/97 THERM	C	2 H	5 O 1 O G 2
CCQ.	-5.49	74.94	18.66	21.81	24.63	27.47	31.44	35.01	0.00	1/ 2/97 THERM	C	2 H	5 O 2 O G 2
C.CQ	7.41	79.63	20.05	23.37	26.32	29.21	33.02	36.26	0.00	1/ 2/97 THERM	C	2 H	5 O 2 O G 3
CC.Q	2.31	78.54	20.85	23.81	26.52	29.26	32.98	36.19	0.00	1/ 2/97 THERM	C	2 H	5 O 2 O G 3
COCO.	-34.47	73.94	18.41	21.69	24.56	27.28	32.14	35.52	0.00	1/ 2/97 THERM	C	2 H	5 O 2 O G 2
C.OCO _H	-42.03	77.54	19.91	22.91	25.37	27.72	32.02	35.05	0.00	1/ 2/97 THERM	C	2 H	5 O 2 O G 3
COC.OH	-44.53	76.18	19.72	22.69	25.15	27.50	31.85	34.93	0.00	1/ 2/97 THERM	C	2 H	5 O 2 O G 3
C ₂ H ₆	-20.40	55.08	12.38	15.68	18.80	21.58	26.04	29.54	35.16	10/31/96	C	2 H	6 0 O G 1
CCOH	-56.20	67.10	15.48	19.19	22.52	25.45	30.15	33.71	0.00	1/ 2/97 THERM	C	2 H	6 O 1 O G 2
COC	-43.40	63.76	15.78	19.38	22.50	25.38	30.46	34.14	0.00	1/ 2/97 THERM	C	2 H	6 O 1 O G 2
CCQ	-41.59	74.72	20.71	24.65	28.18	31.56	36.16	39.98	0.00	1/ 2/97 THERM	C	2 H	6 O 2 O G 3
COCO _H	-86.43	75.40	19.39	22.99	26.17	29.17	34.52	38.32	0.00	1/ 2/97 THERM	C	2 H	6 O 2 O G 3
C*C*C.	81.62	61.13	13.65	16.07	18.08	19.85	22.46	24.44	27.50	10/31/96	C	3 H	3 0 O G 0
C#CC.	81.58	59.57	13.76	16.14	18.14	19.80	22.39	24.34	27.47	1/ 2/97 THERM	C	3 H	3 0 O G 1
C.#CC	124.88	61.39	14.09	15.75	17.43	18.97	21.62	23.68	28.00	1/ 2/97 THERM	C	3 H	3 0 O G 1
C*C*C	46.72	58.47	14.10	17.12	19.72	22.00	25.44	28.04	32.08	10/31/96	C	3 H	4 0 O G 0
C#CC	44.28	59.28	14.60	17.31	19.70	21.75	25.09	27.65	32.78	1/ 2/97 THERM	C	3 H	4 0 O G 1
CC*C*O	-28.20	59.82	13.79	16.13	18.62	20.09	22.45	24.48	27.42	1/17/97 THERM	C	3 H	4 O 1 O G 1
C*CC*O	-20.32	67.39	17.01	20.92	24.08	26.62	30.56	33.28	0.00	1/17/97 THERM	C	3 H	4 O 1 O G 1
CC*OC*O	-64.48	76.23	19.10	22.93	26.39	29.37	34.16	37.44	0.00	10/31/96	C	3 H	4 O 2 O G 2
CC.*C	61.55	65.62	15.11	18.02	20.78	23.27	27.40	30.58	35.63	10/31/96	C	3 H	5 0 O G 1
C*CC.	40.75	62.05	14.83	18.67	21.94	24.67	28.90	32.03	36.90	10/31/96	C	3 H	5 0 O G 1
CC*C.	63.75	65.20	15.26	18.48	21.36	23.87	27.92	31.00	35.86	1/2/97	C	3 H	5 0 O G 1
C*CO.C	-2.91	71.48	17.84	21.27	24.29	27.03	31.82	35.39	40.58	10/31/96	C	3 H	5 O 1 O G 1
C*COHC.	-2.71	72.21	18.56	22.70	25.99	28.70	33.11	36.26	40.88	10/31/96	C	3 H	5 O 1 O G 2
C.*COHC	20.29	73.98	18.99	22.51	25.41	27.90	32.13	35.23	39.84	10/31/96	C	3 H	5 O 1 O G 2
C ₂ C*O	-9.26	72.49	18.29	22.19	25.74	28.77	33.50	36.93	0.00	10/31/96	C	3 H	5 O 1 O G 2
CCYC.OC	22.32	70.04	17.26	21.46	25.41	28.31	33.06	36.45	0.00	10/31/96	C	3 H	5 O 1 O G 1
CCYCOC.	29.52	68.66	17.75	22.25	26.30	29.19	33.79	37.03	0.00	10/31/96	C	3 H	5 O 1 O G 1

Table IIA. 3 Thermodynamic Properties for Species in MTBE System (Cont')

SPECIES	Hf	S	Cp 300	400	500	600	800	1000	1500	DATE	ELEME	N	TS
C*CCO.	22.15	72.99	17.70	21.45	24.85	27.83	32.58	36.01	41.06	10/31/96	C	3 H	5 O 1 0 G 1
C*C.CO	27.09	76.26	18.34	21.54	24.52	27.20	31.62	34.90	39.89	10/31/96	C	3 H	5 O 1 0 G 2
C.*CCOH	29.29	75.84	18.49	22.00	25.10	27.80	32.14	35.32	40.12	10/31/96	C	3 H	5 O 1 0 G 2
C*CC.OH	3.69	70.64	17.14	20.93	24.38	27.40	32.21	35.67	40.80	10/31/96	C	3 H	5 O 1 0 G 2
CCC.*O	-7.60	73.85	18.59	21.98	24.96	27.55	32.16	35.44	0.00	10/31/96	C	3 H	5 O 1 0 G 2
CC.C*O	-4.70	70.36	18.06	21.84	25.19	28.08	32.66	36.06	0.00	10/31/96	C	3 H	5 O 1 0 G 2
C.CC*O	4.50	76.14	18.65	22.05	25.01	27.57	32.16	35.43	0.00	10/31/96	C	3 H	5 O 1 0 G 2
CC*CO.	-1.58	70.39	18.06	21.84	25.19	28.08	32.66	36.06	41.31	12/30/96	C	3 H	5 O 1 0 G 1
C*CCQ.	20.17	82.76	22.05	25.90	29.09	32.15	36.37	40.14	0.00	1/18/97 THERM	C	3 H	5 O 2 0 G 2
C*CC.Q	17.57	78.73	22.56	26.92	30.56	33.92	38.34	41.97	0.00	1/18/97 THERM	C	3 H	5 O 2 0 G 3
C*C.CQ	40.97	84.35	23.76	27.53	30.70	33.72	37.75	41.20	0.00	1/18/97 THERM	C	3 H	5 O 2 0 G 3
C.*CCQ	43.17	83.93	23.91	27.99	31.28	34.32	38.27	41.62	0.00	1/18/97 THERM	C	3 H	5 O 2 0 G 3
YC.COOC	14.71	72.96	19.37	25.33	30.80	34.92	40.19	44.53	0.00	1/18/97 THERM	C	3 H	5 O 2 0 G 0
YCC.OOC	16.81	71.58	19.37	25.33	30.80	34.92	40.19	44.53	0.00	1/18/97 THERM	C	3 H	5 O 2 0 G 0
O*CCCO.	-28.34	81.91	21.54	25.62	29.03	31.95	37.05	40.54	0.00	1/18/97 THERM	C	3 H	5 O 2 0 G 2
O*CCC.OH	-38.40	84.15	22.85	26.62	29.62	32.17	36.76	39.95	0.00	1/18/97 THERM	C	3 H	5 O 2 0 G 3
O*CC.CO	-40.50	81.00	21.16	25.35	28.91	31.95	36.77	40.23	0.00	1/18/97 THERM	C	3 H	5 O 2 0 G 3
O*C.CCOH	-43.40	84.49	21.69	25.49	28.68	31.42	36.27	39.61	0.00	1/18/97 THERM	C	3 H	5 O 2 0 G 3
CO.CYCOC	-5.72	76.13	19.70	24.93	29.56	32.92	38.23	41.81	0.00	1/18/97 THERM	C	3 H	5 O 2 0 G 1
C.OHCYCOC	-15.78	78.37	21.01	25.93	30.15	33.14	37.94	41.22	0.00	1/18/97 THERM	C	3 H	5 O 2 0 G 2
COHCYC.OC	-13.48	80.68	20.36	24.97	29.13	32.18	37.17	40.62	0.00	1/18/97 THERM	C	3 H	5 O 2 0 G 2
COHCYCOC.	-11.28	79.30	20.85	25.76	30.02	33.06	37.90	41.20	0.00	1/18/97 THERM	C	3 H	5 O 2 0 G 2
CC*OCO.	-33.92	80.45	21.30	25.06	28.40	31.39	36.65	40.39	0.00	1/18/97 THERM	C	3 H	5 O 2 0 G 2
CC*OC.OH	-46.98	75.72	20.29	24.91	28.92	32.27	37.37	41.18	0.00	1/18/97 THERM	C	3 H	5 O 2 0 G 3
C.C*OCOH	-43.58	82.93	22.60	26.55	29.86	32.71	37.60	40.97	0.00	1/18/97 THERM	C	3 H	5 O 2 0 G 3
CCO.C*O	-31.24	79.64	21.01	25.73	29.88	32.98	38.10	41.58	0.00	1/18/97 THERM	C	3 H	5 O 2 0 G 2
CC.OHC*O	-44.30	74.91	20.00	25.58	30.40	33.86	38.82	42.37	0.00	1/18/97 THERM	C	3 H	5 O 2 0 G 3
C.COHC*O	-34.20	86.31	21.40	25.71	29.44	32.22	36.98	40.32	0.00	1/18/97 THERM	C	3 H	5 O 2 0 G 3
CCOHC.*O	-46.30	82.22	21.16	25.60	29.53	32.45	37.32	40.65	0.00	1/18/97 THERM	C	3 H	5 O 2 0 G 3
C.CYCOOC	36.41	75.69	19.28	24.95	30.23	34.00	39.63	44.00	0.00	1/18/97 THERM	C	3 H	5 O 2 0 G 1
CCYC.OOC	31.61	73.99	19.73	25.05	30.10	33.77	39.35	43.75	0.00	1/18/97 THERM	C	3 H	5 O 2 0 G 1

Table IIA. 3 Thermodynamic Properties for Species in MTBE System (Cont')

SPECIES	Hf	S	Cp 300	400	500	600	800	1000	1500	DATE	ELEME	N	TS		
CCYCOOC.	31.31	72.62	19.99	25.79	31.03	34.66	39.94	44.05	0.00	1/18/97 THERM	C	3	H	5	O
CC*OCQ.	-34.21	90.80	25.04	29.05	32.41	35.46	40.76	45.02	0.00	10/31/96 C	C	3	H	5	O
C.C*OCQ	-28.01	91.60	27.41	32.08	35.81	38.98	44.05	47.77	0.00	10/31/96 C	C	3	H	5	O
CC*OC.Q	-31.41	94.40	27.23	31.05	34.30	37.25	42.30	46.20	0.00	10/31/96 C	C	3	H	5	O
CC*C	4.65	63.81	15.45	19.23	22.72	25.79	30.74	34.49	40.39	10/31/96 C	C	3	H	6	
C*COHC	-38.81	72.59	19.18	23.26	26.77	29.82	34.95	38.72	44.37	10/31/96 C	C	3	H	6	O
C2C*O	-51.56	70.09	17.97	22.00	25.89	29.34	34.93	39.15	0.00	10/31/96 C	C	3	H	6	O
CCC*O	-44.50	72.73	19.42	23.41	26.92	29.97	35.32	39.17	0.00	10/31/96 C	C	3	H	6	O
CCYCOC	-21.88	66.95	17.58	22.72	27.45	30.94	36.50	40.44	0.00	10/31/96 C	C	3	H	6	O
C*CCOH	-29.81	74.45	18.68	22.75	26.46	29.72	34.96	38.81	44.65	10/31/96 C	C	3	H	6	O
C*COC	-25.54	71.74	19.95	24.97	29.15	32.48	37.52	41.40	0.00	12/22/96 THERM	C	3	H	6	O
CC*COH	-37.48	71.50	19.40	23.83	27.67	30.87	35.79	39.39	45.10	12/24/96 THERM	C	3	H	6	O
C*CQC	-15.57	82.84	23.59	28.35	32.07	35.40	40.81	44.61	0.00	10/31/96 C	C	3	H	6	O
CC*CQ	-15.47	79.71	23.65	28.52	32.79	36.37	41.84	45.69	0.00	12/25/96 THERM	C	3	H	6	O
C*CCQ	-15.93	82.54	24.10	28.74	32.64	36.24	41.09	45.11	0.00	1/18/97 THERM	C	3	H	6	O
YCCOOC	-29.19	69.86	19.43	25.85	31.91	36.66	43.04	48.22	0.00	1/18/97 THERM	C	3	H	6	O
O*CCCOH	-80.30	83.37	22.52	26.92	30.64	33.84	39.43	43.34	0.00	1/18/97 THERM	C	3	H	6	O
COHCYCOC	-57.68	77.59	20.68	26.23	31.17	34.81	40.61	44.61	0.00	1/18/97 THERM	C	3	H	6	O
CCOHCHO	-83.20	82.47	21.99	27.03	31.49	34.87	40.48	44.38	0.00	2/ 9/97 THERM	C	3	H	6	O
CCYCOOC	-12.59	70.90	20.05	26.31	32.14	36.40	42.79	47.74	0.00	2/ 9/97 THERM	C	3	H	6	O
OHYCOCOC	-58.53	73.19	18.75	24.90	30.36	34.39	40.66	44.91	0.00	2/ 9/97 THERM	C	3	H	6	O
YCOCICOH	-66.71	73.46	21.41	26.77	31.42	35.14	40.91	44.89	0.00	2/ 9/97 THERM	C	3	H	6	O
CC*OCOH	-85.88	81.91	22.28	26.36	30.01	33.28	39.03	43.19	0.00	2/ 9/97 THERM	C	3	H	6	O
CQCYCOC	-43.07	85.21	25.91	31.69	36.83	40.92	46.62	50.88	0.00	2/ 9/97 THERM	C	3	H	6	O
QCYCCOC	-43.01	80.00	23.60	30.08	35.59	40.27	46.40	50.91	0.00	2/ 9/97 THERM	C	3	H	6	O
CC*OCQ	-71.31	90.93	27.09	31.89	35.96	39.55	45.48	49.99	0.00	2/ 9/97 THERM	C	3	H	6	O
YCOCICQ	-51.54	81.03	26.22	32.30	37.37	41.41	47.36	51.69	0.00	2/ 9/97 THERM	C	3	H	6	O
CCQCHO	-67.63	90.74	26.80	32.56	37.44	41.14	46.93	51.18	0.00	2/ 9/97 THERM	C	3	H	6	O
CCC.	23.67	70.67	17.11	21.27	25.14	28.53	33.95	38.14	44.70	10/31/96 C	C	3	H	7	
CC.C	21.02	68.94	16.38	20.30	23.95	27.54	33.36	37.43	44.16	10/31/96 C	C	3	H	7	
C2CO.	-13.54	73.06	20.50	25.52	30.11	33.65	39.49	43.75	50.52	12/30/96 THERM	C	3	H	7	O

Table IIA. 3 Thermodynamic Properties for Species in MTBE System (Cont')

SPECIES	Hf	S	Cp	300	400	500	600	800	1000	1500	DATE	ELEME	N	TS
C2C.OH	-24.80	78.99	20.71	24.89	28.90	32.13	37.75	42.02	48.99	12/30/96	THERM	C	3 H	7 O 1 0 G 3
CCCO.	-9.17	75.06	20.00	24.84	29.16	32.91	38.84	43.25	0.00	2/ 9/97	THERM	C	3 H	7 O 1 0 G 2
CCC.OH	-19.23	77.30	21.31	25.84	29.75	33.13	38.55	42.66	0.00	2/ 9/97	THERM	C	3 H	7 O 1 0 G 3
CC.CO	-14.78	81.65	19.44	23.37	27.28	30.90	36.87	41.41	0.00	2/ 9/97	THERM	C	3 H	7 O 1 0 G 3
C.CCOH	-12.13	81.31	20.21	24.78	28.86	32.40	38.06	42.31	0.00	2/ 9/97	THERM	C	3 H	7 O 1 0 G 3
C2.CO	-16.50	79.74	20.89	25.50	29.67	32.89	38.37	42.49	49.24	2/ 9/97	THERM	C	3 H	7 O 1 0 G 3
C2C.Q	-8.48	87.31	26.55	30.69	34.50	38.21	43.48	47.93	0.00	10/31/96	C	3 H	7 O 2 0 G 4	
C2CQ.	-13.88	81.55	24.28	29.16	33.40	37.33	42.89	47.58	0.00	10/31/96	C	3 H	7 O 2 0 G 3	
C.CCQ	2.48	88.93	25.44	30.24	34.52	38.51	44.07	48.58	0.00	10/31/96	C	3 H	7 O 2 0 G 4	
CCCQ.	-10.42	84.36	24.16	28.76	32.88	36.82	42.51	47.35	0.00	2/9/97	C	3 H	7 O 2 0 G 3	
CC.CQ	-0.17	87.21	25.60	30.05	34.15	38.10	43.69	48.27	0.00	2/9/97	C	3 H	7 O 2 0 G 4	
CCC.Q	-2.62	87.96	26.35	30.76	34.77	38.61	44.05	48.53	0.00	2/9/97	C	3 H	7 O 2 0 G 4	
CCOHCQ.	-50.59	94.38	27.76	32.95	37.55	41.43	47.27	52.02	0.00	2/ 9/97	THERM	C	3 H	7 O 3 0 G 4
CCO.CQ	-34.73	92.70	28.83	34.49	39.49	43.63	49.61	54.19	0.00	2/ 9/97	THERM	C	3 H	7 O 3 0 G 4
CCOHC.Q	-42.79	97.98	29.95	34.95	39.44	43.22	48.81	53.20	0.00	2/ 9/97	THERM	C	3 H	7 O 3 0 G 5
CC.OHCQ	-45.99	98.63	29.04	33.86	38.28	42.11	47.87	52.46	0.00	2/ 9/97	THERM	C	3 H	7 O 3 0 G 5
C.COHCQ	-37.69	99.37	29.22	34.47	39.05	42.87	48.49	52.93	0.00	2/ 9/97	THERM	C	3 H	7 O 3 0 G 5
CCQ.CO	-49.68	93.57	27.38	32.67	37.12	41.20	47.00	51.75	0.00	2/ 9/97	THERM	C	3 H	7 O 3 0 G 4
CCQCO.	-33.82	91.89	28.45	34.21	39.06	43.40	49.34	53.92	0.00	2/ 9/97	THERM	C	3 H	7 O 3 0 G 4
CCQC.OH	-43.88	94.13	29.76	35.21	39.65	43.62	49.05	53.33	0.00	2/ 9/97	THERM	C	3 H	7 O 3 0 G 5
CC.QCOH	-44.28	99.33	29.65	34.20	38.22	42.08	47.59	52.10	0.00	2/ 9/97	THERM	C	3 H	7 O 3 0 G 5
C.CQCOH	-36.78	98.29	28.78	34.23	38.79	42.91	48.56	52.97	0.00	2/ 9/97	THERM	C	3 H	7 O 3 0 G 5
CCQCQ.	-35.07	101.19	32.61	38.13	42.78	47.31	53.01	58.02	0.00	2/ 9/97	THERM	C	3 H	7 O 4 0 G 5
CCQ.CQ	-35.07	101.19	32.61	38.13	42.78	47.31	53.01	58.02	0.00	2/ 9/97	THERM	C	3 H	7 O 4 0 G 5
C.CQCQ	-22.17	105.91	34.01	39.69	44.45	49.02	54.57	59.24	0.00	2/ 9/97	THERM	C	3 H	7 O 4 0 G 6
CC.QCQ	-29.67	106.95	34.88	39.66	43.88	48.19	53.60	58.37	0.00	2/ 9/97	THERM	C	3 H	7 O 4 0 G 6
CCQC.Q	-27.27	104.79	34.80	40.13	44.67	49.10	54.55	59.20	0.00	2/ 9/97	THERM	C	3 H	7 O 4 0 G 6
CCC	-25.33	64.50	17.88	22.63	27.05	30.93	37.11	41.88	49.36	10/31/96	C	3 H	8	0 0 G 2
CCCOH	-61.13	76.52	20.98	26.14	30.77	34.80	41.22	46.05	0.00	2/ 9/97	THERM	C	3 H	8 O 1 0 G 3
C2COH	-65.50	74.52	21.48	26.82	31.72	35.54	41.87	46.55	54.11	2/ 9/97	THERM	C	3 H	8 O 1 0 G 3
C2CQ	-49.98	81.33	26.33	32.00	36.95	41.42	47.61	52.55	0.00	10/31/96	C	3 H	8 O 2 0 G 4	

Table IIA. 3 Thermodynamic Properties for Species in MTBE System (Cont')

SPECIES	Hf	S	Cp 300	400	500	600	800	1000	1500	DATE	ELEME	N	TS
CCCQ	-46.52	84.14	26.21	31.60	36.43	40.91	47.23	52.32	0.00	10/31/96	C	3 H	8 O 2 0 G 4
CCOHCQ	-86.69	94.16	29.81	35.79	41.10	45.52	51.99	56.99	0.00	2/ 9/97 THERM	C	3 H	8 O 3 0 G 5
CCQCOH	-85.78	93.35	29.43	35.51	40.67	45.29	51.72	56.72	0.00	2/ 9/97 THERM	C	3 H	8 O 3 0 G 5
CCQCQ	-71.17	100.97	34.66	40.97	46.33	51.40	57.73	62.99	0.00	2/ 9/97 THERM	C	3 H	8 O 4 0 G 6
C*CICC.*O	3.56	73.25	22.95	27.49	31.07	33.96	38.52	41.67	0.00	10/31/96	C	4 H	5 O 1 0 G 2
C2C*C*O	-28.06	73.97	24.08	28.58	33.01	36.14	41.27	45.33	51.36	10/31/96	C	4 H	6 O 1 0 G 2
C*CICC*O	-27.34	74.64	23.14	28.34	32.66	36.17	41.73	45.56	0.00	10/31/96	C	4 H	6 O 1 0 G 2
C*CYCCOC	5.85	67.28	19.11	24.75	29.98	34.31	40.92	45.55	0.00	10/31/96	C	4 H	6 O 1 0 G 0
C2.C*C	32.30	70.99	20.96	26.09	30.52	34.22	40.07	44.43	51.22	10/31/96	C	4 H	7 0 0 G 2
C2C*C.	55.30	72.75	21.39	25.90	29.94	33.42	39.09	43.40	50.18	10/31/96	C	4 H	7 0 0 G 2
C2.CC*O	-2.20	84.87	22.98	28.14	32.91	36.80	43.20	47.87	0.00	10/31/96	C	4 H	7 O 1 0 G 3
C2C.C*O	-13.50	77.94	24.19	29.26	33.73	37.63	43.83	48.46	0.00	10/31/96	C	4 H	7 O 1 0 G 3
C2CC.*O	-14.30	80.77	22.74	28.03	33.00	37.03	43.54	48.20	0.00	10/31/96	C	4 H	7 O 1 0 G 3
C2CC*O.	7.90	81.04	23.38	28.71	33.60	37.53	43.88	48.44	0.00	10/31/96	C	4 H	7 O 1 0 G 3
C2CYCOC.	19.92	74.32	23.47	29.64	34.85	38.95	45.20	49.64	0.00	10/31/96	C	4 H	7 O 1 0 G 2
C*CIC.CO	-2.16	81.63	24.19	29.61	34.26	38.15	44.29	48.75	55.48	10/31/96	C	4 H	7 O 1 0 G 3
C*CICC.OH	-4.76	78.20	23.27	28.35	32.96	36.95	43.38	48.07	55.12	10/31/96	C	4 H	7 O 1 0 G 3
C.*CICCOH	20.84	83.40	24.62	29.42	33.68	37.35	43.31	47.72	54.44	10/31/96	C	4 H	7 O 1 0 G 3
C*CICCO.	13.70	80.55	23.83	28.87	33.43	37.38	43.75	48.41	55.38	10/31/96	C	4 H	7 O 1 0 G 2
C2C*CO.	-10.03	77.94	24.19	29.26	33.77	37.63	43.83	48.46	55.63	12/30/96	C	4 H	7 O 1 0 G 2
C*CICCQ.	11.72	90.32	28.18	33.32	37.67	41.70	47.54	52.54	0.00	10/31/96	C	4 H	7 O 2 0 G 3
C2CO.C*O	-39.04	84.24	26.72	32.79	38.26	42.86	49.80	54.51	0.00	10/31/96	C	4 H	7 O 2 0 G 3
C2.COHC*O	-42.00	90.92	27.11	32.77	37.82	42.10	48.68	53.25	0.00	10/31/96	C	4 H	7 O 2 0 G 4
C*CICC.Q	9.12	86.29	28.69	34.34	39.14	43.47	49.51	54.37	0.00	10/31/96	C	4 H	7 O 2 0 G 4
C*CIC.CQ	11.72	89.72	29.61	35.60	40.44	44.67	50.42	55.05	0.00	10/31/96	C	4 H	7 O 2 0 G 4
C.*CICCQ	34.72	91.49	30.04	35.41	39.86	43.87	49.44	54.02	0.00	10/31/96	C	4 H	7 O 2 0 G 4
C2.CYCOOC	27.81	81.41	25.00	32.34	38.78	43.76	51.04	56.61	0.00	10/31/96	C	4 H	7 O 2 0 G 2
C2CYCOOC	22.71	78.33	25.71	33.18	39.58	44.42	51.35	56.66	0.00	10/31/96	C	4 H	7 O 2 0 G 2
CCYC.COC	18.67	74.37	20.06	26.34	31.97	36.64	43.72	48.73	0.00	10/31/96	C	4 H	7 O 2 0 G 1
CCYCC.OC	18.37	73.00	20.32	27.08	32.90	37.53	44.31	49.03	0.00	10/31/96	C	4 H	7 O 2 0 G 1
CCYC.COOC	9.84	80.37	24.34	31.48	38.19	43.52	50.86	56.71	0.00	10/31/96	C	4 H	7 O 2 0 G 1

Table IIA. 3 Thermodynamic Properties for Species in MTBE System (Cont')

SPECIES	Hf	S	Cp 300	400	500	600	800	1000	1500	DATE	ELEME	N	TS
CCYCC.OOC	9.54	79.00	24.60	32.22	39.12	44.41	51.45	57.01	0.00	10/31/96	C	4 H	7 O 2 0 G 1
CCICO.C*O	-35.04	90.21	25.69	31.67	37.07	41.43	48.43	53.30	0.00	10/31/96	C	4 H	7 O 2 0 G 3
YCOCICCO.	-15.32	81.80	25.42	32.32	38.11	42.68	49.64	54.42	0.00	10/31/96	C	4 H	7 O 2 0 G 2
C2CQC.*O	-38.53	95.49	31.68	38.19	43.86	48.60	55.47	60.38	0.00	10/31/96	C	4 H	7 O 3 0 G 5
C2.CQC*O	-26.43	99.59	31.92	38.30	43.77	48.37	55.13	60.05	0.00	10/31/96	C	4 H	7 O 3 0 G 5
C2CQ.C*O	-39.33	94.59	30.46	36.78	42.27	46.93	53.91	59.14	0.00	10/31/96	C	4 H	7 O 3 0 G 4
C2C.OOC*O	-44.03	102.48	29.65	35.70	41.10	45.24	52.76	58.29	0.00	10/31/96	C	4 H	7 O 3 0 G 5
C2YC2O2O.	-15.03	82.35	29.35	37.15	44.41	49.62	57.04	62.88	0.00	10/31/96	C	4 H	7 O 3 0 G 2
C2C*C	-3.80	69.99	21.58	26.65	31.30	35.34	41.91	46.89	54.71	10/31/96	C	4 H	8 0 0 G 2
C2CC*O	-51.20	79.65	23.57	29.46	34.96	39.45	46.70	51.93	0.00	10/31/96	C	4 H	8 O 1 0 G 3
CC*OCC	-56.88	81.06	24.17	29.70	34.59	38.84	46.03	51.35	0.00	10/31/96	C	4 H	8 O 1 0 G 3
C2CYCOC	-31.48	72.61	23.30	30.11	36.00	40.70	47.91	53.05	0.00	10/31/96	C	4 H	8 O 1 0 G 2
CCYCCOC	-25.53	71.28	20.38	27.60	34.01	39.27	47.16	52.72	0.00	10/31/96	C	4 H	8 O 1 0 G 1
C*CICCOH	-38.26	82.01	24.81	30.17	35.04	39.27	46.13	51.21	58.97	10/31/96	C	4 H	8 O 1 0 G 3
C2C*COH	-45.93	79.05	25.53	31.25	36.25	40.42	46.96	51.79	59.42	10/31/96	C	4 H	8 O 1 0 G 3
C*CICOC	-34.74	81.44	24.98	30.91	35.95	40.22	47.28	52.68	0.00	12/22/96	THERM C	4 H	8 O 1 0 G 3
C2COHC*O	-91.00	85.70	27.70	34.09	39.87	44.75	52.18	57.31	0.00	10/31/96	C	4 H	8 O 2 0 G 4
C*CICCCQ	-24.38	90.10	30.23	36.16	41.22	45.79	52.26	57.51	0.00	10/31/96	C	4 H	8 O 2 0 G 4
C2C*CQ	-23.92	87.26	29.78	35.94	41.37	45.92	53.01	58.09	0.00	10/31/96	C	4 H	8 O 2 0 G 4
C2CYCOOC	-21.19	76.61	25.77	33.70	40.69	46.16	54.20	60.35	0.00	10/31/96	C	4 H	8 O 2 0 G 2
CCYCCOOC	-34.36	77.28	24.66	32.74	40.23	46.15	54.30	60.70	0.00	10/31/96	C	4 H	8 O 2 0 G 1
CCICOHC*O	-87.00	91.67	26.67	32.97	38.68	43.32	50.81	56.10	0.00	10/31/96	C	4 H	8 O 2 0 G 4
YCOCICCCOH	-67.28	83.26	26.40	33.62	39.72	44.57	52.02	57.22	0.00	10/31/96	C	4 H	8 O 2 0 G 3
CCYC3O(Q)	-52.71	85.08	29.60	37.67	44.44	50.11	57.72	63.32	0.00	10/31/96	C	4 H	8 O 3 0 G 3
C2CQC*O	-75.43	94.37	32.51	39.62	45.82	51.02	58.63	64.11	0.00	10/31/96	C	4 H	8 O 3 0 G 5
C2COOC*O	-84.73	100.02	31.14	38.58	45.00	49.75	57.85	63.61	0.00	10/31/96	C	4 H	8 O 3 0 G 5
C2YC2O2OH	-66.99	83.81	30.33	38.45	46.02	51.51	59.42	65.68	0.00	10/31/96	C	4 H	8 O 3 0 G 3
C*CICOHCQ	-58.84	100.74	33.46	39.68	44.96	49.72	56.48	61.83	0.00	10/31/96	C	4 H	8 O 3 0 G 5
C2CYC2O3	-13.43	85.87	27.85	37.56	45.61	51.50	59.72	66.23	0.00	10/31/96	C	4 H	8 O 3 0 G 2
YCOCICCCQ	-52.67	90.88	31.63	39.08	45.38	50.68	58.03	63.49	0.00	10/31/96	C	4 H	8 O 3 0 G 4
C2CYC2O3	-26.46	83.61	27.85	37.56	45.61	51.50	59.72	66.23	0.00	10/31/96	C	4 H	8 O 3 0 G 2

Table IIA. 3 Thermodynamic Properties for Species in MTBE System (Cont')

SPECIES	Hf	S	Cp 300	400	500	600	800	1000	1500	DATE	ELEME	N	TS
C3.C	16.50	77.82	22.52	28.20	33.32	37.77	44.87	50.30	59.05	10/31/96	C	4 H	9 0 0 G 3
C3C.	11.90	75.67	22.33	27.04	31.82	36.27	43.62	49.34	58.53	10/31/96	C	4 H	9 0 0 G 3
C3.CO	-26.10	85.40	26.61	32.89	38.22	42.65	49.78	55.10	0.00	10/31/96	C	4 H	9 0 1 0 G 4
C3CO.	-23.14	76.55	26.22	32.91	38.66	43.41	50.90	56.36	0.00	10/31/96	C	4 H	9 0 1 0 G 3
C2C.CO	-23.90	87.12	25.43	30.55	35.54	40.14	47.73	53.51	0.00	10/31/96	C	4 H	9 0 1 0 G 4
C2CCO.	-16.34	80.42	25.23	31.73	37.48	42.40	50.10	55.73	0.00	10/31/96	C	4 H	9 0 1 0 G 3
C2.CCO	-19.30	88.05	25.44	31.67	37.18	41.89	49.32	54.79	0.00	10/31/96	C	4 H	9 0 1 0 G 4
C2CC.O	-26.40	84.03	26.54	32.73	38.07	42.62	49.81	55.14	0.00	10/31/96	C	4 H	9 0 1 0 G 4
C3.CO	-26.10	85.40	26.61	32.89	38.22	42.65	49.78	55.10	0.00	10/31/96	C	4 H	9 0 1 0 G 4
C2C.O	-19.40	84.82	25.28	30.98	36.10	40.39	48.19	53.99	0.00	10/31/96	C	4 H	9 0 1 0 G 4
C2COC.	-15.70	85.88	27.29	33.78	39.20	43.45	50.78	56.04	0.00	10/31/96	C	4 H	9 0 1 0 G 4
C2.COC	-11.10	87.57	26.18	32.54	37.95	42.25	49.78	55.25	0.00	10/31/96	C	4 H	9 0 1 0 G 4
C3.CQ	-10.68	91.62	31.74	38.27	43.75	48.61	55.43	60.90	0.00	10/31/96	C	4 H	9 0 2 0 G 5
C3CQ.	-23.58	84.45	30.28	36.75	42.25	47.17	54.21	59.99	0.00	10/31/96	C	4 H	9 0 2 0 G 4
C2C.CQ	-9.29	96.11	30.66	36.01	41.20	46.25	53.74	59.78	0.00	10/31/96	C	4 H	9 0 2 0 G 5
C2CCQ.	-17.59	91.09	29.39	35.65	41.20	46.31	53.77	59.83	0.00	10/31/96	C	4 H	9 0 2 0 G 4
C2CC.Q	-9.79	94.69	31.58	37.65	43.09	48.10	55.31	61.01	0.00	10/31/96	C	4 H	9 0 2 0 G 5
C2.CCQ	-4.69	96.09	30.85	37.17	42.70	47.75	54.99	60.74	0.00	10/31/96	C	4 H	9 0 2 0 G 5
C2COHCQ.	-60.19	98.67	33.48	40.34	46.10	51.19	58.68	64.63	0.00	10/31/96	C	4 H	9 0 3 0 G 5
C2CO.CQ	-44.33	96.99	34.55	41.88	48.04	53.39	61.02	66.80	0.00	10/31/96	C	4 H	9 0 3 0 G 5
C2.COHCQ	-47.29	103.67	34.94	41.86	47.60	52.63	59.90	65.54	0.00	10/31/96	C	4 H	9 0 3 0 G 6
C2COHC.Q	-52.39	102.27	35.67	42.34	47.99	52.98	60.22	65.81	0.00	10/31/96	C	4 H	9 0 3 0 G 6
C2CQ.CO	-59.38	97.27	33.38	40.26	45.97	51.04	58.32	64.16	0.00	10/31/96	C	4 H	9 0 3 0 G 5
C2CQCO.	-43.52	95.59	34.45	41.80	47.91	53.24	60.66	66.33	0.00	10/31/96	C	4 H	9 0 3 0 G 5
C2.CQCO	-46.48	102.27	34.84	41.78	47.47	52.48	59.54	65.07	0.00	10/31/96	C	4 H	9 0 3 0 G 6
C2CQC.O	-53.58	97.83	35.76	42.80	48.50	53.46	60.37	65.74	0.00	10/31/96	C	4 H	9 0 3 0 G 6
C2CQ.CQ	-47.67	104.90	38.78	45.97	51.89	57.36	64.38	70.37	0.00	12/27/96 modif	C	4 H	9 0 4 0 G 6
C2CQCQ.	-44.77	104.89	38.61	45.72	51.63	57.15	64.33	70.43	0.00	10/31/96	C	4 H	9 0 4 0 G 6
C2.CQCQ	-31.87	109.89	40.07	47.24	53.13	58.59	65.55	71.34	0.00	10/31/96	C	4 H	9 0 4 0 G 7
C2CQC.Q	-36.97	108.49	40.80	47.72	53.52	58.94	65.87	71.61	0.00	10/31/96	C	4 H	9 0 4 0 G 7
C3C	-32.50	70.43	23.11	29.52	35.37	40.42	48.37	54.36	63.92	10/31/96	C	4 H	10 0 0 G 3

Table IIA. 3 Thermodynamic Properties for Species in MTBE System (Cont')

SPECIES	Hf	S	Cp 300	400	500	600	800	1000	1500	DATE	ELEME	N	TS
C3COH	-75.10	78.01	27.20	34.21	40.27	45.30	53.28	59.16	0.00	10/31/96	C	4	H 10 O 1 0 G 4
C2CCOH	-68.30	83.25	26.21	33.03	39.09	44.29	52.48	58.53	0.00	10/31/96	C	4	H 10 O 1 0 G 4
C2COC	-60.10	82.36	26.77	33.86	40.00	44.90	53.28	59.31	0.00	10/31/96	C	4	H 10 O 1 0 G 4
C3CQ	-59.68	84.23	32.33	39.59	45.80	51.26	58.93	64.96	0.00	10/31/96	C	4	H 10 O 2 0 G 5
C2CCQ	-53.69	90.87	31.44	38.49	44.75	50.40	58.49	64.80	0.00	10/31/96	C	4	H 10 O 2 0 G 5
C2COHCQ	-96.29	98.45	35.53	43.18	49.65	55.28	63.40	69.60	0.00	10/31/96	C	4	H 10 O 3 0 G 6
C2CQCOH	-95.48	97.05	35.43	43.10	49.52	55.13	63.04	69.13	0.00	10/31/96	C	4	H 10 O 3 0 G 6
C2CQCQ	-80.87	104.67	40.66	48.56	55.18	61.24	69.05	75.40	0.00	10/31/96	C	4	H 10 O 4 0 G 7
C2CYCC.OC	10.57	78.19	26.34	35.05	42.49	48.39	56.79	62.51	0.00	10/31/96	C	5	H 9 O 1 0 G 2
C2.CYCCOC	15.67	81.27	25.63	34.21	41.69	47.73	56.48	62.46	0.00	10/31/96	C	5	H 9 O 1 0 G 2
C3.CC*O	-9.30	90.07	29.00	36.11	42.40	47.66	55.68	61.41	0.00	10/31/96	C	5	H 9 O 1 0 G 4
C3CC.*O	-21.40	83.80	28.76	36.00	42.49	47.89	56.02	61.74	0.00	10/31/96	C	5	H 9 O 1 0 G 4
C2CICO.CO	-42.14	94.04	31.71	39.64	46.56	52.29	60.91	66.84	0.00	10/31/96	C	5	H 9 O 2 0 G 4
C5TOH.*O	-57.20	96.62	31.86	39.51	46.21	51.76	60.13	65.91	0.00	10/31/96	C	5	H 9 O 2 0 G 5
C5.TOH*O	-45.10	100.72	32.10	39.62	46.12	51.53	59.79	65.58	0.00	10/31/96	C	5	H 9 O 2 0 G 5
C5TO.*O	-42.14	94.04	31.71	39.64	46.56	52.29	60.91	66.84	0.00	10/31/96	C	5	H 9 O 2 0 G 5
C3CC.I	26.90	93.44	31.39	39.51	46.29	51.93	60.55	66.59	75.51	1/30/95 THERM	C	5	H 10 I 1 0 G 4
C3.CCI	26.90	97.79	31.55	39.33	46.41	51.74	60.13	66.21	0.00	10/31/96	C	5	H 10 I 1 0 G 4
C3CC.I	26.90	93.43	31.55	39.33	46.41	51.74	60.13	66.21	0.00	10/31/96	C	5	H 10 I 1 0 G 4
C3CC*O	-58.30	82.68	29.59	37.43	44.45	50.31	59.18	65.47	0.00	10/31/96	C	5	H 10 O 1 0 G 4
C2CYCCOC	-33.33	76.47	26.40	35.57	43.60	50.13	59.64	66.20	0.00	10/31/96	C	5	H 10 O 1 0 G 2
C2CICQC*O	-79.49	103.12	37.92	46.40	53.83	60.29	69.30	75.91	0.00	10/31/96	C	5	H 10 O 3 0 G 6
C3CC.	8.70	80.84	28.54	36.17	42.91	48.63	57.35	63.78	73.57	10/31/96	C	5	H 11 0 0 0 G 4
C3CCI	-22.10	90.40	32.14	40.65	48.46	54.39	63.63	70.27	0.00	10/31/96	C	5	H 11 I 1 0 G 4
C3CCO.	-24.14	84.81	31.25	39.70	47.07	53.26	62.58	69.21	0.00	10/31/96	C	5	H 11 O 1 0 G 4
C3.CCOH	-27.10	93.66	31.64	39.68	46.63	52.50	61.46	67.95	0.00	10/31/96	C	5	H 11 O 1 0 G 5
C3CC.OH	-34.20	87.05	32.56	40.70	47.66	53.48	62.29	68.62	0.00	10/31/96	C	5	H 11 O 1 0 G 5
C3.COC	-19.90	93.24	31.90	39.93	46.50	52.01	61.19	67.86	0.00	10/31/96	C	5	H 11 O 1 0 G 5
C3COC.	-24.50	89.37	33.01	41.17	47.75	53.21	62.19	68.65	0.00	10/31/96	C	5	H 11 O 1 0 G 5
C3CCOO.	-25.39	94.11	35.41	43.62	50.79	57.17	66.25	73.31	0.00	10/31/96	C	5	H 11 O 2 0 G 5
C3.CCOOH	-12.49	101.28	36.87	45.14	52.29	58.61	67.47	74.22	0.00	10/31/96	C	5	H 11 O 2 0 G 6

Table IIA. 3 Thermodynamic Properties for Species in MTBE System (Cont')

SPECIES	Hf	S	Cp 300	400	500	600	800	1000	1500	DATE	ELEME	N	TS	
C3CC.OOH	-17.59	97.71	37.60	45.62	52.68	58.96	67.79	74.49	0.00	10/31/96	C	5 H	11 O	2 0 G 6
C2CICQCQ.	-46.58	114.55	43.74	52.59	60.17	67.15	76.37	83.75	0.00	10/31/96	C	5 H	11 O	4 0 G 7
C2.CICQCQ	-33.68	119.55	45.20	54.11	61.67	68.59	77.59	84.66	0.00	10/31/96	C	5 H	11 O	4 0 G 8
C2CICQCQ.	-38.78	118.15	45.93	54.59	62.06	68.94	77.91	84.93	0.00	10/31/96	C	5 H	11 O	4 0 G 8
C4C	-40.30	72.87	29.13	37.49	44.96	51.28	60.85	67.84	78.44	10/31/96	C	5 H	12	0 0 G 4
C3CCOH	-76.10	86.27	32.23	41.00	48.68	55.15	64.96	72.01	0.00	10/31/96	C	5 H	12 O	1 0 G 5
C3COC	-68.90	85.85	32.49	41.25	48.55	54.66	64.69	71.92	0.00	10/31/96	C	5 H	12 O	1 0 G 5
C3CCOOH	-61.49	93.89	37.46	46.46	54.34	61.26	70.97	78.28	0.00	10/31/96	C	5 H	12 O	2 0 G 6
C2CICOHCO	-94.10	95.50	32.69	40.94	48.17	54.18	63.29	69.64	0.00	10/31/96	C	5 H	12 O	2 0 G 5
C2CICQCQ	-82.68	114.33	45.79	55.43	63.72	71.24	81.09	88.72	0.00	10/31/96	C	5 H	12 O	4 0 G 8
C6H6	19.80	64.24	19.44	26.64	32.76	37.80	45.24	50.46	58.38	10/31/96	C	6 H	6	0 0 G 0
DE15	20.18	86.63	28.76	36.50	43.28	48.98	57.88	64.40	74.34	10/31/96	C	6 H	10	0 0 G 3
M2DE15	11.73	98.32	34.89	43.92	51.86	58.53	69.05	76.80	88.66	10/31/96	C	7 H	12	0 0 G 4
DM25DE15	3.28	104.50	41.02	51.34	60.44	68.08	80.22	89.20	102.98	10/31/96	C	8 H	14	0 0 G 5
C3.CCC3	-3.20	102.19	45.29	57.98	69.07	78.33	92.16	102.08	116.85	10/31/96	C	8 H	17	0 0 G 7
C3CCC3	-52.20	93.42	45.88	59.30	71.12	80.98	95.66	106.14	121.72	10/31/96	C	8 H	18	0 0 G 7
CYC3OICOH	-68.13	78.86	24.47	32.29	38.91	44.15	52.07	57.52	0.00	3/7/97 THERM	C	4 H	8 O	2 0 G 2
C*CICOOC	-14.57	92.12	28.31	34.90	40.32	44.96	52.55	57.68	0.00	3/16/97 THERM	C	4 H	8 O	2 0 G 4
C*CICOOC.	31.83	95.42	28.93	34.99	39.79	43.87	50.54	54.93	0.00	3/16/97 THERM	C	4 H	7 O	2 0 G 4
C*COOC	-5.37	80.23	23.28	28.96	33.52	37.22	42.79	46.40	0.00	3/16/97 THERM	C	3 H	6 O	2 0 G 3
C*COOC.	41.03	83.53	23.90	29.05	32.99	36.13	40.78	43.65	0.00	3/16/97 THERM	C	3 H	5 O	2 0 G 3
COHCQ	-77.39	85.36	23.81	28.16	31.90	35.43	40.27	44.15	0.00	3/20/97 THERM	C	2 H	6 O	3 0 G 4
CO.CQ	-25.43	83.90	22.83	26.86	30.29	33.54	37.89	41.35	0.00	3/20/97 THERM	C	2 H	5 O	3 0 G 3
COHCQ.	-41.29	85.58	21.76	25.32	28.35	31.34	35.55	39.18	0.00	3/20/97 THERM	C	2 H	5 O	3 0 G 3
COHC.Q	-33.49	89.18	23.95	27.32	30.24	33.13	37.09	40.36	0.00	3/20/97 THERM	C	2 H	5 O	3 0 G 4
C.OHCQ	-35.49	86.14	24.14	27.86	30.88	33.76	37.60	40.76	0.00	3/20/97 THERM	C	2 H	5 O	3 0 G 4
QCCHO	-58.93	82.59	22.34	25.60	28.29	30.68	34.77	37.81	0.00	3/20/97 THERM	C	2 H	4 O	3 0 G 3
Q.CCHO	-22.83	82.81	20.29	22.76	24.74	26.59	30.05	32.84	0.00	3/20/97 THERM	C	2 H	3 O	3 0 G 2
QC.CHO	-20.03	76.40	20.35	24.15	27.20	29.67	33.11	35.80	0.00	3/20/97 THERM	C	2 H	3 O	3 0 G 3
QCC.*O	-22.03	83.71	21.51	24.17	26.33	28.26	31.61	34.08	0.00	3/20/97 THERM	C	2 H	3 O	3 0 G 3
COHCOH	-92.00	76.36	18.58	22.70	26.24	29.32	34.26	37.88	0.00	3/20/97 THERM	C	2 H	6 O	2 0 G 3

Table IIA. 3 Thermodynamic Properties for Species in MTBE System (Cont')

SPECIES	Hf	S	Cp 300	400	500	600	800	1000	1500	DATE	ELEME	N	TS
CO.CO	-40.04	76.28	17.60	21.40	24.63	27.43	31.88	35.08	0.00	3/20/97 THERM	C	2 H	5 O 2
C.OHCOH	-50.10	78.52	18.91	22.40	25.22	27.65	31.59	34.49	0.00	3/20/97 THERM	C	2 H	5 O 3
QCCQ	-62.78	91.60	29.04	33.62	37.56	41.54	46.28	50.42	0.00	3/20/97 THERM	C	2 H	6 O 5
QCCQ.	-26.68	93.20	26.99	30.78	34.01	37.45	41.56	45.45	0.00	3/21/97	C	2 H	5 O 4
QCC.Q	-18.88	96.80	29.18	32.78	35.90	39.24	43.10	46.63	0.00	3/20/97 THERM	C	2 H	5 O 5
COHCHO	-73.50	73.57	17.53	20.07	22.34	24.41	28.32	31.01	0.00	3/20/97 THERM	C	2 H	4 O 2
CO.CHO	-21.54	72.11	16.55	18.77	20.73	22.52	25.94	28.21	0.00	3/20/97 THERM	C	2 H	3 O 1
C.OHCHO	-34.60	67.38	15.54	18.62	21.25	23.40	26.66	29.00	0.00	3/20/97 THERM	C	2 H	3 O 2
COHC.*O	-36.60	74.69	16.70	18.64	20.38	21.99	25.16	27.28	0.00	3/20/97 THERM	C	2 H	3 O 2
COCQ	-71.86	86.60	24.20	28.52	32.12	35.44	40.97	45.12	0.00	3/20/97 THERM	C	2 H	6 O 4
COCQ.	-35.76	86.82	22.15	25.68	28.57	31.35	36.25	40.15	0.00	3/20/97 THERM	C	2 H	5 O 3
COC.Q	-27.96	90.42	24.34	27.68	30.46	33.14	37.79	41.33	0.00	3/20/97 THERM	C	2 H	5 O 4
C.OCQ	-27.46	87.94	24.72	28.44	31.32	33.99	38.47	41.85	0.00	3/20/97 THERM	C	2 H	5 O 4
C2COHC.*O	-54.10	86.82	26.87	32.66	37.91	42.33	49.02	53.58	0.00	3/21/97 THERM	C	4 H	7 O 4
CCQC.*O	-30.73	91.86	25.97	31.13	35.48	38.72	43.77	47.45	0.00	3/21/97 THERM	C	3 H	5 O 4
C2.CQ	-0.98	87.65	25.68	30.72	35.07	39.04	44.45	48.80	0.00	4/2/97	C	3 H	7 O 4
C2C*CB	-3.80	69.99	21.58	26.65	31.30	35.34	41.91	46.89	54.71	10/31/96	C	4 H	8 O 2
HO2B	3.50	54.73	8.37	8.95	9.48	9.96	10.78	11.43	12.47	JANAF	H	1 O	2 O 0
C2C*CQB	-23.92	87.26	29.78	35.94	41.37	45.92	53.01	58.09	0.00	10/31/96	C	4 H	8 O 4
C*ClCCQB	-24.38	90.10	30.23	36.16	41.22	45.79	52.26	57.51	0.00	10/31/96	C	4 H	8 O 4
C*ClCCOHB	-38.26	82.01	24.81	30.17	35.04	39.27	46.13	51.21	58.97	10/31/96	C	4 H	8 O 3
C2C*COHB	-45.93	79.05	25.53	31.25	36.25	40.42	46.96	51.79	59.42	10/31/96	C	4 H	8 O 3
C*COHB	-29.61	61.53	14.15	17.32	19.97	22.08	25.19	27.44	31.09	1/ 2/97 THERM	C	2 H	4 O 1
C*CQB	-7.60	69.74	18.40	22.01	25.09	27.58	31.24	33.74	0.00	1/ 2/97 THERM	C	2 H	4 O 2
CC*CB	4.65	63.81	15.45	19.23	22.72	25.79	30.74	34.49	40.39	10/31/96	C	3 H	6 O 1
C2H4B	12.52	52.47	10.20	12.72	15.02	17.00	20.14	22.54	26.38	10/31/96	C	2 H	4 O 0
C*COHCB	-38.81	72.59	19.18	23.26	26.77	29.82	34.95	38.72	44.37	10/31/96	C	3 H	6 O 2
C*CQCB	-15.57	82.84	23.59	28.35	32.07	35.40	40.81	44.61	0.00	10/31/96	C	3 H	6 O 3
CC*CQB	-15.47	79.71	23.65	28.52	32.79	36.37	41.84	45.69	0.00	12/25/96 THERM	C	3 H	6 O 3
C*CCQB	-15.93	82.54	24.10	28.74	32.64	36.24	41.09	45.11	0.00	1/18/97 THERM	C	3 H	6 O 3
C*CCOHB	-29.81	74.45	18.68	22.75	26.46	29.72	34.96	38.81	44.65	10/31/96	C	3 H	6 O 2

Table IIA. 3 Thermodynamic Properties for Species in MTBE System (Cont')

SPECIES	Hf	S	Cp 300	400	500	600	800	1000	1500 DATE	ELEME	N	T S
CC*COHB	-37.48	71.50	19.40	23.83	27.67	30.87	35.79	39.39	45.10 12/24/96	THERM	C	3 H 6 O 1 0 G 2
CHOC*O	-19.70	65.41	14.71	16.69	18.05	19.19	21.07	21.91	0.00 4/18/97	THERM	C	2 H 1 O 2 0 G 1
C*CC*O	10.58	66.00	16.82	20.07	22.49	24.41	27.35	29.39	0.00 4/18/97	THERM	C	3 H 3 O 1 0 G 1

**Table IIA. 4 Detailed Mechanism for MTBE Pyrolysis and Oxidation
at 1 atm and 300 -20000 K**

04/17/97 mtbe mechanism by ruwei

ELEMENTS

C H O AR N

END

SPECIES

C3COC CH4 CO CO2 HCHO C2H6 C2H4 C2H2 CC*C CH3OH C2C*C C2C*O C*CICC*O
OH HO2 H O CH3O CH3 C2.C*C C*CC. C2.C*O CC.C C3.COC C3COC. C3C. H2 O2
H2O H2O2 C*CICCOH C2C*COH C2CC*O C*CICCCQ C2C*CQ C2C*O C*CC*O C*CICOC
C2CYCOC C3C C*C*O C*C*C CC*C*O CC*OC*O C*COHC C*CCOH C#CC CCC*O C*CICOOOC
C*CYCCOC C3CQ C2CQC*O C2COHC*O YCOCICCCQ YCOCICCOH C2CYC2O3 CCYCCOC
OHCYCCOC C*CQC COC CH3CHO CCOH C*COH C#COH C*COOC COHCHO COHCQ COCQ
CH3OOH CQCHO CC*CQ CC*COH CCQCHO CCOHCHO HCQ*O CQH2OH HCO2H YCOCICQ
YCOCICOH QCYCCOC CQCYCOC CC*OCOH CC*OCQ CCYCOC QCCQ CYC3OICOH C*CO
CYCOC C*CQ QCCHO COHCOH O*CC*O C*CCQ N2 AR C2H5 C2H3 C3CQ. C3.CQ
C2.COC C2COC. C3CO. C3.CO H C3.C C2C.OC C2CCO. C2.CCOH C2C.CO H C2CC.OH C2CCQ.
C2.CCQ C2C.CQ C2CC.Q C2C.C*O C2CC.*O C2CO.C*O C2CQ.C*O C2.CQC*O C2CQC.*O
C*CICCCQ. C*CIC.CQ C*CICCC.Q C*CICCCO. X Y C2C*CO. C*CICCC.*O C2COHCQ. C2CO.CQ
C2.COHCQ C2COHC.Q C2CQ.CO H C2.CQCOH C2CQCO. C2CQC.OH C2CQCQ. C2CQ.CQ
C2CQC.Q C2.CQCQ CCICO.C*O C*CICOOOC. CCYC.COOC CCYCC.OOC C2.CYCOOC
C2CYCOOC. YCOCICCO. C2CYCOC. CYC.OOC C2CQ. C2C.Q C2.CQ C.CCQ CC.CQ CCC.Q
CCCQ. C2C.OH C2CO. C2.CO H C.CCOH CC.CO H CCC.OH CCCO. CC*CO. C*CCQ. C*CC.Q
C*C.CQ C.*CCQ C*CCO. C.CQCQ CC.QCQ CCQ.CQ CCQC.Q CCQCQ. C.CQCOH CC.QCOH
CCQ.CO H CCQC.OH CCQCO. CC*OCO. CCO.C*O CCOHC.*O O*CCCO. CC.C*O CCC.*O C*CO.C
O*CC.*O C*CC.*O CC.*C CC*C. CCC. C*COOC. CCOHCQ. CCO.CQ CCOHC.Q CC.OHCQ
C.COHCQ CCYC.OC CO.CYCOC YC.COOC YCC.OOC CCYC.OOC C.CYCOOC CCYCOOC.
C*CQ. C.*CQ C.*COH C*CO. CYC.OC C.CHO CH3C.*O CCQ. C.CQ CC.Q C.CO H CCO. CC.OH
CH3OO CH2OOH CH2 CHO CH2OH CH2S HCOH COC. O*CCO. HCQ.*O C.Q*O CQ.H2OH
CQH2O. HOC.HQ HOCH2O. C.O2H HCO2. CO.CQ COHCQ. COHC.Q C.OHCQ Q.CCHO QC.CHO
QCC.*O CO.CO H C.OHCOH QCCQ. QCC.Q CO.CHO C.OHCHO COHC.*O COCQ. COC.Q
C.OCQ C2COHC.*O CCQC.*O C2C*CB HO2B C2C*CQB C*CICCCQB C*CICCOHB C2C*COHB
C*CCOHB CC*COHB C*COHB C*CQB CC*CB C2H4B C*COHCB C*CQCB C*CCQB
CC*CQB

END

REACTION

O + O + M	<=> O2 + M	1.88E+13	0.00	-1788.	!86
AR/1./					
H + O2 + M	<=> HO2 + M	6.17E+17	-0.80	0.	!92
AR/1./ N2/2.29/ H2/3.42/ H2O/2.53/					
HO2 + HO2	<=> H2O2 + O2	1.87E+12	0.00	1540.	!92
HO2 + O	<=> OH + O2	3.25E+13	0.00	0.	!92
HO2 + H	<=> H2O + O	3.01E+13	0.00	1721.	!92
HO2 + H	<=> H2 + O2	4.28E+13	0.00	1411.	!92
HO2 + H	<=> OH + OH	1.69E+14	0.00	874.	!92
H2O2 + M	<=> OH + OH + M	1.81E+16	0.00	42924.	!92
AR/1./ N2/6.69/					
H2O2 + H	<=> H2 + HO2	1.69E+12	0.00	3756.	!92
H2O2 + H	<=> H2O + OH	1.02E+13	0.00	3577.	!92
H2O2 + O	<=> OH + HO2	6.62E+11	0.00	3974.	!92
H + O + M	<=> OH + M	4.71E+18	-1.00	0.	!86
H + O2	<=> OH + O	1.99E+14	0.00	16812.	!92

O + H2	<=> OH + H	5.11E+04	2.67	6280.	!92
H + H + M	<=> H2 + M	6.52E+17	-1.00	0.	!92
AR/1./ N2/1.5/ H2/1.47/					
OH + OH	<=> O + H2O	1.51E+09	1.14	99	!92
OH + H + M	<=> H2O + M	8.35E+21	-2.00	0.	!92
AR/1./ N2/2.65/ H2O/16.91/					
OH + H2	<=> H2O + H	1.02E+08	1.60	3299.	!92
OH + HO2	<=> H2O + O2	2.89E+13	0.00	-497.	!92
OH + H2O2	<=> HO2 + H2O	7.83E+12	0.00	1331.	!92
HO2	=> X + Y	1.00E+00	0.00	0.	!
H2O2	=> H2O + X	1.00E+00	0.00	0.	!
X + X	=> O2	1.00E+15	0.00	0.	!
X + Y + Y	=> H2O + O2	1.00E+19	0.00	0.	!
C3COC + H	<=> C3.COC + H2	2.16E+09	1.50	6997.	!F
C3COC + H	<=> C3COC. + H2	7.20E+08	1.50	4352.	!F
C3COC + O	<=> C3.COC + OH	1.53E+09	1.50	5305.	!F
C3COC + O	<=> C3COC. + OH	5.35E+12	0.00	3031.	!n
C3COC + OH	<=> C3.COC + H2O	1.08E+07	2.00	525.	!F
C3COC + OH	<=> C3COC. + H2O	6.27E+12	0.00	739.	!8
C3COC + CH3	<=> C3.COC + CH4	1.36E+00	3.65	7154.	!9
C3COC + CH3	<=> C3COC. + CH4	1.31E+00	4.00	11567.	!b
C3COC + CH3O	<=> C3.COC + CH3OH	9.03E+11	0.00	7866.	!b
C3COC + CH3O	<=> C3COC. + CH3OH	3.01E+11	0.00	5266.	!A
C3COC + HO2	<=> C3.COC + H2O2	3.01E+04	2.55	15500.	!9
C3COC + HO2	<=> C3COC. + H2O2	9.64E+10	0.00	12536.	!8
C3COC + O2	<=> C3COC. + HO2	2.05E+13	0.00	38392.	!8
C3COC + O2	<=> C3.COC + HO2	4.04E+13	0.00	39432.	!9
C3C. + CH3O	<=> C3COC	0.00E+00	.000	0.	! mtbe017d.mec avg err .00%
C3C. + CH3O	<=> C2C*C + CH3OH	9.19E+37	-7.839	8102.	! mtbe017d.mec avg err 47.78%
C3C. + CH3O	<=> C3CO. + CH3	8.72E+05	2.448	7526.	! mtbe017d.mec avg err 112.73%
C3C. + CH3O	<=> C2C.OC + CH3	1.11E+02	3.529	11971.	! mtbe017d.mec avg err 123.04%
C3C. + CH3O	<=> C3.COC + H	7.94E+14	-.786	14903.	! mtbe017d.mec avg err 137.13%
C3C. + CH3O	<=> C3COC. + H	1.50E+06	2.144	27290.	! mtbe017d.mec avg err 74.97%
C3COC	<=> C2C*C + CH3OH	5.35E+03	2.575	23829.	! mtbe017d.mec avg err 85.74%
C3COC	<=> C2C.OC + CH3	3.68E+24	-3.237	60518.	! mtbe017d.mec avg err 42.37%
C3COC	<=> C3.COC + H	2.79E+53	-12.065	90110.	! mtbe017d.mec avg err 56.49%
C3COC	<=> C3COC. + H	4.33E+47	-9.999	109503.	! mtbe017d.mec avg err 36.96%
C3CO. + CH3	<=> C3COC	2.06E+45	-9.593	105188.	! mtbe017d.mec avg err 39.82%
C3CO. + CH3	<=> C2C*C + CH3OH	1.09E+37	-7.502	7800.	! mtbe017d.mec avg err 48.10%
C3CO. + CH3	<=> C2C.OC + CH3	5.46E+04	2.863	7524.	! mtbe017d.mec avg err 118.30%
C3CO. + CH3	<=> C3.COC + H	1.98E+15	-.825	16219.	! mtbe017d.mec avg err 139.60%
C3CO. + CH3	<=> C3COC. + H	7.37E+07	1.736	29651.	! mtbe017d.mec avg err 74.01%
C3.COC	<=> C2C*C + CH3O	1.77E+05	2.216	26030.	! mtbe017d.mec avg err 84.87%
C3.COC	<=> C*ClCOC + CH3	2.45E+36	-7.795	30284.	! mtbe017d.mec avg err 9.77%
C3.COC	<=> C3COC.	1.09E+37	-7.751	32131.	! mtbe017d.mec avg err 9.08%
C3.COC	<=> C3C. + HCHO	4.46E+38	-9.316	23904.	! mtbe017d.mec avg err 6.23%
C3COC.	<=> C2C*C + CH3O	7.89E+37	-8.217	28428.	! mtbe017d.mec avg err 18.17%

C3COC.	<=> C*CICOC + CH3	3.38E+30	-6.142	36763.	! mtbe017d.mec avg err
11.35%					
C3COC.	<=> C3C. + HCHO	3.45E+30	-5.918	37994.	! mtbe017d.mec avg err 8.38%
C2.COC	<=> CC*C + CH3O	6.16E+28	-5.722	15530.	! mtbe017d.mec avg err 26.07%
C2.COC	<=> C*COC + CH3	5.55E+33	-7.097	28720.	! mtbe017d.mec avg err 13.00%
C2.COC	<=> C*CICOC + H	9.35E+32	-6.801	31665.	! mtbe017d.mec avg err 15.60%
C2.COC	<=> C2COC.	7.10E+30	-6.270	34832.	! mtbe017d.mec avg err 18.43%
C2.COC	<=> CC.C + HCHO	1.70E+41	-9.848	25315.	! mtbe017d.mec avg err 6.43%
C2.COC	<=> C2C.OC	1.21E+37	-7.921	28402.	! mtbe017d.mec avg err 20.12%
C2.COC	<=> C2C*O + CH3	2.39E+21	-4.599	36248.	! mtbe017d.mec avg err 34.60%
C2COC.	<=> CC.C + HCHO	1.10E+26	-4.792	39364.	! mtbe017d.mec avg err 22.45%
C2COC.	<=> CCYCOC + CH3	1.37E+50	-12.388	24373.	! mtbe017d.mec avg err
38.54%					
C2COC.	<=> C2C.OC	4.95E+65	-18.009	45221.	! mtbe017d.mec avg err 31.65%
C2C.OC	<=> C2C*O + CH3	6.26E+32	-9.952	13418.	! mtbe017d.mec avg err 34.51%
C2C.OC	<=> C*CICOC + H	2.06E+34	-7.809	11603.	! mtbe017d.mec avg err 27.25%
C3C. + C3COC	<=> C3.COC + C3C	5.06E-06	5.17	9068.	!90
C3C. + C3COC	<=> C3COC. + C3C	7.84E-05	4.70	9320.	!A
C3C. + CH3OH	<=> C3C + CH3O	1.50E+03	1.80	9358.	!90T
C3C. + CH3OH	<=> C3C + CH2OH	7.84E-05	4.70	9085.	!90
C3C. + HCHO	<=> C3C + CHO	3.25E+09	0.00	3553.	!90
C3C. + C2C*O	<=> C3C + C2C*O	6.02E-05	4.90	11362.	!A
C3C. + C2C*C	<=> C3C + C2C*C	6.02E-05	4.90	8362.	!2*
C3C. + CC*C	<=> C3C + C*CC.	3.01E-05	4.90	8362.	!91
C3C. + O2	<=> C2C*C + HO2	4.82E+11	0.00	0.	!90
C3C. + C2CYCOC	<=> C3C + C2CYCOC.	1.07E+11	0.00	11832.	!!/
C3C. + CCYCOC	<=> C3C + CCYC.OC	5.06E-06	5.17	9068.	!90
C3C. + C*CICC*O	<=> C3C + C*CICC.*O	1.02E+10	0.00	6838.	!85
C3C. + C2CC*O	<=> C3C + C2CC.*O	4.00E+10	0.00	6299.	!!/
C3C. + O*CC*O	<=> C3C + O*CC.*O	2.16E+10	0.00	6955.	!!/
C3C. + CCC*O	<=> C3C + CCC.*O	1.08E+10	0.00	6955.	!!/
C3C. + CH3CHO	<=> C3C + CH3C.*O	1.08E+10	0.00	6955.	!!/
C3C. + C2CQC*O	<=> C3C + C2CQC.*O	5.40E+09	0.00	6955.	!!/
C3C. + C2COHC*O	<=> C3C + C2COHC.*O	5.40E+09	0.00	6955.	!!/
C3C. + CCQCHO	<=> C3C + CCQC.*O	5.40E+09	0.00	6955.	!!/
C3C. + CCOHCHO	<=> C3C + CCOHC.*O	5.40E+09	0.00	6955.	!!/
C2C*C + H	<=> C3C.	3.08E+62	-17.123	50708.	! mtbe017d.mec avg err 39.04%
C2C*C + H	<=> C3.C	4.80E+38	-7.952	11164.	! mtbe017d.mec avg err 39.56%
C2C*C + H	<=> CC*C + CH3	5.78E+35	-7.003	21804.	! mtbe017d.mec avg err 43.70%
C3C.	<=> C3.C	2.44E+21	-1.801	22816.	! mtbe017d.mec avg err 55.38%
C3C.	<=> CC*C + CH3	2.16E+60	-14.925	58325.	! mtbe017d.mec avg err 37.88%
C3.C	<=> CC*C + CH3	1.97E+49	-11.006	59961.	! mtbe017d.mec avg err 61.28%
C3C. + O2	<=> C3CQ.	6.32E+65	-16.876	45250.	! mtbe017d.mec avg err 51.90%
C3C. + O2	<=> C2C*CB + HO2B	1.42E+52	-13.155	10033.	! mtbe017d.mec avg err
29.43%					
C3C. + O2	<=> C3CO. + O	4.19E+22	-2.930	10487.	! mtbe017d.mec avg err 10.29%
C3C. + O2	<=> C3.CQ	5.45E+15	-1.025	27929.	! mtbe017d.mec avg err 2.02%
C3C. + O2	<=> C2C*C + HO2	3.41E+36	-8.154	9841.	! mtbe017d.mec avg err 16.15%
C3C. + O2	<=> C2CYCOC + OH	3.07E+32	-5.908	13002.	! mtbe017d.mec avg err
14.48%					
C3C. + O2	<=> C*CQC + CH3	9.43E+23	-3.796	13191.	! mtbe017d.mec avg err 10.01%
C3CQ.	<=> C2C*CB + HO2B	1.88E+14	-629	19932.	! mtbe017d.mec avg err 2.84%
C3CQ.	<=> C3CO. + O	4.52E+50	-11.762	42106.	! mtbe017d.mec avg err 28.99%
C3CQ.	<=> C3.CQ	7.95E+32	-6.762	60220.	! mtbe017d.mec avg err 39.21%

C3CQ. 11.75%	\rightleftharpoons C2CYCOC + OH	6.20E-65	-16.937	41407. ! mtbe017d.mec avg err
C3CQ.	\rightleftharpoons C*CQC + CH3	5.27E-52	-12.828	45984. ! mtbe017d.mec avg err 35.22%
C3.CQ	\rightleftharpoons C2CYCOC + OH	6.72E+34	-7.336	52167. ! mtbe017d.mec avg err 39.07%
C3.CQ	\rightleftharpoons C*CQC + CH3	6.22E+20	-3.690	19206. ! mtbe017d.mec avg err 27.50%
C*CQC	\rightleftharpoons C*CO.C + OH	2.04E+14	-1.342	32073. ! mtbe017d.mec avg err 21.66%
C2C*C + O	\rightleftharpoons C2.C*C + OH	1.21E+11	0.70	7633. !2*91T
C2C*C + O	\rightleftharpoons C2CYCOC	4.20E+12	0.00	503. !73HER
C2C*C + H	\rightleftharpoons C2.C*C + H2	3.50E+05	2.50	2492. !2*91T
C2C*C + H	\rightleftharpoons CC*C + CH3	1.45E+13	0.00	1302. !2*91T
C2C*C + OH	\rightleftharpoons C2.C*C + H2O	6.24E+06	2.00	-298. !91TSA
C2C*C + CH3	\rightleftharpoons C2.C*C + CH4	4.42E+00	3.50	5675. !2*(ch
C2C*C + CH3O	\rightleftharpoons C2.C*C + CH3OH	4.42E+00	3.50	5675. !take
C2C*C + HO2	\rightleftharpoons C2.C*C + H2O2	1.93E+04	2.60	13910. !2*91T
C2C*C + HO2	\rightleftharpoons C2CYCOC + OH	1.05E+12	0.00	14206. !91TSA
C2C*C + O2	\rightleftharpoons C2.C*C + HO2	4.79E+12	0.00	38560. !R.W.W
C2C*C	\rightleftharpoons CC.*C + CH3	5.84E+39	-8.950	23050 ! mtbe017d.mec avg err 38.90%
CC.*C	\rightleftharpoons C*C*C + H	9.85E+35	-5.826	103757. ! mtbe017d.mec avg err 59.26%
CC *C	\rightleftharpoons C*CC.	8.75E+43	-10.144	47445. ! mtbe017d.mec avg err 15.84%
C2C*C + HO2	\rightleftharpoons C3.CQ	1.96E+41	-8.892	43223. ! mtbe017d.mec avg err 27.93%
C2C*C + HO2 30.26%	\rightleftharpoons C2CYCOC + OH	3.76E+17	-2.102	10117. ! mtbe017d.mec avg err
C2C*C + HO2 3.45%	\rightleftharpoons C*CQC + CH3	2.39E+05	2.304	17411. ! mtbe017d.mec avg err
C2C*C + HO2	\rightleftharpoons C3CQ.	3.50E+03	3.274	30182. ! mtbe017d.mec avg err .59%
C2C*C + HO2 35.68%	\rightleftharpoons C3CO. + O	3.36E+47	-11.249	24700. ! mtbe017d.mec avg err
C2C*C + HO2	\rightleftharpoons C2C.CQ	5.72E+04	2.665	40446. ! mtbe017d.mec avg err 5.63%
C2C*C + HO2 22.26%	\rightleftharpoons C2CYCOC + OH	3.49E+23	-3.964	11471. ! mtbe017d.mec avg err
C2C*C + HO2 6.05%	\rightleftharpoons C*CICCQ + H	2.96E+09	1.000	19237. ! mtbe017d.mec avg err
C2C*C + HO2 2.81%	\rightleftharpoons C2C*CQ + H	1.18E+10	1.174	34521. ! mtbe017d.mec avg err
C2C*C + HO2	\rightleftharpoons C2CCQ.	2.39E+08	1.222	36450. ! mtbe017d.mec avg err 2.67%
C2C*C + HO2	\rightleftharpoons C3.C + O2	1.24E+40	-8.945	26000. ! mtbe017d.mec avg err 21.38%
C2C*C + HO2	\rightleftharpoons C2.CCQ	2.94E+23	-2.934	31462. ! mtbe017d.mec avg err 19.55%
C2C*C + HO2 38.79%	\rightleftharpoons CCYCCOC + OH	3.04E+36	-7.380	31559. ! mtbe017d.mec avg err
C2C*C + HO2 28.92%	\rightleftharpoons CC*C + CH2OOH	1.84E+31	-5.618	36765. ! mtbe017d.mec avg err
C2C*C + HO2 12.84%	\rightleftharpoons C*CCQ + CH3	1.04E+25	-3.229	42362. ! mtbe017d.mec avg err
C2C*C + HO2	\rightleftharpoons C2CC.Q	3.72E+24	-3.282	42181. ! mtbe017d.mec avg err 13.04%
C2C*C + HO2 6.39%	\rightleftharpoons C2CC*O + OH	1.31E+09	-1.189	37137. ! mtbe017d.mec avg err
C2C*C + HO2 9.08%	\rightleftharpoons CC*CQ + CH3	1.65E+12	.058	38011. ! mtbe017d.mec avg err
C2C.CQ	\rightleftharpoons C2CYCOC + OH	1.56E-16	7.523	37817. ! mtbe017d.mec avg err 4.45%
C2C.CQ	\rightleftharpoons C*CICCQ + H	2.73E+22	-4.076	21392. ! mtbe017d.mec avg err 24.42%
C2C.CQ	\rightleftharpoons C2C*CQ + H	5.07E+18	-2.626	36845. ! mtbe017d.mec avg err 20.23%
C2C.CQ 20.17%	\rightleftharpoons C2C*CB + HO2B	4.84E+16	-2.483	38765. ! mtbe017d.mec avg err
C2C.CQ	\rightleftharpoons C3.C + O2	2.97E+32	-7.274	31426. ! mtbe017d.mec avg err 12.88%

C2C.CQ	<=> C2.CCQ	3.44E+33	-7.109	33506.	! mtbe017d.mec avg err 9.14%
C2C.CQ	<=> CCYCCOC - OH	4.60E+45	-11.196	32769.	! mtbe017d.mec avg err
29.38%					
C2C.CQ	<=> CC*C + CH2OOH	6.47E+39	-9.317	38266.	! mtbe017d.mec avg err
14.49%					
C2C.CQ	<=> C*CCQ + CH3	5.04E+32	-6.701	44363.	! mtbe017d.mec avg err 5.06%
C2C.CQ	<=> C2CC.Q	1.99E+32	-6.766	44185.	! mtbe017d.mec avg err 4.99%
C2C.CQ	<=> C2CC*O + OH	1.19E+18	-4.055	39608.	! mtbe017d.mec avg err 10.95%
C2C.CQ	<=> CC*CQ + CH3	1.35E+21	-3.800	40448.	! mtbe017d.mec avg err 15.80%
C2CCQ.	<=> C2C.CQ	7.88E-10	4.250	39421.	! mtbe017d.mec avg err 13.42%
C2CCQ.	<=> C2CYCOC + OH	1.00E+54	-13.631	35442.	! mtbe017d.mec avg err
6.86%					
C2CCQ.	<=> C2C*CB + HO2B	1.46E+44	-10.268	42304.	! mtbe017d.mec avg err
20.48%					
C2CCQ.	<=> C3.C + O2	1.66E+41	-9.381	35539.	! mtbe017d.mec avg err 16.14%
C2CCQ.	<=> C2.CCQ	8.78E+44	-9.980	39863.	! mtbe017d.mec avg err 16.19%
C2CCQ.	<=> CCYCCOC + OH	3.38E+49	-11.846	33357.	! mtbe017d.mec avg err
30.38%					
C2CCQ.	<=> CC*C + CH2OOH	1.69E+49	-11.588	43703.	! mtbe017d.mec avg err
17.24%					
C2CCQ.	<=> C*CCQ + CH3	2.91E+44	-9.661	52348.	! mtbe017d.mec avg err 14.82%
C2CCQ.	<=> C*CICCCQ + H	1.14E+44	-9.724	52143.	! mtbe017d.mec avg err 14.71%
C2CCQ.	<=> C2CC.Q	2.30E+40	-9.234	54127.	! mtbe017d.mec avg err 15.93%
C2CCQ.	<=> C2CC*O + OH	1.02E+31	-7.369	48089.	! mtbe017d.mec avg err 21.16%
C2CCQ.	<=> CC*CQ + CH3	1.12E+34	-7.115	48912.	! mtbe017d.mec avg err 27.34%
C2CCQ.	<=> C2C*CQ + H	2.10E+02	1.319	47418.	! mtbe017d.mec avg err 24.63%
C2.CCQ	<=> CCYCCOC + OH	3.02E-02	2.178	49534.	! mtbe017d.mec avg err
23.96%					
C2.CCQ	<=> CC*C + CH2OOH	7.83E+23	-4.387	19296.	! mtbe017d.mec avg err
17.98%					
C2.CCQ	<=> C*CCQ + CH3	1.82E+25	-4.090	31884.	! mtbe017d.mec avg err 12.21%
C2.CCQ	<=> C*CICCCQ + H	4.95E+24	-4.111	31597.	! mtbe017d.mec avg err 12.23%
C2.CCQ	<=> C2CC.Q	2.56E+22	-4.008	34297.	! mtbe017d.mec avg err 11.47%
C2.CCQ	<=> C2CC*O + OH	3.35E+25	-5.957	36196.	! mtbe017d.mec avg err 8.00%
C2CC.Q	<=> C2CC*O + OH	6.14E+28	-5.766	37106.	! mtbe017d.mec avg err 3.48%
C2CC.Q	<=> CC*CQ + CH3	2.10E+08	.188	-837.	! mtbe017d.mec avg err 4.31%
C2CC.Q	<=> C2C*CQ + H	5.51E+08	-.020	33294.	! mtbe017d.mec avg err 5.34%
C3.CQ + O2	<=> C2CQCQ.	7.49E+07	.027	38424.	! mtbe017d.mec avg err 5.55%
C3.CQ + O2	<=> C2CQ.CQ	9.80E+37	-8.502	6836.	! mtbe017d.mec avg err 4.58%
C3.CQ + O2	<=> C2C.CQ + O2	5.81E+70	-19.203	19968.	! mtbe017d.mec avg err
46.38%					
C3.CQ + O2	<=> C*CICCCQB + HO2B	1.47E+60	-15.155	25775.	! mtbe017d.mec avg err
34.46%					
C3.CQ + O2	<=> C2C*CQB + HO2B	2.15E+54	-13.464	26099.	! mtbe017d.mec avg err
31.64%					
C3.CQ + O2	<=> C2.CQCQ	1.85E+53	-13.306	26221.	! mtbe017d.mec avg err 30.65%
C3.CQ + O2	<=> C*CICCCQ + HO2	3.89E+40	-9.229	12322.	! mtbe017d.mec avg err
10.11%					
C3.CQ + O2	<=> C*CQC + CH2OOH	1.26E+34	-6.295	15389.	! mtbe017d.mec avg err
16.35%					
C3.CQ + O2	<=> YCOCICCCQ + OH	1.34E+20	-2.150	24004.	! mtbe017d.mec avg err
7.26%					
C3.CQ + O2	<=> C2CQC.Q	8.35E+27	-5.088	16160.	! mtbe017d.mec avg err 13.78%

C3.CQ + O2 5.90%	<=> C2C* CQ - HO2	7.60E+11	-1.503	18640. ! mtbe017d.mec avg err
C3.CQ + O2 3.02%	<=> C2CQC*O + OH	2.52E-02	3.158	18661. ! mtbe017d.mec avg err
C2CQCQ. 93.78%	<=> C2CQ.CQ	4.75E+13	-8.10	18816. ! mtbe017d.mec avg err 5.89%
C2CQCQ. 44.61%	<=> C* CICCQB + HO2B	1.05E+52	-13.673	24146. ! mtbe017d.mec avg err
C2CQCQ. 41.77%	<=> C2C* CQB - HO2B	1.47E-68	-17.595	53716. ! mtbe017d.mec avg err
C2CQCQ. 42.22%	<=> C2.CQCQ	3.25E+67	-17.561	54145 ! mtbe017d.mec avg err 41.77%
C2CQCQ. 7.57%	<=> C* CICCQ + HO2	4.53E+57	-14.360	35251. ! mtbe017d.mec avg err
C2CQCQ. 10.85%	<=> C* CQC + CH2OOH	2.38E+54	-12.489	43089. ! mtbe017d.mec avg err
C2CQCQ. 4.99%	<=> YCOCICCCQ + OH	3.33E+34	-6.663	53808. ! mtbe017d.mec avg err
C2CQCQ. 9.36%	<=> C2CQC.Q	1.29E+48	-11.271	44973. ! mtbe017d.mec avg err 6.70%
C2CQCQ. 7.61%	<=> C2C* CQ + HO2	1.49E+27	-6.305	47767. ! mtbe017d.mec avg err
C2CQCQ. 21.02%	<=> C2CQC*O + OH	4.94E+09	-5.61	46332. ! mtbe017d.mec avg err
C2CQCQ. 85.53%	<=> C* CICCQB + HO2B	4.33E+28	-5.527	47800. ! mtbe017d.mec avg err
C2CQCQ. 45.15%	<=> C2C* CQB + HO2B	1.34E+44	-9.366	46784. ! mtbe017d.mec avg err
C2CQCQ. 8.02%	<=> C2.CQCQ	3.59E+43	-9.351	47334. ! mtbe017d.mec avg err 19.28%
C2CQCQ. 11.15%	<=> C* CICCQ + HO2	2.44E+74	-19.964	47739. ! mtbe017d.mec avg err
C2CQCQ. 12.09%	<=> C* CQC + CH2OOH	1.46E+81	-21.260	57766. ! mtbe017d.mec avg err
C2CQCQ. 6.52%	<=> YCOCICCCQ + OH	2.19E+63	-16.455	66307. ! mtbe017d.mec avg err
C2CQCQ. 3.53%	<=> C2CQC.Q	3.57E+77	-20.910	60035. ! mtbe017d.mec avg err 32.89%
C2CQCQ. 9.71%	<=> C2C* CQ + HO2	1.03E+59	-16.931	61933. ! mtbe017d.mec avg err
C2CQCQ. 1.77%	<=> C2CQC*O + OH	1.14E+41	-11.203	59537. ! mtbe017d.mec avg err
C2CQCQ. 6.33%	<=> C* CICCQ + HO2	4.52E+60	-16.222	61952. ! mtbe017d.mec avg err
C2CQCQ + O2 8.39%	<=> C* CQC + CH2OOH	5.23E+31	-6.340	19075. ! mtbe017d.mec avg err
C2CQCQ + O2 15.31%	<=> YCOCICCCQ + OH	4.19E+19	-2.569	35048. ! mtbe017d.mec avg err
C2CQCQ + O2 14.92%	<=> C2CQC.Q	2.37E+26	-5.329	22018. ! mtbe017d.mec avg err 4.03%
	<=> C2C* CQ + HO2B	3.40E+21	-5.249	35383. ! mtbe017d.mec avg err
	<=> C2CQC*O + OH	2.62E+11	-768	20933. ! mtbe017d.mec avg err
C2C.CQ + O2	<=> C2CQ.CQ	6.68E+09	-197	-194. ! mtbe017d.mec avg err 6.86%
C2C.CQ + O2	<=> C* CICCQB + HO2B	5.36E+46	-11.225	9319. ! mtbe017d.mec avg err
C2C.CQ + O2	<=> C2C* CQB + HO2B	1.62E+25	-3.710	14978. ! mtbe017d.mec avg err
C2C.CQ + O2	<=> C2.CQCQ	1.89E+24	-3.585	15193. ! mtbe017d.mec avg err 14.92%

C2C.CQ + O2 9.02%	<=> C*CICCCQ + HO2	1.07E+41	-9.357	13671. ! mtbe017d.mec avg err
C2C.CQ + O2 20.32%	<=> C*CQC + CH2OOH	3.96E+37	-7.264	17826. ! mtbe017d.mec avg err
C2C.CQ + O2 14.03%	<=> YCOCICCCQ + OH	1.28E-23	-2.983	25593. ! mtbe017d.mec avg err
C2C.CQ + O2	<=> C2CQC.Q	1.12E+31	-5.954	18245. ! mtbe017d.mec avg err 17.19%
C2C.CQ + O2 23.51%	<=> C2C*CQ + HO2	6.11E-29	-6.368	12889. ! mtbe017d.mec avg err
C2C.CQ + O2 14.00%	<=> C2CQC*O + OH	8.89E-13	-1.040	13879. ! mtbe017d.mec avg err
C2C.CQ + O2	<=> C2CQCQ.	1.74E+31	-5.581	13069. ! mtbe017d.mec avg err 21.34%
C2C*C + OH	<=> C3.CO	1.30E+69	-18.667	20099. ! mtbe017d.mec avg err 47.86%
C2C*C + OH 18.61%	<=> C*COHC + CH3	1.01E+40	-8.842	8454. ! mtbe017d.mec avg err
C2C*C + OH	<=> C3CO.	3.45E+22	-2.806	10906. ! mtbe017d.mec avg err 37.68%
C2C*C + OH	<=> C2C*O + CH3	1.26E+04	.408	13428. ! mtbe017d.mec avg err 2.65%
C3.CO	<=> C*COHC + CH3	7.56E+09	.370	16888. ! mtbe017d.mec avg err 13.56%
C3.CO	<=> C3CO.	4.92E+38	-8.314	34846. ! mtbe017d.mec avg err 20.00%
C3.CO	<=> C2C*O + CH3	6.91E+23	-6.137	42635. ! mtbe017d.mec avg err 25.99%
C3CO.	<=> C2C*O + CH3	1.34E+29	-6.084	45757. ! mtbe017d.mec avg err 21.46%
C2C*C + OH	<=> C2C.CO	6.35E+41	-10.227	13555. ! mtbe017d.mec avg err 36.50%
C2C*C + OH 21.16%	<=> C*CICCOH + H	1.67E+41	-9.197	8473. ! mtbe017d.mec avg err
C2C*C + OH 19.52%	<=> C2C*COH + H	2.58E+21	-2.329	16684. ! mtbe017d.mec avg err
C2C*C + OH	<=> C2.CCOH	4.64E+20	-2.549	13685. ! mtbe017d.mec avg err 29.23%
C2C*C + OH 24.29%	<=> C*CCOH + CH3	4.68E+39	-8.353	27423. ! mtbe017d.mec avg err
C2C*C + OH	<=> C2CC.OH	3.67E+22	-2.520	28201. ! mtbe017d.mec avg err 44.39%
C2C*C + OH 22.48%	<=> CC*COH + CH3	1.24E+39	-8.531	24554. ! mtbe017d.mec avg err
C2C*C + OH	<=> C2CCO.	2.40E+22	-2.655	24698. ! mtbe017d.mec avg err 31.89%
C2C*C + OH 12.30%	<=> CC.C + HCHO	6.16E+11	-1.395	17916. ! mtbe017d.mec avg err
C2C.CO	<=> C*CICCOH + H	2.95E+11	.142	20823. ! mtbe017d.mec avg err
C2C.CO 16.30%	<=> C2C*COH + H	1.18E+41	-8.928	45062. ! mtbe017d.mec avg err
C2C.CO	<=> C2.CCOH	1.86E+40	-9.110	41051. ! mtbe017d.mec avg err 17.04%
C2C.CO 20.04%	<=> C*CCOH + CH3	1.35E+53	-12.959	55072. ! mtbe017d.mec avg err
C2C.CO	<=> C2CC.OH	1.03E+36	-7.302	55406. ! mtbe017d.mec avg err 24.38%
C2C.CO 23.28%	<=> CC*COH + CH3	1.57E+55	-13.870	52766. ! mtbe017d.mec avg err
C2C.CO	<=> C2CCO.	7.93E+38	-8.321	52522. ! mtbe017d.mec avg err 23.09%
C2C.CO 37.53%	<=> CC.C + HCHO	3.61E+30	-7.678	47115. ! mtbe017d.mec avg err
C2.CCOH 19.65%	<=> C*CICCOH + H	2.74E+29	-5.987	49451. ! mtbe017d.mec avg err
C2.CCOH 52.96%	<=> C*CCOH + CH3	3.26E+70	-19.346	49022. ! mtbe017d.mec avg err
C2.CCOH	<=> C2CC.OH	8.32E+68	-18.083	45720. ! mtbe017d.mec avg err 62.19%

C2.CCOH 28.39%	\rightleftharpoons CC*COH + CH3	1.12E+72 -21.191 38378. ! mtbe017d.mec avg err
C2.CCOH	\rightleftharpoons C2CCO.	1.75E+66 -19.475 41279. ! mtbe017d.mec avg err 10.54%
C2.CCOH 17.34%	\rightleftharpoons CC.C + HCHO	8.96E+63 -18.989 36478. ! mtbe017d.mec avg err
C2CC.OH 8.16%	\rightleftharpoons CC*COH + CH3	5.94E+69 -19.792 40824. ! mtbe017d.mec avg err
C2CC.OH 19.62%	\rightleftharpoons C2C*COH + H	1.22E+39 -8.306 36478. ! mtbe017d.mec avg err
C2CC.OH	\rightleftharpoons C2CCO.	1.03E+39 -8.582 41456. ! mtbe017d.mec avg err 17.20%
C2CC.OH 32.53%	\rightleftharpoons CC.C + HCHO	4.09E+18 -4.410 51680. ! mtbe017d.mec avg err
C2CCO. 20.25%	\rightleftharpoons C*CCOH + CH3	9.96E+19 -3.400 55081. ! mtbe017d.mec avg err
C2CCO. 26.48%	\rightleftharpoons CC*COH + CH3	1.00E+59 -18.253 38985. ! mtbe017d.mec avg err
C2CCO.	\rightleftharpoons CC.C + HCHO	2.51E+53 -15.167 31250. ! mtbe017d.mec avg err 45.59%
C3.CO ₂ H + O ₂ 19.86%	\rightleftharpoons C2COHCQ.	7.75E+54 -14.011 22709. ! mtbe017d.mec avg err
C3.CO ₂ H + O ₂	\rightleftharpoons C2CO.CQ	9.36E+37 -8.428 7106. ! mtbe017d.mec avg err 6.03%
C3.CO ₂ H + O ₂ 30.80%	\rightleftharpoons C2C*O + CH2OOH	7.63E+38 -9.475 11260. ! mtbe017d.mec avg err
C3.CO ₂ H + O ₂ 24.48%	\rightleftharpoons C2.COHCQ	5.02E+31 -6.021 11292. ! mtbe017d.mec avg err
C3.CO ₂ H + O ₂ 30.43%	\rightleftharpoons C*CICCCQ + OH	9.52E+39 -8.882 13278. ! mtbe017d.mec avg err
C3.CO ₂ H + O ₂ 16.11%	\rightleftharpoons C*COHC + CH2OOH	1.18E+31 -5.404 24465. ! mtbe017d.mec avg err
C3.CO ₂ H + O ₂ 18.26%	\rightleftharpoons CYC3OICOH + OH	1.15E+32 -5.703 23025. ! mtbe017d.mec avg err
C3.CO ₂ H + O ₂ 27.71%	\rightleftharpoons C2COHC.Q	3.19E+36 -7.476 18531. ! mtbe017d.mec avg err
C3.CO ₂ H + O ₂ 9.48%	\rightleftharpoons C2C*CQ + OH	1.15E+13 -1.427 18296. ! mtbe017d.mec avg err
C3.CO ₂ H + O ₂ 5.91%	\rightleftharpoons C2COHC*O + OH	4.04E-11 5.981 20550. ! mtbe017d.mec avg err
C2COHCQ.	\rightleftharpoons C2CO.CQ	3.49E+15 -1.087 19026. ! mtbe017d.mec avg err 7.95%
C2COHCQ. 23.55%	\rightleftharpoons C2C*O + CH2OOH	3.15E+52 -13.831 28007. ! mtbe017d.mec avg err
C2COHCQ. 8.96%	\rightleftharpoons C2.COHCQ	7.88E+46 -10.843 33914. ! mtbe017d.mec avg err
C2COHCQ. 33.41%	\rightleftharpoons C*CICCCQ + OH	9.11E+46 -11.220 32002. ! mtbe017d.mec avg err
C2COHCQ. 5.32%	\rightleftharpoons C*COHC + CH2OOH	1.52E+43 -9.303 52862. ! mtbe017d.mec avg err
C2COHCQ. 4.88%	\rightleftharpoons CYC3OICOH + OH	2.69E+44 -9.671 51060. ! mtbe017d.mec avg err
C2COHCQ. 17.42%	\rightleftharpoons C2COHC.Q	5.69E+46 -10.810 42579. ! mtbe017d.mec avg err
C2COHCQ. 6.72%	\rightleftharpoons C2C*CQ + OH	5.80E+28 -6.436 47807. ! mtbe017d.mec avg err
C2COHCQ. 18.77%	\rightleftharpoons C2COHC*O + OH	1.47E+00 2.316 48558. ! mtbe017d.mec avg err

C2CO.CQ 12.98%	\rightleftharpoons C2C*O + CH2OOH	1.20E+31	-6.061	48440.	! mtbe017d.mec avg err
C2CO.CQ	\rightleftharpoons C2.COHCQ	1.40E+27	-5.079	10911.	! mtbe017d.mec avg err 13.93%
C2CO.CQ 43.49%	\rightleftharpoons C*CICCCQ + OH	2.07E+50	-12.999	22206.	! mtbe017d.mec avg err
C2CO.CQ 18.58%	\rightleftharpoons C*COHC + CH2OOH	1.41E+42	-9.747	41124.	! mtbe017d.mec avg err
C2CO.CQ 21.03%	\rightleftharpoons CYC3OICOH + OH	2.24E+43	-10.107	39286.	! mtbe017d.mec avg err
C2CO.CQ	\rightleftharpoons C2COHC.Q	2.66E+45	-11.203	30472.	! mtbe017d.mec avg err 41.47%
C2CO.CQ 16.75%	\rightleftharpoons C2C*CQ + OH	1.40E+27	-6.699	35868.	! mtbe017d.mec avg err
C2CO.CQ 8.73%	\rightleftharpoons C2COHC*O + OH	1.02E-02	2.260	36560.	! mtbe017d.mec avg err
C2.COHCQ 17.26%	\rightleftharpoons C2C*O + CH2OOH	2.50E+29	-6.303	36488.	! mtbe017d.mec avg err
C2.COHCQ 35.33%	\rightleftharpoons C*CICCCQ + OH	7.87E+43	-10.184	26797.	! mtbe017d.mec avg err
C2.COHCQ 13.04%	\rightleftharpoons C*COHC + CH2OOH	2.43E+26	-4.455	33296.	! mtbe017d.mec avg err
C2.COHCQ 13.70%	\rightleftharpoons CYC3OICOH + OH	2.79E+26	-4.502	30768.	! mtbe017d.mec avg err
C2.COHCQ 14.40%	\rightleftharpoons C2COHC.Q	2.03E+25	-4.790	19260.	! mtbe017d.mec avg err
C2.COHCQ 13.86%	\rightleftharpoons C2C*CQ + OH	1.67E+28	-6.558	38162.	! mtbe017d.mec avg err
C2.COHCQ 4.23%	\rightleftharpoons C2COHC*O + OH	2.78E+03	1.043	39759.	! mtbe017d.mec avg err
C2COHC.Q 7.83%	\rightleftharpoons C2C*O + CH2OOH	5.60E+30	-6.244	38874.	! mtbe017d.mec avg err
C2COHC.Q 92.10%	\rightleftharpoons C*CICCCQ + OH	6.23E-05	2.284	10221.	! mtbe017d.mec avg err
C2COHC.Q 11.43%	\rightleftharpoons C*COHC + CH2OOH	8.52E+13	-1.786	47668.	! mtbe017d.mec avg err
C2COHC.Q 88.21%	\rightleftharpoons CYC3OICOH + OH	7.39E-24	8.452	15822.	! mtbe017d.mec avg err
C2COHC.Q 100.90%	\rightleftharpoons C2C*CQ + OH	1.06E+29	-7.724	22510.	! mtbe017d.mec avg err
C2COHC.Q 4.16%	\rightleftharpoons C2COHC*O + OH	9.08E+10	-4.45	35847.	! mtbe017d.mec avg err
C2C.COHC + O2	\rightleftharpoons C2CQ.COHC	4.95E+09	-2.203	-356.	! mtbe017d.mec avg err 2.74%
C2C.COHC + O2 17.25%	\rightleftharpoons C*CICCOHB + HO2B	3.63E+46	-11.322	8598.	! mtbe017d.mec avg err
C2C.COHC + O2 9.68%	\rightleftharpoons C2C*COHB + HO2B	8.67E+21	-2.724	12791.	! mtbe017d.mec avg err
C2C.COHC + O2 14.64%	\rightleftharpoons C2.CQCOH	9.98E+27	-4.525	11315.	! mtbe017d.mec avg err
C2C.COHC + O2 21.59%	\rightleftharpoons C*CICCOH + HO2	2.29E+41	-9.750	12643.	! mtbe017d.mec avg err
C2C.COHC + O2 19.01%	\rightleftharpoons YCOCICCOH + OH	2.54E+35	-6.899	16223.	! mtbe017d.mec avg err
C2C.COHC + O2 16.35%	\rightleftharpoons C2CQCO.	2.21E+29	-5.676	16481.	! mtbe017d.mec avg err

C2C.CO ₂ H + O ₂ 26.66%	<=> C2C.Q + HCHO	1.50E+51	-13.022	15334. ! mtbe017d.mec avg err
C2C.CO ₂ H + O ₂ 19.02%	<=> C2CQC.OH	1.69E+38	-8.202	14388. ! mtbe017d.mec avg err
C2C.CO ₂ H + O ₂ 14.78%	<=> C2C*COH + HO ₂	3.09E+37	-8.814	9776. ! mtbe017d.mec avg err
C2CQC.CO ₂ H 18.42%	<=> C*CICCOHB + HO ₂ B	4.95E+34	-6.838	13379. ! mtbe017d.mec avg err
C2CQC.CO ₂ H 20.59%	<=> C2C*COHB + HO ₂ B	2.17E+42	-9.219	42029. ! mtbe017d.mec avg err
C2CQC.CO ₂ H 14.17%	<=> C2.CQCOH	5.23E+46	-10.512	37385. ! mtbe017d.mec avg err
C2CQC.CO ₂ H 20.88%	<=> C*CICCOH + HO ₂	1.63E+65	-16.851	42253. ! mtbe017d.mec avg err
C2CQC.CO ₂ H 24.01%	<=> YCOCICCOH + OH	9.42E+59	-14.507	47137. ! mtbe017d.mec avg err
C2CQC.CO ₂ H 64.73%	<=> C2CQCO.	1.70E+52	-12.833	47258. ! mtbe017d.mec avg err 24.83%
C2CQC.CO ₂ H 18.09%	<=> C2C.Q + HCHO	7.80E+54	-14.278	31733. ! mtbe017d.mec avg err
C2CQC.CO ₂ H 16.88%	<=> C2CQC.OH	2.59E+58	-14.427	42304. ! mtbe017d.mec avg err
C2CQC.CO ₂ H 19.36%	<=> C2C*COH + HO ₂	1.85E+59	-15.352	35676. ! mtbe017d.mec avg err
C2.CQCOH 30.73%	<=> C*CICCOHB + HO ₂ B	3.49E+56	-13.652	40737. ! mtbe017d.mec avg err
C2.CQCOH 24.45%	<=> C2C*COHB + HO ₂ B	1.63E+33	-7.208	30034. ! mtbe017d.mec avg err
C2.CQCOH 25.94%	<=> C*CICCOH + HO ₂	2.27E+43	-10.157	29793. ! mtbe017d.mec avg err
C2.CQCOH 39.01%	<=> YCOCICCOH + OH	6.93E+32	-6.805	19638. ! mtbe017d.mec avg err
C2.CQCOH 20.64%	<=> C2CQCO.	2.77E+26	-5.440	21445. ! mtbe017d.mec avg err 28.98%
C2.CQCOH 8.58%	<=> C2C.Q + HCHO	8.57E+66	-18.445	34615. ! mtbe017d.mec avg err
C2CQCO.	<=> C2CQC.OH	3.71E+54	-14.009	33794. ! mtbe017d.mec avg err
C2CQCO.	<=> C2C*COH + HO ₂	1.43E+57	-15.444	30469. ! mtbe017d.mec avg err
C2CQCO.	<=> C*CICCOHB + HO ₂ B	8.20E+52	-13.247	33213. ! mtbe017d.mec avg err
C2CQCO.	<=> C2C*COHB + HO ₂ B	2.27E+50	-12.203	30858. ! mtbe017d.mec avg err
C2CQCO.	<=> C*CICCOH + HO ₂	1.06E+56	-13.852	27772. ! mtbe017d.mec avg err
C2CQCO.	<=> YCOCICCOH + OH	8.73E+67	-17.490	36090. ! mtbe017d.mec avg err
C2CQCO.	<=> C2C.Q + HCHO	9.47E+59	-15.749	35859. ! mtbe017d.mec avg err
C2CQCO.	<=> C2CQC.OH	1.76E+30	-5.833	15527. ! mtbe017d.mec avg err 7.02%
C2CQCO.	<=> C2C*COH + HO ₂	3.89E+65	-17.863	25711. ! mtbe017d.mec avg err
C2CQC.OH 43.43%	<=> C*CICCOHB + HO ₂ B	1.75E+65	-16.826	31012. ! mtbe017d.mec avg err

C2CQC.OH 26.67%	<=> C2C*COHB + HO2B	7.97E+30	-6.491	34647. ! mtbe017d.mec avg err
C2CQC.OH 17.49%	<=> C2C.Q + HCHO	2.80E+38	-8.707	32445. ! mtbe017d.mec avg err
C2CQC.OH 14.03%	<=> C2C*COH + HO2	1.44E+50	-12.691	36836. ! mtbe017d.mec avg err
C2C*CQ	<=> C2C*CO. + OH	2.56E+32	-6.725	18456. ! mtbe017d.mec avg err 34.96%
C2.C*C + HO2	<=> C*CICCCQ	3.85E+41	-9.419	24393. ! mtbe017d.mec avg err 49.14%
C2.C*C + HO2 24.51%	<=> C*CICCO. + OH	2.59E+49	-11.759	10186. ! mtbe017d.mec avg err
C*CICCCQ 20.67%	<=> C*CICCO. + OH	1.13E+21	-2.170	7943. ! mtbe017d.mec avg err
C*CICCO. 37.92%	<=> C*CICC*O + H	2.48E+48	-10.538	54973. ! mtbe017d.mec avg err
C*CICCO. 27.97%	<=> CC.*C + HCHO	9.65E+30	-6.461	16432. ! mtbe017d.mec avg err
C2C.C*O + HO2 23.58%	<=> C2CQC*O	8.28E+21	-3.687	23122. ! mtbe017d.mec avg err
C2C.C*O + HO2 19.36%	<=> C2C.Q + CHO	9.54E+45	-10.749	8788. ! mtbe017d.mec avg err
C2C.C*O + HO2 20.12%	<=> C2CQC.*O + H	1.16E+08	1.863	16906. ! mtbe017d.mec avg err
C2C.C*O + HO2 104.85%	<=> C2CO.C*O + OH	2.83E+07	1.323	31842. ! mtbe017d.mec avg err
C2CQC*O	<=> C2C.Q + CHO	3.50E+22	-2.640	8138. ! mtbe017d.mec avg err 22.39%
C2CQC*O 22.87%	<=> C2CQC.*O + H	8.13E+44	-9.294	79566. ! mtbe017d.mec avg err
C2CQC*O 25.56%	<=> C2CO.C*O + OH	4.00E+36	-7.735	91686. ! mtbe017d.mec avg err
C2C.C*O + OH 35.50%	<=> C2COHC*O	5.44E+44	-9.450	52149. ! mtbe017d.mec avg err
C2C.C*O + OH 59.21%	<=> C2C.OH + CHO	1.17E+57	-14.008	13588. ! mtbe017d.mec avg err
C2C.C*O + OH 39.91%	<=> C2COHC.*O + H	6.09E+19	-1.741	9443. ! mtbe017d.mec avg err
C2COHC*O 24.31%	<=> C2C.OH + CHO	6.26E+08	.417	12653. ! mtbe017d.mec avg err
C2COHC*O 71.42%	<=> C2COHC.*O + H	7.04E+52	-11.090	84381. ! mtbe017d.mec avg err
C2COHC.*O 47.26%	<=> C2C.OH + CO	2.16E+60	-14.468	101643. ! mtbe017d.mec avg err
C2CQC.*O	<=> C2C.Q + CO	4.61E+12	-1.182	2311. ! mtbe017d.mec avg err 22.23%
YCOCICCCQ 16.82%	<=> CCYC.OC + CH2OOH	3.99E+11	-.803	2247. ! mtbe017d.mec avg err
YCOCICCCQ 31.78%	<=> YCOCICCO. + OH	1.65E+40	-8.278	90863. ! mtbe017d.mec avg err
YCOCICCOH 36.97%	<=> CCYC.OC + CH2OH	2.28E+48	-10.498	54373. ! mtbe017d.mec avg err
C2C.Q	<=> C2C*O + OH	2.32E+36	-6.131	89864. ! mtbe017d.mec avg err 60.79%
CCYC.OC	<=> C2.C*O	3.05E+09	-.134	-376. ! mtbe017d.mec avg err 2.12%
C2CYCOC 8.18%	<=> CCYC.OC + CH3	1.18E+12	-.994	1702. ! mtbe017d.mec avg err
C2C*O	<=> CH3C.*O + CH3	4.81E+40	-7.326	93465. ! mtbe017d.mec avg err 70.70%

C*ClCC*O 38.51%	<=> CC.*C + CHO	5.09E+47 -9.779 90106. ! mtbe017d.mec avg err
C*ClCC*O 53.96%	<=> C*ClCC.*O + H	3.88E+36 -6.109 102355. ! mtbe017d.mec avg err
C*ClCC.*O C2.C*O	<=> CC.*C + CO	1.33E+25 -3.336 85773. ! mtbe017d.mec avg err 39.34%
C2CYCOC. C2CYCOC.	<=> C*ClCC.*O + CH3	2.49E+44 -9.813 41318. ! mtbe017d.mec avg err 19.74%
12.52%	<=> C2C.C*O	6.12E+30 -5.755 42358. ! mtbe017d.mec avg err 26.21%
C2CYCOC. 37.62%	<=> C*ClCC*O + H	3.11E+37 -9.012 10250. ! mtbe017d.mec avg err
C2CYCOC.	<=> C2C*ClCC*O + H	9.07E+12 -1.067 12137. ! mtbe017d.mec avg err
C2CYCOC.	<=> C2CC.*O	5.70E+12 -1.051 12342. ! mtbe017d.mec avg err 37.20%
C2CYCOC.	<=> CC.C + CO	2.85E+06 -3.359 6461. ! mtbe017d.mec avg err 24.55%
C2C.C*O	<=> C*ClCC*O + H	3.75E+11 -5.573 10111. ! mtbe017d.mec avg err 40.72%
C2C.C*O	<=> C2C*ClCC*O + H	3.14E+40 -8.636 47876. ! mtbe017d.mec avg err 27.00%
C2C.C*O	<=> C2CC.*O	3.29E+40 -8.686 48278. ! mtbe017d.mec avg err 26.31%
C2C.C*O	<=> CC.C + CO	3.95E+28 -6.278 37898. ! mtbe017d.mec avg err 15.97%
C2CC.*O	<=> CC.C + CO	1.36E+34 -6.684 41715. ! mtbe017d.mec avg err 32.78%
C2C.C*O + O2	<=> C2CQ.C*O	4.15E+21 -3.789 9000. ! mtbe017d.mec avg err 35.30%
C2C.C*O + O2	<=> C2CQC.*O	1.13E+29 -5.953 2554. ! mtbe017d.mec avg err 16.53%
C2C.C*O + O2	<=> C2C.Q + CO	4.45E+19 -3.548 4470. ! mtbe017d.mec avg err 5.57%
C2C.C*O + O2 6.68%	<=> C2C*ClCC*O + HO2	2.72E+23 -3.346 6161. ! mtbe017d.mec avg err
C2C.C*O + O2	<=> C2.CQC*O	3.92E+08 .429 6318. ! mtbe017d.mec avg err 3.05%
C2C.C*O + O2 5.62%	<=> C*ClCC + CHO	7.11E+11 -.878 6977. ! mtbe017d.mec avg err
C2C.C*O + O2 4.08%	<=> C*ClCC*O + HO2	1.28E+05 2.056 17110. ! mtbe017d.mec avg err
C2CQ.C*O	<=> C2CQC.*O	2.19E+14 -.674 10322. ! mtbe017d.mec avg err 1.30%
C2CQ.C*O	<=> C2C.Q + CO	3.11E+31 -7.778 17941. ! mtbe017d.mec avg err 2.99%
C2CQ.C*O 11.52%	<=> C2C*ClCC*O + HO2	2.72E+33 -7.062 19407. ! mtbe017d.mec avg err
C2CQ.C*O	<=> C2.CQC*O	1.75E+17 -2.877 22496. ! mtbe017d.mec avg err 16.70%
C2CQ.C*O 17.24%	<=> C*ClCC + CHO	2.42E+25 -5.489 27214. ! mtbe017d.mec avg err
C2CQ.C*O 18.69%	<=> C*ClCC*O + HO2	3.44E+11 -.549 36566. ! mtbe017d.mec avg err
C2CQC.*O 20.98%	<=> C2C*ClCC*O + HO2	2.92E+25 -4.628 29752. ! mtbe017d.mec avg err
C2CQC.*O	<=> C2.CQC*O	4.20E+08 -.155 16190. ! mtbe017d.mec avg err 5.80%
C2CQC.*O 38.18%	<=> C*ClCC + CHO	1.28E-12 3.881 -7080. ! mtbe017d.mec avg err
C2CQC.*O 5.13%	<=> C*ClCC*O + HO2	5.95E+05 .566 36445. ! mtbe017d.mec avg err
C2.CQC*O	<=> C2C.Q + CO	4.81E-08 3.938 8569. ! mtbe017d.mec avg err 53.88%
C2.CQC*O 69.20%	<=> C2C*ClCC*O + HO2	3.09E-03 2.630 -4224. ! mtbe017d.mec avg err
C2.CQC*O 43.81%	<=> C*ClCC + CHO	6.10E-29 9.765 -5291. ! mtbe017d.mec avg err
C2.CQC*O 8.74%	<=> C*ClCC*O + HO2	1.07E+11 -.348 21393. ! mtbe017d.mec avg err
C2.C*O + HCHO	<=> CHO + C2C*O	6.30E+07 1.90 18191. ! 1/2
C2.C*O + C2C*ClCC	<=> C2C*O + C2.C*ClCC	1.01E-01 4.00 227. !
C2.C*O + C3COC	<=> C2C*O + C3COC.	1.78E+02 3.30 19844. ! 1/2 (c)

```

C2.C*O + C3COC   <=> C2C*O + C3.COC   8.70E+02  2.90  19314. !1/2 (c
C2.C*O + CH3OH   <=> C2C*O + CH2OH   8.70E+02  2.90  20456. !1/2 (c
C2.C*O + C2CYCOC <=> C2C*O + C2CYCOC.  5.00E-01  4.00  13318. !1/2 (c
C2.C*O + CCYCOC  <=> C2C*O + CCYC.OC  2.21E-01  3.30  17169. !1/2 (c
C2.C*O + C*CICC*O <=> C2C*O + C*CICC.*O 1.25E+07  0.00   0. !1/2 (c
C2.C*O + C2CC*O  <=> C2C*O + C2CC.*O  2.51E+07  0.00   0. !the sa
C2.C*O + O*CC*O  <=> C2C*O + O*CC.*O  5.02E+07  0.00   0. !2*ch3c
C2.C*O + CCC*O   <=> C2C*O + CCC.*O   2.51E+07  0.00   0. !the sa
C2.C*O + CH3CHO  <=> C2C*O + CH3C.*O  2.51E+07  0.00   0. !70 SCH
C2.C*O + C2CQC*O <=> C2C*O + C2CQC.*O 1.25E+07  0.00   0. !1/2 (c
C2.C*O + C2COHC*O <=> C2C*O + C2COHC.*O 1.25E+07  0.00   0. !1/2 (c
C2.C*O + CCQCHO  <=> C2C*O + CCQC.*O  1.25E+07  0.00   0. !1/2 (c
C2.C*O + CCOHCHO <=> C2C*O + CCOHC.*O 1.25E+07  0.00   0. !1/2 (c
C2C*O + O        <=> C2.C*O + OH      2.28E+12  0.00  4961. !88HER
C2C*O + H        <=> C2.C*O + H2      1.86E+13  0.00  6357. !76AMB
C2C*O + OH       <=> C2.C*O + H2O     1.02E+12  0.00  1192. !92&89
C2C*O + CH3      <=> C2.C*O + CH4      3.29E+11  0.00  9600. !nist
C2C*O + CH3O     <=> C2.C*O + CH3OH    3.29E+11  0.00  9600. !take
C2C*O + HO2      <=> C2.C*O + H2O2     3.29E+11  0.00  9600. !nist
C2C*O + O2       <=> C2.C*O + HO2      3.29E+11  0.00  9600. !nist
C2CYCOC + OH     <=> C2CYCOC. + H2O    1.55E+06  2.0  -1458. !84
C2CYCOC+CH3OO    <=> C2CYCOC.+CH3OOH   1.00E+00  4.0  13318. ! !
C2CYCOC + O      <=> C2CYCOC. + OH     4.00E+07  0.0  0. !88 H
C2CYCOC + H      <=> C2CYCOC. + H2     8.00E+13  0.0  9680. !84 B
C2CYCOC + CH3    <=> C2CYCOC. + CH4    1.02E-01  4.0  4915. !AMDC
C2CYCOC + CH3O   <=> C2CYCOC. + CH3OH   1.02E-01  4.0  4915. !AMDC
C2CYCOC + HO2    <=> C2CYCOC. + H2O2    1.00E+00  4.0  13318. !
CCYCOC + O       <=> CCYC.OC + OH      1.56E+05  2.50  1113. !90 T
CCYCOC + H       <=> CCYC.OC + H2      6.02E+05  2.40  2583. !90 T
CCYCOC + OH      <=> CCYC.OC + H2O     5.73E+10  0.51  64. !90 T
CCYCOC + CH3     <=> CCYC.OC + CH4     9.04E-01  3.46  4598. !90 T
CCYCOC + CH3O    <=> CCYC.OC + CH3OH    2.29E+10  0.00  2873. !90 T
CCYCOC + CH3OO   <=> CCYC.OC + CH3OOH   3.61E+03  2.55  10532. !90 T
CCYCOC + HO2     <=> CCYC.OC + H2O2     3.61E+03  2.55  10532. !90 T
CCYCOC + CH2OH   <=> CCYC.OC + CH3OH    1.21E+02  2.76  10796. !90 T
CCYCOC + O2      <=> CCYC.OC + HO2      3.97E+13  0.00  43997. !90 T
C*CICC*O + O     <=> C*CICC.*O + OH    1.40E+13  0.00  2401. !75 GAF
C*CICC*O + H     <=> C*CICC.*O + H2    8.09E+11  0.00   0. !78 KOD
C*CICC*O + OH    <=> C*CICC.*O + H2O    1.60E+13  0.00   0. !80 MAL
C*CICC*O + CH3   <=> C*CICC.*O + CH4    4.25E+10  0.00  4999. !A/2,E-
C*CICC*O + CH3O  <=> C*CICC.*O + CH3OH  4.25E+10  0.00  4999. !A/2,E-
C*CICC*O + O2    <=> C*CICC.*O + HO2    1.50E+13  0.00  38148. !A/2,E-
C*CICC*O + HO2   <=> C*CICC.*O + H2O2   1.50E+12  0.00  10923. !A/2,E-
C2CC*O + O       <=> C2CC.*O + OH      5.00E+12  0.00  1792. !84 WAR
C2CC*O + H       <=> C2CC.*O + H2      4.00E+13  0.00  4207. !84 WAR
C2CC*O + OH      <=> C2CC.*O + H2O     1.00E+13  0.00   0. !84 WAR
C2CC*O + CH3     <=> C2CC.*O + CH4     8.49E+10  0.00  5999. !84 WAR
C2CC*O + CH3O    <=> C2CC.*O + CH3OH    8.49E+10  0.00  5999. !84 WAR
C2CC*O + O2      <=> C2CC.*O + HO2     3.01E+13  0.00  39148. !92BAU/
C2CC*O + HO2     <=> C2CC.*O + H2O2     3.01E+12  0.00  11923. !92BAU/
O*CC*O + O       <=> O*CC.*O + OH      3.01E+08  0.00   0. !85 NTK
O*CC*O + H       <=> O*CC.*O + H2      8.00E+13  0.00  4207. !2*84
O*CC*O + OH      <=> O*CC.*O + H2O     6.62E+12  0.00   0. !92 BAU
O*CC*O + CH3     <=> O*CC.*O + CH4     1.70E+11  0.00  5999. !2*84

```


O*CC*O + CH3O	<=> O*CC.*O + CH3OH	1.70E+11	0.00	5999. ! 2* 84
O*CC*O + O2	<=> O*CC.*O + HO2	6.02E+13	0.00	39148. ! 2* 92
O*CC*O + HO2	<=> O*CC.*O + H2O2	6.02E+12	0.00	11923. ! 2* 92
CCC*O + O	<=> CCC.*O + OH	5.68E+12	0.00	1542. ! 77 SIN
CCC*O + H	<=> CCC.*O + H2	4.00E+13	0.00	4207. ! 84 WAR
CCC*O + OH	<=> CCC.*O + H2O	1.00E+13	0.00	0 ! 84 WAR
CCC*O + CH3	<=> CCC.*O + CH4	8.49E+10	0.00	5999. ! 84 WAR
CCC*O + CH3O	<=> CCC.*O + CH3OH	8.49E+10	0.00	5999. ! 84 WAR
CCC*O + O2	<=> CCC.*O + HO2	3.01E+13	0.00	39148. ! 92BAU/
CCC*O + HO2	<=> CCC.*O + H2O2	3.01E+12	0.00	11923. ! 92BAU/
CH3CHO + O	<=> CH3C.*O + OH	5.00E+12	0.00	1792. ! 84 WAR
CH3CHO + H	<=> CH3C.*O + H2	4.00E+13	0.00	4207. ! 84 WAR
CH3CHO + OH	<=> CH3C.*O + H2O	4.16E+11	0.57	2762. ! 92BAU/
CH3CHO + CH3	<=> CH3C.*O + CH4	8.49E+10	0.00	5999. ! 84 WAR
CH3CHO + CH3O	<=> CH3C.*O + CH3OH	8.49E+10	0.00	5999. ! 84 WAR
CH3CHO + O2	<=> CH3C.*O + HO2	3.01E+13	0.00	39148. ! 92BAU/
CH3CHO + HO2	<=> CH3C.*O + H2O2	3.01E+12	0.00	11923. ! 92BAU/
C2CQC*O + O	<=> C2CQC.*O + OH	2.50E+12	0.00	1792. ! 1/2 84
C2CQC*O + H	<=> C2CQC.*O + H2	2.00E+13	0.00	4207. ! 1/2 84
C2CQC*O + OH	<=> C2CQC.*O + H2O	2.08E+11	0.57	2762. ! 1/2 92
C2CQC*O + CH3	<=> C2CQC.*O + CH4	4.25E+10	0.00	5999. ! 1/2 84
C2CQC*O + CH3O	<=> C2CQC.*O + CH3OH	4.25E+10	0.00	5999. ! 1/2 84
C2CQC*O + O2	<=> C2CQC.*O + HO2	1.50E+13	0.00	39148. ! 1/2 92
C2CQC*O + HO2	<=> C2CQC.*O + H2O2	1.50E+12	0.00	11923. ! 1/2 92
C2COHC*O + O	<=> C2COHC.*O + OH	2.50E+12	0.00	1792. ! 1/2 84
C2COHC*O + H	<=> C2COHC.*O + H2	2.00E+13	0.00	4207. ! 1/2 84
C2COHC*O + OH	<=> C2COHC.*O + H2O	2.08E+11	0.57	2762. ! 1/2 92
C2COHC*O + CH3	<=> C2COHC.*O + CH4	4.25E+10	0.00	5999. ! 1/2 84
C2COHC*O + CH3O	<=> C2COHC.*O + CH3OH	4.25E+10	0.00	5999. ! 1/2 84
C2COHC*O + O2	<=> C2COHC.*O + HO2	1.50E+13	0.00	39148. ! 1/2 92
C2COHC*O + HO2	<=> C2COHC.*O + H2O2	1.50E+12	0.00	11923. ! 1/2 92
CCQCHO + O	<=> CCQC.*O + OH	2.50E+12	0.00	1792. ! 1/2 84
CCQCHO + H	<=> CCQC.*O + H2	2.00E+13	0.00	4207. ! 1/2 84
CCQCHO + OH	<=> CCQC.*O + H2O	2.08E+11	0.57	2762. ! 1/2 92
CCQCHO + CH3	<=> CCQC.*O + CH4	4.25E+10	0.00	5999. ! 1/2 84
CCQCHO + CH3O	<=> CCQC.*O + CH3OH	4.25E+10	0.00	5999. ! 1/2 84
CCQCHO + O2	<=> CCQC.*O + HO2	1.50E+13	0.00	39148. ! 1/2 92
CCQCHO + HO2	<=> CCQC.*O + H2O2	1.50E+12	0.00	11923. ! 1/2 92
CCOHCHO + O	<=> CCOHC.*O + OH	2.50E+12	0.00	1792. ! 1/2 84
CCOHCHO + H	<=> CCOHC.*O + H2	2.00E+13	0.00	4207. ! 1/2 84
CCOHCHO + OH	<=> CCOHC.*O + H2O	2.08E+11	0.57	2762. ! 1/2 92
CCOHCHO + CH3	<=> CCOHC.*O + CH4	4.25E+10	0.00	5999. ! 1/2 84
CCOHCHO + CH3O	<=> CCOHC.*O + CH3OH	4.25E+10	0.00	5999. ! 1/2 84
CCOHCHO + O2	<=> CCOHC.*O + HO2	1.50E+13	0.00	39148. ! 1/2 92
CCOHCHO + HO2	<=> CCOHC.*O + H2O2	1.50E+12	0.00	11923. ! 1/2 92
C*CC*O + O	<=> C*CC.*O + OH	1.40E+13	0.00	2401. ! 75 GAF
C*CC*O + H	<=> C*CC.*O + H2	8.09E+11	0.00	0. ! 78 KOD
C*CC*O + OH	<=> C*CC.*O + H2O	1.60E+13	0.00	0. ! 80 MAL
C*CC*O + CH3	<=> C*CC.*O + CH4	4.25E+10	0.00	4999. ! A/2.E-
C*CC*O + CH3O	<=> C*CC.*O + CH3OH	4.25E+10	0.00	4999. ! A/2.E-
C*CC*O + O2	<=> C*CC.*O + HO2	1.50E+13	0.00	38148. ! A/2.E-
C*CC*O + HO2	<=> C*CC.*O + H2O2	1.50E+12	0.00	10923. ! A/2.E-
C2.C*C + C2C*C	<=> C2C*C + C2.C*C	2.23E+01	3.50	6637. ! RXN6
C2.C*C + C3COC	<=> C2C*C + C3.COC	3.56E+02	3.30	19844. ! data f

$C2.C^*C + C3COC$	$\Leftrightarrow C2C^*C + C3COC.$	1.74E+03	2.90	19314.	!data f
$C2.C^*C + CH3OH$	$\Leftrightarrow C2C^*C + CH2OH$	1.74E+03	2.90	20456.	!data f
$C2.C^*C + HCHO$	$\Leftrightarrow CHO + C2C^*C$	1.26E+08	1.90	18191.	!86TSA/
$C2.C^*C + C2CYCOC$	$\Leftrightarrow C2C^*C + C2CYCOC.$	1.00E+00	4.00	13318.	!AMD CH
$C2.C^*C + CCYCOC$	$\Leftrightarrow C2C^*C + CCYC.OC$	4.22E+01	3.30	17169.	!data f
$C2.C^*C + C^*CICC^*O$	$\Leftrightarrow C2C^*C + C^*CICC.^*O$	1.90E+11	0.00	6218.	!data f
$C2.C^*C + C2CC^*O$	$\Leftrightarrow C2C^*C + C2CC.^*O$	3.80E+11	0.00	7218.	!data f
$C2.C^*C + O^*CC^*O$	$\Leftrightarrow C2C^*C + O^*CC.^*O$	7.90E+11	0.00	7218.	!data f
$C2.C^*C + CCC^*O$	$\Leftrightarrow C2C^*C + CCC.^*O$	3.80E+11	0.00	7218.	!data f
$C2.C^*C + CH3CHO$	$\Leftrightarrow C2C^*C + CH3C.^*O$	3.80E+11	0.00	7218.	!data f
$C2.C^*C + C2CQC^*O$	$\Leftrightarrow C2C^*C + C2CQC.^*O$	1.90E+11	0.00	7218.	!data f
$C2.C^*C + C2COHC^*O$	$\Leftrightarrow C2C^*C + C2COHC.^*O$	1.90E+11	0.00	7218.	!data f
$C2.C^*C + CCQCHO$	$\Leftrightarrow C2C^*C + CCQC.^*O$	1.90E+11	0.00	7218.	!data f
$C2.C^*C + CCOHCHO$	$\Leftrightarrow C2C^*C + CCOHC.^*O$	1.90E+11	0.00	7218.	!data f
$C2.C^*C$	$\Leftrightarrow C^*C^*C + CH3$	2.25E+15	-1.870	4734.	! mtbe017d.mec avg err 16.07%
$C2.C^*C + O2$	$\Leftrightarrow C^*CICCCQ.$	5.30E+24	-3.637	55355.	! mtbe017d.mec avg err 29.88%
$C2.C^*C + O2$	$\Leftrightarrow C^*CICCO.^*O$	6.80E+28	-5.919	3261.	! mtbe017d.mec avg err 15.76%
$C2.C^*C + O2$	$\Leftrightarrow C^*CICCC.Q$	3.17E+16	-1.051	42827.	! mtbe017d.mec avg err 3.03%
$C2.C^*C + O2$	$\Leftrightarrow C^*CICCC^*O + OH$	9.83E+06	.337	20445.	! mtbe017d.mec avg err 6.64%
$C2.C^*C + O2$	$\Leftrightarrow C^*CIC.CQ$	2.17E+11	.499	21331.	! mtbe017d.mec avg err 2.57%
$C2.C^*C + O2$	$\Leftrightarrow C^*C^*C + CH2OOH$	6.74E+31	-6.172	9528.	! mtbe017d.mec avg err 4.97%
$C2.C^*C + O2$	$\Leftrightarrow C^*CYCCOC + OH$	1.91E+15	-.446	41097.	! mtbe017d.mec avg err 8.96%
$C2.C^*C + O2$	$\Leftrightarrow CCYC.COOC$	2.35E+19	-2.109	17979.	! mtbe017d.mec avg err 9.12%
$C2.C^*C + O2$	$\Leftrightarrow C2.CYCOOC$	1.83E+29	-6.422	18935.	! mtbe017d.mec avg err 17.69%
$C2.C^*C + O2$	$\Leftrightarrow CCYCC.OOC$	3.86E+10	-.793	16420.	! mtbe017d.mec avg err 5.76%
$C2.C^*C + O2$	$\Leftrightarrow YCOCICCO.$	3.45E+04	.749	24249.	! mtbe017d.mec avg err 16.77%
$C2.C^*C + O2$	$\Leftrightarrow CCYC.OC+HCHO$	2.13E+08	-.585	13591.	! mtbe017d.mec avg err 17.57%
$C2.C^*C + O2$	$\Leftrightarrow C2CYCOOC.$	2.10E+12	-.313	17050.	! mtbe017d.mec avg err 3.20%
$C2.C^*C + O2$	$\Leftrightarrow CCICO.C^*O$	1.05E+06	3.629	31834.	! mtbe017d.mec avg err 8.07%
$C2.C^*C + O2$	$\Leftrightarrow CC.C^*O + HCHO$	3.07E+02	2.780	20289.	! mtbe017d.mec avg err 11.71%
$C2.C^*C + O2$	$\Leftrightarrow C2CO.C^*O$	8.88E+05	1.598	24012.	! mtbe017d.mec avg err 14.55%
$C2.C^*C + O2$	$\Leftrightarrow C2C^*O + CHO$	1.30E+05	3.424	32184.	! mtbe017d.mec avg err 6.87%
$C^*CICCCQ.$	$\Leftrightarrow C^*CICCO.^*O$	2.16E+04	4.236	32097.	! mtbe017d.mec avg err 8.10%
$C^*CICCCQ.$	$\Leftrightarrow C^*CICCC.Q$	5.26E+15	-1.531	58012.	! mtbe017d.mec avg err 16.37%
$C^*CICCCQ.$	$\Leftrightarrow C^*CICCC^*O + OH$	2.95E+11	-1.638	36430.	! mtbe017d.mec avg err 15.33%
$C^*CICCCQ.$	$\Leftrightarrow C^*CIC.CQ$	5.49E+15	-1.462	37266.	! mtbe017d.mec avg err 19.12%
$C^*CICCCQ.$	$\Leftrightarrow C^*C^*C + CH2OOH$	4.31E+41	-9.638	22293.	! mtbe017d.mec avg err 7.14%
$C^*CICCCQ.$	$\Leftrightarrow C^*CYCCOC + OH$	2.77E+15	-1.196	56577.	! mtbe017d.mec avg err 11.59%
$C^*CICCCQ.$	$\Leftrightarrow CCYC.COOC$	4.04E+25	-4.600	33463.	! mtbe017d.mec avg err 12.38%
$C^*CICCCQ.$	$\Leftrightarrow C2.CYCOOC$	1.99E+35	-8.720	35245.	! mtbe017d.mec avg err 32.93%

C*CICCCQ. 15.74%	<=> CCYCC.OOC	3.31E+16 -3.186 32364. ! mtbe017d.mec avg err
C*CICCCQ.	<=> YCOCICCO.	5.68E+06 -588 39292. ! mtbe017d.mec avg err 8.51%
C*CICCCQ. 44.20%	<=> CCYC.OC+HCHO	1.52E+14 -2.928 29598. ! mtbe017d.mec avg err
C*CICCCQ. 18.90%	<=> C2CYCOOC.	1.02E+18 -2.642 32881. ! mtbe017d.mec avg err
C*CICCCQ	<=> CCICO.C*O	3.88E-06 2.738 47078. ! mtbe017d.mec avg err 15.00%
C*CICCCQ. 20.41%	<=> CC.C*O + HCHO	4.69E+00 1.459 35334. ! mtbe017d.mec avg err
C*CICCCQ.	<=> C2CO.C*O	1.24E+08 .279 39014. ! mtbe017d.mec avg err 10.37%
C*CICCCQ.	<=> C2C*O + CHO	5.16E-05 2.525 47447. ! mtbe017d.mec avg err 16.55%
C*CICCC.Q 15.05%	<=> C*CICCC*O + OH	8.54E-04 3.337 47357. ! mtbe017d.mec avg err
C*CICCC.Q	<=> C*CIC.CQ	7.41E+08 .034 -607. ! mtbe017d.mec avg err 3.53%
C*CICCC.Q	<=> CCYC.COOC	2.61E-01 .639 -4359. ! mtbe017d.mec avg err 28.62%
C*CICCC.Q	<=> C2.CYCOOC	5.58E+13 -4.567 673. ! mtbe017d.mec avg err 9.04%
C*CIC.CQ 31.41%	<=> C*C*C + CH2OOH	2.96E+19 -5.908 4510. ! mtbe017d.mec avg err
C*CIC.CQ 10.50%	<=> C*CYCCOC + OH	1.29E+15 -1.040 53521. ! mtbe017d.mec avg err
C*CIC.CQ	<=> CCYC.COOC	6.26E+19 -2.895 28050. ! mtbe017d.mec avg err 5.71%
C*CIC.CQ 27.28%	<=> C2.CYCOOC	1.59E+38 -9.520 36350. ! mtbe017d.mec avg err
CCYC.COOC 9.67%	<=> C2.CYCOOC	9.90E+18 -3.826 33336. ! mtbe017d.mec avg err
CCYC.COOC 134.24%	<=> YCOCICCO.	2.80E-14 4.504 8165. ! mtbe017d.mec avg err
CCYC.COOC 15.66%	<=> CCYC.OC+HCHO	3.10E+35 -8.775 25698. ! mtbe017d.mec avg err
CCYC.COOC 9.28%	<=> CCYCC.OOC	2.86E+38 -8.300 28883. ! mtbe017d.mec avg err
CCYC.COOC 68.28%	<=> CCICO.C*O	1.11E-18 6.935 13494. ! mtbe017d.mec avg err
CCYC.COOC 81.23%	<=> CC.C*O + HCHO	3.82E-11 5.151 19149. ! mtbe017d.mec avg err
C2.CYCOOC 97.99%	<=> YCOCICCO.	4.01E-03 3.796 23289. ! mtbe017d.mec avg err
C2.CYCOOC 21.81%	<=> CCYC.OC+HCHO	2.34E+10 -1.812 -2283. ! mtbe017d.mec avg err
C2.CYCOOC	<=> C2CYCOOC.	2.07E+11 -.660 608. ! mtbe017d.mec avg err 2.02%
C2.CYCOOC 78.76%	<=> C2CO.C*O	1.07E-67 20.391 -18520. ! mtbe017d.mec avg err
C2.CYCOOC 109.40%	<=> C2C*O + CHO	1.52E-71 21.784 -17283. ! mtbe017d.mec avg err
CCYCC.OOC 111.64%	<=> CCICO.C*O	2.41E-70 22.604 -17332. ! mtbe017d.mec avg err
CCYCC.OOC 9.76%	<=> CC.C*O + HCHO	3.47E+07 -.465 -2618. ! mtbe017d.mec avg err
YCOCICCO. 1.10%	<=> CCYC.OC+HCHO	2.69E+12 -.915 630. ! mtbe017d.mec avg err
C2CYCOOC. 44.34%	<=> C2CO.C*O	8.98E+30 -6.438 15815. ! mtbe017d.mec avg err

C2CYCOOC. .27%	\rightleftharpoons C2C*O + CHO	5.58E+09	-1.311	-272.	! mtbe017d.mec avg err
CCICO.C*O 1.41%	\rightleftharpoons CC.C*O + HCHO	6.55E+10	-457	-385.	! mtbe017d.mec avg err
C2CO.C*O 22.35%	\rightleftharpoons C2C*O + CHO	6.47E+18	-2.948	6595.	! mtbe017d.mec avg err
CC C*O	\rightleftharpoons C*CC*O + H	1.74E+12	-882	152.	! mtbe017d.mec avg err 4.88%
CC C*O	\rightleftharpoons CC*C*O + H	3.99E+40	-8.736	45673.	! mtbe017d.mec avg err 17.53%
CC.C*O	\rightleftharpoons CCC.*O	2.00E+30	-6.266	32648.	! mtbe017d.mec avg err 31.72%
CC.C*O	\rightleftharpoons C2H5 + CO	5.27E+32	-7.546	38484.	! mtbe017d.mec avg err 7.22%
CCC.*O	\rightleftharpoons C2H5 + CO	1.25E+35	-7.052	41157.	! mtbe017d.mec avg err 25.02%
CH3OH + O	\rightleftharpoons CH2OH + OH	1.72E+13	0.00	4914.	!NIST F
CH3OH + O	\rightleftharpoons CH3O + OH	1.00E+13	0.00	5129.	!A from
CH3OH + H	\rightleftharpoons CH2OH + H2	3.40E+13	0.00	5497.	!A from
CH3OH + H	\rightleftharpoons CH3O + H2	4.00E+13	0.00	6095.	!84 WAR
CH3OH + OH	\rightleftharpoons CH2OH + H2O	1.35E+13	0.00	1881.	!NIST F
CH3OH + OH	\rightleftharpoons CH3O + H2O	1.00E+13	0.00	1953.	!A from
CH3OH + CH3	\rightleftharpoons CH2OH + CH4	3.19E+01	3.20	7172.	!87 TSA
CH3OH + CH3	\rightleftharpoons CH3O + CH4	1.44E+01	3.10	6935.	!87 TSA
CH3OH + CH3O	\rightleftharpoons CH2OH + CH3OH	3.01E+11	0.00	4074.	!87 TSA
CH3OH + HO2	\rightleftharpoons CH2OH + H2O2	9.64E+10	0.00	12579.	!87 TSA
CH3OH + O2	\rightleftharpoons CH2OH + HO2	2.05E+13	0.00	44911.	!87 TSA
CH3 + OH	\rightleftharpoons CH3OH	2.84E+27	-5.499	13233.	! mtbe017d.mec avg err 25.65%
CH3 + OH	\rightleftharpoons CH2S + H2O	1.67E+34	-6.747	5582.	! mtbe017d.mec avg err 18.78%
CH3 + OH	\rightleftharpoons HCOH + H2	2.77E+14	-508	2729.	! mtbe017d.mec avg err 5.94%
CH3 + OH	\rightleftharpoons HCHO + H2	2.04E+16	-1.146	2772.	! mtbe017d.mec avg err 6.51%
CH3 + OH	\rightleftharpoons CH2OH + H	1.94E+08	1.030	3927.	! mtbe017d.mec avg err 3.86%
CH3 + OH	\rightleftharpoons CH3O + H	1.95E+13	-087	6228.	! mtbe017d.mec avg err 2.54%
CH3OH	\rightleftharpoons CH2S + H2O	8.91E+12	-302	13599.	! mtbe017d.mec avg err .34%
CH3OH	\rightleftharpoons HCOH + H2	1.46E+36	-6.939	96720.	! mtbe017d.mec avg err 22.15%
CH3OH	\rightleftharpoons HCHO + H2	5.63E+32	-5.899	93292.	! mtbe017d.mec avg err 24.60%
CH3OH	\rightleftharpoons CH2OH + H	1.12E+31	-5.813	99212.	! mtbe017d.mec avg err 18.04%
CH3OH	\rightleftharpoons CH3O + H	1.53E+36	-7.048	102724.	! mtbe017d.mec avg err 15.67%
CH3 + O	\rightleftharpoons CH3O	4.64E+32	-6.514	108860.	! mtbe017d.mec avg err 12.95%
CH3 + O	\rightleftharpoons HCHO + H	7.24E+19	-3.378	758.	! mtbe017d.mec avg err 4.90%
CH3 + O	\rightleftharpoons CH2OH	5.65E+13	-.052	-253.	! mtbe017d.mec avg err 1.95%
CH3O	\rightleftharpoons HCHO + H	1.12E+24	-4.167	2710.	! mtbe017d.mec avg err 5.83%
CH3O	\rightleftharpoons CH2OH	9.20E+29	-6.055	27052.	! mtbe017d.mec avg err 5.24%
CH2OH	\rightleftharpoons HCHO + H	1.57E+38	-9.055	44503.	! mtbe017d.mec avg err 12.57%
CH2OH + O2	\rightleftharpoons CQ.H2OH	2.22E+30	-5.916	40127.	! mtbe017d.mec avg err 14.62%
CH2OH + O2	\rightleftharpoons HOCH2O. + O	3.40E+41	-9.552	7060.	! mtbe017d.mec avg err
9.42%					
CH2OH + O2	\rightleftharpoons CQH2O.	2.99E+13	-.294	25339.	! mtbe017d.mec avg err 18.67%
CH2OH + O2	\rightleftharpoons HCHO + HO2	6.13E+14	-2.035	2213.	! mtbe017d.mec avg err
1.32%					
CH2OH + O2	\rightleftharpoons HOC.HQ	1.76E+18	-1.965	4070.	! mtbe017d.mec avg err 3.86%
CH2OH + O2	\rightleftharpoons HCO2H + OH	5.31E+09	-.515	6821.	! mtbe017d.mec avg err 2.08%
CH2OH + O2	\rightleftharpoons HCQ*O + H	7.57E+10	.390	6433.	! mtbe017d.mec avg err .81%
CQ.H2OH	\rightleftharpoons HOCH2O. + O	1.38E-01	3.327	4843.	! mtbe017d.mec avg err .87%
CQ.H2OH	\rightleftharpoons CQH2O.	2.54E+25	-4.828	61426.	! mtbe017d.mec avg err 20.77%
CQ.H2OH	\rightleftharpoons HCHO + HO2	6.55E+31	-7.403	35589.	! mtbe017d.mec avg err 21.97%
CQ.H2OH	\rightleftharpoons HOC.HQ	5.90E+37	-8.168	38393.	! mtbe017d.mec avg err 24.47%
CQ.H2OH	\rightleftharpoons HCO2H + OH	1.96E+32	-7.955	45255.	! mtbe017d.mec avg err 9.09%
CQ.H2OH	\rightleftharpoons HCQ*O + H	3.37E+33	-7.080	44878.	! mtbe017d.mec avg err 7.79%

CQH2O.	<=> HCHO + HO2	2.59E+22	-4.475	43083.	! mtbe017d.mec avg err	9.27%
CQH2O.	<=> HOC HQ	2.64E+13	-1.392	2869	! mtbe017d.mec avg err	8.86%
CQH2O.	<=> HCO2H + OH	1.42E+18	-4.679	5443.	! mtbe017d.mec avg err	4.37%
HOC.HQ	<=> HCO2H + OH	1.08E+19	-3.706	5015.	! mtbe017d.mec avg err	3.46%
HOC.HQ	<=> HCQ*O + H	2.79E+12	-.931	713.	! mtbe017d.mec avg err	1.06%
CHO + O2	<=> HCQ *O	1.13E+12	-.920	21519	! mtbe017d.mec avg err	1.81%
CHO + O2	<=> HCO2. + O	1.34E+35	-7.676	4877.	! mtbe017d.mec avg err	5.72%
CHO + O2	<=> C.Q*O	1.54E+15	-.591	11927.	! mtbe017d.mec avg err	4.75%
CHO + O2	<=> CO + HO2	2.79E+15	-1.459	2078.	! mtbe017d.mec avg err	3.40%
CHO + O2	<=> CO2 + OH	7.32E+13	-.543	2007	! mtbe017d.mec avg err	1.06%
HCQ.*O	<=> HCO2. + O	3.62E+16	-1.172	2432.	! mtbe017d.mec avg err	1.85%
HCQ.*O	<=> C.Q*O	2.80E+31	-6.300	55096.	! mtbe017d.mec avg err	3.53%
HCQ.*O	<=> CO + HO2	2.12E+35	-7.913	41535.	! mtbe017d.mec avg err	15.50%
HCQ.*O	<=> CO2 + OH	4.73E+34	-7.358	41727.	! mtbe017d.mec avg err	12.45%
C.Q*O	<=> CO + HO2	3.44E+36	-7.663	41916.	! mtbe017d.mec avg err	13.72%
C.Q*O	<=> CO2 + OH	5.08E+11	-.735	12689.	! mtbe017d.mec avg err	1.23%
HCQ*O	<=> HCO2. + OH	4.74E+12	-1.026	1578.	! mtbe017d.mec avg err	.59%
HCO2.	<=> CO2 + H	5.13E+43	-9.732	42403.	! mtbe017d.mec avg err	6.69%
HCO2.	<=> C.O2H	2.27E+30	-6.086	37422.	! mtbe017d.mec avg err	6.18%
HCO2.	<=> CO + OH	6.48E+35	-8.598	41151.	! mtbe017d.mec avg err	5.56%
C.O2H	<=> CO2 + H	5.09E+29	-5.899	40723.	! mtbe017d.mec avg err	8.48%
C.O2H	<=> CO + OH	1.45E+25	-4.994	34719.	! mtbe017d.mec avg err	6.27%
HCO2H	<=> CO + H2O	1.13E+26	-5.016	21027.	! mtbe017d.mec avg err	3.64%
HCO2H	<=> CO2 + H2	7.57E+25	-4.224	65105.	! mtbe017d.mec avg err	17.88%
HCHO + O	<=> CHO + OH	4.16E+11	0.57	2762.	!92BAU/	
HCHO + H	<=> CHO + H2	2.29E+10	1.05	3279.	!92BAU/	
HCHO + OH	<=> CHO + H2O	3.44E+09	1.18	-447.	!86TSA/	
HCHO + CH3	<=> CHO + CH4	5.54E+03	2.81	5862.	!86TSA/	
HCHO + CH3O	<=> CHO + CH3OH	1.02E+11	0.00	2981.	!86TSA/	
HCHO + HO2	<=> CHO + H2O2	1.58E+12	0.00	12665.	!86TSA/	
HCHO + O2	<=> CHO + HO2	2.05E+13	0.00	38949.	!91TSA/	
HCHO + CH3OO	<=> CHO + CH3OOH	1.99E+12	0.00	11665.	!86TSA/	
HCHO + CH2OH	<=> CHO + CH3OH	5.49E+03	2.80	5862.	!87TSA/	
HCHO + C2H3	<=> CHO + C2H4	5.43E+03	2.81	5862.	!86TSA/	
HCHO + C2H5	<=> CHO + C2H6	5.50E+03	2.81	5862.	!86TSA/	
HCHO	<=> CHO + H	6.27E+14	-1.651	50635.	! mtbe017d.mec avg err	10.69%
HCHO	<=> CO + H2	4.30E+20	-3.823	90631.	! mtbe017d.mec avg err	4.54%
CH4	<=> CH3 + H	5.11E+26	-4.845	51446.	! mtbe017d.mec avg err	8.39%
CH3 + O2	<=> CH3OO	9.79E+31	-5.575	109222.	! mtbe017d.mec avg err	12.75%
CH3 + O2	<=> CH3O + O	2.66E+35	-7.866	5504.	! mtbe017d.mec avg err	7.33%
CH3 + O2	<=> CH2OOH	7.83E+13	-.339	29880.	! mtbe017d.mec avg err	11.23%
CH3 + O2	<=> HCHO + OH	1.21E+07	.597	17237.	! mtbe017d.mec avg err	2.42%
CH3OO	<=> CH3O + O	3.38E+10	.613	18230.	! mtbe017d.mec avg err	.81%
CH3OO	<=> CH2OOH	1.32E+26	-4.932	60217.	! mtbe017d.mec avg err	4.49%
CH3OO	<=> HCHO + OH	3.00E+21	-4.531	48449.	! mtbe017d.mec avg err	3.71%
CH2OOH	<=> HCHO + OH	1.10E+25	-4.553	49469.	! mtbe017d.mec avg err	4.65%
CH3 + CH3	<=> C2H6	4.71E+10	-.519	686.	! mtbe017d.mec avg err	2.16%
CH3 + CH3	<=> C2H5 + H	4.17E+39	-8.223	8194.	! mtbe017d.mec avg err	42.15%
CH3 + CH3	<=> C2H4 + H2	5.73E+27	-5.129	16513.	! mtbe017d.mec avg err	5.69%
C2H6	<=> C2H5 + H	2.32E+30	-4.538	16851.	! mtbe017d.mec avg err	4.79%
C2H6	<=> C2H4 + H2	3.65E+52	-12.144	109762.	! mtbe017d.mec avg err	26.52%
CH3OO + OH	<=> CH3OH + O2	6.03E+13	0.00	0.	!86	
CH3O + HO2	<=> HCHO + H2O2	3.01E+11	0.0	0.	!	
CH3 + HO2	<=> CH3O + OH	1.35E+13	0.0	0.	!16/09/	

CH3 + HO2	<=> CH4 + O2	3.61E-12	0.0	0.186	TSA
CH3 + CH2OH	<=> CH4 + HCHO	2.41E-12	0.0	0.186	TSA
CH3 + CH2OH	<=> CCOH	1.21E+12	0.0	0.187	TSA
CH3 + CH3O	<=> CH4 + HCHO	2.41E-13	0.0	0.186	TSA
CH3 + CH3OO	<=> CH3O + CH3O	2.41E+13	0.0	0.186	TSA
OH + CH3O	<=> HCHO + H2O	1.81E+13	0.0	0.186	TSA
OH + CH2OH	<=> HCHO + H2O	2.41E+13	0.0	0.187	TSA
O + CH3OO	<=> CH3O + O2	3.61E+13	0.0	0.186	TSA/
CH3O + CO	<=> CH3 + CO2	1.57E+13	0.00	11804.	186TSA/
O + CO	<=> CO2	1.82E+06	5.84	1632.	!nist f
CO + H + M	<=> CHO + M	2.10E+20	-1.82	3688.	!2
CO + OH	<=> CO2 + H	6.32E+06	1.50	-497.	!2
CO + HO2	<=> CO2 + OH	1.51E+14	0.0	23648.	!2
CO + O2	<=> CO2 + O	2.53E+12	0.0	47693.	!2
OH + CH4	<=> CH3 + H2O	1.93E+05	2.40	2106.	186TSA/
O + CH4	<=> CH3 + OH	2.47E+07	1.96	7540.	!modifi
H + CH4	<=> CH3 + H2	1.33E+04	3.00	8038.	192BAU/
O2 + CH2OH	<=> HCHO + HO2	1.21E+12	0.00	0.187	SA/H
CH3O + O2	<=> HO2 + HCHO	6.62E+10	0.00	2603.	186TSA/
CH3O + O	<=> OH + HCHO	6.03E+12	0.00	0.186	TSA/
HCO2H + O	<=> OH + HCO2.	1.15E+12	0.00	1351.	192 BAU
HCO2H + O	<=> OH + C.O2H	1.15E+12	0.00	1351.	192 BAU
HCO2H + H	<=> H2 + HCO2.	9.00E+12	0.00	3378.	192 BAU
HCO2H + H	<=> H2 + C.O2H	9.00E+12	0.00	3378.	192 BAU
HCO2H + OH	<=> H2O + HCO2.	2.71E+11	0.00	0.192	BAU
HCO2H + OH	<=> H2O + C.O2H	2.71E+11	0.00	0.192	BAU
C2H4 + HO2	<=> CH3CHO + OH	6.03E+09	0.0	7949.	!
C2H4 + CH3	<=> C2H3 + CH4	6.63E+00	3.7	9499.	!
C2H4 + O	<=> C2H3 + OH	5.55E+05	2.17	2597.	!N
C2H4 + O	<=> CH3 + CHO	1.32E+08	1.55	427.	!8
C2H4 + O	<=> CH2 + HCHO	5.11E+10	0.66	1029.	!N
C2H4 + O	<=> C.CHO + H	1.21E+06	2.08	0.	!9
C2H4 + O	<=> CYCOC	7.00E+11	0.00	0.	!7
C2H4 + OH	<=> C2H3 + H2O	1.57E+04	2.75	4173.	!8
C2H4 + H	<=> C2H3 + H2	1.33E+06	2.53	12241.	!8
C2H4 + CH3O	<=> C2H3 + CH3OH	6.63E+00	3.7	9499.	!
C2H4 + OH	<=> C.CO	3.09E+55	-11.747	110099.	! mtbe017d.mec avg err 24.25%
C2H4 + OH	<=> C*COH + H	1.41E+39	-8.532	7358.	! mtbe017d.mec avg err 15.25%
C2H4 + OH	<=> CCO.	1.19E+14	-6.92	7744.	! mtbe017d.mec avg err 6.88%
C2H4 + OH	<=> CH3 + HCHO	3.07E+18	-3.378	14863.	! mtbe017d.mec avg err 11.87%
C2H4 + OH	<=> CH3CHO + H	2.57E+12	-286	15123.	! mtbe017d.mec avg err 4.15%
C.CO	<=> C*COH + H	6.51E+11	-0.75	14970.	! mtbe017d.mec avg err 4.08%
C.CO	<=> CCO.	2.73E+36	-8.222	38774.	! mtbe017d.mec avg err 10.58%
C.CO	<=> CH3 + HCHO	6.64E+35	-9.459	45167.	! mtbe017d.mec avg err 21.58%
C.CO	<=> CH3CHO + H	5.12E+30	-6.716	45565.	! mtbe017d.mec avg err 9.14%
CCO.	<=> C*COH + H	1.46E+30	-6.527	45406.	! mtbe017d.mec avg err 9.20%
CCO.	<=> CH3 + HCHO	2.26E+35	-9.343	34855.	! mtbe017d.mec avg err 7.36%
CCO.	<=> CH3CHO + H	5.25E+38	-8.874	21974.	! mtbe017d.mec avg err 5.25%
C.CO + O2	<=> COHCQ.	6.74E+36	-8.302	22429.	! mtbe017d.mec avg err 4.25%
C.CO + O2	<=> CO.CO + O	3.08E+37	-8.523	5206.	! mtbe017d.mec avg err 15.25%
C.CO + O2	<=> C*COHB + HO2B	2.44E+12	-0.47	28994.	! mtbe017d.mec avg err 40.55%
C.CO + O2	<=> COHC.Q	1.32E+19	-2.353	5114.	! mtbe017d.mec avg err 5.12%

C COH + O2 1.49%	<=> COHCHO + OH	2.09E+05	669	12291. ! mtbe017d.mec avg err
C COH + O2	<=> C OHCQ	1.10E+09	.734	13290. ! mtbe017d.mec avg err 1.11%
C COH + O2 12.03%	<=> C*COH + HO2	3.76E+30	-6.441	5318. ! mtbe017d.mec avg err
C COH + O2	<=> CO CQ	2.28E+26	-4.293	7242. ! mtbe017d.mec avg err 6.59%
C COH + O2 12.39%	<=> HCHO + CH2OOH	6.97E+32	-7.079	8230. ! mtbe017d.mec avg err
COHCQ.	<=> CO COH + O	1.29E+19	-2.264	9989 ! mtbe017d.mec avg err 9.46%
COHCQ. 21.28%	<=> C*COHB + HO2B	3.79E+22	-3.896	59327. ! mtbe017d.mec avg err
COHCQ.	<=> COHC.Q	1.83E+39	-8.855	33769. ! mtbe017d.mec avg err 10.64%
COHCQ. 17.72%	<=> COHCHO + OH	1.81E+21	-4.720	44457. ! mtbe017d.mec avg err
COHCQ.	<=> C.OHCQ	1.14E+25	-4.691	45443. ! mtbe017d.mec avg err 21.23%
COHCQ.	<=> C*COH + HO2	4.65E+47	-11.574	30911. ! mtbe017d.mec avg err 9.74%
COHCQ.	<=> CO.CQ	6.88E+46	-10.784	35240. ! mtbe017d.mec avg err 15.28%
COHCQ. 21.96%	<=> HCHO + CH2OOH	4.66E+38	-9.218	26373. ! mtbe017d.mec avg err
COHC.Q 10.92%	<=> COHCHO + OH	2.88E+35	-7.622	41285. ! mtbe017d.mec avg err
COHC.Q	<=> C.OHCQ	1.32E+09	-.052	-338. ! mtbe017d.mec avg err 2.59%
C.OHCQ	<=> COHCHO + OH	1.56E+09	-2.404	-777. ! mtbe017d.mec avg err 6.21%
C.OHCQ	<=> C*COH + HO2	4.77E+31	-7.433	14306. ! mtbe017d.mec avg err 11.55%
CO.CQ	<=> COHC.Q	4.00E+29	-5.993	17444. ! mtbe017d.mec avg err 18.64%
CO.CQ	<=> COHCHO + OH	6.32E+25	-6.156	31438. ! mtbe017d.mec avg err 7.76%
CO.CQ	<=> C.OHCQ	5.04E+29	-6.157	32463. ! mtbe017d.mec avg err 5.10%
CO.CQ	<=> C*COH + HO2	1.34E+46	-11.503	17348. ! mtbe017d.mec avg err 18.87%
CO.CQ 24.93%	<=> HCHO + CH2OOH	5.07E+43	-10.044	21179. ! mtbe017d.mec avg err
C2H4 + HO2	<=> C.CQ	4.52E+24	-3.942	22525. ! mtbe017d.mec avg err 7.36%
C2H4 + HO2	<=> C*CQ + H	3.62E+26	-5.224	9857. ! mtbe017d.mec avg err 17.92%
C2H4 + HO2	<=> CCQ.	3.18E+14	-.871	35949. ! mtbe017d.mec avg err 4.97%
C2H4 + HO2 22.06%	<=> C2H4B + HO2B	2.13E+42	-9.886	20237. ! mtbe017d.mec avg err
C2H4 + HO2	<=> CC.Q	8.62E+18	-2.212	21093. ! mtbe017d.mec avg err 11.59%
C2H4 + HO2 2.69%	<=> CH3CHO + OH	4.23E+11	-1.096	27498. ! mtbe017d.mec avg err
C.CQ + O2	<=> QCCQ.	3.33E+15	-1.057	28577. ! mtbe017d.mec avg err 3.47%
C.CQ + O2	<=> CO.CQ + O	9.75E+40	-9.490	6776. ! mtbe017d.mec avg err 15.39%
C.CQ + O2 137.69%	<=> C*CQB + HO2B	4.86E+09	.810	29599. ! mtbe017d.mec avg err
C.CQ + O2	<=> QCC.Q	1.81E+16	-1.608	8781. ! mtbe017d.mec avg err 5.79%
C.CQ + O2	<=> C*CQ + HO2	1.28E+24	-4.762	7467. ! mtbe017d.mec avg err 11.80%
C.CQ + O2	<=> QCCHO + OH	7.55E+08	.049	7064. ! mtbe017d.mec avg err 5.54%
QCCQ.	<=> CO.CQ + O	4.14E+26	-4.350	7908. ! mtbe017d.mec avg err 10.42%
QCCQ.	<=> C*CQB + HO2B	1.31E+23	-4.012	58994. ! mtbe017d.mec avg err 24.80%
QCCQ.	<=> QCC.Q	1.45E+37	-8.362	39708. ! mtbe017d.mec avg err 18.89%
QCCQ.	<=> C*CQ + HO2	3.13E+37	-9.194	30469. ! mtbe017d.mec avg err 25.19%
QCCQ.	<=> QCCHO + OH	8.80E+27	-6.252	35981. ! mtbe017d.mec avg err 18.67%
QCC.Q	<=> C*CQ + HO2	2.62E+40	-8.939	31235. ! mtbe017d.mec avg err 18.49%
QCC.Q	<=> QCCHO + OH	2.72E+09	-.455	19421. ! mtbe017d.mec avg err 4.10%
C.CHO + HO2	<=> QCCHO	2.13E+09	-.060	-320. ! mtbe017d.mec avg err 3.35%

C.CHO + HO2 11.07%	<=> QCC.*O + H	2.12E+38	-8.869	5172. ! mtbe017d.mec avg err
C.CHO + HO2 61.81%	<=> CHO + CH2OOH	6.68E-06	5.022	21956. ! mtbe017d.mec avg err
C.CHO + HO2 11.15%	<=> O*CCO. + OH	8.14E+00	3.586	16942. ! mtbe017d.mec avg err
QCCHO	<=> QCC.*O + H	6.10E+14	-.507	1288. ! mtbe017d.mec avg err .92%
QCCHO 9.07%	<=> CHO + CH2OOH	5.44E+30	-6.242	91243. ! mtbe017d.mec avg err
QCCHO	<=> O*CCO. + OH	7.27E+33	-6.704	85505. ! mtbe017d.mec avg err 9.37%
QCC.*O 28.74%	<=> CH2OOH + CO	7.17E+48	-10.832	54367. ! mtbe017d.mec avg err
O*CC*O	<=> CHO + CHO	2.02E+27	-5.374	14295. ! mtbe017d.mec avg err 22.59%
O*CC*O	<=> O*CC.*O + H	3.13E+47	-10.158	76840. ! mtbe017d.mec avg err 17.36%
O*CC.*O	<=> CHO + CO	2.04E+35	-7.663	86611. ! mtbe017d.mec avg err 9.24%
C*CQ	<=> C*CO. + OH	8.89E+13	-1.527	4233. ! mtbe017d.mec avg err 6.68%
CO.COH 25.23%	<=> HCHO + CH2OH	2.94E+38	-8.577	23856. ! mtbe017d.mec avg err
C2H4 + H	<=> C2H5	1.55E+32	-6.810	18611. ! mtbe017d.mec avg err 21.25%
C2H5 + O2	<=> CCQ.	5.57E+32	-6.242	7593. ! mtbe017d.mec avg err 24.24%
C2H5 + O2 15.64%	<=> C2H4B + HO2B	2.14E+45	-10.791	8458. ! mtbe017d.mec avg err
C2H5 + O2	<=> CCO. + O	6.88E+14	-1.072	5663. ! mtbe017d.mec avg err 4.98%
C2H5 + O2	<=> C.CQ	6.40E+13	-.395	28880. ! mtbe017d.mec avg err 11.69%
C2H5 + O2	<=> C2H4 + HO2	2.25E+28	-5.704	6281. ! mtbe017d.mec avg err 9.81%
C2H5 + O2	<=> CC.Q	5.45E+22	-3.222	7884. ! mtbe017d.mec avg err 7.86%
C2H5 + O2	<=> CH3CHO + OH	6.85E+05	.579	12187. ! mtbe017d.mec avg err 1.29%
CCQ.	<=> C2H4B + HO2B	4.52E+09	.640	13244. ! mtbe017d.mec avg err .80%
CCQ.	<=> CCO. + O	2.02E+42	-9.824	40344. ! mtbe017d.mec avg err 14.91%
CCQ.	<=> C.CQ	8.93E+27	-5.531	61317. ! mtbe017d.mec avg err 14.90%
CCQ.	<=> CC.Q	5.69E+45	-10.950	36744. ! mtbe017d.mec avg err 12.08%
CCQ.	<=> CH3CHO + OH	8.74E+26	-6.452	46782. ! mtbe017d.mec avg err 13.46%
C.CQ	<=> CC.Q	7.10E+30	-6.430	47827. ! mtbe017d.mec avg err 16.01%
C.CQ	<=> CH3CHO + OH	7.39E+21	-5.925	11060. ! mtbe017d.mec avg err 28.94%
CC.Q	<=> CH3CHO + OH	2.39E+24	-5.514	11750. ! mtbe017d.mec avg err 35.18%
C2H2 + H	<=> C2H3	2.49E+09	-.150	-240. ! mtbe017d.mec avg err 2.00%
C2H3 + O2	<=> C*CQ.	4.58E+30	-5.820	7302. ! mtbe017d.mec avg err 14.42%
C2H3 + O2	<=> C*CO. + O	2.05E+35	-8.021	4606. ! mtbe017d.mec avg err 8.16%
C2H3 + O2	<=> C.*CQ	1.29E+15	-.762	1316. ! mtbe017d.mec avg err .80%
C2H3 + O2	<=> C2H2 + HO2	3.24E+15	-2.156	663. ! mtbe017d.mec avg err 8.83%
C2H3 + O2	<=> CYC.OOC	1.09E+11	.071	2312. ! mtbe017d.mec avg err 2.75%
C2H3 + O2	<=> O*CCO.	5.47E+11	-1.575	1532. ! mtbe017d.mec avg err 2.14%
C2H3 + O2	<=> CHO + HCHO	1.69E+11	-1.356	-694. ! mtbe017d.mec avg err 9.94%
C2H3 + O2	<=> O*CC*O + H	2.43E+14	-1.056	1523. ! mtbe017d.mec avg err .93%
C*CQ.	<=> C*CO. + O	2.30E+11	-.364	999. ! mtbe017d.mec avg err .74%
C*CQ.	<=> C.*CQ	5.49E+44	-10.058	40558. ! mtbe017d.mec avg err 10.20%
C*CQ.	<=> C2H2 + HO2	1.32E+47	-11.592	42227. ! mtbe017d.mec avg err 4.58%
C*CQ.	<=> CYC.OOC	2.84E+41	-9.490	44347. ! mtbe017d.mec avg err 9.48%
C*CQ.	<=> O*CCO.	4.87E+39	-10.314	39851. ! mtbe017d.mec avg err 13.77%
C*CQ.	<=> CHO + HCHO	4.55E+38	-9.918	37484. ! mtbe017d.mec avg err 6.04%
C*CQ.	<=> O*CC*O + H	2.09E+42	-9.798	39836. ! mtbe017d.mec avg err 11.92%
C.*CQ	<=> C2H2 + HO2	2.45E+40	-9.505	39599. ! mtbe017d.mec avg err 11.10%
C.*CQ	<=> CYC.OOC	2.59E+22	-4.141	12061. ! mtbe017d.mec avg err 15.75%
C.*CQ	<=> O*CCO.	6.89E+22	-5.894	13686. ! mtbe017d.mec avg err 12.41%

C.*CQ	<=> CHO + HCHO	1.42E-22	-5.607	11531.	! mtbe017d.mec avg err 26.80%
C.*CQ	<=> O*CC*O + H	2.01E-25	-5.320	13724.	! mtbe017d.mec avg err 14.54%
CYC.OOC	<=> O*CCO.	1.47E-22	-4.631	13117.	! mtbe017d.mec avg err 17.57%
CYC.OOC	<=> CHO + HCHO	3.63E-11	-1.928	142.	! mtbe017d.mec avg err 11.68%
CYC.OOC	<=> O*CC*O + H	8.14E+13	-1.411	2182.	! mtbe017d.mec avg err 1.02%
O*CCO.	<=> CHO + HCHO	5.24E+08	-124	1214.	! mtbe017d.mec avg err 2.44%
O*CCO.	<=> O*CC*O + H	2.75E+21	-3.775	9003.	! mtbe017d.mec avg err 16.80%
C2H2 + OH	<=> C.*COH	3.80E+13	-1.490	24384.	! mtbe017d.mec avg err 11.86%
C2H2 + OH	<=> C#COH + H	4.80E+36	-7.927	7481.	! mtbe017d.mec avg err 11.46%
C2H2 + OH	<=> C*CO.	3.69E+12	-206	14335.	! mtbe017d.mec avg err 2.42%
C2H2 + OH	<=> C*C*O + H	6.58E+21	-3.384	5119.	! mtbe017d.mec avg err 7.48%
C2H2 + OH	<=> C.CHO	2.34E+13	-672	3926.	! mtbe017d.mec avg err 5.41%
C2H2 + OH	<=> CH3C.*O	7.91E+18	-2.680	3870.	! mtbe017d.mec avg err 6.74%
C2H2 + OH	<=> CH3 + CO	4.32E+27	-6.066	7082.	! mtbe017d.mec avg err 5.87%
C.*COH	<=> C#COH + H	2.92E+26	-4.481	8176.	! mtbe017d.mec avg err 19.13%
C.*COH	<=> C*CO.	1.12E+31	-6.609	50029.	! mtbe017d.mec avg err 12.18%
C.*COH	<=> C*C*O + H	6.86E+39	-9.202	37882.	! mtbe017d.mec avg err 12.36%
C.*COH	<=> C.CHO	8.69E+35	-8.052	37942.	! mtbe017d.mec avg err 10.85%
C.*COH	<=> CH3C.*O	4.82E+36	-8.420	36565.	! mtbe017d.mec avg err 10.97%
C.*COH	<=> CH3 + CO	8.23E+43	-11.377	39334.	! mtbe017d.mec avg err 9.46%
C*CO.	<=> C*C*O + H	4.19E+43	-10.087	40679.	! mtbe017d.mec avg err 23.59%
C*CO.	<=> C.CHO	3.87E+20	-2.762	39499.	! mtbe017d.mec avg err 4.91%
C*CO.	<=> CH3C.*O	1.15E+14	-1.602	641.	! mtbe017d.mec avg err 1.22%
C*CO.	<=> CH3 + CO	4.29E+26	-5.421	36187.	! mtbe017d.mec avg err 4.49%
C.CHO	<=> CH3C.*O	8.01E+24	-3.754	37304.	! mtbe017d.mec avg err 18.20%
C.CHO	<=> CH3 + CO	6.61E+23	-4.727	38065.	! mtbe017d.mec avg err 3.44%
C.CHO	<=> C*C*O + H	1.37E+22	-3.076	39191.	! mtbe017d.mec avg err 16.95%
CH3C.*O	<=> CH3 + CO	1.67E+12	-814	41162.	! mtbe017d.mec avg err 15.20%
CH3C.*O	<=> C*C*O + H	2.58E+26	-5.159	15922.	! mtbe017d.mec avg err 9.32%
COC + O	<=> COC. + OH	5.00E+13	0.0	4571.	!
COC + H	<=> COC. + H2	6.41E+00	4.13	2180.	!
COC + OH	<=> COC. + H2O	6.27E+12	0.0	739.	!
COC + CH3	<=> COC. + CH4	3.55E+12	0.0	11800.	!
COC + CH3O	<=> COC. + CH3OH	3.55E+12	0.0	11800.	!
CH3O + CH3	<=> COC	5.96E+18	-3.062	45056.	! mtbe017d.mec avg err 5.05%
CH3O + CH3	<=> COC. + H	7.34E+34	-6.820	7124.	! mtbe017d.mec avg err 47.68%
CH3O + CH3	<=> CH2S + CH3OH	1.94E+14	-314	19135.	! mtbe017d.mec avg err 12.00%
COC	<=> COC. + H	2.10E+15	-437	19034.	! mtbe017d.mec avg err 11.79%
COC	<=> CH2S + CH3OH	7.80E+45	-9.746	104606.	! mtbe017d.mec avg err 27.78%
COC.	<=> HCHO + CH3	1.01E+47	-9.881	104547.	! mtbe017d.mec avg err 27.88%
COC. + O2	<=> COCQ.	3.09E+28	-5.789	15191.	! mtbe017d.mec avg err 19.66%
COC. + O2	<=> C.OCQ	1.29E+37	-8.005	6211.	! mtbe017d.mec avg err 12.41%
COC. + O2	<=> HCHO + CH2OOH	1.19E+34	-6.912	8351.	! mtbe017d.mec avg err 14.39%
COCQ.	<=> C.OCQ	3.14E+27	-4.269	10684.	! mtbe017d.mec avg err 14.64%
COCQ.	<=> HCHO + CH2OOH	2.24E+36	-7.972	26426.	! mtbe017d.mec avg err 20.43%
C.OCQ	<=> HCHO + CH2OOH	8.58E+42	-9.344	41597.	! mtbe017d.mec avg err 17.04%
C*CC. + C2C*C	<=> CC*C + C2.C*C	2.01E-01	4.00	227.	!
C*CC. + HCHO	<=> CHO + CC*C	1.26E+08	1.90	18191.	!86TSA
C*CC. + C3COC	<=> CC*C + C3.COC	3.56E+02	3.30	19844.	!91 TS
C*CC. + C3COC	<=> CC*C + C3COC.	1.74E+03	2.90	19314.	!A fro

C*CC. + CH3OH	<=>	CC*C - CH2OH	1.74E+03	2.90	20456.191 TS
C*CC. + C2C*O	<=>	CC*C - C2.C*O	7.08E+11	0.00	16492.189 LO
C*CC. + O2	<=>	C*C*C - HO2	1.21E+12	0.00	13553.191 TS
C*CC. + C2CYCOC	<=>	CC*C + C2CYCOC.	1.00E+00	4.00	13318.1AMD C
C*CC. + CCYCOC	<=>	CC*C + CCYC.OC	4.42E+01	3.30	17169.191 TSA
C*CC. + C*CI CC*O	<=>	CC*C + C*CI CC.*O	1.90E+11	0.00	6218.1A=1/2
C*CC. + C2CC*O	<=>	CC*C + C2CC.*O	3.80E+11	0.00	7218.1the
C*CC. + O*CC*O	<=>	CC*C + O*CC.*O	7.90E+11	0.00	7218.12*(c
C*CC. + CCC*O	<=>	CC*C + CCC.*O	3.80E+11	0.00	7218.1the
C*CC. + CH3CHO	<=>	CC*C + CH3C.*O	3.80E+11	0.00	7218.189 L
C*CC. + C2CQC*O	<=>	CC*C + C2CQC.*O	1.90E+11	0.00	7218.11/2
C*CC. + C2COHC*O	<=>	CC*C + C2COHC.*O	1.90E+11	0.00	7218.11/2
C*CC. + CCQCHO	<=>	CC*C + CCQC.*O	1.90E+11	0.00	7218.11/2
C*CC. + CCOHCHO	<=>	CC*C + CCOHC.*O	1.90E+11	0.00	7218.11/2
CC*C + O	<=>	C*CC. + OH	6.03E+10	0.70	7633.191 TSA
CC*C + O	<=>	CCYCOC	4.20E+12	0.00	503.173 HER
CC*C + H	<=>	C*CC. + H2	1.75E+05	2.50	2492.191 TSA
CC*C + H	<=>	C2H4 + CH3	7.23E+12	0.00	1302.191 TSA
CC*C + OH	<=>	C*CC. + H2O	3.12E+06	2.00	-298.191 TSA
CC*C + CH3	<=>	C*CC. + CH4	2.21E+00	3.50	5675.191 TSA
CC*C + CH3O	<=>	C*CC. + CH3OH	2.21E+00	3.50	5675.191 TSA
CC*C + HO2	<=>	C*CC. + H2O2	9.64E+03	2.60	13910.191 TSA
CC*C + HO2	<=>	CCYCOC + OH	1.05E+12	0.00	14206.191 TSA
CC*C + O2	<=>	C*CC. + HO2	1.95E+12	0.00	39110.1R.W.W
CC.C + O2	<=>	C2CQ.	2.90E+28	-5.259	25035.1 mtbe017d.mec avg err 9.28%
CC.C + O2	<=>	CC*CB + HO2B	1.82E+49	-11.956	9442.1 mtbe017d.mec avg err 20.72%
CC.C + O2	<=>	C2C.Q	5.06E+17	-1.718	8038.1 mtbe017d.mec avg err 7.37%
CC.C + O2	<=>	C2C*O + OH	4.84E+08	-245	12041.1 mtbe017d.mec avg err 1.17%
CC.C + O2	<=>	C2.CQ	1.49E+11	.037	12664.1 mtbe017d.mec avg err 2.54%
CC.C + O2	<=>	CCYCOC + OH	2.13E+33	-7.124	8861.1 mtbe017d.mec avg err 12.69%
CC.C + O2	<=>	CC*C + HO2	6.24E+17	-2.221	10575.1 mtbe017d.mec avg err 7.34%
CC.C + O2	<=>	C*CQ + CH3	3.21E+27	-4.564	10895.1 mtbe017d.mec avg err 12.31%
C2CQ.	<=>	CC*CB + HO2B	1.31E+08	.870	17572.1 mtbe017d.mec avg err .77%
C2CQ.	<=>	C2C.Q	1.50E+46	-10.814	41672.1 mtbe017d.mec avg err 21.63%
C2CQ.	<=>	C2C*O + OH	4.96E+32	-8.127	46104.1 mtbe017d.mec avg err 24.48%
C2CQ.	<=>	C2.CQ	1.53E+35	-7.857	46685.1 mtbe017d.mec avg err 28.96%
C2CQ.	<=>	CCYCOC + OH	2.53E+54	-13.557	39427.1 mtbe017d.mec avg err 15.48%
C2CQ.	<=>	C*CQ + CH3	8.72E+45	-11.254	44702.1 mtbe017d.mec avg err 26.45%
C2C.Q	<=>	C2.CQ	2.41E+28	-5.978	50817.1 mtbe017d.mec avg err 28.16%
C2.CQ	<=>	C2C*O + OH	1.24E+13	-3.580	126.1 mtbe017d.mec avg err 8.58%
C2.CQ	<=>	CCYCOC + OH	3.14E+38	-9.865	14698.1 mtbe017d.mec avg err 33.54%
C2.CQ	<=>	C*CQ + CH3	8.35E+19	-3.561	19789.1 mtbe017d.mec avg err 22.73%
C*CC. + O2	<=>	C*CCQ.	1.59E+13	-1.257	31670.1 mtbe017d.mec avg err 19.50%
C*CC. + O2	<=>	C*CCO. + O	3.48E+34	-7.593	5724.1 mtbe017d.mec avg err 12.47%
C*CC. + O2	<=>	C*C.CQ	2.64E+17	-1.255	42868.1 mtbe017d.mec avg err 3.72%
C*CC. + O2	<=>	C.*CCQ	1.59E+12	-1.153	17303.1 mtbe017d.mec avg err 4.41%
C*CC. + O2	<=>	C*CC.Q	6.73E+12	-239	15252.1 mtbe017d.mec avg err 4.40%
C*CC. + O2	<=>	C*CC*O + OH	1.35E+08	-1.106	20031.1 mtbe017d.mec avg err 7.46%
C*CC. + O2	<=>	YC.COOC	1.50E+13	-0.090	20971.1 mtbe017d.mec avg err 4.32%
C*CC. + O2	<=>	C.CYCOOC	6.23E+29	-6.640	17289.1 mtbe017d.mec avg err 14.19%
C*CC. + O2	<=>	CO.CYCOC	6.16E+13	-1.998	13881.1 mtbe017d.mec avg err 6.03%

C*CC. + O2 5.14%	<=> CYC.OC-HCHO	1.67E-16	-1.631	16986. ! mtbe017d.mec avg err
C*CC. + O2	<=> YCC.OOC	1.08E+20	-2.714	18117. ! mtbe017d.mec avg err 9.52%
C*CC. + O2	<=> CCYC.OOC	1.93E+03	1.089	20427. ! mtbe017d.mec avg err 16.43%
C*CC. + O2	<=> CCYCOOC.	2.75E+03	.680	35359. ! mtbe017d.mec avg err 5.30%
C*CC. + O2	<=> C*COOC.	2.17E+03	.743	33376. ! mtbe017d.mec avg err 5.59%
C*CC. + O2	<=> C*CO. + HCHO	1.51E+08	-.678	37094. ! mtbe017d.mec avg err 5.61%
C*CC. + O2	<=> O*CCCO.	4.47E+08	.324	36618. ! mtbe017d.mec avg err 5.73%
C*CC. - O2 10.28%	<=> C.CHO + HCHO	1.44E-01	2.468	16925. ! mtbe017d.mec avg err
C*CC. + O2	<=> CC*OCO.	1.19E+05	1.806	20226. ! mtbe017d.mec avg err 14.15%
C*CC. - O2 8.61%	<=> CH3C.*O + HCHO	6.97E-02	1.999	32308. ! mtbe017d.mec avg err
C*CC. + O2	<=> CCO.C*O	8.19E+05	1.275	35565. ! mtbe017d.mec avg err 5.24%
C*CC. + O2 7.96%	<=> CH3CHO + CHO	1.24E-01	2.095	30988. ! mtbe017d.mec avg err
C*CC. + O2	<=> CCOHC.*O	2.49E+06	1.218	33694. ! mtbe017d.mec avg err 6.17%
C*CCQ.	<=> C*CCO. + O	4.51E-03	3.525	32815. ! mtbe017d.mec avg err 5.20%
C*CCQ.	<=> C*C.CQ	2.15E+22	-3.561	60583. ! mtbe017d.mec avg err 20.50%
C*CCQ.	<=> C.*CCQ	1.08E+22	-3.825	35436. ! mtbe017d.mec avg err 18.38%
C*CCQ.	<=> C*CC.Q	3.75E+23	-4.170	33510. ! mtbe017d.mec avg err 18.64%
C*CCQ.	<=> C*CC*O + OH	5.12E+16	-3.417	38048. ! mtbe017d.mec avg err 14.64%
C*CCQ.	<=> YC.COOC	6.04E+21	-3.415	38979. ! mtbe017d.mec avg err 18.28%
C*CCQ.	<=> C.CYCOOC	1.76E+39	-10.062	35520. ! mtbe017d.mec avg err 36.52%
C*CCQ.	<=> CO.CYCOC	9.90E+23	-5.717	32228. ! mtbe017d.mec avg err 23.10%
C*CCQ. 17.56%	<=> CYC.OC+HCHO	1.56E+26	-5.331	35116. ! mtbe017d.mec avg err
C*CCQ.	<=> YCC.OOC	5.00E+29	-6.309	36088. ! mtbe017d.mec avg err 13.94%
C*CCQ.	<=> CCYC.OOC	6.05E+10	-1.946	37762. ! mtbe017d.mec avg err 10.73%
C*CCQ.	<=> CCYCOOC.	8.72E+08	-1.802	52967. ! mtbe017d.mec avg err 18.34%
C*CCQ.	<=> C*COOC.	1.31E+09	-1.816	51011. ! mtbe017d.mec avg err 18.15%
C*CCQ.	<=> C*CO. + HCHO	3.16E+13	-3.108	54676. ! mtbe017d.mec avg err 17.54%
C*CCQ.	<=> O*CCCO.	9.21E+13	-2.106	54190. ! mtbe017d.mec avg err 17.77%
C*CCQ.	<=> C.CHO + HCHO	4.25E+06	-.553	34272. ! mtbe017d.mec avg err 26.34%
C*CCQ.	<=> CC*OCO.	3.55E+12	-1.225	37548. ! mtbe017d.mec avg err 12.99%
C*CCQ. 31.86%	<=> CH3C.*O + HCHO	1.88E+04	-.458	49905. ! mtbe017d.mec avg err
C*CCQ.	<=> CCO.C*O	2.60E+11	-1.207	53173. ! mtbe017d.mec avg err 18.40%
C*CCQ. 20.18%	<=> CH3CHO + CHO	6.18E+04	-.435	48606. ! mtbe017d.mec avg err
C*CCQ.	<=> CCOHC.*O	1.37E+12	-1.328	51316. ! mtbe017d.mec avg err 17.58%
C*CC.Q	<=> C*C.CQ	3.62E+03	.914	50440. ! mtbe017d.mec avg err 19.49%
C*CC.Q	<=> C.*CCQ	3.05E-05	3.120	28140. ! mtbe017d.mec avg err 77.16%
C*CC.Q	<=> C*CC*O + OH	1.04E+07	-.204	29928. ! mtbe017d.mec avg err 71.79%
C*CC.Q	<=> YC.COOC	1.37E+10	-.367	234. ! mtbe017d.mec avg err 2.84%
C*CC.Q	<=> C.CYCOOC	3.28E+11	-3.555	540. ! mtbe017d.mec avg err 8.68%
YC.COOC	<=> C*C.CQ	7.43E+05	-1.819	-374. ! mtbe017d.mec avg err 13.13%
YC.COOC	<=> C.*CCQ	2.67E+18	-2.872	42303. ! mtbe017d.mec avg err 12.74%
YC.COOC	<=> C.CYCOOC	5.99E+19	-3.149	41064. ! mtbe017d.mec avg err 13.39%
YC.COOC	<=> CO.CYCOC	1.04E-08	2.766	10413. ! mtbe017d.mec avg err 104.85%
YC.COOC 17.31%	<=> CYC.OC+HCHO	1.72E+36	-9.012	26326. ! mtbe017d.mec avg err
YC.COOC	<=> YCC.OOC	1.15E+40	-8.860	29217. ! mtbe017d.mec avg err 13.14%
YC.COOC	<=> O*CCCO.	2.27E-21	7.435	10168. ! mtbe017d.mec avg err 42.25%

YC.COOC 53.12%	<=> C.CHO - HCHO	4.41E-23	8.308	11966. ! mtbe017d.mec avg err
C.CYCOOC	<=> C*C.CQ	1.19E-16	7.489	15715. ! mtbe017d.mec avg err 72.57%
C.CYCOOC	<=> C.*CCQ	1.14E+02	1.808	17601. ! mtbe017d.mec avg err 6.49%
C.CYCOOC 6.33%	<=> CO.CYCOC	7.50E+02	1.680	16170. ! mtbe017d.mec avg err
C.CYCOOC 19.89%	<=> CYC.OC-HCHO	6.71E-18	-2.995	6878. ! mtbe017d.mec avg err
C.CYCOOC 60.09%	<=> CCYC.OOC	7.33E+12	-2.302	4295. ! mtbe017d.mec avg err
C.CYCOOC 114.33%	<=> CCYCOOC.	3.53E-48	14.262	-11146. ! mtbe017d.mec avg err
C.CYCOOC 101.93%	<=> C*COOC.	2.30E-46	13.846	-10579. ! mtbe017d.mec avg err
C.CYCOOC 93.30%	<=> C*CO. + HCHO	5.34E-53	15.812	-11418. ! mtbe017d.mec avg err
C.CYCOOC	<=> CC*OCO.	5.05E-54	17.285	-11876. ! mtbe017d.mec avg err 91.63%
C.CYCOOC 120.87%	<=> CH3C.*O + HCHO	3.13E-64	19.090	-16212. ! mtbe017d.mec avg err
C.CYCOOC	<=> CCO.C*O	1.30E-58	18.809	-13199. ! mtbe017d.mec avg err 95.55%
C.CYCOOC 97.62%	<=> CH3CHO + CHO	6.19E-62	18.679	-14762. ! mtbe017d.mec avg err
C.CYCOOC 86.93%	<=> CCOHC.*O	1.86E-55	18.055	-12178. ! mtbe017d.mec avg err
CO.CYCOC	<=> C*C.CQ	3.89E-68	21.575	-13491. ! mtbe017d.mec avg err 89.50%
CO.CYCOC	<=> C.*CCQ	3.23E+03	1.146	61489. ! mtbe017d.mec avg err 8.67%
CO.CYCOC 8.61%	<=> CYC.OC+HCHO	3.90E+04	.946	60279. ! mtbe017d.mec avg err
YCC.OOC	<=> O*CCCO.	9.96E+24	-4.774	11834. ! mtbe017d.mec avg err 32.36%
YCC.OOC 13.30%	<=> C.CHO + HCHO	2.66E+09	-1.097	-1632. ! mtbe017d.mec avg err
CCYC.OOC	<=> CCYCOOC.	7.17E+12	-1.062	1146. ! mtbe017d.mec avg err 1.73%
CCYC.OOC	<=> CC*OCO.	2.48E-11	2.334	-4642. ! mtbe017d.mec avg err 77.30%
CCYC.OOC 10.09%	<=> CH3C.*O + HCHO	1.55E+05	-.157	-3175. ! mtbe017d.mec avg err
CCYCOOC.	<=> CCO.C*O	8.39E+10	-.516	-160. ! mtbe017d.mec avg err 1.11%
CCYCOOC. 4.45%	<=> CH3CHO + CHO	6.15E+04	.032	-2585. ! mtbe017d.mec avg err
CCYCOOC.	<=> CCOHC.*O	1.76E+11	-.613	-27. ! mtbe017d.mec avg err 1.79%
C*COOC.	<=> C*CO. + HCHO	6.25E-03	3.015	-1600. ! mtbe017d.mec avg err 1.80%
O*CCCO.	<=> C.CHO + HCHO	2.81E+12	-.964	607. ! mtbe017d.mec avg err 3.78%
CCO.C*O 25.08%	<=> CH3CHO + CHO	9.43E+19	-3.342	8106. ! mtbe017d.mec avg err
CCO.C*O	<=> CCOHC.*O	2.93E+12	-1.141	2225. ! mtbe017d.mec avg err 14.41%
C.*CCQ 4.38%	<=> C2H2 + CH2OOH	3.66E+05	1.005	25146. ! mtbe017d.mec avg err
C*C.CQ	<=> C*C*C + HO2	2.71E+39	-8.393	38687. ! mtbe017d.mec avg err 17.03%
CC*C + H	<=> CC.C	1.48E+28	-5.550	17004. ! mtbe017d.mec avg err 18.84%
CC*C + HO2	<=> C2.CQ	2.44E+34	-6.780	8016. ! mtbe017d.mec avg err 31.39%
CC*C + HO2 22.54%	<=> CCYCOC + OH	2.33E+20	-3.123	10686. ! mtbe017d.mec avg err
CC*C + HO2	<=> C*CQ + CH3	1.31E+08	.995	17590. ! mtbe017d.mec avg err 3.29%
CC*C + HO2	<=> C2CQ.	1.35E+08	1.336	30846. ! mtbe017d.mec avg err 6.73%
CC*C + HO2	<=> CC.CQ	6.13E+45	-11.037	23886. ! mtbe017d.mec avg err 28.27%

CC*C + HO2 32.03%	<=> CCYCOC + OH	4.47E-25 -5.202 8361. ! mtbe017d.mec avg err
CC*C + HO2	<=> CCCQ.	4.42E-12 -602 16285. ! mtbe017d.mec avg err 2.14%
CC*C + HO2	<=> CCC. + O2	3.23E+46 -11.560 22047. ! mtbe017d.mec avg err 20.41%
CC.CQ	<=> CCYCOC + OH	3.61E+26 -4.474 24573. ! mtbe017d.mec avg err 13.65%
CC.CQ	<=> CCCQ.	1.56E+16 -2.469 18164. ! mtbe017d.mec avg err 23.49%
CC.CQ	<=> CC*CB + HO2B	4.25E+45 -11.818 22377. ! mtbe017d.mec avg err 5.73%
CC.CQ	<=> CCC. + O2	1.00E+26 -5.703 25530. ! mtbe017d.mec avg err 9.77%
CCCQ.	<=> CC*CB + HO2B	5.67E+28 -5.882 26566. ! mtbe017d.mec avg err 9.78%
CCCQ.	<=> CCC. + O2	5.25E+43 -10.239 38434. ! mtbe017d.mec avg err 19.63%
C2.CQ + O2	<=> CCQCQ.	1.64E+48 -10.949 40647. ! mtbe017d.mec avg err 18.57%
C2.CQ + O2 5.82%	<=> C*QCB + HO2B	3.08E+32 -6.810 4905. ! mtbe017d.mec avg err
C2.CQ + O2	<=> C.CQCQ	1.03E+16 -1.477 11272. ! mtbe017d.mec avg err 9.18%
C2.CQ + O2 8.55%	<=> C*CCQ + HO2	2.12E+33 -7.185 10027. ! mtbe017d.mec avg err
C2.CQ + O2	<=> C*CQ + CH2OOH	3.36E+29 -5.250 13311. ! mtbe017d.mec avg err
C2.CQ + O2 11.50%	<=> CQCYCOC + OH	3.41E+17 -1.984 23185. ! mtbe017d.mec avg err
C2.CQ + O2 6.14%	<=> QCYCCOC + OH	2.55E+23 -3.855 14417. ! mtbe017d.mec avg err
C2.CQ + O2 9.28%	<=> CC.QCQ	9.13E+25 -4.810 13527. ! mtbe017d.mec avg err 10.86%
C2.CQ + O2	<=> YCOCICQ + OH	1.08E+24 -4.565 8746. ! mtbe017d.mec avg err
C2.CQ + O2 15.81%	<=> CC*OCQ + OH	7.40E+09 -1.116 9270. ! mtbe017d.mec avg err 9.88%
C2.CQ + O2	<=> C*CQC + HO2	2.73E+25 -3.934 8899. ! mtbe017d.mec avg err
C2.CQ + O2 12.21%	<=> CCQC.Q	1.45E+09 .289 9730. ! mtbe017d.mec avg err 9.38%
C2.CQ + O2	<=> CCQCHO + OH	1.68E+10 -6.90 17209. ! mtbe017d.mec avg err
C2.CQ + O2 8.52%	<=> CC*CQ + HO2	5.90E+12 -2.15 17566. ! mtbe017d.mec avg err 4.29%
C2.CQ + O2	<=> CCQ.CQ	7.42E-02 3.125 17225. ! mtbe017d.mec avg err 4.01%
C2.CQ + O2 32.43%	<=> CC*CQB + HO2B	3.50E+42 -9.843 14007. ! mtbe017d.mec avg err
CCQCQ.	<=> C*CQCB + HO2B	2.42E+32 -6.264 22215. ! mtbe017d.mec avg err
CCQCQ. 43.32%	<=> C.CQCQ	3.17E+29 -5.844 37771. ! mtbe017d.mec avg err 6.45%
CCQCQ.	<=> C*CCQ + HO2	3.15E+47 -11.518 32702. ! mtbe017d.mec avg err
CCQCQ. 29.48%	<=> C*CQ + CH2OOH	4.09E+46 -10.576 40354. ! mtbe017d.mec avg err
CCQCQ. 9.11%	<=> CQCYCOC + OH	3.28E+27 -5.302 51853. ! mtbe017d.mec avg err
CCQCQ. 16.91%	<=> QCYCCOC + OH	3.84E+39 -8.938 42663. ! mtbe017d.mec avg err
CCQCQ. 12.31%	<=> CC.QCQ	8.36E+42 -10.108 40989. ! mtbe017d.mec avg err 9.76%
CCQCQ.	<=> YCOCICQ + OH	1.29E+31 -7.107 26247. ! mtbe017d.mec avg err
CCQCQ. 21.50%	<=> CC*OCQ + OH	5.06E+19 -3.491 32579. ! mtbe017d.mec avg err 3.72%
CCQCQ.	<=> C*CQC + HO2	1.81E+32 -6.414 26544. ! mtbe017d.mec avg err 15.38%
CCQCQ.	<=> CCQC.Q	4.66E+19 -3.277 34023. ! mtbe017d.mec avg err 5.03%
CCQCQ. 7.15%	<=> CCQCHO + OH	2.56E+22 -4.658 46060. ! mtbe017d.mec avg err

CCQCQ.	<=> CC* <chem>CQ</chem> + <chem>HO2</chem>	5.47E+24	-4.132	46306.	! mtbe017d.mec avg err 13.26%
CCQCQ.	<=> CCQ <chem>CQ</chem>	1.47E+08	-0.094	44841.	! mtbe017d.mec avg err 14.32%
CCQCQ.	<=> C*CCQB + <chem>HO2B</chem>	4.05E+35	-8.078	24842.	! mtbe017d.mec avg err
42.60%					
CCQCQ.	<=> CC* <chem>CQB</chem> + <chem>HO2B</chem>	3.73E+39	-8.590	46843.	! mtbe017d.mec avg err
30.63%					
C.CQCQ	<=> C*CCQ - <chem>HO2</chem>	2.22E+39	-8.589	47354.	! mtbe017d.mec avg err 29.37%
C.CQCQ	<=> C* <chem>CQ</chem> + <chem>CH2OOH</chem>	2.56E+66	-17.416	29411.	! mtbe017d.mec avg err
63.66%					
C.CQCQ	<=> <chem>CQCYCOC</chem> + <chem>OH</chem>	6.33E+74	-22.878	45711.	! mtbe017d.mec avg err
34.30%					
C.CQCQ	<=> <chem>QCYCCOC</chem> + <chem>OH</chem>	3.05E+70	-19.332	35570.	! mtbe017d.mec avg err
57.80%					
C.CQCQ	<=> CC.QCQ	7.90E+65	-17.953	31236.	! mtbe017d.mec avg err 62.51%
C.CQCQ	<=> CC*OCQ + <chem>OH</chem>	1.58E+65	-18.212	32043.	! mtbe017d.mec avg err
95.72%					
C.CQCQ	<=> CCQC.Q	9.66E+67	-18.044	32661.	! mtbe017d.mec avg err 85.27%
C.CQCQ	<=> CCQCHO + <chem>OH</chem>	4.80E+42	-13.159	12526.	! mtbe017d.mec avg err
95.83%					
C.CQCQ	<=> CCQ.CQ	3.75E+46	-13.161	13877.	! mtbe017d.mec avg err 90.86%
CC.QCQ	<=> <chem>YCOCICQ</chem> + <chem>OH</chem>	2.24E+65	-17.684	31148.	! mtbe017d.mec avg err
88.46%					
CC.QCQ	<=> CC*OCQ + <chem>OH</chem>	4.43E+10	-0.756	19901.	! mtbe017d.mec avg err 3.78%
CC.QCQ	<=> C* <chem>CQC</chem> + <chem>HO2</chem>	2.16E+10	-0.331	-47.	! mtbe017d.mec avg err 3.79%
CC.QCQ	<=> CCQC.Q	2.44E+11	-0.738	22172.	! mtbe017d.mec avg err 3.89%
CC.QCQ	<=> CCQCHO + <chem>OH</chem>	5.27E-51	15.533	4713.	! mtbe017d.mec avg err
*****%					
CC.QCQ	<=> CCQ.CQ	6.06E-37	12.723	12269.	! mtbe017d.mec avg err 729.06%
CCQC.Q	<=> CCQCHO + <chem>OH</chem>	1.14E+31	-7.576	27424.	! mtbe017d.mec avg err
88.84%					
CCQC.Q	<=> CC* <chem>CQ</chem> + <chem>HO2</chem>	2.99E+09	-0.096	-297.	! mtbe017d.mec avg err 6.00%
CCQC.Q	<=> CCQ.CQ	1.09E+10	-0.605	19607.	! mtbe017d.mec avg err 5.99%
CCQ.CQ	<=> CC*OCQ + <chem>OH</chem>	6.12E-56	16.518	-15506.	! mtbe017d.mec avg err
125.85%					
CCQ.CQ	<=> CCQCHO + <chem>OH</chem>	5.36E+38	-8.274	36744.	! mtbe017d.mec avg err
62.28%					
CCQ.CQ	<=> C*CCQB + <chem>HO2B</chem>	2.98E+38	-8.369	55194.	! mtbe017d.mec avg err
14.52%					
CCQ.CQ	<=> CC* <chem>CQB</chem> + <chem>HO2B</chem>	6.36E+27	-4.652	38953.	! mtbe017d.mec avg err
22.15%					
CC.CQ + O2	<=> CCQ.CQ	5.64E+27	-4.696	39632.	! mtbe017d.mec avg err 21.51%
CC.CQ + O2	<=> C*CCQB + <chem>HO2B</chem>	9.14E+37	-8.378	6444.	! mtbe017d.mec avg err
4.14%					
CC.CQ + O2	<=> CC* <chem>CQB</chem> + <chem>HO2B</chem>	3.87E+19	-2.247	11731.	! mtbe017d.mec avg err
10.04%					
CC.CQ + O2	<=> C.CQCQ	9.22E+18	-2.126	11946.	! mtbe017d.mec avg err 9.72%
CC.CQ + O2	<=> C*CCQ + <chem>HO2</chem>	7.96E+31	-6.729	10281.	! mtbe017d.mec avg err
8.17%					
CC.CQ + O2	<=> C* <chem>CQ</chem> + <chem>CH2OOH</chem>	3.09E+30	-5.406	14562.	! mtbe017d.mec avg err
14.58%					
CC.CQ + O2	<=> <chem>CQCYCOC</chem> + <chem>OH</chem>	3.47E+16	-1.584	22874.	! mtbe017d.mec avg err
11.84%					
CC.CQ + O2	<=> <chem>QCYCCOC</chem> + <chem>OH</chem>	5.14E+23	-3.826	15111.	! mtbe017d.mec avg err
11.95%					

CC.CQ + O2	<=> CC.QCQ	5.96E-26	-4.925	14638.	! mtbe017d.mec avg err 13.86%
CC.CQ + O2	<=> YCOCICQ + OH	4.74E+13	-1.639	15823.	! mtbe017d.mec avg err
5.49%					
CC.CQ + O2	<=> CC*OCQ + OH	4.84E+00	2.481	15158.	! mtbe017d.mec avg err
3.24%					
CC.CQ + O2	<=> C*QCQ + HO2	1.87E+15	-1.061	15953.	! mtbe017d.mec avg err
5.84%					
CC.CQ - O2	<=> CCQC.Q	5.94E-01	2.942	15219.	! mtbe017d.mec avg err 2.76%
CC.CQ - O2	<=> CCQCHO + OH	1.76E+27	-5.633	9810.	! mtbe017d.mec avg err
18.21%					
CC.CQ + O2	<=> CC*CQ + HO2	2.59E+29	-5.057	10148.	! mtbe017d.mec avg err
14.66%					
CC.CQ + O2	<=> CCQCQ.	1.05E+13	-1.019	10546.	! mtbe017d.mec avg err 9.65%
CC.CQ + O2	<=> C*QCQ + HO2B	3.46E+51	-12.618	16169.	! mtbe017d.mec avg err
31.22%					
CC.CQ + O2	<=> C2.CQ + O2	1.35E+38	-8.463	21716.	! mtbe017d.mec avg err 28.18%
CC*C + OH	<=> C2.CO.H	2.32E+43	-9.486	21511.	! mtbe017d.mec avg err 29.93%
CC*C + OH	<=> C*COH + CH3	2.32E+45	-10.440	9210.	! mtbe017d.mec avg err
18.59%					
CC*C + OH	<=> C*COHC + H	2.22E+21	-2.819	7968.	! mtbe017d.mec avg err 10.07%
CC*C + OH	<=> C2C.OH	1.79E+19	-2.136	8591.	! mtbe017d.mec avg err 7.47%
CC*C + OH	<=> C2C*O + H	1.58E+35	-7.376	15737.	! mtbe017d.mec avg err 15.83%
CC*C + OH	<=> C2CO.	1.90E+19	-1.876	14921.	! mtbe017d.mec avg err 17.77%
CC*C + OH	<=> CH3CHO + CH3	1.97E+08	-3.53	11785.	! mtbe017d.mec avg err
19.65%					
C2.CO.H	<=> C*COH + CH3	9.80E+08	.952	14107.	! mtbe017d.mec avg err 3.26%
C2.CO.H	<=> C*COHC + H	1.93E+44	-10.506	36701.	! mtbe017d.mec avg err 18.38%
C2.CO.H	<=> C2C.OH	7.57E+43	-10.357	38908.	! mtbe017d.mec avg err 18.47%
C2.CO.H	<=> C2C*O + H	3.36E+53	-13.561	45427.	! mtbe017d.mec avg err 24.14%
C2.CO.H	<=> C2CO.	5.15E+39	-8.885	44835.	! mtbe017d.mec avg err 16.71%
C2.CO.H	<=> CH3CHO + CH3	2.64E+28	-7.281	42376.	! mtbe017d.mec avg err
40.84%					
C2C.OH	<=> C*COHC + H	3.70E+29	-6.182	44633.	! mtbe017d.mec avg err 25.63%
C2C.OH	<=> C2C*O + H	1.58E+56	-14.024	51486.	! mtbe017d.mec avg err 29.30%
C2CO.	<=> C2C.OH	1.02E+42	-9.439	36732.	! mtbe017d.mec avg err 45.34%
C2CO.	<=> CH3CHO + CH3	1.53E+37	-10.648	13935.	! mtbe017d.mec avg err 22.97%
C2CO.	<=> C2C*O + H	3.40E+39	-9.287	16735.	! mtbe017d.mec avg err 12.05%
C2.CO.H + O2	<=> CCOHCQ.	5.99E+37	-9.066	18453.	! mtbe017d.mec avg err 13.00%
C2.CO.H + O2	<=> C*COHCB + HO2B	8.99E+35	-7.908	6030.	! mtbe017d.mec avg err
9.15%					
C2.CO.H + O2	<=> CCO.CQ	7.05E+20	-2.769	8604.	! mtbe017d.mec avg err 17.44%
C2.CO.H + O2	<=> CQCHO + CH3	3.65E+26	-5.989	6571.	! mtbe017d.mec avg err
13.44%					
C2.CO.H + O2	<=> CH3CHO + CH2OOH	9.94E+21	-3.479	9807.	! mtbe017d.mec avg err
13.42%					
C2.CO.H + O2	<=> CC*OCQ + H	5.18E+22	-3.508	9783.	! mtbe017d.mec avg err
13.46%					
C2.CO.H + O2	<=> CCOHC.Q	1.98E+18	-2.663	10805.	! mtbe017d.mec avg err 11.92%
C2.CO.H + O2	<=> CC*CQ + OH	1.83E+09	-.331	16000.	! mtbe017d.mec avg err 8.33%
C2.CO.H + O2	<=> CCOHCHO + OH	1.40E-11	6.161	18369.	! mtbe017d.mec avg err
8.77%					
C2.CO.H + O2	<=> C.COHCQ	1.92E+12	-.087	16733.	! mtbe017d.mec avg err 4.66%
C2.CO.H + O2	<=> C*COH + CH2OOH	6.40E+33	-7.003	10967.	! mtbe017d.mec avg err
32.90%					

C2.CO ₂ H + O ₂ 20.31%	<=> C*CCQ + OH	1.23E+28	-4.928	21593. ! mtbe017d.mec avg err
C2.CO ₂ H + O ₂ 18.92%	<=> OHCYCCOC + OH	1.69E+29	-4.837	22410. ! mtbe017d.mec avg err
C2.CO ₂ H + O ₂ 14.06%	<=> CC.OHCQ	7.64E+31	-6.241	16227. ! mtbe017d.mec avg err 31.54%
C2.CO ₂ H + O ₂ 14.06%	<=> YCOCICOH + OH	2.44E+37	-7.939	10915. ! mtbe017d.mec avg err
CCOHCQ. 24.86%	<=> C*COHCB + HO ₂ B	4.62E+31	-5.741	14844. ! mtbe017d.mec avg err
CCOHCQ. 12.40%	<=> CCO.CQ	4.58E+34	-7.334	32364. ! mtbe017d.mec avg err 8.13%
CCOHCQ. 9.96%	<=> CQCHO + CH ₃	3.50E+53	-14.046	35099. ! mtbe017d.mec avg err
CCOHCQ. 9.90%	<=> CH ₃ CHO + CH ₂ OOH	1.73E+44	-10.412	39083. ! mtbe017d.mec avg err
CCOHCQ. 14.42%	<=> CC*OCQ + H	9.59E+44	-10.448	39029. ! mtbe017d.mec avg err
CCOHCQ. 19.83%	<=> CCOHC.Q	4.20E+39	-9.349	40913. ! mtbe017d.mec avg err 12.30%
CCOHCQ. 17.41%	<=> CC*CO + OH	9.35E+25	-5.749	46688. ! mtbe017d.mec avg err
CCOHCQ. 7.25%	<=> CCOHCHO + OH	4.25E+00	2.107	47260. ! mtbe017d.mec avg err
CCOHCQ. 23.87%	<=> C.COHCQ	8.19E+28	-5.496	47353. ! mtbe017d.mec avg err 20.85%
CCOHCQ. 24.24%	<=> C*COH + CH ₂ OOH	1.03E+41	-9.443	30739. ! mtbe017d.mec avg err
CCOHCQ. 20.07%	<=> C*CCQ + OH	2.01E+40	-8.917	50620. ! mtbe017d.mec avg err 6.76%
CCOHCQ. 7.12%	<=> OHCYCCOC + OH	1.84E+41	-8.781	51573. ! mtbe017d.mec avg err
CCOHCQ. 27.74%	<=> CC.OHCQ	1.78E+42	-9.652	41508. ! mtbe017d.mec avg err 11.95%
CCOHCQ. 30.34%	<=> YCOCICOH + OH	2.21E+44	-10.290	29359. ! mtbe017d.mec avg err
CCOHC.Q 30.61%	<=> CQCHO + CH ₃	4.13E+45	-10.268	40328. ! mtbe017d.mec avg err
CCOHC.Q 33.10%	<=> CH ₃ CHO + CH ₂ OOH	7.27E+24	-4.731	13001. ! mtbe017d.mec avg err
CCOHC.Q 57.92%	<=> CC*OCQ + H	5.56E+25	-4.810	12993. ! mtbe017d.mec avg err 20.48%
C.COHCQ 74.63%	<=> CCOHC.Q	1.72E+19	-3.286	15067. ! mtbe017d.mec avg err 13.40%
	<=> CCOHCHO + OH	9.79E+17	-4.392	29263. ! mtbe017d.mec avg err
	<=> C.COHCQ	7.24E+20	-4.112	29916. ! mtbe017d.mec avg err 1.66%
	<=> OHCYCCOC + OH	1.60E+47	-12.268	21280. ! mtbe017d.mec avg err
	<=> CC.OHCQ	1.23E+38	-9.484	25742. ! mtbe017d.mec avg err 28.61%
	<=> YCOCICOH + OH	2.12E+54	-14.187	22594. ! mtbe017d.mec avg err
	<=> CC*CO + OH	1.67E+43	-10.603	25698. ! mtbe017d.mec avg err
	<=> CCOHCHO + OH	6.73E+68	-21.018	46584. ! mtbe017d.mec avg err
	<=> C.COHCQ	4.31E+35	-8.320	8272. ! mtbe017d.mec avg err 75.53%
	<=> CC.OHCQ	2.48E+19	-6.863	4568. ! mtbe017d.mec avg err 81.83%
	<=> YCOCICOH + OH	2.80E+19	-6.779	3678. ! mtbe017d.mec avg err
	<=> CCOHCHO + OH	4.64E+50	-15.756	30683. ! mtbe017d.mec avg err

C.COHCQ 12.03%	\Leftrightarrow C*COH + CH2OOH	2.44E+30	-6.260	37465. ! mtbe017d.mec avg err
C.COHCQ 15.06%	\Leftrightarrow C*CCQ + OH	2.30E+25	-4.469	31175. ! mtbe017d.mec avg err
C.COHCQ 14.25%	\Leftrightarrow OHCYCCOC + OH	7.90E+26	-4.487	32461. ! mtbe017d.mec avg err
C.COHCQ	\Leftrightarrow CC.OHCQ	7.42E+23	-4.364	19295. ! mtbe017d.mec avg err 18.15%
C.COHCQ 44.39%	\Leftrightarrow YCOCICOH + OH	9.97E+43	-10.426	24327. ! mtbe017d.mec avg err
CC.OHCQ 48.39%	\Leftrightarrow YCOCICOH + OH	1.44E+45	-10.380	32432. ! mtbe017d.mec avg err
CC*C + OH	\Leftrightarrow CC.COH	9.87E+26	-4.957	24388. ! mtbe017d.mec avg err 8.99%
CC*C + OH 19.54%	\Leftrightarrow C*CCOH + H	8.15E+45	-10.627	8794. ! mtbe017d.mec avg err
CC*C + OH	\Leftrightarrow CC*COH + H	2.40E+15	-9.13	13166. ! mtbe017d.mec avg err 2.20%
CC*C + OH	\Leftrightarrow CCCO.	7.05E+16	-1.465	9003. ! mtbe017d.mec avg err 5.91%
CC*C + OH 17.64%	\Leftrightarrow C2H5 + HCHO	9.27E+08	-4.23	14783. ! mtbe017d.mec avg err
CC*C + OH	\Leftrightarrow CCC*O + H	3.53E+08	1.064	16918. ! mtbe017d.mec avg err 1.35%
CC*C + OH	\Leftrightarrow CCC.OH	8.92E+04	1.995	16473. ! mtbe017d.mec avg err 1.38%
CC*C + OH	\Leftrightarrow C.CCOH	1.83E+38	-8.366	17897. ! mtbe017d.mec avg err 17.27%
CC*C + OH 13.15%	\Leftrightarrow C2H4 + CH2OH	7.72E+30	-5.889	21275. ! mtbe017d.mec avg err
CC.COH	\Leftrightarrow C*CCOH + H	3.50E+14	-3.14	20485. ! mtbe017d.mec avg err 16.36%
CC.COH	\Leftrightarrow CC*COH + H	6.71E+35	-8.050	42929. ! mtbe017d.mec avg err 21.12%
CC.COH	\Leftrightarrow CCCO.	5.29E+40	-9.559	39078. ! mtbe017d.mec avg err 18.77%
CC.COH	\Leftrightarrow C2H5 + HCHO	3.87E+26	-6.692	44207. ! mtbe017d.mec avg err 38.41%
CC.COH	\Leftrightarrow CCC*O + H	3.34E+26	-5.371	46266. ! mtbe017d.mec avg err 20.78%
CC.COH	\Leftrightarrow CCC.OH	5.18E+22	-4.403	45657. ! mtbe017d.mec avg err 21.22%
CC.COH	\Leftrightarrow C.CCOH	1.43E+55	-14.203	46908. ! mtbe017d.mec avg err 25.79%
CCCO.	\Leftrightarrow C2H5 + HCHO	1.19E+46	-11.363	50074. ! mtbe017d.mec avg err 26.70%
CCCO.	\Leftrightarrow CCC*O + H	5.33E+40	-9.622	17781. ! mtbe017d.mec avg err 9.83%
CCCO.	\Leftrightarrow CCC.OH	3.22E+40	-9.711	22835. ! mtbe017d.mec avg err 13.48%
CCCO.	\Leftrightarrow C*COH + CH3	1.18E+39	-11.298	15162. ! mtbe017d.mec avg err 19.42%
CCCO.	\Leftrightarrow CC*COH + H	1.67E+36	-10.045	27654. ! mtbe017d.mec avg err 30.37%
CCCO.	\Leftrightarrow C.CCOH	2.85E+42	-12.132	33555. ! mtbe017d.mec avg err 23.04%
CCCO.	\Leftrightarrow C2H4 + CH2OH	3.89E+36	-10.615	14400. ! mtbe017d.mec avg err 23.02%
CCC.OH 25.94%	\Leftrightarrow C*COH + CH3	3.85E+38	-10.808	29442. ! mtbe017d.mec avg err
CCC.OH	\Leftrightarrow CCC*O + H	6.32E+40	-9.095	38006. ! mtbe017d.mec avg err 17.83%
CCC.OH	\Leftrightarrow CC*COH + H	1.21E+41	-8.993	36744. ! mtbe017d.mec avg err 19.39%
CCC.OH	\Leftrightarrow C.CCOH	2.15E+40	-9.066	42009. ! mtbe017d.mec avg err 15.41%
C.CCOH 32.15%	\Leftrightarrow C2H4 + CH2OH	2.83E+40	-9.876	54645. ! mtbe017d.mec avg err
C.CCOH	\Leftrightarrow C*CCOH + H	1.71E+47	-11.209	35915. ! mtbe017d.mec avg err 45.78%
CC.COH + O2 24.72%	\Leftrightarrow CCQ.COH	4.39E+59	-15.421	47955. ! mtbe017d.mec avg err
CC.COH + O2 17.52%	\Leftrightarrow CC*COHB + HO2B	5.30E+44	-10.597	8232. ! mtbe017d.mec avg err
CC.COH + O2 13.56%	\Leftrightarrow C*CCOHB + HO2B	8.98E+23	-3.583	9058. ! mtbe017d.mec avg err
CC.COH + O2	\Leftrightarrow CCQCO.	1.07E+17	-1.635	9957. ! mtbe017d.mec avg err 8.16%
CC.COH + O2 12.85%	\Leftrightarrow CC.Q + HCHO	2.06E+34	-8.092	9128. ! mtbe017d.mec avg err

CC.COH + O2 13.30%	<=> CCQC.OH	1.01E+29 -5.439 11391. ! mtbe017d.mec avg err
CC.COH + O2 12.29%	<=> CC*COH + HO2	1.50E+44 -10.243 11864. ! mtbe017d.mec avg err
CC.COH + O2 16.15%	<=> C.CQCOH	3.39E+33 -6.279 14042. ! mtbe017d.mec avg err
CC.COH + O2 16.04%	<=> C*CCOH + HO2	8.48E+35 -8.039 10741. ! mtbe017d.mec avg err
CC.COH + O2 15.38%	<=> C*CQ + CH2OH	2.93E+29 -5.222 13392. ! mtbe017d.mec avg err
CC.COH + O2	<=> CC.QCOH	1.92E+13 -.756 17747. ! mtbe017d.mec avg err 4.63%
CC.COH + O2 2.18%	<=> CC*OCOH + OH	1.47E+10 -.680 13564. ! mtbe017d.mec avg err
CCQ.COH 3.83%	<=> CC*COHB + HO2B	2.76E+12 -.348 14110. ! mtbe017d.mec avg err
CCQ.COH 16.01%	<=> C*CCOHB + HO2B	2.80E+42 -9.594 35727. ! mtbe017d.mec avg err
CCQ.COH	<=> CCQCO.	6.36E+39 -8.951 40988. ! mtbe017d.mec avg err 19.67%
CCQ.COH 24.42%	<=> CC.Q + HCHO	1.31E+52 -13.481 35098. ! mtbe017d.mec avg err
CCQ.COH	<=> CCQC.OH	1.58E+53 -12.997 42526. ! mtbe017d.mec avg err 14.16%
CCQ.COH 30.23%	<=> CC*COH + HO2	1.65E+51 -12.481 32321. ! mtbe017d.mec avg err
CCQ.COH	<=> C.CQCOH	2.53E+53 -12.605 43281. ! mtbe017d.mec avg err 21.93%
CCQ.COH 13.08%	<=> C*CCOH + HO2	1.68E+55 -13.916 39680. ! mtbe017d.mec avg err
CCQ.COH 22.43%	<=> C*CQ + CH2OH	5.53E+52 -12.572 44482. ! mtbe017d.mec avg err
CCQ.COH	<=> CC.QCOH	5.92E+30 -6.584 49173. ! mtbe017d.mec avg err 30.60%
CCQ.COH 24.08%	<=> CC*OCOH + OH	3.62E+29 -7.044 45193. ! mtbe017d.mec avg err
CCQCO.	<=> CC.Q + HCHO	5.61E+31 -6.701 45672. ! mtbe017d.mec avg err 29.24%
CCQCO.	<=> CCQC.OH	1.59E+25 -4.595 13737. ! mtbe017d.mec avg err 14.91%
CCQCO. 44.03%	<=> CC*COH + HO2	1.79E+56 -14.717 23771. ! mtbe017d.mec avg err
CCQCO.	<=> C.CQCOH	4.79E+48 -11.991 28062. ! mtbe017d.mec avg err 26.00%
CCQCO. 24.84%	<=> C*CCOH + HO2	4.01E+53 -14.264 25951. ! mtbe017d.mec avg err
CCQCO. 20.13%	<=> C*CQ + CH2OH	4.45E+46 -11.553 28502. ! mtbe017d.mec avg err
CCQCO.	<=> CC.QCOH	1.10E+22 -4.719 31585. ! mtbe017d.mec avg err 6.78%
CCQCO. 2.45%	<=> CC*OCOH + OH	6.05E+20 -5.177 27703. ! mtbe017d.mec avg err
CCQC.OH 6.38%	<=> CC.Q + HCHO	8.40E+22 -4.815 28178. ! mtbe017d.mec avg err
CCQC.OH 13.09%	<=> CC*COH + HO2	8.41E+51 -12.792 37704. ! mtbe017d.mec avg err
CCQC.OH	<=> C.CQCOH	1.51E+31 -6.146 25501. ! mtbe017d.mec avg err 5.35%
CCQC.OH 17.02%	<=> C*CCOH + HO2	2.70E+55 -14.166 35936. ! mtbe017d.mec avg err
CCQC.OH 18.29%	<=> C*CQ + CH2OH	1.84E+52 -12.595 39851. ! mtbe017d.mec avg err
CCQC.OH	<=> CC.QCOH	5.81E+28 -6.189 42500. ! mtbe017d.mec avg err 23.96%

CCQC.OH 16.83%	\Leftrightarrow CC*OCOH + OH	5.03E+27 -6.685 38825. ! mtbe017d.mec avg err	
C.CQCOH 21.76%	\Leftrightarrow CC.Q + HCHO	8.34E+29 -6.350 39315. ! mtbe017d.mec avg err	
C.CQCOH 17.63%	\Leftrightarrow CC*COH + HO2	1.32E+44 -10.919 30945. ! mtbe017d.mec avg err	
C.CQCOH 19.66%	\Leftrightarrow C*CCOH + HO2	6.35E+46 -11.229 32912. ! mtbe017d.mec avg err	
C.CQCOH 20.92%	\Leftrightarrow C*CQ + CH2OH	2.64E+30 -6.150 18383. ! mtbe017d.mec avg err	
C.CQCOH C.CQCOH 97.54%	\Leftrightarrow CC.QCOH	7.67E+16 -2.315 29967. ! mtbe017d.mec avg err	22.02%
	\Leftrightarrow CC*OCOH + OH	5.47E-19 5.742 -1293. ! mtbe017d.mec avg err	
CC.QCOH 100.24%	\Leftrightarrow CC.Q + HCHO	2.91E-18 6.537 -1073. ! mtbe017d.mec avg err	
CC.QCOH 76.89%	\Leftrightarrow CC*COH + HO2	1.03E-04 2.211 17690. ! mtbe017d.mec avg err	
CC.QCOH 30.36%	\Leftrightarrow C*CCOH + HO2	3.45E-23 8.257 13151. ! mtbe017d.mec avg err	
CC.QCOH 52.77%	\Leftrightarrow C*CQ + CH2OH	7.44E+46 -12.367 30557. ! mtbe017d.mec avg err	
CC.QCOH .87%	\Leftrightarrow CC*OCOH + OH	2.30E-05 3.094 42001. ! mtbe017d.mec avg err	
YCOCICQ 1.83%	\Leftrightarrow CCYC.OC + HO2	2.41E+09 -.098 -482. ! mtbe017d.mec avg err	
YCOCICOH 63.10%	\Leftrightarrow CCYC.OC + OH	5.98E+43 -8.499 82399. ! mtbe017d.mec avg err	
CC.C*O + HO2 53.01%	\Leftrightarrow CCQCHO	2.53E+33 -5.179 102022. ! mtbe017d.mec avg err	
CC.C*O + HO2 19.20%	\Leftrightarrow CHO + CC.Q	2.17E+43 -10.080 7311. ! mtbe017d.mec avg err	
CC.C*O + HO2 9.49%	\Leftrightarrow CCQC.*O + H	1.66E+02 3.302 15057. ! mtbe017d.mec avg err	
CC.C*O + HO2 93.22%	\Leftrightarrow CCO.C*O + OH	8.18E+00 3.294 26639. ! mtbe017d.mec avg err	
CCQCHO 21.19%	\Leftrightarrow CHO + CC.Q	2.38E+18 -1.480 4596. ! mtbe017d.mec avg err	6.90%
CCQCHO 21.18%	\Leftrightarrow CCQC.*O + H	1.01E+40 -8.249 81687. ! mtbe017d.mec avg err	
CCQCHO 21.18%	\Leftrightarrow CCO.C*O + OH	3.40E+34 -7.180 91354. ! mtbe017d.mec avg err	
CC.C*O + OH 35.68%	\Leftrightarrow CCOHCHO	8.19E+45 -9.881 52692. ! mtbe017d.mec avg err	
CC.C*O + OH 56.35%	\Leftrightarrow CHO + CC.OH	6.28E+42 -9.304 9517. ! mtbe017d.mec avg err	
CC.C*O + OH 46.76%	\Leftrightarrow CCOHC.*O + H	1.61E+12 .587 6765. ! mtbe017d.mec avg err	
CCOHCHO 37.11%	\Leftrightarrow CHO + CC.OH	8.55E+06 1.488 9994. ! mtbe017d.mec avg err	
CCOHCHO 54.54%	\Leftrightarrow CCOHC.*O + H	6.26E+38 -7.084 84212. ! mtbe017d.mec avg err	
CCOHC.*O 50.94%	\Leftrightarrow CC.OH + CO	2.67E+46 -9.993 98371. ! mtbe017d.mec avg err	
CCQC.*O	\Leftrightarrow CC.Q + CO	4.50E+21 -3.762 9473. ! mtbe017d.mec avg err	25.66%

CC*OCQ	<=> CC*OCO. + OH	2.39E-21	-3.602	10018.	! mtbe017d.mec avg err
23.25%					
CC*OCO.	<=> CC*OC*O + H	2.61E-47	-10.310	53941.	! mtbe017d.mec avg err
38.00%					
CC*OCO.	<=> CH3C.*O + HCHO	1.51E+10	-.488	19749.	! mtbe017d.mec avg err
12.06%					
C*CC.*O	<=> CO + C2H3	2.58E+16	-2.300	5113.	! mtbe017d.mec avg err 22.87%
END					

APPENDIX IIB
TRANSITION STATES IN THE MTBE SYSTEM

TS IIB. 1 Thermodynamic Properties from MOPAC PM3

SPECIES	H _{f,298} ^a	S ₂₉₈ ^b	C _p ^b 300	400	500	600	800	1000	1500	DATE		ELEMENTS				
HO2	3.5	54.73	8.37	8.95	9.48	9.96	10.78	11.43	12.47	JANAF	H	1 O	2	0	0	G 0
C3CQ.	-23.58	83.36	29.46	36.78	43.1	48.24	55.85	61.25	69.59	3/5/97 CHEN	C	4 H	9 O	2	0	G 4
C3.CQ	-10.68	92.19	31.31	38.68	44.91	49.9	57.1	62.04	69.54	3/5/97 CHEN	C	4 H	9 O	2	0	G 5
C2C*C	-3.8	71.01	20.4	25.42	30.16	34.27	40.89	45.92	53.96	3/5/97 CHEN	C	4 H	8	0	0	G 2
C2C.CQ	-9.29	97.76	29.21	35.75	41.77	46.86	54.58	60.07	68.48	3/5/97 CHEN	C	4 H	9 O	2	0	G 5
C2CCQ.	-17.59	89.44	28.69	36.06	42.43	47.59	55.3	60.85	69.41	3/5/97 CHEN	C	4 H	9 O	2	0	G 4
C2.CCQ	-4.69	96.38	31.24	38.51	44.72	49.68	56.86	61.85	69.47	3/5/97 CHEN	C	4 H	9 O	2	0	G 5
C*ClCCQ.	11.72	89.74	26.09	31.72	36.75	41	47.61	52.49	60.03	3/5/97 CHEN	C	4 H	7 O	2	0	G 3
C*ClCC.Q	9.12	90.11	29.59	35.34	40.24	44.25	50.26	54.53	61.08	3/5/97 CHEN	C	4 H	7 O	2	0	G 4
C*ClC.CQ	11.72	91.2	28.79	35.05	40.28	44.47	50.58	54.83	61.27	3/5/97 CHEN	C	4 H	7 O	2	0	G 4
C2.CYCOOC	27.81	83.74	25.49	32.34	38.12	42.75	49.53	54.29	61.51	3/5/97 CHEN	C	4 H	7 O	2	0	G 2
CCYC.COOC	9.84	81.75	25.27	32.01	37.8	42.51	49.59	54.63	62.22	3/5/97 CHEN	C	4 H	7 O	2	0	G 1
C2COHCQ.	-60.19	96.02	32.85	40.56	47.2	52.53	60.33	65.8	74.22	3/5/97 CHEN	C	4 H	9 O	3	0	G 5
C2CO.CQ	-44.33	96.6	33.58	41.37	47.9	53.09	60.55	62.65	73.37	3/5/97 CHEN	C	4 H	9 O	3	0	G 5
C2CQ.CO	-59.38	96.14	33.23	40.71	47.14	52.34	60.06	65.55	74.06	3/5/97 CHEN	C	4 H	9 O	3	0	G 5
C2CQCO.	-43.52	95.17	34.49	42.65	49.6	55.14	62.98	68.18	75.8	3/5/97 CHEN	C	4 H	9 O	3	0	G 5
C2.COHCQ	-47.29	100.36	34.66	42.21	48.5	53.47	60.69	65.74	73.58	3/5/97 CHEN	C	4 H	9 O	3	0	G 6
C2.CQCOH	-46.48	103.99	35.12	42.76	49.13	54.19	61.48	66.47	74.1	3/5/97 CHEN	C	4 H	9 O	3	0	G 6
C2CQC.OH	-53.58	100.1	35.47	42.78	49.03	54.07	61.39	66.4	74.06	3/5/97 CHEN	C	4 H	9 O	3	0	G 6
C2CQ.CQ	-47.67	102.62	37.48	46.11	53.21	58.78	66.65	71.99	80	3/5/97 CHEN	C	4 H	9 O	4	0	G 6
C2.CQCQ	-31.87	110.04	39.69	48.06	54.91	60.23	67.67	72.58	79.82	3/5/97 CHEN	C	4 H	9 O	4	0	G 7
C2CQCQ.	-44.77	102.68	37.34	46.06	53.34	59.06	67.13	72.5	80.39	3/5/97 CHEN	C	4 H	9 O	4	0	G 6
C2CQC.Q	-36.97	106.93	39.56	47.96	54.96	60.47	68.14	73.07	80.21	3/5/97 CHEN	C	4 H	9 O	4	0	G 7
TC2YCQC	29.53	82.05	28.92	36.75	43.38	48.7	56.48	61.9	70.09	3/5/97 CHEN	C	4 H	9 O	2	0	G 2
TC2YCXQC*	30.39	84.54	29.77	37.14	43.47	48.64	56.32	61.75	70.01	3/5/97 CHEN	C	4 H	9 O	2	0	G 2
TC3*CXQ	20.52	90.91	29.9	36.85	42.79	47.62	54.79	59.88	67.82	3/5/97 CHEN	C	4 H	9 O	2	0	G 4
TC2YC2OXP	11.1	86.99	29.19	36.43	42.6	47.53	54.8	59.99	68.19	3/5/97 CHEN	C	4 H	9 O	2	0	G 3
TC2CJ*CXQ	15.53	91.28	29.1	36.11	42.18	47.12	54.47	59.68	67.74	3/5/97 CHEN	C	4 H	9 O	2	0	G 4
TC2YCCOXP	4.45	87.97	29.11	36.18	42.32	47.29	54.67	59.95	68.24	3/5/97 CHEN	C	4 H	9 O	2	0	G 3
TC2YCCQ	25.61	83.17	28.67	36.47	43.18	48.58	56.49	61.98	70.21	3/5/97 CHEN	C	4 H	9 O	2	0	G 2

Table IIB. 1 Thermodynamic Properties from MOPAC PM3 (Cont')

SPECIES	H _{1,298} ^a	S ₂₉₈ ^b	C _p ^b 300	400	500	600	800	1000	1500	DATE		ELEMENTS					
TC2YC*CXQ	32.54	82.61	27.82	35.05	41.42	46.73	54.8	60.59	69.39	3/5/97 CHEN	C	4 H	9 O	2 O	G	2	
TCYCCQC	21.11	80.34	27.09	35.27	42.3	47.97	56.31	62.12	70.77	3/5/97 CHEN	C	4 H	9 O	2 O	G	1	
TC2*CYCQ	55.09	86.82	26.65	32.85	38.08	42.34	48.72	53.28	60.16	3/5/97 CHEN	C	4 H	7 O	2 O	G	2	
TC*YCCQC	47.97	79.76	25.33	32.43	38.31	43.02	49.94	54.76	61.92	3/5/97 CHEN	C	4 H	7 O	2 O	G	0	
TC2*YCOOC	51.07	82.17	25.24	31.31	36.61	41.01	47.73	52.61	60.12	3/5/97 CHEN	C	4 H	7 O	2 O	G	1	
TCYC*COOC	50.37	79.36	24.59	30.89	36.34	40.84	47.67	52.6	60.15	3/5/97 CHEN	C	4 H	7 O	2 O	G	1	
TC*YC3OXP	37.45	84.33	25.52	32.02	37.4	41.71	48.12	52.74	59.96	3/5/97 CHEN	C	4 H	7 O	2 O	G	1	
TC2YCCQO	-15.29	84.3	30.26	38.86	46.23	52.17	60.82	66.77	75.57	3/5/97 RU	C	4 H	9 O	3 O	G	2	
TICPYCCQC	-19.64	85.37	30.94	39.46	46.65	52.39	60.75	66.53	75.23	3/5/97 RU	C	4 H	9 O	3 O	G	2	
TC2YCQOC	-15.13	84.71	30.51	39.07	46.39	52.29	60.9	66.83	75.61	3/5/97 CHEN	C	4 H	9 O	3 O	G	2	
TICCPYCQC	-8.76	91.89	32.04	40.16	46.96	52.41	60.4	66	74.47	3/5/97 CHEN	C	4 H	9 O	3 O	G	3	
TC2YCQCIP	-12.27	89.51	32.7	40.83	47.69	53.15	61.06	66.52	74.75	3/5/97 CHEN	C	4 H	9 O	3 O	G	3	
TICCCQYCQC	7.89	101	37.38	46.46	53.93	59.75	67.84	73.15	80.85	3/5/97 CHEN	C	4 H	9 O	4 O	G	4	
TC2YCQOOC	5.87	86.09	30.51	39.07	46.39	52.29	60.9	66.83	75.61	3/5/97 CHEN	C	4 H	9 O	4 O	G	2	
TC2YCQCICQ	4.95	98.22	37.71	46.64	54.04	59.84	67.94	73.23	80.89	3/5/97 CHEN	C	4 H	9 O	4 O	G	4	
TICQYCCQC	0.66	95.34	36.07	45.32	53.02	59.09	67.68	73.35	81.46	3/5/97 CHEN	C	4 H	9 O	4 O	G	3	
C2COHC.Q	-52.39	103.01	35.65	42.94	49.05	53.92	61.03	65.99	73.74	3/5/97 RU	C	4 H	9 O	3 O	G	6	
TC2CPYCQ	-13.31	92.02	33.7	41.48	48	53.16	60.66	65.89	73.91	3/5/97 RU	C	4 H	9 O	3 O	G	4	
TICCCQYCPC	-9.9	92.5	33.73	42.11	49.09	54.59	62.33	67.47	74.99	3/5/97 RU	C	4 H	9 O	3 O	G	4	
TC2YCPCICQ	-16.13	88.69	33.14	41.26	48.17	53.68	61.59	66.93	74.72	3/5/97 RU	C	4 H	9 O	3 O	G	4	
TICPYC3OXP	-33.53	90.95	32.03	39.64	46.08	51.27	58.96	64.48	73.21	3/5/97 RU	C	4 H	9 O	3 O	G	3	
C3COC	-68.9	85.64	32.85	41.42	48.89	55.01	64.39	71.31	82.33	3/5/97 RU	C	5 H	12 O	1 O	G	5	
CH3OH	-48	57.26	10.8	12.63	14.59	16.33	19.17	21.38	25.04	3/5/97 RU	C	1 H	4 O	1 O	G	1	
TMTBE	-1.3	86.37	33	41.72	49.23	55.41	64.9	71.86	82.77	3/29/97 RU	C	5 H	12 O	1 O	G	2	
TMEOH	45.06	54.87	10.62	12.89	15.05	16.94	19.96	22.18	25.49	3/29/97 RU	C	1 H	4 O	1 O	G	0	
C3C.	11.9	75.1	22.54	27.44	32.28	36.61	43.65	49.08	57.83	3/5/96 CHEN	C	4 H	9	0	O	G	3
TC2CJ*CXII	49.15	74.35	22.87	28.38	33.35	37.63	44.46	49.61	57.79	3/5/96 CHEN	C	4 H	9	0	O	G	2
C2CY2CO	-24.81	72.63	22.98	29.75	35.67	40.5	47.68	52.78	60.58	3/5/96 CHEN	C	4 H	9 O	1 O	G	2	
TCYCOOH	39.3	71.46	18.1	22.3	25.83	27.73	31.32	34.52	39.29	3/30/96 BOZZ	C	2 H	5 O	2 O	G	1	
TYCCOOH	29.6	70.94	17.44	21.97	25.84	28.96	33.54	36.72	41.41	3/30/96 BOZZ	C	2 H	5 O	2 O	G	0	

Table II.B. 1 Thermodynamic Properties from MOPAC PM3 (Cont')

SPECIES	H_f^{298} ^a	S_{298} ^b	C_p ^b	300	400	500	600	800	1000	1500	DATE	ELEMENTS
TCYCOCXOH	32	73.59		17.72	21.69	25.06	27.78	31.82	34.77	39.48	3/30/96 BOZZ	C 2 H 5 O 2 O G 1
TCQJCQ	1.2	87.57		25.81	31.07	35.48	38.98	43.93	47.19	51.71	3/30/96 BOZZ	C 2 H 5 O 4 O G 2
TIPRXOOH	19	83.21		24.53	29.11	33.24	36.75	42.32	46.51	53.31	3/30/96 BOZZ	C 3 H 7 O 2 O G 2
TIPROXOH	18	78.11		23.31	28.69	33.04	36.97	42.82	46.83	53.51	3/30/96 BOZZ	C 3 H 7 O 2 O G 2
TIPRYQE	18.2	76.86		23.63	29.2	34.02	38.01	44.13	48.55	55.28	3/30/96 BOZZ	C 3 H 7 O 2 O G 1
TIPROOXH	18.2	75.82		23.09	29.03	34.09	38.23	44.4	48.81	55	3/30/96 BOZZ	C 3 H 7 O 2 O G 1
TC*YCOOJ	54.89	67.46		15.06	18.16	20.74	22.8	25.84	28	31.26	3/30/96 BOZZ	C 2 H 3 O 2 O G 0
TYC*COOH	62.23	67.67		15.09	18.64	21.4	23.7	26.85	28.95	31.93	3/30/96 BOZZ	C 2 H 3 O 2 O G 0
TYVVOOH	68	69.4		16.1	19.22	21.71	23.71	26.66	28.71	31.73	3/30/96 BOZZ	C 2 H 3 O 2 O G 0
TC*CXO2	71.6	76.1		16.33	18.7	20.68	22.31	24.92	26.91	30.13	3/30/96 BOZZ	C 2 H 3 O 2 O G 0
TYVVOOHS	66.3	67.96		15.75	19.21	22.09	24.24	27.26	29.26	31.1	3/30/96 BOZZ	C 2 H 3 O 2 O G 0
TC*COXO	62.72	68.4		15.81	18.64	21.01	22.94	25.86	28.82	31.23	3/30/96 BOZZ	C 2 H 3 O 2 O G 0
H	52.1	27.3		4.9	4.9	4.9	4.9	4.9	4.9	4.9		H 1 0 0 O G 0

^a Unit in kcal-mol⁻¹.^b Unit in cal-mol⁻¹-K⁻¹.

TS IIB. 2 TS Information for MTBE \rightarrow C2C=C + CH₃OH

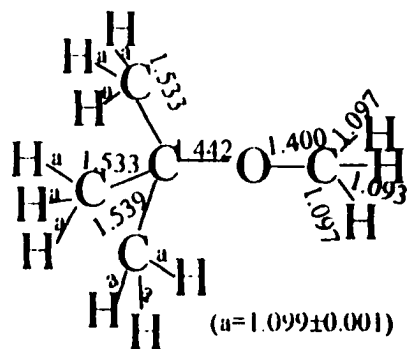
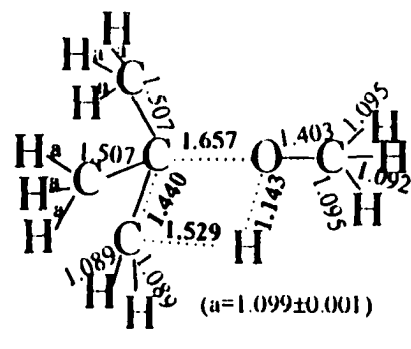
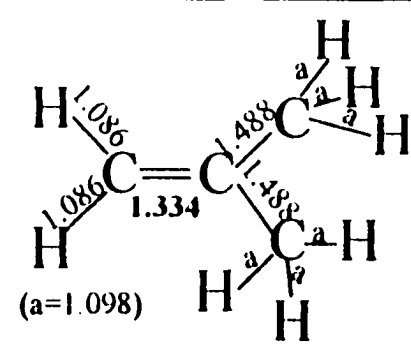
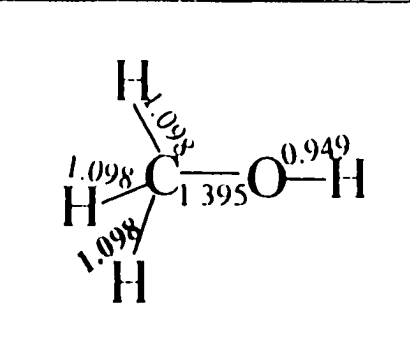
Reactant	Transition State	Product 1	Product 2
 <p>($a=1.099\pm0.001$)</p>	 <p>($a=1.099\pm0.001$)</p>	 <p>($a=1.098$)</p>	
C3COC (MTBE)	TSMTBE	C2C=C	CH ₃ OH
Principle moments of inertia in unit of cm ⁻¹ : A = 0.145357 B = 0.091250 C = 0.090246 in unit of 10 ⁻⁴⁰ -gram-cm ² : A = 192.578843 B = 306.770121 C = 310.182958	Principle moments of inertia in unit of cm ⁻¹ : A = 0.139810 B = 0.087818 C = 0.085587 in unit of 10 ⁻⁴⁰ -gram-cm ² : A = 200.219214 B = 318.758215 C = 327.067124	Principle moments of inertia in unit of cm ⁻¹ : A = 0.312646 B = 0.278927 C = 0.156031 in unit of 10 ⁻⁴⁰ -gram-cm ² : A = 89.534710 B = 100.358468 C = 179.404128	Principle moments of inertia in unit of cm ⁻¹ : A = 4.244786 B = 0.856787 C = 0.825179 in unit of 10 ⁻⁴⁰ -gram-cm ² : A = 6.594594 B = 32.671649 C = 33.923121
Symmetry = 243	Symmetry = 9	Symmetry = 18	Symmetry = 3
Internal rotor(s): V / kcal-mol⁻¹ CH ₃ -C(C2)OH (3): 4.01 C3C-OCH ₃ (1): 3.0 C3CO-CH ₃ (1): 2.0	Internal rotor(s): V / kcal-mol⁻¹ CH ₃ -C(C2)OH (2): 4.01 TC2yCCHO-CH ₃ (1): 2.0	Internal rotor(s): V / kcal-mol⁻¹ CH ₃ -C ₂ H ₃ (C) (2): 1.26	Internal rotor(s): V / kcal-mol⁻¹ CH ₃ -OH (1): 1.09
-147.13 -50.78 132.26 166.25	-1507.06 9.81 85.42 131.81	-116 108 393 423 471 618 932	292.33 988 92 1020.76 1164.45

Table II.B. 2 TS Information for MTBE \rightarrow C2C=C + CH3OH (Cont')

Reactant	Transition State	Product 1	Product 2
174.70 263.64 354.18 384.01	156.12 232.38 289.03 371.28	937.943 985.993 1024.1069	1362.29 1366.05 1366.27
433.99 494.67 570.33	421.06 476.74 506.60 554.17	1312.1323 1382.1390 1397	1409.05 3035.71 3068.61
847.04767 907.40 947.78	595.25 863.31 934.90 939.70	1398.1399 1477.1873 3073	3141.15 3896.48
962.81 976.05 1008.28 1014.88	955.48 974.38 981.57 987.02	3074.3074 3077.3147 3148	
1016.87 1093.17 1165.37	1014.80 1031.24 1063.34	3173.3175	
1277.79 1286.42 1314.16	1131.33 1311.38 1339.61		
1351.20 1359.77 1386.62	1354.05 1356.95 1371.65		
1389.60 1397.88 1402.98	1389.81 1394.12 1397.56		
1403.73 1404.08 1407.60	1401.17 1411.34 1429.60		
1411.79 1416.78 1432.75	1580.09 1849.90 3053.94		
3031.90 3068.05 3073.63	3076.06 3078.28 3080.10		
3078.69 3078.96 3081.08	3082.51 3083.73 3124.29		
3088.68 3089.85 3145.91	3134.41 3138.72 3174.58		
3180.09 3181.10 3184.05	3175.50		

TS IIB. 3 Information for C2C=C Related Transition States

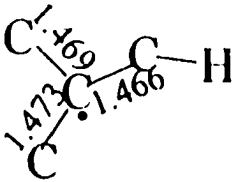
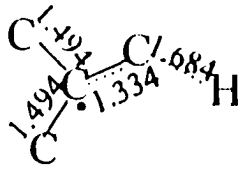
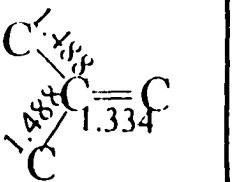
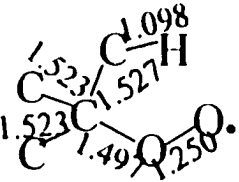
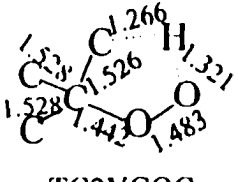
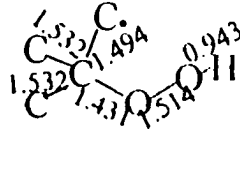
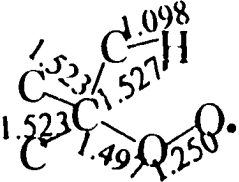
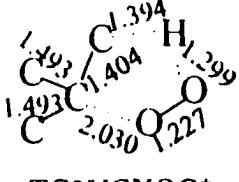
Number	Thermodynamic Properties Information	Reactant	Transition State*	Product
TS 1	<p>Rx C3C. = TC2CJ*CXH S {cal/mol K} 75.100 74.350 for A(T) = Aprime * T^n Aprime = 6.1488E+09 n = 1.33029</p> <p>Rx C3C. = C2C*C + H Hf {Kcal/mol} 11.900 -3.800 52.100 S {cal/mol K} 75.100 71.010 27.300 dU (dE) {kcal/mol} (") = 35.81 dUr avg (298., 1500. K) = 35.82 Fit A/Ar: A = 3.065E-02 n = .75 alpha = 8.028E-04</p>		 TC2J*CXH	
TS 2	<p>Rx C3CQ. = TC2YCQC S {cal/mol K} 83.360 82.050 for A(T) = Aprime * T^n Aprime = 7.5198E+09 n = 1.22128</p> <p>Rx C3CQ. = C3.CQ Hf {Kcal/mol} -23.580 -10.680 S {cal/mol K} 83.360 92.190 dU (dE) {kcal/mol} (") = 12.90 dUr avg (298., 1500. K) = 13.50 Fit A/Ar: A = 6.146E-02 n = 1.31 alpha = 8.741E-04</p>		 TC2YCQC	
TS 3	<p>Rx C3CQ. = TC2YCXQC* S {cal/mol K} 83.360 84.540</p> <p>for A(T) = Aprime * T^n Aprime = 2.8762E+10 n = 1.21961</p> <p>Rx C3CQ. = C2C*C + HO2 Hf {Kcal/mol} -23.580 -3.800 3.500 S {cal/mol K} 83.360 71.010 54.730 dHr {kcal/mol} (298K) = 23.28</p>		 TC2YCXQC*	

Table IIB. 3 Information for C2C=C Related Transition States (Cont')

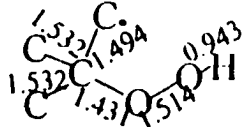
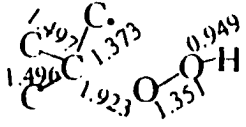
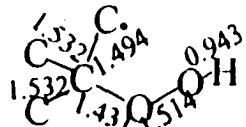

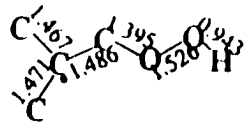
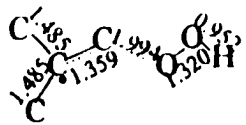
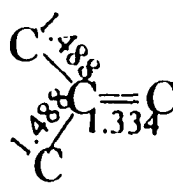
Number	Thermodynamic Properties Information	Reactant	Transition State*	Product
	dHr avg (298., 1500. K) = 21.17 dU (dE) {kcal/mol} (") = 22.69 dUr avg (298., 1500. K) = 19.38 Fit Af/Ar: A = 8.789E+10 n = -2.59 alpha = 1.937E-04			
TS 4	Rx C3.CQ = TC3*CXQ S {cal/mol K} 92.190 90.910 for A(T) = Aprime * T^n Aprime = 1.0628E+13 n = -.02701 Rx C3.CQ = C2C*C + HO2 Hf {Kcal/mol} -10.680 -3.800 3.500 S {cal/mol K} 92.190 71.010 54.730 dHr {kcal/mol} (298K) = 10.38 dHr avg (298., 1500. K) = 7.67 dU (dE) {kcal/mol} (") = 9.79 dUr avg (298., 1500. K) = 5.88 Fit Af/Ar: A = 1.430E+12 n = -3.90 alpha = -6.804E-04		 TC3*CXQ	
TS 5	Rx C3.CQ = TC2YC2OXP S {cal/mol K} 92.190 86.990 for A(T) = Aprime * T^n Aprime = 1.3840E+12 n = -.03057		 TC2YC2OXP	
TS 6	Rx C2C*C + HO2 = TC2CJ*CXQ S {cal/mol K} 71.010 54.730 91.280 for A(T) = Aprime * T^n Aprime = 6.3904E+02 n = 3.10237 Rx C2C*C + HO2 = C2C.CQ		 TC2CJ*CXQ	

Table IIB. 3 Information for C2C=C Related Transition States (Cont')

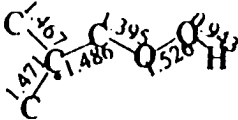
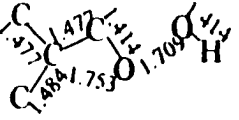
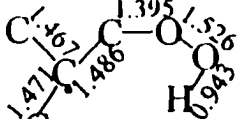
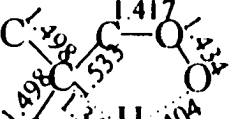
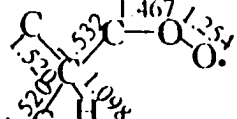
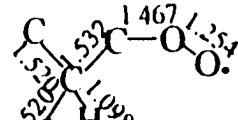
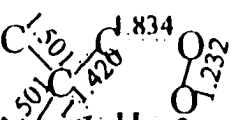
Number	Thermodynamic Properties Information	Reactant	Transition State*	Product
	Hf {Kcal/mol} -3.800 3.500 -9.290 S {cal/mol K} 71.010 54.730 97.760 dHr {kcal/mol} (298K) = -8.99 dHr avg (298., 1500. K) = -7.58 dU (dE) {kcal/mol} (") = -8.40 dUr avg (298., 1500. K) = -5.79 Fit Af/Ar: A = 4.161E-07 n = 2.03 alpha = -1.597E-04			
TS 7	Rx C2C.CQ = TC2YCCOXP S {cal/mol K} 97.760 87.970 for A(T) = Aprime * T^n Aprime = 2.9956E+08 n = 1.06135		 TC2YCCOXP	
TS 8	Rx C2C.CQ = TC2YCCQ S {cal/mol K} 97.760 83.170 for A(T) = Aprime * T^n Aprime = 3.3144E+05 n = 1.79209 Rx C2C.CQ = C2CCQ. Hf {Kcal/mol} -9.290 -17.590 S {cal/mol K} 97.760 89.440 dU (dE) {kcal/mol} (") = -8.30 dUr avg (298., 1500. K) = -7.89 Fit Af/Ar: A = 7.503E-03 n = 10 alpha = -2.761E-04		 TC2YCCQ	
TS 9	Rx C2CCQ. = TC2YC*CXQ S {cal/mol K} 89.440 82.610 for A(T) = Aprime * T^n Aprime = 7.4672E+09 n = .73486 Rx C2CCQ. = C2C*C + HO2 Hf {Kcal/mol} -17.590 -3.800 3.500 S {cal/mol K} 89.440 71.010 54.730		 TC2YC*CXQ	

Table IIB. 3 Information for C2C=C Related Transition States (Cont')

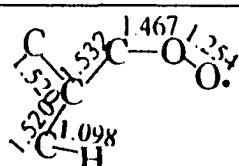
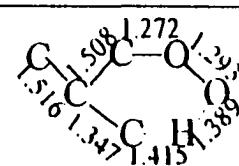
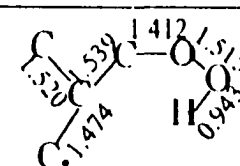
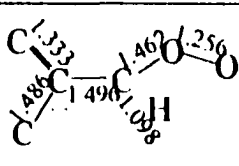
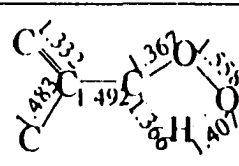
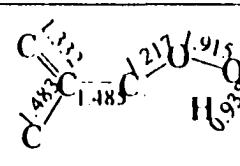
Number	Thermodynamic Properties Information	Reactant	Transition State	Product
	dHr {kcal/mol} (298K) = 17.29 dHr avg (298., 1500. K) = 15.46 dU (dE) {kcal/mol} (") = 16.70 dUr avg (298., 1500. K) = 13.68 Fit A/Ar: A = 3.203E+08 n = -2.13 alpha = 4.358E-04			
TS 10	Rx C2CCQ. = TCYCCQC S {cal/mol K} 89.440 80.340 for A(T) = Aprime * T^n Aprime = 7.2022E+07 n = 1.31680 Rx C2CCQ. = C2.CCQ Hf {Kcal/mol} -17.590 -4.690 S {cal/mol K} 89.440 96.380 dU (dE) {kcal/mol} (") = 12.90 dUr avg (298., 1500. K) = 13.69 Fit A/Ar: A = 3.707E-03 n = 1.65 alpha = 1.074E-03		 TCYCCQC	
TS 11	Rx C*ClCCQ. = TC2*CYCQ S {cal/mol K} 89.740 86.820 for A(T) = Aprime * T^n Aprime = 1.0112E+09 n = 1.45505 Rx C*ClCCQ. = C*ClCC.Q Hf {Kcal/mol} 11.720 9.120 S {cal/mol K} 89.740 90.110 dU (dE) {kcal/mol} (") = -2.60 dUr avg (298., 1500. K) = -1.03 Fit A/Ar: A = 3.062E-06 n = 2.31 alpha = 1.095E-03	 C=C(C)COO	 TC2*CYCQ	 C=C(C)C.OOH

Table II.B. 3 Information for C2C=C Related Transition States (Cont')

Number	Thermodynamic Properties Information	Reactant	Transition State	Product
TS 12	Rx $C^*CICCCQ = TC^*YCCQC$ S {cal/mol K} 89.740 79.760 for $A(T) = A_{prime} * T^n$ $A_{prime} = 1.2748E+06$ $n = 1.95375$ Rx $C^*CICCCQ = C^*CIC.CQ$ Hf {Kcal/mol} 11.720 11.720 S {cal/mol K} 89.740 91.200 dU (dE) {kcal/mol} (") = .00 dUr avg (298., 1500. K) = 1.54 Fit A/Ar: A = 1.037E-05 n = 2.18 alpha = 9.729E-04		 TC*YCCQC	
TS 13	Rx $C^*CICCCQ = TC2^*YCOOC$ S {cal/mol K} 89.740 82.170 for $A(T) = A_{prime} * T^n$ $A_{prime} = 1.2216E+09$ $n = .98999$ Rx $C^*CICCCQ = C2.CYCOOC$ Hf {Kcal/mol} 11.720 27.810 S {cal/mol K} 89.740 83.740 dU (dE) {kcal/mol} (") = 16.09 dUr avg (298., 1500. K) = 17.02 Fit A/Ar: A = 2.393E-03 n = .49 alpha = -3.097E-04		 TC2*TCOOC	
TS 14	Rx $C^*CICCCQ = TCYC^*COOC$ S {cal/mol K} 89.740 79.360 for $A(T) = A_{prime} * T^n$ $A_{prime} = 4.0903E+08$ $n = .92337$ Rx $C^*CICCCQ = CCYC.COOC$ Hf {Kcal/mol} 11.720 9.840 S {cal/mol K} 89.740 81.750 dU (dE) {kcal/mol} (") = -1.88 dUr avg (298., 1500. K) = -.86 Fit A/Ar: A = 5.813E-03 n = .14 alpha = -7.725E-04		 TCYC*COOC	

Table IIB. 3 Information for C2C=C Related Transition States (Cont')

Number	Thermodynamic Properties Information	Reactant	Transition State	Product
TS 15	Rx $C^*CIC.CQ = TC^*YC3OXP$ S {cal/mol K} 91.200 84.330 for $A(T) = A_{prime} * T^n$ $A_{prime} = 1.2156E+12$ $n = -.17298$		 TC*YC3OXP	
TS 16	Rx $C2COHCQ. = TC2YCCQO$ S {cal/mol K} 96.020 84.300 for $A(T) = A_{prime} * T^n$ $A_{prime} = 7.5594E+07$ $n = 1.06165$ Rx $C2COHCQ. = C2CO.CQ$ Hf {Kcal/mol} -60.190 -44.330 S {cal/mol K} 96.020 96.600 dU (dE) {kcal/mol} (") = 15.86 dUr avg (298., 1500. K) = 15.38 Fit A/Ar: A = 3.536E-02 n = .70 alpha = 1.134E-03		 TC2YCCQO	
TS 17	Rx $C2COHCQ. = TICPYCCQC$ S {cal/mol K} 96.020 85.370 $A_{prime} = 1.2631E+08$ $n = 1.08388$ Rx $C2COHCQ. = C2.COHCQ$ Hf {Kcal/mol} -60.190 -47.290 S {cal/mol K} 96.020 100.360 dU (dE) {kcal/mol} (") = 12.90 dUr avg (298., 1500. K) = 13.09 Fit A/Ar: A = 2.829E-02 n = 1.07 alpha = 9.692E-04		 TICPYCCQC	

Table IIB. 3 Information for C2C=C Related Transition States (Cont')

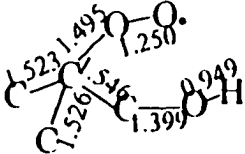
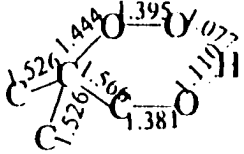
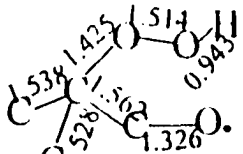
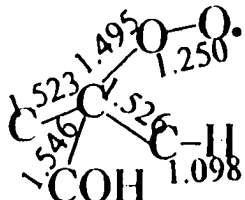
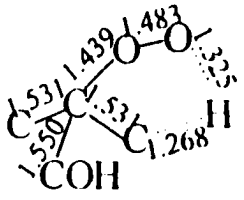
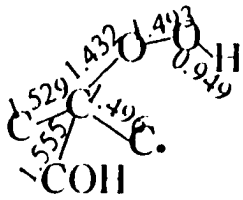
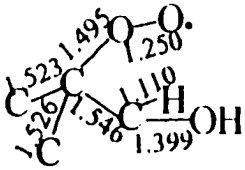
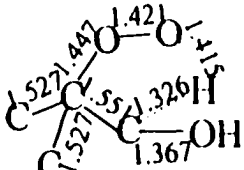
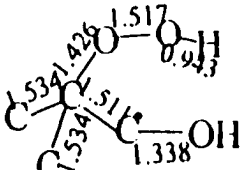
Number	Thermodynamic Properties Information	Reactant	Transition State	Product
TS 18	<p>Rx C2CQ.CO₂H = TC2YCQOC</p> <p>S {cal/mol K} 96.140 84.710</p> <p>for A(T) = Aprime * T^n</p> <p>Aprime = 4.2170E+07 n = 1.18430</p> <p>Rx C2CQ.CO₂H = C2CQCO₂</p> <p>Hf {Kcal/mol} -59.380 -43.520</p> <p>S {cal/mol K} 96.140 95.170</p> <p>dU (dE) {kcal/mol} (") = 15.86</p> <p>dUr avg (298., 1500. K) = 17.30</p> <p>Fit A/Ar: A = 2.475E-04 n = 1.36 alpha = 1.870E-04</p>		<p>TC2YCQOC</p> 	
TS 19	<p>Rx C2CQ.CO₂H = TICCPYCQC</p> <p>S {cal/mol K} 96.140 91.890</p> <p>for A(T) = Aprime * T^n</p> <p>Aprime = 3.8358E+09 n = 1.07094</p> <p>Rx C2CQ.CO₂H = C2.CQCO₂H</p> <p>Hf {Kcal/mol} -59.380 -46.480</p> <p>S {cal/mol K} 96.140 103.990</p> <p>dU (dE) {kcal/mol} (") = 12.90</p> <p>dUr avg (298., 1500. K) = 13.59</p> <p>Fit A/Ar: A = 2.231E-02 n = 1.40 alpha = 8.977E-04</p>		<p>TICCPYCQC</p> 	
TS 20	<p>Rx C2CQ.CO₂H = TC2YCQCIP</p> <p>S {cal/mol K} 96.140 89.510</p> <p>for A(T) = Aprime * T^n</p> <p>Aprime = 2.3281E+08 n = 1.35787</p> <p>Rx C2CQ.CO₂H = C2CQC.OH</p> <p>Hf {Kcal/mol} -59.380 -53.580</p> <p>S {cal/mol K} 96.140 100.100</p> <p>dU (dE) {kcal/mol} (") = 5.80</p>		<p>TC2YCQCIP</p> 	

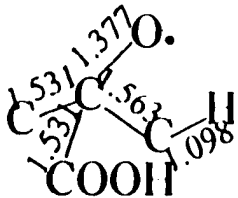
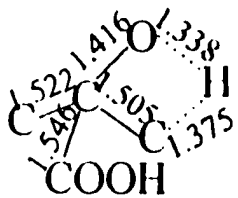
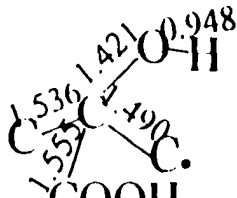
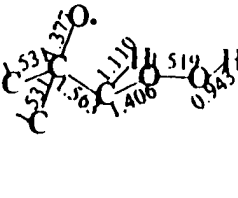
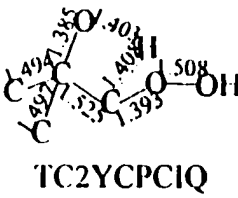
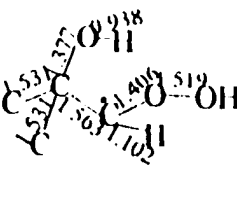
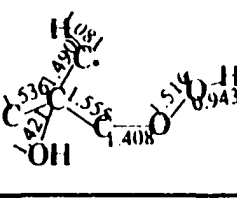
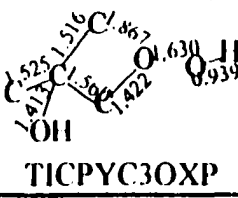
Table IIB. 3 Information for C2C=C Related Transition States (Cont')

Number	Thermodynamic Properties Information	Reactant	Transition State*	Product
	dUr avg (298., 1500. K) = 6.46 Fit A/Ar: A = 3.233E-03 n = 1.41 alpha = 9.274E-04			
TS 21	Rx C2CQ.CQ = TICCQYCQC S {cal/mol K} 102.620 101.000 for A(T) = Aprime * T^n Aprime = 1.8018E+08 n = 1.83229 Rx C2CQ.CQ = C2.CQCQ Hf {Kcal/mol} -47.670 -31.870 S {cal/mol K} 102.620 110.040 dU (dE) {kcal/mol} (") = 15.80 dUr avg (298., 1500. K) = 16.33 Fit A/Ar: A = 3.369E-02 n = 1.30 alpha = 9.308E-04			
TS 22	Rx C2CQ.CQ = TC2YCQOOC S {cal/mol K} 102.620 86.090 for A(T) = Aprime * T^n Aprime = 3.5366E+12 n = -1.24370 Rx C2CQ.CQ = C2CQCQ. Hf {Kcal/mol} -47.670 -44.770 S {cal/mol K} 102.620 102.680 dU (dE) {kcal/mol} (") = 2.90 dUr avg (298., 1500. K) = 3.11 Fit A/Ar: A = 8.358E-01 n = .02 alpha = -1.595E-04			
TS 23	Rx C2CQ.CQ = TC2YCQCIQ S {cal/mol K} 102.620 98.220 for A(T) = Aprime * T^n Aprime = 1.3902E+07 n = 2.03199 Rx C2CQ.CQ = C2CQC.Q Hf {Kcal/mol} -47.670 -36.970			

Table II.B. 3 Information for C2C=C Related Transition States (Cont')

Number	Thermodynamic Properties Information	Reactant	Transition State*	Product
	<p>S {cal/mol K} 102.620 106.930 dU (dE) {kcal/mol} (") = 10.70 dUr avg (298., 1500. K) = 11.43 Fit A/Ar: A = 6.883E-03 n = 1.29 alpha = 7.553E-04</p>			
TS 24	<p>Rx C2CQCQ. = TICQYCCQC S {cal/mol K} 102.680 95.340 for A(T) = Aprime * T^n Aprime = 6.1059E+07 n = 1.49680</p> <p>Rx C2CQCQ. = C2.CQCQ Hf {Kcal/mol} -44.770 -31.870 S {cal/mol K} 102.680 110.040 dU (dE) {kcal/mol} (") = 12.90 dUr avg (298., 1500. K) = 13.22 Fit A/Ar : A = 4.031E-02 n = 1.28 alpha = 1.090E-03</p>		<p>TICQYCCQC</p>	
TS 25	<p>Rx C2COHCQ. = TC2CPYCQ S {cal/mol K} 96.020 92.020 for A(T) = Aprime * T^n Aprime = 3.1162E+09 n = 1.17380</p> <p>Rx C2COHCQ. = C2COHC.Q Hf {Kcal/mol} -60.190 -52.390 S {cal/mol K} 96.020 103.010 dU (dE) {kcal/mol} (") = 7.80 dUr avg (298., 1500. K) = 8.21 Fit A/Ar: A = 1.172E-02 n = 1.47 alpha = 1.211E-03</p>		<p>TC2CPYCQ</p>	

Table IIB. 3 Information for C2C=C Related Transition States (Cont')

Number	Thermodynamic Properties Information	Reactant	Transition State	Product
TS 26	<p>Rx C2CO.CQ = TICCQYCPC S {cal/mol K} 96.600 92.500 for A(T) = Aprime * T^n Aprime = 7.3487E+05 n = 2.54484</p> <p>Rx C2CO.CQ = C2.COHCQ Hf {Kcal/mol} -44.330 -47.290 S {cal/mol K} 96.600 100.360 dU (dE) {kcal/mol} (") = -2.96 dUr avg (298., 1500. K) = -2.29 Fit A/Ar: A = 8.001E-01 n = .36 alpha = -1.651E-04</p>			
TS 27	<p>Rx C2CO.CQ = TC2YCPCIQ S {cal/mol K} 96.600 88.690 for A(T) = Aprime * T^n Aprime = 2.5418E+06 n = 1.99355</p> <p>Rx C2CO.CQ = C2COHC.Q Hf {Kcal/mol} -44.330 -52.390 S {cal/mol K} 96.600 103.010 dU (dE) {kcal/mol} (") = -8.06 dUr avg (298., 1500. K) = -7.17 Fit A/Ar: A = 3.315E-01 n = .77 alpha = 7.659E-05</p>			
TS 28	<p>Rx C2.COHCQ = TICPYC3OXP S {cal/mol K} 100.360 90.950 for A(T) = Aprime * T^n Aprime = 4.2531E+10 n = .18330</p>			

* T - Transition state; Y - Cyclic, Q - OOH; Q - OO., P - OH; I - iso-C; X - represents the elimination of the species after X (except for TC2YCNQC*)

TS IIB. 4 Transition State Information for Reaction $\text{CH}_3\text{OH} \rightarrow \text{CH}_2\text{O} + \text{H}_2$

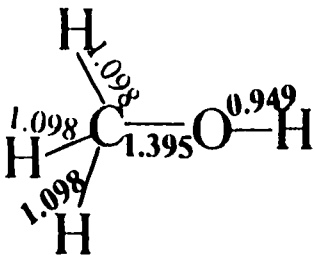
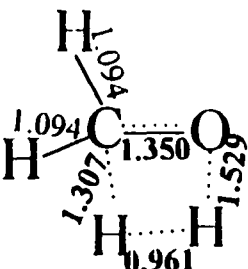
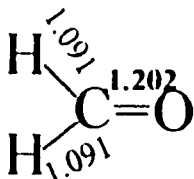
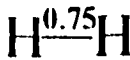
Reactant	Transition State	Product 1	Product 2
			
CH_3OH	TSMEOH	CH_2O	H_2
Principle moments of inertia in unit of cm^{-1} : A = 4.244786 B = 0.856787 C = 0.825179 in unit of 10^{-40} -gram-cm ² : A = 6.594594 B = 32.671649 C = 33.923121	Principle moments of inertia in unit of cm^{-1} : A = 3.173265 B = 0.929231 C = 0.837343 in unit of 10^{-40} -gram-cm ² : A = 8.821400 B = 30.124509 C = 33.430301	Principle moments of inertia in unit of cm^{-1} : A = 9.720866 B = 1.305991 C = 1.151313 in unit of 10^{-40} -gram-cm ² : A = 2.879645 B = 21.434012 C = 24.313656	* Thermodynamic data from THERM - Group Additivity
Symmetry = 3	Symmetry = 1	Symmetry = 1	
Internal rotor(s): V / kcal-mol ⁻¹ CH ₃ -OH (1): 1.09	No Internal Rotor	No Internal Rotor	
frequencies 292.33 988.92 1020.76 1164.45 1362.29 1366.05 1366.27	frequencies -3495.48 598.78 916.88 1002.25 1127.97 1145.21	frequencies 1070 1098 1289 1987 2999 3026	

Table II B. 4 Transition State Information for $\text{CH}_3\text{OH} \rightarrow \text{CH}_2\text{O} + \text{H}_2$ (Cont')

1409.05 3035.71 3068.61	1315.87 1487.04 1844.70		
3141.15 3896.48	2486.70 3003.12 3012.59		

TS IIB. 5 Thermodynamic Analysis for C3COC → C2C=C + CH3OH

Rx C3COC = TMTBE Hf {Kcal/mol} -68.900 -1.300 S {cal/mol K} 85.640 86.370 dU (dE) {kcal/mol} (298K) = 67.60 dUr avg (298., 1500. K) = 67.86 for A(T) = Aprime * T^n Aprime = 2.20E+10 n = 1.22396				Rx C3COC = C2C=C + CH3OH Hf {Kcal/mol} -68.9 -3.8 -48 S {cal/mol K} 85.85 69.99 57.3 dHr {kcal/mol} (298K) = 17.1 dHr avg (298., 1500. K) = 15.19 dU (dE) {kcal/mol} (") = 16.51 dUr avg (298., 1500. K) = 13.4 Al/Ar (") = 1.717E+04 Al/Ar avg (298., 1500. K) = 1.750E+03 Fit Al/Ar: A = 6.14E+09 n = -2.19 alpha = 4.42E-04				
Temp(K)	AF(T)	AF-fit(T)	dS(cal/mol K)	dH(Kcal/mol)	dU(Kcal/mol)	dS(cal/mol K)	(Al/Ar)	dG(Kcal/mol)
300	2.45E+13	2.36E+13	8.11E-50	1.71E+01	1.65E+01	4.14E+01	1.70E+04	4.67E+00
400	3.34E+13	3.36E+13	1.67E-37	1.70E+01	1.62E+01	4.11E+01	1.08E+04	5.38E-01
500	4.34E+13	4.42E+13	4.11E-30	1.67E+01	1.57E+01	4.06E+01	6.61E+03	-3.55E+00
600	5.42E+13	5.52E+13	3.50E-25	1.64E+01	1.52E+01	4.00E+01	4.11E+03	-7.58E+00
800	7.78E+13	7.85E+13	5.16E-19	1.57E+01	1.41E+01	3.89E+01	1.82E+03	-1.55E+01
1000	1.03E+14	1.03E+14	2.63E-15	1.50E+01	1.30E+01	3.81E+01	9.62E+02	-2.32E+01
1200	1.29E+14	1.29E+14	7.84E-13	1.43E+01	1.19E+01	3.75E+01	5.84E+02	-3.07E+01
1500	1.69E+14	1.70E+14	2.36E-10	1.33E+01	1.03E+01	3.68E+01	3.23E+02	-4.19E+01
2000	2.47E+14	2.41E+14	7.23E-08	1.18E+01	7.79E+00	3.59E+01	1.56E+02	-6.00E+01

TS IIB. 6 Thermodynamic Analysis for $\text{CH}_3\text{OH} \rightarrow \text{CH}_2\text{O} + \text{H}_2$

Rx $\text{CH}_3\text{OH} = \text{TMEOH}$				Rx $\text{CH}_3\text{OH} = \text{CH}_2\text{O} + \text{H}_2$				
Hf {Kcal/mol} -48.000 45.060				Hf {Kcal/mol} -48.00 -26.00 0				
S {cal/mol K} 57.260 54.870				S {cal/mol K} 57.30 50.92 31.20				
dU (dE) {kcal/mol} (298K) = 93.06				dHr {kcal/mol} (298K) = 22.0 dHr avg (298., 1500 K) = 22.89				
dUr avg (298., 1500. K) = 93.41				dU (dE) {kcal/mol} (") = 21.41 dUr avg (298., 1500 K) = 21.11				
for A(T) = Aprime * T^n				Af/Ar (") = 4.000E+00 Af/Ar avg (298., 1500 K) = 3.244E+00				
Aprime = 3.02E+09 n = 1.29165				Fit Af/Ar: A = 1.23E-03 n = 1.54 alpha = 1.94E-03				
Temp(K)	AF(T)	AF-fit(T)	dS(cal/mol K)	dH(Kcal/mol)	dU(Kcal/mol)	dS(cal/mol K)	(Af/Ar)	dG(Kcal/mol)
300	5.10E+12	4.78E+12	4.76E-69	2.20E+01	2.14E+01	2.49E+01	4.04E+00	1.46E+01
400	6.75E+12	6.93E+12	4.23E-52	2.25E+01	2.17E+01	2.61E+01	5.76E+00	1.20E+01
500	8.83E+12	9.24E+12	6.28E-42	2.28E+01	2.18E+01	2.69E+01	6.93E+00	9.34E+00
600	1.13E+13	1.17E+13	3.83E-35	2.31E+01	2.19E+01	2.75E+01	7.55E+00	6.62E+00
800	1.69E+13	1.70E+13	1.19E-26	2.35E+01	2.19E+01	2.81E+01	7.64E+00	1.06E+00
1000	2.30E+13	2.26E+13	1.50E-21	2.37E+01	2.18E+01	2.83E+01	6.95E+00	-4.58E+00
1200	2.93E+13	2.86E+13	3.84E-18	2.38E+01	2.14E+01	2.84E+01	6.04E+00	-1.03E+01
1500	3.89E+13	3.82E+13	9.94E-15	2.38E+01	2.08E+01	2.84E+01	4.76E+00	-1.88E+01
2000	5.48E+13	5.54E+13	2.61E-11	2.34E+01	1.94E+01	2.82E+01	3.19E+00	-3.29E+01

APPENDIX IIC
FIGURES IN THE MTBE SYSTEM

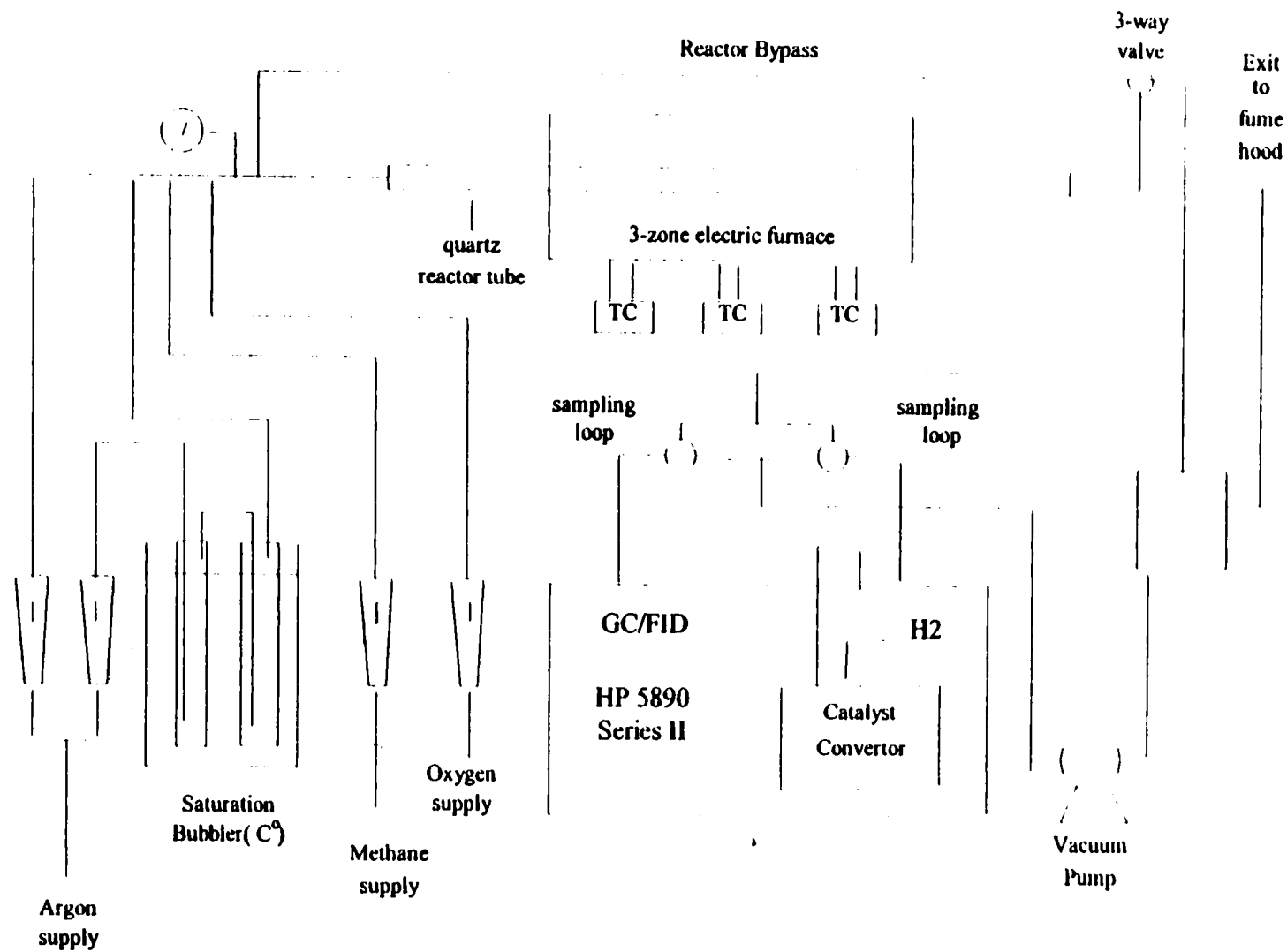


Figure IIC. 1 Experimental Apparatus

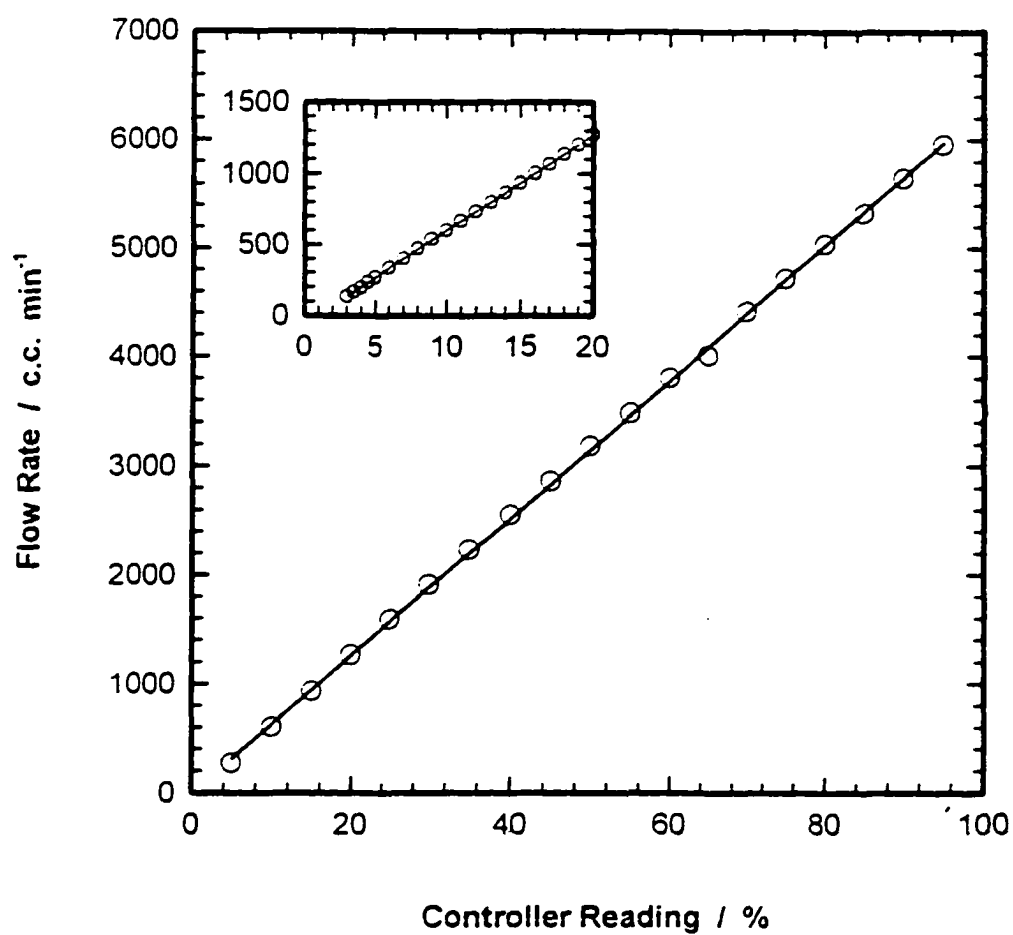


Figure IIC. 2 Calibration curve of mass flow controller 1 (AR) with inlet pressure of 200 psi.

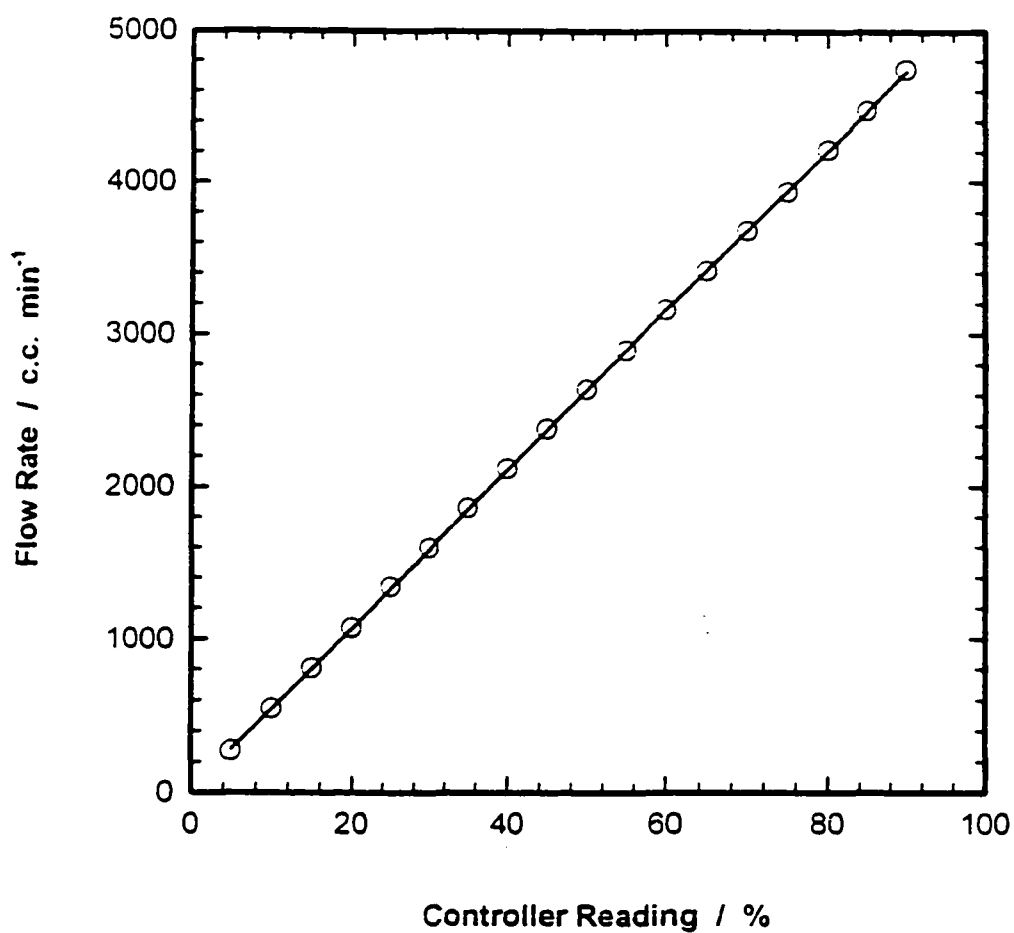


Figure IIC. 3 Calibration curve of mass flow controller 2 (AR) with inlet pressure of 200 psi.

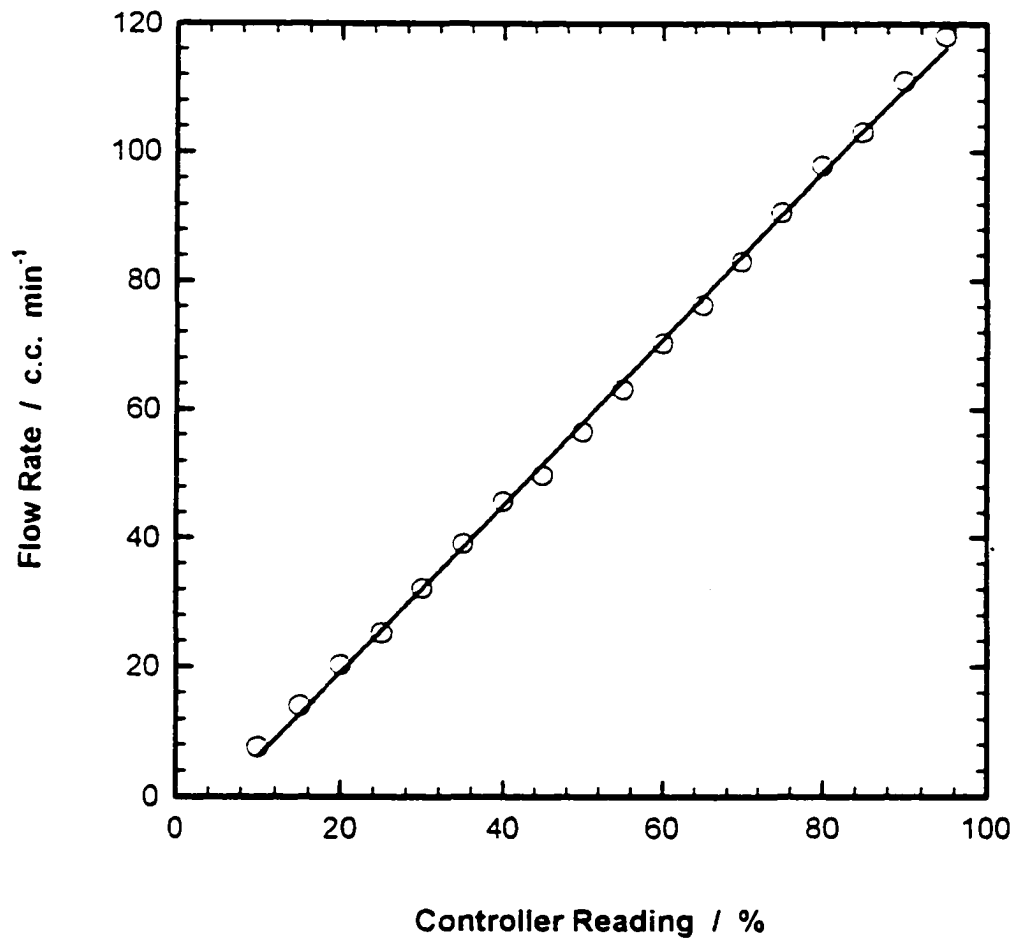


Figure IIC. 4 Calibration curve of mass flow controller 3 (O₂) with inlet pressure of 200 psi.

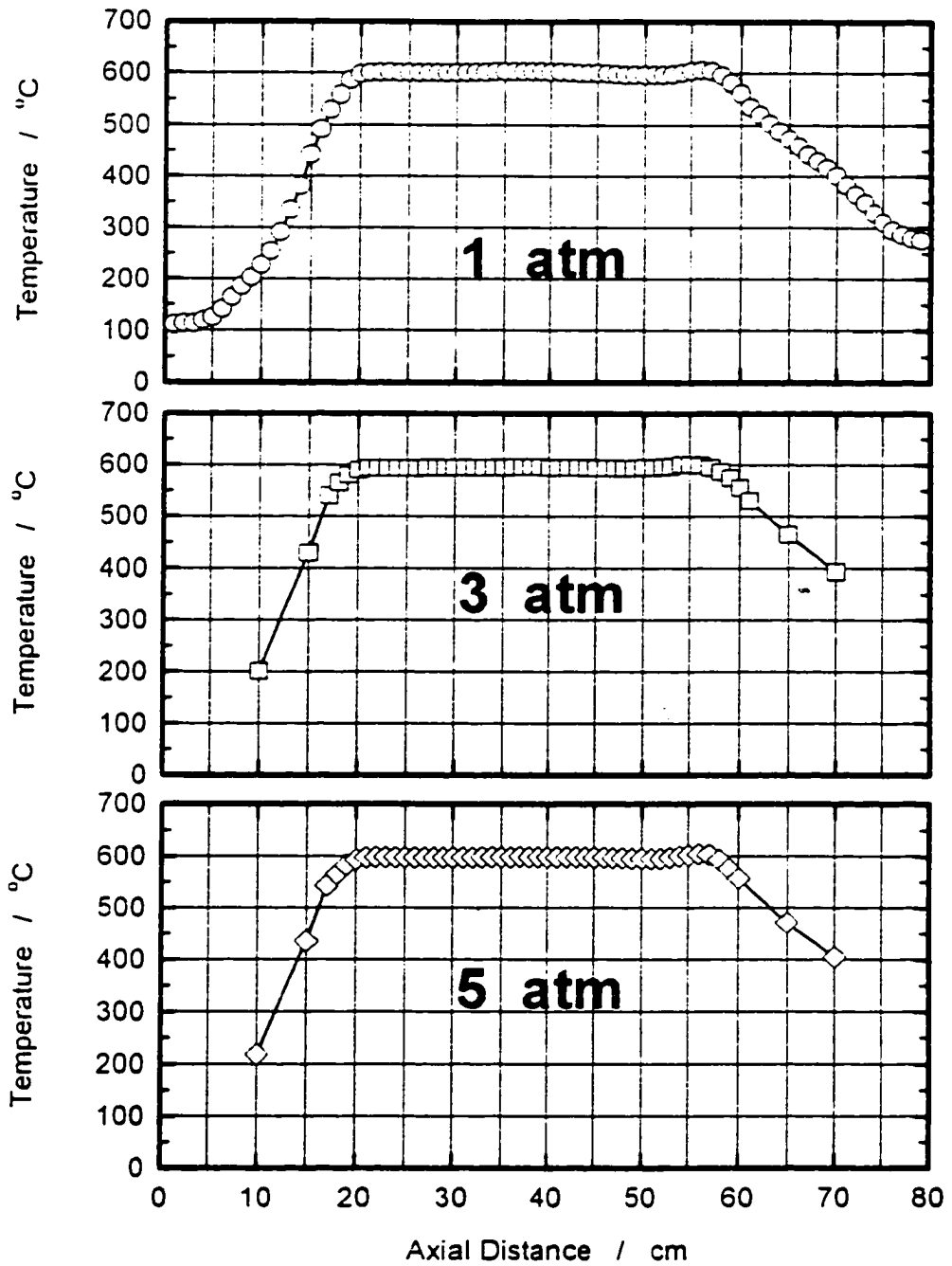


Figure IIC. 5 Reactor temperature profile at 1.3 gm Ar / min.

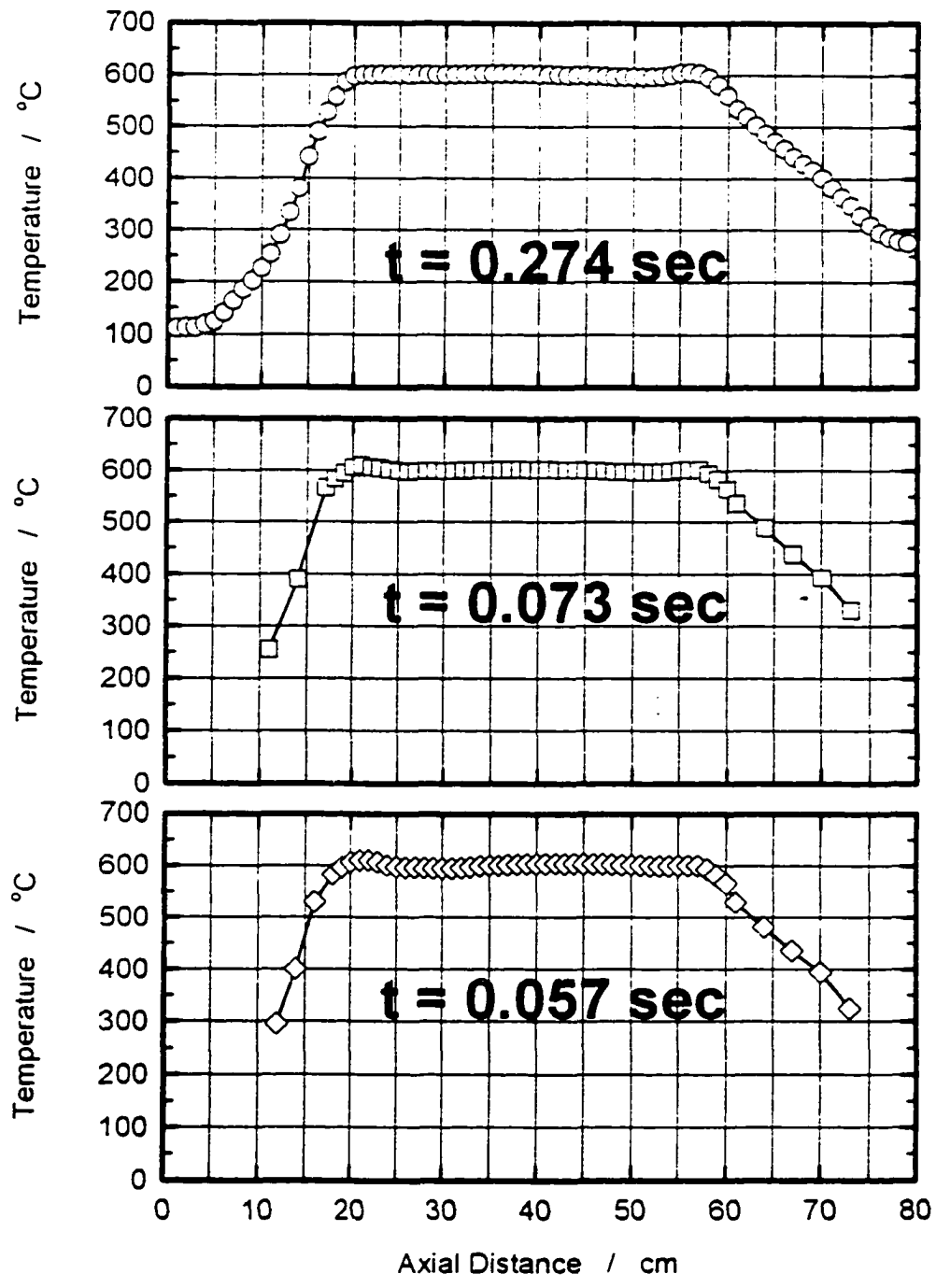


Figure IIC. 6 Reactor temperature profiles at 1 atm.

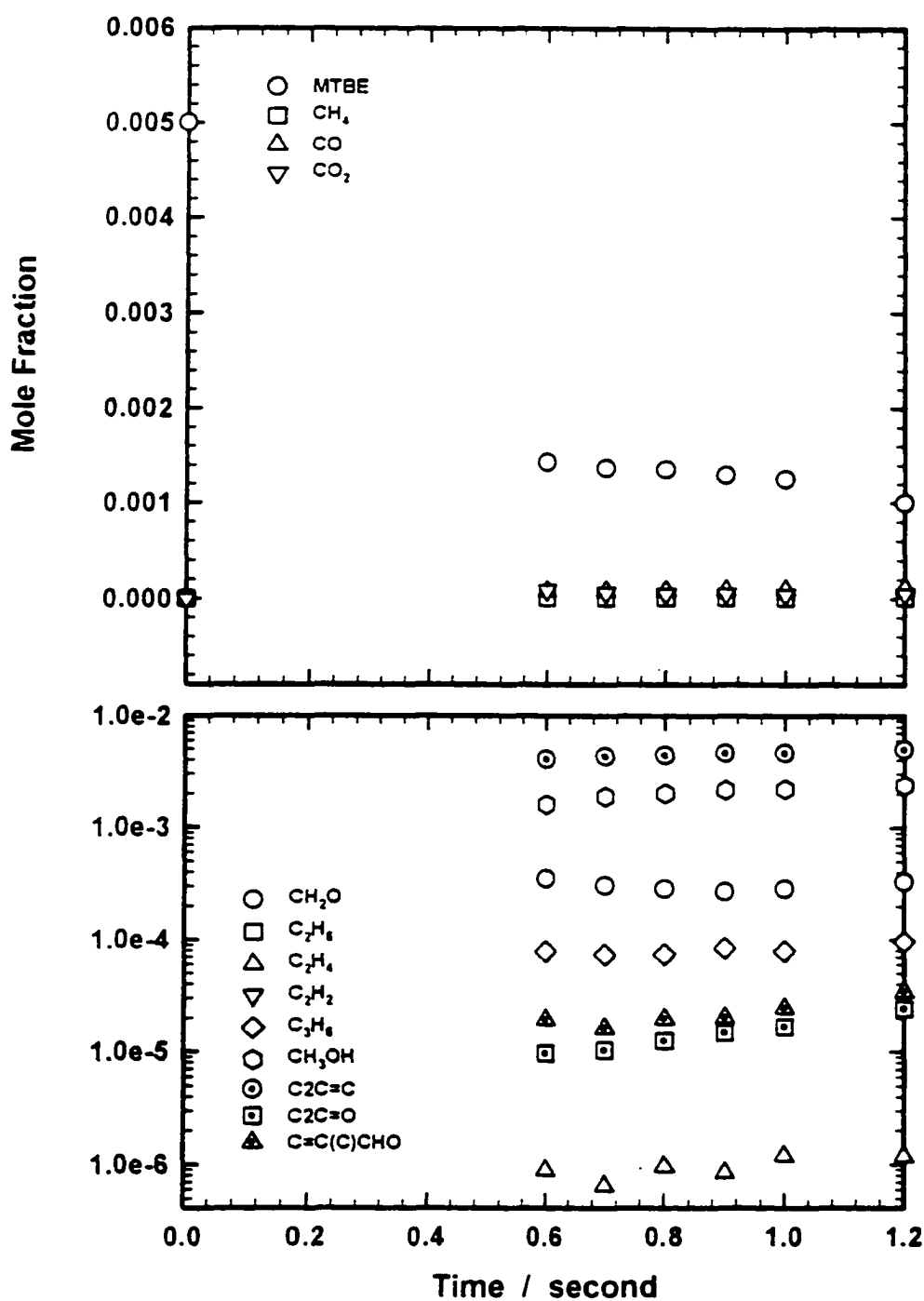


Figure IIC. 7 Experimental result of 0.5% MTBE oxidation product distribution at $\phi = 0.75$, $P = 4$ atm, $T = 823$ K

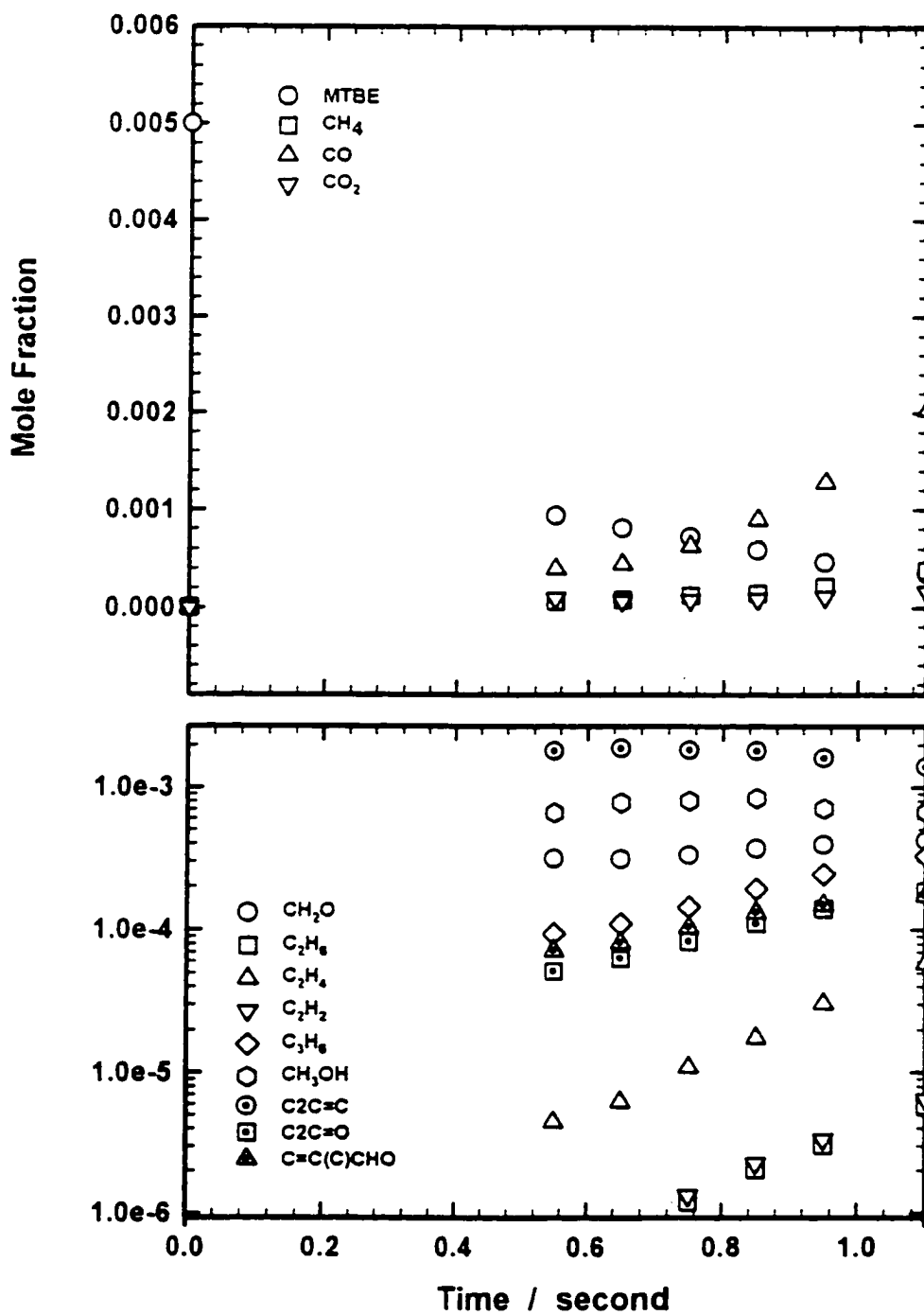


Figure IIC. 8 Experimental result of 0.5% MTBE oxidation product distribution at $\phi = 0.75$, $P = 4$ atm, $T = 873$ K

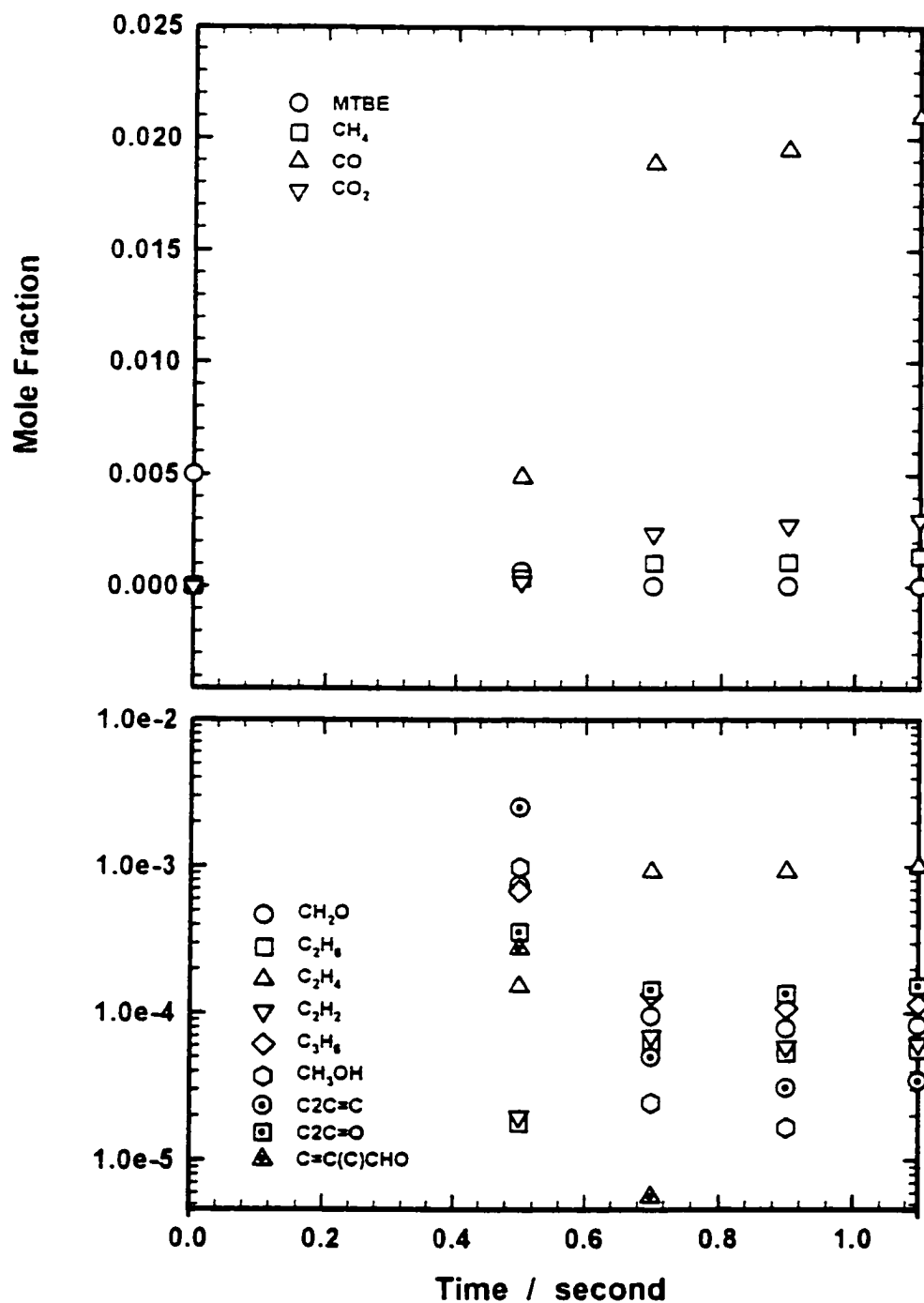


Figure IIC. 9 Experimental result of 0.5% MTBE oxidation product distribution at $\phi = 0.75$, $P = 4$ atm, $T = 898$ K

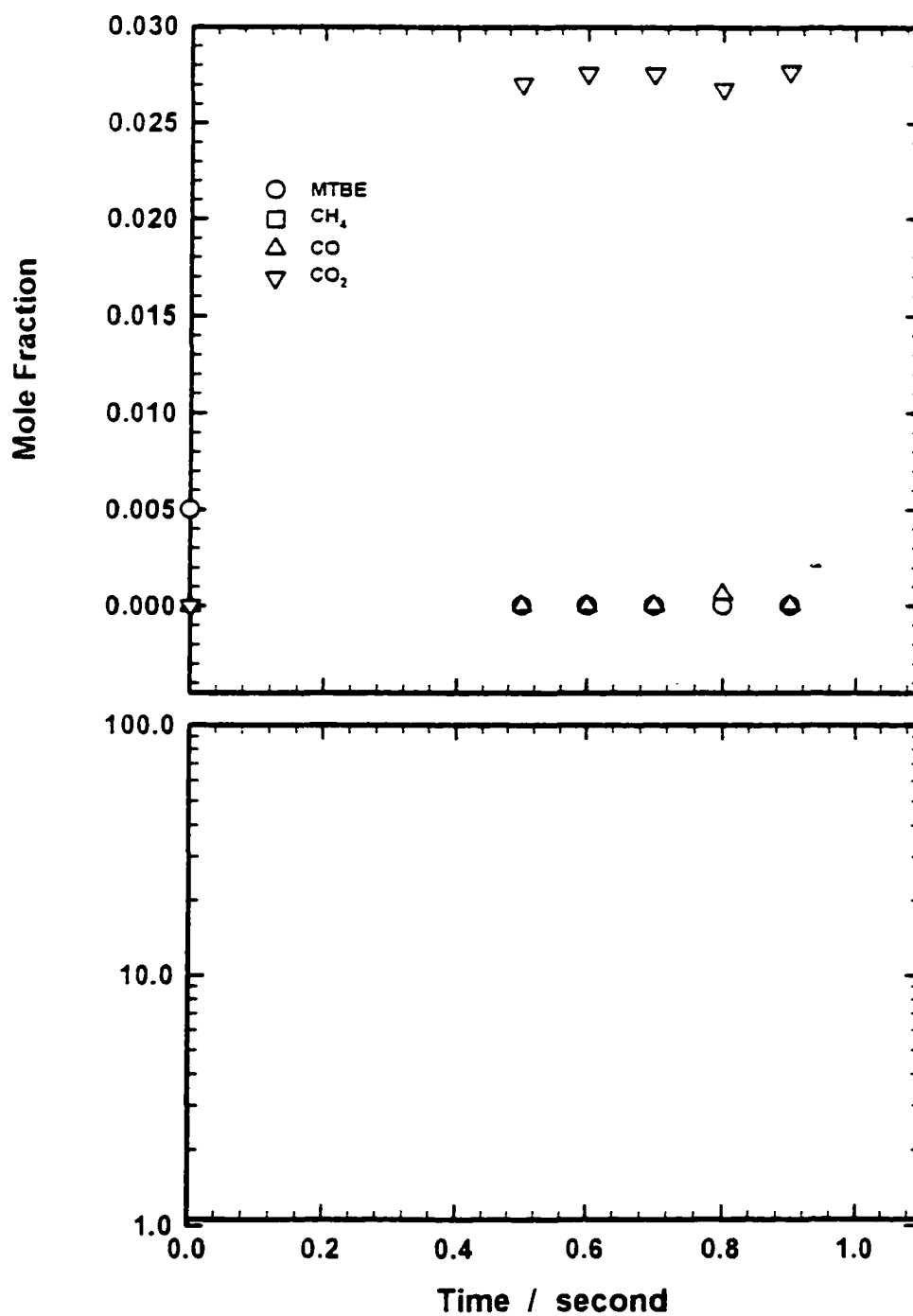


Figure IIC. 10 Experimental result of 0.5% MTBE oxidation product distribution at $\phi = 0.75$, $P = 4$ atm, $T = 923$ K

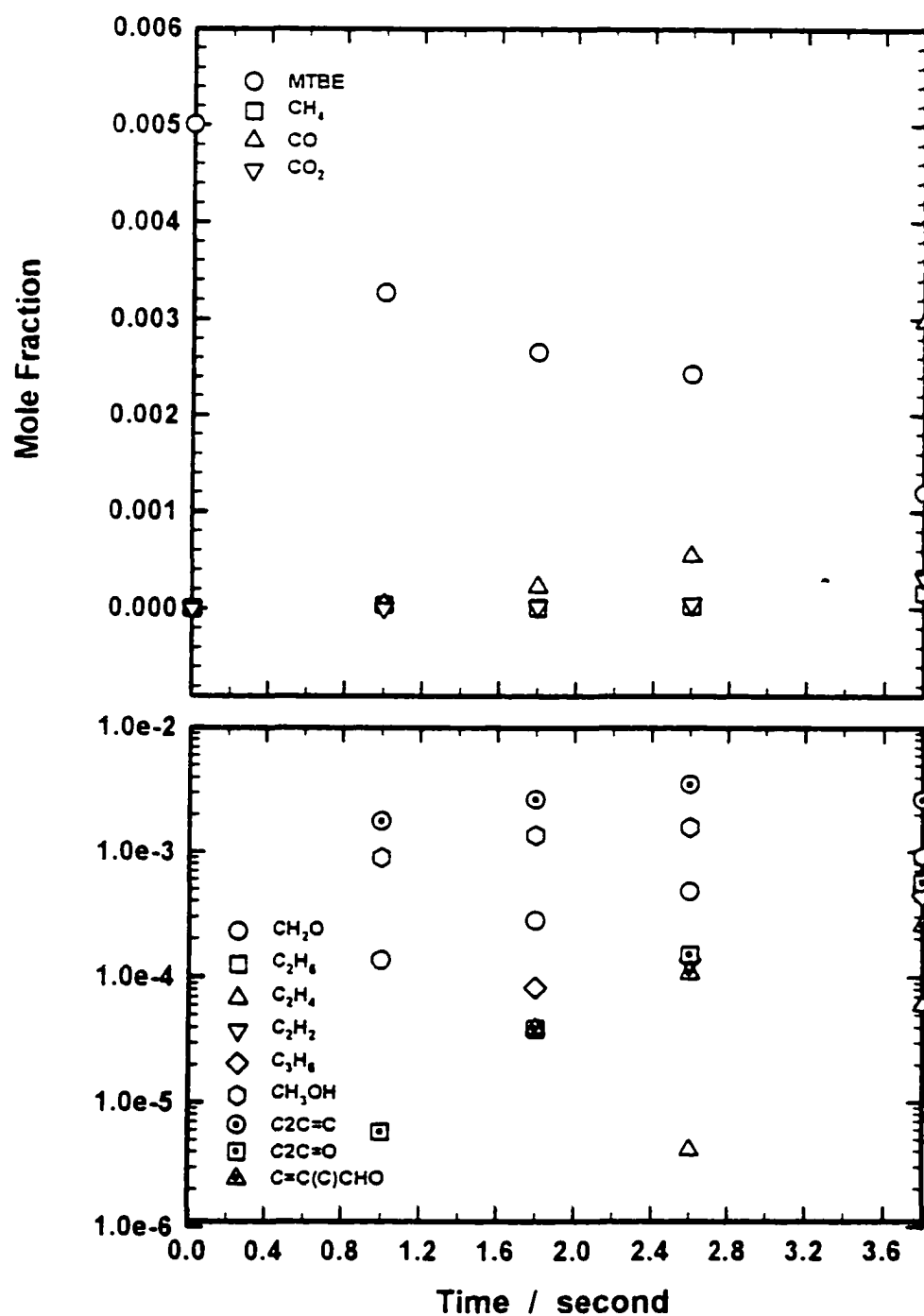


Figure IIC. 11 Experimental result of 0.5% MTBE oxidation product distribution at $\phi = 0.75$, $P = 7$ atm, $T = 798$ K

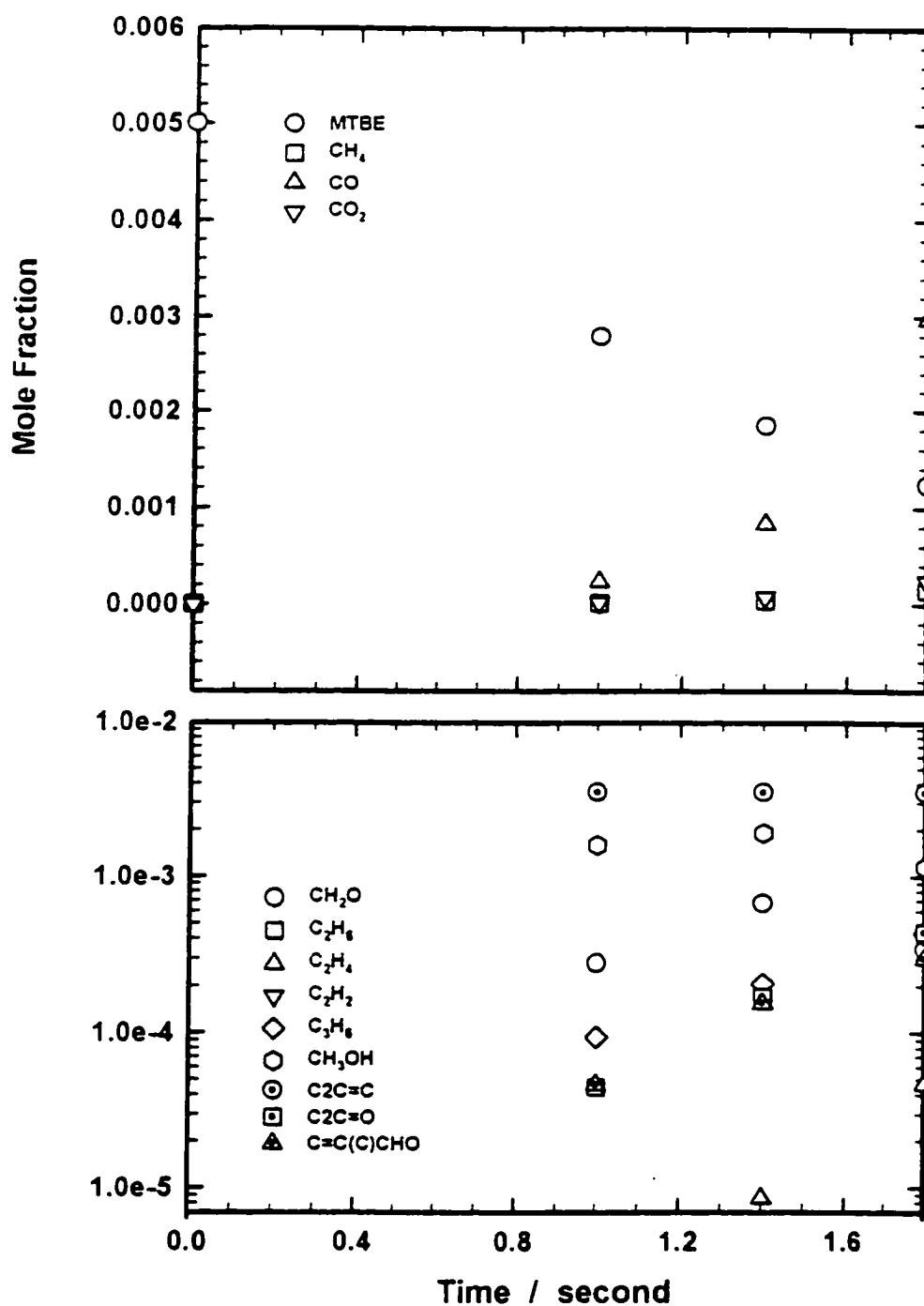


Figure IIC. 12 Experimental result of 0.5% MTBE oxidation product distribution at $\phi = 0.75$, $P = 7$ atm, $T = 823$ K

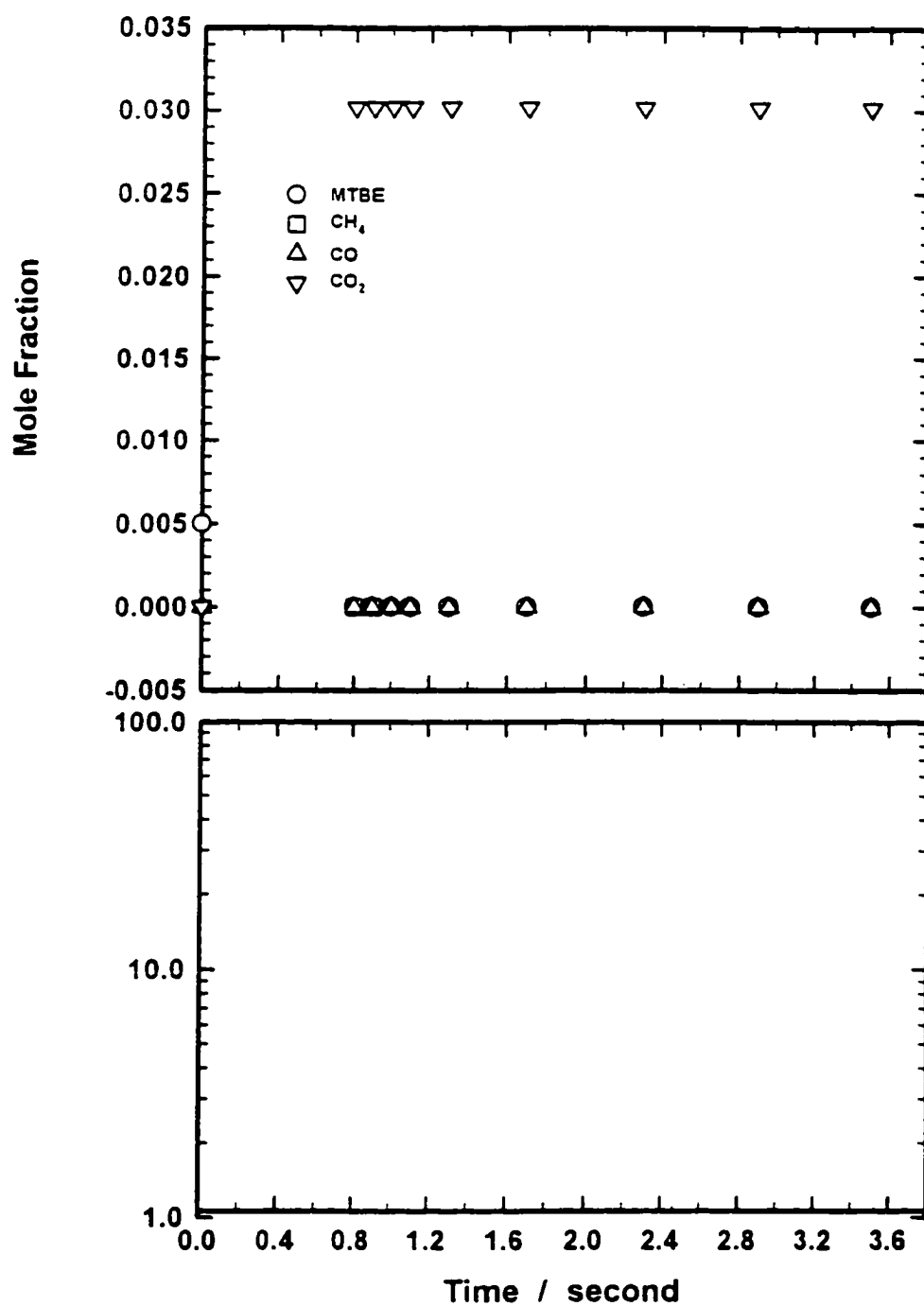


Figure IIC. 13 Experimental result of 0.5% MTBE oxidation product distribution at $\phi = 0.75$, $P = 7$ atm, $T = 873$ K

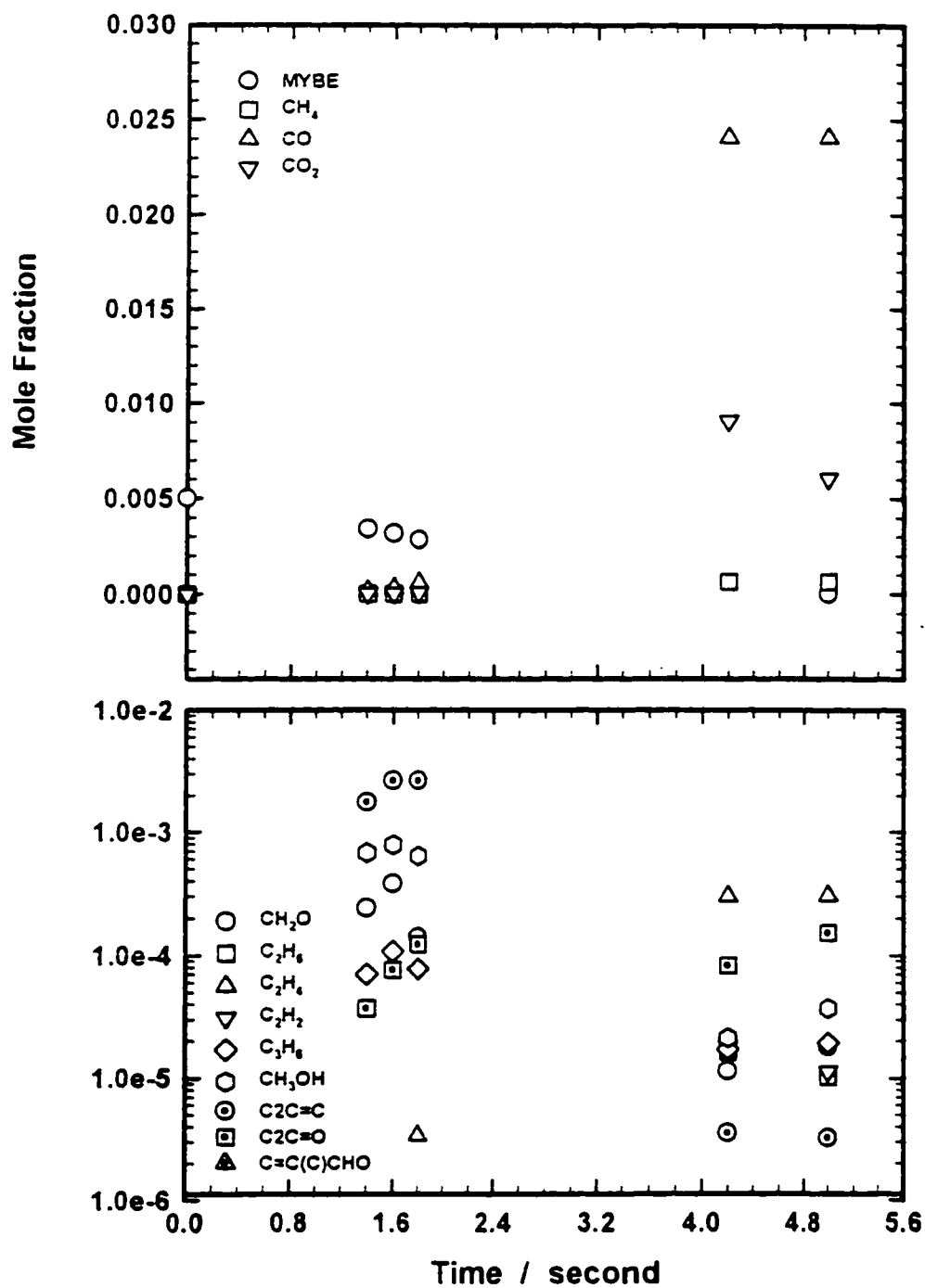


Figure IIC. 14 Experimental result of 0.5% MTBE oxidation product distribution at $\phi = 0.75$, $P = 10$ atm, $T = 798$ K

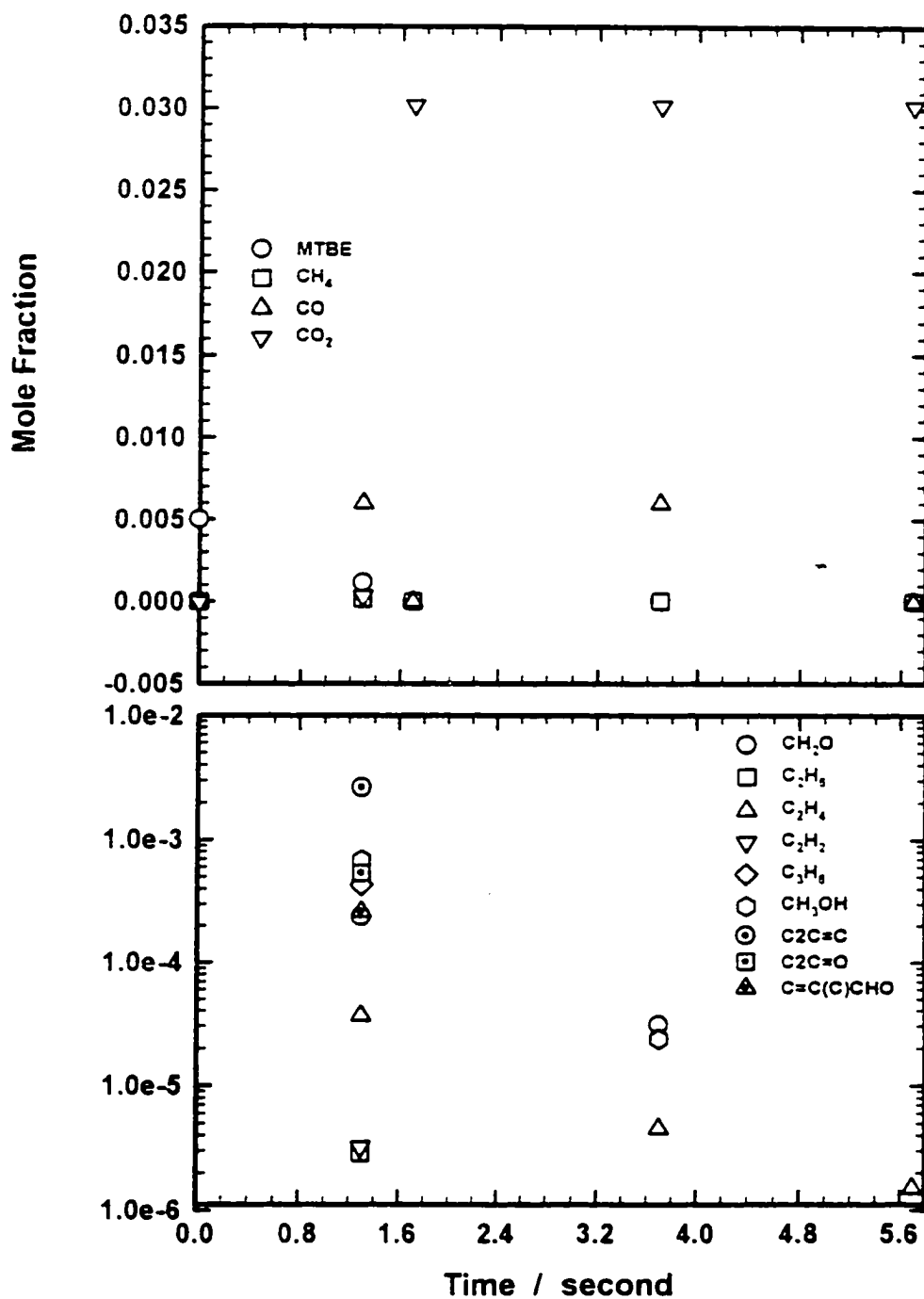


Figure IIC. 15 Experimental result of 0.5% MTBE oxidation product distribution at $\phi = 0.75$, $P = 10$ atm, $T = 823$ K

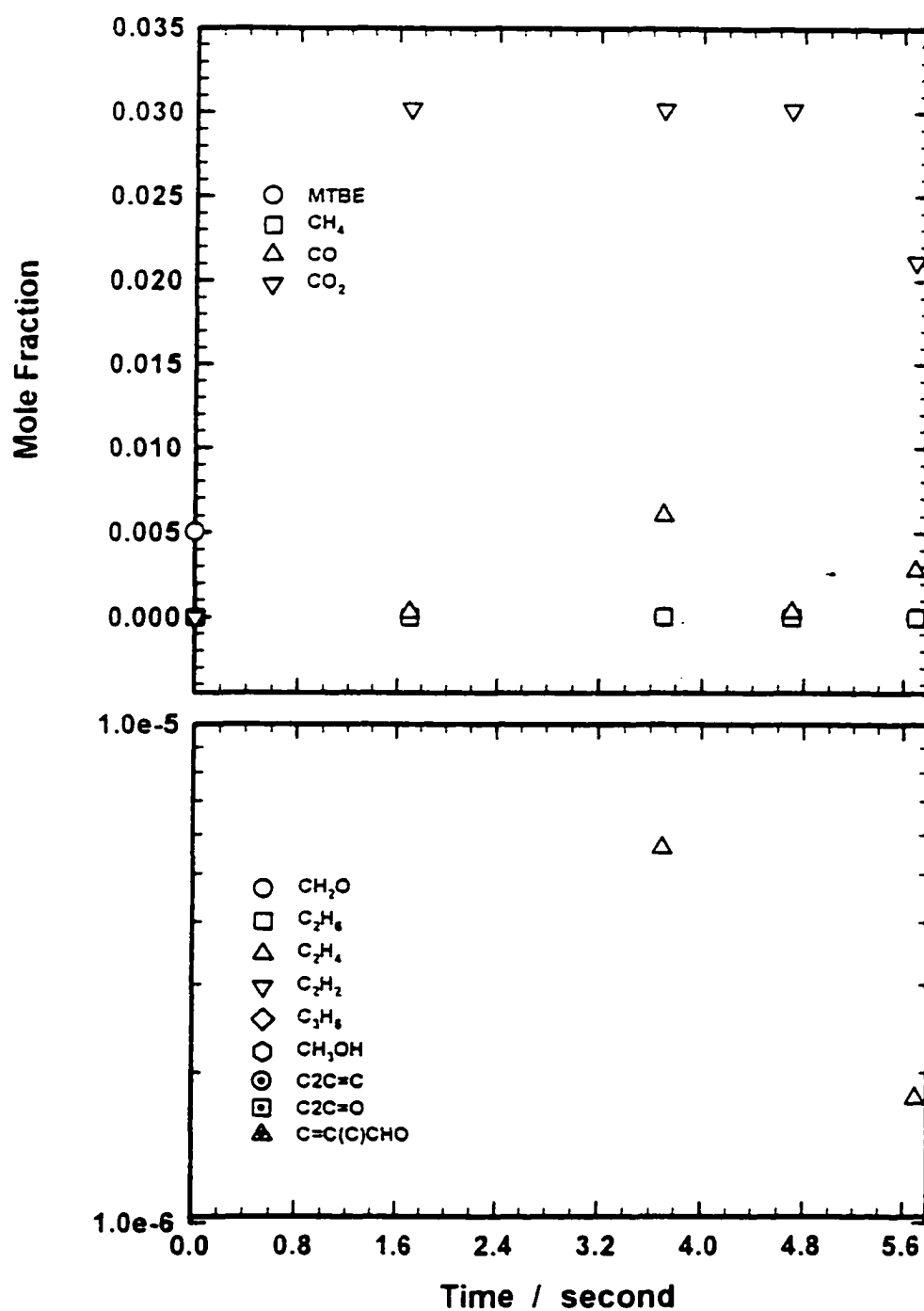


Figure IIC. 16 Experimental result of 0.5% MTBE oxidation product distribution at $\phi = 0.75$, $P = 10$ atm, $T = 873$ K

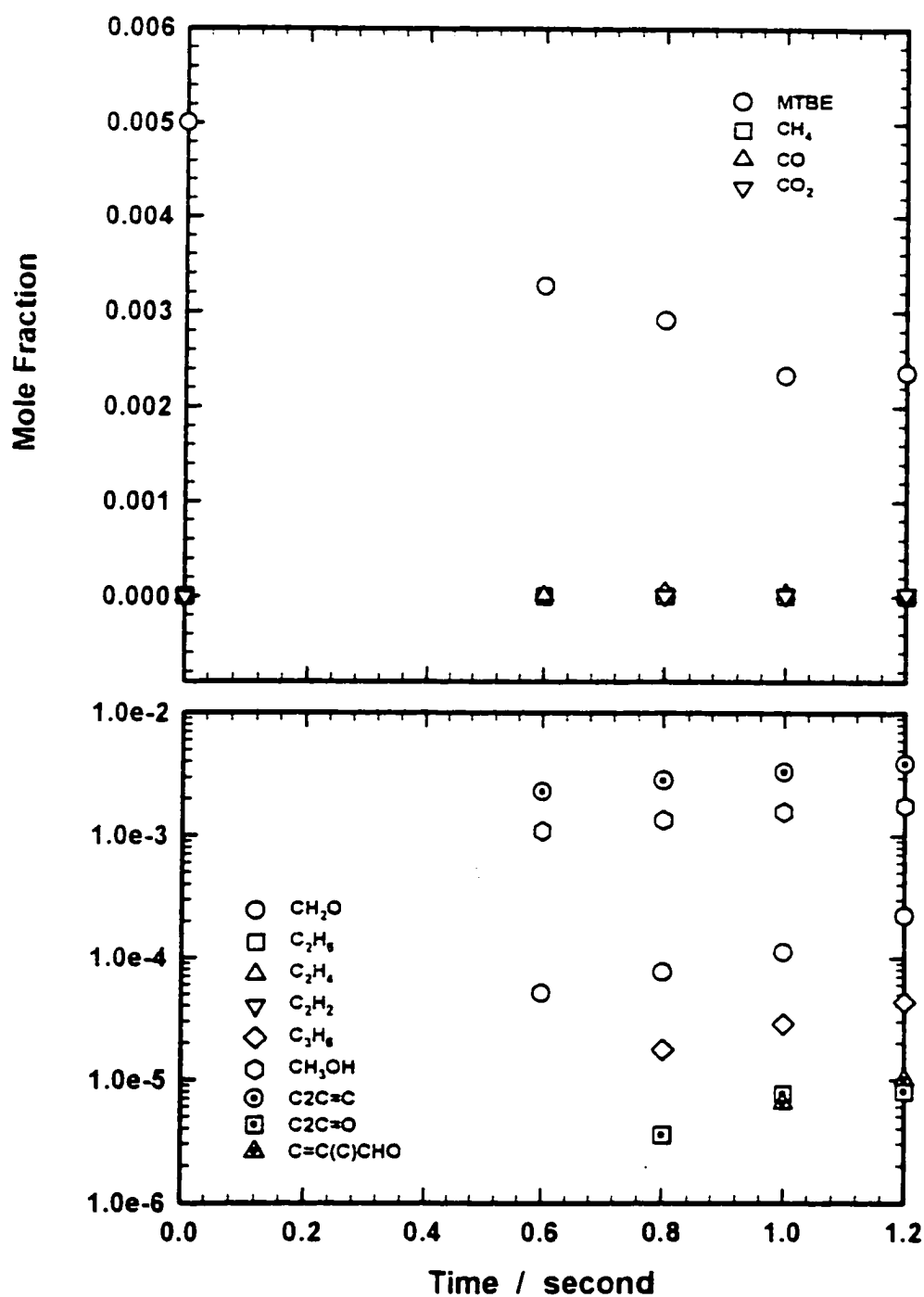


Figure IIC. 17 Experimental result of 0.5% MTBE oxidation product distribution at $\phi = 1.00$, $P = 4$ atm, $T = 823$ K

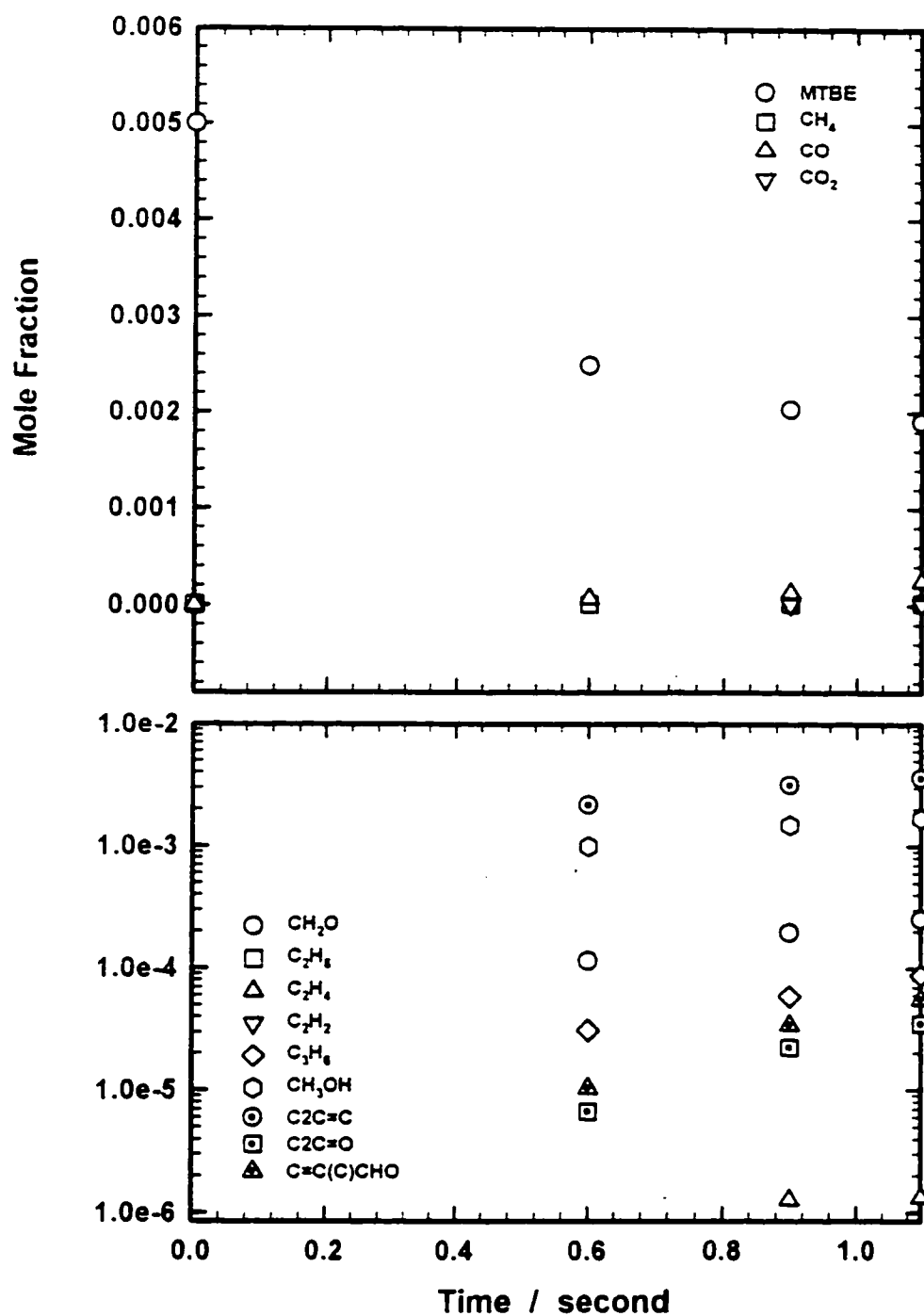


Figure IIC. 18 Experimental result of 0.5% MTBE oxidation product distribution at $\phi = 1.00$, $P = 4$ atm, $T = 848$ K

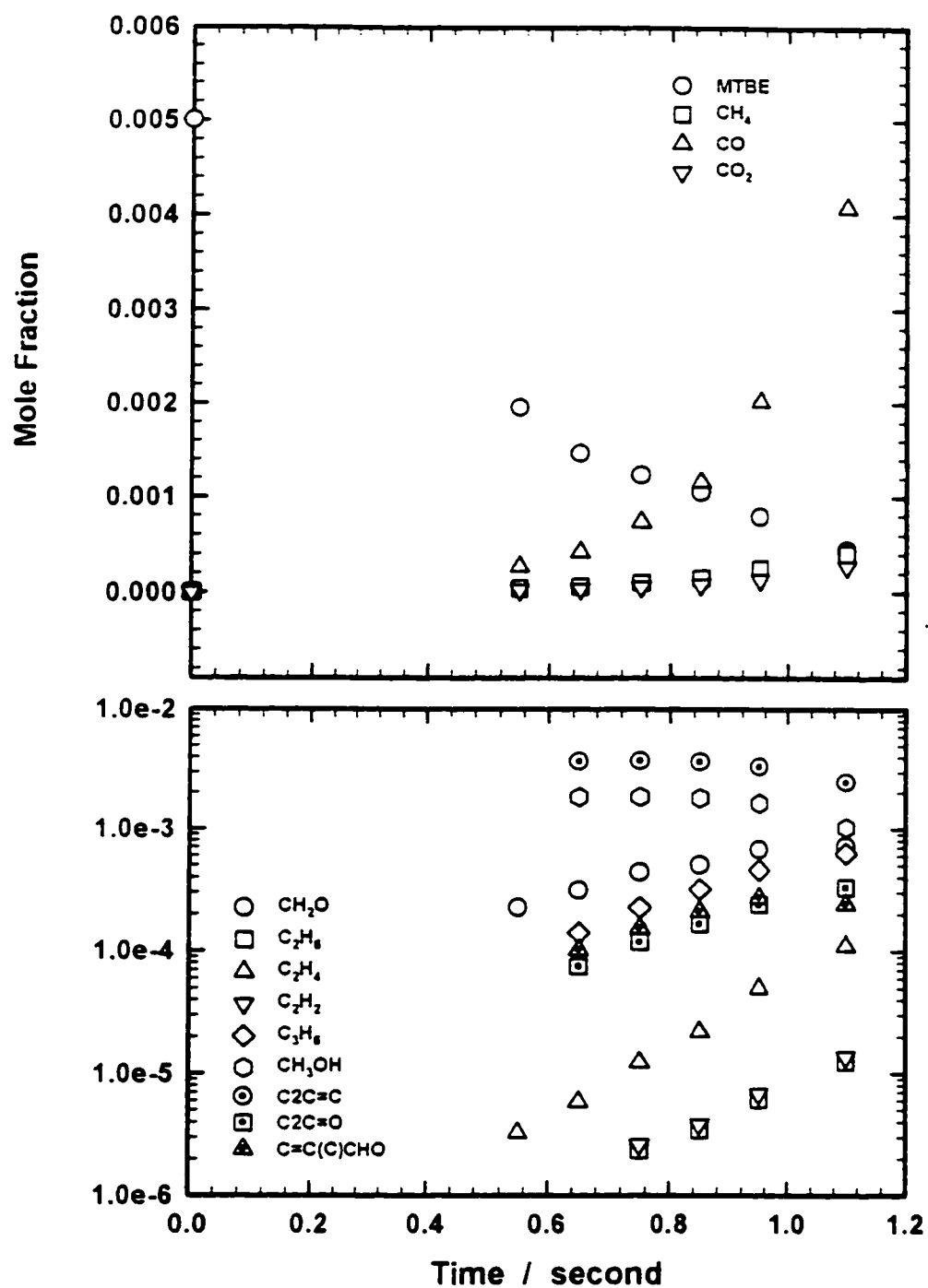


Figure IIC. 19 Experimental result of 0.5% MTBE oxidation product distribution at $\phi = 1.00$, $P = 4$ atm, $T = 873$ K

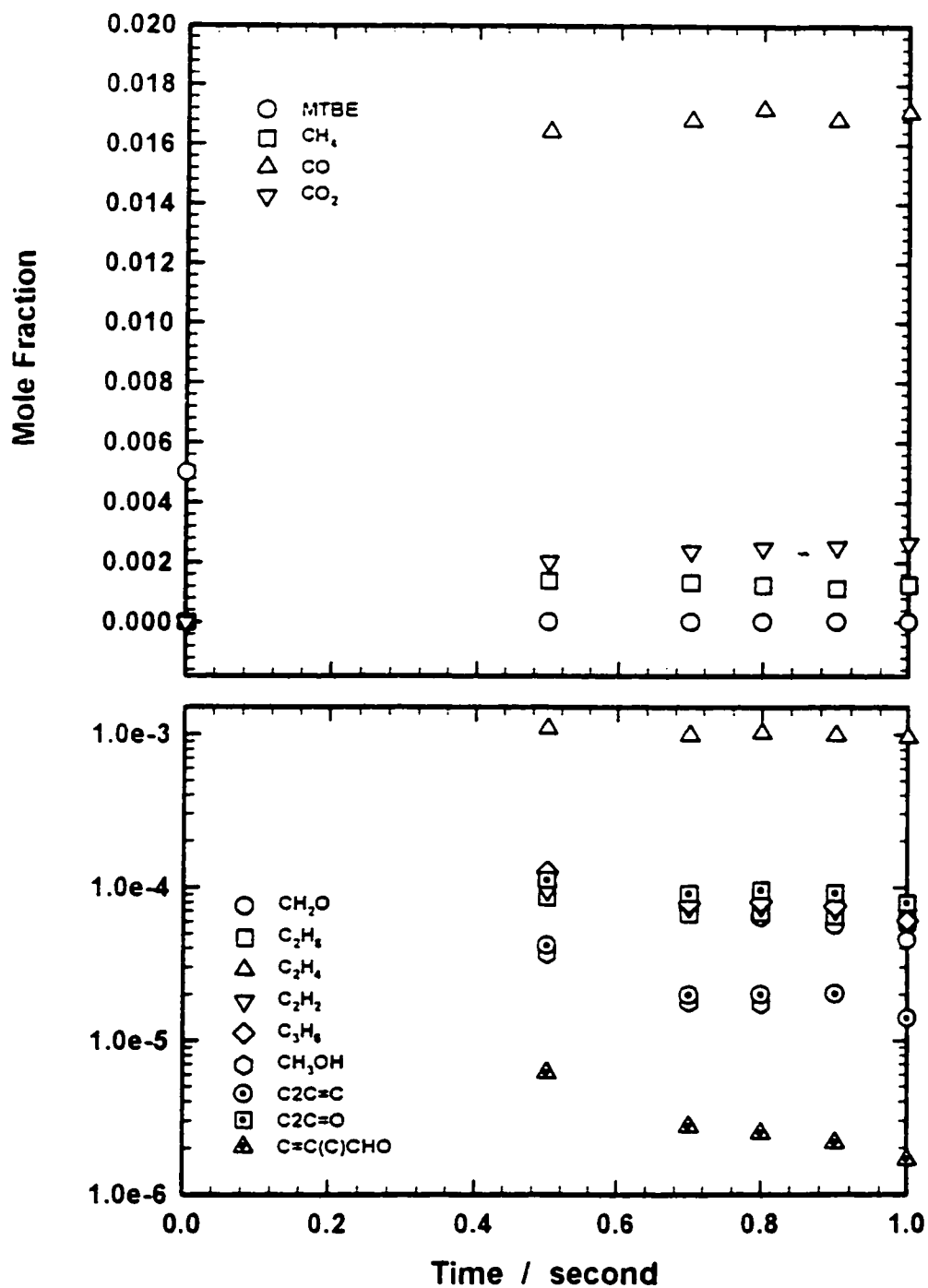


Figure IIC. 20 Experimental result of 0.5% MTBE oxidation product distribution at $\phi = 1.00$, $P = 4$ atm, $T = 923$ K

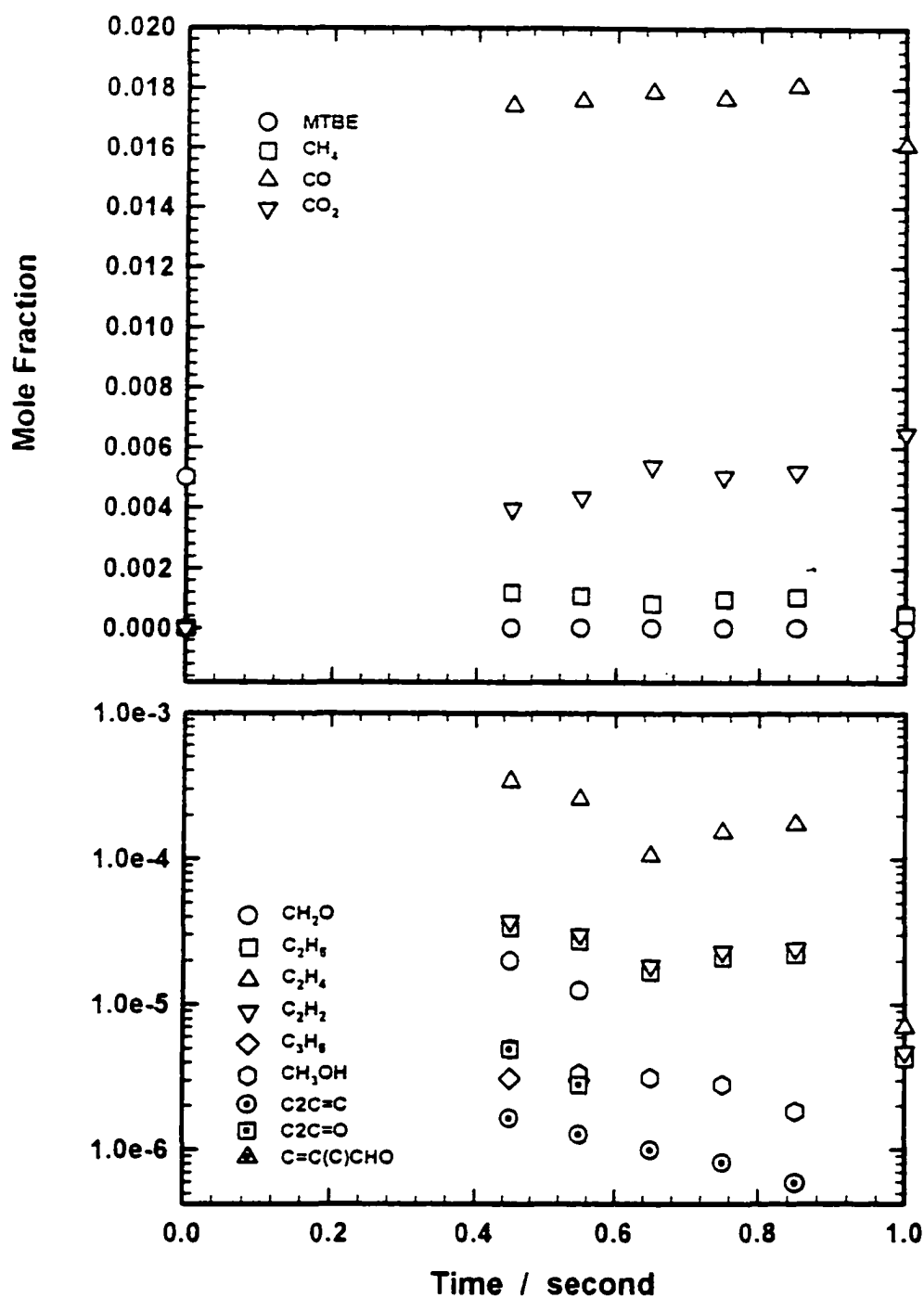


Figure IIC. 21 Experimental result of 0.5% MTBE oxidation product distribution at $\phi = 1.00$, $P = 4$ atm, $T = 973$ K

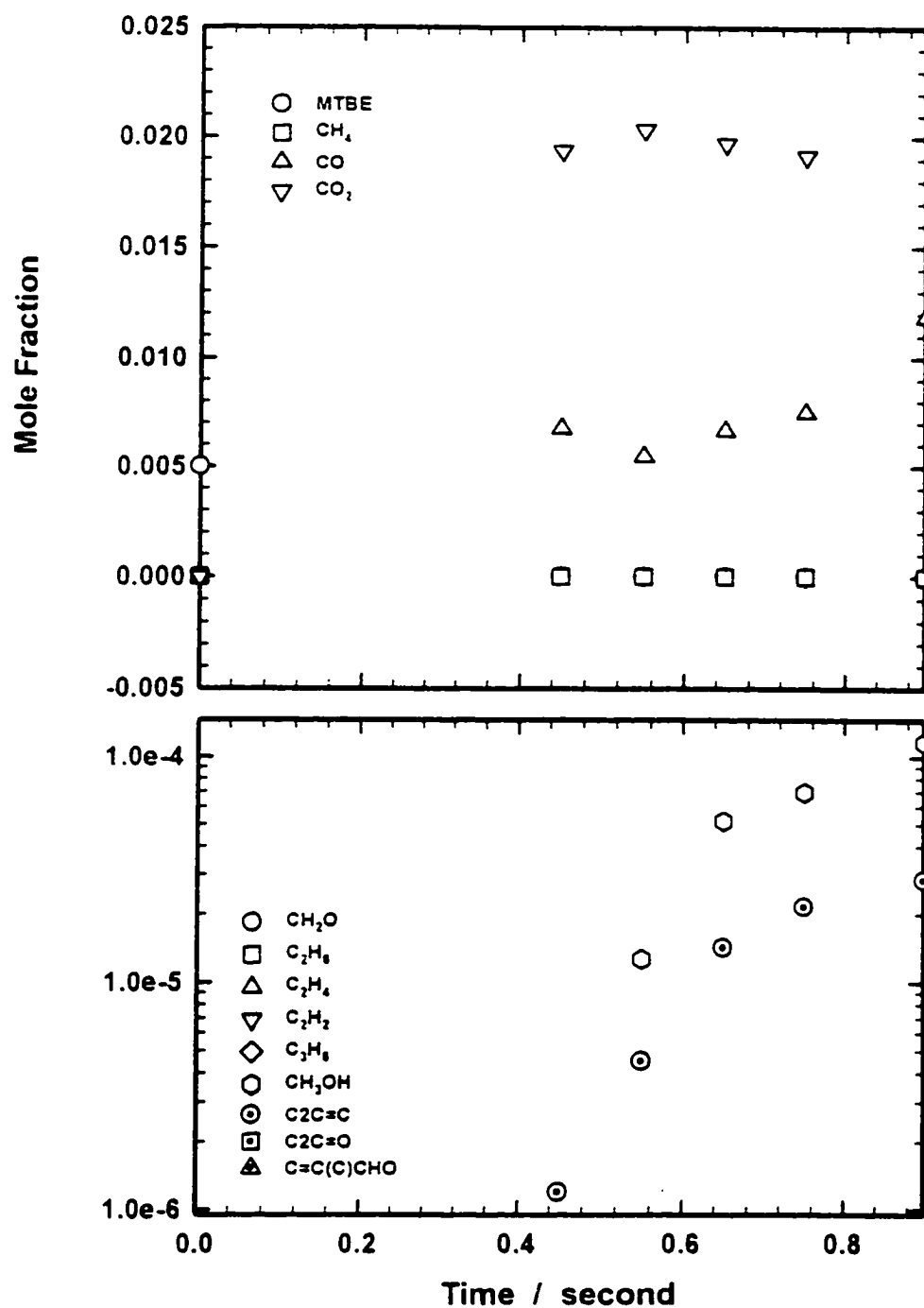


Figure IIC. 22 Experimental result of 0.5% MTBE oxidation product distribution at $\phi = 1.00$, $P = 4$ atm, $T = 1023$ K

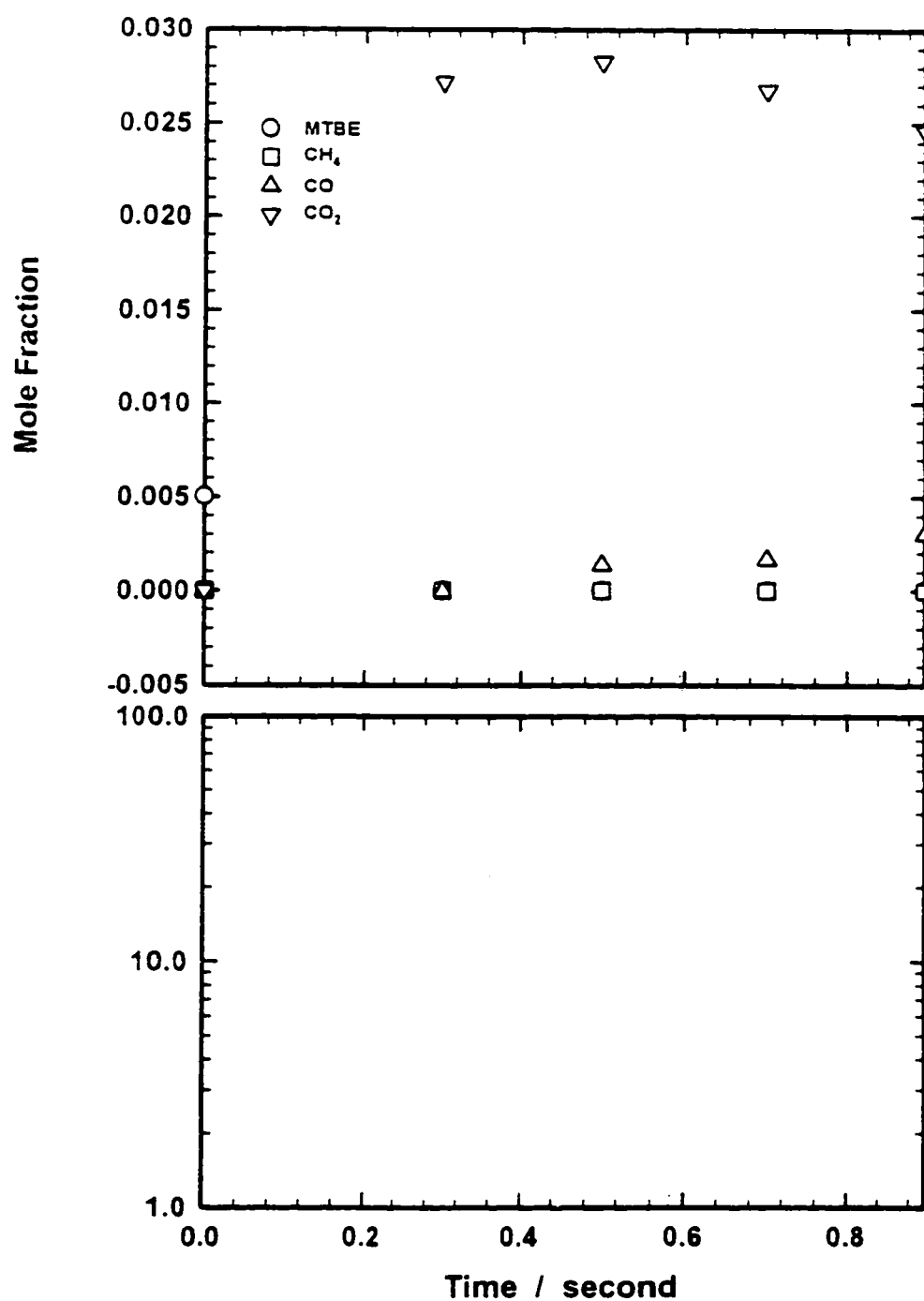


Figure IIC. 23 Experimental result of 0.5% MTBE oxidation product distribution at $\phi = 1.00$, $P = 4$ atm, $T = 1073$ K

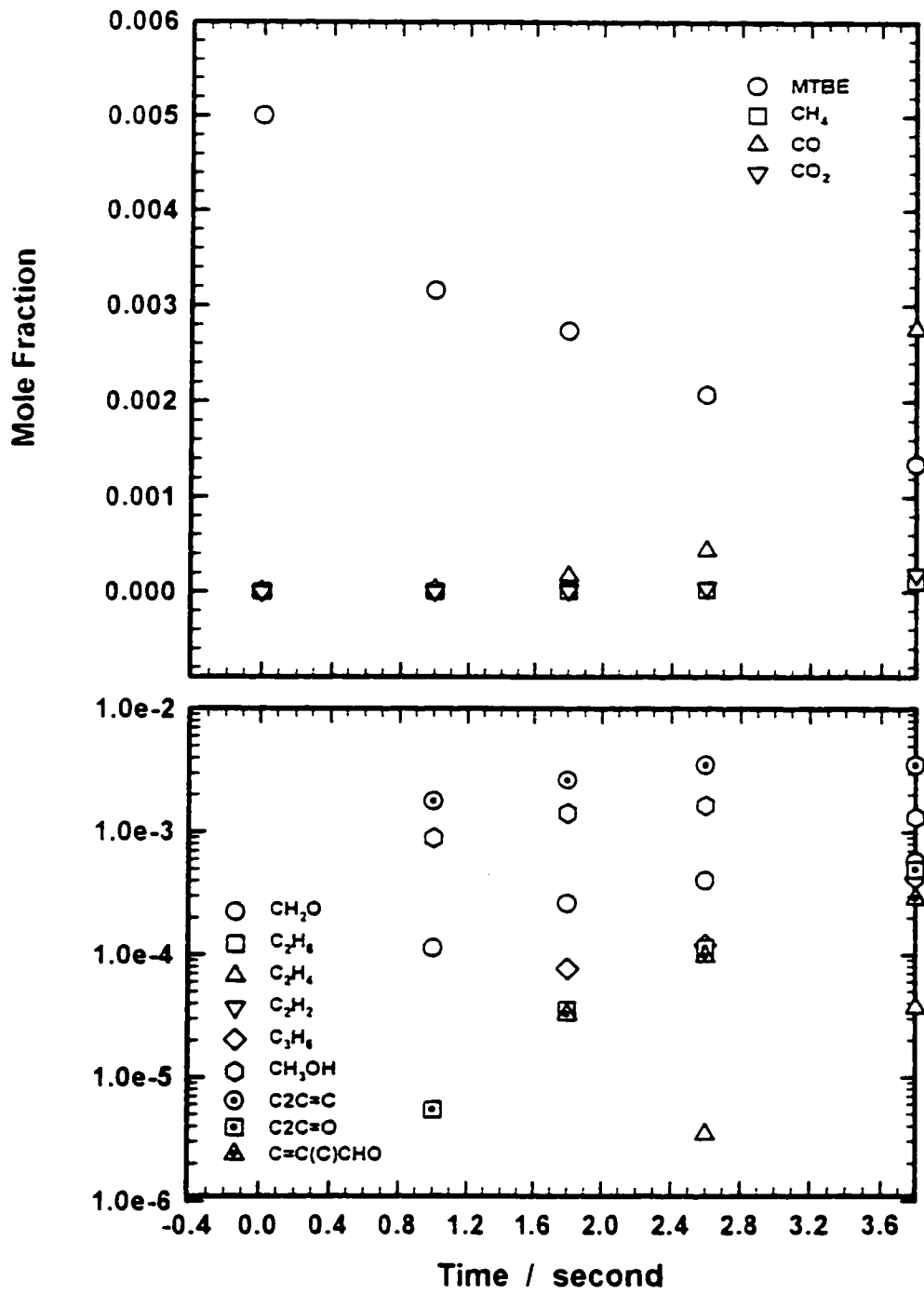


Figure IIC. 24 Experimental result of 0.5% MTBE oxidation product distribution at $\phi = 1.00$, $P = 7$ atm, $T = 798$ K

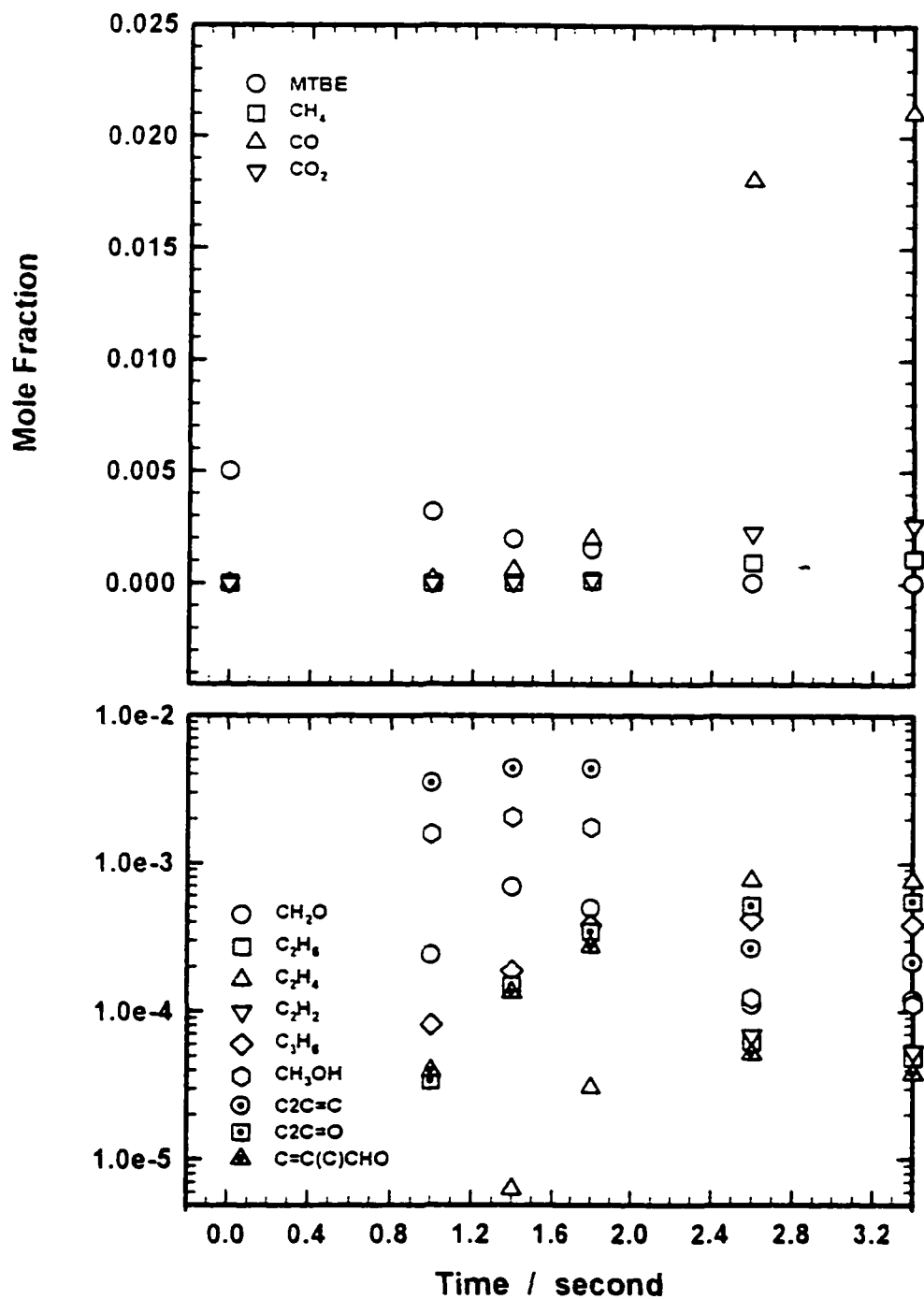


Figure IIC. 25 Experimental result of 0.5% MTBE oxidation product distribution at $\phi = 1.00$, $P = 7$ atm, $T = 823$ K

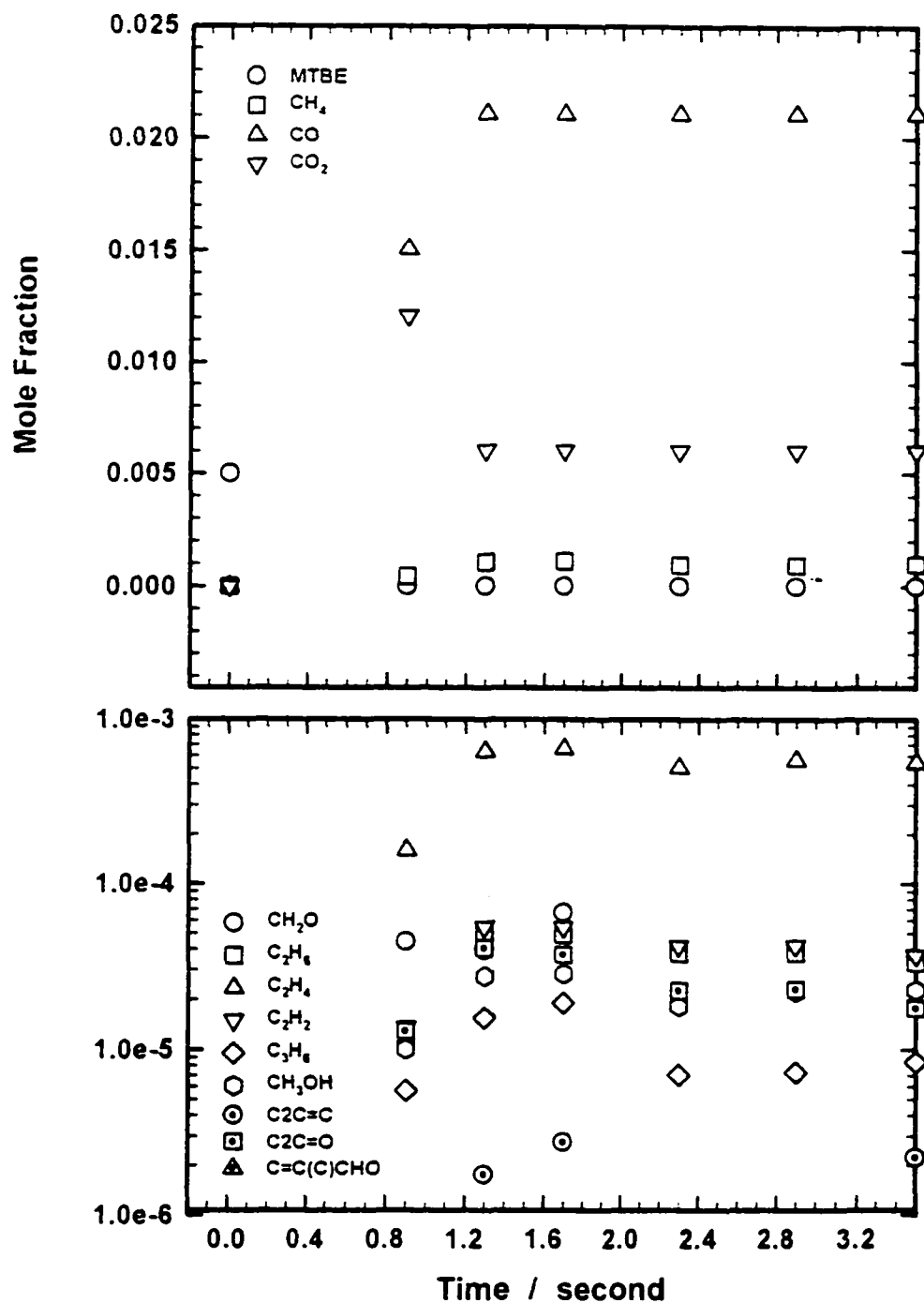


Figure IIC. 26 Experimental result of 0.5% MTBE oxidation product distribution at $\phi = 1.00$, $P = 7$ atm, $T = 873$ K

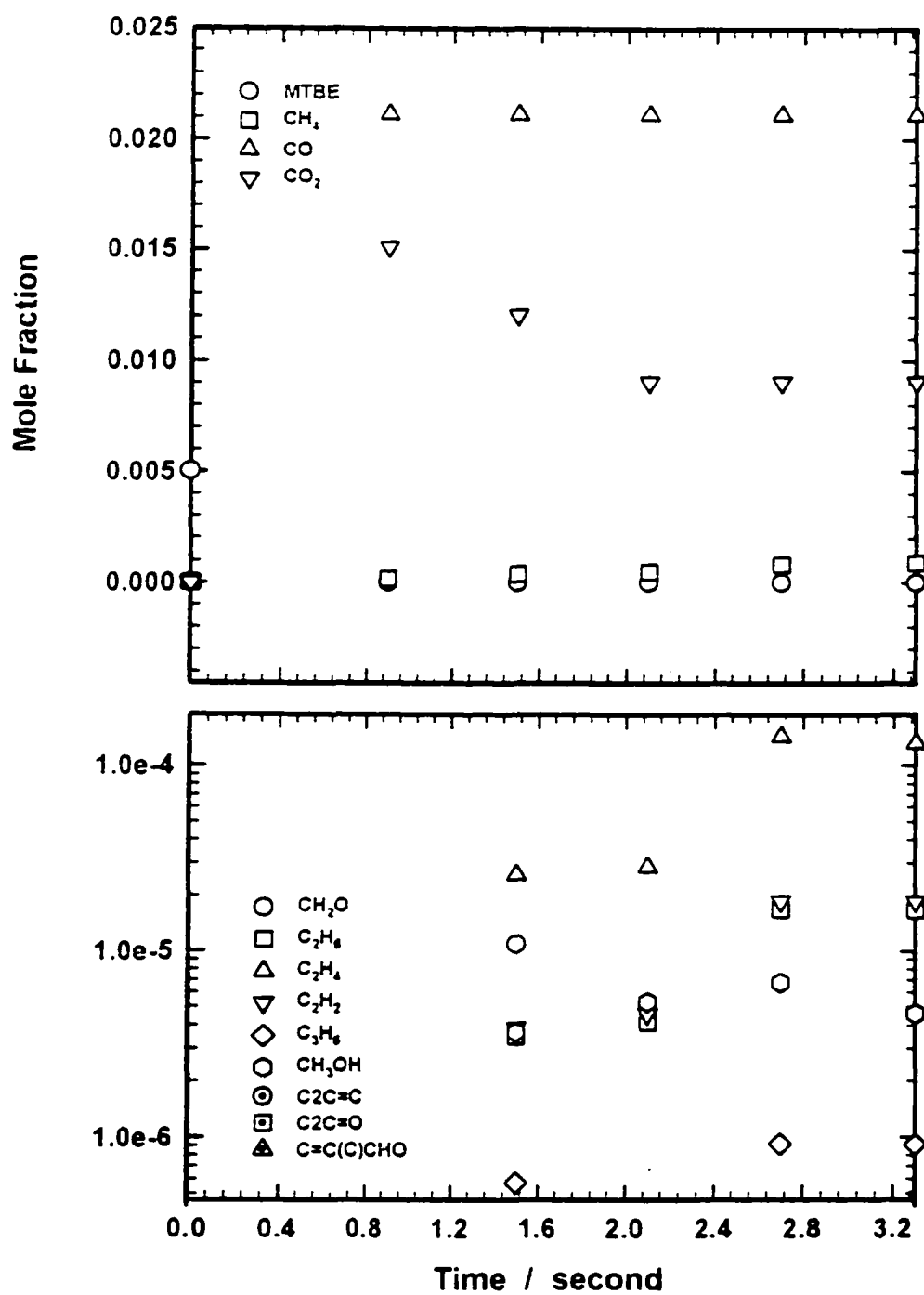


Figure IIC. 27 Experimental result of 0.5% MTBE oxidation product distribution at $\phi = 1.00$, $P = 7$ atm, $T = 923$ K

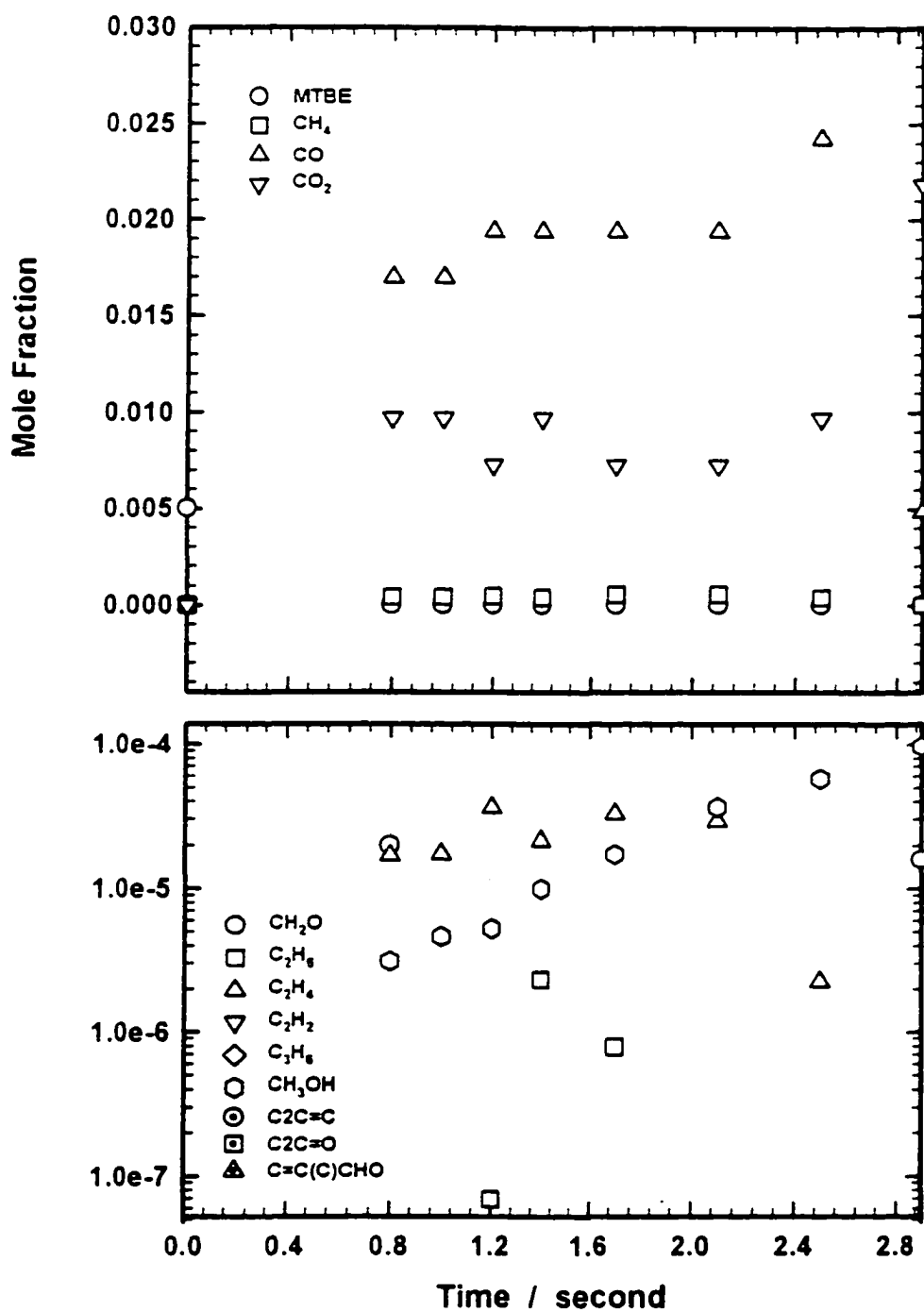


Figure IIC. 28 Experimental result of 0.5% MTBE oxidation product distribution at $\phi = 1.00$, $P = 7$ atm, $T = 1023$ K

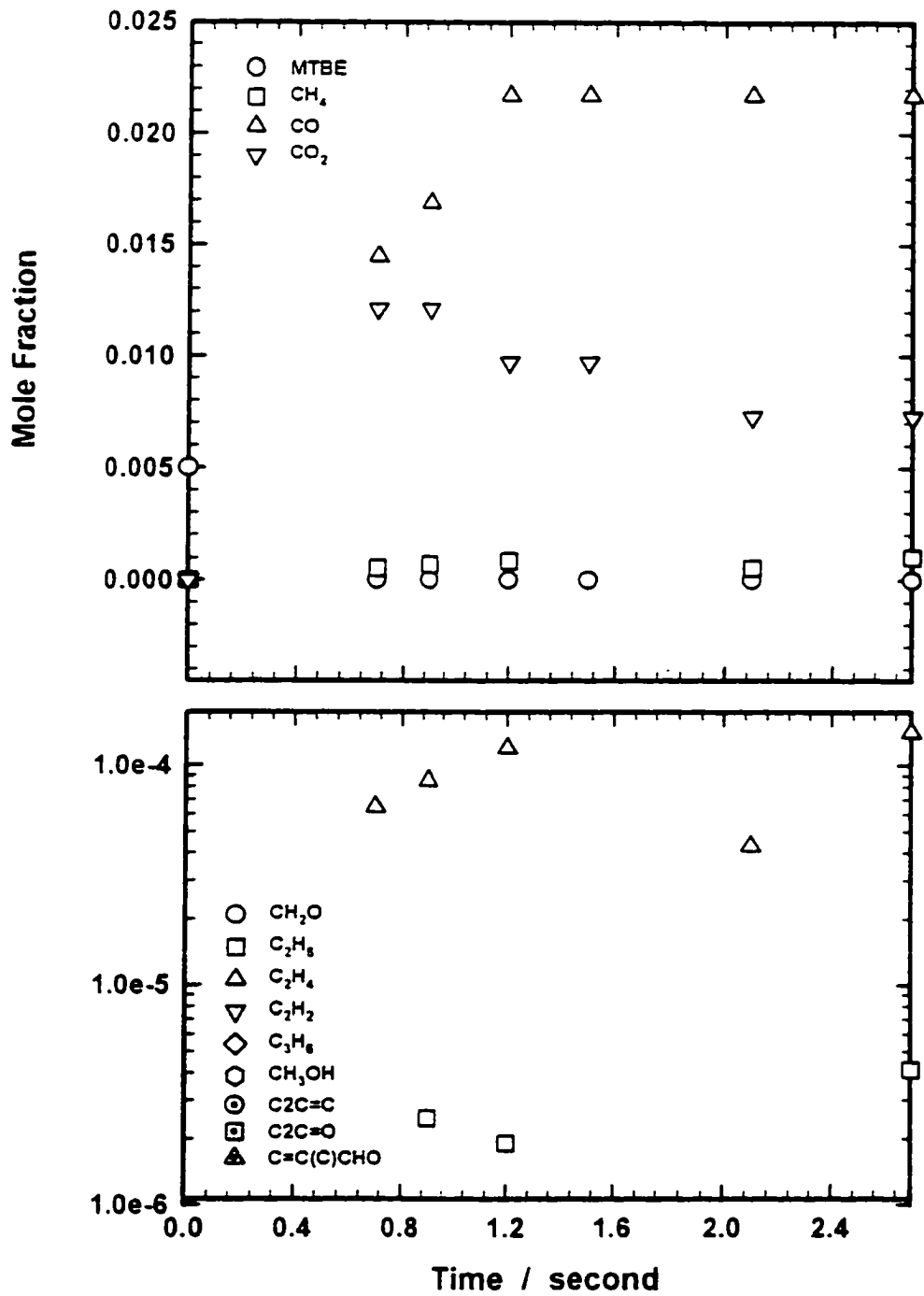


Figure IIC. 29 Experimental result of 0.5% MTBE oxidation product distribution at $\phi = 1.00$, $P = 7$ atm, $T = 1073$ K

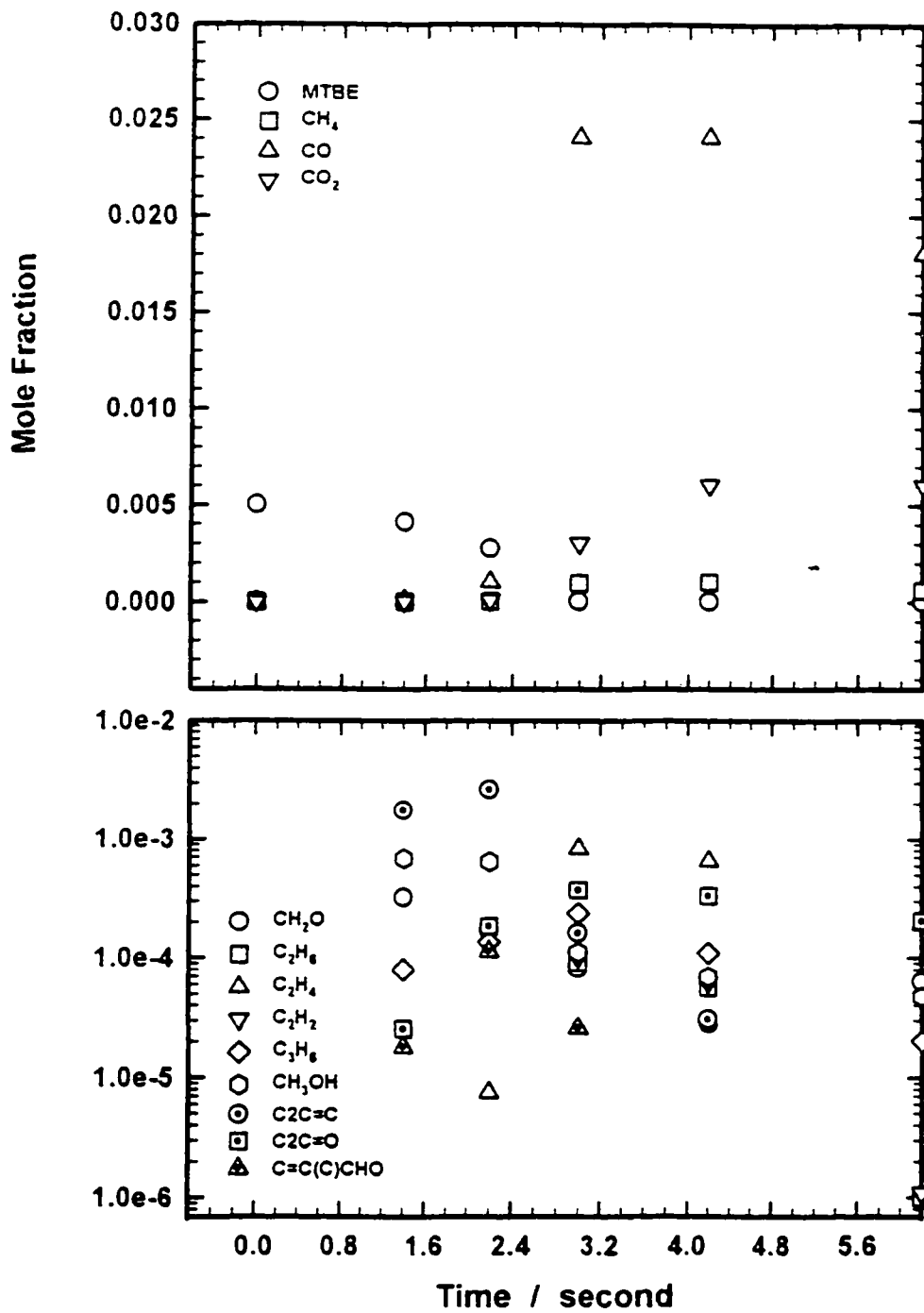


Figure IIC. 30 Experimental result of 0.5% MTBE oxidation product distribution at $\phi = 1.00$, $P = 10$ atm, $T = 798$ K

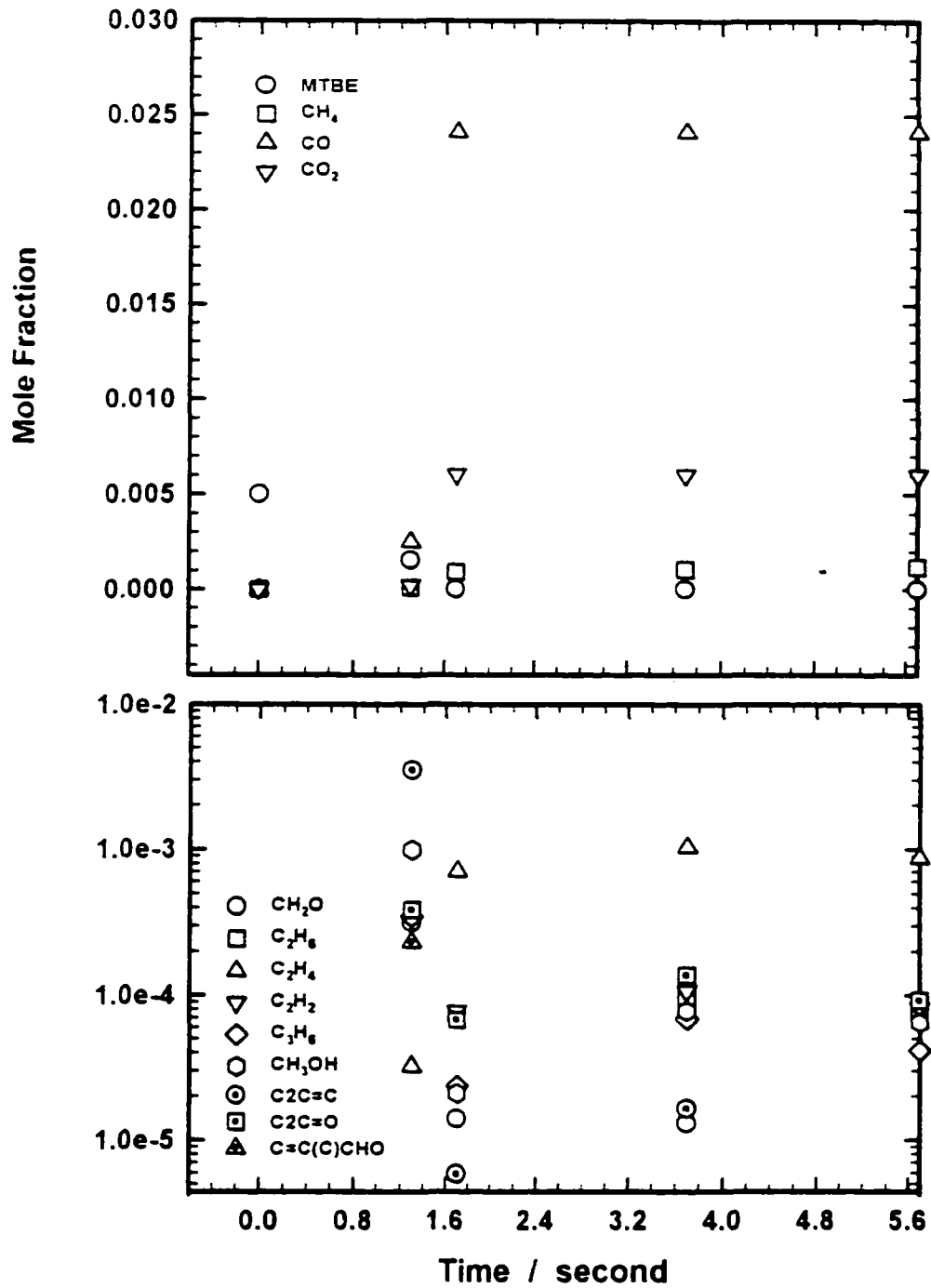


Figure IIC. 31 Experimental result of 0.5% MTBE oxidation product distribution at $\phi = 1.00$, $P = 10$ atm, $T = 823$ K

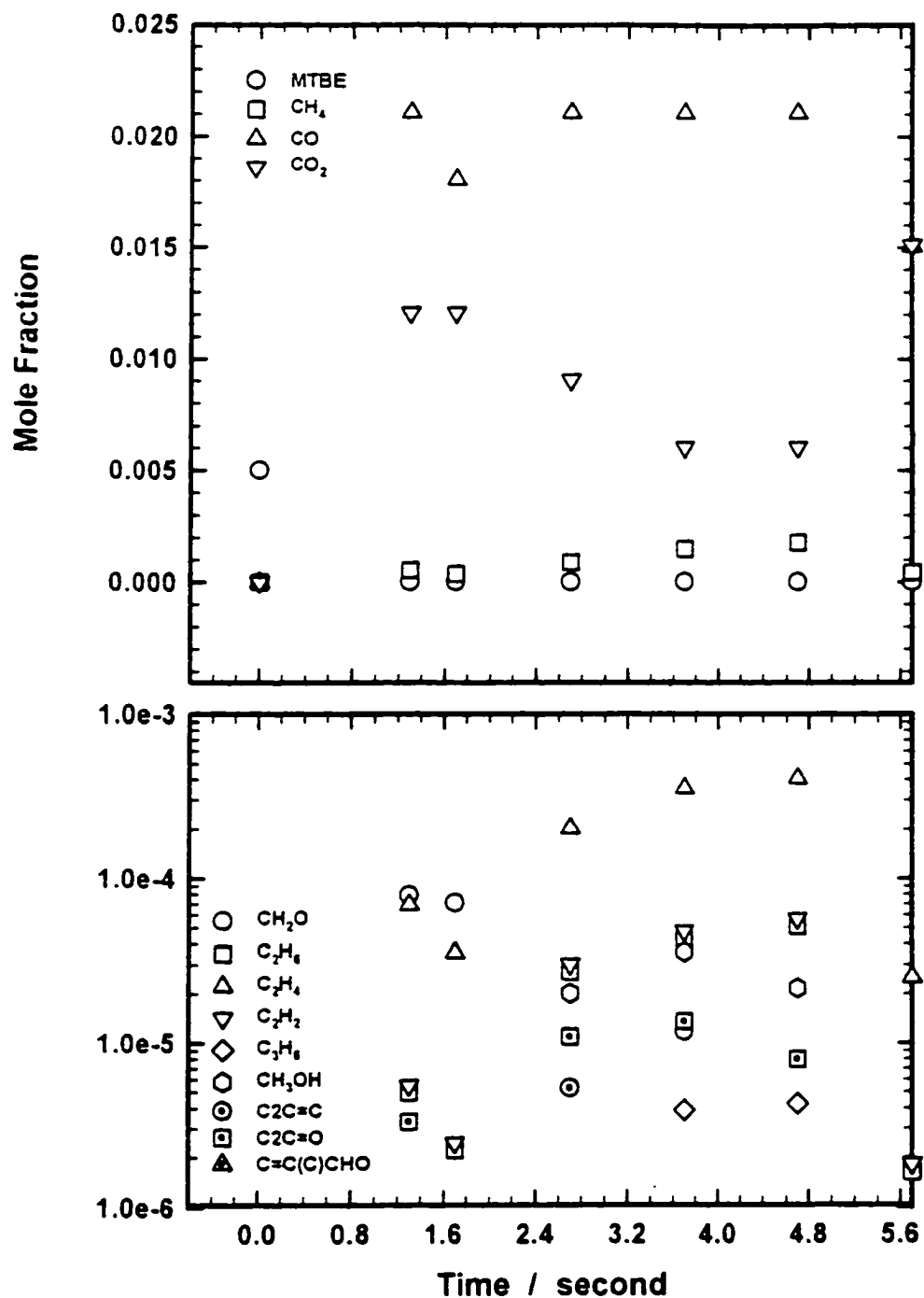


Figure IIC. 32 Experimental result of 0.5% MTBE oxidation product distribution at $\phi = 1.00$, $P = 10$ atm, $T = 873$ K

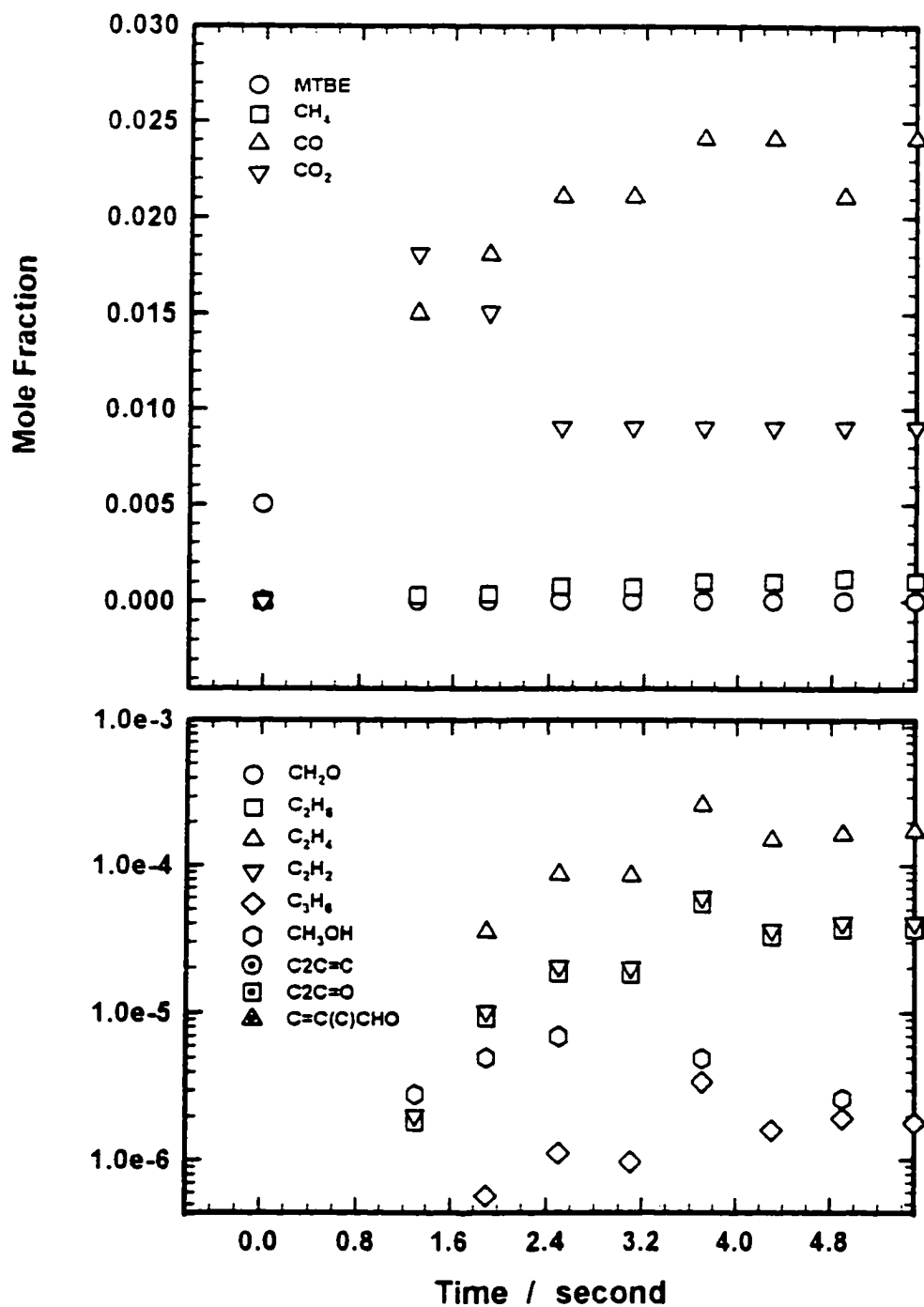


Figure IIC. 33 Experimental result of 0.5% MTBE oxidation product distribution at $\phi = 1.00$, $P = 10$ atm, $T = 923$ K

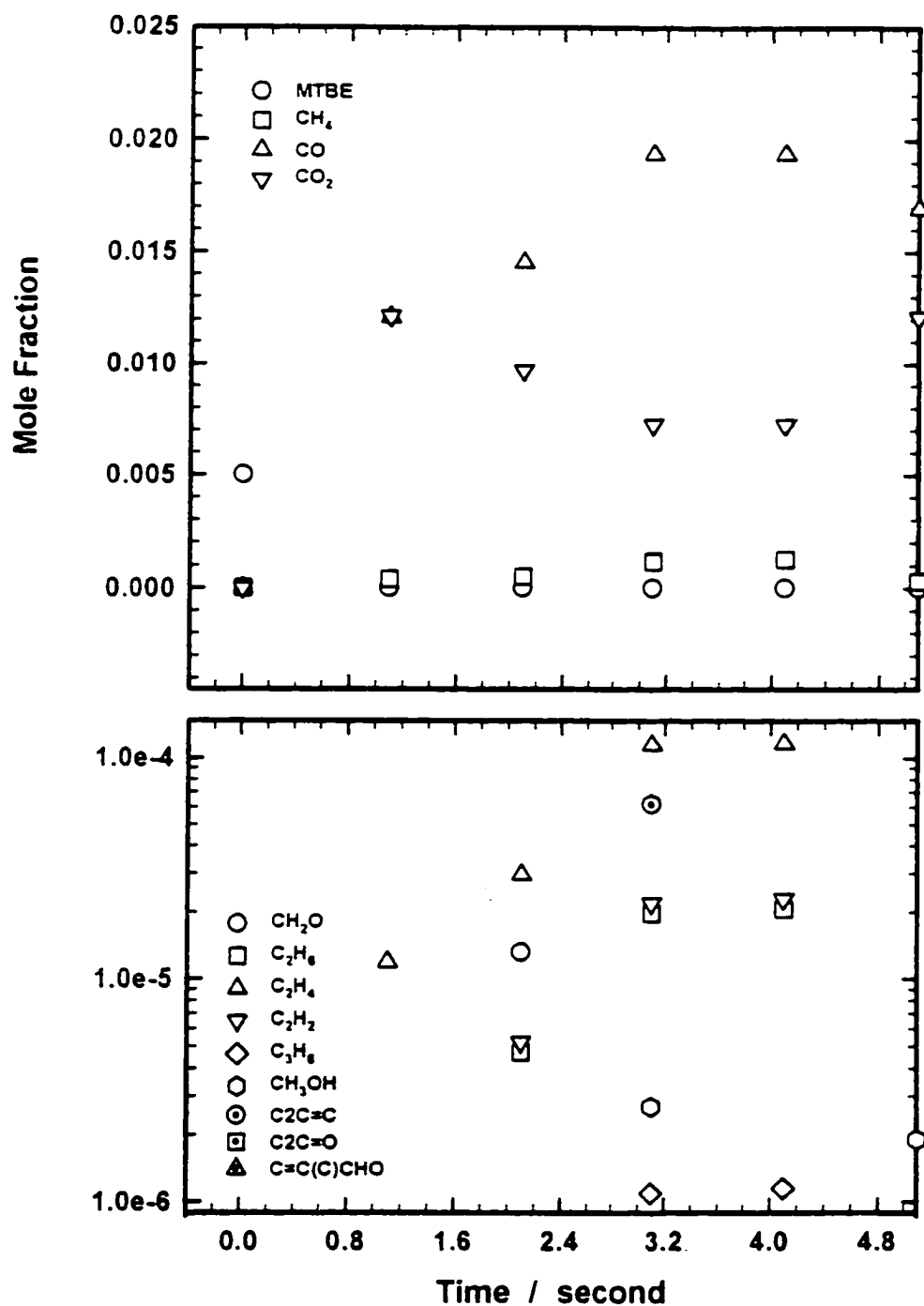


Figure IIC. 34 Experimental result of 0.5% MTBE oxidation product distribution at $\phi = 1.00$, $P = 10$ atm, $T = 973$ K

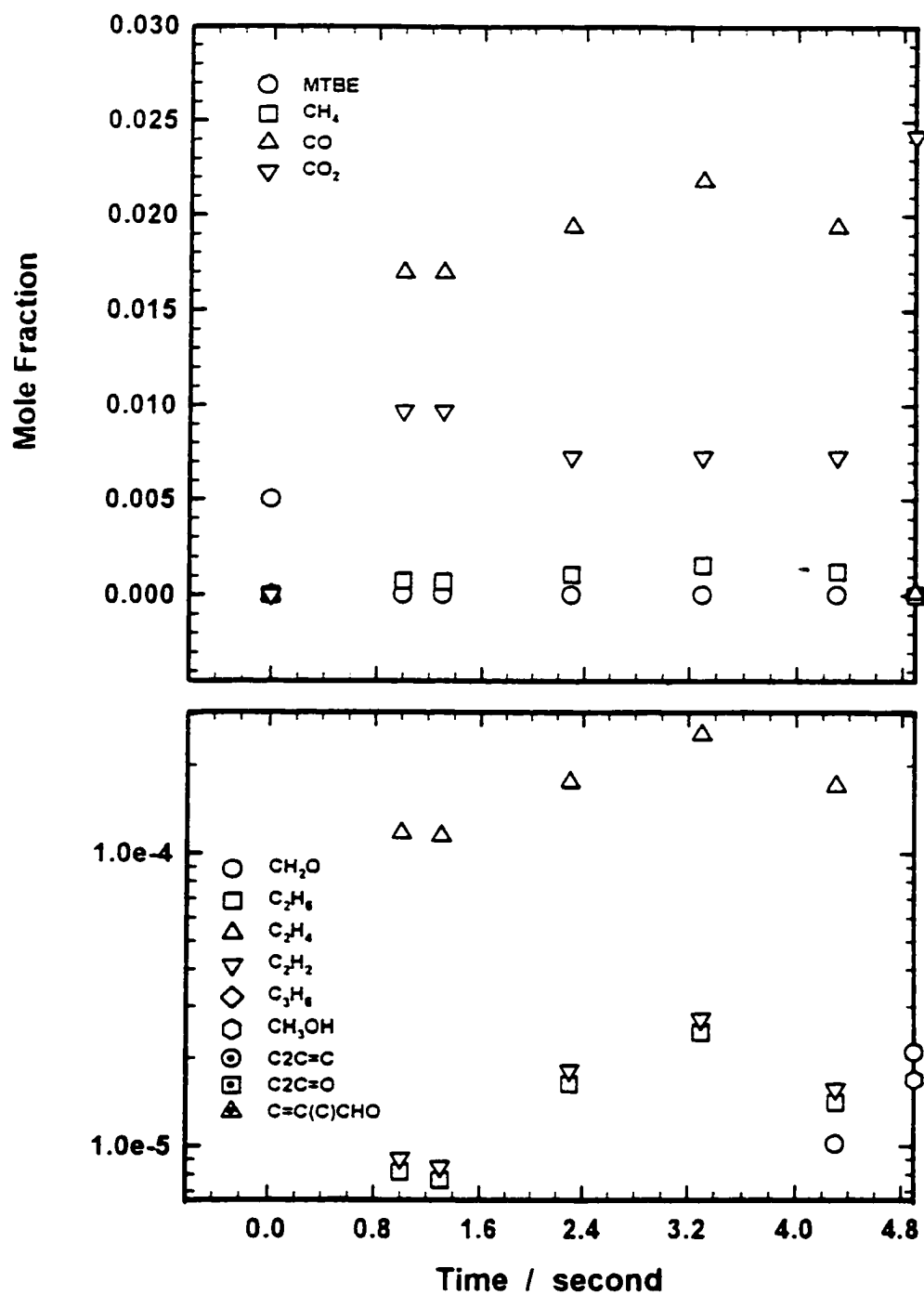


Figure IIC. 35 Experimental result of 0.5% MTBE oxidation product distribution at $\phi = 1.00$, $P = 10$ atm, $T = 1023$ K

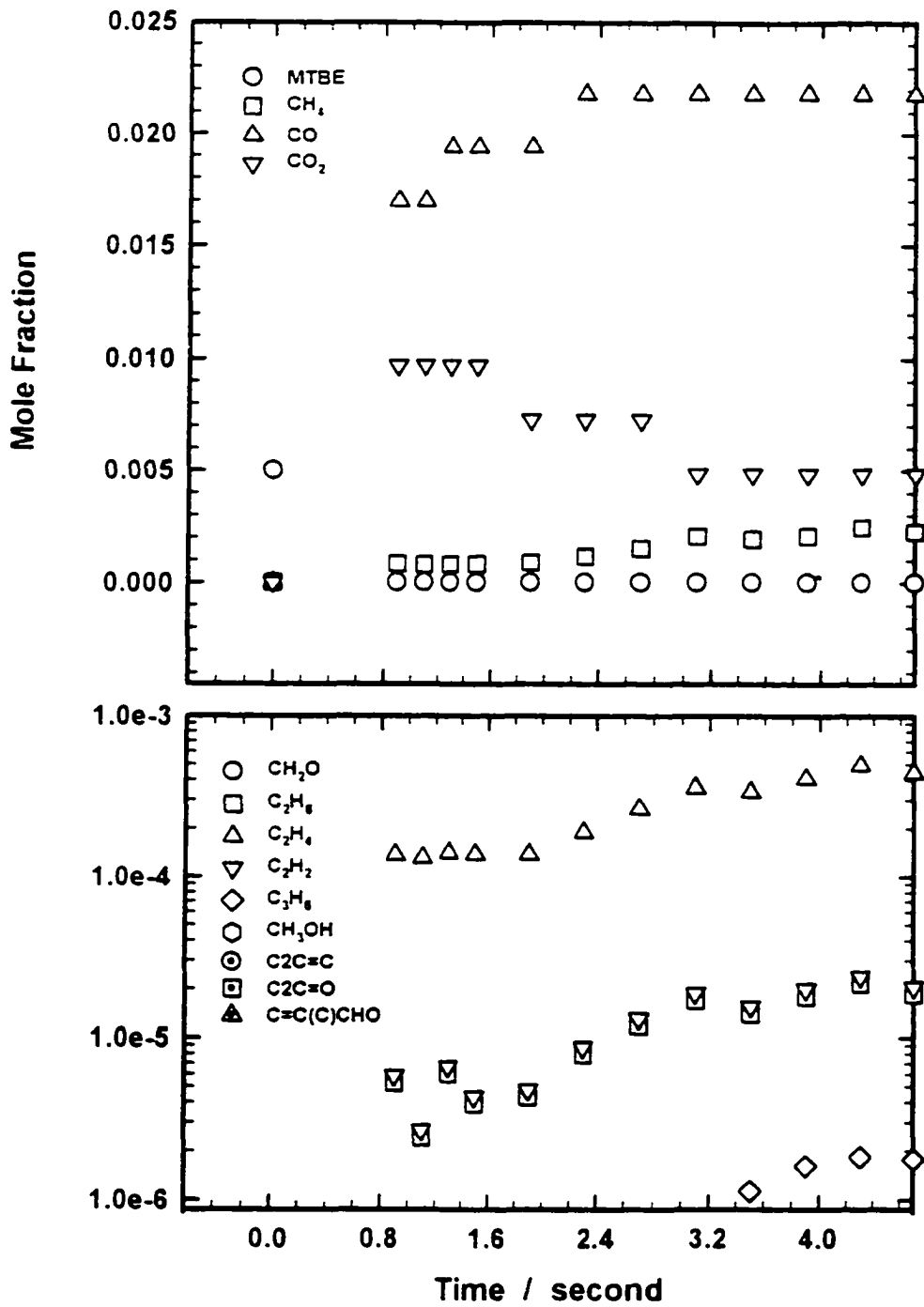


Figure IIC. 36 Experimental result of 0.5% MTBE oxidation product distribution at $\phi = 1.00$, $P = 10$ atm, $T = 1073$ K

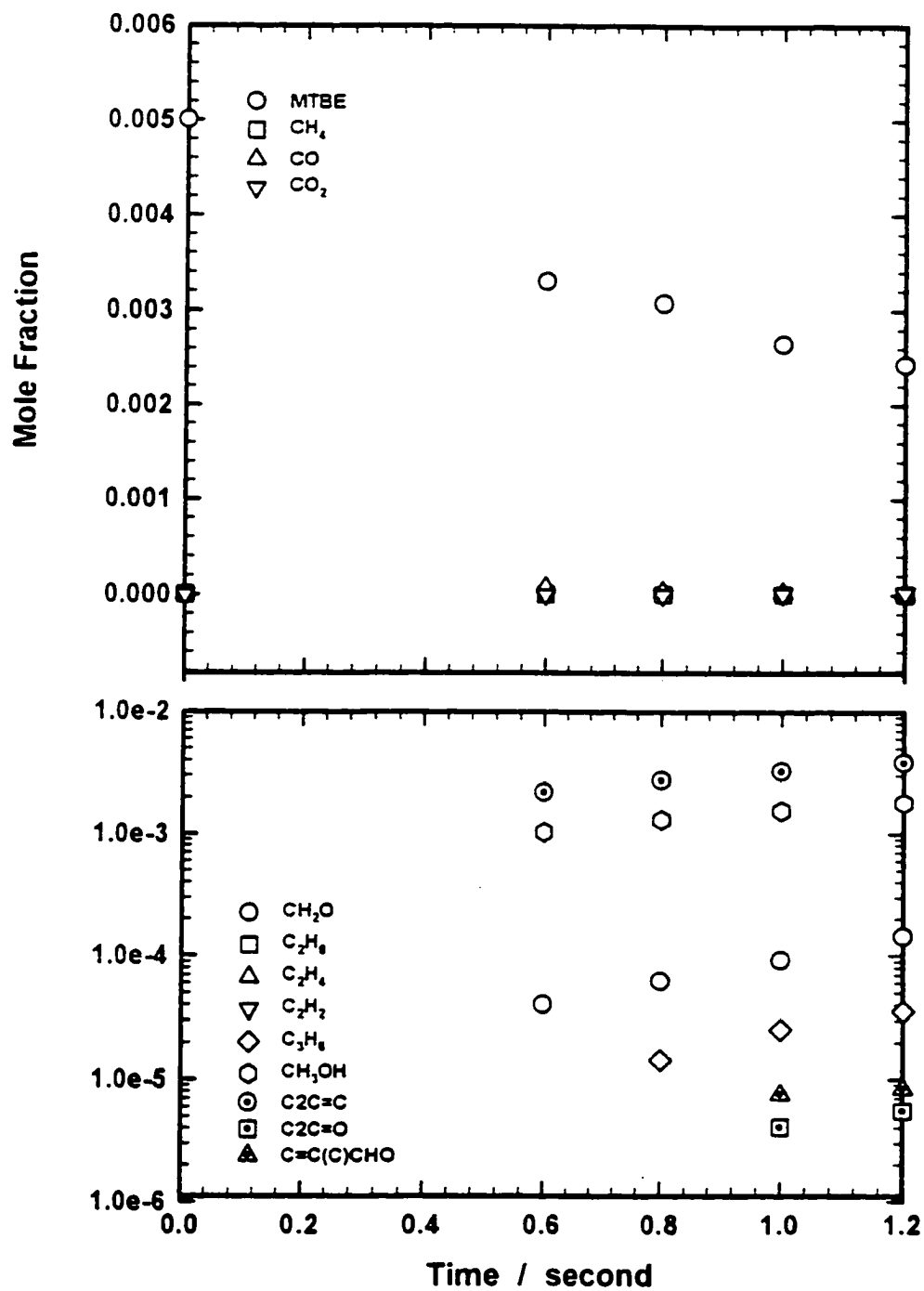


Figure IIC. 37 Experimental result of 0.5% MTBE oxidation product distribution at $\phi = 1.50$, $P = 4$ atm, $T = 823$ K

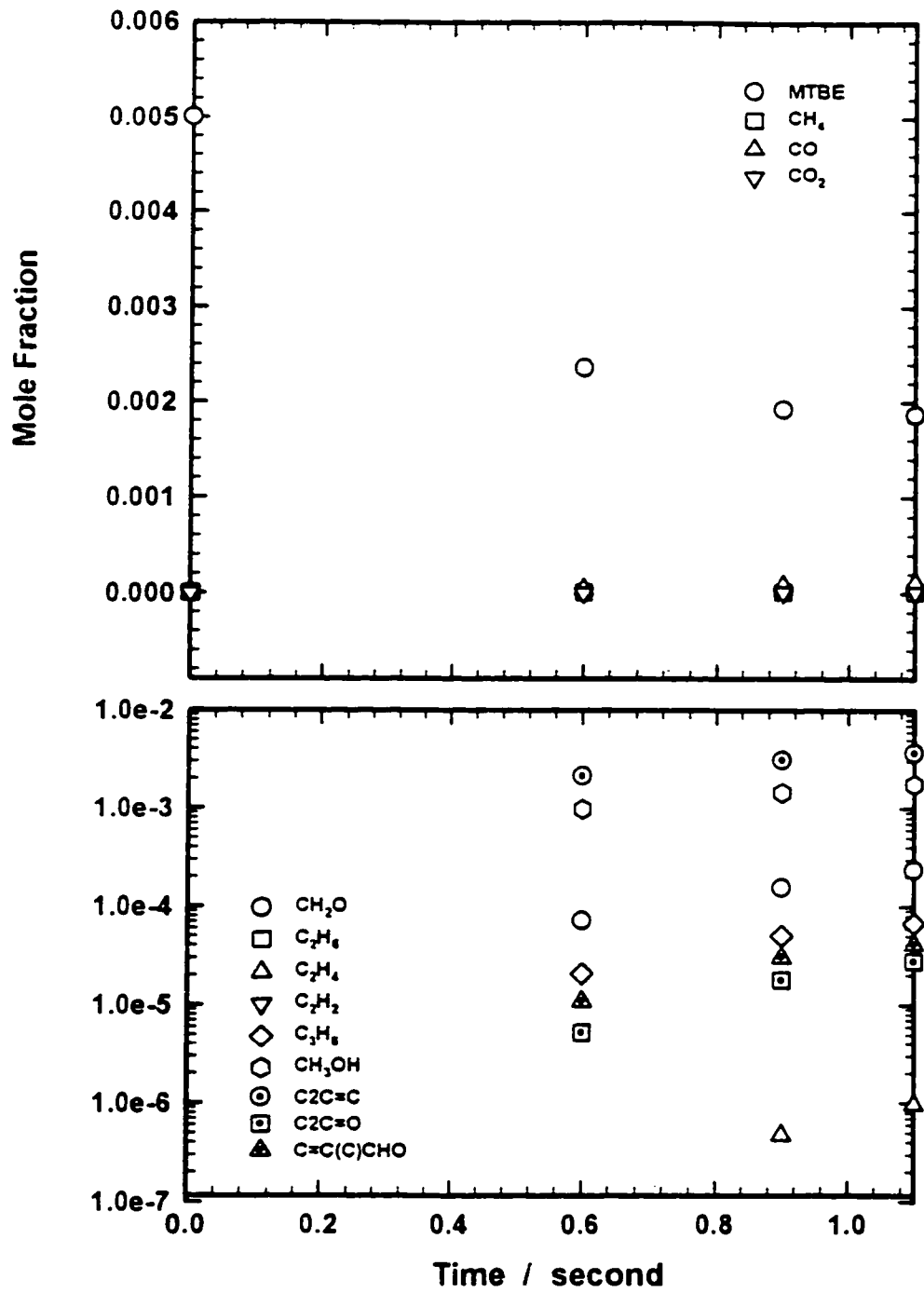


Figure IIC. 38 Experimental result of 0.5% MTBE oxidation product distribution at $\phi = 1.50$, $P = 4$ atm, $T = 848$ K

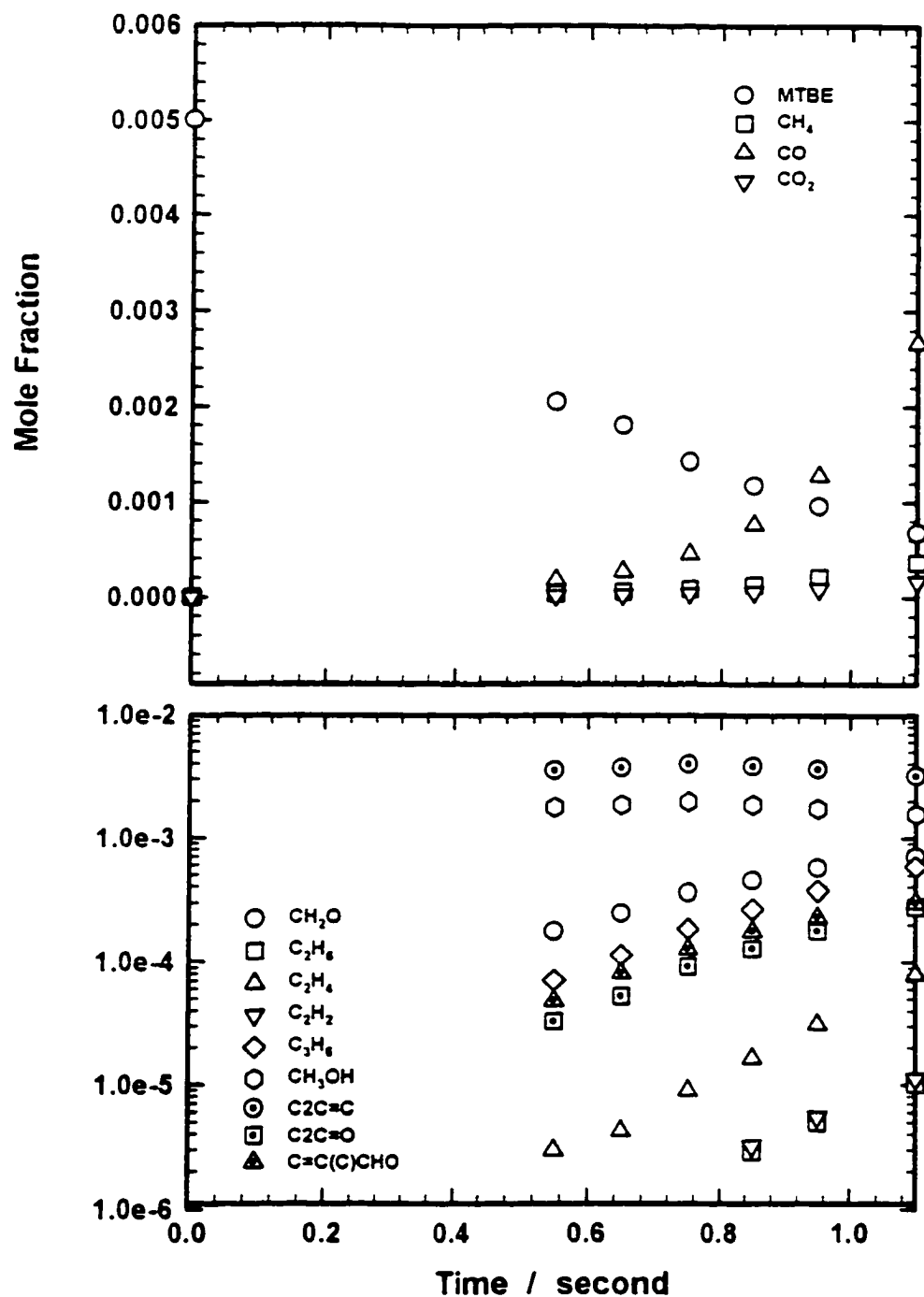


Figure IIC. 39 Experimental result of 0.5% MTBE oxidation product distribution at $\phi = 1.50$, $P = 4$ atm, $T = 873$ K

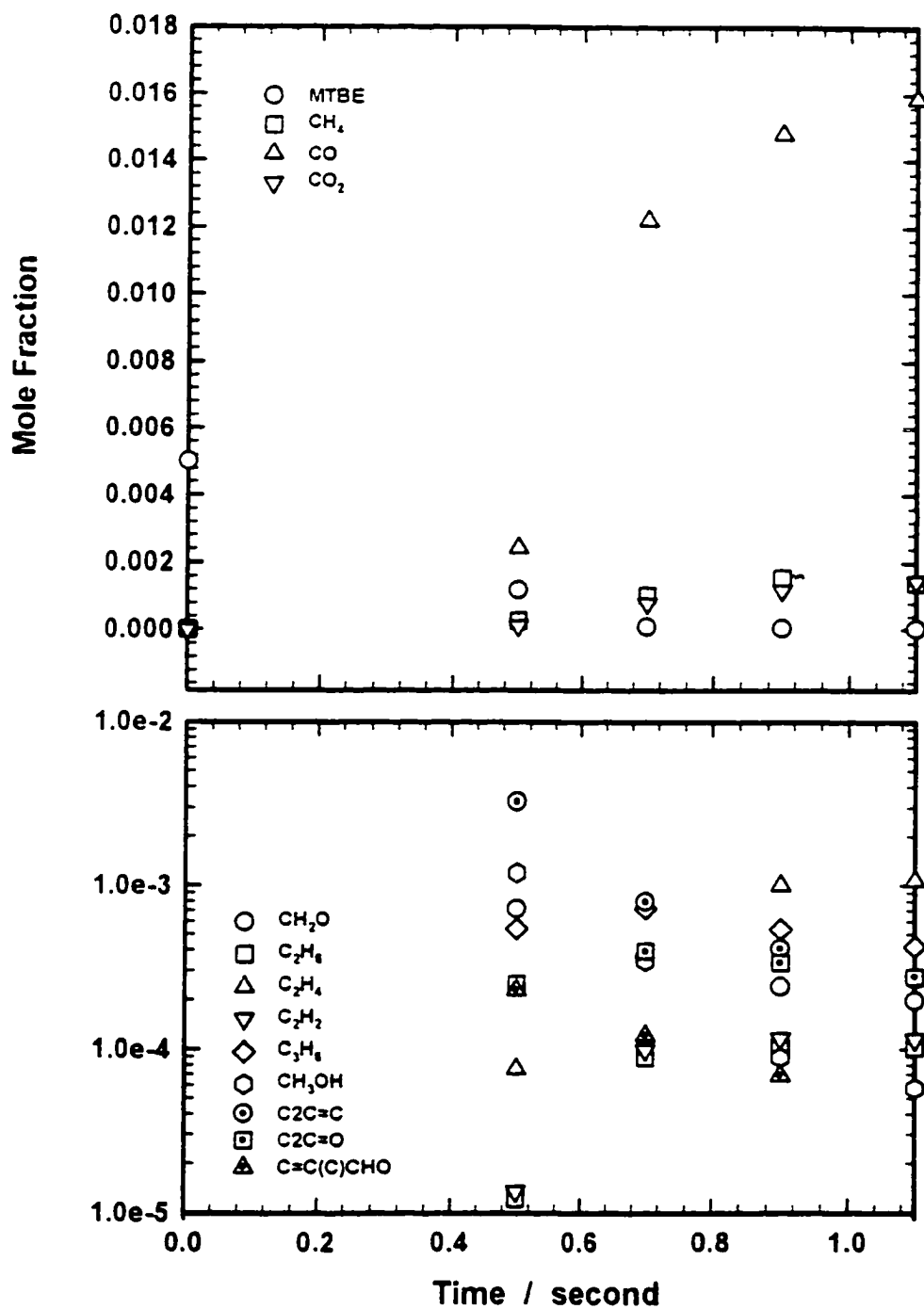


Figure IIC. 40 Experimental result of 0.5% MTBE oxidation product distribution at $\phi = 1.50$, $P = 4$ atm, $T = 898$ K

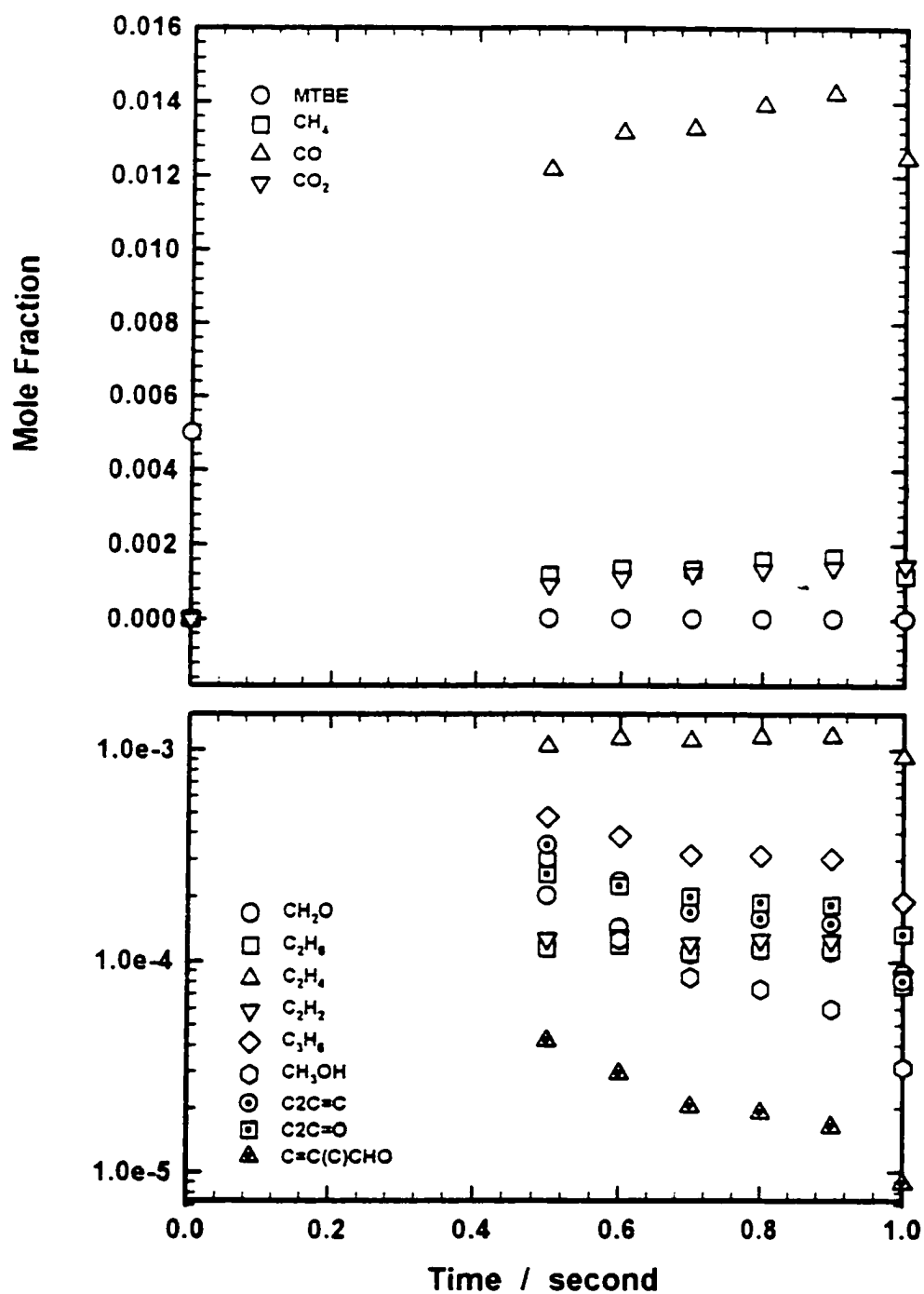


Figure IIC. 41 Experimental result of 0.5% MTBE oxidation product distribution at $\phi = 1.50$, $P = 4$ atm, $T = 923$ K

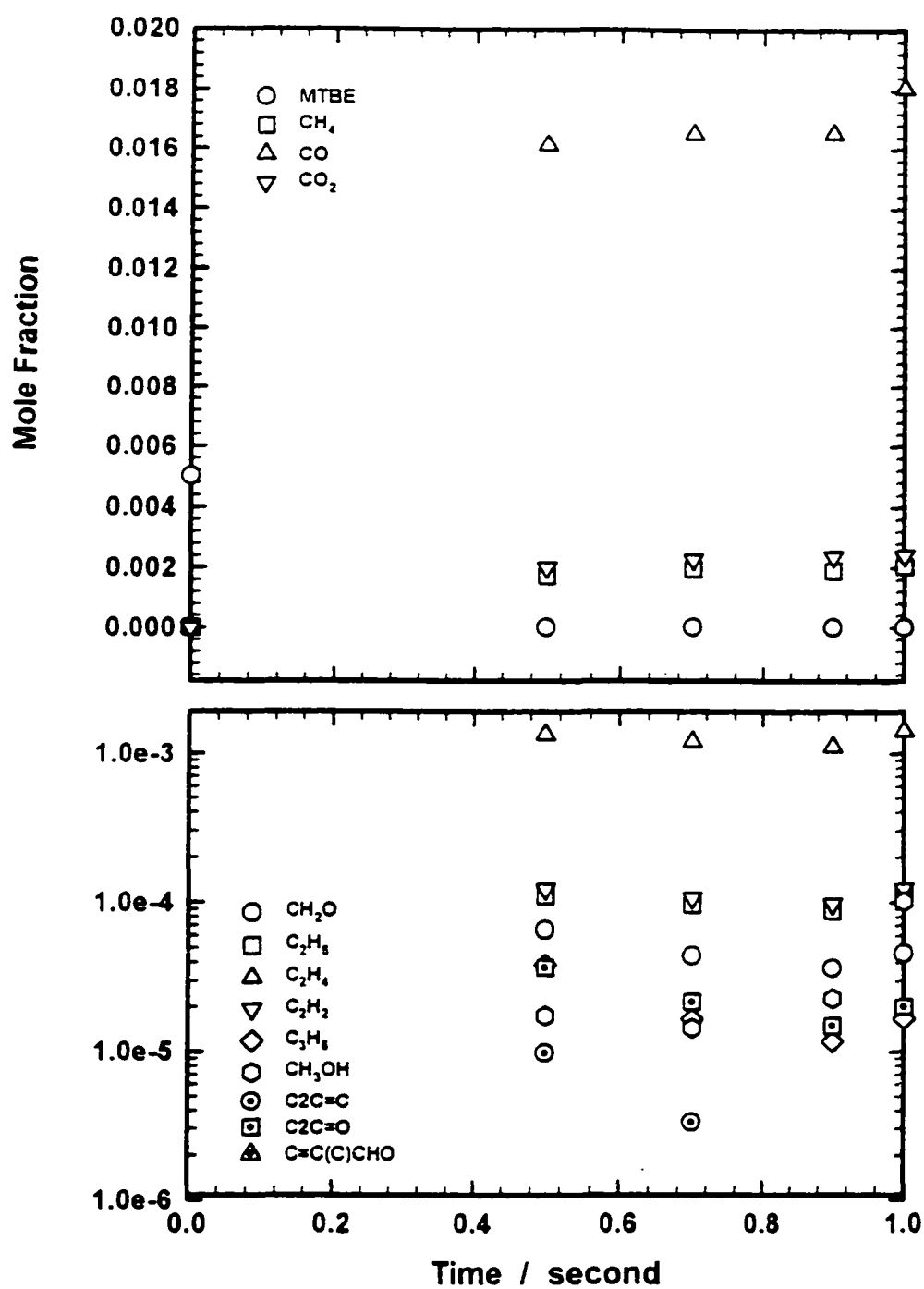


Figure IIC. 42 Experimental result of 0.5% MTBE oxidation product distribution at $\phi = 1.50$, $P = 4$ atm, $T = 998$ K

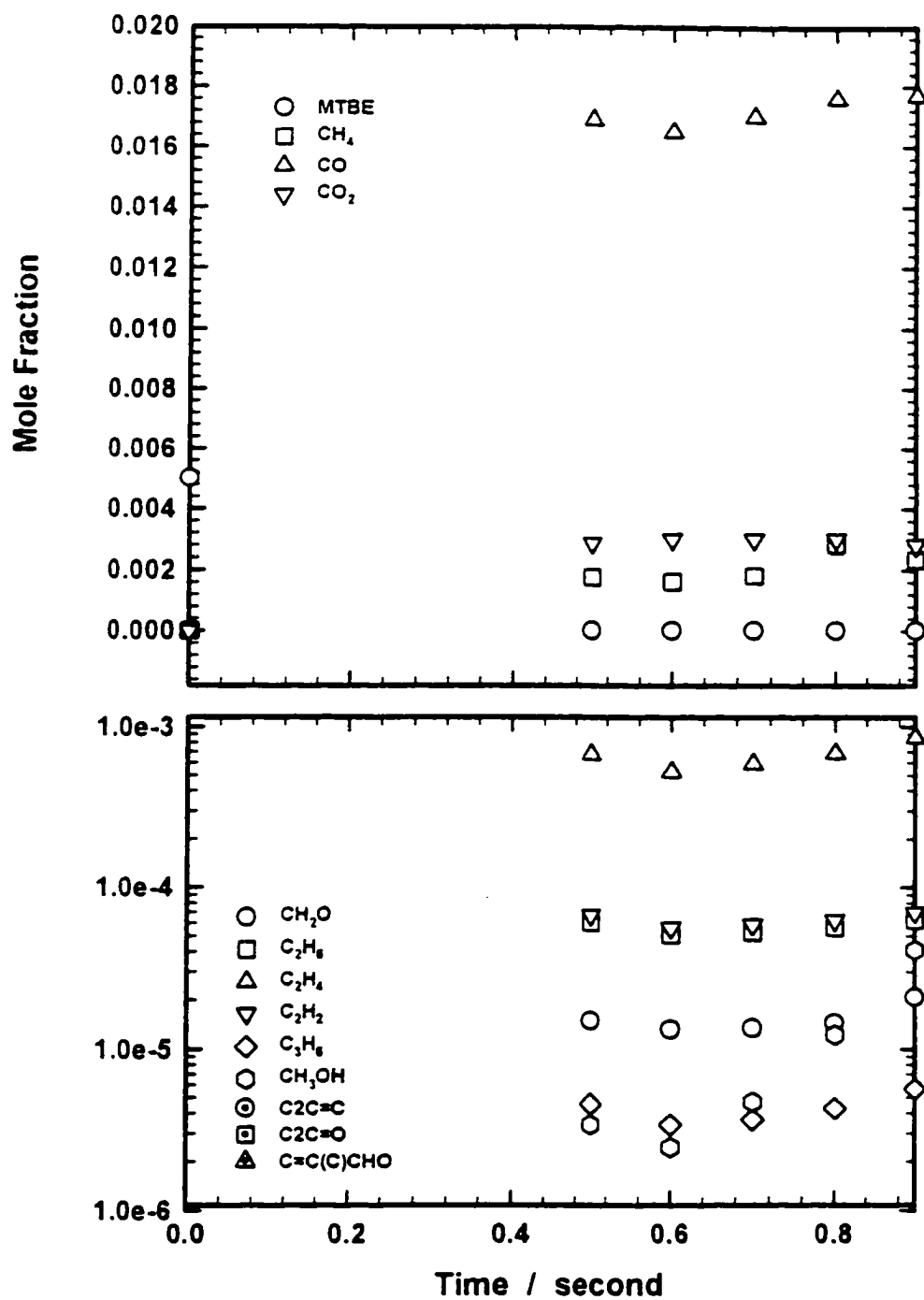


Figure IIC. 43 Experimental result of 0.5% MTBE oxidation product distribution at $\phi = 1.50$, $P = 4$ atm, $T = 1048$ K

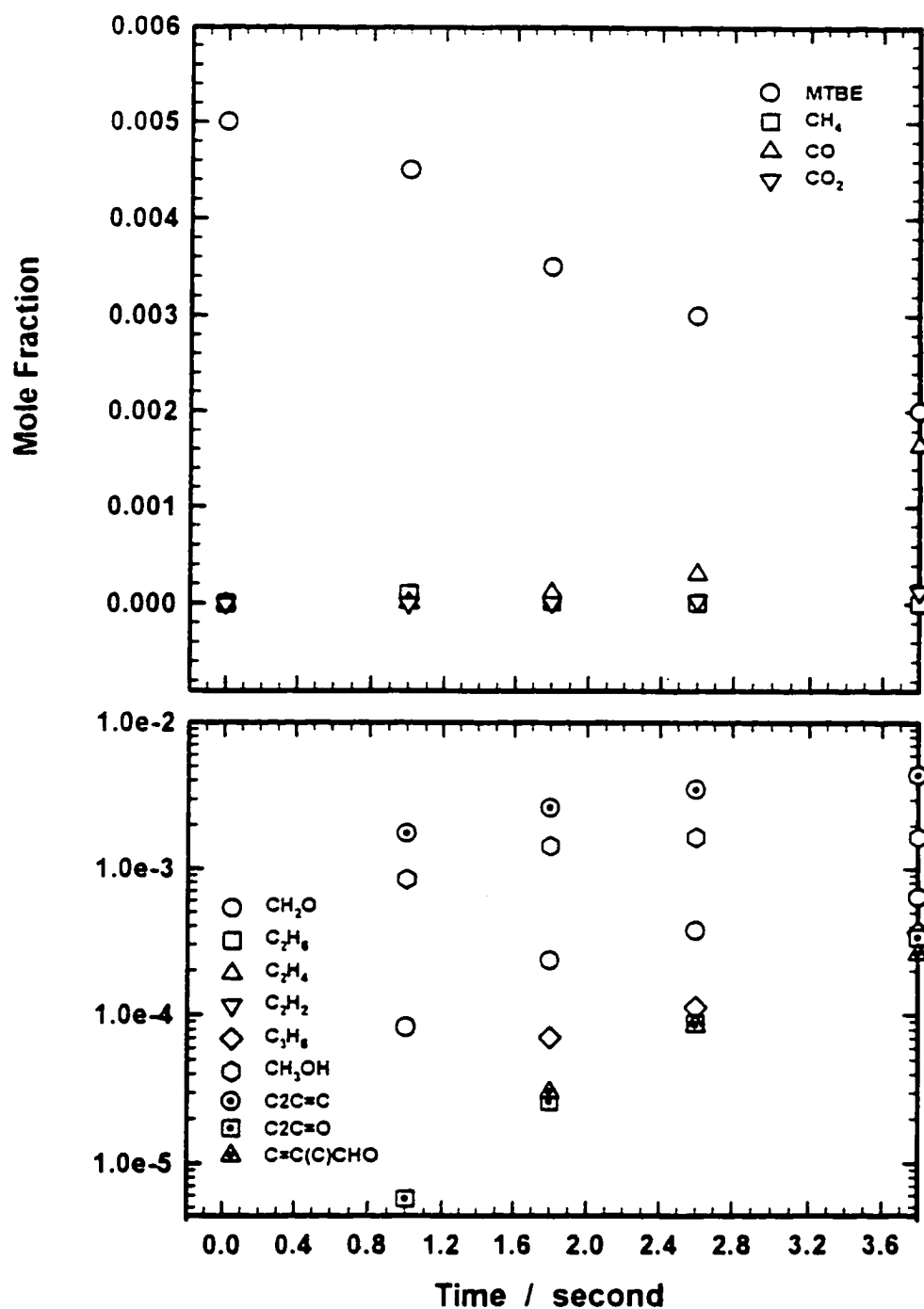


Figure IIC. 44 Experimental result of 0.5% MTBE oxidation product distribution at $\phi = 1.50$, $P = 7$ atm, $T = 798$ K

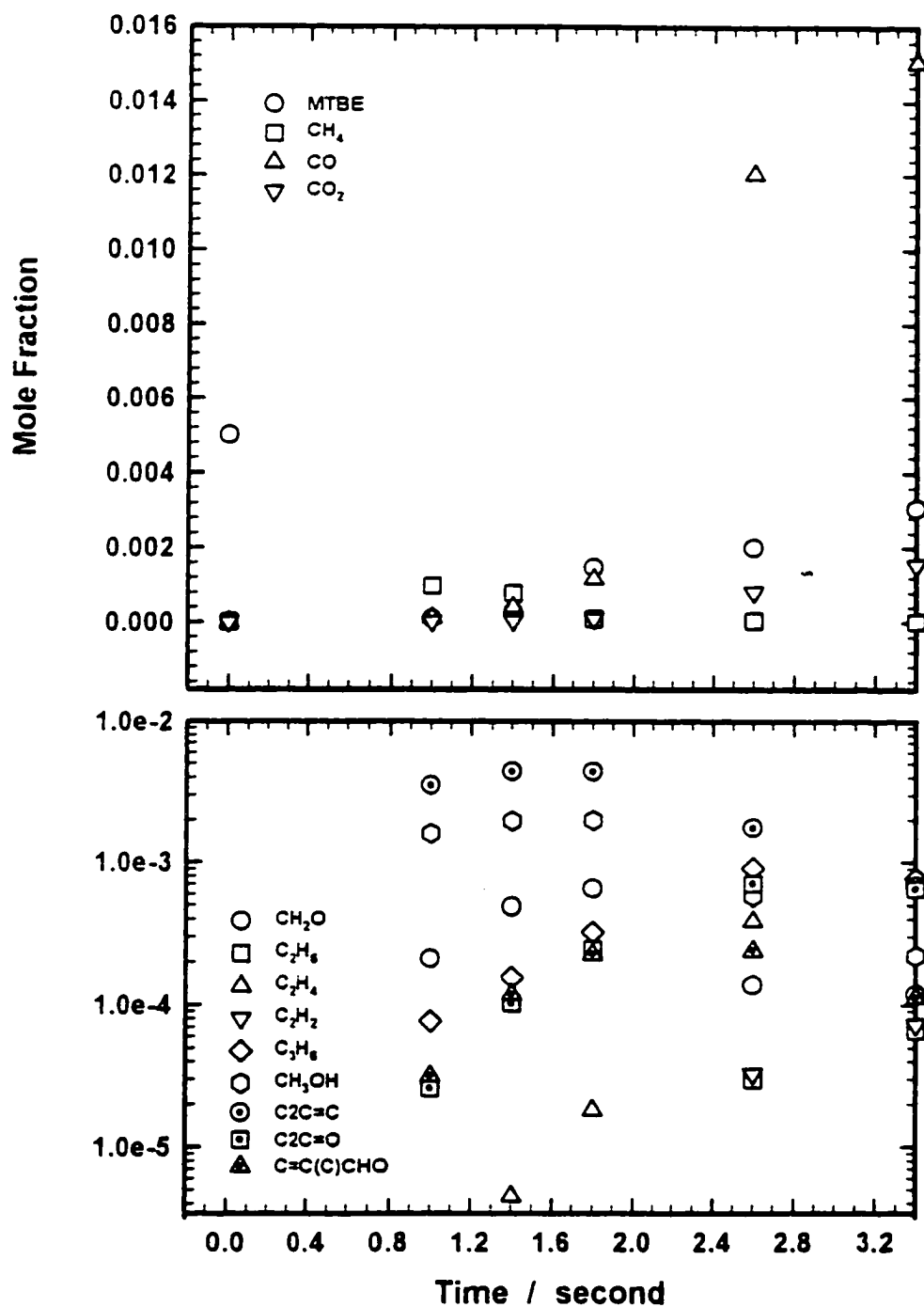


Figure IIC. 45 Experimental result of 0.5% MTBE oxidation product distribution at $\phi = 1.50$, $P = 7$ atm, $T = 823$ K

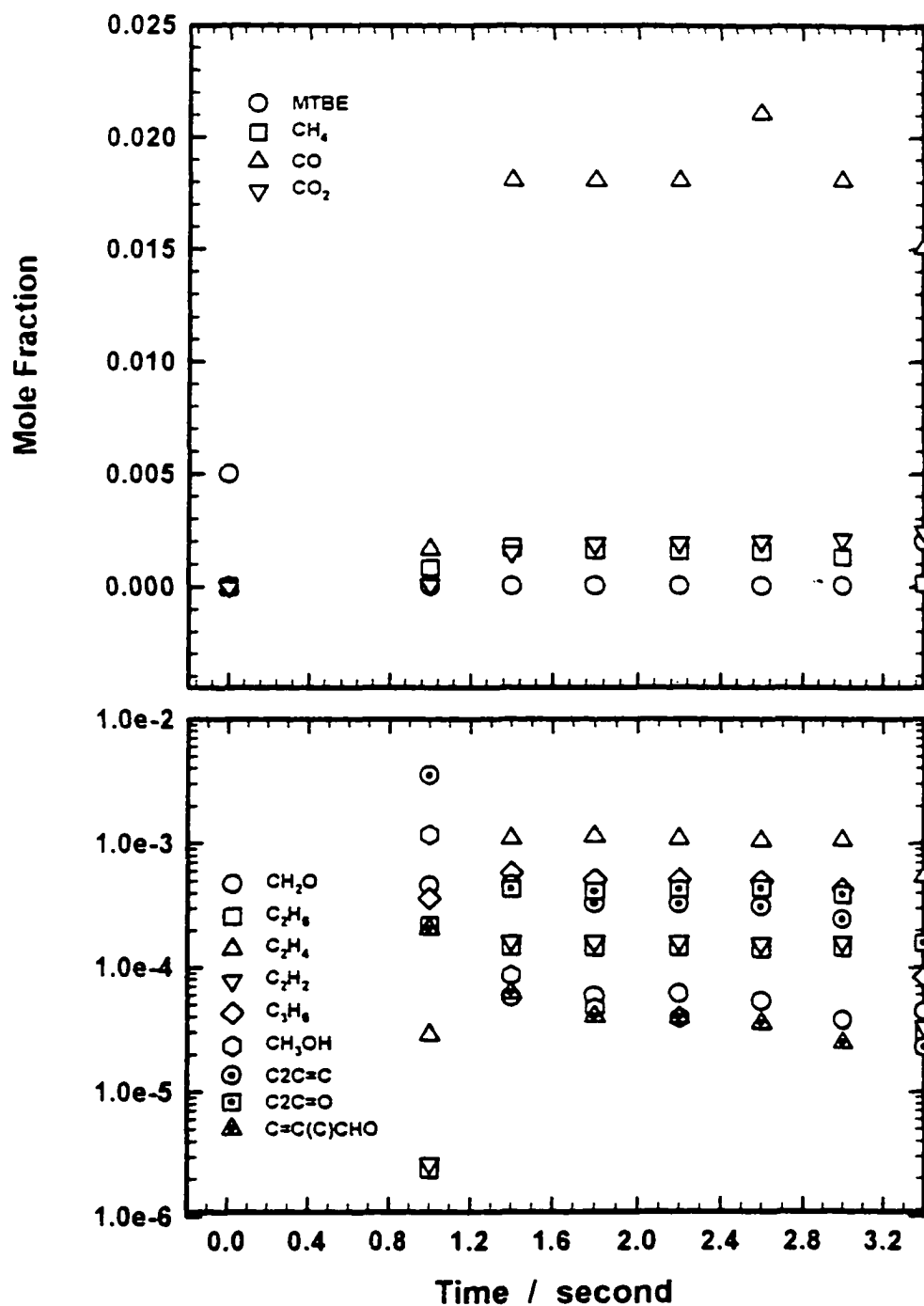


Figure IIC. 46 Experimental result of 0.5% MTBE oxidation product distribution at $\phi = 1.50$, $P = 7$ atm, $T = 848$ K

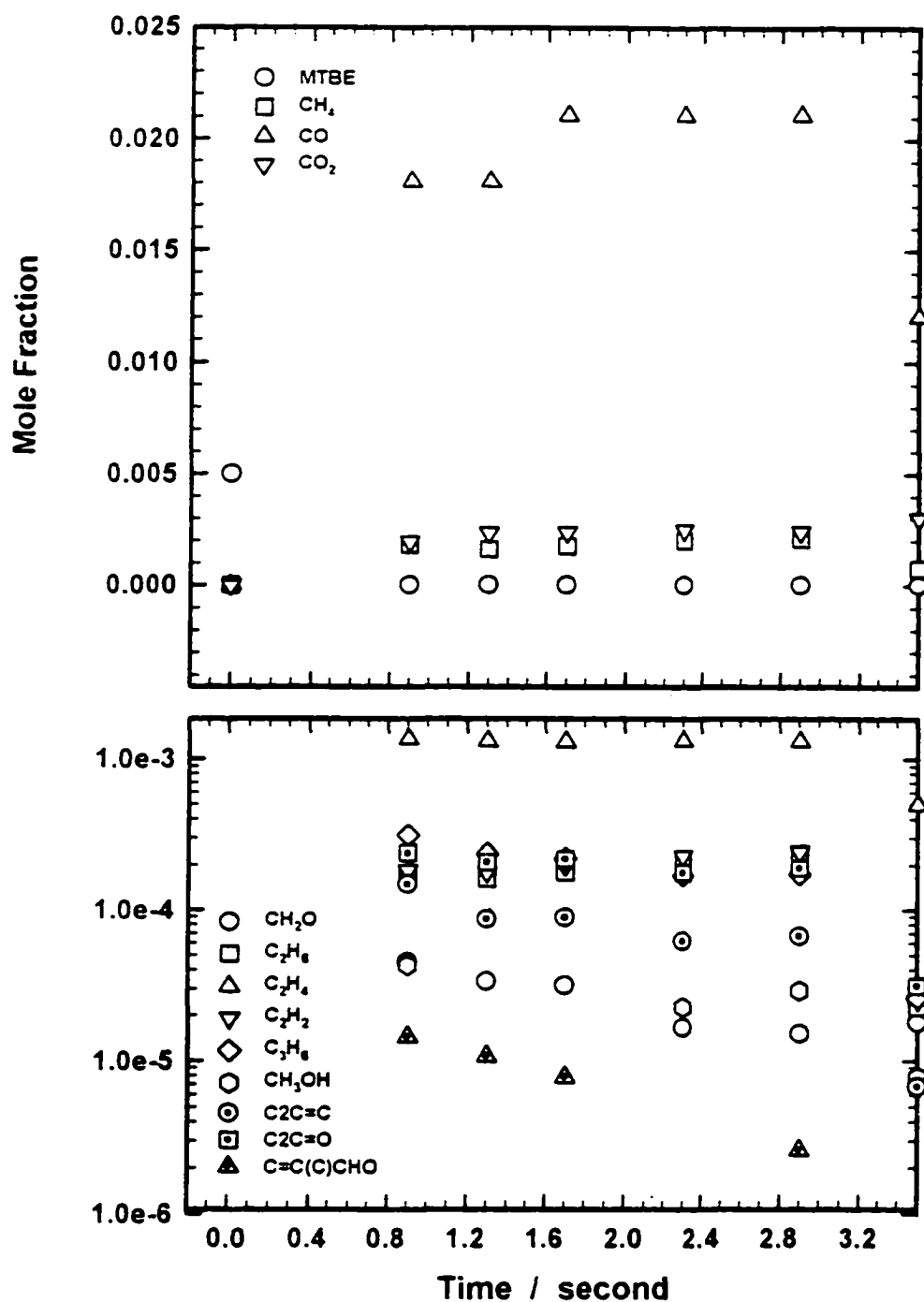


Figure II. 47 Experimental result of 0.5% MTBE oxidation product distribution at $\phi = 1.50$, $P = 7$ atm, $T = 873$ K

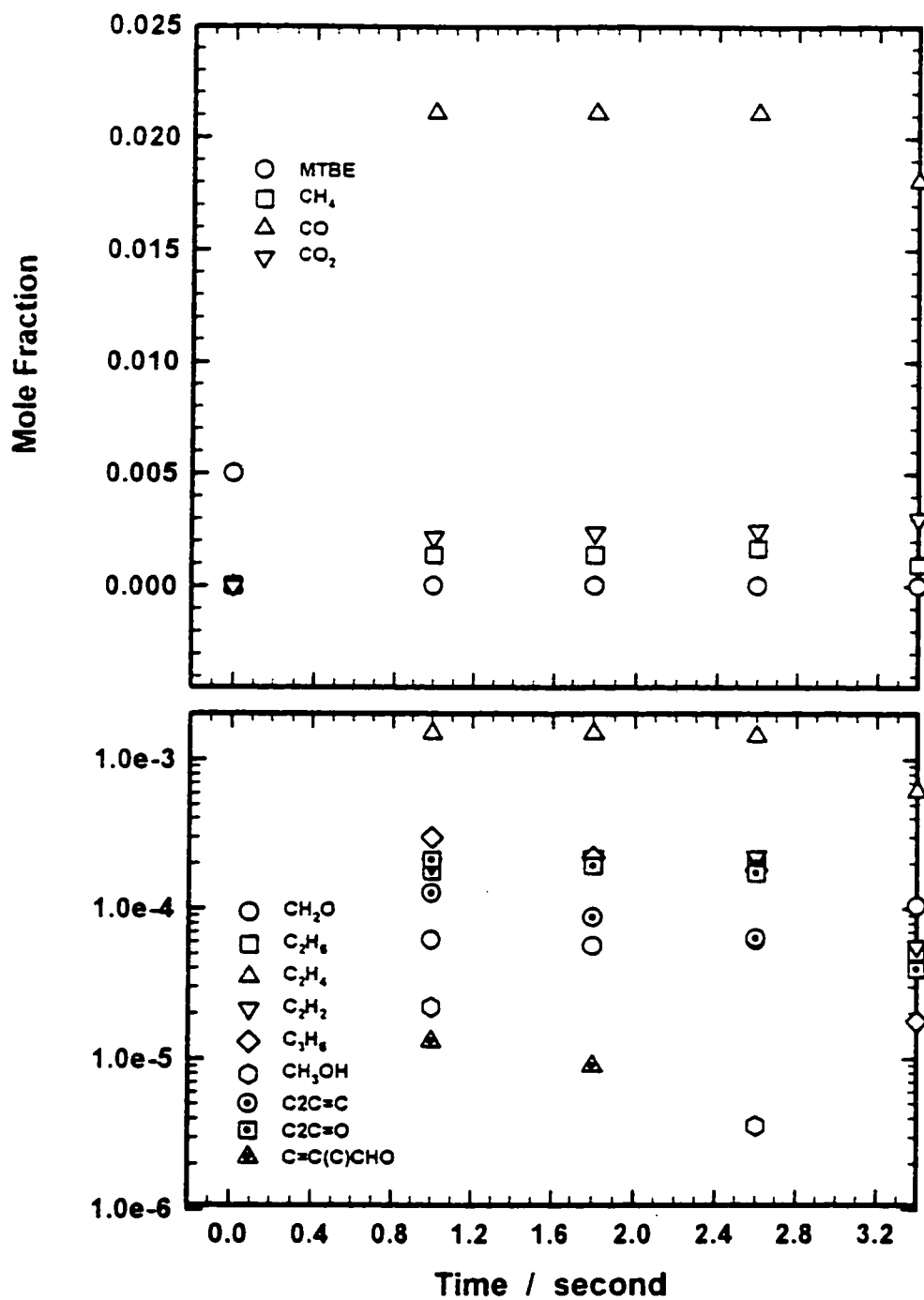


Figure IIC. 48 Experimental result of 0.5% MTBE oxidation product distribution at $\phi = 1.50$, $P = 7$ atm, $T = 898$ K

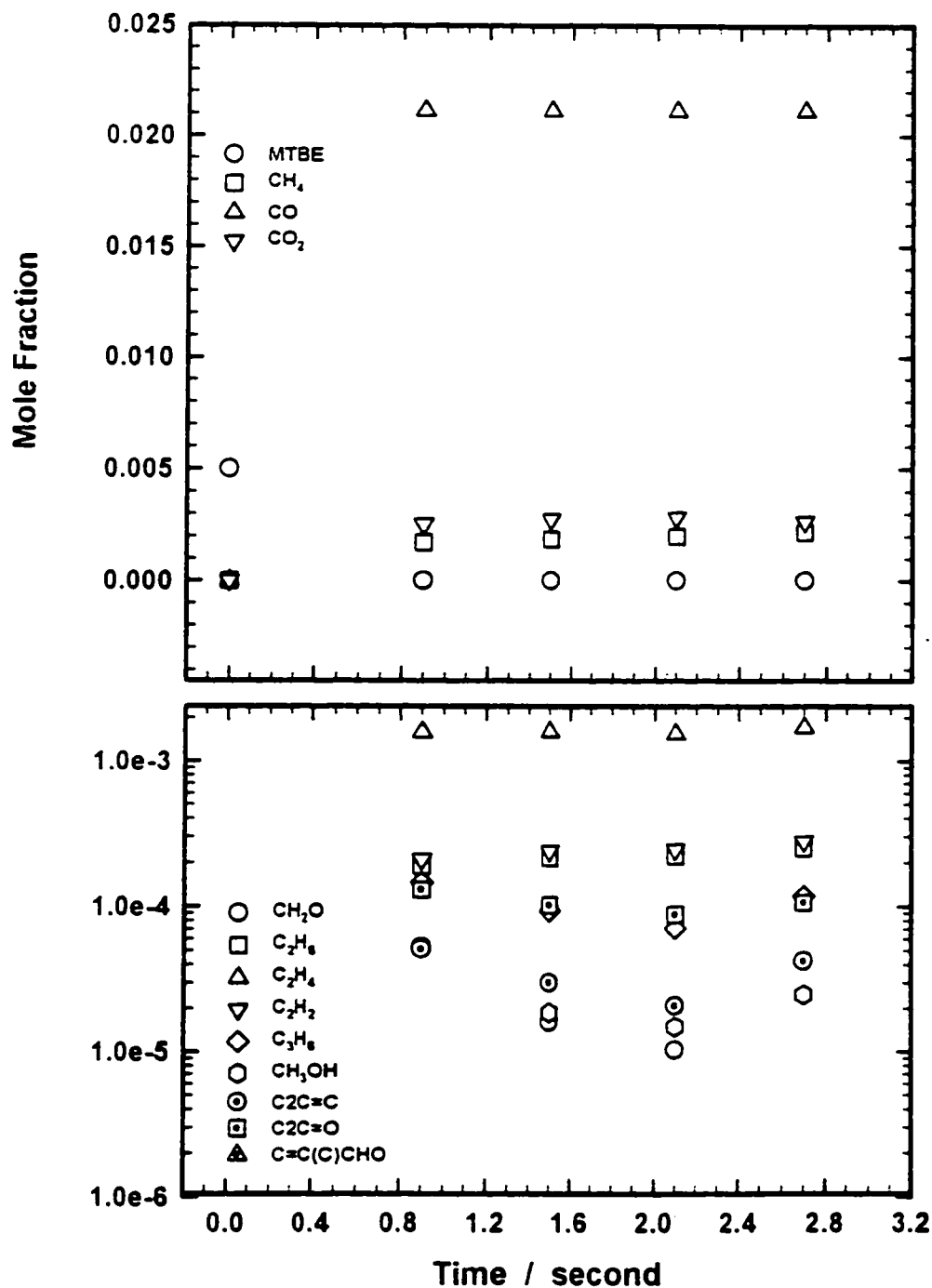


Figure IIC. 49 Experimental result of 0.5% MTBE oxidation product distribution at $\phi = 1.50$, $P = 7$ atm, $T = 923$ K

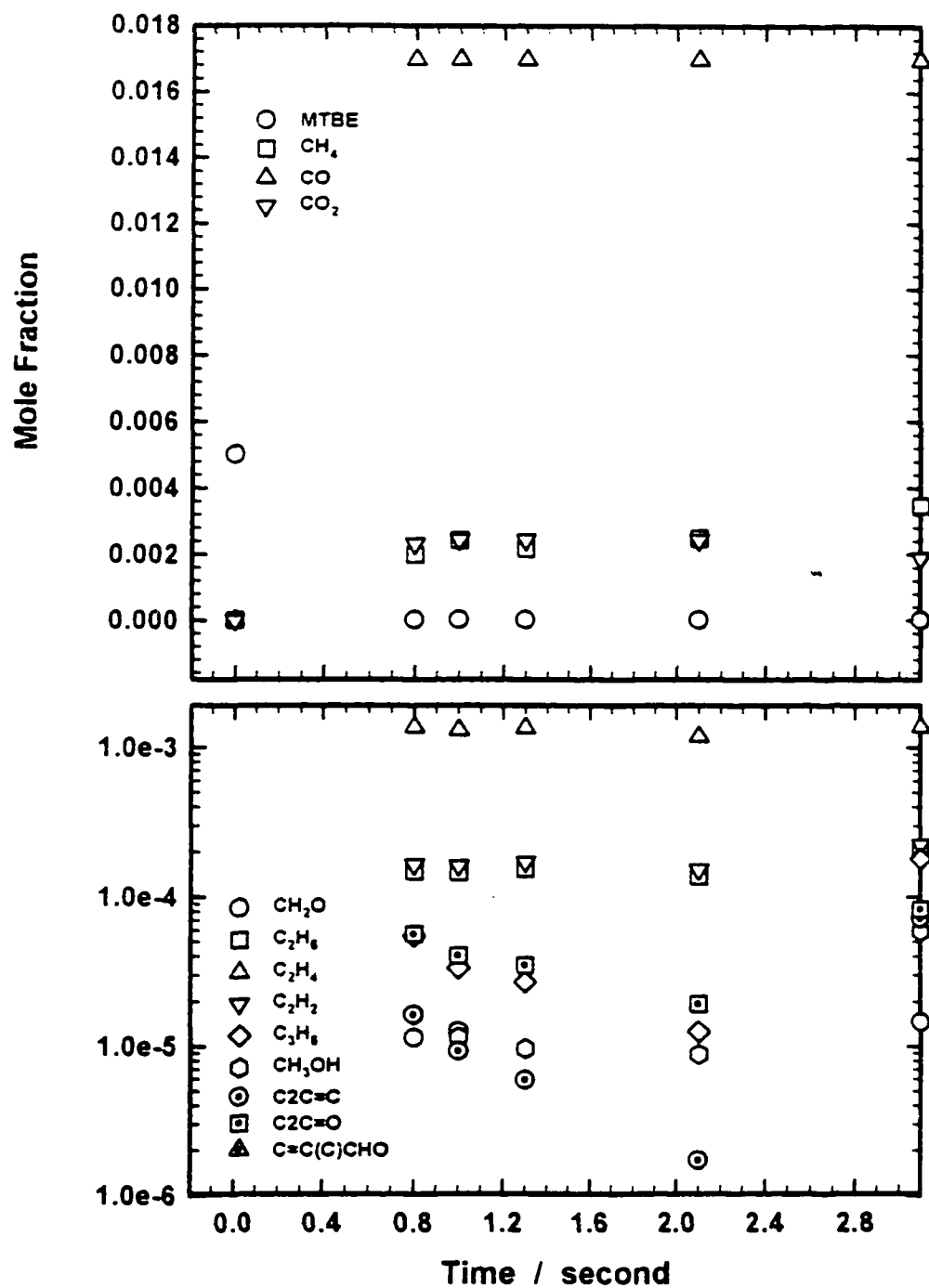


Figure IIC. 50 Experimental result of 0.5% MTBE oxidation product distribution at $\phi = 1.50$, $P = 7$ atm, $T = 973$ K

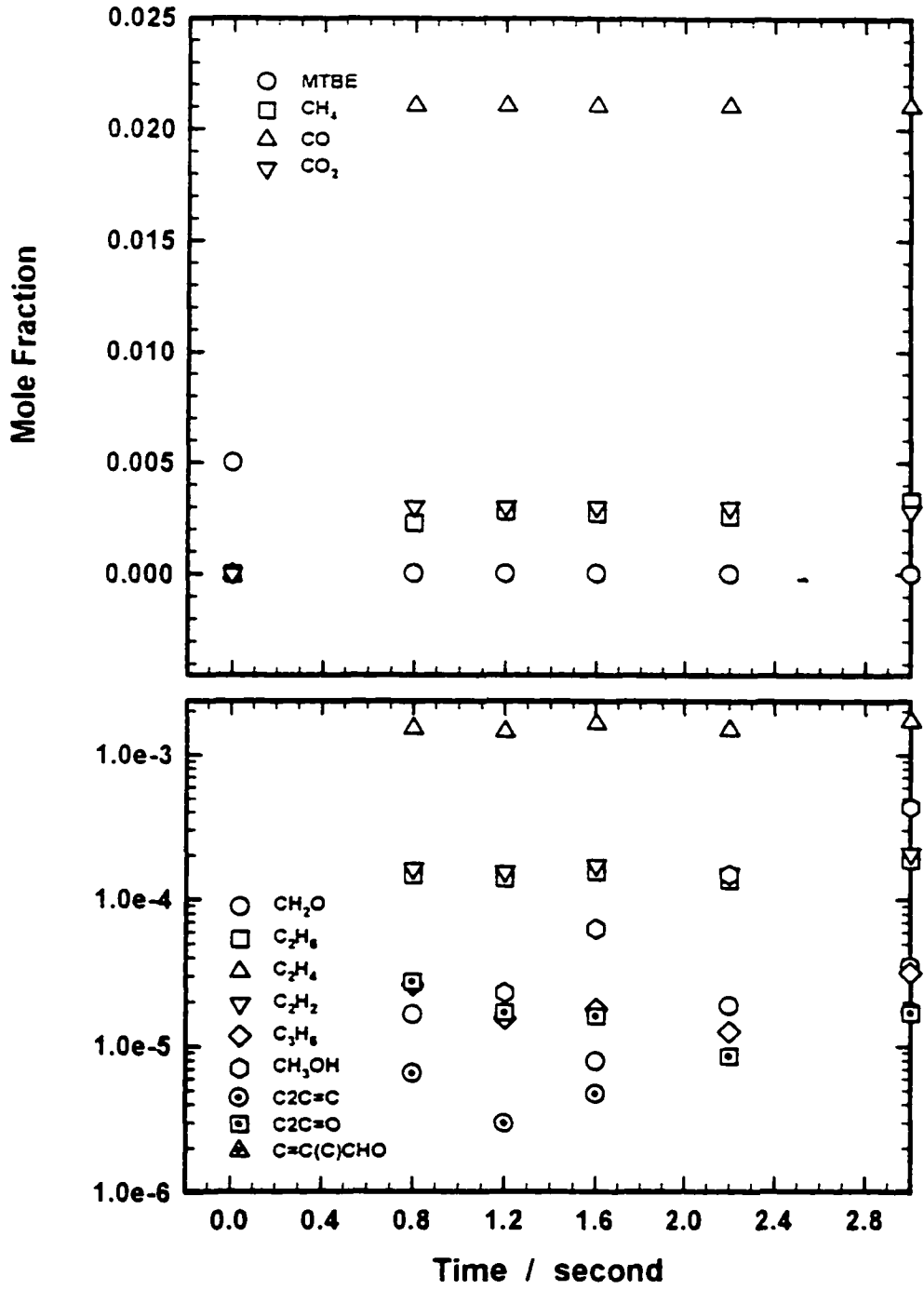


Figure IIC. 51 Experimental result of 0.5% MTBE oxidation product distribution at $\phi = 1.50$, $P = 7$ atm, $T = 998$ K

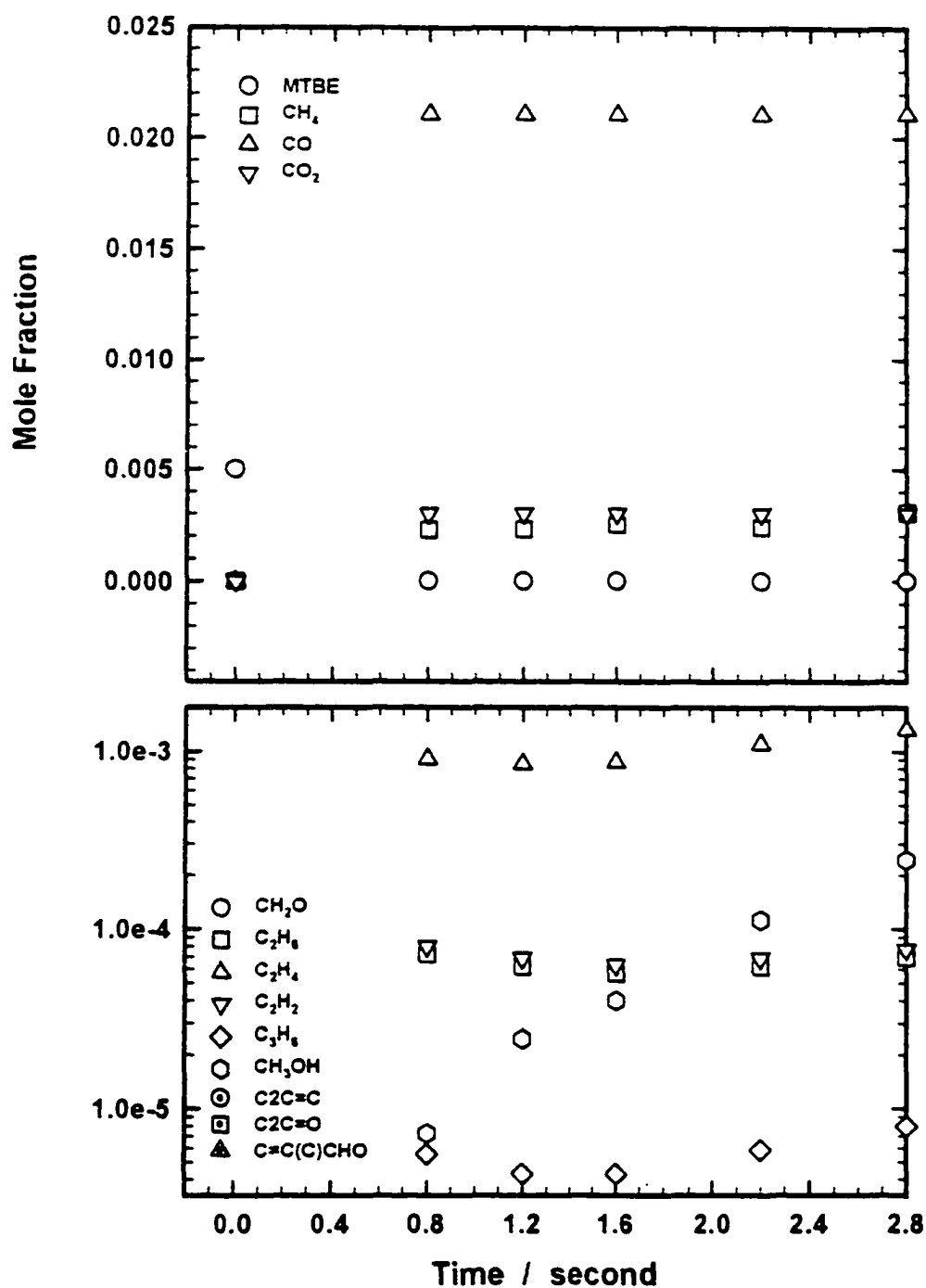


Figure IIC. 52 Experimental result of 0.5% MTBE oxidation product distribution at $\phi = 1.50$, $P = 7$ atm, $T = 1048$ K

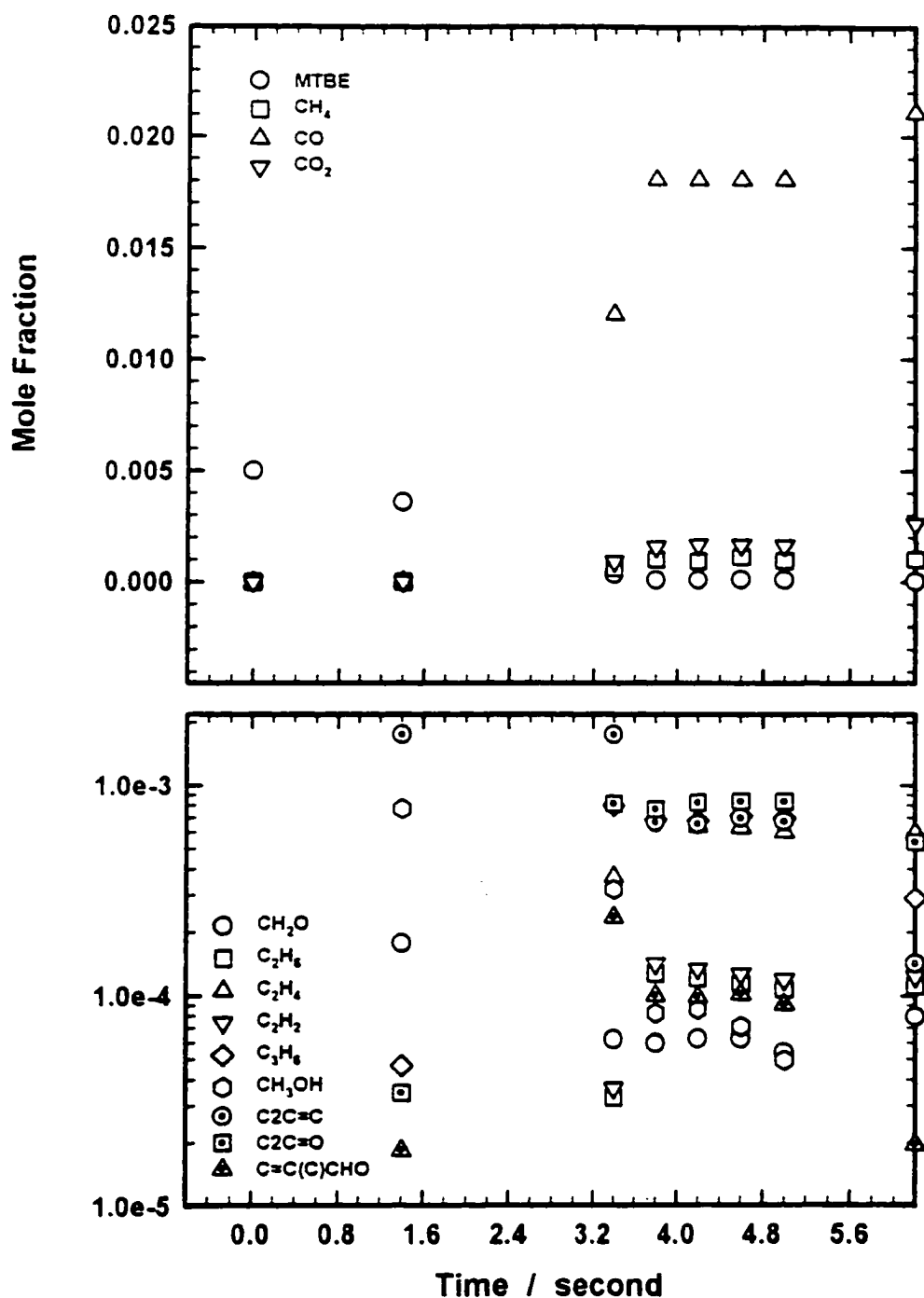


Figure IIC. 53 Experimental result of 0.5% MTBE oxidation product distribution at $\phi = 1.50$, $P = 10$ atm, $T = 798$ K

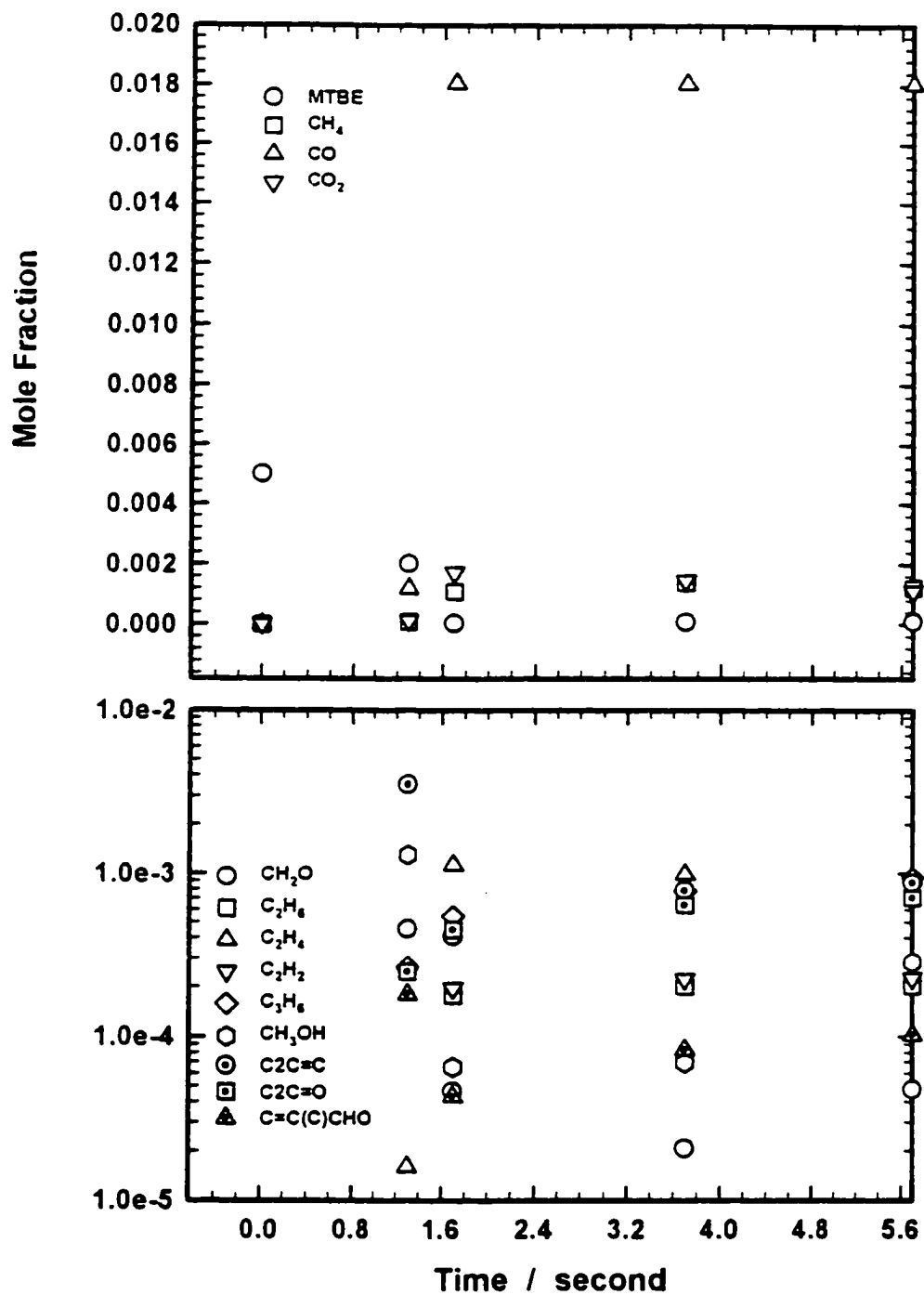


Figure II. 54 Experimental result of 0.5% MTBE oxidation product distribution at $\phi = 1.50$, $P = 10$ atm, $T = 823$ K

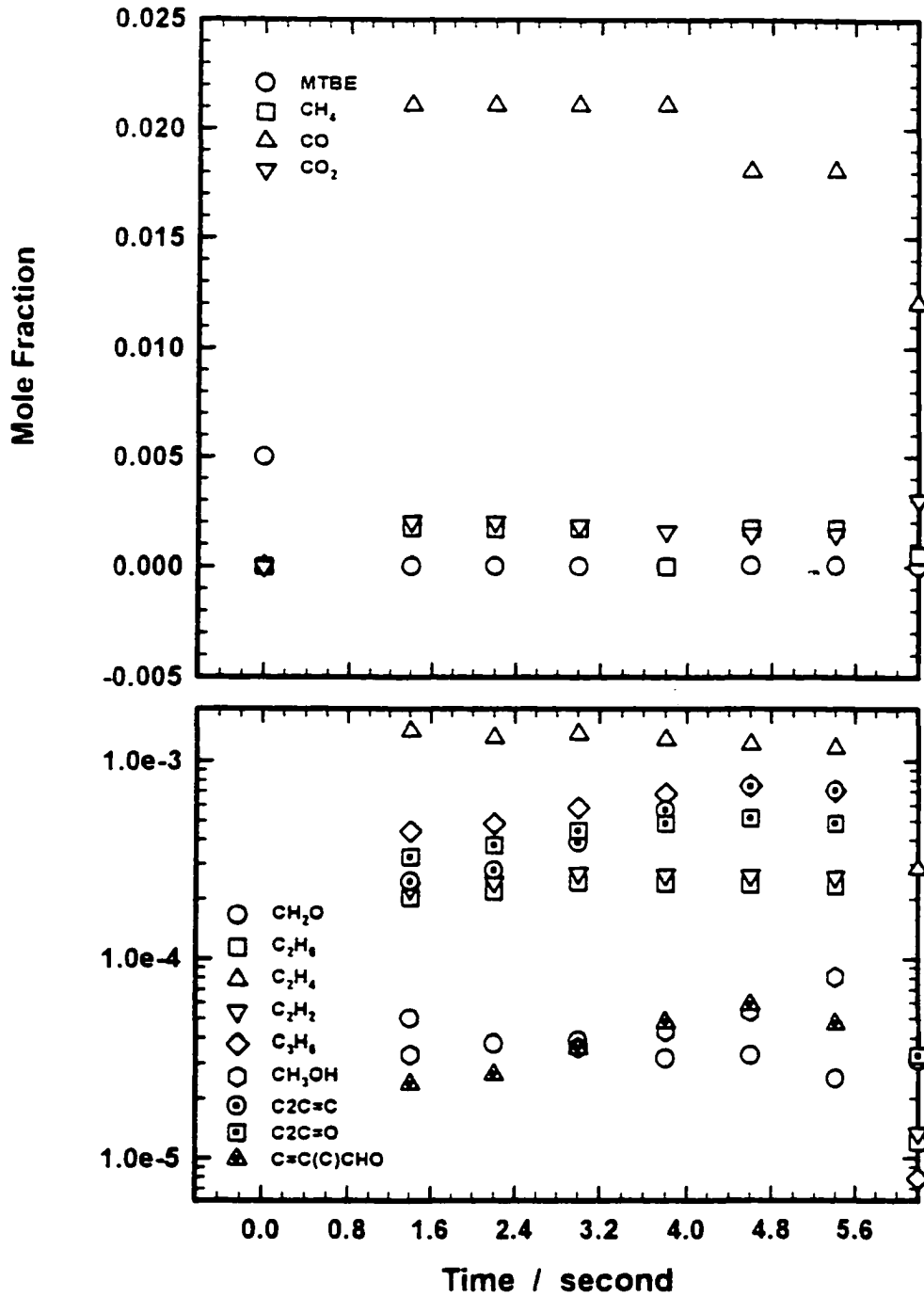


Figure IIC. 55 Experimental result of 0.5% MTBE oxidation product distribution at $\phi = 1.50$, $P = 10$ atm, $T = 848$ K

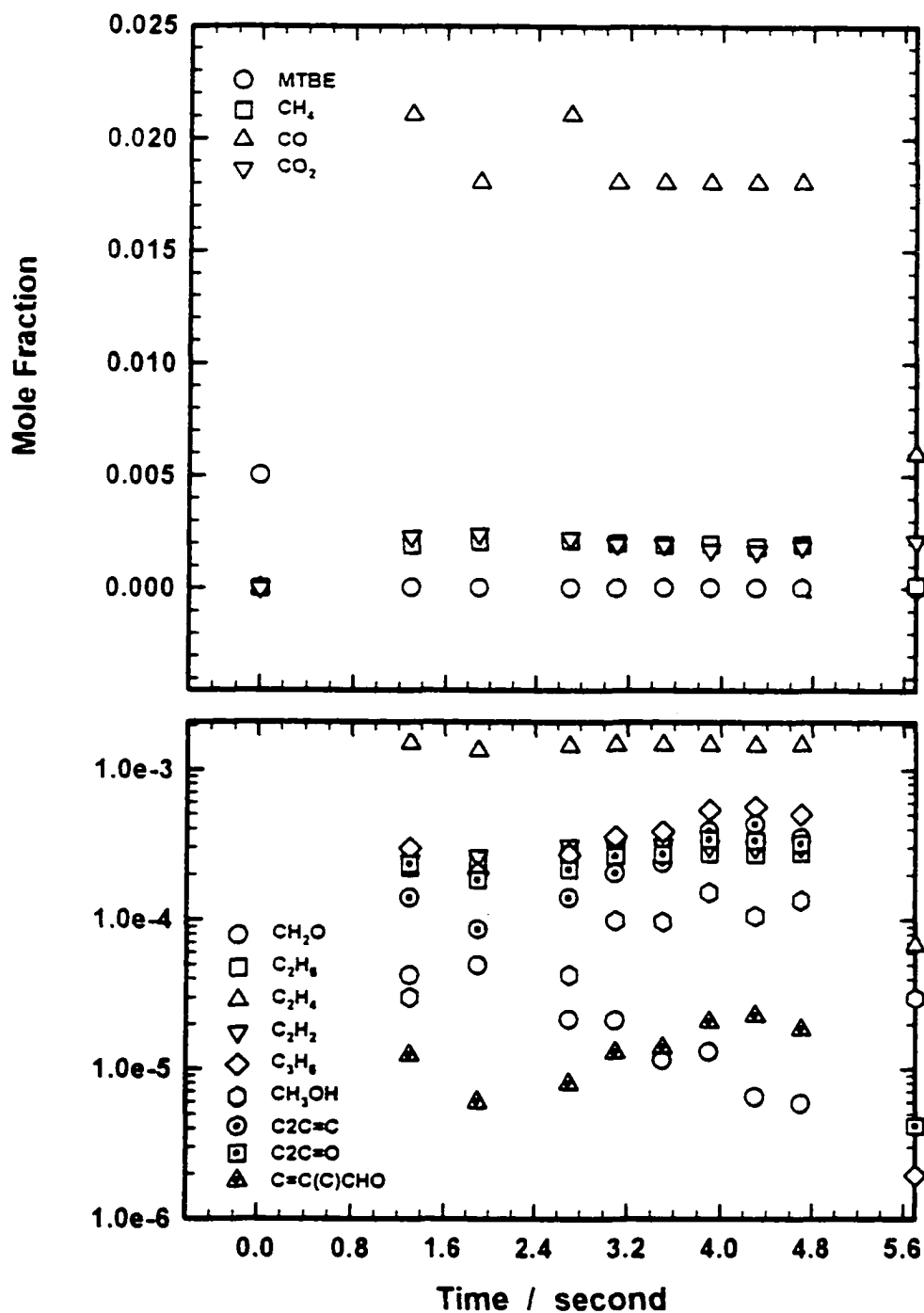


Figure II. 56 Experimental result of 0.5% MTBE oxidation product distribution at $\phi = 1.50$, $P = 10$ atm, $T = 873$ K

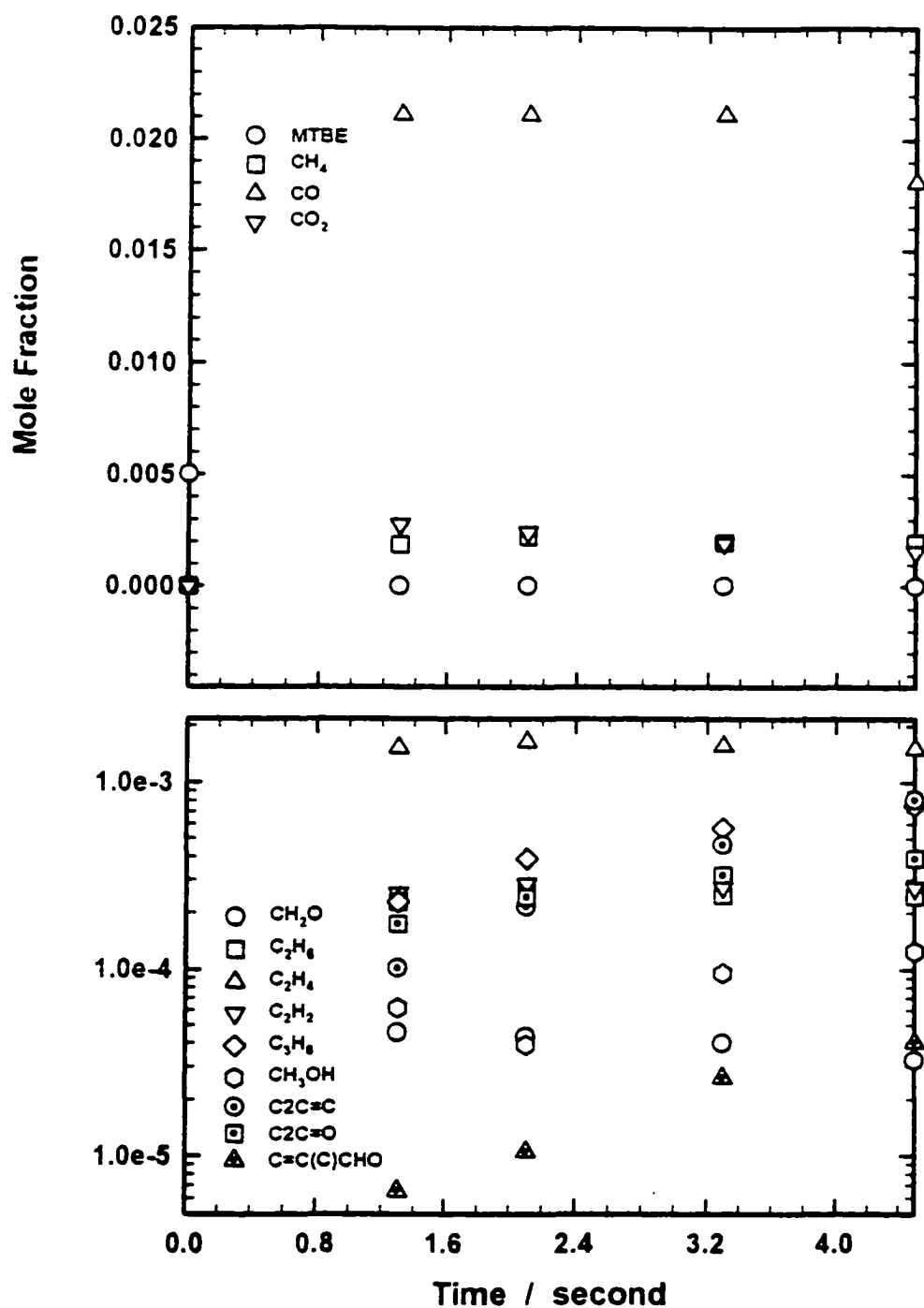


Figure IIC. 57 Experimental result of 0.5% MTBE oxidation product distribution at $\phi = 1.50$, $P = 10$ atm, $T = 898$ K

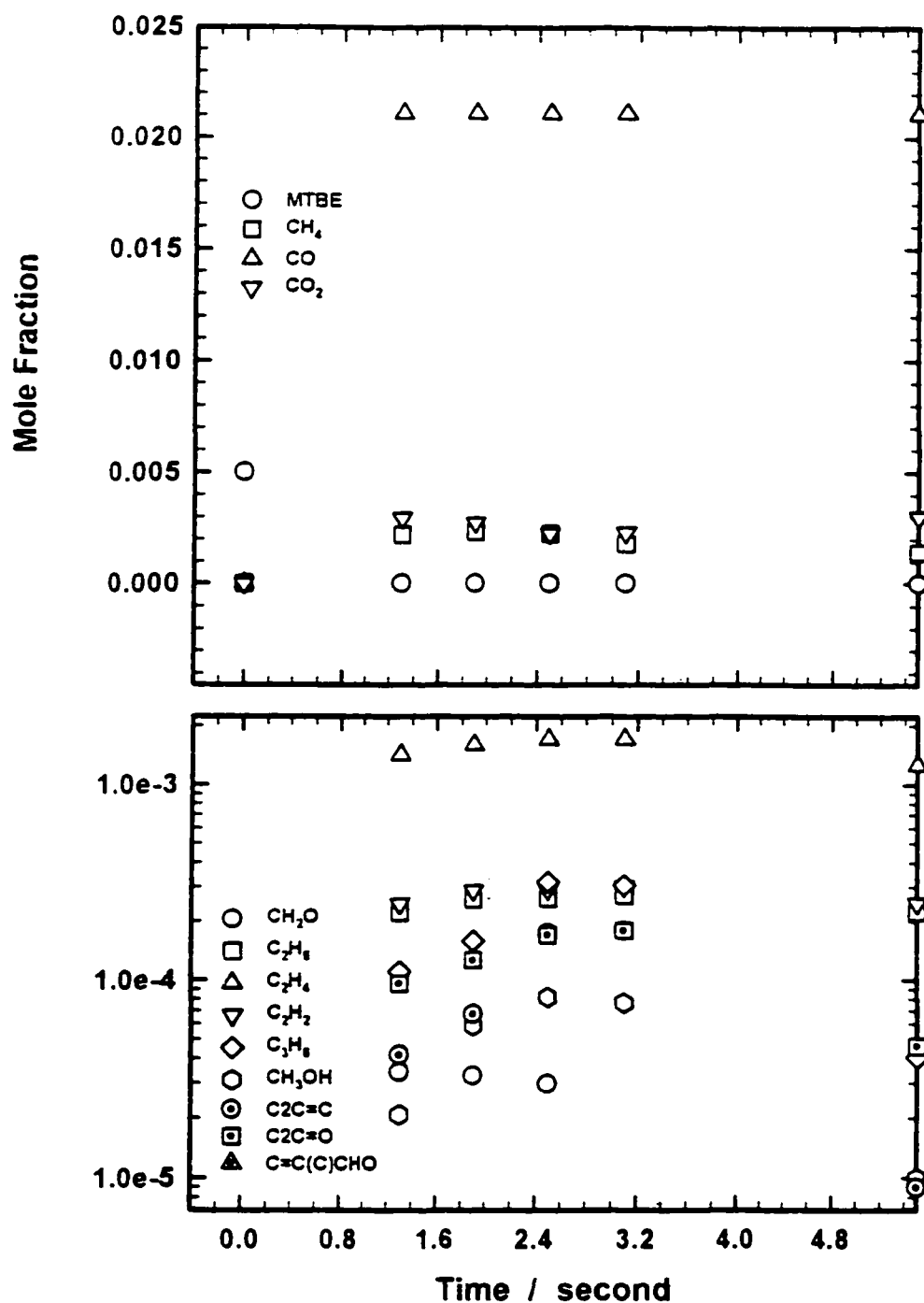


Figure IIC. 58 Experimental result of 0.5% MTBE oxidation product distribution at $\phi = 1.50$, $P = 10$ atm, $T = 923$ K

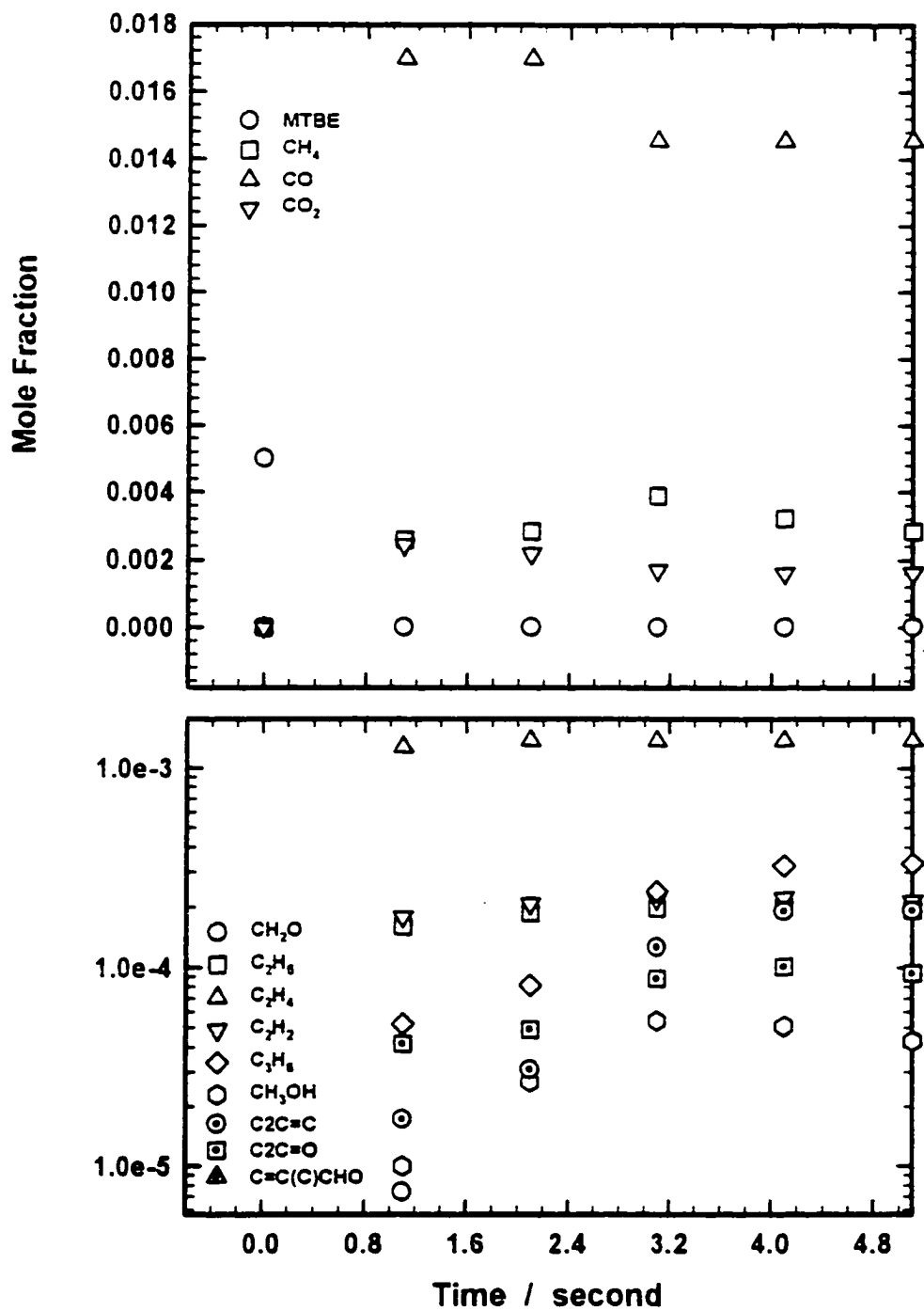


Figure IIC. 59 Experimental result of 0.5% MTBE oxidation product distribution at $\phi = 1.50$, $P = 10$ atm, $T = 973$ K

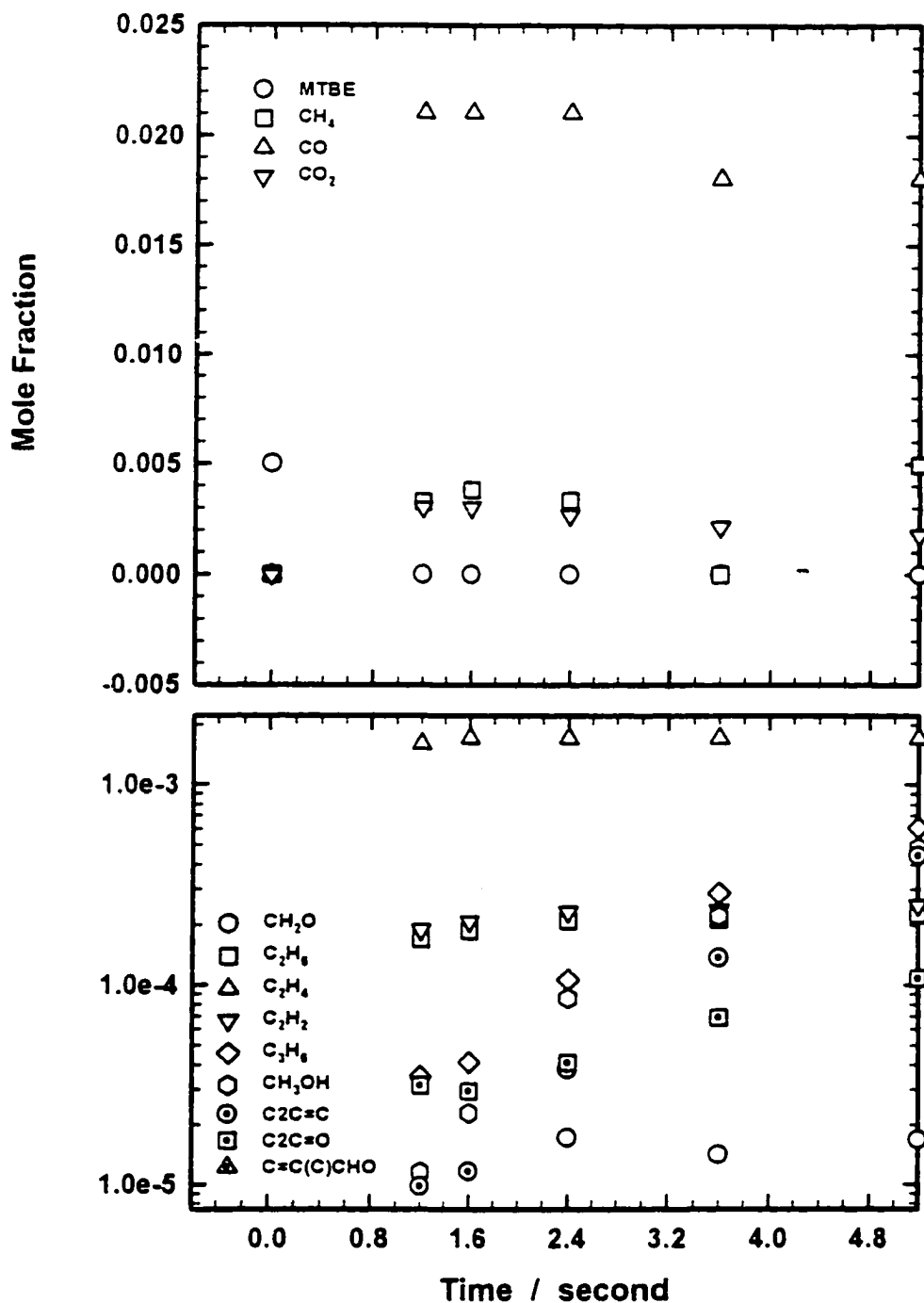


Figure IIC. 60 Experimental result of 0.5% MTBE oxidation product distribution at $\phi = 1.50$, $P = 10$ atm, $T = 998$ K

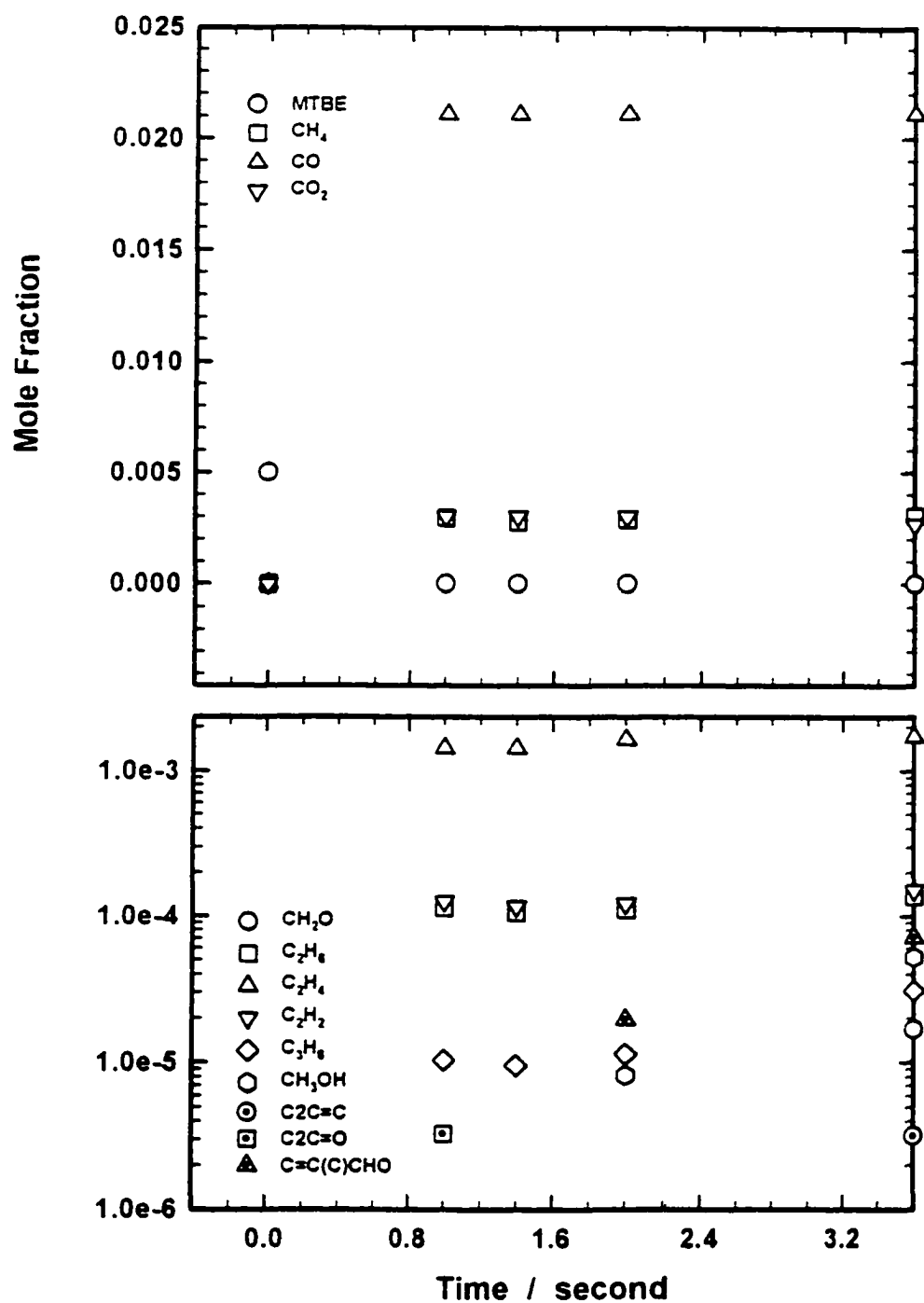


Figure IIC. 61 Experimental result of 0.5% MTBE oxidation product distribution at $\phi = 1.50$, $P = 10$ atm, $T = 1048$ K

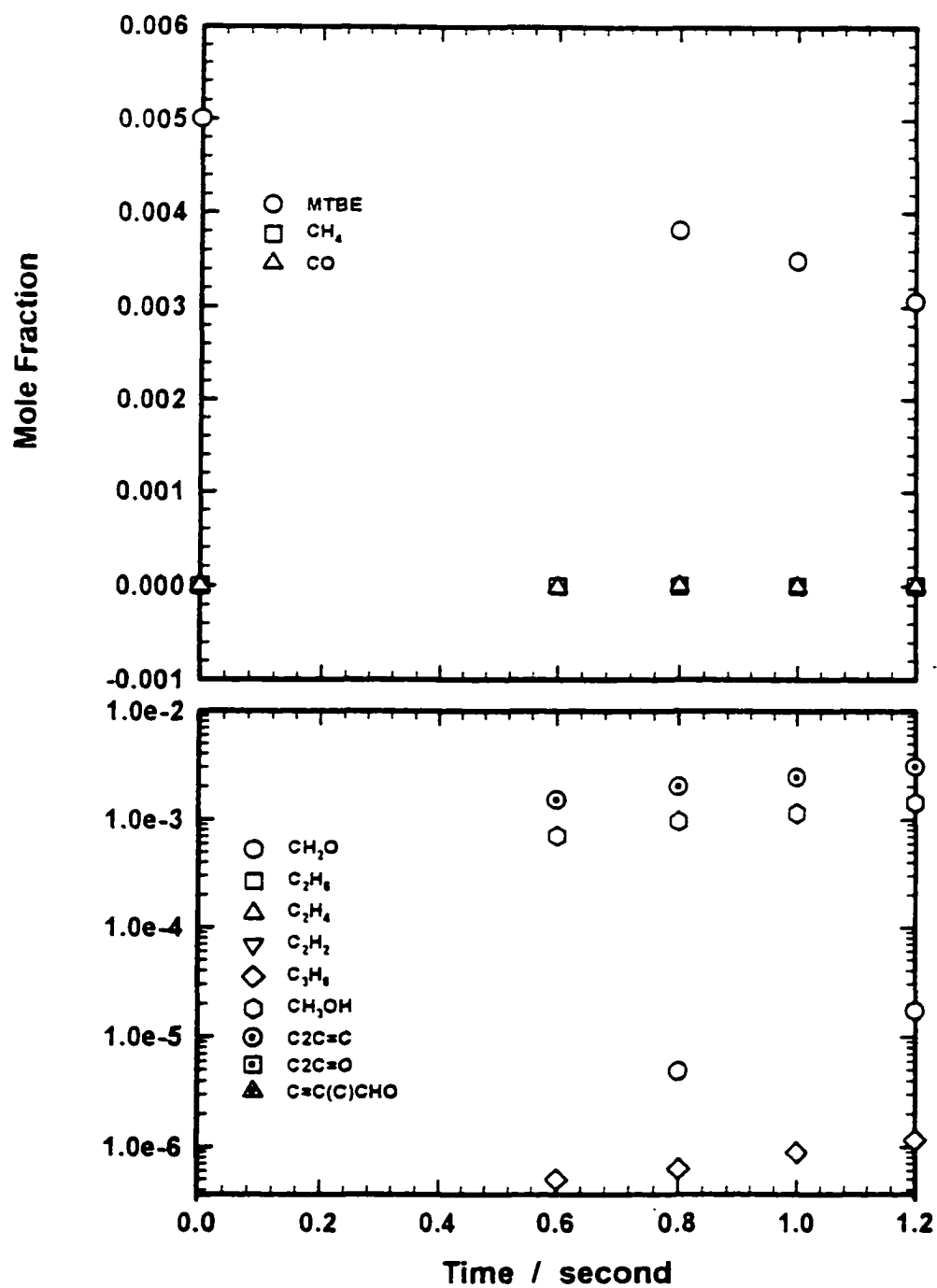


Figure IIC. 62 Experimental result of 0.5% MTBE pyrolysis product distribution at $P = 4$ atm, $T = 823$ K

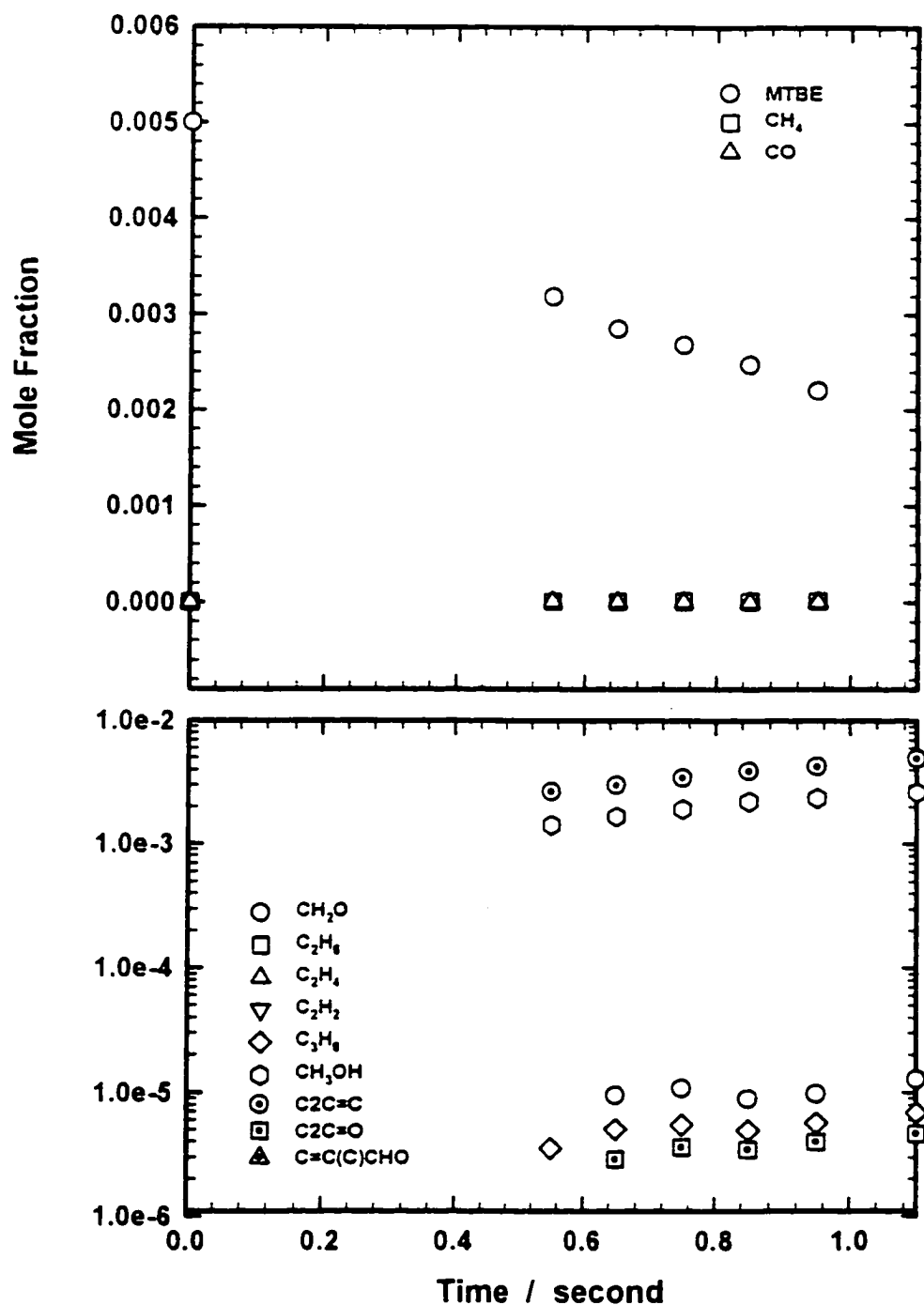


Figure IIC. 63 Experimental result of 0.5% MTBE pyrolysis product distribution at $P = 4$ atm, $T = 873$ K

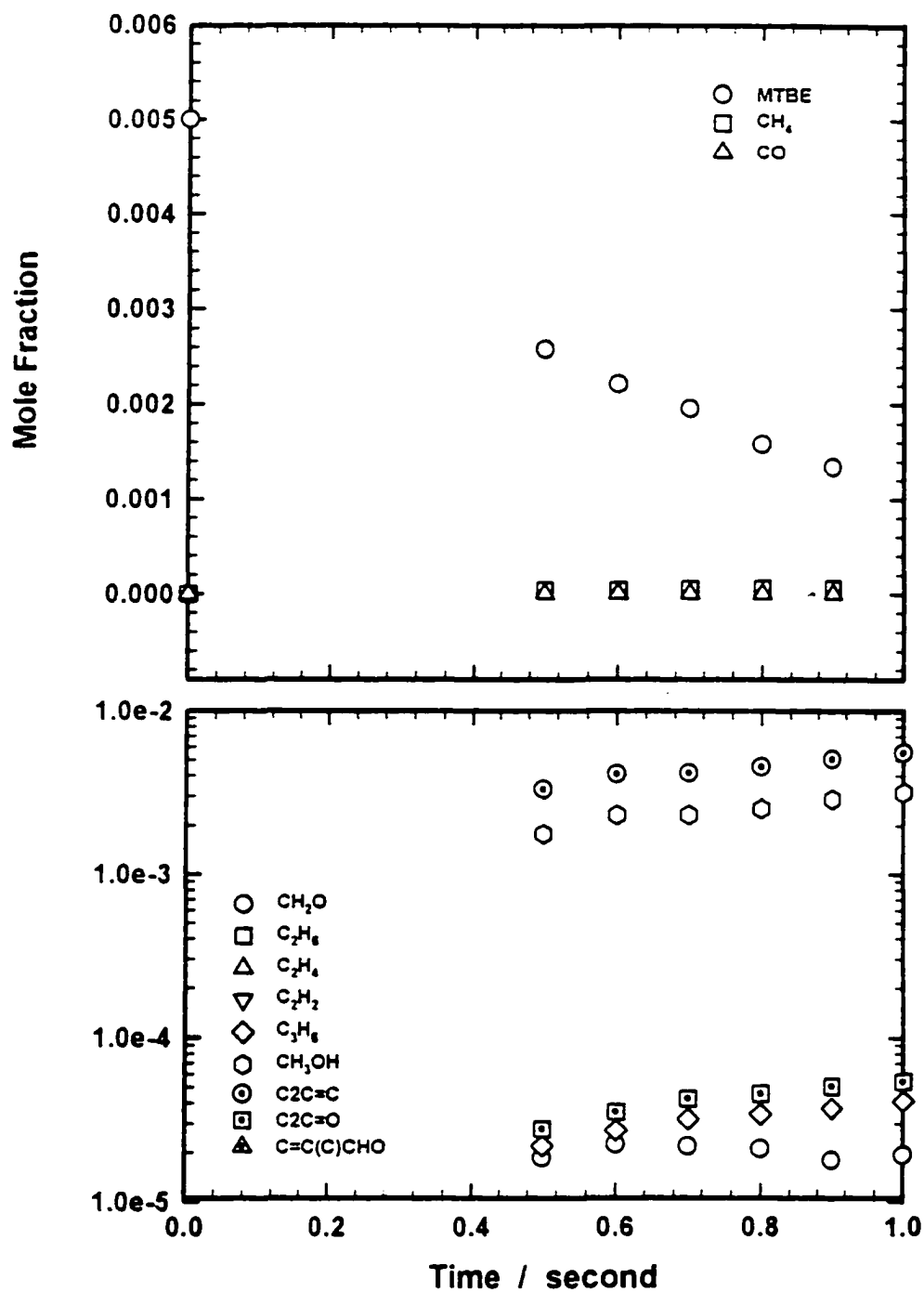


Figure IIC. 64 Experimental result of 0.5% MTBE pyrolysis product distribution at $P = 4$ atm, $T = 923$ K

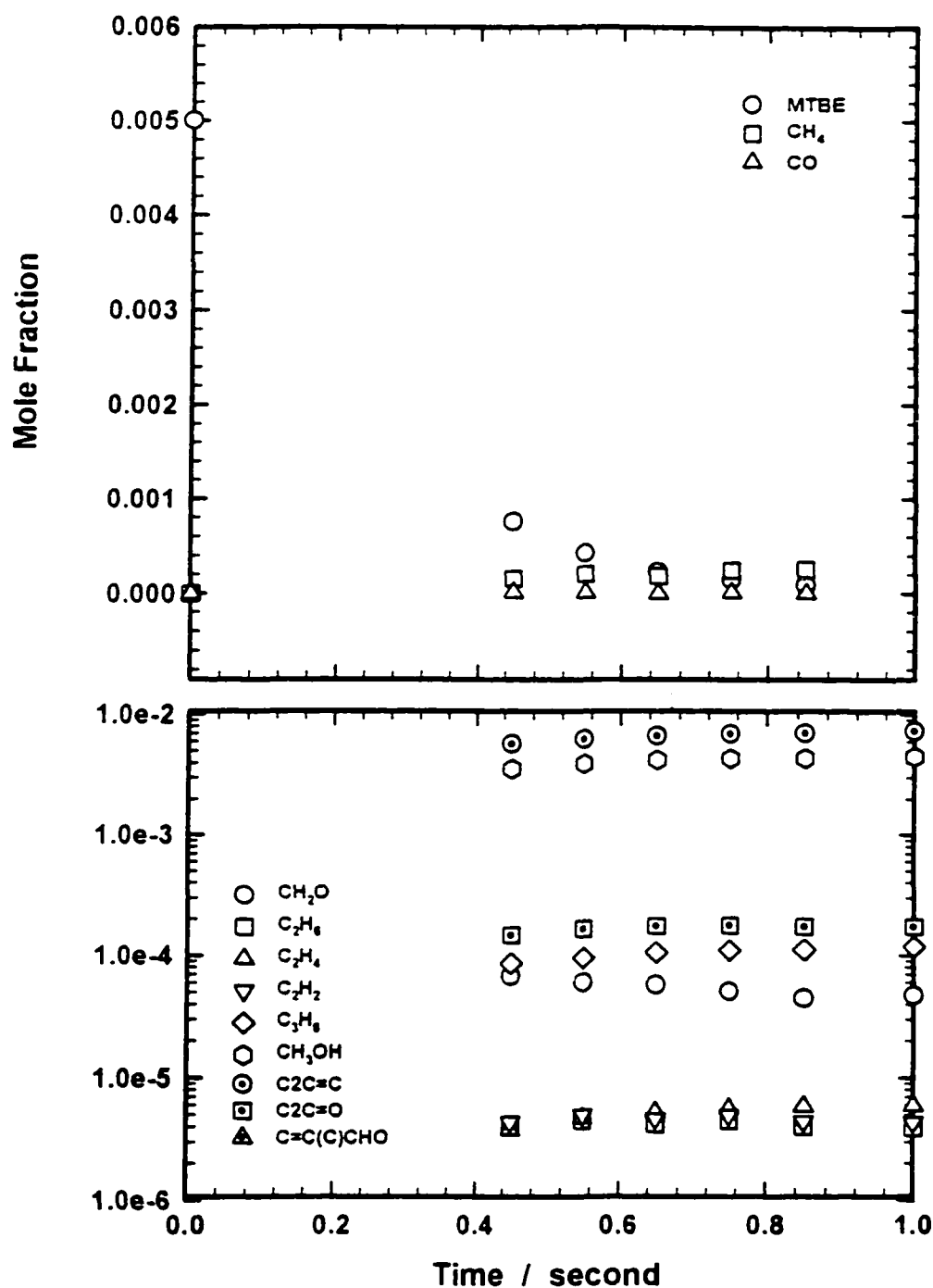


Figure IIC. 65 Experimental result of 0.5% MTBE pyrolysis product distribution at $P = 4$ atm, $T = 973$ K

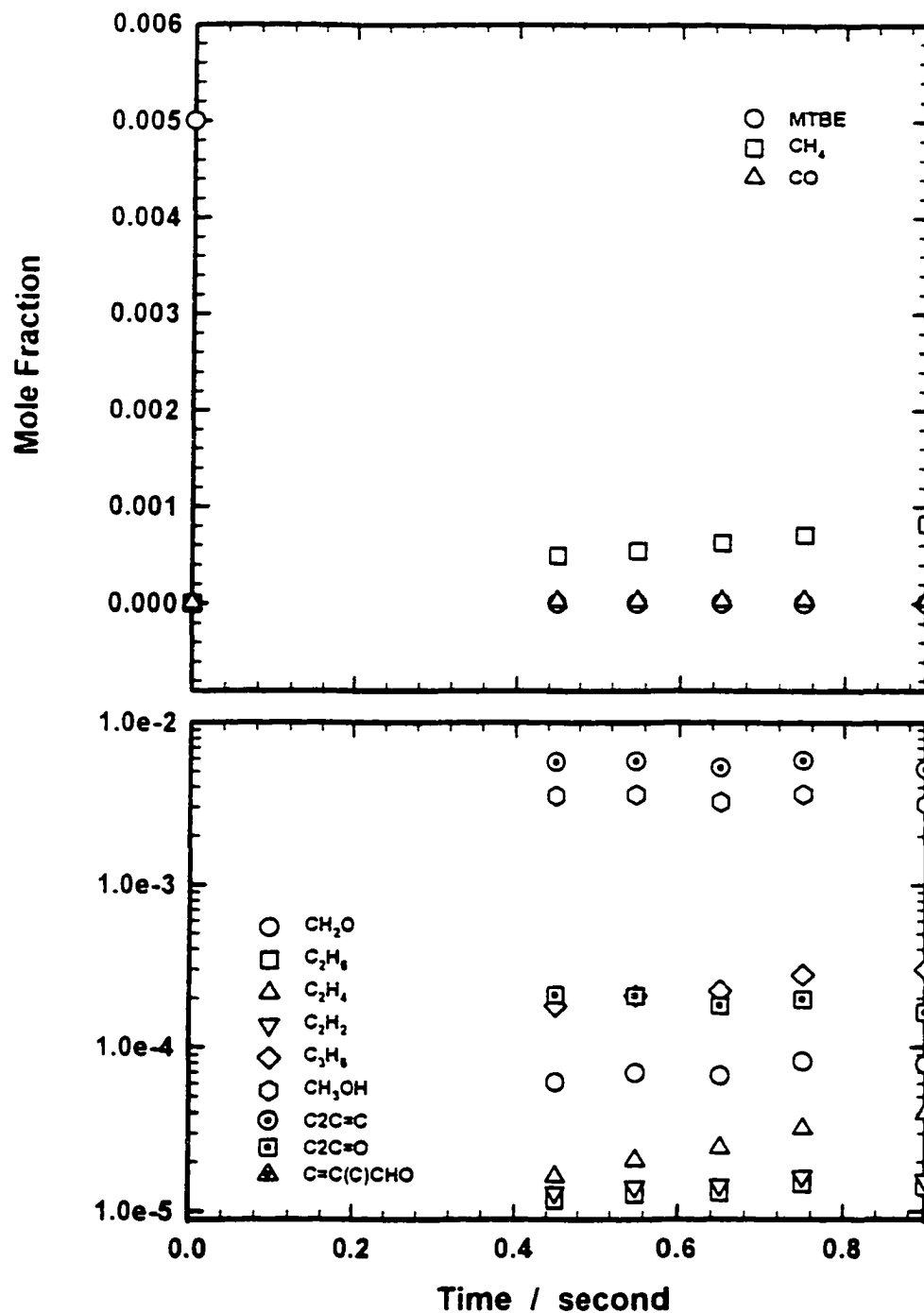


Figure IIC. 66 Experimental result of 0.5% MTBE pyrolysis product distribution at $P = 4$ atm, $T = 1023$ K

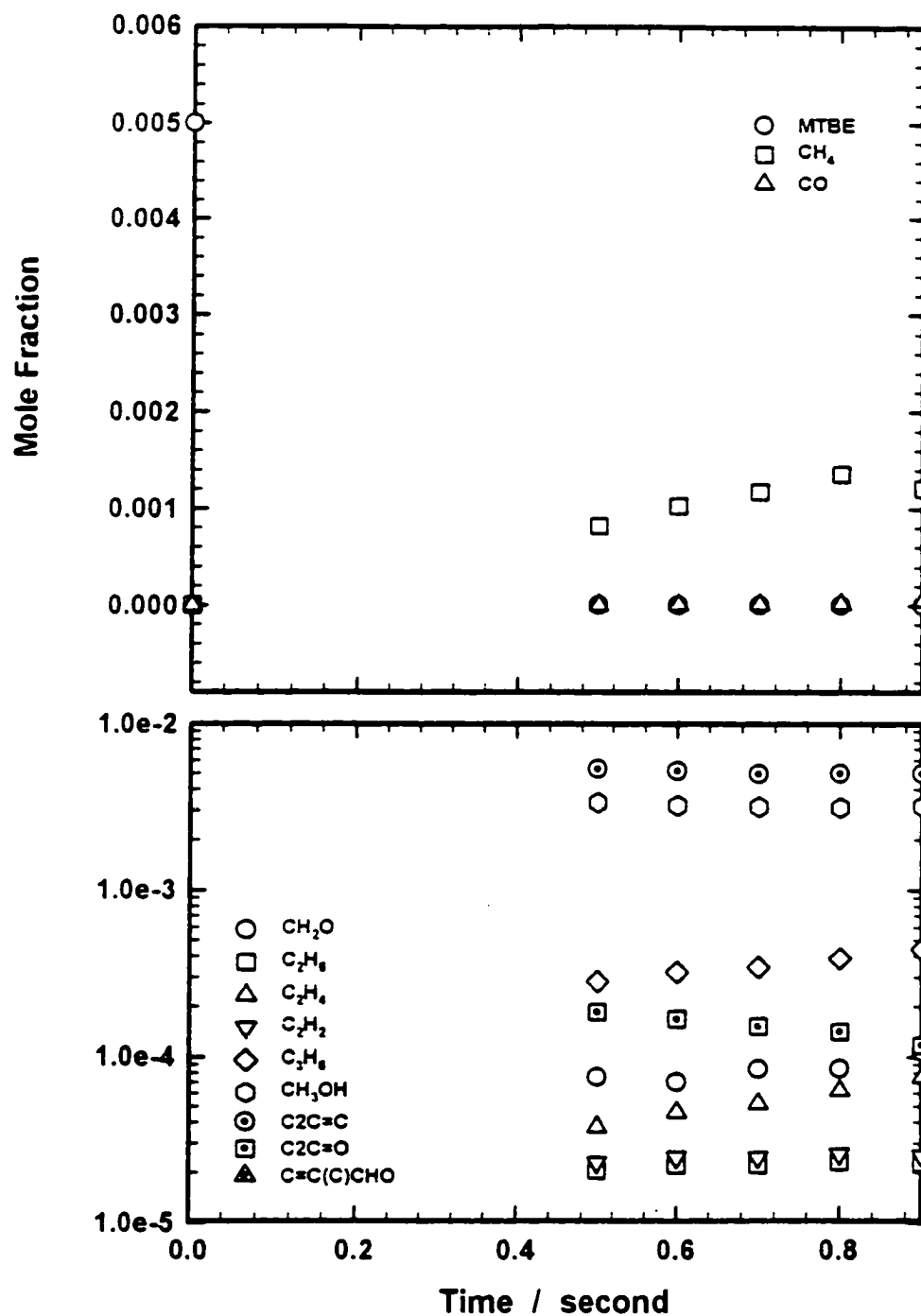


Figure IIC. 67 Experimental result of 0.5% MTBE pyrolysis product distribution at $P = 4$ atm, $T = 1048$ K

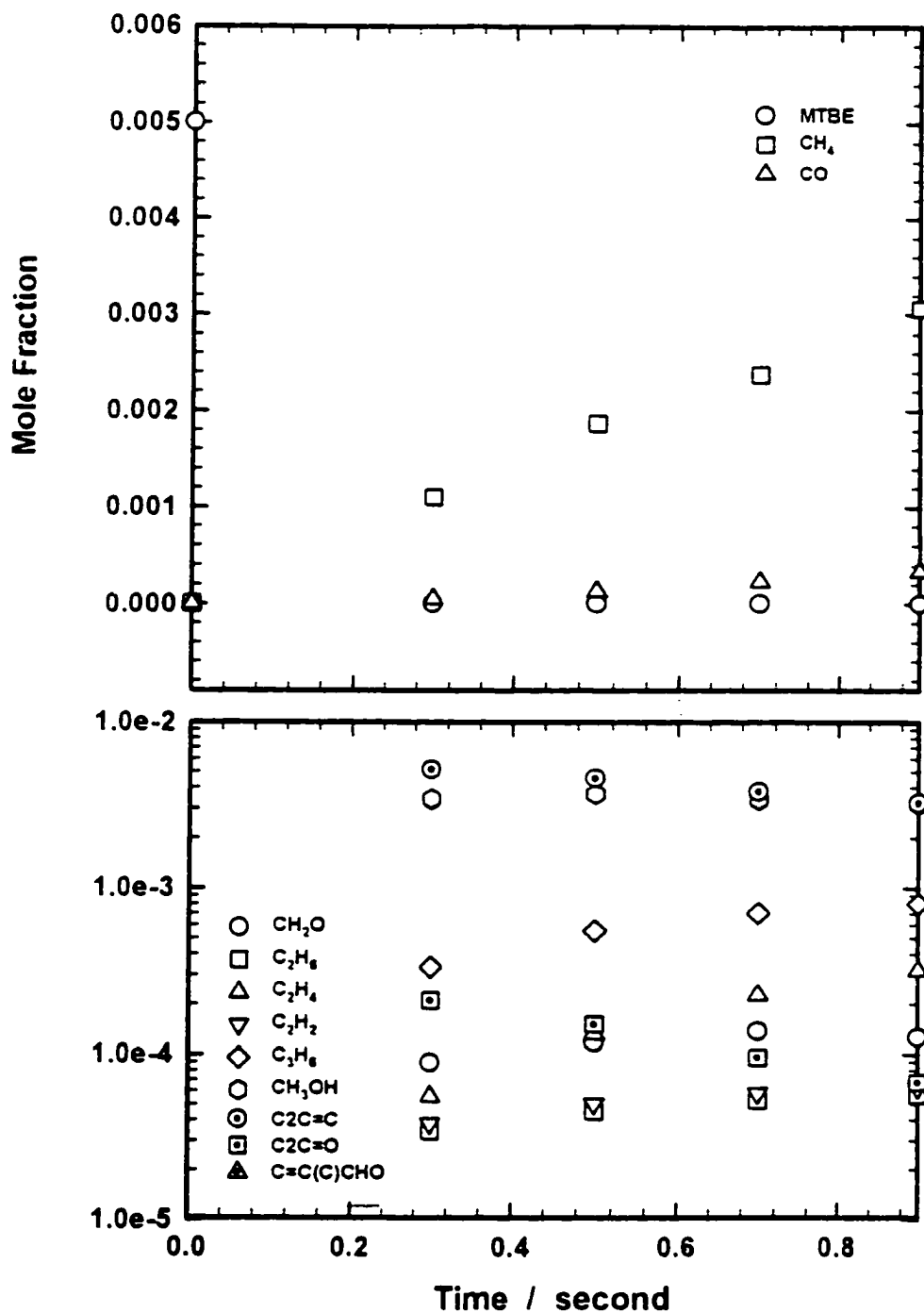


Figure IIC. 68 Experimental result of 0.5% MTBE pyrolysis product distribution at P = 4 atm, T = 1073 K

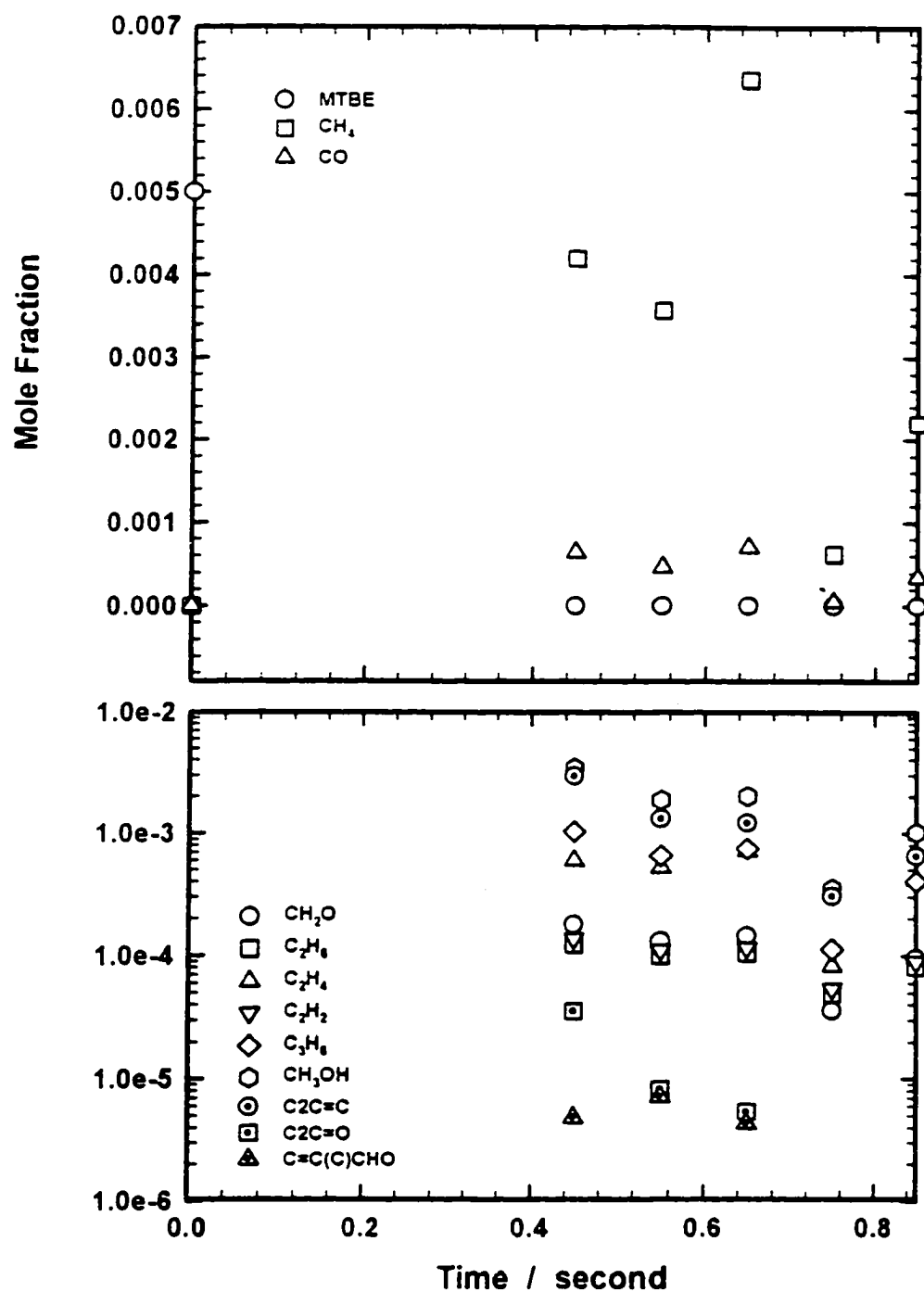


Figure IIC. 69 Experimental result of 0.5% MTBE pyrolysis product distribution at $P = 4$ atm, $T = 1123$ K

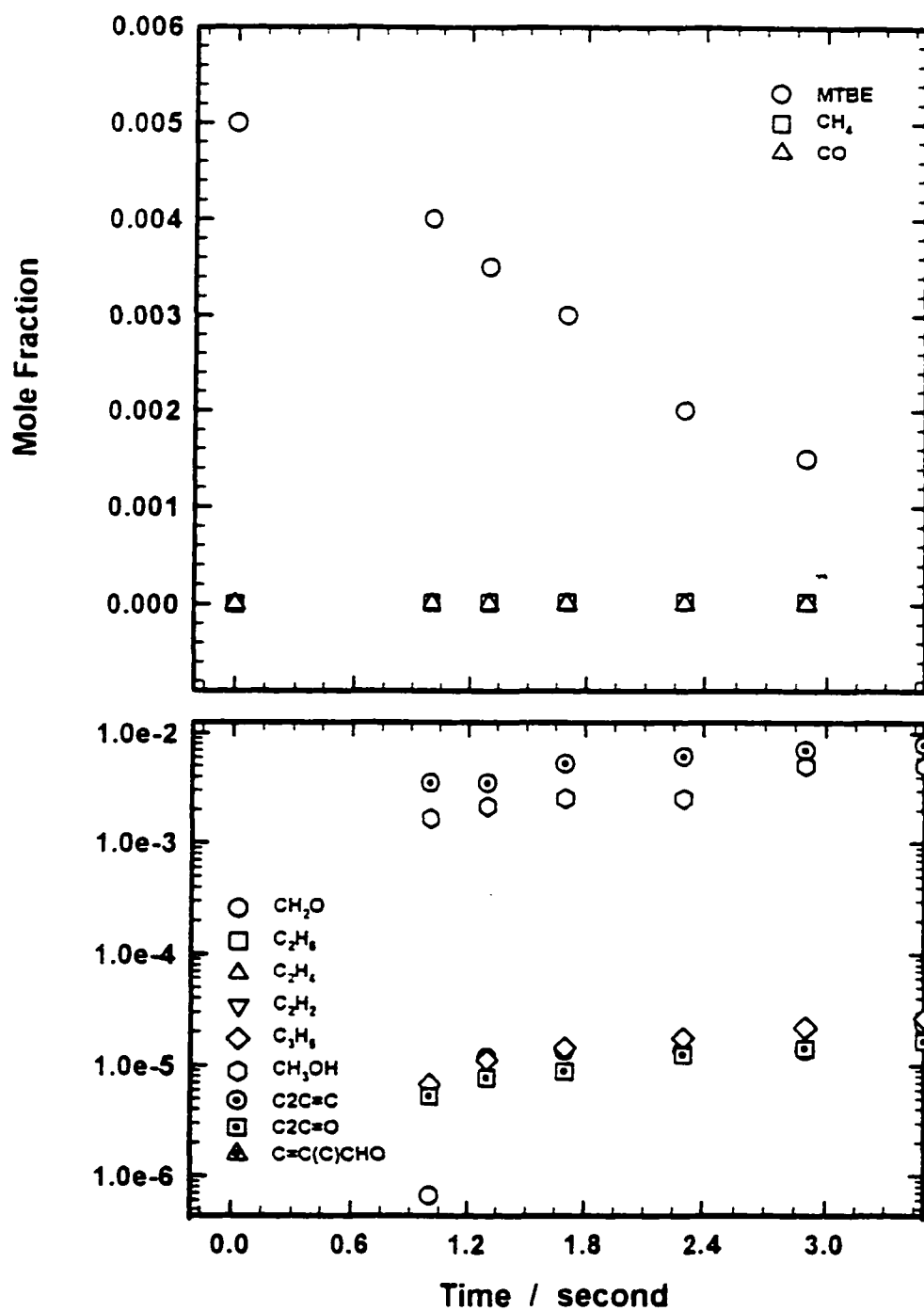


Figure IIC. 70 Experimental result of 0.5% MTBE pyrolysis product distribution at $P = 7$ atm, $T = 873$ K

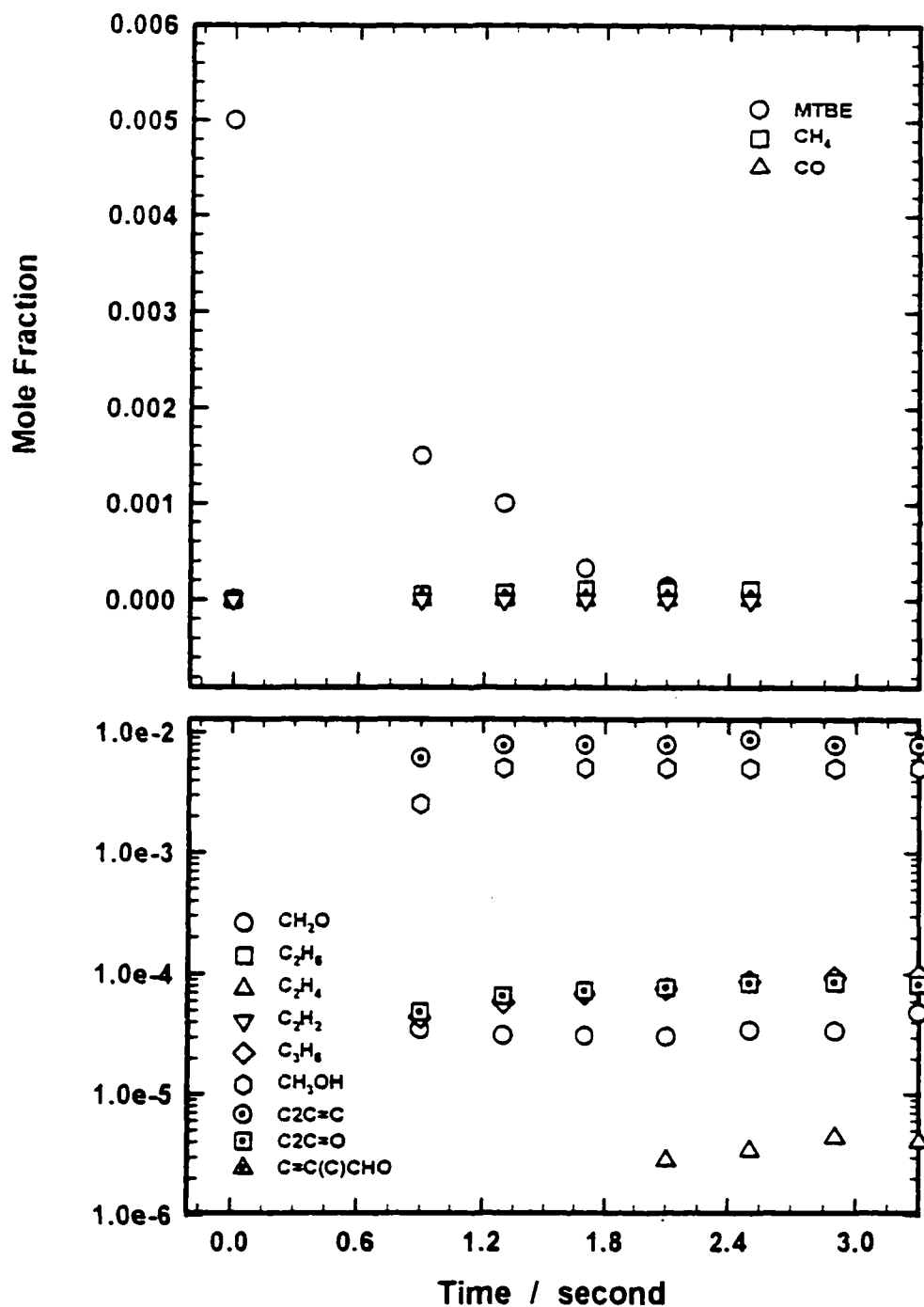


Figure IIC. 71 Experimental result of 0.5% MTBE pyrolysis product distribution at $P = 7$ atm, $T = 923$ K

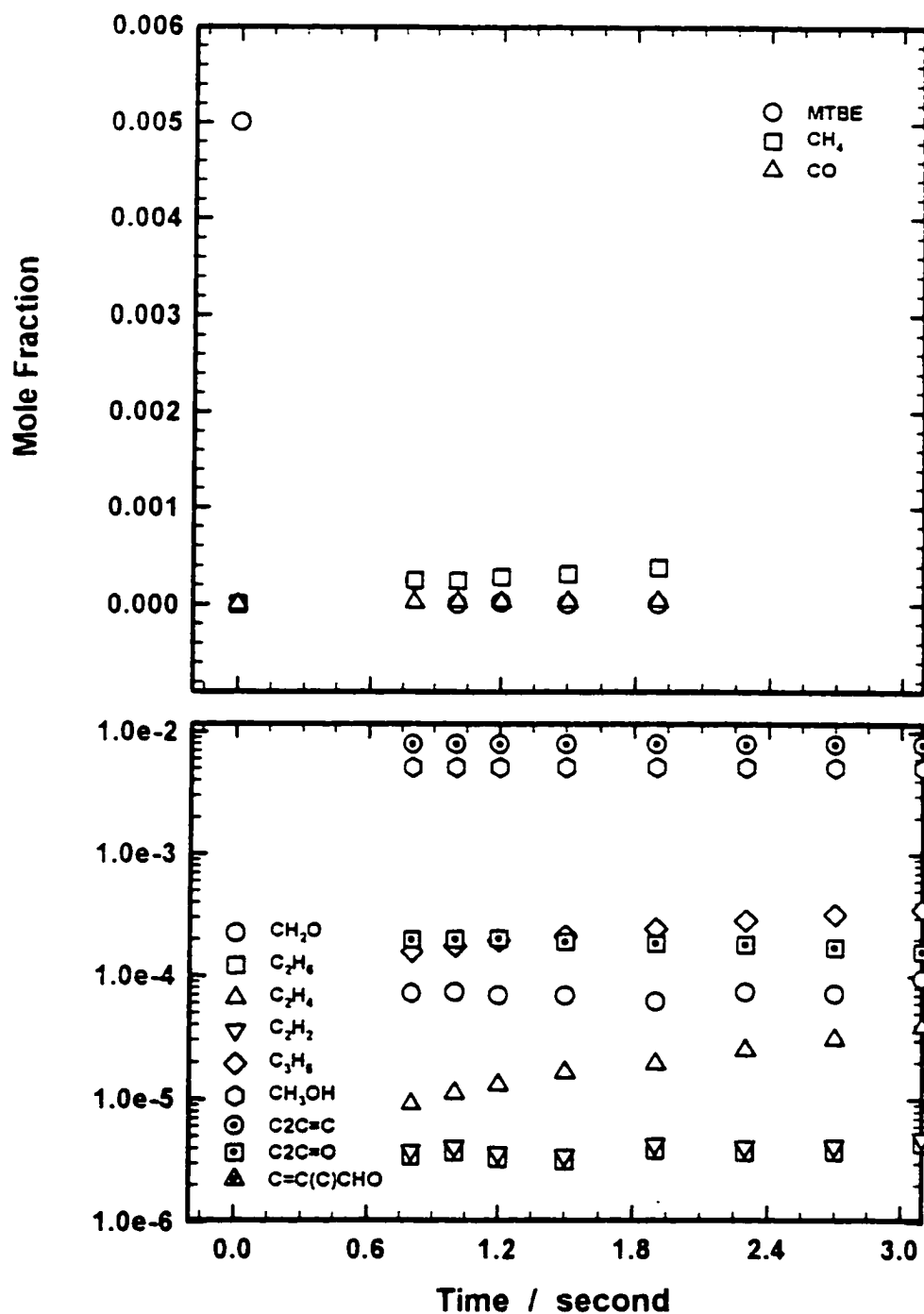


Figure IIC. 72 Experimental result of 0.5% MTBE pyrolysis product distribution at $P = 7$ atm, $T = 973$ K

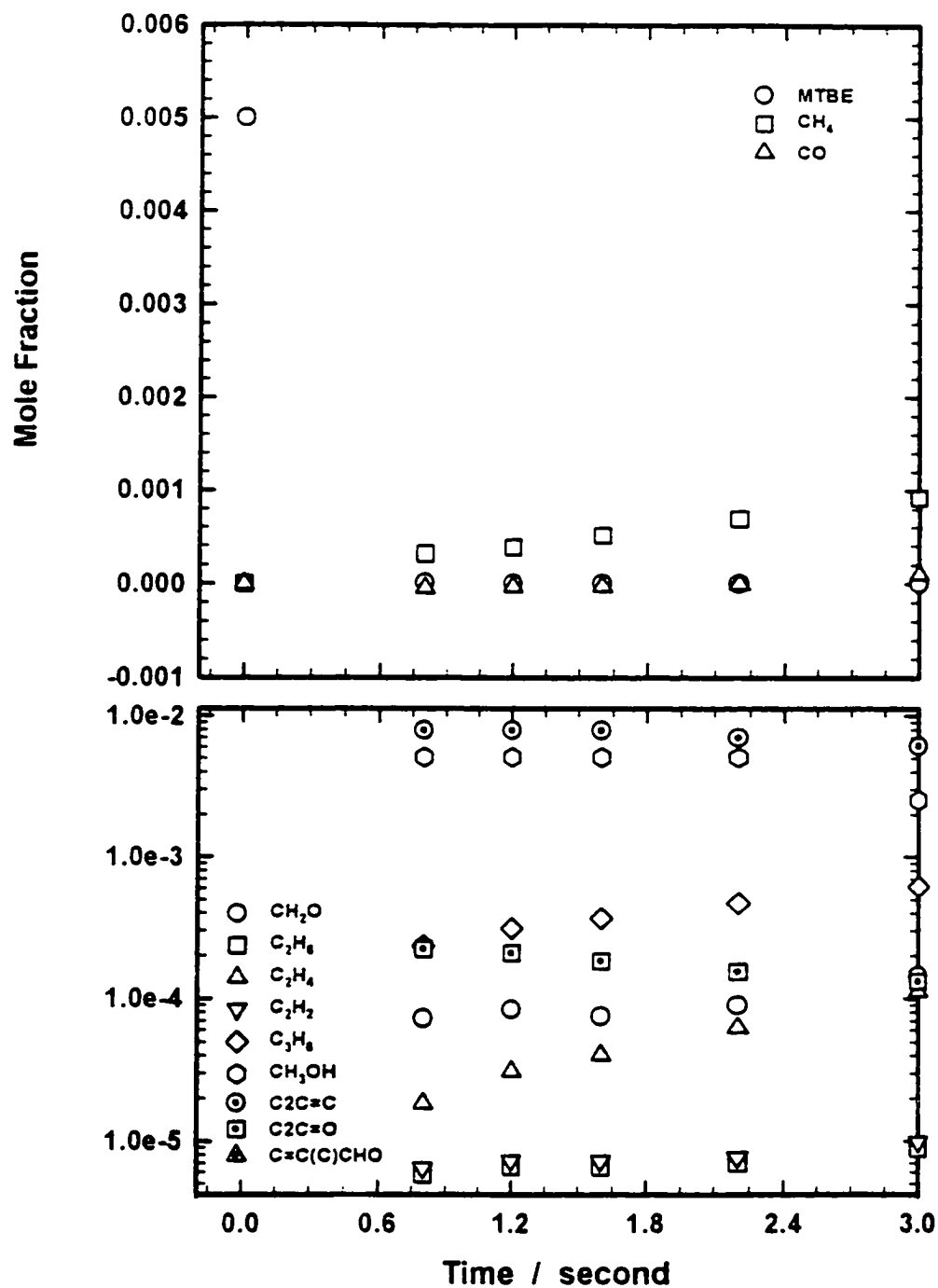


Figure IIC. 73 Experimental result of 0.5% MTBE pyrolysis product distribution at $P = 7$ atm, $T = 998$ K

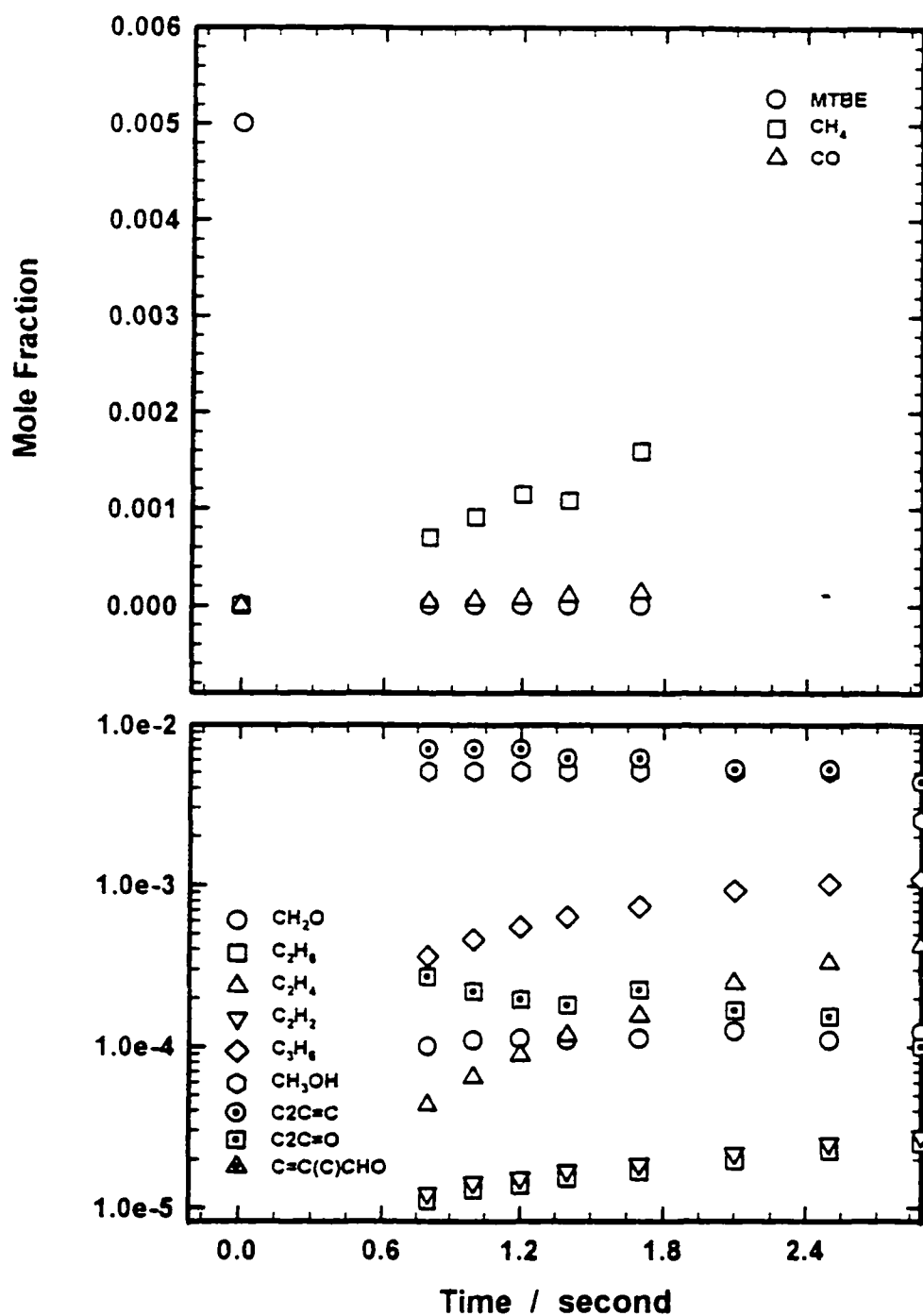


Figure IIC. 74 Experimental result of 0.5% MTBE pyrolysis product distribution at $P = 7$ atm, $T = 1023$ K

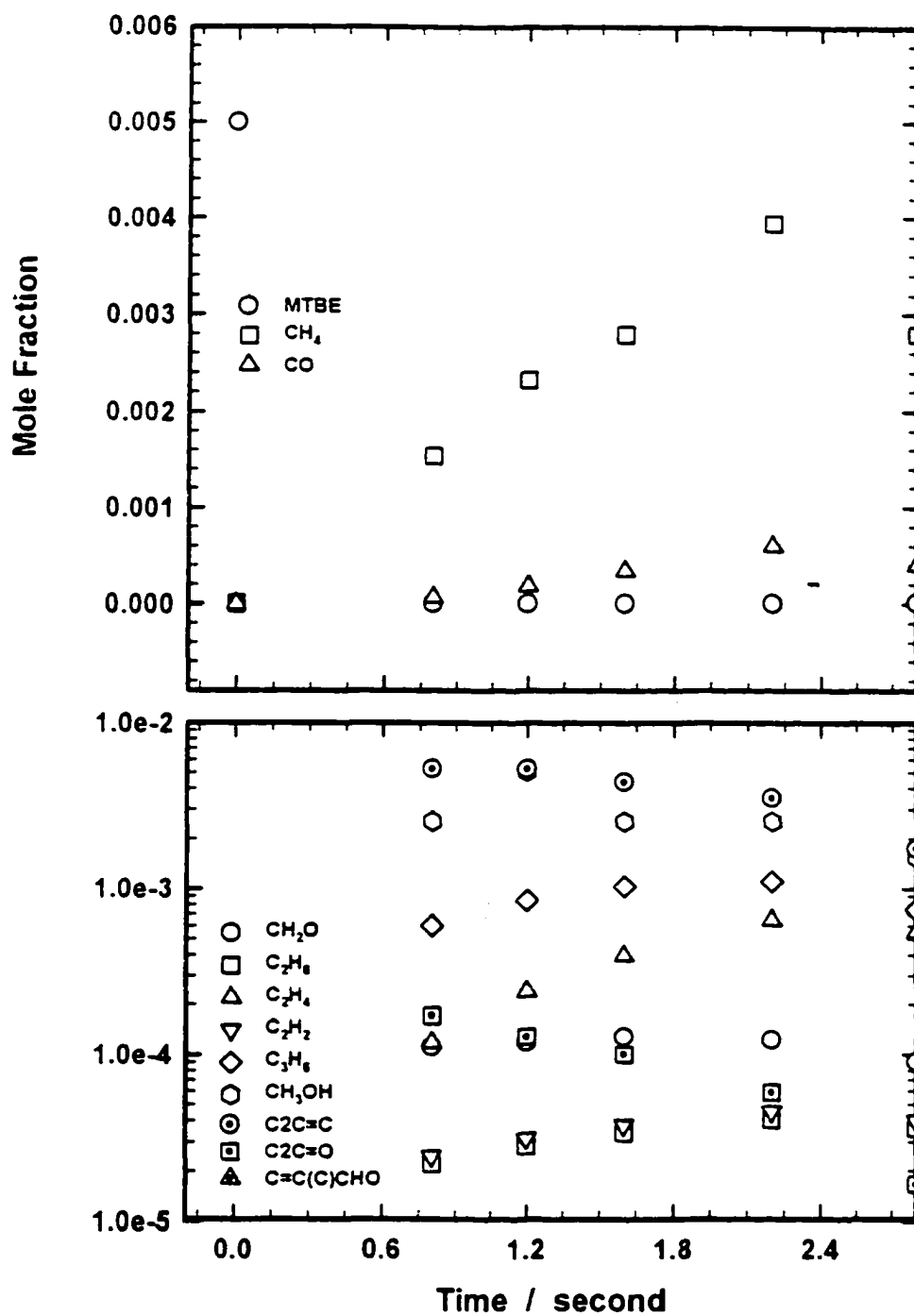


Figure IIC. 75 Experimental result of 0.5% MTBE pyrolysis product distribution at $P = 7$ atm, $T = 1048$ K

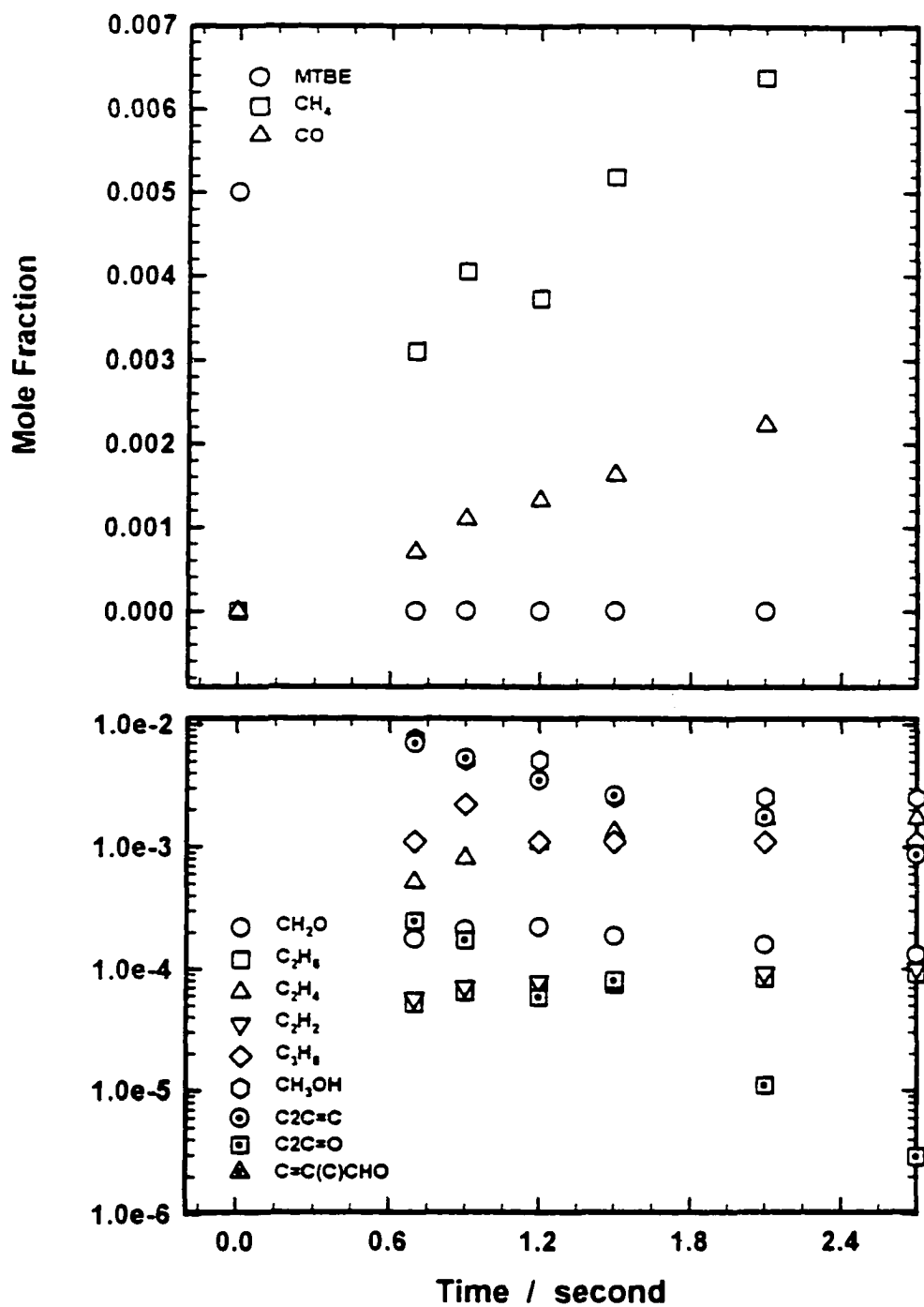


Figure II.C. 76 Experimental result of 0.5% MTBE pyrolysis product distribution at $P = 7$ atm, $T = 1073$ K

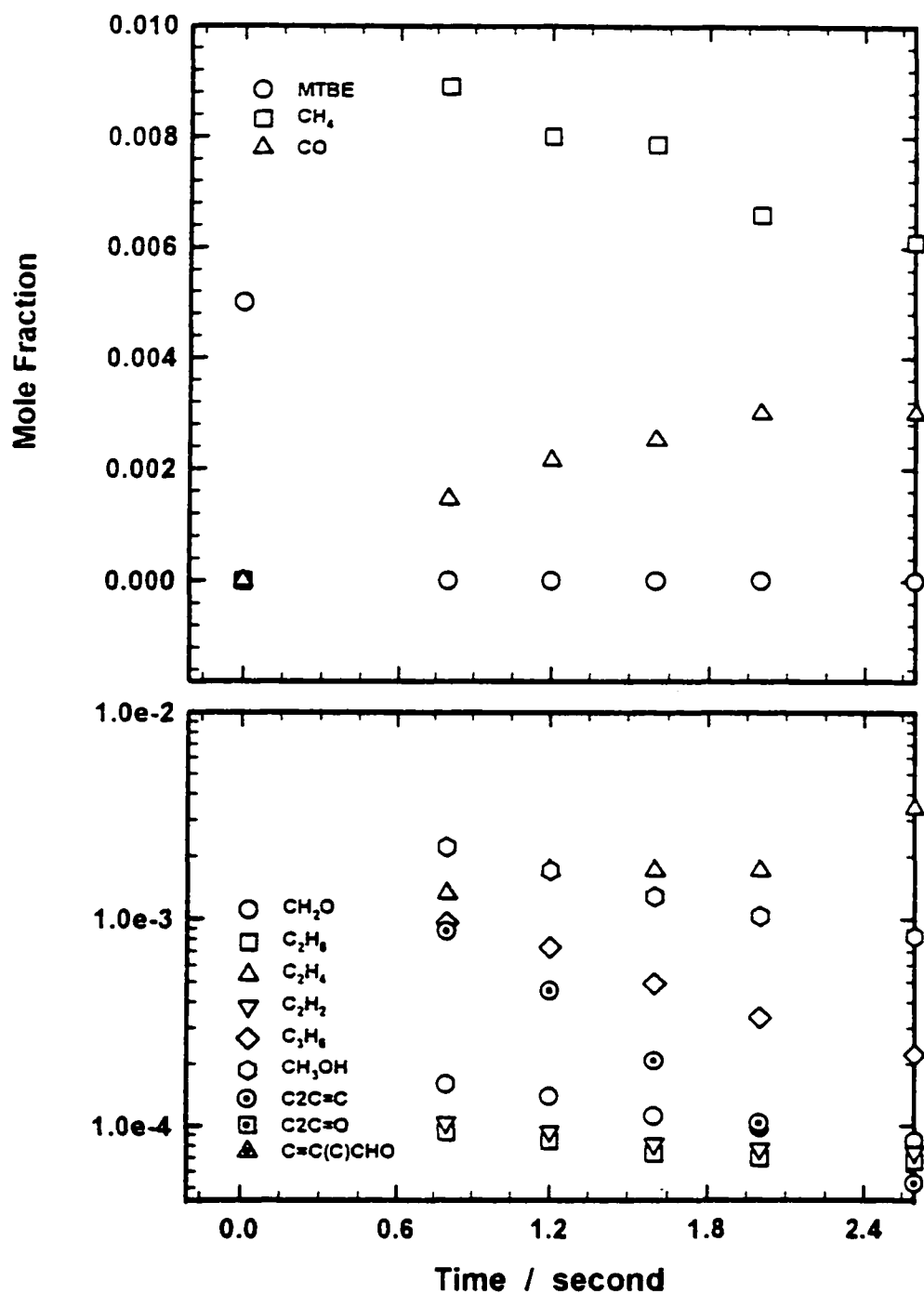


Figure IIC. 77 Experimental result of 0.5% MTBE pyrolysis product distribution at $P = 7$ atm, $T = 1123$ K

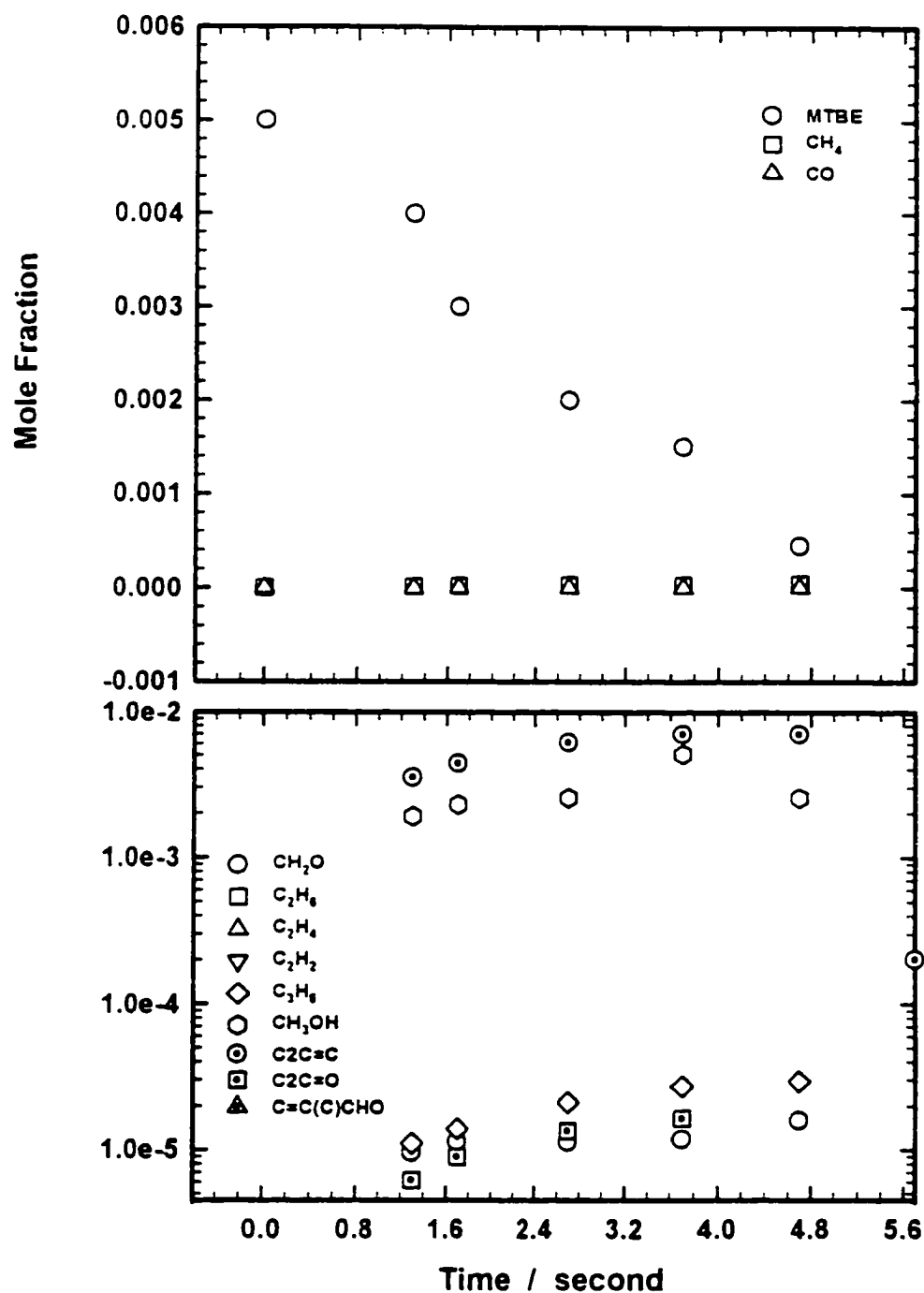


Figure II.C. 78 Experimental result of 0.5% MTBE pyrolysis product distribution at $P = 10$ atm, $T = 873$ K

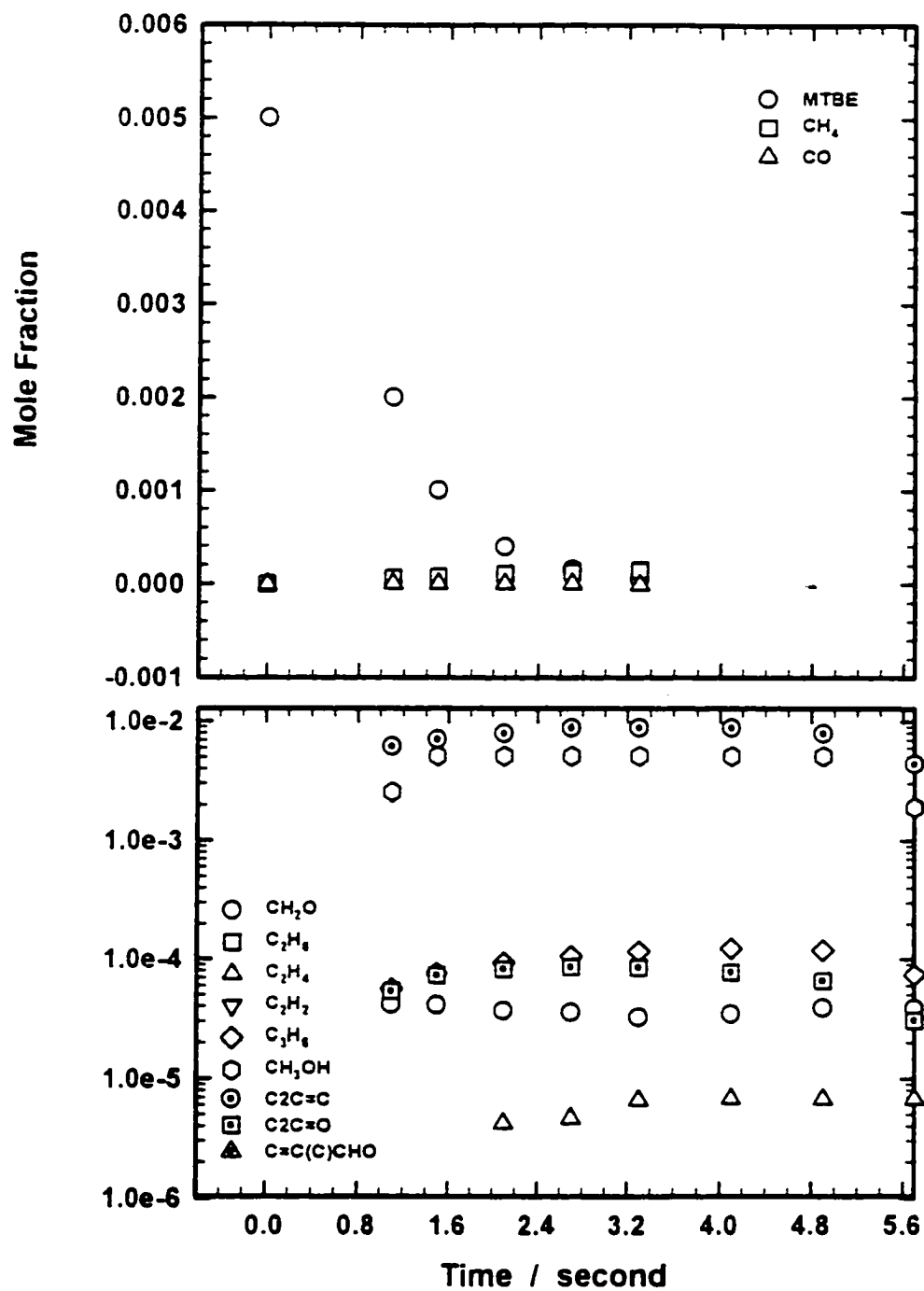


Figure II. 79 Experimental result of 0.5% MTBE pyrolysis product distribution at P = 10 atm, T = 923 K

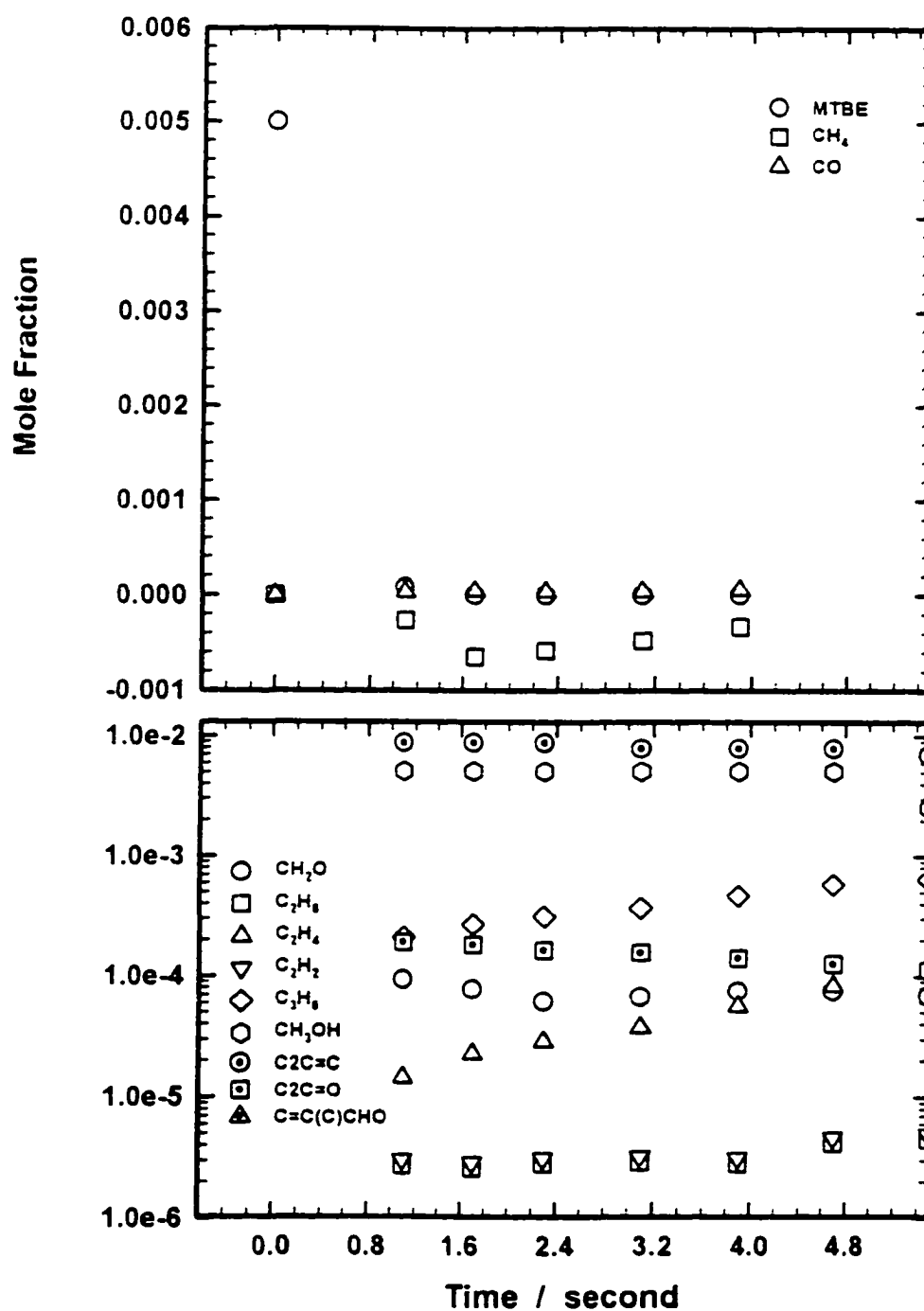


Figure IIC. 80 Experimental result of 0.5% MTBE pyrolysis product distribution at $P = 10$ atm, $T = 973$ K

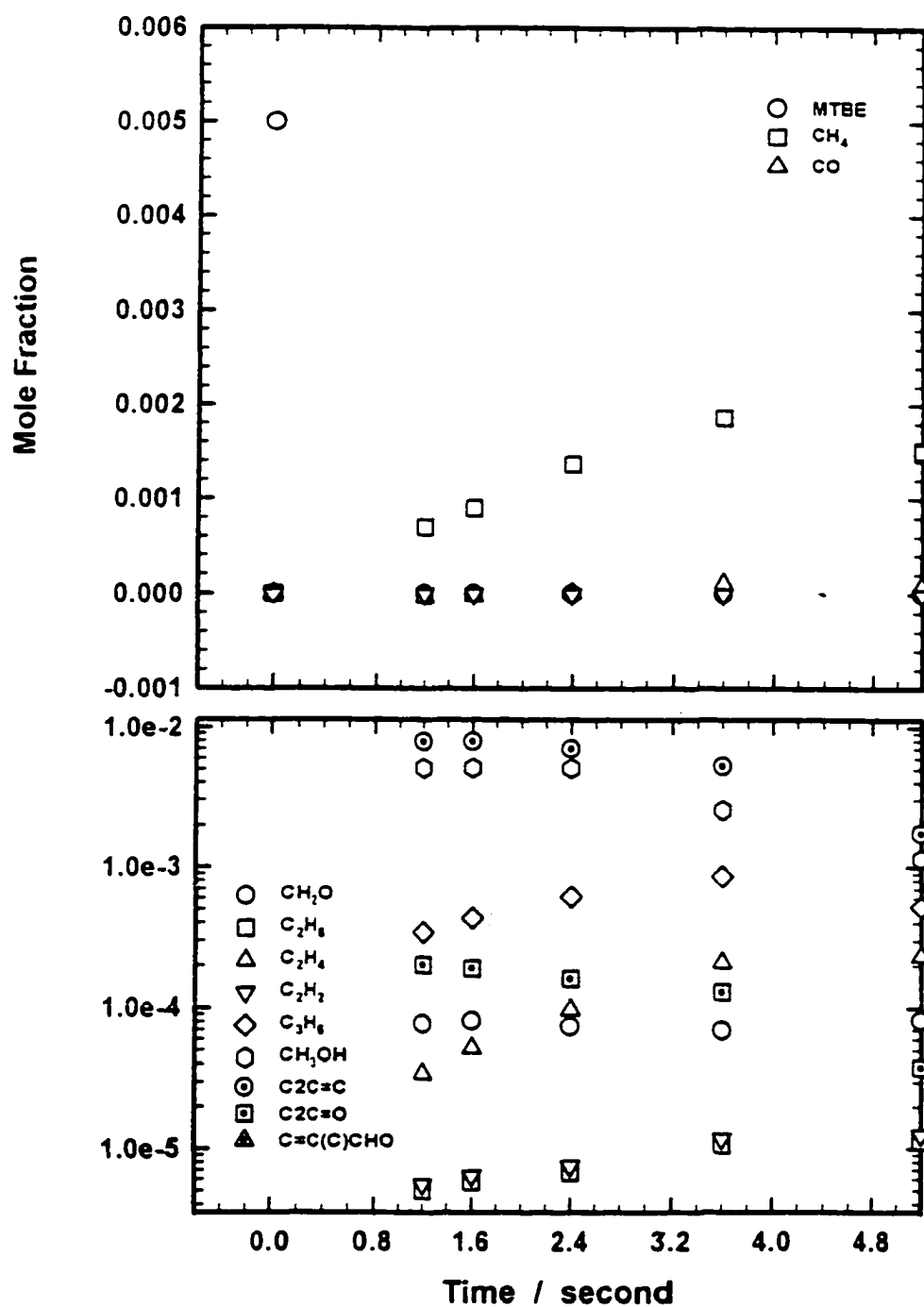


Figure IIC. 81 Experimental result of 0.5% MTBE pyrolysis product distribution at $P = 10$ atm, $T = 998$ K

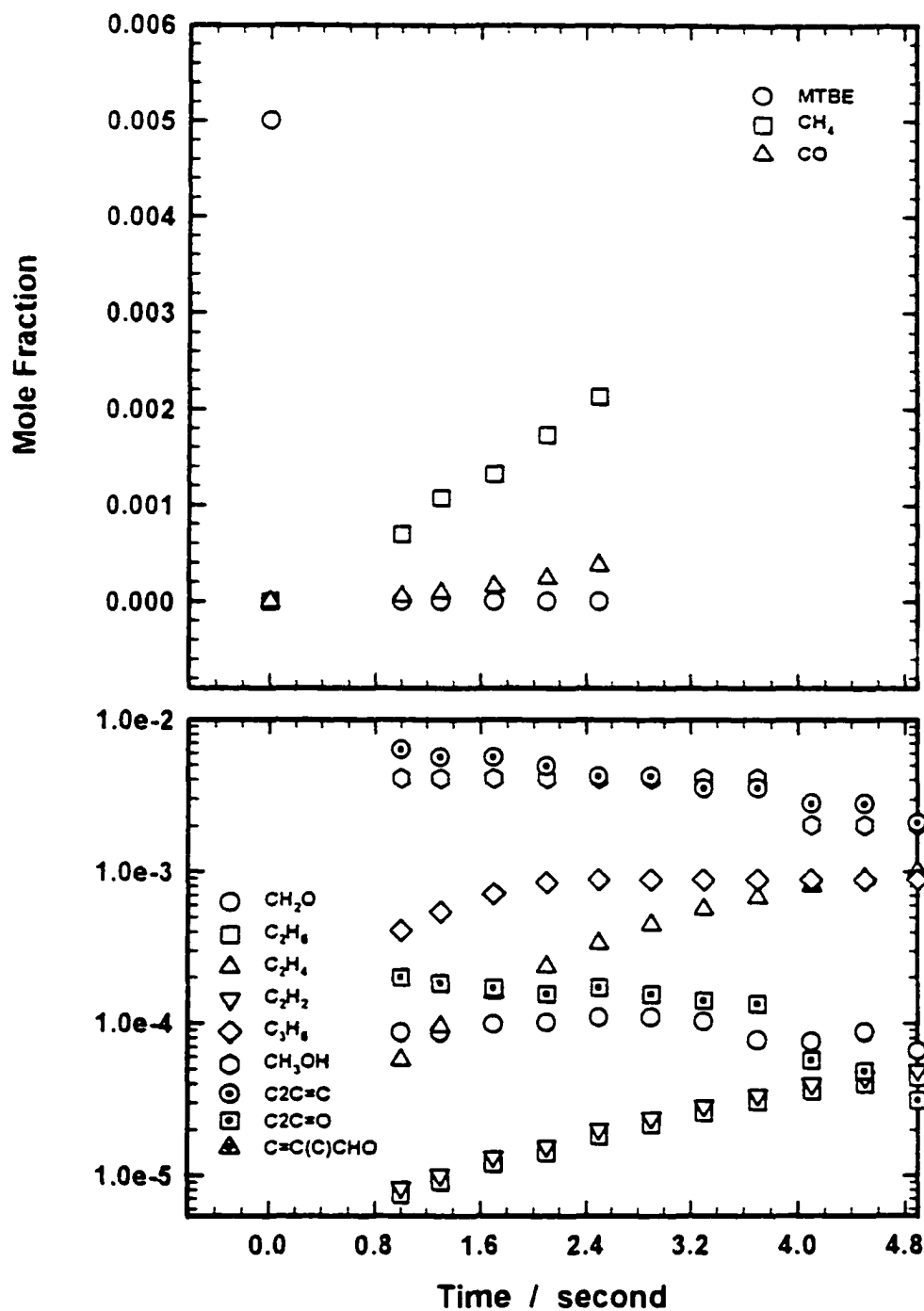


Figure IIC. 82 Experimental result of 0.5% MTBE pyrolysis product distribution at $P = 10$ atm, $T = 1023$ K

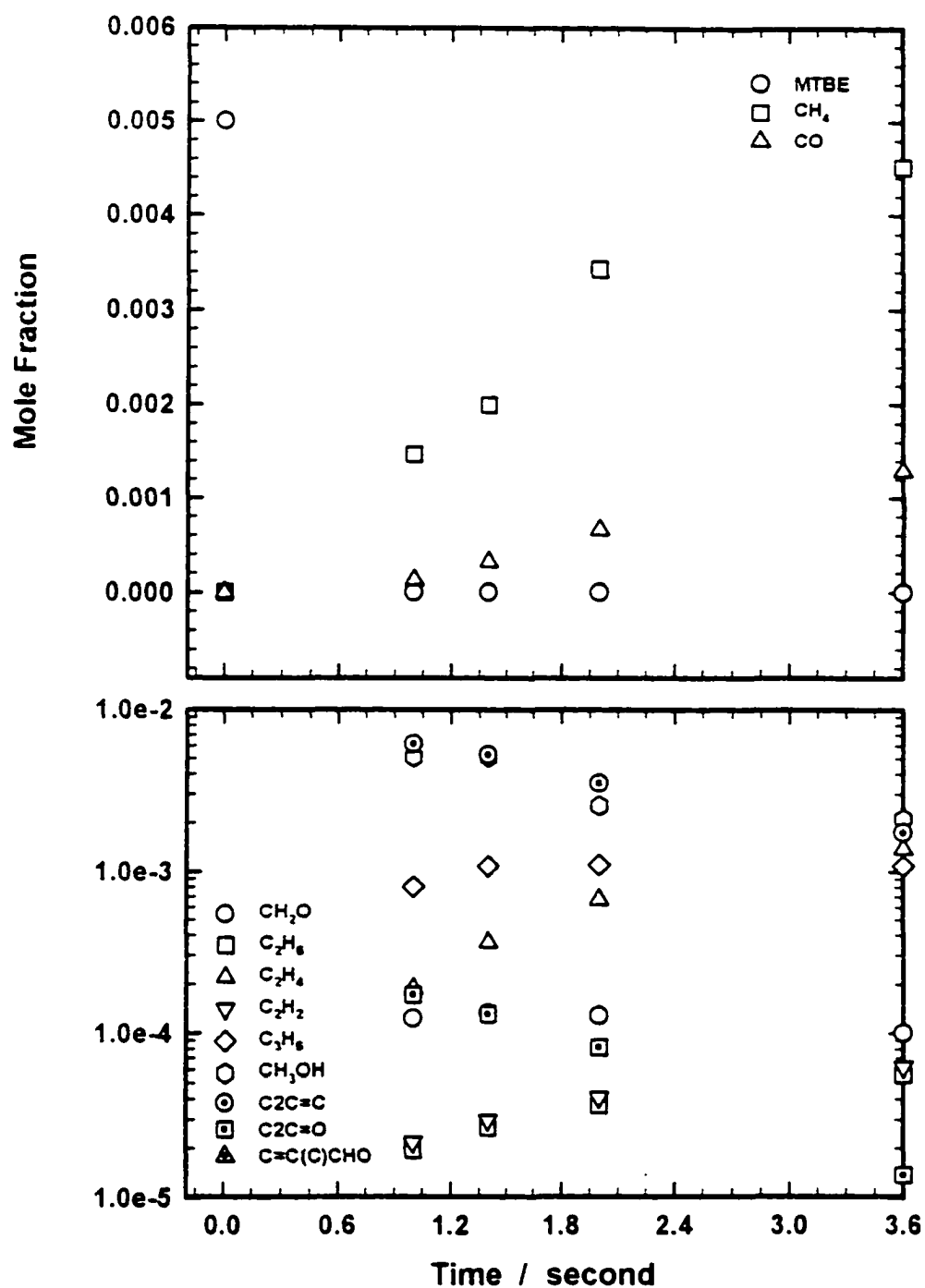


Figure II. 83 Experimental result of 0.5% MTBE pyrolysis product distribution at $P = 10$ atm, $T = 1048$ K

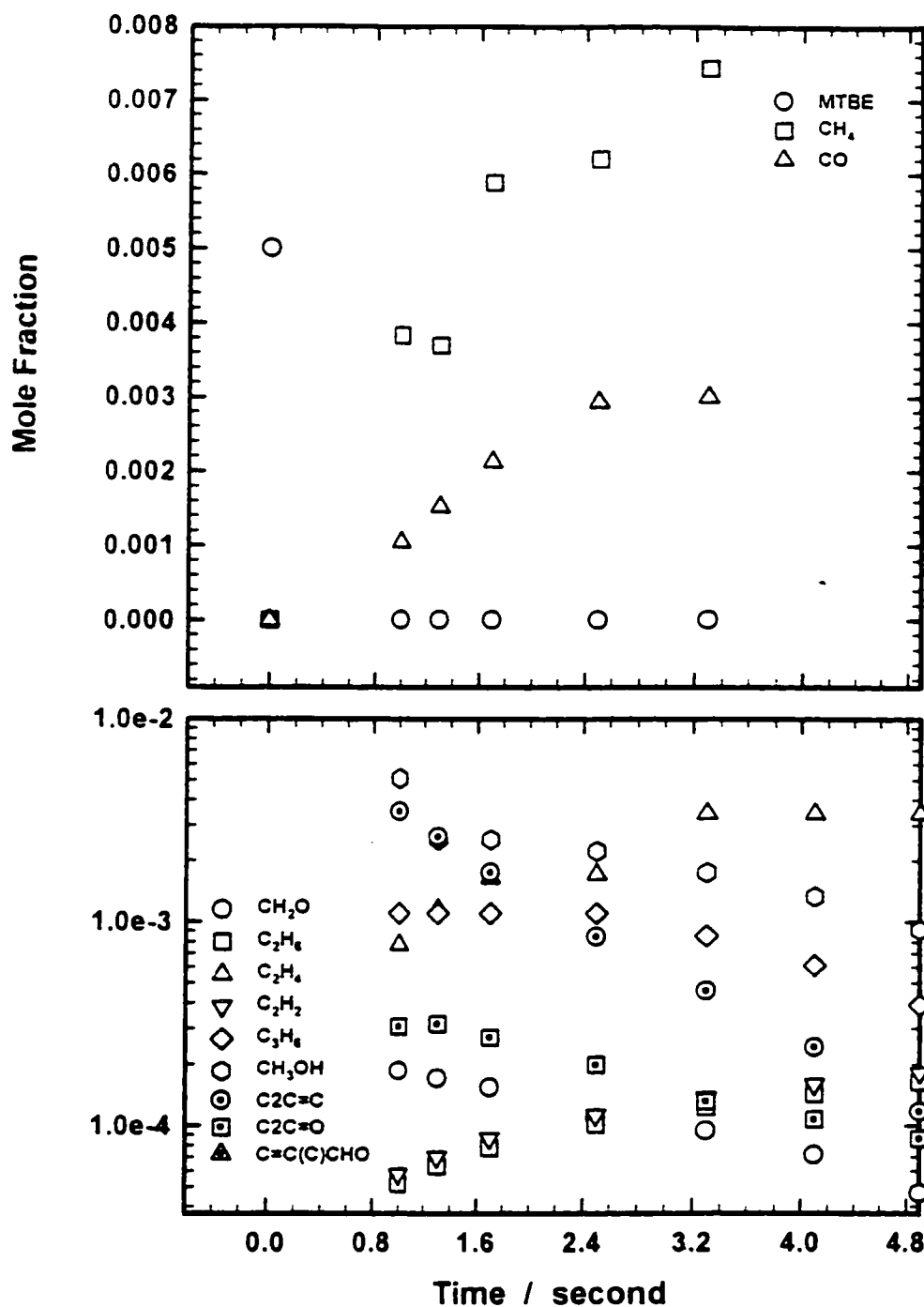


Figure IIC. 84 Experimental result of 0.5% MTBE pyrolysis product distribution at $P = 10$ atm, $T = 1073$ K

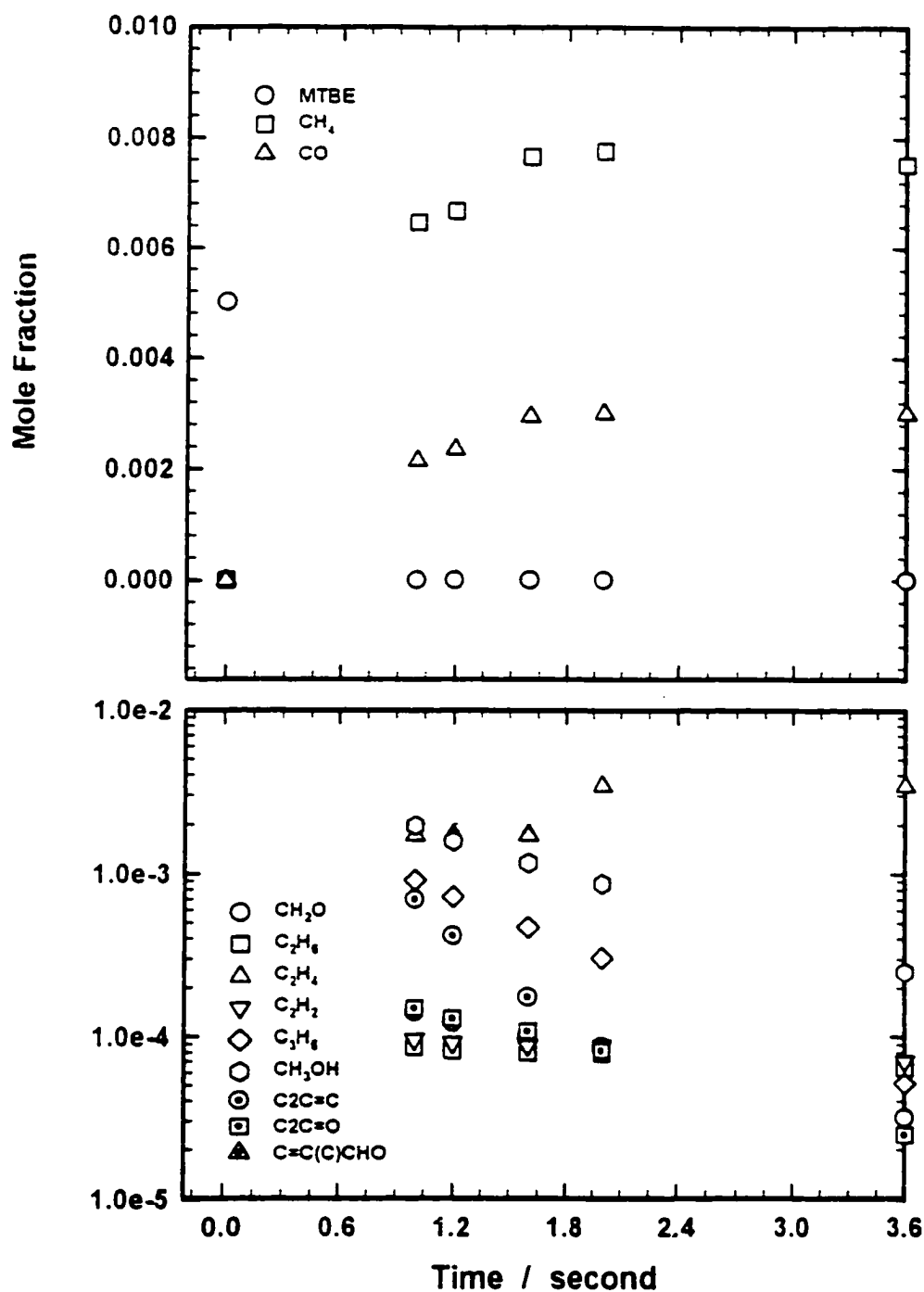


Figure II.C. 85 Experimental result of 0.5% MTBE pyrolysis product distribution at $P = 10$ atm, $T = 1123$ K

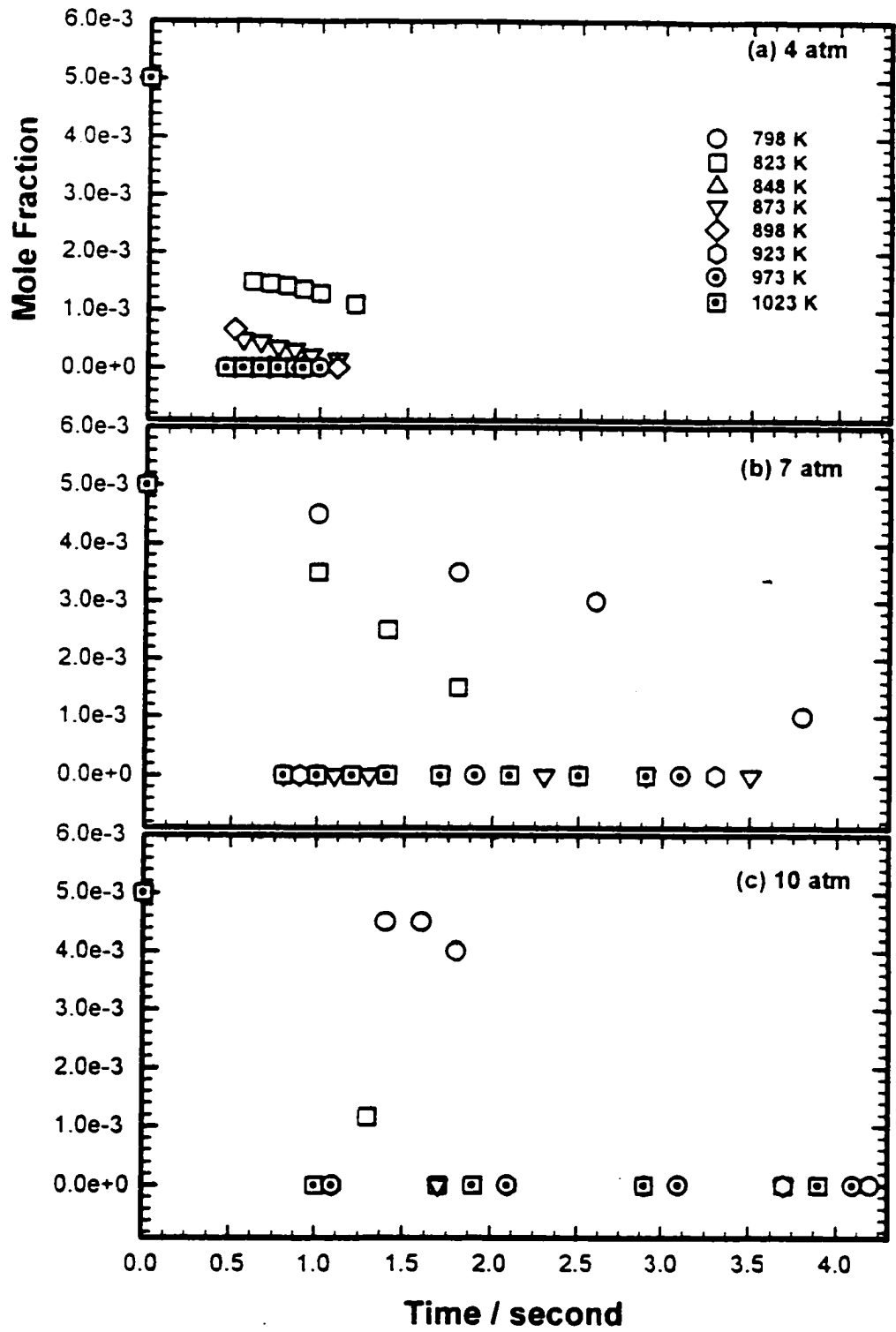


Figure IIC. 86 Experimental result of 0.5% MTBE oxidation: temperature and pressure dependence of MTBE at $\phi = 0.75$

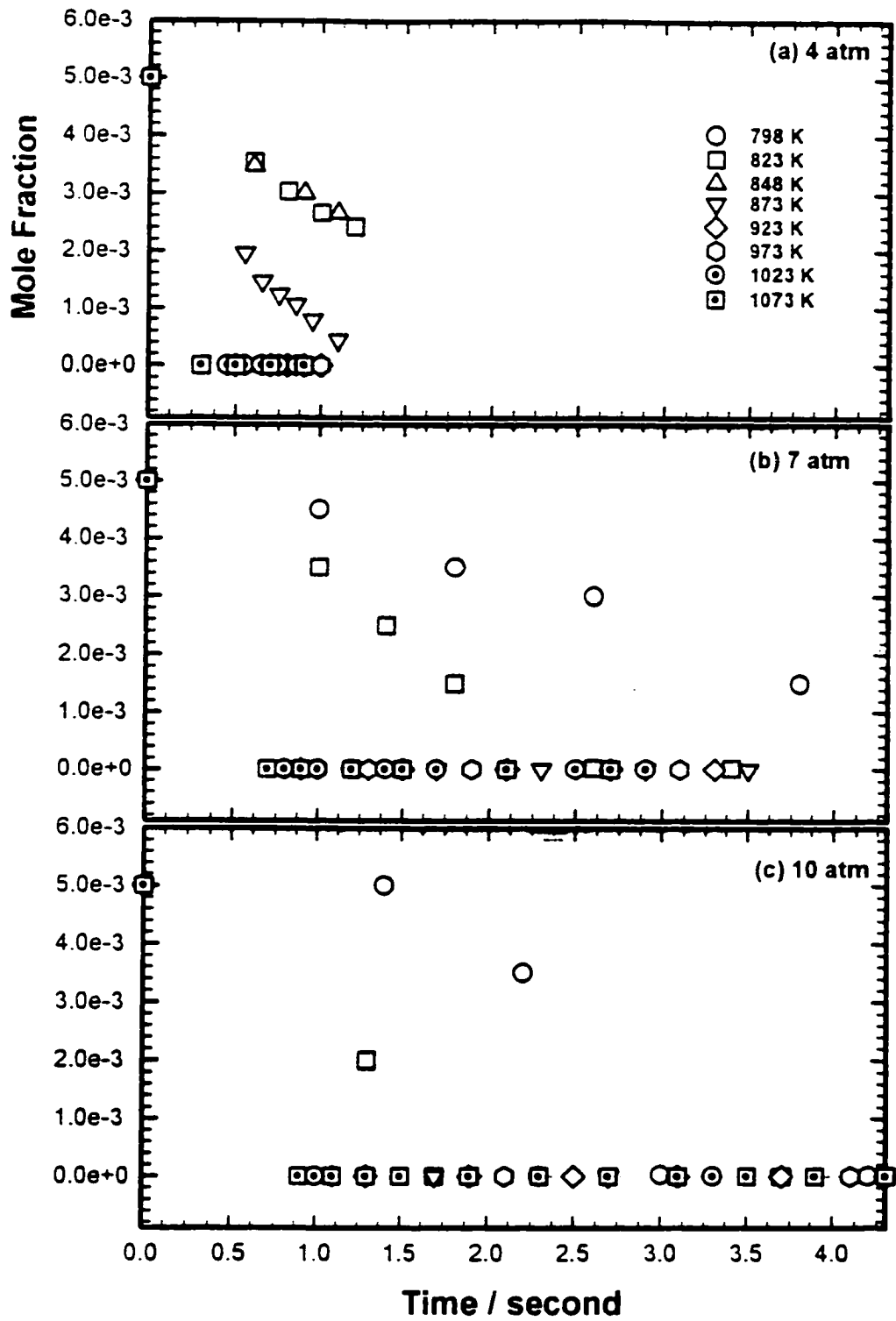


Figure IIC. 87 Experimental result of 0.5% MTBE oxidation: temperature and pressure dependence of MTBE at $\phi = 1.00$

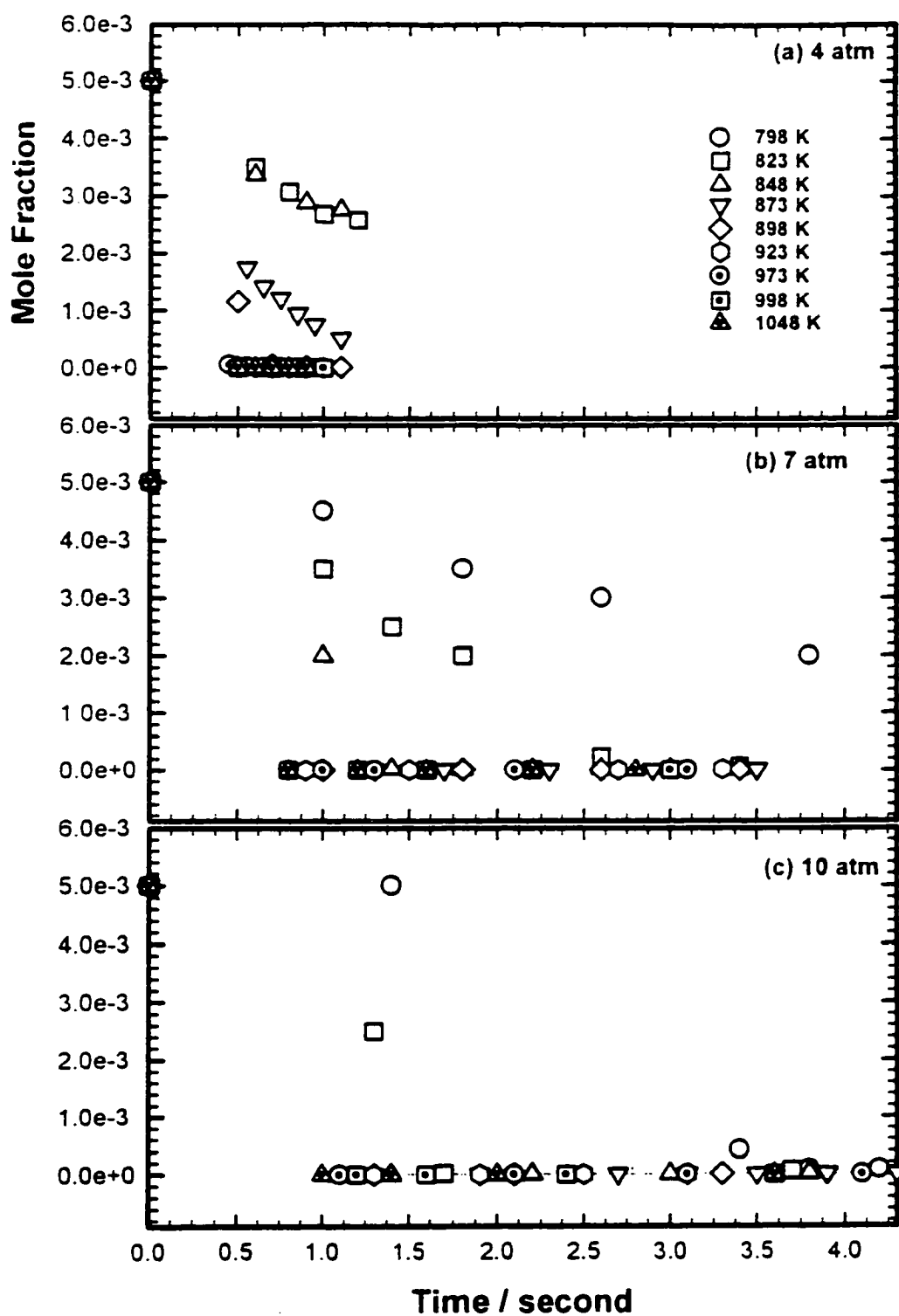


Figure IIC. 88 Experimental result of 0.5% MTBE oxidation: temperature and pressure dependence of MTBE at $\phi = 1.50$

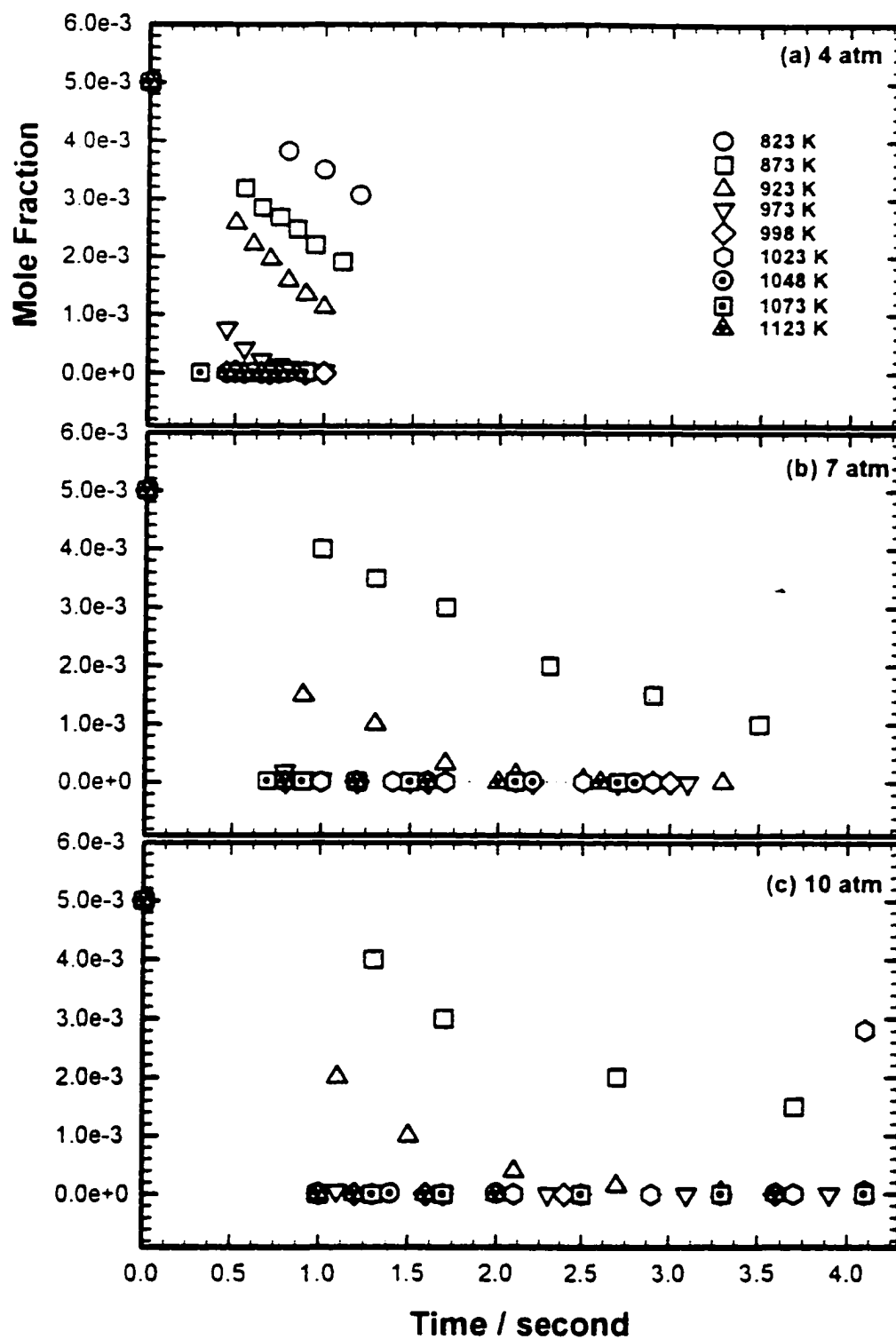


Figure IIC. 89 Experimental result of 0.5% MTBE pyrolysis: temperature and pressure dependence of MTBE

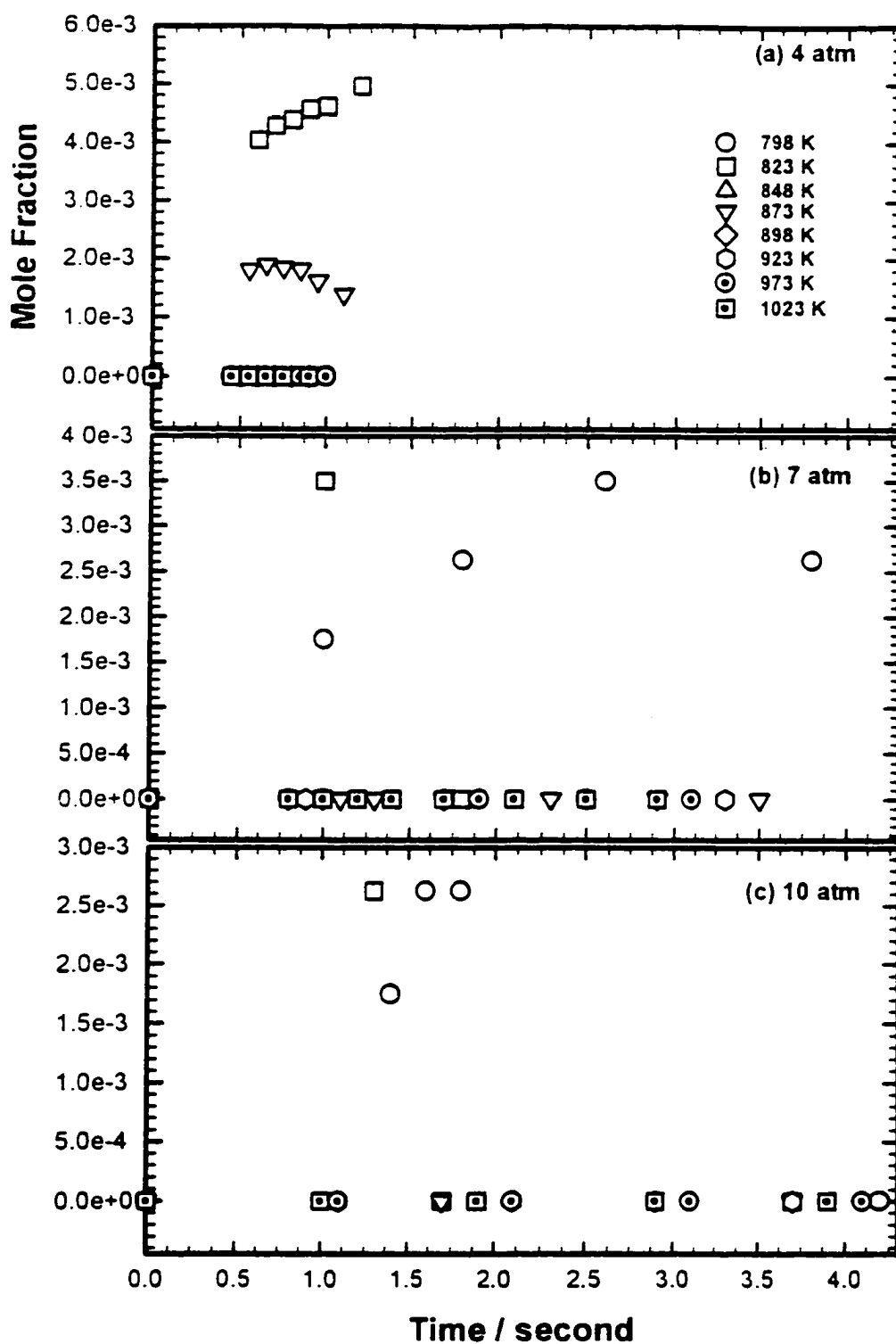


Figure II.C. 90 Experimental result of 0.5% MTBE oxidation: temperature and pressure dependence of $C_2C=C$ at $\phi = 0.75$

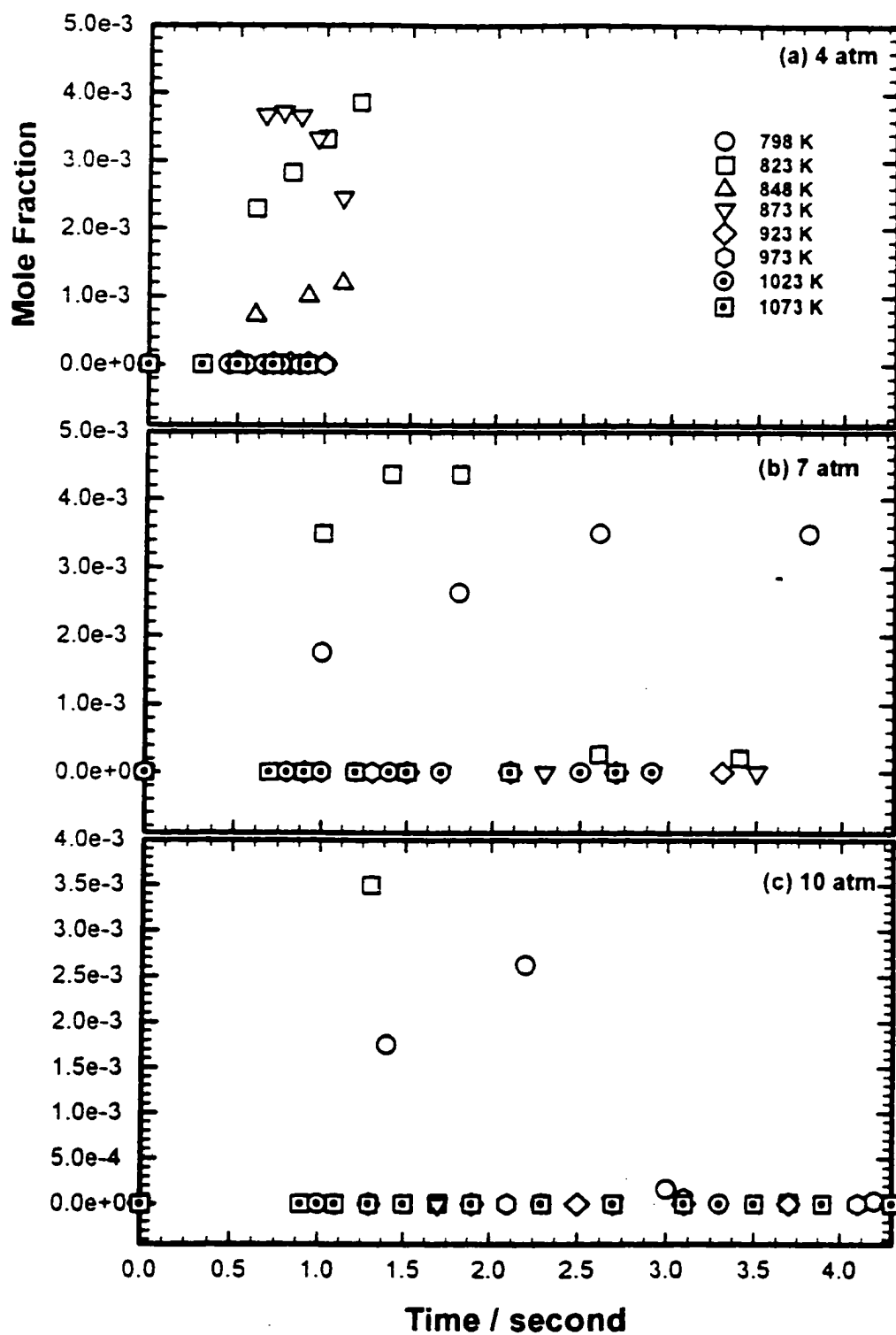


Figure IIC. 91 Experimental result of 0.5% MTBE oxidation: temperature and pressure dependence of $C_2C=C$ at $\phi = 1.00$

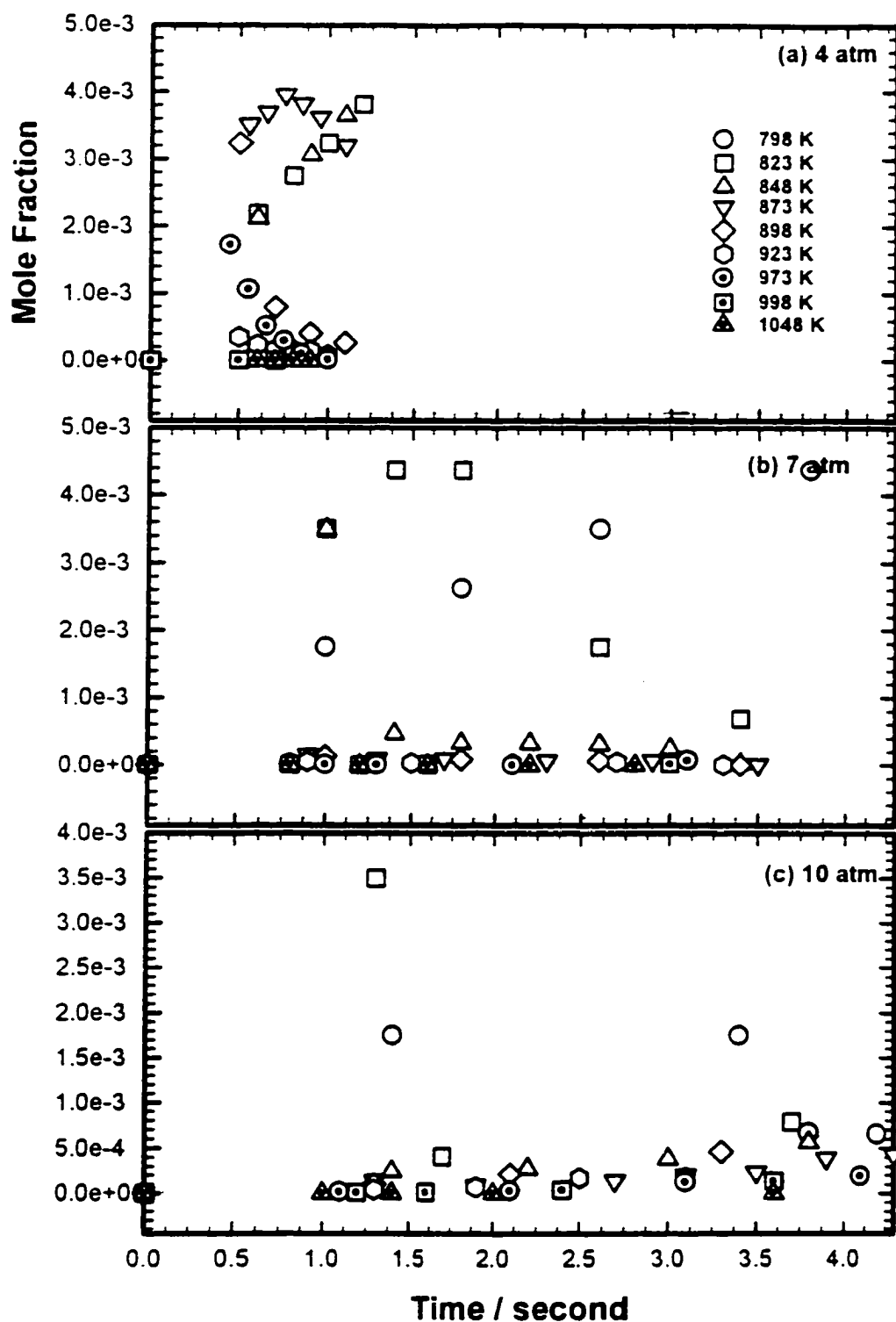


Figure IIC. 92 Experimental result of 0.5% MTBE oxidation: temperature and pressure dependence of $C_2C=C$ at $\phi = 1.50$

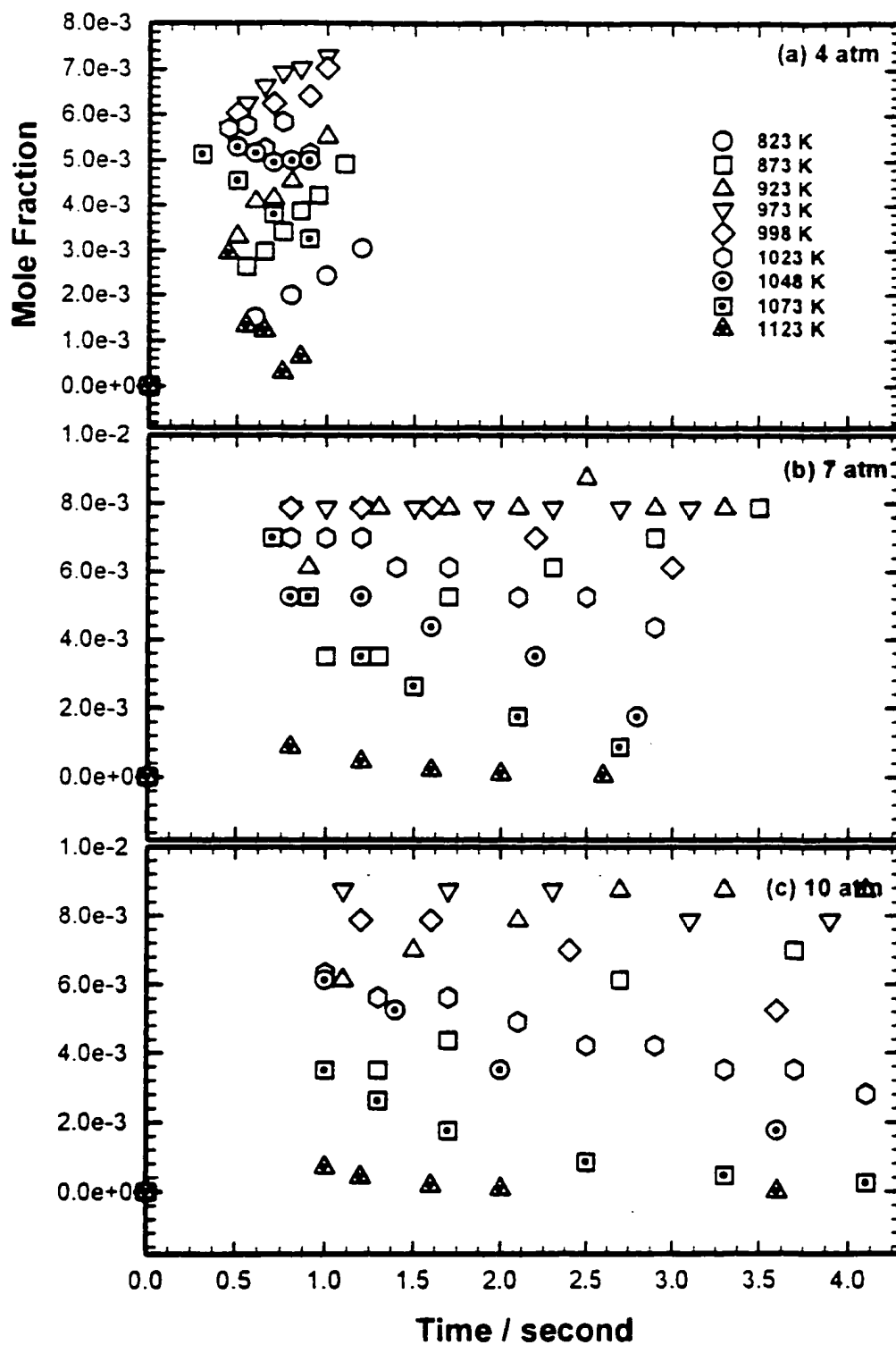


Figure IIC. 93 Experimental result of 0.5% MTBE pyrolysis: temperature and pressure dependence of $C_2C=C$

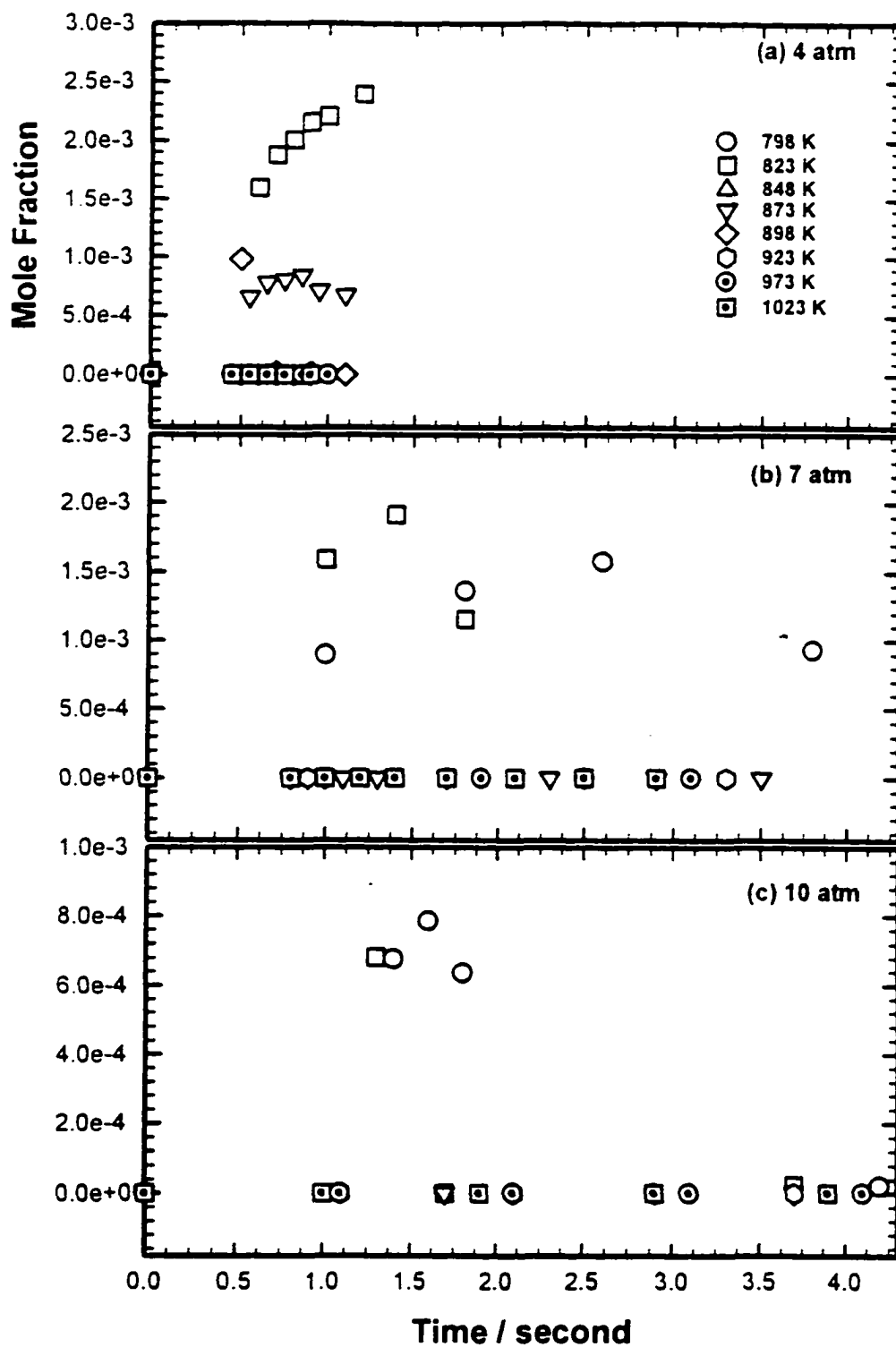


Figure IIC. 94 Experimental result of 0.5% MTBE oxidation: temperature and pressure dependence of CH_3OH at $\phi = 0.75$

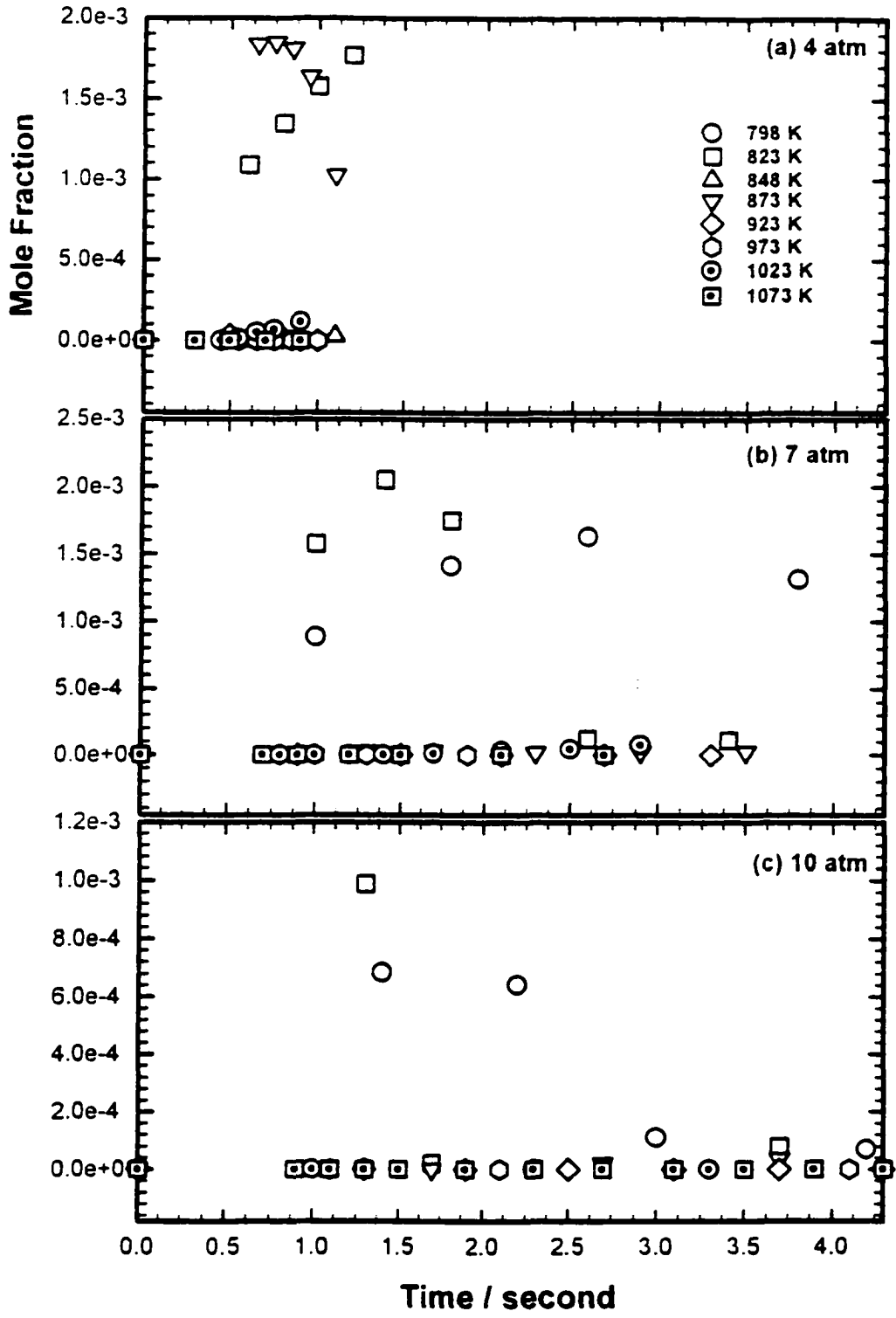


Figure II.C. 95 Experimental result of 0.5% MTBE oxidation: temperature and pressure dependence of CH_3OH at $\phi = 1.00$

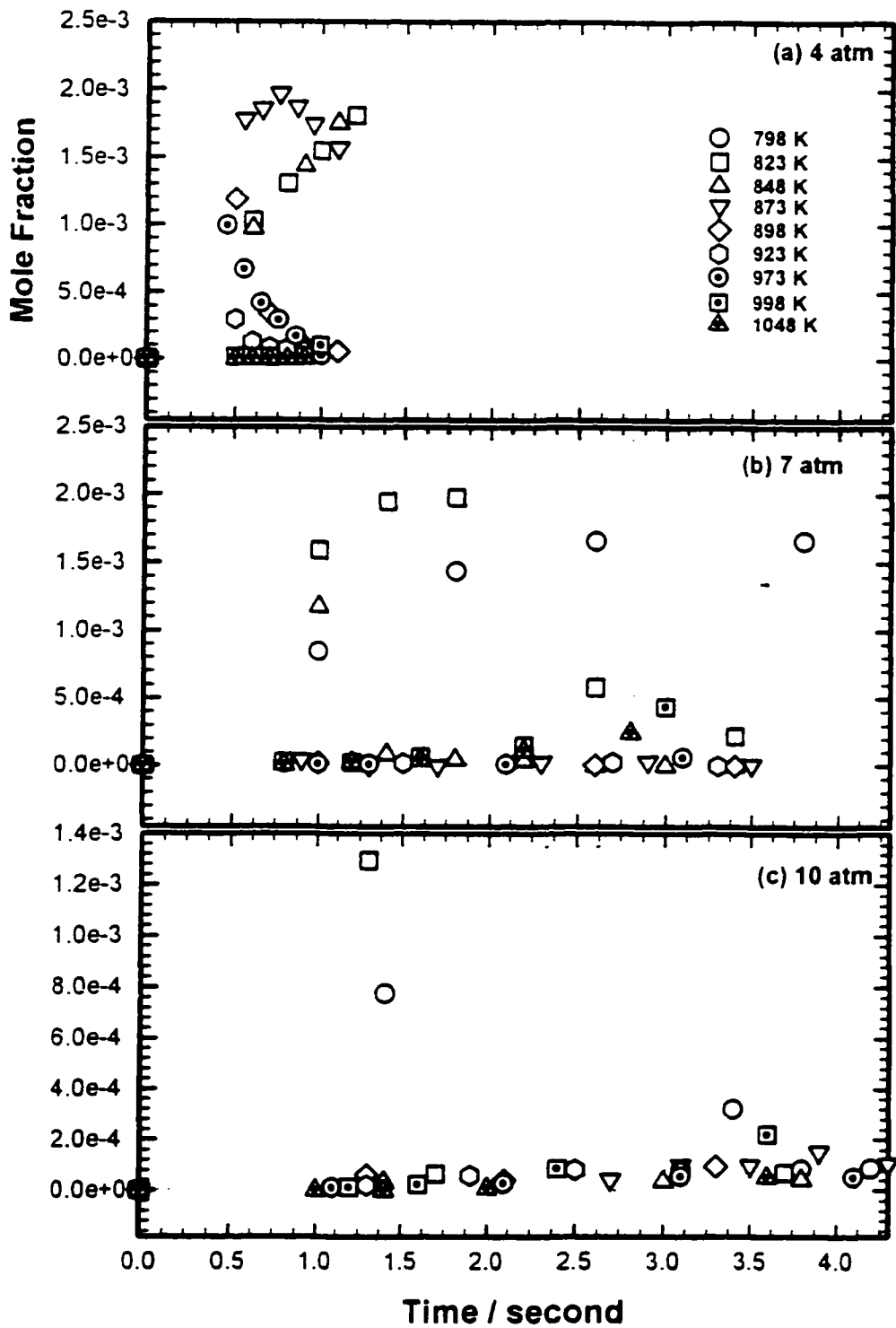


Figure IIC. 96 Experimental result of 0.5% MTBE oxidation: temperature and pressure dependence of CH_3OH at $\phi = 1.50$

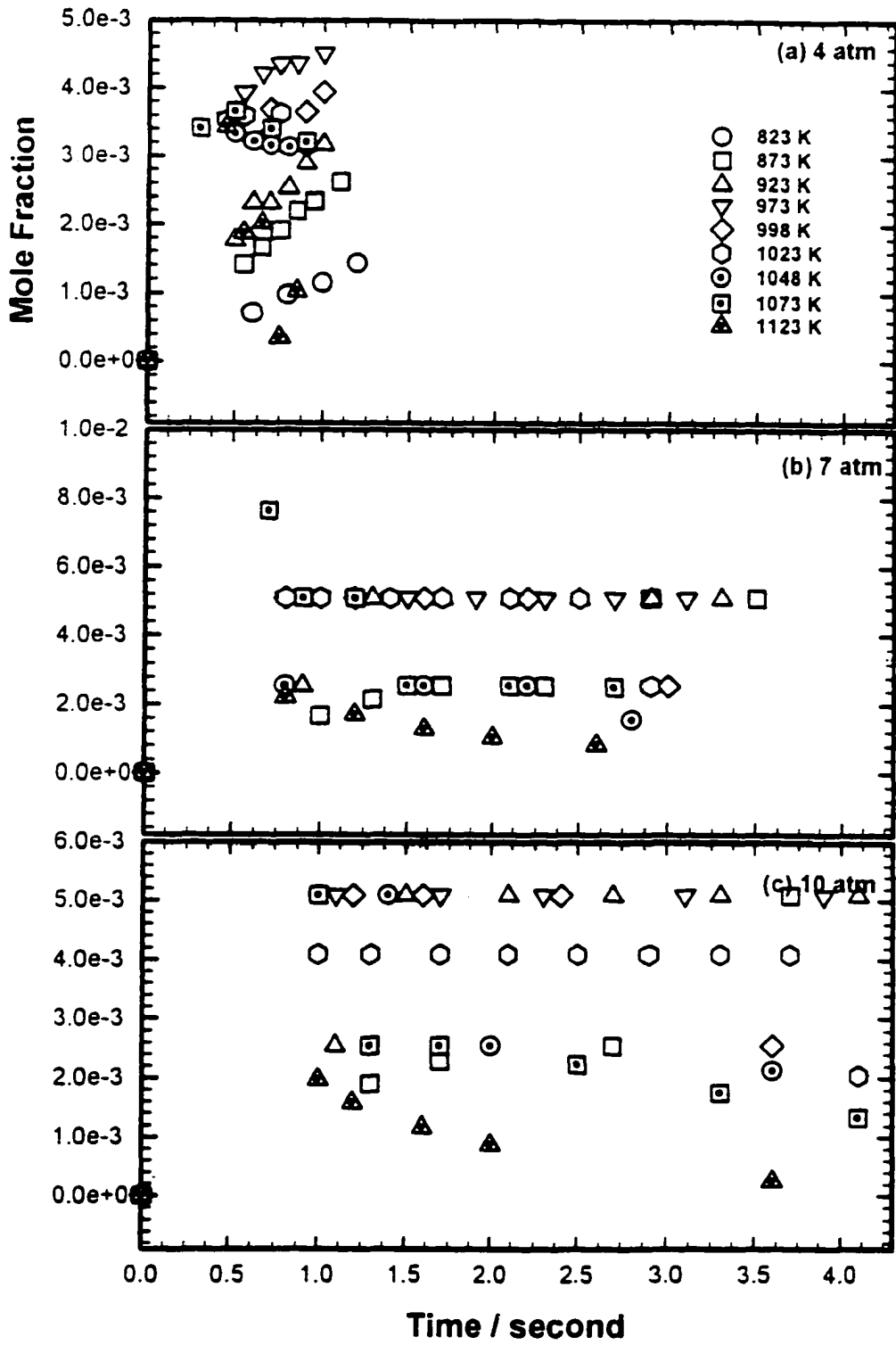


Figure IIC. 97 Experimental result of 0.5% MTBE pyrolysis: temperature and pressure dependence of CH_3OH

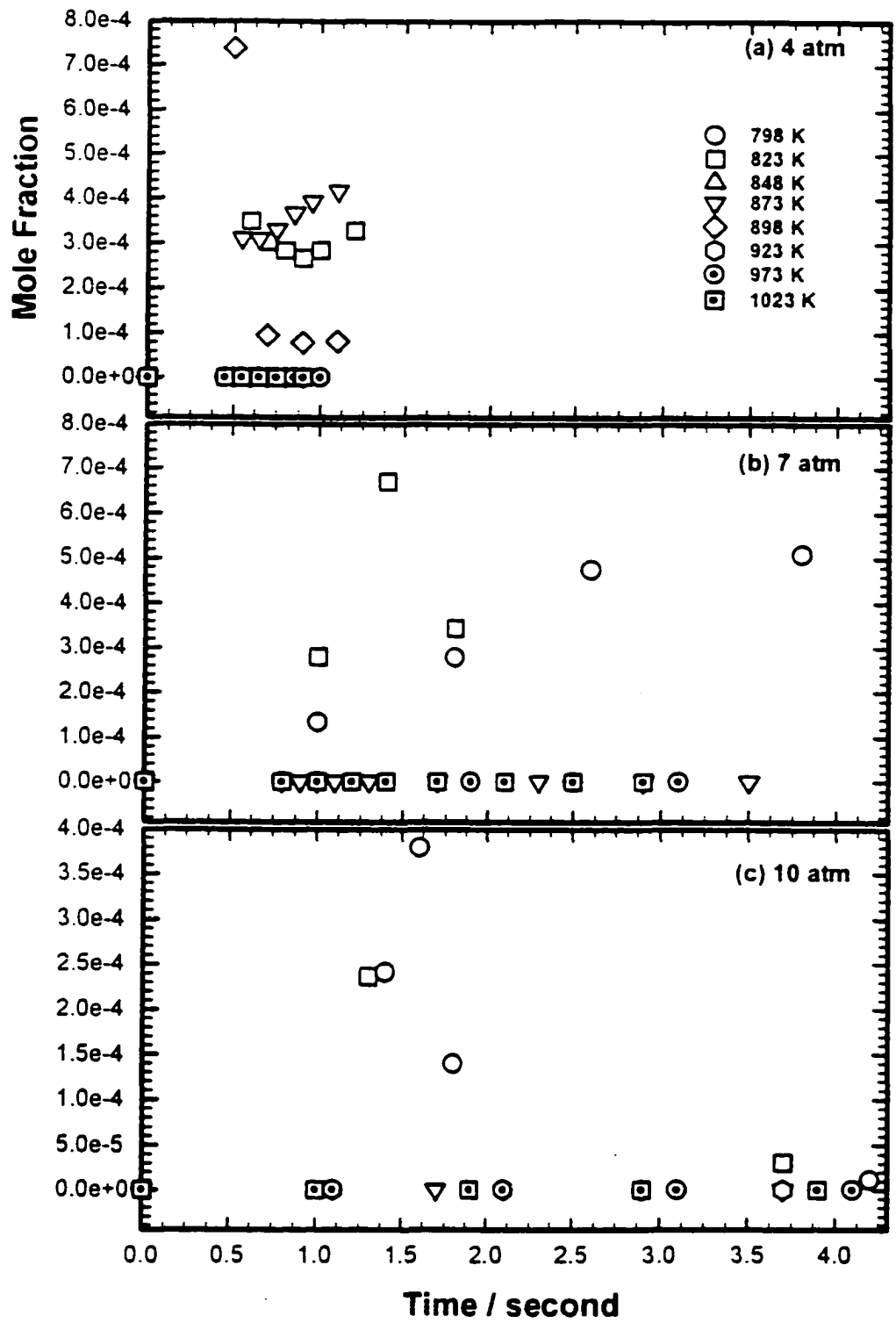


Figure II.C. 98 Experimental result of 0.5% MTBE oxidation: temperature and pressure dependence of CH_2O at $\phi = 0.75$

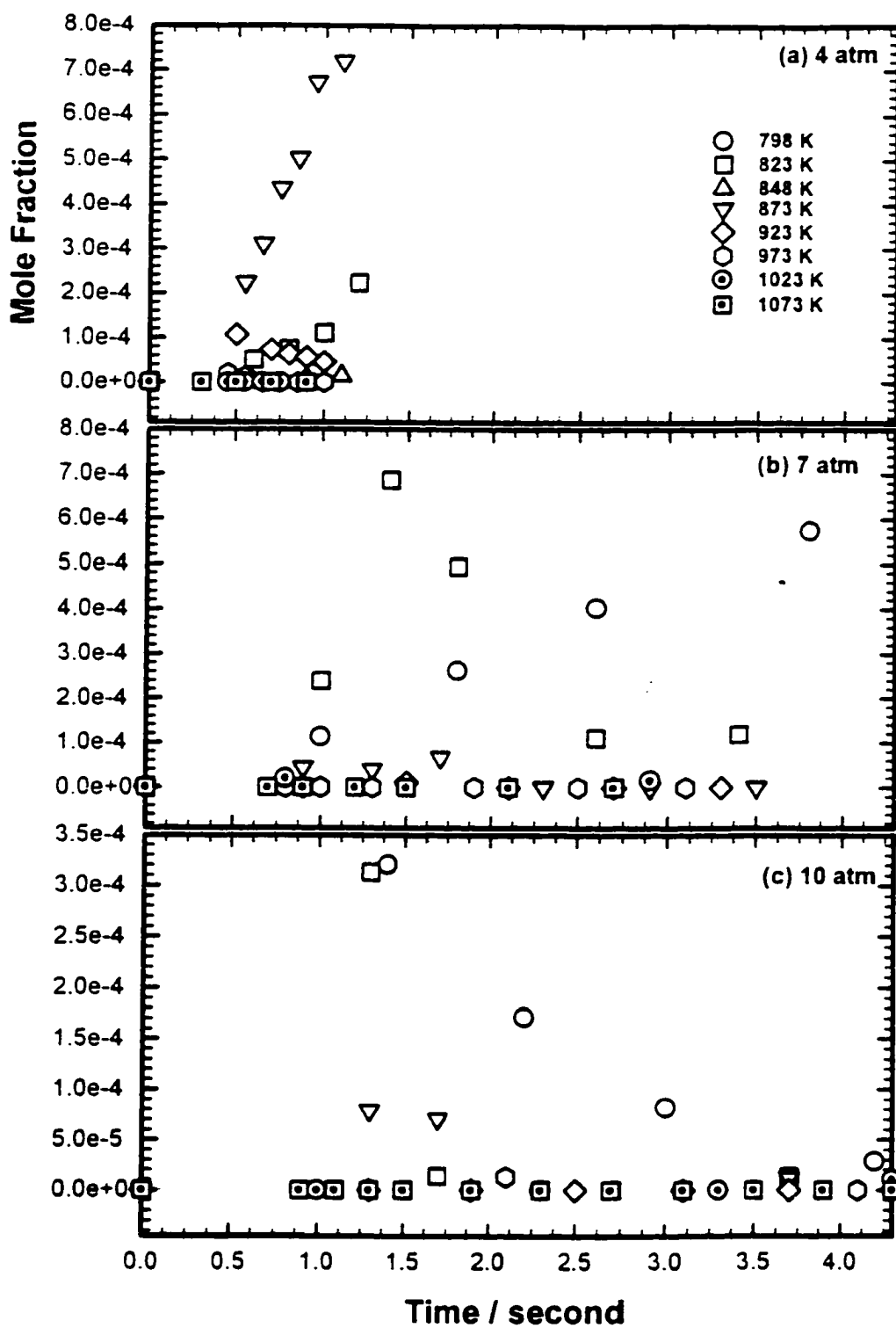


Figure IIC. 99 Experimental result of 0.5% MTBE oxidation: temperature and pressure dependence of CH_2O at $\phi = 1.00$

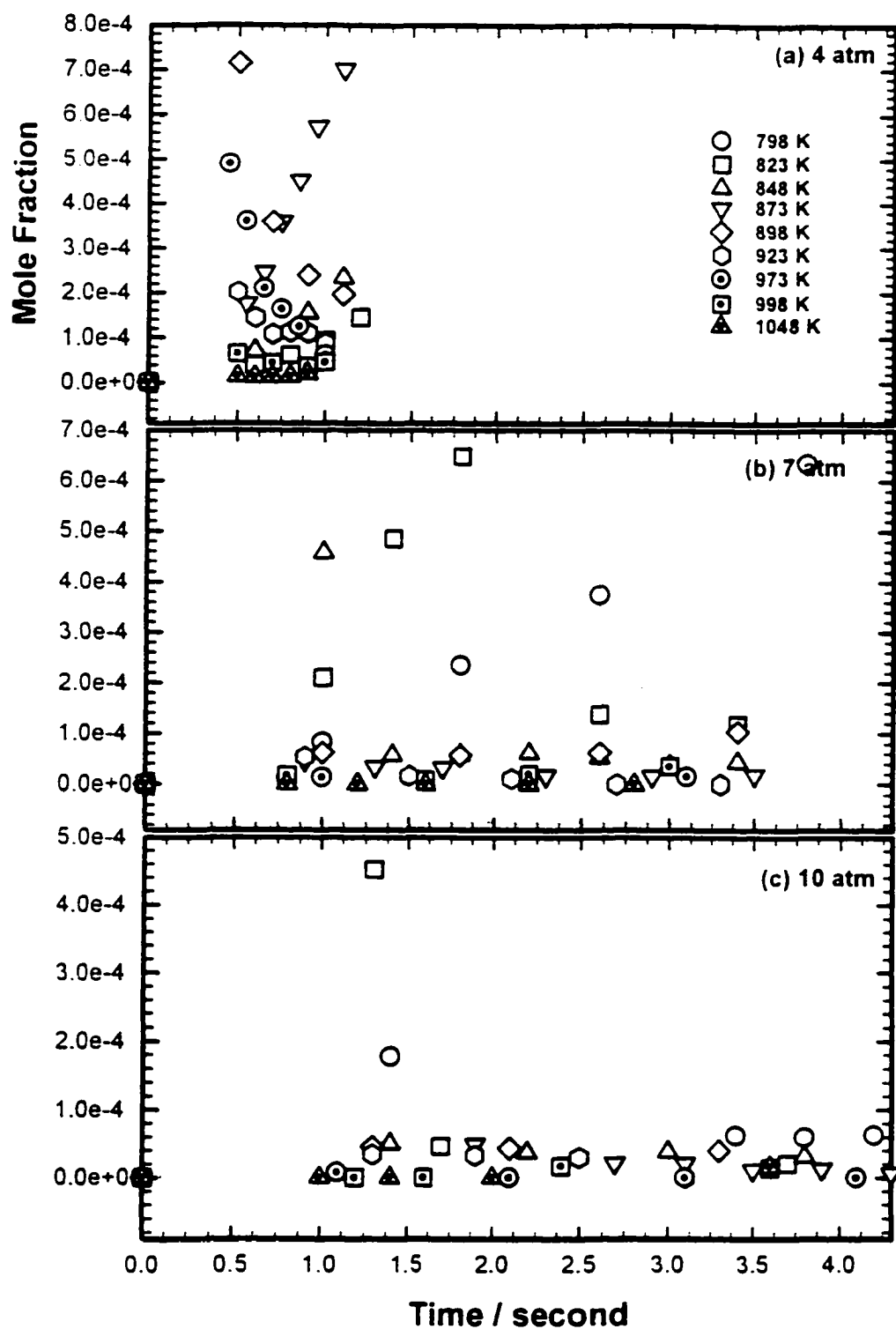


Figure IIC. 100 Experimental result of 0.5% MTBE oxidation: temperature and pressure dependence of CH_2O at $\phi = 1.50$

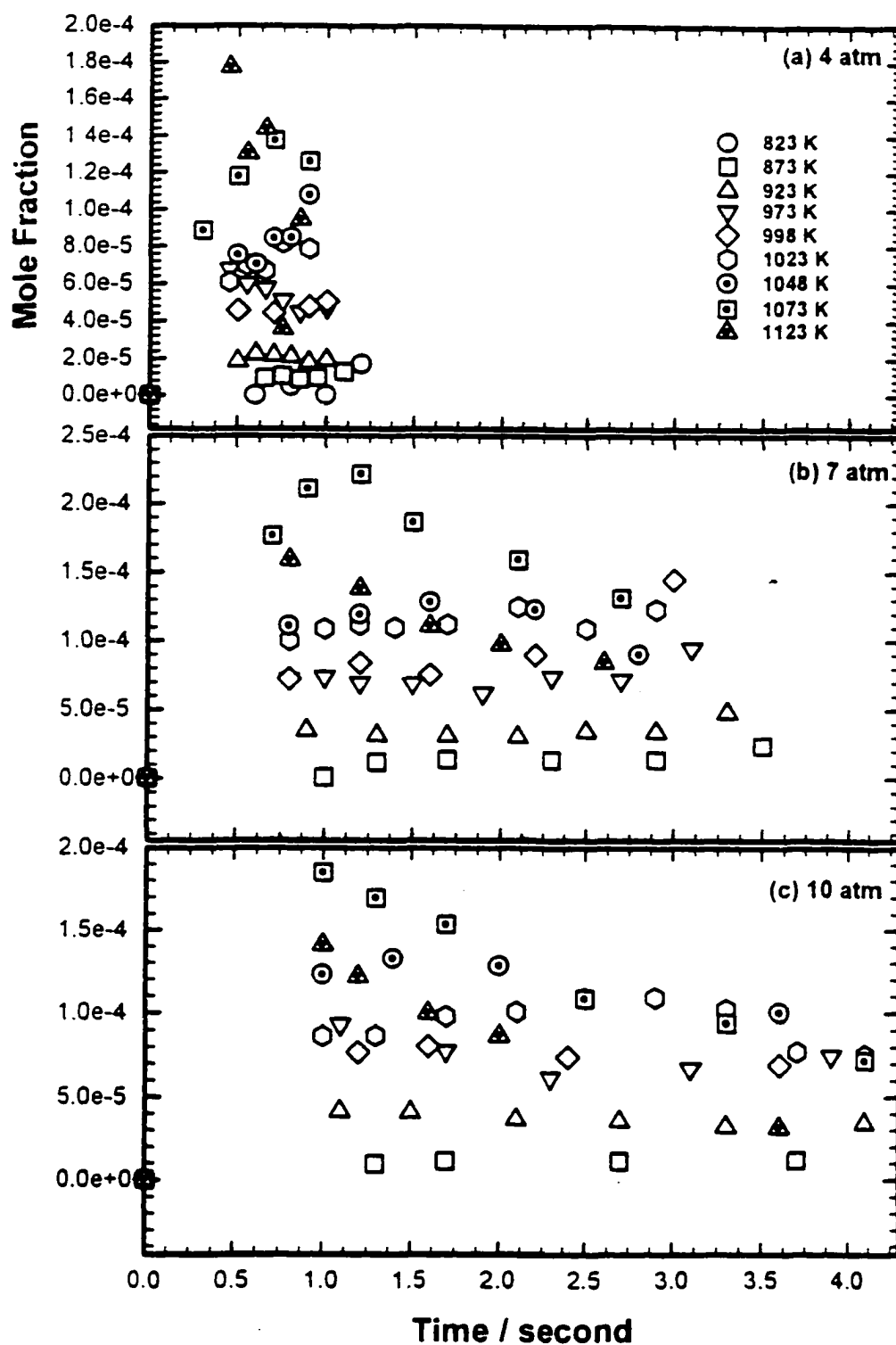


Figure IIC. 101 Experimental result of 0.5% MTBE pyrolysis: temperature and pressure dependence of CH_2O

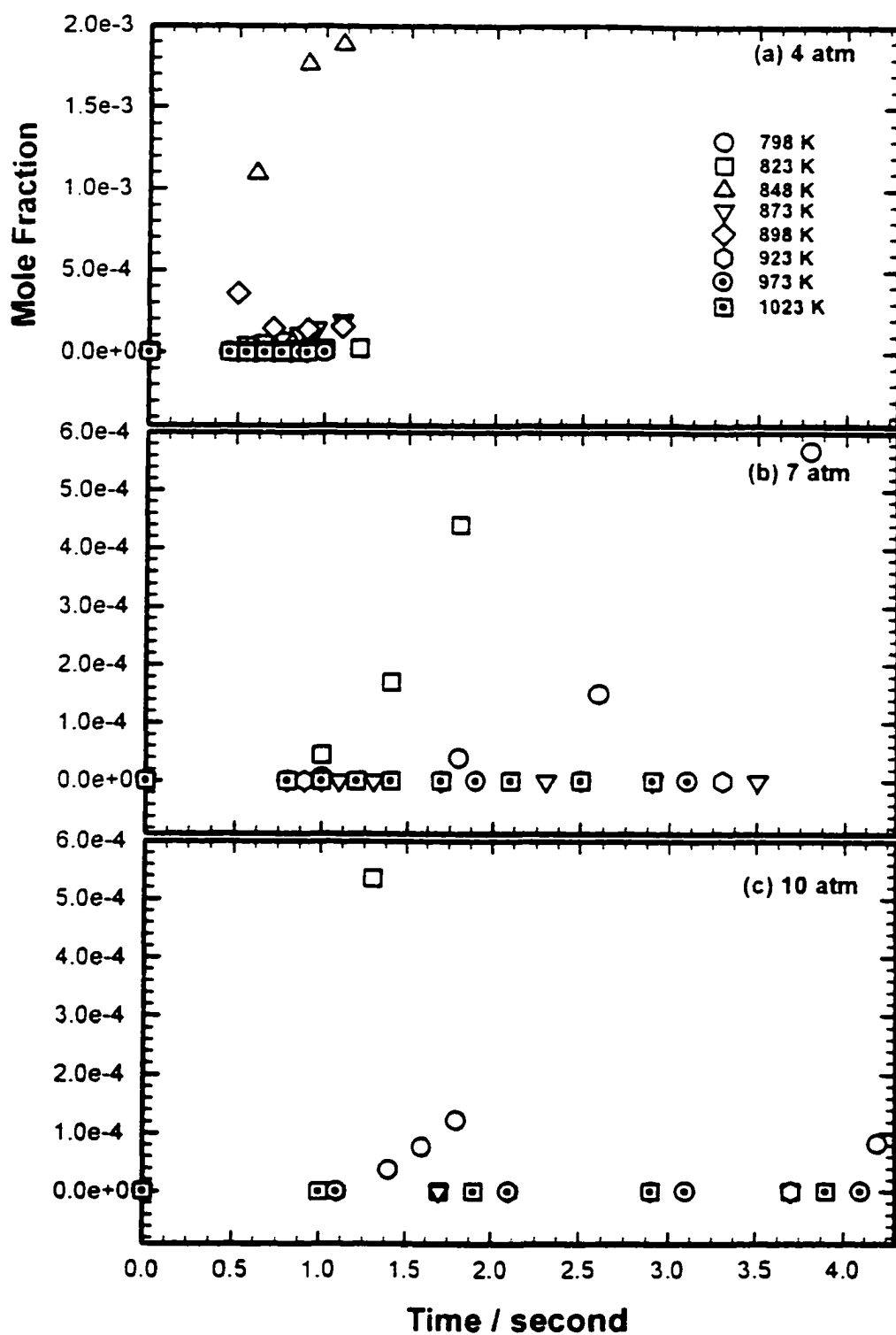


Figure IIC. 102 Experimental result of 0.5% MTBE oxidation: temperature and pressure dependence of $C_2C=O$ at $\phi = 0.75$

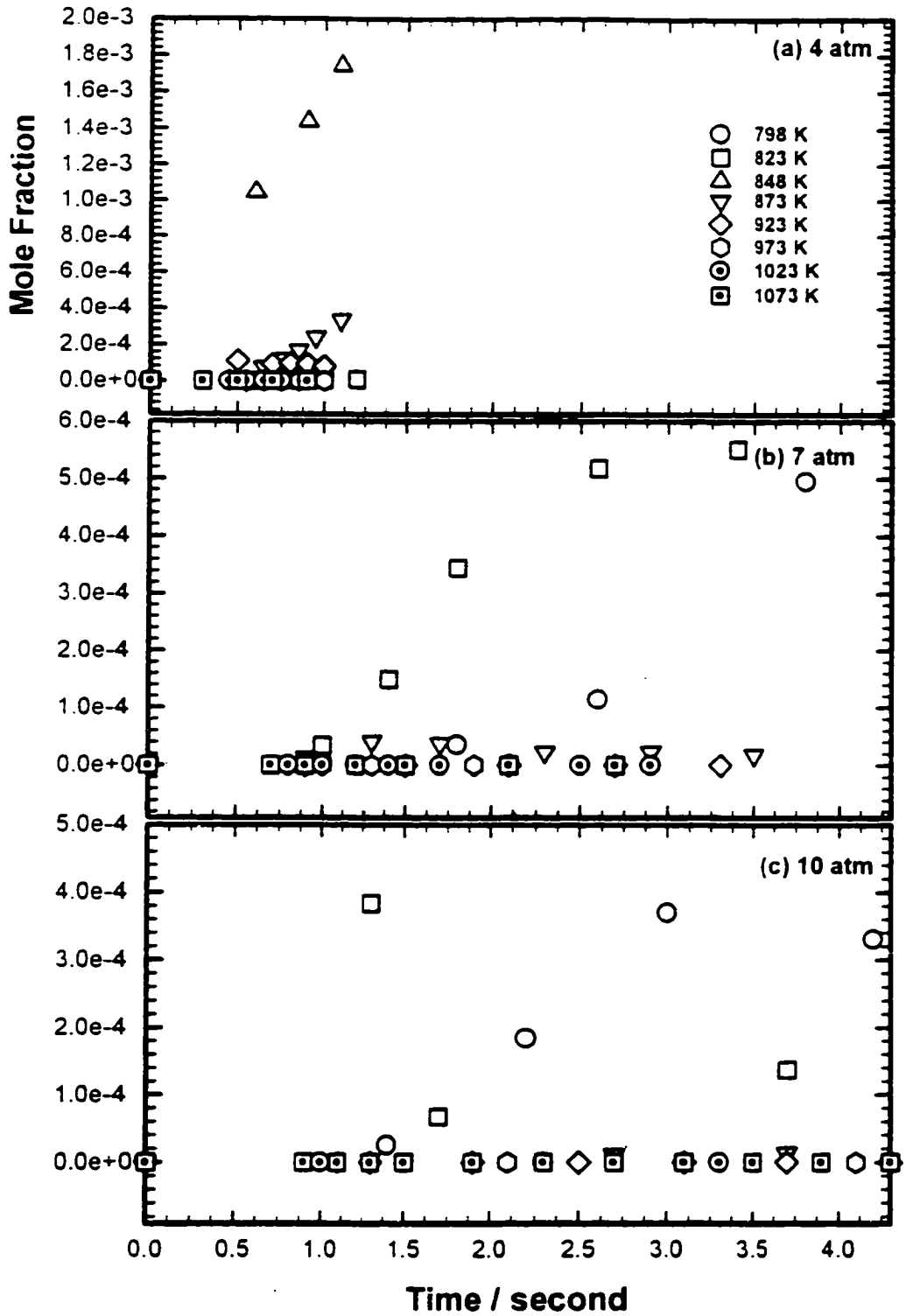


Figure IIC. 103 Experimental result of 0.5% MTBE oxidation: temperature and pressure dependence of $C_2C=O$ at $\phi = 1.00$

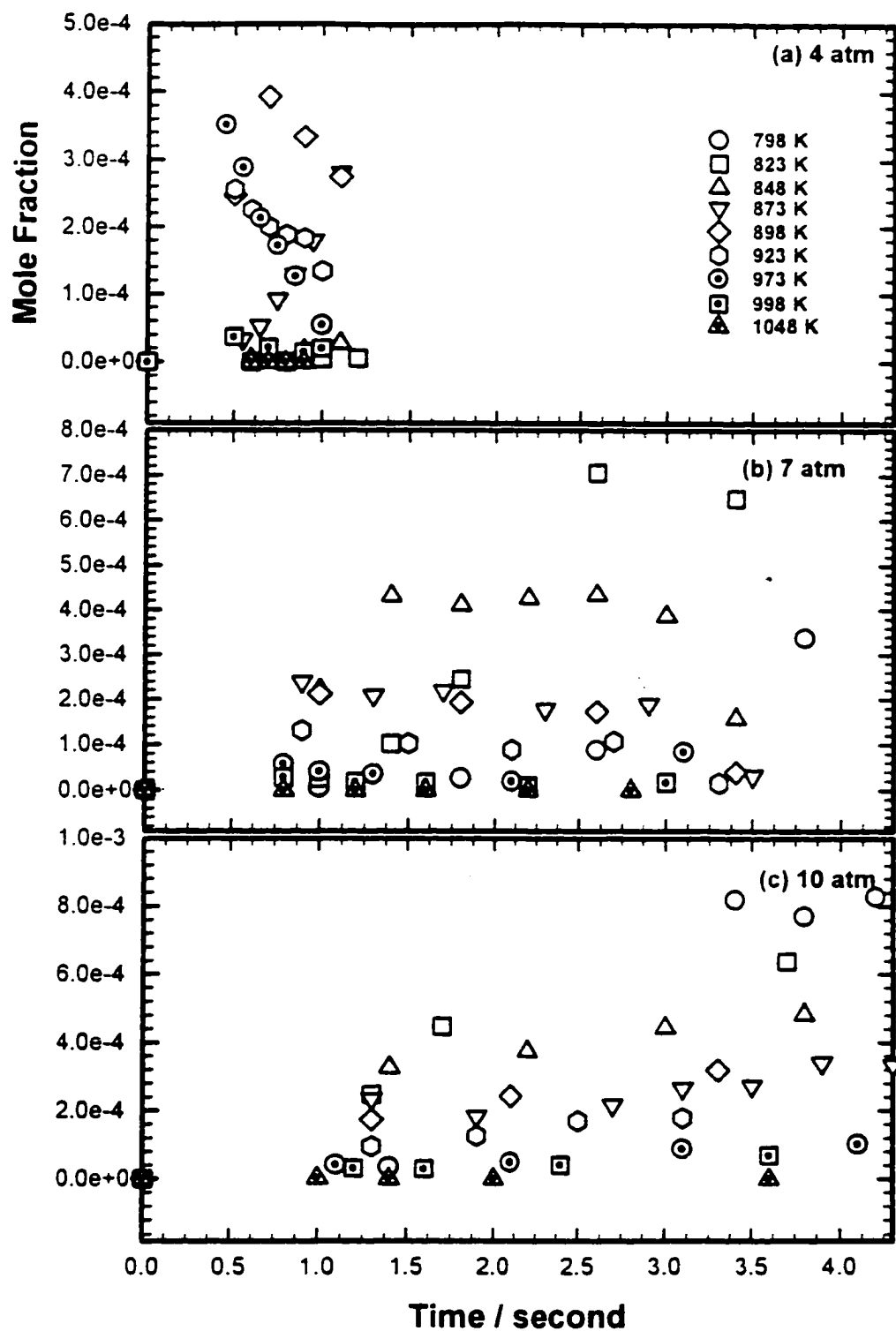


Figure IIC. 104 Experimental result of 0.5% MTBE oxidation: temperature and pressure dependence of $C_2C=O$ at $\phi = 1.50$

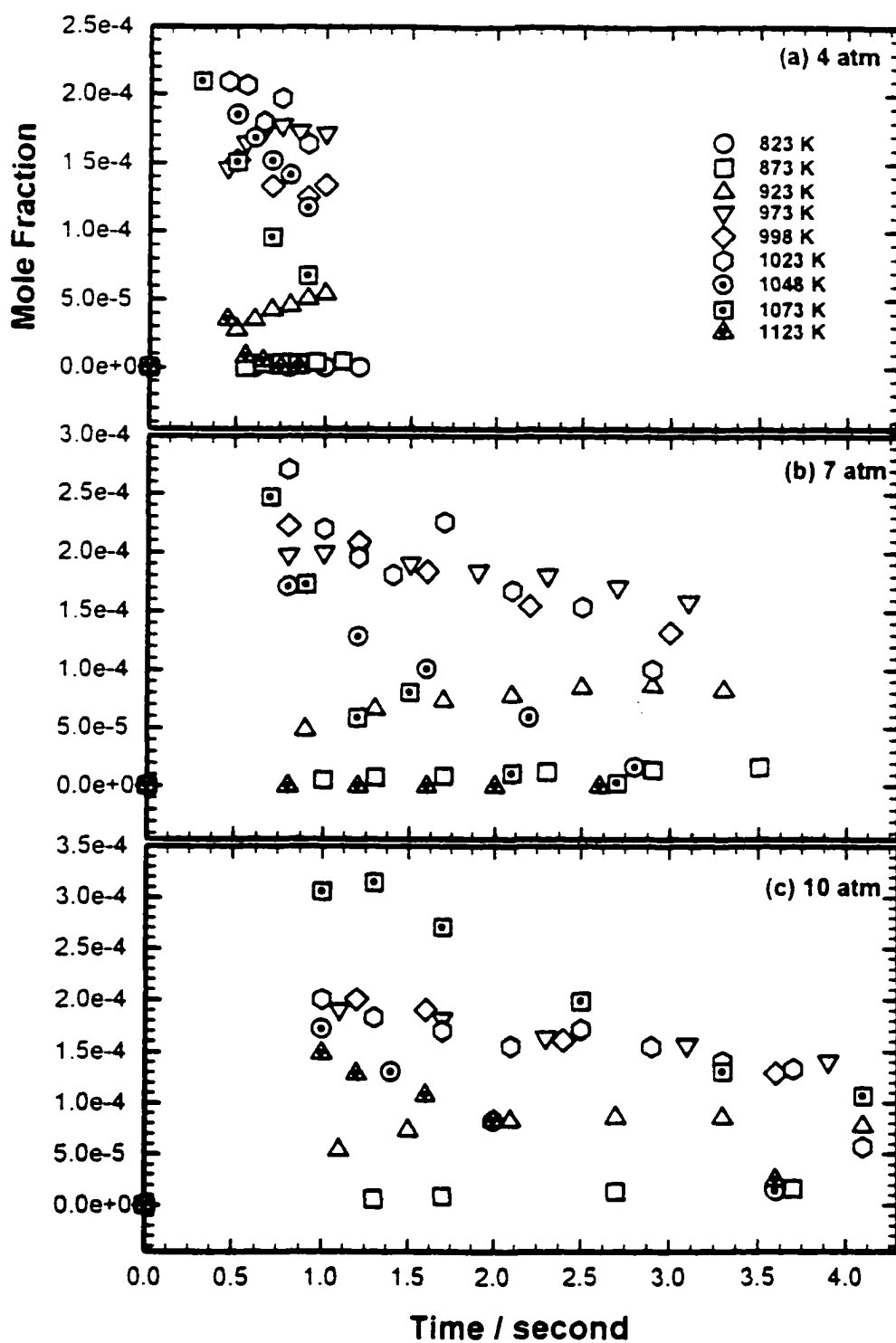


Figure IIC. 105 Experimental result of 0.5% MTBE pyrolysis: temperature and pressure dependence of $C_2C=O$

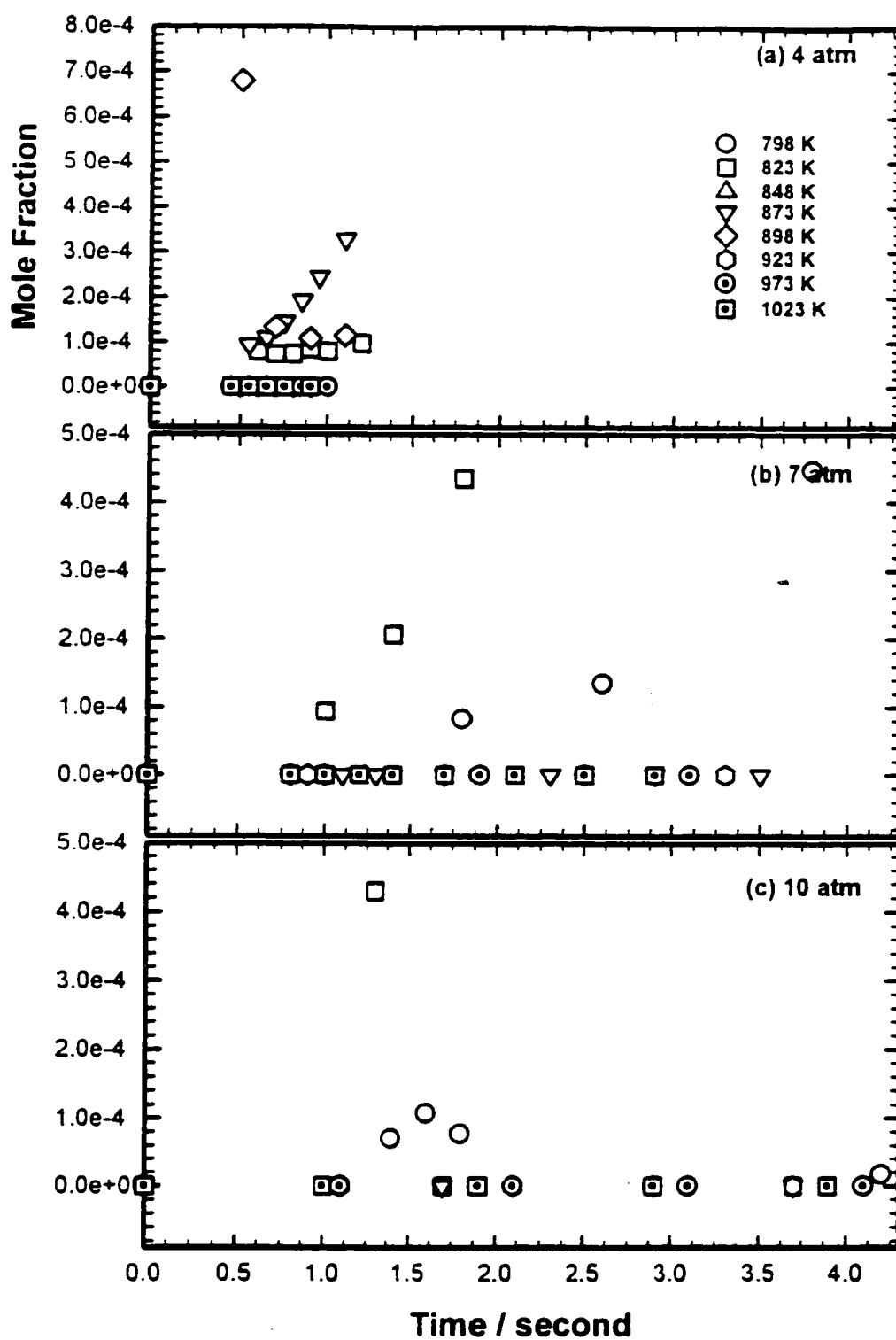


Figure IIC. 106 Experimental result of 0.5% MTBE oxidation: temperature and pressure dependence of C_3H_6 at $\phi = 0.75$

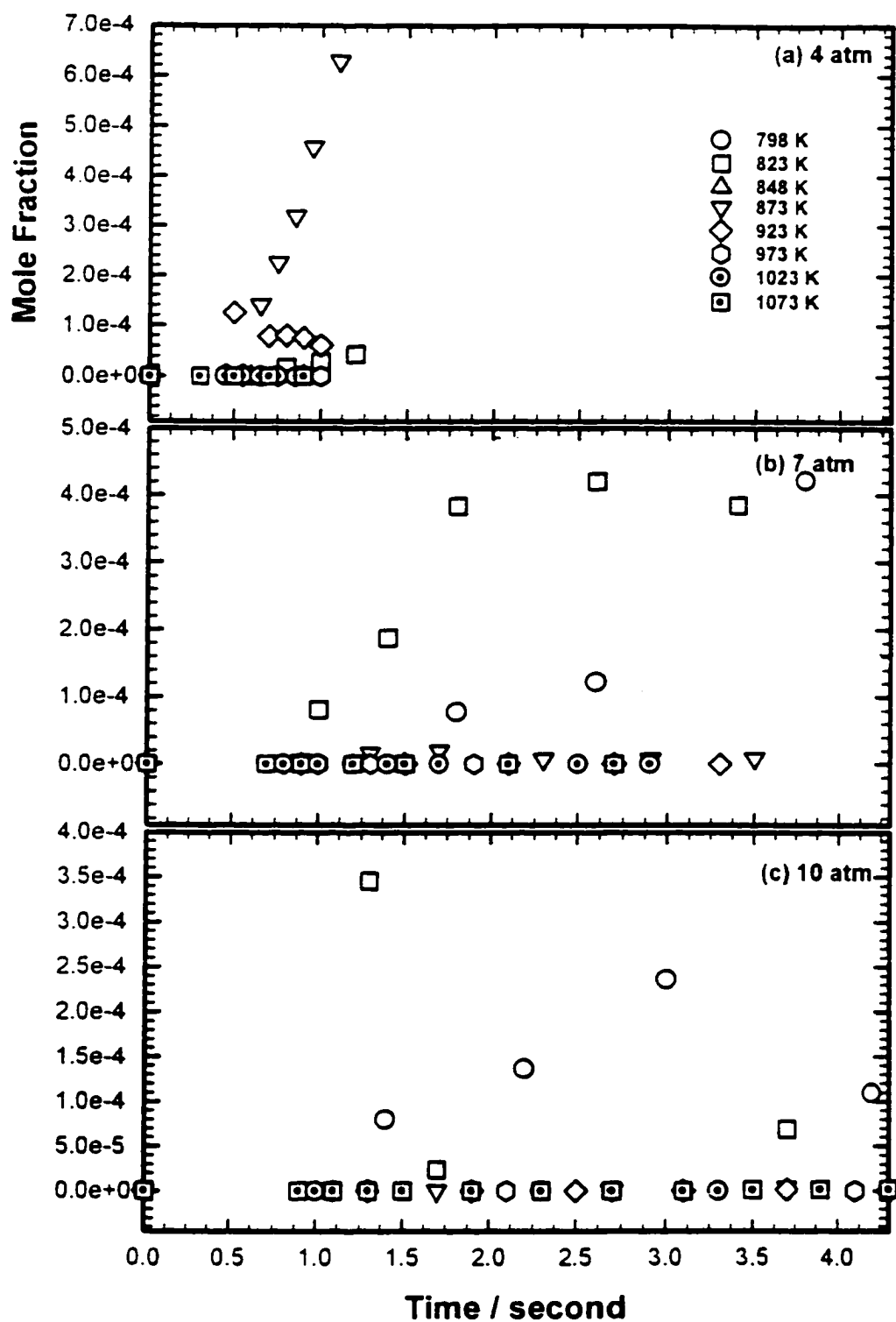


Figure II.C. 107 Experimental result of 0.5% MTBE oxidation: temperature and pressure dependence of C_3H_6 at $\phi = 1.00$

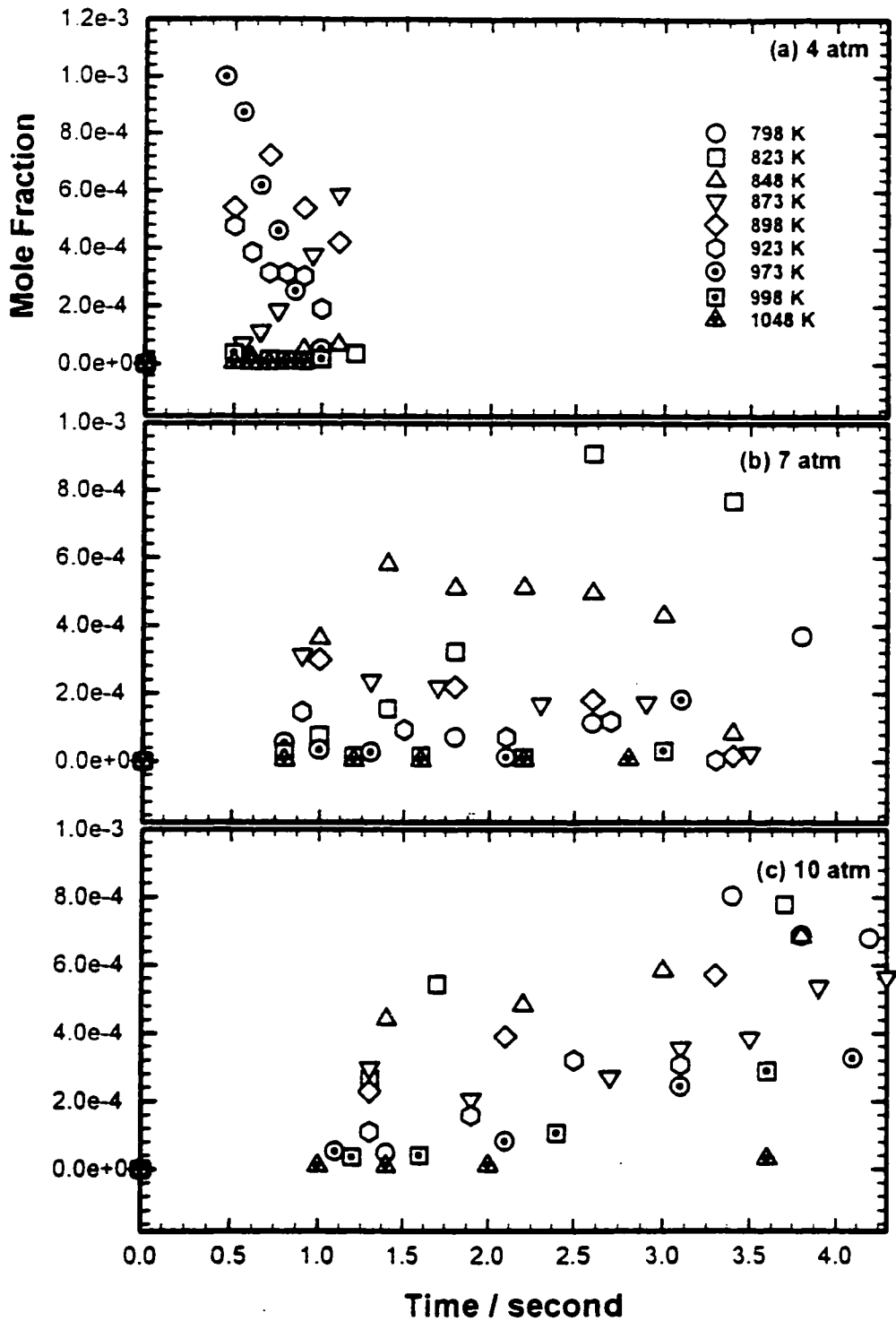


Figure IIC. 108 Experimental result of 0.5% MTBE oxidation: temperature and pressure dependence of C_3H_6 at $\phi = 1.50$

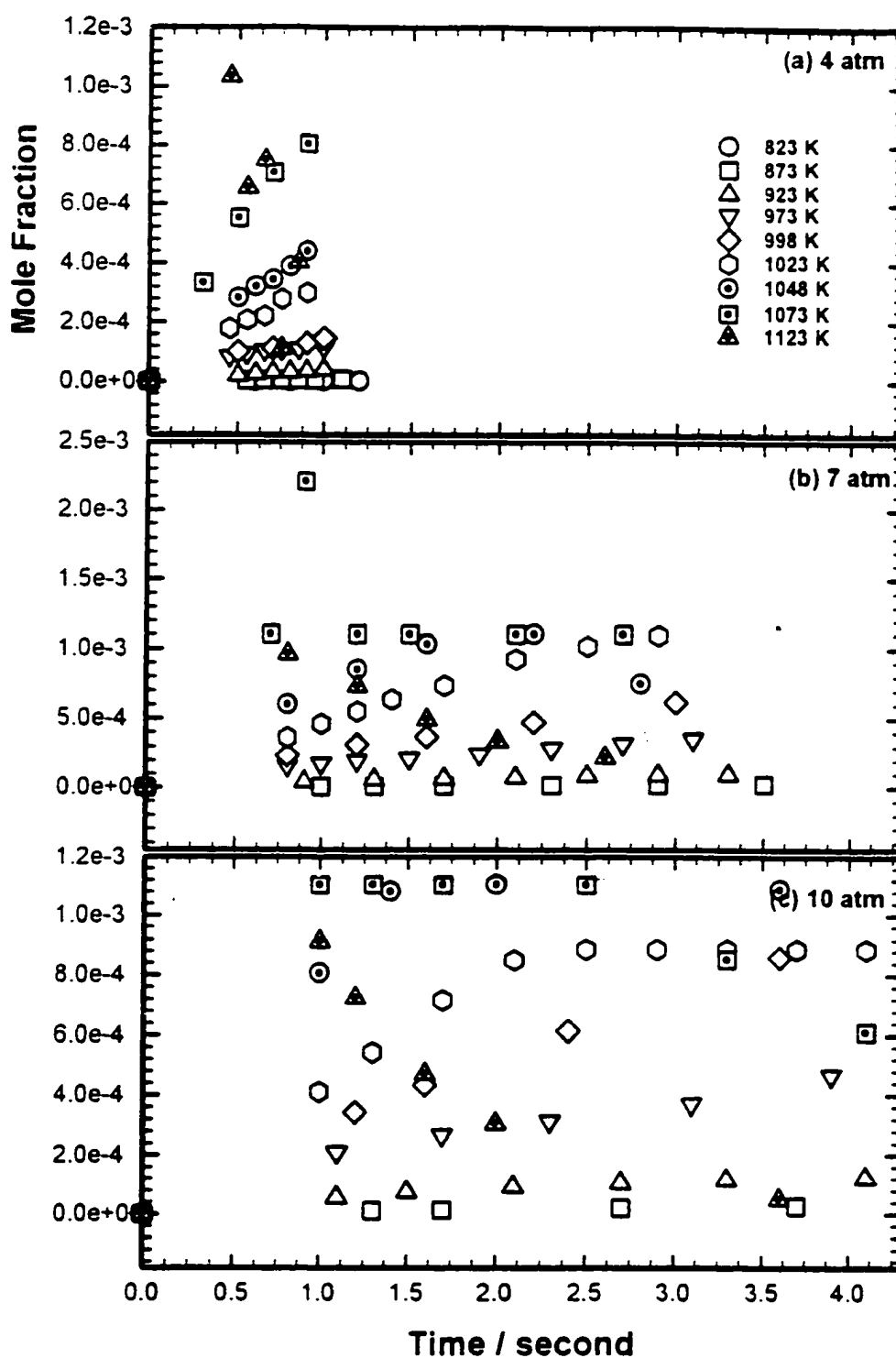


Figure IIC. 109 Experimental result of 0.5% MTBE pyrolysis: temperature and pressure dependence of C_3H_6

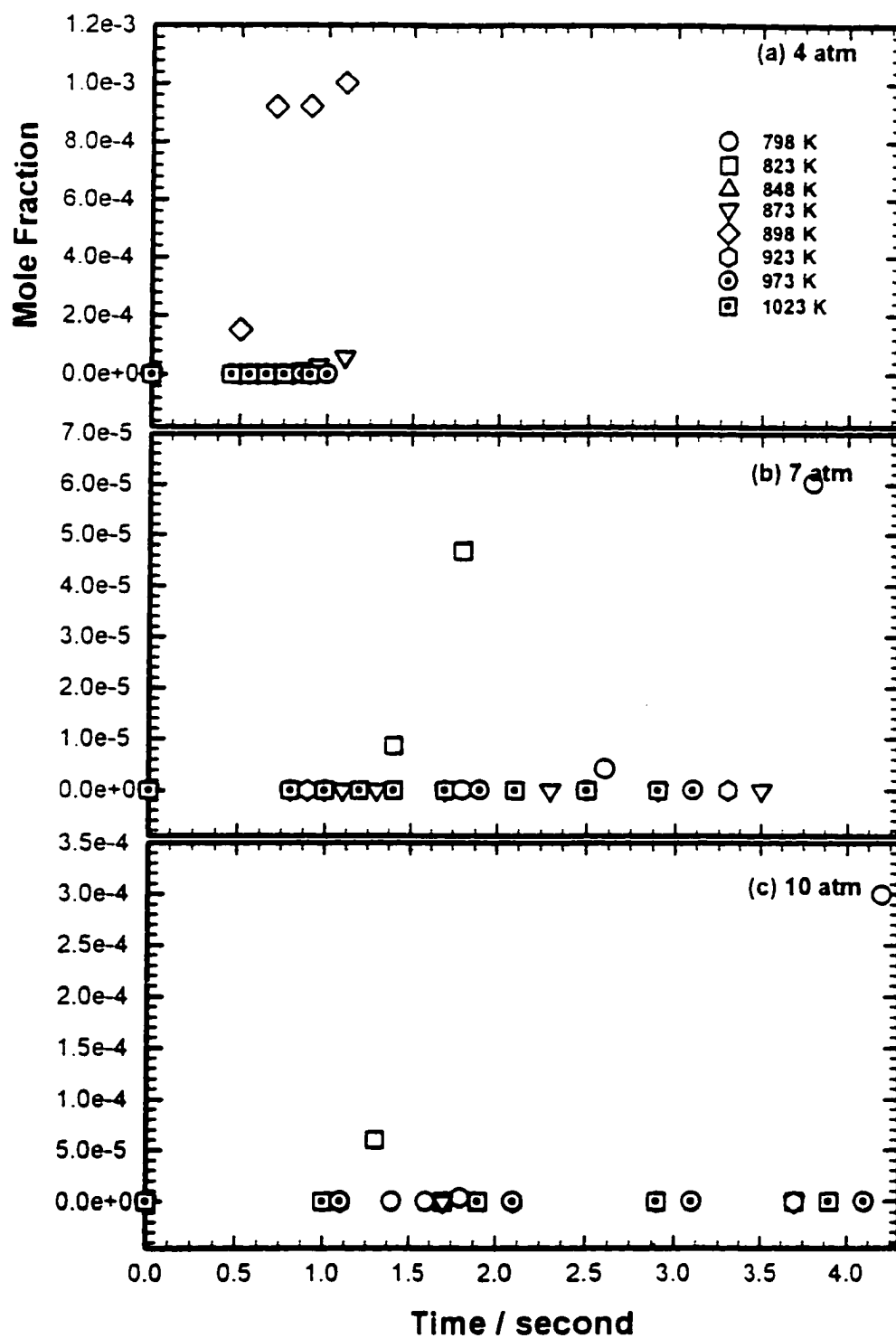


Figure IIC. 110 Experimental result of 0.5% MTBE oxidation: temperature and pressure dependence of C_2H_4 at $\phi = 0.75$

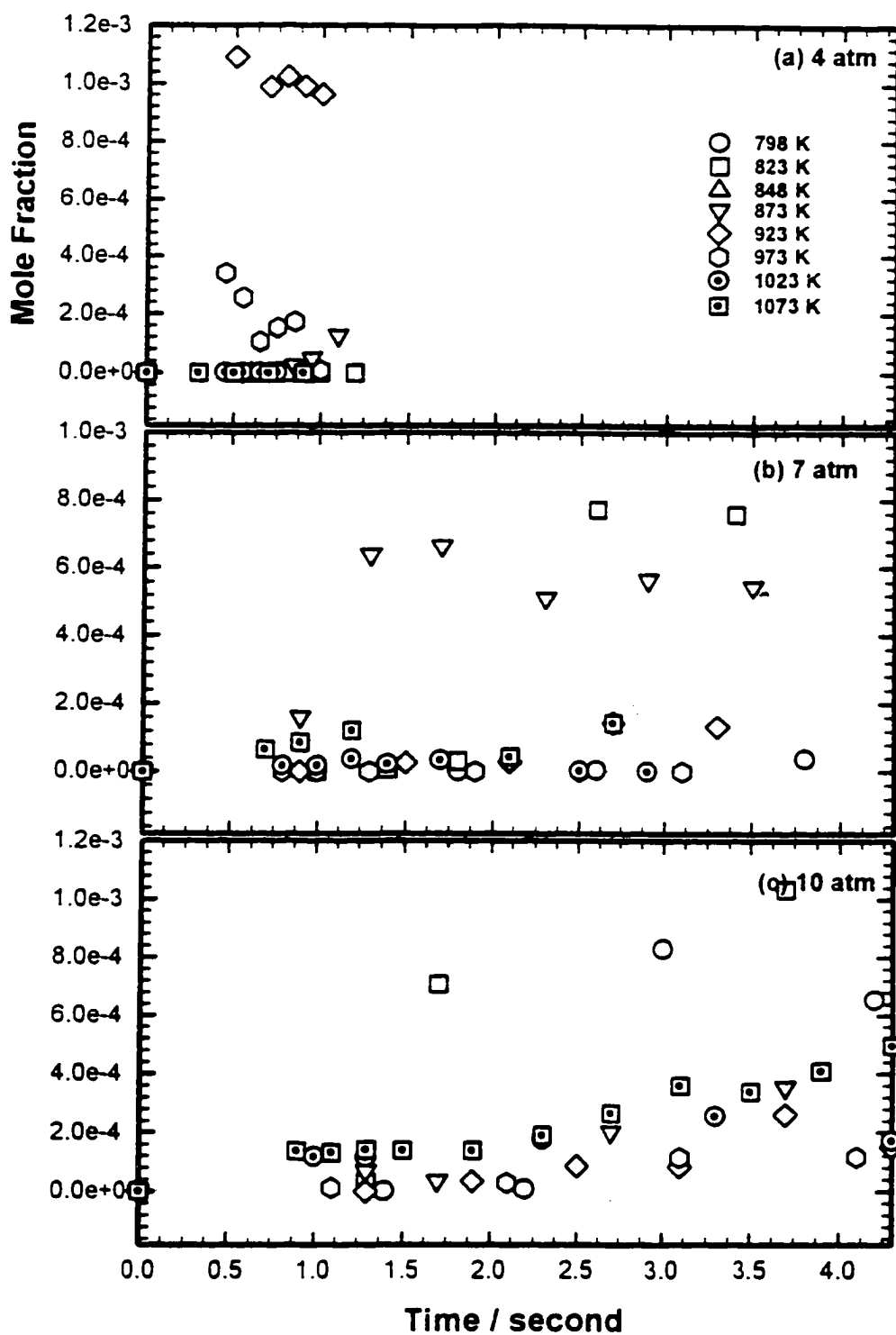


Figure II.C. 111 Experimental result of 0.5% MTBE oxidation: temperature and pressure dependence of C_2H_4 at $\phi = 1.00$

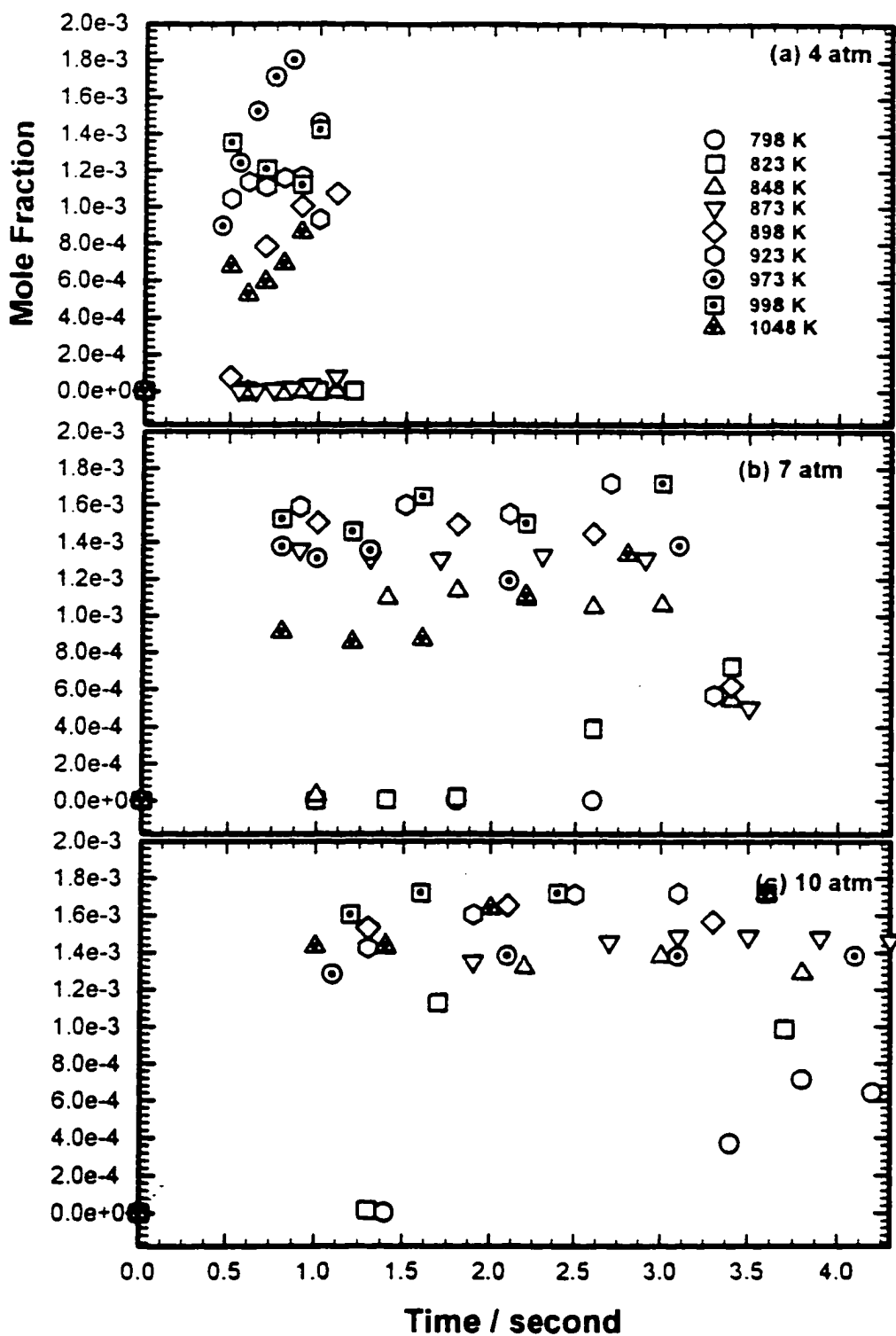


Figure IIC. 112 Experimental result of 0.5% MTBE oxidation: temperature and pressure dependence of C_2H_4 at $\phi = 1.50$

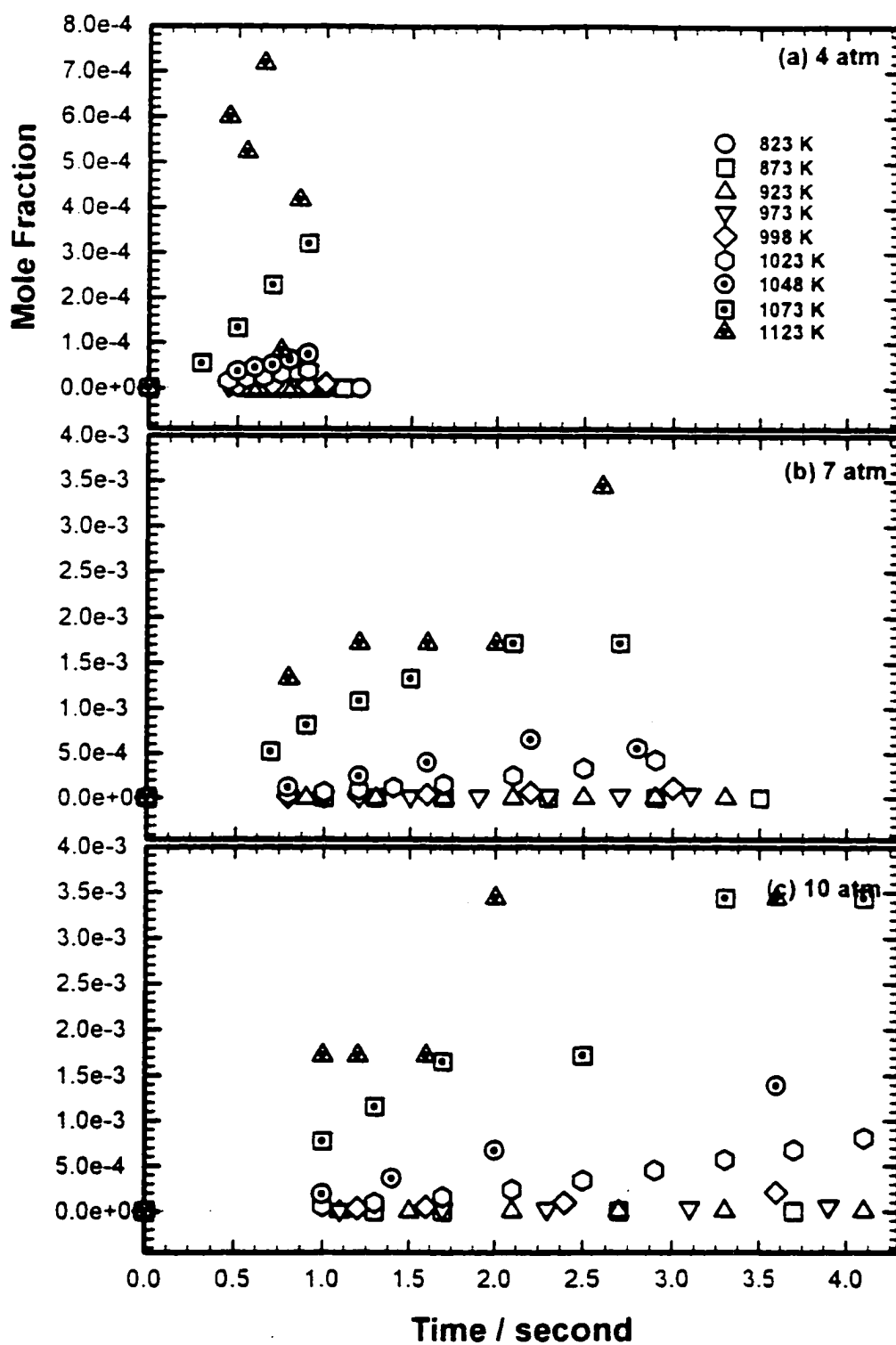


Figure IIC. 113 Experimental result of 0.5% MTBE pyrolysis: temperature and pressure dependence of C_2H_4

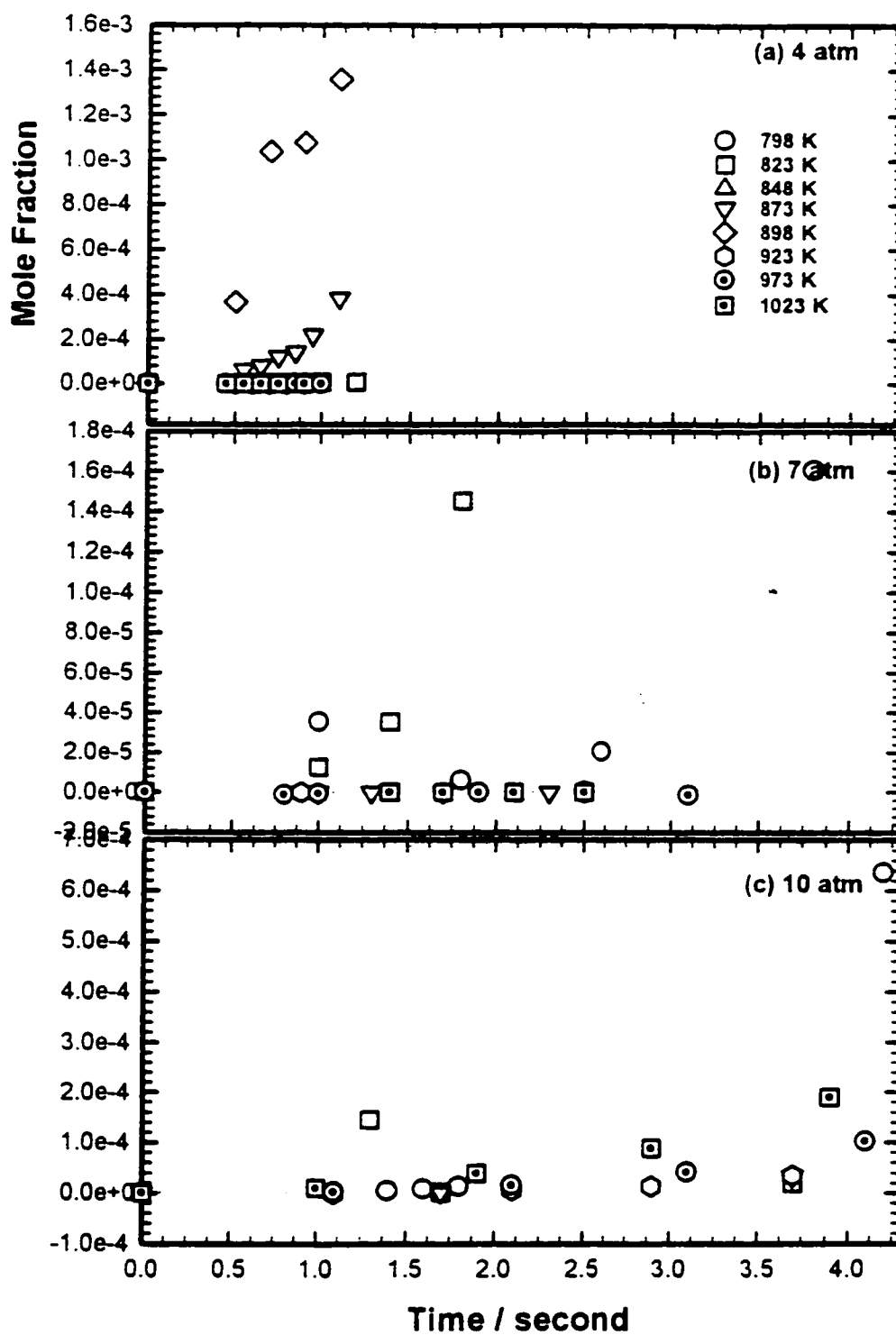


Figure IIC. 114 Experimental result of 0.5% MTBE oxidation: temperature and pressure dependence of CH_4 at $\phi = 0.75$

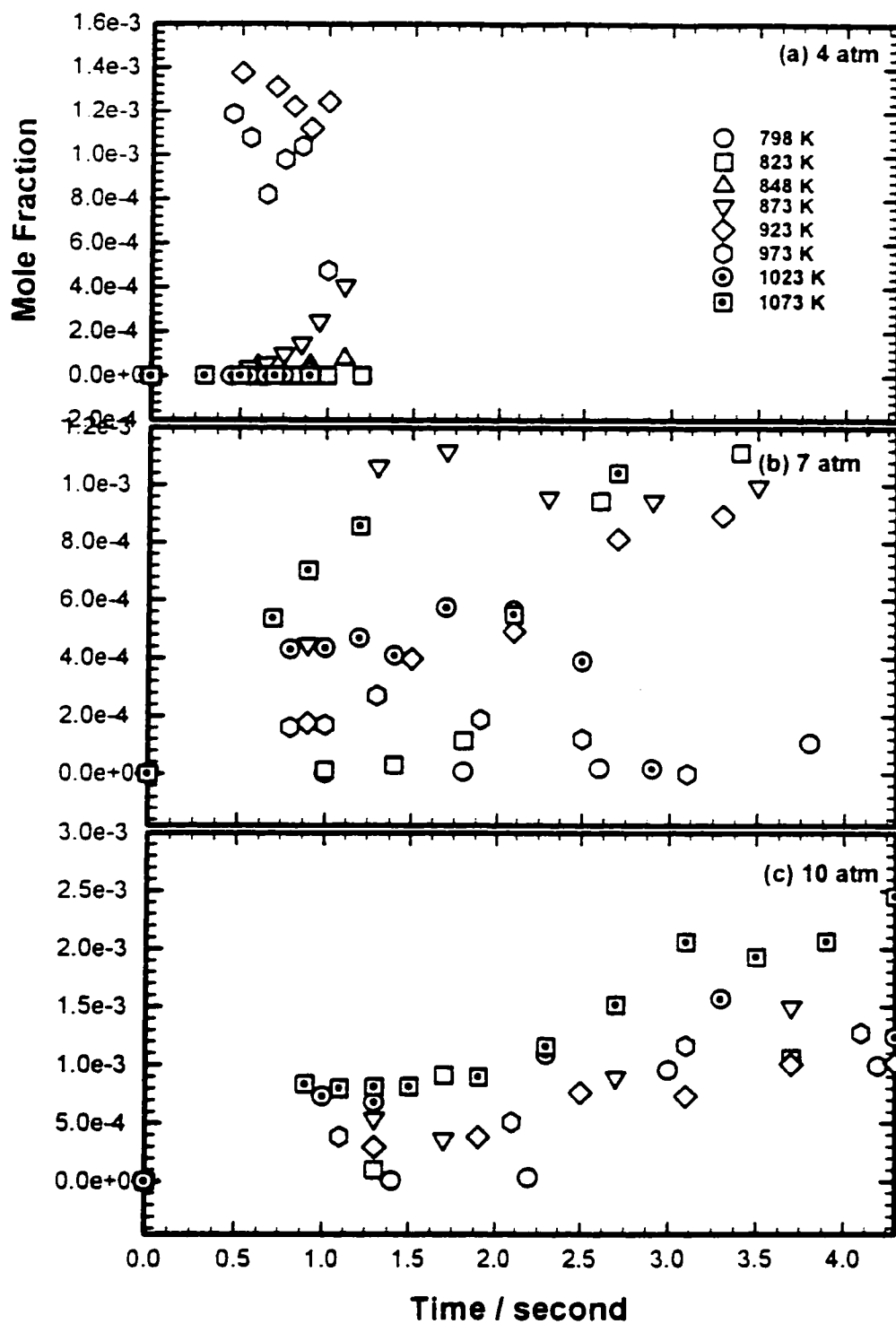


Figure IIC. 115 Experimental result of 0.5% MTBE oxidation: temperature and pressure dependence of CH_4 at $\phi = 1.00$

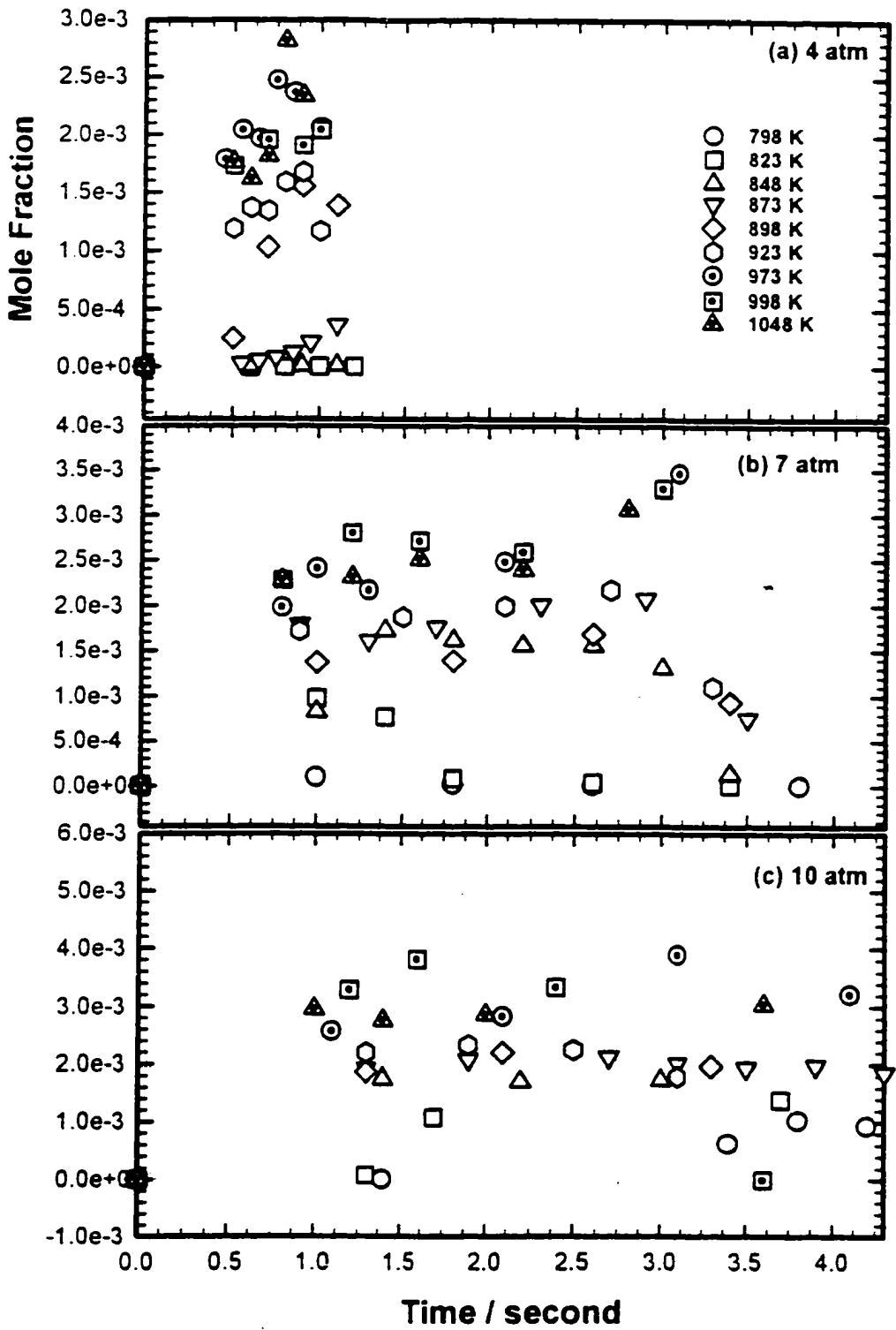


Figure IIC. 116 Experimental result of 0.5% MTBE oxidation: temperature and pressure dependence of CH_4 at $\phi = 1.50$

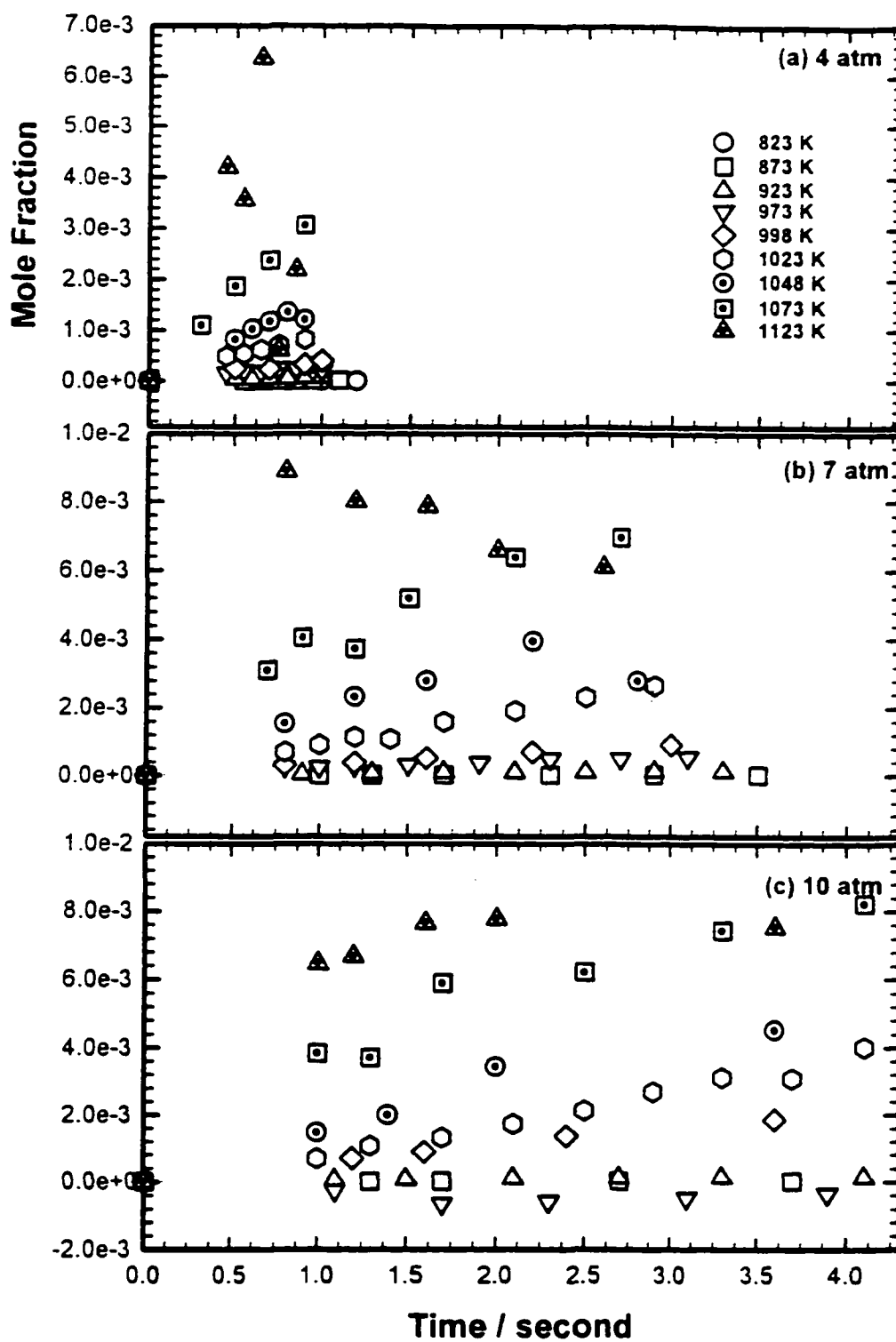


Figure IIC. 117 Experimental result of 0.5% MTBE pyrolysis: temperature and pressure dependence of CH_4

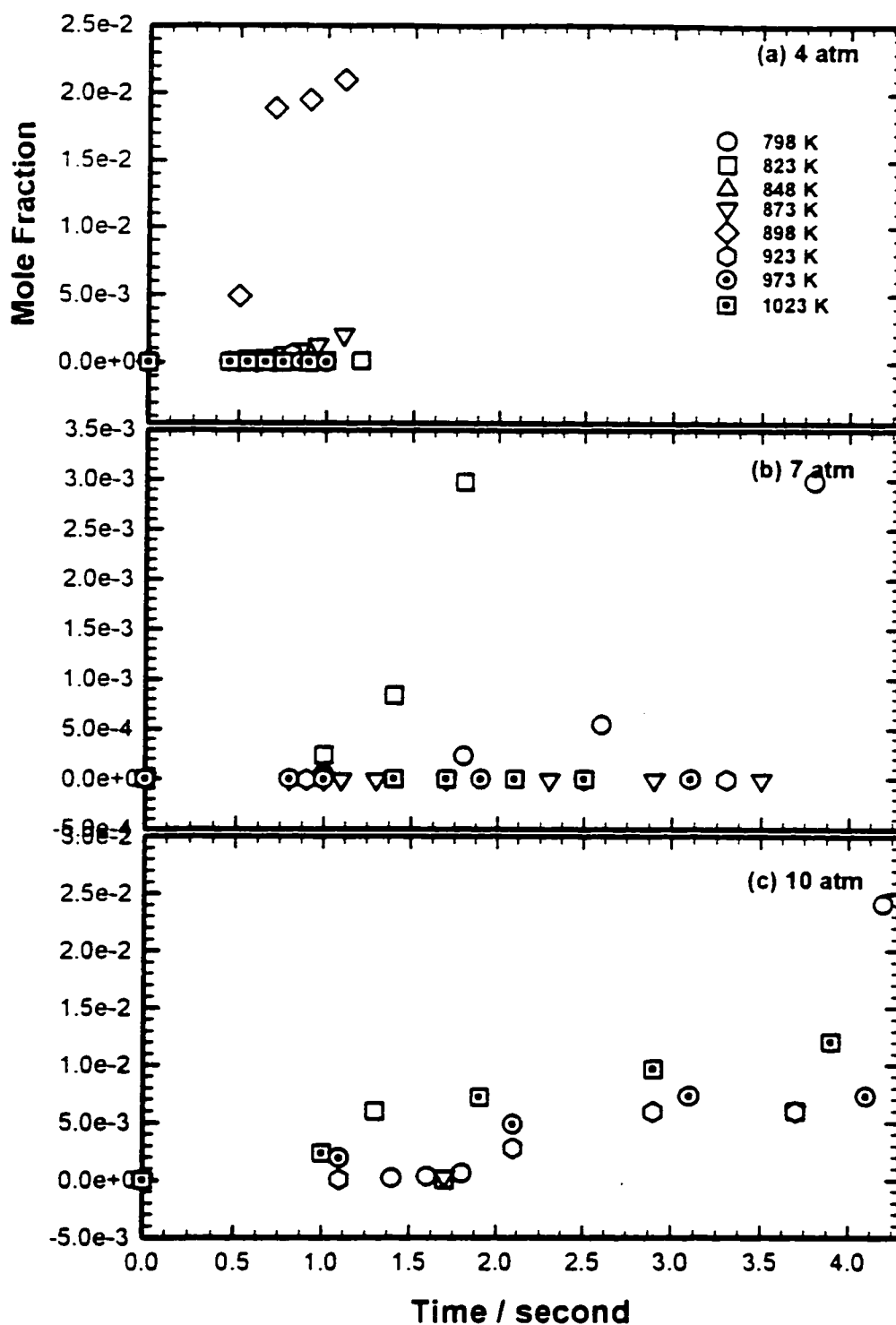


Figure IIC. 118 Experimental result of 0.5% MTBE oxidation: temperature and pressure dependence of CO at $\phi = 0.75$

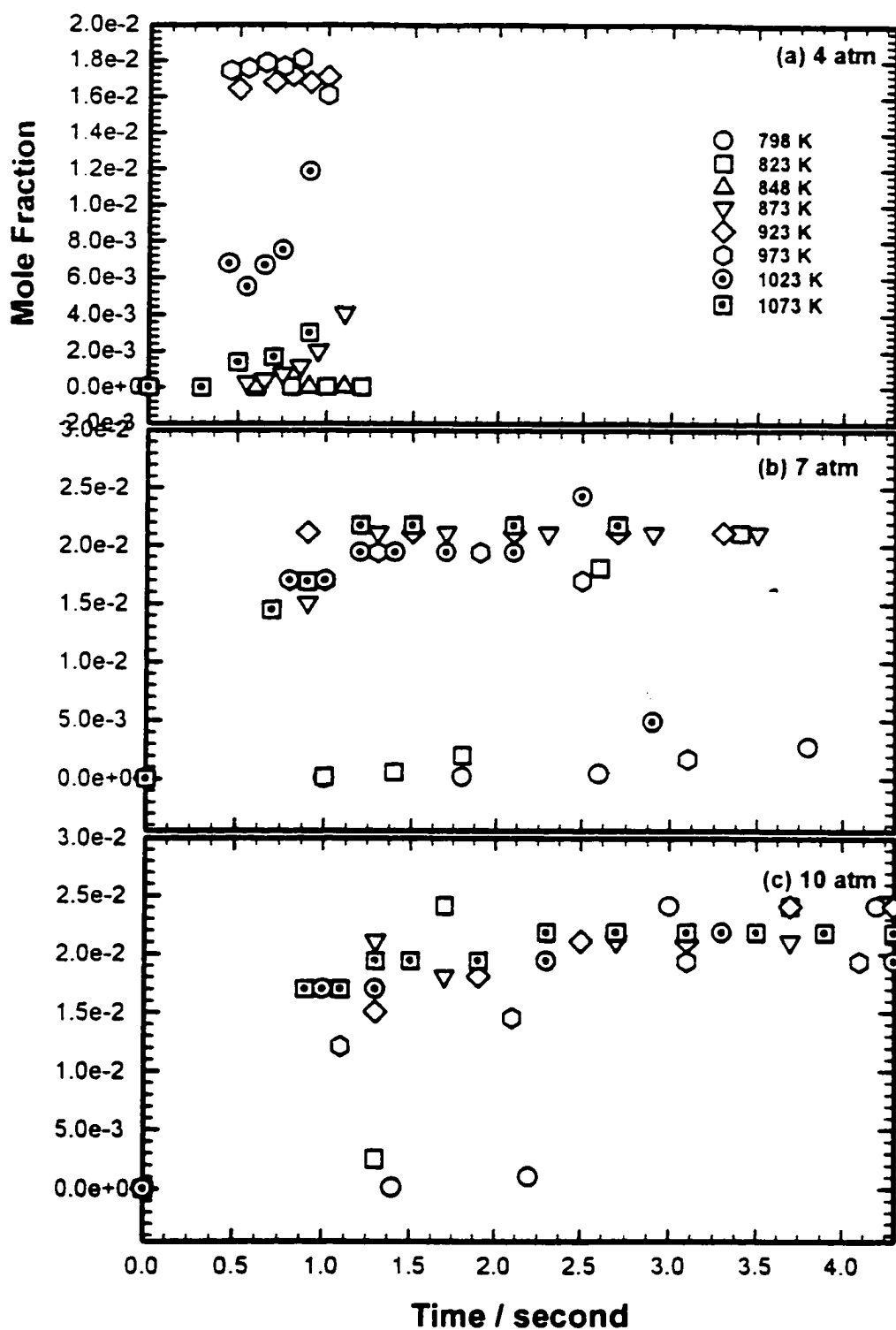


Figure IIC. 119 Experimental result of 0.5% MTBE oxidation: temperature and pressure dependence of CO at $\phi = 1.00$

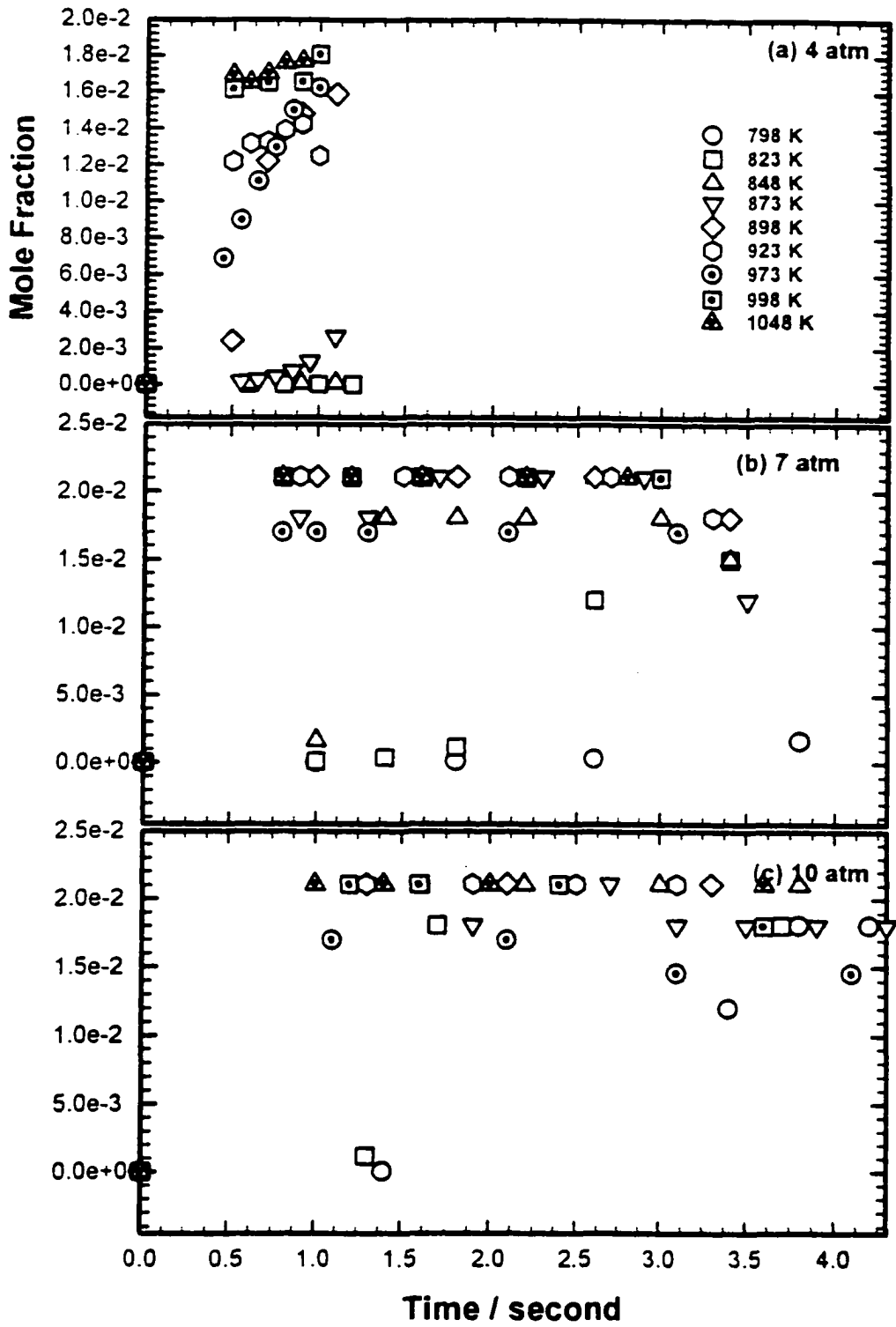


Figure IIC. 120 Experimental result of 0.5% MTBE oxidation: temperature and pressure dependence of CO at $\phi = 1.50$

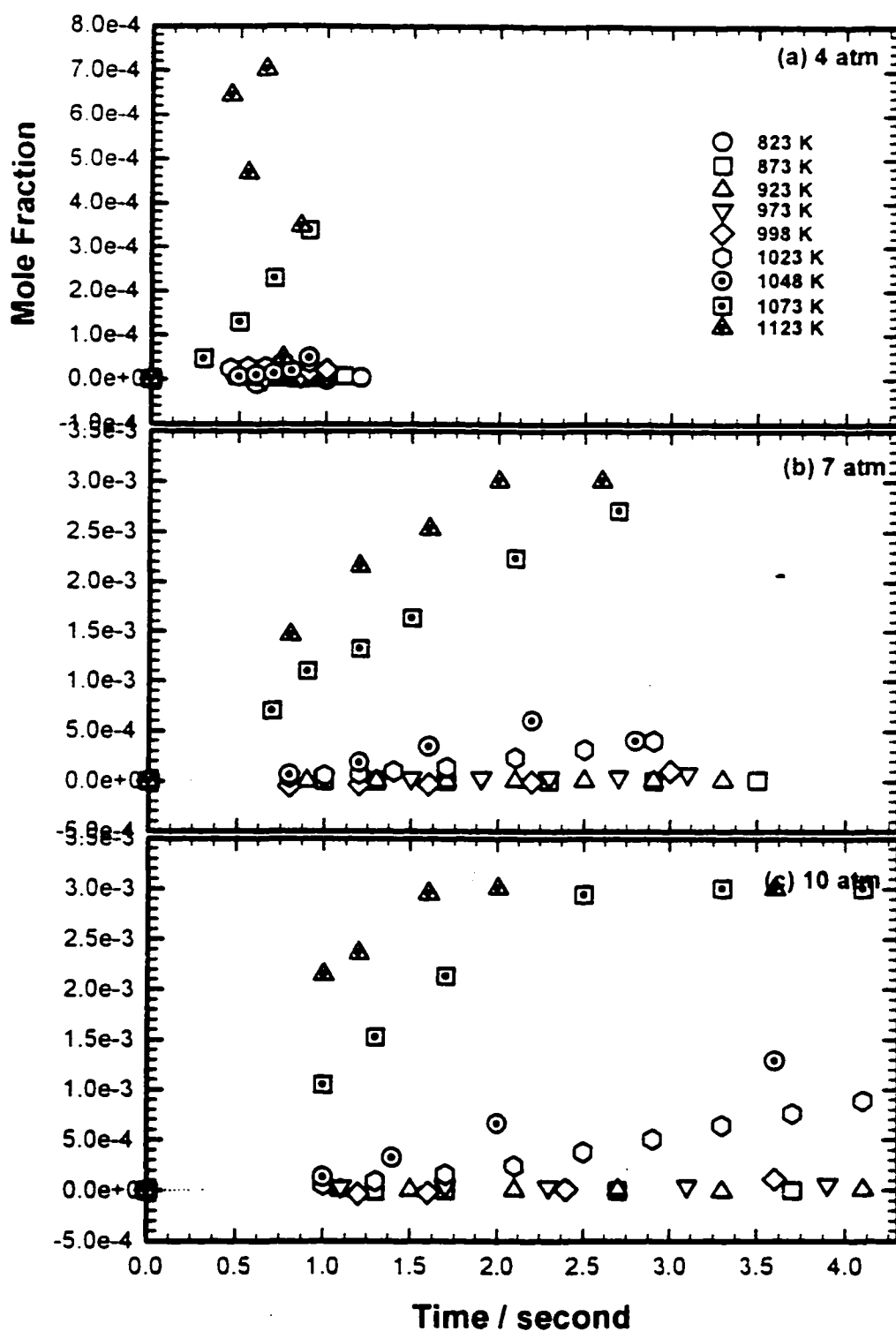


Figure IIC. 121 Experimental result of 0.5% MTBE pyrolysis: temperature and pressure dependence of CO

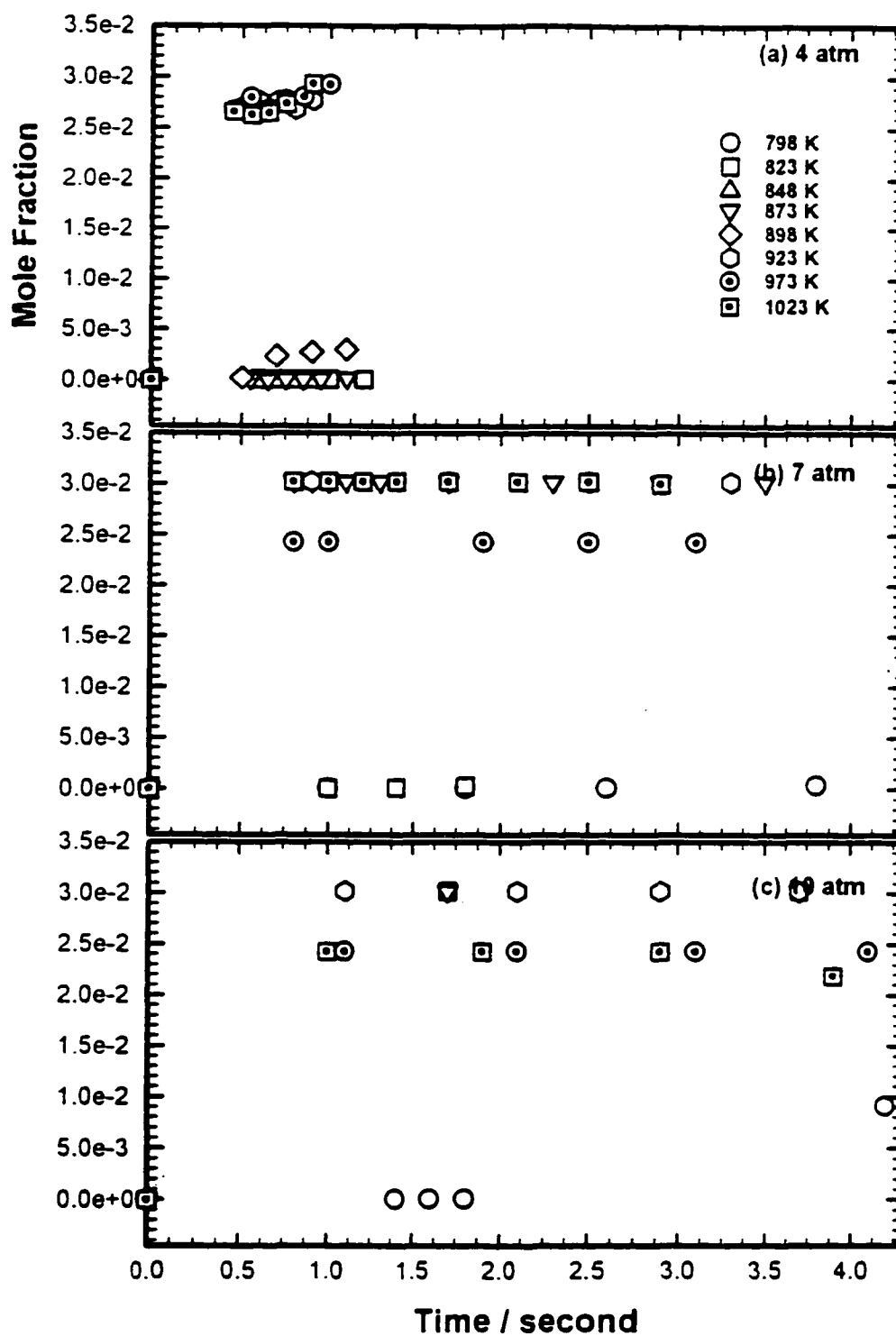


Figure IIC. 122 Experimental result of 0.5% MTBE oxidation: temperature and pressure dependence of CO₂ at $\phi = 0.75$

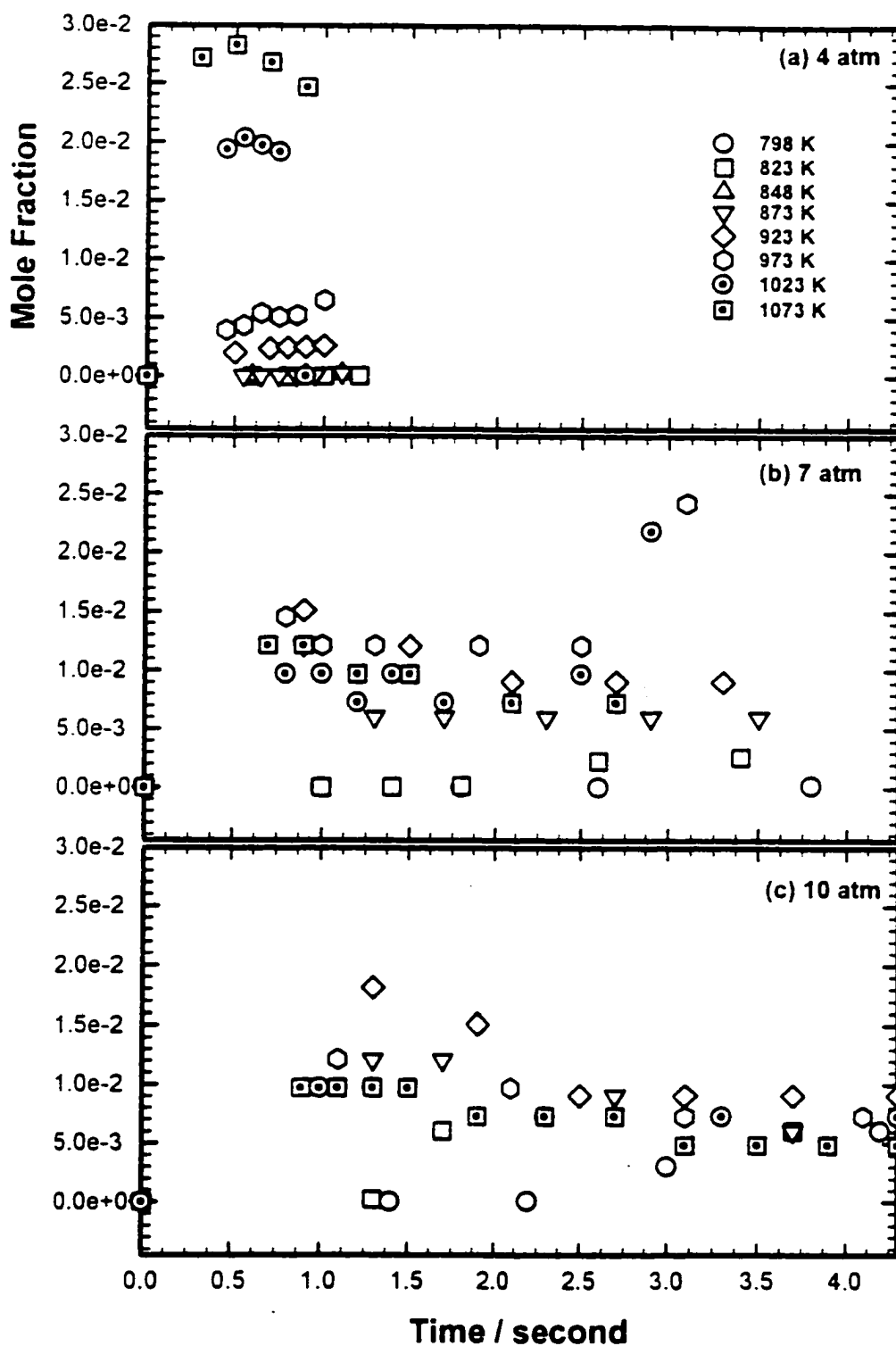


Figure IIC. 123 Experimental result of 0.5% MTBE oxidation: temperature and pressure dependence of CO_2 at $\phi = 1.00$

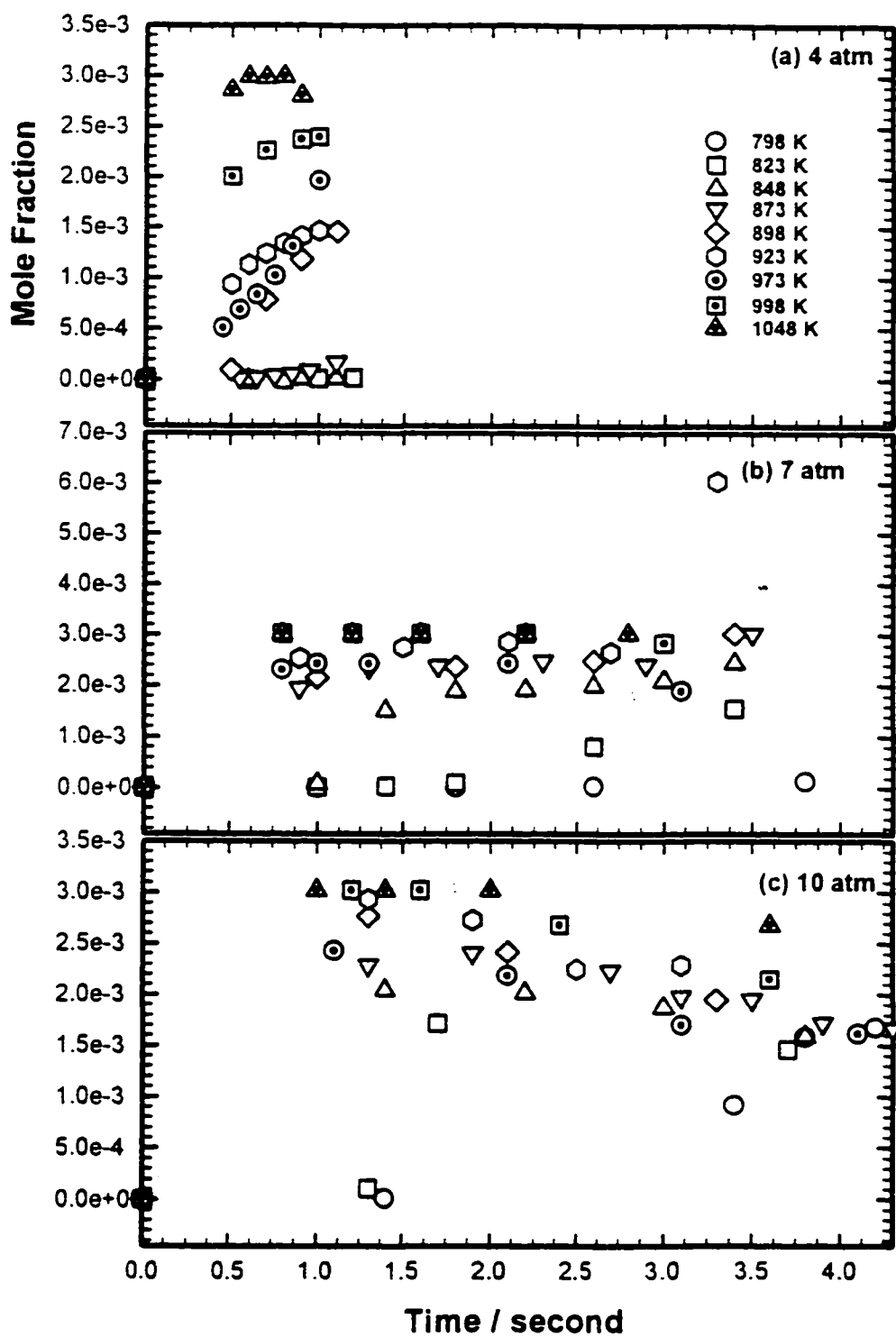
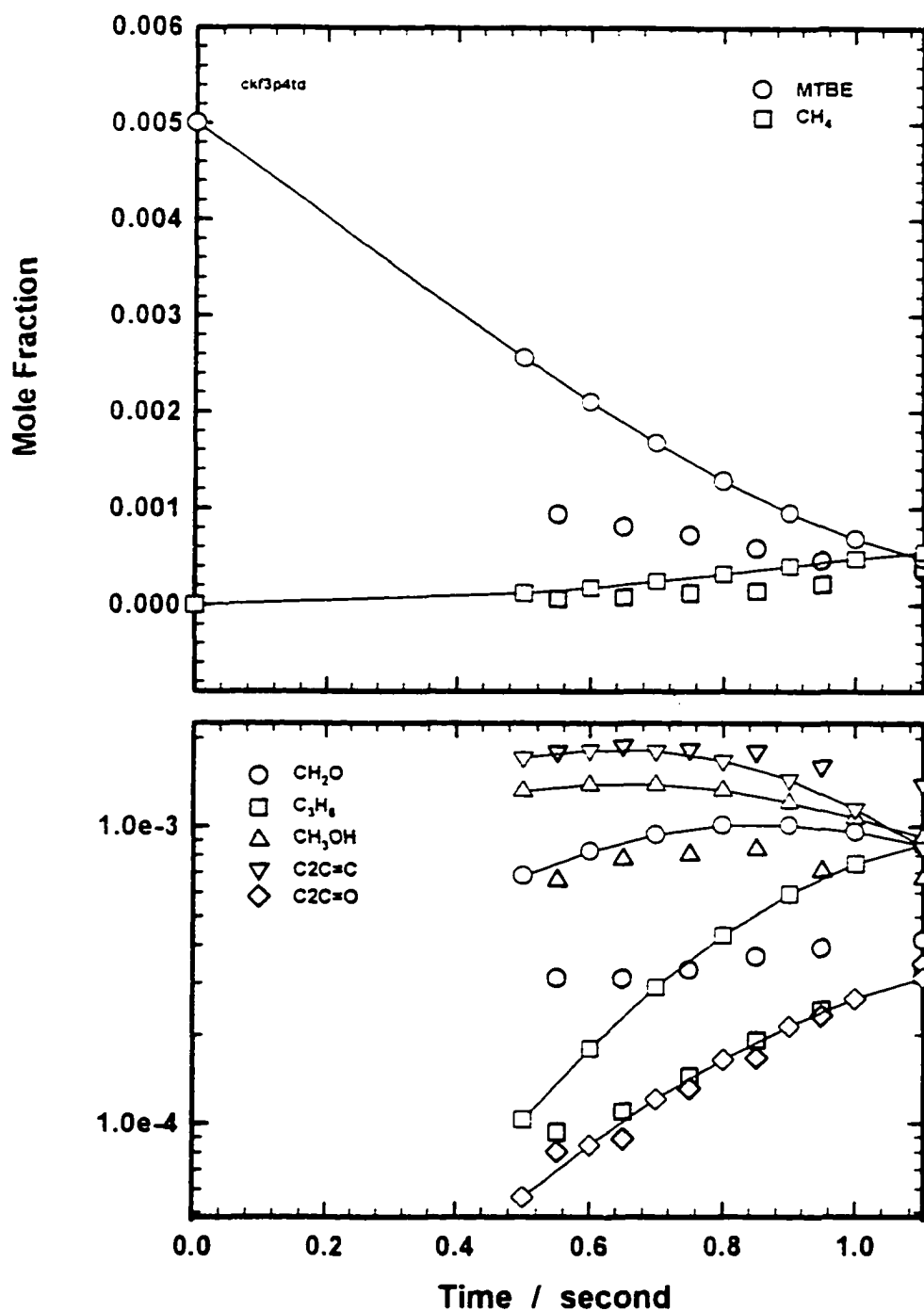
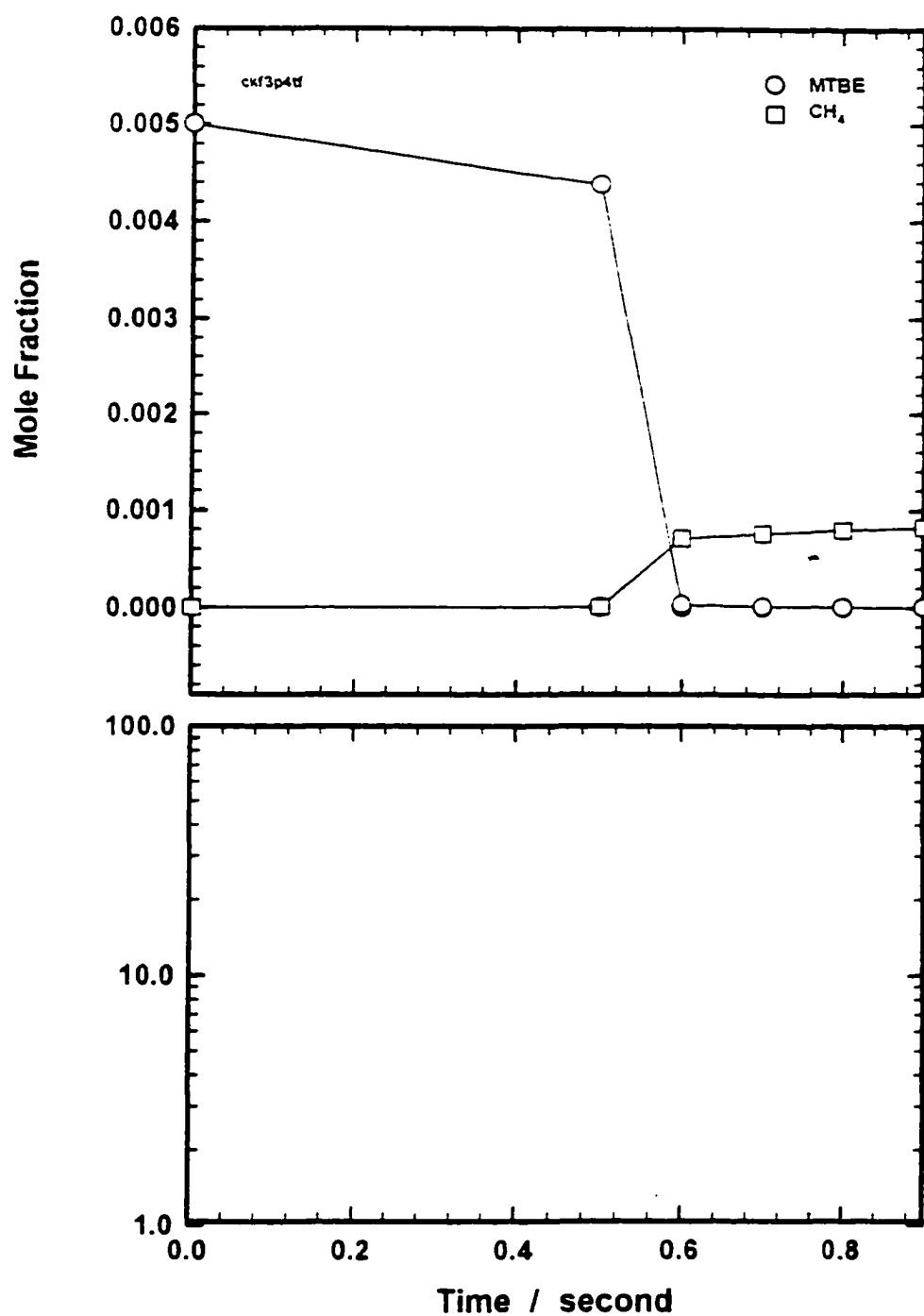


Figure IIC. 124 Experimental result of 0.5% MTBE oxidation: temperature and pressure dependence of CO_2 at $\phi = 1.50$



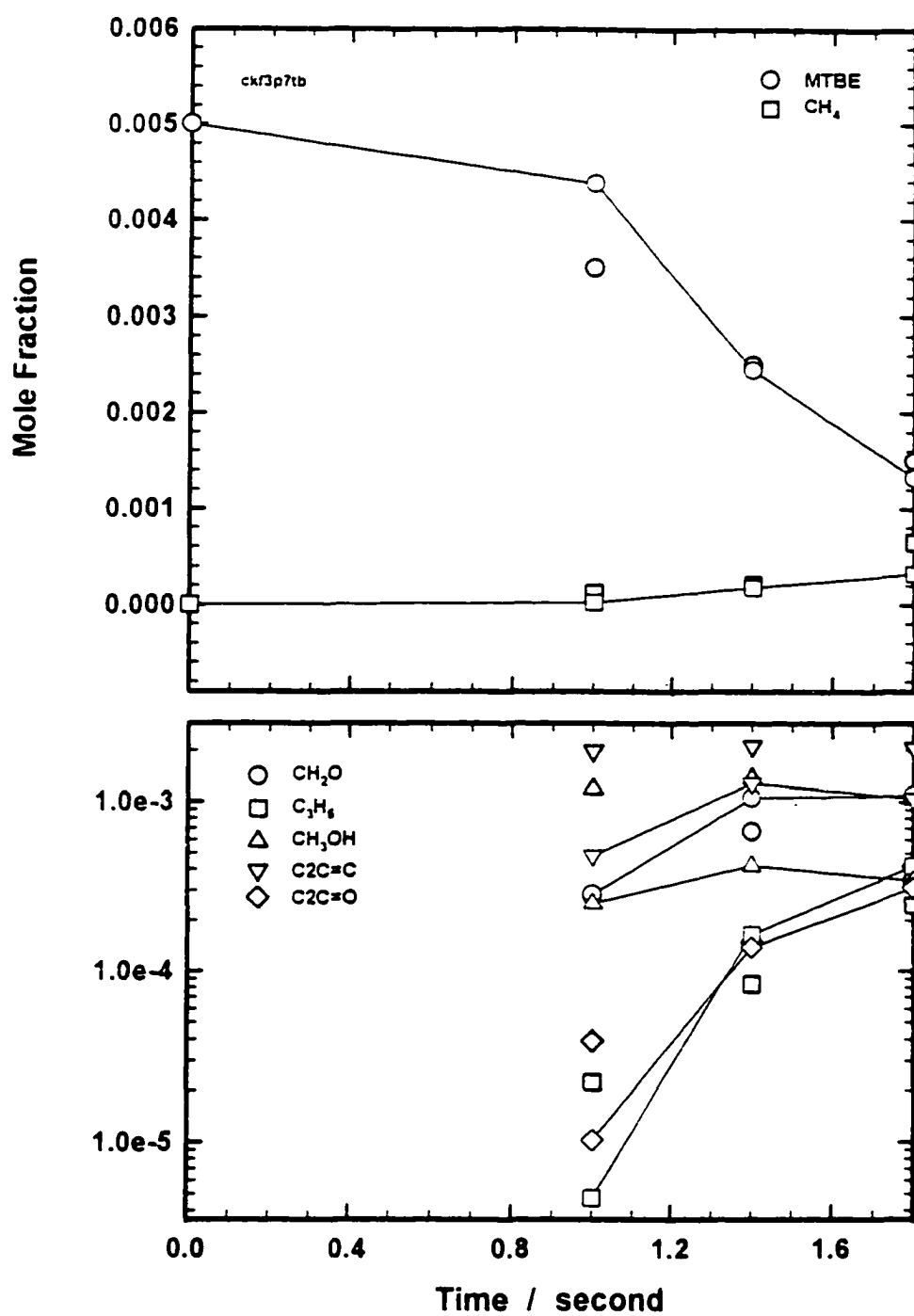
line is modeling result, symbols are experimental data

Figure II. 125 Comparison of experiment and modeling result
 $\phi = 0.75$, $P = 4$ atm, $T = 873$ K



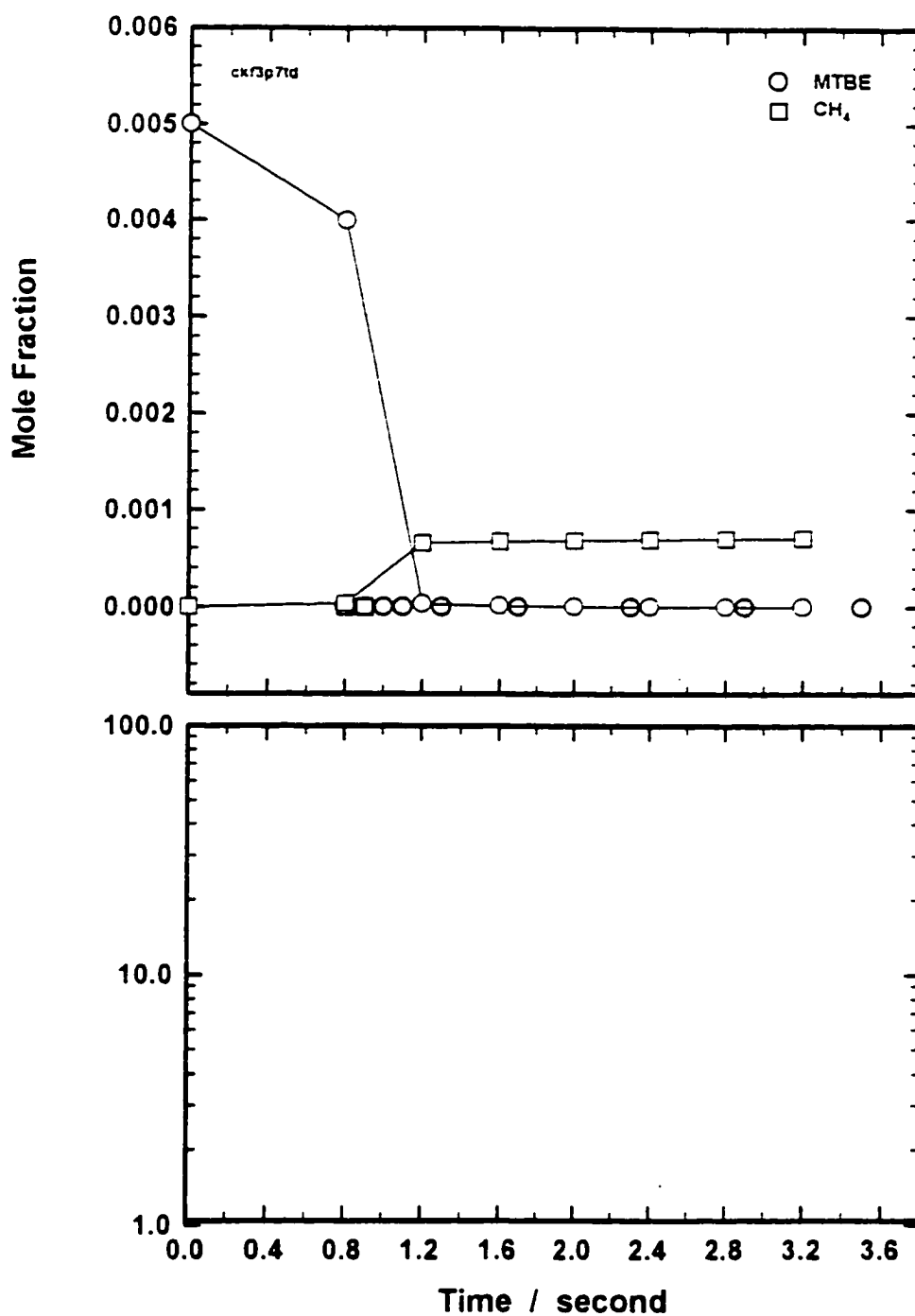
line is modeling result, symbols are experimental data

Figure IIC. 126 Comparison of experiment and modeling result
 $\varphi = 0.75$, $P = 4$ atm, $T = 923$ K



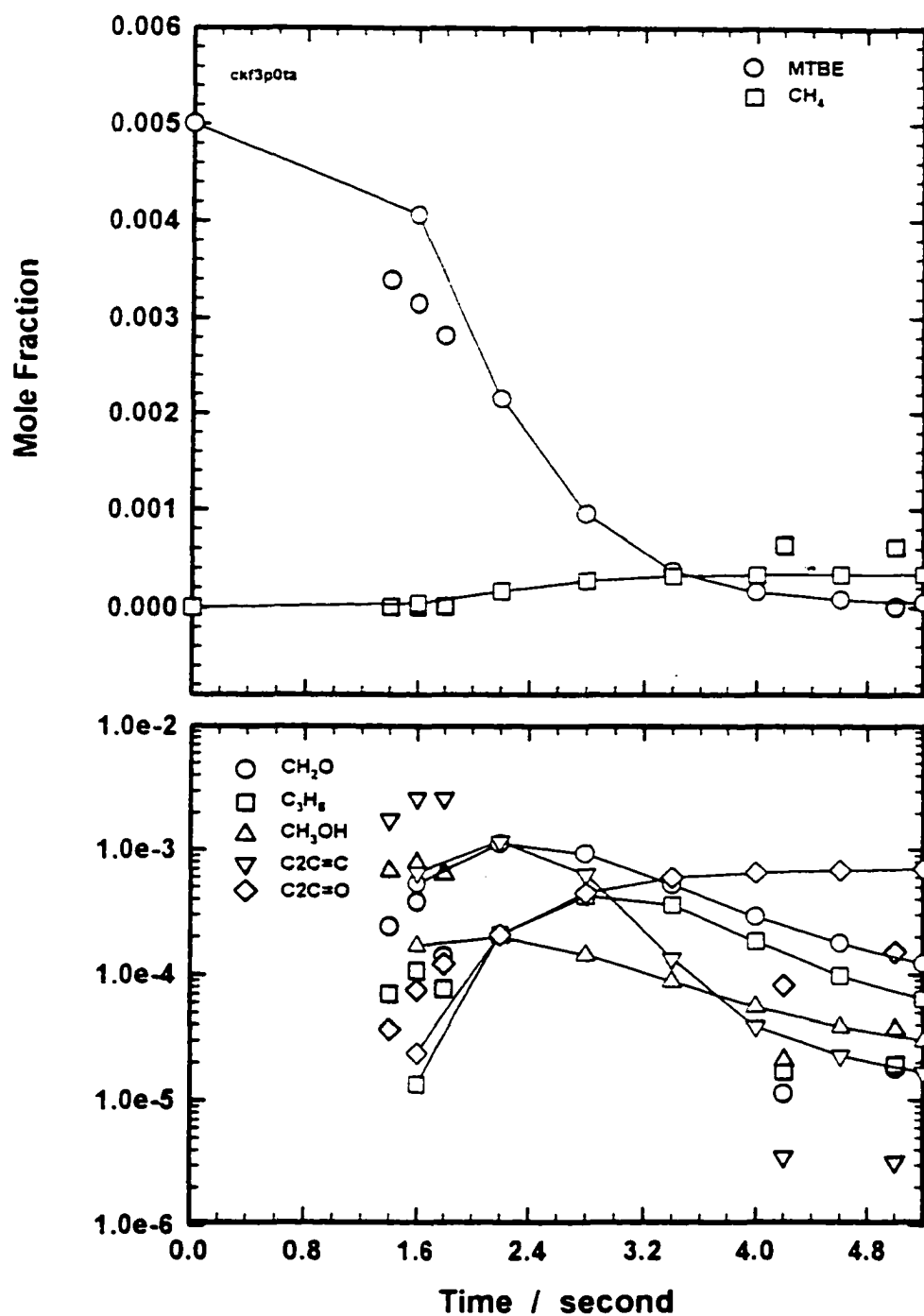
line is modeling result, symbols are experimental data

Figure IIC. 127 Comparison of experiment and modeling result
 $\phi = 0.75$, $P = 7$ atm, $T = 823$ K



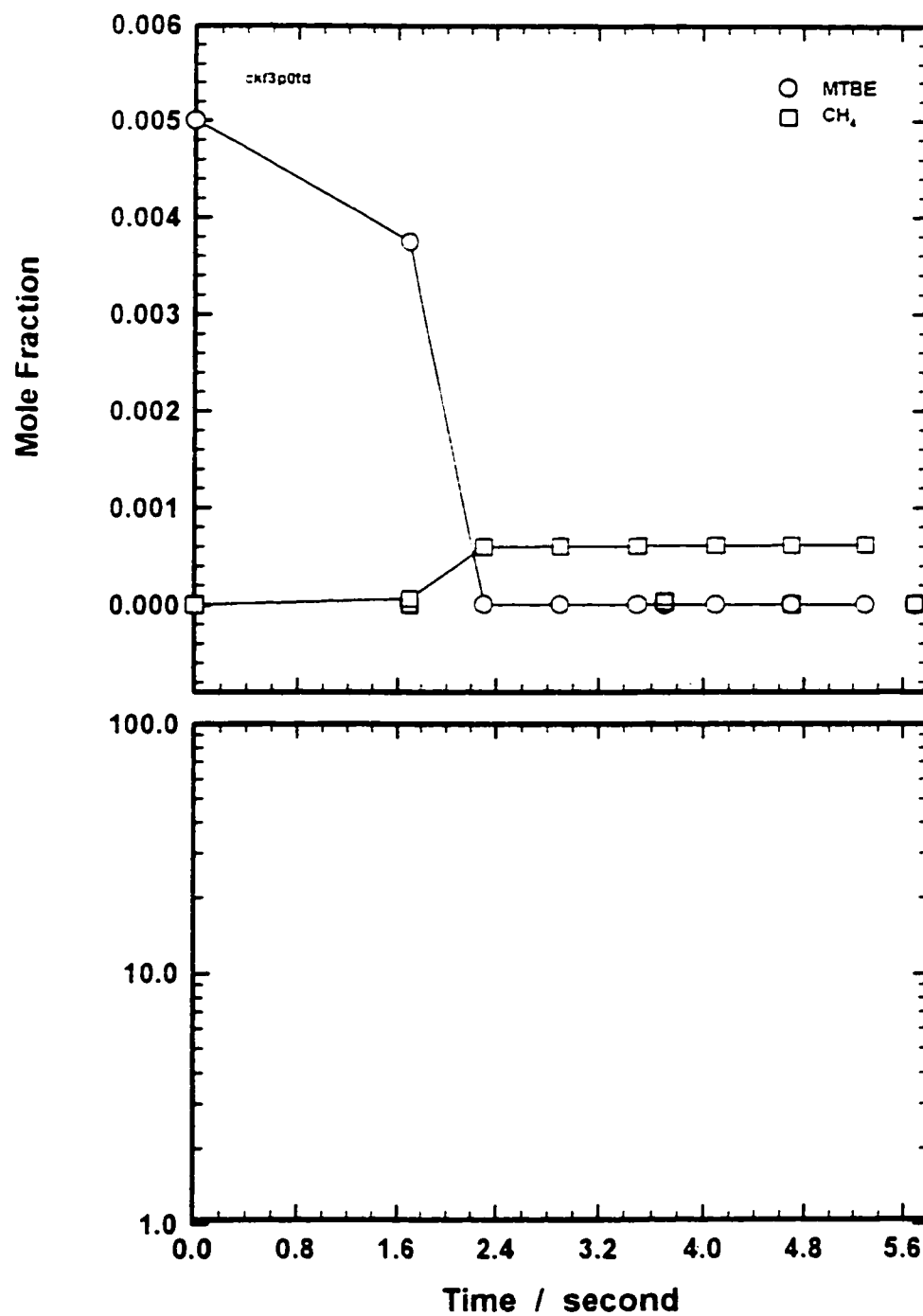
line is modeling result, symbols are experimental data

Figure IIC. 128 Comparison of experiment and modeling result
 $\phi = 0.75$, $P = 7$ atm, $T = 873$ K



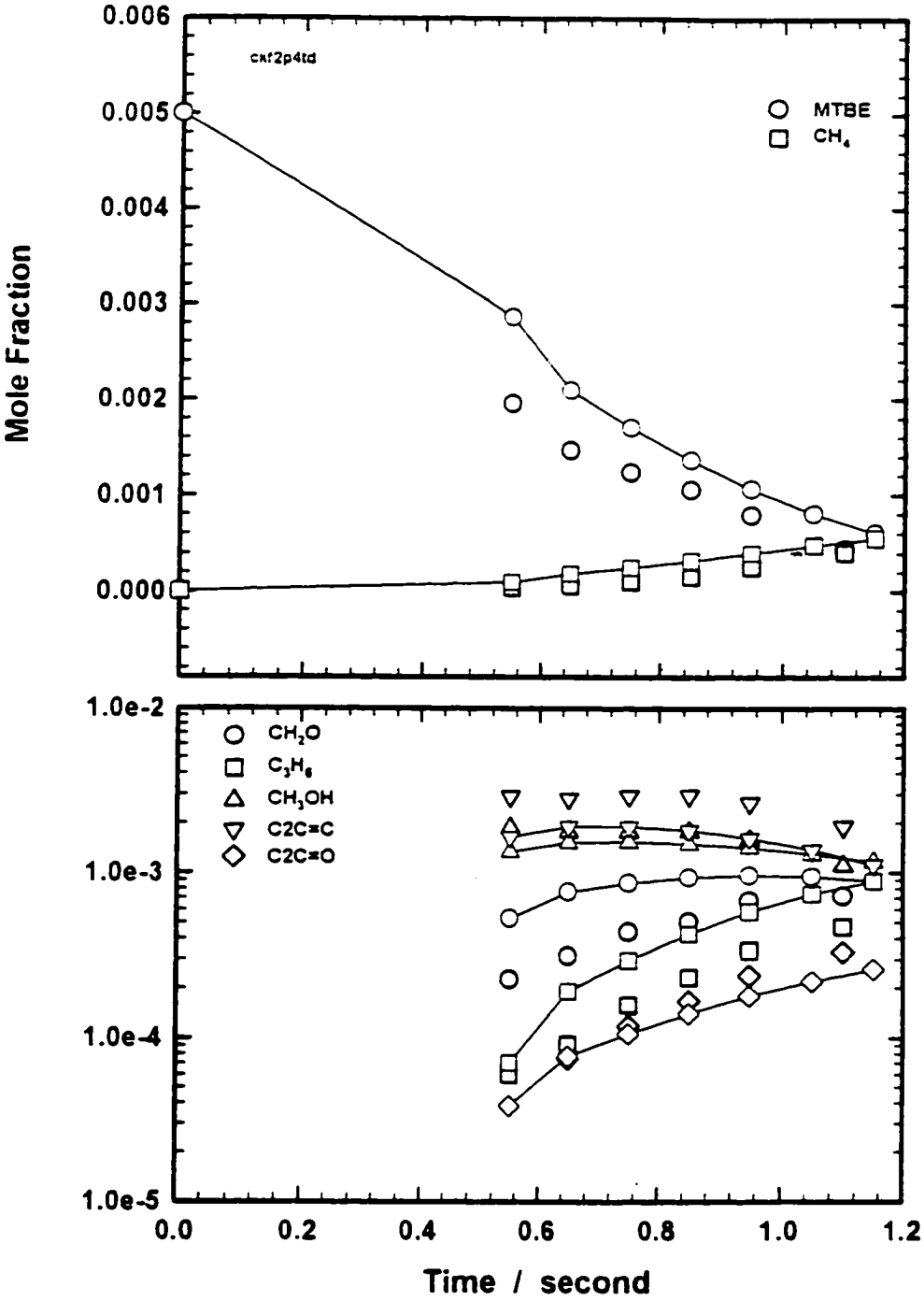
line is modeling result, symbols are experimental data

Figure IIC. 129 Comparison of experiment and modeling result
 $\phi = 0.75$, $P = 10$ atm, $T = 798$ K

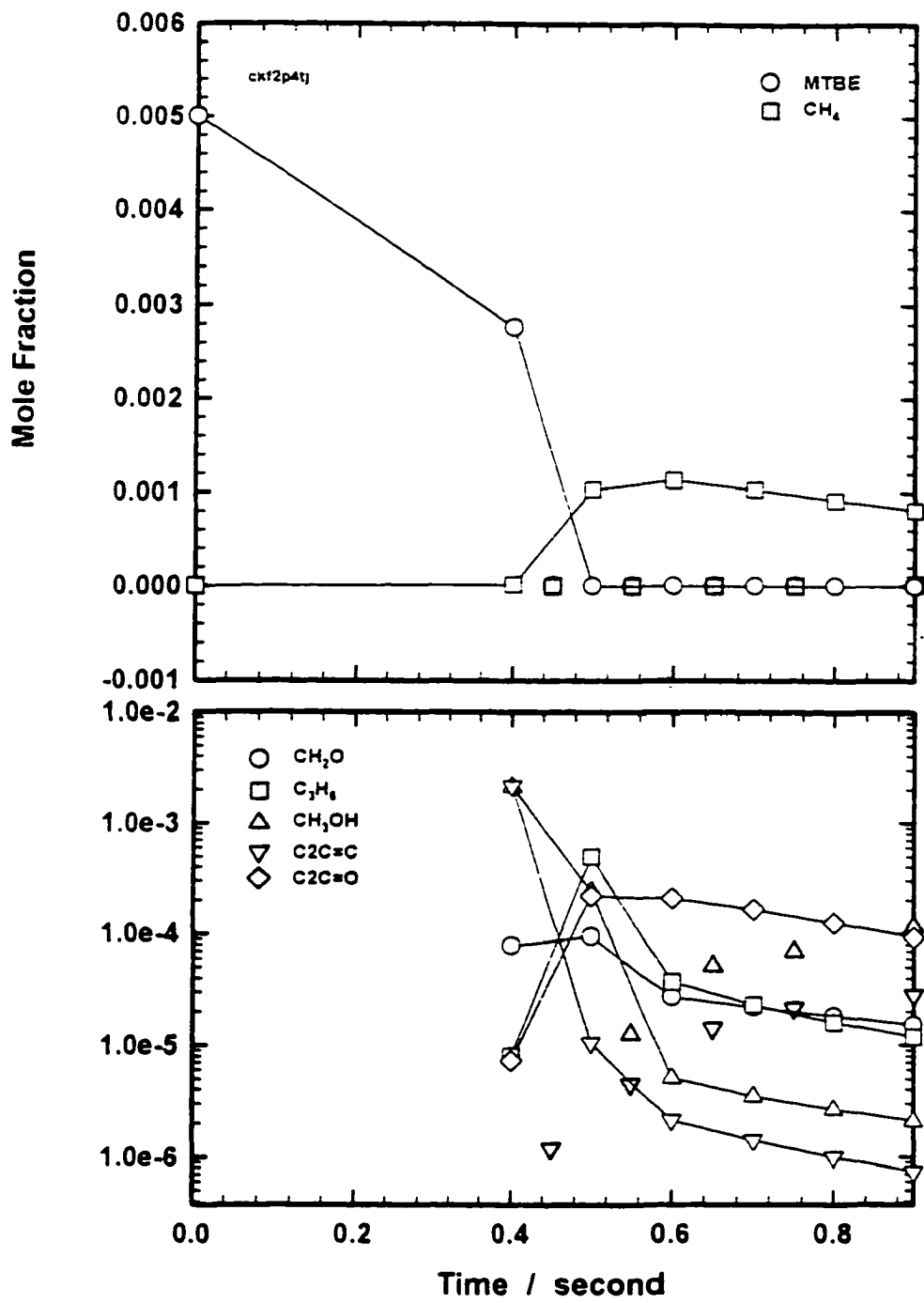


line is modeling result, symbols are experimental data

Figure IIC. 130 Comparison of experiment and modeling result
 $\phi = 0.75$, $P = 10$ atm, $T = 873$ K

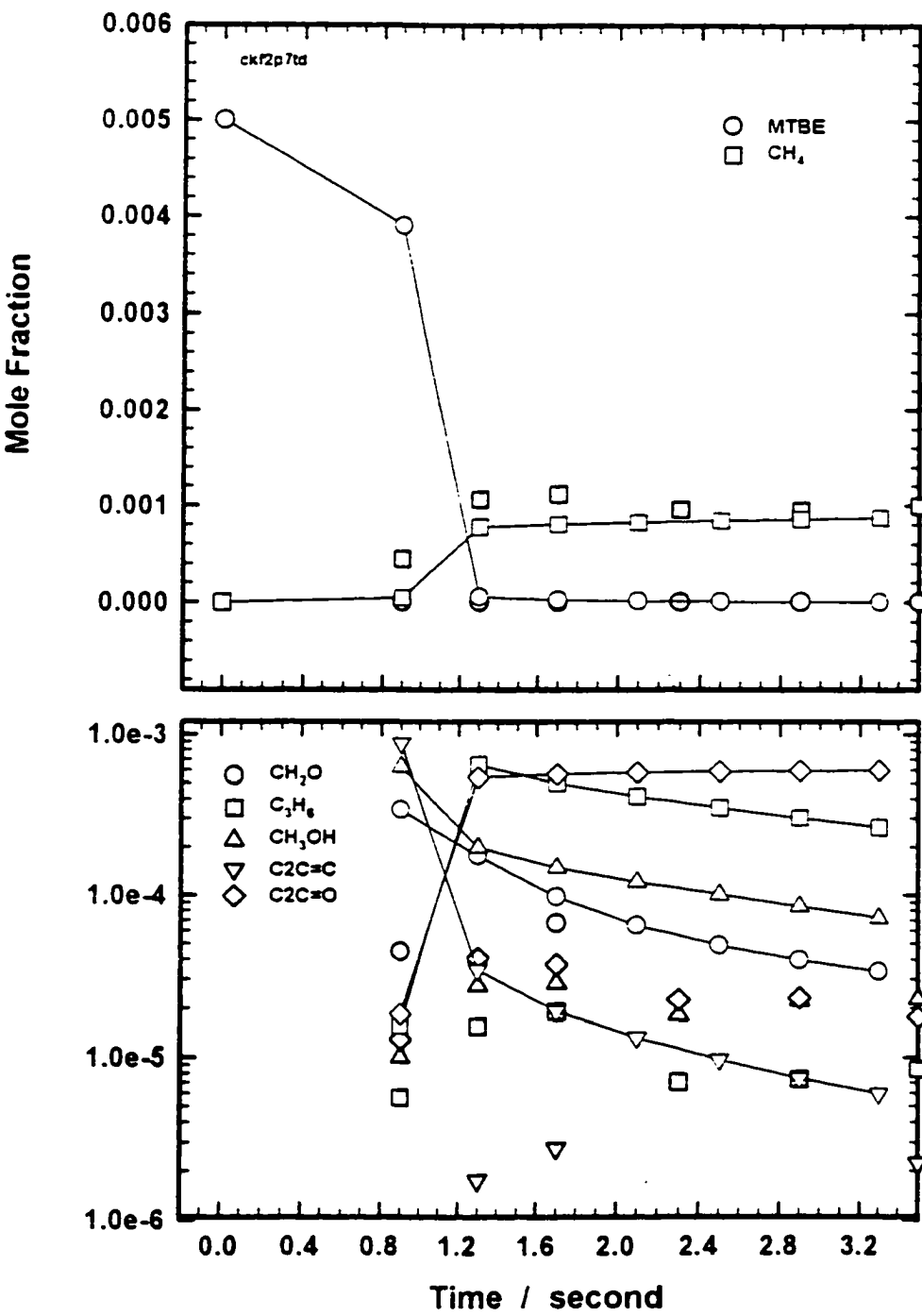


line is modeling result, symbols are experimental data
Figure IIC. 131 Comparison of experiment and modeling result
 $\phi = 1.0$, $P = 4$ atm, $T = 873$ K



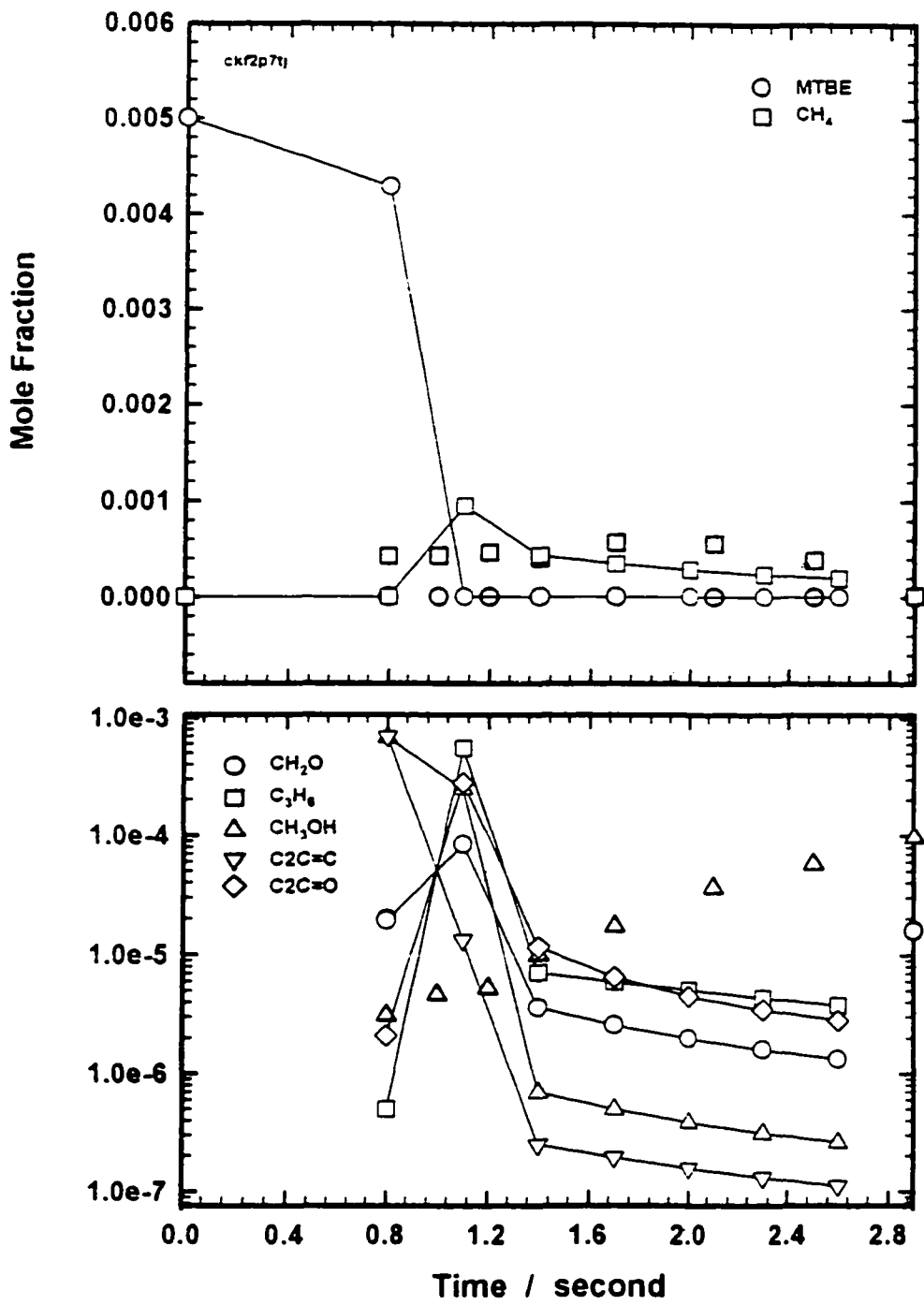
line is modeling result, symbols are experimental data

Figure IIC. 132 Comparison of experiment and modeling result
 $\phi = 1.0$, $P = 4$ atm, $T = 1023$ K

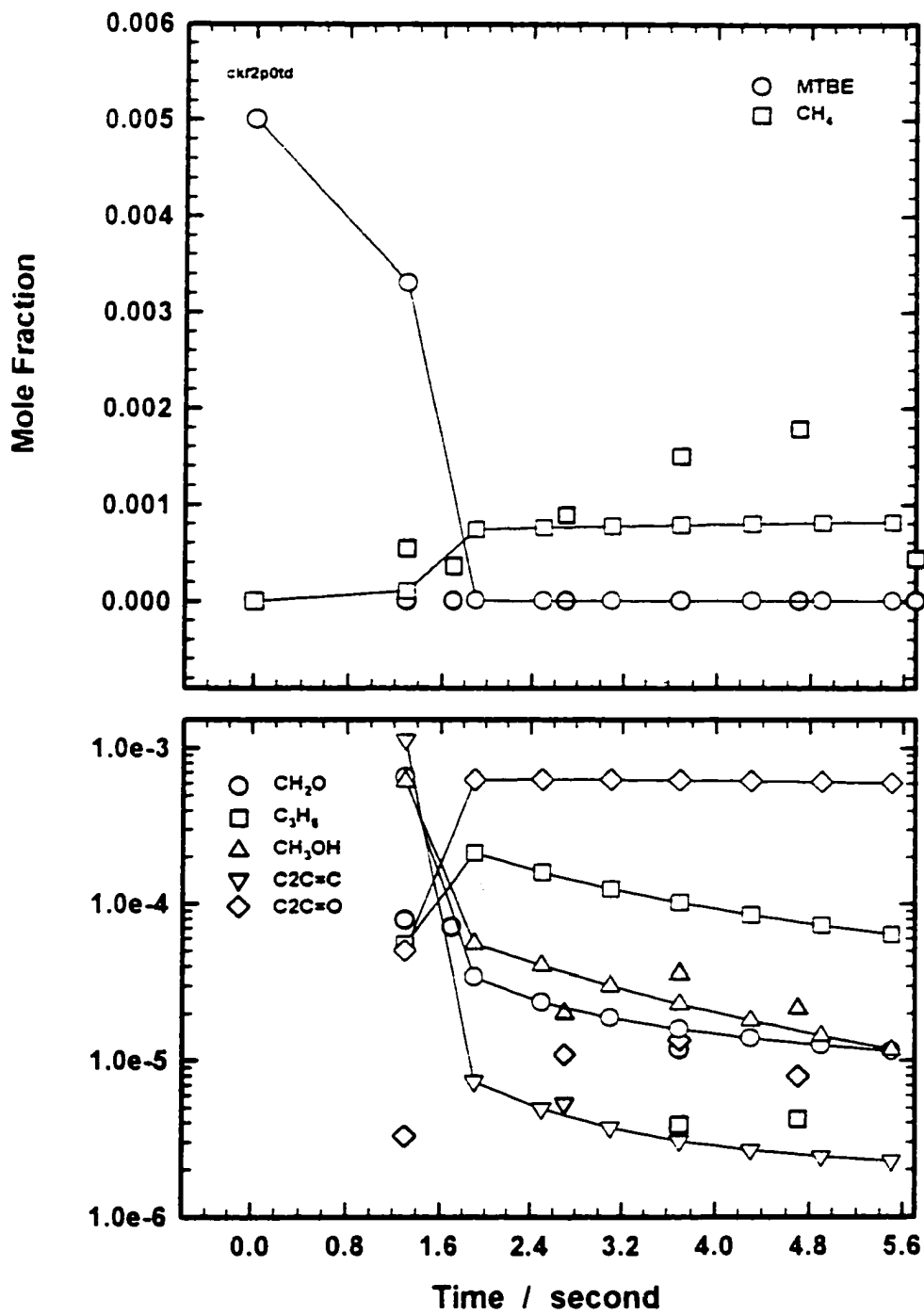


line is modeling result, symbols are experimental data

Figure IIC. 133 Comparison of experiment and modeling result
 $\phi = 1.0$, $P = 7$ atm, $T = 873$ K

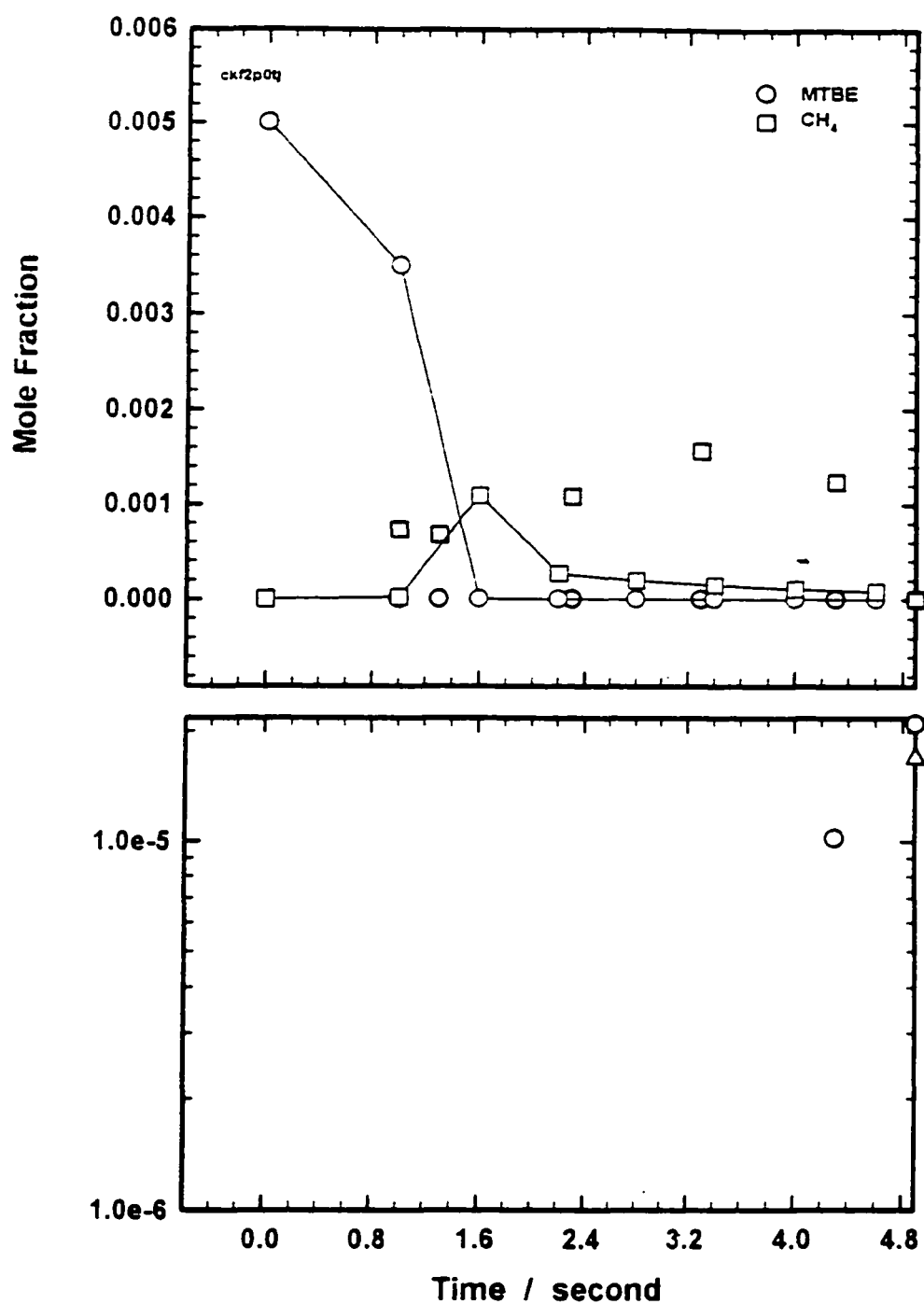


line is modeling result, symbols are experimental data
Figure IIC. 134 Comparison of experiment and modeling result
 $\phi = 1.0$, $P = 7$ atm, $T = 1023$ K



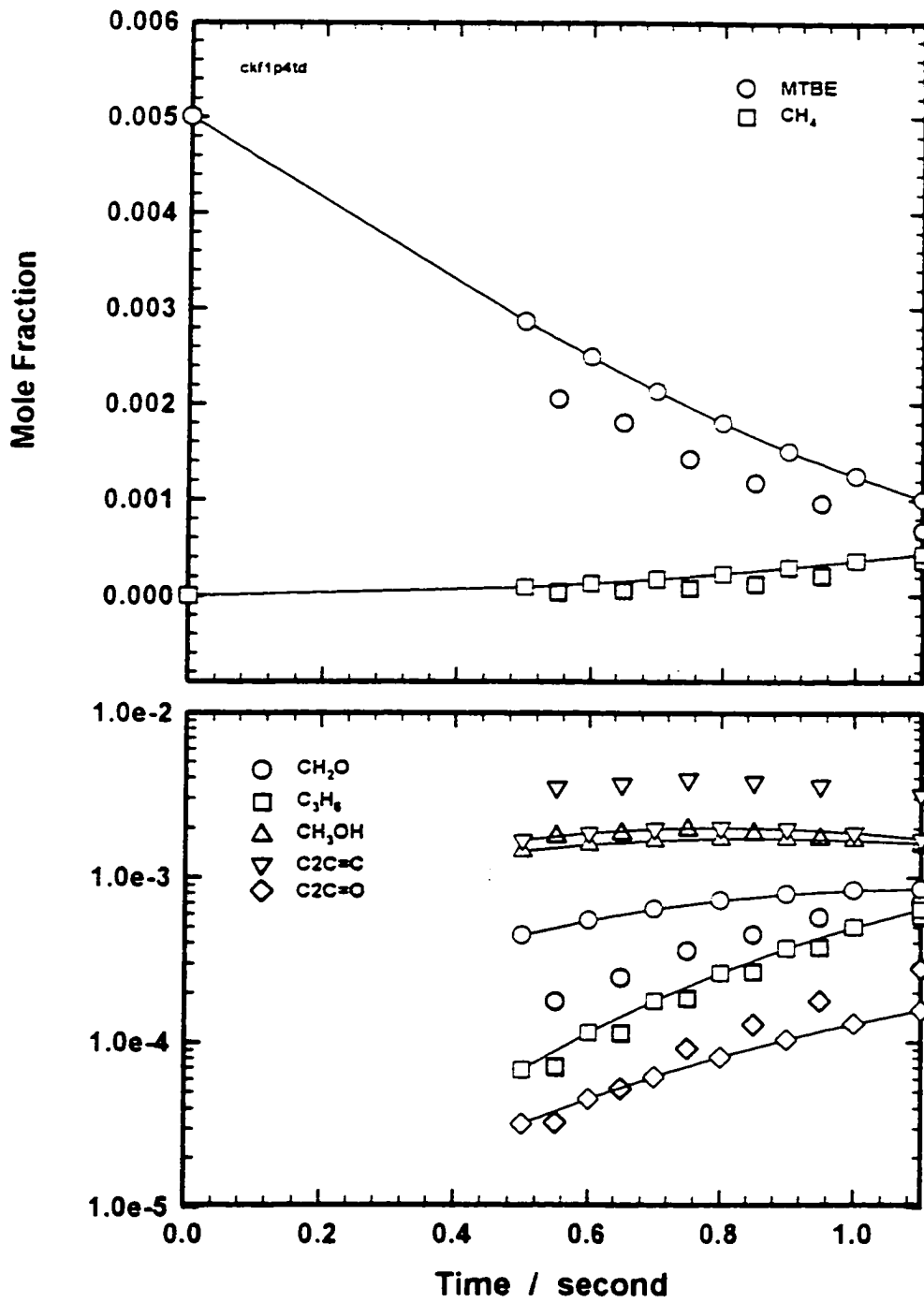
line is modeling result, symbols are experimental data

Figure IIC. 135 Comparison of experiment and modeling result
 $\phi = 1.0$, $P = 10 \text{ atm}$, $T = 873 \text{ K}$



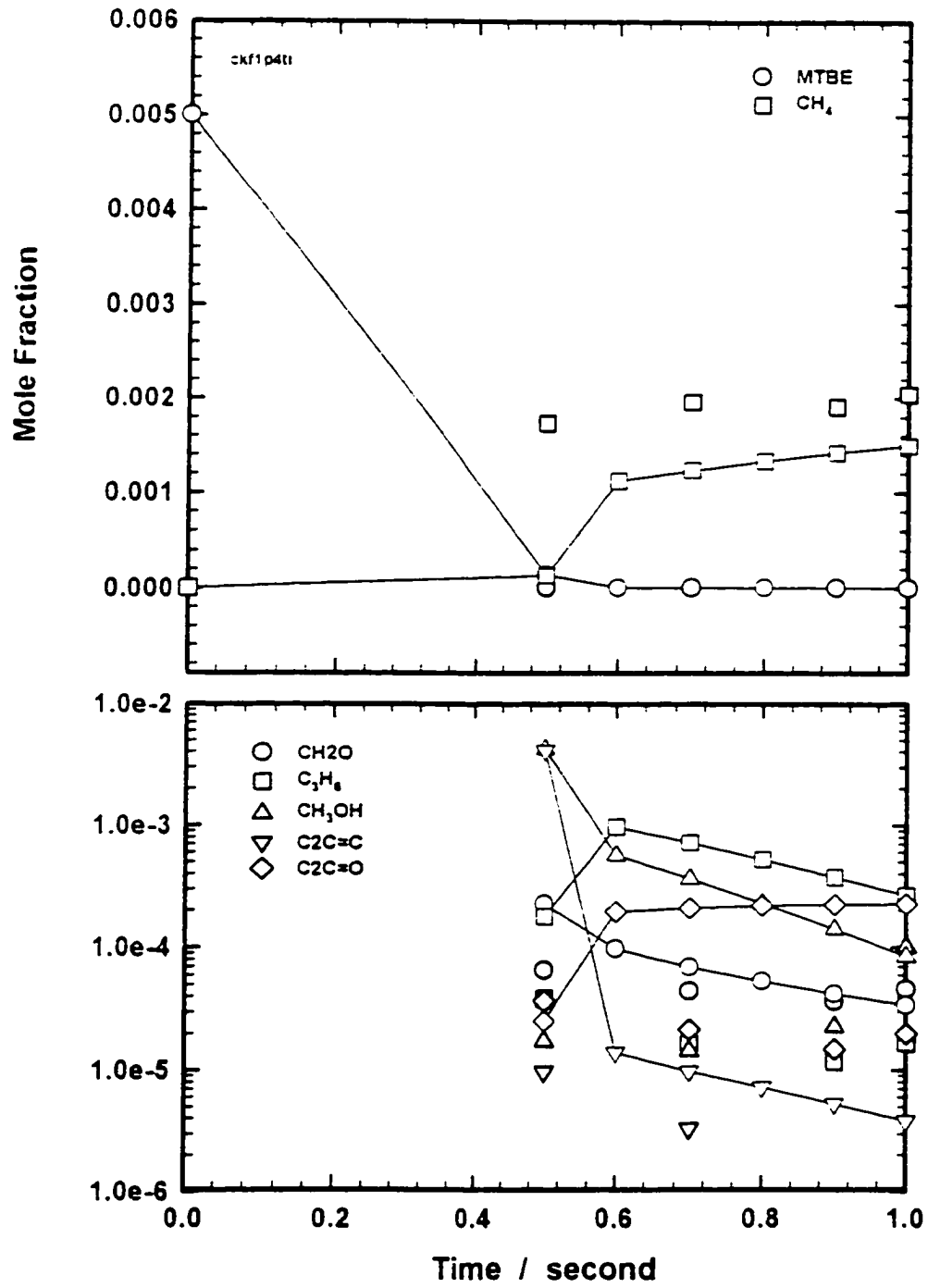
line is modeling result, symbols are experimental data

Figure IIC. 136 Comparison of experiment and modeling result
 $\phi = 1.0$, $P = 10$ atm, $T = 1023$ K



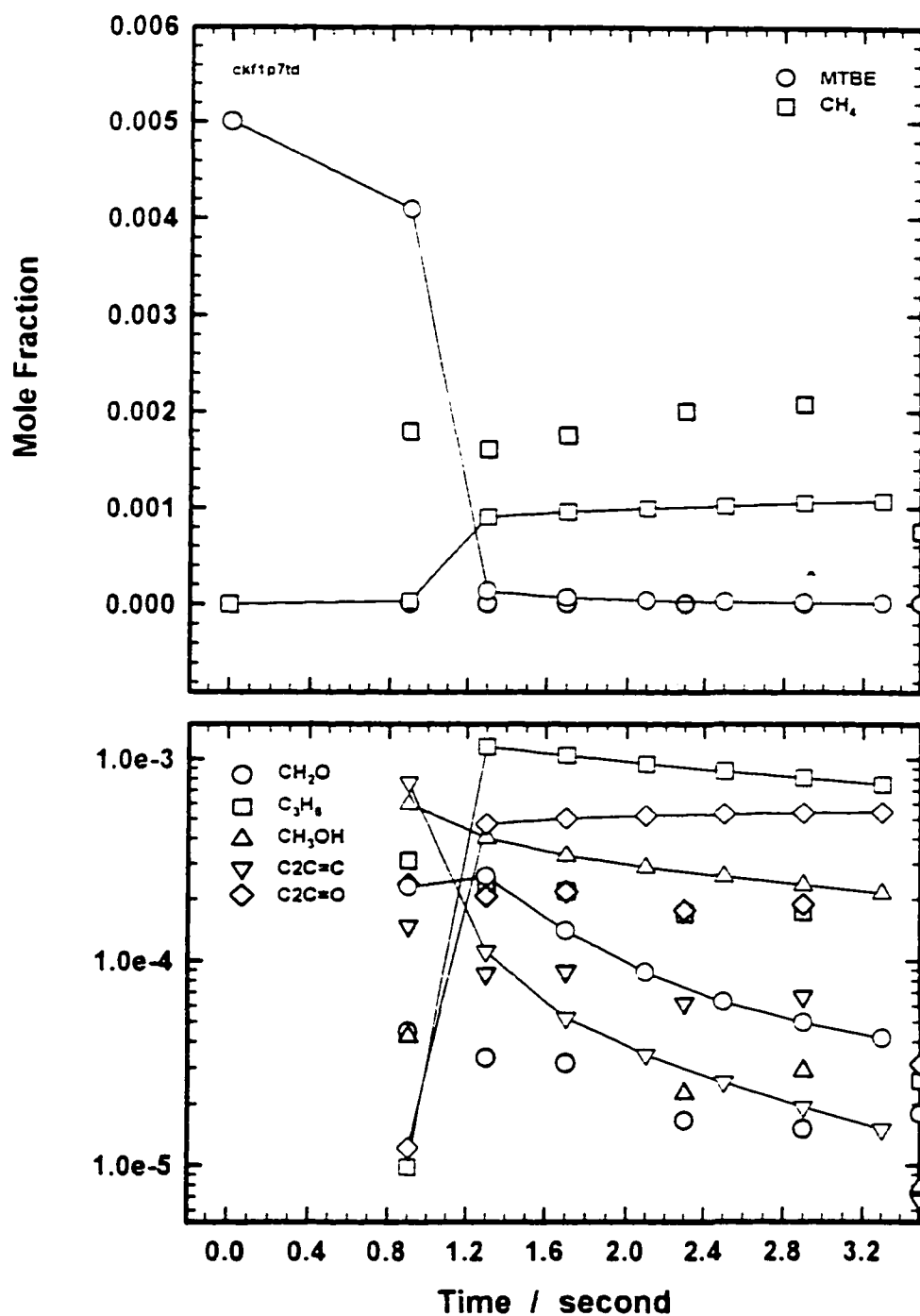
line is modeling result, symbols are experimental data

Figure IIC. 137 Comparison of experiment and modeling result
 $\varphi = 1.5$, $P = 4$ atm, $T = 873$ K



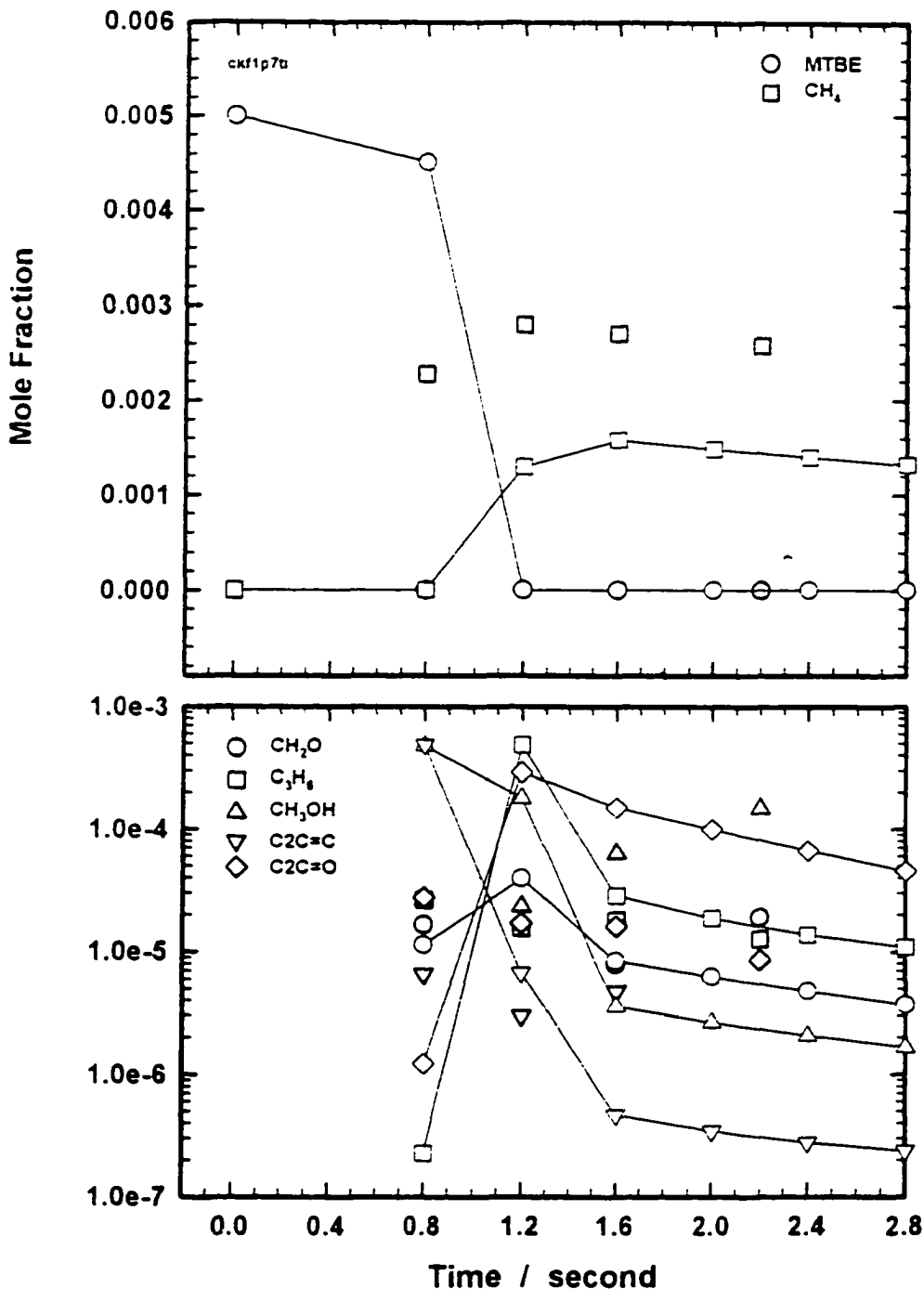
line is modeling result, symbols are experimental data

Figure IIC. 138 Comparison of experiment and modeling result
 $\phi = 1.5$, $P = 4$ atm, $T = 998$ K

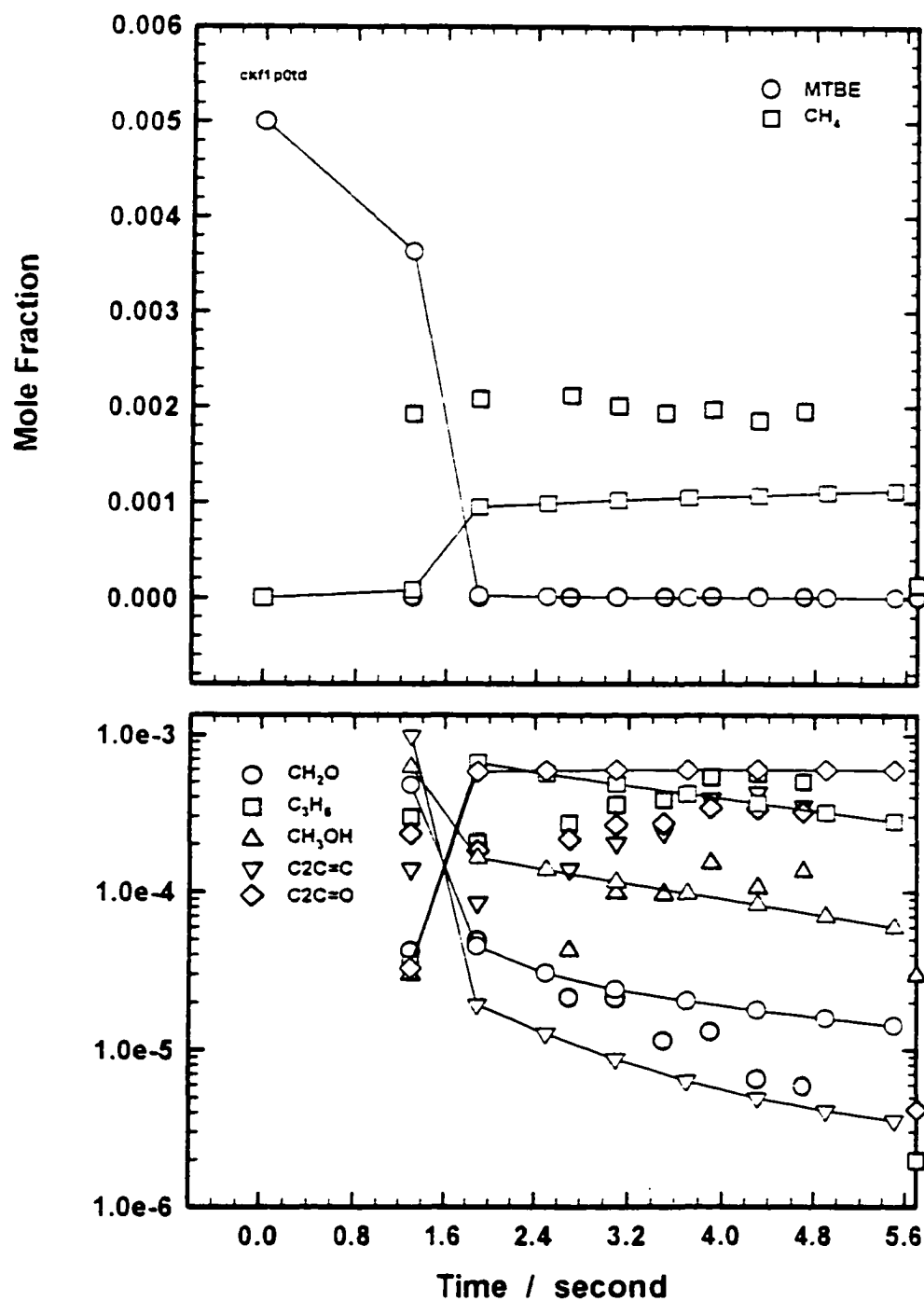


line is modeling result, symbols are experimental data

Figure IIC. 139 Comparison of experiment and modeling result
 $\phi = 1.5$, $P = 7$ atm, $T = 873$ K

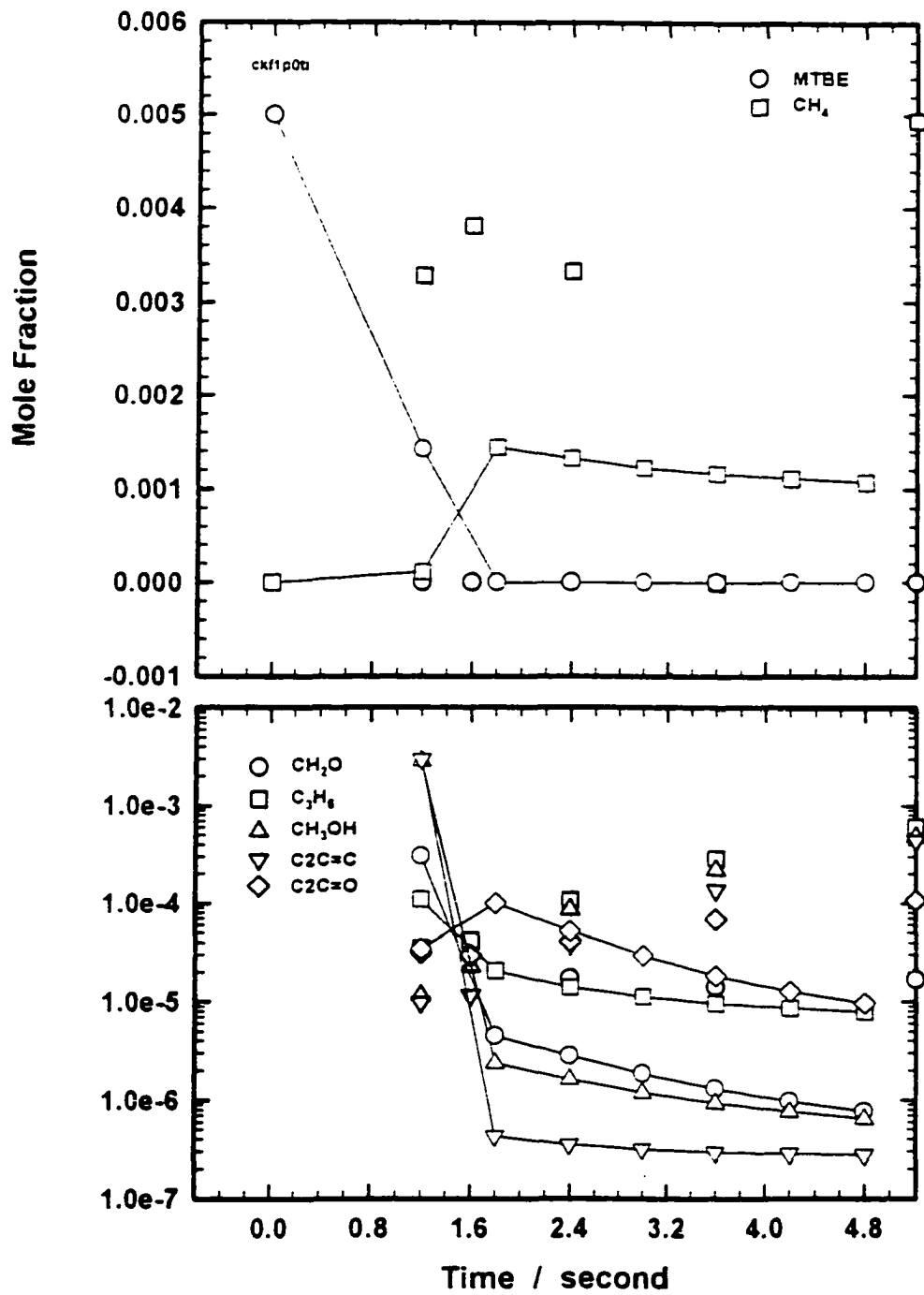


line is modeling result, symbols are experimental data
Figure IIC. 140 Comparison of experiment and modeling result
 $\phi = 1.5$, $P = 7$ atm, $T = 998$ K



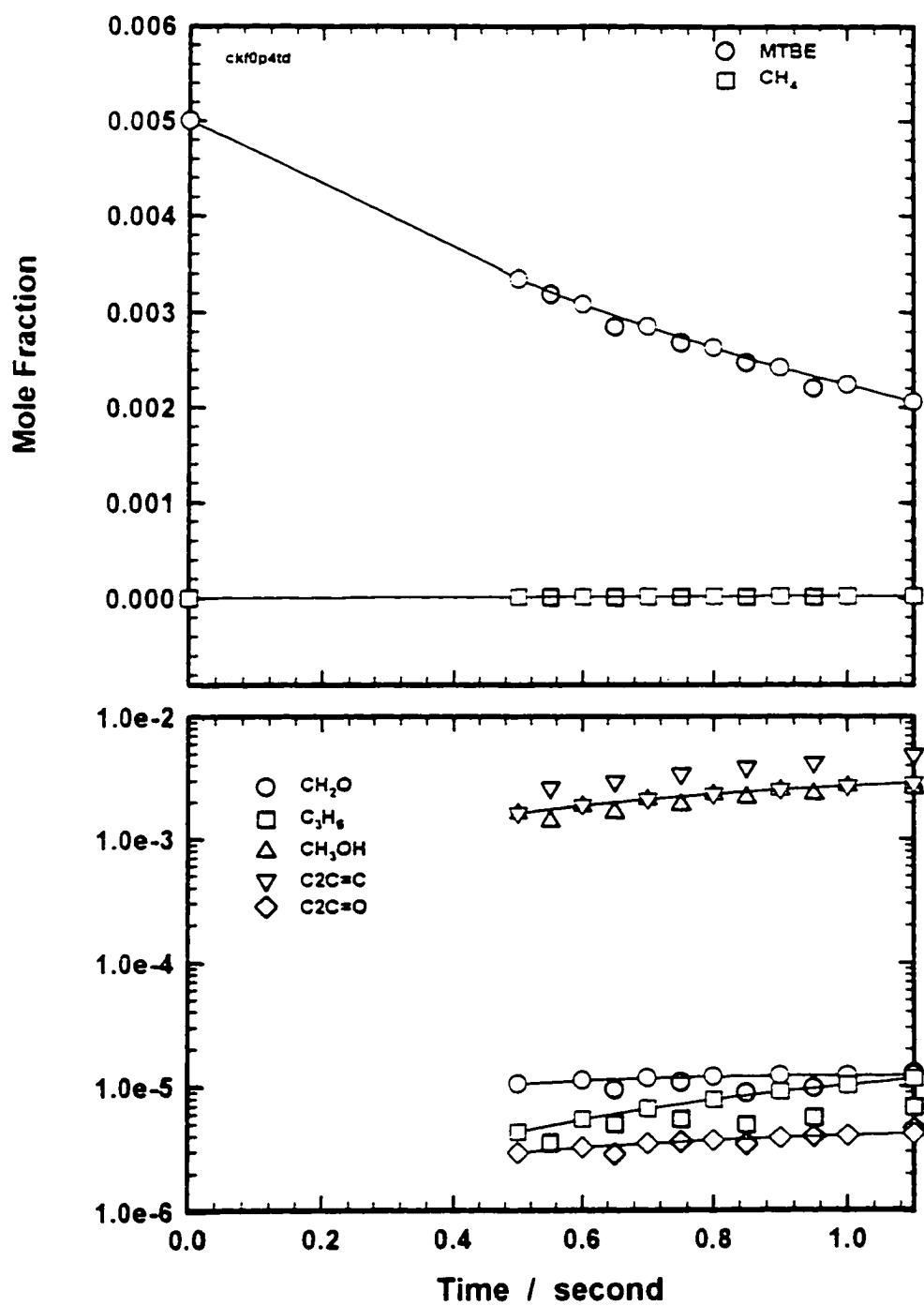
line is modeling result, symbols are experimental data

Figure II.C. 141 Comparison of experiment and modeling result
 $\phi = 1.5$, $P = 10$ atm, $T = 873$ K



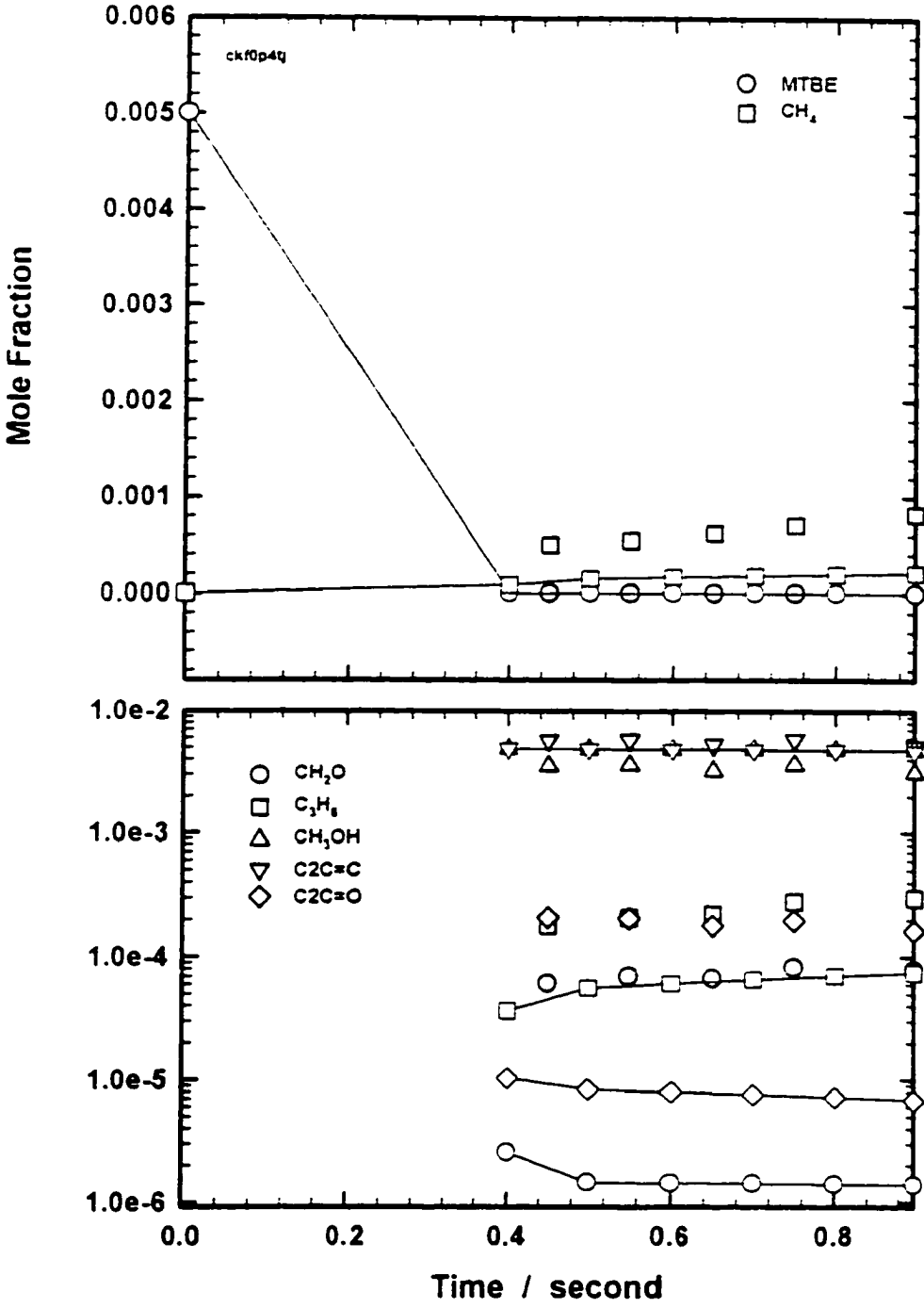
line is modeling result, symbols are experimental data

Figure IIC. 142 Comparison of experiment and modeling result
 $\varphi = 1.5$, $P = 10$ atm, $T = 998$ K



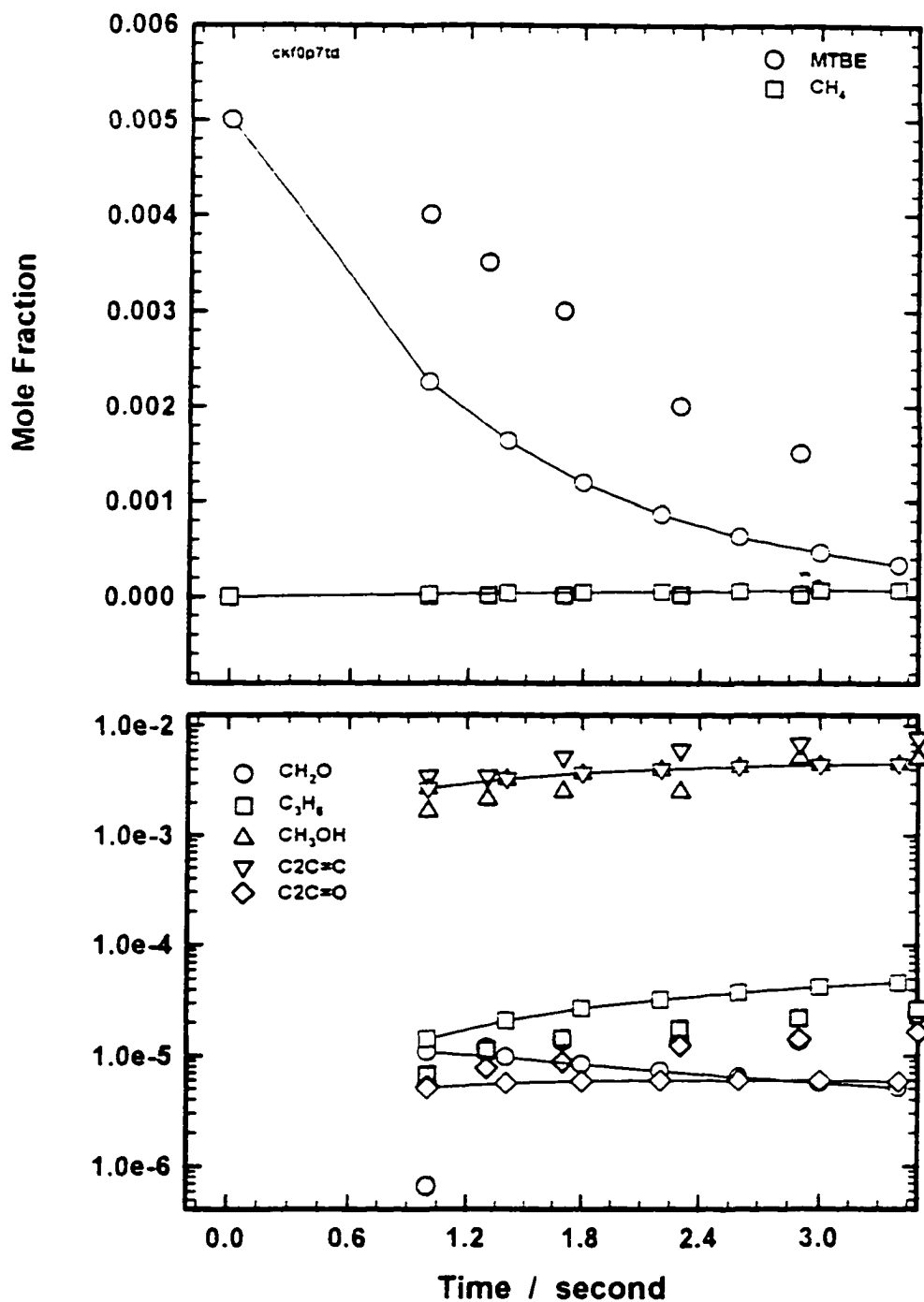
line is modeling result, symbols are experimental data

Figure IIC. 143 Comparison of experiment and modeling result
Pyrolysis, P = 4 atm, T = 873 K



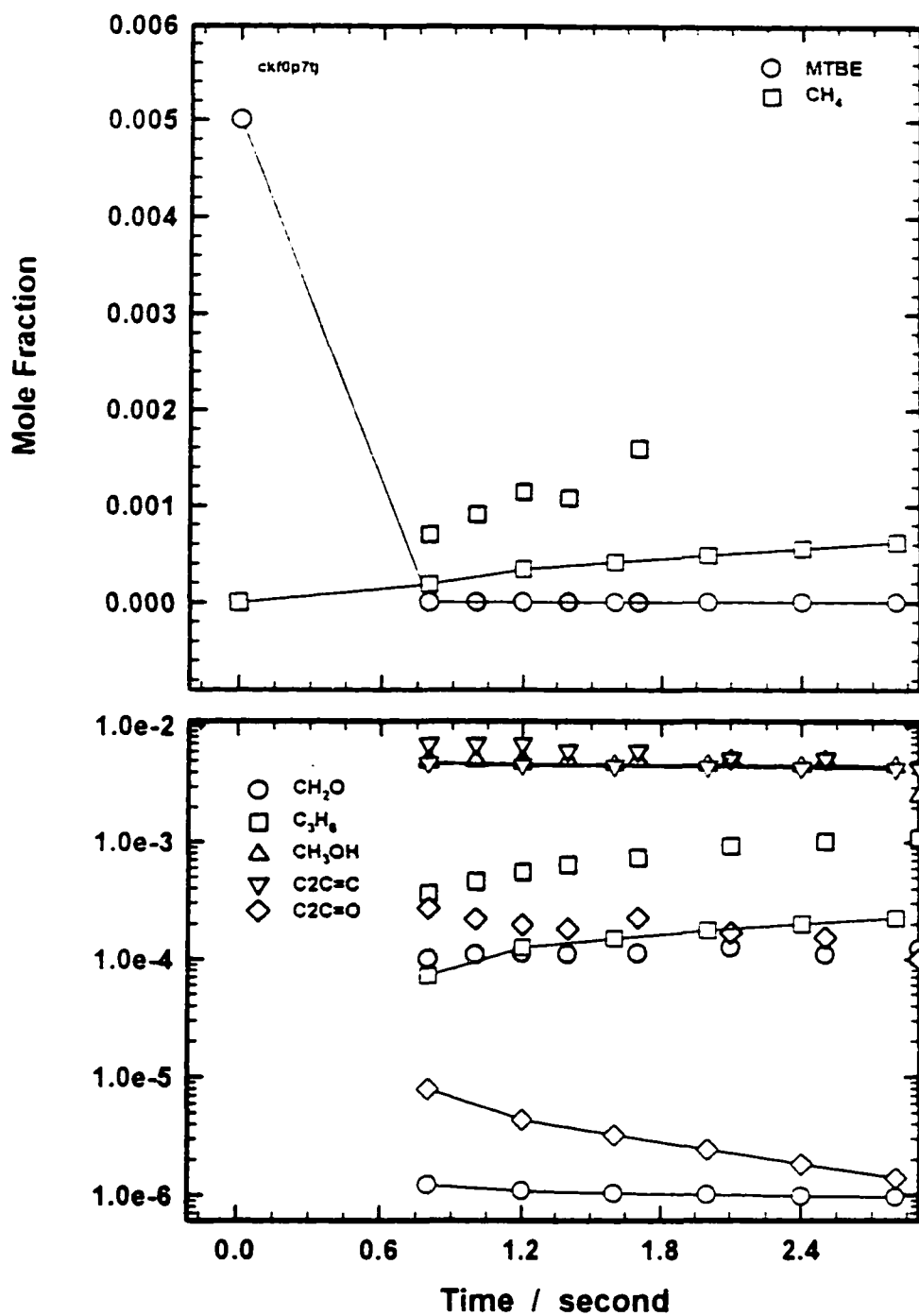
line is modeling result, symbols are experimental data

Figure IIC. 144 Comparison of experiment and modeling result
Pyrolysis, P = 4 atm, T = 1023 K



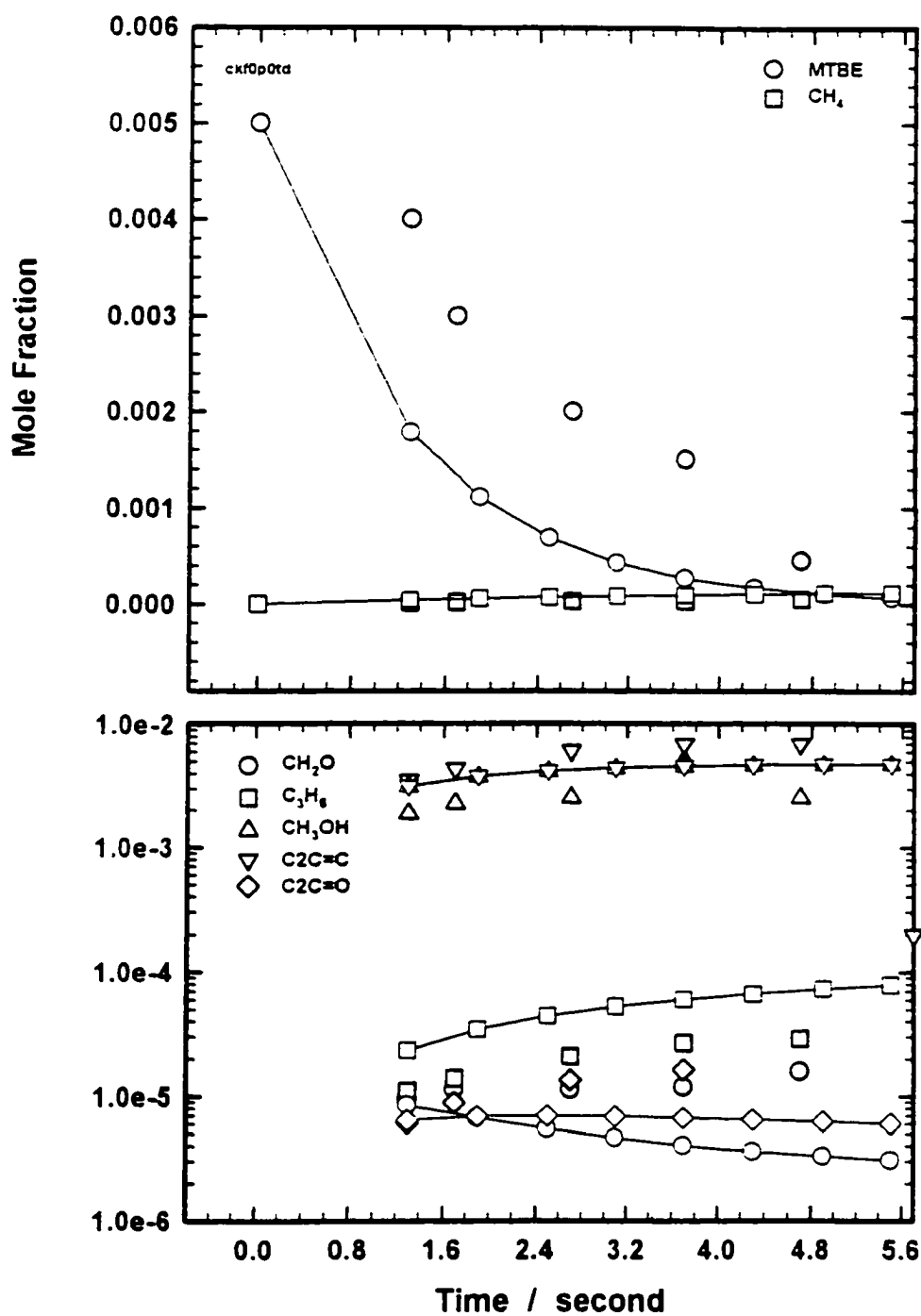
line is modeling result, symbols are experimental data

Figure IIC. 145 Comparison of experiment and modeling result
Pyrolysis, P = 7 atm, T = 873 K



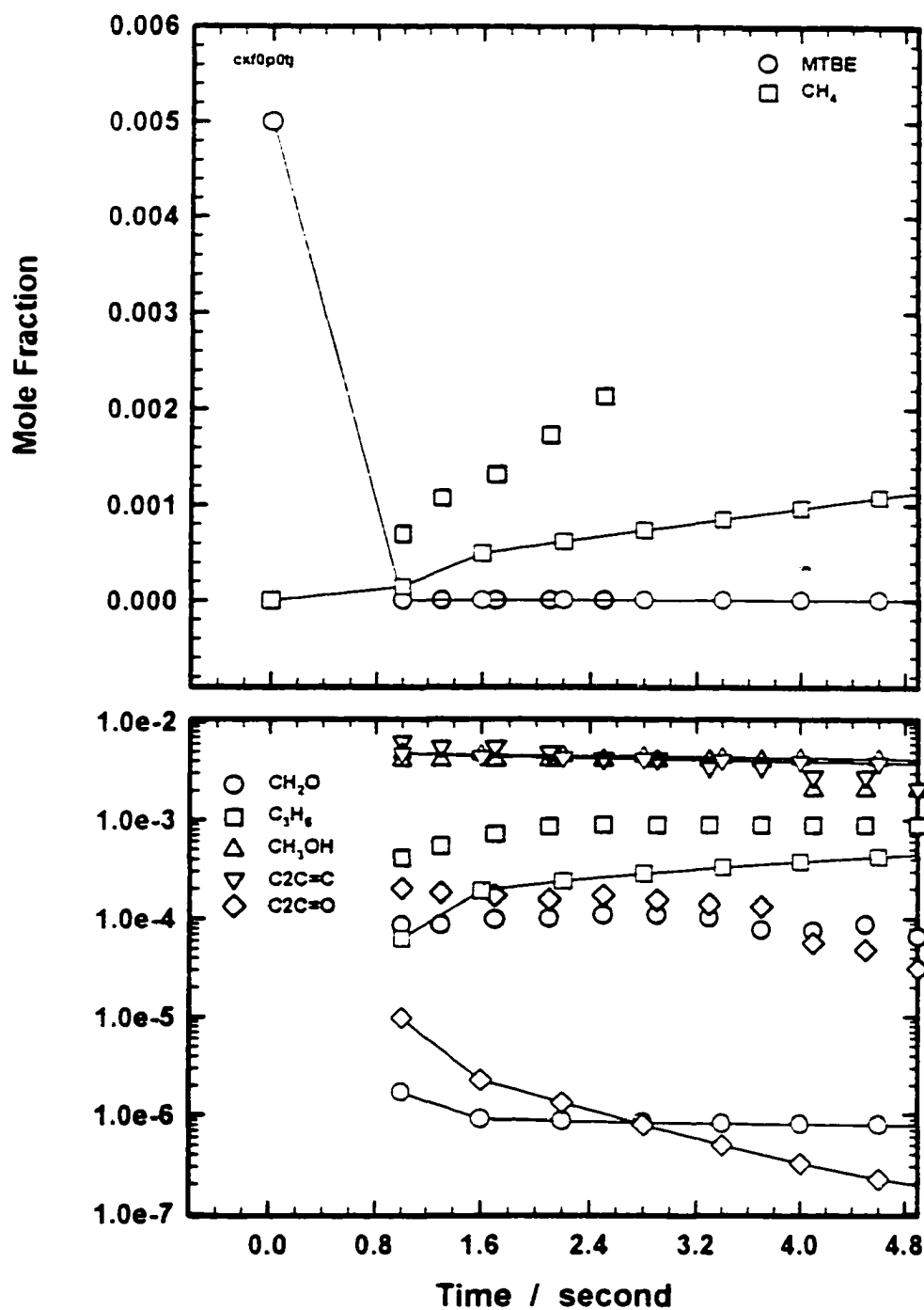
line is modeling result, symbols are experimental data

Figure IIC. 146 Comparison of experiment and modeling result
Pyrolysis, $P = 7$ atm, $T = 1023$ K



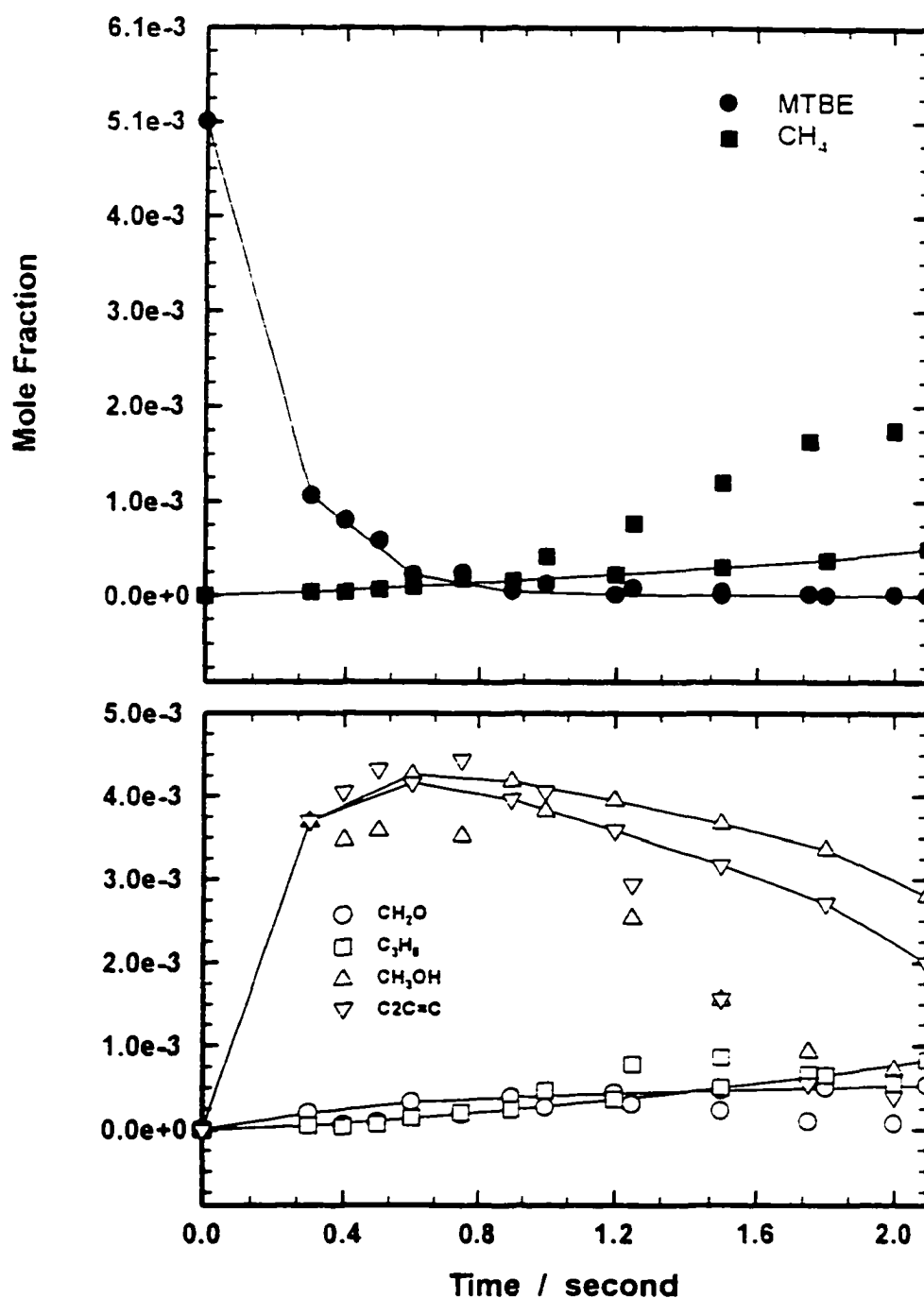
line is modeling result, symbols are experimental data

Figure IIC. 147 Comparison of experiment and modeling result
Pyrolysis, P = 10 atm, T = 873 K



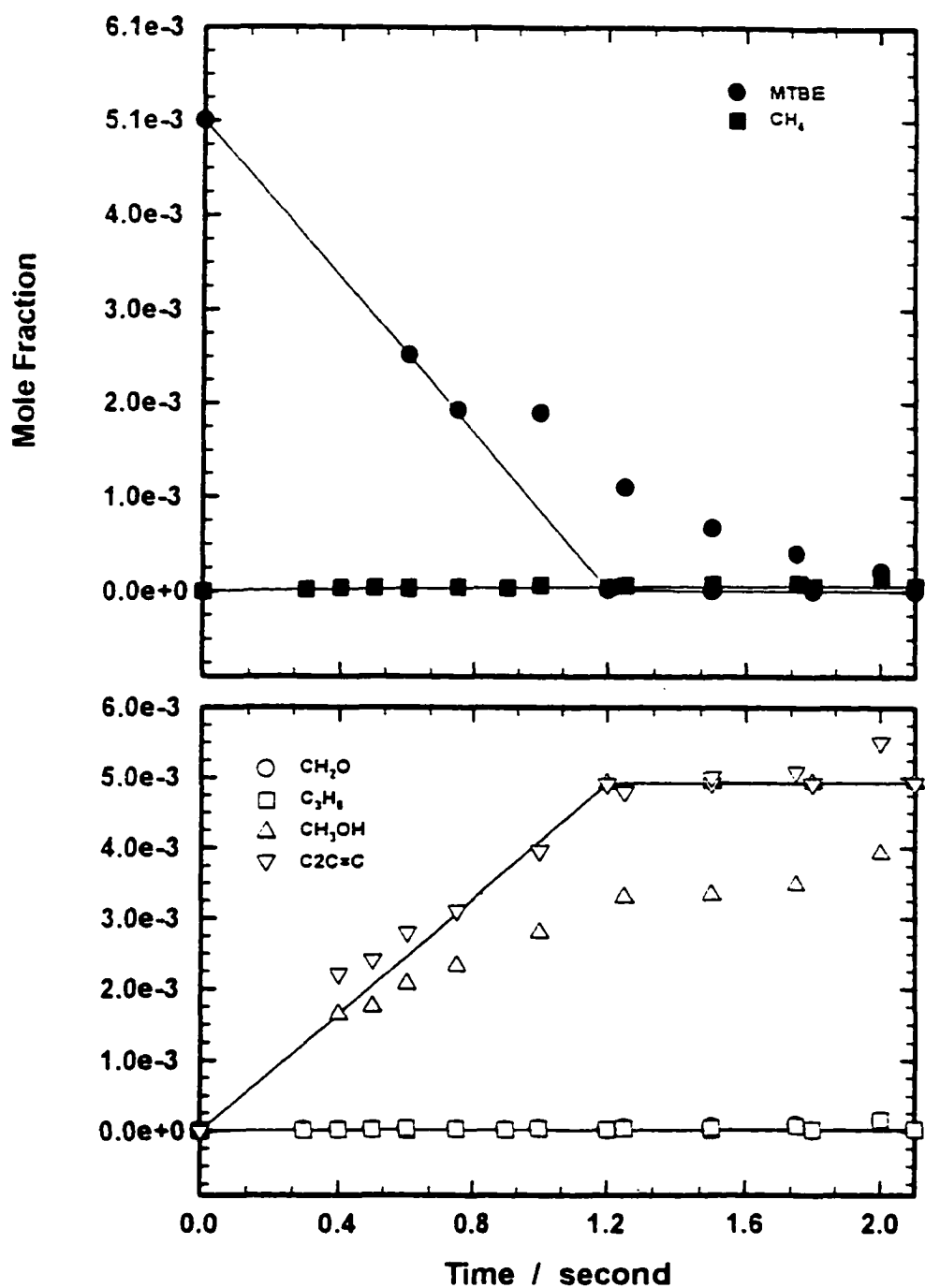
line is modeling result, symbols are experimental data

Figure IIC. 148 Comparison of experiment and modeling result
Pyrolysis, P = 10 atm, T = 1023 K



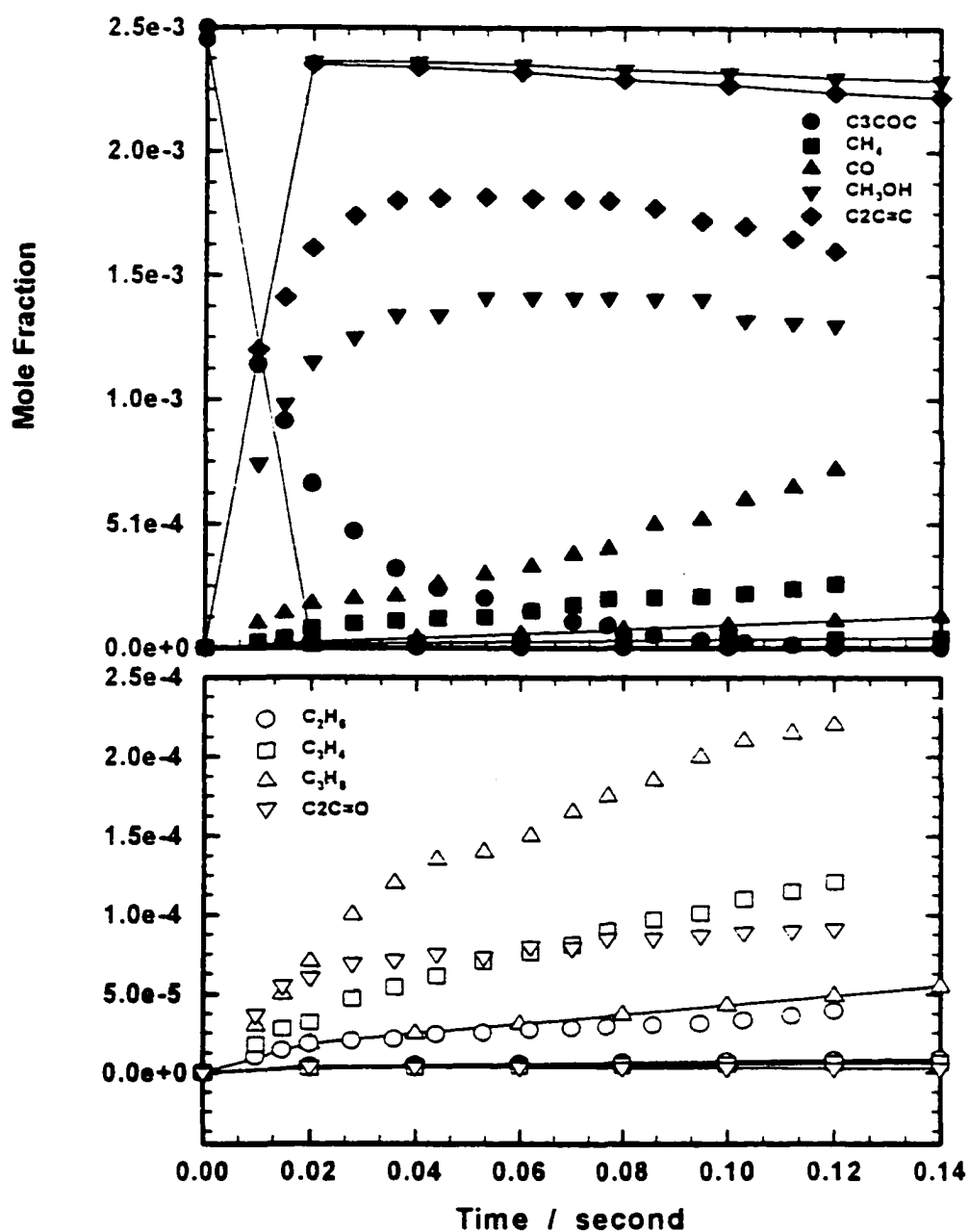
line is modeling result, symbols are experimental data

Figure IIC. 149 Comparison of experiment and modeling result
 $\phi = 1.0$, $P = 1 \text{ atm}$, $T = 923 \text{ K}$



line is modeling result, symbols are experimental data

Figure II.C. 150 Comparison of experiment and modeling result
Pyrolysis, $P = 1 \text{ atm}$, $T = 923 \text{ K}$



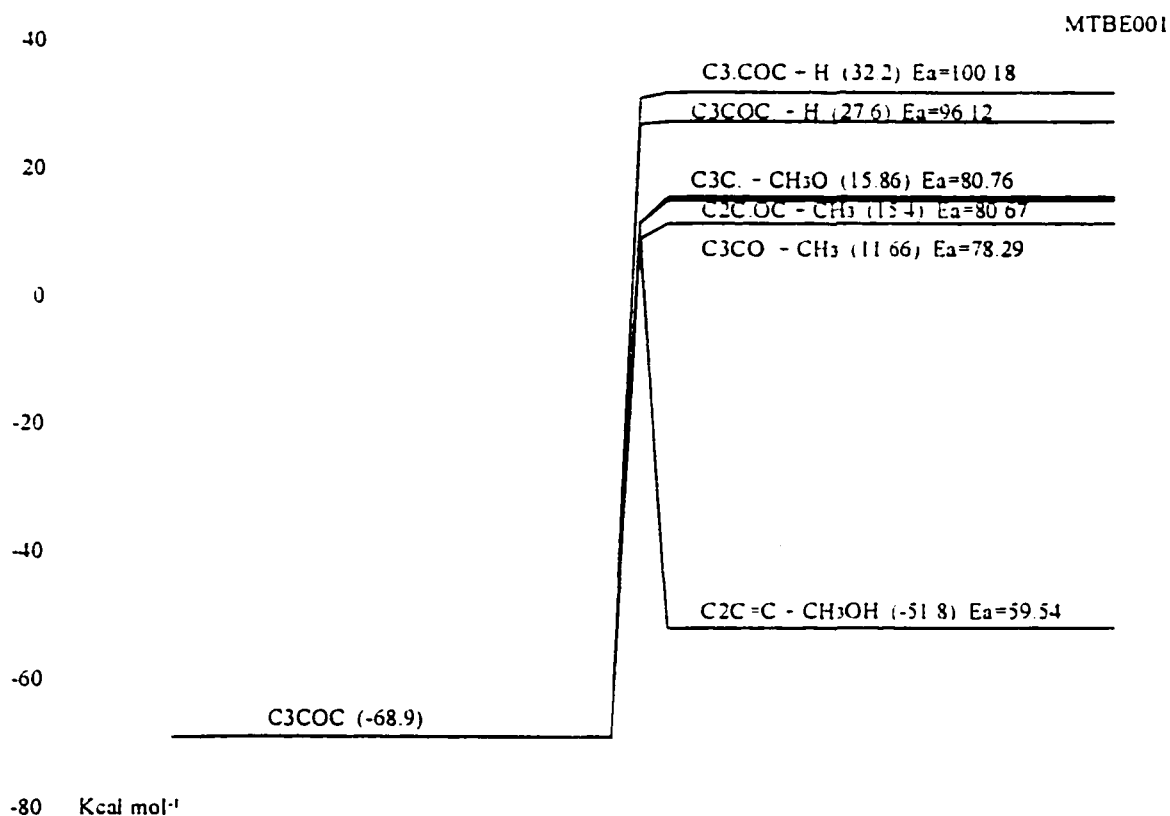
line is modeling result, symbols are experimental data

Figure IIC. 151 Comparison of experiment and modeling result
 $\phi = 0.96$, $P = 1$ atm, $T = 1028$ K

APPENDIX IID

QRRK INPUT PARAMETERS IN THE MTBE SYSTEM

IID. 1 MTBE → Products



Reaction		$A T^n e^{-\alpha T}$ (s ⁻¹)	E_a (kcal mol ⁻¹)
k ₁	C3COC → C2C=C + CH ₃ OH	$2.20 \times 10^{10} T^{1.22} e^{-0T}$	59.54
k ₂	C3COC → C3C. + CH ₃ O	$5.99 \times 10^{16} T^0 e^{-0T}$	80.76
k ₃	C3COC → C3CO. + CH ₃	$7.06 \times 10^{15} T^0 e^{-0T}$	78.29
k ₄	C3COC → C2C.OC + CH ₃	$3.70 \times 10^{21} T^{-1.81} e^{-0.00143T}$	80.67
k ₅	C3COC → C3.COC + H	$1.56 \times 10^{16} T^0 e^{-0T}$	100.18
k ₆	C3COC → C3COC. + H	$1.21 \times 10^{15} T^0 e^{-0T}$	96.12

frequency/degeneracy (CPFIT)

C3COC: 559.6 (21.177); 1680.8 (17.127); 3331.4 (7.196)

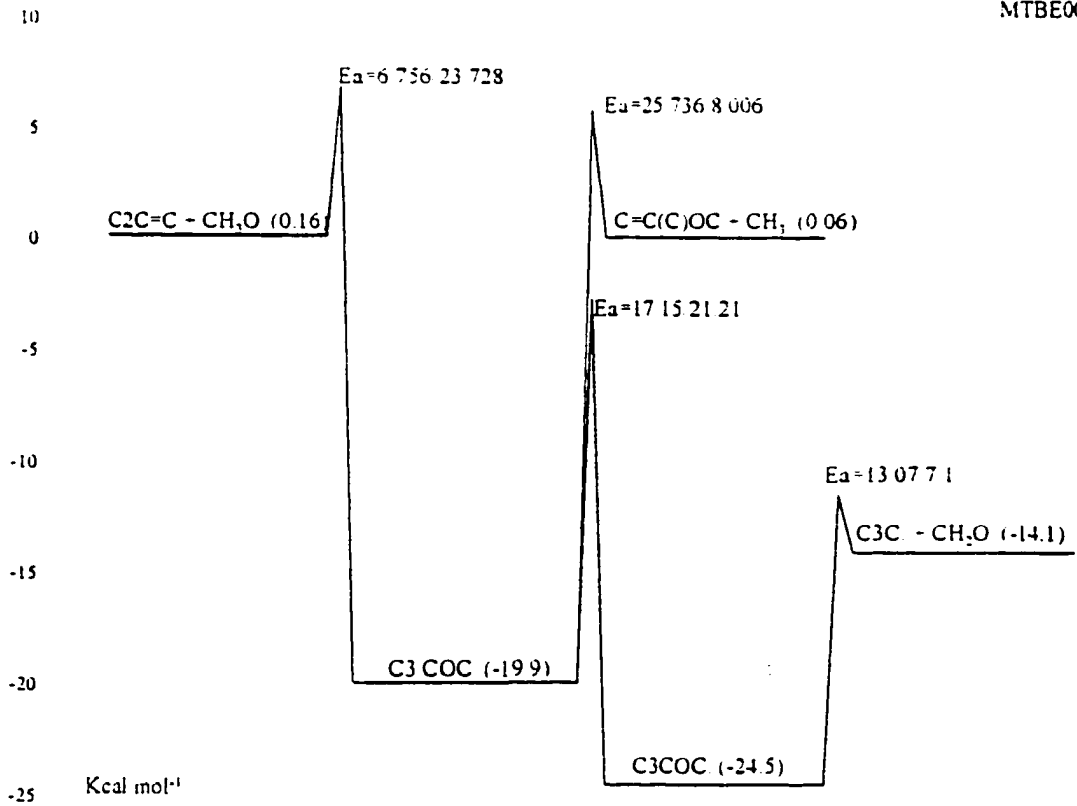
Lennard-Jones parameter

$\sigma(\text{\AA}) = 5.5471$, ϵ/k (K) = 584.86

- k_1 A_f is from AFACT2f thermodynamic analysis with thermodynamic properties calculated by MOPAC PM3, $E_{a,f}$ from NIST fit
- k_2 A_f via A_r and Microscopic Reversibility (MR), $A_r = 9.04 \times 10^{12}$, 90 TSA. $E_{a,f} = \Delta U_{\text{rxn}} = 80.76 \text{ kcal mol}^{-1}$.
- k_3 A_f via A_r and Microscopic Reversibility (MR), $A_r = 1.21 \times 10^{13}$, 86 TSA/HAM for $\text{CH}_3\text{O} + \text{CH}_3 \rightarrow \text{COC}$. $E_{a,f} = \Delta U_{\text{rxn}} = 78.29 \text{ kcal mol}^{-1}$.
- k_4 A_f via A_r and Microscopic Reversibility (MR), $A_r = 1.63 \times 10^{13} \text{ T}^{-0.596}$, 90 TSA for $\text{C3C} + \text{CH}_3 \rightarrow \text{neo-C5}$. $E_{a,f} = \Delta U_{\text{rxn}} = 80.67 \text{ kcal mol}^{-1}$.
- k_5 A_f via A_r and Microscopic Reversibility (MR), $A_r = 3.61 \times 10^{13}$, 90 TSA for $\text{C3C} + \text{H} \rightarrow \text{Prod.}$. $E_{a,f} = \Delta U_{\text{rxn}} = 100.18 \text{ kcal mol}^{-1}$.
- k_6 A_f via A_r and Microscopic Reversibility (MR), $A_r = 1.30 \times 10^{13}$, Bozzelli lecture note CCC. $+ \text{H} \rightarrow \text{CCC}$. $E_{a,f} = \Delta U_{\text{rxn}} = 96.12 \text{ kcal mol}^{-1}$.

IID. 2 C3.COC/C3COC. → Products

MTBE008



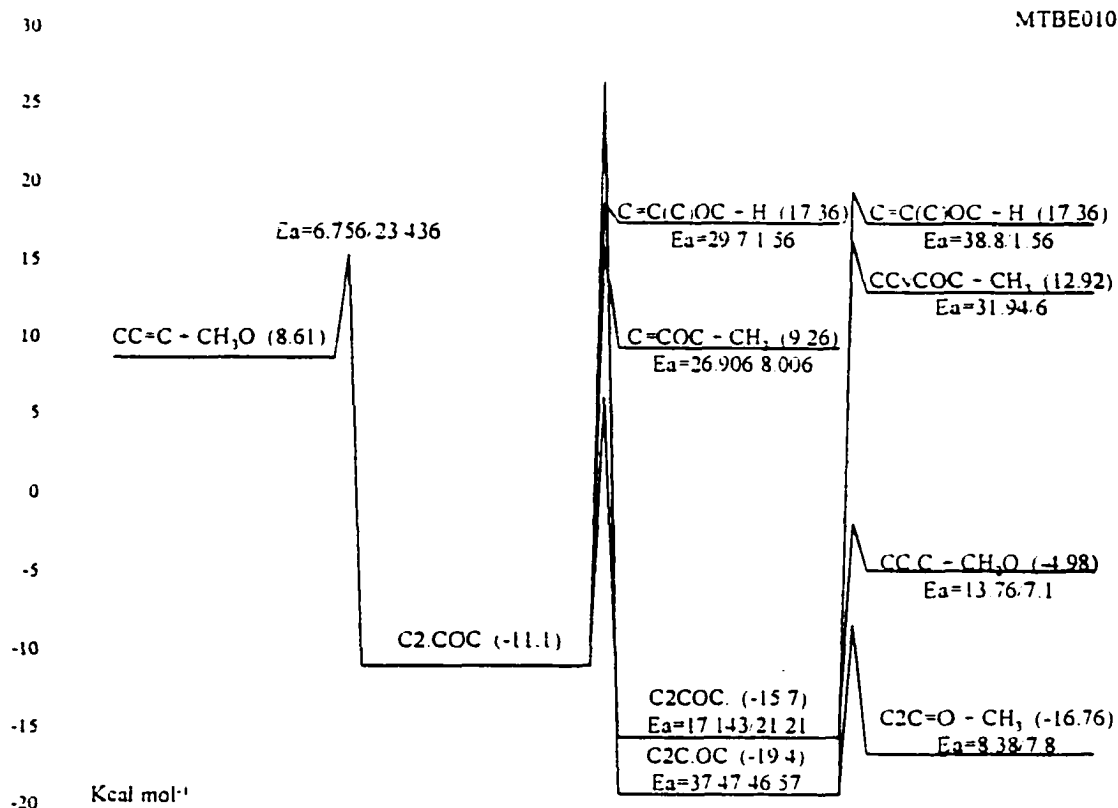
Reaction		$A T^n e^{-\alpha T}$ (s ⁻¹ or cm ³ mol ⁻¹ s ⁻¹)	E_a (kcal mol ⁻¹)
k_1	C2C=C + CH ₃ O → C3.COC	$1.21 \times 10^{11} T^0 e^{-0T}$	6.76
k_{-1}	C3.COC → C2C=C + CH ₃ O	$1.90 \times 10^{12} T^0 e^{-0T}$	23.73
k_2	C3.COC → C=C(C)OC + CH ₃	$1.48 \times 10^{13} T^0 e^{-0T}$	25.74
k_3	C3.COC → C3COC.	$1.44 \times 10^6 T^{1.78} e^{-0.00035T}$	17.15
k_{-3}	C3COC. → C3.COC	$7.72 \times 10^8 T^{1.0} e^{-0T}$	21.21
k_4	C3COC. → C3C. + CH ₂ O	$3.12 \times 10^{12} T^0 e^{-0T}$	13.07

frequency/degeneracy (CPFIT)
C3.COC: 560.0 (20.916); 1815.8 (16.374); 3598.5 (5.200)
C3COC.: 552.0 (21.562); 1791.0 (15.756); 3590.0 (5.182)
Lennard-Jones parameter
 $\sigma(\text{\AA}) = 5.54$, $\epsilon/k \text{ (K)} = 584.86$

k_1 taken from 86 TSA/HAM for CH₃O + C=C → Prod.

- k_1 A_r via A_f and Microscopic Reversibility (MR) $E_{a,r} = E_{a,f} - \Delta U_{rxn}$, $\Delta U_{rxn} = -16.97$ kcal mol⁻¹
- k_2 A_f via A_r and Microscopic Reversibility (MR), $A_r = 9.64 \times 10^{10}$, 91 TSA for $C_3H_6 + CH_3 \rightarrow C3.C$. $E_{a,f} = E_{a,r} + \Delta U_{rxn}$, $\Delta U_{rxn} = 17.73$ kcal mol⁻¹. $E_{a,r} = 8.006$ kcal mol⁻¹. (referenced as the same as the A_r).
- k_3 A_f via A_r and Microscopic Reversibility (MR), $E_{a,f} = E_{a,r} + \Delta U_{rxn}$, $\Delta U_{rxn} = 4.06$ kcal mol⁻¹
- k_3 A_r estimated using TST, $A = (\text{deg.}) (ek_B/h) T^n \exp(\Delta S^\ddagger(T)/R)$, $\text{deg.} = 9$, $ek_B/h = 5.66 \times 10^{10}$, $n = 1.0$, $\Delta S^\ddagger(T)$ is estimated as loss of three rotors (-4.3×3 cal mol⁻¹ K⁻¹). $E_{a,f} = RS(6) + E_{abst}(11.15) + \Delta U_{rxn}(4.06)$ kcal mol⁻¹.
- k_4 A_f via A_r and Microscopic Reversibility (MR), $A_r = 2.82 \times 10^{10}$, 72 KER for $C3C. + C=C \rightarrow C3CCC.$. $E_{a,f} = E_{a,r} + \Delta U_{rxn}$, $\Delta U_{rxn} = 5.97$ kcal mol⁻¹. $E_{a,r} = 7.10$ kcal mol⁻¹. (referenced as the same as the A_r).

IID. 3 C2.COC → Products



Reaction		$A T^n e^{-u/T}$ (s ⁻¹ or cm ³ mol ⁻¹ s ⁻¹)	E_a (kcal mol ⁻¹)
k ₁	CC=C + CH ₃ O → C2.COC	$1.21 \times 10^{11} T^0 e^{-0/T}$	6.76
k ₋₁	C2.COC → CC=C + CH ₃ O	$1.50 \times 10^{12} T^0 e^{-0/T}$	23.36
k ₂	C2.COC → C=C(C)OC + H	$2.28 \times 10^{12} T^0 e^{-0/T}$	31.05
k ₃	C2.COC → C=COC + CH ₃	$3.42 \times 10^{12} T^0 e^{-0/T}$	26.91
k ₄	C2.COC → C2COC.	$2.74 \times 10^6 T^{1.79} e^{-0.00037T}$	17.14
k ₋₄	C2COC. → C2.COC	$5.15 \times 10^8 T^{1.0} e^{-0/T}$	21.21
k ₅	C2COC. → CC ₂ COC + CH ₃	$4.68 \times 10^{11} T^0 e^{-0/T}$	31.94
k ₆	C2COC. → CC ₂ C + CH ₂ O	$7.88 \times 10^{11} T^0 e^{-0/T}$	13.76
k ₇	C2.COC → C2C.OC	$3.49 \times 10^{12} T^{-0.04} e^{-0.0004T}$	37.47
k ₋₇	C2C.OC → C2.COC	$3.90 \times 10^{10} T^{1.0} e^{-0/T}$	46.57
k ₈	C2C.OC → C2C=O + CH ₃	$6.71 \times 10^{12} T^0 e^{-0/T}$	8.38
k ₉	C2C.OC → C=C(C)OC + H	$2.92 \times 10^{13} T^0 e^{-0/T}$	38.80

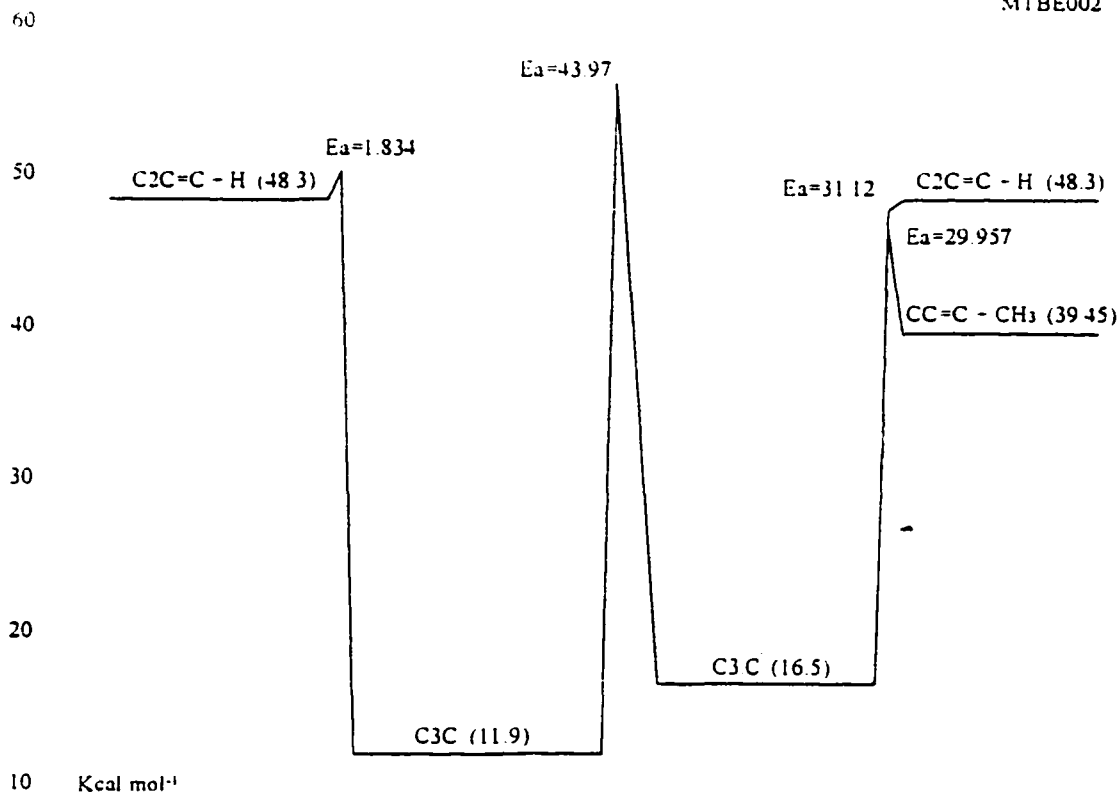
frequency/degeneracy (CPFIT)
 C2.COC: 518.9 (14.066); 1404.9 (10.574); 2806.5 (9.36)

C2COC.. 525 2 (15 353); 1474 1 (10.557); 2908 5 (8 09)
 C2C OC 516 8 (13 691); 1614 9 (12.169); 2927 8 (8.141)
 Lennard-Jones parameter
 $\sigma(\text{\AA}) = 5.20$, $\epsilon/k(\text{K}) = 533.08$

- k_1 taken from 86 TSA/HAM for $\text{CH}_3\text{O} + \text{C}=\text{C} \rightarrow \text{Prod.}$
- k_{-1} A_r via A_f and Microscopic Reversibility (MR), $E_{a,r} = E_{a,f} - \Delta U_{\text{rxn}} (-16.60) \text{ kcal mol}^{-1}$.
- k_2 A_f via A_r and Microscopic Reversibility (MR), $A_r = 7.23 \times 10^{12} = 1/2 (\text{H} + \text{CC}=\text{C} \rightarrow \text{CCC.})$, 91 TSA/HAM, $E_{a,f} = E_{a,r} (2.906) + \Delta U_{\text{rxn}} (28.14) \text{ kcal mol}^{-1}$.
- k_3 A_f via A_r and Microscopic Reversibility (MR), $A_r = 9.64 \times 10^{10}$, 91 TSA for $\text{C}_3\text{H}_6 + \text{CH}_3 \rightarrow \text{C3.C.}$ $E_{a,f} = E_{a,r} (8.006) + \Delta U_{\text{rxn}} (18.90) \text{ kcal mol}^{-1}$.
- k_4 A_f via A_r and Microscopic Reversibility (MR), $E_{a,f} = E_{a,r} + \Delta U_{\text{rxn}} (4.07) \text{ kcal mol}^{-1}$.
- k_{-4} A_r estimated using TST, $A = (\text{deg.}) (ek_b/h) T^n \exp(\Delta S^\ddagger(T)/R)$, $\text{deg.} = 6$, $ek_b/h = 5.66 \times 10^{10}$, $n = 1.0$, $\Delta S^\ddagger(T)$ is estimated as loss of three rotors $(-4.3 \times 3 \text{ cal mol}^{-1} \text{ K}^{-1})$. $E_{a,f} = \text{RS} (6) + E_{\text{abst}} (11.14) + \Delta H_{\text{rxn}} (4.07) \text{ kcal mol}^{-1}$.
- k_5 A_f estimated using TST, $A = (\text{deg.}) (ek_b T/h) \exp(\Delta S^\ddagger(T)/R)$, $\text{deg.} = 1$, $ek_b T/h = 10^{13.55} ?$, $\Delta S^\ddagger(T)$ is estimated as loss of two rotors $(-4.3 \times 2 \text{ cal mol}^{-1} \text{ K}^{-1})$. $E_{a,f} = E_{a,r} + \Delta U_{\text{rxn}} (25.94) \text{ kcal mol}^{-1}$. $E_{a,r} = 6.0 \text{ kcal mol}^{-1}$ (estimated by Bozzelli).
- k_6 A_f via A_r and Microscopic Reversibility (MR), $A_r = 2.82 \times 10^{10}$, 72 KER for $\text{C3C.} + \text{C}=\text{C} \rightarrow \text{C3CCC.}$ $E_{a,f} = E_{a,r} (7.10) + \Delta U_{\text{rxn}} (6.66) \text{ kcal mol}^{-1}$.
- k_7 A_f via A_r and Microscopic Reversibility (MR), $E_{a,f} = E_{a,r} + \Delta U_{\text{rxn}} (9.10) \text{ kcal mol}^{-1}$.
- k_{-7} A_r estimated using TST, $A = (\text{deg.}) (ek_b/h) T^n \exp(\Delta S^\ddagger(T)/R)$, $\text{deg.} = 6$, $ek_b/h = 5.66 \times 10^{10}$, $n = 1.0$, $\Delta S^\ddagger(T)$ is estimated as loss of one rotor $(-4.3 \text{ cal mol}^{-1} \text{ K}^{-1})$. $E_{a,f} = \text{RS} (28) + E_{\text{abst}} (9.47) + \Delta H_{\text{rxn}} (9.10) \text{ kcal mol}^{-1}$.
- k_8 A_f via A_r and Microscopic Reversibility (MR), $A_r = 1.69 \times 10^{11}$, 91 TSA for $\text{CH}_3 + \text{CC}=\text{C} \rightarrow \text{CC.CC.}$ $E_{a,f} = E_{a,r} + \Delta U_{\text{rxn}} (0.58) \text{ kcal mol}^{-1}$. $E_{a,r} = 7.8 \text{ kcal mol}^{-1}$ (estimated by Bozzelli).
- k_9 A_f via A_r and Microscopic Reversibility (MR), $A_r = 6.50 \times 10^{12} = 1/2 (\text{H} + \text{CC}=\text{C} \rightarrow \text{CC.C.})$, 91 TSA/HAM. $E_{a,f} = E_{a,r} (1.56) + \Delta U_{\text{rxn}} (37.24) \text{ kcal mol}^{-1}$.

IID. 4 C3C./C3.C → Products

MTBE002



Reaction		$A T^n e^{-aT}$ (s ⁻¹ or cm ³ mol ⁻¹ s ⁻¹)	E_a (kcal mol ⁻¹)
k_1	$C2C=C + H \rightarrow C3C.$	$6.15 \times 10^9 T^{1.33} e^{-0T}$	2.33
k_{-1}	$C3C. \rightarrow C2C=C + H$	$2.01 \times 10^{11} T^{-0.58} e^{-0.00008T}$	38.15
k_2	$C3C. \rightarrow C3.C$	$5.85 \times 10^{10} T^{1.0} e^{-0T}$	43.97
k_{-2}	$C3.C \rightarrow C3C.$	$1.70 \times 10^{12} T^{-0.21} e^{-0.00029T}$	38.77
k_3	$C3.C \rightarrow CC=C + CH_3$	$2.00 \times 10^{13} T^0 e^{-0T}$	29.98
k_4	$C3.C \rightarrow C2C=C + H$	$2.86 \times 10^{10} T^0 e^{-0T}$	31.12

frequency/degeneracy (CPFIT)

C3C.: 250.0 (6.593); 1226.0 (14.014); 2721.0 (10.893)

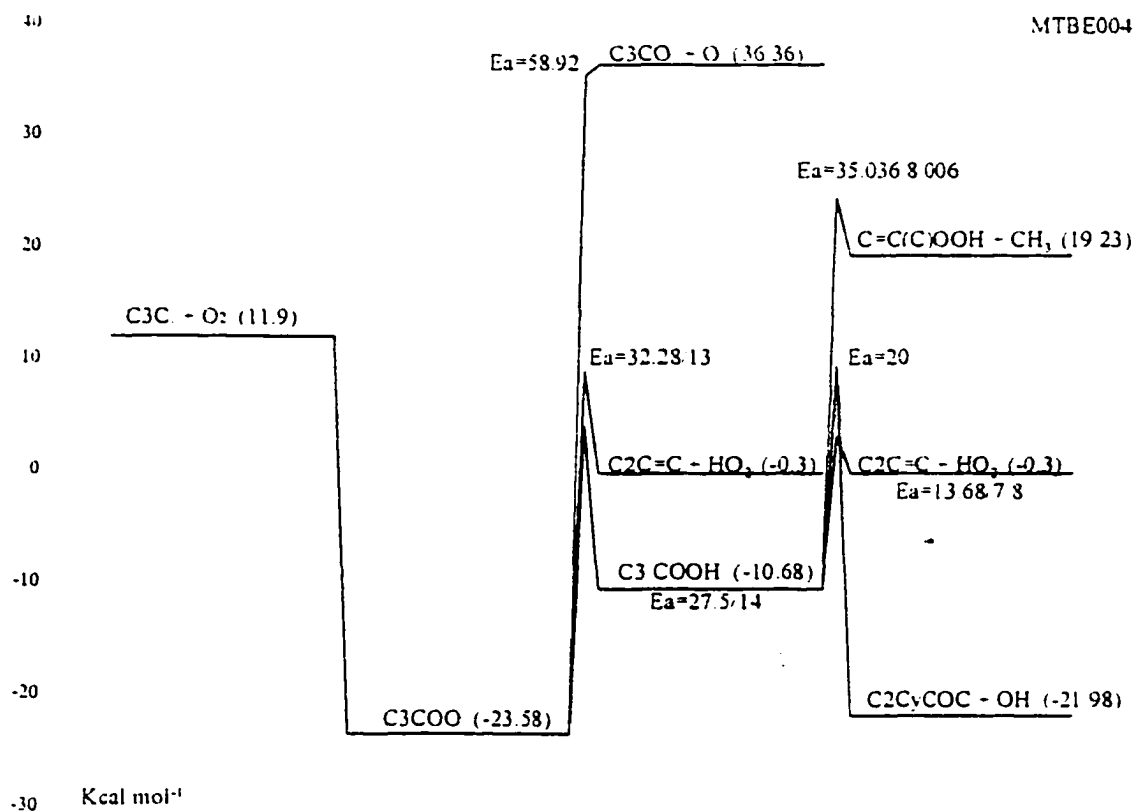
C3.C: 250.0 (5.631); 1074.1 (14.902); 2708.2 (10.968)

Lennard-Jones parameter

 $\sigma(\text{\AA}) = 5.18$, $\epsilon/k(\text{K}) = 357.0$ k_1 A_f from AFACT2f thermodynamic analysis with thermodynamic properties from

chiungchu, $E_{a,f}$ from 90 TSA.

- k₁ A_r via A_r and Microscopic Reversibility (MR), $E_{a,f} = E_{a,f} - \Delta U_{\text{rot}}$ (35.82) kcal mol⁻¹.
- k₂ A_r estimated using TST, $A = (\text{deg.}) (ek_B/h) \exp(\Delta S^\ddagger(T)/R) T^n$, deg. = 9, $ek_B/h = 5.66 \times 10^{10}$, $n = 1.0$, $\Delta S^\ddagger(T)$ is estimated as loss of one rotor (-4.3 cal mol⁻¹ K⁻¹).
 $E_{a,f} = RS(28) + E_{\text{abst}}(10.77) + \Delta H_{\text{rot}}(5.2)$ kcal mol⁻¹.
- k₂ A_r via A_r and Microscopic Reversibility (MR), $E_{a,f} = E_{a,f} - \Delta U_{\text{rot}}$, $\Delta U_{\text{rot}} = 5.2$ kcal mol⁻¹.
- k₃ 90 TSA
- k₄ A_r via A_r and Microscopic Reversibility (MR), $A_r = 1.26 \times 10^{11} T^0$, 72 KER. $E_{a,f} = \Delta U_{\text{rot}} = 31.12$ kcal mol⁻¹.

IID. 5 C3C. + O₂ → Products

Reaction	$A T^n e^{-\alpha T}$ (s ⁻¹ or cm ³ mol ⁻¹ s ⁻¹)	E_a (kcal mol ⁻¹)
k_1 C3C. + O ₂ → C3COO.	$1.81 \times 10^{12} T^0 e^{-0T}$	0.00
k_{-1} C3COO. → C3C. + O ₂	$2.03 \times 10^{15} T^0 e^{-0T}$	32.26
k_2 C3COO. → C3CO. + O	$5.82 \times 10^{15} T^0 e^{-0T}$	58.92
k_3 C3COO. → C2C=C + HO ₂	$2.59 \times 10^{11} T^{1.22} e^{-0T}$	32.28
k_4 C3COO. → C3.COOH	$6.77 \times 10^{10} T^{1.22} e^{-0T}$	27.50
k_{-4} C3.COOH → C3COO.	$1.10 \times 10^{12} T^{-0.09} e^{-0.00087T}$	14.00
k_5 C3.COOH → C2CyCOC + OH	$1.38 \times 10^{12} T^{-0.03} e^{-0T}$	20.00
k_6 C3.COOH → C2C=C + HO ₂	$1.06 \times 10^{13} T^{-0.03} e^{-0T}$	13.68
k_7 C3.COOH → C=C(C)OOH + CH ₃	$4.33 \times 10^{13} T^0 e^{-0T}$	35.04

frequency/degeneracy (CPFIT)

C3COO.: 250.4 (9.685); 1072.1 (16.487); 2880.5 (10.829)

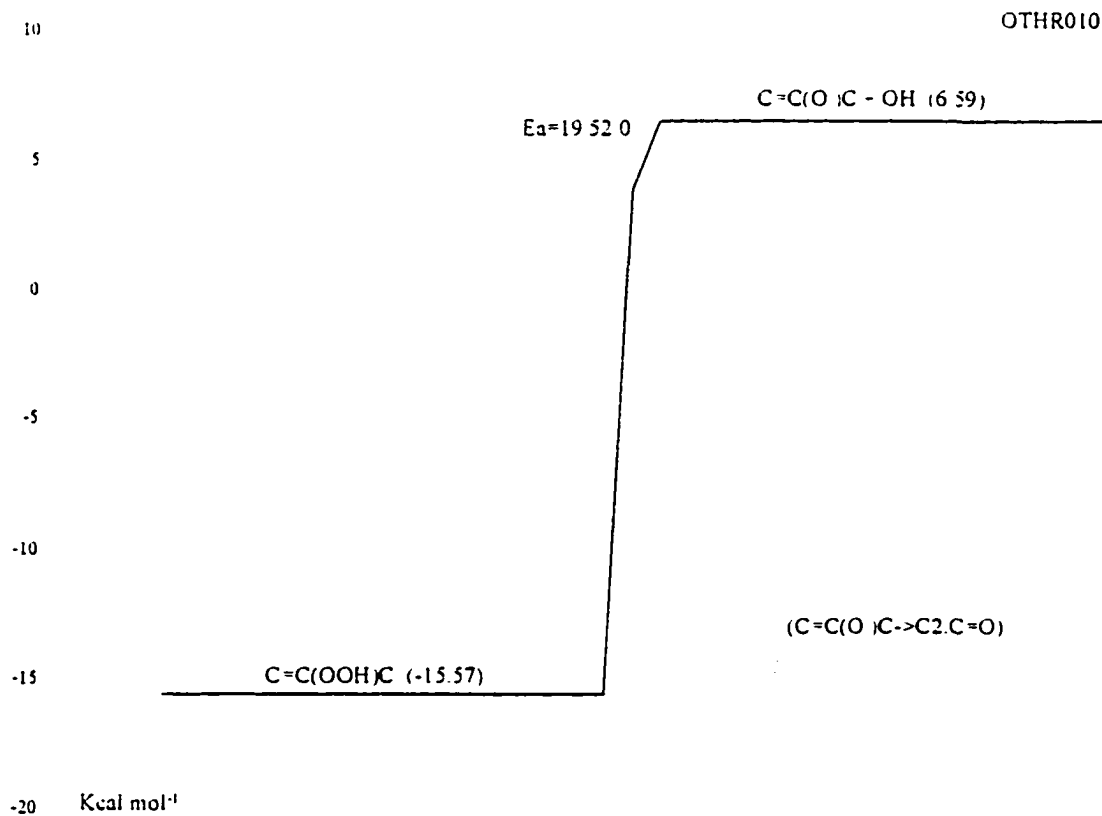
C3.COOH: 251.5 (10.679); 1084.5 (16.339); 2872.0 (9.482)

Lennard-Jones parameter

$\sigma(\text{\AA}) = 5.54$, $\epsilon/k(\text{K}) = 584.86.0$

- k_1 92 WAL/AND, for $C_3C. + O_2$.
- k_{-1} A_r via A_f and Microscopic Reversibility (MR), $E_{a,r} = E_{a,f} - \Delta U_{rxn}$, $\Delta U_{rxn} = 32.26 \text{ kcal mol}^{-1}$.
- k_2 A_f via A_r and Microscopic Reversibility (MR), $A_r = 1.51 \times 10^{13}$, 92 BAU/COB for $O + CH_3O \rightarrow \text{Prod.}$, $E_{a,f} = \Delta U_{rxn} = 58.92 \text{ kcal mol}^{-1}$.
- k_3 A_f estimated using TST, $A = (\text{deg.}) A' T^n$, $\text{deg.} = 9$, $A' = 2.876 \times 10^{10}$, $n = 1.22$, A' and n are from thermal reaction analysis (AFACT2f) based on the thermodynamic properties calculated from MOPAC PM3 (corrected with internal rotor, electronic spin and optical isomer). $E_{a,f}$ via $E_{a,r}$, $+ \Delta U_{rxn}$, $E_{a,r}$ is estimated as 13 kcal mol^{-1} in this study, $\Delta U_{rxn} = 19.38 \text{ kcal mol}^{-1}$.
- k_4 A_f estimated using TST, $A = (\text{deg.}) A' T^n$, $\text{deg.} = 6$, $A' = 3.836 \times 10^9$, $n = 1.071$, A' and n are from thermal reaction analysis (AFACT2f) based on the thermodynamic properties calculated from MOPAC PM3 (corrected with internal rotor, electronic spin and optical isomer). $E_{a,f} = RS(6) + E_{aba}(8.0) + \Delta H_{rxn}(13.50) \text{ kcal mol}^{-1}$.
- k_{-4} A_r via A_f and Microscopic Reversibility (MR), $E_{a,r} = E_{a,f} - \Delta U_{rxn}$, $\Delta U_{rxn} = 13.50 \text{ kcal mol}^{-1}$.
- k_5 A_f estimated using TST, $A = (\text{deg.}) A' T^n$, $\text{deg.} = 1$, $A' = 1.384 \times 10^{12}$, $n = -0.031$, A' and n are from thermal reaction analysis (AFACT2f) based on the thermodynamic properties calculated from MOPAC PM3 (corrected with internal rotor, electronic spin and optical isomer). $E_{a,f}$ via $E_{a,r} + \Delta U_{rxn}$, $E_{a,r}$ is estimated in this study.
- k_6 A_f estimated using TST, $A = (\text{deg.}) A' T^n$, $\text{deg.} = 1$, $A' = 1.063 \times 10^{13}$, $n = -0.027$, A' and n are from thermal reaction analysis (AFACT2f) based on the thermodynamic properties calculated from MOPAC PM3 (corrected with internal rotor, electronic spin and optical isomer). $E_{a,f}$ via $E_{a,r} + \Delta U_{rxn}$, $E_{a,r} = 7.8 \text{ kcal mol}^{-1}$. (Bozzelli), $\Delta U_{rxn} = 5.88 \text{ kcal mol}^{-1}$.
- k_7 A_f via A_r and Microscopic Reversibility (MR), $A_r = 9.64 \times 10^{10}$, 91 TSA for $C_3H_6 + CH_3 \rightarrow C_3C.$, $E_{a,f} = E_{a,r} + \Delta U_{rxn}$, $\Delta U_{rxn} = 35.036 \text{ kcal mol}^{-1}$. $E_{a,r} = 8.006 \text{ kcal mol}^{-1}$. (referenced as the same as the A_r).

IID. 6 $\text{C}=\text{C}(\text{OOH})\text{C} \rightarrow \text{C}_2\text{C}=\text{O} (\text{C}=\text{C}(\text{O.})\text{C}) + \text{OH}$



	Reaction	$A T^n e^{-\alpha T}$	E_a
		(s ⁻¹ or cm ³ mol ⁻¹ s ⁻¹)	(kcal mol ⁻¹)
k ₁	$\text{C}=\text{C}(\text{OOH})\text{C} \rightarrow (\text{C}=\text{C}(\text{O.})\text{C}) + \text{OH}$	$5.98 \times 10^{14} T^0 e^{-0T}$	19.52

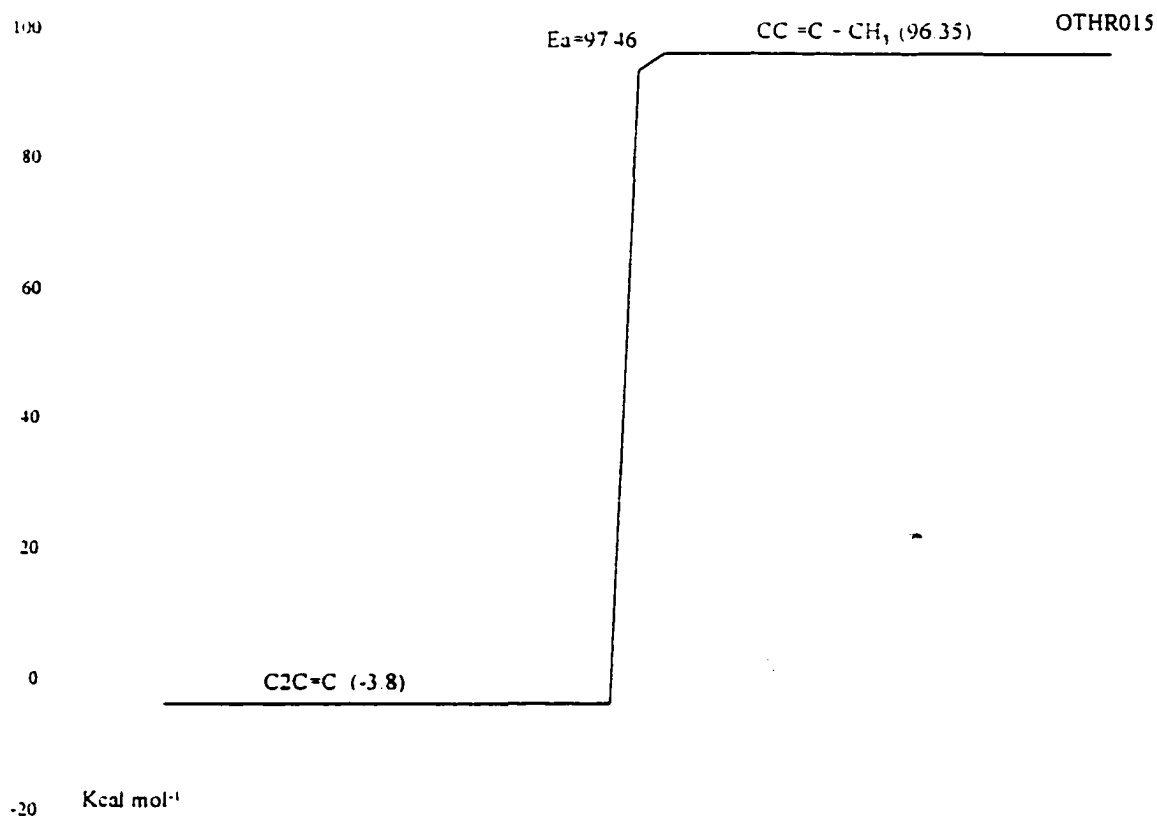
frequency/degeneracy (CPFIT)

$\text{C}=\text{C}(\text{OOH})\text{C}$: 526.0 (12.851); 1827.0 (10.334); 4000.0 (2.315)

Lennard-Jones parameter

$\sigma(\text{\AA}) = 5.20$, $\epsilon/k (\text{K}) = 533.08$

k₁ A_f via A_r and Microscopic Reversibility (MR), A_r = 1.51×10^{13} , 91 TSA for $\text{C}=\text{CC} + \text{OH}$. E_{a,f} = $\Delta U_{\text{rxn}} = 19.52 \text{ kcal mol}^{-1}$.

IID. 7 $\text{C}_2\text{C}=\text{C} \rightarrow \text{CC}=\text{C} + \text{CH}_3$ 

	Reaction	$A T^n e^{-\alpha T}$ (s^{-1})	E_a (kcal mol^{-1})
k_1	$\text{C}_2\text{C}=\text{C} \rightarrow \text{CC}=\text{C} + \text{CH}_3$	$1.93 \times 10^{17} T^0 e^{-0T}$	97.46

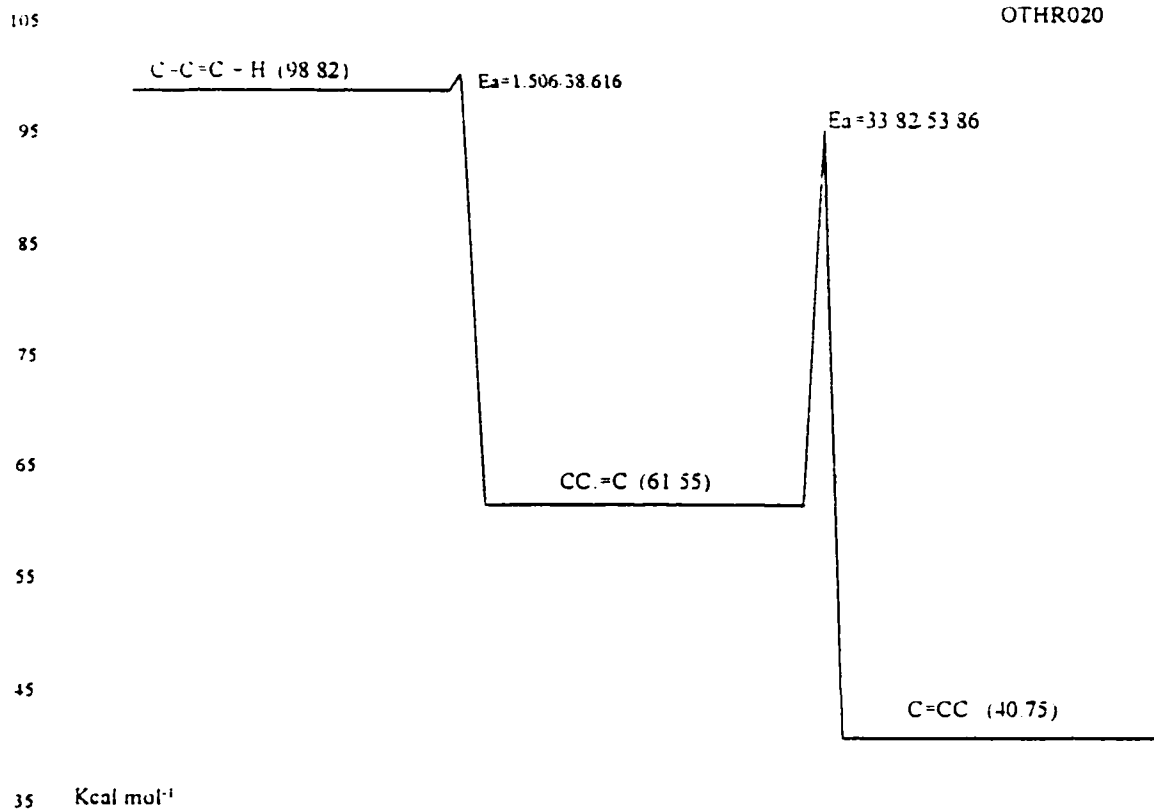
frequency/degeneracy (CPFIT)

 $\text{C}_2\text{C}=\text{C}$: 435.4 (8.508); 1327.6 (12.429); 2967.5 (8.063)

Lennard-Jones parameter

 $\sigma(\text{\AA}) = 5.18$, $\epsilon/k(\text{K}) = 407.0$

k_1 A_f via A_r and Microscopic Reversibility (MR), $A_r = 3.61 \times 10^{13}$, 92 BAU/COB for $\text{CH}_3 + \text{CH}_3 \rightarrow \text{C}_2\text{H}_6$. $E_{a,f} = \Delta U_{\text{rxn}} = 97.46 \text{ kcal mol}^{-1}$.

IID. 8 $\text{CC}=\text{C} \rightarrow \text{Products}$ 

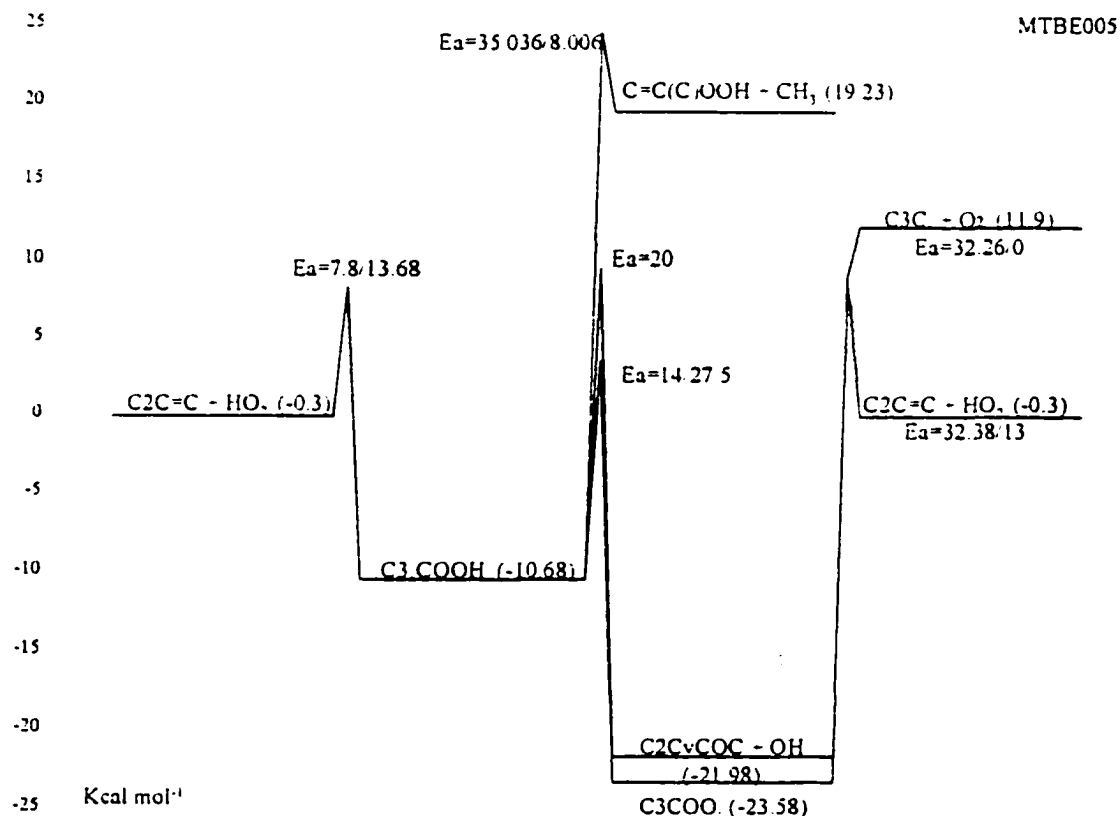
Reaction		$A T^n e^{-\alpha T}$ (s ⁻¹ or cm ³ mol ⁻¹ s ⁻¹)	E_a (kcal mol ⁻¹)
k_1	$\text{C}=\text{C}=\text{C} + \text{H} \rightarrow \text{CC}=\text{C}$	$1.00 \times 10^{13} T^0 e^{-0T}$	1.506
k_{-1}	$\text{CC}=\text{C} \rightarrow \text{C}=\text{C}=\text{C} + \text{H}$	$4.46 \times 10^{12} T^0 e^{-0T}$	38.62
k_2	$\text{CC}=\text{C} \rightarrow \text{C}=\text{CC}.$	$1.95 \times 10^{10} T^{1.0} e^{-0T}$	33.82

frequency/degeneracy (CPFIT)
 $\text{C}=\text{C}.\text{C}:$ 473.2 (4.836); 1413.1 (7.638); 3019.1 (5.025)
 Lennard-Jones parameter
 $\sigma(\text{\AA}) = 4.57, \epsilon/k (\text{K}) = 307.60$

- k_1 $A_f = 1.00 \times 10^{13}$, 84 WAR for $\text{C}=\text{C} + \text{H}$. $E_{a,f} = 1.506 \text{ kcal mol}^{-1}$ taken from the same reference.
- k_{-1} A_r via A_f and Microscopic Reversibility (MR), $E_{a,r} = E_{a,f} - \Delta U_{\text{rxn}}$, $\Delta U_{\text{rxn}} = -37.11 \text{ kcal mol}^{-1}$.

k_2 A_r estimated using TST, $A = (\text{deg.}) (ek_B/h) T^n \exp(\Delta S^\ddagger(T)/R)$, $\text{deg.} = 3$, $ek_B/h = 5.66 \times 10^{10}$, $n = 1.0$, $\Delta S^\ddagger(T)$ is estimated as loss of one rotor ($-4.3 \text{ cal mol}^{-1} \text{ K}^{-1}$).
 $E_{a,f} = RS(28) + E_{a,bst}(13.82) \text{ kcal mol}^{-1}$.

IID. 9 $C_2C=C + HO_2 \rightarrow [C_3.COOH]^* \rightarrow \text{Products}$



Reaction	$A T^n e^{-a/T}$ (s ⁻¹ or cm ³ mol ⁻¹ s ⁻¹)	E_a (kcal mol ⁻¹)
$k_1 \quad C_2C=C + HO_2 \rightarrow C_3.COOH$	$7.43 \times 10^0 T^{3.87} e^{0.00068T}$	7.80
$k_{-1} \quad C_3.COOH \rightarrow C_2C=C + HO_2$	$1.06 \times 10^{13} T^{-0.03} e^{-0T}$	13.68
$k_2 \quad C_3.COOH \rightarrow C_2C=COC + OH$	$1.38 \times 10^{12} T^{-0.03} e^{-0T}$	20.00
$k_3 \quad C_3.COOH \rightarrow C=C(C)OOH + CH_3$	$4.33 \times 10^{13} T^0 e^{-0T}$	35.04
$k_4 \quad C_3.COOH \rightarrow C_3COO$	$1.10 \times 10^{12} T^{-0.09} e^{-0.00087T}$	14.00
$k_{-4} \quad C_3COO \rightarrow C_3.COOH$	$6.77 \times 10^{10} T^{1.22} e^{-0T}$	27.50
$k_5 \quad C_3COO \rightarrow C_2C=C + HO_2$	$2.59 \times 10^{11} T^{1.22} e^{-0T}$	32.28
$k_6 \quad C_3COO \rightarrow C_3C + O_2$	$2.03 \times 10^{15} T^0 e^{-0T}$	32.26

frequency/degeneracy (CPFIT)

$C_3.COOH$: 251.5 (10.679); 1084.5 (16.339); 2872.0 (9.482)

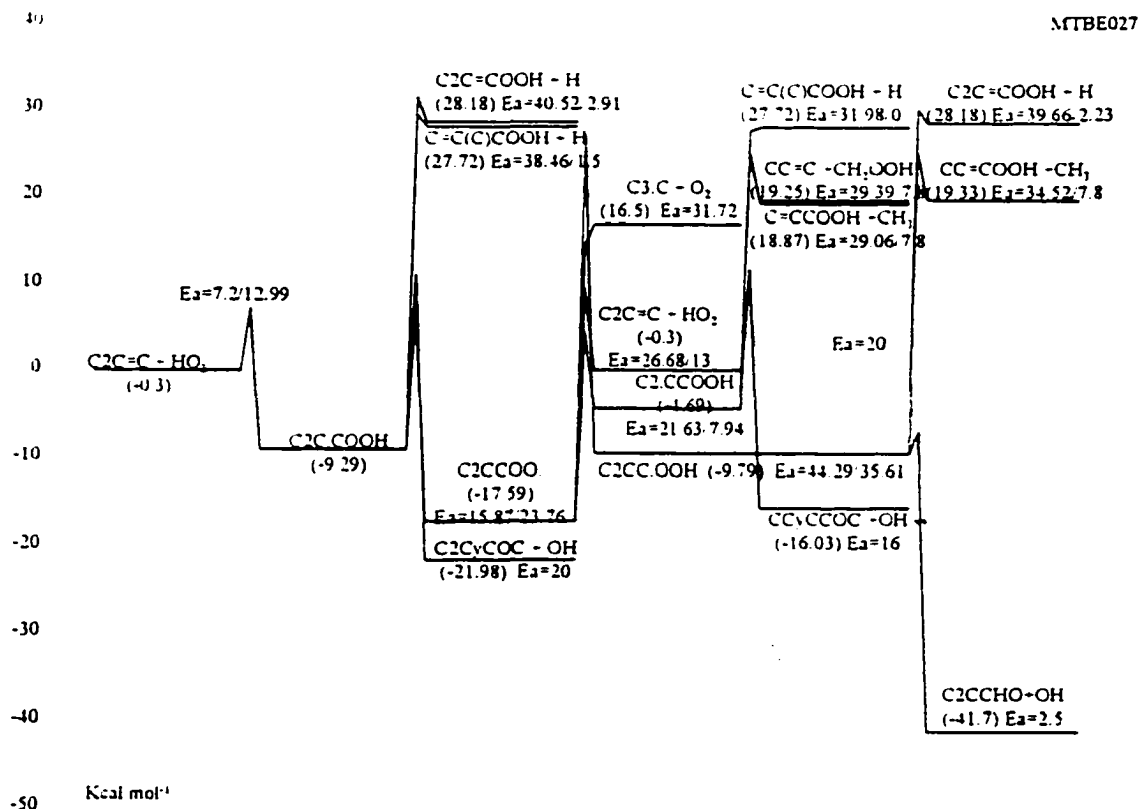
C_3COO : 250.4 (9.685); 1072.1 (16.487); 2880.5 (10.829)

Lennard-Jones parameter

$\sigma(\text{\AA}) = 5.54$, $\epsilon/k(\text{K}) = 584.86.0$

- k_1 A_f via A_r and Microscopic Reversibility (MR), $E_{a,f} = 7.8 \text{ kcal mol}^{-1}$ (Bozzelli).
- k_{-1} A_r estimated using TST, $A = (\text{deg.}) A' T^n$, $\text{deg.} = 1$, $A' = 1.063 \times 10^{13}$, $n = -0.027$, A' and n are from thermal reaction analysis (AFACT2f) based on the thermodynamic properties calculated from MOPAC PM3 (corrected with internal rotor, electronic spin and optical isomer). $E_{a,r}$ via $E_{a,f} - \Delta U_{\text{rxn}}$, $E_{a,f} = 7.8 \text{ kcal mol}^{-1}$ (Bozzelli), $\Delta U_{\text{rxn}} = 5.88 \text{ kcal mol}^{-1}$.
- k_2 A_f estimated using TST, $A = (\text{deg.}) A' T^n$, $\text{deg.} = 1$, $A' = 1.384 \times 10^{12}$, $n = -0.031$, A' and n are from thermal reaction analysis (AFACT2f) based on the thermodynamic properties calculated from MOPAC PM3 (corrected with internal rotor, electronic spin and optical isomer). $E_{a,f}$ via $E_{a,r} + \Delta U_{\text{rxn}}$, $E_{a,r}$ is estimated in this study.
- k_3 A_f via A_r and Microscopic Reversibility (MR), $A_r = 9.64 \times 10^{10}$, 91 TSA for $\text{C}_3\text{H}_6 + \text{CH}_3 \rightarrow \text{C}_3\text{C}$. $E_{a,f} = E_{a,r} + \Delta U_{\text{rxn}}$, $\Delta U_{\text{rxn}} = 35.036 \text{ kcal mol}^{-1}$. $E_{a,r} = 8.006 \text{ kcal mol}^{-1}$ (referenced as the same as the A_r).
- k_4 A_f via A_r and Microscopic Reversibility (MR), $E_{a,f} = E_{a,r} - \Delta U_{\text{rxn}}$, $\Delta U_{\text{rxn}} = 13.50 \text{ kcal mol}^{-1}$.
- k_{-4} A_r estimated using TST, $A = (\text{deg.}) A' T^n$, $\text{deg.} = 6$, $A' = 3.836 \times 10^9$, $n = 1.071$, A' and n are from thermal reaction analysis (AFACT2f) based on the thermodynamic properties calculated from MOPAC PM3 (corrected with internal rotor, electronic spin and optical isomer). $E_{a,r} = \text{RS (6)} + E_{\text{abs}} (8.0) + \Delta H_{\text{rxn}} (13.50) \text{ kcal mol}^{-1}$.
- k_5 A_f estimated using TST, $A = (\text{deg.}) A' T^n$, $\text{deg.} = 9$, $A' = 2.876 \times 10^{10}$, $n = 1.22$, A' and n are from thermal reaction analysis (AFACT2f) based on the thermodynamic properties calculated from MOPAC PM3 (corrected with internal rotor, electronic spin and optical isomer). $E_{a,f}$ via $E_{a,r} + \Delta U_{\text{rxn}}$, $E_{a,r}$ is estimated as 13 kcal mol^{-1} in this study, $\Delta U_{\text{rxn}} = 19.38 \text{ kcal mol}^{-1}$.
- k_6 A_r via A_f and Microscopic Reversibility (MR), $A_f = 1.81 \times 10^{12}$, 92 WAL/AND, for $\text{C}_3\text{C} + \text{O}_2$, $E_{a,f} = E_{a,r} + \Delta U_{\text{rxn}}$, $\Delta U_{\text{rxn}} = 32.26 \text{ kcal mol}^{-1}$.

IID. 10 $C_2C=C + HO_2 \rightarrow [C_2C.COOH]^* \rightarrow \text{Products}$



Reaction	$A T^n e^{-\alpha/T}$ (s ⁻¹ or cm ³ mol ⁻¹ s ⁻¹)	E_a (kcal mol ⁻¹)
$k_1 \quad C_2C=C + HO_2 \rightarrow C_2C.COOH$	$6.39 \times 10^2 T^{3.10} e^{-0T}$	7.20
$k_{-1} \quad C_2C.COOH \rightarrow C_2C=C + HO_2$	$1.54 \times 10^9 T^{1.07} e^{-0.00016T}$	12.99
$k_2 \quad C_2C.COOH \rightarrow C_2CyCOC + OH$	$3.00 \times 10^8 T^{1.06} e^{-0T}$	20.00
$k_3 \quad C_2C.COOH \rightarrow C=C(C)COOH + H$	$3.02 \times 10^{13} T^0 e^{-0T}$	38.46
$k_4 \quad C_2C.COOH \rightarrow C_2C=COOH + H$	$9.14 \times 10^{11} T^0 e^{-0T}$	40.52
$k_5 \quad C_2C.COOH \rightarrow C_2CCOO.$	$3.31 \times 10^5 T^{1.79} e^{-0T}$	15.87
$k_{-5} \quad C_2CCOO. \rightarrow C_2C.COOH$	$4.42 \times 10^7 T^{1.69} e^{-0.00028T}$	23.76
$k_6 \quad C_2CCOO. \rightarrow C_2C=C + HO_2$	$7.47 \times 10^9 T^{0.74} e^{-0T}$	26.68
$k_7 \quad C_2CCOO. \rightarrow C_3.C + O_2$	$2.30 \times 10^{14} T^0 e^{-0T}$	31.72
$k_8 \quad C_2CCOO. \rightarrow C_2.CCOOH$	$4.32 \times 10^8 T^{1.32} e^{-0T}$	21.63
$k_{-8} \quad C_2.CCOOH \rightarrow C_2CCOO.$	$1.17 \times 10^{11} T^{-0.33} e^{-0.00107T}$	7.94
$k_9 \quad C_2.CCOOH \rightarrow C=CCOOH + CH_3$	$6.32 \times 10^{12} T^0 e^{-0T}$	29.06
$k_{10} \quad C_2.CCOOH \rightarrow CC=C + CH_2OOH$	$2.78 \times 10^{13} T^0 e^{-0T}$	29.39
$k_{11} \quad C_2.CCOOH \rightarrow CCyCCOC + OH$	$5.38 \times 10^{10} T^0 e^{-0T}$	16.00
$k_{12} \quad C_2.CCOOH \rightarrow C=C(C)COOH + H$	$8.62 \times 10^{10} T^0 e^{-0T}$	31.98

Reaction		$A T^n e^{-E_a/T}$ (s^{-1} or $cm^3 mol^{-1} s^{-1}$)	E_a ($kcal mol^{-1}$)
k_{13}	$C_2CCOO. \rightarrow C_2CC.OOH$	$2.60 \times 10^{10} T^{1.0} e^{-0.7T}$	44.29
k_{-13}	$C_2CC.OOH \rightarrow C_2CCOO.$	$9.11 \times 10^{12} T^{-0.38} e^{-0.00071T}$	35.61
k_{14}	$C_2CC.OOH \rightarrow C_2CCHO + OH$	$1.34 \times 10^{15} T^0 e^{-0.7T}$	2.50
k_{15}	$C_2CC.OOH \rightarrow C_2C=COOH + H$	$9.30 \times 10^{11} T^0 e^{-0.7T}$	39.66
k_{16}	$C_2CC.OOH \rightarrow CC=COOH + CH_3$	$4.73 \times 10^{12} T^0 e^{-0.7T}$	34.52

frequency/degeneracy (CPFIT)

$C_2C.COOH$: 250.0 (11.309); 1364.5 (17.843); 2818.8 (7.349)

$C_2CCOO.$: 250.2 (9.560); 1119.2 (16.494); 2788.5 (10.946)

$C_2.CCOOH$: 250.0 (10.534); 1133.0 (16.419); 2777.2 (9.548)

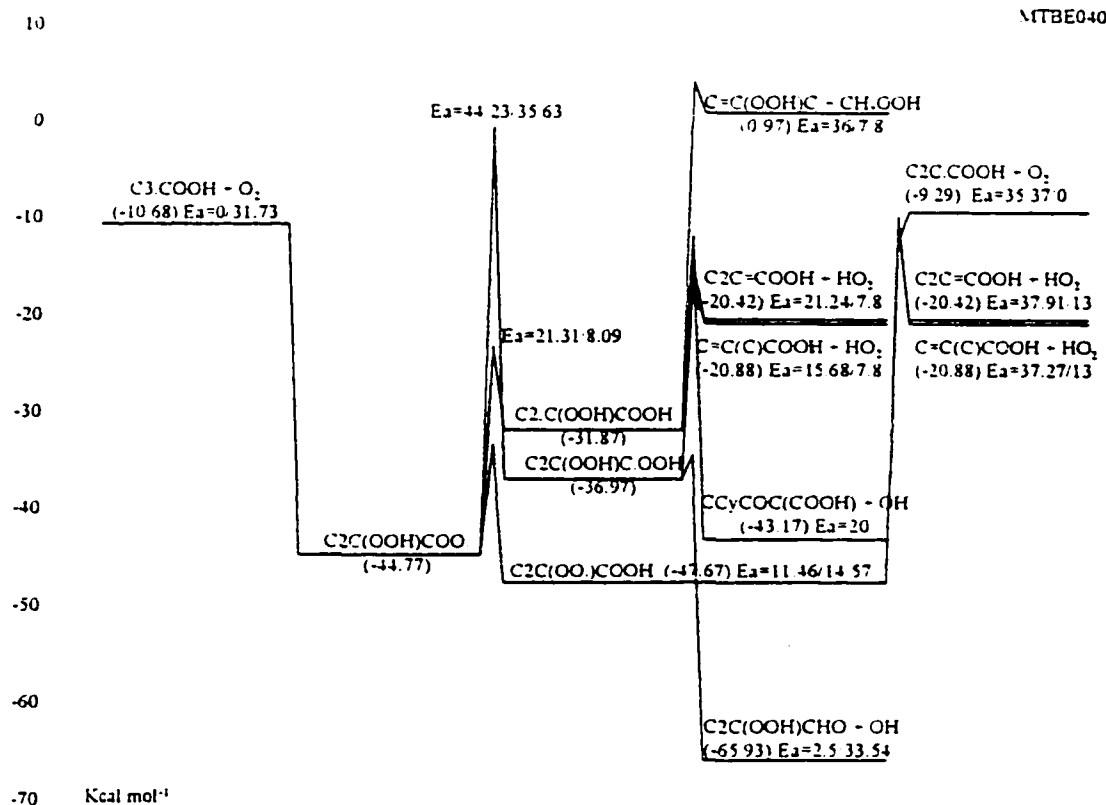
$C_2CC.OOH$: 250.2 (11.370); 1195.7 (16.616); 2826.5 (8.513)

Lennard-Jones parameter

$\sigma(\text{\AA}) = 5.54$, $\epsilon/k(K) = 584.86.0$

- k_1 A_f , estimated using TST, $A = (\text{deg.}) A' T^n$, $\text{deg.} = 1$, $A' = 6.39 \times 10^2$, $n = 3.102$, A' and n are from thermal reaction analysis (AFACT2f) based on the thermodynamic properties calculated from MOPAC PM3 (corrected with internal rotor, electronic spin and optical isomer). $E_{a,f} = 7.2 \text{ kcal mol}^{-1}$ (Bozzelli).
- k_{-1} A_r via A_f and Microscopic Reversibility (MR), $E_{a,r} = E_{a,f} - \Delta U_{rxn}$, $\Delta U_{rxn} = 5.79 \text{ kcal mol}^{-1}$.
- k_2 A_f estimated using TST, $A = (\text{deg.}) A' T^n$, $\text{deg.} = 1$, $A' = 2.996 \times 10^8$, $n = 1.061$, A' and n are from thermal reaction analysis (AFACT2f) based on the thermodynamic properties calculated from MOPAC PM3 (corrected with internal rotor, electronic spin and optical isomer). $E_{a,f}$ is estimated in this study.
- k_3 A_f via A_r and Microscopic Reversibility (MR), $A_r = 3.09 \times 10^{13}$, 72 KER for $C_2C=C + H \rightarrow C_3C.$, $E_{a,f} = E_{a,r} + \Delta U_{rxn}$, $\Delta U_{rxn} = 36.96 \text{ kcal mol}^{-1}$. $E_{a,r} = 1.50 \text{ kcal mol}^{-1}$. (referenced as the same as the A_r).
- k_4 A_f via A_r and Microscopic Reversibility (MR), $A_r = 3.615 \times 10^{12} = 1/2(C_3H_6 + H \rightarrow CCC.)$, 91 TSA. $E_{a,f} = E_{a,r} + \Delta U_{rxn}$, $\Delta U_{rxn} = 37.61 \text{ kcal mol}^{-1}$. $E_{a,r} = 2.906 \text{ kcal mol}^{-1}$. (referenced as the same as the A_r).
- k_5 A_f estimated using TST, $A = (\text{deg.}) A' T^n$, $\text{deg.} = 1$, $A' = 3.314 \times 10^5$, $n = 1.792$, A' and n are from thermal reaction analysis (AFACT2f) based on the thermodynamic properties calculated from MOPAC PM3 (corrected with internal rotor, electronic spin and optical isomer). $E_{a,f} = E_{a,r} + \Delta U_{rxn}$, $\Delta U_{rxn} = -7.89 \text{ kcal mol}^{-1}$.
- k_{-5} A_r via A_f and Microscopic Reversibility (MR), $E_{a,r} = RS(6) + E_{a,bst}(9.87) + \Delta H_{rxn}(7.89) \text{ kcal mol}^{-1}$.
- k_6 A_f estimated using TST, $A = (\text{deg.}) A' T^n$, $\text{deg.} = 1$, $A' = 7.467 \times 10^9$, $n = 0.735$, A' and n are from thermal reaction analysis (AFACT2f) based on the thermodynamic properties calculated from MOPAC PM3 (corrected with internal rotor, electronic spin and optical isomer). $E_{a,f}$ via $E_{a,r} + \Delta U_{rxn}$, $E_{a,r}$ is estimated as

- 13 kcal mol⁻¹ in this study, $\Delta U_{\text{rxn}} = 13.68$ kcal mol⁻¹.
- k₇ A_f via A_r and Microscopic Reversibility (MR), $A_r = 1.0 \times 10^{12}$, 88 XI for $\text{C}_3\text{CC} + \text{O}_2 \rightarrow \text{C}_3\text{CCOO}$. $E_{a,f} = \Delta U_{\text{rxn}} = 31.72$ kcal mol⁻¹.
- k₈ A_f estimated using TST, $A = (\text{deg.}) A' T^n$, deg. = 6, $A' = 7.202 \times 10^7$, $n = 1.317$, A' and n are from thermal reaction analysis (AFACT2f) based on the thermodynamic properties calculated from MOPAC PM3 (corrected with internal rotor, electronic spin and optical isomer). $E_{a,f} = \text{RS (0)} + E_{\text{abst (7 94)}} + \Delta H_{\text{rxn}} (13.69)$ kcal mol⁻¹.
- k₈ A_r via A_f and Microscopic Reversibility (MR), $E_{a,r} = E_{a,f} - \Delta U_{\text{rxn}}$, $\Delta U_{\text{rxn}} = 13.69$ kcal mol⁻¹.
- k₉ A_f via A_r and Microscopic Reversibility (MR), $A_r = 9.64 \times 10^{10}$, 91 TSA for $\text{C}_3\text{H}_6 + \text{CH}_3 \rightarrow \text{C}_3\text{C}$. $E_{a,f} = E_{a,r} + \Delta U_{\text{rxn}}$, $\Delta U_{\text{rxn}} = 21.26$ kcal mol⁻¹. $E_{a,r} = 7.8$ kcal mol⁻¹. (estimated by Bozzelli).
- k₁₀ A_f via A_r and Microscopic Reversibility (MR), $A_r = 9.64 \times 10^{10}$, 91 TSA for $\text{C}_3\text{H}_6 + \text{CH}_3 \rightarrow \text{C}_3\text{C}$. $E_{a,f} = E_{a,r} + \Delta U_{\text{rxn}}$, $\Delta U_{\text{rxn}} = 21.59$ kcal mol⁻¹. $E_{a,r} = 7.8$ kcal mol⁻¹. (estimated by Bozzelli).
- k₁₁ A_f estimated using TST, $A = (\text{deg.}) (ek_b T/h) \exp(\Delta S^\ddagger(T)/R)$, deg. = 1, $ek_b T/h = 10^{13.55}$?, $\Delta S^\ddagger(T)$ is estimated as loss of three rotors (-4.3×3 cal mol⁻¹ K⁻¹). $E_{a,f}$ is evaluated in this study.
- k₁₂ A_f via A_r and Microscopic Reversibility (MR), $A_r = 1.26 \times 10^{11}$, 72 KER. $E_{a,f} = \Delta U_{\text{rxn}} = 31.98$ kcal mol⁻¹.
- k₁₃ A_f estimated using TST, $A = (\text{deg.}) (ek_b/h) T^n \exp(\Delta S^\ddagger(T)/R)$, deg. = 2, $ek_b/h = 5.66 \times 10^{10}$, $n = 1.0$, $\Delta S^\ddagger(T)$ is estimated as loss of one rotor (-4.3 cal mol⁻¹ K⁻¹) and gain an optical isomer (OI). $E_{a,f} = \text{RS (26)} + E_{\text{abst (9 61)}} + \Delta H_{\text{rxn}} (8.68)$ kcal mol⁻¹.
- k₁₃ A_r via A_f and Microscopic Reversibility (MR), $E_{a,r} = E_{a,f} - \Delta U_{\text{rxn}}$, $\Delta U_{\text{rxn}} = 8.68$ kcal mol⁻¹.
- k₁₄ A_f via A_r and Microscopic Reversibility (MR), $A_r = 2.75 \times 10^{12} = 1/2 (\text{OH} + \text{C}=\text{C})$. $E_{a,f}$ estimated the same 2.5 kcal mol⁻¹ as $E_{a,r}$ for $\text{CH}_2\text{OOH} \rightarrow \text{CH}_2\text{O} + \text{OH}$ (1990 Page)
- k₁₅ A_f via A_r and Microscopic Reversibility (MR), $A_r = 3.215 \times 10^{12} = 1/4 (\text{H} + \text{CC}=\text{C} \rightarrow \text{CC}\cdot\text{C})$, 91 TSA. $E_{a,f}$ is estimated as the average of terminal and non-terminal addition of H to carbon double bond of $\text{CC}=\text{C}$, $1/2 (1.506 + 2.906)$, 91 TSA.
- k₁₆ A_f via A_r and Microscopic Reversibility (MR), $A_r = 1.69 \times 10^{11}$, 91 TSA for $\text{CH}_3 + \text{CC}=\text{C} \rightarrow \text{CC}\cdot\text{CC}$. $E_{a,f} = E_{a,r} + \Delta U_{\text{rxn}}$, $\Delta U_{\text{rxn}} = 26.72$ kcal mol⁻¹. $E_{a,r} = 7.8$ kcal mol⁻¹. (estimated by Bozzelli).

IID. 11 C3.COOH + O₂ → Products

Reaction		$A T^n e^{-aT}$ (s ⁻¹ or cm ³ mol ⁻¹ s ⁻¹)	E_a (kcal mol ⁻¹)
k ₁	C3.COOH + O ₂ → C2C(OOH)COO.	$1.00 \times 10^{12} T^0 e^{-0T}$	0.00
k ₋₁	C2C(OOH)COO. → C3.COOH + O ₂	$2.31 \times 10^{14} T^0 e^{-0T}$	31.73
k ₂	C2C(OOH)COO. → C2C(OOH)C.OOH	$6.11 \times 10^9 T^{1.0} e^{-0T}$	44.23
k ₋₂	C2C(OOH)C.OOH → C2C(OOH)COO.	$1.59 \times 10^{12} T^{-0.33} e^{-0.00073T}$	35.63
k ₃	C2C(OOH)C.OOH → C2C(OOH)CHO + OH	$3.22 \times 10^{13} T^0 e^{-0T}$	2.50
k ₄	C2C(OOH)C.OOH → C2C=COOH + HO ₂	$9.82 \times 10^{12} T^0 e^{-0T}$	21.24
k ₅	C2C(OOH)COO. → C2.C(OOH)COOH	$3.66 \times 10^8 T^{1.50} e^{-0T}$	21.31
k ₋₅	C2.C(OOH)COOH → C2C(OOH)COO.	$9.09 \times 10^9 T^{0.22} e^{-0.00109T}$	8.09
k ₆	C2.C(OOH)COOH → CCyCOC(COOH) + OH	$4.68 \times 10^{11} T^0 e^{-0T}$	20.00
k ₇	C2.C(OOH)COOH → C=C(C)COOH + HO ₂	$3.05 \times 10^{13} T^0 e^{-0T}$	15.68
k ₈	C2.C(OOH)COOH → C=C(OOH)C + CH ₂ OOH	$2.84 \times 10^{14} T^0 e^{-0T}$	36.00
k ₉	C2C(OOH)COO. → C2C(OO.)COOH	$4.23 \times 10^{12} T^{-1.26} e^{0.000160T}$	11.46
k ₋₉	C2C(OO.)COOH → C2C(OOH)COO.	$3.54 \times 10^{12} T^{-1.24} e^{-0T}$	14.57
k ₁₀	C2C(OO.)COOH → C2C.COOH + O ₂	$2.08 \times 10^{15} T^0 e^{-0T}$	35.37
k ₁₁	C2C(OO.)COOH → C=C(C)COOH + HO ₂	$1.73 \times 10^{11} T^{1.22} e^{-0T}$	37.27
k ₁₂	C2C(OO.)COOH → C2C=COOH + HO ₂	$5.75 \times 10^{10} T^{1.22} e^{-0T}$	37.91

frequency/degeneracy (CPFIT)

C2C(OOH)COO: 100.3 (12.287); 1038.0 (19.413); 2858.4 (10.300)

C2C(OOH)C OOH: 100.1 (13.652); 1056.4 (19.084); 2833.5 (8.765)

C2C(OOH)COOH: 100.4 (12.975); 1031.0 (19.408); 2821.6 (9.117)

C2C(OO)COOH: 100.6 (12.290); 1031.9 (19.577); 2928.8 (10.133)

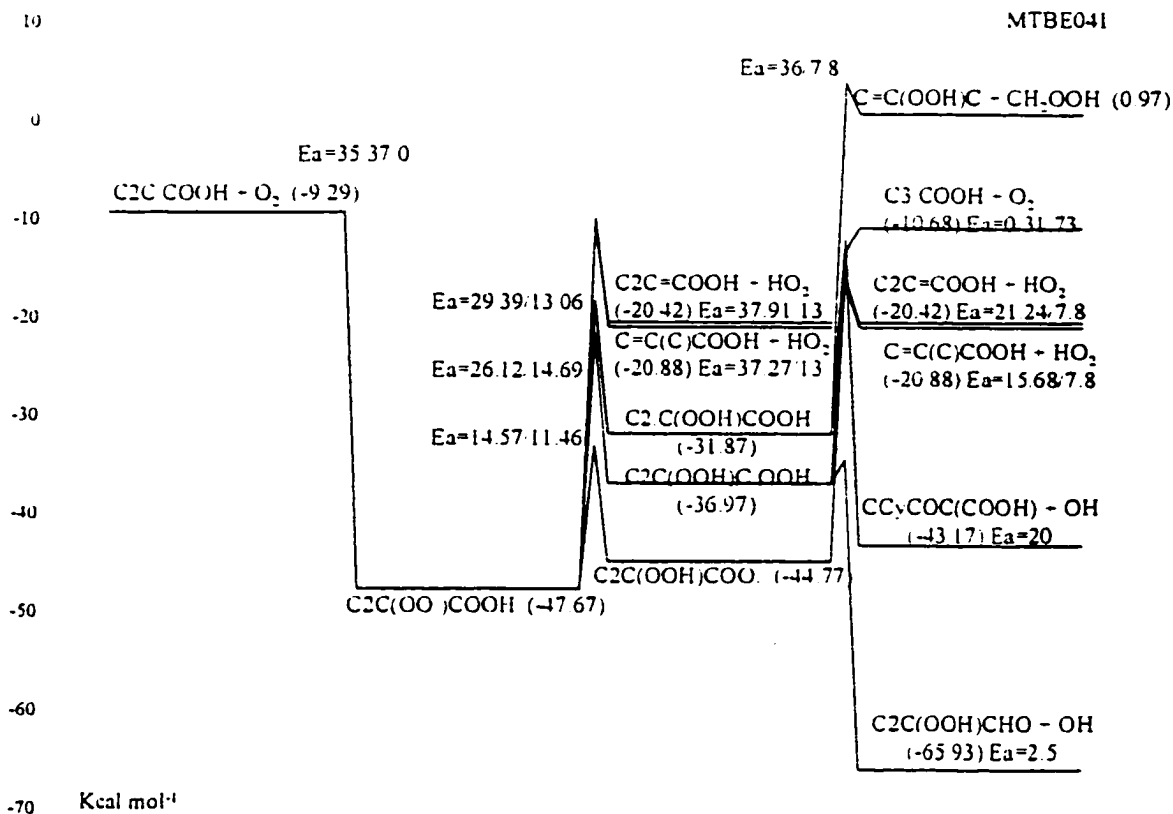
Lennard-Jones parameter

$\sigma(\text{\AA}) = 6.14$, $\epsilon/k(\text{K}) = 678.63$

- k_1 taken from 88 XI
- k_{-1} A_r via A_r and Microscopic Reversibility (MR), $E_{a,r} = E_{a,f} - \Delta U_{rxn}$, $\Delta U_{rxn} = -31.73$ kcal mol⁻¹.
- k_2 A_f estimated using TST, $A = (\text{deg.}) (ek_b/h) T^n \exp(\Delta S^\ddagger(T)/R)$, $\text{deg.} = 2$, $ek_b/h = 5.66 \times 10^{10}$, $n = 1.0$, $\Delta S^\ddagger(T)$ is estimated as loss of one rotor (-4.3 cal mol⁻¹ K⁻¹) and gain an optical isomer (OI). $E_{a,f} = RS(26) + E_{abst}(9.63) + \Delta H_{rxn}(8.60)$ kcal mol⁻¹.
- k_{-2} A_r via A_f and Microscopic Reversibility (MR), $E_{a,r} = E_{a,f} - \Delta U_{rxn}$, $\Delta U_{rxn} = 8.60$ kcal mol⁻¹.
- k_3 A_f via A_r and Microscopic Reversibility (MR), $A_r = 2.75 \times 10^{12} = 1/2(\text{OH} + \text{C}=\text{C})$. $E_{a,f}$ estimated the same 2.5 kcal mol⁻¹ as $E_{a,f}$ for $\text{CH}_2\text{OOH} \rightarrow \text{CH}_2\text{O} + \text{OH}$ (1990 Page)
- k_4 A_f via A_r and Microscopic Reversibility (MR), $A_r = 2.5 \times 10^{11} = 1/2(\text{C}=\text{C} + \text{HO}_2)$, 72 KER/PAR. $E_{a,f} = E_{a,r} + \Delta U_{rxn}$, $\Delta U_{rxn} = 13.44$ kcal mol⁻¹. $E_{a,r} = 7.8$ kcal mol⁻¹. (estimated by Bozzelli).
- k_5 A_f estimated using TST, $A = (\text{deg.}) A' T^n$, $\text{deg.} = 6$, $A' = 6.106 \times 10^7$, $n = 1.497$, A' and n are from thermal reaction analysis (AFACT2f) based on the thermodynamic properties calculated from MOPAC PM3 (corrected with internal rotor, electronic spin and optical isomer). $E_{a,f} = RS(0) + E_{abst}(8.09) + \Delta H_{rxn}(13.22)$ kcal mol⁻¹.
- k_{-5} A_r via A_f and Microscopic Reversibility (MR), $E_{a,r} = E_{a,f} - \Delta U_{rxn}$, $\Delta U_{rxn} = 13.22$ kcal mol⁻¹.
- k_6 A_f estimated using TST, $A = (\text{deg.}) (ek_b T/h) \exp(\Delta S^\ddagger(T)/R)$, $\text{deg.} = 1$, $ek_b T/h = 10^{13.55}$?, $\Delta S^\ddagger(T)$ is estimated as loss of two rotors (-4.3×2 cal mol⁻¹ K⁻¹). $E_{a,f}$ is evaluated in this study.
- k_7 A_f via A_r and Microscopic Reversibility (MR), $A_r = 3.5 \times 10^{11}$, Bozzelli. $E_{a,f} = E_{a,r} + \Delta U_{rxn}$, $\Delta U_{rxn} = 7.88$ kcal mol⁻¹. $E_{a,r} = 7.8$ kcal mol⁻¹. (estimated by Bozzelli).
- k_8 A_f via A_r and Microscopic Reversibility (MR), $A_r = 9.64 \times 10^{10}$, 91 TSA for $\text{C}_3\text{H}_6 + \text{CH}_3 \rightarrow \text{C}_3\text{C}$. $E_{a,f} = E_{a,r} + \Delta U_{rxn}$, $\Delta U_{rxn} = 28.2$ kcal mol⁻¹. $E_{a,r} = 7.8$ kcal mol⁻¹. (estimated by Bozzelli).
- k_9 A_f via A_r and Microscopic Reversibility (MR), $E_{a,f} = E_{a,r} + \Delta U_{rxn}$, $\Delta U_{rxn} = -3.11$ kcal mol⁻¹.
- k_{-9} A_r estimated using TST, $A = (\text{deg.}) A' T^n$, $\text{deg.} = 1$, $A' = 3.537 \times 10^{12}$, $n = -1.244$, A' and n are from thermal reaction analysis (AFACT2f) based on the

thermodynamic properties calculated from MOPAC PM3 (corrected with internal rotor, electronic spin and optical isomer). $E_{a,r} = RS(6) + E_{abt}(11.46) - 6(\text{H bond}) - \Delta U_{\text{rot}}(-3.11)$ kcal mol⁻¹.

- k_{10} A_f via A_r and Microscopic Reversibility (MR), $A_r = 1.81 \times 10^{12}$, 92 WAL/AND for $\text{C3C} + \text{O}_2 \rightarrow \text{C3COO}$. $E_{a,f} = \Delta U_{\text{rot}} = 35.37$ kcal mol⁻¹.
- k_{11} A_f estimated using TST, $A = (\text{deg.}) A' T^n$, deg. = 6, $A' = 2.876 \times 10^{10}$, $n = 1.220$, A' and n are from thermal reaction analysis (AFACT2f) based on the thermodynamic properties calculated from MOPAC PM3 (corrected with internal rotor, electronic spin and optical isomer). $E_{a,f}$ via $E_{a,r} + \Delta U_{\text{rot}}$. $E_{a,r}$ is estimated as 13 kcal mol⁻¹ in this study, $\Delta U_{\text{rot}} = 24.27$ kcal mol⁻¹.
- k_{12} A_f estimated using TST, $A = (\text{deg.}) A' T^n$, deg. = 2, $A' = 2.876 \times 10^{10}$, $n = 1.220$, A' and n are from thermal reaction analysis (AFACT2f) based on the thermodynamic properties calculated from MOPAC PM3 (corrected with internal rotor, electronic spin and optical isomer). $E_{a,f}$ via $E_{a,r} + \Delta U_{\text{rot}}$. $E_{a,r}$ is estimated as 13 kcal mol⁻¹ in this study, $\Delta U_{\text{rot}} = 24.91$ kcal mol⁻¹.

IID. 12 C2C.COOH + O₂ → Products

Reaction		A T ⁿ e ^{-αT} (s ⁻¹ or cm ³ mol ⁻¹ s ⁻¹)	E _a (kcal mol ⁻¹)
k ₁	C2C.COOH + O ₂ → C2C(OO.)COOH	1.81 × 10 ¹² T ⁰ e ^{-0T}	0.00
k ₋₁	C2C(OO.)COOH → C2C.COOH + O ₂	2.08 × 10 ¹⁵ T ⁰ e ^{-0T}	35.37
k ₂	C2C(OO.)COOH → C=C(C)COOH + HO ₂	1.73 × 10 ¹¹ T ^{1.22} e ^{-0T}	37.27
k ₃	C2C(OO.)COOH → C2C=COOH + HO ₂	5.75 × 10 ¹⁰ T ^{1.22} e ^{-0T}	37.91
k ₄	C2C(OO.)COOH → C2C(OOH)C.OOH	2.78 × 10 ⁷ T ^{2.03} e ^{-0T}	26.12
k ₋₄	C2C(OOH)C.OOH → C2C(OO.)COOH	4.04 × 10 ⁹ T ^{0.74} e ^{-0.00076T}	14.69
k ₅	C2C(OOH)C.OOH → C2C(OOH)CHO + OH	3.22 × 10 ¹³ T ⁰ e ^{-0T}	2.50
k ₆	C2C(OOH)C.OOH → C2C=COOH + HO ₂	9.82 × 10 ¹² T ⁰ e ^{-0T}	21.24
k ₇	C2C(OO.)COOH → C2.C(OOH)COOH	1.08 × 10 ⁹ T ^{1.83} e ^{-0T}	29.39
k ₋₇	C2.C(OOH)COOH → C2C(OO.)COOH	3.21 × 10 ¹⁰ T ^{0.53} e ^{-0.00093T}	13.06
k ₈	C2.C(OOH)COOH → CCyCOC(COOH) + OH	4.68 × 10 ¹¹ T ⁰ e ^{-0T}	20.00
k ₉	C2.C(OOH)COOH → C=C(C)COOH + HO ₂	3.05 × 10 ¹³ T ⁰ e ^{-0T}	15.68
k ₁₀	C2.C(OOH)COOH → C=C(OOH)C + CH ₂ O	2.84 × 10 ¹⁴ T ⁰ e ^{-0T}	36.00
k ₁₁	C2C(OO.)COOH → C2C(OOH)COO.	3.54 × 10 ¹² T ^{-1.24} e ^{-0T}	14.57
k ₋₁₁	C2C(OOH)COO. → C2C(OO.)COOH	4.23 × 10 ¹² T ^{-1.26} e ^{0.00016T}	11.46

	Reaction	$A T^n e^{-u/T}$ (s^{-1} or $cm^3 mol^{-1} s^{-1}$)	E_a ($kcal mol^{-1}$)
k_{12}	<chem>C2C(OOH)COO. -> C3 COOH + O2</chem>	$2.31 \times 10^{14} T^0 e^{-0/T}$	31.73

frequency/degeneracy (CPFIT)

C2C(OO.)COOH: 100.6 (12.290); 1031.9 (19.577); 2928.8 (10.133)

C2C(OOH)C.OOH: 100.1 (13.652); 1056.4 (19.084); 2833.5 (8.765)

C2 C(OOH)COOH: 100.4 (12.975); 1031.0 (19.408); 2821.6 (9.117)

C2C(OOH)COO.: 100.3 (12.287); 1038.0 (19.413); 2858.4 (10.300)

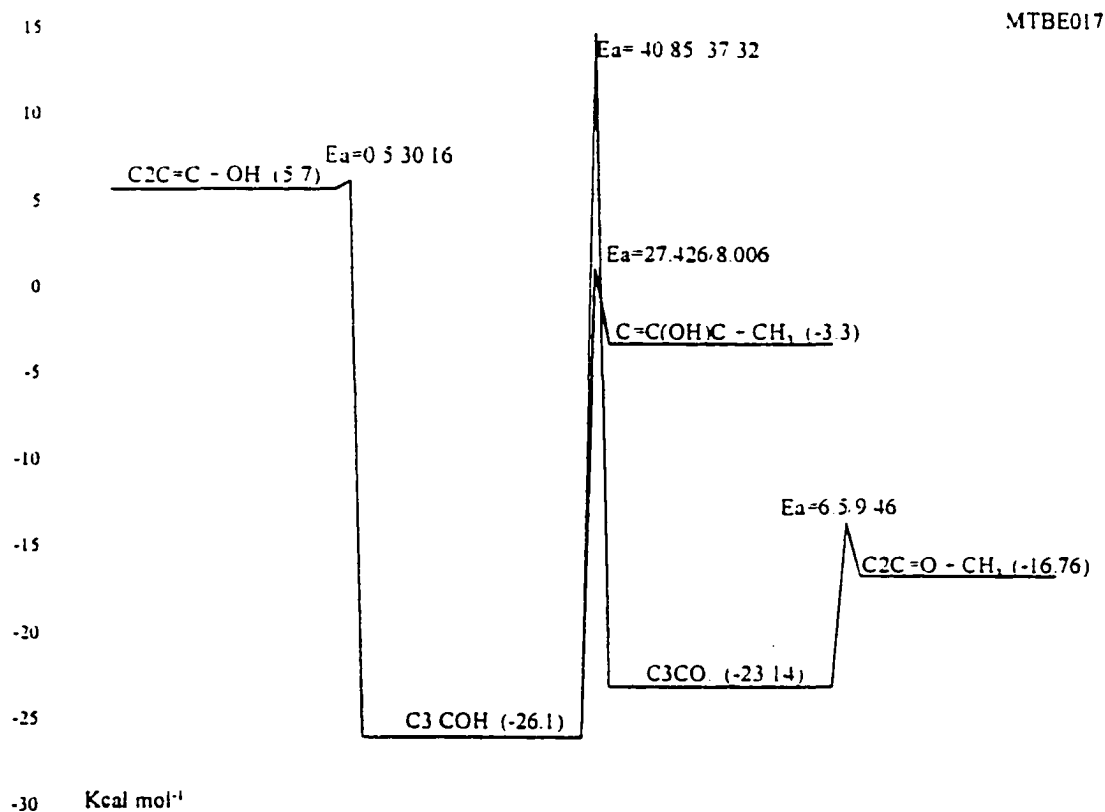
Lennard-Jones parameter

$\sigma(\text{\AA}) = 6.14$, $\epsilon/k (K) = 678.63$

- k_1 92 WAL/AND for C3C. + O2 -> C3COO..
- k_{-1} A_r via A_f and Microscopic Reversibility (MR), $E_{a,r} = E_{a,f} - \Delta U_{rxn}$, $\Delta U_{rxn} = -35.37 kcal mol^{-1}$.
- k_2 A_f estimated using TST, $A = (deg.) A' T^n$, $deg. = 6$, $A' = 2.876 \times 10^{10}$, $n = 1.220$, A' and n are from thermal reaction analysis (AFACT2f) based on the thermodynamic properties calculated from MOPAC PM3 (corrected with internal rotor, electronic spin and optical isomer). $E_{a,f}$ via $E_{a,r} + \Delta U_{rxn}$, $E_{a,f}$ is estimated as $13 kcal mol^{-1}$ in this study, $\Delta U_{rxn} = 24.27 kcal mol^{-1}$.
- k_3 A_f estimated using TST, $A = (deg.) A' T^n$, $deg. = 2$, $A' = 2.876 \times 10^{10}$, $n = 1.220$, A' and n are from thermal reaction analysis (AFACT2f) based on the thermodynamic properties calculated from MOPAC PM3 (corrected with internal rotor, electronic spin and optical isomer). $E_{a,f}$ via $E_{a,r} + \Delta U_{rxn}$, $E_{a,f}$ is estimated as $13 kcal mol^{-1}$ in this study, $\Delta U_{rxn} = 24.91 kcal mol^{-1}$.
- k_4 A_f estimated using TST, $A = (deg.) A' T^n$, $deg. = 2$, $A' = 1.390 \times 10^7$, $n = 2.032$, A' and n are from thermal reaction analysis (AFACT2f) based on the thermodynamic properties calculated from MOPAC PM3 (corrected with internal rotor, electronic spin and optical isomer). $E_{a,f} = RS(6) + E_{abst}(8.69) + \Delta H_{rxn}(11.43) kcal mol^{-1}$.
- k_{-4} A_r via A_f and Microscopic Reversibility (MR), $E_{a,r} = E_{a,f} - \Delta U_{rxn}$, $\Delta U_{rxn} = 11.43 kcal mol^{-1}$.
- k_5 A_f via A_r and Microscopic Reversibility (MR), $A_r = 2.75 \times 10^{12} = 1/2 (OH + C=C)$. $E_{a,f}$ estimated the same $2.5 kcal mol^{-1}$ as $E_{a,r}$ for CH2OOH -> CH2O + OH (1990 Page)
- k_6 A_f via A_r and Microscopic Reversibility (MR), $A_r = 2.5 \times 10^{11} = 1/2 (C=C + HO_2)$, 72 KER/PAR. $E_{a,f} = E_{a,r} + \Delta U_{rxn}$, $\Delta U_{rxn} = 13.44 kcal mol^{-1}$. $E_{a,r} = 7.8 kcal mol^{-1}$ (estimated by Bozzelli).
- k_7 A_f estimated using TST, $A = (deg.) A' T^n$, $deg. = 6$, $A' = 1.802 \times 10^8$, $n = 1.832$, A' and n are from thermal reaction analysis (AFACT2f) based on the thermodynamic properties calculated from MOPAC PM3 (corrected with internal rotor, electronic spin and optical isomer). $E_{a,f} = RS(6) + E_{abst}(7.06) + \Delta H_{rxn}(16.33) kcal mol^{-1}$.

- k₇ A_r via A_f and Microscopic Reversibility (MR), $E_{a,r} = E_{a,f} - \Delta U_{\text{ren}}$, $\Delta U_{\text{ren}} = 16.33 \text{ kcal mol}^{-1}$.
- k₈ A_f estimated using TST, $A = (\text{deg.}) (ek_b T/h) \exp(\Delta S^\ddagger(T)/R)$, $\text{deg.} = 1$, $ek_b T/h = 10^{13.55} ?$, $\Delta S^\ddagger(T)$ is estimated as loss of two rotors ($-4.3 \times 2 \text{ cal mol}^{-1} \text{ K}^{-1}$). $E_{a,f}$ is evaluated in this study.
- k₉ A_f via A_r and Microscopic Reversibility (MR), $A_r = 3.5 \times 10^{11}$, Bozzelli. $E_{a,f} = E_{a,r} + \Delta U_{\text{ren}}$, $\Delta U_{\text{ren}} = 7.88 \text{ kcal mol}^{-1}$. $E_{a,r} = 7.8 \text{ kcal mol}^{-1}$ (estimated by Bozzelli).
- k₁₀ A_f via A_r and Microscopic Reversibility (MR), $A_r = 9.64 \times 10^{10}$, 91 TSA for $\text{C}_3\text{H}_6 + \text{CH}_3 \rightarrow \text{C3.C}$. $E_{a,f} = E_{a,r} + \Delta U_{\text{ren}}$, $\Delta U_{\text{ren}} = 28.2 \text{ kcal mol}^{-1}$. $E_{a,r} = 7.8 \text{ kcal mol}^{-1}$ (estimated by Bozzelli).
- k₁₁ A_f estimated using TST, $A = (\text{deg.}) A' T^n$, $\text{deg.} = 1$, $A' = 3.537 \times 10^{12}$, $n = -1.244$, A' and n are from thermal reaction analysis (AFACT2f) based on the thermodynamic properties calculated from MOPAC PM3 (corrected with internal rotor, electronic spin and optical isomer). $E_{a,f} = \text{RS (6)} + E_{\text{abst}} (11.46) - 6 (\text{H bond}) + \Delta U_{\text{ren}} (3.11) \text{ kcal mol}^{-1}$.
- k₁₁ A_r via A_f and Microscopic Reversibility (MR), $E_{a,r} = E_{a,f} - \Delta U_{\text{ren}}$, $\Delta U_{\text{ren}} = 3.11 \text{ kcal mol}^{-1}$.
- k₁₂ A_f via A_r and Microscopic Reversibility (MR), $A_r = 1.0 \times 10^{12}$, 88 XI for $\text{C3CC.} + \text{O}_2 \rightarrow \text{C3CCOO.}$. $E_{a,f} = \Delta U_{\text{ren}}$, $= 31.73 \text{ kcal mol}^{-1}$.

IID. 13 $\text{C}_2\text{C}=\text{C} + \text{OH} \rightarrow [\text{C}_3.\text{COH}]^* \rightarrow \text{Products}$



Reaction		$A T^n e^{-\alpha T}$ (s ⁻¹ or cm ³ mol ⁻¹ s ⁻¹)	E_a (kcal mol ⁻¹)
k_1	$\text{C}_2\text{C}=\text{C} + \text{OH} \rightarrow \text{C}_3.\text{COH}$	$2.92 \times 10^{12} T^0 e^{-0T}$	0.50
k_{-1}	$\text{C}_3.\text{COH} \rightarrow \text{C}_2\text{C}=\text{C} + \text{OH}$	$2.12 \times 10^{13} T^0 e^{-0T}$	30.16
k_2	$\text{C}_3.\text{COH} \rightarrow \text{C}=\text{C}(\text{OH})\text{C} + \text{CH}_3$	$6.72 \times 10^{12} T^{1.0} e^{-0T}$	27.43
k_3	$\text{C}_3.\text{COH} \rightarrow \text{C}_3\text{CO.}$	$5.92 \times 10^7 T^{1.01} e^{-0.00049T}$	40.85
k_{-3}	$\text{C}_3\text{CO.} \rightarrow \text{C}_3.\text{COH}$	$6.72 \times 10^9 T^{1.0} e^{-0T}$	37.32
k_4	$\text{C}_3\text{CO.} \rightarrow \text{C}_2\text{C}=\text{O} + \text{CH}_3$	$3.20 \times 10^{14} T^0 e^{-0T}$	9.46

frequency/degeneracy (CPFIT)

$\text{C}_3.\text{COH}$: 442.8 (11.944); 1273.0 (12.834); 2967.6 (9.222)

$\text{C}_3\text{CO.}$: 452.6 (11.685); 1274.7 (14.286); 2979.3 (8.528)

Lennard-Jones parameter

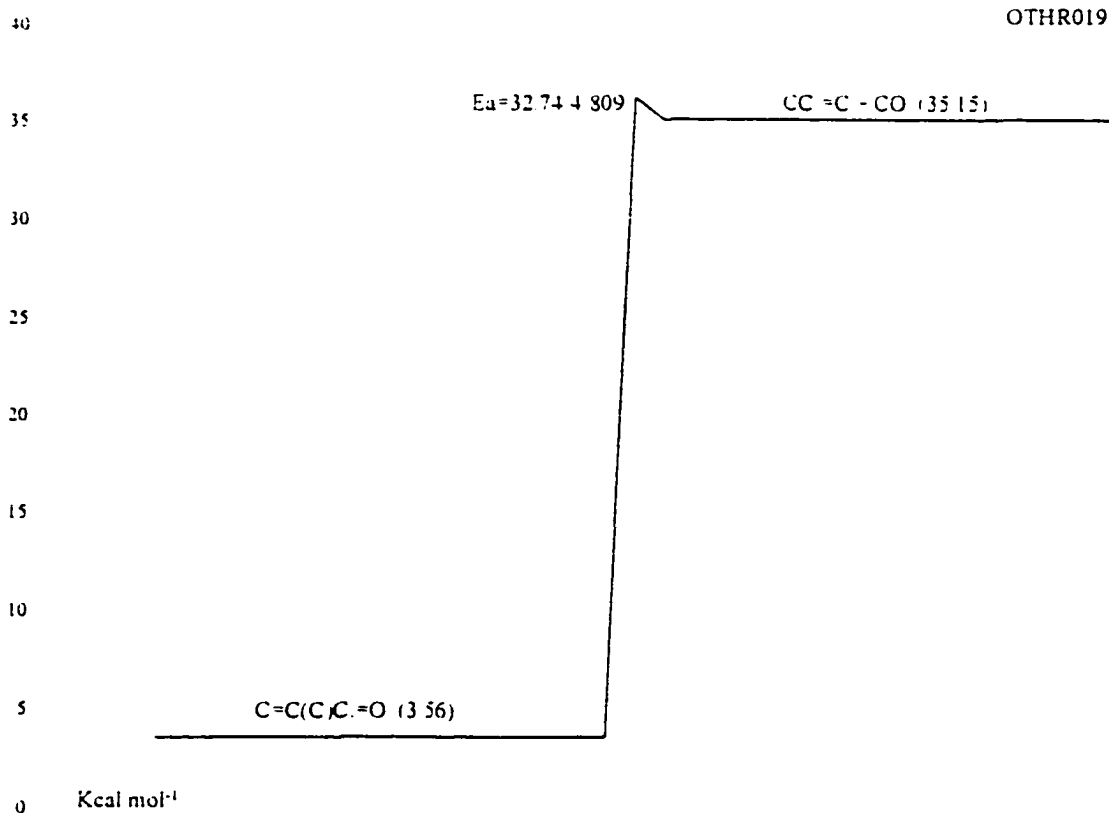
$\sigma(\text{\AA}) = 5.20$, $\epsilon/k(\text{K}) = 533.08$

k_1 A_f estimated as 1/2 ($\text{C}_3\text{H}_6 + \text{OH}$), 91 TSA. $E_{a,f}$ estimated as 0.5 kcal mol⁻¹ by

Bozzelli

- k_1 A_r via A_f and Microscopic Reversibility (MR), $E_{a,r} = E_{a,f} - \Delta U_{\text{run}}$, $\Delta U_{\text{run}} = -29.66$ kcal mol⁻¹.
- k_2 A_f via A_r and Microscopic Reversibility (MR), $A_r = 9.64 \times 10^{10}$, 91 TSA for $C_3H_6 + CH_3 \rightarrow C_3H_5 + CH_4$. $E_{a,f} = E_{a,r} + \Delta U_{\text{run}}$, $\Delta U_{\text{run}} = 19.42$ kcal mol⁻¹. $E_{a,r} = 8.006$ kcal mol⁻¹. (referenced as the same as the A_r).
- k_3 A_f via A_r and Microscopic Reversibility (MR), $E_{a,f} = E_{a,r} + \Delta U_{\text{run}}$, $\Delta U_{\text{run}} = 3.53$ kcal mol⁻¹.
- k_3 A_r estimated using TST, $A = (\text{deg.}) (ek_B/h) T^n \exp(\Delta S^\ddagger(T)/R)$, $\text{deg.} = 9$, $ek_B/h = 5.66 \times 10^{10}$, $n = 1.0$, $\Delta S^\ddagger(T)$ is estimated as loss of one rotors (-4.3 cal mol⁻¹ K⁻¹). $E_{a,f} = RS(26) + E_{\text{abst}}(11.32)$ kcal mol⁻¹.
- k_4 A_f via A_r and Microscopic Reversibility (MR), $A_r = 3.16 \times 10^{11}$ Bozzelli. $E_{a,f} = E_{a,r} + \Delta U_{\text{run}}$, $\Delta U_{\text{run}} = 2.96$ kcal mol⁻¹. $E_{a,r} = 6.5$ kcal mol⁻¹. (estimated by Bozzelli).

IID. 14 $C_2C=C + OH \rightarrow [C_2C.COH]^* \rightarrow \text{Products}$



	Reaction	$A T^n e^{-\alpha/T}$ (s ⁻¹ or cm ³ mol ⁻¹ s ⁻¹)	E_a (kcal mol ⁻¹)
k_1	$C_2C=C + OH \rightarrow C_2C.COH$	$2.92 \times 10^{12} T^0 e^{-0/T}$	0.00
k_{-1}	$C_2C.COH \rightarrow C_2C=C + OH$	$1.95 \times 10^{13} T^0 e^{-0/T}$	28.52
k_2	$C_2C.COH \rightarrow C_2C=COH + H$	$1.64 \times 10^{12} T^{1.0} e^{-0/T}$	33.43
k_3	$C_2C.COH \rightarrow C=C(C)COH + H$	$8.30 \times 10^{13} T^0 e^{-0/T}$	38.15

frequency/degeneracy (CPFIT)

$C_2C.COH$: 389.3 (10.799); 1475.6 (15.383); 3185.2 (7.818)

Lennard-Jones parameter

$\sigma(\text{\AA}) = 5.20$, $\epsilon/k \text{ (K)} = 533.08$

- k_1 A_f estimated as 1/2 ($C_3H_6 + OH$), 91 TSA. $E_{a,f}$ estimated as 0 kcal mol⁻¹ by Bozzelli
- k_{-1} A_r via A_f and Microscopic Reversibility (MR), $E_{a,r} = E_{a,f} - \Delta U_{\text{run}}$, $\Delta U_{\text{run}} = -28.52$ kcal mol⁻¹.
- k_2 A_f via A_r and Microscopic Reversibility (MR), $A_f = 3.615 \times 10^{12} = 1/2 (C_3H_6 + H$

→ CCC.), 91 TSA. $E_{\text{J,r}} = E_{\text{J,r}} + \Delta U_{\text{rnn}}$, $\Delta U_{\text{rnn}} = 30.52 \text{ kcal mol}^{-1}$ $E_{\text{J,r}} = 2.906 \text{ kcal mol}^{-1}$. (referenced as the same as the A_r).

k_3 90 TSA for C3C. → C2C=C + H

—
—

frequency/degeneracy (CPFIT)

C2C(OH)COO.. 270.0 (12.085); 1109.5 (16.601); 2859.8 (10.814)

C2.C(OH)COOH. 298.6 (13.666); 1139.6 (15.948); 2851.4 (9.386)

C2C(OH)C.OOH. 278.7 (13.932); 1159.7 (16.043); 2864.7 (9.025)

C2C(O.)COOH. 277.7 (12.704); 1121.3 (17.851); 2824.5 (8.945)

Lennard-Jones parameter

$\sigma(\text{\AA}) = 5.86$, $\epsilon/k(\text{K}) = 632.06$

- k_1 taken from 88 XI for $\text{C3CC.} + \text{O}_2 \rightarrow \text{C3CCOO.}$.
- k_{-1} A_r via A_f and Microscopic Reversibility (MR), $E_{a,r} = E_{a,f} - \Delta U_{\text{rxn}}$, $\Delta U_{\text{rxn}} = -31.71$ kcal mol⁻¹.
- k_2 A_f estimated using TST, $A = (\text{deg.}) A' T^n$, deg. = 2, $A' = 3.116 \times 10^9$, $n = 1.174$, A' and n are from thermal reaction analysis (AFACT2f) based on the thermodynamic properties calculated from MOPAC PM3 (corrected with internal rotor, electronic spin and optical isomer). $E_{a,f} = \text{RS (26)} + E_{\text{abst}} (9.76) + \Delta H_{\text{rxn}} (8.21)$ kcal mol⁻¹.
- k_{-2} A_r via A_f and Microscopic Reversibility (MR), $E_{a,r} = E_{a,f} - \Delta U_{\text{rxn}}$, $\Delta U_{\text{rxn}} = 8.21$ kcal mol⁻¹.
- k_3 A_f via A_r and Microscopic Reversibility (MR), $A_r = 2.75 \times 10^{12} = 1/2 (\text{OH} + \text{C}=\text{C})$. $E_{a,f}$ estimated the same 2.5 kcal mol⁻¹ as $E_{a,r}$ for $\text{CH}_2\text{OOH} \rightarrow \text{CH}_2\text{O} + \text{OH}$ (1990 Page)
- k_4 A_f via A_r and Microscopic Reversibility (MR), $A_r = 1.46 \times 10^{12} = 1/4 (\text{C}=\text{C} + \text{OH})$. $E_{a,f} = E_{a,r} + \Delta U_{\text{rxn}}$, $\Delta U_{\text{rxn}} = 36.05$ kcal mol⁻¹. $E_{a,r} = 0.5$ kcal mol⁻¹. (estimated by Bozzelli).
- k_5 A_f estimated using TST, $A = (\text{deg.}) A' T^n$, deg. = 6, $A' = 1.263 \times 10^8$, $n = 1.084$, A' and n are from thermal reaction analysis (AFACT2f) based on the thermodynamic properties calculated from MOPAC PM3 (corrected with internal rotor, electronic spin and optical isomer). $E_{a,f} = \text{RS (0)} + E_{\text{abst}} (8.14) + \Delta H_{\text{rxn}} (13.09)$ kcal mol⁻¹.
- k_{-5} A_r via A_f and Microscopic Reversibility (MR), $E_{a,r} = E_{a,f} - \Delta U_{\text{rxn}}$, $\Delta U_{\text{rxn}} = 13.09$ kcal mol⁻¹.
- k_6 A_f via A_r and Microscopic Reversibility (MR), $A_r = 9.64 \times 10^{10}$, 91 TSA for $\text{C}_3\text{H}_6 + \text{CH}_3 \rightarrow \text{C3.C}$. $E_{a,f} = E_{a,r} + \Delta U_{\text{rxn}}$, $\Delta U_{\text{rxn}} = 20.57$ kcal mol⁻¹. $E_{a,r} = 7.8$ kcal mol⁻¹. (estimated by Bozzelli).
- k_7 A_f via A_r and Microscopic Reversibility (MR), $A_r = 2.92 \times 10^{12}$, 91 TSA for $\text{C}_3\text{H}_6 + \text{OH} \rightarrow \text{Prod.}$. $E_{a,f} = E_{a,r} + \Delta U_{\text{rxn}}$, $\Delta U_{\text{rxn}} = 30.49$ kcal mol⁻¹. $E_{a,r} = 0.5$ kcal mol⁻¹. (estimated by Bozzelli).
- k_8 A_f estimated using TST, $A = (\text{deg.}) A' T^n$, deg. = 1, $A' = 4.253 \times 10^{10}$, $n = 0.183$, A' and n are from thermal reaction analysis (AFACT2f) based on the thermodynamic properties calculated from MOPAC PM3 (corrected with internal rotor, electronic spin and optical isomer). $E_{a,f}$ is estimated in this study.
- k_9 A_f estimated using TST, $A = (\text{deg.}) A' T^n$, deg. = 1, $A' = 7.559 \times 10^7$, $n = 1.062$, A' and n are from thermal reaction analysis (AFACT2f) based on the thermodynamic properties calculated from MOPAC PM3 (corrected with internal

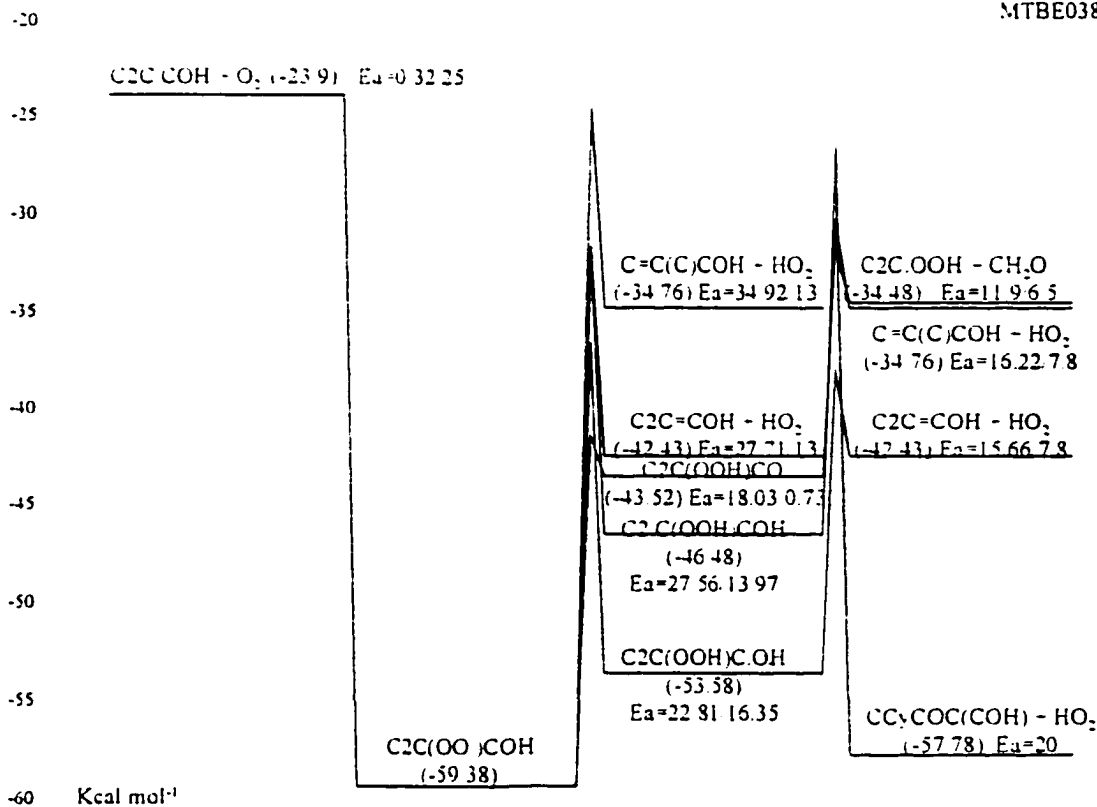
rotor, electronic spin and optical isomer). $E_{a,f} = RS(0) - E_{\text{bst}}(7.37) - 6(\text{H bond}) + \Delta H_{\text{ren}}(15.38) \text{ kcal mol}^{-1}$.

k_9 A_r via A_f and Microscopic Reversibility (MR), $E_{a,r} = E_{a,f} - \Delta U_{\text{ren}}$, $\Delta U_{\text{ren}} = 15.38 \text{ kcal mol}^{-1}$.

k_{10} A_f via A_r and Microscopic Reversibility (MR), $A_r = 3.16 \times 10^{11}$, Bozzelli. $E_{a,f} = E_{a,r} + \Delta U_{\text{ren}}$, $\Delta U_{\text{ren}} = 4.10 \text{ kcal mol}^{-1}$. $E_{a,r} = 6.5 \text{ kcal mol}^{-1}$. (estimated by Bozzelli).

IID. 16 C2C.CO₂H + O₂ → Products

MTBE038



Reaction		A T ⁿ e ^{-αT} (s ⁻¹ or cm ³ mol ⁻¹ s ⁻¹)	E _a (kcal mol ⁻¹)
k ₁	C2C.CO ₂ H + O ₂ → C2C(OO)COH	1.81×10 ¹² T ⁰ e ^{-0T}	0.00
k ₋₁	C2C(OO)COH → C2C.CO ₂ H + O ₂	1.02×10 ¹⁵ T ⁰ e ^{-0T}	32.25
k ₂	C2C(OO)COH → C=C(C)COH + HO ₂	1.73×10 ¹¹ T ^{1.22} e ^{-0T}	34.92
k ₃	C2C(OO)COH → C2C=COH + HO ₂	5.75×10 ¹⁰ T ^{1.22} e ^{-0T}	27.71
k ₄	C2C(OO)COH → C2C(OOH)C.OH	4.66×10 ⁸ T ^{1.36} e ^{-0T}	22.81
k ₋₄	C2C(OOH)C.OH → C2C(OO)COH	1.44×10 ¹¹ T ^{-0.05} e ^{-0.00093T}	16.35
k ₅	C2C(OOH)C.OH → C2C=COH + HO ₂	3.18×10 ¹¹ T ⁰ e ^{-0T}	15.66
k ₆	C2C(OO)COH → C2C(OOH)COH	2.30×10 ¹⁰ T ^{1.07} e ^{-0T}	27.56
k ₋₆	C2C(OOH)COH → C2C(OO)COH	1.03×10 ¹² T ^{-0.33} e ^{-0.0009T}	13.97
k ₇	C2C(OOH)COH → C=C(C)COH + HO ₂	2.09×10 ¹³ T ⁰ e ^{-0T}	16.22
k ₈	C2C(OOH)COH → CC ₂ COC(COH) + OH	4.68×10 ¹¹ T ⁰ e ^{-0T}	20.00
k ₉	C2C(OO)COH → C2C(OOH)CO	4.22×10 ⁷ T ^{1.18} e ^{-0T}	18.03
k ₋₉	C2C(OOH)CO → C2C(OO)COH	1.70×10 ¹¹ T ^{-0.18} e ^{-0.00019T}	0.73
k ₁₀	C2C(OOH)CO → C2C.OOH + CH ₂ O	8.22×10 ¹³ T ⁰ e ^{-0T}	11.90

frequency/degeneracy (CPFIT)

C2C(OO.)COH: 291.4 (12.538); 1135.9 (16.437); 2997.8 (10.525)

C2.C(OOH)COH: 312.6 (14.003); 1162.7 (15.884); 3008.3 (9.113)

C2C(OOH)C OH: 309.2 (14.390); 1147.0 (15.883); 3022.3 (8.727)

C2C(OOH)CO.: 295.9 (13.107); 1144.8 (17.750); 2992.0 (8.643)

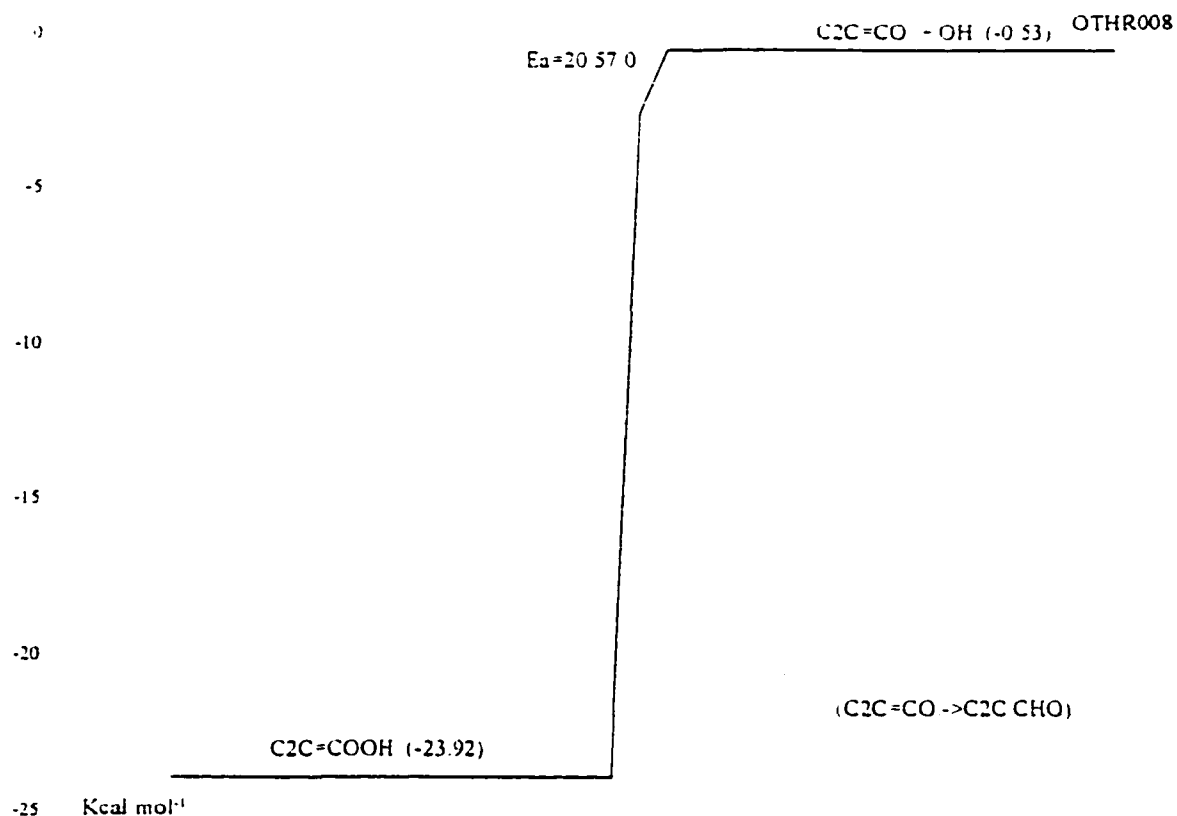
Lennard-Jones parameter

$\sigma(\text{\AA}) = 5.86$, $\varepsilon/k(\text{K}) = 632.06$

- k_1 92 WAL/AND for $\text{C3C.} + \text{O}_2 \rightarrow \text{C3COO.}$
- k_{-1} A_r via A_f and Microscopic Reversibility (MR), $E_{a,r} = E_{a,f} - \Delta U_{\text{rxn}}$, $\Delta U_{\text{rxn}} = -32.25$ kcal mol⁻¹.
- k_2 A_f estimated using TST, $A = (\text{deg.}) A' T^n$, deg. = 6, $A' = 2.876 \times 10^{10}$, $n = 1.22$, A' and n are from thermal reaction analysis (AFACT2f) based on the thermodynamic properties calculated from MOPAC PM3 (corrected with internal rotor, electronic spin and optical isomer). $E_{a,f}$ via $E_{a,r} + \Delta U_{\text{rxn}}$, $E_{a,r}$ is estimated as 13 kcal mol⁻¹ in this study, $\Delta U_{\text{rxn}} = 21.92$ kcal mol⁻¹.
- k_3 A_f estimated using TST, $A = (\text{deg.}) A' T^n$, deg. = 2, $A' = 2.876 \times 10^{10}$, $n = 1.22$, A' and n are from thermal reaction analysis (AFACT2f) based on the thermodynamic properties calculated from MOPAC PM3 (corrected with internal rotor, electronic spin and optical isomer). $E_{a,f}$ via $E_{a,r} + \Delta U_{\text{rxn}}$, $E_{a,r}$ is estimated as 13 kcal mol⁻¹ in this study, $\Delta U_{\text{rxn}} = 14.71$ kcal mol⁻¹.
- k_4 A_f estimated using TST, $A = (\text{deg.}) A' T^n$, deg. = 2, $A' = 2.328 \times 10^8$, $n = 1.358$, A' and n are from thermal reaction analysis (AFACT2f) based on the thermodynamic properties calculated from MOPAC PM3 (corrected with internal rotor, electronic spin and optical isomer). $E_{a,f} = \text{RS}(6) + E_{\text{abst}}(10.35) + \Delta H_{\text{rxn}}(6.46)$ kcal mol⁻¹.
- k_{-4} A_r via A_f and Microscopic Reversibility (MR), $E_{a,r} = E_{a,f} - \Delta U_{\text{rxn}}$, $\Delta U_{\text{rxn}} = 6.46$ kcal mol⁻¹.
- k_5 A_f via A_r and Microscopic Reversibility (MR), $A_r = 2.5 \times 10^{11} = 1/2(\text{C}=\text{C} + \text{HO}_2)$, 72 KER/PAR. $E_{a,f} = E_{a,r} + \Delta U_{\text{rxn}}$, $\Delta U_{\text{rxn}} = 7.86$ kcal mol⁻¹. $E_{a,r} = 7.8$ kcal mol⁻¹. (estimated by Bozzelli).
- k_6 A_f estimated using TST, $A = (\text{deg.}) A' T^n$, deg. = 6, $A' = 3.836 \times 10^9$, $n = 1.071$, A' and n are from thermal reaction analysis (AFACT2f) based on the thermodynamic properties calculated from MOPAC PM3 (corrected with internal rotor, electronic spin and optical isomer). $E_{a,f} = \text{RS}(6) + E_{\text{abst}}(7.97) + \Delta H_{\text{rxn}}(13.59)$ kcal mol⁻¹.
- k_{-6} A_r via A_f and Microscopic Reversibility (MR), $E_{a,r} = E_{a,f} - \Delta U_{\text{rxn}}$, $\Delta U_{\text{rxn}} = 13.59$ kcal mol⁻¹.
- k_7 A_f via A_r and Microscopic Reversibility (MR), $A_r = 3.5 \times 10^{11}$, Bozzelli. $E_{a,f} = E_{a,r} + \Delta U_{\text{rxn}}$, $\Delta U_{\text{rxn}} = 8.42$ kcal mol⁻¹. $E_{a,r} = 7.8$ kcal mol⁻¹. (estimated by Bozzelli).
- k_8 A_f estimated using TST, $A = (\text{deg.}) (ek_b T/h) \exp(\Delta S^\ddagger(T)/R)$, deg. = 1, $ek_b T/h = 10^{13.55}$, $\Delta S^\ddagger(T)$ is estimated as loss of two rotors (-4.3×2 cal mol⁻¹ K⁻¹). $E_{a,f}$ is evaluated in this study.

- k₉ A_f estimated using TST, $A = (\text{deg.}) A' T^n$, $\text{deg.} = 1$, $A' = 4.217 \times 10^7$, $n = 1.184$, A' and n are from thermal reaction analysis (AFACT2f) based on the thermodynamic properties calculated from MOPAC PM3 (corrected with internal rotor, electronic spin and optical isomer). $E_{a,f} = RS(0) + E_{\text{bst}}(6.73) - 6(\text{H bond}) + \Delta H_{\text{rxn}}(17.30) \text{ kcal mol}^{-1}$.
- k₉ A_f via A_r and Microscopic Reversibility (MR), $E_{a,f} = E_{a,r} - \Delta U_{\text{rxn}}$, $\Delta U_{\text{rxn}} = 17.30 \text{ kcal mol}^{-1}$.
- k₁₀ A_f via A_r and Microscopic Reversibility (MR), $A_r = 2.41 \times 10^{10} = 1/2 (\text{CH}_2\text{OH} + \text{C}=\text{C} \rightarrow \text{C CCOH})$, 87 TSA. $E_{a,f} = E_{a,r} + \Delta U_{\text{rxn}}$, $\Delta U_{\text{rxn}} = 5.40 \text{ kcal mol}^{-1}$. $E_{a,r} = 6.5 \text{ kcal mol}^{-1}$. (estimated by Bozzelli).

IID. 17 $\text{C2C=COOH} \rightarrow \text{C2C.CHO} (\text{C2C=CO.}) + \text{OH}$



Reaction		$A T^n e^{-a/T}$ (s^{-1} or $\text{cm}^3 \text{mol}^{-1} \text{s}^{-1}$)	E_a (kcal mol^{-1})
k_1	$\text{C2C=COOH} \rightarrow \text{C2C=CO.} + \text{OH}$	$1.56 \times 10^{15} T^0 e^{-u/T}$	20.57

frequency/degeneracy (CPFIT)

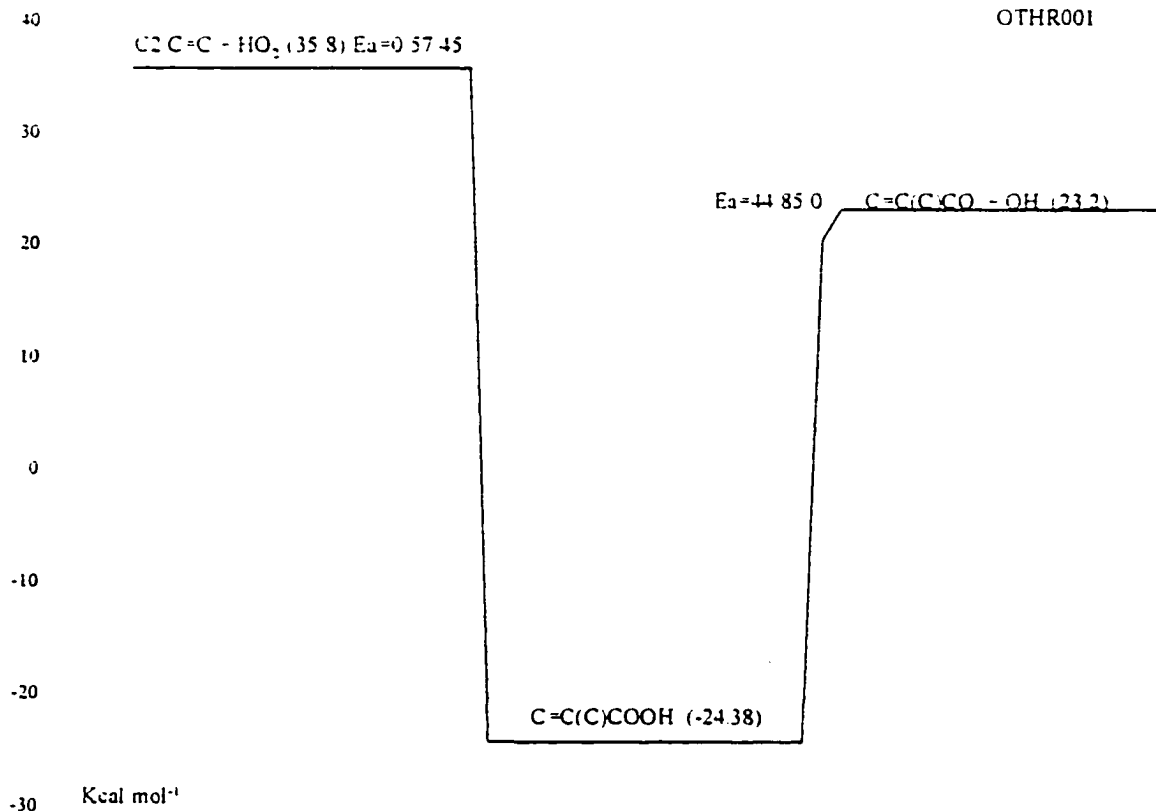
C2C=COOH : 337.9 (11.813); 1223.0 (14.753); 2824.6 (7.434)

Lennard-Jones parameter

$\sigma(\text{\AA}) = 5.55$, $\epsilon/k (\text{K}) = 584.86$

k_1 A_f via A_r and Microscopic Reversibility (MR), $A_r = 1.51 \times 10^{13}$, 91 TSA for $\text{C=CC.} + \text{OH}$. $E_{a,f} = \Delta U_{\text{rxn}} = 20.57 \text{ kcal mol}^{-1}$.

IID. 18 $\text{C2.C=C} + \text{HO}_2 \rightarrow \text{C=C(C)COOH} \rightarrow \text{C=C(C)CO.} + \text{OH}$



	Reaction	$A T^n e^{-a/T}$ (s ⁻¹ or cm ³ mol ⁻¹ s ⁻¹)	E_a (kcal mol ⁻¹)
k_1	$\text{C2.C=C} + \text{HO}_2 \rightarrow \text{C=C(C)COOH}$	$1.00 \times 10^{13} T^0 e^{-0/T}$	0.00
k_{-1}	$\text{C=C(C)COOH} \rightarrow \text{C2.C=C} + \text{HO}_2$	$1.67 \times 10^{15} T^0 e^{-0/T}$	57.45
k_2	$\text{C=C(C)COOH} \rightarrow \text{C=C(C)CO.} + \text{OH}$	$1.66 \times 10^{15} T^0 e^{-0/T}$	44.85

frequency/degeneracy (CPFIT)

C=C(C)COOH : 250.9 (10.249); 1109.7 (14.976); 2777.4 (8.775)

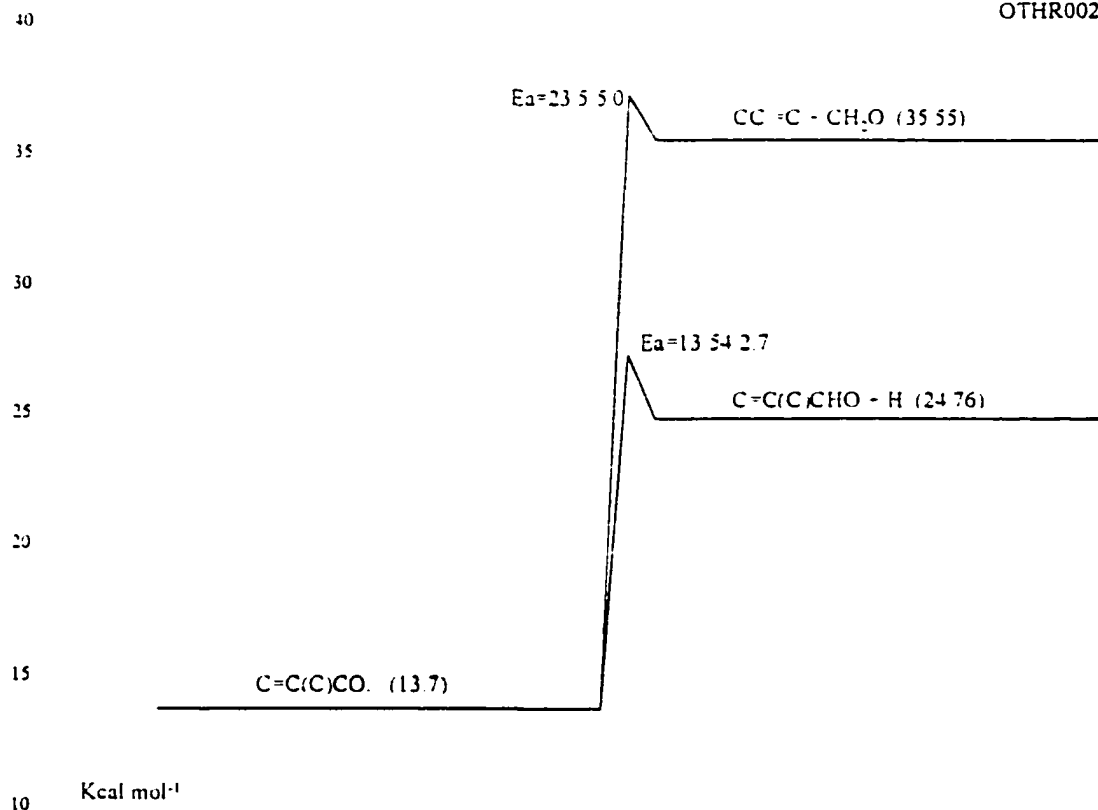
Lennard-Jones parameter

$\sigma(\text{\AA}) = 5.54$, $\epsilon/k(\text{K}) = 584.86$

- k_1 A_f estimated as $1/2 (\text{CH}_3 + \text{HO}_2 \rightarrow \text{CH}_3\text{O} + \text{OH})$.
- k_{-1} A_r via A_f and Microscopic Reversibility (MR), $E_{a,r} = E_{a,f} - \Delta U_{\text{rxn}}$, $\Delta U_{\text{rxn}} = -57.45$ kcal mol⁻¹.
- k_2 A_f via A_r and Microscopic Reversibility (MR), $A_r = 1.81 \times 10^{13}$, taken as the same as A for $\text{CH}_3\text{O} + \text{OH}$. $E_{a,f} = \Delta U_{\text{rxn}} = 44.85$ kcal mol⁻¹.

IID. 19 C=C(C)CO. → Products

OTHR002



Reaction		$A T^n e^{-u/T}$ (s ⁻¹ or cm ³ mol ⁻¹ s ⁻¹)	E _a (kcal mol ⁻¹)
k ₁	C=C(C)CO. → CC=C + CH ₂ O	$1.54 \times 10^{13} T^0 e^{-0/T}$	23.50
k ₂	C=C(C)CO. → C=C(C)CHO + H	$4.18 \times 10^{12} T^0 e^{-0/T}$	13.54

frequency/degeneracy (CPFIT)

C=C(C)CO.: 468.5 (11.349); 1549.9 (12.883); 3526.8 (4.768)

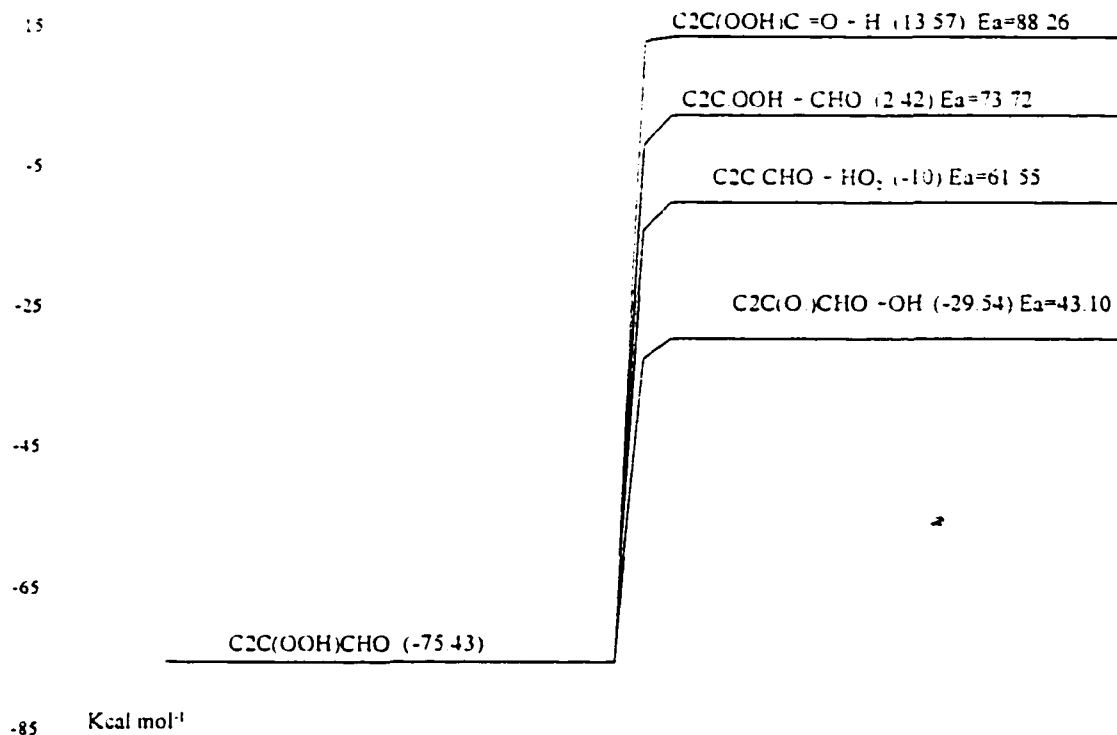
Lennard-Jones parameter

 $\sigma(\text{\AA}) = 5.20$, ϵ/k (K) = 533.08

- k₁ A_r via A_r and Microscopic Reversibility (MR), A_r = 1.81×10^{13} , taken as the same as A for CC=C + CH₂O → CCC + CHO. E_{a,f} = E_{a,r} + ΔU_{rxn}, ΔU_{rxn} = 18.5 kcal mol⁻¹. E_{a,r} = 5.0 kcal mol⁻¹. (estimated in this study).
- k₂ A_r via A_r and Microscopic Reversibility (MR), A_r = 5.00×10^{12} = 1/2 (H + C=C). E_{a,f} = E_{a,r} + ΔU_{rxn}, ΔU_{rxn} = 10.84 kcal mol⁻¹. E_{a,r} = 2.7 kcal mol⁻¹. (estimated based on 84 WAR for H + CC=C → CCC.).

IID. 20 C2C(OOH)CHO → Products

OTHR005



	Reaction	$A T^n e^{-E_a/T}$ (s⁻¹ or cm³ mol⁻¹ s⁻¹)	E_a (kcal mol⁻¹)
k ₁	C2C(OOH)CHO → C2C(OOH) + CHO	$3.35 \times 10^{17} T^0 e^{-0/T}$	73.72
k ₂	C2C(OOH)CHO → C2C(OH) + HO ₂	$3.45 \times 10^{15} T^0 e^{-0/T}$	61.55
k ₃	C2C(OOH)CHO → C2C(OOH)C=O + H	$1.02 \times 10^{15} T^0 e^{-0/T}$	88.26
k ₄	C2C(OOH)CHO → C2C(O)CHO + OH	$1.06 \times 10^{15} T^0 e^{-0/T}$	43.10

frequency/degeneracy (CPFIT)

C2C(OOH)CHO: 251.1 (10.745); 1069.7 (17.622); 2476.7 (8.133)

Lennard-Jones parameter

 $\sigma(\text{\AA}) = 5.86$, $\epsilon/k(\text{K}) = 632.06$

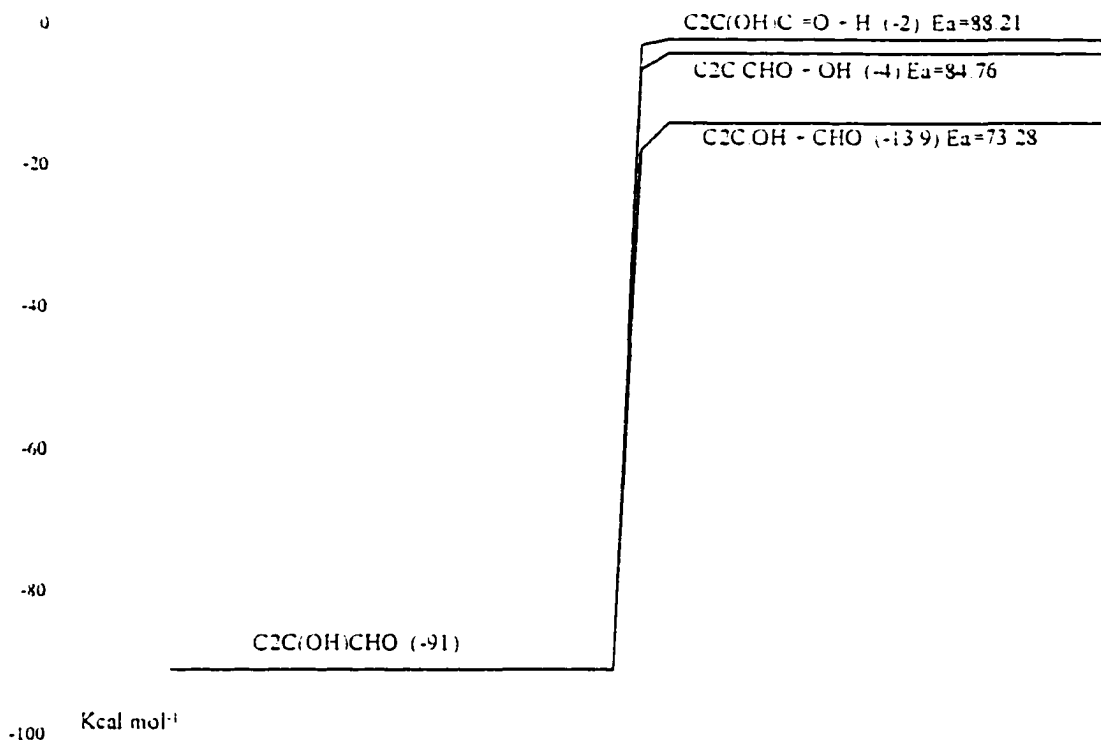
- k₁ A_f via A_r and Microscopic Reversibility (MR), A_r = 1.81 × 10¹³, 88 TSA for CC.C + CHO → C2CCHO. E_{a,f} = ΔU_{rxn} = 73.72 kcal mol⁻¹.
- k₂ A_f via A_r and Microscopic Reversibility (MR), A_r = 1.00 × 10¹³ = 1/2 (HO₂ + CH₃). E_{a,f} = ΔU_{rxn} = 61.55 kcal mol⁻¹.
- k₃ A_f via A_r and Microscopic Reversibility (MR), A_r = 5.00 × 10¹³ 1/2 (H + CHO),

NIST FIT. $E_{a,f} = E_{a,f}(0) + \Delta U_{\text{rot}}(88.26) \text{ kcal mol}^{-1}$.

k_4 A_f via A_r and Microscopic Reversibility (MR), $A_r = 1.51 \times 10^{13}$, 92 BAU/COB for $\text{CH}_3\text{O} + \text{O}$, $E_{a,f} = E_{a,f}(0) + \Delta U_{\text{rot}}(43.10) \text{ kcal mol}^{-1}$

IID. 21 C2C(OH)CHO → Products

OTHR006



	Reaction	$A T^n e^{-\alpha/T}$ (s ⁻¹ or cm ³ mol ⁻¹ s ⁻¹)	E_a (kcal mol ⁻¹)
k ₁	C2C(OH)CHO → C2C.OH + CHO	$4.48 \times 10^{17} T^0 e^{-0/T}$	73.28
k ₂	C2C(OH)CHO → C2C.CHO + OH	$2.75 \times 10^{15} T^0 e^{-0/T}$	84.76
k ₂	C2C(OH)CHO → C2C(OH)C.=O + H	$9.83 \times 10^{14} T^0 e^{-0/T}$	88.21

frequency/degeneracy (CPFIT)

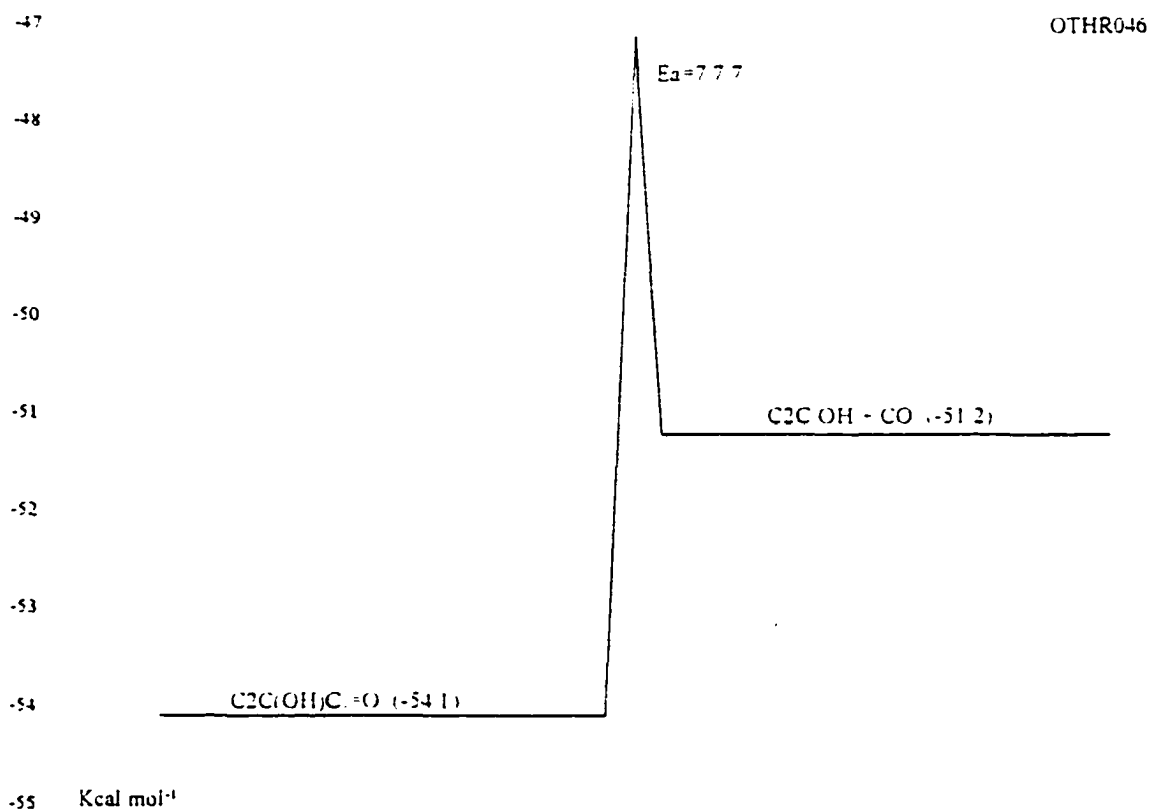
C2C(OH)CHO: 417.6 (12.380); 1378.6 (16.307); 3379.2 (5.313)

Lennard-Jones parameter

 $\sigma(\text{\AA}) = 5.55$, ϵ/k (K) = 584.86

- k₁ A_r via A_r and Microscopic Reversibility (MR), A_r = 1.81×10^{13} , 88 TSA for CC.C + CHO → C2CCHO. E_{a,r} = ΔU_{rxn} = 73.28 kcal mol⁻¹.
- k₂ A_r via A_r and Microscopic Reversibility (MR), A_r = 7.55×10^{12} = 1/2 (OH + C=CC.), 86 TSA. E_{a,r} = ΔU_{rxn} = 84.76 kcal mol⁻¹.
- k₃ A_r via A_r and Microscopic Reversibility (MR), A_r = 5.00×10^{13} 1/2 (H + CHO), NIST FIT. E_{a,r} = E_{a,r}(0) + ΔU_{rxn} (88.21) kcal mol⁻¹.

IID. 22 $\text{C}_2\text{C}(\text{OH})\text{C}=\text{O} \rightarrow \text{C}_2\text{C.OH} + \text{CO}$



	Reaction	$A T^n e^{-u/T}$	E_a
		(s ⁻¹ or cm ³ mol ⁻¹ s ⁻¹)	(kcal mol ⁻¹)
k ₁	$\text{C}_2\text{C}(\text{OH})\text{C}=\text{O} \rightarrow \text{C}_2\text{C.OH} + \text{CO}$	$7.22 \times 10^{13} T^0 e^{-0/T}$	7.00

frequency/degeneracy (CPFIT)

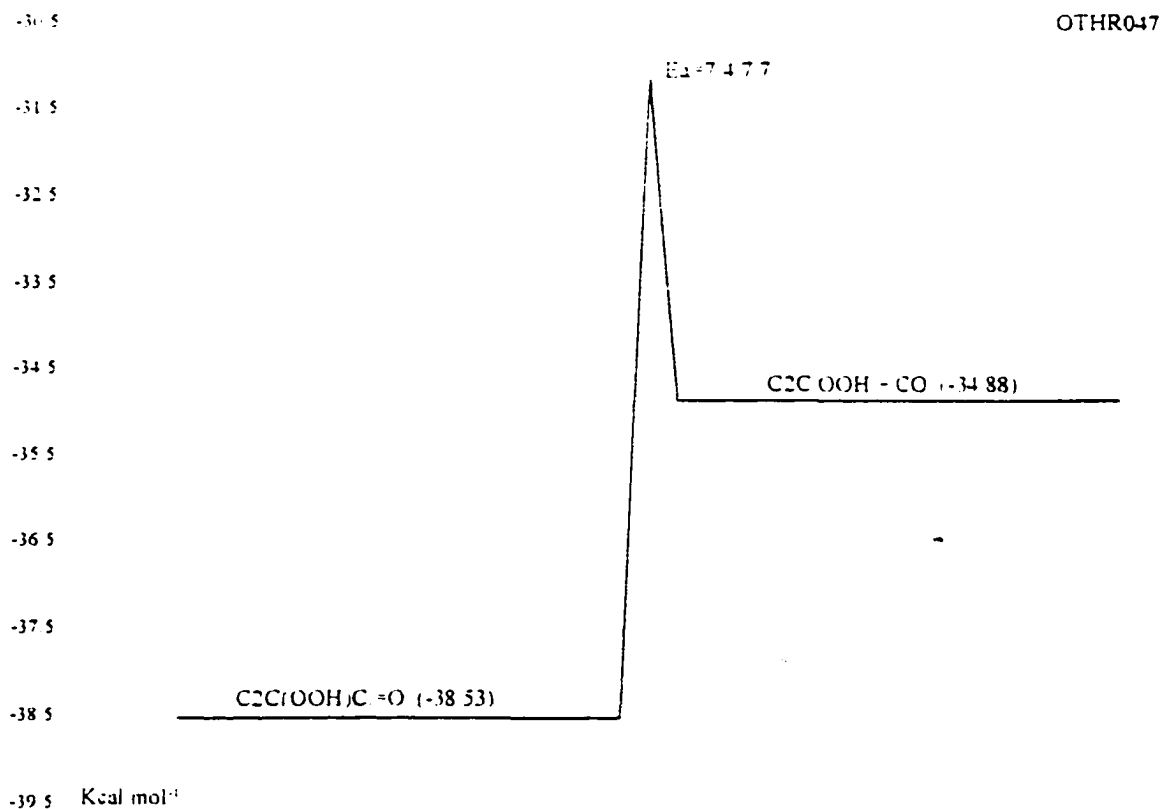
$\text{C}_2\text{C}(\text{OH})\text{C}=\text{O}$: 412.6 (11.980); 1408.4 (14.872); 3549.7 (4.148)

Lennard-Jones parameter

$\sigma(\text{\AA}) = 5.55$, $\epsilon/k(\text{K}) = 584.86$

k₁ A_f via A_r and Microscopic Reversibility (MR), A_r = 1.00×10^{11} , 72 KER/PAR for $\text{C}_3\text{C} + \text{C}_2\text{H}_2$. $E_{a,f} = E_{a,r}(7.7) + \Delta U_{\text{rm}}(-0.68)$ kcal mol⁻¹.

IID. 23 $\text{C}_2\text{C}(\text{OOH})\text{C}=\text{O} \rightarrow \text{C}_2\text{C}.\text{OOH} + \text{CO}$



	Reaction	$A T^n e^{-\alpha/T}$	E_a
		(s ⁻¹ or cm ³ mol ⁻¹ s ⁻¹)	(kcal mol ⁻¹)
k ₁	$\text{C}_2\text{C}(\text{OOH})\text{C}=\text{O} \rightarrow \text{C}_2\text{C}.\text{OOH} + \text{CO}$	$5.23 \times 10^{13} T^0 e^{-\alpha/T}$	7.40

frequency/degeneracy (CPFIT)

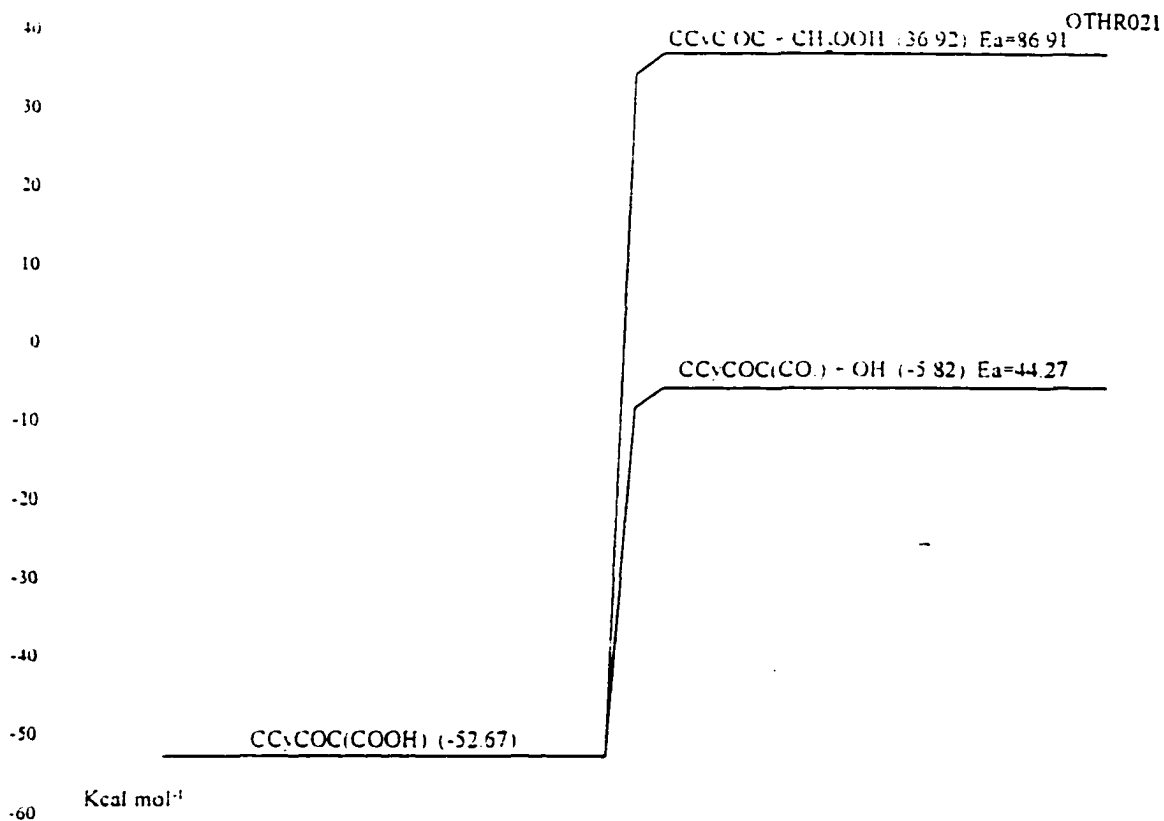
$\text{C}_2\text{C}(\text{OOH})\text{C}=\text{O}$: 250.0 (10.700); 1079.7 (15.893); 2400.1 (6.907)

Lennard-Jones parameter

$\sigma(\text{\AA}) = 5.86$, $\epsilon/k(\text{K}) = 632.06$

k₁ A_f via A_r and Microscopic Reversibility (MR), $A_r = 1.00 \times 10^{11}$, 72 KER/PAR for $\text{C}_3\text{C} + \text{C}_2\text{H}_2$. $E_{a,f} = E_{a,r}(7.7) + \Delta U_{\text{rxn}}(-0.29)$ kcal mol⁻¹.

IID. 24 CCyCOC(COOH) → Products



	Reaction	$A T^n e^{-\alpha T}$	E_a
		(s^{-1} or $cm^3 mol^{-1} s^{-1}$)	($kcal mol^{-1}$)
k_1	$CCyCOC(COOH) \rightarrow CCyC OC + CH_2OOH$	$8.02 \times 10^{16} T^0 e^{-0.7T}$	86.91
k_2	$CCyCOC(COOH) \rightarrow CCyCOC(CO) + OH$	$1.98 \times 10^{15} T^0 e^{-0.7T}$	44.27

frequency/degeneracy (CPFIT)

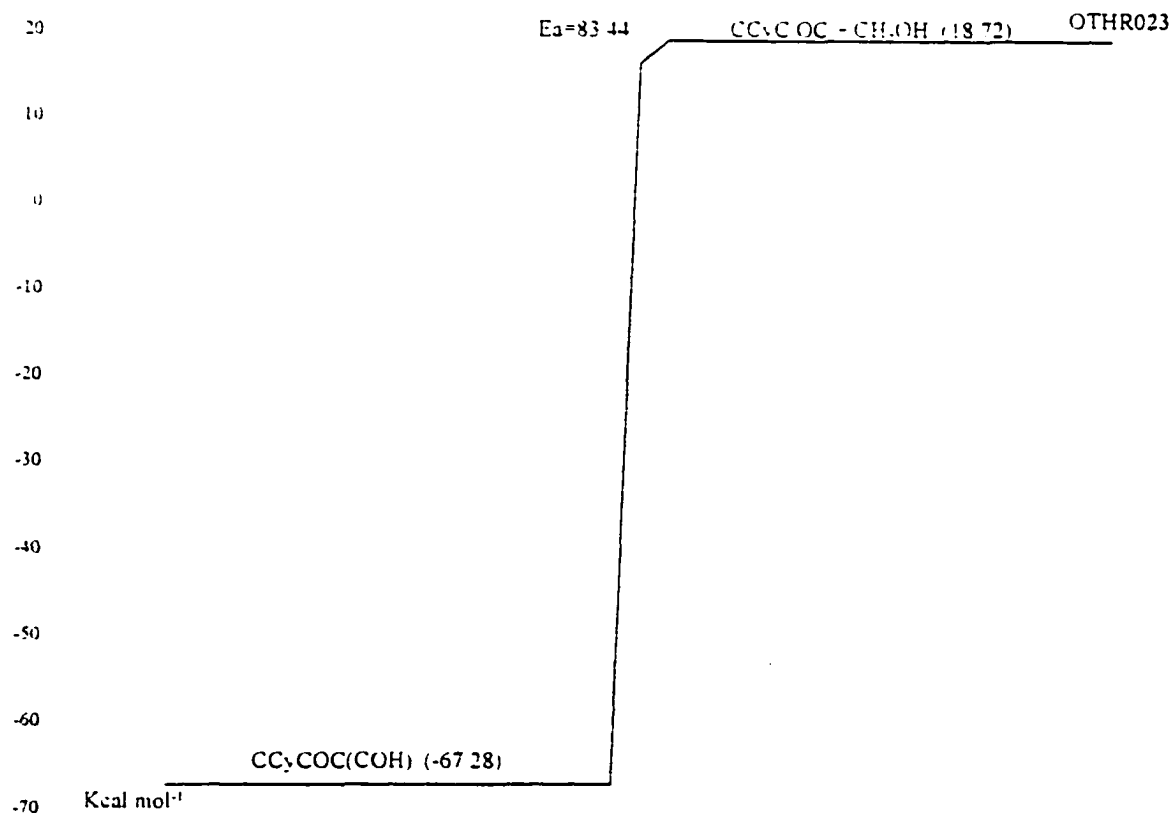
CCyCOC(COOH): 250.9 (9.960); 1066.2 (19.075); 2811.3 (7.964)

Lennard-Jones parameter

$\sigma(\text{\AA}) = 5.86$, $\epsilon/k (K) = 632.06$

- k_1 A_f via A_r and Microscopic Reversibility (MR), $A_r = 1.00 \times 10^{12} = 1/3$ (C3C. + CH₂OH), 91 TSA. $E_{a,f} = \Delta U_{rxn} = 86.91 kcal mol^{-1}$.
- k_2 A_f via A_r and Microscopic Reversibility (MR), $A_r = 1.51 \times 10^{13}$, 91 TSA for OH + C=CC.. $E_{a,f} = \Delta U_{rxn} = 44.27 kcal mol^{-1}$.

IID. 25 CCyCOC(COH) → Products



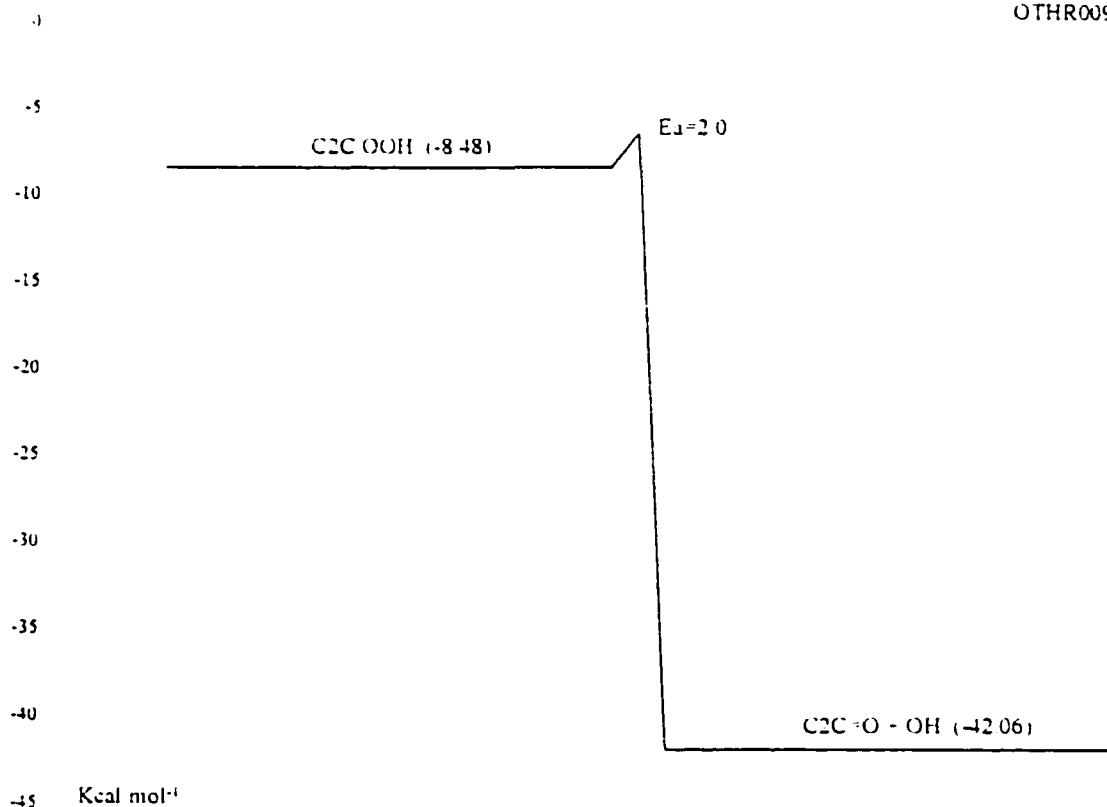
	Reaction	$A T^n e^{-\alpha T}$	E_a
		(s ⁻¹ or cm ³ mol ⁻¹ s ⁻¹)	(kcal mol ⁻¹)
k ₁	CCyCOC(COH) → CCyC OC + CH ₂ OH	$5.98 \times 10^{16} T^0 e^{-0.7T}$	83.44

frequency/degeneracy (CPFIT)
 CCyCOC(COH): 479.0 (12.212); 1268.8 (14.955); 3148.6 (7.334)
 Lennard-Jones parameter
 $\sigma(\text{\AA}) = 5.55$, $\epsilon/k(\text{K}) = 584.86$

k₁ A_f via A_r and Microscopic Reversibility (MR), A_r = 1.51×10^{12} = 1/2 (C3C. + CH₂OH), 91 TSA. E_{a,f} = ΔU_{rxn} = 83.44 kcal mol⁻¹.

IID. 26 C2C.OOH \rightarrow C2C=O + OH

OTHR009



Reaction		$A T^n e^{-\alpha T}$ (s ⁻¹ or cm ³ mol ⁻¹ s ⁻¹)	E_a (kcal mol ⁻¹)
k_1	C2C.OOH \rightarrow C2C=O + OH	$4.48 \times 10^{12} T^0 e^{-0T}$	2.00

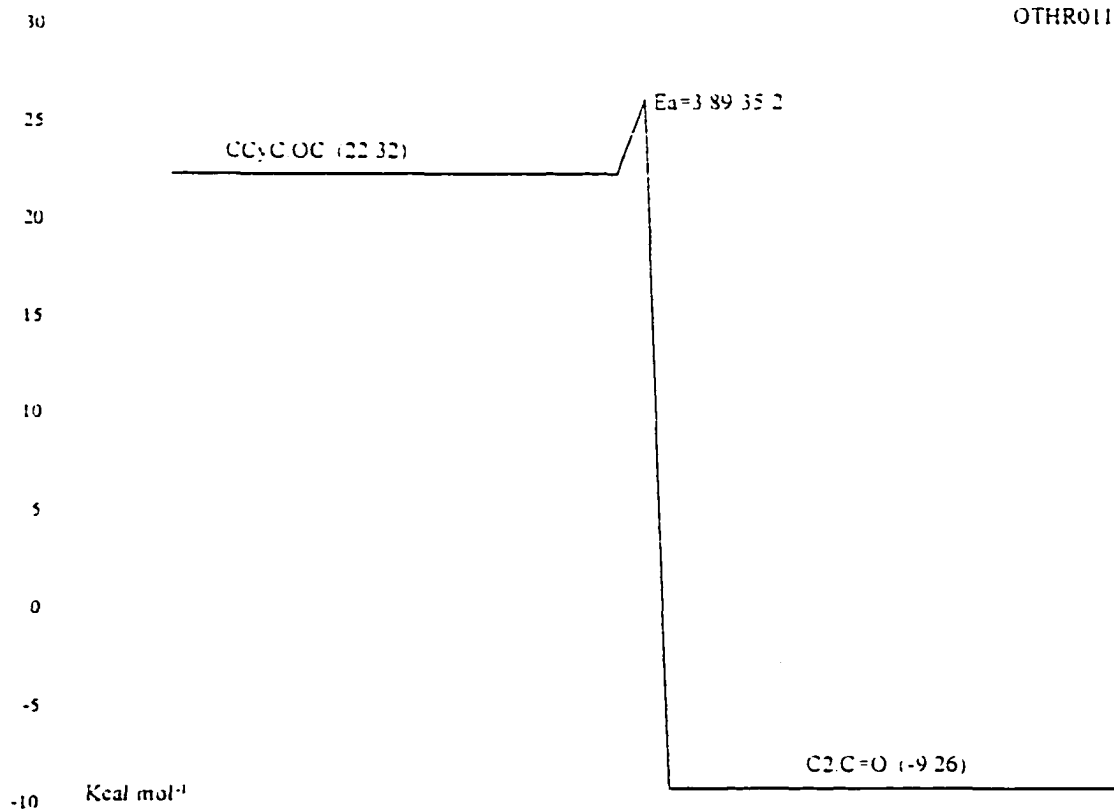
frequency/degeneracy (CPFIT)

C2C.OOH: 100.3 (7.507); 1069.9 (12.133); 2730.8 (8.360)

Lennard-Jones parameter

 $\sigma(\text{\AA}) = 5.20$, $\epsilon/k(\text{K}) = 533.08$

k_1 A_f via A_r and Microscopic Reversibility (MR), $A_r = 2.75 \times 10^{12} = 1/2 (\text{OH} + \text{C}=\text{C})$.
 $E_{a,f}$ estimated the same 2.0 kcal mol⁻¹ based on $E_{a,r}$ for CH₂OOH \rightarrow CH₂O + OH
 (1990 Page)

IID. 27 CCyC.OC \rightarrow C2.C=O

Reaction		$A T^n e^{-a/T}$ (s^{-1} or $cm^3 mol^{-1} s^{-1}$)	E_a ($kcal mol^{-1}$)
k_1	CCyC.OC \rightarrow C2.C=O	$1.73 \times 10^{13} T^{1.0} e^{-0/T}$	3.89

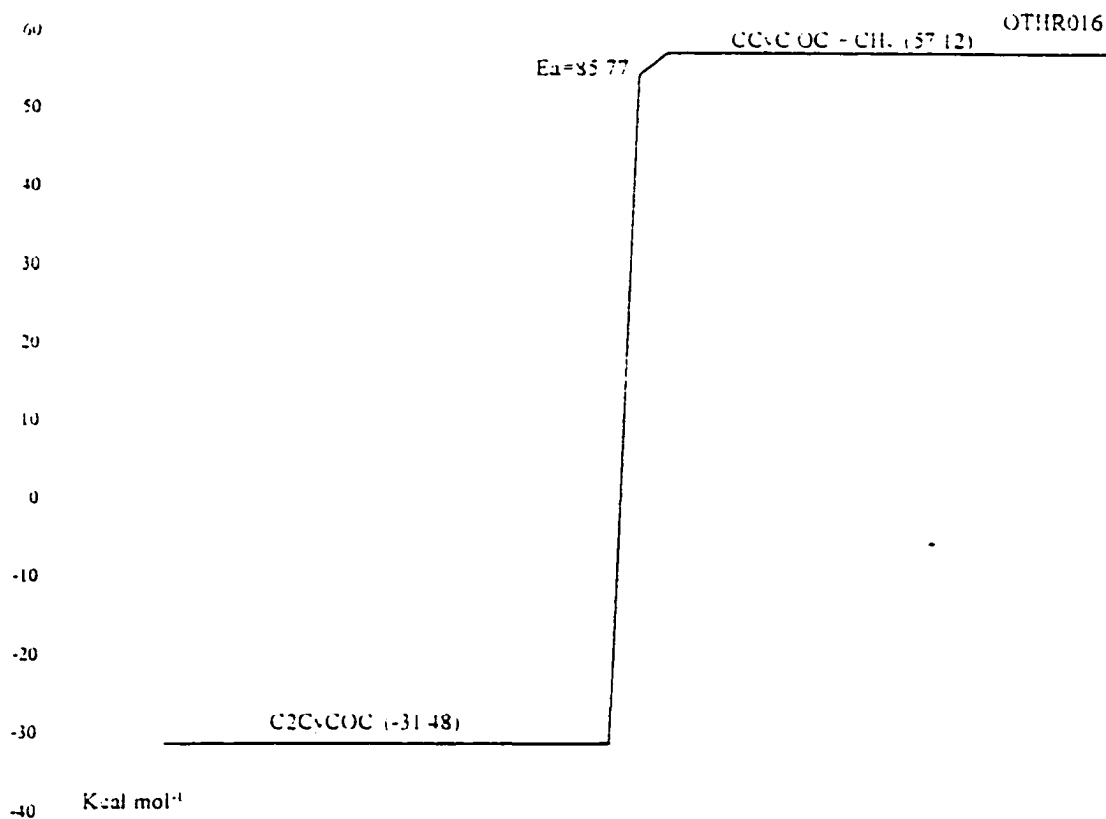
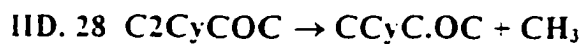
frequency/degeneracy (CPFIT)

CCyC.OC: 250.1 (3.28); 1087.9 (11.744); 2928.9 (5.476)

Lennard-Jones parameter

 $\sigma(\text{\AA}) = 4.80$, ϵ/k (K) = 481.73

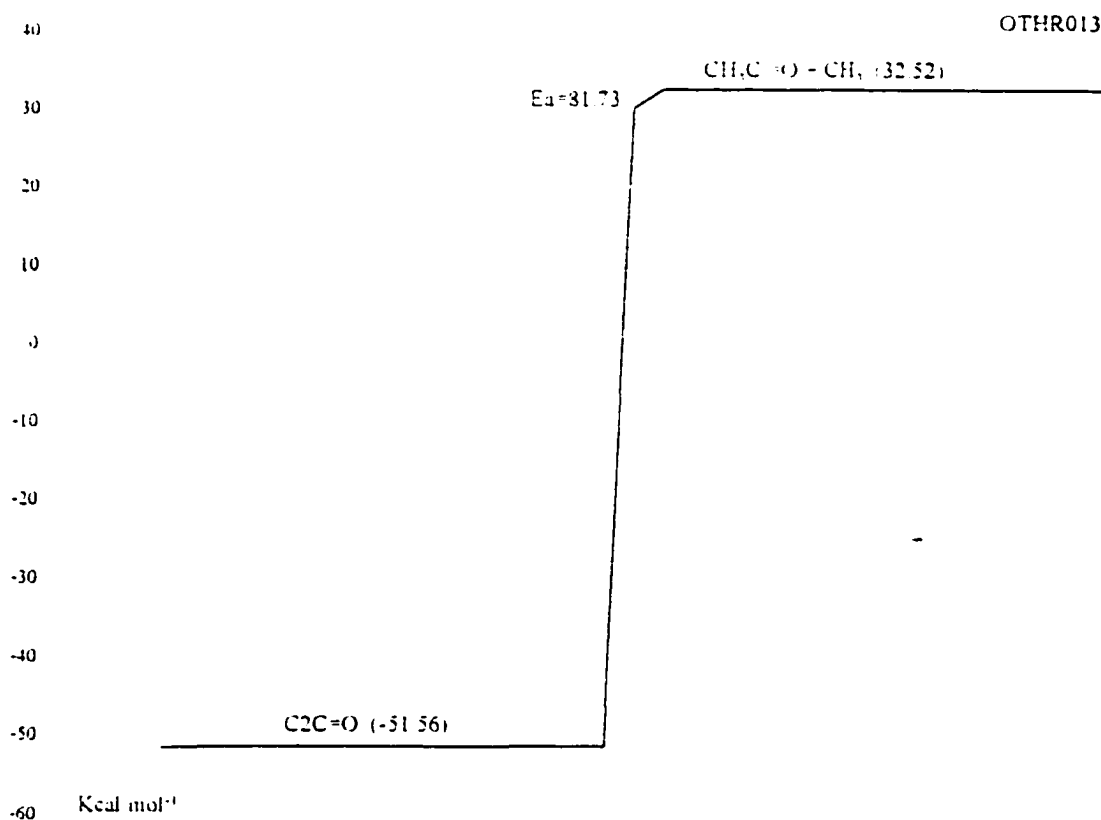
- k_1 A_f via A_r and Microscopic Reversibility (MR), A_r estimated using TST, $A = (\text{deg.}) (ek_b T/h) \exp(\Delta S^\ddagger(T)/R)$, $\text{deg.} = 1$, $ek_b T/h = 10^{13.55} ?$, $\Delta S^\ddagger(T)$ is estimated as loss of one rotor ($-4.3 \text{ cal mol}^{-1} \text{ K}^{-1}$). $E_{a,f} = E_{a,r} + \Delta U_{\text{rxn}}$, $\Delta U_{\text{rxn}} = -31.31 \text{ kcal mol}^{-1}$, $E_{a,r}$ estimated as ring strain difference plus considered addition to C=O double bond.



Reaction		$A T^n e^{-aT}$ (s^{-1} or $\text{cm}^3 \text{mol}^{-1} \text{s}^{-1}$)	E_a (kcal mol^{-1})
k_1	$\text{C2CyCOC} \rightarrow \text{CCyC.OC} + \text{CH}_3$	$2.02 \times 10^{17} T^0 e^{-0T}$	85.77

frequency/degeneracy (CPFIT)
 C2CyCOC : 469.6 (9.195) 1197.2 (15.095) 2986.5 (7.709)
 Lennard-Jones parameter
 $\sigma(\text{\AA}) = 5.20$, $\epsilon/k (\text{K}) = 533.08$

k_1 A_f via A_r and Microscopic Reversibility (MR), $A_r = 1.63 \times 10^{13}$, 90 TSA for $\text{C3C} + \text{CH}_3 \rightarrow \text{neo-C5}$. $E_{a,f} = E_{a,r} + \Delta U_{\text{rxn}}$, $\Delta U_{\text{rxn}} = 85.77 \text{ kcal mol}^{-1}$. $E_{a,r} = 0 \text{ kcal mol}^{-1}$ (estimated by Bozzelli).

IID. 29 $\text{C}_2\text{C}=\text{O} \rightarrow \text{CH}_3\text{C}=\text{O}$ 

Reaction		$A T^n e^{-\alpha/T}$ (s ⁻¹ or cm ³ mol ⁻¹ s ⁻¹)	E_a (kcal mol ⁻¹)
k_1	$\text{C}_2\text{C}=\text{O} \rightarrow \text{CH}_3\text{C}=\text{O}$	$4.54 \times 10^{18} T^{-0.27} e^{-0.00215/T}$	81.73

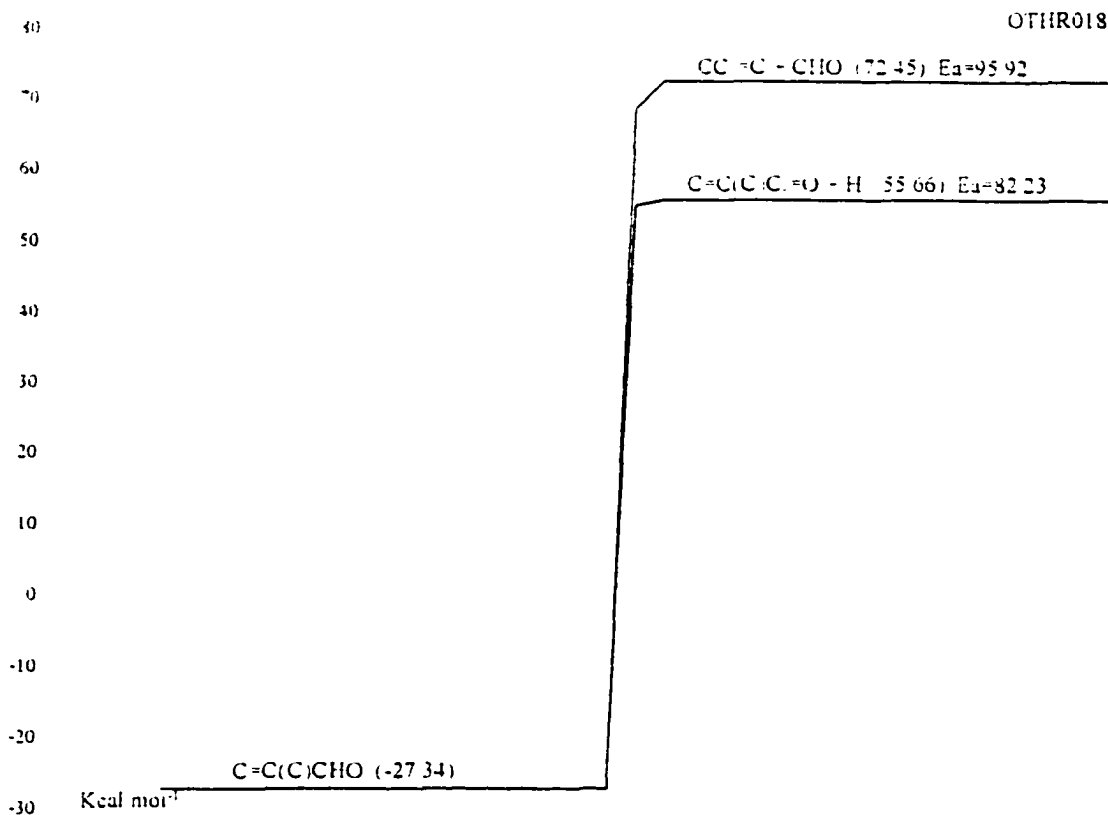
frequency/degeneracy (CPFIT)

$\text{C}_2\text{C}=\text{O}$: 478.2 (6.771); 1383.8 (10.063); 2760.1 (6.166)

Lennard-Jones parameter

$\sigma(\text{\AA}) = 4.80$, $\epsilon/k(\text{K}) = 481.73$

k_1 A_f via A_r and Microscopic Reversibility (MR), $A_r = 4.04 \times 10^{15} T^{-0.8}$, 86 TSA. $E_{a,f} = \Delta U_{\text{rxn}} = 81.73 \text{ kcal mol}^{-1}$.

IID. 30 $C=C(C)CHO \rightarrow \text{Products}$ 

Reaction		$A T^n e^{-a/T}$ (s ⁻¹ or cm ³ mol ⁻¹ s ⁻¹)	E_a (kcal mol ⁻¹)
k_1	$C=C(C)CHO \rightarrow CCyC.OC + CH_2OOH$	$1.24 \times 10^{17} T^0 e^{-a/T}$	95.92
k_2	$C=C(C)CHO \rightarrow CCyCOC(CO.) + OH$	$2.97 \times 10^{14} T^0 e^{-a/T}$	82.23

frequency/degeneracy (CPFIT)

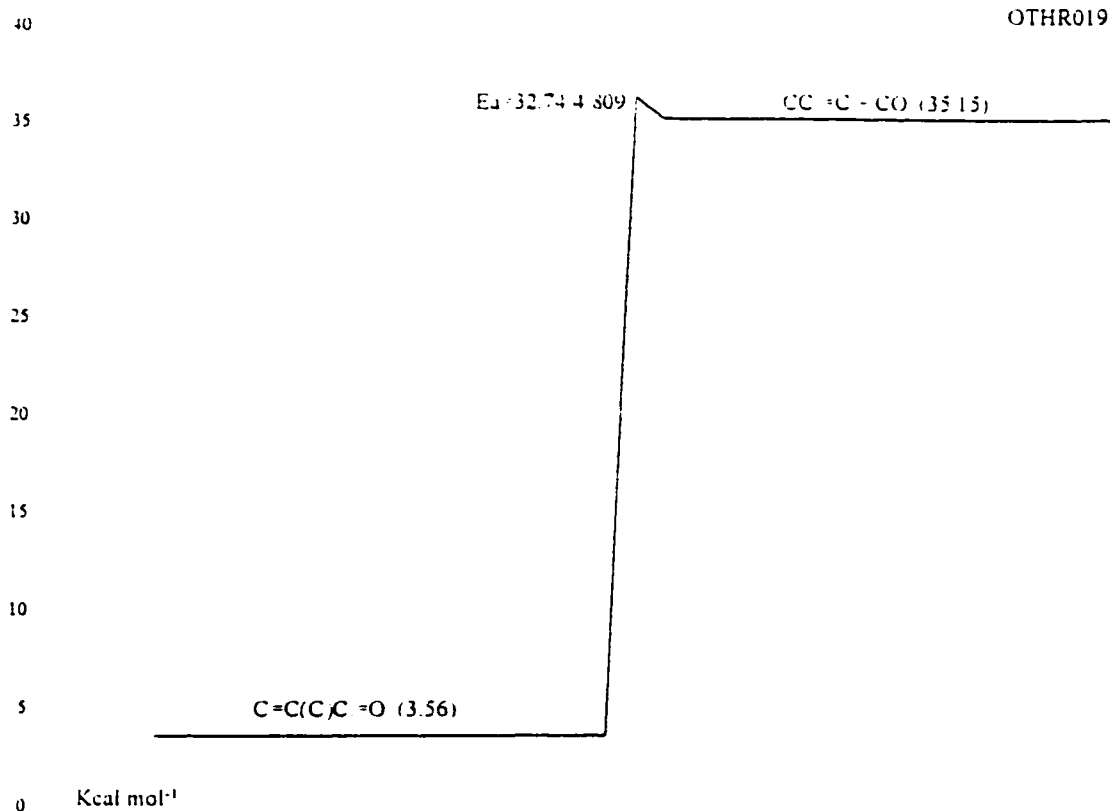
 $C=C(C)CHO$: 425.2 (9.229); 1227.6 (10.817); 2929.6 (5.954)

Lennard-Jones parameter

 $\sigma(\text{\AA}) = 5.20$, ϵ/k (K) = 533.08

- k_1 A_f via A_r and Microscopic Reversibility (MR), $A_r = 1.81 \times 10^{13}$, 88 TSA for $CC.C + CHO \rightarrow C2CCHO$. $E_{a,f} = \Delta U_{\text{ren}} = 95.92$ kcal mol⁻¹.
- k_2 A_f via A_r and Microscopic Reversibility (MR), $A_r = 5.00 \times 10^{13}$ 1/2 (H + CHO). $E_{a,f} = \Delta U_{\text{ren}} = 82.23$ kcal mol⁻¹.

IID. 31 $\text{C}=\text{C}(\text{C})\text{C}=\text{O} \rightarrow \text{CC}=\text{C} + \text{CO}$



	Reaction	$A T^n e^{-u/T}$	E_a
		(s ⁻¹ or cm ³ mol ⁻¹ s ⁻¹)	(kcal mol ⁻¹)
k ₁	$\text{C}=\text{C}(\text{C})\text{C}=\text{O} \rightarrow \text{CC}=\text{C} + \text{CO}$	$9.95 \times 10^{13} T^0 e^{-0/T}$	32.74

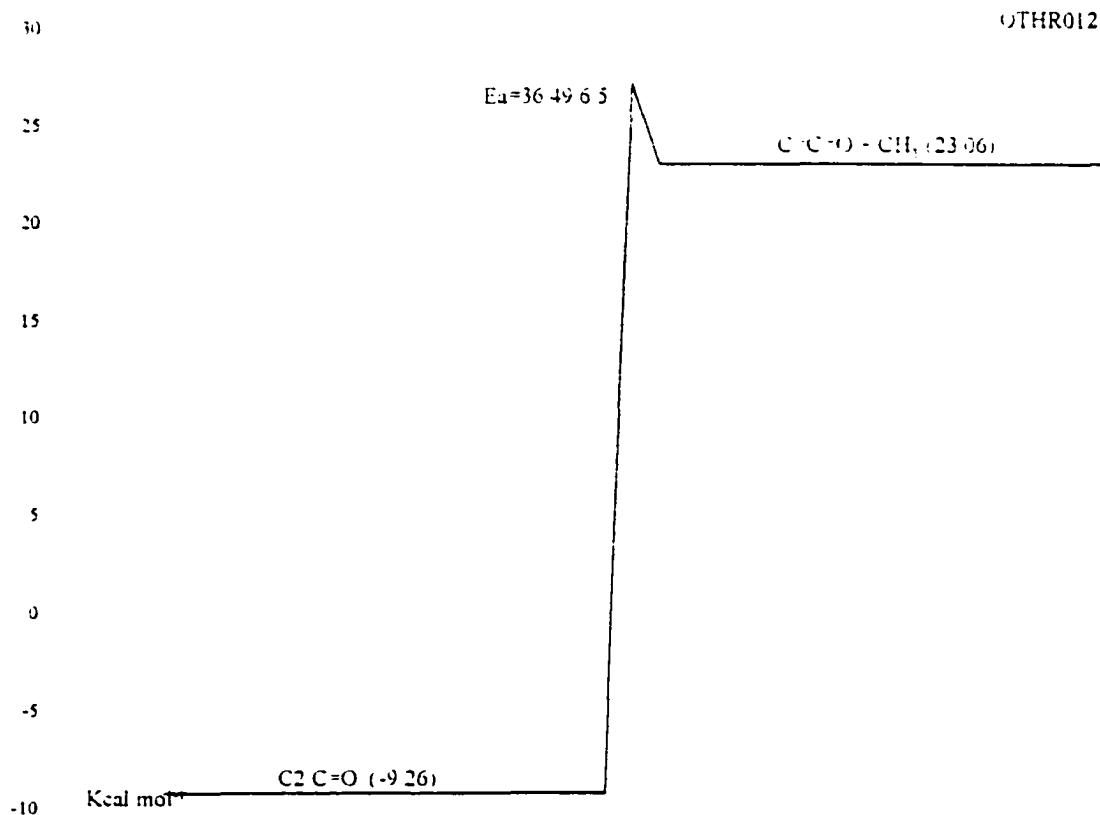
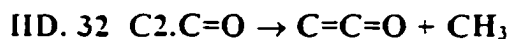
frequency/degeneracy (CPFIT)

$\text{C}=\text{C}(\text{C})\text{C}=\text{O}$: 408.6 (9.006); 1183.9 (8.561); 2919.2 (5.433)

Lennard-Jones parameter

$\sigma(\text{\AA}) = 5.20$, $\epsilon/k(\text{K}) = 533.08$

- k₁ A_f via A_r and Microscopic Reversibility (MR), $A_r = 1.51 \times 10^{11}$, 86 TSA for $\text{C}=\text{C} + \text{CO} \rightarrow \text{C}=\text{CC}=\text{O}$. $E_{a,f} = E_{a,r} + \Delta U_{\text{rxn}}$, $\Delta U_{\text{rxn}} = 27.93 \text{ kcal mol}^{-1}$. $E_{a,r} = 4.809 \text{ kcal mol}^{-1}$ (from the same reference as A_r)
- k₂ A_f via A_r and Microscopic Reversibility (MR), $A_r = 5.00 \times 10^{13} \text{ } 1/2 (\text{H} + \text{CHO})$. $E_{a,f} = \Delta U_{\text{rxn}} = 82.23 \text{ kcal mol}^{-1}$.



Reaction		$A T^n e^{-E_a/T}$ (s^{-1} or $\text{cm}^3 \text{mol}^{-1} \text{s}^{-1}$)	E_a (kcal mol^{-1})
k_1	$\text{C2.C=O} \rightarrow \text{C=C=O} + \text{CH}_3$	$3.26 \times 10^{12} T^0 e^{-E_a/T}$	36.49

frequency/degeneracy (CPFIT)

C2.C=O : 372.4 (5.286); 1158.0 (9.242); 2500.5 (5.471)

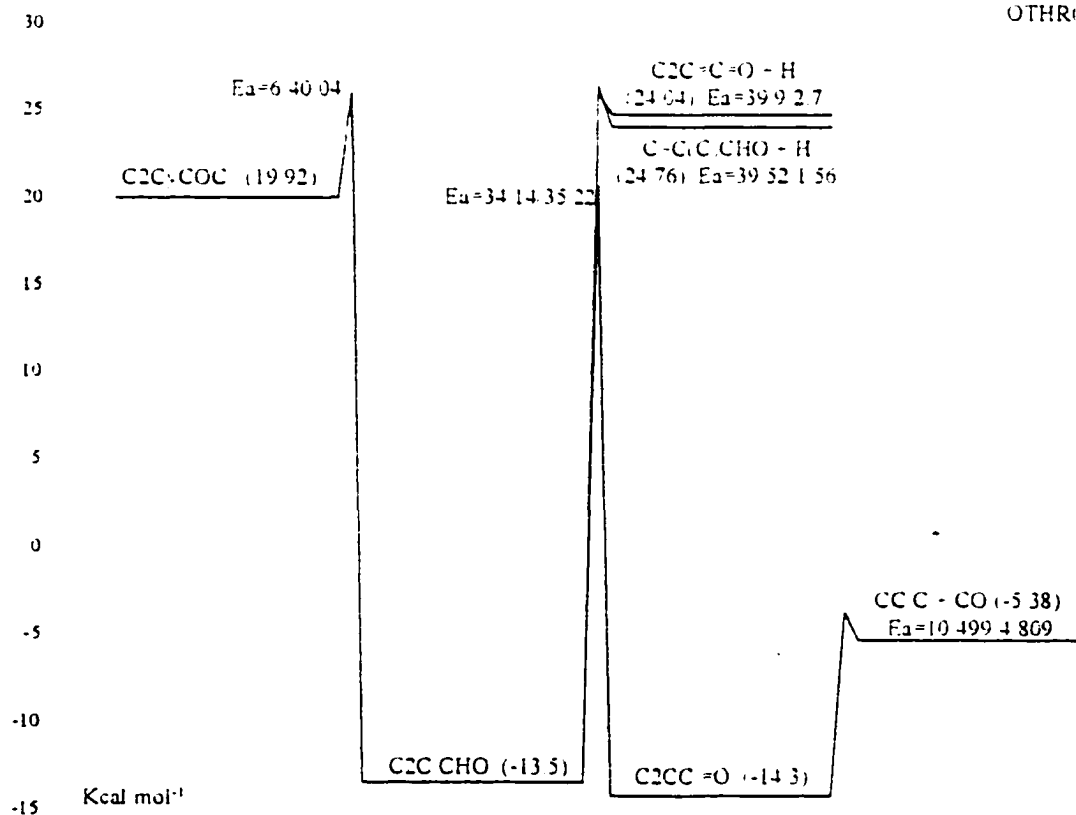
Lennard-Jones parameter

$\sigma(\text{\AA}) = 4.80$, $\epsilon/k(\text{K}) = 481.73$

k_1 A_f via A_r and Microscopic Reversibility (MR), $A_r = 1.58 \times 10^{11}$, 73 TSA2 for $\text{C=C=C} + \text{CH}_3 \rightarrow \text{C2.C=C}$. $E_{a,f} = E_{a,r} + \Delta U_{\text{rxn}}$, $\Delta U_{\text{rxn}} = 29.99 \text{ kcal mol}^{-1}$. $E_{a,r} = 6.5 \text{ kcal mol}^{-1}$ (estimated by Bozzelli).

IID. 33 C2CyCOC. → C2C.CHO → Products

OTHR017



Reaction		$A T^n e^{-a/T}$ (s ⁻¹ or cm ³ mol ⁻¹ s ⁻¹)	E_a (kcal mol ⁻¹)
k_1	C2CyCOC → C2C.CHO	$1.71 \times 10^{13} T^0 e^{-0/T}$	6.00
k_{-1}	C2C.CHO → C2CyCOC.	$4.08 \times 10^{12} T^0 e^{-0/T}$	40.04
k_2	C2C.CHO → C2C=C=O + H	$1.40 \times 10^{13} T^0 e^{-0/T}$	39.90
k_3	C2C.CHO → C=C(C)CHO + H	$1.87 \times 10^{13} T^0 e^{-0/T}$	39.52
k_4	C2C.CHO → C2CC.=O	$6.50 \times 10^9 T^{1.0} e^{-0/T}$	34.14
k_{-4}	C2CC.=O → C2C.CHO	$7.34 \times 10^7 T^{1.56} e^{-0.00036/T}$	35.22
k_5	C2CC.=O → CC.C + CO	$1.77 \times 10^{13} T^0 e^{-0/T}$	10.50

frequency/degeneracy (CPFIT)

C2CYCOC.: 432.8 (8.787); 1159.6 (13.398); 2960.2 (6.816)

C2C.CHO: 394.7 (9.643); 1273.2 (11.447); 2762.4 (7.410)

Lennard-Jones parameter

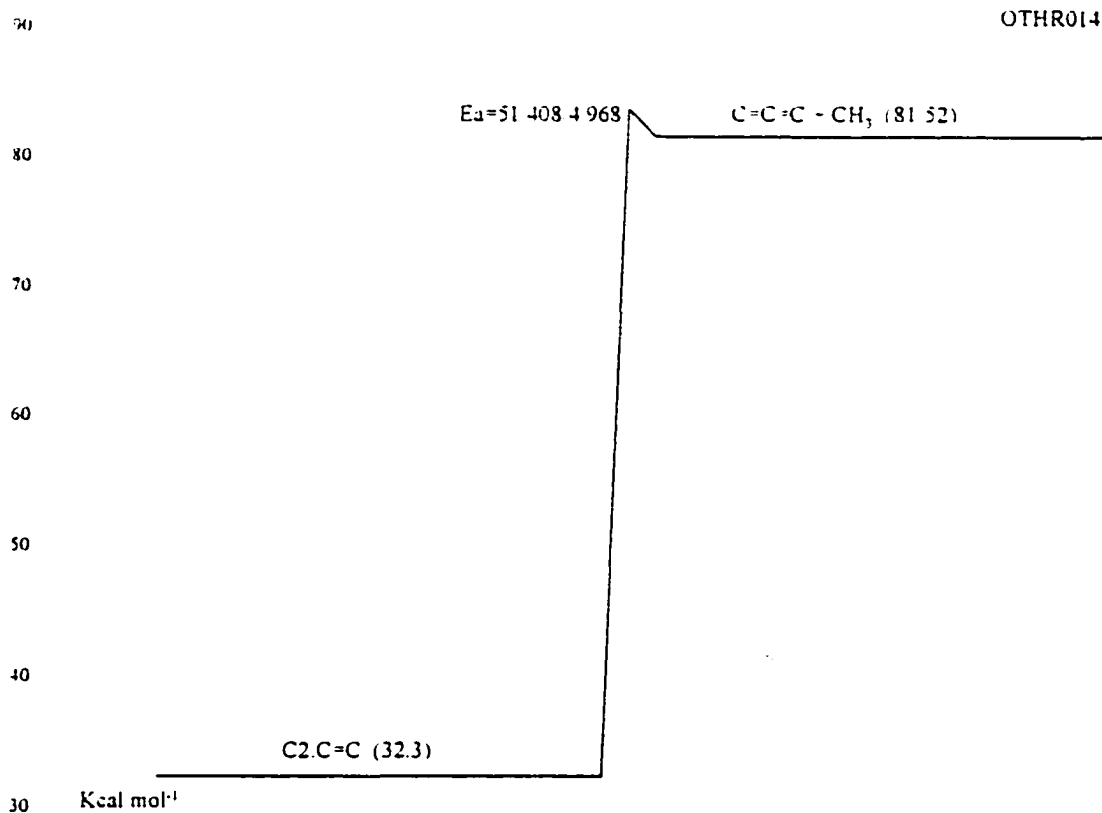
 $\sigma(\text{\AA}) = 5.20$, ϵ/k (K) = 533.08

- k_1 A_f via A_r and Microscopic Reversibility (MR). $E_{a,f}$ is estimated by Bozzelli (Chiungchu)
- k_{-1} A_r estimated using TST, $A = (\text{deg.}) (ek_b T/h) \exp(\Delta S^\ddagger(T)/R)$, $\text{deg.} = 1$, $ek_b T/h = 10^{13.55}$?, $\Delta S^\ddagger(T)$ is estimated as loss of one rotor ($-4.3 \text{ cal mol}^{-1} \text{ K}^{-1}$). $E_{a,r} = E_{a,f} - \Delta U_{\text{rot}}$, $\Delta U_{\text{rot}} = -34.04 \text{ kcal mol}^{-1}$.
- k_2 A_f via A_r and Microscopic Reversibility (MR), $A_r = 6.50 \times 10^{12} = 1/2 (\text{H} + \text{CC}=\text{C} \rightarrow \text{CC}\cdot\text{C})$, 91 TSA/HAM. $E_{a,f}$ is estimated by Bozzelli.
- k_3 A_f via A_r and Microscopic Reversibility (MR), $A_r = 6.50 \times 10^{12} = 1/2 (\text{H} + \text{CC}=\text{C} \rightarrow \text{CC}\cdot\text{C})$, 91 TSA/HAM. $E_{a,f}$ is estimated by Bozzelli.
- k_4 A_r estimated using TST, $A = (\text{deg.}) (ek_b/h) T^n \exp(\Delta S^\ddagger(T)/R)$, $\text{deg.} = 1$, $ek_b/h = 5.66 \times 10^{10}$, $n = 1.0$, $\Delta S^\ddagger(T)$ is estimated as loss of one rotor ($-4.3 \text{ cal mol}^{-1} \text{ K}^{-1}$). $E_{a,f} = \text{RS (28)} + E_{\text{abst}} (6.14) \text{ kcal mol}^{-1}$.
- k_{-4} A_r via A_f and Microscopic Reversibility (MR), $E_{a,r} = E_{a,f} - \Delta U_{\text{rot}}$, $\Delta U_{\text{rot}} = -1.08 \text{ kcal mol}^{-1}$.
- k_5 A_f via A_r and Microscopic Reversibility (MR), $A_r = 1.51 \times 10^{11}$, 86 TSA/HAM for $\text{CO} + \text{CC}\cdot$. $E_{a,f} = E_{a,r} + \Delta U_{\text{rot}}$, $\Delta U_{\text{rot}} = 5.69 \text{ kcal mol}^{-1}$. $E_{a,r} = 4.809 \text{ kcal mol}^{-1}$. (taken from the same reference as A_r).

Lennard-Jones parameter
 $\sigma(\text{\AA}) = 5.86, \epsilon/k (\text{K}) = 632.06$

- k_1 92 WAL/AND, for C3C. + O₂.
- k_{-1} A_r via A_r and Microscopic Reversibility (MR), $E_{a,r} = \Delta U_{\text{run}} = 22.91 \text{ kcal mol}^{-1}$.
- k_2 A_r estimated using TST, $A = (\text{deg.}) (ek_B/h) T^n \exp(\Delta S^\ddagger(T)/R)$, $\text{deg.} = 1$, $ek_B/h = 5.66 \times 10^{10}$, $n = 1.0$, $\Delta S^\ddagger(T)$ is estimated as loss of one rotor ($-4.3 \text{ cal mol}^{-1} \text{ K}^{-1}$) and gain an optical isomer (OI). $E_{a,f} = \text{RS (6)} + E_{\text{abst}} (5.98) + \Delta U_{\text{run}} (1.55) \text{ kcal mol}^{-1}$
- k_{-2} A_r via A_r and Microscopic Reversibility (MR), $E_{a,r} = E_{a,f} - \Delta U_{\text{run}}$, $\Delta U_{\text{run}} = 1.55 \text{ kcal mol}^{-1}$.
- k_3 A_r via A_r and Microscopic Reversibility (MR), $A_r = 1.33 \times 10^{11}$, Bozzelli. $E_{a,f} = E_{a,r} + \Delta U_{\text{run}}$, $\Delta U_{\text{run}} = 10.50 \text{ kcal mol}^{-1}$. $E_{a,r} = 7.80 \text{ kcal mol}^{-1}$. (estimated by Bozzelli).
- k_4 A_r via A_r and Microscopic Reversibility (MR), $A_r = 1.00 \times 10^{11}$, 72 KER for C3C. + C#C. $E_{a,f} = E_{a,r} + \Delta U_{\text{run}}$, $\Delta U_{\text{run}} = 0.29 \text{ kcal mol}^{-1}$. $E_{a,r} = 4.809 \text{ kcal mol}^{-1}$. (referenced on 88 TSA CC. + CO).
- k_5 A_r estimated using TST, $A = (\text{deg.}) (ek_B/h) T^n \exp(\Delta S^\ddagger(T)/R)$, $\text{deg.} = 6$, $ek_B/h = 5.66 \times 10^{10}$, $n = 1.0$, $\Delta S^\ddagger(T)$ is estimated as loss of two rotors ($-4.3 \times 2 \text{ cal mol}^{-1} \text{ K}^{-1}$) and gain an optical isomer (OI). $E_{a,f} = \text{RS (6)} + E_{\text{abst}} (8) + \Delta U_{\text{run}} (13.52) \text{ kcal mol}^{-1}$
- k_{-5} A_r via A_r and Microscopic Reversibility (MR), $E_{a,r} = E_{a,f} - \Delta U_{\text{run}}$, $\Delta U_{\text{run}} = 13.52 \text{ kcal mol}^{-1}$.
- k_6 A_r via A_r and Microscopic Reversibility (MR), $A_r = 3.50 \times 10^{11}$, Bozzelli. $E_{a,f} = E_{a,r} + \Delta U_{\text{run}}$, $\Delta U_{\text{run}} = -0.71 \text{ kcal mol}^{-1}$. $E_{a,r} = 7.80 \text{ kcal mol}^{-1}$. (estimated by Bozzelli).
- k_7 A_r via A_r and Microscopic Reversibility (MR), $A_r = 1.02 \times 10^{11}$, 86 LES/ROU for CHO + CC=C → Prod.. $E_{a,f} = E_{a,r} + \Delta U_{\text{run}}$, $\Delta U_{\text{run}} = 17.74 \text{ kcal mol}^{-1}$. $E_{a,r} = 6.21 \text{ kcal mol}^{-1}$. (referenced as the same as the A_r).

IID. 35 C2.C=C → Products



Reaction		$A T^n e^{-u/T}$ (s ⁻¹ or cm ³ mol ⁻¹ s ⁻¹)	E_a (kcal mol ⁻¹)
k_1	C2C.=C → C=C=C + CH ₃	$1.30 \times 10^{13} T^0 e^{-u/T}$	51.41

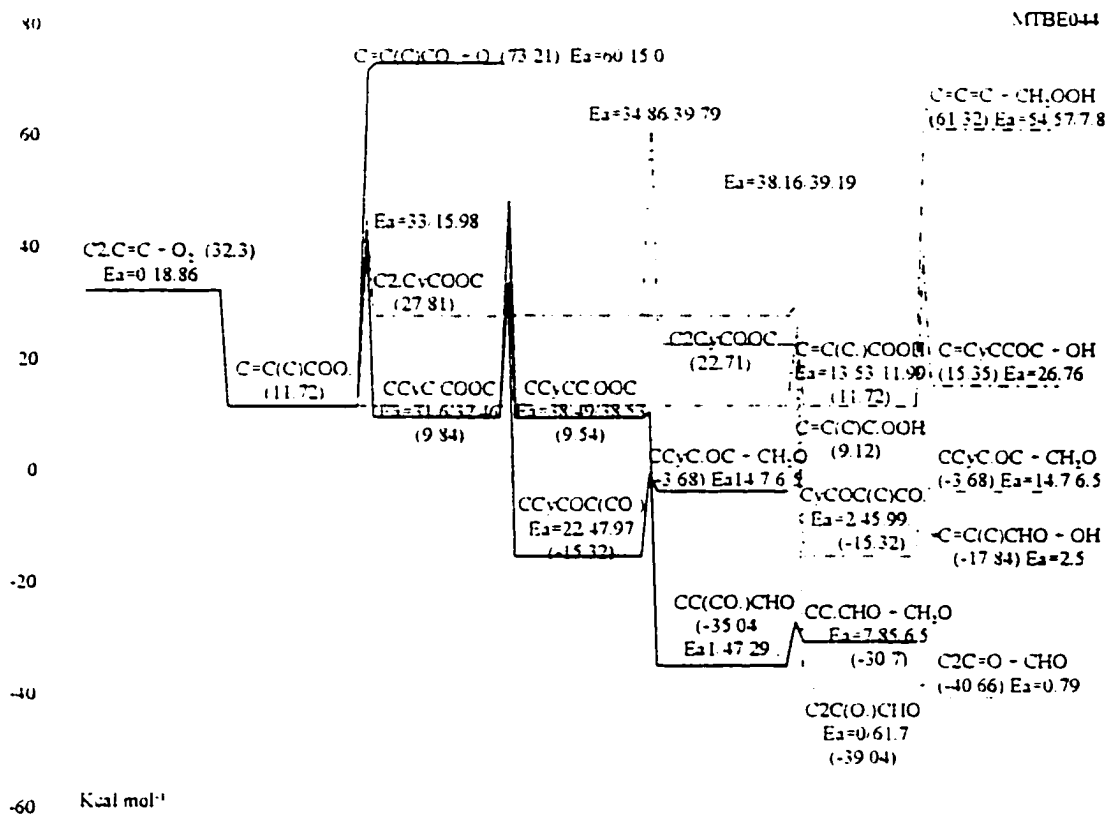
frequency/degeneracy (CPFIT)

C2C.=C: 250.1 (4.454); 981.6 (12.636); 2533.9 (8.910)

Lennard-Jones parameter

$\sigma(\text{\AA}) = 5.18$, $\epsilon/k(\text{K}) = 407.0$

k_1 A_f via A_r and Microscopic Reversibility (MR), $A_r = 1.58 \times 10^{11}$, 73 TSA2. $E_{a,f} = E_{a,r} + \Delta U_{\text{rxn}}$, $\Delta U_{\text{rxn}} = 46.44 \text{ kcal mol}^{-1}$. $E_{a,r} = 4.968 \text{ kcal mol}^{-1}$. (taken from the same reference as A_r).

IID. 36 C2.C=C + O₂ → Products

Reaction		$A T^n e^{-aT}$ (s ⁻¹ or cm ³ mol ⁻¹ s ⁻¹)	E _a (kcal mol ⁻¹)
k ₁	C ₂ .C=C + O ₂ → C=C(C)COO.	5.00×10 ¹¹ T ⁰ e ^{-0T}	0.00
k ₋₁	C=C(C)COO. → C ₂ .C=C + O ₂	7.82×10 ¹² T ⁰ e ^{-0T}	18.86
k ₂	C=C(C)COO. → C=C(C)CO. + O	1.84×10 ¹⁴ T ⁰ e ^{-0T}	60.15
k ₃	C=C(C)COO. → C=C(C)C.OOH	2.60×10 ¹⁰ T ^{1.0} e ^{-0T}	37.95
k ₋₃	C=C(C)C.OOH → C=C(C)COO.	2.31×10 ¹³ T ^{0.18} e ^{-0.00007T}	39.61
k ₄	C=C(C)C.OOH → C=C(C)CHO + OH	1.23×10 ¹⁴ T ⁰ e ^{-0T}	2.50
k ₅	C=C(C)COO. → C=C(C.)COOH	5.15×10 ⁸ T ^{1.0} e ^{-0T}	12.48
k ₋₅	C=C(C.)COOH → C=C(C)COO.	8.64×10 ¹² T ^{-0.66} e ^{-0.00048T}	11.00
k ₆	C=C(C.)COOH → C=C=C + CH ₂ OOH	3.43×10 ¹³ T ⁰ e ^{-0T}	54.57
k ₇	C=C(C.)COOH → C=CyCCOC + OH	1.22×10 ¹² T ^{-0.17} e ^{-0T}	26.76
k ₈	C=C(C)COO. → CCyC.COOC	4.68×10 ¹¹ T ⁰ e ^{-0T}	31.60
k ₋₈	CCyC.COOC → C=C(C)COO.	3.78×10 ¹³ T ⁰ e ^{-0T}	31.96
k ₉	CCyC.COOC → CCyCOC(CO.)	1.00×10 ¹³ T ⁰ e ^{-0T}	22.00
k ₋₉	CCyCOC(CO.) → CCyC.COOC	6.85×10 ¹² T ^{1.0} e ^{-0T}	47.97
k ₁₀	CCyCOC(CO.) → CCyC.OC + CH ₂ O	7.36×10 ¹³ T ⁰ e ^{-0T}	14.70

Reaction		$A T^n e^{-u/T}$ (s^{-1} or $cm^3 mol^{-1} s^{-1}$)	E_a ($kcal mol^{-1}$)
k_{11}	$CCyC.COOC \rightarrow CCyCC.OOC$	$2.26 \times 10^{11} T^{1.0} e^{-u/T}$	38.49
k_{-11}	$CCyCC.OOC \rightarrow CCyC.COOC$	$9.28 \times 10^{12} T^{0.46} e^{-0.00034T}$	38.53
k_{12}	$CCyCC.OOC \rightarrow CC(CO.)CHO$	$5.20 \times 10^{13} T^0 e^{-u/T}$	1.00
k_{-12}	$CC(CO.)CHO \rightarrow CCyCC.OOC$	$4.68 \times 10^{11} T^0 e^{-u/T}$	47.29
k_{13}	$CC(CO.)CHO \rightarrow CC.CHO + CH_2O$	$1.73 \times 10^{12} T^0 e^{-u/T}$	7.85
k_{14}	$C=C(C)COO. \rightarrow C2.CyCOOC$	$4.68 \times 10^{11} T^0 e^{-u/T}$	33.00
k_{-14}	$C2.CyCOOC \rightarrow C=C(C)COO.$	$2.02 \times 10^{13} T^0 e^{-u/T}$	15.33
k_{15}	$C2.CyCOOC \rightarrow CCyCOC(CO.)$	$4.08 \times 10^{12} T^0 e^{-u/T}$	2.00
k_{-15}	$CCyCOC(CO.) \rightarrow C2.CyCOOC$	$5.23 \times 10^{12} T^0 e^{-u/T}$	45.99
k_{16}	$CCyCOC(CO.) \rightarrow C2C(OOH)CO.$	$7.36 \times 10^{13} T^0 e^{-u/T}$	14.70
k_{17}	$C2.CyCOOC \rightarrow C2CyCOOC.$	$1.30 \times 10^{10} T^{1.0} e^{-u/T}$	34.86
k_{-17}	$C2CyCOOC. \rightarrow C2.CyCOOC$	$1.14 \times 10^{12} T^{0.46} e^{-0.00042T}$	39.79
k_{18}	$C2CyCOOC. \rightarrow C2C(O.)CHO$	$4.78 \times 10^{13} T^0 e^{-u/T}$	0.00
k_{-18}	$C2C(O.)CHO \rightarrow C2CyCOOC.$	$4.08 \times 10^{12} T^0 e^{-u/T}$	62.70
k_{19}	$C2C(O.)CHO \rightarrow C2C=O + CHO$	$2.20 \times 10^{13} T^0 e^{-u/T}$	0.79

frequency/degeneracy (CPFIT)

$C=C(C)COO.$: 250.2 (9.328); 1085.2 (12.518); 2775.4 (9.654)
 $C=C(C)C.OOH$: 250.1 (9.281); 1072.2 (13.818); 2573.4 (7.901)
 $C=C(C.)COOH$: 250.1 (9.354); 1014.6 (14.110); 2587.6 (7.537)
 $CCyC.COOC$: 250.2 (5.838); 1079.1 (19.700); 2566.7 (6.963)
 $C2.CyCOOC$: 250.2 (5.146); 955.4 (18.106); 2284.9 (8.748)
 $CCyCOC(CO.)$: 479.0 (11.457); 1251.1 (14.140); 3091.0 (6.403)
 $CCyCC.OOC$: 250.1 (5.427); 1047.2 (20.847); 2766.5 (6.227)
 $C2CyCOOC.$: 250.6 (5.473); 961.6 (18.784); 2467.2 (7.743)
 $CC(CO.)CHO$: 392.3 (10.257); 1270.1 (14.560); 2975.3 (6.683)
 $C2C(O.)CHO$: 431.6 (12.207); 1412.1 (15.266); 3486.6 (4.027)

Lennard-Jones parameter

$\sigma(\text{\AA}) = 5.86$, $\epsilon/k (K) = 632.06$

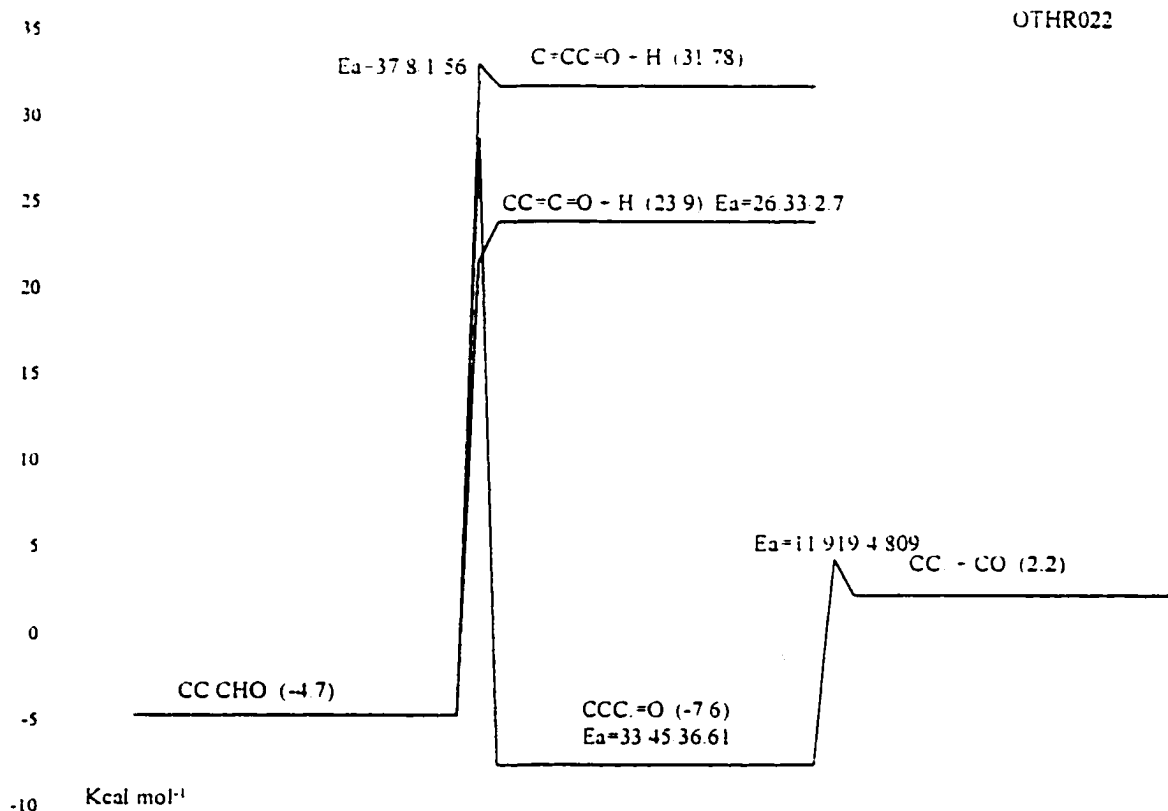
- k_1 $1/2(C3C. + O_2 \rightarrow C3COO.)$, 88 XI
 k_{-1} A_r via A_f and Microscopic Reversibility (MR), $E_{a,r} = E_{a,f} - \Delta U_{rxn}$, $\Delta U_{rxn} = -18.86$ $kcal mol^{-1}$.
 k_2 A_f via A_r and Microscopic Reversibility (MR), $A_r = 1.51 \times 10^{13}$, 92 BAU/COB for $(CH_3O + O \rightarrow Prod.)$, $E_{a,f} = \Delta U_{rxn} = 60.15$ $kcal mol^{-1}$.
 k_3 A_f estimated using TST, $A = (deg.) A' T^n$, $deg. = 2$, $A' = 1.011 \times 10^9$, $n = 1.455$, A' and n are from thermal reaction analysis (AFACT2f) based on the thermodynamic properties calculated from MOPAC PM3 (corrected with internal rotor, electronic spin and optical isomer). $E_{a,f} = RS(26) + E_{abs}(12.16)$ $kcal mol^{-1}$.
 k_{-3} A_r via A_f and Microscopic Reversibility (MR), $E_{a,r} = E_{a,f} - \Delta U_{rxn}$, $\Delta U_{rxn} = -1.03$ $kcal mol^{-1}$.

- k_4 A_f via A_r and Microscopic Reversibility (MR), $A_r = 2.75 \times 10^{12} = 1/2$ (OH + C=C). $E_{a,f}$ estimated the same 2.5 kcal mol⁻¹ as $E_{a,r}$ for CH₂OOH → CH₂O + OH (1990 Page)
- k_5 A_f estimated using TST, $A = (\text{deg.}) A' T^n$, deg. = 3, $A' = 1.275 \times 10^6$, $n = 1.954$, A' and n are from thermal reaction analysis (AFACT2f) based on the thermodynamic properties calculated from MOPAC PM3 (corrected with internal rotor, electronic spin and optical isomer). $E_{a,f} = RS(0) + E_{\text{abst}}(11.97) + \Delta H_{\text{rxn}}(1.54)$ kcal mol⁻¹.
- k_{-5} A_r via A_f and Microscopic Reversibility (MR), $E_{a,r} = E_{a,f} - \Delta U_{\text{rxn}}$, $\Delta U_{\text{rxn}} = 1.54$ kcal mol⁻¹.
- k_6 A_f via A_r and Microscopic Reversibility (MR), $A_r = 9.64 \times 10^{10}$, 91 TSA for C₃H₆ + CH₃ → C3.C. $E_{a,f} = E_{a,r} + \Delta U_{\text{rxn}}$, $\Delta U_{\text{rxn}} = 46.77$ kcal mol⁻¹. $E_{a,r} = 7.8$ kcal mol⁻¹. (estimated by Bozzelli).
- k_7 A_f estimated using TST, $A = (\text{deg.}) A' T^n$, deg. = 1, $A' = 1.216 \times 10^{12}$, $n = -0.173$, A' and n are from thermal reaction analysis (AFACT2f) based on the thermodynamic properties calculated from MOPAC PM3 (corrected with internal rotor, electronic spin and optical isomer). $E_{a,f}$ is estimated by Bozzelli (Chiungchu).
- k_8 A_f estimated using TST, $A = (\text{deg.}) A' T^n$, deg. = 1, $A' = 4.090 \times 10^8$, $n = 0.923$, A' and n are from thermal reaction analysis (AFACT2f) based on the thermodynamic properties calculated from MOPAC PM3 (corrected with internal rotor, electronic spin and optical isomer). $E_{a,f}$ is estimated by Bozzelli (Chiungchu).
- k_{-8} A_r via A_f and Microscopic Reversibility (MR), $E_{a,r} = E_{a,f} - \Delta U_{\text{rxn}}$, $\Delta U_{\text{rxn}} = -0.86$ kcal mol⁻¹.
- k_9 A_f is taken from ref. [55] $E_{a,f}$ is estimated as the difference of ring strain (28 - 6) kcal mol⁻¹. (estimated by Bozzelli).
- k_{-9} A_r via A_f and Microscopic Reversibility (MR), $E_{a,r} = E_{a,f} - \Delta U_{\text{rxn}}$, $\Delta U_{\text{rxn}} = -25.97$ kcal mol⁻¹.
- k_{10} A_f via A_r and Microscopic Reversibility (MR), $A_r = 1.08 \times 10^{11}$, 88 TSA for CH₂O + CC.C → CCC + CHO. $E_{a,f} = E_{a,r} + \Delta U_{\text{rxn}}$, $\Delta U_{\text{rxn}} = 8.2$ kcal mol⁻¹. $E_{a,r} = 6.5$ kcal mol⁻¹. (estimated by Bozzelli).
- k_{11} A_r estimated using TST, $A = (\text{deg.}) (ek_b/h) T^n \exp(\Delta S^\ddagger(T)/R)$, deg. = 4, $ek_b/h = 5.66 \times 10^{10}$, $n = 1.0$, $\Delta S^\ddagger(T)$ is estimated as loss of rotor (no rotor loss here, thus $\Delta S^\ddagger(T) = 0$). $E_{a,r} = RS(28) + E_{\text{abst}}(10.49)$ kcal mol⁻¹.
- k_{-11} A_r via A_f and Microscopic Reversibility (MR), $E_{a,r} = E_{a,f} - \Delta U_{\text{rxn}}$, $\Delta U_{\text{rxn}} = -0.04$ kcal mol⁻¹.
- k_{12} A_f via A_r and Microscopic Reversibility (MR), $E_{a,f}$ is estimated as 1 kcal mol⁻¹ by Bozzelli.
- k_{-12} A_r estimated using TST, $A = (\text{deg.}) (ek_b T/h) \exp(\Delta S^\ddagger(T)/R)$, deg. = 1, $ek_b T/h = 10^{13.55}$?, $\Delta S^\ddagger(T)$ is estimated as loss of two rotors (-4.3×2 cal mol⁻¹ K⁻¹). $E_{a,r} = E_{a,f} - \Delta U_{\text{rxn}}$, $\Delta U_{\text{rxn}} = -46.29$ kcal mol⁻¹.
- k_{13} A_f via A_r and Microscopic Reversibility (MR), $A_r = 1.08 \times 10^{11}$, 88 TSA for CH₂O + CC.C → CCC + CHO. $E_{a,f} = E_{a,r} + \Delta U_{\text{rxn}}$, $\Delta U_{\text{rxn}} = 1.35$ kcal mol⁻¹. $E_{a,r} = 6.5$ kcal mol⁻¹. (estimated by Bozzelli).
- k_{14} A_f estimated using TST, $A = (\text{deg.}) A' T^n$, deg. = 1, $A' = 1.222 \times 10^9$, $n = 0.99$, A'

and n are from thermal reaction analysis (AFACT2f) based on the thermodynamic properties calculated from MOPAC PM3 (corrected with internal rotor, electronic spin and optical isomer). $E_{a,f}$ is estimated as difference of ring strain plus 7 kcal mol⁻¹ for addition to C=C double bond.

- k_{-14} A_r via A_f and Microscopic Reversibility (MR), $E_{a,r} = E_{a,f} - \Delta U_{\text{rxn}}$, $\Delta U_{\text{rxn}} = 17.02$ kcal mol⁻¹.
- k_{15} A_f estimated using TST, $A = (\text{deg.}) (ek_b T/h) \exp(\Delta S^\ddagger(T)/R)$, $\text{deg.} = 1$, $ek_b T/h = 10^{13.55}$, $\Delta S^\ddagger(T)$ is estimated as loss of one rotor (-4.3 cal mol⁻¹ K⁻¹). $E_{a,f}$ is estimated by Bozzelli.
- k_{-15} A_r via A_f and Microscopic Reversibility (MR), $E_{a,r} = E_{a,f} - \Delta U_{\text{rxn}}$, $\Delta U_{\text{rxn}} = -43.99$ kcal mol⁻¹.
- k_{16} A_f via A_r and Microscopic Reversibility (MR), $A_r = 1.08 \times 10^{11}$, 88 TSA for CH2O + CC.C -> CCC + CHO. $E_{a,f} = E_{a,r} + \Delta U_{\text{rxn}}$, $\Delta U_{\text{rxn}} = 8.2$ kcal mol⁻¹. $E_{a,r} = 6.5$ kcal mol⁻¹. (estimated by Bozzelli).
- k_{17} A_r estimated using TST, $A = (\text{deg.}) (ek_b/h) T^n \exp(\Delta S^\ddagger(T)/R)$, $\text{deg.} = 2$, $ek_b/h = 5.66 \times 10^{10}$, $n = 1.0$, $\Delta S^\ddagger(T)$ is estimated as loss of one rotor (-4.3 cal mol⁻¹ K⁻¹). $E_{a,r} = \text{RS}(26) + E_{\text{abst}}(8.86)$ kcal mol⁻¹.
- k_{-17} A_r via A_f and Microscopic Reversibility (MR), $E_{a,r} = E_{a,f} - \Delta U_{\text{rxn}}$, $\Delta U_{\text{rxn}} = -4.93$ kcal mol⁻¹.
- k_{18} A_f via A_r and Microscopic Reversibility (MR), $E_{a,f}$ is estimated as 0 kcal mol⁻¹ by Bozzelli.
- k_{-18} A_r estimated using TST, $A = (\text{deg.}) (ek_b T/h) \exp(\Delta S^\ddagger(T)/R)$, $\text{deg.} = 1$, $ek_b T/h = 10^{13.55}$, $\Delta S^\ddagger(T)$ is estimated as loss of one rotors (-4.3 cal mol⁻¹ K⁻¹). $E_{a,r} = E_{a,f} - \Delta U_{\text{rxn}}$, $\Delta U_{\text{rxn}} = -62.7$ kcal mol⁻¹.
- k_{19} A_f via A_r and Microscopic Reversibility (MR), $A_r = 5.10 \times 10^{10} = 1/2$ (CC=C + CHO -> Prod.), 86 LES/ROU. $E_{a,f} = E_{a,r} + \Delta U_{\text{rxn}}$, $\Delta U_{\text{rxn}} = -5.71$ kcal mol⁻¹. $E_{a,r} = 6.5$ kcal mol⁻¹. (estimated by Bozzelli).

IID. 37 CC.CHO → Products



Reaction		$A T^n e^{-\alpha/T}$ (s ⁻¹ or cm ³ mol ⁻¹ s ⁻¹)	E_a (kcal mol ⁻¹)
k_1	CC.CHO → CCC.=O	$6.50 \times 10^9 T^{1.0} e^{-0T}$	33.45
k_{-1}	CCC.=O → CC.CHO	$9.86 \times 10^8 T^{1.0} e^{-0.00023T}$	36.61
k_2	CCC.=O → CC. + CO	$8.14 \times 10^{12} T^0 e^{-0T}$	11.92
k_3	CC.CHO → C=CCHO + H	$2.58 \times 10^{13} T^0 e^{-0T}$	37.80
k_4	CC.CHO → CC=C=O + H	$2.96 \times 10^{10} T^0 e^{-0T}$	26.33

frequency/degeneracy (CPFIT)

CC.CHO: 433.2 (6.147); 1255.8 (8.449); 2726.7 (5.404)

CCC.=O: 518.7 (8.551); 1777.1 (8.864); 3567.0 (2.585)

Lennard-Jones parameter

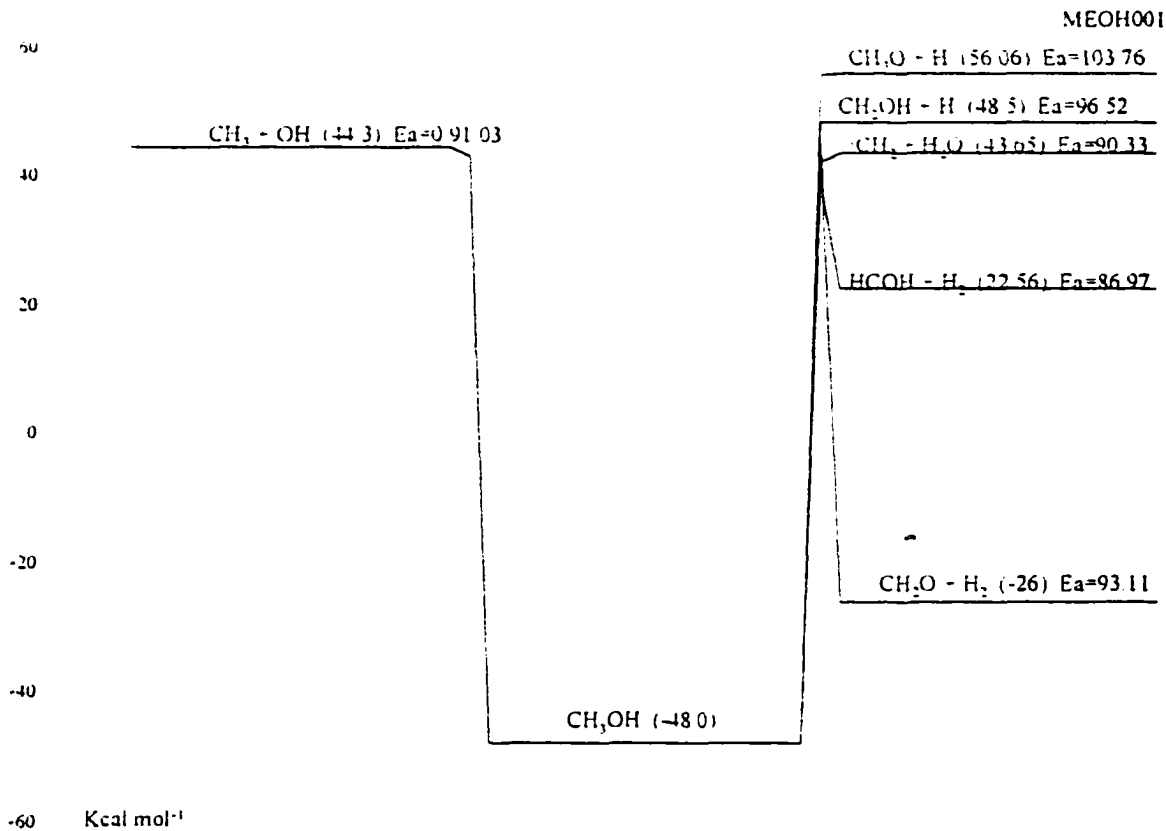
$\sigma(\text{\AA}) = 4.80$, $\epsilon/k(\text{K}) = 481.73$

k_1 A_r estimated using TST, $A = (\text{deg.}) (ek_B/h) T^n \exp(\Delta S^\ddagger(T)/R)$, $\text{deg.} = 1$, $ek_B/h = 5.66 \times 10^{10}$, $n = 1.0$, $\Delta S^\ddagger(T)$ is estimated as loss of one rotor (-4.3 cal mol⁻¹ K⁻¹).

$$E_{a,f} = RS(28) + E_{abst}(5.45) \text{ kcal mol}^{-1}.$$

- k_1 A_f via A_r and Microscopic Reversibility (MR), $E_{a,f} = E_{a,r} - \Delta U_{rxn}$, $\Delta U_{rxn} = -3.16 \text{ kcal mol}^{-1}$.
- k_2 A_f via A_r and Microscopic Reversibility (MR), $A_r = 1.51 \times 10^{11}$, 86 TSA/HAM for $CO + CC \rightarrow CC + CO$. $E_{a,f} = E_{a,r} + \Delta U_{rxn}$, $\Delta U_{rxn} = 7.11 \text{ kcal mol}^{-1}$. $E_{a,r} = 4.809 \text{ kcal mol}^{-1}$. (taken from the same reference as A_r).
- k_3 A_f via A_r and Microscopic Reversibility (MR), $A_r = 7.42 \times 10^{12}$, 72 KER for $C=C + H \rightarrow C-C + H$. $E_{a,f} = E_{a,r} + \Delta U_{rxn}$, $\Delta U_{rxn} = 36.24 \text{ kcal mol}^{-1}$. $E_{a,r} = 1.56 \text{ kcal mol}^{-1}$. (taken from the same reference as A_r).
- k_4 A_f via A_r and Microscopic Reversibility (MR), $A_r = 6.50 \times 10^{12} = 1/2 (H + CC=C \rightarrow CC + C)$, 91 TSA/HAM. $E_{a,f}$ is estimated by Bozzelli.

IID. 38 CH₃OH → Products



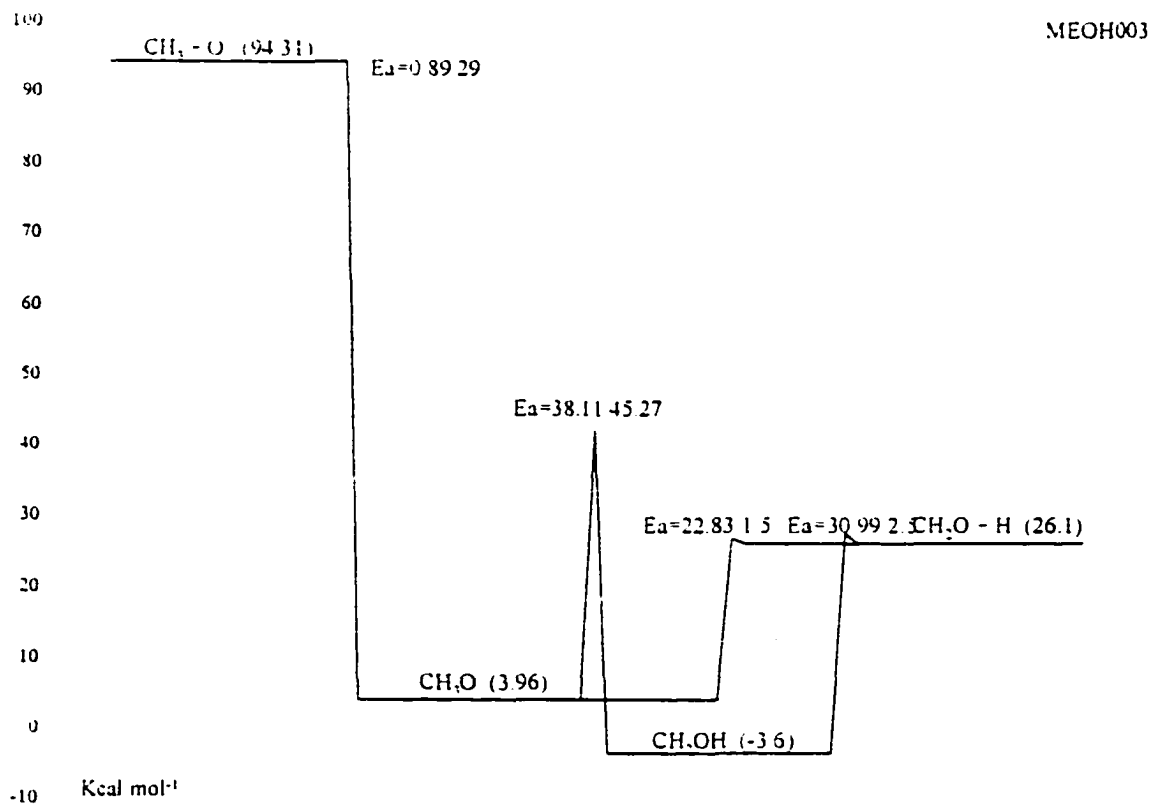
	Reaction	$A T^n e^{-\alpha/T}$ (s ⁻¹)	E_a (kcal mol ⁻¹)
k ₁	CH ₃ OH → CH ₂ O + H ₂	$3.02 \times 10^9 T^{1.29} e^{-\alpha/T}$	93.11
k ₂	CH ₃ OH → ¹ HCOH + H ₂	$1.09 \times 10^{14} T^0 e^{-\alpha/T}$	86.97
k ₃	CH ₃ OH → ¹ CH ₂ + H ₂ O	$4.40 \times 10^{14} T^0 e^{-\alpha/T}$	90.33
k ₄	CH ₃ OH → CH ₃ + OH	$5.60 \times 10^{15} T^0 e^{-\alpha/T}$	91.03
k ₅	CH ₃ OH → CH ₂ OH + H	$1.55 \times 10^{15} T^0 e^{-\alpha/T}$	96.52
k ₆	CH ₃ OH → CH ₂ O + H	$1.39 \times 10^{14} T^0 e^{-\alpha/T}$	103.76

frequency/degeneracy (CPFIT)
 CH₃OH: 753.6 (3.317); 1827.7 (6.176); 3999.9 (2.006)
 Lennard-Jones parameter
 $\sigma(\text{\AA}) = 3.76$, $\epsilon/k(\text{K}) = 369.16$

k₁ A_f is from AFACT2f thermodynamic analysis with thermodynamic properties calculated by MOPAC PM3, E_{a,f} = E_{a,r} + ΔU_{rxn} (21.11) kcal·mol⁻¹, E_{a,r} is estimated

as 72.0 kcal-mol⁻¹ based on reference Walch (1993) [95].

- k₂ A_f is taken from Bozzelli (1991) [21]. E_{a,f} = E_{a,r} + ΔU_{rxn} (70.43) kcal-mol⁻¹, E_{a,r} is estimated as 16.54 kcal-mol⁻¹ based on reference Walch (1993) [95].
- k₃ A_f is taken from Bozzelli (1991) [21]. E_{a,f} = E_{a,r} + ΔU_{rxn} (90.33) kcal-mol⁻¹, E_{a,r} is estimated as 0 kcal-mol⁻¹ based on reference Walch (1993) [95].
- k₄ A_f via A_r and Microscopic Reversibility (MR), A_r = 3.61 × 10¹³, 92 BAU/COB, NIST, E_{a,f} = ΔU_{rxn} = 91.03 kcal mol⁻¹.
- k₅ A_f via A_r and Microscopic Reversibility (MR), A_r = 3.00 × 10¹³, 81 HOY/COF, E_{a,f} = ΔU_{rxn} = 96.52 kcal mol⁻¹.
- k₆ A_f via A_r and Microscopic Reversibility (MR), A_r = 2.00 × 10¹³, 91 DOB/BER, E_{a,f} = ΔU_{rxn} = 103.76 kcal mol⁻¹.

IID. 39 $\text{CH}_3\text{O}/\text{CH}_2\text{OH} \rightarrow \text{Products}$ 

	Reaction	$A T^n e^{-\alpha T}$ (s^{-1})	E_a (kcal mol^{-1})
k_1	$\text{CH}_3 + \text{O} \rightarrow \text{CH}_3\text{O}$	$7.83 \times 10^{13} T^0 e^{-0T}$	0.00
k_{-1}	$\text{CH}_3\text{O} \rightarrow \text{CH}_3 + \text{O}$	$2.97 \times 10^{15} T^0 e^{-0T}$	89.29
k_2	$\text{CH}_3\text{O} \rightarrow \text{CH}_2\text{O} + \text{H}$	$1.55 \times 10^{13} T^0 e^{-0T}$	22.83
k_3	$\text{CH}_3\text{O} \rightarrow \text{CH}_2\text{OH}$	$1.71 \times 10^{11} T^{1.0} e^{-0T}$	38.11
k_{-3}	$\text{CH}_2\text{OH} \rightarrow \text{CH}_3\text{O}$	$2.37 \times 10^{14} T^{-0.72} e^{-0.00015T}$	45.27
k_6	$\text{CH}_2\text{OH} \rightarrow \text{CH}_2\text{O} + \text{H}$	$1.16 \times 10^{12} T^0 e^{-0T}$	30.99

frequency/degeneracy (CPFIT)

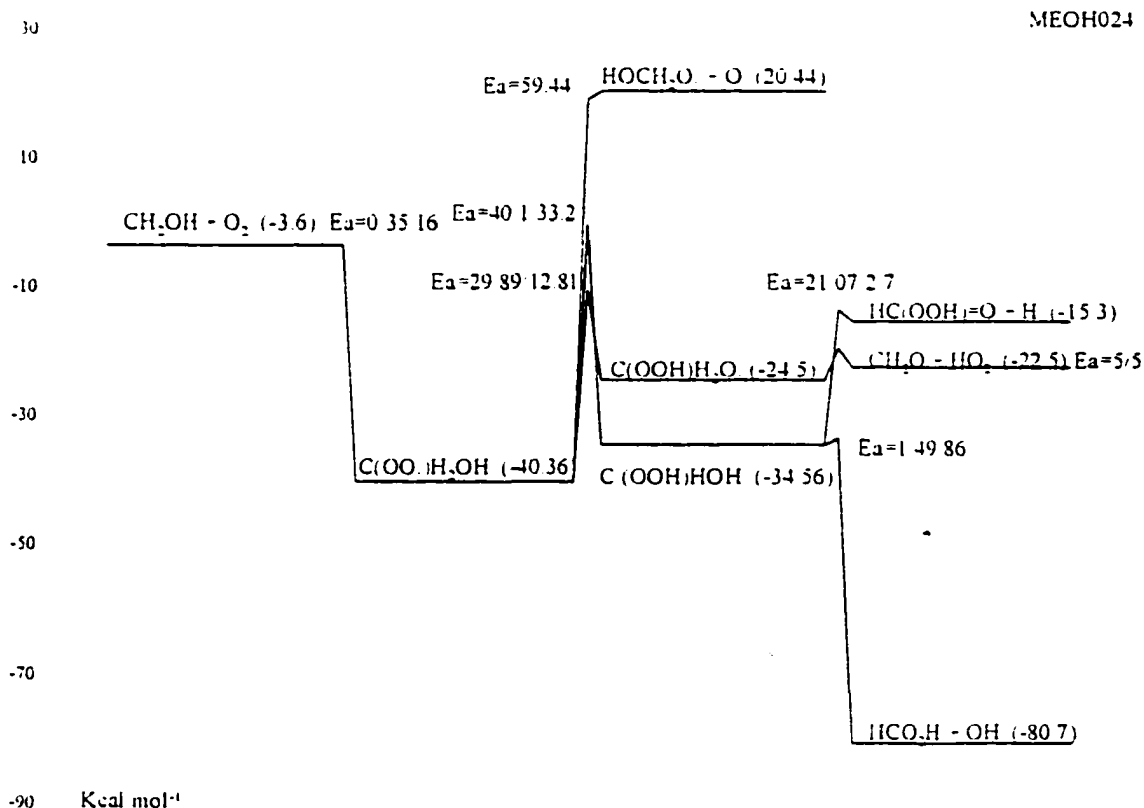
 CH_3O : 1189.6 (4.569); 2053.5 (3.381); 3999.3 (1.050)

Lennard-Jones parameter

 $\sigma(\text{\AA}) = 3.76$, $\epsilon/k(\text{K}) = 369.16$ k_1 86 TSA/HAM k_{-1} A_r via A_f and Microscopic Reversibility (MR), $E_{a,r} = E_{a,f} - \Delta U_{\text{rxn}}$, $\Delta U_{\text{rxn}} = 89.29 \text{ kcal}$

mol⁻¹.

- k₂ A_f via A_r and Microscopic Reversibility (MR), A_r = 1.00 × 10¹³, 84 WAR for H + CH₂O. E_{a,f} = E_{a,r} + ΔU_{rot}, ΔU_{rot} = 21.33 kcal mol⁻¹. E_{a,r} = 1.50 kcal mol⁻¹ (from the same reference as A_r)
- k₃ A_f estimated using TST, A = (deg.) (ek_B/h) exp(ΔS[‡](T)/R) Tⁿ, deg. = 3, ek_B/h = 5.66 × 10¹⁰, n = 1.0, ΔS[‡](T) is estimated as loss of rotor (no rotor lost here, so ΔS[‡](T) is 0 kcal mol⁻¹). E_{a,f} = RS (28) + E_{abs} (10.11) kcal mol⁻¹.
- k₃ A_f via A_r and Microscopic Reversibility (MR), E_{a,r} = E_{a,f} - ΔU_{rot}, ΔU_{rot} = -7.16 kcal mol⁻¹.
- k₄ A_f via A_r and Microscopic Reversibility (MR), A_r = 1.00 × 10¹³, 84 WAR for H + CH₂O. E_{a,f} = E_{a,r} + ΔU_{rot}, ΔU_{rot} = 21.33 kcal mol⁻¹. E_{a,r} = 2.50 kcal mol⁻¹ (estimated by Bozzelli)

IID. 40 $\text{CH}_2\text{OH} + \text{O}_2 \rightarrow \text{Products}$ 

	Reaction	$A T^n e^{-E_a/T}$ (s^{-1})	E_a (kcal mol^{-1})
k_1	$\text{CH}_2\text{OH} + \text{O}_2 \rightarrow \text{C}(\text{OO})\text{H}_2\text{OH}$	$6.00 \times 10^{12} T^0 e^{-0T}$	0.00
k_1	$\text{C}(\text{OO})\text{H}_2\text{OH} \rightarrow \text{CH}_2\text{OH} + \text{O}_2$	$2.75 \times 10^{14} T^0 e^{-0T}$	35.16
k_2	$\text{C}(\text{OO})\text{H}_2\text{OH} \rightarrow \text{HOCH}_2\text{O}$	$1.23 \times 10^{14} T^0 e^{-0T}$	59.44
k_3	$\text{C}(\text{OO})\text{H}_2\text{OH} \rightarrow \text{C}(\text{OOH})\text{H}_2\text{O}$	$1.49 \times 10^9 T^{1.0} e^{-0T}$	29.89
k_3	$\text{C}(\text{OOH})\text{H}_2\text{O} \rightarrow \text{C}(\text{OO})\text{H}_2\text{OH}$	$2.54 \times 10^{12} T^{-0.15} e^{-0.00016T}$	12.81
k_4	$\text{C}(\text{OOH})\text{H}_2\text{O} \rightarrow \text{C}(\text{OO})\text{H}_2\text{OH}$	$4.10 \times 10^{12} T^0 e^{-0T}$	5.00
k_5	$\text{C}(\text{OO})\text{H}_2\text{OH} \rightarrow \text{HOC.HOOH}$	$2.60 \times 10^{10} T^{1.0} e^{-0T}$	40.10
k_5	$\text{HOC.HOOH} \rightarrow \text{C}(\text{OO})\text{H}_2\text{OH}$	$3.79 \times 10^{14} T^{-0.78} e^{-0.00093T}$	33.20
k_6	$\text{HOC.HOOH} \rightarrow \text{HCO}_2\text{H} + \text{OH}$	$3.80 \times 10^{13} T^0 e^{-0T}$	1.00
k_7	$\text{HOC.HOOH} \rightarrow \text{HOOCHO} + \text{H}$	$1.48 \times 10^{13} T^0 e^{-0T}$	21.07

frequency/degeneracy (CPFIT)

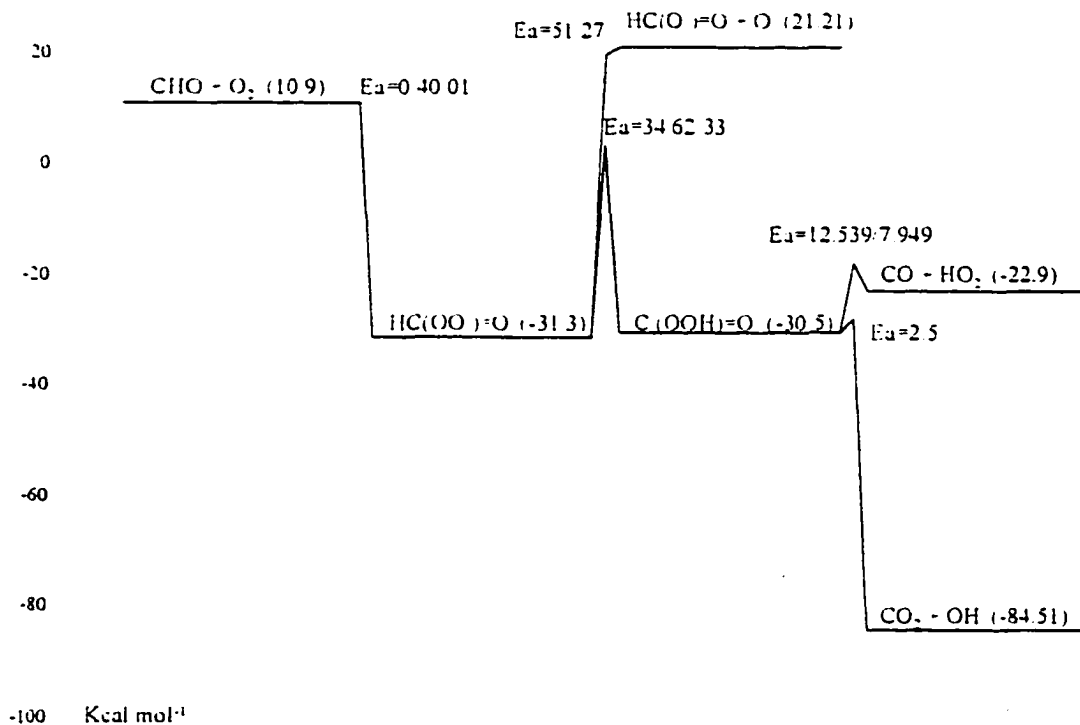
 $\text{C}(\text{OO})\text{H}_2\text{OH}$: 250.5 (4.365); 1024.3 (3.133); 2314.0 (6.502) $\text{C}(\text{OOH})\text{H}_2\text{O}$: 257.7 (4.476); 801.4 (3.128); 1871.3 (6.396) HOC.HOOH : 100.1 (3.079); 580.9 (4.827); 2001.8 (5.594)

Lennard-Jones parameter
 $\sigma(\text{\AA}) = 4.80$, $\epsilon/k(\text{K}) = 481.73$

- k_1 $2 \times (\text{CC} + \text{O}_2)$, 90 DEM/SAN and 89 ATK/BAU.
- k_1 A_r via A_f and Microscopic Reversibility (MR), $E_{a,r} = E_{a,f}(0) - \Delta U_{\text{run}} (-35.16) \text{ kcal mol}^{-1}$.
- k_2 A_f via A_r and Microscopic Reversibility (MR), $A_r = 1.51 \times 10^{13}$, 92 BAU/COB for $\text{O} + \text{CH}_3\text{O} \rightarrow \text{Prod.}$, $E_{a,f} = E_{a,r}(0) + \Delta U_{\text{run}} (59.44) \text{ kcal mol}^{-1}$.
- k_3 A_f estimated using TST, $A = (\text{deg.}) (ek_B/h) \exp(\Delta S^\ddagger(T)/R) T^n$, $\text{deg.} = 1$, $ek_B/h = 5.66 \times 10^{10}$, $n = 1.0$, $\Delta S^\ddagger(T)$ is estimated as loss of two rotors ($-4.3 \times 2 \text{ kcal mol}^{-1}$) and gain an optical isomer (OI). $E_{a,f} = \text{RS}(6) + E_{\text{abst}}(6.81) + \Delta H_{\text{run}}(17.08) \text{ kcal mol}^{-1}$.
- k_{-3} A_r via A_f and Microscopic Reversibility (MR), $E_{a,r} = E_{a,f} - \Delta U_{\text{run}}(17.08) \text{ kcal mol}^{-1}$.
- k_4 A_f via A_r and Microscopic Reversibility (MR), $A_r = 5.01 \times 10^{11}$, 72 KER/PAR for $\text{C}=\text{C} + \text{HO}_2 \rightarrow \text{Prod.}$, $E_{a,f}$ is estimated by Bozzelli.
- k_5 A_f estimated using TST, $A = (\text{deg.}) (ek_B/h) \exp(\Delta S^\ddagger(T)/R) T^n$, $\text{deg.} = 1$, $ek_B/h = 5.66 \times 10^{10}$, $n = 1.0$, $\Delta S^\ddagger(T)$ is estimated as loss of one rotor ($-4.3 \text{ kcal mol}^{-1}$) and gain an optical isomer (OI). $E_{a,f} = \text{RS}(26) + E_{\text{abst}}(7.20) + \Delta H_{\text{run}}(6.90) \text{ kcal mol}^{-1}$.
- k_{-5} A_r via A_f and Microscopic Reversibility (MR), $E_{a,r} = E_{a,f} - \Delta U_{\text{run}}(6.90) \text{ kcal mol}^{-1}$.
- k_6 A_f via A_r and Microscopic Reversibility (MR), $A_r = 2.75 \times 10^{12} = 1/2 (\text{OH} + \text{C}=\text{C})$, $E_{a,f}$ estimated the same $1.0 \text{ kcal mol}^{-1}$ based on $E_{a,f}$ for $\text{CH}_2\text{OOH} \rightarrow \text{CH}_2\text{O} + \text{OH}$ (1990 Page)
- k_7 A_f via A_r and Microscopic Reversibility (MR), $A_r = 1.00 \times 10^{13}$, 84 WAR for $\text{H} + \text{CH}_2\text{O}$. $E_{a,f} = E_{a,r} + \Delta U_{\text{run}}(18.37) \text{ kcal mol}^{-1}$. $E_{a,r} = 2.7 \text{ kcal mol}^{-1}$ (estimated by Bozzelli)

IID. 41 CHO + O₂ → Products

MEOH023



	Reaction	$A T^n e^{-E_a/T}$ (s ⁻¹)	E_a (kcal mol ⁻¹)
k_1	CHO + O ₂ → HC(OO.)=O	$6.00 \times 10^{12} T^0 e^{-E_a/T}$	0.00
k_{-1}	HC(OO.)=O → CHO + O ₂	$3.95 \times 10^{13} T^0 e^{-E_a/T}$	40.01
k_2	HC(OO.)=O → HC(O)=O + O	$2.98 \times 10^{14} T^0 e^{-E_a/T}$	51.27
k_3	HC(OO.)=O → C.(OOH)=O	$1.30 \times 10^{10} T^{1.0} e^{-E_a/T}$	34.62
k_{-3}	C.(OOH)=O → HC(OO.)=O	$1.13 \times 10^{13} T^{-0.29} e^{-0.00066T}$	33.00
k_4	C.(OOH)=O → CO + HO ₂	$2.33 \times 10^{11} T^0 e^{-E_a/T}$	12.54
k_5	C.(OOH)=O → CO ₂ + OH	$2.10 \times 10^{11} T^0 e^{-E_a/T}$	1.50

frequency/degeneracy (CPFIT)

HC(OO.)=O: 396.2 (2.750); 802.3 (1.921); 2085.1 (3.828)

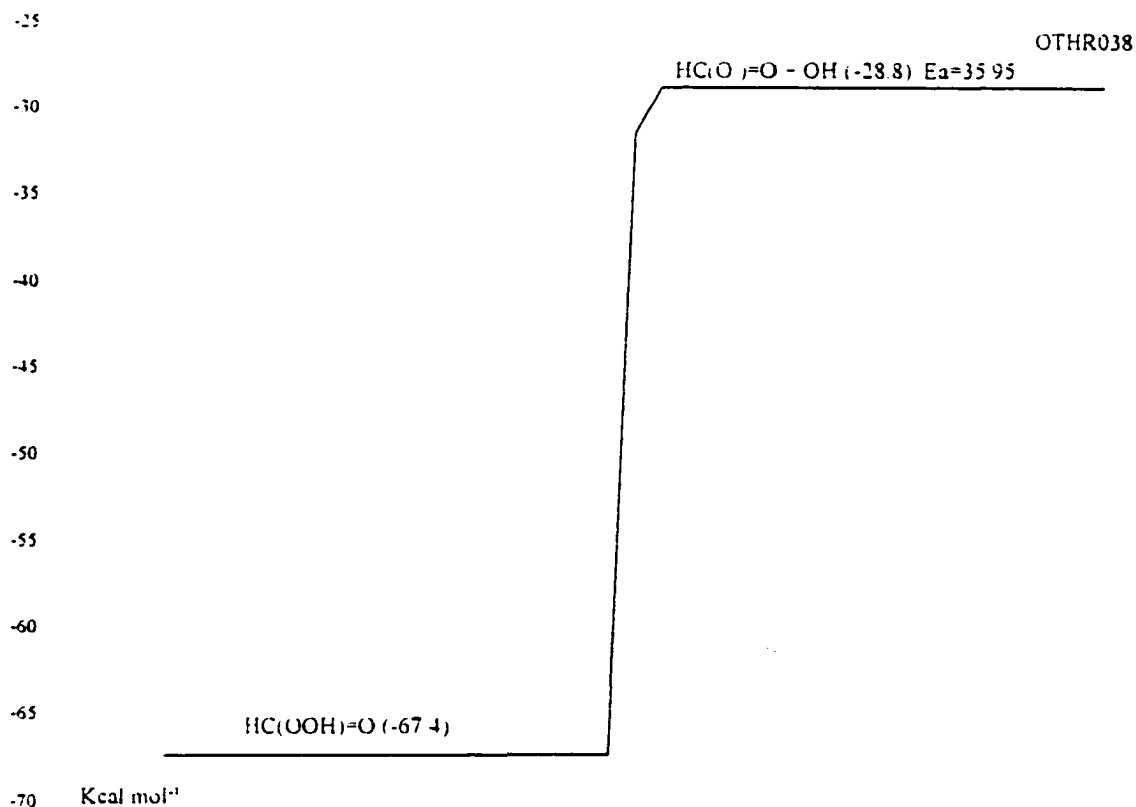
Lennard-Jones parameter

 $\sigma(\text{\AA}) = 4.80$, ϵ/k (K) = 481.73 k_1 A_f is taken as 2 times 90 DEM/ASN & 89 ATK/BAU for CC. + O₂. $E_{a,f}$ is 0 from

the same reference.

- k_1 A_f via A_r and Microscopic Reversibility (MR), $E_{a,f} = E_{a,r} - \Delta U_{rxn}$, $\Delta U_{rxn} = -40.01$ kcal mol⁻¹.
- k_2 A_f via A_r and Microscopic Reversibility (MR), $A_r = 1.51 \times 10^{13}$, 92 BAU/COB for $O + CH_3O \rightarrow \text{Prod.}$ $E_{a,f} = \Delta U_{rxn} = 51.27$ kcal mol⁻¹.
- k_3 A_f estimated using TST, $A = (\text{deg.}) (ek_B/h) \exp(\Delta S^\ddagger(T)/R) T^n$, deg. = 3, $ek_B/h = 5.66 \times 10^{10}$, $n = 1.0$, $\Delta S^\ddagger(T)$ is estimated as loss of one rotor (-4.3 kcal mol⁻¹) and gain one optical isomer (OI). $E_{a,f} = RS(26) + E_{a,bst}(7) + \Delta U_{rxn}(1.62)$ kcal mol⁻¹.
- k_3 A_f via A_r and Microscopic Reversibility (MR), $E_{a,f} = E_{a,r} - \Delta U_{rxn}$, $\Delta U_{rxn} = 1.62$ kcal mol⁻¹.
- k_4 A_f via A_r and Microscopic Reversibility (MR), $A_r = 1.21 \times 10^{11}$, 86 TSA/HAM for $C_2H_2 + CH_3O \rightarrow \text{Prod.}$ $E_{a,f} = E_{a,r} + \Delta U_{rxn}$, $\Delta U_{rxn} = 4.59$ kcal mol⁻¹. $E_{a,r} = 7.949$ kcal mol⁻¹ (referenced from 86 TSA for $C_2H_2 + HO_2 \rightarrow CH_2CO + OH$)
- k_5 A_f via A_r and Microscopic Reversibility (MR), $A_r = 2.75 \times 10^{12} = 1/2 (OH + C=C)$. $E_{a,f}$ estimated the same 1.5 kcal mol⁻¹ based on $E_{a,f}$ for $CH_2OOH \rightarrow CH_2O + OH$ (1990 Page)

IID. 42 $\text{HC}(\text{OOH})=\text{O} \rightarrow \text{HC}(\text{O.})=\text{O} + \text{OH}$



	Reaction	$A T^n e^{-a/T}$ (s^{-1} or $\text{cm}^3 \text{mol}^{-1} \text{s}^{-1}$)	E_a (kcal mol^{-1})
k_1	$\text{HC}(\text{OOH})=\text{O} \rightarrow \text{HC}(\text{O.})=\text{O} + \text{OH}$	$2.20 \times 10^{15} T^0 e^{-0/T}$	35.95

frequency/degeneracy (CPFIT)

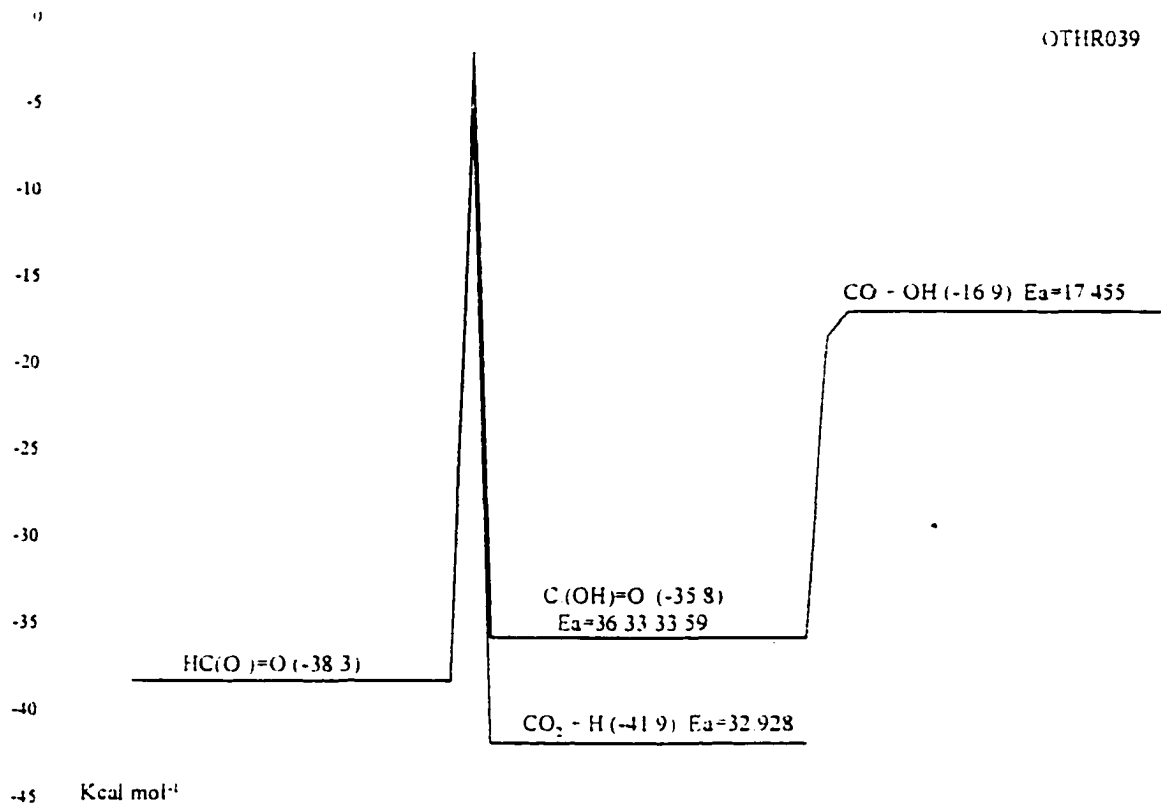
$\text{HC}(\text{OOH})=\text{O}$: 425.5 (3.716); 800.4 (2.821); 1723.9 (4.464)

Lennard-Jones parameter

$\sigma(\text{\AA}) = 4.80$, $\epsilon/k(\text{K}) = 481.73$

k_1 A_f via A_r and Microscopic Reversibility (MR), $A_r = 1.51 \times 10^{13}$, 91 TSA/HAM for $\text{C}=\text{CC.} + \text{OH}$. $E_{a,f} = E_{a,r}(0) + \Delta U_{\text{rxn}}$ (35.95) kcal mol^{-1} .

IID. 43 HC(O.)=O → Products



Reaction		$A T^n e^{-\alpha T}$ (s ⁻¹ or cm ³ mol ⁻¹ s ⁻¹)	E_a (kcal mol ⁻¹)
k_1	HC(O.)=O → CO ₂ + H	$1.74 \times 10^{12} T^{0.31} e^{-0.7T}$	32.93
k_2	HC(O.)=O → C.(OH)=O	$5.66 \times 10^{10} T^{1.0} e^{-0.7T}$	36.33
k_2	C.(OH)=O → HC(O.)=O	$3.15 \times 10^{12} T^{0.16} e^{-0.00069T}$	33.59
k_3	C.(OH)=O → CO + OH	$4.11 \times 10^{11} T^0 e^{-0.7T}$	17.46

frequency/degeneracy (CPFIT)

HC(O.)=O: 962.8 (1.855); 954.9 (1.796); 2215.5 (2.349)

C.(OH)=O: 500.5 (1.780); 800.0 (1.194); 1777.2 (2.525)

Lennard-Jones parameter

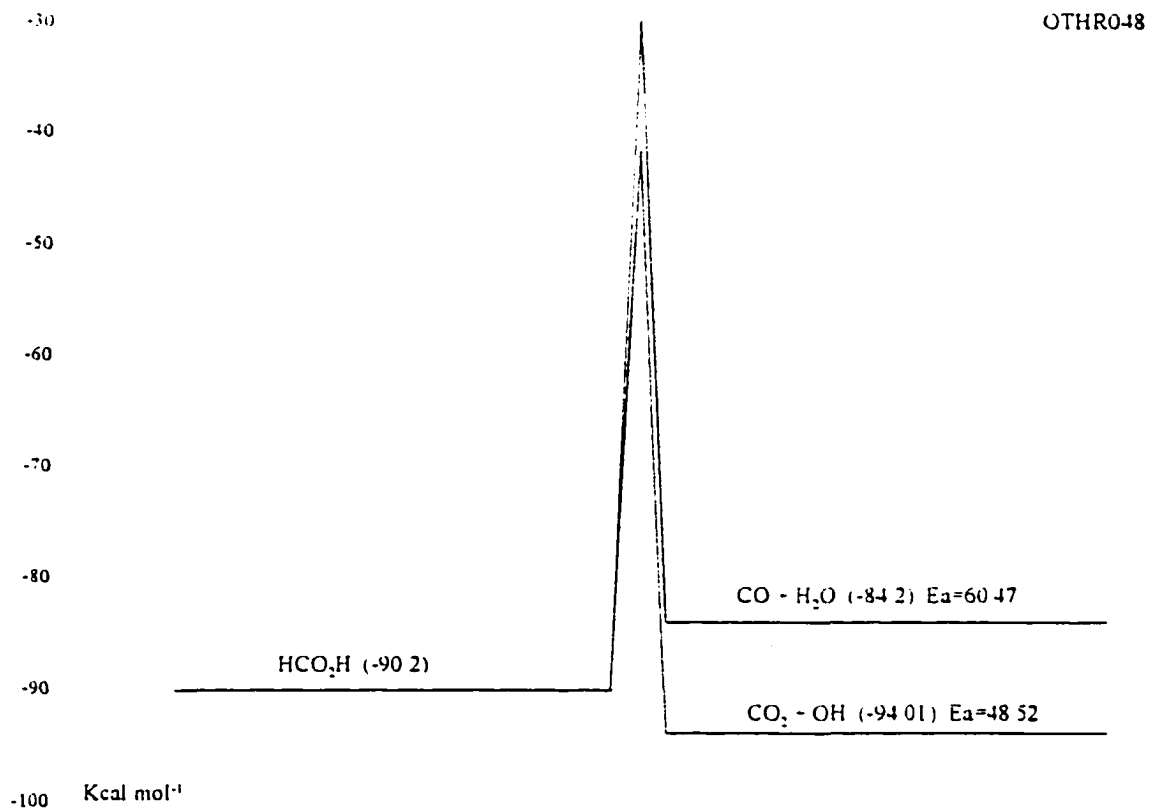
 $\sigma(\text{\AA}) = 4.35$, ϵ/k (K) = 422.61 k_1^* 88 LAR/STE.

k_2 A_r estimated using TST, $A = (\text{deg.}) (ek_B/h) T^n \exp(\Delta S^\ddagger(T)/R)$, $\text{deg.} = 1$, $ek_B/h = 5.66 \times 10^{10}$, $n = 1.0$, $\Delta S^\ddagger(T)$ is estimated as loss of rotor (no rotor loss here, so

$\Delta S^\ddagger(T) = 0$), $E_{a,f} = RS(28) - E_{abs} (5.59) \text{ kcal mol}^{-1}$.

k_{-2} A_r via A_f and Microscopic Reversibility (MR), $E_{a,r} = E_{a,f} - \Delta U_{rxn} (-25.0) + \Delta H_{rxn} (2.74) \text{ kcal mol}^{-1}$.

k_3 A_f via A_r and Microscopic Reversibility (MR), $A_r = 3.09 \times 10^{11}$, 72 DIX for $\text{CO} + \text{OH} \rightarrow \text{CO}_2 + \text{H}$, $E_{a,f} = E_{a,r} (0.735) + \Delta U_{rxn} (16.72) \text{ kcal mol}^{-1}$.

IID. 44 $\text{HCO}_2\text{H} \rightarrow \text{Products}$ 

	Reaction	$A T^n e^{-\alpha T}$ (s ⁻¹)	E_a (kcal mol ⁻¹)
k_1	$\text{HCO}_2\text{H} \rightarrow \text{CO} + \text{H}_2\text{O}$	$2.45 \times 10^{12} T^0 e^{-0T}$	60.47
k_2	$\text{HCO}_2\text{H} \rightarrow \text{CO}_2 + \text{H}_2$	$2.95 \times 10^9 T^0 e^{-0T}$	48.52

frequency/degeneracy (CPFIT)

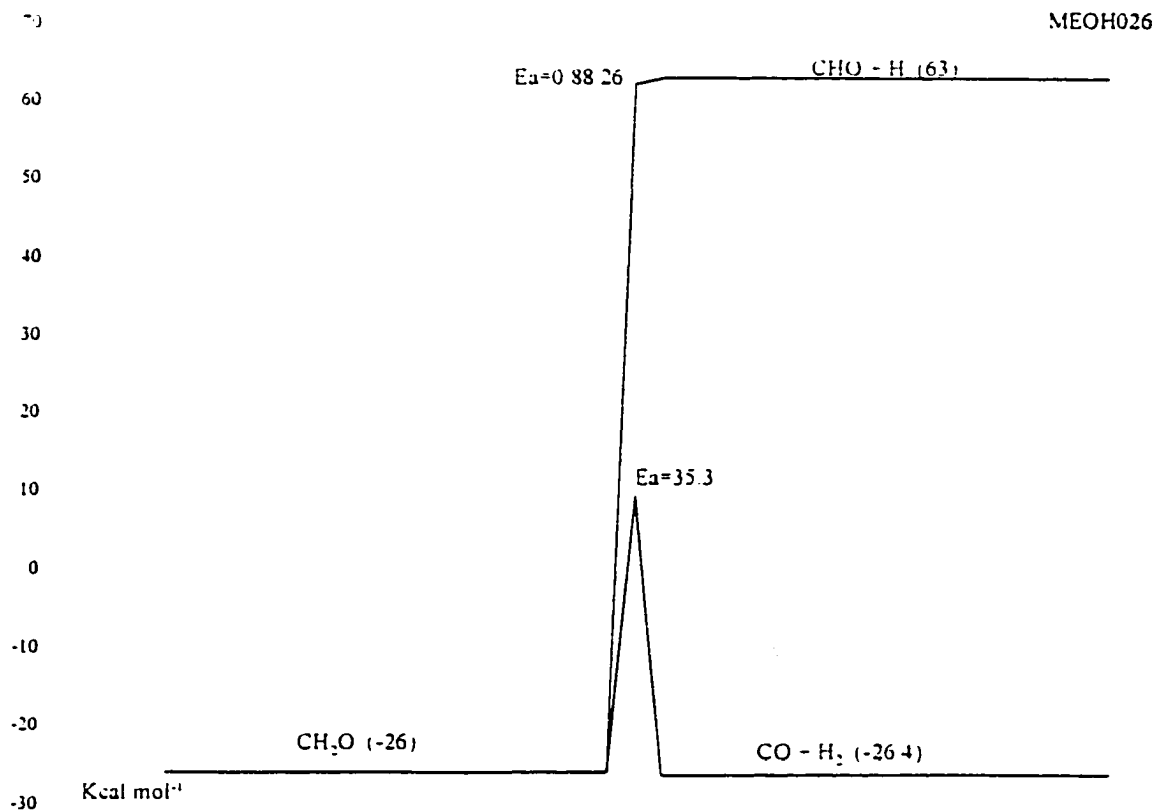
HCO_2H : 747.0 (2.569); 996.2 (2.452); 2148.2 (3.479)

Lennard-Jones parameter

$\sigma(\text{\AA}) = 4.34$, $\epsilon/k(\text{K}) = 422.61$

k_1 71 BLA/DAL, NIST

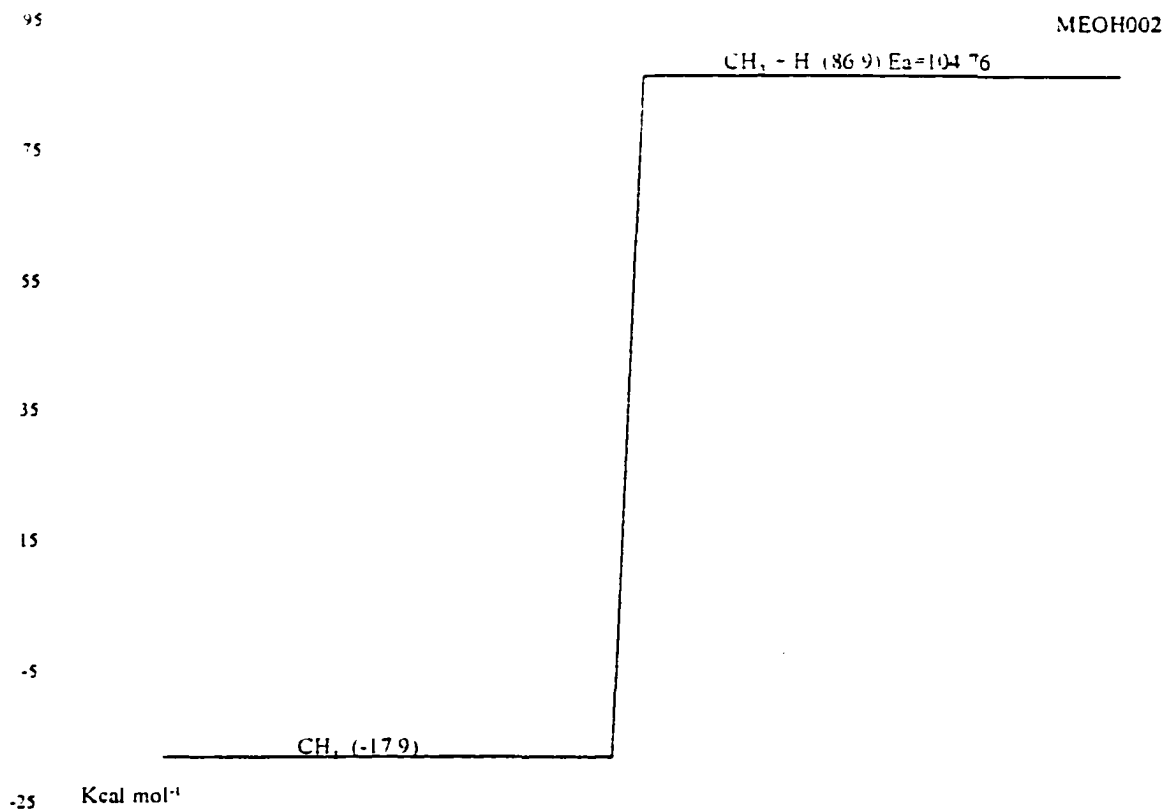
k_2 71 BLA/DAL, NIST

IID. 45 $\text{CH}_2\text{O} \rightarrow \text{Products}$ 

	Reaction	$A T^n e^{-\alpha T}$ (s ⁻¹)	E_a (kcal mol ⁻¹)
k_1	$\text{CH}_2\text{O} \rightarrow \text{CHO} + \text{H}$	$3.59 \times 10^{14} T^0 e^{-0T}$	88.26
k_2	$\text{CH}_2\text{O} \rightarrow \text{CO} + \text{H}_2$	$4.52 \times 10^{15} T^0 e^{-0T}$	35.30

frequency/degeneracy (CPFIT)
 CH_2O : 1071.8 (0.995); 1468.5 (2.766); 2740.8 (2.239)
 Lennard-Jones parameter
 $\sigma(\text{\AA}) = 3.59$, $\epsilon/k(\text{K}) = 498.0$

- k_1 A_f is taken from NIST fit. $E_{a,f} = \Delta U_{\text{rxn}} = 88.26 \text{ kcal mol}^{-1}$.
 k_2 NIST fit.

IID. 46 $\text{CH}_4 \rightarrow \text{CH}_3 + \text{H}$ 

	Reaction	$A T^n e^{-E_a/T}$ (s ⁻¹)	E _a (kcal mol ⁻¹)
k ₁	CH ₄ → CH ₃ + H	$1.07 \times 10^{16} T^0 e^{-0.7T}$	104.76

frequency/degeneracy (CPFIT)

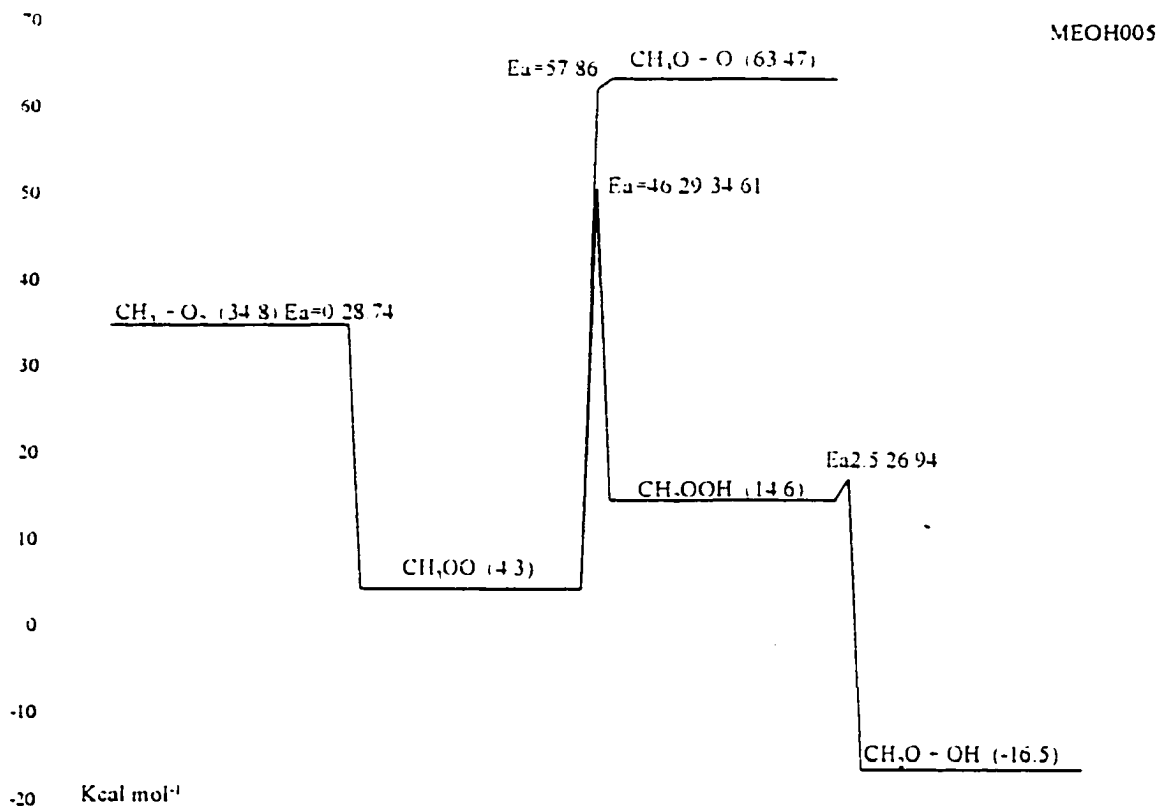
CH₄: 1106.6 (2.973); 2499.9 (4.410); 3693.3 (1.617)

Lennard-Jones parameter

$\sigma(\text{\AA}) = 3.75$, ϵ/k (K) = 141.40

k₁ A_f via A_r and Microscopic Reversibility (MR), A_r = 2.11 × 10¹⁴, 92 BAU/COB. E_{a,f} = E_{a,r}(0) + ΔU_{rxn} (104.76) kcal mol⁻¹.

ID. 47 $\text{CH}_3 + \text{O}_2 \rightarrow \text{Products}$



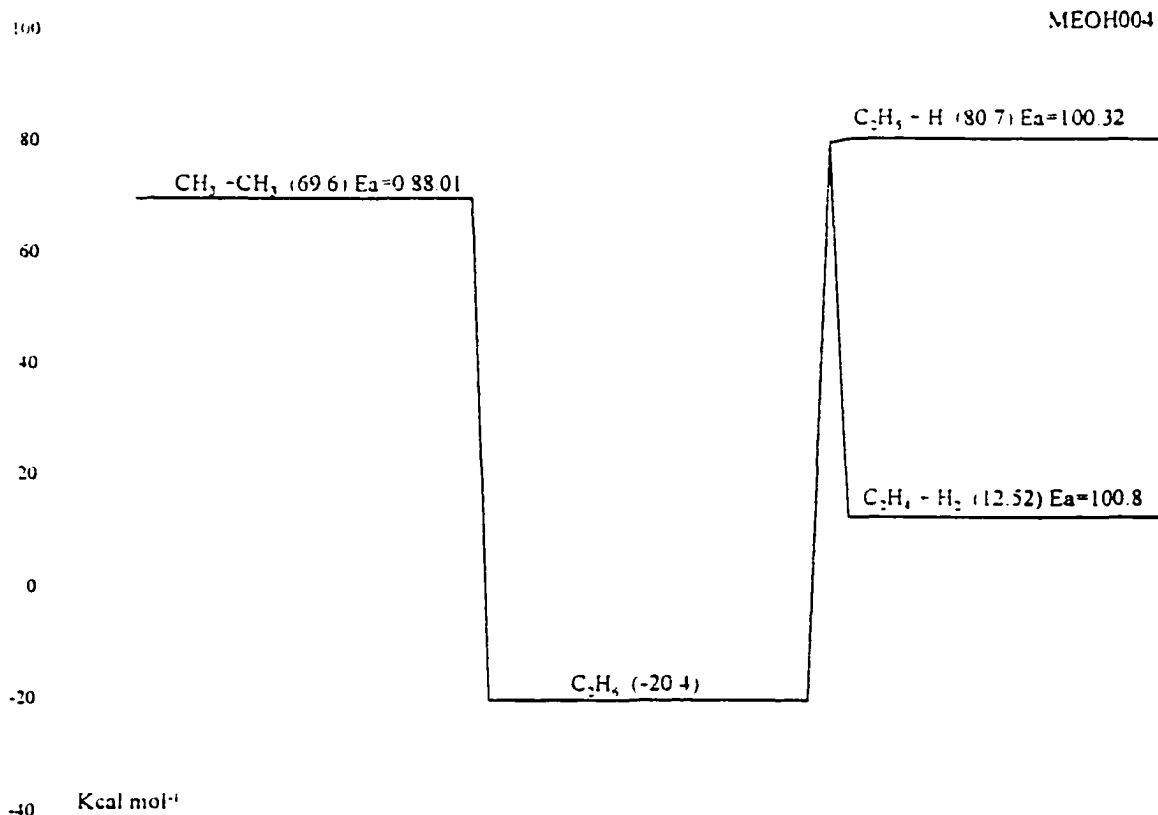
	Reaction	$A T^n e^{-uT}$ (s ⁻¹)	E_a (kcal mol ⁻¹)
k_1	$\text{CH}_3 + \text{O}_2 \rightarrow \text{CH}_3\text{OO}\cdot$	$1.08 \times 10^{12} T^0 e^{-0T}$	0.00
k_{-1}	$\text{CH}_3\text{OO}\cdot \rightarrow \text{CH}_3 + \text{O}_2$	$2.49 \times 10^{13} T^0 e^{-0T}$	28.74
k_2	$\text{CH}_3\text{OO}\cdot \rightarrow \text{CH}_3\text{O} + \text{O}$	$1.36 \times 10^{14} T^0 e^{-0T}$	57.86
k_3	$\text{CH}_3\text{OO}\cdot \rightarrow \text{CH}_2\text{OOH}$	$3.90 \times 10^{10} T^{1.0} e^{-0T}$	46.29
k_{-3}	$\text{CH}_2\text{OOH} \rightarrow \text{CH}_3\text{OO}\cdot$	$3.82 \times 10^{14} T^{-0.92} e^{-0.00084T}$	34.61
k_4	$\text{CH}_2\text{OOH} \rightarrow \text{CH}_2\text{O} + \text{OH}$	$3.07 \times 10^{12} T^0 e^{-0T}$	2.50

frequency/degeneracy (CPFIT)
 $\text{CH}_3\text{OO}\cdot$: 250.3 (2.713); 1091.2 (3.941); 2772.2 (4.846)
 Lennard-Jones parameter
 $\sigma(\text{\AA}) = 4.34$, $\epsilon/k(\text{K}) = 422.61$

k_1 90 DEM/ASN & 89 ATK/BAU.

k_{-1} A_r via A_f and Microscopic Reversibility (MR), $E_{a,r} = E_{a,f} - \Delta U_{\text{rxn}}$, $\Delta U_{\text{rxn}} = -28.74$

- kcal mol⁻¹.
- k₂ A_f via A_r and Microscopic Reversibility (MR), A_r = 1.51×10^{13} , 92 BAU/COB for O + CH₃O → Prod.). E_{a,f} = ΔU_{rot} = 57.86 kcal mol⁻¹
- k₃ A_f estimated using TST, A = (deg.) (ek_B/h) exp(ΔS[‡](T)/R) Tⁿ, deg. = 3, ek_B/h = 5.66×10^{10} , n = 1.0, ΔS[‡](T) is estimated as loss of one rotor (-4.3 kcal mol⁻¹) and gain one optical isomer (OI). E_{a,f} = RS (26) + E_{abst} (8.61) + ΔU_{rot} (11.68) kcal mol⁻¹
- k₃ A_r via A_f and Microscopic Reversibility (MR), E_{a,r} = E_{a,f} - ΔU_{rot}, ΔU_{rot} = 11.68 kcal mol⁻¹.
- k₄ A_f via A_r and Microscopic Reversibility (MR), A_r = 2.75×10^{12} = 1/2 (OH + C=C). E_{a,f} estimated the same 2.5 kcal mol⁻¹ based on E_{a,f} for CH₂OOH → CH₂O + OH (1990 Page)

IID. 48 $\text{CH}_3 + \text{CH}_3 \rightarrow \text{Products}$ 

	Reaction	$A T^n e^{-a/T}$ (s ⁻¹)	E_a (kcal mol ⁻¹)
k_1	$\text{CH}_3 + \text{CH}_3 \rightarrow \text{C}_2\text{H}_6$	$3.61 \times 10^{13} T^0 e^{-0/T}$	0.00
k_{-1}	$\text{C}_2\text{H}_6 \rightarrow \text{CH}_3 + \text{CH}_3$	$4.08 \times 10^{16} T^0 e^{-0/T}$	88.01
k_2	$\text{C}_2\text{H}_6 \rightarrow \text{C}_2\text{H}_5 + \text{H}$	$1.26 \times 10^{16} T^0 e^{-0/T}$	100.32
k_3	$\text{C}_2\text{H}_6 \rightarrow \text{C}_2\text{H}_4 + \text{H}_2$	$4.95 \times 10^{20} T^0 e^{-0/T}$	100.80

frequency/degeneracy (CPFIT)
 C_2H_6 : 729.3 (4.525); 1333.9 (6.571); 2825.0 (6.404)

Lennard-Jones parameter
 $\sigma(\text{\AA}) = 4.3$, $\epsilon/k(\text{K}) = 252.3$

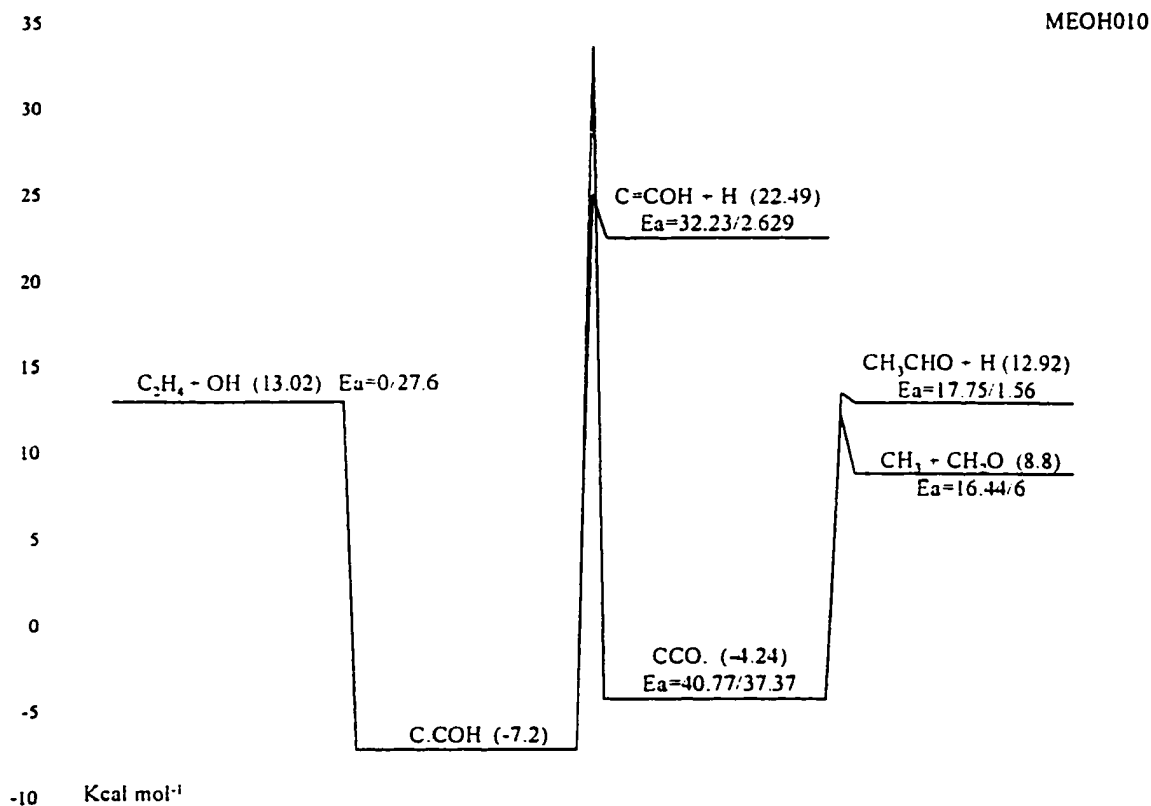
k_1 92 BAU/COB

k_{-1} A_r via A_f and Microscopic Reversibility (MR), $E_{a,r} = E_{a,f} - \Delta U_{\text{rxn}}$, $\Delta U_{\text{rxn}} = 88.01$ kcal mol⁻¹.

k_2 A_f via A_r and Microscopic Reversibility (MR), $A_r = 1.00 \times 10^{14}$, 93 SIL/RAT. $E_{a,f} =$

$$\Delta U_{\text{rxn}} = 100.32 \text{ kcal mol}^{-1}.$$

k_3 A_f is taken from NIST fit. $E_{a,f} = \Delta U_{\text{rxn}} = 100.80 \text{ kcal mol}^{-1}$.

IID. 49 $C_2H_4 + OH \rightarrow \text{Products}$ 

	Reaction	$A T^n e^{-\alpha T}$ (s ⁻¹ or cm ³ mol ⁻¹ s ⁻¹)	E_a (kcal mol ⁻¹)
k_1	$C_2H_4 + OH \rightarrow C.CO.H$	$5.42 \times 10^{12} T^0 e^{-0T}$	0.00
k_{-1}	$C.CO.H \rightarrow C_2H_4 + OH$	$7.65 \times 10^{12} T^0 e^{-0T}$	27.60
k_2	$C.CO.H \rightarrow C=COH + H$	$3.85 \times 10^{11} T^0 e^{-0T}$	32.23
k_3	$C.CO.H \rightarrow CCO.$	$8.58 \times 10^8 T^{0.97} e^{-0.00042T}$	40.77
k_{-3}	$CCO. \rightarrow C.CO.H$	$1.95 \times 10^{10} T^{1.0} e^{-0T}$	37.37
k_4	$CCO. \rightarrow CH_2O + CH_3$	$1.04 \times 10^{13} T^0 e^{-0T}$	16.44
k_5	$CCO. \rightarrow CH_3CHO + H$	$1.73 \times 10^{13} T^0 e^{-0T}$	17.75

frequency/degeneracy (CPFIT)

C.CO.H: 583.0 (5.793); 1512.1 (6.964); 3255.1 (4.243)

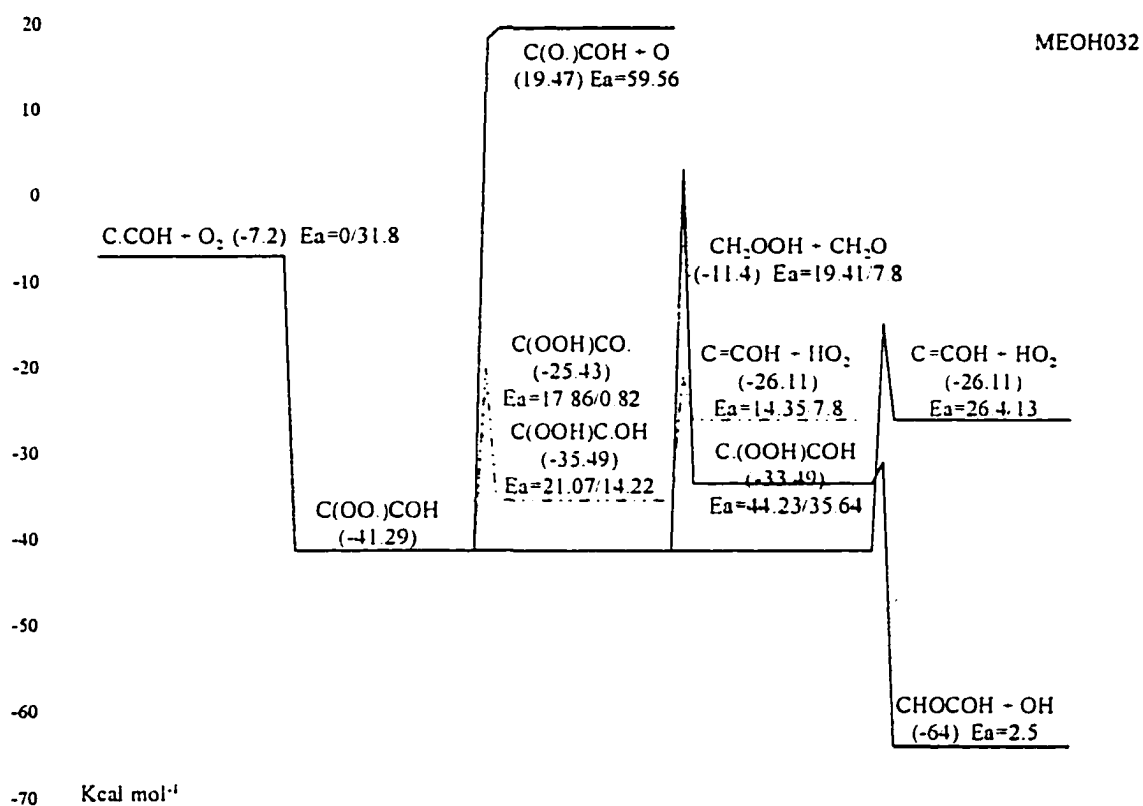
CCO.: 619.0 (5.969); 1499.7 (7.377); 3180.0 (4.154)

Lennard-Jones parameter

$\sigma(\text{\AA}) = 4.35$, ϵ/k (K) = 422.61

- k_1 92 BAU/COB.
- k_{-1} A_r via A_f and Microscopic Reversibility (MR), $E_{a,r} = E_{a,f}(0) - \Delta U_{rxn} (-27.6) \text{ kcal mol}^{-1}$.
- k_2 A_f via A_r and Microscopic Reversibility (MR), $A_r = 4.00 \times 10^{12}$, 84 WAR for $CC=C + H \rightarrow CCC$. $E_{a,f} = E_{a,r} (2.629) + \Delta U_{rxn} (29.6) \text{ kcal mol}^{-1}$.
- k_{-3} A_f via A_r and Microscopic Reversibility (MR), $E_{a,f} = E_{a,r} + \Delta U_{rxn} (3.4) \text{ kcal mol}^{-1}$.
- k_{-3} A_r estimated using TST, $A = (\text{deg.}) (ek_b/h) T^n \exp(\Delta S^\ddagger(T)/R)$, $\text{deg.} = 3$, $ek_b/h = 5.66 \times 10^{10}$, $n = 1.0$, $\Delta S^\ddagger(T)$ is estimated as loss of one rotors $(-4.3 \text{ cal mol}^{-1} \text{ K}^{-1})$. $E_{a,f} = RS (26) + E_{abst} (11.37) \text{ kcal mol}^{-1}$.
- k_4 A_f via A_r and Microscopic Reversibility (MR), $A_r = 3.31 \times 10^{11}$ 86 TSA/HAM for $CH_3 + C=C$. $E_{a,f} = E_{a,r} + \Delta U_{rxn} (10.44) \text{ kcal mol}^{-1}$. $E_{a,r} = 6.0 \text{ kcal mol}^{-1}$. (estimated by Bozzelli).
- k_5 A_f via A_r and Microscopic Reversibility (MR), $A_r = 6.50 \times 10^{12} = 1/2 (H + CC=C \rightarrow CC.C, 91 \text{ TSA/HAM})$. $E_{a,f} = E_{a,r} (1.56) + \Delta U_{rxn} (16.19) \text{ kcal mol}^{-1}$.

IID. 50 C.CO₂H + O₂ → Products



	Reaction	$A T^n e^{-aT}$ (s ⁻¹ or cm ³ mol ⁻¹ s ⁻¹)	E_a (kcal mol ⁻¹)
k ₁	C.CO ₂ H + O ₂ → C(OO.)CO ₂ H	$3.01 \times 10^{12} T^0 e^{-0T}$	0.00
k ₋₁	C(OO.)CO ₂ H → C.CO ₂ H + O ₂	$5.93 \times 10^{14} T^0 e^{-0T}$	31.81
k ₂	C(OO.)CO ₂ H → C(O.)CO ₂ H + O	$2.63 \times 10^{14} T^0 e^{-0T}$	59.56
k ₃	C(OO.)CO ₂ H → C=COH + HO ₂	$1.49 \times 10^{10} T^{0.74} e^{-0T}$	26.40
k ₄	C(OO.)CO ₂ H → C.(OOH)CO ₂ H	$2.60 \times 10^{10} T^{1.0} e^{-0T}$	44.23
k ₋₄	C.(OOH)CO ₂ H → C(OO.)CO ₂ H	$6.71 \times 10^{12} T^{-0.33} e^{-0.00073T}$	35.64
k ₅	C.(OOH)CO ₂ H → CHOCO ₂ H + OH	$1.16 \times 10^{13} T^0 e^{-0T}$	2.50
k ₆	C(OO.)CO ₂ H → C(OOH)C.OH	$2.99 \times 10^9 T^{1.0} e^{-0T}$	21.07
k ₋₆	C(OOH)C.OH → C(OO.)CO ₂ H	$2.52 \times 10^{13} T^{-0.68} e^{-0.00087T}$	14.22
k ₇	C(OOH)C.OH → C=COH + HO ₂	$2.41 \times 10^{12} T^0 e^{-0T}$	14.35
k ₈	C(OO.)CO ₂ H → C(OOH)CO.	$1.72 \times 10^3 T^{1.0} e^{-0T}$	17.86
k ₋₈	C(OOH)CO. → C(OO.)CO ₂ H	$1.72 \times 10^{11} T^{-0.06} e^{-0.00009T}$	0.82
k ₉	C(OOH)CO. → CH ₂ O + CH ₂ OOH	$6.82 \times 10^{13} T^0 e^{-0T}$	19.41

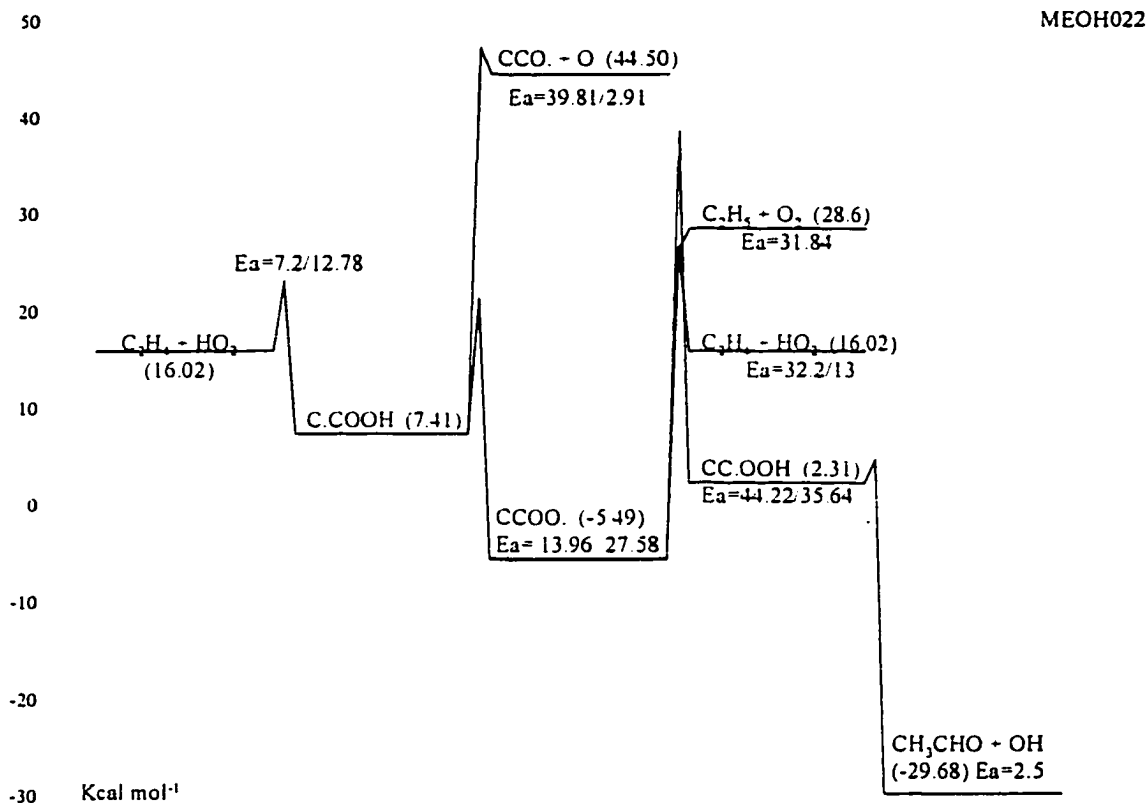
frequency/degeneracy (CPFIT)

C(OO.)COH: 265.0 (6.738); 1167.8 (9.006); 2891.9 (6.756)
 C.(OOH)COH: 257.1 (8.192); 1237.6 (8.815); 2903.7 (4.993)
 C(OOH)C.OH: 299.8 (8.560); 1190.9 (8.506); 2901.2 (4.933)
 C(OOH)CO.: 277.1 (7.323); 1180.9 (10.312); 2843.6 (4.865)

Lennard-Jones parameter

$\sigma(\text{\AA}) = 5.20$, ϵ/k (K) = 533.08

- k_1 89 ATK/BAU and 90 DEM/SAN for CC. + O₂.
- k_{-1} A_r via A_f and Microscopic Reversibility (MR), $E_{a,r} = E_{a,f} - \Delta U_{\text{rxn}}$ (-31.81) kcal mol⁻¹.
- k_2 A_f via A_r and Microscopic Reversibility (MR), $A_r = 1.51 \times 10^{13}$, 92 BAU/COB for O + CH₃O → Prod., $E_{a,f} = E_{a,f}(0) + \Delta U_{\text{rxn}}$ (59.56) kcal mol⁻¹.
- k_3 A_f is referenced from reaction C2CCOO. → C2C=C + HO₂, (from thermal reaction analysis (AFACT2f) based on the thermodynamic properties calculated from MOPAC PM3 (corrected with internal rotor, electronic spin and optical isomer). $E_{a,f} = E_{a,r} + \Delta U_{\text{rxn}}$ (13.40) $E_{a,r}$ is estimated as ring strain (6) + $E_{a,\text{add}}$ (7).
- k_4 A_f estimated using TST, $A = (\text{deg.}) (ek_B/h) T^n \exp(\Delta S^\ddagger(T)/R)$, deg. = 2, $ek_B/h = 5.66 \times 10^{10}$, $n = 1.0$, $\Delta S^\ddagger(T)$ is estimated as loss of one rotor (-4.3 cal mol⁻¹ K⁻¹) and gain an optical isomer (OI). $E_{a,f} = RS$ (26) + $E_{a,\text{bst}}$ (9.64) + ΔH_{rxn} (8.59) kcal mol⁻¹.
- k_{-4} A_r via A_f and Microscopic Reversibility (MR), $E_{a,r} = E_{a,f} - \Delta U_{\text{rxn}}$ (8.59) kcal mol⁻¹.
- k_5 A_f via A_r and Microscopic Reversibility (MR), $A_r = 2.75 \times 10^{12} = 1/2$ (OH + C=C). $E_{a,f}$ estimated the same 2.5 kcal mol⁻¹ as $E_{a,r}$ for CH₂OOH → CH₂O + OH (1990 Page)
- k_6 A_f estimated using TST, $A = (\text{deg.}) (ek_B/h) T^n \exp(\Delta S^\ddagger(T)/R)$, deg. = 2, $ek_B/h = 5.66 \times 10^{10}$, $n = 1.0$, $\Delta S^\ddagger(T)$ is estimated as loss of two rotors (-4.3 × 2 cal mol⁻¹ K⁻¹) and gain an optical isomer (OI). $E_{a,f} = RS$ (6) + $E_{a,\text{bst}}$ (8.22) + ΔH_{rxn} (6.85) kcal mol⁻¹.
- k_{-6} A_r via A_f and Microscopic Reversibility (MR), $E_{a,r} = E_{a,f} - \Delta U_{\text{rxn}}$ (6.85) kcal mol⁻¹.
- k_7 A_f via A_r and Microscopic Reversibility (MR), $A_r = 2.50 \times 10^{11} = 1/2$ (HO₂ + C=C), 72 KER/PAR. $E_{a,f} = E_{a,r} + \Delta U_{\text{rxn}}$ (6.55) kcal mol⁻¹. $E_{a,r} = 7.8$ kcal mol⁻¹. (estimated by Bozzelli).
- k_8 A_f estimated using TST, $A = (\text{deg.}) (ek_B/h) T^n \exp(\Delta S^\ddagger(T)/R)$, deg. = 3, $ek_B/h = 5.66 \times 10^{10}$, $n = 1.0$, $\Delta S^\ddagger(T)$ is estimated as loss of three rotors (-4.3 × 3 cal mol⁻¹ K⁻¹) and gain an optical isomer (OI). $E_{a,f} = RS$ (0) + $E_{a,\text{bst}}$ (6.82) - H bond (6) + ΔH_{rxn} (17.04) kcal mol⁻¹.
- k_{-8} A_r via A_f and Microscopic Reversibility (MR), $E_{a,r} = E_{a,f} - \Delta U_{\text{rxn}}$ (17.04) kcal mol⁻¹.
- k_9 A_f via A_r and Microscopic Reversibility (MR), $A_r = 3.31 \times 10^{11}$, 86 TSA/HAM and 72 KER/PAR for C=C + CH₃. $E_{a,f} = E_{a,r}$ (7.8) + ΔU_{rxn} (11.61) kcal mol⁻¹.

IID. 51 $C_2H_4 + HO_2 \rightarrow$ Products

	Reaction	$A T^n e^{-\alpha T}$ (s ⁻¹)	E_a (kcal mol ⁻¹)
k ₁	$C_2H_4 + HO_2 \rightarrow C.COOH$	$3.50 \times 10^{11} T^0 e^{-0T}$	7.20
k ₋₁	$C.COOH \rightarrow C_2H_4 + HO_2$	$8.23 \times 10^{11} T^0 e^{-0T}$	12.78
k ₂	$C.COOH \rightarrow C=COOH + H$	$7.61 \times 10^{11} T^0 e^{-0T}$	39.81
k ₃	$C.COOH \rightarrow CCOO.$	$2.14 \times 10^{11} T^{-0.12} e^{-0.00057T}$	13.96
k ₋₃	$CCOO. \rightarrow C.COOH$	$4.49 \times 10^9 T^{1.0} e^{-0T}$	27.58
k ₄	$CCOO. \rightarrow C_2H_5 + O_2$	$2.99 \times 10^{14} T^0 e^{-0T}$	31.84
k ₅	$CCOO. \rightarrow C_2H_4 + HO_2$	$2.24 \times 10^{10} T^{0.74} e^{-0T}$	32.20
k ₆	$CCOO. \rightarrow CC.OOH$	$2.60 \times 10^{10} T^{1.0} e^{-0T}$	44.22
k ₋₆	$CC.OOH \rightarrow CCOO.$	$6.77 \times 10^{12} T^{-0.33} e^{-0.00075T}$	35.64
k ₇	$CC.OOH \rightarrow CH_3CHO + OH$	$1.15 \times 10^{13} T^0 e^{-0T}$	2.50

frequency/degeneracy (CPFIT)

CCOO.: 250.3 (4.749); 1127.3 (8.486); 2761.8 (6.765)

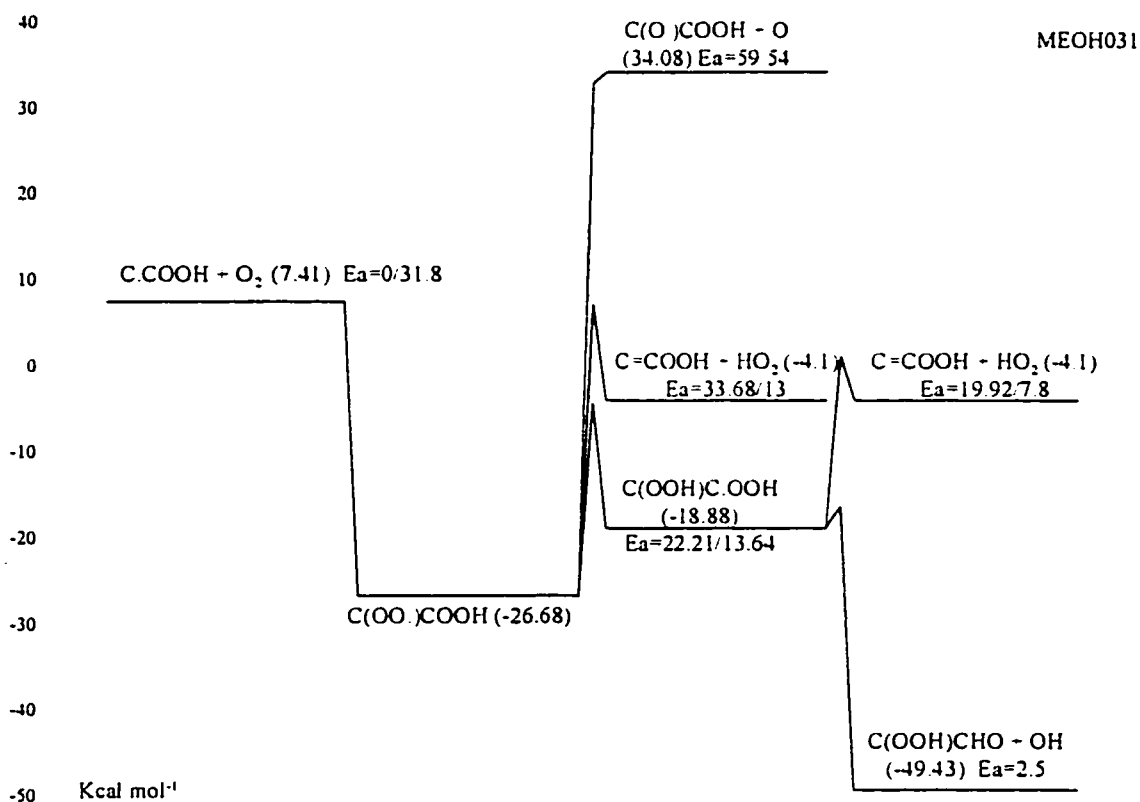
C.COOH: 251.0 (5.710); 1184.3 (9.067); 2804.0 (4.723)

CC.OOH: 100.4 (5.313); 1071.3 (8.260); 2583.3 (5.926)

Lennard-Jones parameter
 $\sigma(\text{\AA}) = 4.80$, $\varepsilon/k(\text{K}) = 481.73$

- k_1 estimated by Bozzelli.
- k_{-1} A_r via A_f and Microscopic Reversibility (MR), $E_{a,r} = E_{a,f} - \Delta U_{rxn}$ (-5.58) kcal mol⁻¹.
- k_2 A_f via A_r and Microscopic Reversibility (MR), $A_r = 7.23 \times 10^{12}$, 91 TSA/HAM for $H + CC=C \rightarrow CCC..$ $E_{a,f} = E_{a,r} + \Delta U_{rxn}$ (36.9) kcal mol⁻¹. $E_{a,r} = 2.906$ kcal mol⁻¹. (taken from the same reference).
- k_3 A_f estimated using TST, $A = (\text{deg.}) (ek_b/h) \exp(\Delta S^\ddagger(T)/R) T^n$, deg. = 3, $ek_b/h = 5.66 \times 10^{10}$, $n = 1.0$, $\Delta S^\ddagger(T)$ is estimated as loss of two rotors (-4.3×2 kcal mol⁻¹) and gain one optical isomer (OI). $E_{a,f} = RS(6) + E_{abst}(7.96) + \Delta H_{rxn}(13.62)$ kcal mol⁻¹.
- k_{-3} A_r via A_f and Microscopic Reversibility (MR), $E_{a,r} = E_{a,f} - \Delta U_{rxn}$ (13.62) kcal mol⁻¹.
- k_4 A_f via A_r and Microscopic Reversibility (MR), $A_r = 3.01 \times 10^{12}$, 90 DEM/ASN and 89 ATK/BAU. $E_{a,f} = E_{a,r}(0) + \Delta U_{rxn}$ (31.84) kcal mol⁻¹.
- k_5 A_f is referenced from reaction $C2CCOO. \rightarrow C2C=C + HO_2$, (from thermal reaction analysis (AFACT2f) based on the thermodynamic properties calculated from MOPAC PM3 (corrected with internal rotor, electronic spin and optical isomer). $E_{a,f} = E_{a,r} + \Delta U_{rxn}$ (19.20) $E_{a,r}$ is estimated as ring strain (6) + $E_{a,add}$ (7).
- k_6 A_f estimated using TST, $A = (\text{deg.}) (ek_b/h) \exp(\Delta S^\ddagger(T)/R) T^n$, deg. = 2, $ek_b/h = 5.66 \times 10^{10}$, $n = 1.0$, $\Delta S^\ddagger(T)$ is estimated as loss of one rotor (-4.3 kcal mol⁻¹) and gain one optical isomer (OI). $E_{a,f} = RS(26) + E_{abst}(9.64) + \Delta H_{rxn}(8.58)$ kcal mol⁻¹.
- k_{-6} A_r via A_f and Microscopic Reversibility (MR), $E_{a,r} = E_{a,f} - \Delta U_{rxn}$ (8.58) kcal mol⁻¹.
- k_7 A_f via A_r and Microscopic Reversibility (MR), $A_r = 2.75 \times 10^{12} = 1/2 (OH + C=C)$. $E_{a,f}$ estimated the same 2.5 kcal mol⁻¹ based on $E_{a,f}$ for $CH_2OOH \rightarrow CH_2O + OH$ (1990 Page)

IID. 52 C.COOH + O₂ → Products



	Reaction	$A T^n e^{-\alpha T}$ (s ⁻¹ or cm ³ mol ⁻¹ s ⁻¹)	E_a (kcal mol ⁻¹)
k ₁	C.COOH + O ₂ → C(OO.)COOH	$3.01 \times 10^{12} T^0 e^{-0T}$	0.00
k ₋₁	C(OO.)COOH → C.COOH + O ₂	$6.34 \times 10^{14} T^0 e^{-0T}$	31.80
k ₂	C(OO.)COOH → C(O.)COOH + O	$2.61 \times 10^{14} T^0 e^{-0T}$	59.54
k ₃	C(OO.)COOH → C=COOH + HO ₂	$1.49 \times 10^{10} T^{0.74} e^{-0T}$	33.68
k ₄	C(OO.)COOH → C(OOH)C.OOH	$2.99 \times 10^9 T^{1.0} e^{-0T}$	22.21
k ₋₄	C(OOH)C.OOH → C(OO.)COOH	$8.68 \times 10^{11} T^{-0.36} e^{-0.00078T}$	13.64
k ₅	C(OOH)C.OOH → C=COOH + HO ₂	$7.40 \times 10^{11} T^0 e^{-0T}$	19.92
k ₆	C(OOH)C.OOH → C(OOH)CHO + OH	$1.88 \times 10^{13} T^0 e^{-0T}$	2.50

frequency/degeneracy (CPFIT)

C(OO.)COOH: 100.4 (7.902); 1049.4 (10.517); 2637.2 (6.581)

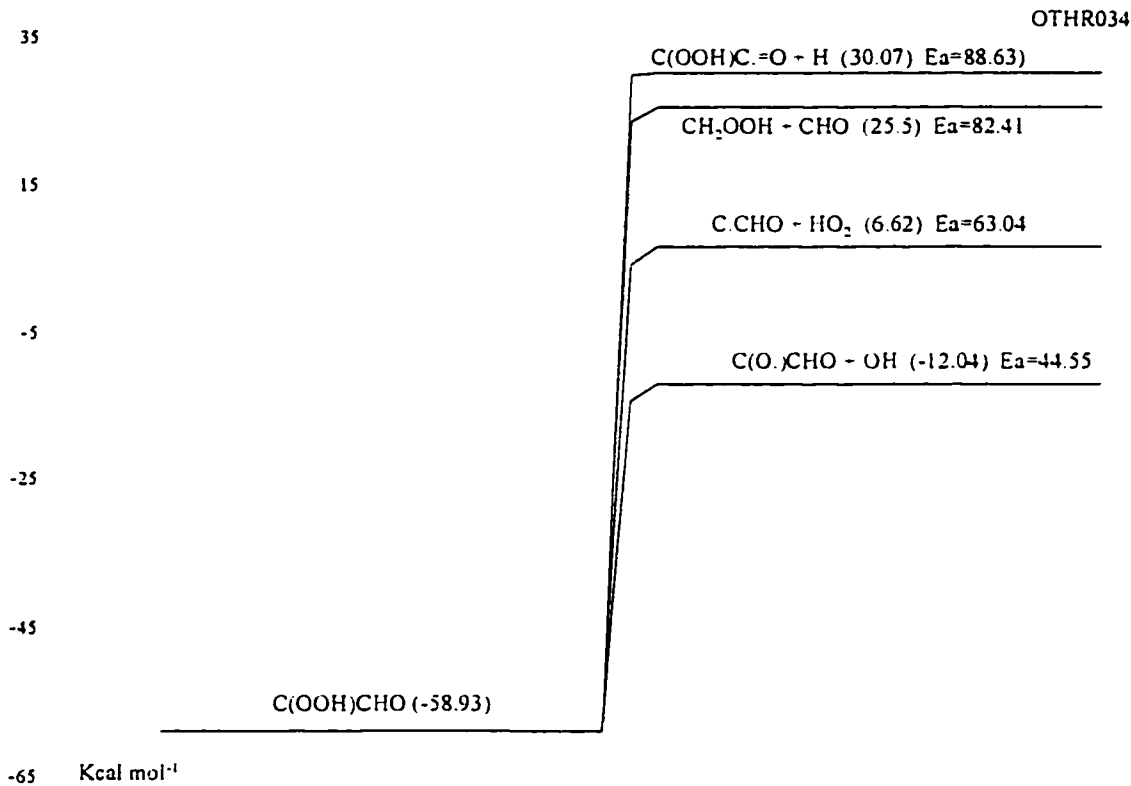
C(OOH)C.OOH: 100.1 (9.454); 1121.1 (10.325); 2623.9 (4.720)

Lennard-Jones parameter

$\sigma(\text{\AA}) = 5.55$, ϵ/k (K) = 584.86

- k₁ 89 ATK/BAU and 90 DEM/SAN for CC. + O₂.
- k₁ A_r via A_f and Microscopic Reversibility (MR), E_{a,r} = E_{a,f} - ΔU_{rxn} (-31.80) kcal mol⁻¹.
- k₂ A_f via A_r and Microscopic Reversibility (MR), A_r = 1.51 × 10¹³, 92 BAU/COB for O + CH₃O → Prod.. E_{a,f} = E_{a,f}(0) + ΔU_{rxn} (59.54) kcal mol⁻¹.
- k₃ A_f is referenced from reaction C2CCOO. → C2C=C + HO₂, (from thermal reaction analysis (AFACT2f) based on the thermodynamic properties calculated from MOPAC PM3 (corrected with internal rotor, electronic spin and optical isomer). E_{a,f} = E_{a,f}(13) + ΔU_{rxn} (20.68) kcal mol⁻¹. E_{a,R} is estimated as ring strain (6) + E_{a,add} (7).
- k₄ A_f estimated using TST, A = (deg.) (ek_B/h) Tⁿ exp(ΔS[‡](T)/R), deg. = 2, ek_B/h = 5.66 × 10¹⁰, n = 1.0, ΔS[‡](T) is estimated as loss of two rotors (-4.3 × 2 cal mol⁻¹ K⁻¹) and gain an optical isomer (OI). E_{a,f} = RS (6) + E_{abs} (7.64) + ΔH_{rxn} (8.57) kcal mol⁻¹.
- k₄ A_r via A_f and Microscopic Reversibility (MR), E_{a,r} = E_{a,f} - ΔU_{rxn} (-8.57) kcal mol⁻¹.
- k₅ A_f via A_r and Microscopic Reversibility (MR), A_r = 2.50 × 10¹¹ = 1/2 (HO₂ + C=C), 72 KER/PAR. E_{a,f} = E_{a,r} + ΔU_{rxn} (12.12) kcal mol⁻¹. E_{a,r} = 7.8 kcal mol⁻¹. (estimated by Bozzelli).
- k₆ A_f via A_r and Microscopic Reversibility (MR), A_r = 2.75 × 10¹² = 1/2 (OH + C=C). E_{a,f} estimated the same 2.5 kcal mol⁻¹ as E_{a,f} for CH₂OOH → CH₂O + OH (1990 Page)

IID. 53 C(OOH)CHO → Products



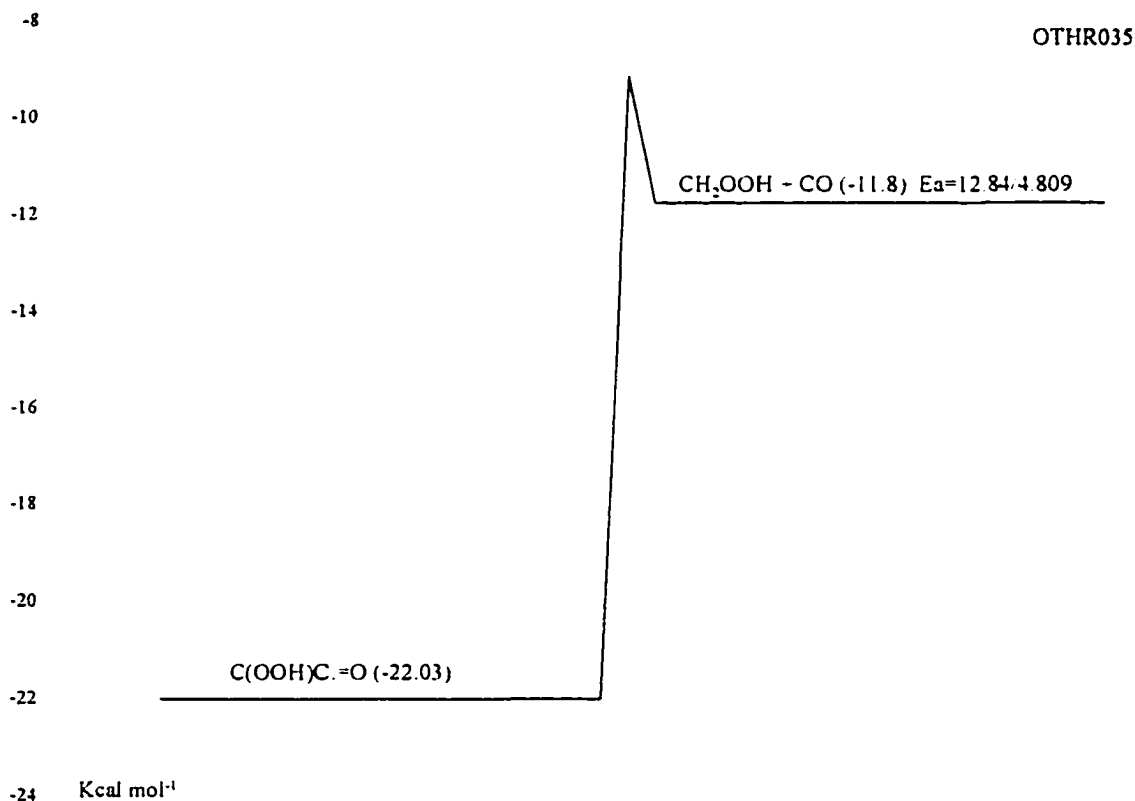
	Reaction	$A T^n e^{-\alpha/T}$ (s ⁻¹ or cm ³ mol ⁻¹ s ⁻¹)	E _a (kcal mol ⁻¹)
k ₁	C(OOH)CHO → C(OOH)C=O + H	1.36×10 ¹⁵ T ⁰ e ^{-0/T}	88.63
k ₂	C(OOH)CHO → CHO + CH ₂ OOH	3.48×10 ¹⁶ T ⁰ e ^{-0/T}	82.41
k ₃	C(OOH)CHO → C.CHO + HO ₂	4.30×10 ¹⁴ T ⁰ e ^{-0/T}	63.04
k ₃	C(OOH)CHO → C(O.)CHO + OH	1.49×10 ¹⁵ T ⁰ e ^{-0/T}	44.55

frequency/degeneracy (CPFIT)
C(OOH)CHO: 317.6 (6.233); 800.4 (4.689); 2043.0 (8.578)
Lennard-Jones parameter
σ(Å) = 5.20, ε/k (K) = 533.08

- k₁ A_f via A_r and Microscopic Reversibility (MR), A_r = 5.00 × 10¹³ = 1/2 (H + CHO), NIST FIT. E_{a,f} = E_{a,f}(0) + ΔU_{rxn} (88.63) kcal mol⁻¹.
- k₂ A_f via A_r and Microscopic Reversibility (MR), A_r = 1.81 × 10¹³, 86 TSA/HAM for CH₃ + CHO. E_{a,f} = E_{a,f}(0) + ΔU_{rxn} (82.41) kcal mol⁻¹.

- k_3 A_f via A_r and Microscopic Reversibility (MR), $A_r = 9.64 \times 10^{12}$, 91 TSA/HAM for $C=CC. + HO_2 \rightarrow C=CCO. + OH$. $E_{a,f} = E_{a,f}(0) + \Delta U_{rxn}$ (63.04) kcal mol⁻¹.
- k_4 A_f via A_r and Microscopic Reversibility (MR), $A_r = 1.81 \times 10^{13}$, 86 TSA/HAM for $CH_3O + OH \rightarrow H_2O + CH_2O$. $E_{a,f} = E_{a,f}(0) + \Delta U_{rxn}$ (44.55) kcal mol⁻¹.

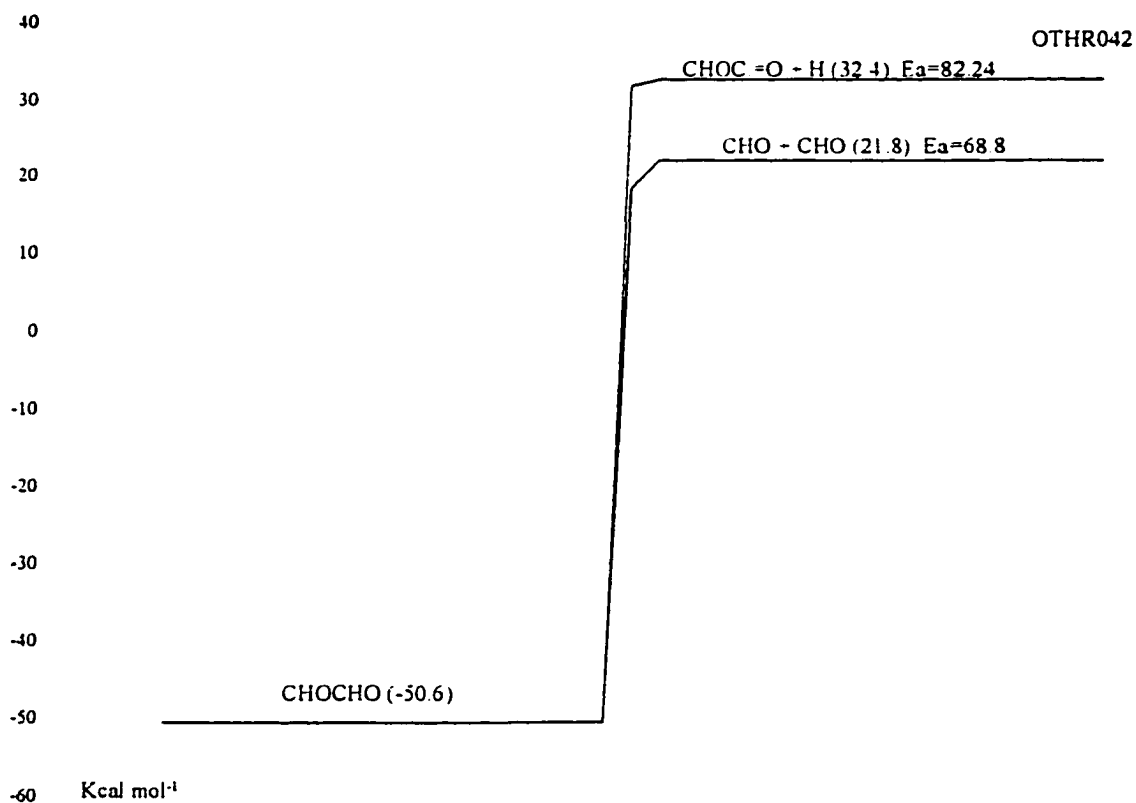
IID. 54 $\text{C}(\text{OOH})\text{C}=\text{O} \rightarrow \text{CH}_2\text{OOH} + \text{CO}$



	Reaction	$A T^n e^{-\alpha/T}$ (s ⁻¹ or cm ³ mol ⁻¹ s ⁻¹)	E_a (kcal mol ⁻¹)
k_1	$\text{C}(\text{OOH})\text{C}=\text{O} \rightarrow \text{CH}_2\text{OOH} + \text{CO}$	$6.10 \times 10^{12} T^0 e^{-0/T}$	12.84

frequency/degeneracy (CPFIT)
 $\text{C}(\text{OOH})\text{C}=\text{O}$: 413.5 (6.396); 407.2 (2.854); 1856.0 (7.249)
 Lennard-Jones parameter
 $\sigma(\text{\AA}) = 5.20$, $\epsilon/k \text{ (K)} = 533.08$

k_1 A_f via A_r and Microscopic Reversibility (MR), $A_r = 1.51 \times 10^{11}$, 86 TSA/HAM for $\text{CC} + \text{CO}$. $E_{a,f} = E_{a,r} (4.809) + \Delta U_{\text{rxn}} (8.03) \text{ kcal mol}^{-1}$.

IID. 55 CHOCHO \rightarrow Products

	Reaction	$A T^n e^{-\alpha/T}$ (s ⁻¹ or cm ³ mol ⁻¹ s ⁻¹)	E_a (kcal mol ⁻¹)
k ₁	CHOCHO \rightarrow CHOC=O + H	$5.94 \times 10^{14} T^0 e^{-0/T}$	82.24
k ₂	CHOCHO \rightarrow CHO + CHO	$5.66 \times 10^{16} T^0 e^{-0/T}$	68.80

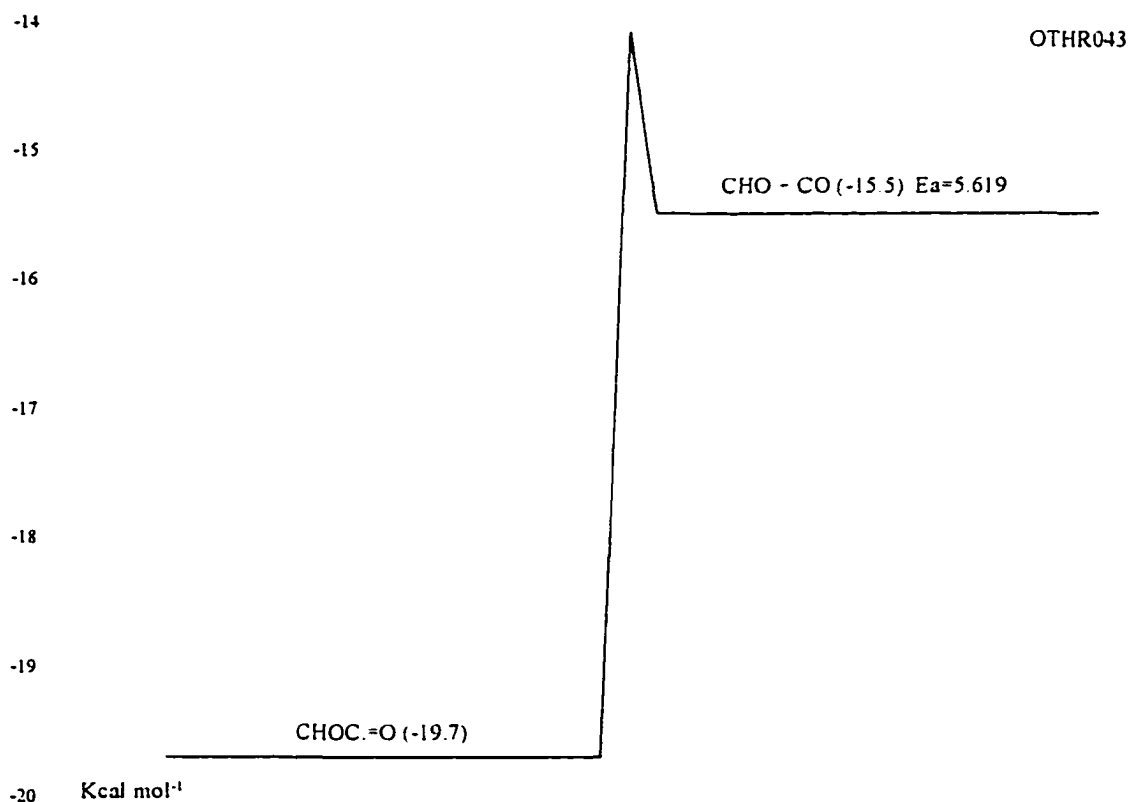
frequency/degeneracy (CPFIT)

CHOCHO: 516.1 (5.362); 1504.9 (5.604); 3990.9 (0.534)

Lennard-Jones parameter

 $\sigma(\text{\AA}) = 4.80$, ϵ/k (K) = 481.73

- k₁ A_f via A_r and Microscopic Reversibility (MR), $A_r = 5.00 \times 10^{13} = 1/2$ (H + CHO), NIST FIT. $E_{a,f} = E_{a,r}(0) + \Delta U_{\text{rxn}}$ (82.24) kcal mol⁻¹.
- k₂ A_f via A_r and Microscopic Reversibility (MR), $A_r = 3.01 \times 10^{11}$, 85 STO/SCH. $E_{a,f} = E_{a,r}(0) + \Delta U_{\text{rxn}}$ (68.8) kcal mol⁻¹.

IID. 56 $\text{CHOC}=\text{O} \rightarrow \text{CHO} + \text{CO}$ 

	Reaction	$A T^n e^{-\alpha T}$ (s^{-1} or $\text{cm}^3 \text{mol}^{-1} \text{s}^{-1}$)	E_a (kcal mol^{-1})
k_1	$\text{CHOC}=\text{O} \rightarrow \text{CHO} + \text{CO}$	$1.37 \times 10^{13} T^0 e^{-0T}$	5.62

frequency/degeneracy (CPFIT)

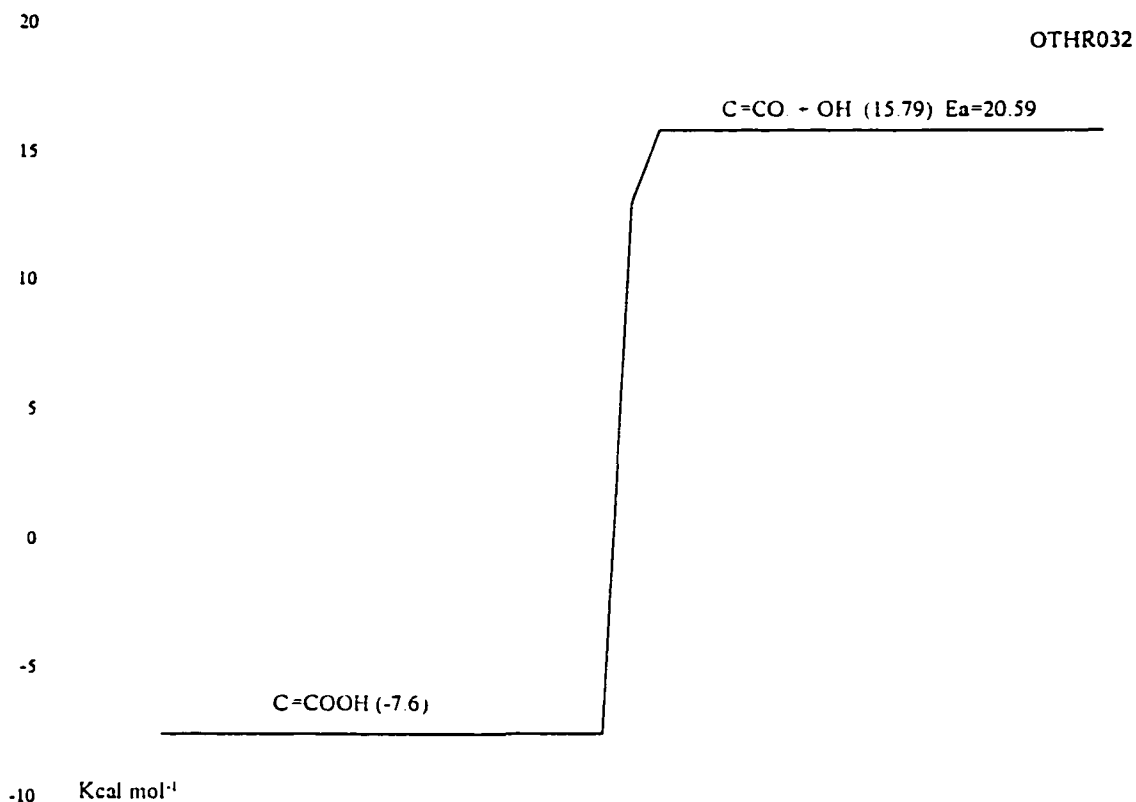
 $\text{CHOC}=\text{O}$: 435.1 (3.791); 800.3 (2.166); 1849.1 (2.544)

Lennard-Jones parameter

 $\sigma(\text{\AA}) = 4.80$, $\varepsilon/k(\text{K}) = 481.73$

k_1 A_f via A_r and Microscopic Reversibility (MR), $A_r = 1.51 \times 10^{11}$, 86 TSA/HAM for $\text{CO} + \text{C}=\text{C}$. $E_{a,f} = E_{a,r} (4.809) + \Delta U_{\text{rxn}} (0.81) \text{ kcal mol}^{-1}$.

IID. 57 $\text{C}=\text{COOH} \rightarrow \text{C}=\text{CO} + \text{OH}$



Reaction		$A T^n e^{-\alpha T}$ (s ⁻¹ or cm ³ mol ⁻¹ s ⁻¹)	E_a (kcal mol ⁻¹)
k_t	$\text{C}=\text{COOH} \rightarrow \text{C}=\text{CO} + \text{OH}$	$1.58 \times 10^{15} T^0 e^{-0T}$	20.59

frequency/degeneracy (CPFIT)

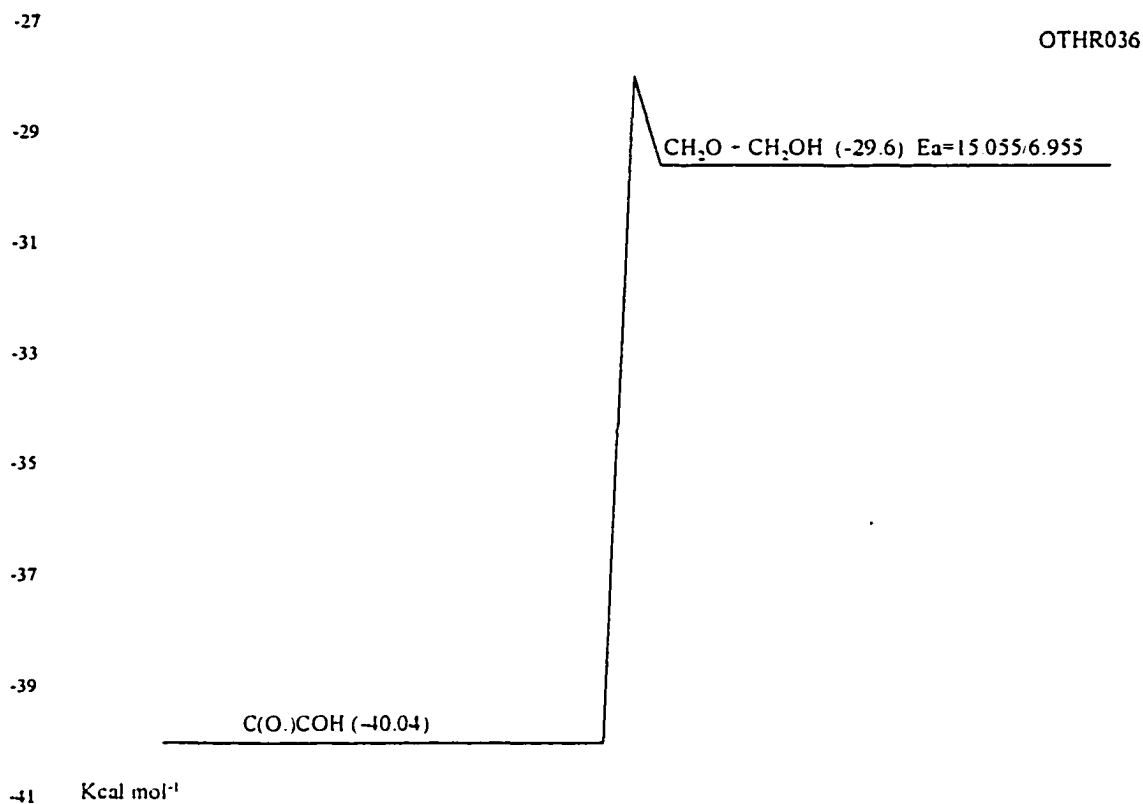
$\text{C}=\text{COOH}$: 385.4 (5.761); 1193.2 (8.293); 2866.8 (2.946)

Lennard-Jones parameter

$\sigma(\text{\AA}) = 4.80$, $\epsilon/k(\text{K}) = 481.73$

k_t A_f via A_r and Microscopic Reversibility (MR), $A_r = 1.51 \times 10^{13}$, 91 TSA/HAM for $\text{C}=\text{CC} + \text{OH}$. $E_{a,f} = E_{a,r}(0) + \Delta U_{\text{rxn}}$ (20.59) kcal mol⁻¹.

IID. 58 $\text{C}(\text{O.})\text{COH} \rightarrow \text{CH}_2\text{O} + \text{CH}_2\text{OH}$



	Reaction	$A T^n e^{-\alpha T}$ (s ⁻¹ or cm ³ mol ⁻¹ s ⁻¹)	E_a (kcal mol ⁻¹)
k ₁	$\text{C}(\text{O.})\text{COH} \rightarrow \text{CH}_2\text{O} + \text{CH}_2\text{OH}$	$4.84 \times 10^{12} T^0 e^{-0T}$	15.06

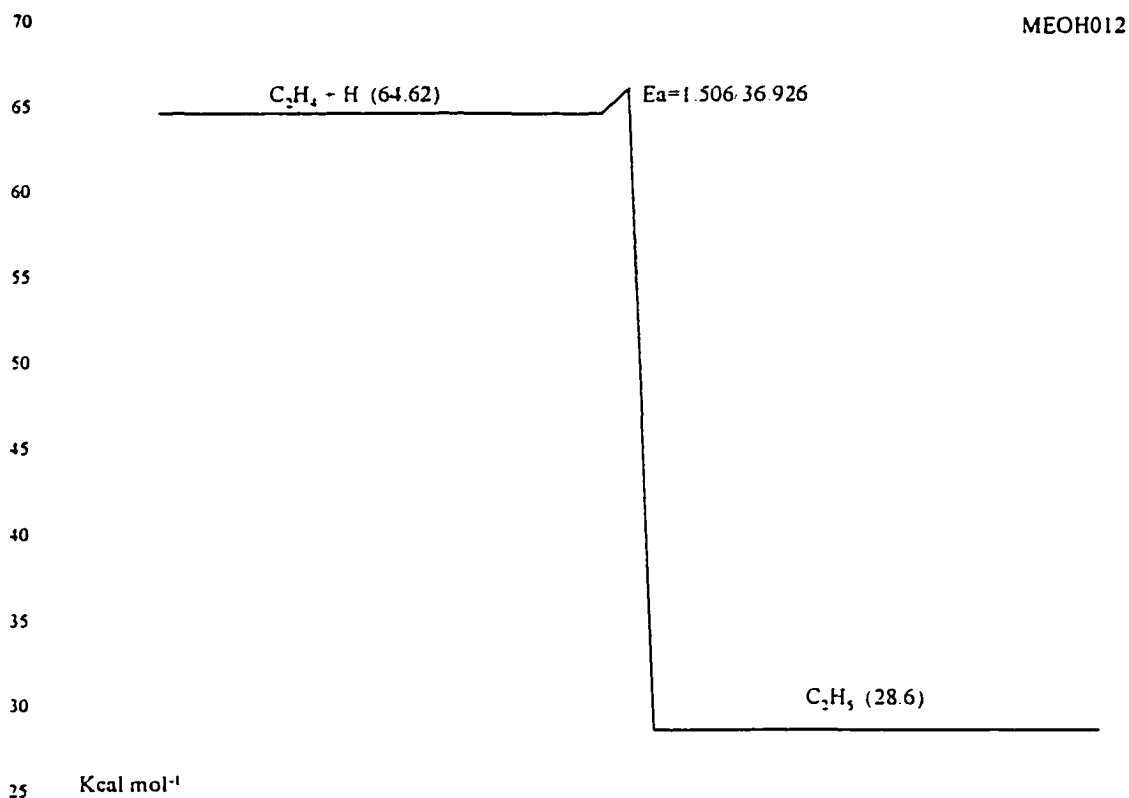
frequency/degeneracy (CPFIT)

$\text{C}(\text{O.})\text{COH}$: 509.7 (7.126); 1415.0 (8.212); 3225.7 (4.662)

Lennard-Jones parameter

$\sigma(\text{\AA}) = 4.80$, ϵ/k (K) = 481.73

k₁ A_f via A_r and Microscopic Reversibility (MR), A_r = 4.82 × 10¹⁰, 86 TSA/HAM for C=C + CH₂OH. E_{a,f} = E_{a,r} (6.955) + ΔU_{rxn} (8.10) kcal mol⁻¹.

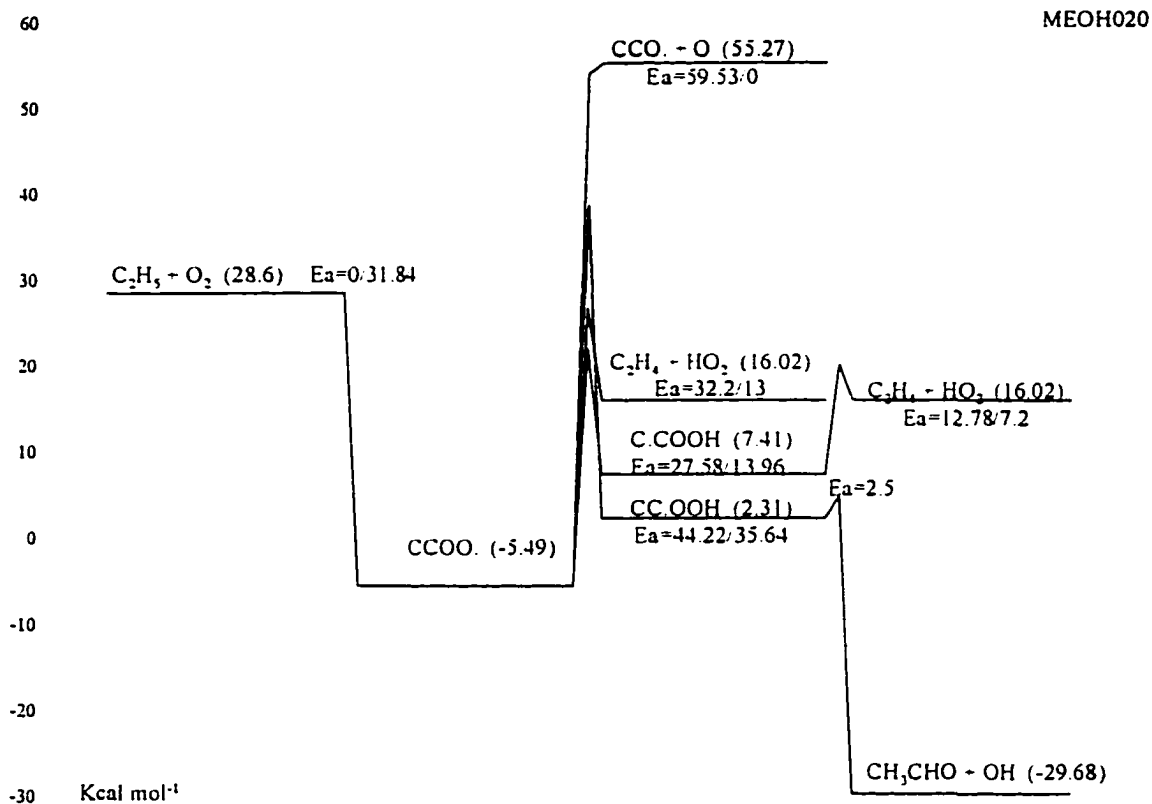
IID. 59 $\text{C}_2\text{H}_5 \rightarrow \text{C}_2\text{H}_4 + \text{H}$ 

Reaction		$A T^n e^{-\alpha T}$ (s ⁻¹ or cm ³ mol ⁻¹ s ⁻¹)	E_a (kcal mol ⁻¹)
k_1	$\text{C}_2\text{H}_5 \rightarrow \text{C}_2\text{H}_4 + \text{H}$	$2.92 \times 10^{12} T^0 e^{-0T}$	36.93

frequency/degeneracy (CPFIT)
 C_2H_5 : 728.5 (3.698); 1311.6 (5.239); 2771.8 (5.563)
 Lennard-Jones parameter
 $\sigma(\text{\AA}) = 4.30$, $\epsilon/k(\text{K}) = 252.30$

k_1 A_f via A_r and Microscopic Reversibility (MR), $A_r = 1.00 \times 10^{13}$, 84 WAR. $E_{a,f} = E_{a,r}$
 $(1.506) + \Delta U_{\text{rxn}} (36.93) \text{ kcal mol}^{-1}$.

IID. 60 $C_2H_5 + O_2 \rightarrow$ Products



	Reaction	$A T^n e^{-aT}$ (s ⁻¹)	E_a (kcal mol ⁻¹)
k_1	$C_2H_5 + O_2 \rightarrow CCOO.$	$3.01 \times 10^{12} T^0 e^{-0T}$	0.00
k_{-1}	$CCOO. \rightarrow C_2H_5 + O_2$	$2.99 \times 10^{14} T^0 e^{-0T}$	31.84
k_2	$CCOO. \rightarrow CCO. + O$	$2.59 \times 10^{14} T^0 e^{-0T}$	59.53
k_3	$CCOO. \rightarrow C_2H_4 + HO_2$	$2.24 \times 10^{10} T^{0.74} e^{-0T}$	32.20
k_4	$CCOO. \rightarrow C.CO OH$	$4.49 \times 10^9 T^{1.0} e^{-0T}$	27.58
k_{-4}	$C.CO OH \rightarrow CCOO.$	$2.14 \times 10^{11} T^{-0.12} e^{-0.00057T}$	13.96
k_5	$C.CO OH \rightarrow C_2H_4 + HO_2$	$8.23 \times 10^{11} T^0 e^{-0T}$	12.78
k_6	$CCOO. \rightarrow CC.O OH$	$2.60 \times 10^{10} T^{1.0} e^{-0T}$	44.22
k_{-6}	$CC.O OH \rightarrow CCOO.$	$6.77 \times 10^{12} T^{-0.33} e^{-0.00075T}$	35.64
k_7	$CC.O OH \rightarrow CH_3CHO + OH$	$1.15 \times 10^{13} T^0 e^{-0T}$	2.50

frequency/degeneracy (CPFIT)

CCOO.: 250.3 (4.749); 1127.3 (8.486); 2761.8 (6.765)
 C.CO OH: 251.0 (5.710); 1184.3 (9.067); 2804.0 (4.723)
 CC.O OH: 100.4 (5.313); 1071.3 (8.260); 2583.3 (5.926)

Lennard-Jones parameter
 $\sigma(\text{\AA}) = 4.80$, $\epsilon/k \text{ (K)} = 481.73$

- k_1 90 DEM/ASN and 89 ATK/BAU
- k_{-1} A_f via A_r and Microscopic Reversibility (MR), $E_{a,f} = E_{a,f}(0) - \Delta U_{\text{rxn}} (-31.84) \text{ kcal mol}^{-1}$.
- k_2 A_f via A_r and Microscopic Reversibility (MR), $A_r = 1.51 \times 10^{13}$, 92 BAU/COB for $O + \text{CH}_3\text{O} \rightarrow \text{Prod.}$. $E_{a,f} = E_{a,r}(0) + \Delta U_{\text{rxn}} (59.53) \text{ kcal mol}^{-1}$.
- k_3 A_f is referenced from reaction $\text{C2CCOO.} \rightarrow \text{C2C=C} + \text{HO}_2$, (from thermal reaction analysis (AFACT2f) based on the thermodynamic properties calculated from MOPAC PM3 (corrected with internal rotor, electronic spin and optical isomer). $E_{a,f} = E_{a,r} + \Delta U_{\text{rxn}} (19.20)$ $E_{a,r}$ is estimated as ring strain (6) + $E_{a,\text{add}}$ (7).
- k_4 A_f estimated using TST, $A = (\text{deg.}) (ek_b/h) \exp(\Delta S^\ddagger(T)/R) T^n$, $\text{deg.} = 3$, $ek_b/h = 5.66 \times 10^{10}$, $n = 1.0$, $\Delta S^\ddagger(T)$ is estimated as loss of two rotors ($-4.3 \times 2 \text{ kcal mol}^{-1}$) and gain one optical isomer (OI). $E_{a,f} = \text{RS} (6) + E_{a,\text{bst}} (7.96) + \Delta H_{\text{rxn}} (13.62) \text{ kcal mol}^{-1}$.
- k_{-4} A_f via A_r and Microscopic Reversibility (MR), $E_{a,f} = E_{a,r} - \Delta U_{\text{rxn}} (13.62) \text{ kcal mol}^{-1}$.
- k_5 A_f via A_r and Microscopic Reversibility (MR), $A_r = 3.50 \times 10^{11}$, Bozzelli. $E_{a,f} = E_{a,r} + \Delta U_{\text{rxn}} (5.58) \text{ kcal mol}^{-1}$. $E_{a,r} = 7.2 \text{ kcal mol}^{-1}$. (estimated by Bozzelli).
- k_6 A_f estimated using TST, $A = (\text{deg.}) (ek_b/h) \exp(\Delta S^\ddagger(T)/R) T^n$, $\text{deg.} = 2$, $ek_b/h = 5.66 \times 10^{10}$, $n = 1.0$, $\Delta S^\ddagger(T)$ is estimated as loss of one rotor ($-4.3 \text{ kcal mol}^{-1}$) and gain one optical isomer (OI). $E_{a,f} = \text{RS} (26) + E_{a,\text{bst}} (9.64) + \Delta H_{\text{rxn}} (8.58) \text{ kcal mol}^{-1}$.
- k_{-6} A_f via A_r and Microscopic Reversibility (MR), $E_{a,f} = E_{a,r} - \Delta U_{\text{rxn}} (8.58) \text{ kcal mol}^{-1}$.
- k_7 A_f via A_r and Microscopic Reversibility (MR), $A_r = 2.75 \times 10^{12} = 1/2 (\text{OH} + \text{C}=\text{C})$. $E_{a,f}$ estimated the same $2.5 \text{ kcal mol}^{-1}$ based on $E_{a,f}$ for $\text{CH}_2\text{OOH} \rightarrow \text{CH}_2\text{O} + \text{OH}$ (1990 Page)

IID. 61 $\text{C}_2\text{H}_3 \rightarrow \text{C}_2\text{H}_2 + \text{H}$

115

MEOH011

110

 $E_a = 2.583/36.603$

105

 $\text{C}_2\text{H}_3 + \text{H} (105.96)$

100

95

90

85

80

75

70

 $\text{C}_2\text{H}_3 (71.62)$ 65 Kcal mol⁻¹

Reaction		$A T^n e^{-aT}$ (s ⁻¹ or cm ³ mol ⁻¹ s ⁻¹)	E_a (kcal mol ⁻¹)
k_1	$\text{C}_2\text{H}_3 \rightarrow \text{C}_2\text{H}_2 + \text{H}$	$3.60 \times 10^{12} T^0 e^{-0T}$	36.60

frequency/degeneracy (CPFIT)

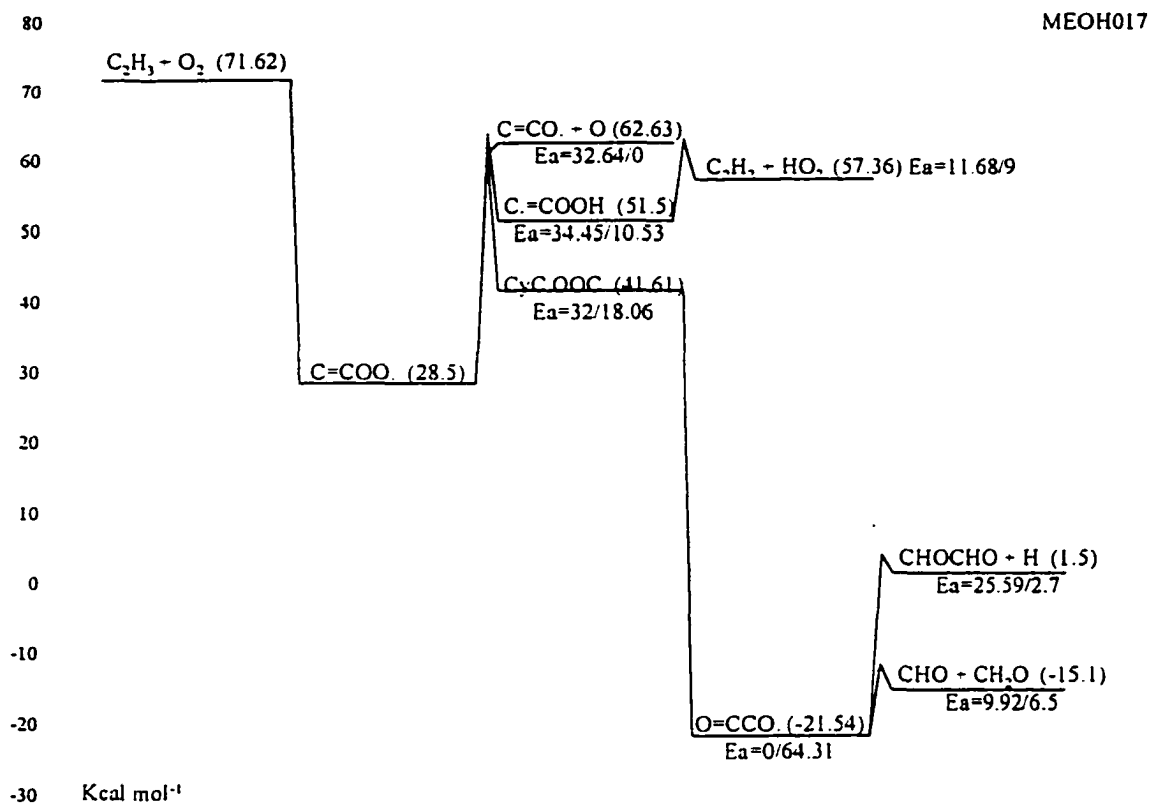
 C_2H_3 : 871.1 (2.528); 1155.4 (2.961); 2876.1 (3.511)

Lennard-Jones parameter

 $\sigma(\text{\AA}) = 4.10$, $\epsilon/k(\text{K}) = 209.00$

k_1 A_f via A_r and Microscopic Reversibility (MR), $A_r = 8.43 \times 10^{12}$, 92 BAU/COB. $E_{a,f} = E_{a,r}(2.583) + \Delta U_{\text{rxn}}(34.02)$ kcal mol⁻¹.

IID. 62 $C_2H_3 + O_2 \rightarrow$ Products



	Reaction	$A T^n e^{-\alpha T}$ (s ⁻¹)	E_a (kcal mol ⁻¹)
k ₁	$C_2H_3 + O_2 \rightarrow C=COO.$	$4.00 \times 10^{12} T^0 e^{-0T}$	0.00
k ₋₁	$C=COO. \rightarrow C_2H_3 + O_2$	$4.31 \times 10^{14} T^0 e^{-0T}$	40.65
k ₂	$C=COO. \rightarrow C=CO. + O$	$2.00 \times 10^{14} T^0 e^{-0T}$	32.64
k ₃	$C=COO. \rightarrow C.=COOH$	$2.60 \times 10^{10} T^{1.0} e^{-0T}$	34.45
k ₋₃	$C.=COOH \rightarrow C=COO.$	$2.20 \times 10^{13} T^{-0.44} e^{-0.00073T}$	10.53
k ₄	$C.=COOH \rightarrow C_2H_2 + HO_2$	$1.13 \times 10^{12} T^0 e^{-0T}$	11.68
k ₅	$C=COO. \rightarrow CyC.OOC$	$4.08 \times 10^{12} T^0 e^{-0T}$	32.00
k ₋₅	$CyC.OOC \rightarrow C=COO.$	$3.16 \times 10^{13} T^0 e^{-0T}$	18.06
k ₆	$CyC.OOC \rightarrow O=CCO.$	$7.45 \times 10^{13} T^0 e^{-0T}$	1.00
k ₋₆	$O=CCO. \rightarrow CyC.OOC$	$4.08 \times 10^{12} T^0 e^{-0T}$	65.31
k ₇	$O=CCO. \rightarrow CH_2O + CHO$	$2.35 \times 10^{12} T^0 e^{-0T}$	8.87
k ₈	$O=CCO. \rightarrow CHOCHO + H$	$2.77 \times 10^{12} T^0 e^{-0T}$	25.59

frequency/degeneracy (CPFIT)
 $C=COO.$: 402.7 (4.812); 1181.7 (5.956); 2794.2 (3.732)

C=COOH: 328.5 (5.086); 1086.0 (6.740); 2682.1 (2.173)

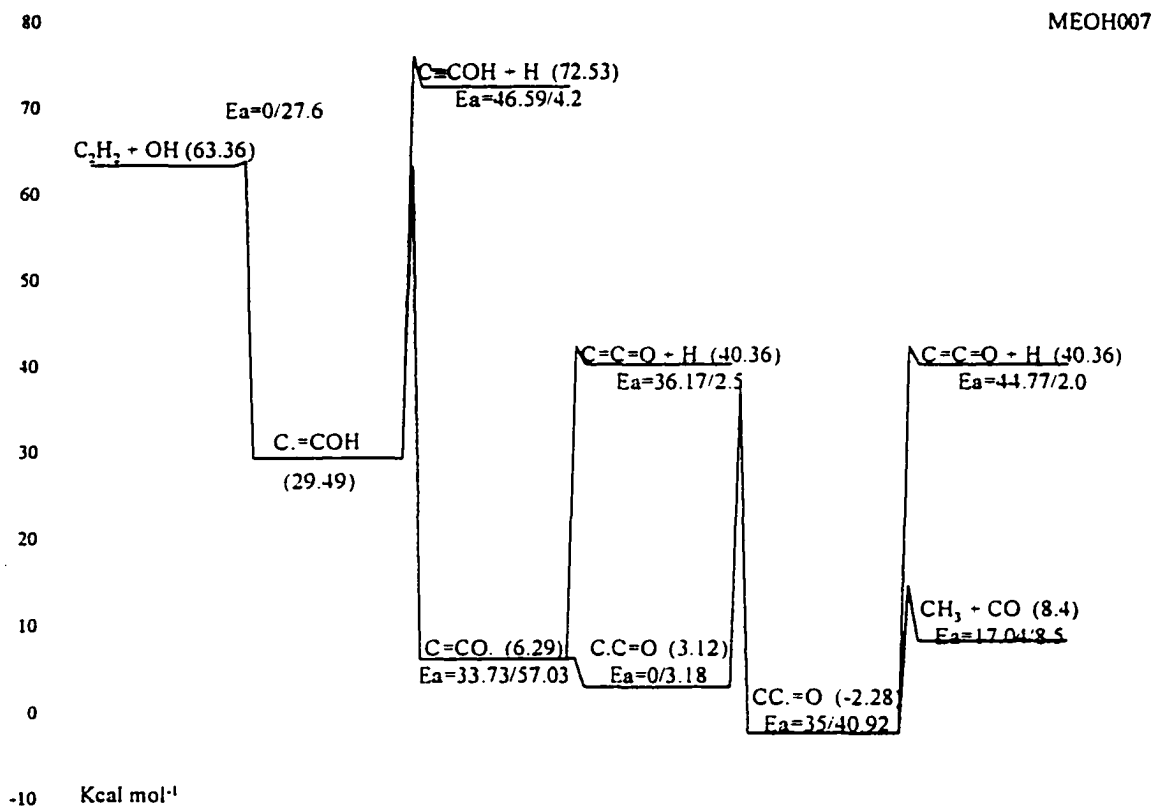
CyC.OOC: 250.3 (0.359); 904.8 (10.622); 2067.8 (4.019)

O=CCO.: 458.0 (6.266); 1848.3 (7.107); 3996.1 (1.126)

Lennard-Jones parameter

$\sigma(\text{\AA}) = 4.80$, ϵ/k (K) = 481.73

- k_1 90 DEM/ASN for $C_2H_3 + O_2 \rightarrow \text{Prod.}$
- k_{-1} A_r via A_f and Microscopic Reversibility (MR), $E_{a,r} = E_{a,f}(0) - \Delta U_{rxn} (-40.65) \text{ kcal mol}^{-1}$.
- k_2 A_f via A_r and Microscopic Reversibility (MR), $A_r = 1.51 \times 10^{13}$, 92 BAU/COB for $O + CH_3O \rightarrow \text{Prod.}$, $E_{a,f} = E_{a,r}(0) + \Delta U_{rxn} (32.64) \text{ kcal mol}^{-1}$.
- k_3 A_f estimated using TST, $A = (\text{deg.}) (ek_b/h) \exp(\Delta S^\ddagger(T)/R) T^n$, $\text{deg.} = 2$, $ek_b/h = 5.66 \times 10^{10}$, $n = 1.0$, $\Delta S^\ddagger(T)$ is estimated as loss of one rotor ($-4.3 \text{ kcal mol}^{-1}$) and gain one optical isomer (OI). $E_{a,f} = RS(6) + E_{abst}(4.53) + \Delta H_{rxn}(23.92) \text{ kcal mol}^{-1}$.
- k_{-3} A_r via A_f and Microscopic Reversibility (MR), $E_{a,r} = E_{a,f} - \Delta U_{rxn} (23.92) \text{ kcal mol}^{-1}$.
- k_4 A_f via A_r and Microscopic Reversibility (MR), $A_r = 1.21 \times 10^{11}$, 86 TSA for $C_2H_2 + CH_3O \rightarrow \text{Prod.}$, $E_{a,f} = E_{a,r} + \Delta U_{rxn} (2.68) \text{ kcal mol}^{-1}$. $E_{a,r} = 9.0 \text{ kcal mol}^{-1}$. (estimated by Bozzelli).
- k_5 A_f estimated using TST, $A = (\text{deg.}) (ek_bT/h) \exp(\Delta S^\ddagger(T)/R)$, $\text{deg.} = 1$, $ek_bT/h = 10^{13.55} ?$, $\Delta S^\ddagger(T)$ is estimated as loss of one rotor ($-4.3 \text{ cal mol}^{-1} \text{ K}^{-1}$). $E_{a,f}$ is estimated as ring strain (26) + $E_{a,add}(6)$.
- k_{-5} A_r via A_f and Microscopic Reversibility (MR), $E_{a,r} = E_{a,f} - \Delta U_{rxn} (13.94) \text{ kcal mol}^{-1}$.
- k_6 A_f via A_r and Microscopic Reversibility (MR), $E_{a,f}$ is estimated as $1.0 \text{ kcal mol}^{-1}$ by Bozzelli.
- k_{-6} A_r estimated using TST, $A = (\text{deg.}) (ek_bT/h) \exp(\Delta S^\ddagger(T)/R)$, $\text{deg.} = 1$, $ek_bT/h = 10^{13.55} ?$, $\Delta S^\ddagger(T)$ is estimated as loss of one rotor ($-4.3 \text{ cal mol}^{-1} \text{ K}^{-1}$). $E_{a,r} = E_{a,f} - \Delta U_{rxn} (-64.31) \text{ kcal mol}^{-1}$.
- k_7 A_f via A_r and Microscopic Reversibility (MR), $A_r = 9.04 \times 10^{10}$, 86 LES/ROU for $CHO + C=C \rightarrow \text{Prod.}$, $E_{a,f} = E_{a,r} + \Delta U_{rxn} (3.42) \text{ kcal mol}^{-1}$. $E_{a,r} = 5.45 \text{ kcal mol}^{-1}$. (taken from the same reference).
- k_8 A_f via A_r and Microscopic Reversibility (MR), $A_r = 5.00 \times 10^{12} = 1/2 (H + C=C)$, NIST. $E_{a,f} = E_{a,r} + \Delta U_{rxn} (22.89) \text{ kcal mol}^{-1}$. $E_{a,r} = 2.7 \text{ kcal mol}^{-1}$. (estimated by Bozzelli).

IID. 63 $C_2H_2 + OH \rightarrow$ Products

Reaction		$A T^n e^{-\alpha T}$ (s ⁻¹ or cm ³ mol ⁻¹ s ⁻¹)	E_a (kcal mol ⁻¹)
k_1	$C_2H_2 + OH \rightarrow C \equiv COH$	$5.12 \times 10^{12} T^0 e^{-0T}$	1.40
k_1	$C \equiv COH \rightarrow C_2H_2 + OH$	$3.18 \times 10^{13} T^0 e^{-0T}$	33.41
k_2	$C \equiv COH \rightarrow C \equiv COH + H$	$3.99 \times 10^{12} T^0 e^{-0T}$	45.49
k_3	$C \equiv COH \rightarrow C = CO.$	$2.06 \times 10^{12} T^{0.1} e^{-0.00087T}$	30.73
k_3	$C = CO. \rightarrow C \equiv COH$	$1.13 \times 10^{10} T^{1.0} e^{-0T}$	54.03
k_4	$C = CO. \rightarrow C = C = O + H$	$1.42 \times 10^{12} T^0 e^{-0T}$	36.68
k_5	$C = CO. \rightarrow C.CHO$	$3.60 \times 10^{16} T^0 e^{-0T}$	0.00
k_5	$C.CHO \rightarrow C = CO.$	$3.66 \times 10^{16} T^0 e^{-0T}$	3.18
k_6	$C.CHO \rightarrow CH_3C.=O$	$6.50 \times 10^9 T^{1.0} e^{-0T}$	35.00
k_6	$CH_3C.=O \rightarrow C.CHO$	$2.38 \times 10^7 T^{2.2} e^{-0.00065T}$	40.92
k_7	$CH_3C.=O \rightarrow CH_3 + CO$	$2.05 \times 10^{12} T^0 e^{-0T}$	13.35
k_8	$CH_3C.=O \rightarrow C = C = O + H$	$4.33 \times 10^{12} T^0 e^{-0T}$	44.28

frequency/degeneracy (CPFIT)

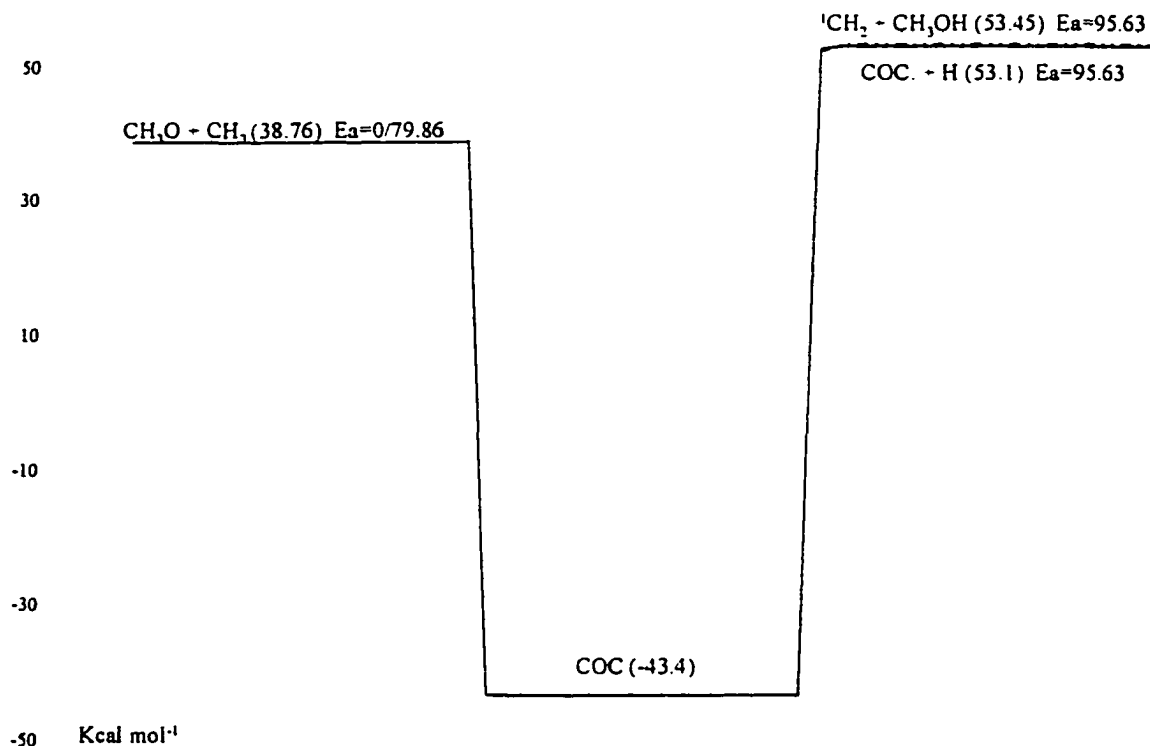
C≡COH: 504.0 (3.819); 1135.7 (4.866); 3449.5 (2.815)

$\text{C}=\text{CO}.$: 578.8 (3.802); 1311.9 (5.098); 3085.1 (3.100)
 $\text{C}.\text{CHO}$: 556.8 (3.618); 1205.4 (4.219); 2442.0 (3.663)
 $\text{CH}_3\text{C}=\text{O}$: 485.8 (3.061); 1486.0 (5.839); 2844.5 (2.600)
 Lennard-Jones parameter
 $\sigma(\text{\AA}) = 4.35$, $\epsilon/k (\text{K}) = 422.61$

- k_1 88 LIU/MUL2.
 k_{-1} A_r via A_f and Microscopic Reversibility (MR), $E_{a,r} = E_{a,f} (1.4) - \Delta U_{\text{rxn}} (-32.01) \text{ kcal mol}^{-1}$.
 k_2 A_f via A_r and Microscopic Reversibility (MR), $A_r = 5.79 \times 10^{12}$, 72 WAG for $\text{CC}\equiv\text{C} + \text{H} \rightarrow \text{C}=\text{CC}$. $E_{a,f} = E_{a,r} (3.1) + \Delta U_{\text{rxn}} (42.39) \text{ kcal mol}^{-1}$.
 k_3 A_f via A_r and Microscopic Reversibility (MR), $E_{a,f} = E_{a,r} + \Delta U_{\text{rxn}} (-23.3) \text{ kcal mol}^{-1}$.
 k_{-3} A_r estimated using TST, $A = (\text{deg.}) (ek_b/h) T^n \exp(\Delta S^\ddagger(T)/R)$, $\text{deg.} = 2$, $ek_b/h = 5.66 \times 10^{10}$, $n = 1.0$, $\Delta S^\ddagger(T)$ is estimated as loss of rotors (no rotor loss here, $\Delta S^\ddagger(T) = 0$). $E_{a,f} = \text{RS} (26) + E_{\text{abst}} (4.73) + \Delta H_{\text{rxn}} (23.3) \text{ kcal mol}^{-1}$.
 k_4 A_f via A_r and Microscopic Reversibility (MR), $A_r = 7.00 \times 10^{12}$, 84 WAR for $\text{C}=\text{C}=\text{O} + \text{H} \rightarrow \text{Prod.}$. $E_{a,f} = E_{a,r} (3.011) + \Delta U_{\text{rxn}} (33.67) \text{ kcal mol}^{-1}$.
 k_5 Jeff Ing. PHD thesis.
 k_{-5} A_r via A_f and Microscopic Reversibility (MR), $E_{a,r} = E_{a,f} - \Delta U_{\text{rxn}} (-3.18) \text{ kcal mol}^{-1}$.
 k_6 A_f estimated using TST, $A = (\text{deg.}) (ek_b/h) T^n \exp(\Delta S^\ddagger(T)/R)$, $\text{deg.} = 1$, $ek_b/h = 5.66 \times 10^{10}$, $n = 1.0$, $\Delta S^\ddagger(T)$ is estimated as loss of one rotor ($-4.3 \text{ cal mol}^{-1} \text{ K}^{-1}$). $E_{a,f} = \text{RS} (28) + E_{\text{abst}} (7.0) \text{ kcal mol}^{-1}$.
 k_{-6} A_r via A_f and Microscopic Reversibility (MR), $E_{a,r} = E_{a,f} - \Delta U_{\text{rxn}} (-5.92) \text{ kcal mol}^{-1}$.
 k_7 A_f via A_r and Microscopic Reversibility (MR), $A_r = 1.51 \times 10^{11}$, 86 TSA/HAM for $\text{CC.} + \text{CO} \rightarrow \text{CCC}=\text{O}$, $E_{a,f} = E_{a,r} (4.809) + \Delta U_{\text{rxn}} (8.54) \text{ kcal mol}^{-1}$.
 k_8 A_f via A_r and Microscopic Reversibility (MR), $A_r = 1.00 \times 10^{13}$, 84 WAR for $\text{C}=\text{C} + \text{H}$, $E_{a,f} = E_{a,r} (1.506) + \Delta U_{\text{rxn}} (42.77) \text{ kcal mol}^{-1}$.

IID. 64 COC → Products

MEOH033



Reaction		$A T^n e^{-\alpha T}$ (s ⁻¹ or cm ³ mol ⁻¹ s ⁻¹)	E_a (kcal mol ⁻¹)
k ₁	CH ₃ O + CH ₃ → COC	$1.21 \times 10^{13} T^0 e^{-0T}$	0.00
k ₋₁	COC → CH ₃ O + CH ₃	$8.14 \times 10^{15} T^0 e^{-0T}$	79.86
k ₂	COC → COC. + H	$5.60 \times 10^{15} T^0 e^{-0T}$	96.13
k ₃	COC → CH ₂ S + CH ₃ OH	$2.16 \times 10^{16} T^0 e^{-0T}$	95.63

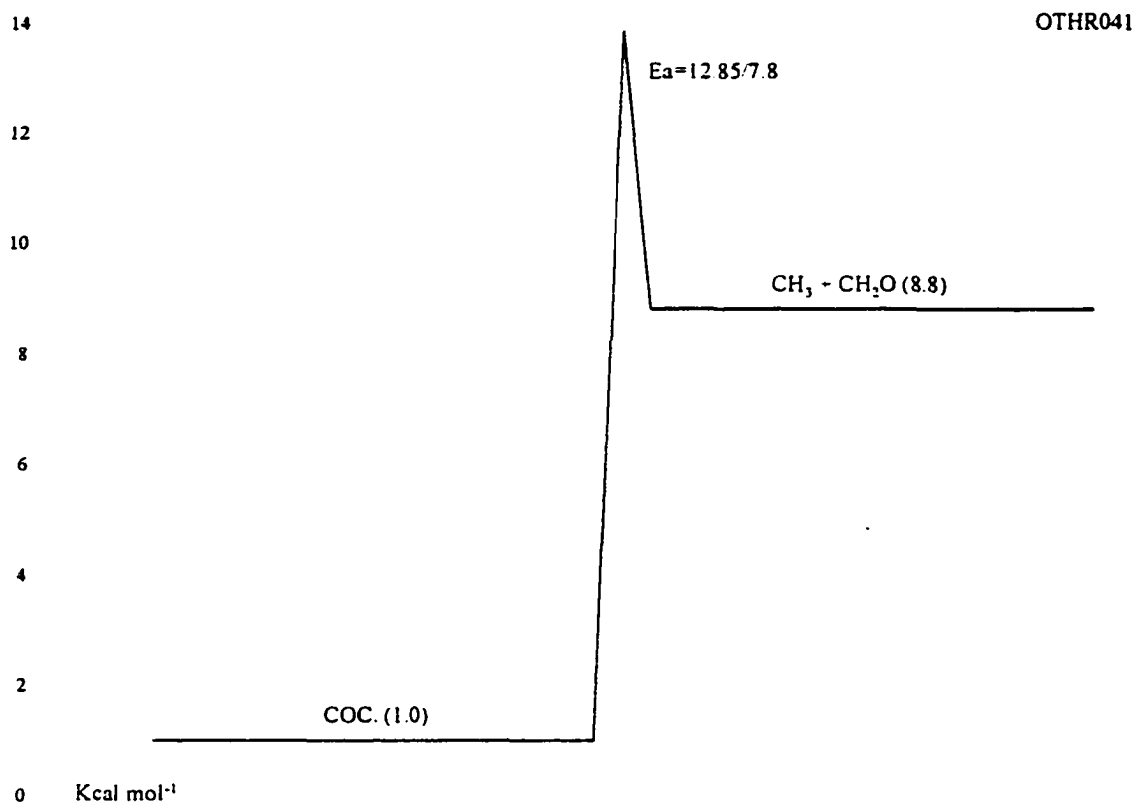
frequency/degeneracy (CPFIT)

COC: 635.8 (7.937); 1878.7 (9.590); 3509.4 (2.473)

Lennard-Jones parameter

 $\sigma(\text{\AA}) = 4.34$, ϵ/k (K) = 422.61k₁ 86 TSA/HAM.k₋₁ A_r via A_f and Microscopic Reversibility (MR), $E_{a,r} = E_{a,f} - \Delta U_{rxn}$ (-79.86) kcal mol⁻¹.k₂ A_f via A_r and Microscopic Reversibility (MR), $A_r = 6.00 \times 10^{13} = 2 \times (\text{H} + \text{CH}_2\text{OH})$, 81 HOY/COF. $E_{a,r} = E_{a,f}(0) + \Delta U_{rxn}$ (96.13) kcal mol⁻¹.k₃ A_f via A_r and Microscopic Reversibility (MR), $A_r = 2.50 \times 10^{13}$, Jeff Ing. PHD THESIS. $E_{a,f} = E_{a,r}(1.0) + \Delta U_{rxn}$ (94.63) kcal mol⁻¹.

IID. 65 $\text{COC.} \rightarrow \text{CH}_2\text{O} + \text{CH}_3$

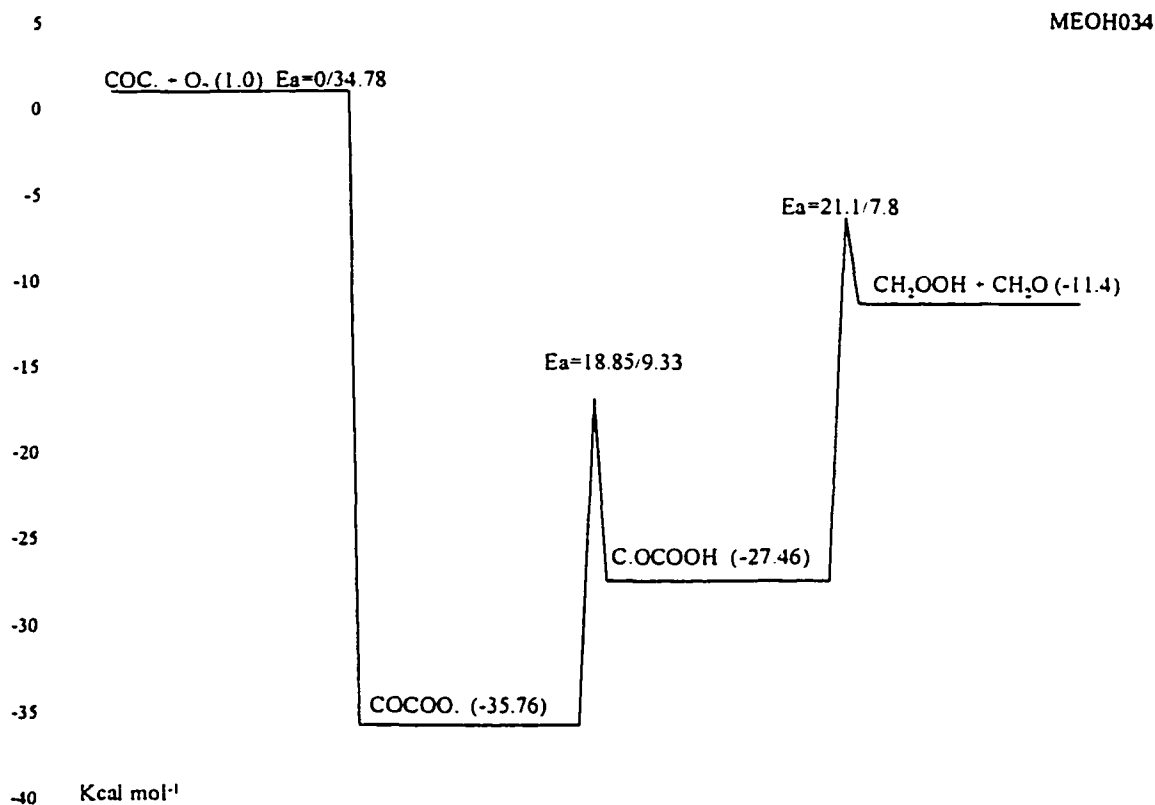


	Reaction	$A T^n e^{-\alpha T}$ (s ⁻¹ or cm ³ mol ⁻¹ s ⁻¹)	E_a (kcal mol ⁻¹)
k_1	$\text{COC.} \rightarrow \text{CH}_2\text{O} + \text{CH}_3$	$3.69 \times 10^{12} T^0 e^{-0T}$	12.85

frequency/degeneracy (CPFIT)
 $\text{COC.}: 516.9 (6.322); 1262.4 (3.723); 2460.9 (6.954)$
 Lennard-Jones parameter
 $\sigma(\text{\AA}) = 4.35, \epsilon/k (\text{K}) = 422.61$

k_1 A_f via A_r and Microscopic Reversibility (MR), $A_r = 3.31 \times 10^{11}$ 86 TSA/HAM for $\text{CH}_3 + \text{C}=\text{C}$. $E_{a,f} = E_{a,r} (7.8) + \Delta U_{\text{rxn}} (5.05) \text{ kcal mol}^{-1}$.

IID. 66 COC. + O₂ → Products



Reaction		$A T^n e^{-\alpha T}$ (s ⁻¹ or cm ³ mol ⁻¹ s ⁻¹)	E_a (kcal mol ⁻¹)
k_1	$\text{COC.} + \text{O}_2 \rightarrow \text{COCO.}$	$6.00 \times 10^{12} T^0 e^{-0T}$	0.00
k_{-1}	$\text{COCO.} \rightarrow \text{COC.} + \text{O}_2$	$8.52 \times 10^{13} T^0 e^{-0T}$	34.78
k_2	$\text{COCO.} \rightarrow \text{C.OCO.}$	$5.15 \times 10^8 T^{1.0} e^{-0T}$	18.85
k_{-2}	$\text{C.OCO.} \rightarrow \text{COCO.}$	$2.07 \times 10^{13} T^{-1.01} e^{-0.0011T}$	9.33
k_3	$\text{C.OCO.} \rightarrow \text{CH}_2\text{O} + \text{CH}_2\text{OOH}$	$6.66 \times 10^{12} T^0 e^{-0T}$	21.10

frequency/degeneracy (CPFIT)

COCO.: 366.7 (7.587); 800.0 (3.436); 2104.7 (11.478)

C.OCO.: 450.0 (9.178); 473.6 (3.020); 1959.6 (9.802)

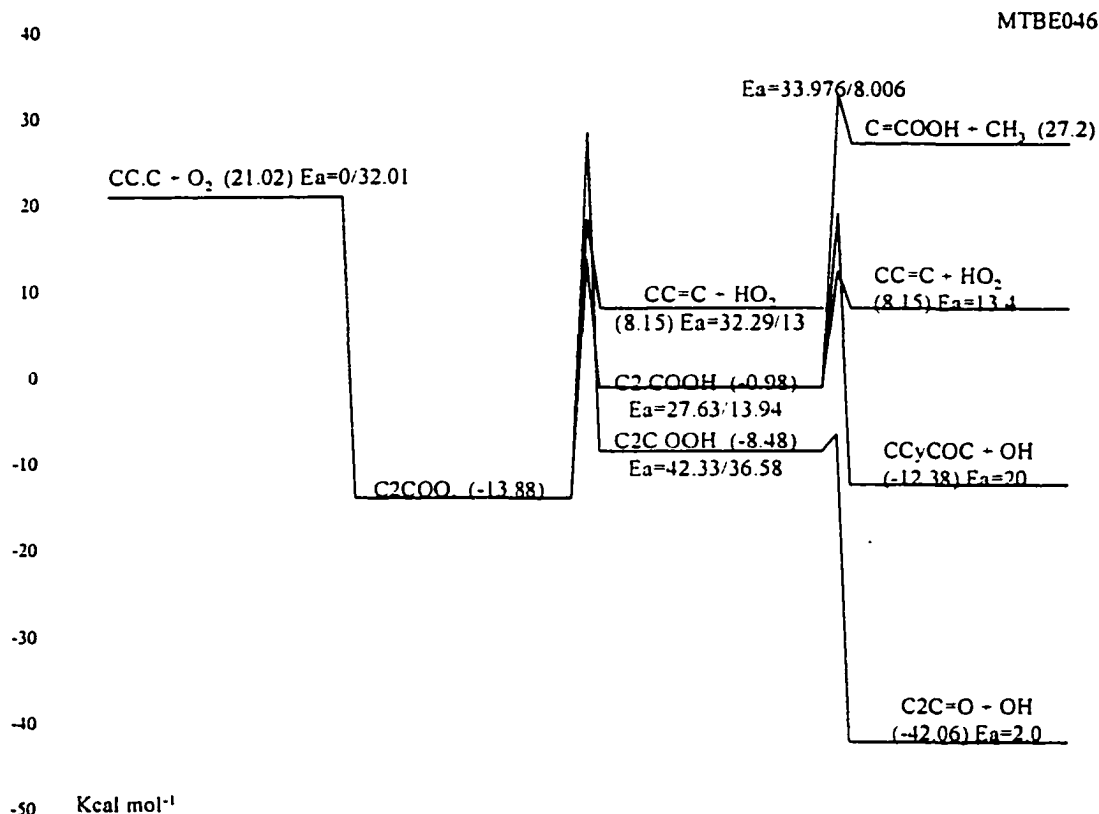
Lennard-Jones parameter

$\sigma(\text{\AA}) = 5.20$, $\epsilon/k(\text{K}) = 533.08$

k_1 $2 \times (\text{CC.} + \text{O}_2)$, 89 ATK/BAU and 90 DEM/SAN.

k_{-1} A_r via A_f and Microscopic Reversibility (MR), $E_{a,r} = E_{a,f} - \Delta U_{rxn}$ (-34.78) kcal mol⁻¹.

- k_2 A_f estimated using TST, $A = (\text{deg.}) (ek_B/h) T^n \exp(\Delta S^\ddagger(T)/R)$, $\text{deg.} = 3$, $ek_B/h = 5.66 \times 10^{10}$, $n = 1.0$, $\Delta S^\ddagger(T)$ is estimated as loss of three rotors ($-4.3 \times 3 \text{ cal mol}^{-1} \text{ K}^{-1}$) and gain an optical isomer (OI). $E_{a,f} = RS(0) + E_{\text{abst}}(9.33) + \Delta H_{\text{rxn}}(9.52) \text{ kcal mol}^{-1}$.
- k_{-2} A_r via A_f and Microscopic Reversibility (MR), $E_{a,r} = E_{a,f} - \Delta U_{\text{rxn}}(9.52) \text{ kcal mol}^{-1}$.
- k_3 A_f via A_r and Microscopic Reversibility (MR), $A_r = 3.31 \times 10^{11}$, 86 TSA/HAM and 72 KER/PAR for $\text{C}=\text{C} + \text{CH}_3$. $E_{a,f} = E_{a,r}(7.8) + \Delta U_{\text{rxn}}(13.30) \text{ kcal mol}^{-1}$.

IID. 67 $\text{CC.C} + \text{O}_2 \rightarrow \text{Products}$ 

Reaction		$A T^n e^{-\alpha T}$ (s ⁻¹ or cm ³ mol ⁻¹ s ⁻¹)	E_a (kcal mol ⁻¹)
k_1	$\text{CC.C} + \text{O}_2 \rightarrow \text{C}_2\text{COO.}$	$6.62 \times 10^{12} T^0 e^{-0T}$	0.00
k_{-1}	$\text{C}_2\text{COO.} \rightarrow \text{CC.C} + \text{O}_2$	$1.41 \times 10^{15} T^0 e^{-0T}$	32.01
k_2	$\text{C}_2\text{COO.} \rightarrow \text{CC=C} + \text{HO}_2$	$4.98 \times 10^9 T^{1.18} e^{-0T}$	32.29
k_3	$\text{C}_2\text{COO.} \rightarrow \text{C}_2\text{C.OOH}$	$1.30 \times 10^{10} T^{1.0} e^{-0T}$	42.33
k_{-3}	$\text{C}_2\text{C.OOH} \rightarrow \text{C}_2\text{COO.}$	$1.33 \times 10^{11} T^{0.04} e^{-0.00073T}$	36.58
k_4	$\text{C}_2\text{C.OOH} \rightarrow \text{C}_2\text{C=O} + \text{OH}$	$4.48 \times 10^{12} T^0 e^{-0T}$	2.00
k_5	$\text{C}_2\text{COO.} \rightarrow \text{C}_2\text{C.OOH}$	$5.27 \times 10^9 T^{1.08} e^{-0T}$	27.63
k_{-5}	$\text{C}_2\text{C.OOH} \rightarrow \text{C}_2\text{COO.}$	$1.32 \times 10^{11} T^{-0.04} e^{-0.00052T}$	13.94
k_6	$\text{C}_2\text{C.OOH} \rightarrow \text{CCyCOC} + \text{OH}$	$6.80 \times 10^{11} T^{-0.27} e^{-0T}$	20.00
k_7	$\text{C}_2\text{C.OOH} \rightarrow \text{CC=C} + \text{HO}_2$	$4.56 \times 10^{12} T^{-0.14} e^{-0T}$	13.41
k_8	$\text{C}_2\text{C.OOH} \rightarrow \text{C=COOH} + \text{CH}_3$	$1.55 \times 10^{12} T^0 e^{-0T}$	33.98

frequency/degeneracy (CPFIT)
 $\text{C}_2\text{COO.}$: 250.0 (7.189); 1111.8 (12.877); 2859.1 (8.434)
 $\text{C}_2\text{C.OOH}$: 100.3 (7.507); 1069.9 (12.133); 2730.8 (8.360)

Lennard-Jones parameter
 $\sigma(\text{\AA}) = 5.20$, $\epsilon/k \text{ (K)} = 533.08$

- k_1 92 ATK/BAU
- k_{-1} A_r via A_f and Microscopic Reversibility (MR), $E_{a,r} = E_{a,f} - \Delta U_{rxn}$ (32.01) kcal mol⁻¹.
- k_2 A_f calculated by Bozzelli based on TST, $A = (\text{deg.}) (ek_b T/h) \exp(\Delta S^\ddagger(T)/R)$, with $\Delta S^\ddagger(T)$ from MOPAC calculation, $E_{a,f} = E_{a,r} + \Delta U_{rxn}$ (19.29) $E_{a,r}$ is estimated as ring strain (6) + $E_{a,add}$ (7).
- k_3 A_f estimated using TST, $A = (\text{deg.}) (ek_b/h) T^n \exp(\Delta S^\ddagger(T)/R)$, $\text{deg.} = 1$ $ek_b/h = 5.66 \times 10^{10}$, $n = 1.0$, $\Delta S^\ddagger(T)$ is estimated as loss of one rotor (-4.3 cal mol⁻¹ K⁻¹) and gain of an optical isomer (OI), $E_{a,f} = RS$ (26) + $E_{a,bst}$ (10.58) + ΔH_{rxn} (5.75) kcal mol⁻¹.
- k_{-3} A_r via A_f and Microscopic Reversibility (MR), $E_{a,r} = E_{a,f} - \Delta U_{rxn}$ (5.75) kcal mol⁻¹.
- k_4 A_f via A_r and Microscopic Reversibility (MR), $A_r = 2.75 \times 10^{12} = 1/2$ (OH + C=C). $E_{a,f}$ estimated the same 2.0 kcal mol⁻¹ based on $E_{a,f}$ for $\text{CH}_2\text{OOH} \rightarrow \text{CH}_2\text{O} + \text{OH}$ (1990 Page)
- k_5 A_f calculated by Bozzelli based on TST, $A = (\text{deg.}) (ek_b T/h) \exp(\Delta S^\ddagger(T)/R)$, with $\Delta S^\ddagger(T)$ from MOPAC calculation, $E_{a,f} = RS$ (6) + $E_{a,bst}$ (7.94) + ΔH_{rxn} (13.69) kcal mol⁻¹.
- k_{-5} A_r via A_f and Microscopic Reversibility (MR), $E_{a,r} = E_{a,f} - \Delta U_{rxn}$ (13.69) kcal mol⁻¹.
- k_6 A_f calculated by Bozzelli based on TST, $A = (\text{deg.}) (ek_b T/h) \exp(\Delta S^\ddagger(T)/R)$, with $\Delta S^\ddagger(T)$ from MOPAC calculation, $E_{a,f}$ is evaluated in this study.
- k_7 A_f calculated by Bozzelli based on TST, $A = (\text{deg.}) (ek_b T/h) \exp(\Delta S^\ddagger(T)/R)$, with $\Delta S^\ddagger(T)$ from MOPAC calculation, $E_{a,f} = E_{a,r} + \Delta U_{rxn}$ (7.88) kcal mol⁻¹. $E_{a,r} = 7.8$ kcal mol⁻¹. (estimated by Bozzelli).
- k_8 A_f via A_r and Microscopic Reversibility (MR), $A_r = 9.64 \times 10^{10}$, 91 TSA for $\text{C}_3\text{H}_6 + \text{CH}_3 \rightarrow \text{C}_3\text{C}$. $E_{a,f} = E_{a,r} + \Delta U_{rxn}$, $\Delta U_{rxn} = 25.97$ kcal mol⁻¹. $E_{a,r} = 8.006$ kcal mol⁻¹. (referenced as the same as the A_r).

	Reaction	$A T^n e^{-\alpha T}$ (s^{-1} or $cm^3 mol^{-1} s^{-1}$)	E_a ($kcal mol^{-1}$)
k ₁₀	CyCOC(CO.) \rightarrow CyC.COOC	$3.89 \times 10^{12} T^0 e^{-0T}$	43.58
k ₁₁	CyCOC(CO.) \rightarrow CCyCC.OOC	$1.76 \times 10^{13} T^0 e^{-0T}$	11.79
k ₁₂	CyC.COOC \rightarrow CyCC.OOC	$2.26 \times 10^{11} T^{1.0} e^{-0T}$	39.90
k ₁₂	CyCC.OOC \rightarrow CyC.COOC	$4.53 \times 10^{11} T^{1.0} e^{-0T}$	37.80
k ₁₃	CyCC.OOC \rightarrow O=CCCO.	$3.54 \times 10^{13} T^0 e^{-0T}$	1.00
k ₁₃	O=CCCO. \rightarrow CyCC.OOC	$4.68 \times 10^{11} T^0 e^{-0T}$	47.84
k ₁₄	O=CCCO. \rightarrow C.CHO + CH ₂ O	$1.28 \times 10^{12} T^0 e^{-0T}$	8.81
k ₁₅	C=CCOO. \rightarrow C.CyCOOC	$4.68 \times 10^{11} T^0 e^{-0T}$	33.00
k ₁₅	C.CyCOOC \rightarrow C=CCOO.	$8.27 \times 10^{12} T^0 e^{-0T}$	15.27
k ₁₆	C.CyCOOC \rightarrow C=COOC.	$5.49 \times 10^{12} T^0 e^{-0T}$	38.12
k ₁₆	C=COOC. \rightarrow C.CyCOOC	$5.38 \times 10^{10} T^0 e^{-0T}$	33.00
k ₁₇	C=COOC. \rightarrow C=CO. + CH ₂ O	$1.53 \times 10^{13} T^0 e^{-0T}$	1.00
k ₁₈	C.CyCOOC \rightarrow CyCOC(CO.)	$4.08 \times 10^{12} T^0 e^{-0T}$	8.00
k ₁₈	CyCOC(CO.) \rightarrow C.CyCOOC	$5.02 \times 10^{12} T^0 e^{-0T}$	50.95
k ₁₉	CyCOC(CO.) \rightarrow CyCOC. + CH ₂ O	$1.76 \times 10^{13} T^0 e^{-0T}$	11.79
k ₂₀	C.CyCOOC \rightarrow CCyC.OOC	$6.50 \times 10^9 T^{1.0} e^{-0T}$	36.87
k ₂₀	CCyC.OOC \rightarrow C.CyCOOC	$1.43 \times 10^{10} T^{1.0} e^{-0.00009T}$	41.77
k ₂₁	CCyC.OOC \rightarrow CC(=O)CO.	$4.96 \times 10^{13} T^0 e^{-0T}$	1.00
k ₂₁	CC(=O)CO. \rightarrow CCyC.OOC	$4.08 \times 10^{12} T^0 e^{-0T}$	67.95
k ₂₂	CC(=O)CO. \rightarrow CH ₃ C.=O + CH ₂ O	$1.00 \times 10^{13} T^0 e^{-0T}$	8.63
k ₂₃	C.CyCOOC \rightarrow CCyCOOC.	$1.30 \times 10^{10} T^{1.0} e^{-0T}$	34.86
k ₂₃	CCyCOOC. \rightarrow C.CyCOOC	$1.17 \times 10^{12} T^{0.46} e^{-0.00041T}$	39.78
k ₂₄	CCyCOOC. \rightarrow CC(O.)CHO	$8.09 \times 10^{13} T^0 e^{-0T}$	1.00
k ₂₄	CC(O.)CHO \rightarrow CCyCOOC.	$4.08 \times 10^{12} T^0 e^{-0T}$	64.58
k ₂₅	CC(O.)CHO \rightarrow CH ₃ CHO + CHO	$9.16 \times 10^{12} T^0 e^{-0T}$	5.32
k ₂₆	CC(O.)CHO \rightarrow C2C(OH)C.=O	$6.50 \times 10^9 T^{1.0} e^{-0T}$	27.33
k ₂₆	C2C(OH)C.=O \rightarrow CC(O.)CHO	$1.49 \times 10^9 T^{1.01} e^{-0.00038T}$	42.83
k ₂₇	C2C(OH)C.=O \rightarrow C2C=O + CHO	$3.28 \times 10^{12} T^0 e^{-0T}$	7.52

frequency/degeneracy (CPFIT)

C=CCOO.: 250.2 (6.265); 1062.0 (9.404); 2787.9 (7.331)
 C=CC.OOH: 250.2 (6.237); 1049.3 (10.657); 2504.4 (5.606)
 C=C.COOH: 250.1 (7.596); 1156.5 (9.768); 2748.4 (5.136)
 C.=CCOOH: 251.1 (7.383); 1087.0 (9.979); 2746.1 (5.138)
 CyC.COOC: 250.1 (3.158); 1034.0 (16.543); 2708.5 (4.299)
 CyCOC(CO.): 250.9 (3.423); 1006.8 (14.393); 2896.7 (5.684)
 CyCC.OOC: 250.1 (3.158); 1034.0 (16.543); 2708.5 (4.299)
 O=CCCO.: 513.3 (10.877); 1805.9 (9.913); 3999.6 (2.210)
 C.CyCOOC: 250.7 (2.831); 959.2 (14.424); 2187.3 (6.245)
 C=COOC.: 510.4 (12.353); 1463.5 (8.291); 3296.4 (1.857)
 CCyC.OOC: 251.4 (3.448); 967.9 (13.280); 2172.2 (6.773)
 CC(=O)CO.: 469.2 (9.796); 1694.2 (9.877); 3139.4 (3.327)

CCyCOOC.: 250.0 (3.140); 964.1 (15.134); 2436.5 (5.226)
 CC(O.)CHO: 251.8 (5.080); 1041.8 (12.047); 2706.1 (5.874)
 CC(OH)C.=O: 250.3 (5.384); 1058.9 (11.400); 2797.0 (5.716)

Lennard-Jones parameter

$$\sigma(\text{\AA}) = 5.86, \varepsilon/k (\text{K}) = 632.06$$

- k_1 93 JEN/MUR
- k_{-1} A_r via A_f and Microscopic Reversibility (MR), $E_{a,r} = E_{a,f} - \Delta U_{rxn}$, $\Delta U_{rxn} = -18.87$ kcal mol⁻¹.
- k_2 A_f via A_r and Microscopic Reversibility (MR), $A_r = 1.51 \times 10^{13}$, 92 BAU/COB for (CH₃O + O → Prod., $E_{a,f} = \Delta U_{rxn} = 60.16$ kcal mol⁻¹.
- k_3 A_r estimated using TST, $A = (\text{deg.}) (ek_b/h) T^n \exp(\Delta S^\ddagger(T)/R)$, deg. = 2 $ek_b/h = 5.66 \times 10^{10}$, $n = 1.0$, $\Delta S^\ddagger(T)$ is estimated as loss of one rotor (-4.3 kcal mol⁻¹) and gain of an optical isomer (OI). $E_{a,f} = RS (26) + E_{abst} (11.94)$ kcal mol⁻¹.
- k_{-3} A_r via A_f and Microscopic Reversibility (MR), $E_{a,r} = E_{a,f} - \Delta U_{rxn}$, $\Delta U_{rxn} = -1.67$ kcal mol⁻¹.
- k_4 A_f via A_r and Microscopic Reversibility (MR), $A_r = 2.75 \times 10^{12} = 1/2$ (OH + C=C). $E_{a,f}$ estimated the same 2.5 kcal mol⁻¹ as $E_{a,f}$ for CH₂OOH → CH₂O + OH (1990 Page)
- k_5 A_r estimated using TST, $A = (\text{deg.}) (ek_b/h) T^n \exp(\Delta S^\ddagger(T)/R)$, deg. = 1 $ek_b/h = 5.66 \times 10^{10}$, $n = 1.0$, $\Delta S^\ddagger(T)$ is estimated as loss of two rotors (-4.3 × 2 kcal mol⁻¹) and gain of an optical isomer (OI). $E_{a,f} = RS (6) + E_{abst} (6.28) + \Delta H_{rxn} (21.65)$ kcal mol⁻¹.
- k_{-5} A_r via A_f and Microscopic Reversibility (MR), $E_{a,r} = E_{a,f} - \Delta U_{rxn}$, $\Delta U_{rxn} = 21.65$ kcal mol⁻¹.
- k_6 A_f via A_r and Microscopic Reversibility (MR), $A_r = 3.50 \times 10^{11}$, Bozzelli. $E_{a,f} = E_{a,r} + \Delta U_{rxn}$, $\Delta U_{rxn} = 6.31$ kcal mol⁻¹. $E_{a,r} = 7.80$ kcal mol⁻¹. (estimated by Bozzelli).
- k_7 A_r estimated using TST, $A = (\text{deg.}) (ek_b/h) T^n \exp(\Delta S^\ddagger(T)/R)$, deg. = 2 $ek_b/h = 5.66 \times 10^{10}$, $n = 1.0$, $\Delta S^\ddagger(T)$ is estimated as loss of two rotors (-4.3 × 2 kcal mol⁻¹) and gain of an optical isomer (OI). $E_{a,f} = RS (0) + E_{abst} (7.47)$ kcal mol⁻¹ + $\Delta H_{rxn} (24.08)$ kcal mol⁻¹.
- k_{-7} A_r via A_f and Microscopic Reversibility (MR), $E_{a,r} = E_{a,f} - \Delta U_{rxn}$, $\Delta U_{rxn} = 24.08$ kcal mol⁻¹.
- k_8 A_f via A_r and Microscopic Reversibility (MR), $A_r = 3.01 \times 10^{11} = 1/2$ (C≡C + CH₃), 92 BAU/COB. $E_{a,f} = E_{a,r} + \Delta U_{rxn}$, $\Delta U_{rxn} = 23.29$ kcal mol⁻¹. $E_{a,r} = 7.8$ kcal mol⁻¹. (estimated by Bozzelli).
- k_9 A_r estimated using TST, $A = (\text{deg.}) (ek_b T/h) \exp(\Delta S^\ddagger(T)/R)$, deg. = 1, $ek_b T/h = 10^{13.55}$?, $\Delta S^\ddagger(T)$ is estimated as loss of two rotors (-4.3 × 2 cal mol⁻¹ K⁻¹). $E_{a,f}$ is estimated by Bozzelli.
- k_{-9} A_r via A_f and Microscopic Reversibility (MR), $E_{a,r} = E_{a,f} - \Delta U_{rxn}$, $\Delta U_{rxn} = -3.64$ kcal mol⁻¹.
- k_{10} A_f is taken from ref [55]. $E_{a,f}$ is estimated as the difference of ring strain (28 - 6) kcal mol⁻¹.

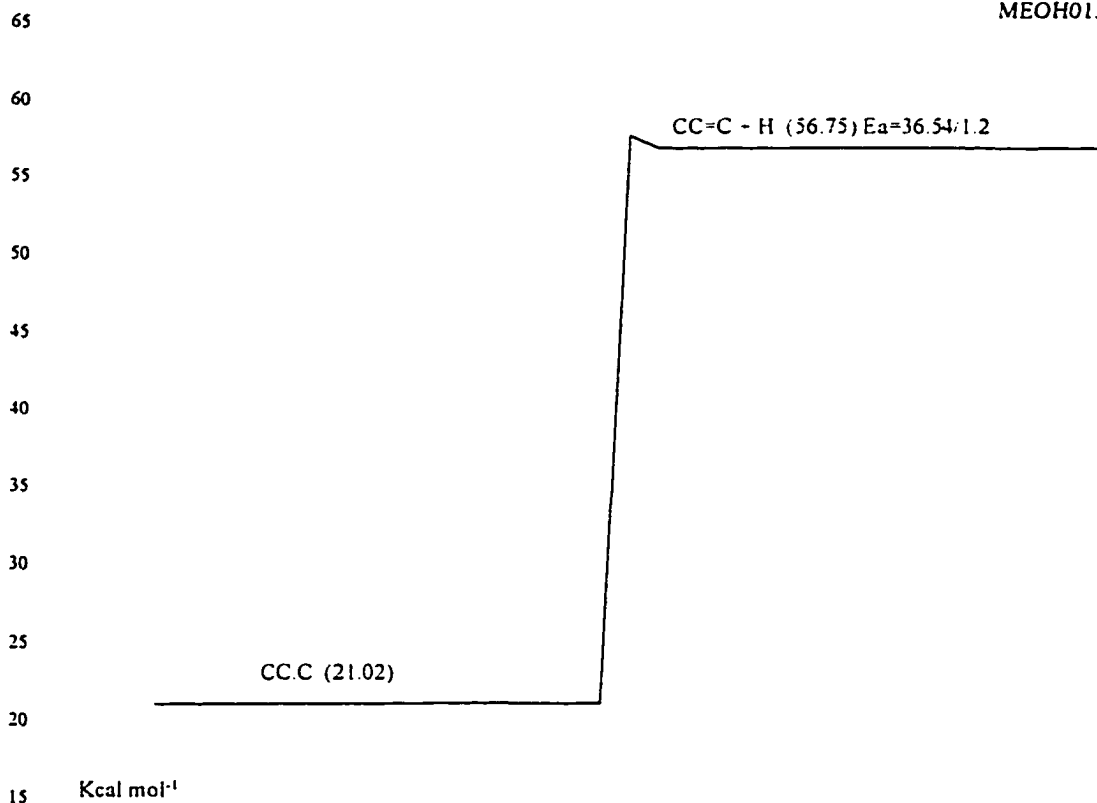
- k₁₀ A_r via A_f and Microscopic Reversibility (MR), E_{a,r} = E_{a,f} - ΔU_{rxn}, ΔU_{rxn} = -21.58 kcal mol⁻¹.
- k₁₁ A_f via A_r and Microscopic Reversibility (MR), A_r = 1.08 × 10¹¹, 88 TSA for CH₂O + CC.C → CCC + CHO. E_{a,f} = E_{a,r} + ΔU_{rxn}, ΔU_{rxn} = 5.79 kcal mol⁻¹. E_{a,r} = 6.0 kcal mol⁻¹. (estimated by Bozzelli).
- k₁₂ A_r estimated using TST, A = (deg.) (ek_b/h) Tⁿ exp(ΔS[‡](T)/R), deg. = 1 ek_b/h = 5.66 × 10¹⁰, n = 1.0, ΔS[‡](T) is estimated as loss of rotor (no rotor loss here, so ΔS[‡](T) = 0), E_{a,f} = RS (0) + E_{abt} (9.80) + ΔH_{rxn} (2.10) kcal mol⁻¹.
- k₁₂ A_r via A_f and Microscopic Reversibility (MR), E_{a,r} = E_{a,f} - ΔU_{rxn}, ΔU_{rxn} = 2.10 kcal mol⁻¹.
- k₁₃ A_f via A_r and Microscopic Reversibility (MR), E_{a,f} is estimated as 1 kcal mol⁻¹ by Bozzelli.
- k₁₃ A_r estimated using TST, A = (deg.) (ek_bT/h) exp(ΔS[‡](T)/R), deg. = 1, ek_bT/h = 10^{13.55} ?, ΔS[‡](T) is estimated as loss of two rotors (-4.3 × 2 cal mol⁻¹ K⁻¹). E_{a,r} = E_{a,f} - ΔU_{rxn}, ΔU_{rxn} = -46.84 kcal mol⁻¹.
- k₁₄ A_f via A_r and Microscopic Reversibility (MR), A_r = 1.58 × 10¹¹, 72 KER/PAR for CC. + C=C → CCCC.. E_{a,f} = E_{a,r} + ΔU_{rxn}, ΔU_{rxn} = 2.81 kcal mol⁻¹. E_{a,r} = 6.0 kcal mol⁻¹. (estimated by Bozzelli).
- k₁₅ A_f estimated using TST, A = (deg.) (ek_bT/h) exp(ΔS[‡](T)/R), deg. = 1, ek_bT/h = 10^{13.55} ?, ΔS[‡](T) is estimated as loss of two rotors (-4.3 × 2 cal mol⁻¹ K⁻¹). E_{a,f} is estimated as ring strain (26) + E_{a,add} (7).
- k₁₅ A_r via A_f and Microscopic Reversibility (MR), E_{a,r} = E_{a,f} - ΔU_{rxn}, ΔU_{rxn} = 17.73 kcal mol⁻¹.
- k₁₆ A_f via A_r and Microscopic Reversibility (MR), E_{a,f} = E_{a,r} + ΔU_{rxn}, ΔU_{rxn} = 5.12 kcal mol⁻¹.
- k₁₆ A_r estimated using TST, A = (deg.) (ek_bT/h) exp(ΔS[‡](T)/R), deg. = 1, ek_bT/h = 10^{13.55} ?, ΔS[‡](T) is estimated as loss of three rotors (-4.3 × 3 cal mol⁻¹ K⁻¹). E_{a,r} is estimated as ring strain (26) + E_{a,add} (7).
- k₁₇ A_f via A_r and Microscopic Reversibility (MR), A_r = 1.60 × 10¹¹, NIST fit for CH₃O + CO. E_{a,f} is estimated as 1.0 kcal mol⁻¹ by Bozzelli.
- k₁₈ A_f estimated using TST, A = (deg.) (ek_bT/h) exp(ΔS[‡](T)/R), deg. = 1, ek_bT/h = 10^{13.55} ?, ΔS[‡](T) is estimated as loss of one rotor (-4.3 cal mol⁻¹ K⁻¹). E_{a,f} is estimated by Bozzelli.
- k₁₈ A_r via A_f and Microscopic Reversibility (MR), E_{a,r} = E_{a,f} - ΔU_{rxn}, ΔU_{rxn} = -42.95 kcal mol⁻¹.
- k₁₉ A_f via A_r and Microscopic Reversibility (MR), A_r = 1.08 × 10¹¹, 88 TSA for CH₂O + CC.C → CCC + CHO. E_{a,f} = E_{a,r} + ΔU_{rxn}, ΔU_{rxn} = 5.79 kcal mol⁻¹. E_{a,r} = 6.0 kcal mol⁻¹. (estimated by Bozzelli).
- k₂₀ A_f estimated using TST, A = (deg.) (ek_b/h) Tⁿ exp(ΔS[‡](T)/R), deg. = 1 ek_b/h = 5.66 × 10¹⁰, n = 1.0, ΔS[‡](T) is estimated as loss of one rotor (-4.3 cal mol⁻¹ K⁻¹), E_{a,f} = RS (28) + E_{abt} (8.87) kcal mol⁻¹.
- k₂₀ A_r via A_f and Microscopic Reversibility (MR), E_{a,r} = E_{a,f} - ΔU_{rxn}, ΔU_{rxn} = -4.90 kcal mol⁻¹.
- k₂₁ A_f via A_r and Microscopic Reversibility (MR), E_{a,f} is estimated as 1.0 kcal mol⁻¹ by

Bozzelli.

- k₂₁ A_r estimated using TST, $A = (\text{deg.}) (ek_b T/h) \exp(\Delta S^\ddagger(T)/R)$, $\text{deg.} = 1$, $ek_b T/h = 10^{13.55}$?, $\Delta S^\ddagger(T)$ is estimated as loss of one rotor ($-4.3 \text{ cal mol}^{-1} \text{ K}^{-1}$). $E_{a,r} = E_{a,f} - \Delta U_{\text{rxn}}$, $\Delta U_{\text{rxn}} = -66.95 \text{ kcal mol}^{-1}$.
- k₂₂ A_f via A_r and Microscopic Reversibility (MR), $A_r = 1.08 \times 10^{11}$, 88 TSA for $\text{CH}_2\text{O} + \text{CC.C} \rightarrow \text{CCC} + \text{CHO}$. $E_{a,f} = E_{a,r} + \Delta U_{\text{rxn}}$, $\Delta U_{\text{rxn}} = 2.63 \text{ kcal mol}^{-1}$. $E_{a,r} = 6.0 \text{ kcal mol}^{-1}$. (estimated by Bozzelli).
- k₂₃ A_f estimated using TST, $A = (\text{deg.}) (ek_b/h) T^n \exp(\Delta S^\ddagger(T)/R)$, $\text{deg.} = 1$, $ek_b/h = 5.66 \times 10^{10}$, $n = 1.0$, $\Delta S^\ddagger(T)$ is estimated as loss of one rotor ($-4.3 \text{ cal mol}^{-1} \text{ K}^{-1}$), $E_{a,f} = \text{RS (26)} + E_{\text{abst}} (8.86) \text{ kcal mol}^{-1}$.
- k₂₃ A_r via A_f and Microscopic Reversibility (MR), $E_{a,r} = E_{a,f} - \Delta U_{\text{rxn}}$, $\Delta U_{\text{rxn}} = -4.92 \text{ kcal mol}^{-1}$.
- k₂₄ A_f via A_r and Microscopic Reversibility (MR), $E_{a,f}$ is estimated as $1.0 \text{ kcal mol}^{-1}$ by Bozzelli.
- k₂₄ A_r estimated using TST, $A = (\text{deg.}) (ek_b T/h) \exp(\Delta S^\ddagger(T)/R)$, $\text{deg.} = 1$, $ek_b T/h = 10^{13.55}$?, $\Delta S^\ddagger(T)$ is estimated as loss of one rotor ($-4.3 \text{ cal mol}^{-1} \text{ K}^{-1}$). $E_{a,r} = E_{a,f} - \Delta U_{\text{rxn}}$, $\Delta U_{\text{rxn}} = -63.58 \text{ kcal mol}^{-1}$.
- k₂₅ A_f via A_r and Microscopic Reversibility (MR), $A_r = 5.01 \times 10^{11} = 1/2 (\text{CC}=\text{C} + \text{CHO} \rightarrow \text{Prod.})$, NIST. $E_{a,f} = E_{a,r} + \Delta U_{\text{rxn}}$, $\Delta U_{\text{rxn}} = -0.68 \text{ kcal mol}^{-1}$. $E_{a,r} = 6.0 \text{ kcal mol}^{-1}$. (estimated by Bozzelli).
- k₂₆ A_f estimated using TST, $A = (\text{deg.}) (ek_b/h) T^n \exp(\Delta S^\ddagger(T)/R)$, $\text{deg.} = 1$, $ek_b/h = 5.66 \times 10^{10}$, $n = 1.0$, $\Delta S^\ddagger(T)$ is estimated as loss of one rotor ($-4.3 \text{ cal mol}^{-1} \text{ K}^{-1}$), $E_{a,f} = \text{RS (26)} + E_{\text{abst}} (1.33) \text{ kcal mol}^{-1}$.
- k₂₆ A_r via A_f and Microscopic Reversibility (MR), $E_{a,r} = E_{a,f} - \Delta U_{\text{rxn}}$, $\Delta U_{\text{rxn}} = -15.50 \text{ kcal mol}^{-1}$.
- k₂₇ A_f via A_r and Microscopic Reversibility (MR), $A_r = 7.50 \times 10^{10} = 1/2 (\text{CC.} + \text{CO.})$, 86 TSA/HAM. $E_{a,f} = E_{a,r} + \Delta U_{\text{rxn}}$, $\Delta U_{\text{rxn}} = 2.71 \text{ kcal mol}^{-1}$. $E_{a,r} = 4.809 \text{ kcal mol}^{-1}$. (taken from the same reference as A_r).

IID. 69 $\text{CC.C} \rightarrow \text{CC}=\text{C} + \text{H}$

MEOH013



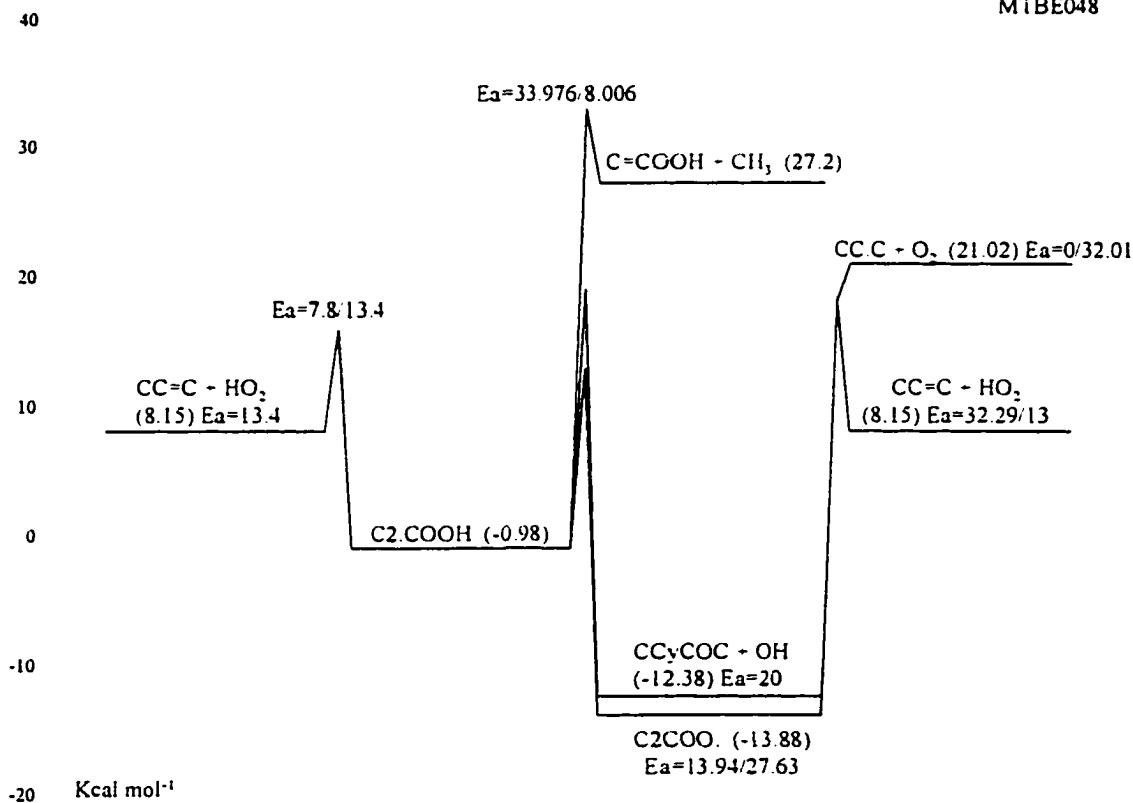
Reaction		$A T^n e^{-\alpha T}$ (s^{-1} or $\text{cm}^3 \text{mol}^{-1} \text{s}^{-1}$)	E_a (kcal mol^{-1})
k_1	$\text{CC.C} \rightarrow \text{CC}=\text{C} + \text{H}$	$7.78 \times 10^{12} T^0 e^{-0T}$	36.54

frequency/degeneracy (CPFIT)
 CC.C: 554.4 (6.897); 1622.0 (11.862); 3563.2 (4.241)
 Lennard-Jones parameter
 $\sigma(\text{\AA}) = 4.98$, $\epsilon/k(\text{K}) = 266.8$

k_1 A_f via A_r and Microscopic Reversibility (MR), $A_r = 7.24 \times 10^{12}$, 72 KER/PAR. $E_{a,f} = E_{a,r}(1.2) + \Delta U_{\text{rxn}}(36.54) \text{ kcal mol}^{-1}$.

IID. 70 $\text{CC}=\text{C} + \text{HO}_2 \rightarrow [\text{C2C.OOH}]^* \rightarrow \text{Products}$

MTBE048



Reaction	$A T^n e^{-\frac{E_a}{T}}$ (s^{-1} or $\text{cm}^3 \text{mol}^{-1} \text{s}^{-1}$)	E_a (kcal mol^{-1})
$k_1 \text{ CC}=\text{C} + \text{HO}_2 \rightarrow \text{C2.COOH}$	$2.13 \times 10^4 T^{2.44} e^{0.00014T}$	7.80
$k_{-1} \text{ C2.COOH} \rightarrow \text{CC}=\text{C} + \text{HO}_2$	$4.56 \times 10^{12} T^{-0.14} e^{-0T}$	13.40
$k_2 \text{ C2.COOH} \rightarrow \text{CCyCOC} + \text{OH}$	$6.80 \times 10^{11} T^{-0.27} e^{-0T}$	20.00
$k_3 \text{ C2.COOH} \rightarrow \text{C=COOH} + \text{CH}_3$	$1.55 \times 10^{12} T^0 e^{-0T}$	33.98
$k_4 \text{ C2.COOH} \rightarrow \text{C2COO.}$	$1.32 \times 10^{11} T^{-0.04} e^{-0.00052T}$	13.94
$k_{-4} \text{ C2COO.} \rightarrow \text{C2.COOH}$	$5.27 \times 10^9 T^{1.08} e^{-0T}$	27.63
$k_5 \text{ C2COO.} \rightarrow \text{CC}=\text{C} + \text{HO}_2$	$4.98 \times 10^9 T^{1.18} e^{-0T}$	32.29
$k_6 \text{ C2COO.} \rightarrow \text{CC.C} + \text{O}_2$	$1.41 \times 10^{15} T^0 e^{-0T}$	32.01

frequency/degeneracy (CPFIT)

C2C.OOH : 100.3 (7.507); 1069.9 (12.133); 2730.8 (8.360)

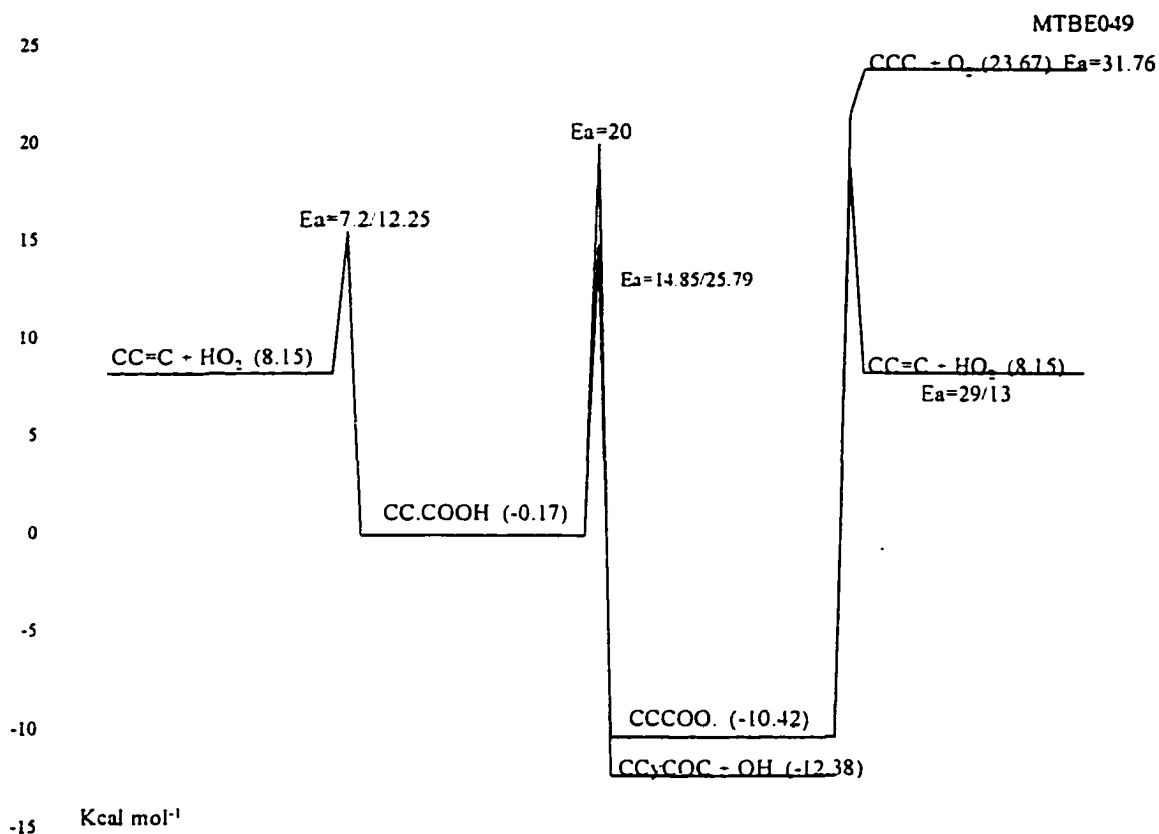
C2COO. : 250.0 (7.189); 1111.8 (12.877); 2859.1 (8.434)

Lennard-Jones parameter

$\sigma(\text{\AA}) = 5.20$, $\epsilon/k (\text{K}) = 533.08$

- k_1 A_f via A_r and Microscopic Reversibility (MR), $E_{a,f}$ estimated by Bozzelli.
- k_{-1} A_r calculated by Bozzelli based on TST with MOPAC, $E_{a,r} = E_{a,f} - \Delta U_{rxn}$ (-32.01) kcal mol⁻¹.
- k_2 A_f calculated by Bozzelli based on TST, $A = (\text{deg.}) (ek_b T/h) \exp(\Delta S^\ddagger(T)/R)$, with $\Delta S^\ddagger(T)$ from MOPAC calculation, $E_{a,f}$ is evaluated in this study.
- k_3 A_f via A_r and Microscopic Reversibility (MR), $A_r = 9.64 \times 10^{10}$, 91 TSA for $C_3H_6 + CH_3 \rightarrow C3.C$. $E_{a,f} = E_{a,r} + \Delta U_{rxn}$, $\Delta U_{rxn} = 25.97$ kcal mol⁻¹. $E_{a,r} = 8.006$ kcal mol⁻¹. (referenced as the same as the A_r).
- k_4 A_f via A_r and Microscopic Reversibility (MR), $E_{a,f} = E_{a,r} + \Delta U_{rxn}$ (-5.75) kcal mol⁻¹.
- k_{-4} A_r calculated by Bozzelli based on TST, $A = (\text{deg.}) (ek_b T/h) \exp(\Delta S^\ddagger(T)/R)$, with $\Delta S^\ddagger(T)$ from MOPAC calculation, $E_{a,r} = RS(26) + E_{abst}(10.58) + \Delta H_{rxn}(5.75)$ kcal mol⁻¹.
- k_5 A_f calculated by Bozzelli based on TST, $A = (\text{deg.}) (ek_b T/h) \exp(\Delta S^\ddagger(T)/R)$, with $\Delta S^\ddagger(T)$ from MOPAC calculation, $E_{a,f} = E_{a,r} + \Delta U_{rxn}$ (19.29) $E_{a,r}$ is estimated as ring strain (6) + $E_{a,add}$ (7).
- k_6 A_f via A_r and Microscopic Reversibility (MR), $A_r = 6.62 \times 10^{12}$, 92 ATK/BAU. $E_{a,f} = \Delta U_{rxn} = 32.01$ kcal mol⁻¹.

IID. 71 $\text{CC}=\text{C} + \text{HO}_2 \rightarrow [\text{CC}.\text{COOH}]^* \rightarrow \text{Products}$



Reaction		$A T^n e^{-\alpha T}$ (s ⁻¹ or cm ³ mol ⁻¹ s ⁻¹)	E_a (kcal mol ⁻¹)
k_1	$\text{CC}=\text{C} + \text{HO}_2 \rightarrow \text{CC}.\text{COOH}$	$5.01 \times 10^{11} T^0 e^{-0T}$	7.20
k_{-1}	$\text{CC}.\text{COOH} \rightarrow \text{CC}=\text{C} + \text{HO}_2$	$6.69 \times 10^{12} T^0 e^{-0T}$	12.25
k_2	$\text{CC}.\text{COOH} \rightarrow \text{CCyCOC} + \text{OH}$	$4.68 \times 10^{11} T^0 e^{-0T}$	20.00
k_3	$\text{CC}.\text{COOH} \rightarrow \text{CCCOO}.$	$9.16 \times 10^{10} T^{0.01} e^{-0.00047T}$	14.85
k_{-3}	$\text{CCCOO}.\rightarrow \text{CC}.\text{COOH}$	$1.50 \times 10^9 T^0 e^{-0T}$	25.79
k_4	$\text{CCCOO}.\rightarrow \text{CC}=\text{C} + \text{HO}_2$	$7.47 \times 10^9 T^{0.73} e^{-0T}$	29.00
k_5	$\text{CCCOO}.\rightarrow \text{CCC}.\text{ + O}_2$	$5.74 \times 10^{14} T^0 e^{-0T}$	31.76

frequency/degeneracy (CPFIT)

CC.CO₂H: 250.3 (8.681); 1245.6 (12.964); 2818.4 (6.355)

CCCOO.: 251.0 (7.429); 1148.5 (12.338); 2789.4 (8.734)

Lennard-Jones parameter

$\sigma(\text{\AA}) = 5.20$, $\epsilon/k(\text{K}) = 533.08$

- k_1 A_f via A_r and Microscopic Reversibility (MR), $A_r = 5.01 \times 10^{11}$, 72 KER/PAR for $C=C + HO_2 \rightarrow \text{Prod.}$. $E_{a,f}$ is estimated by Bozzelli.
- k_{-1} A_r via A_f and Microscopic Reversibility (MR), $E_{a,r} = E_{a,f} - \Delta U_{\text{rxn}}$, $\Delta U_{\text{rxn}} = -5.05 \text{ kcal mol}^{-1}$.
- k_2 A_f estimated using TST, $A = (\text{deg.}) (ek_b T/h) \exp(\Delta S^\ddagger(T)/R)$, $\text{deg.} = 1$, $ek_b T/h = 10^{13.55} ?$, $\Delta S^\ddagger(T)$ is estimated as loss of two rotors ($-4.3 \times 2 \text{ cal mol}^{-1} \text{ K}^{-1}$). $E_{a,f}$ is evaluated in this study.
- k_3 A_f via A_r and Microscopic Reversibility (MR), $E_{a,f} = E_{a,r} + \Delta U_{\text{rxn}} (-10.94) \text{ kcal mol}^{-1}$.
- k_{-3} A_r estimated using TST, $A = (\text{deg.}) (ek_b/h) T^n \exp(\Delta S^\ddagger(T)/R)$, $\text{deg.} = 1$, $ek_b/h = 5.66 \times 10^{10}$, $n = 1.0$, $\Delta S^\ddagger(T)$ is estimated as loss of two rotors ($-4.3 \times 2 \text{ cal mol}^{-1} \text{ K}^{-1}$) and gain of an optical isomer (OI), $E_{a,r} = \text{RS (6)} + E_{\text{abst}} (8.85) + \Delta H_{\text{rxn}} (10.94) \text{ kcal mol}^{-1}$.
- k_4 A_f is referenced from reaction $C_2CCOO. \rightarrow C_2C=C + HO_2$, (from thermal reaction analysis (AFACT2f) based on the thermodynamic properties calculated from MOPAC PM3 (corrected with internal rotor, electronic spin and optical isomer). $E_{a,f} = E_{a,r} + \Delta U_{\text{rxn}} (16.0)$ $E_{a,r}$ is estimated as ring strain (6) + $E_{a,\text{add}}$ (7).
- k_5 A_f via A_r and Microscopic Reversibility (MR), $A_r = 3.01 \times 10^{12}$, NIST fit for $CC. + O_2$. $E_{a,f} = \Delta U_{\text{rxn}} = 32.01 \text{ kcal mol}^{-1}$.

	Reaction	$A T^n e^{-\alpha T}$ (s^{-1} or $cm^3 mol^{-1} s^{-1}$)	E_a ($kcal mol^{-1}$)
k_{12}	$CC.(OOH)COOH \rightarrow CC(=O)COOH + OH$	$8.71 \times 10^{12} T^0 e^{-0T}$	2.00
k_{13}	$CC.(OOH)COOH \rightarrow CyCOC(C)OOH + OH$	$4.68 \times 10^{11} T^0 e^{-0T}$	20.00
k_{14}	$CC.(OOH)COOH \rightarrow C=C(OOH)C + HO_2$	$2.94 \times 10^{12} T^0 e^{-0T}$	22.25
k_{15}	$CC(OOH)COO. \rightarrow CC(OO.)COOH$	$9.85 \times 10^6 T^{1.0} e^{-0T}$	15.90
k_{15}	$CC(OO.)COOH \rightarrow CC(OOH)COO.$	$9.85 \times 10^6 T^{1.0} e^{-0T}$	15.90
k_{16}	$CC(OO.)COOH \rightarrow CC.COOH + O_2$	$4.90 \times 10^{14} T^0 e^{-0T}$	32.46
k_{17}	$CC(OO.)COOH \rightarrow C=CCOOH + HO_2$	$2.49 \times 10^9 T^{1.18} e^{-0T}$	33.17
k_{18}	$CC(OO.)COOH \rightarrow CC=COOH + HO_2$	$1.66 \times 10^9 T^{1.18} e^{-0T}$	33.83

frequency/degeneracy (CPFIT)

$CC(OOH)COO.:$ 100.1 (10.107); 1059.7 (15.280); 2808.7 (8.113)
 $CC(OOH)C.OOH:$ 100.1 (11.462); 1084.1 (14.972); 2766.1 (6.566)
 $C.C(OOH)COOH:$ 100.0 (10.777); 1065.9 (15.825); 2784.7 (6.397)
 $CC.(OOH)COOH:$ 100.2 (11.914); 1126.4 (13.906); 2772.2 (7.180)
 $CC(OO.)COOH:$ 100.1 (10.107); 1059.7 (15.280); 2808.7 (8.113)

Lennard-Jones parameter

$\sigma(\text{\AA}) = 5.86$, ϵ/k (K) = 632.06

- k_1 taken from 88 XI for $C3CC. + O_2$.
- k_{-1} A_r via A_f and Microscopic Reversibility (MR), $E_{a,r} = E_{a,f} - \Delta U_{rxn}$, $\Delta U_{rxn} = -31.9 kcal mol^{-1}$.
- k_2 A_f is referenced from reaction $C2CCOO. \rightarrow C2C=C + HO_2$, (from thermal reaction analysis (AFAC2f) based on the thermodynamic properties calculated from MOPAC PM3 (corrected with internal rotor, electronic spin and optical isomer). $E_{a,f} = E_{a,r} + \Delta U_{rxn}$ (20.2) $E_{a,r}$ is estimated as ring strain (6) + $E_{a,add}$ (7).
- k_3 A_f estimated using TST, $A = (deg.) (ek_b/h) T^n \exp(\Delta S^\ddagger(T)/R)$, $deg. = 2$, $ek_b/h = 5.66 \times 10^{10}$, $n = 1.0$, $\Delta S^\ddagger(T)$ is estimated as loss of one rotor ($-4.3 cal mol^{-1} K^{-1}$) and gain an optical isomer (OI). $E_{a,f} = RS$ (26) + E_{abst} (9.63) + ΔH_{rxn} (8.60) $kcal mol^{-1}$.
- k_{-3} A_r via A_f and Microscopic Reversibility (MR), $E_{a,r} = E_{a,f} - \Delta U_{rxn}$, $\Delta U_{rxn} = 8.60 kcal mol^{-1}$.
- k_4 A_f via A_r and Microscopic Reversibility (MR), $A_r = 2.75 \times 10^{12} = 1/2 (OH + C=C)$. $E_{a,f}$ estimated the same $2.5 kcal mol^{-1}$ as $E_{a,r}$ for $CH_2OOH \rightarrow CH_2O + OH$ (1990 Page)
- k_5 A_f via A_r and Microscopic Reversibility (MR), $A_r = 2.5 \times 10^{11} = 1/2 (C=C + HO_2)$, 72 KER/PAR. $E_{a,f} = E_{a,r} + \Delta U_{rxn}$, $\Delta U_{rxn} = 12.23 kcal mol^{-1}$. $E_{a,r} = 7.8 kcal mol^{-1}$. (estimated by Bozzelli).
- k_6 A_f estimated using TST, $A = (deg.) (ek_b/h) T^n \exp(\Delta S^\ddagger(T)/R)$, $deg. = 3$, $ek_b/h = 5.66 \times 10^{10}$, $n = 1.0$, $\Delta S^\ddagger(T)$ is estimated as loss of three rotors ($-4.3 \times 3 cal mol^{-1} K^{-1}$) and gain an optical isomer (OI). $E_{a,f} = RS$ (0) + E_{abst} (7.95) + ΔH_{rxn} (13.65) $kcal mol^{-1}$.

- k₆ A_f via A_r and Microscopic Reversibility (MR), E_{a,r} = E_{a,f} - ΔU_{rxn}, ΔU_{rxn} = 13.65 kcal mol⁻¹.
- k₇ A_f estimated using TST, A = (deg.) (ek_bT/h) exp(ΔS[‡](T)/R), deg. = 1, ek_bT/h = 10^{13.55} ?, ΔS[‡](T) is estimated as loss of two rotors (-4.3 × 2 cal mol⁻¹ K⁻¹). E_{a,f} is evaluated in this study.
- k₈ A_f via A_r and Microscopic Reversibility (MR), A_r = 3.5 × 10¹¹, Bozzelli. E_{a,f} = E_{a,r} + ΔU_{rxn}, ΔU_{rxn} = 6.52 kcal mol⁻¹. E_{a,r} = 7.8 kcal mol⁻¹. (estimated by Bozzelli).
- k₉ A_f via A_r and Microscopic Reversibility (MR), A_r = 9.64 × 10¹⁰, 91 TSA for C₃H₆ + CH₃ → C3.C. E_{a,f} = E_{a,r} + ΔU_{rxn}, ΔU_{rxn} = 27.22 kcal mol⁻¹. E_{a,r} = 7.8 kcal mol⁻¹. (estimated by Bozzelli).
- k₁₀ A_f estimated using TST, A = (deg.) (ek_bT/h) exp(ΔS[‡](T)/R), deg. = 1, ek_bT/h = 10^{13.55} ?, ΔS[‡](T) is estimated as loss of three rotors (-4.3 × 3 cal mol⁻¹ K⁻¹). E_{a,f} is evaluated in this study.
- k₁₁ A_f estimated using TST, A = (deg.) (ek_b/h) Tⁿ exp(ΔS[‡](T)/R), deg. = 1, ek_b/h = 5.66 × 10¹⁰, n = 1.0, ΔS[‡](T) is estimated as loss of two rotors (-4.3 × 2 cal mol⁻¹ K⁻¹) and gain an optical isomer (OI). E_{a,f} = RS (6) + E_{abst} (7.98) + ΔH_{rxn} (5.76) kcal mol⁻¹.
- k₁₁ A_r via A_f and Microscopic Reversibility (MR), E_{a,r} = E_{a,f} - ΔU_{rxn}, ΔU_{rxn} = 5.76 kcal mol⁻¹.
- k₁₂ A_f via A_r and Microscopic Reversibility (MR), A_r = 2.75 × 10¹² = 1/2 (OH + C=C). E_{a,f} estimated the same 2.0 kcal mol⁻¹ as E_{a,r} for CH₂OOH → CH₂O + OH (1990 Page)
- k₁₃ A_f estimated using TST, A = (deg.) (ek_bT/h) exp(ΔS[‡](T)/R), deg. = 1, ek_bT/h = 10^{13.55} ?, ΔS[‡](T) is estimated as loss of two rotors (-4.3 × 2 cal mol⁻¹ K⁻¹). E_{a,f} is evaluated in this study.
- k₁₄ A_f via A_r and Microscopic Reversibility (MR), A_r = 3.16 × 10¹¹ Bozzelli. E_{a,f} = E_{a,r} + ΔU_{rxn}, ΔU_{rxn} = 14.45 kcal mol⁻¹. E_{a,r} = 7.8 kcal mol⁻¹. (estimated by Bozzelli).
- k₁₅ A_f estimated using TST, A = (deg.) (ek_b/h) Tⁿ exp(ΔS[‡](T)/R), deg. = 1, ek_b/h = 5.66 × 10¹⁰, n = 1.0, ΔS[‡](T) is estimated as loss of four rotors (-4.3 × 4 cal mol⁻¹ K⁻¹) and an optical isomer (OI) but gain an optical isomer (OI). E_{a,f} = RS (6) + E_{abst} (9.9) + ΔH_{rxn} (0.0) kcal mol⁻¹.
- k₁₅ A_r via A_f and Microscopic Reversibility (MR), E_{a,r} = E_{a,f} - ΔU_{rxn}, ΔU_{rxn} = 0.0 kcal mol⁻¹.
- k₁₆ A_f via A_r and Microscopic Reversibility (MR), A_r = 3.31 × 10¹² = 1/2 (CC.C + O₂), 92 ATK/BAU. E_{a,f} = ΔU_{rxn}, = 32.46 kcal mol⁻¹.
- k₁₇ A_f is referenced from reaction C2COO. → CC=C + HO₂, (from thermal reaction analysis (AFACT2f) based on the thermodynamic properties calculated from MOPAC PM3 (corrected with internal rotor, electronic spin and optical isomer). E_{a,f} = E_{a,r} + ΔU_{rxn} (20.17) E_{a,r} is estimated as ring strain (6) + E_{a,add} (7).
- k₁₈ A_f is referenced from reaction C2COO. → CC=C + HO₂, (from thermal reaction analysis (AFACT2f) based on the thermodynamic properties calculated from MOPAC PM3 (corrected with internal rotor, electronic spin and optical isomer). E_{a,f} = E_{a,r} + ΔU_{rxn} (20.83) E_{a,r} is estimated as ring strain (6) + E_{a,add} (7).

Reaction		$A T^n e^{-\alpha T}$ (s^{-1} or $cm^3 mol^{-1} s^{-1}$)	E_a ($kcal mol^{-1}$)
k_{12}	$CC.(OOH)COOH \rightarrow CC(OO.)COOH$	$1.28 \times 10^{11} T^{0.04} e^{-0.00072T}$	36.58
k_{13}	$CC.(OOH)COOH \rightarrow CC(=O)COOH + OH$	$8.71 \times 10^{12} T^0 e^{-0T}$	2.00
k_{14}	$CC.(OOH)COOH \rightarrow CyCOC(C)OOH + OH$	$4.68 \times 10^{11} T^0 e^{-0T}$	20.00
k_{15}	$CC.(OOH)COOH \rightarrow C=C(OOH)C + HO_2$	$2.94 \times 10^{12} T^0 e^{-0T}$	22.25
k_{16}	$CC(OO.)COOH \rightarrow CC(OOH)COO.$	$9.85 \times 10^6 T^{1.0} e^{-0T}$	15.90
k_{16}	$CC(OOH)COO. \rightarrow CC(OO.)COOH$	$9.85 \times 10^6 T^{1.0} e^{-0T}$	15.90
k_{17}	$CC(OOH)COO. \rightarrow C2.COOH + O_2$	$1.04 \times 10^{14} T^0 e^{-0T}$	31.90
k_{18}	$CC(OOH)COO. \rightarrow C=C(OOH)C + HO_2$	$7.48 \times 10^9 T^{0.73} e^{-0T}$	33.20

frequency/degeneracy (CPFIT)

CC(OO.)COOH: 100.1 (10.107); 1059.7 (15.280); 2808.7 (8.113)

CC(OOH)C.OOH: 100.1 (11.462); 1084.1 (14.972); 2766.1 (6.566)

C.C(OOH)COOH: 100.0 (10.777); 1065.9 (15.825); 2784.7 (6.397)

CC.(OOH)COOH: 100.2 (11.914); 1126.4 (13.906); 2772.2 (7.180)

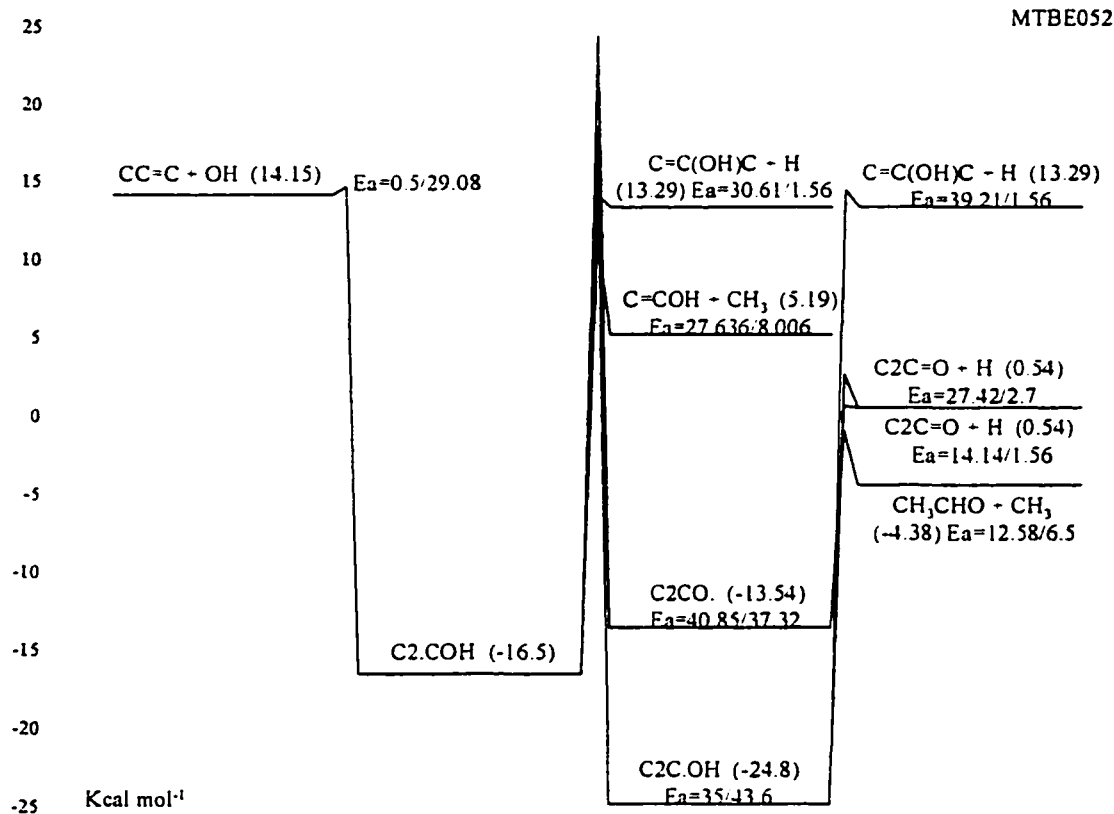
CC(OOH)COO.: 100.1 (10.107); 1059.7 (15.280); 2808.7 (8.113)

Lennard-Jones parameter

 $\sigma(\text{\AA}) = 5.86$, ϵ/k (K) = 632.06 k_1 1/2 (CC.C + O₂), 92 ATK/BAU. k_{-1} A_r via A_f and Microscopic Reversibility (MR), $E_{a,r} = E_{a,f} - \Delta U_{rxn}$, $\Delta U_{rxn} = -32.46$ kcal mol⁻¹. k_2 A_f is referenced from reaction C2COO. \rightarrow CC=C + HO₂, (from thermal reaction analysis (AFACT2f) based on the thermodynamic properties calculated from MOPAC PM3 (corrected with internal rotor, electronic spin and optical isomer). $E_{a,f} = E_{a,r} + \Delta U_{rxn}$ (20.83) $E_{a,r}$ is estimated as ring strain (6) + $E_{a,add}$ (7). k_3 A_f is referenced from reaction C2COO. \rightarrow CC=C + HO₂, (from thermal reaction analysis (AFACT2f) based on the thermodynamic properties calculated from MOPAC PM3 (corrected with internal rotor, electronic spin and optical isomer). $E_{a,f} = E_{a,r} + \Delta U_{rxn}$ (20.17) $E_{a,r}$ is estimated as ring strain (6) + $E_{a,add}$ (7). k_4 A_f estimated using TST, $A = (\text{deg.}) (ek_b/h) T^n \exp(\Delta S^\ddagger(T)/R)$, deg. = 2, $ek_b/h = 5.66 \times 10^{10}$, $n = 1.0$, $\Delta S^\ddagger(T)$ is estimated as loss of two rotors (-4.3×2 cal mol⁻¹ K⁻¹) and gain an optical isomer (OI). $E_{a,f} = RS$ (6) + E_{abst} (7.03) + ΔH_{rxn} (8.60) kcal mol⁻¹. k_{-4} A_r via A_f and Microscopic Reversibility (MR), $E_{a,r} = E_{a,f} - \Delta U_{rxn}$, $\Delta U_{rxn} = 8.60$ kcal mol⁻¹. k_5 A_f via A_r and Microscopic Reversibility (MR), $A_r = 2.75 \times 10^{12} = 1/2$ (OH + C=C). $E_{a,f}$ estimated the same 2.5 kcal mol⁻¹ as $E_{a,r}$ for CH₂OOH \rightarrow CH₂O + OH (1990 Page) k_6 A_f via A_r and Microscopic Reversibility (MR), $A_r = 2.5 \times 10^{11} = 1/2$ (C=C + HO₂), 72 KER/PAR. $E_{a,f} = E_{a,r} + \Delta U_{rxn}$, $\Delta U_{rxn} = 12.23$ kcal mol⁻¹. $E_{a,r} = 7.8$ kcal mol⁻¹. (estimated by Bozzelli).

- k₇ A_f estimated using TST, $A = (\text{deg.}) (ek_b/h) T^n \exp(\Delta S^\ddagger(T)/R)$, $\text{deg.} = 3$, $ek_b/h = 5.66 \times 10^{10}$, $n = 1.0$, $\Delta S^\ddagger(T)$ is estimated as loss of three rotors ($-4.3 \times 2 \text{ cal mol}^{-1} \text{ K}^{-1}$) and gain an optical isomer (OI). $E_{a,f} = RS(6) + E_{abst}(7.95) + \Delta H_{rxn}(13.65) \text{ kcal mol}^{-1}$.
- k₇ A_r via A_f and Microscopic Reversibility (MR), $E_{a,r} = E_{a,f} - \Delta U_{rxn}$, $\Delta U_{rxn} = 13.65 \text{ kcal mol}^{-1}$.
- k₈ A_f estimated using TST, $A = (\text{deg.}) (ek_b T/h) \exp(\Delta S^\ddagger(T)/R)$, $\text{deg.} = 1$, $ek_b T/h = 10^{13.55} ?$, $\Delta S^\ddagger(T)$ is estimated as loss of two rotors ($-4.3 \times 2 \text{ cal mol}^{-1} \text{ K}^{-1}$). $E_{a,f}$ is evaluated in this study.
- k₉ MR 3.5×10^{11} , Bozzelli). $E_{a,f} = E_{a,r} + \Delta U_{rxn}$, $\Delta U_{rxn} = 6.52 \text{ kcal mol}^{-1}$. $E_{a,r} = 7.8 \text{ kcal mol}^{-1}$. (estimated by Bozzelli).
- k₁₀ A_f via A_r and Microscopic Reversibility (MR), $A_r = 9.64 \times 10^{10}$, 91 TSA for $C_3H_6 + CH_3 \rightarrow C3.C$. $E_{a,f} = E_{a,r} + \Delta U_{rxn}$, $\Delta U_{rxn} = 27.22 \text{ kcal mol}^{-1}$. $E_{a,r} = 7.8 \text{ kcal mol}^{-1}$. (estimated by Bozzelli).
- k₁₁ A_f estimated using TST, $A = (\text{deg.}) (ek_b T/h) \exp(\Delta S^\ddagger(T)/R)$, $\text{deg.} = 1$, $ek_b T/h = 10^{13.55} ?$, $\Delta S^\ddagger(T)$ is estimated as loss of three rotors ($-4.3 \times 3 \text{ cal mol}^{-1} \text{ K}^{-1}$). $E_{a,f}$ is evaluated in this study.
- k₁₂ A_f estimated using TST, $A = (\text{deg.}) (ek_b/h) T^n \exp(\Delta S^\ddagger(T)/R)$, $\text{deg.} = 1$, $ek_b/h = 5.66 \times 10^{10}$, $n = 1.0$, $\Delta S^\ddagger(T)$ is estimated as loss of one rotor ($-4.3 \text{ cal mol}^{-1} \text{ K}^{-1}$) and gain an optical isomer (OI). $E_{a,f} = RS(26) + E_{abst}(7.98) + \Delta H_{rxn}(5.76) \text{ kcal mol}^{-1}$.
- k₁₂ A_r via A_f and Microscopic Reversibility (MR), $E_{a,r} = E_{a,f} - \Delta U_{rxn}$, $\Delta U_{rxn} = 5.76 \text{ kcal mol}^{-1}$.
- k₁₃ A_f via A_r and Microscopic Reversibility (MR), $A_r = 2.75 \times 10^{12} = 1/2 (\text{OH} + \text{C}=\text{C})$. $E_{a,f}$ estimated the same $2.0 \text{ kcal mol}^{-1}$ as $E_{a,r}$ for $\text{CH}_2\text{OOH} \rightarrow \text{CH}_2\text{O} + \text{OH}$ (1990 Page)
- k₁₄ A_f estimated using TST, $A = (\text{deg.}) (ek_b T/h) \exp(\Delta S^\ddagger(T)/R)$, $\text{deg.} = 1$, $ek_b T/h = 10^{13.55} ?$, $\Delta S^\ddagger(T)$ is estimated as loss of two rotors ($-4.3 \times 2 \text{ cal mol}^{-1} \text{ K}^{-1}$). $E_{a,f}$ is evaluated in this study.
- k₁₅ A_f via A_r and Microscopic Reversibility (MR), $A_r = 3.16 \times 10^{11}$ Bozzelli. $E_{a,f} = E_{a,r} + \Delta U_{rxn}$, $\Delta U_{rxn} = 14.45 \text{ kcal mol}^{-1}$. $E_{a,r} = 7.8 \text{ kcal mol}^{-1}$. (estimated by Bozzelli).
- k₁₆ A_f via A_r and Microscopic Reversibility (MR), $E_{a,f} = E_{a,r} + \Delta U_{rxn}(0)$.
- k₁₆ A_r estimated using TST, $A = (\text{deg.}) (ek_b/h) T^n \exp(\Delta S^\ddagger(T)/R)$, $\text{deg.} = 1$, $ek_b/h = 5.66 \times 10^{10}$, $n = 1.0$, $\Delta S^\ddagger(T)$ is estimated as loss of four rotor ($-4.3 \times 4 \text{ cal mol}^{-1} \text{ K}^{-1}$) and loss of one optical isomer but gain a new optical isomer (OI). $E_{a,f} = RS(6) + E_{abst}(9.90) + \Delta H_{rxn}(0.00) \text{ kcal mol}^{-1}$.
- k₁₇ A_f via A_r and Microscopic Reversibility (MR), $A_r = 1.00 \times 10^{12}$, 88 XI for $\text{C3CC.} + \text{O}_2$. $E_{a,f} = \Delta U_{rxn} = 31.90 \text{ kcal mol}^{-1}$.
- k₁₈ A_f is referenced from reaction $\text{C2CCOO.} \rightarrow \text{C2C}=\text{C} + \text{HO}_2$, (from thermal reaction analysis (AFACT2f) based on the thermodynamic properties calculated from MOPAC PM3 (corrected with internal rotor, electronic spin and optical isomer). $E_{a,f} = E_{a,r} + \Delta U_{rxn}(20.2)$ $E_{a,r}$ is estimated as ring strain (6) + $E_{a,add}(7)$.

IID. 74 $\text{CC}=\text{C} + \text{OH} \rightarrow [\text{C2.COH}]^* \rightarrow \text{Products}$

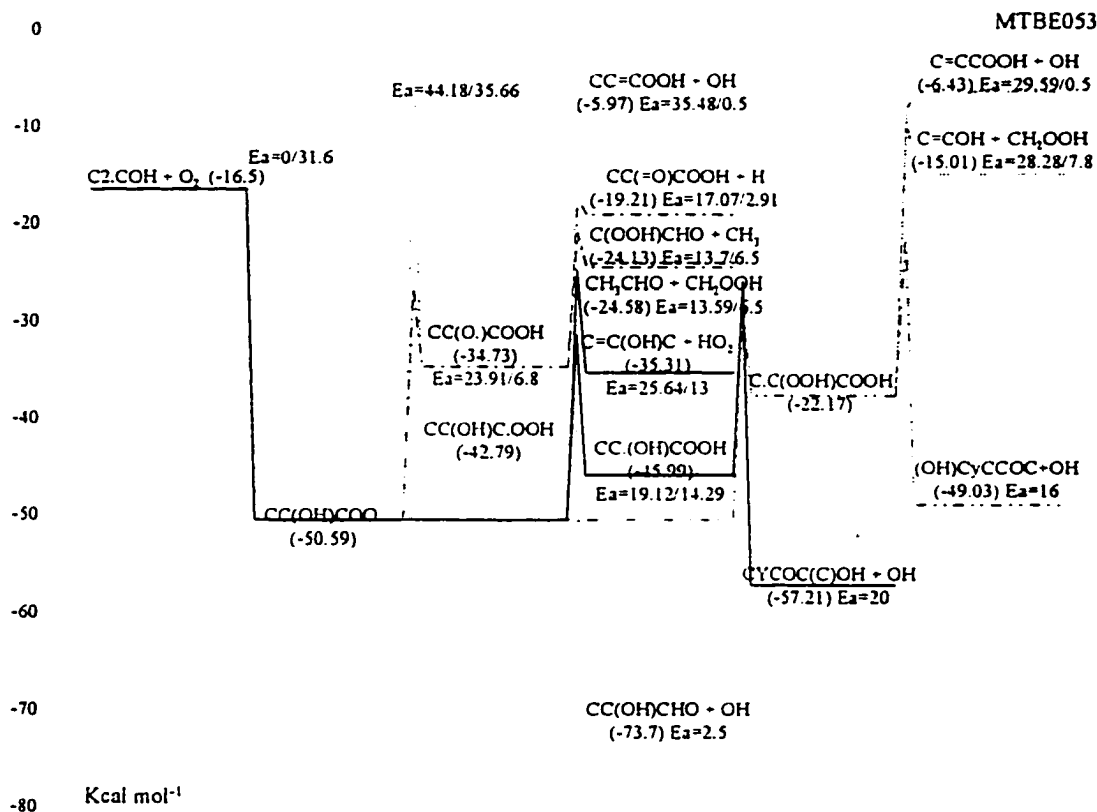


Reaction		$A T^n e^{-\alpha/T}$ (s ⁻¹ or cm ³ mol ⁻¹ s ⁻¹)	E_a (kcal mol ⁻¹)
k ₁	$\text{CC}=\text{C} + \text{OH} \rightarrow \text{C2.COH}$	$1.81 \times 10^{13} T^0 e^{-0T}$	0.50
k ₋₁	$\text{C2.COH} \rightarrow \text{CC}=\text{C} + \text{OH}$	$1.04 \times 10^{14} T^0 e^{-0T}$	29.08
k ₂	$\text{C2.COH} \rightarrow \text{C}=\text{COH} + \text{CH}_3$	$7.11 \times 10^{11} T^0 e^{-0T}$	27.64
k ₃	$\text{C2.COH} \rightarrow \text{C}=\text{C}(\text{OH})\text{C} + \text{H}$	$1.86 \times 10^{12} T^0 e^{-0T}$	30.61
k ₄	$\text{C2.COH} \rightarrow \text{C2CO.}$	$1.03 \times 10^9 T^{1.01} e^{-0.0005T}$	40.85
k ₋₄	$\text{C2CO.} \rightarrow \text{C2.COH}$	$3.90 \times 10^{10} T^{1.0} e^{-0T}$	37.32
k ₅	$\text{C2CO.} \rightarrow \text{CH}_3\text{CHO} + \text{CH}_3$	$7.44 \times 10^{13} T^0 e^{-0T}$	12.58
k ₆	$\text{C2CO.} \rightarrow \text{C2C}=\text{O} + \text{H}$	$9.02 \times 10^{12} T^0 e^{-0T}$	14.14
k ₇	$\text{C2.COH} \rightarrow \text{C2C.OH}$	$6.50 \times 10^9 T^{1.0} e^{-0T}$	35.00
k ₋₇	$\text{C2C.OH} \rightarrow \text{C2.COH}$	$9.09 \times 10^8 T^{1.42} e^{0.00017T}$	43.60
k ₈	$\text{C2C.OH} \rightarrow \text{C}=\text{C}(\text{OH})\text{C} + \text{H}$	$6.77 \times 10^{12} T^0 e^{-0T}$	39.21
k ₉	$\text{C2C.OH} \rightarrow \text{C2C}=\text{O} + \text{H}$	$1.77 \times 10^{12} T^0 e^{-0T}$	27.42

frequency/degeneracy (CPFIT)
 C2.COH: 250.9 (5.095); 1053.9 (11.950); 2837.8 (8.455)

C2CO.: 250.2 (4.688); 1065.6 (13.397); 2814.4 (7.915)
 C2C.OH: 250.2 (5.519); 1129.1 (11.377); 2824.2 (8.604)
 Lennard-Jones parameter
 $\sigma(\text{\AA}) = 4.80$, $\epsilon/k(\text{K}) = 481.73$

- k_1 A_f is referenced from 89 ATK/BAU, E_a is estimated by Bozzelli.
- k_{-1} A_r via A_f and Microscopic Reversibility (MR), $E_{a,r} = E_{a,f} - \Delta U_{\text{rxn}}$, $\Delta U_{\text{rxn}} = -28.18$ kcal mol⁻¹.
- k_2 A_f via A_r and Microscopic Reversibility (MR), $A_r = 9.64 \times 10^{10}$, 91 TSA for $\text{C}_3\text{H}_6 + \text{CH}_3 \rightarrow \text{C3.C}$. $E_{a,f} = E_{a,r} + \Delta U_{\text{rxn}}$, $\Delta U_{\text{rxn}} = 19.63$ kcal mol⁻¹. $E_{a,r} = 8.006$ kcal mol⁻¹. (referenced as the same as the A_r).
- k_3 A_f via A_r and Microscopic Reversibility (MR), $A_r = 6.50 \times 10^{12} = 1/2 (\text{H} + \text{CC}=\text{C} \rightarrow \text{CC.C}$, 91 TSA/HAM). $E_{a,f}$ is estimated by Bozzelli.
- k_4 A_f via A_r and Microscopic Reversibility (MR), $E_{a,f} = E_{a,r} + \Delta U_{\text{rxn}}$ (3.53) kcal mol⁻¹.
- k_{-4} A_r estimated using TST, $A = (\text{deg.}) (ek_b/h) T^n \exp(\Delta S^\ddagger(T)/R)$, deg. = 6, $ek_b/h = 5.66 \times 10^{10}$, $n = 1.0$, $\Delta S^\ddagger(T)$ is estimated as loss of one rotor (-4.3 cal mol⁻¹ K⁻¹) and gain of an optical isomer (OI), $E_{a,r} = \text{RS (26)} + E_{\text{abst}}$ (11.32) kcal mol⁻¹.
- k_5 A_f via A_r and Microscopic Reversibility (MR), $A_r = 3.16 \times 10^{11}$ Bozzelli. $E_{a,f} = E_{a,r} + \Delta U_{\text{rxn}}$, $\Delta U_{\text{rxn}} = 6.08$ kcal mol⁻¹. $E_{a,r} = 6.5$ kcal mol⁻¹. (estimated by Bozzelli).
- k_6 A_f via A_r and Microscopic Reversibility (MR), $A_r = 6.50 \times 10^{12} = 1/2 (\text{H} + \text{CC}=\text{C} \rightarrow \text{CC.C}$, 91 TSA/HAM). $E_{a,f}$ is taken from the same reference as A_r .
- k_7 A_f estimated using TST, $A = (\text{deg.}) (ek_b/h) T^n \exp(\Delta S^\ddagger(T)/R)$, deg. = 1, $ek_b/h = 5.66 \times 10^{10}$, $n = 1.0$, $\Delta S^\ddagger(T)$ is estimated as loss of one rotor (-4.3 cal mol⁻¹ K⁻¹), $E_{a,r} = \text{RS (28)} + E_{\text{abst}}$ (7.0) kcal mol⁻¹.
- k_{-7} A_r via A_f and Microscopic Reversibility (MR), $E_{a,r} = E_{a,f} - \Delta U_{\text{rxn}}$, $\Delta U_{\text{rxn}} = -8.6$ kcal mol⁻¹.
- k_8 A_f via A_r and Microscopic Reversibility (MR), $A_r = 1.30 \times 10^{13}$, 91 TSA/HAM for $\text{H} + \text{CC}=\text{C} \rightarrow \text{CC.C}$, $E_{a,f}$ is estimated by Bozzelli.
- k_9 A_f via A_r and Microscopic Reversibility (MR), $A_r = 1.30 \times 10^{13}$, 91 TSA/HAM for $\text{H} + \text{CC}=\text{C} \rightarrow \text{CC.C}$, $E_{a,f}$ is taken from the same reference as A_r .

IID. 75 C2.CO₂H + O₂ → Products

Reaction		A T ⁿ e ^{-αT} (s ⁻¹ or cm ³ mol ⁻¹ s ⁻¹)	E _a (kcal mol ⁻¹)
k ₁	C ₂ .CO ₂ H + O ₂ → CC(OH)COO.	1.00×10 ¹² T ⁰ e ^{-0T}	0.00
k ₋₁	CC(OH)COO. → C ₂ .CO ₂ H + O ₂	1.08×10 ¹⁴ T ⁰ e ^{-0T}	31.60
k ₂	CC(OH)COO. → C=C(OH)C + HO ₂	7.48×10 ⁹ T ^{0.74} e ^{-0T}	25.64
k ₃	CC(OH)COO. → CC(OH)C.OOH	2.60×10 ¹⁰ T ^{1.0} e ^{-0T}	44.18
k ₋₃	CC(OH)C.OOH → CC(OH)COO.	4.38×10 ¹² T ^{-0.26} e ^{-0.00072T}	35.66
k ₄	CC(OH)C.OOH → CC(OH)CHO + OH	1.24×10 ¹³ T ⁰ e ^{-0T}	2.50
k ₅	CC(OH)C.OOH → CC=COOH + OH	1.76×10 ¹³ T ⁰ e ^{-0T}	35.48
k ₆	CC(OH)COO. → C.C(OH)COOH	5.15×10 ⁸ T ^{1.0} e ^{-0T}	21.67
k ₋₆	C.C(OH)COOH → CC(OH)COO.	1.41×10 ¹⁰ T ^{-0.03} e ^{-0.00037T}	7.92
k ₇	C.C(OOH)COOH → C=CCOOH + OH	6.58×10 ¹³ T ⁰ e ^{-0T}	29.59
k ₈	C.C(OOH)COOH → CyCCOC(OH) + OH	5.38×10 ¹⁰ T ⁰ e ^{-0T}	16.00
k ₉	C.C(OOH)COOH → C=COH + CH ₂ OOH	1.98×10 ¹² T ⁰ e ^{-0T}	28.28
k ₁₀	CC(OH)COO. → CC.(OH)COOH	1.50×10 ⁹ T ^{1.0} e ^{-0T}	19.12
k ₋₁₀	CC.(OH)COOH → CC(OH)COO.	3.55×10 ⁹ T ^{0.45} e ^{-0.0004T}	14.29
k ₁₁	CC.(OH)COOH → CyCOC(C)OH	4.68×10 ¹¹ T ⁰ e ^{-0T}	20.00

	Reaction	$A T^n e^{-\alpha T}$ (s^{-1} or $cm^3 mol^{-1} s^{-1}$)	E_a ($kcal mol^{-1}$)
k_{12}	$CC(OH)COO. \rightarrow CC(O.)COOH$	$1.72 \times 10^8 T^{1.0} e^{-0T}$	23.91
k_{12}	$CC(O.)COOH \rightarrow CC(OH)COO.$	$1.67 \times 10^{11} T^{-0.05} e^{-0.00002T}$	6.80
k_{13}	$CC(O.)COOH \rightarrow CH_3CHO + CH_2OOH$	$2.24 \times 10^{14} T^0 e^{-0T}$	13.59
k_{14}	$CC(O.)COOH \rightarrow C(OOH)CHO + CH_3$	$5.48 \times 10^{13} T^0 e^{-0T}$	13.70
k_{15}	$CC(O.)COOH \rightarrow CC(=O)COOH + H$	$1.04 \times 10^{13} T^0 e^{-0T}$	17.07

frequency/degeneracy (CPFIT)

$CC(OH)COO.$: 250.8 (9.217); 1122.7 (13.406); 2922.8 (8.377)
 $CC(OH)C.OOH$: 100.2 (8.968); 1063.5 (14.069); 2832.3 (7.463)
 $C.C(OH)COOH$: 250.2 (10.056); 1150.8 (13.940); 2841.4 (6.504)
 $CC.(OH)COOH$: 100.9 (8.688); 1083.8 (13.748); 2790.4 (8.064)
 $CC(O.)COOH$: 251.0 (9.668); 1140.1 (15.036); 2871.3 (6.296)

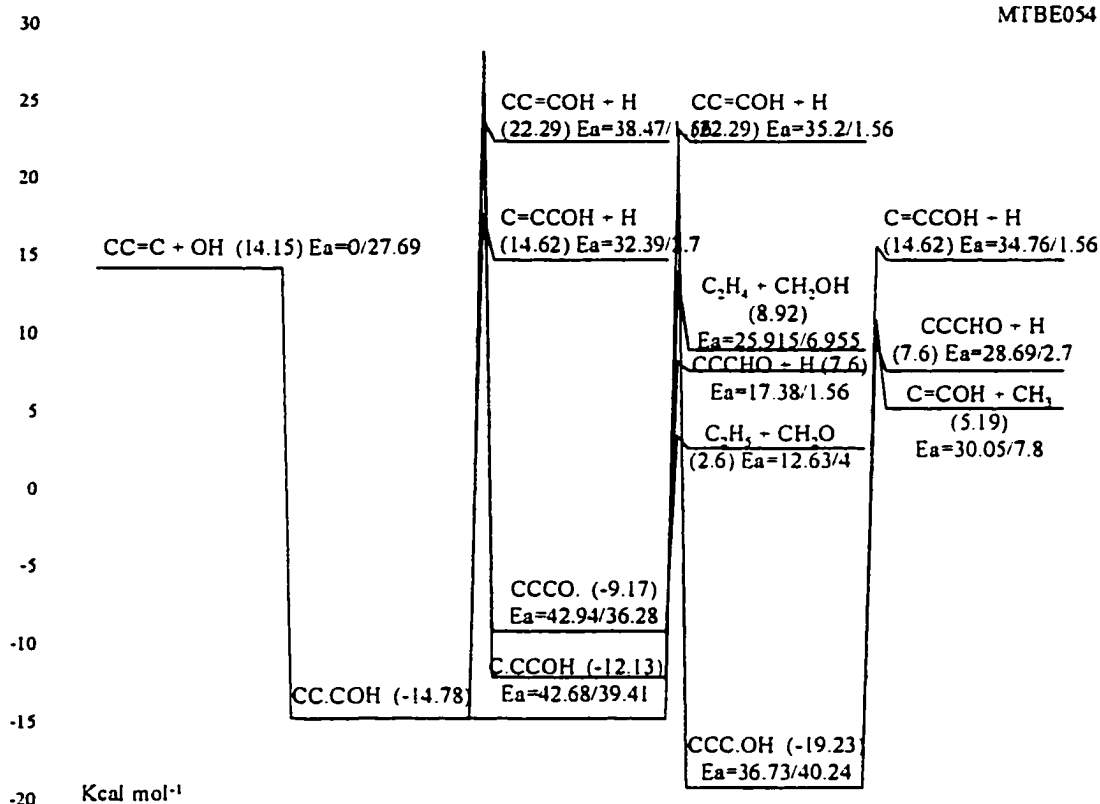
Lennard-Jones parameter

$\sigma(\text{\AA}) = 5.55$, ϵ/k (K) = 584.86

- k_1 taken from 88 XI for $C3CC. + O_2 \rightarrow C3CCOO.$.
- k_{-1} A_r via A_f and Microscopic Reversibility (MR), $E_{a,r} = E_{a,f} - \Delta U_{rxn}$, $\Delta U_{rxn} = -31.60$ $kcal mol^{-1}$.
- k_2 A_f is referenced from reaction $C2CCOO. \rightarrow C2C=C + HO_2$, (from thermal reaction analysis (AFACT2f) based on the thermodynamic properties calculated from MOPAC PM3 (corrected with internal rotor, electronic spin and optical isomer). $E_{a,f} = E_{a,r} + \Delta U_{rxn}$ (12.64) $E_{a,r}$ is estimated as ring strain (6) + $E_{a,add}$ (7).
- k_3 A_f estimated using TST, $A = (\text{deg.}) (ek_b/h) T^n \exp(\Delta S^\ddagger(T)/R)$, $\text{deg.} = 2$, $ek_b/h = 5.66 \times 10^{10}$, $n = 1.0$, $\Delta S^\ddagger(T)$ is estimated as loss of one rotor (-4.3 $cal mol^{-1} K^{-1}$) and gain an optical isomer (OI), $E_{a,r} = RS$ (26) + E_{abst} (9.66) + ΔH_{rxn} (8.52) $kcal mol^{-1}$.
- k_{-3} A_r via A_f and Microscopic Reversibility (MR), $E_{a,r} = E_{a,f} - \Delta U_{rxn}$, $\Delta U_{rxn} = -8.52$ $kcal mol^{-1}$.
- k_4 A_f via A_r and Microscopic Reversibility (MR), $A_r = 2.75 \times 10^{12} = 1/2$ (OH + C=C). $E_{a,f}$ estimated the same 2.5 $kcal mol^{-1}$ based on $E_{a,f}$ for $CH_2OOH \rightarrow CH_2O + OH$ (1990 Page)
- k_5 A_f via A_r and Microscopic Reversibility (MR), $A_r = 9.05 \times 10^{12} = 1/2$ (OH + CC=C \rightarrow C2.CO), 89 ATK/BAU. $E_{a,f} = E_{a,r} + \Delta U_{rxn}$ (34.98) $kcal mol^{-1}$. $E_{a,r} = 0.5$ $kcal mol^{-1}$. (estimated by Bozzelli).
- k_6 A_f estimated using TST, $A = (\text{deg.}) (ek_b/h) T^n \exp(\Delta S^\ddagger(T)/R)$, $\text{deg.} = 3$, $ek_b/h = 5.66 \times 10^{10}$, $n = 1.0$, $\Delta S^\ddagger(T)$ is estimated as loss of three rotors (-4.3×3 $cal mol^{-1} K^{-1}$) and gain an optical isomer (OI), $E_{a,r} = RS$ (0) + E_{abst} (7.92) + ΔH_{rxn} (13.75) $kcal mol^{-1}$.
- k_{-6} A_r via A_f and Microscopic Reversibility (MR), $E_{a,r} = E_{a,f} - \Delta U_{rxn}$, $\Delta U_{rxn} = 13.75$ $kcal mol^{-1}$.
- k_7 A_f via A_r and Microscopic Reversibility (MR), $A_r = 1.81 \times 10^{13}$, 89 ATK/BAU for

- OH + C=C. $E_{a,f} = E_{a,r} + \Delta U_{rxn}$ (29.09) kcal mol⁻¹. $E_{a,r} = 0.5$ kcal mol⁻¹. (estimated by Bozzelli).
- k₈ A_f estimated using TST, $A = (\text{deg.}) (ek_b T/h) \exp(\Delta S^\ddagger(T)/R)$, deg. = 1, $ek_b T/h = 10^{13.55}$?, $\Delta S^\ddagger(T)$ is estimated as loss of three rotors (-4.3×3 cal mol⁻¹ K⁻¹). $E_{a,f}$ is evaluated in this study.
- k₉ A_f via A_r and Microscopic Reversibility (MR), $A_r = 9.64 \times 10^{10}$, 91 TSA for C₃H₆ + CH₃ → C3.C. $E_{a,f} = E_{a,r} + \Delta U_{rxn}$ (21.26) kcal mol⁻¹. $E_{a,r} = 7.8$ kcal mol⁻¹. (estimated by Bozzelli).
- k₁₀ A_f estimated using TST, $A = (\text{deg.}) (ek_b/h) T^n \exp(\Delta S^\ddagger(T)/R)$, deg. = 1, $ek_b/h = 5.66 \times 10^{10}$, $n = 1.0$, $\Delta S^\ddagger(T)$ is estimated as loss of two rotors (-4.3×2 cal mol⁻¹ K⁻¹) and gain an optical isomer (OI), $E_{a,r} = RS(6) + E_{abst}(8.29) + \Delta H_{rxn}(4.83)$ kcal mol⁻¹.
- k₁₀ A_r via A_f and Microscopic Reversibility (MR), $E_{a,r} = E_{a,f} - \Delta U_{rxn}$, $\Delta U_{rxn} = 4.83$ kcal mol⁻¹.
- k₁₁ A_f estimated using TST, $A = (\text{deg.}) (ek_b T/h) \exp(\Delta S^\ddagger(T)/R)$, deg. = 1, $ek_b T/h = 10^{13.55}$?, $\Delta S^\ddagger(T)$ is estimated as loss of two rotors (-4.3×2 cal mol⁻¹ K⁻¹). $E_{a,f}$ is evaluated in this study.
- k₁₂ A_f estimated using TST, $A = (\text{deg.}) (ek_b/h) T^n \exp(\Delta S^\ddagger(T)/R)$, deg. = 1, $ek_b/h = 5.66 \times 10^{10}$, $n = 1.0$, $\Delta S^\ddagger(T)$ is estimated as loss of two rotors (-4.3×2 cal mol⁻¹ K⁻¹) and gain an optical isomer (OI), $E_{a,r} = RS(0) + E_{abst}(6.80) + \Delta H_{rxn}(17.11)$ kcal mol⁻¹.
- k₁₂ A_r via A_f and Microscopic Reversibility (MR), $E_{a,r} = E_{a,f} - \Delta U_{rxn}$, $\Delta U_{rxn} = 17.11$ kcal mol⁻¹.
- k₁₃ A_f via A_r and Microscopic Reversibility (MR), $A_r = 3.16 \times 10^{11}$, Bozzelli. $E_{a,f} = E_{a,r} + \Delta U_{rxn}$, $\Delta U_{rxn} = 7.09$ kcal mol⁻¹. $E_{a,r} = 6.5$ kcal mol⁻¹. (estimated by Bozzelli).
- k₁₄ A_f via A_r and Microscopic Reversibility (MR), $A_r = 3.16 \times 10^{11}$, Bozzelli. $E_{a,f} = E_{a,r} + \Delta U_{rxn}$, $\Delta U_{rxn} = 7.20$ kcal mol⁻¹. $E_{a,r} = 6.5$ kcal mol⁻¹. (estimated by Bozzelli).
- k₁₅ A_f via A_r and Microscopic Reversibility (MR), $A_r = 3.62 \times 10^{12} = 1/2$ (H + CC=C → CCC., 91 TSA/HAM). $E_{a,f}$ is estimated by Bozzelli.

III. 76 $\text{CC}=\text{C} + \text{OH} \rightarrow [\text{CC}.\text{COH}]^* \rightarrow \text{Products}$



Reaction		$A T^n e^{-\alpha T}$ (s^{-1} or $cm^3 mol^{-1} s^{-1}$)	E_a ($kcal mol^{-1}$)
k_1	$CC=C + OH \rightarrow CC.COH$	$1.81 \times 10^{13} T^0 e^{-0T}$	0.00
k_{-1}	$CC.COH \rightarrow CC=C + OH$	$7.59 \times 10^{13} T^0 e^{-0T}$	27.69
k_2	$CC.COH \rightarrow C=CCOH + H$	$5.83 \times 10^{12} T^0 e^{-0T}$	38.47
k_3	$CC.COH \rightarrow CC=COH + H$	$1.56 \times 10^{12} T^0 e^{-0T}$	32.39
k_4	$CC.COH \rightarrow CCCO.$	$3.16 \times 10^{10} T^{1.86} e^{-0.00002T}$	42.94
k_{-4}	$CCCO. \rightarrow CC.COH$	$1.30 \times 10^{10} T^{1.0} e^{-0T}$	36.28
k_5	$CCCO. \rightarrow CH_2O + C_2H_5$	$2.30 \times 10^{13} T^0 e^{-0T}$	12.63
k_6	$CCCO. \rightarrow CCCHO + H$	$2.04 \times 10^{13} T^0 e^{-0T}$	17.38
k_7	$CC.COH \rightarrow CCC.OH$	$1.30 \times 10^{10} T^{1.0} e^{-0T}$	36.73
k_{-7}	$CCC.OH \rightarrow CC.COH$	$4.60 \times 10^{14} T^{-0.49} e^{0.00075T}$	40.24
k_8	$CCC.OH \rightarrow C=COH + CH_3$	$3.90 \times 10^{12} T^0 e^{-0T}$	30.05
k_9	$CCC.OH \rightarrow CCCHO + H$	$1.26 \times 10^{13} T^0 e^{-0T}$	28.69
k_{10}	$CCC.OH \rightarrow CC=COH + H$	$4.00 \times 10^{12} T^0 e^{-0T}$	34.76
k_{11}	$CC.COH \rightarrow C.CCOH$	$1.95 \times 10^{10} T^{1.0} e^{-0T}$	42.68
k_{-11}	$C.CCOH \rightarrow CC.COH$	$2.31 \times 10^{10} T^{0.11} e^{-0.0004T}$	39.41

	Reaction	$A T^n e^{-\alpha T}$	E_a
		(s^{-1} or $cm^3 mol^{-1} s^{-1}$)	($kcal mol^{-1}$)
k_{12}	$C.CCOH \rightarrow C_2H_4 + CH_2OH$	$9.47 \times 10^{11} T^0 e^{-0T}$	25.92
k_{13}	$C.CCOH \rightarrow C=CCOH + H$	$2.18 \times 10^{12} T^0 e^{-0T}$	35.20

frequency/degeneracy (CPFIT)

CC.COH: 410.4 (7.198); 1475.4 (12.281); 3204.6 (6.022)

CCCO.: 494.7 (8.503); 1392.3 (11.260); 3093.2 (6.238)

CCC.OH: 469.0 (9.204); 1376.7 (9.627); 3068.0 (6.668)

C.CCOH: 475.9 (8.453); 1397.0 (10.702); 3138.2 (6.345)

Lennard-Jones parameter

$\sigma(\text{\AA}) = 4.80$, $\epsilon/k (K) = 481.73$

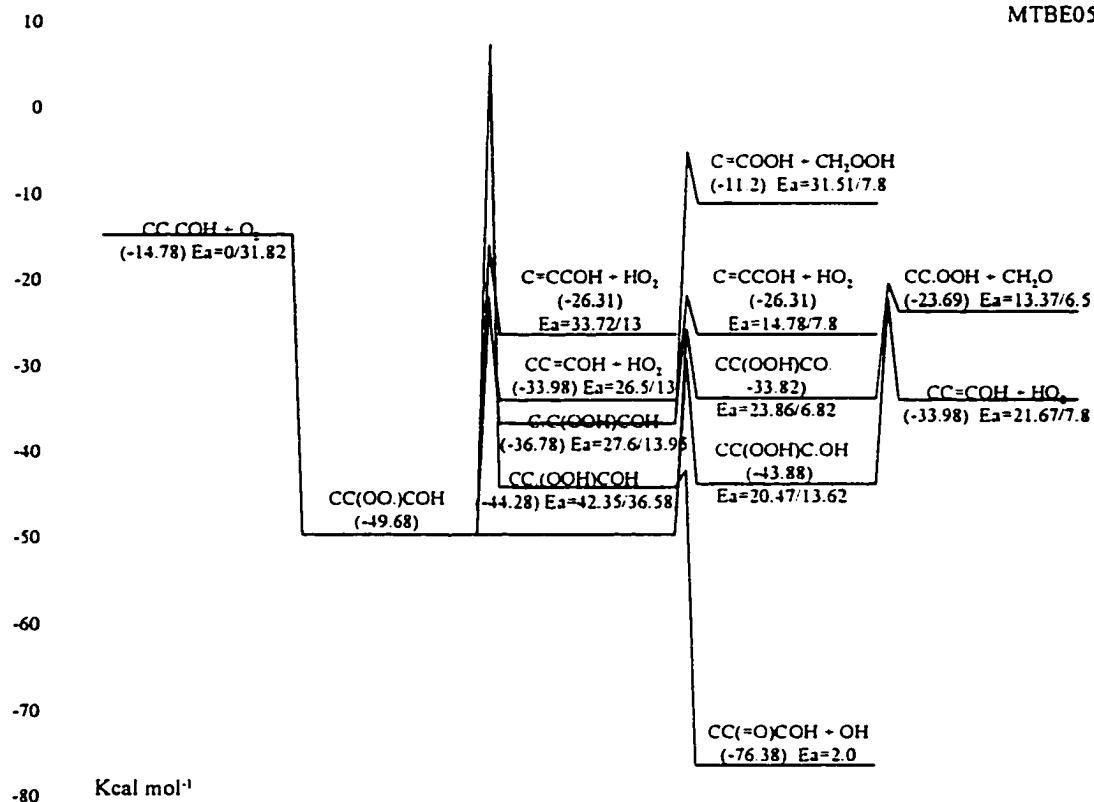
- k_1 A_f is referenced from 89 ATK/BAU, E_a is estimated by Bozzelli.
- k_{11} A_f via A_r and Microscopic Reversibility (MR), $E_{a,r} = E_{a,f} - \Delta U_{rxn}$, $\Delta U_{rxn} = -27.69$ $kcal mol^{-1}$.
- k_2 A_f via A_r and Microscopic Reversibility (MR), $A_r = 1.30 \times 10^{13}$, 91 TSA/HAM for $H + CC=C \rightarrow CC.C$, $E_{a,f}$ is taken from the same reference as A_r .
- k_3 A_f via A_r and Microscopic Reversibility (MR), $A_r = 3.62 \times 10^{12} = 1/2 (H + CC=C \rightarrow CCC.)$, 91 TSA/HAM. $E_{a,f}$ is estimated by Bozzelli.
- k_4 A_f via A_r and Microscopic Reversibility (MR), $E_{a,f} = E_{a,r} + \Delta U_{rxn}$ (6.66) $kcal mol^{-1}$.
- k_{44} A_r estimated using TST, $A = (\text{deg.}) (ek_b/h) T^n \exp(\Delta S^\ddagger(T)/R)$, $\text{deg.} = 6$, $ek_b/h = 5.66 \times 10^{10}$, $n = 1.0$, $\Delta S^\ddagger(T)$ is estimated as loss of one rotor (-4.3 $cal mol^{-1} K^{-1}$) and gain of an optical isomer (OI), $E_{a,r} = RS (26) + E_{abst} (10.28)$ $kcal mol^{-1}$.
- k_5 A_f via A_r and Microscopic Reversibility (MR), $A_r = 1.58 \times 10^{11}$, 72 KER/PAR for $CC. + C=C \rightarrow CCCC.$ $E_{a,f} = E_{a,r} + \Delta U_{rxn}$, $\Delta U_{rxn} = 8.63$ $kcal mol^{-1}$. $E_{a,r} = 4.968$ $kcal mol^{-1}$. (estimated by Bozzelli).
- k_6 A_f via A_r and Microscopic Reversibility (MR), $A_r = 6.50 \times 10^{12} = 1/2 (H + CC=C \rightarrow CC.C)$, 91 TSA/HAM. $E_{a,f}$ is taken from the same reference as A_r .
- k_7 A_f estimated using TST, $A = (\text{deg.}) (ek_b/h) T^n \exp(\Delta S^\ddagger(T)/R)$, $\text{deg.} = 2$, $ek_b/h = 5.66 \times 10^{10}$, $n = 1.0$, $\Delta S^\ddagger(T)$ is estimated as loss of one rotor (-4.3 $cal mol^{-1} K^{-1}$), $E_{a,r} = RS (28) + E_{abst} (8.73)$ $kcal mol^{-1}$.
- k_{77} A_r via A_f and Microscopic Reversibility (MR), $E_{a,r} = E_{a,f} - \Delta U_{rxn}$, $\Delta U_{rxn} = -3.51$ $kcal mol^{-1}$.
- k_8 A_f via A_r and Microscopic Reversibility (MR), $A_r = 1.69 \times 10^{11}$, 91 TSA for $CH_3 + CC=C \rightarrow CC.CC$. $E_{a,f} = E_{a,r} + \Delta U_{rxn}$, $\Delta U_{rxn} = 22.25$ $kcal mol^{-1}$. $E_{a,r} = 7.8$ $kcal mol^{-1}$. (estimated by Bozzelli).
- k_9 A_f via A_r and Microscopic Reversibility (MR), $A_r = 1.30 \times 10^{13}$, 91 TSA/HAM for $H + CC=C \rightarrow CC.C$, $E_{a,f}$ is estimated by Bozzelli.
- k_{10} A_f via A_r and Microscopic Reversibility (MR), $A_r = 6.50 \times 10^{12} = 1/2 (H + CC=C \rightarrow CC.C)$, 91 TSA/HAM. $E_{a,f}$ is taken from the same reference as A_r .
- k_{11} A_f estimated using TST, $A = (\text{deg.}) (ek_b/h) T^n \exp(\Delta S^\ddagger(T)/R)$, $\text{deg.} = 3$, $ek_b/h =$

5.66×10^{10} , $n = 1.0$, $\Delta S^\ddagger(T)$ is estimated as loss of one rotor ($-4.3 \text{ cal mol}^{-1} \text{ K}^{-1}$),
 $E_{a,r} = RS(28) + E_{abst}(12.41) + \Delta H_{rxn}(3.27) \text{ kcal mol}^{-1}$.

- k_{11} A_r via A_f and Microscopic Reversibility (MR), $E_{a,r} = E_{a,f} - \Delta U_{rxn}$, $\Delta U_{rxn} = 3.27 \text{ kcal mol}^{-1}$.
- k_{12} A_f via A_r and Microscopic Reversibility (MR), $A_r = 4.82 \times 10^{10}$, 87 TSA/HAM, $E_{a,f} = E_{a,r} + \Delta U_{rxn}(18.96) \text{ kcal mol}^{-1}$, $E_{a,r} = 6.955 \text{ kcal mol}^{-1}$ from the same reference as A_r .
- k_{13} A_f via A_r and Microscopic Reversibility (MR), $A_r = 6.50 \times 10^{12} = 1/2 (\text{H} + \text{CC}=\text{C} \rightarrow \text{CC.C})$, 91 TSA/HAM. $E_{a,f}$ is taken from the same reference as A_r .

IID. 77 CC.CO₂H + O₂ → Products

MTBE055



Reaction		$A T^n e^{-\alpha T}$ (s^{-1} or $cm^3 mol^{-1} s^{-1}$)	E_a ($kcal mol^{-1}$)
k_1	$CC.CO_2H + O_2 \rightarrow CC(OO.)C OH$	$3.31 \times 10^{12} T^0 e^{-0T}$	0.00
k_{-1}	$CC(OO.)C OH \rightarrow CC.CO_2H + O_2$	$8.71 \times 10^{14} T^0 e^{-0T}$	31.82
k_2	$CC(OO.)C OH \rightarrow C=CCOH + HO_2$	$2.49 \times 10^9 T^{1.18} e^{-0T}$	33.72
k_3	$CC(OO.)C OH \rightarrow CC=COH + HO_2$	$1.66 \times 10^9 T^{1.18} e^{-0T}$	26.50
k_4	$CC(OO.)COH \rightarrow CC.(OOH)COH$	$1.30 \times 10^{10} T^{1.0} e^{-0T}$	42.35
k_{-4}	$CC.(OOH)COH \rightarrow CC(OH)COO.$	$1.39 \times 10^{11} T^{0.03} e^{-0.00072T}$	36.58
k_5	$CC.(OOH)COH \rightarrow CC=COOH + OH$	$4.50 \times 10^{12} T^0 e^{-0T}$	2.00
k_6	$CC(OO.)COH \rightarrow C.C(OOH)COH$	$4.49 \times 10^9 T^{1.0} e^{-0T}$	27.60
k_{-6}	$C.C(OOH)COH \rightarrow CC(OO.)C OH$	$2.20 \times 10^{11} T^{-0.12} e^{-0.00055T}$	13.95
k_7	$C.C(OOH)COH \rightarrow C=CCOH + HO_2$	$3.33 \times 10^{12} T^0 e^{-0T}$	14.87
k_8	$C.C(OOH)COH \rightarrow C=COOH + CH_2OH$	$2.41 \times 10^{12} T^0 e^{-0T}$	31.51
k_9	$CC(OO.)COH \rightarrow CC(OOH)C.OH$	$2.99 \times 10^9 T^{1.0} e^{-0T}$	20.47
k_{-9}	$CC(OOH)C.OH \rightarrow CC(OO.)COH$	$2.52 \times 10^{13} T^{-0.68} e^{-0.00087T}$	13.62
k_{10}	$CC(OOH)C.OH \rightarrow CC=COH + HO_2$	$1.50 \times 10^{13} T^0 e^{-0T}$	21.67
k_{11}	$CC(OO.)COH \rightarrow CC(OOH)CO.$	$1.72 \times 10^8 T^{1.0} e^{-0T}$	23.86

	Reaction	$A T^n e^{-a/T}$ (s^{-1} or $cm^3 mol^{-1} s^{-1}$)	E_a ($kcal mol^{-1}$)
k_{11}	$CC(OOH)CO. \rightarrow CC(OO.)COH$	$1.72 \times 10^{11} T^{-0.06} e^{-0.00009T}$	6.82
k_{12}	$CC(OOH)CO. \rightarrow CC.OOH + CH_2O$	$3.76 \times 10^{13} T^0 e^{-0T}$	13.37

frequency/degeneracy (CPFIT)

CC(OO.)COH: 263.2 (9.166); 1129.6 (13.243); 2947.7 (8.591)
 CC.(OOH)COH: 250.0 (11.027); 1240.8 (12.207); 2978.8 (7.266)
 C.C(OOH)COH: 292.6 (10.537); 1176.0 (13.350); 3006.3 (6.612)
 CC(OOH)C.OH: 292.8 (11.036); 1145.0 (12.686); 2968.5 (6.777)
 CC(OOH)CO.: 274.5 (9.794); 1144.0 (14.514); 2929.5 (6.692)

Lennard-Jones parameter

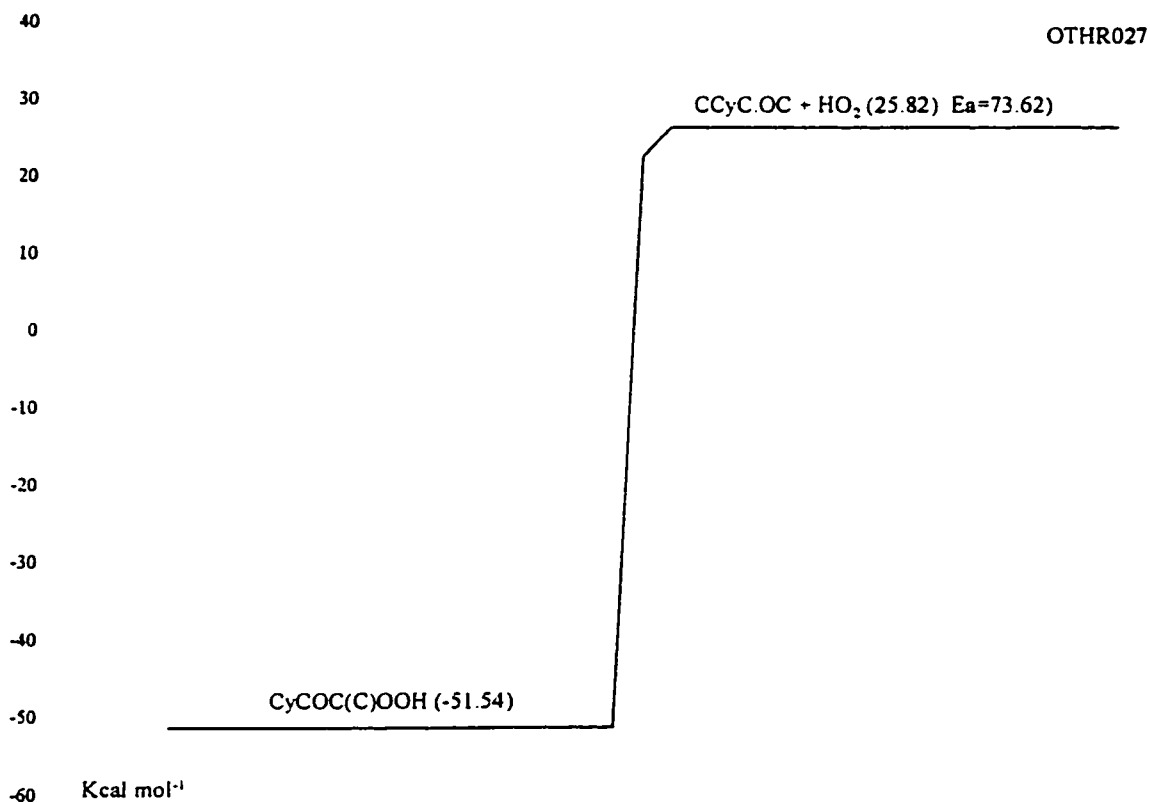
$\sigma(\text{\AA}) = 5.55$, ϵ/k (K) = 584.86

- k_1 $A_f = 1/2$ (CC.C + O₂), 92 ATK/BAU, $E_{a,f}$ is taken from the same reference.
- k_{-1} A_r via A_f and Microscopic Reversibility (MR), $E_{a,r} = \Delta U_{rxn} = 31.82$ kcal mol⁻¹.
- k_2 A_f is referenced from reaction C2COO. \rightarrow CC=C + HO₂, (from thermal reaction analysis (AFACT2f) based on the thermodynamic properties calculated from MOPAC PM3 (corrected with internal rotor, electronic spin and optical isomer). $E_{a,f} = E_{a,r} + \Delta U_{rxn}$ (20.72) $E_{a,r}$ is estimated as ring strain (6) + $E_{a,add}$ (7).
- k_3 A_f is referenced from reaction C2COO. \rightarrow CC=C + HO₂, (from thermal reaction analysis (AFACT2f) based on the thermodynamic properties calculated from MOPAC PM3 (corrected with internal rotor, electronic spin and optical isomer). $E_{a,f} = E_{a,r} + \Delta U_{rxn}$ (13.50) $E_{a,r}$ is estimated as ring strain (6) + $E_{a,add}$ (7).
- k_4 A_f estimated using TST, $A = (\text{deg.}) (ek_b/h) T^n \exp(\Delta S^\ddagger(T)/R)$, deg. = 1, $ek_b/h = 5.66 \times 10^{10}$, $n = 1.0$, $\Delta S^\ddagger(T)$ is estimated as loss of one rotor (-4.3 cal mol⁻¹ K⁻¹) and gain an optical isomer (OI), $E_{a,r} = RS$ (26) + E_{abst} (10.58) + ΔH_{rxn} (5.77) kcal mol⁻¹.
- k_{-4} A_r via A_f and Microscopic Reversibility (MR), $E_{a,r} = E_{a,f} - \Delta U_{rxn}$, $\Delta U_{rxn} = -5.77$ kcal mol⁻¹.
- k_5 A_f via A_r and Microscopic Reversibility (MR), $A_r = 2.75 \times 10^{12} = 1/2$ (OH + C=C). $E_{a,f}$ estimated the same 2.0 kcal mol⁻¹ based on $E_{a,f}$ for CH₂OOH \rightarrow CH₂O + OH (1990 Page)
- k_6 A_f estimated using TST, $A = (\text{deg.}) (ek_b/h) T^n \exp(\Delta S^\ddagger(T)/R)$, deg. = 3, $ek_b/h = 5.66 \times 10^{10}$, $n = 1.0$, $\Delta S^\ddagger(T)$ is estimated as loss of three rotors (-4.3 \times 3 cal mol⁻¹ K⁻¹) and gain an optical isomer (OI), $E_{a,r} = RS$ (6) + E_{abst} (7.95) + ΔH_{rxn} (13.65) kcal mol⁻¹.
- k_{-6} A_r via A_f and Microscopic Reversibility (MR), $E_{a,r} = E_{a,f} - \Delta U_{rxn}$, $\Delta U_{rxn} = 13.65$ kcal mol⁻¹.
- k_7 A_f via A_r and Microscopic Reversibility (MR), $A_r = 3.50 \times 10^{11}$, Bozzelli. $E_{a,f} = E_{a,r} + \Delta U_{rxn}$, $\Delta U_{rxn} = 7.07$ kcal mol⁻¹. $E_{a,r} = 7.80$ kcal mol⁻¹. (estimated by Bozzelli).
- k_8 A_f via A_r and Microscopic Reversibility (MR), $A_r = 9.64 \times 10^{10}$, 91 TSA for C₃H₆ + CH₃ \rightarrow C3.C. $E_{a,f} = E_{a,r} + \Delta U_{rxn}$ (23.71) kcal mol⁻¹. $E_{a,r} = 7.8$ kcal mol⁻¹. (estimated

by Bozzelli).

- k₉ A_f estimated using TST, $A = (\text{deg.}) (ek_b/h) T^n \exp(\Delta S^\ddagger(T)/R)$, deg. = 2, $ek_b/h = 5.66 \times 10^{10}$, $n = 1.0$, $\Delta S^\ddagger(T)$ is estimated as loss of two rotors ($-4.3 \times 2 \text{ cal mol}^{-1} \text{ K}^{-1}$) and gain an optical isomer (OI), $E_{a,r} = RS(6) + E_{abst}(7.62) + \Delta H_{rxn}(6.85) \text{ kcal mol}^{-1}$.
- k₉ A_r via A_f and Microscopic Reversibility (MR), $E_{a,r} = E_{a,f} - \Delta U_{rxn}$, $\Delta U_{rxn} = 6.85 \text{ kcal mol}^{-1}$.
- k₁₀ A_f via A_r and Microscopic Reversibility (MR), $A_r = 2.50 \times 10^{11} = 1/2 (\text{HO}_2 + \text{C}=\text{C})$, 72 KER/PAR. $E_{a,f} = E_{a,r} + \Delta U_{rxn}(13.87) \text{ kcal mol}^{-1}$. $E_{a,r} = 7.8 \text{ kcal mol}^{-1}$. (estimated by Bozzelli).
- k₁₁ A_f estimated using TST, $A = (\text{deg.}) (ek_b/h) T^n \exp(\Delta S^\ddagger(T)/R)$, deg. = 1, $ek_b/h = 5.66 \times 10^{10}$, $n = 1.0$, $\Delta S^\ddagger(T)$ is estimated as loss of three rotors ($-4.3 \times 3 \text{ cal mol}^{-1} \text{ K}^{-1}$) and gain an optical isomer (OI), $E_{a,r} = RS(0) + E_{abst}(6.82) + \Delta H_{rxn}(17.04) \text{ kcal mol}^{-1}$.
- k₁₁ A_r via A_f and Microscopic Reversibility (MR), $E_{a,r} = E_{a,f} - \Delta U_{rxn}$, $\Delta U_{rxn} = 17.04 \text{ kcal mol}^{-1}$.
- k₁₂ A_f via A_r and Microscopic Reversibility (MR), $A_r = 1.08 \times 10^{11}$, 88 TSA for $\text{CH}_2\text{O} + \text{CC.C} \rightarrow \text{CCC} + \text{CHO}$. $E_{a,f} = E_{a,r} + \Delta U_{rxn}$, $\Delta U_{rxn} = 8.2 \text{ kcal mol}^{-1}$. $E_{a,r} = 6.5 \text{ kcal mol}^{-1}$. (taken from the same reference).

IID. 78 $\text{CyCOC(C)OOH} \rightarrow \text{CCyCOC.} + \text{HO}_2$



	Reaction	$A T^n e^{-\alpha T}$ (s ⁻¹ or cm ³ mol ⁻¹ s ⁻¹)	E_a (kcal mol ⁻¹)
k_1	$\text{CyCOC(C)OOH} \rightarrow \text{CCyCOC.} + \text{HO}_2$	$5.61 \times 10^{16} T^0 e^{-0T}$	73.62

frequency/degeneracy (CPFIT)

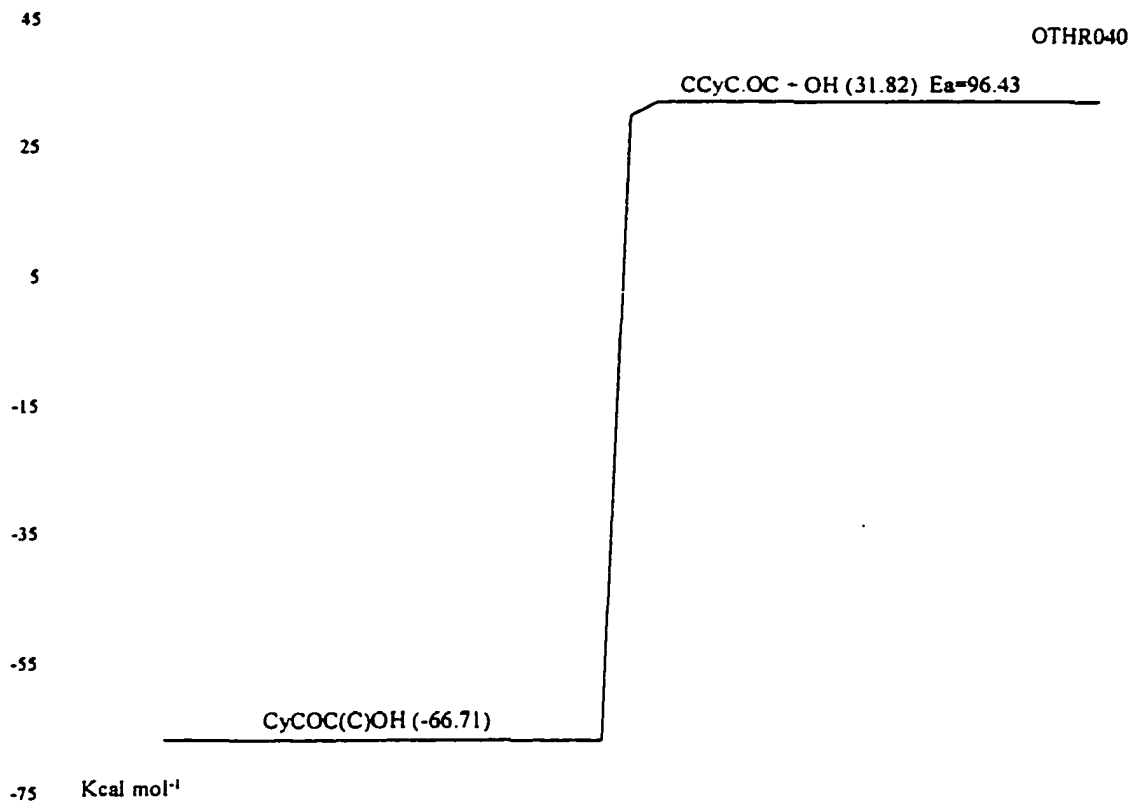
CyCOC(C)OOH : 250.2 (6.957); 976.8 (14.529); 2436.2 (7.015)

Lennard-Jones parameter

$\sigma(\text{\AA}) = 5.55$, $\epsilon/k(\text{K}) = 584.86$

k_1 A_f via A_r and Microscopic Reversibility (MR), $A_r = 1.00 \times 10^{13} = 1/2 (\text{CH}_3 + \text{HO}_2 \rightarrow \text{CH}_3\text{O} + \text{OH})$, 86 TSA/HAM, $E_{a,f} = E_{a,r}(0) + \Delta U_{\text{rxn}} (73.62) \text{ kcal mol}^{-1}$.

IID. 79 $\text{CyCOC}(\text{C})\text{OH} \rightarrow \text{CCyC}.\text{OC} + \text{OH}$



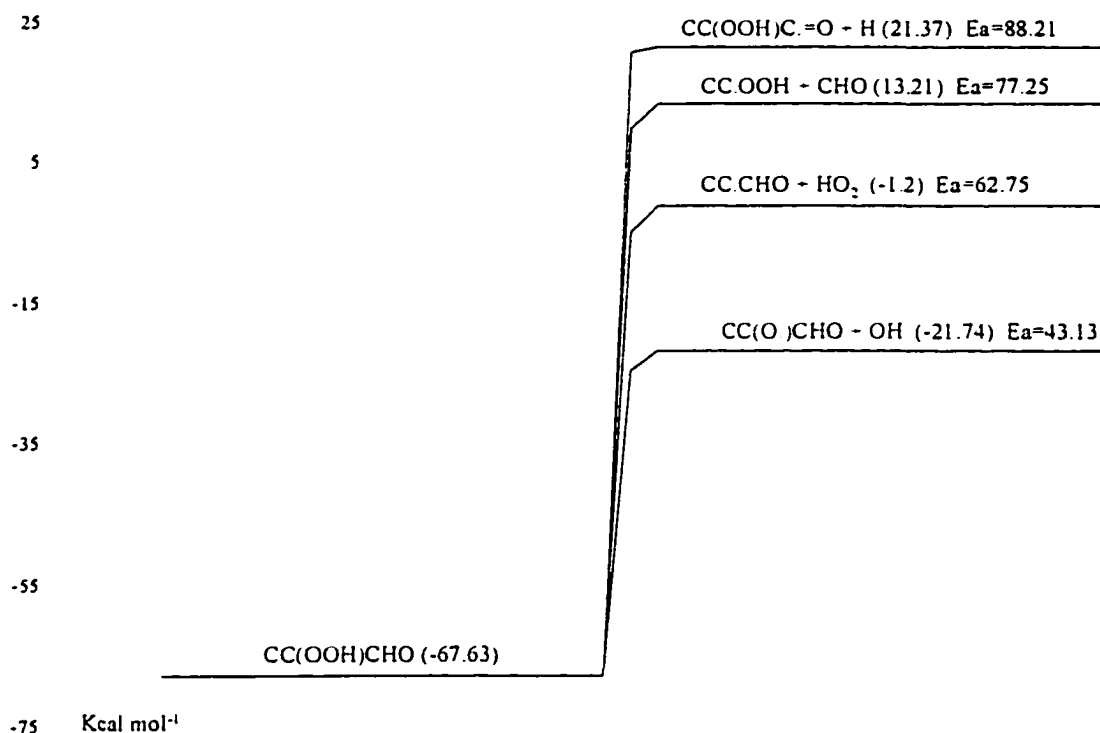
	Reaction	$A T^n e^{-a/T}$ (s ⁻¹ or cm ³ mol ⁻¹ s ⁻¹)	E_a (kcal mol ⁻¹)
k_1	$\text{CyCOC}(\text{C})\text{OH} \rightarrow \text{CCyC}.\text{OC} + \text{OH}$	$6.18 \times 10^{16} T^0 e^{-0/T}$	96.43

frequency/degeneracy (CPFIT)
 $\text{CyCOC}(\text{C})\text{OH}$: 489.2 (9.211); 1324.4 (11.691); 3257.3 (5.098)
 Lennard-Jones parameter
 $\sigma(\text{\AA}) = 5.20$, $\epsilon/k(\text{K}) = 533.08$

k_1 A_f via A_r and Microscopic Reversibility (MR), $A_r = 1.81 \times 10^{13}$, 90 TSA/HAM for $\text{C3C} + \text{OH}$. $E_{a,f} = E_{a,r}(0) + \Delta U_{\text{rxn}}$ (96.43) kcal mol⁻¹.

IID. 80 CC(OOH)CHO → Products

OTHR028



	Reaction	$A T^n e^{-\alpha T}$ (s^{-1} or $cm^3 mol^{-1} s^{-1}$)	E_a ($kcal mol^{-1}$)
k_1	$CC(OOH)CHO \rightarrow CC.OOH + CHO$	$3.44 \times 10^{16} T^0 e^{-0T}$	77.25
k_2	$CC(OOH)CHO \rightarrow CC.CHO + HO_2$	$5.11 \times 10^{14} T^0 e^{-0T}$	62.75
k_3	$CC(OOH)CHO \rightarrow CC(OOH)C=O + H$	$9.78 \times 10^{14} T^0 e^{-0T}$	88.21
k_4	$CC(OOH)CHO \rightarrow CC(O.)CHO + OH$	$6.57 \times 10^{14} T^0 e^{-0T}$	43.13

frequency/degeneracy (CPFIT)

CC(OOH)CHO: 250.2 (7.103); 924.9 (13.196); 2314.3 (7.701)

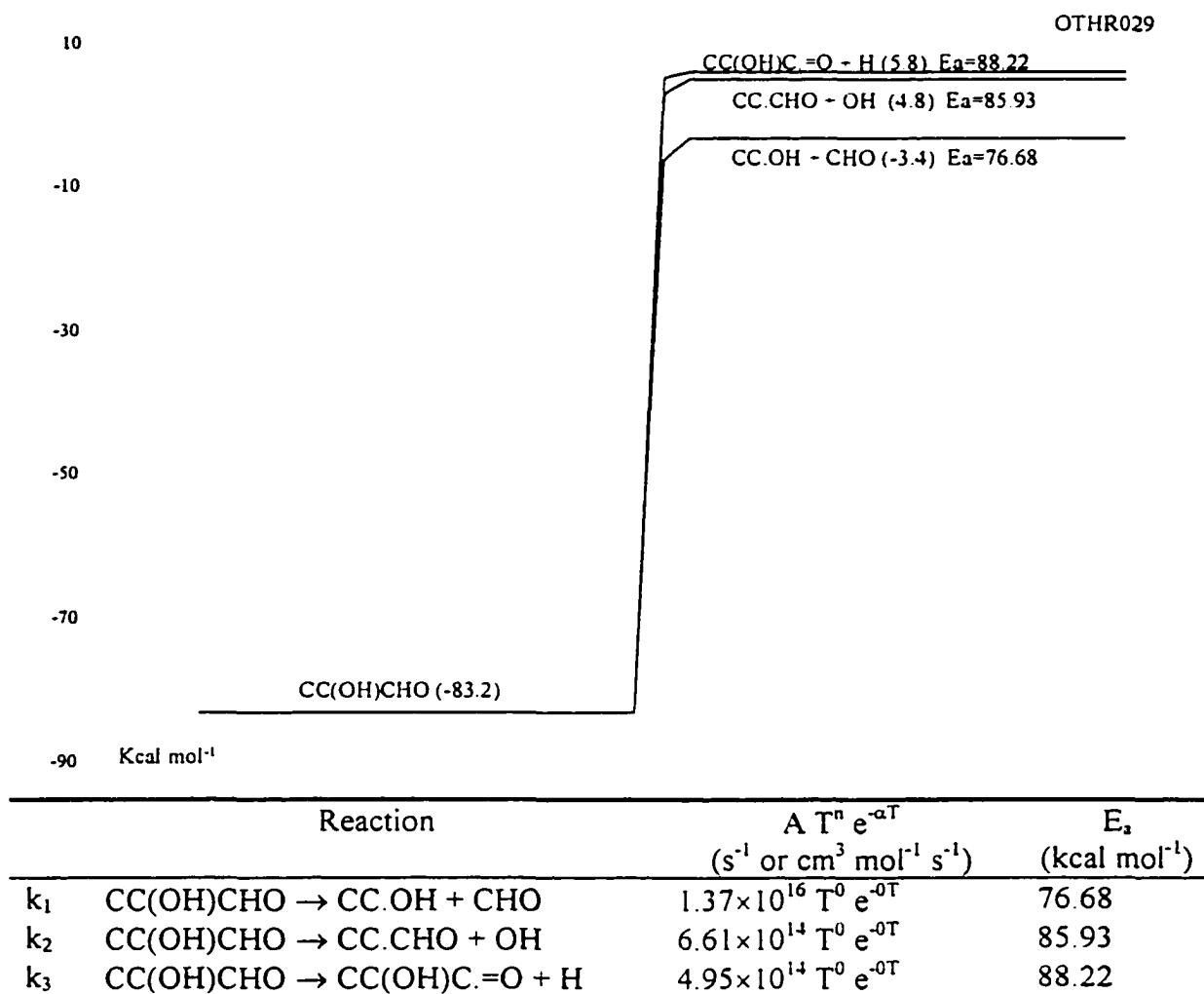
Lennard-Jones parameter

 $\sigma(\text{\AA}) = 5.55$, $\epsilon/k (K) = 584.86$

- k_1 A_f via A_r and Microscopic Reversibility (MR), $A_r = 1.81 \times 10^{13}$, 88 TSA/HAM for $CC.C + CHO$. $E_{a,f} = E_{a,r}(0) + \Delta U_{rxn}$ (77.25) $kcal mol^{-1}$.
- k_2 A_f via A_r and Microscopic Reversibility (MR), $A_r = 1.00 \times 10^{13} = 1/2 (CH_3 + HO_2 \rightarrow CH_3O + OH, 86 \text{ TSA/HAM})$. $E_{a,f} = E_{a,r}(0) + \Delta U_{rxn}$ (62.75) $kcal mol^{-1}$.

- k_3 A_f via A_r and Microscopic Reversibility (MR), $A_r = 5.00 \times 10^{13} \text{ 1/2 (H + CHO)}$, NIST FIT. $E_{a,f} = E_{a,r}(0) + \Delta U_{\text{rxn}} (88.21) \text{ kcal mol}^{-1}$.
- K_4 A_f via A_r and Microscopic Reversibility (MR), $A_r = 1.51 \times 10^{13} \text{ 92 BAU/COB for CH}_3\text{O + O}$. $E_{a,f} = E_{a,r}(0) + \Delta U_{\text{rxn}} (43.13) \text{ kcal mol}^{-1}$.

IID. 81 CC(OH)CHO → Products

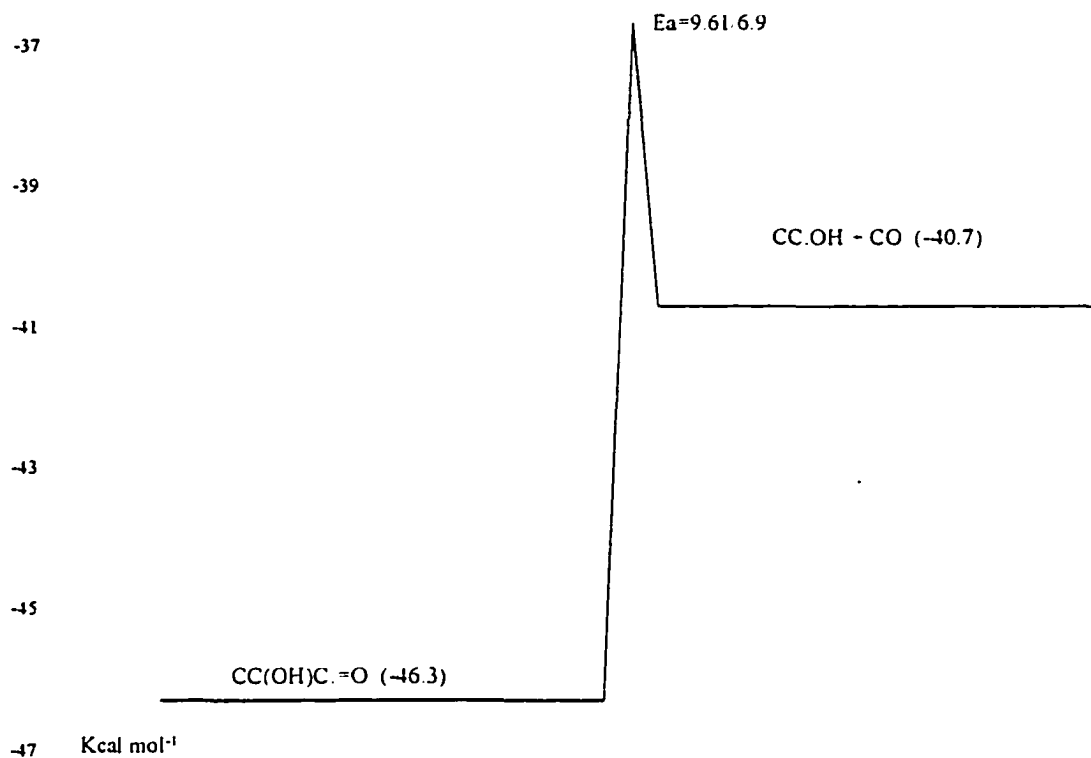


frequency/degeneracy (CPFIT)
 CC(OH)CHO: 250.3 (5.563); 1060.1 (13.058); 2806.5 (6.878)
 Lennard-Jones parameter
 $\sigma(\text{\AA}) = 5.20$, ϵ/k (K) = 533.08

- k_1 A_f via A_r and Microscopic Reversibility (MR), $A_r = 1.81 \times 10^{13}$, 88 TSA/HAM for CC.C + CHO. $E_{a,f} = E_{a,f}(0) + \Delta U_{rxn}$ (76.68) $kcal mol^{-1}$.
- k_2 A_f via A_r and Microscopic Reversibility (MR), $A_r = 1.51 \times 10^{13}$, 91 TSA/HAM for C=CC. + OH. $E_{a,f} = E_{a,f}(0) + \Delta U_{rxn}$ (85.93) $kcal mol^{-1}$.
- k_3 A_f via A_r and Microscopic Reversibility (MR), $A_r = 5.00 \times 10^{13}$ 1/2 (H + CHO), NIST FIT. $E_{a,f} = E_{a,f}(0) + \Delta U_{rxn}$ (88.22) $kcal mol^{-1}$.

IID. 82 $\text{CC}(\text{OH})\text{C}=\text{O} \rightarrow \text{CC}.\text{OH} + \text{CO}$

OTHR044

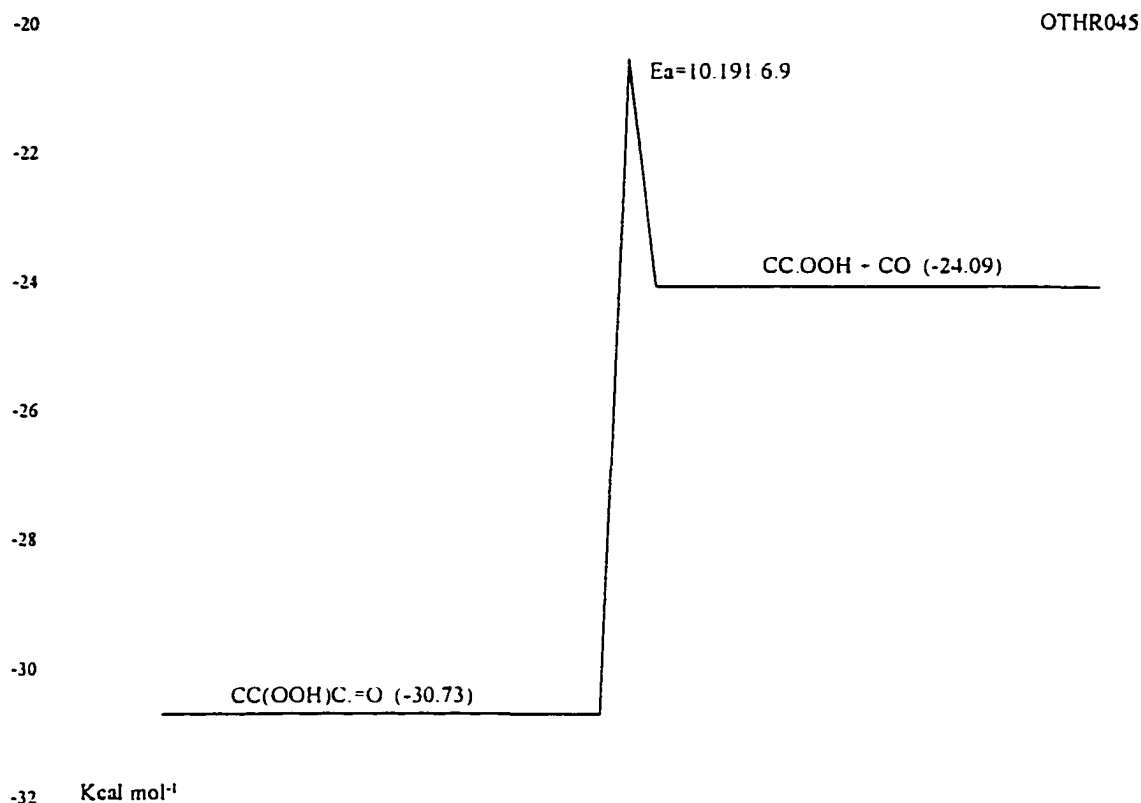


	Reaction	$A T^n e^{-\alpha/T}$ (s ⁻¹ or cm ³ mol ⁻¹ s ⁻¹)	E_a (kcal mol ⁻¹)
k_1	$\text{CC}(\text{OH})\text{C}=\text{O} \rightarrow \text{CC}.\text{OH} + \text{CO}$	$2.19 \times 10^{12} T^0 e^{-0/T}$	9.61

frequency/degeneracy (CPFIT)
 $\text{CC}(\text{OH})\text{C}=\text{O}$: 250.3 (5.384); 1058.9 (11.400); 2797.0 (5.716)
 Lennard-Jones parameter
 $\sigma(\text{\AA}) = 5.20$, $\epsilon/k(\text{K}) = 533.08$

k_1 A_f via A_r and Microscopic Reversibility (MR), $A_r = 5.01 \times 10^{10}$, 72 KER/PAR for $\text{CC}.\text{C} + \text{C}_2\text{H}_2$. $E_{a,f} = E_{a,r}(6.9) + \Delta U_{\text{rxn}}(2.71)$ kcal mol⁻¹.

IID. 83 $\text{CC}(\text{OOH})\text{C}=\text{O} \rightarrow \text{CC}.\text{OOH} + \text{CO}$

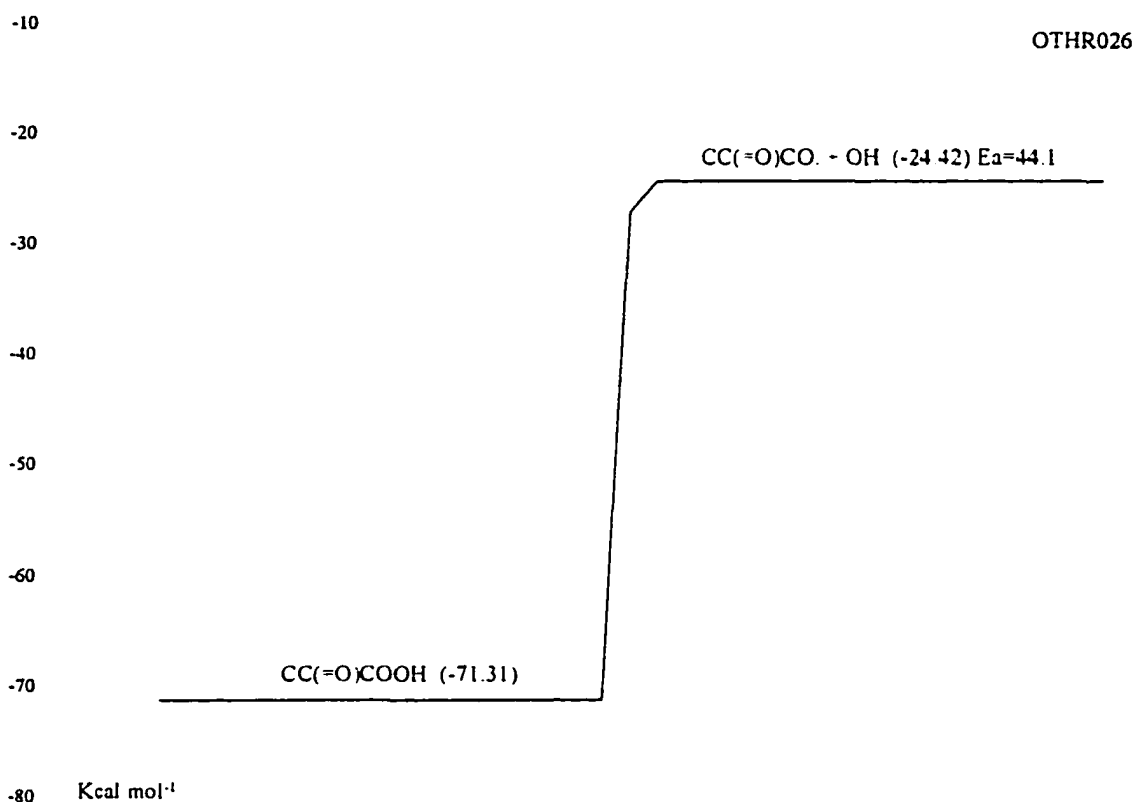


	Reaction	$A T^n e^{-\alpha/T}$ (s ⁻¹ or cm ³ mol ⁻¹ s ⁻¹)	E_a (kcal mol ⁻¹)
k_1	$\text{CC}(\text{OOH})\text{C}=\text{O} \rightarrow \text{CC}.\text{OOH} + \text{CO}$	$2.79 \times 10^{12} T^0 e^{-0/T}$	10.19

frequency/degeneracy (CPFIT)
 $\text{CC}(\text{OOH})\text{C}=\text{O}$: 250.8 (6.693); 887.0 (11.549); 2197.9 (6.758)
 Lennard-Jones parameter
 $\sigma(\text{\AA}) = 5.55$, $\epsilon/k(\text{K}) = 584.86$

k_1 A_f via A_r and Microscopic Reversibility (MR), $A_r = 5.01 \times 10^{10}$, 72 KER/PAR for $\text{CC}.\text{C} + \text{C}_2\text{H}_2$. $E_{a,f} = E_{a,r}(6.9) + \Delta U_{\text{rxn}}(3.29)$ kcal mol⁻¹.

IID. 84 $\text{CC}(=\text{O})\text{COOH} \rightarrow \text{CC}(=\text{O})\text{CO.} + \text{OH}$



	Reaction	$A T^n e^{-\alpha T}$ (s ⁻¹ or cm ³ mol ⁻¹ s ⁻¹)	E_a (kcal mol ⁻¹)
k_1	$\text{CC}(=\text{O})\text{COOH} \rightarrow \text{CC}(=\text{O})\text{CO.} + \text{OH}$	$1.06 \times 10^{15} T^0 e^{-0T}$	44.10

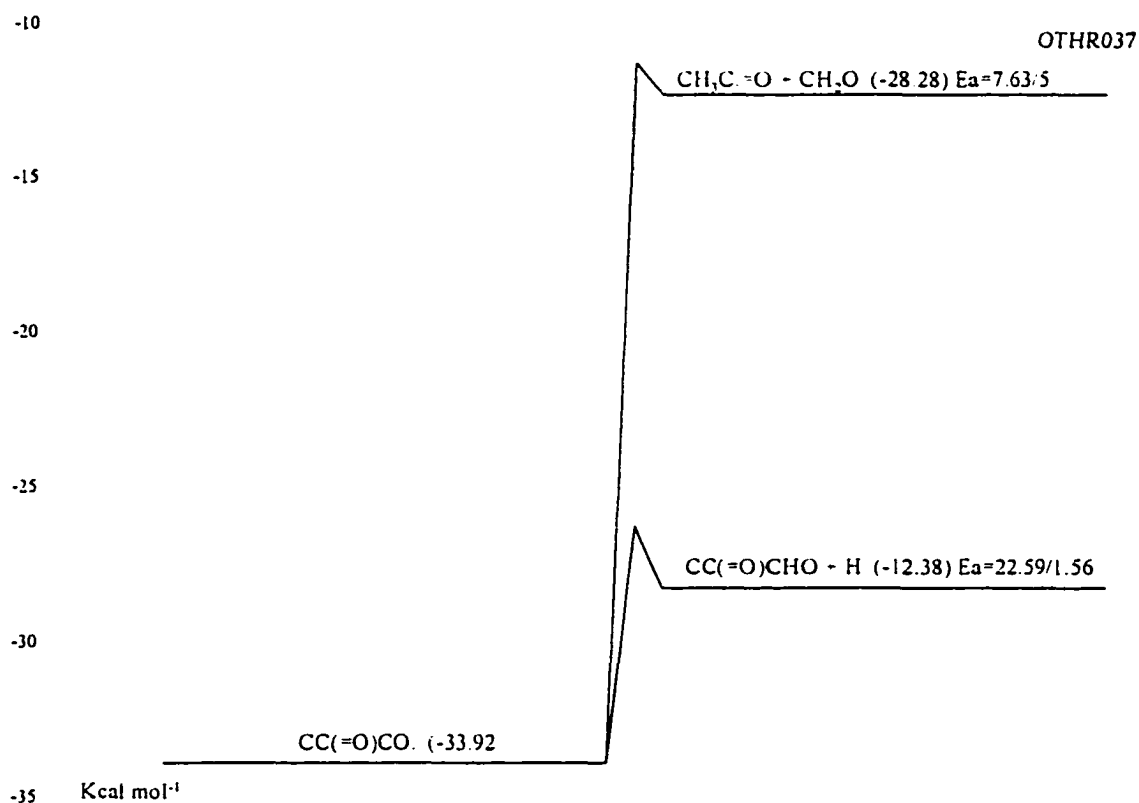
frequency/degeneracy (CPFIT)

$\text{CC}(=\text{O})\text{COOH}$: 325.0 (9.173); 877.0 (7.704); 2125.7 (11.123)

Lennard-Jones parameter

$\sigma(\text{\AA}) = 5.55$, ϵ/k (K) = 584.86

k_1 A_f via A_r and Microscopic Reversibility (MR), $A_r = 1.81 \times 10^{13}$, 92 BAU/COB for $\text{CH}_3\text{O} + \text{OH}$. $E_{a,f} = E_{a,r}(0) + \Delta U_{\text{rxn}}$ (44.10) kcal mol⁻¹.

IID. 85 $\text{CC}(=\text{O})\text{CO.} \rightarrow \text{Products}$ 

	Reaction	$A T^n e^{-\alpha/T}$ (s ⁻¹ or cm ³ mol ⁻¹ s ⁻¹)	E_a (kcal mol ⁻¹)
k_1	$\text{CC}(=\text{O})\text{CO.} \rightarrow \text{CC}(=\text{O})\text{CHO} + \text{H}$	$7.28 \times 10^{12} T^0 e^{-0/T}$	22.59
k_3	$\text{CC}(=\text{O})\text{CO.} \rightarrow \text{CH}_3\text{C}(=\text{O}) + \text{CH}_2\text{O}$	$1.00 \times 10^{13} T^0 e^{-0/T}$	7.63

frequency/degeneracy (CPFIT)

 $\text{CC}(=\text{O})\text{CO.}$: 469.2 (9.796); 1694.2 (9.877); 3139.4 (3.327)

Lennard-Jones parameter

 $\sigma(\text{\AA}) = 5.20, \epsilon/k(\text{K}) = 533.08$

- k_1 A_f via A_r and Microscopic Reversibility (MR), $A_r = 5.00 \times 10^{12} = 1/2 (\text{H} + \text{C}=\text{C})$.
 $E_{a,f} = E_{a,r} (1.56) + \Delta U_{\text{rxn}} (21.03) \text{ kcal mol}^{-1}$.
- k_2 A_f via A_r and Microscopic Reversibility (MR), $A_r = 1.08 \times 10^{11}$, 88 TSA for $\text{CH}_2\text{O} + \text{CC.C} \rightarrow \text{CCC} + \text{CHO}$. $E_{a,f} = E_{a,r} + \Delta U_{\text{rxn}} (2.63) \text{ kcal mol}^{-1}$. $E_{a,r} = 6.0 \text{ kcal mol}^{-1}$.
 (estimated by Bozzelli).

k_3 A_f via A_r and Microscopic Reversibility (MR), $A_r = 5.00 \times 10^{13} \text{ l/2 (H + CHO)}$,
 NIST FIT. $E_{a,f} = E_{a,f}(0) + \Delta U_{\text{rxn}} (88.22) \text{ kcal mol}^{-1}$.

IID. 86 $\text{C}=\text{CC}=\text{O} \rightarrow \text{C}_2\text{H}_3 + \text{CO}$

55

OTHR050

50

45

40

35

30

25

20

15

10

5

Kcal mol⁻¹ $E_a = 36.329/4.809$ $\text{C}_2\text{H}_3 + \text{CO} (45.22)$ $\text{C}=\text{CC}=\text{O} (10.58)$

	Reaction	$A T^n e^{-\alpha/T}$ (s ⁻¹ or cm ³ mol ⁻¹ s ⁻¹)	E_a (kcal mol ⁻¹)
k_1	$\text{C}=\text{CC}=\text{O} \rightarrow \text{C}_2\text{H}_3 + \text{CO}$	$3.13 \times 10^{13} T^0 e^{-0/T}$	36.33

frequency/degeneracy (CPFIT)

 $\text{C}=\text{CC}=\text{O}$: 450.7 (5.070); 1031.9 (5.583); 2692.0 (3.848)

Lennard-Jones parameter

 $\sigma(\text{\AA}) = 4.80$, ϵ/k (K) = 481.73

k_1 A_f via A_r and Microscopic Reversibility (MR), $A_r = 1.51 \times 10^{11}$, 86 TSA/HAM for $\text{CO} + \text{C}_2\text{H}_3$. $E_{a,f} = E_{a,r} (4.809) + \Delta U_{\text{rxn}} (31.52)$ kcal mol⁻¹.

APPENDIX III
TS INFORMATION AND QRRK ANALYSIS IN CH₂OOH ELIMINATION
REACTION SYSTEM

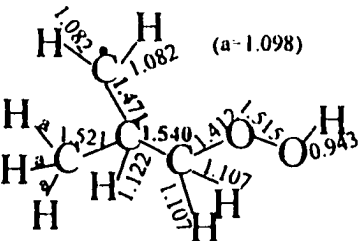
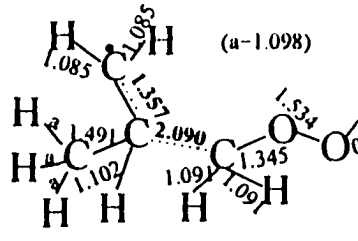
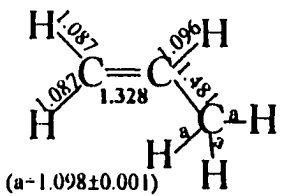
TS III. 1 TS Infomation for C.CCOOH \rightarrow C₂H₄ + CH₂OOH

	Reactant	Transition State	Product 1 (Alkene)
Bond Lengths (Å)			
Species ID	C.CCOOH	TCJ*CXCQ	C ₂ H ₄
Principal Moments Of Inertia	in unit of cm ⁻¹ : A = 0.755548 B = 0.072565 C = 0.068077 in unit of 10 ⁻⁴⁰ -gram-cm ² : A = 37.049450 B = 385.762064 C = 411.192869	in unit of cm ⁻¹ : A = 0.279402 B = 0.098401 C = 0.082060 in unit of 10 ⁻⁴⁰ -gram-cm ² : A = 100.187777 B = 284.475509 C = 341.123046	in unit of cm ⁻¹ : A = 5.050953 B = 1.001305 C = 0.835646 in unit of 10 ⁻⁴⁰ -gram-cm ² : A = 5.542050 B = 27.956154 C = 33.498204
Symmetry	1	1	4
Internal Rotor(s) And Barrier(s) V (kcal-mol ⁻¹)	CH ₂ -CCOOH (1): 0.16 C.C-COOH (1): 3.26 C.CC-OOH (1): 5.40 C.CCO-OH (1): 6.38	CH ₂ -CCOOH (1): 5.80 C.C-COOH (1): 0.20 C.CC-OOH (1): 5.40 C.CCO-OH (1): 6.38	NO ROTOR
Frequencies (cm ⁻¹)	39 78 120 165 219 425 461 632 754 800 909 951 1057 1097 1134 1152 1160 1275 1329 1362 1384 1451 1494 2923	-915 39 92 149 209 280 394 437 651 745 821 915 934 955 1026 1074 1096 1189 1288 1321 1348 1451 1658 3040	822 881 984 1054 1093 1307 1328 1829 3128. 3138 3146 3157

TS III. 1 TS Information for C.CCOOH → C₂H₄ + CH₂OOH (Cont')

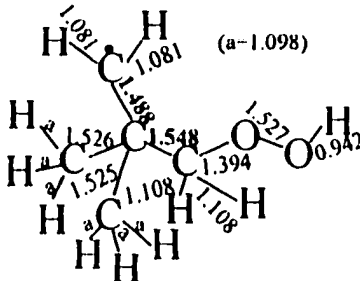
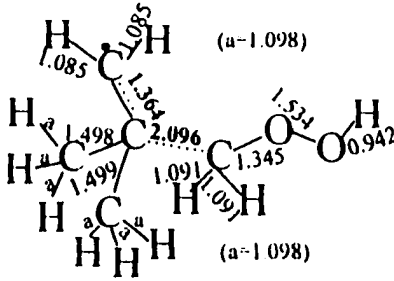
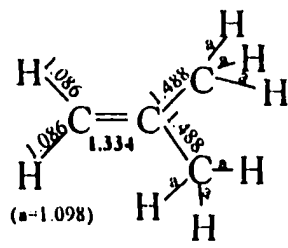
	2937 2991 3014 3147 3183 3990	3107 3112 3114 3150 3153 3988	
--	----------------------------------	----------------------------------	--

TS III. 2 TS Information for C2.CCOOH \rightarrow CC=C + CH₂OOH

	Reactant	Transition State	Product 1 (Alkene)
Bond Lengths (Å)			
Species ID	C2.CCOOH	TC2J*CXCQ	CC=C
Principal Moments Of Inertia	in unit of cm ⁻¹ : A = 0.250388 B = 0.061569 C = 0.053235 in unit of 10 ⁻⁴⁰ -gram-cm ² : A = 111.797064 B = 454.654301 C = 525.829879	in unit of cm ⁻¹ : A = 0.176505 B = 0.071129 C = 0.062813 in unit of 10 ⁻⁴⁰ -gram-cm ² : A = 158.594369 B = 393.546252 C = 445.651061	in unit of cm ⁻¹ : A = 1.518362 B = 0.319380 C = 0.277607 in unit of 10 ⁻⁴⁰ -gram-cm ² : A = 18.436071 B = 87.646884 C = 100.835643
Symmetry	3	3	6
Internal Rotor(s) And Barrier(s) V (kcal-mol ⁻¹)	CH ₃ -C(C.)COOH (1): 3.87 CH ₂ -C(C)COOH (1): 0.20 C2.C-COOH (1): 4.20 C2.CC-OOH (1): 5.40 C2.CCO-OH (1): 6.38	CH ₃ -C(C.)COOH (1): 2.87 CH ₂ -C(C)COOH (1): 6.00 C2.C-COOH (1): 0.20 C2.CC-OOH (1): 5.40 C2.CCO-OH (1): 6.38	CH ₃ -C ₂ H ₃ (1): 1.26
Frequencies (cm ⁻¹)	28 74 119 163 167 216 347 403 480 492 643 798 905 927 955 989 1012 1071 1103	-945 38 95 129 131 202 215 331 429 461 531 664 750 901 923 936 968 997 1034 1079	-113 430 585 895 925 987 1009 1057 1156 1220 1324 1388 1400 1422 1860 3046

TS III. 2 TS Information for C2.CCOOH → CC=C + CH₂OOH (Cont')

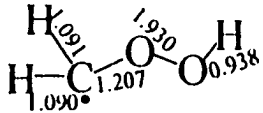
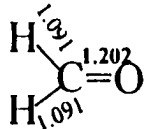
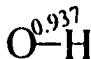
	1130 1156 1273 1305 1339 1376 1400 1407 1409 1441 1493 2833 2930 2986 3082 3087 3143 3182 3183 3989	1158 1192 1210 1322 1348 1395 1400 1414 1450 1684 3004 3038 3072 3080 3105 3147 3156 3174 3989	3068 3080 3139 3148 3174
--	--	---	--------------------------

	Reactant	Transition State	Product 1 (Alkene)
Bond Lengths (Å)			
Species ID	C3.CCOOH	TC3J*CXCQ	C2C=C
Principal Moments Of Inertia	in unit of cm^{-1} : A = 0.134413 B = 0.057918 C = 0.055484 in unit of 10^{-40} -gram-cm ² : A = 208.258377 B = 483.312996 C = 504.519395	in unit of cm^{-1} : A = 0.134601 B = 0.050499 C = 0.049792 in unit of 10^{-40} -gram-cm ² : A = 207.967001 B = 554.324829 C = 562.190911	in unit of cm^{-1} : A = 0.312646 B = 0.278927 C = 0.156031 in unit of 10^{-40} -gram-cm ² : A = 89.534710 B = 100.358468 C = 179.404128
Symmetry	9	9	18
Internal Rotor(s) And Barrier(s) V (kcal-mol ⁻¹)	CH ₃ -C(C2.)COOH (2): 4.70 CH ₂ -C(C2)COOH (1): 0.20 C3.C-COOH (1): 4.20 C3.CC-OOH (1): 5.40 C3.CCO-OH (1): 6.38	CH ₃ -C(C2.)COOH (2): 3.87 CH ₂ -C(C2)COOH (1): 6.20 C3.C-COOH (1): 0.20 C3.CC-OOH (1): 5.40 C3.CCO-OH (1): 6.38	CH ₃ -C ₂ H ₃ (C) (2): 1.26
	13 48 115 157 183 201 264 307 339 410 435 461 569 626 733	-947 36 96 128 136 155 189 207 255 406 416 439 451 549	-116 108 393 423 471 618 932 937 943 985 993 1024 1069

TS III. 3 TS Information for C3.CCOOH → C2C=C + CH₂OOH (Cont')

Frequencies (cm ⁻¹)	863 922 937 962 976 993 1008	670 752 903 925 935 952 965	1312 1323 1382 1390 1397
	1135 1143 1259 1284 1304	984 1032 1057 1079 1190 1317	1398 1399 1477 1873 3073
	1327 1346 1391 1398 1402	1327 1343 1388 1395 1400	3074 3074 3077 3147 3148
	1405 1410 1412 1426 1460	1404 1415 1445 1446 1690	3173 3175
	2946 3014 3082 3083 3085	3033 3070 3071 3078 3080	
	3086.13858 3142 3178 3179	3098 3145 3157 3171 3172	
	3184 3991	3989	

TS III. 4 TS Information For $\text{CH}_2\text{OOH} \rightarrow \text{CH}_2\text{O} + \text{OH}$

	Reactant	Product 1 (Formaldehyde)	Product 2 (OH Radical)
Bond Lengths (Å)			
Species ID	CH_2OOH	CH_2O	OH
Principal Moments Of Inertia	in unit of cm^{-1} : A = 1.952583 B = 0.269966 C = 0.237180	in unit of cm^{-1} : A = 9.720866 B = 1.305991 C = 1.151313	in unit of cm^{-1} : A = 0.000000 B = 20.236922 C = 20.236922
	in unit of 10^{-40} -gram-cm ² : A = 14.336207 B = 103.689311 C = 118.022837	in unit of 10^{-40} -gram-cm ² : A = 2.879645 B = 21.434012 C = 24.313656	in unit of 10^{-40} -gram-cm ² : A = 0.000000 B = 1.383246 C = 1.383246
Symmetry	1	2	1
Internal Rotor(s) And Barrier(s) V (kcal-mol ⁻¹)	$\text{CH}_2\text{-OOH}$ (1): 6.46 $\text{CH}_2\text{O-OH}$ (1): 5.98	NO ROTOR	NO ROTOR
Frequencies (cm ⁻¹)	162 195 197 546 647 1091 1102 1282 1961 3001 3038 3988	1070 1098 1289 1987 2999 3026	3989.03618

TS III. 5 Summary of the Important Bond Lengths

Bond	In reactant	In transition state	In product	Comment
RC.--CCOOH	1.462Å for C.CCOOH	1.347Å for C.CCOOH	1.322Å for C=C	The forming double bond
	1.471Å for C2.CCOOH	1.357Å for C2.CCOOH	1.328Å for CC=C	
	1.488Å for C3.CCOOH	1.364Å for C3.CCOOH	1.334Å for C2C=C	
RC.C--COOH	1.530Å for C.CCOOH	2.096Å for C.CCOOH		The breaking bond
	1.540Å for C2.CCOOH	2.090Å for C2.CCOOH		
	1.548Å for C3.CCOOH	2.096Å for C3.CCOOH		
RC.CC--OOH	1.411Å for C.CCOOH	1.344Å for C.CCOOH		The forming double bond in the second step
	1.412Å for C2.CCOOH	1.345Å for C2.CCOOH	1.207Å for C.H ₂ OOH	
	1.394Å for C3.CCOOH	1.345Å for C3.CCOOH		
RC.CCO--OH	1.514Å for C.CCOOH	1.535Å for C.CCOOH		The breaking bond in the second step
	1.515Å for C2.CCOOH	1.534Å for C2.CCOOH	1.930Å for C.H ₂ OOH	
	1.527Å for C3.CCOOH	1.534Å for C3.CCOOH		

TS III. 6 Thermodynamic Properties from MOPAC Calculation

SPECIES	H_{298}^a	S_{298}^b	C_p^b							DATE	E L E M E N T					
			300	400	500	600	800	1000	1500							
C3.CCOOH	-12.49	101.47	36.53	45.66	53.42	59.59	68.46	74.56	83.88	3/31/97 RU	C	5 H	11 O	2 O G	6	
TC3J*CXCQ ^c	9.54	102.25	36.22	45.04	52.43	58.33	66.92	72.90	82.08	3/31/97 RU	C	5 H	11 O	2 O G	6	
C2.CCOOH	-4.69	96.65	30.82	38.23	44.53	49.55	56.81	61.83	69.47	3/31/97 RU	C	4 H	9 O	2 O G	5	
TC2J*CXCQ ^d	16.29	96.74	30.47	37.58	43.57	48.37	55.37	60.25	67.69	3/31/97 RU	C	4 H	9 O	2 O G	5	
C.CCOOH	2.48	90.39	25.35	31.00	35.81	39.67	45.28	49.17	55.07	3/31/97 RU	C	3 H	7 O	2 O G	4	
TCJ*CXCQ ^e	23.07	90.06	25.03	30.7	35.43	39.17	44.49	48.10	53.56	3/31/97 RU	C	3 H	7 O	2 O G	4	
C2C=C	-3.80	71.00	20.31	25.37	30.13	34.25	40.88	45.91	53.96	3/31/97 RU	C	4 H	8	0 O G	2	
CC=C	4.65	64.20	15.1	18.89	22.43	25.49	30.39	34.11	40.07	3/31/97 RU	C	3 H	6	0 O G	1	
C ₂ H ₄	12.52	52.37	10.44	12.86	15.09	16.98	20.01	22.35	26.15	3/31/97 RU	C	2 H	4	0 O G	0	
CH ₂ OOH	-14.60	70.56	16.46	18.54	20.26	21.63	23.59	24.90	26.85	3/31/97 RU	C	1 H	3 O	2 O G	2	
CH ₂ O	-26.00	52.25	8.72	9.74	10.79	11.77	13.44	14.76	16.89	3/31/97 RU	C	1 H	2 O	1 O G	0	
OH	9.50	44.60	6.96	6.96	6.96	6.97	7.03	7.17	7.62	3/31/97 RU	H	1 O	1	0 O G	0	

- a Unit in kcal-mol⁻¹.
b Unit in cal-mol⁻¹.
c Transition state for reaction C3.CCOOH → C2C-C + CH₂OOH
d Transition state for reaction C2.CCOOH → CC-C + CH₂OOH
e Transition state for reaction C.CCOOH → C=C + CH₂OOH

TS III. 7 Thermodynamic Analysis for C.CCOOH \rightarrow C=C + CH₂OOH

Rx C.CCOOH = TCJ*CXCQ Hf {Kcal/mol} 2.480 23.070 S {cal/mol K} 90.390 90.060 dU (dE) {kcal/mol} (298K) = 20.59 dUr avg (298., 1500. K) = 20.06 for A(T) = Aprime * T^n Aprime = 6.1334E+11 n = .57148				Rx C.CCOOH = C2H4 + CH2OOH Hf {Kcal/mol} 2.480 12.520 14.600 S {cal/mol K} 90.390 52.370 70.560 dHr {kcal/mol} (298K) = 24.64 dHr avg (298., 1500. K) = 23.81 dU (dE) {kcal/mol} (") = 24.05 dUr avg (298., 1500. K) = 22.03 Af/Ar (") = 1.947E+02 Af/Ar avg (298., 1500. K) = 4.417E+01 Fit Af/Ar: A = 2.369E+04 n = -.77 alpha = 9.928E-04 avg error 6.94 %				
Temp(K)	AF(T)	AF-fit(T)	dS(cal/mol K)	dH(Kcal/mol)	dU(Kcal/mol)	dS(cal/mol K)	(Af/Ar)	dG(Kcal/mol)
300	1.44E+13	1.60E+13	8.45E-16	2.46E+01	2.41E+01	3.26E+01	1.94E+02	1.49E+01
400	1.84E+13	1.88E+13	4.73E-12	2.47E+01	2.39E+01	3.28E+01	1.67E+02	1.16E+01
500	2.19E+13	2.14E+13	8.31E-10	2.47E+01	2.37E+01	3.28E+01	1.32E+02	8.33E+00
600	2.50E+13	2.37E+13	2.59E-08	2.47E+01	2.35E+01	3.27E+01	1.03E+02	5.05E+00
800	3.01E+13	2.80E+13	1.86E-06	2.44E+01	2.28E+01	3.23E+01	6.29E+01	-1.44E+00
1000	3.41E+13	3.18E+13	2.38E-05	2.40E+01	2.20E+01	3.19E+01	4.09E+01	-7.85E+00
1200	3.72E+13	3.53E+13	1.28E-04	2.36E+01	2.12E+01	3.15E+01	2.85E+01	-1.42E+01
1500	4.00E+13	4.01E+13	6.71E-04	2.30E+01	2.00E+01	3.10E+01	1.81E+01	-2.36E+01
2000	4.10E+13	4.72E+13	3.34E-03	2.20E+01	1.80E+01	3.04E+01	1.01E+01	-3.89E+01

TS III. 8 Thermodynamic Analysis for C2.CCOOH → CC=C + CH₂OOH

Rx C2.CCOOH = TC2J*CXCQ Hf {Kcal/mol} -4.690 16.290 S {cal/mol K} 96.650 96.740 dU (dE) {kcal/mol} (298K) = 20.98 dUr avg (298., 1500. K) = 20.62 for A(T) = Aprime * T^n Aprime = 3.4940E+11 n = .68817				Rx C2.CCOOH = CC*C + CH2OOH Hf {Kcal/mol} - 4.690 4.650 14.600 S {cal/mol K} 96.650 64.200 70.560 dHr {kcal/mol} (298K) = 23.94 dHr avg (298., 1500. K) = 22.55 dU (dE) {kcal/mol} (") = 23.35 dUr avg (298., 1500. K) = 20.77 Af/Ar (") = 3.212E+03 Af/Ar avg (298., 1500. K) = 4.790E+02 Fit Af/Ar : A = 3.480E+07 n = -1.57 alpha = 6.394E-04 avg error 8.16 %				
Temp(K)	AF(T)	AF-fit(T)	dS(cal/mol K)	dH(Kcal/mol)	dU(Kcal/mol)	dS(cal/mol K)	(Af/Ar)	dG(Kcal/mol)
300	1.78E+13	1.77E+13	5.43E-16	2.39E+01	2.34E+01	3.81E+01	3.20E+03	1.25E+01
400	2.19E+13	2.16E+13	3.56E-12	2.39E+01	2.31E+01	3.81E+01	2.36E+03	8.69E+00
500	2.52E+13	2.52E+13	6.83E-10	2.38E+01	2.28E+01	3.78E+01	1.63E+03	4.90E+00
600	2.83E+13	2.85E+13	2.25E-08	2.36E+01	2.24E+01	3.74E+01	1.12E+03	1.14E+00
800	3.41E+13	3.48E+13	1.73E-06	2.31E+01	2.15E+01	3.66E+01	5.71E+02	-6.26E+00
1000	4.02E+13	4.05E+13	2.30E-05	2.25E+01	2.05E+01	3.60E+01	3.32E+02	-1.35E+01
1200	4.61E+13	4.60E+13	1.29E-04	2.19E+01	1.96E+01	3.55E+01	2.16E+02	-2.07E+01
1500	5.41E+13	5.36E+13	7.09E-04	2.12E+01	1.82E+01	3.49E+01	1.29E+02	-3.12E+01
2000	6.57E+13	6.53E+13	3.83E-03	2.00E+01	1.60E+01	3.42E+01	6.82E+01	-4.85E+01

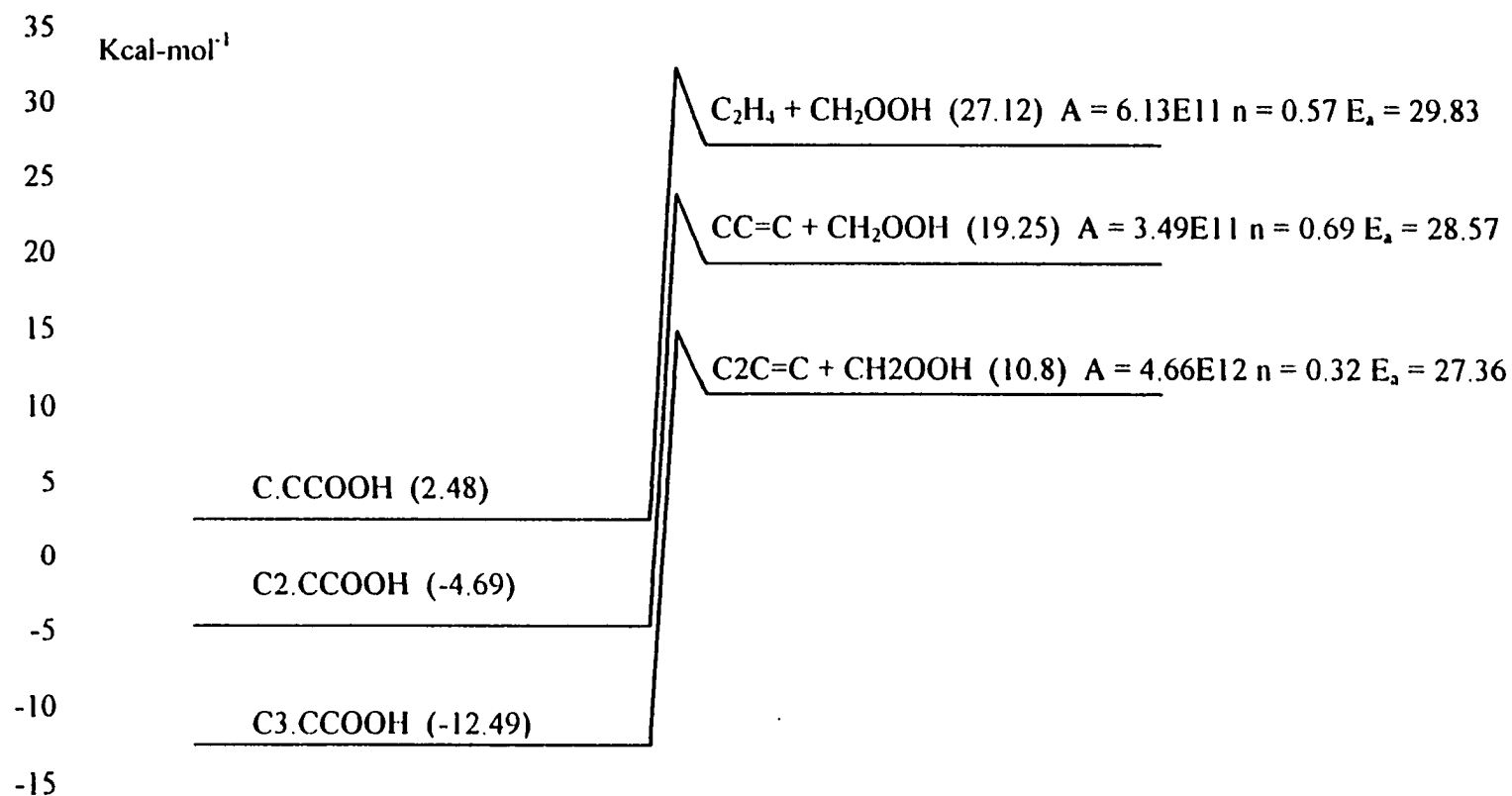
TS III. 9 Thermodynamic Analysis for C3.CCOOH → C2C=C + CH2OOH

Rx C3.CCOOH = TC3J*CXCQ Hf {Kcal/mol} -12.490 9.540 S {cal/mol K} 101.470 102.250 dU (dE) {kcal/mol} (298K) = 22.03 dUr avg (298., 1500. K) = 21.16 for A(T) = Aprime * T^n Aprime = 4.6599E+12 n = .31773				Rx C3.CCOOH = C2C*C + CH2OOH Hf {Kcal/mol} -12.490 -3.800 14.600 S {cal/mol K} 101.470 71.000 70.560 dHr {kcal/mol} (298K) = 23.29 dHr avg (298., 1500. K) = 21.34 dU (dE) {kcal/mol} (") = 22.70 dUr avg (298., 1500. K) = 19.56 Af/Ar (") = 8.701E+03 Af/Ar avg (298., 1500. K) = 8.744E+02 Fit Af/Ar: A = 4.701E+09 n = -2.26 alpha = 3.985E-04 avg error 10.53 %				
Temp(K)	AF(T)	AF-fit(T)	dS(cal/mol K)	dH(Kcal/mol)	dU(Kcal/mol)	dS(cal/mol K)	(Af/Ar)	dG(Kcal/mol)
300	2.51E+13	2.85E+13	1.32E-16	2.33E+01	2.27E+01	4.01E+01	8.65E+03	1.13E+01
400	3.10E+13	3.13E+13	1.35E-12	2.32E+01	2.24E+01	3.98E+01	5.71E+03	7.26E+00
500	3.53E+13	3.36E+13	3.36E-10	2.30E+01	2.20E+01	3.93E+01	3.49E+03	3.31E+00
600	3.84E+13	3.56E+13	1.31E-08	2.26E+01	2.14E+01	3.87E+01	2.14E+03	-5.95E-01
800	4.21E+13	3.90E+13	1.23E-06	2.18E+01	2.03E+01	3.76E+01	9.13E+02	-8.22E+00
1000	4.39E+13	4.18E+13	1.81E-05	2.11E+01	1.91E+01	3.67E+01	4.71E+02	-1.56E+01
1200	4.48E+13	4.43E+13	1.06E-04	2.04E+01	1.80E+01	3.61E+01	2.84E+02	-2.29E+01
1500	4.57E+13	4.76E+13	5.94E-04	1.94E+01	1.64E+01	3.54E+01	1.59E+02	-3.36E+01
2000	4.81E+13	5.22E+13	3.16E-03	1.80E+01	1.40E+01	3.45E+01	7.92E+01	-5.11E+01

TS III. 10 Thermodynamic Analysis for $\text{CH}_2\text{OOH} \rightarrow \text{CH}_2\text{O} + \text{OH}$

Rx	CH ₂ OOH = CH ₂ O + OH			Temp(K)	dH(Kcal/mol)	dU(Kcal/mol)	dS(cal/mol K)	(Af/Ar)	dG(Kcal/mol)
Hf {Kcal/mol}	14.600	-26.000	9.500	300	-3.11E+01	-3.17E+01	2.63E+01	8.31E+00	-3.90E+01
S {cal/mol K}	70.560	52.250	44.600	400	-3.12E+01	-3.20E+01	2.59E+01	5.24E+00	-4.16E+01
dHr {kcal/mol} (298K) = -31.10				500	-3.14E+01	-3.24E+01	2.55E+01	3.30E+00	-4.42E+01
dHr avg (298., 1500. K) = -32.68				600	-3.17E+01	-3.29E+01	2.50E+01	2.15E+00	-4.67E+01
dU (dE) {kcal/mol} (") = -31.69				800	-3.23E+01	-3.39E+01	2.41E+01	1.04E+00	-5.16E+01
dUr avg (298., 1500. K) = -34.47				1000	-3.29E+01	-3.49E+01	2.34E+01	5.86E-01	-5.63E+01
Af/Ar (") = 8.382E+00				1200	-3.35E+01	-3.59E+01	2.29E+01	3.76E-01	-6.10E+01
Af/Ar avg (298., 1500. K) = 1.024E+00				1500	-3.43E+01	-3.72E+01	2.23E+01	2.26E-01	-6.78E+01
Fit Af/Ar: A = 2.191E+06 n = -2.16 alpha = 1.667E-04				2000	-3.53E+01	-3.93E+01	2.17E+01	1.26E-01	-7.88E+01

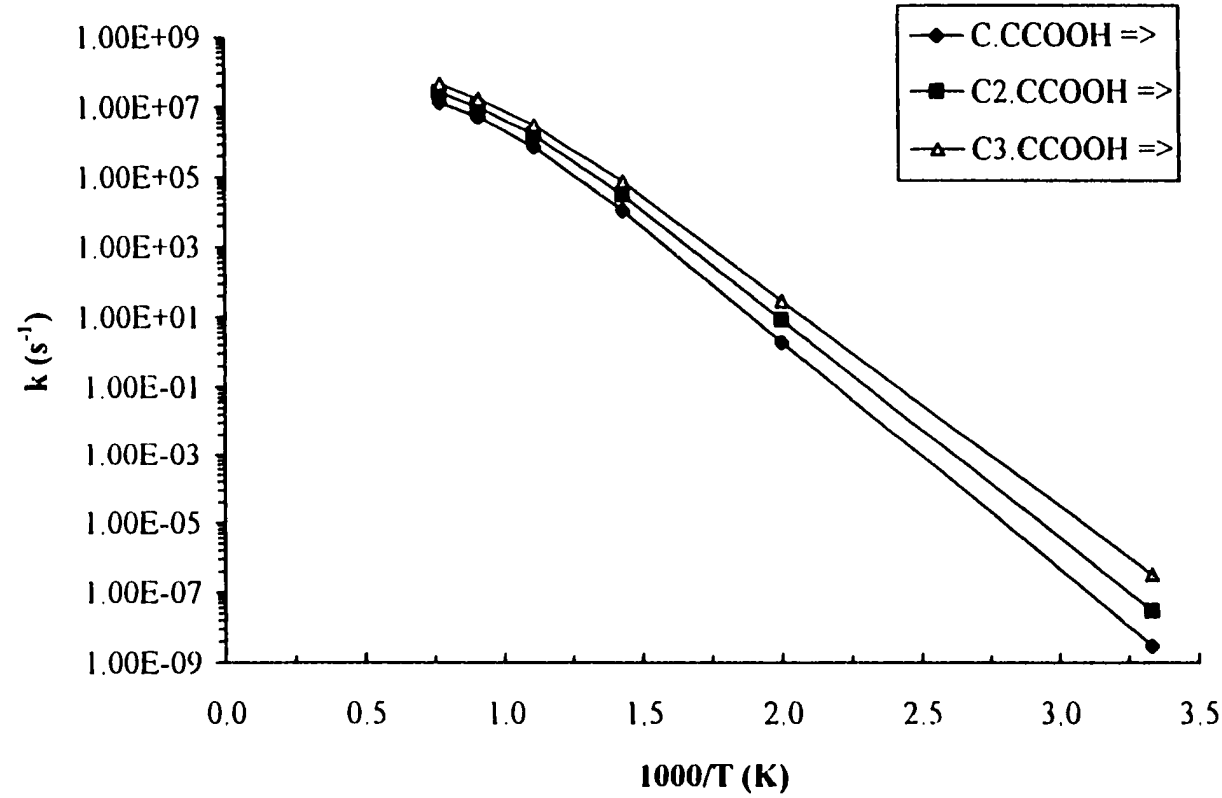
TS III. 11 Potential Energy Diagrams for $(R_1R_2C)CCOOH \rightarrow R_1R_2C=C + CH_2OOH$



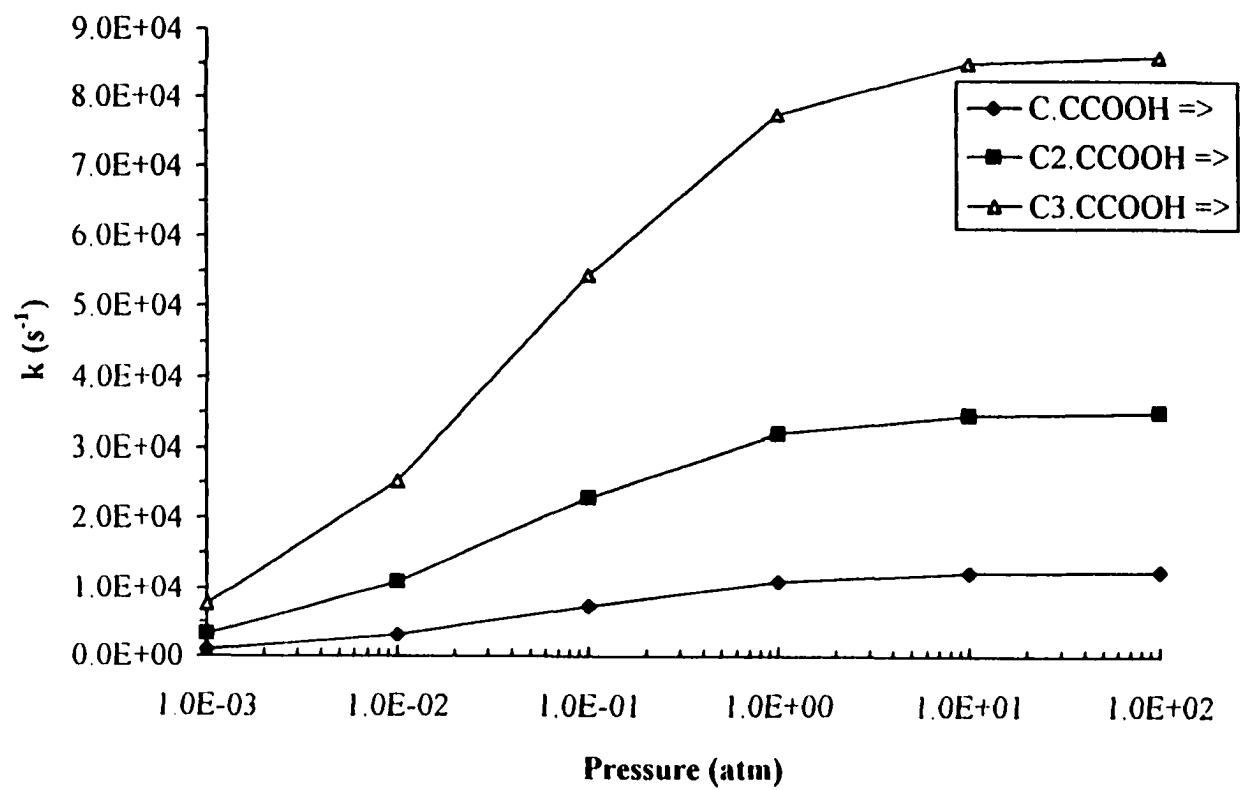
A are from thermodynamic analysis as in TS III. 6 - III. 8

E_a are from $(E_{a,r}(7.8) + \Delta U) Kcal-mol^{-1}$

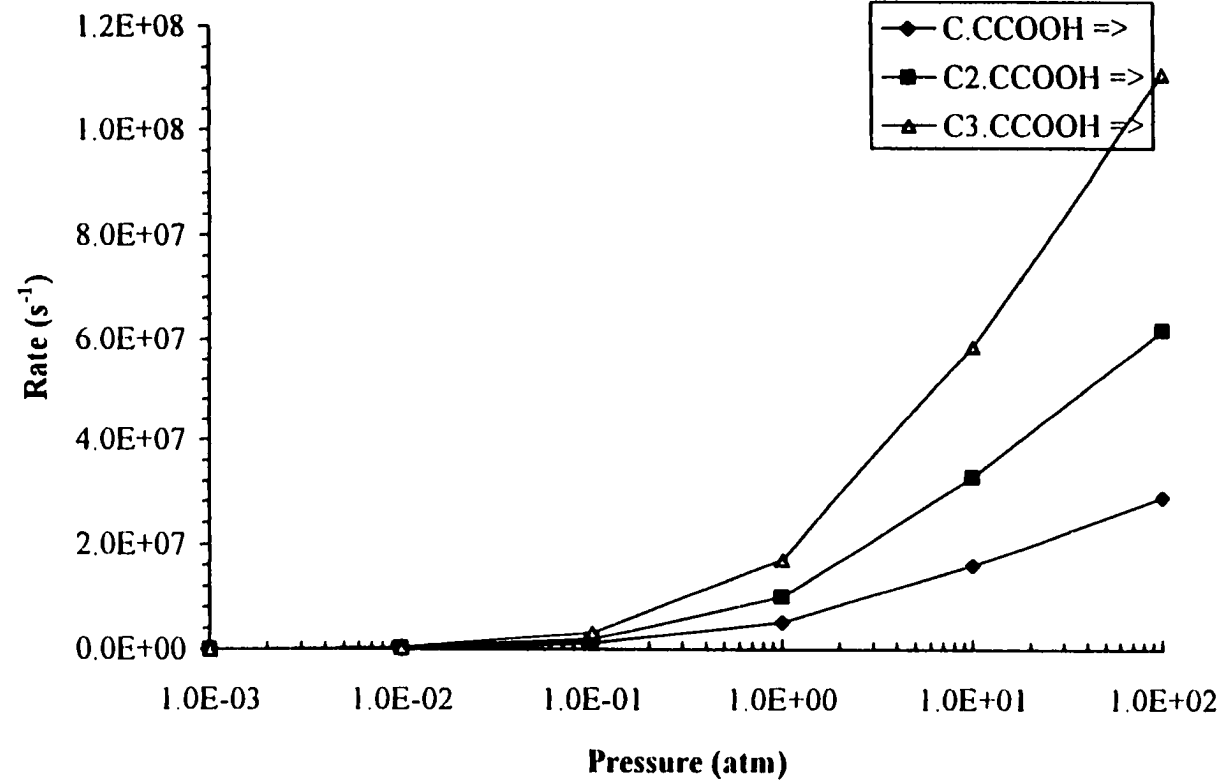
TS III. 12 Temperature Dependence of Rate Constants at 1 Atm



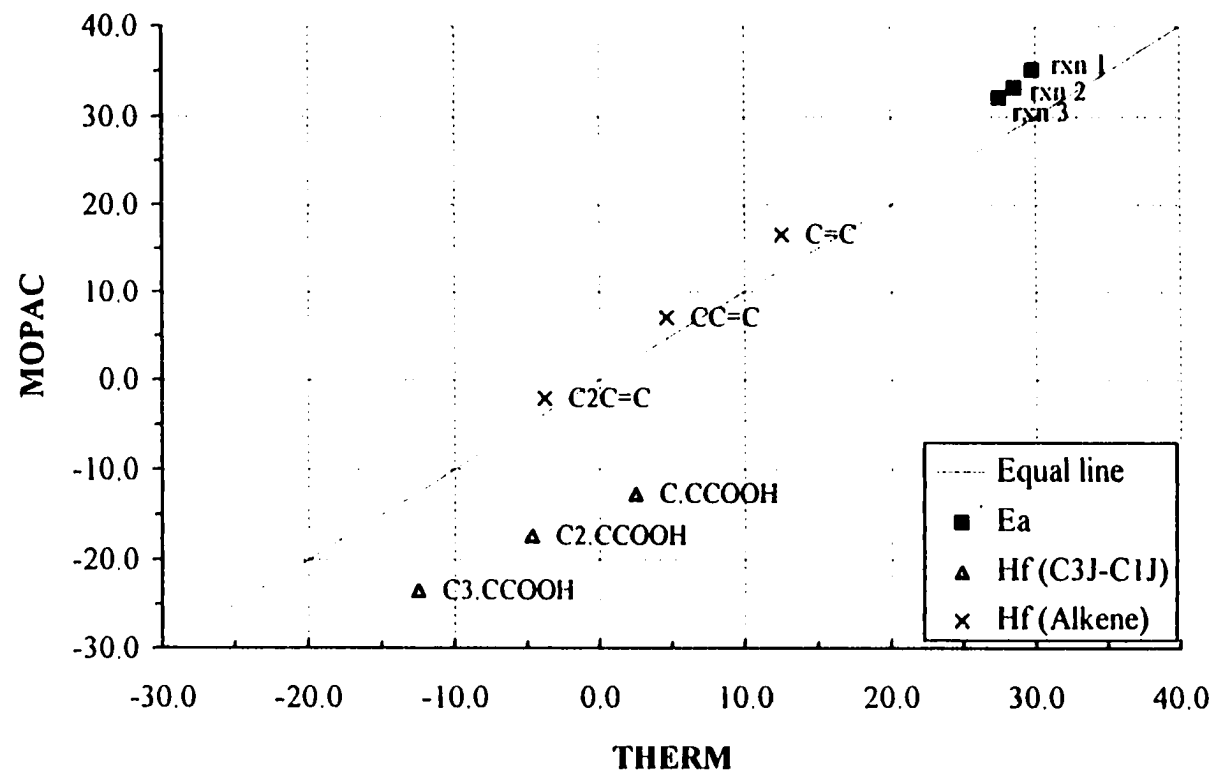
TS III. 13 Pressure Dependence of Rate Constants at 700 K



TS III. 14 Pressure Dependence of Rate Constants at 1100 K



TS III. 15 Activation Energy Analysis



REFERENCE

- 1 Benson, S. W. and Buss, J.H., "Additivity Rules for the Estimation of Molecular Properties." *J. Chem. Phys.*, 29, 546 (1958).
- 2 Ritter, E. R., "CPFIT Computer Code." *J. Chem. Inf. Computat. Sci.* 31, 400 (1991).
- 3 Lay, T. H.; Ritter, E. R.; Bozzelli, J. W. and Dean, A.M., "Hydrogen Atom Bond Increments (HBI) for Calculation of Thermodynamic Properties of Hydrocarbon Radical Species." *J. Phys. Chem.*, 99, 14514 (1995).
- 4 Lay, T. H. and Bozzelli, J. W., "Thermodynamic Properties of Oxygenated Hydrocarbon Radical Species Using Hydrogen Atom Bond Dissociation Groups." *AICHE Annal. Meeting*, San Francisco, California, November, 13-19, 1994.
- 5 Pitzer, K. S., "Thermodynamic Functions for Molecules having Restricted Internal Rotations." *J. Chem. Phys.*, 5, 469 (1937).
- 6 Pitzer, K. S. and Gwinn, W. D., "Energy Levels and Thermodynamic Function for Molecular With Internal Rotation I. Rigid Frame with Attached Tops." *J. Chem. Phys.*, 10, 428 (1942).
- 7 Pitzer, K. S., "Energy Levels and Thermodynamic Function for Molecular With Internal Rotation II. Unsymmetrical Tops Attached to a Rigid Frame." *J. Chem. Phys.*, 14, 239 (1946).
- 8 Kilpatrick, J. E. and Pitzer, K. S., "Energy Levels and Thermodynamic Function for Molecular with Internal Rotation III. Compound Rotation." *J. Chem. Phys.*, 11, 1064 (1949).
- 9 (a) Stewart, J. J. P., "Optimization of Parameters for Semiempirical Methods I. Principles." *J. Comput. Chem.*, 10, 209 (1989). (b) *ibid.* "Optimization of Parameters for Semiempirical Methods II. Applications" 10, 221 (1989).
- 10 Stewart, J. J. P., "MOPAC 6.0: A General Molecular Orbital Package." October, 1990. Frank J. Seiler Research Lab., US Air Force Academy, Colorado.
- 11 Dean, A. M. and Bozzelli, J. W., "Analysis of Hydrogen Atom Abstraction Reactions." *Comb. Chem. Nitro.* 1, 12-15 (1997).
- 12 (a) Maricq, M. M.; Szenté, J. J. and Kaiser, E. W., "A Diode Laser Study of Cl + C₂H₅ Reaction." *J. Phys. Chem.* 97, 7970 (1993). (b) Kaiser, E. W., "Relative Rate Constants for Reactions of HFC 152a, 143, 143a, 134a and HCFC 124 with F or Cl Atoms and for CF₂CH₃, CF₂HCH₂ and CF₃CFH radicals with F₂, Cl₂ and O₂." *Int. J. Chem. Kinet.* 25, 667 (1993). (c) Bozzelli, J. W. and Dean, A. M., "Hydrocarbon Radical Reactions with O₂: Comparison of Allyl, Formyl, and Vinyl to Ethyl." *J. Phys. Chem.* 97, 4427 (1993). (d) Wagner, W. H.; Slagle, I. R.; Sarzynski, D. and Gutman, D., "Experimental and Theoretical Studies of the C₂H₅ + O₂ Reaction Kinetics." *J. Phys. Chem.* 94, 1853 (1990). (e) Green, W. H., "Predictive Chemical Kinetics: Density Functional and Hartree-Fock Calculations on

- Free-Radical Reaction Transition States." *Int. J. Quat. Chem.*, 52, 837, (1994). (f) Quelch, G. E.; Gallo, M. M. and Schaefer III, H. F., "Aspects of the Reaction Mechanism of Ethane Combustion Conformations of the Ethylperoxy Radical." *J. Am. Chem. Soc.*, 114, 8239, (1992). (g) Prichard, H. O.; Shen, D. and Moise, A., "Theoretical Calculation of Intramolecular Reactions in Methylperoxyl and Ethylperoxyl Radicals." *J. Chem. Soc., Faraday Trans.*, 91, 1425-30 (1995).
- 13 Slater, N. B., "The Rates of Unimolecular Reactions in Gases." *Proc. Camb. Phil. Soc.*, 35, 56 (1939).
 - 14 Slater, N. B., *Theory of Unimolecular Reactions*. Methuen, London, 1959.
 - 15 Lindemann, F. A., "Discussion on 'the Radiation Theory of Chemical Action'" *Trans. Faraday Soc.*, 17, 598 (1922).
 - 16 Christiansen, J. A., *Ph.D. Thesis*, Dept. of Chemistry, Copenhagen (1921).
 - 17 Hinshelwood, C. N., "On the Theory of Unimolecular Reactions." *Proc. Roy. Soc. (A)*, 113, 230 (1927).
 - 18 Rice, O. K. and Ramsperger, H. C., "Theories of Unimolecular Gas Reactions at Low Pressure I." *J. Amer. Chem. Soc.*, 49, 1617 (1927); (b) *ibid.*, "Theories of Unimolecular Gas Reactions at Low Pressure II." 50, 617 (1928).
 - 19 (a) Kassel, L. S., "Studies in Homogeneous Gas Reactions (I)." *J. Phys. Chem.* 32, 225 (1928); (b) *ibid.*, "Studies in Homogeneous Gas Reactions (II)." 32, 1065 (1928).
 - 20 Kassel, L. S., "Kinetics of Homogenous Gas Reaction." Chemical Catalog Co., New York, 1932.
 - 21 Dean, A. M., "Predictions of Pressure and Temperature Effects upon Radical Addition and Recombination Reactions." *J. Phys. Chem.* 89, 4600 (1985).
 - 22 Dean, A.M.; Bozzelli, J. W. and Ritter, E. R., "Chemact: A Computer Code to Estimate Rate Constants for Chemically-Activated Reactions." *Combust. Sci. Technol.* 80, 63-85 (1991).
 - 23 Bozzelli, J. W.; Chang, A. Y. and Dean, A.M., "Molecular Density of States from Estimated Vapor Phase Heat Capacities." personal communication, Annandale, NJ, 1994.
 - 24 Gilbert, R. G.; Luther, K. and Troe, J., *Ber. Bunsenges. Phys. Chem.* 87, 164 (1983).
 - 25 Benson, S. W., *Thermochemical Kinetics* John Wiley, New York, 1976.
 - 26 Bozzelli, J. W.; Chang, A. Y. and Dean, A.M., "Molecular Density of States from Estimated Vapor Phase Heat Capacities." *Int. J. Chem. Kinet.*, 29, 161 (1996).
 - 27 Reid, R. C.; Prausnitz, J. M. and Poling, B. E., *The Properties of Gases and Liquids*. 5th ed., McGraw-Hill, Singapore, 1988.

- 28 Ben-Amotz, D. and Herschbach, D., "Estimation of Effective Diameters for Molecular Fluids." *J. Phys. Chem.* 94, 1038 (1990).
- 29 Hirschfelder, J. O.; Curtiss, C. F. and Bird, R. B., *Molecular Theory of Gases and Liquids*. 2nd ed., Wiley, London, 1963.
- 30 Harrington, R. E.; Rabinovitch, B. S. and Hoare, M. R., "Collisional Deaction of Vibrationally Excited Sec-Butyl-d1 Radicals Produced by Chemical Activation." *J. Phys. Chem.* 33, 744, (1960). Kohlmaier, G. H.; Rabinovitch, B. S., "Collisional Transition Probabilities for Vibrational Deactivation of Chemically Activated sec-Butyl Radicals, Different Initial Vibration Energy Levels." *ibid.* 39, 490 (1963). Ireton, R. C., Rabinovitch, B. S., "Transfer of Vibrational Energy from Highly Excited Butyl Radicals. Structural Effects on the Magnitudes of Relative Collision Diameters." *J. Phys. Chem.* 78, 1984 (1974).
- 31 Bozzelli, J. W. and Dean, A. M., "Chemical Activation of the Reaction of C_2H_5 with O_2 ." *J. Phys. Chem.* 94, 3313 (1990).
- 32 Ho, W. P.; Barat, R. B. and Bozzelli, J. W., "Thermal Reactions of CH_2Cl_2 in H_2/O_2 Mixtures: Implications for Chlorine Inhibition of CO Conversion to CO_2 ." *Combust. and Flame* 88, 265 (1992).
- 33 Tavakoli, J.; Chiang, H.M. and Bozzelli, J. W., "Thermal Reactions Of Methylene Chloride In Methane/Argon Mixtures." *Combust. Sci. and Tech.* 101, 135 (1994).
- 34 (a) Won, Y. S. and Bozzelli, J. W., "Chloroform pyrolysis. Experiment and detailed reaction model." *Combust. Sci. and Tech.* 85, 345 (1992). (b) Ho, W. P.; Yu, Q. R. and Bozzelli, J. W., "Kinetics Study on Pyrolysis and Oxidation of CH_3Cl in $Ar/H_2/O_2$ Mixtures." *Combust. Sci. and Tech.* 85, 23-63 (1992).
- 35 Westmoreland, P. R.; Howard, J. B.; Longwell, J. P. and Dean, A. M., "Prediction of Rate Constants for Combustion and Pyrolysis Reactions by Bimolecular QRRK." *AIChE Journal*, 32, 1971 (1986).
- 36 Dean, A. M. and Westmoreland, P. R., "Bimolecular QRRK Analysis of Methyl Radical Reactions." *Int. J. Chem. Kinet.* 19, 207 (1987).
- 37 Westmoreland, P. R., "Thermochemistry and Kinetics of $C_2H_3 + O_2$ Reactions." *Combust. Sci. and Tech.* 82, 151 (1992).
- 38 Ritter, E. R.; Bozzelli, J. W. and Dean, A. M., "Kinetic Study on Thermal Decomposition of Chlorobenzene Diluted in H_2 ." *J. Phys. Chem.* 94, 2493 (1990).
- 39 Bozzelli, J. W. and Dean, A. M., "Energized Complex Quantum Rice-Ramsperger-Kassel Analysis on Reactions of NH_2 with HO_2 , O_2 , and O Atoms." *J. Phys. Chem.* 93(3), 1058 (1989).
- 40 Bozzelli, J. W.; Chang, A. Y. and Dean, A.M., "Molecular Density of States from Estimated Vapor Phase Heat Capacities." *Twenty-fifth Symposium (International) on Combustion, the Combustion Institute*, p965-74, 1994.

- 41 Bozzelli, J. W. and Pitz, W. J., "The Reaction of Hydroperoxy-Propyl Radicals with Molecular Oxygen." *Twenty-fifth symposium (International) on Combustion, the Combustion Institute*, 783-791 (1994).
- 42 Baldwin, R. R.; Dean, C. E. and Walker, R. W., "Relative Rate Study of the Addition of HO₂ Radicals to C₂H₄ and C₃H₆." *J. Chem. Soc. Faraday Trans. 2* 82, 1445 (1986).
- 43 Chiang, H. M., "Dichloromethane Pyrolysis and Oxidation: Formation of Chlorinated Aromatic Pprecursors to PCDD/F." 1995 *Ph.D. Thesis*, Dept. of Chemistry, New Jersey Institute of Technology, Newark, NJ, May, 1995.
- 44 Warnatz, J., *Symp. (Int.) Combust., [Proc]*, 20, 845 (1985).
- 45 Norton, T. S. and Dryer, F. L., "An Experimental and Modeling Study of Ethanol Oxidation — Kinetics in an Atmospheric Pressure Flow Reactor." *Int. J. Chem. Kinet.*, 24, 319-344 (1992).
- 46 Koert, D. N.; Pitz, W. J.; Bozzelli, J. W. and Cernansky, N. P., "Chemical Kinetics Modeling of High Pressure Propane and Comparison to Experimental Results." *Twenty-sixth International Symposium on Combustion, Universita Federico II, Napoli, Italy* 28 July - 2 August, 1996.
- 47 Anderson, K. H. and Benson, S. W., "Catalytical Transfer by HCl in the Pyrolysis of Neopentane. The Rate of Dissociation of the Neopentyl Radical." *J. Chem. Phys.*, 40, 3747 (1964).
- 48 (a) Furimsky, E.; Laidler, K. J., "Kinetics of the Mercury-Photosensitized Decomposition of Neopentane. Part I. The Overall Mechanism." *Can. J. Chem.* 50, 1115, (1972). (b) Furimsky, E.; Laidler, K. J., "Kinetics of the Mercury-Photosensitized Decomposition of Neopentane. Part II. Reactions of the Methyl and Neopentyl Radicals." *Can. J. Chem.* 50, 1123, (1972). (c) Furimsky, E.; Laidler, K. J., "Kinetics of the Mercury-Photosensitized Decomposition of Neopentane. Part III. The Secondary Reactions." *Can. J. Chem.* 50, 1129, (1972).
- 49 Slagle, I. R.; Batt, L.; Gmurczyk, G. W.; Gutman, D. and Tsang, W., "Unimolecular Decomposition of the Neopentyl Radical." *J. Phys. Chem.* 95, 7732 (1991).
- 50 Baldwin, R. R.; Hisham, M. W. and Walker, R. W., "Arrhenius Parameters of Elementary Reactions Involved in the Oxidation of Neopentane." *J. Chem. Soc. Faraday Trans. 1*, 78, 1615 (1982).
- 51 Mitchell, T. J. and Benson, S. W., "Modeling of the Homogeneously Catalyzed and Uncatalyzed Pyrolysis of Neopentane: Thermochemistry of the Neopentyl Radical." *Intel. J. Chem. Kinet.*, 25, 931 (1993).
- 52 Wu, D. and Bayes, K. D., "Rate Constants for the Reactions of Isobutyl, Neopentyl, Cyclopentyl, and Cyclohexyl Radicals with Molecular Oxygen." *Int. J. Chem. Kinet.*, 18, 547 (1986).

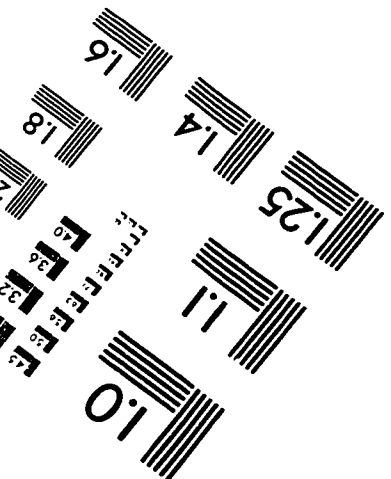
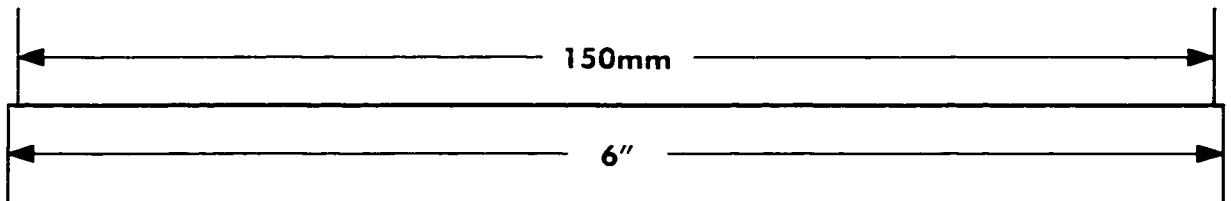
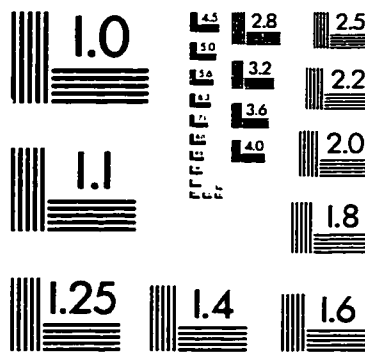
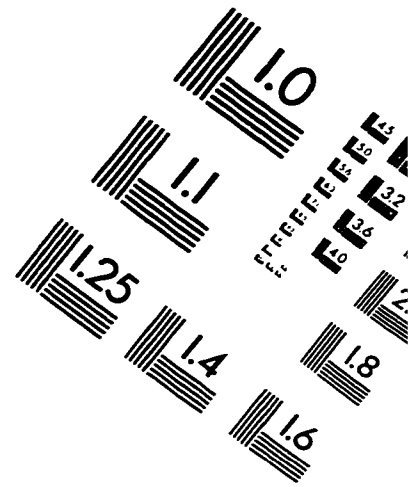
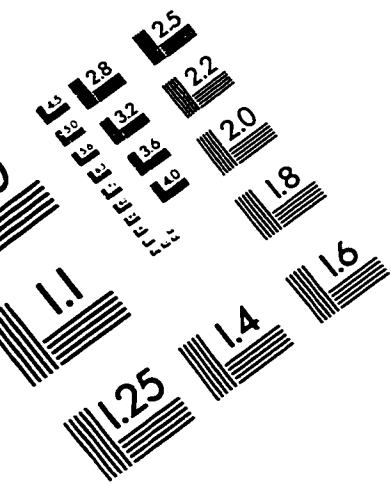
- 53 Xi, Z.; Han, W. J. and Bayes, K. D., Temperature Dependence of the Rate Constant for the Reaction of Neopentyl Radical + O₂." *J. Phys. Chem.* 92, 3450 (1988).
- 54 Hughes, K. J.; Halford-Maw, P. A.; Lightfoot, P. D.; Turanyi, T. and Pilling, M. J., "Direct Measurements of the Neopentyl Peroxy-Hydroperoxy Radical Isomerization over the Temperature Range 660-750 K." *Twenty-fourth Symposium (International) on Combustion, The Combustion Institute, Pittsburgh, PA*, p.645, 1992.
- 55 Zeelenberg, A. P., "Slow Oxidation of Hydrocarbons in the Gas Phase II Neopentane." *Rec. Trav. Chim.*, 81, 720 (1962).
- 56 Antonik, S. and Lucquin, M., "N 421.-Oxydation et Combustion de Basse Temperature du Neopentane en Pressure de Bromured' Hydrogene I - Existence de deux Mecanismes." *Bull. Soc. Chim.*, 2796 (1968).
- 57 Antonik, S. and Lucquin, M., "N 421.-Oxydation et Combustion de Basse Temperature du Neopentane en Pressure de Bromured' Hydrogene I - Resutats Analytiques et Cinetiques." *Bull. Soc. Chim.*, 3139 (1971).
- 58 Drysdale, D. D. and Norrish, R. G. W., "The Oxidation of Neopentane." *Proc. Roy. Soc. (London)* A308, 305 (1969).
- 59 Fish, A., *Combust. Flame*, 13, 23 (1969).
- 60 Baker, R. R.; Baldwin, R. R. and Walker, R. W., "The Use of the H₂ + O₂ Reaction in Determing the Velocity of Elementary Reactions in Dydrocarbon Oxidaiton." *Combust. Flame* 14, 31 (1970).
- 61 Baker, R. R.; Baldwin, R.R.; Everret, C. J. and Walker, R. W., "The Addition of Neopentane to Slower Reacting Mixtures of H₂ + O₂ at 480 °C. Part I. Formation of Primary Products from Neopentane." *Combust. Flame* 25, 285 (1975).
- 62 Baker, R. R.; Baldwin, R.R. and Walker, R. W., "Addition of Neopentane to Slower Reacting Mixtures of H₂ + O₂ at 480 °C. Part II. The Addition of the Primary Products from Neopentane, and the Rate Constants for H and OH Attack on Neopentane." *Combust. Flame* 27, 147 (1976).
- 63 Baldwin, R. R.; Pickering, I. R. and Walker, R. W., "Reactions of Ethyl Radicals with Oxygen over the Temperature Range 400 540 °C." *J. Chem. Soc. Faraday Trans. I*, 76, 2374 (1980).
- 64 Curran, H. J.; Pitz, W. J.; Westbrook, C. K.; Hisman, M. W. M. and Walker, R. W., "An Intermediate Temperature Modeling Study of the Combustion of Neopentane." submitted for The 26th International Symposium on Combustion, University of Naples, Italy. Vol. 1, p653, 1997.
- 65 Curran, H. J.; Gaffuri, P.; Pitz, W. J.; Westbrook, C. K.; Callahan, C.; Dryer, F. L. and Held, T., "Kinetics of the Formation of Oxetan Species from Alkyl

- Hydroperoxide Radicals." *Central States/Western States/Mexican Ntl. Sections Comb. Inst.* 263, (1995).
- 66 Ritter, E. R. and Bozzelli, J. W., "THERM. Thermodynamic Property Estimation for Gas Phase Radicals and Molecules." *Int. J. Chem. Kinet.* 23, 767 (1991).
 - 67 Lay, T. H.; Krasnoperov, L.; Venanzi, C. and Bozzelli, J. W., "Ab Initio Study of alpha-Chlorinated Ethyl Hydroperoxides $\text{CH}_3\text{CH}_2\text{OOH}$, $\text{CH}_3\text{CHClOOH}$ and $\text{CH}_3\text{CCl}_2\text{OOH}$: Conformational Analysis, Internal Rotation Barrier, Vibrational Frequencies, and Thermodynamic Properties." *J. Phys. Chem.*, 100, 8240 (1997).
 - 68 Lay, T. H.; Ritter, E. R.; Bozzelli, J. W. and Dean, A. M., "Hydrogen Atom Bond Increments (HBI) for Calculation of Thermodynamic Properties of Hydrocarbon Radical Species." *Chemical and Physical Process in combustion, The Eastern States Section Meeting of the Combustion Institute*, Paper No. 100 (1-4), 1993.
 - 69 Atkins, P. W., *Physical Chemistry*. 2nd, ed., W. H. Freeman and Company, San Francisco, 1982.
 - 70 Lay, T. H., "Thermodynamic Properties of Hydrocarbon Radicals, Peroxy Hydrocarbon and Peroxy Chlorohydrocarbon Molecules and Radicals: Kinetics and Reaction Mechanisms for: (1) Chloroform Pyrolysis and Oxidation (2) Benzene and Toluene Oxidation under Atmospheric Conditions." *Ph.D Thesis*, Dept. of Chemistry, New Jersey Institute of Technology, Newark, NJ.
 - 71 "Chemkin II", Sandia National Labs, Combustion Research Facility, Livermore, CA, 1990.
 - 72 Szivoczka, L. and Marta, F., "Kinetics of the Decomposition of neo-Pentane Sensitized by Azoisopropane." *React. Kinet. Catal. Lett.*, 3, 9 (1975); (b) *ibid.*, "Kinetics of the Decomposition of Neopentane Sensitized by Azoisopropane." *Magy. Kem. Foly.*, 85, 369 (1979).
 - 73 Muller, J.; Baronnet, F.; Scacchi, G.; Dzierzynski, M. and Niclaude, M., "Influences of ClH and BrH on the Pyrolysis of Neopentane and Ethane at Small Extents of Reaction." *Int. J. Chem. Kinet.*, 9, 425 (1977).
 - 74 Tsang, W., "The Stability of Alkyl Radicals." *J. Am. Chem. Soc.*, 107, 2872 (1985).
 - 75 Whitley, S. Craig, "MTBE, The Evolution of a Commodity and its Impact on US Butane." *Proc. Annu. Conv. - Gas Process Assoc.* (73rd), p283-289 (1994).
 - 76 Sheiley, Suzanne; Fouhy, Ken, "The Drive for Cleaner-Burning Fuel." *Chemical Engineering*, 101(1), 61 (1994)
 - 77 Parkinson, Gerald, "Oxygenates in Gasoline Cut CO Emissions." *Chemical Engineering*, 101(4), 46 (1994)
 - 78 Hamid, Syed Halim and Ali, Mohammed Ashraf, "Effect of MTBE Blending on the Properties of Gasoline." *Fuel Science and Tech. (Int'l)*, 13(5), 509-544 (1995).

- 79 Newman, Alan, "MTBE Detected in Survey of Urban Groundwater." *Environmental Science & Technology*, 29, 305A (1995)
- 80 Yeh, Carol K.; Novak, John T., "Anaerobic Biodegradation of Gasoline Oxygenates in Soils." *Water Environment Research*, 66, 744-52 (1994)
- 81 Mehlman, Myron A., "Dangerous and Cancer-Causing Properties of Products and Chemicals in the Oil Refining and Petrochemical Industrial: Part XV. Health Hazards and Health Risks from Oxygenated Automobile fuels (MTBE): Lessons not Heeded." *Int. J. Occup. Med. Toxicol.*, 4(2), 219-36 (1995)
- 82 Benson, Sidney W., "Mechanism of Inhibition of Knock by Lead Additives, a Chain Debranching Reaction." *J. Phys. Chem.*, 92 (3), 1531-3 (1988).
- 83 Ing, J. "Reaction Kinetics of Methanol and MTBE Oxidation and Pyrolysis." *PHD Thesis*, New Jersey Institute of Technology, Newark, 1996.
- 84 (a) Daly, N. J. and Wentrup, C., "Pyrolysis of Methyl Tert-Butyl Ether." *Aust. J. Chem.*, 21, 2711 (1968); (b) *ibid.*, 21, 1535 (1968).
- 85 Choo, K. Y.; Golden, D. M. and Benson, S. W., "Very Low-Pressure Pyrolysis (VLPP) of t-Butylmethyl Ether." *Int. J. Chem. Kinet.*, VI, 631-641 (1974).
- 86 (a) Brocard, J. C. and Baronnet, F., "Pyrolysis of Methyl Tert-Butyl Ether." *Oxidation Commun.*, 1, 321 (1980); (b) Brocard, J. C. and Baronnet, F., "Effets de Parois Dans la Pyrolyse du Methyl tert-Butyl Ether (MTBE)." *J. Chim. Phys. Phys.-Chim. Biol.*, 84, 19 (1987).
- 87 Cox, R. A. and Goldstone, A., "Atmospheric Reactivity of Oxygenated Motor Fuel Additive." *Proceeding of the 2nd European Symposium on the Physico Chemical Behavior of Atmospheric Pollutants*, Riedel, Dorecht, Holland, 112 (1982).
- 88 Wallington, T. J.; Dagant, P.; Liu, R. and Kurylo, M., "Gas-Phase Reactions of Hydroxyl Radical with the Fuel Additives Methyl tert-Butyl Ether and tert-Butyl Alcohols over the Temperature Range 240-440 K." *Combust. Sci. Tech.*, 22, 842 (1988).
- 89 Wallington, T. J.; Andino, J. M.; Skewes, L. M.; Siegl, W. O. and Japar, S. M., "Kinetics of the Reaction of OH Radicals with a Series of Ethers under Simulated Atmospheric Conditions at 295 K." *Int. J. Chem. Kinet.*, 21, 993-1001 (1989).
- 90 Tuazon, E. C.; Carter, W. P.; Aschmann, S. M. and Atkinson, R., "Products of the Gas-Phase Reaction of Methyl tert-Butyl Ether with the OH Radical in the Presence of NO_x." *Int. J. Chem. Kinet.*, 23, 1003-1015 (1991).
- 91 Smith, D. F.; Kleindienst, T. E.; Hudgens, E. E.; McIver, C. D. and Bufalini, J., "The Photooxidation of Methyl Tertiary Butyl Ether." *Int. J. Chem. Kinet.*, 23, 907-924 (1991).
- 92 Dunphy, M. and Simmie, J. M., "High Temperature Oxidation of Methyl Tert-Butyl Ether." *Combust. Sci. Tech.*, 66, 157 (1989)

- 93 Norton, T. S. and Dryer, F. L. "The Flow Reactor Oxidation of C1-C4 Alcohols and MTBE." *The Twenty-third Symposium (International) on Combustion*, The Combustion Institute: Pittsburgh. PA, P179-85, 1990.
- 94 Held, T. J.; Dryer, F. L. and Noton, T. S., "Oxidation of Methyl Tert-Butyl Ether." To be published.
- 95 (a) Chen, C. J. and Bozzelli, J. W., "Thermochemical Kinetic Analysis on the Reaction of Tertiary Butyl Radical with Oxygen and an Elementary Reaction Mechanism for Tertiary Butyl Oxidation." to be published. (b) Chen, C. J. and Bozzelli, J. W., "Thermochemical Kinetic Analysis on the Reaction of Allylic Isobutenyl Radical with O₂ : an Elementary Reaction Mechanism for Isobutene Oxidation." to be published.
- 96 Baker, R. R.; Baldwin, R. R. and Walker, R. W., Addition of I-Butane to Slowly Reacting Mixtures of Hydrogen and Oxygen at 480 °C." *J. Chem. Soc. Faraday Trans. 74*, 2229 (1978).
- 97 Walch, S. P. *American Inst. Phys.* 98, 3163 (1993).
- 98 Soto, M. R. and Page, M. J., "Features of the Potential Energy Surface for Reactions of OH with CH₂O." *J. Phys. Chem.* 94, 3242 - 3246 (1990).

IMAGE EVALUATION TEST TARGET (QA-3)



APPLIED IMAGE, Inc
1653 East Main Street
Rochester, NY 14609 USA
Phone: 716/482-0300
Fax: 716/288-5989

© 1993, Applied Image, Inc., All Rights Reserved

